Volumes 113–116 (12 Issues), Spring 2004, ISSN: 0273–2289

Applied Biochemistry and Biotechnology

Executive Editor: **Ashok Mulchandani**

Biotechnology for Fuels and Chemicals

The Twenty-Fifth Symposium

Editors

Mark Finkelstein
James D. McMillan
Brian H. Davison
Barbara Evans

HUMANA PRESS

Biotechnology for Fuels and Chemicals

The Twenty-Fifth Symposium

Presented as Volumes 113–116
of *Applied Biochemistry and Biotechnology*
Proceedings of the Twenty-Fifth Symposium
on Biotechnology for Fuels and Chemicals
Held May 4–7, 2003, in Breckenridge, CO

Sponsored by

US Department of Energy's Office of the Biomass Program (DOE-OBP)
National Renewable Energy Laboratory (NREL)
Oak Ridge National Laboratory (ORNL)
Argonne National Laboratory (ANL)
Idaho National Engineering and Environment Laboratory (INEEL)
Pacific Northwest National Laboratory (PNNL)
US Department of Agriculture (USDA)
Alltech
Archer Daniels Midland (ADM)
BBI International
Biotechnology Industrial Organization (BIO)
Breckenridge Brewery
Cargill, Inc.
Cargill Dow, LLC
Coors Brewing Company
Corn Refiners Association (CRA)
E. I. du Pont de Nemours & Co., Inc. (DuPont)
Genencor International
Iogen Corporation
Katzen International
Natural Resources Canada
Novozymes Biotech
Proctor and Gamble
Syngenta
Tate and Lyle
Tembec Industries

Editors

Mark Finkelstein and James D. McMillan
National Renewable Energy Laboratory

Brian H. Davison and Barbara Evans
Oak Ridge National Laboratory

Humana Press • Totowa, New Jersey

Applied Biochemistry and Biotechnology
Volumes 113–116, Complete, Spring 2004

Applied Biochemistry and Biotechnology is abstracted or indexed regularly in *Chemical Abstracts*, *Biological Abstracts*, *Current Contents*, *Science Citation Index*, *Excerpta Medica*, *Index Medicus*, and appropriate related compendia.

Introduction to the Proceedings of the Twenty-Fifth Symposium on Biotechnology for Fuels and Chemicals

Mark Finkelstein

National Renewable Energy Laboratory

Brian H. Davison

Oak Ridge National Laboratory

The 25th Symposium on Biotechnology for Fuels and Chemicals was held in Breckenridge, CO, May 4–7, 2003. Over 450 attendees helped underscore the growing importance of bioenergy and a biobased economy during this special Silver Anniversary Symposium. Forty states and twenty-three countries were represented at the Symposium, with over 40% of the attendees from industry, almost 40% from universities and colleges, and the remainder from government agencies and laboratories. The robust participation and sponsorship by industry highlights the relevancy and importance of this Symposium.

While improving the economics of producing fuels and chemicals is vital to many industrial sectors, the ability to do so in a sustainable and environmentally responsible manner is becoming increasingly important. The program for the 25th Symposium on Biotechnology for Fuels and Chemicals was designed to deliver the latest research breakthroughs and results in biotechnology that stimulate such improvements. The technical focus of Symposium was evident at each session, as evolutionary as well as revolutionary research findings were revealed. The eight technical sessions contained 52 oral presentations and we had 272 poster presentations. Whether one represented the industrial, academic, or government sector, each was invited to participate in this stimulating exchange of information and ideas. Valuable opportunities for productive interactions with colleagues, both from a national and international perspective, were evident throughout the meeting.

With the 25th Symposium, we continued the tradition of providing an informal, congenial atmosphere that our participants found conducive to discussing technical program topics. This year's topics included:

Session 1A	Feedstock Supply, Logistics, Processing, and Composition
Session 1B	Enzyme Catalysis and Engineering
Session 2	Microbial Catalysis and Engineering
Session 3	Bioprocessing including Separations
Session 4	Biotechnology for Fuels and Chemicals—Past, Present, and Future
Session 5	Biobased Industrial Chemicals
Session 6A	Biomass Pretreatment and Hydrolysis
Session 6B	Plant Biotechnology and Feedstock Genomics
Special Topics A	Microbial Pentose Metabolism
Special Topics B	International Bioenergy Agency Bioethanol Meeting

A summary of these sessions is included at the beginning of each section of the Proceedings. The technical core of the Symposium remains the creation, manipulation, and practical use of new biocatalysts to produce useful fuels and chemicals. This was shown in both fundamental science discoveries as well as progress reports from commercialization efforts. However, we have continued to expand interest into the biofeedstock (plant genomics, production, and pretreatment). While the production of sugars from biomass and their subsequent bioconversion into chemicals remains the dominant thrust, areas such as gasification and direct production in plants were presented. The use of molecular biology and genomics to provide new biocatalysts as well as understanding the fundamentals of the microbes, enzymes, and biomass has increased the likely achievement of both near and long-term commercialization goals.

This year Dr. J. Craig Venter, Genome Sequencer, Entrepreneur, and Chief Executive Officer augmented our technical program with a spellbinding after dinner presentation entitled "Genomic Approaches to the Environment." This touched on his latest efforts in metagenomics and in constructing a minimal genome.

Charles D. Scott Award Presentation

For the past 10 symposia we have recognized an individual who has distinguished him or herself in the application of biotechnology towards the production of fuels and chemicals. This award acknowledges contributions to the field as a whole or this symposium, with particular attention to innovation in fundamental and applied biotechnology, insight into bioprocessing fundamentals, or commitment to facilitate commercialization of products from renewable resources. The award is named in honor of Dr. Charles D. Scott, the founder of this symposium and its chair for the first 10 years.

Dr. Tom Jeffries received this year's award. Dr. Jeffries is a microbiologist whose research focuses on using plant matter to make the fuel ethanol. He directs the Institute for Microbial and Biochemical Technology at the USDA Forest Service Forest Products Laboratory in Madison, WI, and is a

professor in the Bacteriology and Food Science departments at the University of Wisconsin, Madison. His recent research has aimed at modifying yeast DNA to increase the amount of ethanol produced when the yeast metabolizes certain components of wood. He was also one of four attendees who attended the inaugural Symposium 25 years ago (along with Bob Tanner, Y.Y. Lee, and Chuck Scott).

Session Chairpersons

Session 1A: Feedstock Supply, Logistics, Processing, and Composition.

Topics encompassed production and collection issues (availability, farming, silviculture, harvesting, densification, consistency and storage).

Chair: Jim Hettenhaus, *E-mail: jrhetten@ceassist.com*
Co-Chair: David Morris, *E-mail: dmorris@ilsr.org*

Session 1B: Enzyme Catalysis and Engineering.

Speakers focused on how to identify, modify, develop, and cost-effectively produce the use of enzymes to carry out a myriad of biological/chemical transformations.

Chair: Mike Himmel, *E-mail: Mike_Himmel@nrel.gov*
Co-Chair: David Wilson, *E-mail: dbw3@cornell.edu*

Session 2: Microbial Catalysis and Engineering.

This session focused on finding new and developing existing microorganisms for improved performance to produce fuels and chemicals.

Chair: Tom Jeffries, *E-mail: Twjeffri@facstaff.wisc.edu*
Co-Chair: Lee Lynd, *E-mail: lee.lynd@dartmouth.edu*

Session 3: Bioprocessing, Including Separations.

This session covered reactor configurations and the integration of engineering with microbiology, biochemistry, and chemistry to produce fuels and chemicals.

Chair: Dale Monceaux, *E-mail: monceaux@katzen.com*
Co-Chair: David Short, *E-mail: david.r.short@usa.dupont.com*

Session 4: Biotechnology for Fuels and Chemicals—Past, Present, and Future.

This session gazed into the crystal ball while occasionally looking into the rear-view mirror to review the past 25 years.

Chair: Chuck Scott, *E-mail: cdscott1@aol.com*
Co-Chair: Charles Wyman, *E-mail: charles.e.wyman@dartmouth.edu*

Session 5: Biobased Industrial Chemicals.

The production of chemicals and other value-added bioproducts from biological rather than petrochemical uses was discussed at this session. Advances in process integration, demonstration, economics, and commercialization were highlighted.

Chair: Doug Cameron, *E-mail: Doug_Cameron@cargill.com*
Co-Chair: Marion Bradford, *Tate & Lyle, Retired*

Session 6A: Biomass Pretreatment and Hydrolysis.

Novel reactor configurations as well as new process approaches to pretreat and saccharify biomass was the focus of this session.

Chair: Y. Y. Lee, *E-mail: yylee@eng.auburn.edu*
Co-Chair: Bruce Dale, *E-mail: bdale@egr.msu.edu*

Session 6B: Plant Biotech and Feedstock Genetics.

The sustainable success of Bioenergy and Bioproducts requires new integrated approaches. The potential impact of transgenic, genetic, and genomic-based modifications to the archi-tectural, compositional, or metabolic functions of plants was discussed in relation to an enhanced renewable base.

Chair: Jim McLaren, *E-mail: mclaren@inverizon.com*
Co-Chair: Steve Thomas, *E-mail: Steve_Thomas@nrel.gov*

Special Topics: Pentose Metabolism.

Microorganisms capable of converting biomass pentose sugars to fuels and chemicals are essential for robust biomass-based processes. This session discussed recent technological developments and understanding that will allow for the construction of superior microorganisms.

Chair: Barbel Hahn-Hagerdal, *Lund University, Sweden*
Co-Chair: Neville Pamment, *University of Melbourne, Australia*

Special Topics: IEA Task 39 Bioethanol

Chair: Jack Saddler, *E-mail: saddler@interchg.ubc.ca*
Co-Chair: David Gregg, *E-mail: djgregg@interchange.ubc.ca*

Organizing Committee

Mark Finkelstein, Conference Chair, *National Renewable Energy Laboratory, Golden, CO*
Brian Davison, Conference Co-Chair, *Oak Ridge National Laboratory, Oak Ridge, TN*
William Apel, *Idaho National Engineering and Environmental Laboratory, Idaho Falls, ID*
Doug Cameron, *Cargill, Minneapolis, MN*
Tom Jeffries, *USDA, Forest Service, Madison, WI*
James Lee, *Oak Ridge National Laboratory, Oak Ridge, TN*
Lee Lynd, *Dartmouth College, Hanover, NH*
James McMillan, *National Renewable Energy Laboratory, Golden, CO*
Amy Mannheim, *US Department of Energy, Washington, DC*
Dale Monceaux, *Katzen International, Cincinnati, OH*
Jack Saddler, *University of British Columbia, Vancouver, British Columbia, Canada*
Sharon Shoemaker, *University of California, Davis, CA*
David Short, *DuPont, Newark, DE*
Jim Spaeth, *US Department of Energy, Golden, CO*

Jeff Tolan, *Iogen Corporation, Ottawa, Ontario, Canada*
Nancy Watlington, *Oak Ridge National Laboratory, Oak Ridge, TN*
Liz Willson, *National Renewable Energy Laboratory, Golden, CO*
Charles E. Wyman, *Dartmouth College, Hanover, NH*
Guido Zacchi, *Lund University, Lund, Sweden*
Gisella M. Zanin, *State University of Maringa, Maringa, Parana, Brazil*

Acknowledgments

The continued success of the symposium is due to the many participants, organizers, and sponsors, but is also a success and pleasure due to the diligent and creative staff. In particular, Liz Willson of NREL and Nancy Watlington of ORNL, provided organization, advice, persistence, and unfailing good humor. Howard Brown of NREL provided communications and website acumen, Ivilina Thornton provided the overall conference coordination, and the overall assistance from Lyn Lumberg of NREL is gratefully acknowledged.

The National Renewable Energy Laboratory is operated for the US Department of Energy by Midwest Research Institute and Battelle under contract DE-AC36-99GO10337.

Oak Ridge National Laboratory is operated for the US Department of Energy by UT-Battelle, LLC under contract DE-AC05-00OR22725.

Other Proceedings in this Series

1. Proceedings of the First Symposium on Biotechnology in Energy Production and Conservation (1978), *Biotechnol. Bioeng. Symp.* **8.**
2. Proceedings of the Second Symposium on Biotechnology in Energy Production and Conservation (1980), *Biotechnol. Bioeng. Symp.* **10.**
3. Proceedings of the Third Symposium on Biotechnology in Energy Production and Conservation (1981), *Biotechnol. Bioeng. Symp.* **11.**
4. Proceedings of the Fourth Symposium on Biotechnology in Energy Production and Conservation (1982), *Biotechnol. Bioeng. Symp.* **12.**
5. Proceedings of the Fifth Symposium on Biotechnology for Fuels and Chemicals (1983), *Biotechnol. Bioeng. Symp.* **13.**
6. Proceedings of the Sixth Symposium on Biotechnology for Fuels and Chemicals (1984), *Biotechnol. Bioeng. Symp.* **14.**
7. Proceedings of the Seventh Symposium on Biotechnology for Fuels and Chemicals (1985), *Biotechnol. Bioeng. Symp.* **15.**
8. Proceedings of the Eighth Symposium on Biotechnology for Fuels and Chemicals (1986), *Biotechnol. Bioeng. Symp.* **16.**
9. Proceedings of the Ninth Symposium on Biotechnology for Fuels and Chemicals (1988), *Appl. Biochem. Biotechnol. Symp.* **17,18.**

10. Proceedings of the Tenth Symposium on Biotechnology for Fuels and Chemicals (1989), *Appl. Biochem. Biotechnol. Symp.* **20,21.**
11. Proceedings of the Eleventh Symposium on Biotechnology for Fuels and Chemicals (1990), *Appl. Biochem. Biotechnol. Symp.* **24,25.**
12. Proceedings of the Twelfth Symposium on Biotechnology for Fuels and Chemicals (1991), *Appl. Biochem. Biotechnol. Symp.* **28,29.**
13. Proceedings of the Thirteenth Symposium on Biotechnology for Fuels and Chemicals (1992), *Appl. Biochem. Biotechnol. Symp.* **34,35.**
14. Proceedings of the Fourteenth Symposium on Biotechnology for Fuels and Chemicals (1993), *Appl. Biochem. Biotechnol. Symp.* **39,40.**
15. Proceedings of the Fifteenth Symposium on Biotechnology for Fuels and Chemicals (1994), *Appl. Biochem. Biotechnol. Symp.* **45,46.**
16. Proceedings of the Sixteenth Symposium on Biotechnology for Fuels and Chemicals (1995), *Appl. Biochem. Biotechnol. Symp.* **51,52.**
17. Proceedings of the Seventeenth Symposium on Biotechnology for Fuels and Chemicals (1996), *Appl. Biochem. Biotechnol. Symp.* **57,58.**
18. Proceedings of the Eighteenth Symposium on Biotechnology for Fuels and Chemicals (1997), *Appl. Biochem. Biotechnol. Symp.* **63–65.**
19. Proceedings of the Nineteenth Symposium on Biotechnology for Fuels and Chemicals (1998), *Appl. Biochem. Biotechnol. Symp.* **70–72.**
20. Proceedings of the Twentieth Symposium on Biotechnology for Fuels and Chemicals (1999), *Appl. Biochem. Biotechnol. Symp.* **77–79.**
21. Proceedings of the Twenty–First Symposium on Biotechnology for Fuels and Chemicals (2000), *Appl. Biochem. Biotechnol. Symp.* **84–86.**
22. Proceedings of the Twenty–second Symposium on Biotechnology for Fuels and Chemicals (2001), *Appl. Biochem. Biotechnol. Symp.* **91–93.**
23. Proceedings of the Twenty–Third Symposium on Biotechnology for Fuels and Chemicals (2002), *Appl. Biochem. Biotechnol. Symp.* **98–100.**
24. Proceedings of the Twenty–Fourth Symposium on Biotechnology for Fuels and Chemicals (2003), *Appl. Biochem. Biotechnol. Symp.* **105–108.**

This symposium has been held annually since 1978. We are pleased to have the Proceedings of the Twenty-Fifth Symposium currently published in this special issue to continue the tradition of providing a record of the contributions made.

The Twenty-Sixth Symposium will be held May 7–11, 2004, in Chattanooga, Tennessee. For more information, visit the following Websites: http://www.ct.ornl.gov/symposium or http://nrel.gov/biotech_symposium. We encourage comments or discussions relevant to the format or content of the meetings.

Contents

*For papers with multiple authorship, the asterisk identifies the author to whom correspondence and reprint requests should be addressed.

Volume 113

Session 1A

Feedstock Supply, Logistics, Processing, and Composition

Session 1A

Feedstock Supply, Logistics, Processing, and Composition

Jim Hettenhaus[1] and David Morris[2]

[1]*cea Inc, Charlotte, NC; and*
[2]*Institute for Local Self Reliance, Minneapolis, MN*

For large, economic, and sustainable harvest of biomass feedstock, major changes in cropping practice, collection, storage, and transportation are required. The challenges faced in supplying 0.7–1 million dry short tons (dt) for a single biorefinery are huge—five times larger than previous attempts.

Ultimately, the farmer controls biomass sourcing for biorefineries. The availability of large quantities of residues, stover, and straw is greatly dependent on tillage practice. No tillage results in most of the residue available for removal, especially when cover crops are employed for erosion control. By contrast, no excess is available with conventional tillage. Since <20% of cropland is no till and >60% is conventional till, a major shift in cropping practice is needed for sustainable removal of significant quantities.

Present collection costs are 1.5–2 times the delivered cost target—$35/dt, including $20/acre or more net income for the farmer. Bulk collection is likely needed, because baling adds cost, $15/dt, and no value. One-pass harvest can lower the delivered feedstock cost to <$20/dt within a 15- to 20-mi radius. Prototypes for one-pass harvest of straw and stover are under development, adapting existing equipment. Many variations are possible, but until a better market definition is available, a new design is probably limited to paper studies.

One-pass harvest also reduces the risk of corn stover harvest if storage of wet harvested material is resolved. For the sugar platform, feedstock can be wet, above 65%, or dry, below 20%. Some are looking at adapting wet, bagasse-type storage, large 250,000-dt piles built via circulating liquor that conveys the feedstock from wagons or trailers directly from the field after it is washed and milled to a particle size that ensures good compaction and preservation in storage. Less area is required; fire is eliminated when stored above 65% moisture. The material processes easier because 80% of the solubles is removed in storage. Water management and other issues remain. Validation of this method is required for other crops such as stover and straw.

Because of the bulky nature, the cost of transportation is 20–40% of the cost within a 50-mi radius. Transportation from the field to a storage site following harvest needs to be kept short if truck requirements are to remain manageable. Collection within a 50-mi radius for one site requires about five times the trucks and wagons compared with a 15-mi radius. While bulk density can be increased, the cost of densification generally offsets any transport savings. Pipelines require huge initial investment. Short-line rail delivery from three or more collection sites to supply the plant appears most advantageous compared to trucking or pipelines.

In conclusion, potential processors want clean liquid, mostly fermentable sugars, delivered to the processing plant. Thus, in addition to the above, using part of the storage time for value-added treatment offers more potential. Although this processing is probably under different regulatory requirements than storage, it may be segregated and controlled separately. Including preprocessing with harvesting, collection, and storage provides farmers ample opportunity to participate in the value chain, moving away from simply supplying a commodity.

0273-2289/04/113/0005–0012/$25.00

Designing an Effective Federal Biomass Program

David Morris*

Institute for Local Self-Reliance, Suite 303,
1313 5th Street SE, Minneapolis, MN 55415,
E-mail: dmorris@ilsr.org

Abstract

This article addresses two questions: Has the effectiveness of the US government's federal research and development (R&D) spending suffered from the post-1980 strategic change from freely shared and publicly owned to privately owned scientific advances? What criteria would a federal R&D program use to design a strategy that most effectively enhances the well-being of farmers and rural communities? Several studies found that the pre-1980 US Department of Agriculture research strategy was very effective. No comparable studies have analyzed the comparative effectiveness of the post-1980 strategy of restricting access to the results of public research. Recent experience and several analytical studies suggest that to significantly enhance the health of rural economies from an expanded use of plant matter as an industrial material, federal policy should channel scientific and engineering research into small- and medium-sized production and processing technologies and should encourage farmer-owned, value-added enterprises.

Index Entries: Ethanol; scale; ownership; research and development; effectiveness.

Introduction

One of the twentieth century's greatest scientists and thinkers, Albert Einstein, observed, "Perfection of means and confusion of ends seem to characterize our society." Are the US government's federal programs supporting industrial uses of biomass an example of such thinking?

The ends of the federal biomass programs are clear enough: enhanced national security, improved environmental protection, stronger rural economies. Research is a means to these ends. Are the federal biomass programs designed to most effectively achieve these ends?

*Author to whom all correspondence and reprint requests should be addressed.

Federal programs and policies channel scientific genius and entrepreneurial energy and investment capital in specific directions. Regarding biomass, the overall impact of direct spending and tax incentives is not insubstantial.

The federal government spends more than $200 million annually directly on research and development (R&D) directed toward expanding industrial uses of biomass. Assuming a three- to one-average private-to-public investment match, this federal direct spending attracts an additional $600 million in private spending. Federal biomass-related tax incentives presently "spend" more than $1 billion per year. This in turn attracts several billion dollars of private investment in these areas. The vast majority at present goes into expanding ethanol production.

This article examines some aspects of federal R&D efforts in the biomass area. It raises two areas of question. One is whether the post-1980 changes in the way the federal government conducts biomass research has made the biomass R&D effort more or less effective in achieving its stated goals. The observations are primarily directed toward the Department of Agriculture because the vast majority of its research is conducted in-house by permanent scientific staff.

The second area of question focuses on one of those goals, improving the well-being of America's farmers and rural communities, and suggests that social criteria can and should inform and guide engineering research strategies. The observations are primarily directed toward the Department of Energy (DOE), although they are broadly applicable to agency heads and policy makers.

Public vs Private Knowledge

Before 1980, the results of federal agricultural research were freely available and widely shared. Virtually all of the research was directed toward improving crop production and yields as well as harvesting and storage costs of crops intended for food and feed markets.

There are considerable uncertainties regarding cost-benefit analyses. Nevertheless, it is instructive that the many studies done both inside and outside the United States Department of Agriculture (USDA) found its pre-1980 R&D efforts very effective and influential.

USDA economists found that publicly funded agricultural research earned an annual rate of return of at least 35 %.[1] A 1966 study by the Agricultural Research Service (ARS) on the impact of its research from 1941 to 1966 concluded that 109 products and processes developed by ARS had been commercialized and 26 represented major contributions in basic research. Their value was estimated by the ARS at more than $6 billion, 20 times the $309 million spent by the ARS laboratories during this period.[2]

A 1980 study by the Congressional Office of Technology Assessment on the benefits stemming from agricultural research concluded that, "the

range of estimated rates of return is from a low of 23 percent to a high of 100 percent."[3] A 1992 study by Chapman and Associates *(1)* examined 178 cases of ARS research projects completed from 1980 to 1990 (including cooperative programs or joint programs with State Agricultural Experiment Stations). Of the 178 cases, benefits data were identified for 87, resulting in $14.8 billion in sales or savings. These savings were greater than the total amount spent on the ARS during that time period *(1)*.

Another study *(2)* found that although the ARS had a relatively small number of patents compared to the private sector in agricultural-related areas, the ARS patents were cited more often than private patents. Thus, the ARS patents were considered more often "key" patents marking significant advances in knowledge *(2)*.

Despite these successes, in the late 1970s there was a growing and increasingly influential school of thought that a focus on more basic research and the nonexclusive sharing of the fruits of such research was not encouraging the levels of private investment sufficient to commercialize new technologies. Many potentially valuable scientific advances were therefore remaining in the laboratories. Commercialization would occur only if private investors could be guaranteed exclusive access to the knowledge generated from what would increasingly become investments in federal research efforts made by both private and public sectors.

In rapid fashion, beginning in 1980, the federal government dramatically changed its R&D strategies to encourage one in which private interests would become increasingly influential in directly assisting public research:

1. The University and Small Business Patent Procedure Act, commonly known as the Bayh-Dole Act of 1980, gave nonprofit organizations such as universities as well as small businesses the right to retain patents for technology developed with government funds.
2. The Stevenson-Wydler Technology Innovation Act of 1980 provided federal departments, agencies, and affiliated laboratories with a legislative mandate to pursue technology transfer activities. Each agency was to make available not less than 9.5% of its R&D budget for technology transfer activities.
3. In 1983, an Executive Order extended the coverage of the Bayh-Dole Act to all government contractors. The Act also granted federal agencies the right to offer exclusive or coexclusive licenses to patents on inventions made by laboratory employees considered necessary for the commercialization of the invention.
4. The Federal Technology Transfer Act of 1986 allowed federal laboratories to enter into Cooperative Research and Development Agreements (CRADAs) with private firms. A CRADA confers two important rights to businesses: First, the right of first refusal of an exclusive license on any patentable inventions that arise from the research partnership; and, second, the right to keep research findings secret for 5 yr. The Act also permitted royalty income from

> patent licensing and assignment to be distributed directly to the inventors. The 1986 Act also made technology transfer a responsibility of every laboratory scientist and engineer. It required at least one full-time equivalent technology transfer position for every laboratory having 200 or more full-time scientific, engineering and related positions.

Today much if not most federal research, including biomass-related research, is done in partnership with private companies that have the right to exclusively own the intellectual property generated from that collaboration.

How effective has the post-1980 approach been compared to its predecessor?

Unfortunately, there are few if any studies that adequately address this important question. Vast changes in agricultural technologies have occurred over the last 20 yr, especially in the area of biotechnology in crops and animals. Yet, in this area federal R&D spending may have played a modest role that largely followed the massive amounts of venture capital that flowed into the biotech sector.

Efforts to compare the pre- and post-1980 R&D strategies are confounded by the fact that the metrics used to evaluate the performance of federal research have changed. In the older period, the measures used largely reflected the impact on the country and the countryside, such as the number of acres planted in the new hybrid and the rate of adoption of a new technology by farmers or processors. The new approach largely measures the impact on the agency or its private partner, considering factors such as the number of patents issued, the number of licenses issued, and the amount of royalties received.

It is now more than 20 yr since the federal government adopted a dramatically different approach to R&D by emphasizing technology transfer, private partnerships, and exclusive licensing. This is sufficient time to allow evaluation of the comparative effectiveness of both approaches.

Impact of Federal Biomass R&D on Rural Communities

One of the principal objectives of the federal biomass program is to improve the lot of farmers and rural communities. History teaches us that simply expanding demand for plant matter will not automatically benefit the cultivators of that plant matter. As farmers are aware more than anyone, expanded markets in the past have not resulted in increased net income to the farmer. This is because, as John F. Kennedy once observed, "The farmer is the only man in our economy who buys everything retail, sells everything he sells wholesale and pays the freight both ways."[4]

In 1910, of every dollar generated by agriculture, the farmer received 41¢. By 1990, the farmer's share had dwindled by more than 75%, to just 9¢. And today it is closer to 7¢. Yet this reduction in the farmer's income has not resulted in a reduction in the retail prices of the products made from the

farmer's raw materials. The price of a pound of corn flakes has gone up some 50% in the last 15 yr while the price of a pound of corn has gone down.[5] What this means is that for the farmer to significantly benefit from federal biomass policies, these policies must enable the farmer to gain an income from the value-added steps in converting the commodity crop into a wholesale and retail product.

I serve on a congressionally created committee that advises the Secretaries of Energy and Agriculture on biomass R&D efforts. In 2002, the Biomass R&D Technical Advisory Committee delivered its first annual report, which acknowledged, "Expanding the use of biomass for non-food and feed purposes will benefit farmers and rural areas only indirectly and modestly. A more significant development would occur if farmers themselves were able to produce the biofuels or bioproducts, either on the farm or as owners in a local production plant."[6]

Consider the emergence of bioethanol as an instructive example. The federal excise exemption for ethanol plus Clean Air Act regulations has created a 2.5 billion gal/yr ethanol industry. Evidence from Minnesota and Missouri indicates that this has increased the price that farmers are getting for their corn from local ethanol plants by 5–10¢/bushel.[7]

However, if farmers own the ethanol plant, they receive the additional price that results from increased markets plus they receive a part of the profit generated at the manufacturing level. Information on returns on ethanol investments is closely guarded and the returns vary dramatically from year to year and from plant to plant. Nevertheless, it is not unusual for the dividend in an average year to be 25–50¢/bushel. One unreleased study of the farmer-owned Minnesota Corn Processors ethanol plant found that farmer-investors earned about 18% annually over the 20-yr life of the plant as a cooperative.

Scale: The Minnesota Lesson

Unlike the federal government, several states have altered their biomass incentives to enhance the positive impact on rural communities. The Minnesota experience, often called the Minnesota Model, is instructive.

In the early 1980s, Minnesota's state ethanol incentive mirrored that of the federal incentive—a partial exemption from the gasoline tax. That incentive succeeded in making the price of ethanol competitive with other gasoline additives. The demand for ethanol-blended gasoline soared. But the demand was met entirely by ethanol imported into the state from out-of-state, large manufacturing facilities owned by one multinational corporation. Minnesota farmers and Minnesota's farming communities did not benefit from the expanded consumption of ethanol inside the state.

To remedy this problem, in the mid-1980s, Minnesota converted its state ethanol incentive from a consumer-oriented excise tax exemption to a producer-oriented direct payment. Instead of reducing state gasoline taxes by a couple of pennies for a 10% ethanol blend, the state paid 20¢/gal for ethanol produced within the state. To encourage the construction of

many plants in different parts of the state, the incentive, which ran for 10 yr, applied only to the first 15 million gal produced.

Some argued that by encouraging many small biorefineries, the government was encouraging higher-cost and more inefficient biorefineries because of the engineering economies of scale involved. Indeed, an internal study by the Institute for Local Self-Reliance concluded that a 150 million gal/yr ethanol facility had unit costs about 15–20¢/gal less than those of a 15 gal/yr facility.

Thus, the 20¢ incentive made up for the difference between small and large biorefineries. The result was that rather than one or two 100 million gal/yr plants, by 2002 Minnesota was home to 15 ethanol plants, the average capacity of which was 15 million gal/yr. The scale of the plants also encouraged farmer ownership. In 2002, 12 of the 15 plants were owned by more than 9000 grain farmers. These plants provided almost 10% of the transportation fuel sold in the state.

The proliferation of small plants led to an unanticipated technological dynamic. Because of the large number of plants built, several engineering firms competed with each other to design and build the least expensive and most efficient facility. Yields of ethanol in dry mills quickly rose from 2.5 to >2.8 gal/bushel. The large number of plants, coupled with equal numbers of plants being built in surrounding states, accelerated the engineering and operational learning curves. The result was to rapidly reduce the cost of ethanol produced from small dry mills.

A 1998 study by the USDA, a follow-up to a 1987 ethanol plant survey, examined the comparative economics of small- and medium-sized dry mills and large wet mills. In 1987, small- and mid-sized dry mills had cash operating costs of 50¢/gal. Large wet mills had a cash operating cost of 47¢/gal. By 1998, dry mills had dropped their operating costs to 41.7¢, whereas wet mills had dropped theirs only marginally, from 47.2 to 46¢. The 1998 report concluded, "Wet mill variable costs appear to have remained very stable at about 46 cents per gallon. Improved energy cost management was offset by several factors, including waste management and overhead... In contrast, dry mills have experienced a l5-percent reduction in operating costs, due to the effects of reduced energy, labor and maintenance expenditures and possibly economy of scale" *(3)*.

Scale: The Federal Challenge

Can federal research efforts focus on technologies applicable for smaller facilities? What would such research look like? This is a key challenge for researchers and policy makers. Engineering economies of scale do exist, as do management and marketing economies of scale. However, there are technologies that lend themselves more to modular expansion. Technologies should as much as possible allow the farmer to capture the value added from storing, preprocessing, and perhaps even processing the crop on site.

In the late 1970s, the DOE launched its wind energy initiative. Wind energy has dramatic economies of scale. The power output varies by the square of the diameter of the turbine's blades and by the cube of the increase in the wind speed. The DOE focused on building very large-diameter wind turbines. These megaturbines contributed relatively little to the technological advances in the wind energy field. Much more important for wind energy development was the design of buyback tariff structures in California in the early 1980s and the wind energy mandate in Minnesota in the mid-1990s.

As the wind energy industry grew, advances in the electronics and construction design of wind turbines grew even more rapidly. As they did, wind turbines became larger in a more organic way, moving from the 200-kW machines of the early 1980s to the 750-kW machines of the late 1990s to the new 1.5-MW machines.

In 2001, the DOE launched a small wind turbine initiative. The objective was to make wind energy economical in the many areas of the country that have lower wind speeds. This initiative is a 180° turn from the wind energy program of the late 1970s. It is too early to evaluate its results.

Regarding biomass, the DOE favors larger facilities, again because of their engineering economies of scale. The biomass program's orientation to the scale of production systems mirrors that of the fossil fuel and nuclear programs. Yet biomass has characteristics that may lend itself to a different orientation. The cost of transporting biomass, e.g., is much higher than the cost of transporting fossil fuels or uranium. In addition, the farmer-oriented and rural economy objectives of the biomass program are not part of the fossil fuel or nuclear development program.

Both DOE and the Department of Agriculture are conducting research in biochemical production. How would a focus on smaller scale and modular production units affect the research done under these programs?

The DOE and, to a lesser extent, the Department of Agriculture, have largely ignored questions of scale and ownership in their R&D efforts. The result could be that success in dramatically increasing the use of biomass for energy and industrial purposes may well not translate into higher farmer income or healthier rural communities. Yet these are formal objectives of both agencies' missions. Taking these socioeconomic factors into account could well encourage a different R&D and commercialization strategy by the federal agencies in charge of the biomass program.

Notes

1. Catherine E. Woteki, Deputy Undersecretary, Research, Education and Economics, USDA, Testimony Before the House Agriculture Committee, Resource Conservation, Research and Forestry Subcommittee, May 14, 1996.
2. *Achievements in Agricultural Utilization Research*, ARS Committee on Research Achievements, ARS, Washington, DC, November 1966.

The same 25-yr period, 1941–1966 was examined in a PhD thesis at the University of Georgia by Harold B. Jones, Jr., of the USDA's Economic Research Service. He found that by 1966, 9% of the projects undertaken by the regional laboratories had produced an economic return. That figure compared favorably with returns on food industry research. The cost-benefit ratio was 20 to 1 or better (cited in *Always Something New: A Cavalcade of Scientific Discovery*, USDA, Agricultural Research Service, Miscellaneous Publication 1507. November 1993).

3. Fred C. White, B. R. Eddleman, Joseph Purcell, et al, "Nature and Flow of Benefits from Ag-Food Research," in *An Assessment of the United States Food and Agricultural Research System*. Volume 2. Commissioned Papers, IR-6 Information Report No. 5. Office of Technology Assessment, Washington, DC, December 1980, pp. vii–x.
4. Speech by Senator John F. Kennedy at the National Plowing Contest, Sioux Falls, SD, September 22, 1960.
5. David M. Russo and Edward McLaughlin, *Farmers Can Get Bigger Share of Food Dollar*. New York State College of Agriculture and Life Sciences, Cornell University, April 1991, estimates the retail price of corn flakes at $1.56 per 18-oz box. Corn represents about 10¢ of the cost. The Economic Research Service, in *Food Marketing and Price Spreads: Farm-to-Retail Price Spreads for Individual Food Items* (2003) Washington, DC, estimated the year 2000 cost of an 18-oz box of corn flakes to be $2.14, with corn flakes representing 8¢ of that cost.
6. *Biomass RoadMap*. Biomass Research and Development Technical Advisory Committee, Washington, DC, November 2002.
7. Personal communication from several ethanol plant managers in Minnesota. Also see Van Dyne, D. L., *Employment and Economic Benefits of Ethanol Production in Missouri*. Department of Agricultural Economics, University of Missouri-Columbia, February 2002.

References

1. Chapman and Associates (1992), *An Exploration of Benefits from ARS and Cooperative Research*, Littleton, CO.
2. Ramanujam, S., et al. eds. (1980), *Science and Agriculture : M.S. Swaminathan and the Movement for Self-Reliance*. Arid Zone Research Association of India. New Delhi, India.
3. Hosein Shapouri, Paul Gallagher and Michael S. Graboski, USDA's 1998 Ethanol Cost-of-Production Survey. USDA. Washington, D.C. 1998.

0273-2289/04/113/0013–0026/$25.00

Methodology for Estimating Removable Quantities of Agricultural Residues for Bioenergy and Bioproduct Use

Richard G. Nelson,*[,1] Marie Walsh,[3] John J. Sheehan,[2] and Robin Graham[3]

[1]Kansas State University, 133 Ward Hall, Manhattan, KS 66506, E-mail: rnelson@ksu.edu; [2]National Renewable Energy Laboratory, 1617 Cole Boulevard, Golden, CO 80401; and [3]Oak Ridge National Laboratory, Oak Ridge, TN 37831-6194

Abstract

A methodology was developed to estimate quantities of crop residues that can be removed while maintaining rain or wind erosion at less than or equal to the tolerable soil-loss level. Six corn and wheat rotations in the 10 largest corn-producing states were analyzed. Residue removal rates for each rotation were evaluated for conventional, mulch/reduced, and no-till field operations. The analyses indicated that potential removable maximum quantities range from nearly 5.5 million dry metric t/yr for a continuous corn rotation using conventional till in Kansas to more than 97 million dry metric t/yr for a corn-wheat rotation using no-till in Illinois.

Index Entries: Corn stover; wheat straw; rainfall erosion; wind erosion; tolerable soil loss.

Introduction

Current US primary energy consumption is about 102 exajoules (EJ) (97 Quads) and is expected to increase to >137 EJ (130 Quads) by 2020. Transportation fuels produced from oil are projected to account for nearly one-third of the projected energy use by 2020, with nearly 68% of the oil imported from unstable and/or unfriendly countries, resulting in a trade imbalance of more than $206 billion (US $ in $2001). Additionally, the use of fossil fuels for transportation and electricity is a significant contributor of greenhouse gasses such as carbon dioxide, nitrogen oxides, and carbon monoxide *(1–4)*.

*Author to whom all correspondence and reprint requests should be addressed.

Table 1
Total Production, Residue Generation, and Gross Energy Amounts for Three Major Commodity Crops in the United States[a]

Crop	1997	1998	1999	2000	2001	Average for 1997–2001
Corn						
Production (billion bu)	9.20	9.75	9.43	9.91	9.50	9.56
Residue (million dry Mg)	234.30	248.40	240.00	252.30	241.90	243.40
EJ	3.50	3.70	3.60	3.80	3.60	3.60
Winter Wheat						
Production (billion bu)	1.84	1.88	1.69	1.56	1.30	1.65
Residue (million dry Mg)	85.50	87.10	78.60	72.60	63.10	77.30
EJ	1.30	1.30	1.20	1.10	0.90	1.10
Spring Wheat						
Production (billion bu)	0.54	0.52	0.50	0.55	0.51	0.52
Residue (million dry Mg)	19.40	18.70	17.80	19.70	18.10	18.70
EJ	0.30	0.30	0.30	0.30	0.30	0.30

[a] Production (billion bu), gross residue levels (million metric dry t), and energy (EJ).

An important component of becoming less dependent on fossil-based resources is to produce bioenergy and bioproducts from renewable energy resources such as biomass. Domestically produced bioenergy and bioproducts have lower environmental impacts, have a higher energy-profit ratio (ratio of renewable energy output to total energy inputs) than traditional fossil fuel technologies, and provide for economic development and enhanced energy security.

Among potential biomass resources that can be used to produce bioenergy and bioproducts are agricultural residues such as corn stover and wheat straw. Corn, soybeans, and wheat are the three largest crops produced in the United States, in terms of both acres and total production. Total production (billion bushels), residue quantities (million dry Mg), and energy density (EJ) produced from corn for grain and spring and winter wheat for the period of 1997–2001 are presented in Table 1.

While residue quantities produced are substantial, only a percentage of them can be collected for bioenergy and bioproduct use. Agricultural residues play an important role in controlling erosion and maintaining soil carbon, nutrients, and soil tilth. Removal of agricultural residues for bioenergy and bioproduct use will require consideration of the quantities that must be left to maintain soil quality. A recent analysis has demonstrated that under appropriate conditions, removal of agricultural residue can potentially occur *(5)*.

Methodology

Removal of agricultural residues for bioenergy and bioproduct use is directly influenced by a number of factors including grain yield, crop rota-

tion, field-management practices within a rotation (e.g., tillage), climate, and physical characteristics of the soil such as erodibility and topology.

The goal of the analysis is to develop and apply a methodology to estimate quantities of agricultural crop residues that can be removed for bioenergy and bioproduct use from both continuous crop and multi-crop rotations, while maintaining rain and/or wind erosion rates (Mg/[ha·yr]) at or below the tolerable soil-loss level, *T*. *T* is the maximum rate of soil erosion that will *not* lead to prolonged soil deterioration and/or loss of productivity as defined by the United States Department of Agriculture's Natural Resource Conservation Service (USDA-NRCS). For the purpose of this article, the methodology developed is applied to the top 10 corn-producing states (Iowa, Illinois, Indiana, Kansas, Minnesota, Missouri, Nebraska, Ohio, South Dakota, Wisconsin) based on total production (bushels) between 1997–2001. Three of these states—Kansas, Minnesota, and South Dakota—are among the top 10 wheat-producing states as well.

For each county in the 10 states evaluated, all cropland soil types in land capability classes (LCCs) I–VIII are identified. For each individual soil type, acres of that particular soil type, field topology characteristics (percentage low and high slopes), erodibility, and tolerable soil-loss limit are obtained from the USDA. These data are used in the rain and wind erosion equations described later. In each of the states analyzed, the following crop rotations are considered (where applicable): continuous corn, corn-soybean, corn–winter wheat, corn–spring wheat, continuous winter wheat, winter wheat–soybeans.

For each of these crop rotations, three tillage scenarios (conventional, reduced/mulch, and no-till) are considered. Conventional tillage scenarios consist mainly of moldboard plowing and/or heavy disking, reduced/mulch tillage scenarios include light disking and chisel plowing, and the no-till scenarios use field operations that provide little or no disturbance to the field surface. Harvest, planting, tillage, and chemical application dates for each field operation are adjusted to reflect the most likely time of year and month that they are expected to occur within each of the 10 states. Tables 2 and 3 describe field operations for each crop rotation and tillage combination analyzed.

Residue Production

The quantity of residue that is produced and can potentially be removed is directly related to the production yields of crops in the rotation. County-level harvested acres, yield, and total production for 1997–2001 were obtained from USDA-NASS, and 5-yr averages were determined from these data for all counties in the 10 states. These average yields were then converted to gross residue estimates using ratios of fresh grain weight to bushel factors and ratios of dry weight residues to fresh grain weight. For the three major crops considered, these factors were as follows: for corn, 25.1 kg of dry stover/bu of grain (56 lb/bu) and a 1-to-1 ratio of dry stover to fresh grain mass; for spring wheat, 35.4 kg of dry residue/bu (60 lb/bu)

Table 2
Field Operations Associated with Corn Rotations for Conventional, Reduced/Mulch, and No-till Field-Management Practices

Continuous corn for grain (conventional till)	Corn for grain–soybeans (conventional till)	Corn for grain–winter wheat (conventional till)
moldboard plow; 8" N Disk har-tand.fnsh N cult; secdry-sw6-12 N planter; st dbl dsk N cult; row-mult sweepN harvest	moldboard plow; 8" F disk har-tand.fnsh F cult; secdry-sw6-12 F planter; st dbl dsk F cult; row-mult sweepF harvest	moldboard plow; 8" N disk har-tand.fnsh N cult; scdry-sw6-12 N planter; st dbl dsk N cult; row-mult sweepN harvest
	moldboard plow; 8" F disk har-tand.fnsh F cult; secdry-sw6-12 F planter; st dbl dsk F cult;row-mult sweepF harvest	moldboard plow; 8" N disk har-tand.fnsh N cult; scdry-sw6-12 N drill; dbl dsk opn N harvest
Continuous corn for grain (mulch till)	**Corn for grain–soybeans (mulch till)**	**Corn for grain–winter wheat (mulch til)**
chis-disk; str.pt. N cult; secdry-sw6-12 N planter; st dbl dsk N harvest	chis-disk; str.pt. F cult; secdry-sw6-12 F planter; st dbl dsk F harvest	chis-disk; sweeps N disk har-tand.fnsh N cult; secdry-sw6-12 N planter; st dbl dsk N harvest
	chis-disk; str.pt. N cult; secdry-sw6-12 N planter; st dbl dsk N harvest drill; dbl dsk opn N harvest	chis-disk; sweeps N disk har-tand.fnsh N cult; secdry-sw6-12 N
Continuous corn for grain (no till)	**Corn for grain–soybeans (no till)**	**Corn for grain–winter wheat (no-till)**
anhydrous applic. N planter; NT-fluted c N harvest	anhydrous applic; disk F planter; strip-t flute F harvest	planter; NT-fluted c N harvest
	drill; NT-f.res. ri N harvest	drill; NT-f.res. fl N harvest

and a 1.3-to 1-ratio of dry residue (chaff and straw) to grain; and for winter wheat, 46.3 kg/bu of grain (60 lb/bu) and a 1.7-to-1 ratio of dry residue to grain. For soybeans, these factors were 40.8 kg of dry residue/bu (60 lb/bu) and a 1.5-to-1 ratio of dry residue to beans *(6)*.

Table 3
Field Operations Associated with Wheat Rotations
for Conventional, Reduced/Mulch, and No-till Field-Management Practices

Continuous wheat (conventional till)	Winter wheat–soybeans (conventional till)
moldboard plow; 8" N disk har-tand.fnsh N disk har-tand.fnsh N drill; dbl dsk opn N harvest	moldboard plow; 8" N disk har-tand.fnsh N cult; secdry-sw6-12 N planter; dbl dsk op N cult; row-mult sweepN harvest moldboard plow; 8" N disk har-tand.fnsh N cult; secdry-sw6-12 N drill; dbl dsk opn N harvest
Continuous wheat (mulch till)	**Winter wheat–soybeans (mulch till)**
disk har-tand.prim N drill; dbl dsk opn N harvest	chis-disk; sweeps N cult; secdry-sw6-12 N Planter; st dbl dsk N harvest chis-disk; sweeps F cult; secdry-sw6-12 F drill; dbl dsk opn F harvest
Continuous wheat (no-till)	**Winter wheat–soybeans (no-till)**
drill; NT-s.stub fl N harvest	drill; NT sngl dsk n harvest drill; NT sngl dsk f harvest

To quantify the amount of residue that can be sustainably removed, quantities of residues that must be left on the field to maintain rain and/or wind erosion at or below tolerable soil-loss levels (T) must first be estimated. The revised universal soil loss equation (RUSLE) and the wind erosion equation (WEQ) are used to estimate these residue quantities *(7,8)*.

RUSLE and WEQ are designed primarily to estimate long-term, average annual soil erosion on a site-specific field characterized by a particular soil type, slope and runoff length, field length, cropping and management practices used, and localized climate conditions. Residues that must be left on the field, with respect to rainfall and wind erosion, are estimated for each soil type, each crop rotation, and each tillage combination considered in this analysis, with the higher of the two estimates being the quantity needed to remain on the field.

Rainfall Erosion (RUSLE)

The RUSLE (Eq. 1) is used to estimate the quantities of residue that must remain on the field to keep rainfall-induced erosion at or below *T*.

$$A = R \times K \times S \times L \times C \times P \quad (1)$$

in which *A* is the average annual soil loss (metric t/[ha/yr]), *R* is the rainfall-runoff erosivity factor (location/county specific), *K* is the soil erodibility factor, *S* is the slope steepness factor, *L* is the slope-length factor, *C* is the cover-management factor, and *P* is the support-practices factor. The *A* in RUSLE can be replaced by *T* (tolerable soil loss limit) to give

$$T = R \times K \times L \times S \times C \times P \quad (2)$$

in which *K* and *S* are as described for Eq. 1 and are specific to each soil type examined. *P* is assumed to be 1.0, which provides the most conservative estimate for residue removal. All factors except *C* are independent of crop grain yield or crop-management practices and can be combined into a single value termed ASTAR (A*), which is specific to each particular soil type. ASTAR was calculated for each LCC I–VIII soil type in each of the 10 states.

C is a function of the yield at harvest and is directly influenced by field operations that affect field surface cover throughout the year (i.e., tillage). To estimate the annual erosion and quantities of removable crop residues attributable to specific field operations and harvest yields, the C-factor must be determined in relation to these conditions. Equation 2 can be rewritten as

$$C = (R \times K \times L \times S \times P)/T \quad (3)$$

in which *C* is now the only unknown parameter. To solve for *C*, the RUSLE C-Batch Program (developed by USDA National Soil Survey Center) is used. C-Batch estimates C-factors for various crop rotations, crop grain yield variations, and tillage operations and timing combinations. For this analysis, crop grain yields of 124, 198, 247, 309, and 371 bu/ha for corn; 62, 74, 99, 124, and 148 bu/ha for winter wheat; and 49, 62, 86, 111, and 124 bu/ha for spring wheat are assumed. Soybean yields were 37, 62, 74, 86, and 111 bu/ha. These yields reflect typical ranges for these crops in most states considered in the study.

Table 4 shows variation in the C-factor with respect to a continuous corn and continuous winter wheat rotation for each of the three tillage

Table 4
Variation in Cover-Management Factors for Continuous Corn and Continuous Winter Wheat Rotation for Conventional, Reduced/Mulch, and No-Till Field-Management Practices in Brown County, Kansas

	Conventional till			Reduced/mulch till			No-till		
C-factors for continuous corn	0.455	0.291	0.203	0.318	0.167	0.104	0.148	0.057	0.027
Yield (bu/ha)	124	247	371	124	247	371	124	247	371
C-factors for continuous winter wheat	0.206	0.133	0.092	0.083	0.039	0.022	0.042	0.017	0.008
Yield (bu/ha)	62	99	148	62	99	148	62	99	148

scenarios and three grain yield levels in Brown County, Kansas. The C-factors vary between the two crops owing to different protective cover for corn stover vs wheat straw, with lower C-factors associated with greater protective cover. They also vary across the three tillage scenarios for each crop (on average, the C-factor decreases as the tillage scenario becomes less aggressive, going from conventional till to reduced/mulch to no-till). This is logical because as residue burial increases (such as with a moldboard plow and/or heavy disking representative of conventional till), less protective cover is present on the field and, therefore, it is more likely for soil erosion to occur. From the standpoint of the RUSLE equation, erosion increases when the cover-management factor increases, because ASTAR is constant for a single soil type and erosion is the product of ASTAR and the C-factor. In practical terms, for the same soil type and cropping rotation, more residue is potentially available for removal under no-till field management vs mulch till or conventional till field-management practices because less residue is buried and more residue stays on the field surface to protect against the impact of rainfall and wind forces.

Estimation of Minimum Retainable Residue Levels for Continuous (Single)-Crop Rotation—Rainfall Erosion

The estimated C-factors corresponding to each crop rotation, tillage, and grain yield combination are multiplied by the soil-specific ASTAR values to obtain expected erosion rates (Mg/[ha·yr]) for each soil type. To determine crop residue levels (Mg/[ha·yr]) for which expected erosion rates are at or below T, a regression curve is fitted to the data, with the variables of the independent variable, the natural logarithm of the residue produced (quantity of stover and/or straw present in the field at the time of harvest), and of the dependent variable, the erosion rate. The level of soil erosion varies depending on the quantities of residue left on the field at the time of harvest and throughout the year. Given that expected erosion (for each soil type, crop rotation, and tillage practice combination) is estimated for five grain crop yields (bu/ha), the regression is fitted to five data pairs.

Table 5
Calculation of Minimum Remaining Residue
Levels for Rainfall-Induced Soil Erosion

(Continuous Corn, Mulch Till, Shidler-Catoosa Silt Loam, Allen County, Kansas)					
Corn yield (bu/ha)	124	198	247	309	371
Erosion (Mg/[ha·yr])	20.79	15.19	11.70	9.16	7.68
Corn residue produced (dry Mg/ha)	3.14	5.03	6.29	7.86	9.43
Natural logarithm of corn residue produced	1.145	1.615	1.839	2.062	2.244

Estimated results			
T, tolerable soil loss (Mg/[ha·yr])	Intercept	Slope	Average minimum residue remaining (dry Mg/[ha·yr])
11.2	34.755	–12.269	6.82

A natural logarithmic function provides the best fit. For a single/continuous-crop rotation (continuous corn or continuous wheat), the minimum quantities of residue (R_{min}) that must remain on the field throughout the year to keep erosion at or below T are estimated by rearranging the fitted regression equation (Eq. 4). The quantities of residues that can be removed (R_{rem}) are estimated as the quantity of residue produced (R_{prod}) minus the minimum quantity that must remain (R_{min}) (Eq. 5). If R_{prod} is less than R_{min}, no residue can be removed.

$$R_{min} = \exp[(T - \text{intercept})/\text{slope}] \quad (4)$$

$$R_{rem} = R_{prod} - R_{min} \quad (5)$$

Table 5 presents the regression analysis and estimated quantities of residues that must remain on the field subject to a reduced/mulch till, continuous corn rotation on a Shidler-Catoosa silt-loam soil in Allen County, Kansas. In this example, the regression equation is fitted to the following five pairs of erosion and dry residue–equivalent yield data (20.79 and 1.145, 15.19 and 1.615, 11.70 and 1.839, 9.16 and 2.062, and 7.68 and 2.244). This provides an estimated intercept of 34.755 and a slope of –12.269. Using Eq. 5 and a T value of 11.2 Mg/(ha·yr), the quantity of residue that must remain on the field is estimated as 6.82 Mg/(ha·yr).

Estimation of Minimum Retainable Residue Levels for Multiple-Crop Rotation—Rainfall Erosion

Estimated residues that can be removed for a 2-yr, multiple-crop rotation differ from the continuous-crop, single-year analysis in that removal rates must remain at or below T for each year of the rotation.

Table 6
Variation in Cover-Management Factor for Corn-Soybean Rotation for Conventional, Reduced/Mulch, and No-Till Field-Management Practices

	Conventional till			Reduced/mulch till			No-till		
Yield (bu/ha)	124/37	247/74	371/111	124/37	247/74	371/111	124/37	247/74	371/111
Average residue levels (Mg/ha)	2.33	4.66	7.0	2.33	4.66	7.0	2.33	4.66	7.0
C-factors for corn-soybean	0.484	0.326	0.247	0.377	0.238	0.162	0.283	0.165	0.103

The average annual residue present at harvest over the 2-yr period is calculated at each of the five yield pairs from the C-batch program (e.g., for a corn-soybean rotation, the yield pairs of 124/37, 198/62, 247/74, 309/87, and 371/111 bu/ha equate to average residue levels of 2.33, 3.78, 4.66, 5.7, and 7.0 dry Mg/(ha·yr), respectively, over the 2-yr period). As with continuous-crop rotations, the C-factors vary between rotations (i.e., soybean residue provides less protective cover than corn stover, resulting in higher C-factors for a corn-soybean rotation than a continuous-corn rotation), and across all tillage practices (i.e., the C-factor decreases as tillage becomes less intensive). (Note that the total residue produced during the two-year rotation is twice the 2-yr average). Table 6 illustrates how rotational C-factors vary with respect to tillage for a corn-soybean rotation in the Midwest.

For a multiple-crop rotation, residues that must remain (R_{min}) are calculated by the same equation used for a continuous-crop rotation (Eq. 4), except the intercept and slope are functions of the 2-yr average residue levels of each residue pair. R_{min} represents the amount of residue that must be left in the field each year of the rotation to ensure that rainfall erosion does not exceed T. Note that R_{min} is the same for both cropping years. This follows because the C-factor was calculated on the basis of a rotation, not two independent crops. Unlike the continuous-crop rotation, however, three potential situations can arise that will affect residue quantities that can be removed.

Situation No. 1

Both crops produce more residue each year than R_{min}. If the residue-equivalent production yields of both crops are greater than R_{min}, then the residues from each crop can be removed and are estimated according to Eqs. 6 and 7.

$$ARR1 = R1_{prod} - R_{min} \quad (6)$$

$$ARR2 = R2_{prod} - R_{min} \quad (7)$$

in which *ARR*1 and *ARR*2 are the average annual removable residue from crops one and two, $R1_{prod}$ and $R2_{prod}$ are the gross residues produced for crops one and two (based on the average production yield of crops one and two in the county), and R_{min} is the average minimum residue over the 2-yr period.

Situation No. 2

The average residue produced by the two crops is less than R_{min}. If the residue quantity produced for either crop ($R1_{prod}$ or $R2_{prod}$) is less than the average minimum residue, R_{min}, then a test is conducted to determine whether the average annual residue produced by the rotation (the sum of the gross residue produced by each crop divided by two), *ARR*, is less than R_{min}. If it is, then no residue can be removed in either year. If the average is greater than R_{min}, situation #3 arises.

Situation No. 3

The average residue produced by the two crops is greater than R_{min}, but one crop,Äôs residue is less than R_{min}. This situation also involves the position that one of the crops produces an amount of residue less than R_{min} (the average minimum residue), but the difference between *ARR* and R_{min} is greater than zero. In this situation, it is acceptable to remove residue from *only* the crop that produces more residue than R_{min}, provided that enough residue from that crop is left to ensure that the average amount of residue left on the field over the 2 yr is at least as great as R_{min}. No residue can be removed from the crop that produces less residue than R_{min}. Mathematically, in this situation, the amount of residue removed from the crop that produces "excess" residue is equal to twice the average annual residue – R_{min}. For example, if R_{min} = 2.2 Mg/(ha·yr), $R1_{prod}$ = 3.36, and $R2_{prod}$ = 1.8 Mg/(ha·yr), respectively, then no residue could be removed from crop two and 0.76 Mg/(ha·yr) could be removed from crop one the year it was grown.

Wind Erosion (WEQ)

Estimation of Minimum Retainable Residue Levels for Continuous-Crop Rotation

In general, crop residue removal was affected by wind erosion more than rainfall erosion in the western two-thirds of Kansas, Nebraska, and South Dakota. Rainfall erosion was the dominant erosive force in the eastern one-third of these three states, as well as all the other seven states considered. Equation 8 presents WEQ:

$$E = f(WI, WK, WC, WL, WV) \quad (8)$$

in which *E* is the average annual soil loss (Mg/[ha·yr]); *WI* is the wind erodibility index (a measure of soil susceptibility to detach and be transported by wind) and varies by individual soil type; *WK* is the soil ridge-roughness factor and describes the condition of the field surface at a particular time;

WC is the climate factor and represents the amount of erosive wind energy present at a particular (county-level) location; *W L* is a function of wind direction, field length, and width and is the unsheltered median travel distance of wind across a field; and *WV* is the vegetative factor. The relationship between *E* and the other variables is highly nonlinear.

The amount of residue potentially available for removal with respect to applying WEQ was determined by analyzing total soil loss attributable to wind forces in each field-management period (time between each field operation) for all individual soil types and then summing across all field-management periods including crop growth. These values were then compared to erosion values obtained in the rainfall erosion analysis, and the greater required minimum residue level at harvest was chosen. A detailed discussion of the application of WEQ to agricultural crop residue removal is provided in an article by Nelson *(9)*.

Results

Tables 7 and 8 present data concerning maximum quantities of corn stover and wheat residue, respectively, that could *potentially* be removed from agricultural cropland in each of the 10 largest corn-producing states in the United States subject to the constraints of the tillage scenarios, production yields, soil types, and field topologies considered in this analysis. The removable residue quantities presented in this article reflect removable residue with respect to only soil erosion and no accounting/methodology was performed with respect to the impact removing residue would have on, e.g., soil tilth and nutrients. These are amounts that could be removed if *all* agricultural cropland (not just those in corn, wheat, and soybeans) in each state were planted to a particular rotation and subject to conventional, reduced/mulch, and no-till field-management practices (tillage scenarios), and the counties achieved crop yields equivalent to the 1997–2001 5-yr average. The quantities are the lesser of the two quantities that can be removed under the rain and wind erosion analyses.

For example, if all agricultural cropland in Iowa were managed in a continuous-corn, no-till rotation, 84.4 million dry Mg of corn stover could be harvested annually. If all the agricultural cropland were managed in a corn–winter wheat rotation using mulch till practices, 30.2 million dry Mg of corn stover and 13.4 million dry Mg of wheat residue could be harvested annually. (Note, that if a county did not produce a specific crop during 1997–2001, then it is assumed that crop is not produced in that county and thus any rotation with that crop is also not produced in that county; the same constraint is not applied regarding to tillage practices.) An assumption was made that all tillage practices are possible in all counties.

In addition, it should be noted that not all estimated residue quantities will actually be removed owing to the potential of some farmers being unwilling to remove residues from their fields, as well as weather conditions that may prohibit collection. Other factors may come into play as well.

Table 7
Maximum Removable Corn Stover Quantities (Million Metric Tons at Harvest) by Rotation and Tillage Practice When All Cropland Acres in Each State Are Planted to the Rotation[a]

Crop rotation and tillage scenario	Iowa	Illinois	Minnesota	Nebraska	Indiana	Ohio	Kansas	South Dakota	Wisconsin	Missouri
Continuous corn										
Conventional till	44.3	50.7	61.4	19.3	31.5	17.5	5.5	13.4	26.8	13.5
Reduced/mulch till	59.5	67.6	71.9	48.7	39.2	21.4	39.3	28.4	35.3	19.0
No-till	84.4	90.8	84.8	71.1	50.4	29.4	65.1	38.2	50.8	31.6
Corn–soybean (corn stover)										
Conventional till	43.1	49.2	57.2	19.3	31.8	17.8	5.6	7.4	26.1	13.3
Reduced/mulch till	55.5	61.9	65.3	44.8	37.0	20.0	38.5	26.5	31.7	17.2
No-till	65.6	73.5	72.4	55.2	42.2	23.1	65.1	34.2	39.3	20.9
Corn–winter wheat (corn stover)										
Conventional till	25.0	65.6	8.0	20.3	39.9	21.3	8.4	13.2	20.3	20.3
Reduced/mulch till	30.3	74.5	8.3	47.7	44.6	24.5	42.9	27.0	25.9	23.7
No-till	49.4	97.6	8.6	70.6	56.8	33.2	74.0	35.2	31.3	49.3
Corn–spring wheat (corn stover)										
Conventional tillage	NA	NA	51.5	NA	NA	NA	NA	13.7	NA	NA
Reduced/mulch tillage	NA	NA	55.8	NA	NA	NA	NA	27.6	NA	NA
No-till	NA	NA	61.6	NA	NA	NA	NA	36.9	NA	NA

[a] NA, not available.

Table 8
Maximum Removable Wheat Straw Quantities (Million Metric Tons at Harvest) by Rotation and Tillage Practice When All Cropland Acres in Each State Are Planted to the Rotation[a]

Crop rotation and tillage scenario	Iowa	Illinois	Minnesota	Nebraska	Indiana	Ohio	Kansas	South Dakota	Wisconsin	Missouri
Continuous winter wheat										
Conventional tillage	14.4	55.7	NA	25.4	35.3	20.7	30.3	NA	19.8	16.0
Reduced/mulch tillage	22.2	72.6	NA	35.9	44.5	27.9	50.2	NA	34.4	31.7
No-till	28.3	81.9	NA	39.1	50.0	31.6	56.8	NA	37.9	47.7
Continuous spring wheat										
Conventional tillage	NA	NA	25.2	NA	NA	NA	NA	18.0	NA	NA
Reduced/mulch tillage	NA	NA	27.7	NA	NA	NA	NA	22.5	NA	NA
No-till	NA	NA	28.5	NA	NA	NA	NA	23.9	NA	NA
Wheat-soybeans (wheat straw)										
Conventional tillage	13.2	51.4	21.4	23.2	32.1	19.3	29.1	16.9	22.1	14.2
Reduced/mulch tillage	16.1	60.0	23.3	28.2	36.6	22.9	42.1	19.3	23.8	17.2
No-till	26.4	78.7	26.3	37.0	46.7	30.3	54.1	20.9	32.0	38.0
Corn–winter wheat (wheat straw)										
Conventional tillage	10.9	49.1	4.2	21.4	31.7	18.1	24.2	14.0	14.3	13.7
Reduced/mulch tillage	13.4	56.2	4.4	25.9	35.4	20.8	34.0	17.3	18.3	16.1
No-till	23.2	75.2	4.5	36.9	45.2	28.6	51.3	19.0	22.5	32.4
Corn–spring wheat (wheat straw)										
Conventional tillage	NA	NA	20.9	NA	NA	NA	NA	13.3	NA	NA
Reduced/mulch tillage	NA	NA	23.0	NA	NA	NA	NA	16.4	NA	NA
No-till	NA	NA	27.4	NA	NA	NA	NA	22.7	NA	NA

[a] NA, not available.

Quantities can be adjusted for these factors by assuming that only a certain percentage of the estimated quantities is actually removed.

The estimated quantities of removable corn stover and wheat straw presented in Tables 7 and 8 conform to intuitive expectations in that as tillage operations become less intensive (i.e., go from conventional to no-till), the amounts of removable residue increase across all rotations in all states. Differences in estimated removable quantities among states is a function of several factors including production location (whether the majority of production occurs in areas that have highly erodible soils and field topology nonconducive to removal), climatic/erosive conditions at the locations of production, and actual yields at these specific locations among others. These factors must be considered before residues can be removed at any specific location.

Conclusion

A methodology was developed to assess the amount of agricultural crop residue that can be removed without exceeding the tolerable soil-loss limit in both single and multicrop (2-yr) rotations. Application of this methodology to select corn- and wheat-based cropping rotations on land capability class I–VIII soils subject to conventional, reduced/mulch, and no-till field-management practices in Iowa, Illinois, Nebraska, Minnesota, Indiana, Ohio, Kansas, South Dakota, Missouri, and Wisconsin indicates that significant removable quantities of corn stover and wheat straw exist, but there is considerable variation in the amounts of removable residue with respect to each tillage scenario across all states analyzed. These amounts only consider the need to keep erosion to a tolerable level and do not encompass soil carbon considerations.

References

1. Energy Information Administration. (2003), in *Annual Energy Outlook 2003 with Projections to 2025*, US Department of Energy, Washington, DC, p. 18.
2. Energy Information Administration. (2003), *Annual Energy Outlook 2003 with Projections to 2025*, US Department of Energy, Washington, DC.
3. Energy Information Administration. (2003), in *Annual Energy Outlook 2003 with Projections to 2025*, U S Department of Energy, Washington, DC, p. 4.
4. Energy Information Administration. (2003), in *Annual Energy Outlook 2003 with Projections to 2025*, US Department of Energy, Washington, DC, p. 3.
5. Nelson, R. G., Enersol Resources. (2001), *Resource Assessment, Removal Analysis, Edge-of-Field Cost Analysis, and Supply Curves for Corn Stover and Wheat Straw in the Eastern and Midwestern United States*, National Renewable Energy Laboratory, Golden, CO.
6. Larson et al. (1979), in *Journal of Soil and Water Conservation*, Special Publication No. 25, Soil Conservation Society of America, Ankeny, IA.
7. US Department of Agriculture. (1997), *Predicting Soil Erosion by Water: A Guide to Conservation Planning with the Revised Universal Soil Loss Equation (RUSLE)*, Agricultural Handbook Number 703, US Department of Agriculture, Agricultural Research Service.
8. Skidmore, E. L. (1988), in *Soil Erosion Research Methods*, Soil and Water Conservation Society of America, Ankeny, IA.
9. Nelson, R. G. (2002), *Biomass Bioenergy* **22,** 349–363.

0273-2289/04/113/0027–0039/$25.00

Pipeline Transport of Biomass

Amit Kumar, Jay B. Cameron, and Peter C. Flynn*

Department of Mechanical Engineering,
University of Alberta, Edmonton,
Alberta, T6G 2G8, Canada,
E-mail: peter.flynn@ualberta.ca

Abstract

The cost of transporting wood chips by truck and by pipeline as a water slurry was determined. In a practical application of field delivery by truck of biomass to a pipeline inlet, the pipeline will only be economical at large capacity (>0.5 million dry t/yr for a one-way pipeline, and >1.25 million dry t/yr for a two-way pipeline that returns the carrier fluid to the pipeline inlet), and at medium to long distances (>75 km [one-way] and >470 km [two-way] at a capacity of 2 million dry t/yr). Mixed hardwood and softwood chips in western Canada rise in moisture level from about 50% to 67% when transported in water; the loss in lower heating value (LHV) would preclude the use of water slurry pipelines for direct combustion applications. The same chips, when transported in a heavy gas oil, take up as much as 50% oil by weight and result in a fuel that is >30% oil on mass basis and is about two-thirds oil on a thermal basis. Uptake of water by straw during slurry transport is so extreme that it has effectively no LHV. Pipeline-delivered biomass could be used in processes that do not produce contained water as a vapor, such as supercritical water gasification.

Index Entries: Wood chips; pipeline; biomass; lower heating value; straw.

Introduction

Carbon-based power generation facilities do not typically rely on delivery of fuel by highway truck. Oil- and gas-fired plants rely on pipelines, and coal-based facilities typically either are located at the mine mouth or rely on rail or ship for fuel delivery. The reason for this is the high cost and high congestion that would be associated with delivery of large tonnages of fuel to modern, large power plants.

Numerous biomass power plants are small and utilize truck delivery of fuel. However, in a previous work *(1)*, we noted that optimum size for straw- and wood-based biomass power plants in a western Canadian set-

*Author to whom all correspondence and reprint requests should be addressed.

ting were 450 MW or greater for straw and wood from harvesting the whole forest, and that cost of power increased sharply at sizes below about 200 MW. For forest harvest residues (limbs and tops), which are more widely dispersed, the optimum size was 137 MW.

A 450-MW biomass power plant burning 2.1 million dry t/yr of wood chips would require 17 truck deliveries per hour at 20 t/truck *(2)*. Highway transportation of fuel is a significant cost element, contributing at optimum power plant size 25, 14, and 38% of the total cost of power generation from direct combustion of straw, wood from harvesting the whole forest, and forest harvest residues, respectively *(1)*. In the present work, we evaluated pipeline delivery of biomass to a power generation plant, to avoid road congestion (and likely resistance by nearby residents), and to reduce overall fuel transportation cost.

Two carrier mediums are considered for biomass: water and oil. We review the inherent economics of truck vs pipeline transport, and then evaluate a case of field delivery of biomass by short-haul truck to a pipeline terminal. We also evaluate the impact of water and oil absorption by the biomass fuel. Finally, we discuss the prospects for pipeline transport of biomass.

In this article, all costs are reported in year 2000 US dollars; Canadian dollars are converted to US at an exchange rate of 1.52 Cdn$/US$.

Inherent Economics of Truck and Pipeline Transport

Truck delivery of material has a fixed cost associated with the time required to load and unload the truck, and a variable cost that is related to the time the truck is being driven and/or the distance driven. For most biomass delivery applications, truck speed is relatively constant over the route; thus, e.g., a truck picking up straw would average about 80 km/hr on rural and district roads, and a truck picking up wood chips in a forest would average about 50 km/h on logging roads. Only if the wood chips required a significant drive over highways would there be a second higher speed portion of the trip; this effect is ignored here. Figure 1 shows cost data per kilometer for truck transport of wood chips in a typical western Canadian setting (*[3]*; D. Evashiak, personal communication, 3/03); the intercept of the lines is the fixed cost of loading and unloading, and the slope is the incremental variable cost per kilometer. Table 1 provides the equations for transport costs, including straw *(1)*. Figure 1 is adjusted to dry tonnes of biomass to make a comparison of pipeline costs easier; pipeline costs are discussed later. Typical field moisture levels for straw and wood in western Canada are 16 and 50%, respectively. The range of costs for truck transport of wood chips comes from two different types of estimate: the lower bound is from a Forest Engineering Research Institute of Canada (FERIC) study of chip transport costs from a long-term dedicated fleet, and the upper bound is based on current short-term contract hauling rates. The FERIC data are more representative of steady biomass supply to a long-term end use such as a power plant. Note that there is no change in cost with scale for any

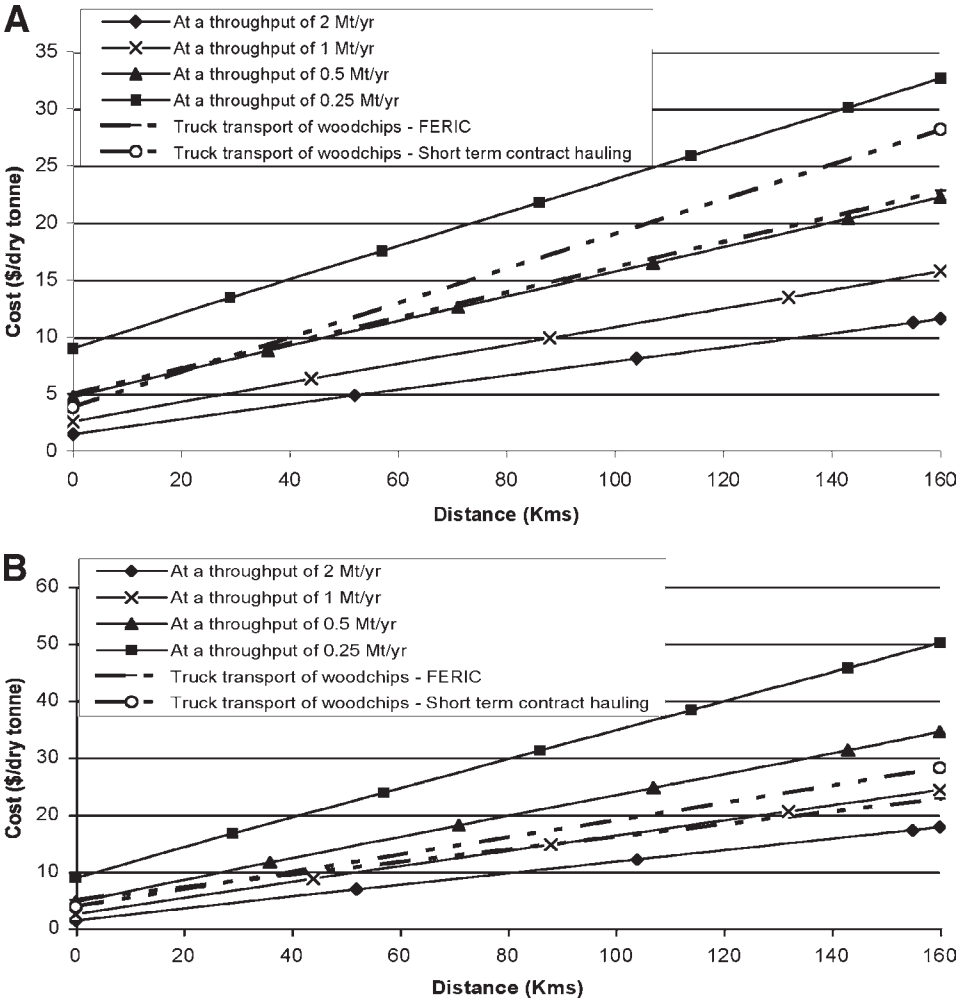

Fig. 1. **(A)** Pipeline transport cost of wood chips without carrier fluid return pipeline. **(B)** Pipeline transport cost of wood chips with carrier fluid return pipeline.

biomass application of interest; that is, the amount of biomass moved fully utilizes multiple trucks and no savings occur with larger throughput.

Pipeline transport of wood chips was studied in the 1960. Brebner *(4)*, Elliott *(5)*, and Wasp et al. *(6)* examined solids carrying capacity and pressure losses, and Wasp et al. *(6)* did a cost analysis for a 160-km pipeline with one-way transport, i.e., no water return. These studies were focused on the supply of wood chips to pulp mills, and hence water uptake by chips did not have a downstream processing impact. More recently Hunt *(7)* did an extensive analysis of friction factors in wood chip slurries in water; in the present work, we utilize his formula for the friction factor.

Table 1
Formulae for Truck and Pipeline Costs as Function of Distance

Cases	Cost ($/dry t)[a]	Distance between slurry pumping stations (km)
Two-way pipeline transport cost of water wood chip slurry		
2 million dry t/yr capacity	0.1023d + 1.47	51
1 million dry t/yr capacity	0.1355d + 2.65	44
0.5 million dry t/yr capacity	0.1858d + 4.80	36
0.25 million dry t/yr capacity	0.2571d + 9.05	29
One-way pipeline transport cost of water wood chip slurry		
2 million dry t/yr capacity	0.0630d + 1.50	51
1 million dry t/yr capacity	0.0819d + 2.63	44
0.5 million dry t/yr capacity	0.1088d + 4.80	36
0.25 million dry t/yr capacity	0.1473d + 9.07	29
Truck transport cost of wood chips (50% moisture)		
FERIC (long-term hauling)	0.1114d + 4.98	—
Short-term contract hauling	0.1542d + 3.81	—
Truck transport cost of straw (16% moisture)	0.1309d + 4.76	—

[a] d, the distance in kilometers.

More recently, Liu et al. *(8)* completed an analysis of two-phase pipelining of coal logs (compressed coal cylinders) by pipeline. In the present article, we draw on the work of Wasp et al. *(6)*, Liu et al. *(8)*, and discussions with a Canadian engineering contractor (D. Williams, personal communication, 3/03) to develop pipeline cost estimates for transporting water slurries of wood chips; these costs are also shown in Fig. 1 and Table 1.

Delivery of material by slurry pipeline has a cost structure similar to that for truck transport. The fixed cost is associated with the investment in the material receiving and slurrying equipment at the pipeline inlet, and the separation and material transport equipment at the terminus. The slope of the curve comes from the operating cost of pumping, and the recovery of the incremental capital investment in the pipeline and booster pumping stations plus associated infrastructure such as power and road access, all of which increase linearly with distance. Technically, pipeline costs would have a slight "sawtooth" shape, with a slight, discrete increase in overall cost occurring when an additional pumping station is required. Practically, most of the incremental capital cost is in the pipeline rather than pumping stations, and the sawtooth effect can be ignored. (In our analysis, the pipeline component of the total capital cost is 85% at 50 km, and 94% at 500 km.)

One key element in the pipeline scope and estimate is whether a return line for the carrying fluid is provided. This would be required in virtually

Table 2
Capital Costs for Inlet, Outlet, and Booster Station Facilities[a]

Item	Cost ($ 1000)	Remark
Inlet facilities		
Land for inlet facility	19.7	Estimated
Access roads	39.9	*(15)*
Conveyor belt	245.3	*(16)*
Mixing tank (water and chips)	61.3	*(16)*
Piping	405.1	*(8)*
Foundation for pump area	100.0	Estimated
Storage tank for water	769.3	*(16)*
Auxiliary pump (with one redundant pump)	137.1	*(8)*
Power supply line and substation	400.0	Estimated
Communication lines	40.0	Estimated
Building	236.8	Estimated
Road along pipeline	266.0	*(15)*
Fire suppression system	65.8	Estimated
Mobile stacker for dead storage	100.0	Estimated
Main pump for transport of wood chips and water mixture	2678.8	*(8)*
Pipeline for transport of wood chips to plant	58,863.9	*(8)*
Total capital cost at inlet	64,429.0	
Outlet facilities		
Building	236.8	Estimated
HVAC system to blow air	48.6	*(16)*
Conveyor belt	490.6	*(16)*
Filtration tank	3.4	*(16)*
Water intake tank	769.3	*(16)*
Water supply lines from water source	42.6	*(8)*
Auxiliary pump (with one redundant pump)	137.1	*(8)*
Main pump for water return	2262.3	*(8)*
Return water pipeline	41,897.2	Estimated
Total capital cost at outlet	45,887.9	
Booster station facilities		
Substation	400.0	Estimated
Booster pump for mixture	1283.0	*(8)*
Booster pump for water	1017.5	*(8)*
Building	19.7	Estimated
Access roads	4.0	*(15)*
Land	0.7	Estimated
Foundation for pump area	100.0	Estimated
Total capital cost at booster station	2824.9	

[a] Two-way pipeline, 819 mm of slurry, 606 mm of water, 2 million dry t/yr, 104 km.

all circumstances if the carrying fluid were a hydrocarbon (e.g., oil) and would be required for water if upstream sources were not available, as might occur in a forest cut area, or if downstream discharge of separated water were prohibited. Tables 2—4 show the scope and cost estimate included in a two-way pipeline (i.e., one with return of the carrier fluid).

Table 3
O/M Cost for Inlet, Outlet and Booster Station Facilities[a]

Item	Cost ($ 1000)	Remark
Inlet facilities		
Electricity	1775.9	
Maintenance cost	423.0	
Salary and wages	1080.0	4 per shift
Total O/M at inlet	3278.9	
Outlet facilities		
Electricity	1448.0	
Maintenance cost	331.1	
Salary and wages	540.0	2 per shift
Total O/M at outlet	2319.1	
Booster station		
Electricity	2627.7	
Maintenance cost	38.5	
Total O/M at booster station	2666.2	

[a] Two-way pipeline, 819 mm of slurry, 606 mm of water, 2 million dry t/yr, 104 km.

Table 4
General Economic and Technical Parameters

Item	Values
Life of pipeline	30 yr
Contingency cost	20% of total cost
Engineering cost	10% of total capital cost
Discount rate	10%
Operating factor	0.85
Power cost	$50/MWh
Velocity of slurry	1.5 m/s
Velocity of water in water return pipeline	2.0 m/s
Maximum pressure	4100 kPa
Pump efficiency	80%
Scale factor applied to inlet, outlet, and booster station facilities excluding pumps	0.75

Key elements at the upstream end are materials receiving from trucks, dead and live storage, slurrying, and pipeline initial pumps. Key elements along the pipeline are the slurry and return pipeline and booster pumping stations. Key elements at the discharge end are slurry separation and drainage of the wood chips, and material transport to the biomass processing facility. As already noted, pressure drops, pumping requirements, and the overall estimate are based on water as the carrier fluid.

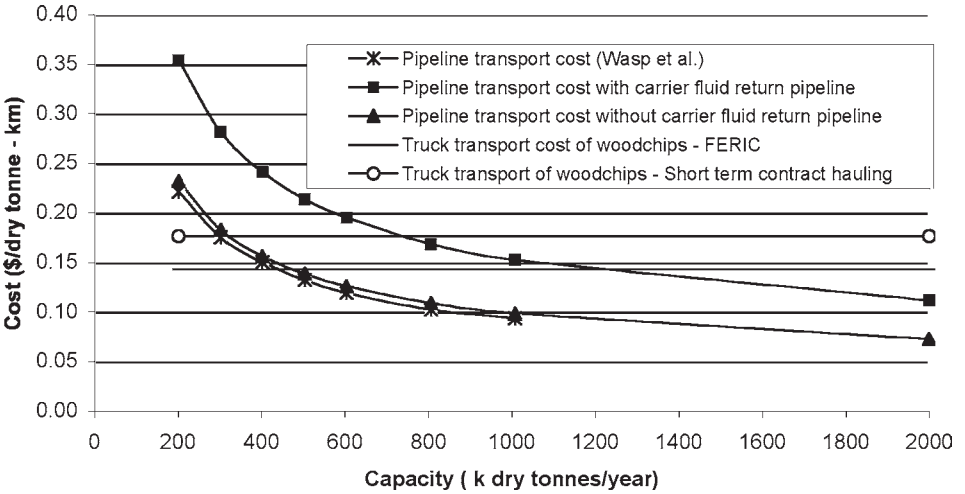

Fig. 2. Pipeline and truck transport cost of wood chips at fixed distance of 160 km.

Note that unlike truck transport, there is an economy of scale in slurry transport of materials, since larger throughputs benefit from an economy of scale in construction of the pipeline and associated equipment, and in lower friction losses in larger pipelines.

Figure 2 compares the total transport costs of wood chips by truck and by pipeline, for an arbitrary fixed distance of 160 km. The basis of the cost estimate is a wood chip concentration of 27% by volume at the inlet end and 30% by volume at the outlet end. The close agreement between the estimating formulae of Liu et al. *(8)* and the results of Wasp et al. *(6)* for a one-way pipeline is evident. The one-way pipeline cost estimates were cross-checked against a recent estimate of two short large-diameter liquid pipelines in western Canada (D. Williams, personal communication, 3/03), and showed good agreement. Figure 2 shows the impact of scale on pipeline costs, as compared with the cost of truck transport, which is independent of scale. (The formulae of Liu et al. *(8)* and the data from Bantrel [D. Williams, personal communication] suggest a capital cost scale factor for pipelines of 0.59—0.62; the data of Wasp et al. *(6)* as not specific enough to calculate a comparable figure.) Figure 2 also shows the significantly higher cost for a two-way pipeline that returns carrier liquid to the inlet end.

From Figs. 1 and 2 it is clear that the marginal cost of transporting biomass by pipeline at a concentration of 30% is higher than truck transport at capacities <0.5 million dry t/yr (one-way pipeline) and 1.25 million dry t/yr (two-way pipeline) at a distance of 160 km. The implications of this finding are discussed in the next section.

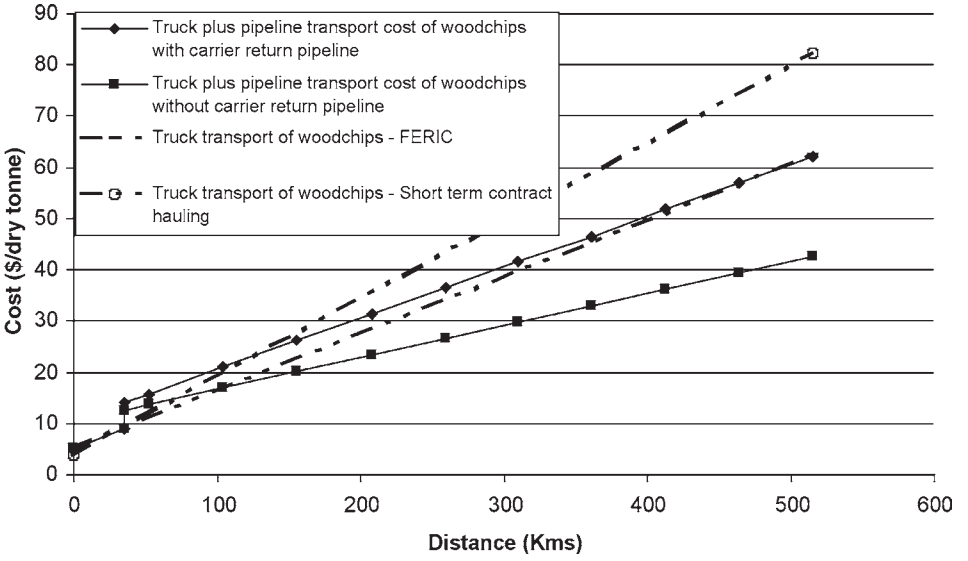

Fig. 3. Comparison of integrated truck/pipeline transport vs truck-only transport of wood chips at capacity of 2 million dry t/yr.

Practical Application: Integrated Truck/Pipeline Transport of Biomass

Any real application of pipeline transport of biomass from a field location (as opposed to mill residue) will normally require an initial truck haul to get the biomass to the pipeline inlet. This means that the fixed costs associated with both truck and pipeline transport are incurred. Thus, e.g., truck hauling of 2 million dry t/yr of biomass to a pipeline inlet at an average haul distance of 35 km *(1)*, as might occur in a whole-forest harvest operation, with further transport of biomass by one- or two-way pipeline would have cost curves as shown in Fig. 3. The alternative of transport by truck alone is shown by the dashed line in Fig. 3.

Since by inspection of Fig. 1 all pipelines with a capacity of <0.5 million dry t/yr (one-way) or 1.25 million dry t/yr (two-way) have a higher incremental cost (slope) per kilometer than the alternative of hauling by truck, it is clear that pipelines below this capacity cannot compete with the alternative of leaving the biomass on the truck for the extra distance. In the example illustrated in Fig. 3, at 2 million dry t/yr the minimum pipeline distance to recover the fixed costs of the pipeline as compared to truck haul are 75 km for a one-way pipeline (in addition to the initial 35-km truck haul to the pipeline inlet), and 470 km for a two-way pipeline (again in addition to the initial truck haul); pipeline distances shorter than this are less economic than continued hauling by truck. Hence, pipelining of truck-delivered biomass at a concentration of 30% is only feasible at both large capacity and medium to long distances.

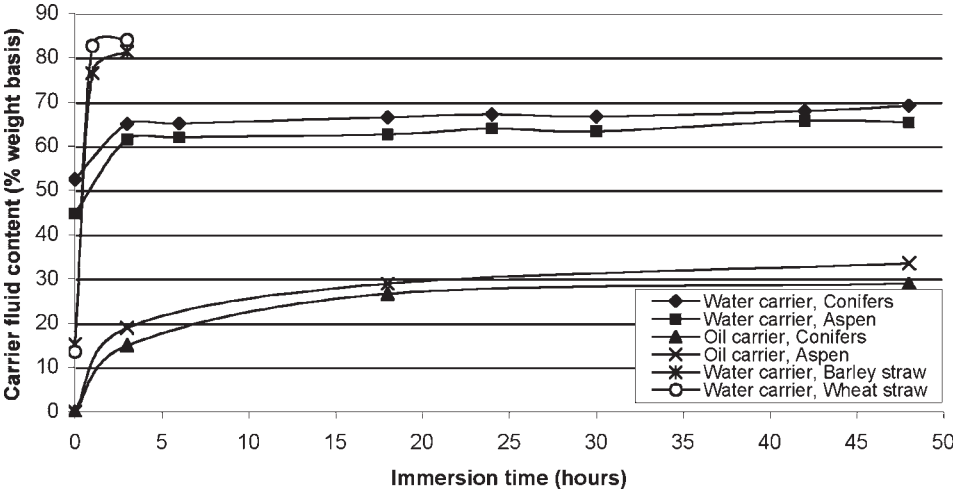

Fig. 4. Carrier fluid content of biomass after different hours of immersion in carrier fluid.

Absorption of Carrier Fluid by Biomass

We performed a series of simple experiments to explore the uptake of carrier fluid by biomass. Fresh wood chips, both hardwood (aspen) and softwood (spruce), were kept sealed and cool until immersion in room temperature water or oil; they were drained and dried to determine moisture level. Water drainage was brief, about 1 min., although one test of a longer drainage period showed a negligible impact of longer drainage times. The oil used in our study is a heavy gas oil fraction from Syncrude Canada, with a nominal boiling range of approx 325—550°C and a viscosity of 1.3 Pa s at 20°C. This type of oil is typical of an industrial-grade furnace oil. Wood chips were drained of oil for 1 hr before weighing. Figure 4 shows the carrier fluid content of biomass after exposure to carrier fluid for varying periods of time. Note that immersion time can be related to pipeline distance because at a typical slurry velocity of 1.5 m/s, the slurry would travel 5.4 km/h.

The choice of an oil carrier requires a tradeoff between the viscosity of the carrier, which drops with lower boiling range of the oil fraction, and the value of the carrier, which increases with lower boiling range. At one extreme, a diesel fraction would have low viscosity but has such a high value as a transportation fuel that its use as a thermal fuel would be cost prohibitive. At the other extreme, a residuum fraction would have low value but such a high viscosity that transport of the slurry would likely be prohibitive in operating (pumping) cost. In the present study, we have arbitrarily selected a heavy gas oil as the balance between these competing considerations.

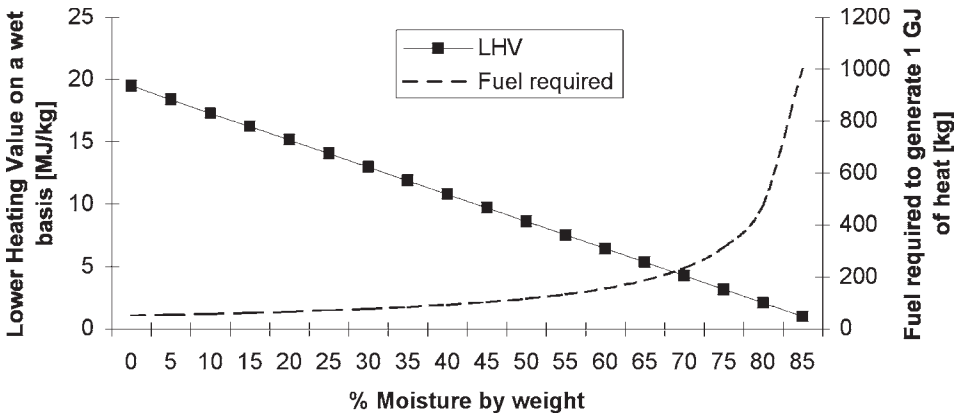

Fig. 5. Moisture content vs LHV and fuel requirement of wood chips.

During water immersion, 1 kg of mixed spruce and aspen wood chips at an average 50% water content would pick up an additional 0.51 kg of water and reach a terminal moisture level of about 67%. Water uptake is quick; even after immersion for 3 h moisture levels exceed 63%. This is similar to the findings of Brebner *(4)* and Wasp et al. *(6)*, who reported saturated wood values of 65%. We conducted two experiments with straw and found that moisture level rose from 14% as received to >80% after exposure of 3 h. This is similar to the findings of Jenkins et al. *(9)* for rice straw from California.

Absorption of water has serious implications for any process such as direct combustion that converts absorbed liquid water in the fuel into emitted water vapor in the flue gas, in that it reduces the lower heating value (LHV) of the biomass and requires more biomass per unit of heat released by combustion, an effect also noted by Yoshida et al. *(10)*. Figure 5 shows the loss in LHV and the corresponding increase in biomass that must be delivered to a direct combustion-based biomass operation at 67% moisture level. Werther et al. *(11)* note some other problems with increasing moisture in the direct combustion of biomass: reduced combustion temperature, delayed release of volatiles, poor ignition, and higher volumes of flue gas. These secondary impacts on efficiency and operability of a direct combustion unit are not considered in Fig. 5.

One can conceptually break down biomass utilization into three component cost categories: (1) field harvest of biomass, (2) transportation from the field to the biomass processing site, (3) cost of processing/conversion. For direct combustion of truck-transported biomass from harvesting of the whole forest in western Canada at or near optimum scale, the percentage and cost per megawatt-hour are as follows: category 1: 33.4%, 15.77$/MWh; category 2: 14.3%, 6.74$/MWh; and category 3: 52.3%, 24.65$/MWh *(1)*.

Since, as shown in Fig. 5, changing the moisture level of wood chips from 50% to 67% increases the requirement for field biomass in direct combustion by 78% for a given output of heat and power, it is evident that water-based pipelining of wood chips cannot be economical for direct combustion, because the increase in field harvest cost associated with the higher biomass requirement is larger than any possible transportation cost saving. For straw, so much water is taken up that the LHV is effectively zero; pipeline transport of straw to a direct combustion application would destroy the heating value of the fuel.

This impact is not true for a fuel process such as supercritical water gasification of biomass *(12—14)* that does not produce water vapor from absorbed water, since the higher heating value (HHV) value of the biomass is effectively realized by countercurrent exchange of heat between products and feed that results in condensation of produced water. The impact of absorbed water is also not an issue for fermentation of biomass, since this is a water-based process. Pipelining of biomass to fermentation processes offers the promise of larger-scale, more economic processing of ethanol, chemicals, and byproducts such as lignin. However, the pipeline design would require more detailed assessment since saccharification in the pipeline would be a logical processing alternative, and this would require temperature control during pipeline transport. This more detailed assessment is the subject of future study.

During oil immersion for 48 h, 1 kg of mixed conifer and aspen wood chips at an average 50% water content would pick up an additional 0.45 kg of oil and reach an oil level of 31%. Comparable figures for 124 hours are an uptake of 0.52 kg to reach a oil level of 34%. Direct combusting wood chips delivered in a heavy gas oil can be thought of as cofiring a mix of about two/thirds oil and one/third wood on a thermal basis. Pipeline cost would increase because of additional pumping; the increase would depend on the viscosity of the oil fraction that was selected as the transport carrier fluid.

Discussion

Pipeline transport of oil and natural gas is clearly far more economical than truck transport, even in relatively small pipelines. Three factors combine to make the transport of energy in the form of biomass far less economic:

1. The density of energy in the pipeline is far lower for biomass than for oil. The present work is based on 30% biomass by volume in a carrier liquid. Wasp et al. *(6)* based their work on 22% biomass. Brebner *(4)* and Elliott *(5)* indicated that at about 47% concentration by volume a slurry of wood chips and water cannot flow. Given the low heat content of wood per unit volume relative to oil and the low concentration of wood chips in water, the energy density in a 30% wood chip slurry is about 8% compared to oil, even based on HHV, and hence far larger pipelines are required to transport the same amount of energy.

2. The pressure drop in the pipeline is high for suspended solids in a carrier fluid. For example, Wasp et al. *(6)* indicate that at 30% concentration of wood and a velocity of 1.4 m/s, a wood chip slurry in a 214-mm-diameter pipeline has a pressure drop that is three times larger than for water alone.
3. Recycle of the carrier fluid will often be required in biomass transport by pipeline, both because large quantities of water will not be available at the inlet end and because discharge of water that has carried the biomass will, in some jurisdictions, be prohibited. This requires that a second pipeline and set of pumping stations be constructed.

In addition to these cost elements, transport of biomass for a direct combustion application by water creates a prohibitive drop in the LHV of the fuel because of absorbed water. These issues limit the application of pipeline transport of biomass to large applications that use oil as a carrier medium, or that supply a process for which the heat content of the fuel is not degraded by the requirement to remove absorbed water as vapor, such as a supercritical water gasification process.

Transport of wood chips by oil precludes firing a high percentage of biomass owing to high oil uptake by wood chips. We consider it unlikely that a two-thirds oil and one-third wood fuel mixture would have high interest today as a power plant fuel, since even a heavy gas oil fraction has too high a value as a transportation fuel precursor to be diverted into power generation.

Conclusion

Pipeline transport of truck-delivered wood chips is only economical at large capacities and medium to long distances. For a one-way pipeline, the minimum economic capacity is >0.5 million dry t/yr. For a two-way pipeline, the minimum economic capacity is >1.25 million dry t/yr. At 2 million dry t/yr, the minimum economical distance for a one-way pipeline without carrier fluid return is 75 km, and for a two-way pipeline with carrier fluid return is 470 km.

Furthermore, water transport of mixed hardwood and softwood chips causes an increase in moisture level to 65% or greater, which so degrades the LHV of the biomass that it cannot be economical for any process, such as direct combustion, that produces water vapor from water contained in the biomass. The impact on straw is greater, in that moisture levels are so high that the LHV is negative. Pipeline transport of biomass water slurries can only be utilized when produced water is removed as a liquid, such as from supercritical water gasification.

Finally, oil transport of mixed hardwood and softwood chips gives a fuel that is more than 30% oil by mass and is two-thirds oil and one-third wood on a thermal basis.

Acknowledgments

We gratefully acknowledge the Poole family and Bud Kushnir, whose financial support made this research possible. Sean Sanders of Syncrude Canada provided insight into pump size and pressure drop in the slurry pipeline and also provided heavy gas oil for the experiments. Mark Coolen, woodlands operations superintendent for Millar Western Forest Products, provided wood chips for the experiments and valuable discussions. David Williams, Chief Estimator for Bantrel (an affiliate of Bechtel), provided valuable comments concerning capital cost estimation of pipeline. Vic Lieffers and Pak Chow of the University of Alberta helped carry out the experiments. All conclusions and opinions are solely the authors and have not been reviewed or endorsed by any other party.

References

1. Kumar, A., Cameron, J. B., and Flynn, P. C. (2003), *Biomass Bioenergy* **24(6),** 445–464.
2. Cameron, J., Kumar, A., and Flynn, P. C. (2002), in *Proceedings of the 12th European Biomass Conference for Energy, Industry and Climate Protection*, vol. 1, June 17–21, Amsterdam, The Netherlands, pp. 123–126.
3. Favreau, J. F. E. (1992), Technical report no. TR-105, Forest Engineering Research Institute of Canada, Canada.
4. Brebner, A. (1964), *Can. J. Chem. Eng.* **42,** 139–142.
5. Elliott, D. R. (1960), *Pulp Paper Mag. Canada* **61,** 170–175.
6. Wasp, E. J., Aude, T. C., Thompson, T. L., and Bailey, C. D. (1967), *Tappi* **50 (7),** 313–318.
7. Hunt, W.A. (1976), in *Proceedings of Hydrotransport 4, 1976: 4th International Conference on the Hydraulic Transport of Solids in Pipes*, BHRA Fluid Engineering, Cranfield, UK, pp. 1–18.
8. Liu, H., Noble, J., Zuniga, R., and Wu, J. (1995), Report no. 95-1, Capsule Pipeline Research Center (CPRC), University of Missouri, Columbia.
9. Jenkins, B. M., Bakker, R. R., and Wei, J.B. (1996), *Biomass Bioenergy* **10(4),** 177–200.
10. Yoshida, Y., Dowaki, K., Matsumura, Y., Matsuhashi, R., Li, D., Ishitani, H. and Komiyama, H. (2003), *Biomass Bioenergy* **25(3),** 257–272.
11. Werther, J., Saenger, M., Haetge, E.-U., Ogada, T., and Siagi, Z. (2000), *Prog. Energy Combust. Sci.* **26,** 1–27.
12. Antal, M. J., Jr., Allen, S. G., Schulman, D. and Xu, X. (2000), *Ind. Eng. Chem. Res.* **39(11),** 819–824.
13. Matsumura, Y., Xu, X., and Antal, M. J., Jr. (1997), *Carbon* **35(6),** 819–824.
14. Matsumura, Y., Minowa, T., Xu, X., Nuessle, F. W., Adschiri, T., and Antal, M. J., Jr. (1997), in *Developments in Thermochemical Biomass Conversion*, Bridgwater A. V. M. and Boocock, D. G. B., eds., Blackie Academic and Professional, London, UK, pp. 864–877.
15. RS Means Company. (2000), in *Heavy Construction Data—14th Annual Edition*, Chandler, H. M., et al., eds.
16. Peters, M. S. and Timmerhaus, K. D. (1991), *Plant Design and Economics for Chemical Engineers*, 4th Ed., McGraw-Hill, New York, NY.

0273-2289/04/113/0041–0054/$25.00

Hydrodynamic Separation of Grain and Stover Components in Corn Silage

Philippe Savoie,*[,1] Kevin J. Shinners,[2] and Benjamin N. Binversie[2]

[1]Agriculture and Agri-Food Canada, 2560 Hochelaga Boulevard, Sainte-Foy, Québec, Canada G1V 2J3, E-mail: psavoie@grr.ulaval.ca; and [2]Biological Systems Engineering Department, University of Wisconsin, 460 Henry Mall, Madison, WI 53706

Abstract

Mixing fresh silage in water resulted in partial segregation of grain from stover. Grain concentration was 75% in the sunk material when silage was relatively dry (64% moisture content [MC]) and 41% when silage was relatively wet (74% MC). Partial drying to remove 20 percentage units of moisture prior to water separation increased grain concentration to 92%, and complete drying increased grain concentration to 99%. Sieving without drying followed by water separation resulted in a grain concentration of 79%. A byproduct of water separation is a large amount of soluble and deposited fine particles in the effluent: 18% of original dry matter after one separation, and between 21 and 26% after eight separations. In an industrial setting, hydrodynamic separation of silage with minimal pretreatment could provide a feedstock with a high concentration of grain (75–80%). In a laboratory setting, hydrodynamic separation with prior oven drying could provide a method to separate grain from stover in corn silage by reaching a grain concentration higher than 99%.

Index Entries: Corn; stover; grain; separation; silage.

Introduction

Various methods for separating corn grain from stover have been proposed. One approach is to shell the grain with a combine and subsequently to harvest the residual stover with either a forage harvester or a baler *(1)*. Another approach is to harvest, chop, and ensile the whole crop, and to separate components at removal from storage *(2)*. Advantages of separation after storage include fast and efficient harvest in a single stream;

*Author to whom all correspondence and reprint requests should be addressed. Contribution number 761, Soils and Crops Research and Development Centre, AAFC.

low-cost storage in high-capacity bunker silos without the need for grain drying; and separation throughout the year at relatively low work rates, with small size equipment, compared with the high rates handled during the short harvest season.

After ensiling, grain has been sorted from stover, at least partially, by mechanical sieving *(3)* or aerodynamic separation *(4)*. Hydrodynamic separation has not previously been used for corn silage, but it is used industrially to separate heavier particles such as phosphatides from corn oil in the wet-milling process *(5)*.

Hydrodynamic separation of grain from stover could be feasible if components exhibit significant differences in specific gravity or buoyancy. The specific gravity of corn grain has been observed to range from 1278 to 1380 kg/m^3 *(6)*. The specific gravity of corn stover components (stalk, cob, leaf, husk) is less well documented. Meanwhile, the specific gravity of forage particles is in the order of 1500 kg/m^3 *(7)*. This would suggest poor hydrodynamic separation of grain from stover in water because both components would sink. However, empirical evidence shows that grain sinks more rapidly than stover, which tends to float because of buoyancy.

The objective of the present work was to evaluate the potential of hydrodynamic separation with water to sort grain from stover after ensiling. New data are presented on the specific gravity of corn grain and stover components after coarse chopping or grinding. Factors considered include harvest conditions (chop length and processing) and pretreatment of the silage (partial drying, sieving) prior to hydrodynamic separation.

Materials and Methods

Experiment 1: Specific Gravity of Corn Components

Several stalks of whole-plant corn were cut with a scythe at 10 cm from the ground at full maturity (early December 2002) near Madison, WI. Plants were separated manually into five components: grain, stalk, leaf, husk, and cob. The components were oven-dried at 103°C for 24 h *(8)* to estimate moisture content and the respective proportions of dry matter (DM). Specific gravity was estimated with a PMI Automated Gas Pycnometer (Porous Materials, Ithaca, NY), which measured the pressure change in helium gas as it surrounded the crop component in an enclosed volume *(9)*. Three iterations were done for each sample in the pycnometer, and three replications were done for each component in two states: intact grain or coarsely chopped stover, and ground components. Chopping was done with a laboratory chopper set at 13-mm theoretical length of cut. Grinding was carried out with a Model 4 Thomas Wiley Mill using a 1-mm screen (Thomas Scientific). The specific gravity was corrected to a dry basis by mass balance:

$$\rho_{DM} = \frac{\rho_{WM}\,\rho_{H_2O}\,(100 - MC)}{100\,\rho_{H_2O} - \rho_{WM}\,MC} \quad (1)$$

in which ρ_{DM} is the corrected specific gravity on a dry matter basis, ρ_{WM} is the wet matter specific gravity as measured experimentally, ρ_{H2O} is the specific gravity of water (1000 kg/m^3), and MC is the moisture content on a wet basis (%).

Experiment 2: Sequential Water Separation

Four silages harvested in fall 2002 were retrieved from the silo in March 2003 for the sequential water separation. The silages were selected to represent four mechanical harvest treatments: short chop and unprocessed, long chop and unprocessed, short chop and processed, and long chop and processed. Processing involved crushing and shearing the chopped whole plant through a pair of toothed rolls operating at small clearance and differential speed *(10)*. Silages came from two experimental farms (Arlington, Prairie-du-Sac) and two commercial farms (Binversie, Ziegler) in Wisconsin. A measured mass of 1 kg of fresh silage was placed in a water basin containing initially 7 L of water. After 1 min of manual gentle mixing, the material still floating on the water surface was removed by hand. The rest of the basin contents was poured gently over a screen made of 0.40-mm (1/64-in.) thick wire spaced 1.59 mm (1/16 in.) center to center in a square grid with about 50% open area. The screen separated material into two components, the effluent water and the suspended solids, and a third component was the sunk material that remained at the bottom of the basin after pouring. The latter two components were spread onto separate paper cloths to partially dry in ambient air. The floating material was then deposited again in the water basin with the same effluent water. After 1 min, the floating and suspended solids were set aside for the next water separation and the sunk material was put on a cloth to dry. This process was repeated until eight water separations had been completed. The eight-step sequential separation was replicated three times for each of the four silages.

The sunk material from each of the eight separations, the suspended solids from the first separation, and the residual floating material after the eighth separation (i.e., 10 components) were oven-dried at 103°C for 24 h to estimate the proportions of DM at each step. A well-mixed amount of 2 kg of water effluent was also measured after the eighth separation and oven-dried to estimate the total DM in the effluent.

For each replication (four silages × three replications), the 10 dried components were hand sorted to separate grain from stover. Sorted grain included full and broken grains, grain hull, and grain endosperm pieces that were large enough (1 to 2 mm) to be clearly identified as starch. The rest was considered to be stover. Because sorting occurred over a period of several weeks after oven-drying, rehydration occurred and component masses were corrected to a DM basis. Grain concentration was estimated as the proportion of sunk grain over the total of sunk grain and sunk stover.

Experiment 3: Separation After Drying or Sieving

Six pretreatments were done to compare the effect of drying or sieving on subsequent grain and stover separation:

1. A fresh untreated silage.
2. Silage that was partially dried until it lost 10 percentage units of moisture.
3. Silage that was partially dried until it lost 20 percentage units of moisture content.
4. Silage that was oven-dried to approx 0% moisture.
5. Silage that was sieved by a standard method *(11)* and whose material from only screen no. 3 was hydrodynamically separated (particle size between 9.0 and 18.0 mm).
6. The same sieved material as in item 5 that was also partially dried to lose 10 percentage units of moisture.

The silage for all six pretreatments was unprocessed and came from a commercial farm (Manthe) in south-central Wisconsin.

A single water separation was done with these treated silages. Using the same amounts of silage (1 kg) and water (7 L) as in the second experiment, the material was separated into three components: sunk, suspended, and floating material. DM in the effluent was estimated by mass balance. The three measured components were further subdivided into grain and stover by hand sorting after oven-drying. The water separation was replicated three times for each of the six silage treatments. In the case of sieved material, 1 kg was placed in the separator, and only the fraction retained on screen no. 3 was separated by water.

MC, Particle Length, and Statistical Analyses

As indicated previously, moisture was measured by oven-drying at 103°C for 24 h *(8)*. Three samples from each of the five silages were taken for moisture measurement. Mean particle length (MPL) was measured by the standard separator method using five screens and a pan *(11)*. Three samples of about 2 kg each were taken to measure MPL for each of the five silages.

Statistical analyses were done using analysis of variance (ANOVA) with a single factor. The single factor in the first experiment was corn component at five levels: grain, stalk, leaf, husk, and cob. The single factor in the second experiment was silage source at four levels: Binversie Farm (unprocessed, short), Prairie-du-Sac Farm (unprocessed, long), Ziegler Farm (processed, short), and Arlington Farm (processed, long). The single factor in the third experiment was treatment at six levels: fresh silage, partially dried to lose 10 percentage units of moisture, partially dried to lose 20 percentage units of moisture, completely dried in the oven, sieved and fresh, sieved and partially dried to lose 10 percentage units of moisture. ANOVA was used to determine significant differences. The least significant difference method was used to rank results *(12)*.

Table 1
Specific Gravity of Corn Components Either Coarsely Chopped or Ground on DM Basis

	Specific gravity (kg DM/m^3)	
Component	Chopped	Ground
Grain	1305 [a]	1486 [a]
Stalk	606 [c]	1625 [a]
Husk	814 [b]	1606 [a]
Cob	837 [b]	1504 [a]
Leaf	664 [c]	1510 [a]
SEM	38	67
LSD	86	149

[a]Average of three replications. Values with the same superscript letter in a given column indicate no significant difference ($p < 0.05$). SEM, standard error of means; LSD, least significant difference.

Chemical Analyses

The following components were selected for chemical analyses: five corn components from the first experiment (grain, stalk, leaf, husk, and cob), five whole-plant corn silages from the second experiment, four effluent DMs obtained from the four corn silages in the second experiment, four components from the third experiment (sunk grain, sunk stover, suspended stover, and floating stover). Three replications of each component were analyzed by the UW Soil and Plant Analysis Lab in Marshfield, WI, using wet chemistry for acid detergent fiber (ADF), neutral detergent fiber (NDF), crude protein (CP), minerals (P, Ca, K, Mg), and starch.

Results

Experiment 1: Specific Gravity of Corn Components

Table 1 presents the specific gravity of corn components as measured by the gas pycnometer. All components were oven-dried prior to measurements. Because of ambient rehydration, the MC of components varied between 2 and 8% at the time of measurements. The data presented in Table 1 were corrected on a DM basis using Eq. 1. Intact grain was significantly denser (1305 kg of DM/m^3) than chopped stalk and leaf (average of 635 kg of DM/m^3) or chopped husk and cob (average of 826 kg of DM/m^3). However, when all material was ground through a 1-mm screen, there was no significant difference among the five components (average of 1546 kg of DM/m^3). The corn used to measure specific gravity was very mature, being harvested in December, and had DM fractions of grain, stalk, husk, cob, and leaf of 65, 18, 4, 10, and 3%, respectively. Measures might be different for earlier maturity corn. However, the data show a remarkable homogeneity in specific gravity when material becomes very fine.

Table 2
Characteristics of Corn Silages Used for Hydrodynamic Separation of Grain and Stover in Eight Stages in Experiment 2[a]

Silage source	MC (% wet basis)			Processed	MPL (mm)	Geometric SD (mm)
	Silage	Grain	Stover			
Ziegler Farm	67.3	50.3	69.5	Yes	12.9	1.70
Prairie-du-Sac Farm	73.8	52.8	75.8	No	17.4	1.81
Arlington Farm	63.8	45.8	67.6	Yes	13.6	1.97
Binversie Farm	66.0	46.8	70.7	No	8.1	1.66

[a]Average of three replications.

Experiment 2: Sequential Water Separation

Table 2 presents the physical characteristics of the four silages used for the sequential water separation experiment. The two processed silages (Ziegler Farm and Arlington Farm) had very similar MPL (13 and 14 mm, respectively). They also had a relatively low MC; the Arlington silage had the highest DM content (36% DM). The Prairie-du-Sac Farm silage was unprocessed and had a long particle size (17 mm), whereas the Binversie Farm silage was unprocessed and had a short particle size (8 mm). The moisture reported for grain and stover in Table 2 may slightly underestimate the actual values because components were exposed to natural air-drying for about 1 h during manual sorting prior to oven-drying.

Table 3 shows the proportion of grain and stover in the sunk material from the four silages. After the first separation, the grain concentration in the sunk material was 75% and highest for the Arlington silage, which also was the driest. The grain concentration was only 41% and lowest for the Prairie-du-Sac silage, which was the wettest. The Binversie silage was different from the other three silages because it produced a higher amount of sunk grain (31% of total DM) than the three other silages (19% of total DM). This might be the result of a later maturity harvest; a greater presence of fully formed kernels; and no used of a processor, thereby leaving more intact grain.

After the eighth separation, grain concentrations ranged from 27 to 46% and were lower than after the first separation. At each separation, more stover sank and mixed with the corn grain. Only the Arlington silage released more than 1.5% of total DM as grain beyond the first separation. The actual concentration of DM in the effluent ranged from 0.71 to 1.22%, with an average of 1.01%. DM in the effluent reported in Table 3 represents the DM as a proportion of the original DM in the silage.

Figures 1 and 2 illustrate the curves of sunk grain, sunk stover, DM in the effluent, and floating material over the course of the eight water separations for two contrasting cases: the Arlington Farm silage with a low MC and the Prairie-du-Sac Farm silage with a high MC. The sunk grain and sunk stover reported in Figs. 1 and 2 were measured at each separation.

Table 3
Grain and Stover Proportions After the First and Eighth Separations of Fresh Silage in Water in Experiment 3

	After first separation			After eighth separation				
	DM (%)		Grain concentration in sunk material (%)	DM (%)				Grain concentration in sunk material (%)
Silage source	Sunk grain	Sunk stover		Sunk grain	Sunk stover	Floating stover	DM in effluent	
Ziegler Farm	18.5 ^{b}	11.4 ^{bc}	62.0 ^{b}	20.0 ^{c}	36.3 ^{b}	17.6 ^{b}	26.0 ^{a}	35.6 ^{b}
Prairie-du-Sac Farm	19.1 ^{b}	27.1 ^{a}	41.3 ^{c}	19.5 ^{c}	53.2 ^{a}	6.7 ^{c}	20.7 ^{b}	26.8 ^{c}
Arlington Farm	19.3 ^{b}	6.6 ^{c}	75.2 ^{a}	25.2 ^{b}	29.6 ^{c}	23.8 ^{a}	21.6 ^{b}	45.9 ^{a}
Binversie Farm	30.7 ^{a}	14.7 ^{b}	67.7 ^{ab}	31.6 ^{a}	37.2 ^{b}	10.2 ^{c}	21.0 ^{b}	45.9 ^{a}
SEM	1.7	2.3	4.9	2.1	2.1	1.7	0.4	3.5
LSD	3.9	5.3	11.2	4.9	4.9	3.9	1.2	7.5

[a] Average of three replications. Values with the same superscript letter in a given column indicate no significant difference ($p < 0.05$). SEM, standard error of means; LSD, least significant difference.

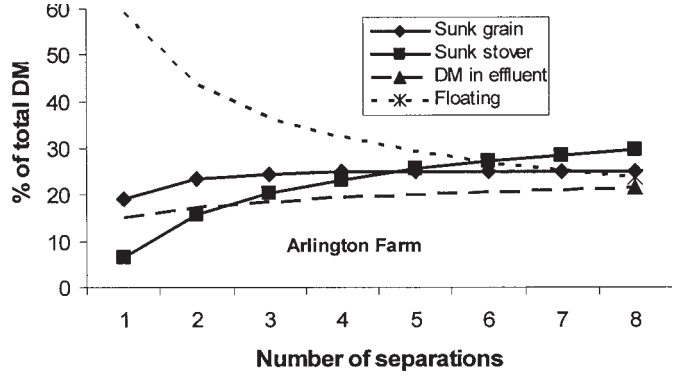

Fig. 1. Corn silage components after eight successive water separations: Arlington Farm. Silage was processed and had an MPL of 13.6 mm and an MC of 63.8%.

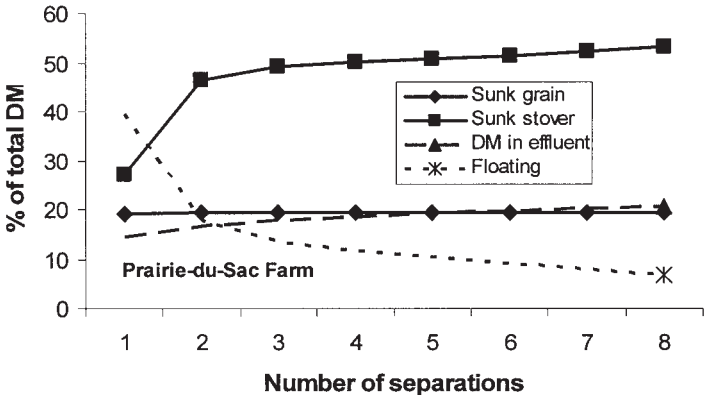

Fig. 2. Corn silage components after eight successive water separations: Prairie-du-Sac Farm. Silage was not processed and had an MPL of 17.4 mm and an MC of 73.9%.

The floating material and the effluent DM were measured only after the eighth separation. The curve for DM in the effluent was inferred by assuming that 70% of DM in the effluent was released after the first separation (*see* experiment 3 for a justification) and by assuming that the release followed a logarithmic curve. The curve for floating material was obtained by mass balance. The suspended stover recovered after the first separation was considered to be part of the floating material.

Experiment 3: Separation After Drying or Sieving

Table 4 presents fractions of sunk, suspended, and floating material after a single separation. The residual grain represents grain that was hand sorted from either the suspended or floating material. The DM in the effluent was obtained by mass balance after other components had been dried and separated.

Table 4
Grain and Stover Proportions After One Water Separation and Various Pretreatments

Pretreatment	Silage used (%)	MC (%)	DM after one separation (%)						Grain concentration in sunk material (%)
			Sunk grain	Sunk stover	Suspended stover	Floating stover	Residual grain	DM in effluent	
1. Untreated silage	100	64.6	21.3 ^{c}	8.4 ^{a}	7.1 ^{b}	44.1 ^{cd}	1.5 ^{b}	17.6 ^{a}	71.8 ^{d}
2. Partially dried to lose 10% units of MC	100	54.8	22.9 ^{c}	9.5 ^{a}	5.2 ^{c}	45.4 ^{c}	0.5 ^{c}	16.5 ^{ab}	70.6 ^{d}
3. Partially dried to lose 20% units of MC	100	45.3	25.8 ^{b}	2.2 ^{c}	2.1 ^{d}	54.6 ^{b}	1.0 ^{bc}	14.3 ^{bc}	92.3 ^{b}
4. Oven-dried	100	0.0	23.8 ^{bc}	0.1 ^{c}	0.6 ^{d}	62.3 ^{a}	2.5 ^{a}	10.8 ^{d}	99.4 ^{a}
5. Sieved and fresh	50.3	64.6	37.0 ^{a}	9.8 ^{a}	9.5 ^{a}	29.5 ^{e}	0.6 ^{c}	13.6 ^{cd}	79.1 ^{c}
6. Sieved, partially dried to lose 10% units of MC	50.3	55.5	34.6 ^{a}	4.7 ^{b}	5.1 ^{c}	41.1 ^{d}	1.7 ^{ab}	12.8 ^{cd}	88.0 ^{b}
SEM			1.4	1.0	0.8	1.8	0.4	1.3	2.7
LSD			3.1	2.2	1.7	3.9	0.9	2.8	5.8

[a] Experiment 3 with silage from Manthe Farm: 64.6% MC, unprocessed and 10.3mm MPL; average of three replications. Values with the same superscript letter in a given column indicate no significant difference ($p < 0.05$). SEM, standard error of means; LSD, least significant difference.

Sieving increased the proportion of grain collected (37 vs 21%, without drying), and improved the grain concentration in the sunk material (79 vs 72%). However, the total amount of grain obtained in the sunk material was lower after sieving (18.6 vs 21.3%) because about half the silage remained in the other sieves that were not used for the water separation. The smaller-size sieves would contain a significant amount of broken grain.

The proportion of sunk stover decreased significantly with partial drying (20 percentage units of moisture loss) and with complete drying in the oven. The grain concentration was enhanced as high as 99.4% for bone-dry material. The proportion of suspended stover was highest for sieved and fresh pretreatment. This material was of relatively uniform length (between 9 and 18 mm), so grain could sink rapidly in the absence of long stover pieces that tended to float and hinder the descent of smaller grain. The proportion of floating material was significantly higher for dry material. Residual grain was highest also in dry material. The proportion of DM in the effluent decreased as the silage was dried. The reduction in soluble and fine particles after drying might be owing to a loss of volatile organic acids.

In experiment 3, effluent contained an average of 17.6% of fresh silage DM after one separation. In experiment 2, in which eight successive water separations occurred, the effluent water contained between 20.7 and 26.0% of the fresh silage DM. A large proportion of the soluble and fine particles mixed rapidly in the effluent water. These values suggest a range between 68 and 85% for the ratio between DM in the effluent after one separation and DM in the effluent after eight separations. A ratio of 70% was assumed in Figs. 1 and 2 to illustrate initial DM in effluent and is within the experimental range of 68 to 85%.

Chemical Composition

Table 5 reports the chemical composition of five components from corn. The level of starch in grain was not as high as expected (50–60% is typical), perhaps because of the crop's late maturity. Fiber concentrations, either ADF or NDF, are good indicators to estimate the proportion of grain and stover in a whole-plant mix.

Table 6 shows the chemical composition of components after water separation. The sunk grain had a level of starch as expected but more fiber than expected. The sunk stover probably contained small fractions of grain that could not be separated manually. The suspended and floating materials also probably contained some small grain particles that had not sunk after the first water separation. The effluent DM containing soluble and very fine particles had on average 26% starch and 3% ADF, indicating a larger proportion of grain than stover components. Prior to water separation, silages in experiment 2 had an average composition of 8.5% CP, 19.1% starch, 23.6% ADF, and 40.3% NDF.

Table 5
Chemical Composition on DM Basis of Mature Whole-Plant Corn Components*

Component	CP (%)	P (%)	Ca (%)	K (%)	Mg (%)	Starch (%)	ADF (%)	NDF (%)
Grain	4.9 ^{b}	0.25 ^{a}	0.03 ^{d}	0.31 ^{d}	0.11 ^{d}	42.5^{a}	2.5 ^{d}	21.0 ^{d}
Stalk	3.3 ^{c}	0.10 ^{bc}	0.16 ^{b}	1.04 ^{a}	0.17 ^{b}	0.4^{b}	45.5 ^{b}	78.3 ^{c}
Husk	3.9 ^{c}	0.07 ^{cd}	0.13 ^{c}	0.74 ^{b}	0.16 ^{c}	1.3^{b}	42.2 ^{c}	84.4 ^{b}
Cob	2.8 ^{d}	0.05 ^{d}	0.05 ^{d}	0.60 ^{c}	0.08 ^{e}	0.1^{b}	44.5 ^{b}	90.6 ^{a}
Leaf	5.7 ^{a}	0.13 ^{b}	0.44 ^{a}	0.23 ^{d}	0.25 ^{a}	1.3^{b}	46.8 ^{a}	77.8 ^{c}
SEM	0.3	0.02	0.01	0.05	0.01	2.3	0.8	2.7
LSD	0.7	0.03	0.02	0.12	0.01	5.2	1.8	6.1

*Average of three replications. Values with the same superscript letter in a given column indicate no significant difference ($p < 0.05$). SEM, standard error of means; LSD, least significant difference.

Table 6
Chemical Composition on DM Basis of Corn Silage Components After One or Eight Water Separations*

Component	CP (%)	P (%)	Ca (%)	K (%)	Mg (%)	Starch (%)	ADF (%)	NDF (%)
After one water separation (experiment 3)								
Sunk grain	1.9 [d]	0.06 [c]	0.02 [c]	0.15 [c]	0.03 [d]	55.0 [a]	5.3 [c]	16.9 [c]
Sunk stover	4.0 [c]	0.10 [b]	0.07 [b]	0.22 [b]	0.07 [c]	16.7 [b]	29.7 [b]	50.9 [b]
Suspended stover	5.1 [b]	0.11 [b]	0.18 [a]	0.23 [b]	0.09 [b]	6.8 [d]	39.0 [a]	63.4 [a]
Floating material	6.0 [a]	0.16 [a]	0.18 [a]	0.38 [a]	0.14 [a]	9.5 [c]	36.5 [a]	61.5 [a]
SEM	0.1	0.01	0.01	0.01	0.00	1.2	1.6	2.2
LSD	0.3	0.02	0.02	0.03	0.01	2.7	3.6	5.1
After eighth water separation (experiment 2)								
Effluent DM	15.5	0.64	0.95	3.13	0.73	25.9	3.2	5.0

*Average of three replications after one separation, average of 12 replications after eighth separation. Values with the same superscript letter in a given column indicate no significant difference ($p < 0.05$). SEM, standard error of means; LSD, least significant difference.

Discussion

The specific gravity of particles changed with their size. Intact grain was much denser than coarsely chopped stover components. However, when material was finely ground, the density of all components increased and no further difference in density was observed. The results suggest that stalk and leaf have more micropores than husk and cob while grain had the least micropores. In principle, fine chopping and processing would contribute to an increase in the density of all components and the proportion of stover that sinks with grain in a water separation process.

In experiment 2, most of the corn grain sunk rapidly. Between the first and the eighth water separation, the amount of sunk grain increased by only 0.4% for the Prairie-du-Sac silage, 0.9% for the Binversie silage, 1.5% for the Ziegler silage, and 5.9% for the Arlington silage. Therefore, only one or two water separations would be needed to separate most grain.

When fresh silage was separated in water, the highest grain concentration achieved in the sunk material was 75%; this was observed with processed and relatively dry corn silage (64% MC). Short chopped material (8 mm) actually had a higher grain concentration (68%) than long material (17 mm), whose grain concentration was only 41% largely because of a high initial MC (74%). The moisture content had a greater impact than the physical form in the range that was observed (8- to 17-mm MPL, processed or not processed).

The effect of MC was even more apparent in experiment 3 when fresh material was compared with material partially dried (10 or 20 percentage units of moisture removal) or completely dried prior to water separation. Greater than 99% grain concentration was observed with bone-dry material. As corn silage becomes drier, stover pieces are likely to become more buoyant because of their large area compared to grain. Oven-drying is therefore a good pretreatment followed by water separation to concentrate grain from corn silage. Because of the large amount of water in silage and the high cost to dry this material, the procedure could be used for small samples in the laboratory but would not likely be feasible in an industrial setting.

Without any pretreatment, hydrodynamic separation could allow the production of a concentrate of about 75% grain and 25% stover. It is difficult to achieve a higher grain concentration without having to partially dry or sieve the silage. Sieving increased the grain concentration in the sunk material to 79%. From an industrial point of view, water separation would require recuperation of considerable amounts of soluble and deposited fine particles (18% of original DM after one separation, and between 21 and 26% after eight separations). Hydrodynamic separation could provide a feedstock with a high concentration in grain (75–80%), but it could not provide a stover-free feedstock without drying. Compared to pneumatic separation and sieving alone, hydrodynamic separation is likely to require less energy when drying is not used. If pure corn

components are needed, the traditional combine thresher is more suitable for providing pure grain than any poststorage separation method applied to silage. Various harvest devices can be designed to collect the stover either simultaneously with threshing or afterward with another pass machine.

Acknowledgments

This research was partially supported by the USDA-ARS, UW Graduate School, John Deere Technical Center, and Wisconsin Corn Promotion Board. We also acknowledge support from the Natural Science and Engineering Research Council of Canada and Agriculture and Agri-Food Canada.

References

1. Richey, C. B., Liljedhal, J. B., and Lechtenberg, V. L. (1982), *Trans. ASAE* **25(4),** 834–839, 844.
2. Jenkins, B. M. and Sumner, H. R. (1986), *Trans. ASAE* **29(3),** 824–836.
3. Ganesh, D. and Mowat, D. N. (1983), *Can. J. Plant Sci.* **63,** 935–941.
4. Bilanski, W. K., Jones, D. K., and Mowat, D. N. (1986), *Trans. ASAE* **29(5),** 1188–1192.
5. Corn Refiners Association. (1996), *Corn Oil. 4th Edition*. Corn Refiners Association, Washington, DC.
6. Gustafson, R. J. and Hall, G. E. (1972), *Trans. ASAE* **15(3),** 523–525.
7. Pitt, R. E. (1983), *Trans. ASAE* **26(5),** 1522–1527, 1532.
8. ASAE. (2002), *Moisture Measurement—Forages*. ASAE S358.2. Standards, 49th Edition. American Society of Agricultural Engineers, St. Joseph, MI.
9. ASTM. (2003), *Standard Test Method for Specific Gravity of Soil Solids by Gas Pycnometer. Designation D5550-00. Volume 04.08*. American Society for Testing Materials, accessed at Website: www.astm.org.
10. Shinners, K. J., Jirovec, A. G., Shaver, R. D., and Bal, M. (2000), *Appl. Eng. Agr.* **16(4),** 323–331.
11. ASAE. (2002), *Method of Determining and Expressing Particle Size of Chopped Forage Material by Screening. ANSI/ASAE S424.1. Standards, 49th Edition*. American Society of Agricultural Engineers, St. Joseph, MI.
12. Steel, R. G. D., Torrie, J. H., and Dickey, D. A. (1996), *Principles and Procedures of Statistics: A Biometrical Approach. 3rd Edition*. McGraw Hill, New York, NY.

0273-2289/04/113/0055–0070/$25.00

A New Class of Plants for a Biofuel Feedstock Energy Crop

James Kamm

University of Toledo,
Toledo, OH 43606,
E-mail: jkamm@utnet.utoledo.edu

Abstract

Directly burnable biomass to be used primarily in steam boilers for power production has been researched and demonstrated in a variety of projects in the United states. The biomass typically comes from wood wastes, such as tree trimmings or the byproducts of lumber production, or from a cash crop, grown by farmers. Of this latter group, the main emphasis has been utilizing corn stover, or a prairie grass called switchgrass, or using tree seedlings such as willow. In this article, I propose an alternative to these energy crops that consists of several different herbaceous plants with the one consistent property that they annually generate an appreciable bulk of dried-down burnable mass. The fact that they are a set of plants (nine are offered as candidates) gives this energy crop a great deal of flexibility as far as growing conditions and annual harvest time line. Their predicted yield is impressive and leads to speculation that they can be economically feasible.

Index Entries: Biomass; biofuel; energy crop; sclerified stalked plants; stiff stalked plants.

Introduction

The prospect of biomass as a fuel source is an alluring one. In the first place, it is geopolitically simple; most countries desiring to utilize it can provide their own biomass. In addition, many forms of biomass-to-energy conversions are CO_2 friendly, adding no net CO_2 to the atmosphere or at least no additional CO_2 other than would have naturally taken place. Probably the most exciting aspect of biomass fuels is that they are replaceable; there is no doomsday worry about using up all of Earthís resources. Indeed, some types of biomass are not only replaceable but also renewable; they are or can be created at the same rate that they are used.

*Author to whom all correspondence and reprint requests should be addressed.

For all of the advantages of biomass fuel sources, there are two distinct drawbacks. First, biofuels do not economically compete with conventional (oil, gas, coal) fuels. It costs more to generate electricity from biomass compared to coal, and it costs more to power automobiles using biomass fuels compared to gasoline. Second, and probably more important, the sources of biomass are quite diffuse and may not be available in sufficient quantities to make a national impact as an energy use. Biomass is defined as organic material from animals, such as manure, or plants such as trees, grasses, and agricultural crops. Common examples are sawdust as a byproduct of milling wood, rice husks as a byproduct of food production, and pallet and wood crate discards. Ohio claims to produce <1% of its electricity with biomass, and it does it with "forest wastes, such as tops and limbs, and wood wastes, such as sawdust, chips, barks, and edgings" *(1)*. Most of this electrical generation is done within the wood-manufacturing industry *(2)* and is primarily used internally by the company that generates it.

Plant biomass can also come from "energy crops." Energy crops are "crops developed and grown specifically for fuel. These crops are selected to be fast growing, drought and pest resistant and readily harvested to allow competitive prices when used as fuel" *(3)*. The prospect that farmers will use portions of their vast acreage to produce a material that can be used for fuel seems to have a ring of creditability to it. Whether the power industry can pay the farmers enough to turn their heads away from the familiar markets of soybean, wheat, and corn is another issue. Farmers can provide the *quantity* of material to make biofuel a significant factor in the energy source equation.

Energy crops, or biofuel feedstocks, "under development in the US include hybrid poplar, willow, switchgrass, and eucalyptus" *(3)*. Indeed, prospective energy crops appear to come from both ends of the spectrum of the plant kingdom—monocot herbaceous plants, on the one hand, to more sophisticated hardwood trees, on the other. Switchgrass is a prairie grass (monocot) that grows favorably in the plains states and southwestern states. It dries down to give a burnable product, and the crop has benefited from significant amounts of research performed in states such as Iowa *(4)*, Wisconsin, and Texas and from the Department of Energy through Oak Ridge National Laboratory. On the other hand, willow is a tree, a woody plant whose trunk has annular rings such that it adds woody matter annually to its stem. It appears to be the favored energy crop under investigation in East Coast states, particularly New York where coburning with coal has produced some electricity *(5)*. Both of these energy crops have their proponents, both have been the subject of a considerable amount of research and demonstration over the past 10–15 yr, and both are looking more and more promising.

The intent of this article is to introduce another type of plant into the energy crop mix. Of this new type, I suggest nine specific species. These species come from the center of the plant kingdom, *between* monocots

(grasses) and woody plants. All are herbaceous, either annual or perennial. The one common characteristic to all is that their stems die off annually and dry down to give a brittle stiff and relatively hard skeleton. These "remains" of the plant consist primarily of organic carbon-rich compounds and become a source of energy (fuel). Herein, they are referred to as stiff stalked plants (SSPs).

Before introducing and discussing these plants on an individual basis, and in order to understand the significance of the measurements made on and the comments made about each, some consideration should be given to plant botany as it relates to the characteristics of a good energy crop. Plant botany or physiology takes on a completely different thrust when viewed from the perspective of using the dead and dried stem for the ultimate purpose. A plant skeleton is really much different, and much simpler, than its living counterpart.

Plant Skeletal Physiology

The skeletal remains of a plant may look quite different than it did as a living entity. For trees, the skeletal remains look, for many years, almost exactly like the living plant. Truly the only telltale sign that the plant is dead is the lack of leaves. Conversely, the skeletal remains of a succulent herbaceous plant are almost nonexistent. It "melts away," leaving virtually no trace of its previous existence.

The difference between these two examples is the tissue construction of the living plant. Although there are a variety of tissue structures in each plant, the basic cells in succulents are thin walled and filled with a dilute solution of carbohydrates and other organic molecules. The cellulose present in the cell walls outside those cells is bathed in aqueous solution. At the first frost, the water freezes and enlarges the cell past its burst point, which then thaws to allow the water to drain out and leave no remaining structure. The plant "melts" to the ground and disappears rapidly.

The cells of woody plants have thick walls and encase a stronger, thicker solution of carbohydrate and cellulose. The freezing point of this solution is much lower than that of water, and if the cells do freeze, the cell walls are able to withstand the hydrostatic force, and therefore remain intact *(6)*.

To be more specific, the wall of a plant cell consists of three layers: primary wall, middle lamella, and secondary wall. The primary wall is thin and the middle lamella is more an adhesive gel than an actual structure. It is the secondary wall that is thick and gives the rigid structure to the cell. In a succulent, the secondary cell wall does not develop and the cell wall has little mass or strength. In cells of a woody plant, not only is the secondary wall thick but often it contains the organic compound lignin. Lignin is a material that is high in carbon, very hard, and very strong. Succulent plants contain virtually no lignin and therefore have a fragile structure and leave almost no skeletal remains. Nut shells are high in lignin and take on an almost rocklike hardness, and their skeletal remains look identical to those

of their live counterpart. Lignin is the second most abundant organic compound on earth, second only to cellulose. Woody plant species typically contain 15–25% lignin. Lignin has a higher carbon concentration than cellulose and therefore has a high heating value.

In herbaceous plants that have persistent lignified stalks ("sclerified stalks") (stems), the variety of tissues in the stem may have characteristics of succulents and some may have characteristics of wood. The result is that the skeletal remains may have some components that remain intact after death and others that essentially disappear.

To describe what the stem of a skeletal herbaceous stalked plant looks like, we begin with the stem parts of a living plant. The parts of a vascular plant stem, be it herbaceous or woody, are basically the same. The stem consists of epidermis (for outer protection), phloem (for transport of food to the plant), xylem (for transport of water to the upper reaches of the plant), and pith (a center core for the incubation of new cells). Of these four parts, the bulk of the mass of the stem cross section consists of xylem and pith. The pith is usually a very light, spongy, almost styrofoam-like material. In wood, pith is almost nonexistent except in new bud stems. In stalked herbaceous plants, the pith is a significant part of the stem.

It is in the xylem that the mass of the stem resides. Both in woods and in stalked herbaceous plants, the burnable portion of the stem is primarily xylem. If the overall purpose of an energy crop is to fix carbon from the CO_2 of the air into a solid form that can be burned for the release of heat, then an energy crop must be one that accomplishes this fixation the best. The fixing of carbon is done through the photosynthesis process while the storing of that carbon is accomplished by the creation of cells and cell walls, which comprise tissue. The photosynthesis process is powered by sunlight; therefore, biofuel energy sources are really one type of solar energy. A good energy crop must not just "fix" carbon but store it as burnable mass. Considering the other demands for the energy the plant may have, such as making leaves, and making fruit or seeds, an energy crop is a plant that efficiently makes harvestable biomass.

To best describe the ability of a plant to create xylem, there are some technical indicators that can be used. Figure 1 illustrates that an SSP skeletal stem is basically tubular. The "tube" itself is primarily xylem because the epidermal phloem and pith cell walls are usually very thin. For energy crops, it is best to have this tube as large and substantial as possible. In monocot plants and some dicots, the xylem and phloem are not created in tubes but are "bundled" together as highly efficient string elements that are located in the pith. There is not much mass to these bundles and, therefore, not much mass to their skeletal remains. SSPs typically are the dicots that do not form xylem bundles but, rather, xylem rings.

Critical parameters concerning the skeletal stem include the stem diameter (*D*); the ratio of the stem diameter to the pith core diameter (*D/P*); the xylem thickness/pith diameter ratio (*X/P*); and the xylem-to-pith ratio, defined as *XPR*. The reason for both *X/P* and *XPR* is that *X/P*

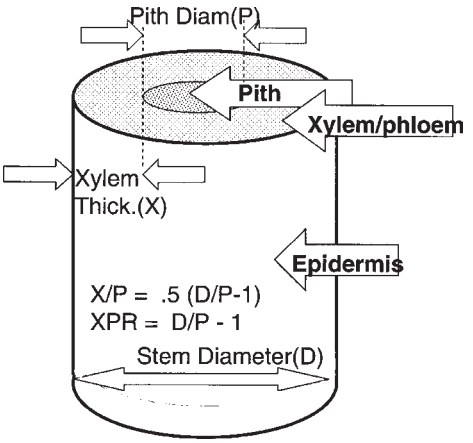

Fig. 1. Geometry of sclerified stalked plants.

ratios the single wall thickness against the total pith diameter, while *XPR* ratios twice the xylem wall thickness against the pith diameter (or the wall thickness against the pith radius). Another important physical property of the stem is the density of the dried xylem tissue (kg/m^3).

Description of Nine Candidate SSPs

The search for a crop that can be grown as an energy fuel begins by finding fast-growing plants that develop a significant xylem ring in their stem. Growth capacity can be estimated from several measurable factors. First is the size or weight of the individual dried-down stalk. Second is the field density at which it can be planted (stalks/ft^2. Third is the density of the material itself (kg/m^3). As each plant species is introduced in the following sections, the physical characteristics of the plant are given to make the growth capacity estimation.

Although one important criterion for an energy crop will be the bulk of burnable mass that can be harvested, per acre, there will be other factors as well. For instance, it may be important for a plant to "dry down" quickly, so it can be taken immediately from field to burner. It may be important that the burnable portion of the plant be easily cut and handled with conventional harvest equipment. It may be important that the plant cause no ill effects to the local population where it is grown and to the workers who harvest it. The type of seed and their dormancy period may be an important consideration. Does it keep for periods of time without rotting? There are some political implications for some of the candidate plants, for they may have been categorized as "invasive plants" or more seriously placed on a list of "noxious plants." Their introduction into certain geographic regions may be forbidden. Therefore as each plant species is introduced next, general information is provided that may be significant in evaluating its potential *(7)*.

Fig. 2. New England Aster blooms.

New England Aster (Asteraceae novae-angliae) *(Fig. 2)*

New England Aster is a wildflower that has such a beautiful and hardy purple-violet flower that it has been domesticated and offered to gardeners as an autumn flower. Although it is a perennial, a multitude of seeds are dried from the flower and scattered each year. The stem has extended branches primary at its top and grows to a height of 2 m. Mostly it grows in a single stalk, but certain types grow as bushes and others grow in several stalk clusters.

Seeds are available commercially and there is sufficient experience with the cultivation of New England Aster to suggest the best planting time, germination rate, and compatible herbicides. Suited for full sun to partial shade, it is a vigorous plant when grown in wet to mildly wet soil, either fertile clay or loam and preferably slightly acid. Flowers bloom from early September through early November. The stalk dies in the middle of October and is reasonably dried by the first of December.

Stem construction consists of a waxy epidermis with xylem cylinder and spongy pith with a "pinhole" tube at the center. The xylem/pith radius ratio (*XPR*) is about 0.46 and typical stem diameter is 0.95 cm. Typical stalk weight is 26 g, height is 130 cm, and cultivation density is 72/m^2. The density of the aster woody material (xylem) was determined to be 474 kg/m^3, which is similar to that of a light hardwood (lighter than pine).

New England Aster is probably the latest maturing of the SSPs. This could be an important factor in extending the harvest season.

Fig. 3. Kinghead Ambrosia growing within corn crop.

Kinghead Ambrosia (Asteracea Ambrosia trifida) *(Fig 3)*

Kinghead Ambrosia is a wildflower, but the flower color is green, and therefore it is not recognizable in the field as such. Definitely considered a "weed" by farmers and woodsmen alike, it lines ditch banks and invades cornfields with equal vigor. It is a floodplain species but does well also in moderately wet fields. The plant height is amazingly impressive, easily exceeding 3 m and sometimes reaching 5 m.

Kinghead Ambrosia is an annual but drops sufficient seed (up to 275/plant) to ensure its steady existence. Pollination occurs in mid-July. Pollen is very small and easily windborne, making it an allergen for humans, although not as serious as its related Common Ambrosia. Seeds are 0.3 to 0.5 mm long, with a woody hull bearing blunt ridges that end in several short, thick spines at the tip. They germinate after a cold, moist dormant period. The stem has extended branches primarily at its top and grows thick enough to make a canopy to maximize its absorption of solar radiation. The stalk dies in late September or early October and dries down quickly (typically 2 wk).

Stem construction consists of a porous epidermis (not waxy), which probably is the cause of its quick drydown. The xylem cylinder has an *XPR* of 0.23, and a typical stalk diameter of 1.6 cm. Xylem material has a density of about 240 kg/m^3, which makes it one of the lightest materials of all the SSPs introduced here. The pith is a solid spongy inner core that rots after about 2 mo of drydown.

Kinghead Ambrosia was suggested as an energy fuel more than 10 yr ago *(6)*. Yields on the order of 2.5 t/acre were quoted. In the analysis done here, I find this number a gross understatement and project yields of 13.4 t/acre without adaptation or modification of the plant as it currently exists.

Kinghead Ambrosia is the largest plant on the list of SSPs, in both height and stem diameter. Although this corresponds to a great bulk of material from this plant, it does not generate a tremendous weight because of its relatively low density. However, the pollen from this plant is very small and easily airborne, causing allergies in humans. Before this plant could be cultivated commercially, it probably would need some alteration.

Evening Primrose (Onagracea Oenothera)

Evening Primrose is a biannual wildflower named for its habit of opening yellow blossoms at dusk. The four-petaled flowers are strongly scented with a sweet perfume that attracts pollinating moths. Evening Primrose is easily cultivated; it prefers acid, neutral, or alkaline, well-drained soils and requires full sun. It does best when not having to compete for soil or space.

Because the Evening Primrose is a biannual, the stem shoots up only in the second year of growth. In the first year, a taproot is put down. In the second year a sprout shoots up. Producing a biomass material only every other year is a definite drawback to its use as a biofuel; however, the density of its xylem material is significantly greater than that of the other candidate plants, actually giving the evening primrose a competitive output.

Evening primrose is grown commercially for its seed oil (treats asthma, arthritis, headaches). Consequently, there is a great bed of knowledge concerning its seed production, cultivation, and even some insights into strategies for making it provide an annual shoot.

Stem construction consists of a thin, barklike epidermis. The xylem cylinder has an *XPR* of 1.3 and a typical stalk diameter of 1.5 cm. Xylem material has a density of about 536 kg/m^3, which makes it almost comparable to hardwood. The pith is a solid spongy inner core that rots after about 2 mo of drydown.

Evening primrose has a dense "stem," probably indicating a high percentage of lignin, and a correspondingly higher heating value than the other SSPs. Being a biannual is a mixed bag. The harvest is less frequent, which is an advantage, but the population density of harvestable plants is only half of what an annual or perennial would be.

Horseweed (Asteracea Conyza canaensis)

Horseweed is a native annual plant that can grow to a height of over 2 m. When mature, several flowering stems appear at the apex, which branch frequently and create a multitude of tiny composite flowers. In each flower, there are numerous yellow disk florets in the center, which are surrounded by tiny white ray florets. There is no noticeable floral scent. The blooming period can occur any time from midsummer to fall, lasting about 3 wk.

Table 1
Physical Properties of SSP

Plant	Stalk diameter (cm)	XPR	Average height (cm)	Material density (kg/m^3) [a]	Growth density ($stalks/m^2$)	Projected yield (mg/ha[$t/acre$]) [b]
New England Aster	0.85	0.46	127	593	55	19.9 (7.8)
Kinghead Ambrosia	1.25	0.23	180	394	46	29.8 (13.4)
Evening Primrose	1.27	1.31	175	748	28	17.1 (7.5)
Horseweed	0.9	0.92	160	675	55	30.4 (13.3)
Cockleburr	1.3	0.46	145	390	14	4.6 (2)
Field Thistle	2.0	0.76	190	425	11	7.3 (3.2)
Dames Rocket	1.1	0.22	110	345	26	2.7 (1.2)
Goldenrod	0.8	0.78	135	694	75	21.2 (9.3)
Annual Sunflower	1.1	0.46	170	784	40	19.5 (8.5)

[a] Measured by sampling of stalks, mass was measured by scale, and volume by stalk diameter, XPR, and length.

[b] Density × avg stalk height × cross section of xylem cylinder × growth density × hectare conversion factor.

The leaves alternate all around the stem (appearing almost whorled) and differ little in length, creating a columnar effect. The stout central stem is ridged and unbranched, except for the flower stems near the apex. Seeds are tiny and distribution is by wind. The preference of the plant is full sun, moist to dry conditions, and rich fertile soil. However, this plant flourishes in other kinds of soil, including those containing considerable amounts of gravel and clay. This weedy plant is easy to grow and sometimes forms large colonies in favorable disturbed sites. Drought resistance is very good. The plant dies in early September and drydown is rapid.

Stem construction consists of a moderately waxy epidermis. The xylem cylinder has a *XPR* of 0.92 and a typical stalk diameter of 0.9 cm. The xylem material has a density of almost 675 kg/m^3, which is a little light. The pith is a solid spongy inner core that appears to be resilient to rot for many months.

According to estimates, horseweed may have one of the highest yields of all the plants presented here (*see* Table 1). Projections indicate that 13.3 t/acre can be taken with current cultivation techniques and no engineering of the plant. Another benefit of horseweed is that it flourishes in dry conditions and in rough soil such as clay and gravel. It is also an early maturing plant and can be harvested as a fuel as early as September.

Cockleburr (Asteraceae Xanthium strumarium)

The cockleburr is a hitchhiker. The seed pod is a burr with hooked spines. It tangles the fur of animals unfortunate enough to brush against the dying plant.

Male flower heads occur at the ends of branches, and the female flower heads occur in the lower parts of these branches. The female heads develop into hard, woody, spiny burrs. These burrs are oval shaped, brown, 20–30 mm long, and covered in hooked spines.

Cockleburr is an annual species that generally germinates from late winter to late summer. Germination often occurs after rainfall and irrigation. The burrs contain two seeds, one larger than the other. The larger seed has limited dormancy and usually germinates in the season it is produced or the following season. The smaller seed has a longer period of dormancy. The plant grows in a wide range of soil types.

Stem construction consists of a moderately waxy, dark brownish-red epidermis. The xylem cylinder has an *XPR* of 0.46 and a typical stalk diameter of 1.75 cm. Xylem material has a density of almost 390 kg/m^3, which corresponds to a corkwood. The pith is a solid spongy inner core that appears to be resilient to rot for many months.

Although an SSP, cocklebur does not have good technical characteristics. In particular, the low *XPR* and density indicate that there is not much dry matter in this stalk. In addition, the burrs are a hazard, or at least an inconvenience, to the workers who must deal with this material. Surely the most serious disadvantage is that it is rated a Class C noxious weed, indicating that the introduction of burrs must be prevented.

Field thistle (Asteraceae Cirsium discolor)

Field thistle is a robust annual and member of the sunflower family. It grows to monster proportions (easily 2 m) with good soil and proper moisture. Flowering heads bear elongated, purple to lavender disk flowers that bloom in July and August. Leaves emerge individually along the entire stem. Leaf margins, the tips of leaf lobes, and parts of the stem all bear spines. The plant dies off in early September and dries down to low moisture content within four weeks.

One plant has the potential to produce up to 5200 seeds in a season, but the average seed production is about 1500 seeds per plant. Seeds are dispersed primarily by wind.

Thistle grows in a wide variety of soils, including sand dunes, but it is most abundant in clay soils. It can tolerate saline soils and wet or dry soils, but it grows best in dry soils. There are many other varieties, including Canadian and Bull.

In large thistle plants, the stem can be 3 cm in diameter. Although this stem size is admirable from the prospect of bulk, it may make cutting by conventional cutter-baler equipment difficult. The stalk consists of a large, spongy pith that does not rot or dry up for up to 1 yr. Although the stem diameter is impressive, the density of burnable mass is only moderate and the expected yield/acre is low.

Although thistle does thrive in sandy soil, most varieties of thistle are highly competitive and in some areas are classified as a noxious weed. It is also referred to as a "highly disruptive exotic plant."

Fig. 4. Field of mixed plants but mostly goldenrod and New England Aster.

Dames Rocket (Cruciferae Hesperis matronalis)

Dames Rocket is a showy, spring perennial wildflower with large, loose clusters of fragrant white, pink, or purple flowers that bloom in April and May on flowering stalks about 1 m high. This member of the mustard family has flowers with four petals. Many seeds are produced in long, narrow fruits. The leaves are oblong, sharply toothed, and alternately arranged. Leaves decrease in size as they ascend the stem.

This plant usually grows in moist soil and does best in sun conditions. The seed is commercially available since it is often planted ornamentally and included in many wildflower seed mixes.

Dames Rocket dies off and dries out by early August. It is one of the earliest of the sclerified stalked plants that is ready to harvest. The plant grows to over 1 m, and the stem diameter is about 1.1 cm. The *XPR* for this plant is a lowly 0.22, with a correspondingly low expected yield.

Goldenrod (Asteraceae Solidago) *(Fig. 4)*

Goldenrod is a perennial wildflower with a multitude of varieties. It is the state flower of Alabama, Nebraska, and Kentucky. Most species have feathery, rich sprays of florets atop sturdy stems. These small clusters of yellow flowers are prominent features of the landscape in September and October, and signal the end of summer. Goldenrod blooms late and dries down slowly, probably owing to the protective waxy epidermis of its stem.

Goldenrod is an erect perennial with simple, alternate, toothed or smooth-margined leaves. Its dried leaves have been used for a tealike beverage by the Indians.

There are many varieties, including early and Canadian. All enjoy full sun and a variety of soil conditions. In general, they present no difficulties in growing. The plant propagates itself by both a spreading root system and seed.

Fig. 5. Wild sunflower is much different from domestic sunflower.

It can grow to 2 m with a stalk that is about 0.8 cm in diameter. In the stem cylinder, the XPR is 0.78 and it has a density that rates well.

Some varieties of late goldenrod (Canadian) are late blooming and even later drying down, so they may not be ready for harvest until almost December. There is a misperception that goldenrod causes hay fever; it is actually the pollen of ragweed and grasses that causes this. Goldenrod's pollen grains are relatively large, heavier than air, and therefore are carried off by flies, bees, butterflies, even ants or birds, but not by the wind.

Annual Sunflower (Asteraceae Helianthus) *(Fig. 5)*

To most people, sunflower conjures an image of a domestic plant with a large stalk crowned by a single large flower. The wild sunflower, or annual sunflower, however, exhibits a branched growing form with numerous smaller flowers at each branch tip. The average diameter of wild sunflower is about 1 cm, unlike cultivated forms, which commonly reach 30 cm.

The stem is erect, columnar at the base and branched at the top. The leaves are alternate, simple, rough, hairy, and ovate or heart-shaped with toothed edges. The heads are showy, with yellow to orange-yellow ray flowers and brown or dark reddish-brown disk flowers. Sunflowers begin to grow in early June, flower in August and September, and mature seed and die in late September.

Wild sunflower, or common sunflower, is an annual, reproducing by seed. The seeds are shaped like the commercial sunflower seeds bought in stores, but much smaller and spread by the wind.

These plants can grow to 3 m with a stalk that is about 1.1 cm in diameter. Stem construction consists of a moderately waxy, dark red epidermis. The xylem cylinder has an XPR of 0.46. Xylem material has a density of 540 kg/m^3, which is about half that of pine wood. The pith is a solid spongy inner core that appears to be resilient to rot for many months.

Methods

Table 1 is important to the analysis of SSPs because it establishes a basis for future evaluation of the fuel source. Yet, much of the information is subject to growing conditions such as soil, water, and amount of competition with other plants. Because there are no cultivated acres of these plants, the projected yields listed in Table 1 are based on stalk weights, which were measured, and growth density (stalks/m^2), which were estimated. The estimations came from grid layouts made in productive parcels of wild-grown fields. They represent what I feel to be a conservative estimate of what densities can be achieved in cultivation.

The material density was determined from stalk weight and *XPR* based on the assumption that the stalk is a composite material of hard biomass and soft pith. The weight, but not the volume, of the pith was neglected:

$$\text{Density} = \text{Avg stalk weight} / (\text{avg stalk height} \times \text{cross-sectional area of stalk} - \text{cross-sectional area of pith})$$

Projected yield (PY) was determined using the following formula:

$$\text{PY} = (\text{density} \times \text{biomass stalk volume} \times \text{no. of stalks/acre})$$

$$\text{PY (t/acre)} = \text{Mat density} \times \text{Avg Stalk Height} \times \pi \times \text{diam}^2 (1 - 1/XPR^2)/4 \ /2.2/2000$$

Analysis

It is not the objective of this article to analyze the plants in the set of SSPs to determine which would be the most acceptable as an energy crop. One reason for this is that SSPs, as a fuel source, are a variety of plants rather than just one. As a variety, they have much more flexibility. It is expected that power plants fueled by SSPs will actually have farm contracts for several of the species within the set. Some species will be harvested and delivered early in the season and others late. This facilitates the storage of the fuel since the window of harvest can be up to 6 mo.

In addition, some SSPs dry down better than others. Having a variety of moisture conditions may be of benefit to the burner. Burning some green material with fully dried material is often the best solution for determining burner feed rates and utilizing the full combustion chamber.

Another reason for keeping all the varieties in the SSP set is that some grow better in certain soils and climates. This is not to say that the nine species identified here will all be viable energy crops, or that other species will not be added. For example, it is hard to imagine any farmer wanting to work with field thistle, no matter how much protective clothing the farmer has. Yet, thistle shows some signs of having the capability of delivering high yield, and, therefore, it should stay a member of the list awaiting further research.

Cocklebur may not be an acceptable member because it is a Class C noxious weed in many parts of the United States. Couple this with the fact that it does not have good physical characteristics for a biofuel and cockleburrís place on the SSP list is precarious.

Some may argue that Evening Primrose is not a true candidate owing to its biannual nature. However, its SSP harvestable material is the densest of all the members of the list, as if the additional year that it takes to mature may have been well spent. More research is needed to determine the density at which it can be planted, and what effect the first-yr plant will have in occupying space in the field.

A further argument for keeping active all members of the SSP list is that there is some interest in targeting acreage that is currently in government "set-aside" programs as sources of the biomass material. In this case, without preparation of the field, the herbaceous stalked material may simply grow wild on the acreage. If this is to be the case, it may not be possible to select the actual plants that will be harvested, and they may include all members of the list along with grasses and more.

It is also not the objective of this article to compare SSPs as a biofuel crop against other energy crops that are currently under research. The primary reason for this is that there is no competition among energy crops. If biofuel is to become significant in the mix of energy sources, all biofuels will need to be collected. In fact, it can be imagined that if a power plant is built to burn biofuels, it may well prefer a proper mix of woody and herbaceous materials along with quantities of animal waste.

However, to demonstrate that SSPs deserve their place in the mix of energy crops, one comparison with other biofuel crops should be made. Table 1 gives the physical characteristics of the nine plants in the SSP set. Of particular importance in Table 1 is the last column, which represents the projected yield of each (in t/acre).

With this caveat, Table 1 indicates that the highest yields are >10 dry t/acre. This compares to corn stover at 2.8 t/acre *(8)*, switchgrass at 2.5 t/acre *(9)*, and willow seedling at 6 t/acre/annum *(10)*. Figure 6 puts Table 1 to life, showing the cross sections of each of the SSPs discussed.

Conclusion

SSPs have been introduced as a group of herbaceous plants that should be given recognition as a biofuel feedstock. They should be given their

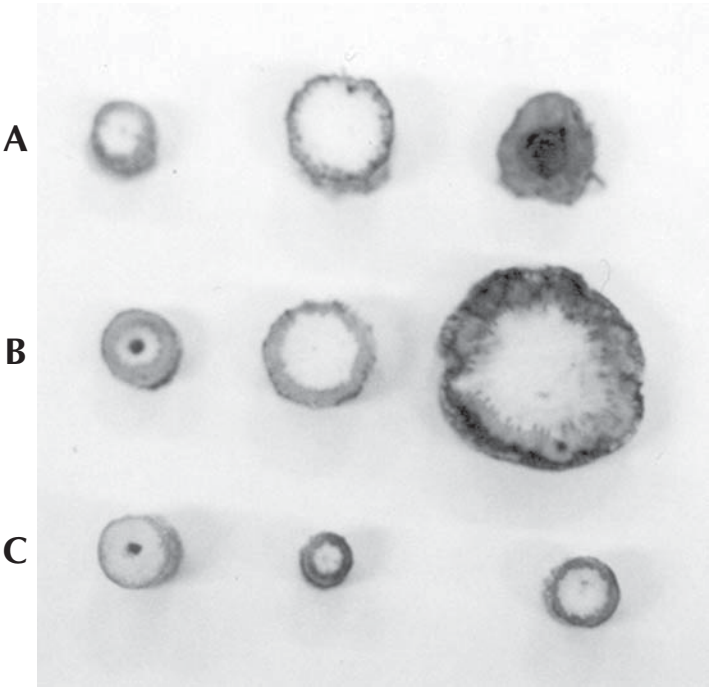

Fig. 6. Cross sections of SSPs, to scale (left to right): **(A)** New England Aster, Ambrosia Kinghead, evening primrose; **(B)** horseweed, cockleburr, thistle; **(C)** Dames Rocket, goldenrod, sunflower.

place in the development of renewable biomass material for direct energy conversion ("directly burnable crop" *[11]*).

In this article, this new energy crop has been introduced and its benefits extolled, in particular, the yield data of Table 1. However, the specifics were done within the economic and time constraints of the grant and are left open for more detailed scrutiny. In particular, the botany and plant physiology of the SSPs need clarification by experts, as do the physical characteristics of Table 1. Further studies are needed to establish heating values for the SSPs and to determine combustion characteristics. Knowledge of the cultivation and harvest of these plants must be expanded. The hope is, however, that the set of plants discussed here makes direct burnable biomass an economically feasible alternative on a broad scale.

Acknowledgments

I wish to thank Gary Haase of The Nature Conservancy at Kitty Todd Nature Preserve in the Oak Openings Region of Lucas Country, OH, for his great insight into the identification and management of the indigenous plants of northwest Ohio. This research was funded by the Ohio Biomass Energy Program.

References

1. OHIO Biobased Fuels, Power and Products Fact Sheet (2003), access to state facts sheet from Website: www.bioproducts-bioenergy.gov/default.asp.
2. Shakya, B. (2000), *Directory of Wood Manufacturing Industry of Ohio*, Ohio Biomass Energy Program, The Public Utilities Commission of Ohio, Cols, OH.
3. DOE. *Department of Energy, Biopower—Renewable Electricity from Plant Material*, Website: www.eren.doe.gov/biopower/feedstocks/fe_energy.htm.
4. Teel, A. (1998), Paper presented at *BioEnergy '98: Expanding Bioenergy Partnerships*, Madison, WI, October 4–8, 1998 (unpublished).
5. Neuhauser, A., White, R., and Peterson, B. (1996), Paper presented at the *1st Conference of the Short Rotation Woody Crops Operations Working Group*, Paducah, KY, September 23–25, 1996 (unpublished).
6. Salisbury, F. and Ross, C. (1992), *Plant Physiology*, Wadsworth Publishing, Beverly, MA.
7. Rickett, H. (1975), *Wildflowers of the United States*, McGraw-Hill, New York, NY.
8. Farm Progress Companies. *Farm Progress: What Are Corn Stalks Worth?*, Farm Progress Companies, Website: www.farmprogress.com/frmp/articleDetail/1,1494,11451+19,00.html.
9. Center for Integrated Agricultural Systems. *Switchgrass Production for Biomass, Research Brief #51*, Center for Integrated Agricultural Systems, University of Wisconsin-Madison, Website: www.wisc.edu/cias/pubs/briefs/051.html.
10. Tharakan, A., Isebrands, R. (1998), Paper presented at *BioEnergy '98: Expanding BioEnergy Partnerships*, Madison, WI (unpublished).
11. Kamm, J. (1993), *Small Farm Today* **10(3)**, 16,17.

0273-2289/04/113/0071–0093/$25.00

Fungal Upgrading of Wheat Straw for Straw-Thermoplastics Production

Tracy P. Houghton,[1] David N. Thompson,[*,1] J. Richard Hess,[1] Jeffrey A. Lacey,[1] Michael P. Wolcott,[2] Anke Schirp,[2] Karl Englund,[2] David Dostal,[2] and Frank Loge[2]

[1]*Idaho National Engineering and Environmental Laboratory, Idaho Falls, ID 83415-2203, E-mail: thomdn@inel.gov; and*
[2]*Washington State University, Pullman, WA 99164-1806*

Abstract

Combining biologic pretreatment with storage is an innovative approach for improving feedstock characteristics and cost, but the magnitude of responses of such systems to upsets is unknown. Unsterile wheat straw stems were upgraded for 12 wk with *Pleurotus ostreatus* at constant temperature to estimate the variation in final compositions with variations in initial moisture and inoculum. Degradation rates and conversions increased with both moisture and inoculum. A regression analysis indicated that system performance was quite stable with respect to inoculum and moisture content after 6 wk of treatment. Scale-up by 150× indicated that system stability and final straw composition are sensitive to inoculum source, history, and inoculation method. Comparative testing of straw-thermoplastic composites produced from upgraded stems is under way.

Index Entries: Fungal upgrading; engineered storage; biological preprocessing; *Pleurotus ostreatus*; straw composite.

Introduction

Agricultural crop residues are a valuable renewable biomass resource. In 1999, American farmers harvested 53,909,000 acres of wheat *(1)*. The straw from this acreage of wheat represents >50 million t annually. Currently, some of the straw is harvested (baled) for use as livestock bedding or low-grade animal feed. However, these low-value uses provide only a

*Author to whom all correspondence and reprint requests should be addressed.

minimal return. Nationally, only about 3.2% of the economic return on wheat is from straw *(1)*. Producers have long recognized the potential economic and environmental benefits of producing forage, bioenergy, and bioproducts from excess wheat straw residue. However, because of the low bulk density of straw and the loss of fermentable sugars to microbial activity during storage, there are harvest, transportation, storage, and preprocessing methods and logistics issues that must be worked out before the excess straw can be economically utilized on a national scale.

The U.S. Department of Energy and U.S. Department of Agriculture recently began a concentrated national effort under the Biomass Research and Development Act of 2000 to develop and demonstrate working biorefineries in the near term. The "vision" and "roadmap" documents for near-term utilization of agricultural residues to produce fuels, chemicals, and bioproducts have recently been completed and focus primarily on corn stover and cereal straws as the feedstocks *(2,3)*. Objectives and research pathways identified in the roadmap document for stover and straw preprocessing and storage issues include the following *(3)*:

1. Cost-Effective Pre-Delivery Treatment Processes—The development and testing of cost-effective pre-conversion treatment processes to increase energy- and chemical-density of raw materials at the point of harvest.
2. Best Practices for Harvesting and Storage—The biomass/agricultural communities must identify, develop, test, and implement best practices for cost-effective and environmentally sound pre-treatment, collection, storage, and transport of plant and animal residue-based feedstocks. This should lead to improved plant and animal residue recovery, more effective separation, improved handling and storage technologies/procedures, and reduced environmental impacts.

Thus, several issues related to preprocessing and storage have been identified as important research and development priorities for the near term. An innovative and potentially useful approach to addressing these issues would be to combine preprocessing and storage into a single system. In this way, energy use and infrastructure could be reduced by modifying the feedstock while it is waiting to be utilized. These modifications could be biological or chemical in nature. In the case of biological treatments, for such a system to be workable, it would be necessary for microbes carrying out the desired modifications to outcompete indigenous microorganisms vying for the same resources.

Straw utilization for composites is limited by poor resin and polymer penetration, and excessive resin consumption owing to the straw cuticle, fines, and the lignin-hemicellulose matrix *(4)*. Some white-rot fungi, including *Pleurotus ostreatus*, degrade the cuticle and selectively degrade lignin and hemicellulose, leaving behind relatively more cellulose *(4)*. Thus, treatments by these fungi could potentially be used to improve resin penetration and resin binding without the use of physical or chemical pretreat-

ments. Although long treatment times and large footprints limit the use of fungal treatments on a large scale, distributed fungal pretreatments could alleviate land requirements.

In a previous study *(4)*, we presented the results of a preliminary investigation to determine whether *P. ostreatus* could be competitive with indigenous organisms in unsterilized wheat straw stems. A detailed description of the potential benefits of preparing straw-thermoplastic composites from wheat straw stems upgraded by selective degradation by a white-rot fungus was provided in that study *(4)*. In general, the potential benefits focus primarily on the reduction of fines (reduced external surface area) via a selective harvest method *(5)*, and removal of amorphous matrix components by *P. ostreatus* to increase internal surface area and allow better penetration of composite formulation components into the lignocellulose matrix *(4)*. Our previous study was conducted with the aim of moving toward the development of a passive, potentially distributed fungal upgrading system to improve feedstock characteristics for production of straw-thermoplastic composites *(4)*. As envisioned, the system would be constructed and operated similarly to passive composting systems and could be operated for 12 wk or longer in a distributed or centralized manner, depending on land use requirements. Such a system fits within the frameworks of both engineered storage systems and pre-conversion processing.

In the preliminary study it was found that above about 11 mg of *P. ostreatus*/g of stems and 0.77 g of H_2O/g of stems, the inoculated *P. ostreatus* was generally competitive with indigenous microbes *(4)*, which is consistent with a previous report showing good competitiveness of *Pleurotus* sp. with soil microorganisms *(6)*. In the present article, we describe completed laboratory studies conducted at the Idaho National Engineering and Environmental Laboratory (INEEL) that were tasked with determining acceptable moisture and inoculum ranges for pilot-scale fungal upgrading tests. Inoculated *P. ostreatus* was found to more completely dominate degradation of the straw stems as inoculum size and moisture content increased, but to be less selective with respect to polysaccharide degradation. Inoculum and moisture levels of 40 mg of *P. ostreatus*/g of stems and 1.6 g of H_2O/g of stems, respectively, allowed successful competition of the inoculum with indigenous organisms and gave acceptable amounts of degradation of xylan and glucan (on a total degradation basis). Statistical analysis of the data was conducted to predict the variability of final compositions in response to ±30% variations in initial moisture and inoculum levels. Minimal variations in final composition would be desirable to ensure consistent product composition in outdoor systems having few environmental controls. In addition, we present the experimental design for the composite formulation/extrusion testing, as well as initial results from several extrusion tests conducted at the Wood Materials & Engineering Laboratory at Washington State University (WSU). In the near term, these data will be used to devise and test a pilot-scale fungal upgrading windrow system at WSU for demonstration of larger-scale operation and extrusion.

Table 1
Composition of Westbred 936 Straw Stem Fraction Used in Fungal Treatment Studies[a]

Component	Wt %[b]
Glucan	37.2 ± 0.8
Xylan	22.1 ± 0.5
Galactan	1.2 ± 0.8
Arabinan	3.0 ± 0.4
Mannan	1.6 ± 0.4
Lignin with extractives	18.9 ± 0.1
Ash	10.1 ± 0.0
Other [c]	5.8 ± 2.1
SUM	100.0 ± 0.2

[a] Uncertainties given are the SDs for four independent replicate measurements.
[b] Based on 100% dry wt of material.
[c] Remaining fraction attributed to unknown uronic acids, proteins, and so on, and to recovery errors in analysis techniques.

Materials and Methods

Wheat Straw

Westbred 936 wheat straw, a hard red spring variety, was obtained from Grant 4-D Farms (Rupert, ID). All the straw utilized was produced during the year 2000 cropping season and rebaled and stored as previously described *(4)*. Straw stems utilized for these tests were mechanically separated as previously described *(5)* during the fall of 2000 and were stored indoors at 21 ± 2°C and 13% moisture until used (all tests were begun by the fall of 2002). The composition of the untreated straw stem fraction, determined as described under Compositional Analyses, is shown in Table 1.

Cultures and Maintenance

P. ostreatus NRRL 2366 was chosen for use in the fungal degradation tests based on its ability to selectively degrade the noncellulose components of wheat straw *(7,8)*. It was obtained from the Northern Regional Research Laboratory (Peoria, IL). Stock cultures were maintained at Utah State University at room temperature on agar slants containing 20 g/L of YM agar (Difco, Detroit, MI) and the following trace minerals: 0.02 g/L of $FeSO_4 \cdot 7H_2O$, 0.004 g/L of $CuSO_4 \cdot 5H_2O$, 0.002 g/L of $ZnSO_4 \cdot 7H_2O$, 0.002 g/L of $MnSO_4 \cdot H_2O$, and 0.001 g/L of $(NH_4)_2MoO_4 \cdot 4H_2O$. Stock cultures were subcultured every 2 wk. Stock mycelial inocula were produced at Utah State University as follows: Fungal mycelia were transferred from the maintenance slants to 100 mL of 20 g/L YM broth (Difco) using a sterile loop and grown in agitated culture for 2 to 3 d at room temperature

and 180 rpm. This culture was transferred to a sterile Fernbach flask containing 1 L of 20 g/L YM broth with trace minerals as already described, and agitated for 4 d at room temperature and 180 rpm. The fungal pellets were harvested by light centrifugation (380*g*) in sterile centrifuge bottles, transferred to sterile bottles with sufficient spent medium to submerge the pellets, shipped under refrigeration to the INEEL, and stored at 4°C until use (typically 2 to 3 wk or less).

Small-Column Experiments

Unsterile straw stems were used in all experiments because sterilization of large quantities of straw for construction of large windrows would be uneconomical and impractical. For this strategy to be effective, it was necessary that the inoculated fungus be able to compete with the indigenous organisms in the straw. Since white-rot fungi dominate in nature under conditions of nitrogen deprivation *(9)*, experiments were previously performed *(4)* to determine inoculum production conditions necessary to limit nitrogen addition during inoculation of the straw with the fungus. C/N ratios in the media tested ranged from about 29 to 89 and were adjusted by adding yeast extract to 20 g/L glucose solutions. The nitrogen-limited medium finally utilized for straw stem inoculum production contained 3.0 g/L of yeast extract, for a C/N of 32.6. Mycelial inocula for inoculation of straw stems were produced in this nitrogen-limited medium, using as inoculum the fungal pellets produced at Utah State University in YM broth *(4)*.

Approximately 500 mL of wet fungal pellets of *P. ostreatus* grown at Utah State University in YM broth were transferred to a sterile blender and blended for 2 min, producing a slurry of finely chopped mycelial fragments. The optical density (OD) at 550 nm was determined for dilutions of this slurry using a standard UV/VIS spectrophotometer. The undiluted slurry was then inoculated to 1.0 OD into the fresh nitrogen-limited medium in sterile shake flasks and incubated for 5–7 d at 30°C, 135 rpm. The fungal pellets in the inoculum cultures were then transferred with the spent medium to a sterile blender and blended for 2 min. The OD at 550 nm was determined for dilutions of this slurry, and the concentration of biomass was estimated from a previously measured calibration. The undiluted slurry was transferred to a sterile hand-pump garden sprayer for addition to the straw stems. No extraordinary measures were taken beyond this point to maintain sterility, except the use of initially sterile equipment.

Air-dried straw stems (150 g dry wt at about 9–13 wt% moisture) were weighed onto a clean, dry, tared tray and spread in a thin (5-cm) layer. The homogenized mycelial inoculum slurry was then sprayed onto the stems, with frequent mixing of both the inoculum and the stems. Sufficient inoculum was added to reach the desired initial level of fungal inoculum in the stems. Periodically during addition of inoculum, a fan was used to blow nonsterile air across the tray of inoculated straw to evaporate excess water,

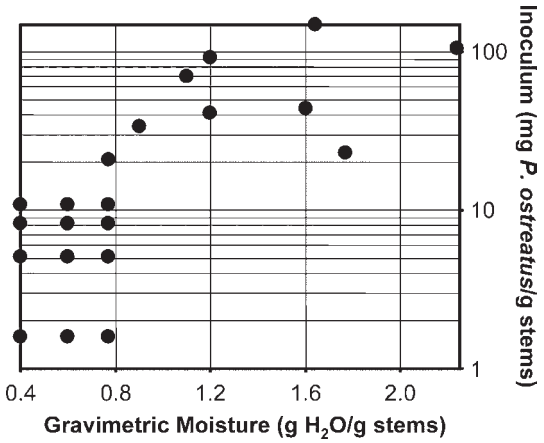

Fig. 1. Combinations of inoculum amount and moisture content tested.

with frequent mixing of the straw. After the desired amount of inoculum was added, additional sterile distilled water was sprayed onto the straw as needed to reach the desired initial moisture content for the particular experiment. A separate sample of the well-mixed inoculum slurry was then added to a tared bottle and dried to constant weight at 105°C to determine the actual biomass concentration of the slurry. In addition, several small samples of the inoculated stems were transferred to tared bottles and dried to constant weight at 105°C to determine the actual moisture content of the inoculated stems.

Combinations of inoculum amounts and moisture contents tested in this exploratory study are shown in Fig. 1; controls lacking inoculum were also conducted at 0.4–0.77 g of H_2O/g of stems and are not shown in Fig. 1. The first tests performed *(4)* are represented by the 12 points in the lower left-hand corner of Fig. 1. When these tests indicated that higher inoculum was needed for better selectivity and that higher moisture was needed for faster degradation *(4)*, parameter testing moved to the combinations plotted in the upper middle and right-hand corner of Fig. 1.

The inoculated straw was added to clean, initially sterile columns fabricated from glass process pipe as previously described *(4)*. The columns were prepared in triplicate with approx 50 g dry wt of inoculated stems in each column. The loaded columns were supplied with humidified oil-free instrument air at 193 kPa and a flow rate sufficient to turn over the air in the system once per day (about 10 mL/min). Approximately 2.5 g (dry wt) of straw was sampled from the top and bottom of each column initially and approx every 3 to 4 wk thereafter for 12 wk. The samples were combined, dried to constant weight overnight at 105°C, and ground to 60 mesh in a Wiley mill for compositional analyses.

Large-Scale Treatment in Drums

Straw stems were first treated for 6 wk in small columns with *P. ostreatus* at 40 mg of *P. ostreatus*/g of stems and 1.6 g of H_2O/g of dry stems, as described. These stems were then inoculated 1:10 into fresh stems, the moisture content was adjusted to 1.6 g of H_2O/g of dry stems, and the mixture was added to the drums for treatment. Because of the large amount of nitrogen-limited inoculum needed for the initial small-column step, the nitrogen-limited inoculum was produced in a slightly different manner than described above. This mycelial inoculum was produced at Utah State University as previously, but the mycelia from the maintenance slants were transferred directly into the nitrogen-limited medium without first being enriched in YM broth. Thus, both of the enrichment steps in the preparation of this mycelial inoculum were carried out in the nitrogen-limited medium. The fungal pellets produced in this manner were harvested as before, shipped under refrigeration to the INEEL, and stored at 4°C until use (up to 4 wk).

After 6 wk the treated stems were removed from the glass columns and mixed by hand at 1:10 (w/w) with fresh, air-dried, uninoculated straw stems. Random samples of the 6-wk-degraded stems were dried, ground to 60 mesh, and analyzed for composition as described under Compositional Analyses. While it was not known how much inoculum would be necessary for the altered inoculation method, a 10 wt% inoculation of wood chips containing an active culture of the desired white-rot fungus has been successful in soil bioremediation *(10)*. The moisture content was brought to 1.60 g of H_2O/g of stems by spraying distilled water with a pressurized garden sprayer onto the fresh stems as they were mixed with the treated straw from the glass columns. The inoculated stems were then packed into 208.5-L drums at about 7.5 kg dry wt of inoculated straw per drum. Before loading the drums, a 56-cm-diameter perforated steel disk was placed in the bottom of each drum and elevated to about 5.7 cm above the bottom of the drum using screws. Humidified oil-free instrument air at 127.6 kPa was supplied at 400–500 mL/min to the bottom of each drum beneath the perforated disk; the pressure drop over each drum was about 41.4 kPa. The air exited the system separately through the centers of the lids of each drum through in-line 16-cm^2 Whatman HEPA-Vent Filters with a porosity of 0.3 μm (Whatman, Newton, MA). After 6 or 12 wk of treatment, the drums were opened and several samples were removed from various locations within the straw beds. The samples were dried, ground to 60 mesh, and analyzed for composition as described under Compositional Analyses. The drums were then resealed and shipped to the Wood Materials and Engineering Laboratory at WSU for analyses of various composite formulations and extrusion testing. Untreated straw was also sent to WSU for these analyses. For the composite testing, the straw samples were referred to as Neat (untreated), Degrade1 (treated for 6 wk), and Degrade2 (treated for 12 wk).

Compositional Analyses

Ash content was determined as follows: At least 1 g of dry stems, ground to 60 mesh, was ashed in a muffle furnace at 650°C for 18–24 h. Ash content was calculated by weight difference. Carbohydrate and lignin compositions of untreated and treated straw samples were determined by quantitative saccharification using the method of Saeman et al. *(11)*. Two aliquots of each sample were analyzed by quantitative saccharification for each of the three replicate columns at each condition, for a total of 12 independent measurements of each composition. Carbohydrate analyses were done by high-performance liquid chromatography using a Bio-Rad HPX-87P carbohydrate column as previously described *(12)*. The acid-insoluble fraction from the quantitative saccharification was ashed at 650°C, and Klason lignin with extractives was calculated by weight difference. The amounts of glucan and xylan degraded per 100 g of initial weight were calculated by mass balance assuming that the sum of lignin, ash, and extractives remained constant. The percentage conversions of glucan and xylan (ΔG and ΔX, respectively) were then calculated by dividing by the initial basis weight of each and multiplying by 100.

Preliminary Extrusion Tests

To evaluate how the formulation components affect extrusion product performance, a fractional factorial design was created for statistical analysis. The fractional design is shown for the Neat and treated straw composite testing in Table 2. As already noted, Degrade1 and Degrade2 represent wheat straw that was inoculated with *P. ostreatus* and incubated for 6 and 12 wk, respectively. The values in Table 2 are percentages required to make a 2-kg batch for extrusion.

Composite formulations were prepared as follows: The straw samples as received from INEEL were ground to 0.69 mm in a hammer mill and oven dried to 1.1% moisture. The dried straw samples were then blended with various amounts of high-density polyethylene (HDPE), lubricants, and maleated polyethylene blends (MAPE) (*see* Table 2). The mixed formulations were then extruded with a 35-mm Cincinnati Milacron® Model CMT 35 counterrotating conical twin screw extruder (Cincinnati Milacron, Batavia, OH), which produced a 9.525×38.1 mm^2 solid cross-section. Flexural strength, density, and water sorption were measured for the extruded samples according to ASTM Standard Methods *(13,14)*.

Results and Discussion

The experimental data presented herein are the result of exploratory research aimed at bracketing the necessary moisture and inoculum loads for effective pilot-scale distributed upgrading of wheat straw stems for production of straw-thermoplastic composites *(4,15)*. An exploratory approach was chosen for these tests because full-scale outdoor systems having few environmental controls would be difficult if not impossible to closely control. Both temperature and moisture levels vary owing to variations in heat,

Table 2
Design of Experiment for Wheat Straw Extrusion[a]

Run no.	Straw stem treatment	Straw stems (wt%)	HDPE (wt%)	MAPE (wt %)	Lubricant (wt %)
3	Degrade1	60	36.25	3	0.75
5	Degrade1	55	42	0	3
8	Degrade1	75	22	0	3
9	Degrade1	70	26.75	1	2.25
10	Degrade1	55	42	0	3
14	Degrade1	60	38.25	1	0.75
24	Degrade1	55	41	4	0
25	Degrade1	55	38	4	3
26	Degrade1	75	18	4	3
27	Degrade1	60	36.25	3	0.75
29	Degrade1	55	45	0	0
30	Degrade1	60	38.25	1	0.75
32	Degrade1	75	18	4	3
33	Degrade1	75	21	4	0
1	Degrade2	55	38	4	3
4	Degrade2	75	21	4	0
6	Degrade2	65	35	0	0
7	Degrade2	55	42	0	3
11	Degrade2	55	41	4	0
13	Degrade2	75	22	0	3
15	Degrade2	55	45	0	0
16	Degrade2	65	35	0	0
20	Degrade2	55	38	4	3
31	Degrade2	75	18	4	3
2	Neat	75	18	4	3
12	Neat	55	38	4	3
17	Neat	55	41	4	0
18	Neat	55	45	0	0
19	Neat	65	32	0	3
21	Neat	55	42	0	3
22	Neat	65	31.5	2	1.5
23	Neat	65	31.5	2	1.5
28	Neat	75	25	0	0
34	Neat	65	31	4	0

[a]Five replicates were run for each formulation.

humidity, and wind. Precise real-time control of temperature and moisture in such a system would be very expensive, and thus counter to the goal of using distributed systems. We therefore decided to choose conditions of moisture and inoculum that provided average fungal degradation of the stems and rapid competitiveness of the inoculated fungus at a single temperature. We then conducted statistical analyses of the data in order to predict the expected variability of final composition in response to variations in initial moisture and inoculum.

Proxy Variable for Degradation Tests

Tests were designed to determine moisture levels and inoculum amounts that maximized hemicellulose degradation. In preliminary testing *(4)* it was shown that 10.9 mg of *P. ostreatus*/g of dry stems was sufficient to allow successful competition of the inoculated fungus with indigenous microbes. However, 10.9 mg of *P. ostreatus*/g of dry stems and a gravimetric moisture content of 0.77 g of H_2O/g of straw were too low to effect significant degradation of the straw in 12 wk *(15)*. In those tests a proxy variable, the ratio of cellulose and hemicellulose compositions (*C/H*), was used to indicate the relative change in composition occurring from indigenous microbes and by *P. ostreatus*. This ratio was used because *P. ostreatus* has been shown to be somewhat selective for hemicellulose and lignin degradation vs cellulose degradation *(7,8)*, while the indigenous microbes were shown in uninoculated controls to be nonselective for one polysaccharide or the other *(4)*.

Owing in part to the low and thus more uncertain measurements of the nonxylan carbohydrate components of hemicellulose (galactan, arabinan, and mannan), we decided to change the proxy variable to one exhibiting less variability as the result of measurement uncertainty. Two additional proxy ratios were assessed: the ratio of glucan and xylan compositions (*G/X*) and an estimate of the relative degradation of xylan vs glucan ($\Delta X/\Delta G$). This "degradation ratio" was calculated from the estimated conversions, which assumed little change in the sum of ash, lignin, and extractives. Implicit in this is an assumption of minimal mineralization of lignin to CO_2, and thus losses of lignin are assumed to be from depolymerization to extractives; extractives would increase, keeping the sum of lignin and extractives constant. This allowed a closed mass balance to be estimated and the amounts of xylan and glucan degraded to be calculated on an initial weight basis.

A comparison of these ratios for the preliminary testing at 0–10.9 mg of *P. ostreatus*/g of stems and 0.77 g of H_2O/g of stems is shown in Table 3. The majority of the glucan/xylan-based ratios had lower standard deviations than the corresponding cellulose/hemicellulose-based ratios, which was expected because xylan represents a greater fraction of the straw stems than galactan, arabinan, and mannan (Table 1). The relative changes in the three proxy variables were consistent among the data. For example, when *C/H* and *G/X* did not change significantly, indicating nonselective degradation of glucan and xylan, the estimated degradation ratio $\Delta X/\Delta G$ was about 1. Similarly, when *C/H* and *G/X* exhibited only a small increase, $\Delta X/\Delta G$ was only slightly larger than 1, while larger increases in *C/H* and *G/X* corresponded with large increases in $\Delta X/\Delta G$. This may provide some support for the assumption used to estimate $\Delta X/\Delta G$. The proxy ratio chosen for use was the degradation ratio $\Delta X/\Delta G$; with this change, the con-clusions of the preliminary study were unchanged, that is, *P. ostreatus* was shown to outcompete the indigenous organisms by 56 d. In addition, from 0 to 22 d the $\Delta X/\Delta G$ ratios did not change significantly from 1.0, suggesting that under

Table 3
Comparison of Cellulose/Hemicellulose, Glucan/Xylan, and Xylan Degradation/Glucan Degradation Ratios for Preliminary Tests *(4)* at 0.77 g of H_2O/g of Dry Stems [a]

	Amount of Inoculum (mg of *P. ostreatus*/g of dry stems)				
Day/ratio [b]	0	1.6	5.1	8.2	10.9
Day 0					
C/H	1.33 ± 0.08	1.33 ± 0.08	1.33 ± 0.08	1.33 ± 0.08	1.33 ± 0.08
G/X	1.69 ± 0.06	1.69 ± 0.06	1.69 ± 0.06	1.69 ± 0.06	1.69 ± 0.06
$\Delta X/\Delta G$	NA [c]	NA	NA	NA	NA
Day 22					
C/H	1.47 ± 0.04	1.45 ± 0.04	1.44 ± 0.05	1.37 ± 0.08	1.43 ± 0.05
G/X	1.71 ± 0.06	1.72 ± 0.06	1.69 ± 0.06	1.72 ± 0.06	1.68 ± 0.05
$\Delta X/\Delta G$	1.11 ± 0.14	1.11 ± 0.07	1.02 ± 0.06	1.14 ± 0.04	0.95 ± 0.08
Day 56					
C/H	1.36 ± 0.03	1.43 ± 0.06	1.52 ± 0.04	1.55 ± 0.06	1.50 ± 0.07
G/X	1.64 ± 0.03	1.73 ± 0.04	1.80 ± 0.12	1.84 ± 0.13	1.87 ± 0.07
$\Delta X/\Delta G$	0.85 ± 0.11	1.19 ± 0.04	1.26 ± 0.07	1.18 ± 0.08	1.78 ± 0.42
Day 84					
C/H	1.43 ± 0.05	1.49 ± 0.05	1.53 ± 0.09	1.46 ± 0.09	1.75 ± 0.11
G/X	1.70 ± 0.02	1.73 ± 0.01	1.77 ± 0.05	1.73 ± 0.03	1.82 ± 0.07
$\Delta X/\Delta G$	1.04 ± 0.02	1.15 ± 0.05	1.17 ± 0.13	1.12 ± 0.03	1.52 ± 0.10

[a] Uncertainties given are the SDs for 12 independent replicate measurements.
[b] *C/H*, cellulose/hemicellulose composition ratio; *G/X*, glucan/xylan composition ratio; $\Delta X/\Delta G$, xylan/glucan degradation ratio (this ratio was calculated assuming little change in the sum of ash, lignin, and extractives).
[c] NA, not applicable since on d 0 no degradation had occurred.

the conditions tested, in the initial 22 d of culture *P. ostreatus* did not dominate degradation of the stems.

Effect of Process Variables on Xylan and Glucan Removal and Selectivity

The time courses of the polysaccharide, lignin with extractives, and ash contents for experiments conducted at 44.0 mg of *P. ostreatus*/g of stems and 1.60 g of H_2O/g of stems are presented in Fig. 2. Time courses such as these were used to estimate xylan and glucan conversions for separate replicate samples, which were then averaged. The xylan and glucan conversions and $\Delta X/\Delta G$ ratios for 23.0–149 mg of *P. ostreatus*/g of stems and 1.10–2.24 g of H_2O/g of stems are presented in Table 4; refer to Fig. 1 for the complete set of inoculum and moisture combinations tested. Of the moisture and inoculum combinations shown in Fig. 1, the (moisture, inoculum) combinations (0.77, 21.0), (0.90, 34.0), and (1.20, 41.0) were performed early in the study and displayed visually uneven growth of

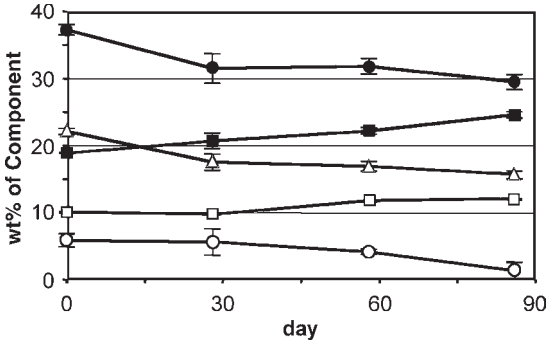

Fig. 2. Time courses of straw stem components for upgrading stems using 44 mg of *P. ostreatus*/g of stems at a moisture content of 1.6 g of H_2O/g of stems. (●) glucan; (△) xylan; (■) lignin with extractives; (□) ash; (○) sum of galactan, arabinan, and mannan.

Table 4
Xylan and Glucan Conversions for Upgrading of Wheat Straw Stems Using *P. ostreatus* at 23.0–149 mg/g of Stems and Moisture Contents of 1.10–2.24 g of H_2O/g of Stems[a]

Inoculum (mg *P. ostreatus*/g stems)	Moisture (g H_2O/g stems)	ΔX (%)	ΔG (%)	$\Delta X/\Delta G$
4 wk				
23.0	1.77	23.4 ± 3.0	16.4 ± 3.2	1.44 ± 0.09
44.0	1.60	24.3 ± 7.6	19.2 ± 8.4	1.31 ± 0.18
70.0	1.10	19.6 ± 1.8	15.3 ± 1.6	1.28 ± 0.01
92.0	1.20	25.2 ± 4.0	18.2 ± 4.2	1.40 ± 0.12
105	2.24	26.4 ± 1.0	19.0 ± 0.6	1.39 ± 0.01
149	1.64	22.9 ± 0.2	17.9 ± 1.0	1.28 ± 0.06
8 weeks				
23.0	1.77	29.7 ± 0.9	21.8 ± 3.1	1.38 ± 0.15
44.0	1.60	34.5 ± 3.5	27.1 ± 3.7	1.28 ± 0.05
70.0	1.10	35.4 ± 0.9	26.6 ± 1.3	1.33 ± 0.05
92.0	1.20	32.3 ± 3.2	25.8 ± 3.1	1.25 ± 0.03
105	2.24	38.8 ± 0.5	32.2 ± 0.5	1.21 ± 0.01
149	1.64	39.7 ± 0.5	33.6 ± 3.0	1.19 ± 0.09
12 weeks				
23.0	1.77	36.3 ± 1.7	29.3 ± 2.7	1.25 ± 0.06
44.0	1.60	43.8 ± 2.6	37.3 ± 3.1	1.18 ± 0.03
70.0	1.10	37.0 ± 2.7	32.5 ± 3.6	1.14 ± 0.04
92.0	1.20	46.7 ± 3.1	38.3 ± 3.0	1.22 ± 0.04
105	2.24	48.3 ± 4.3	41.2 ± 5.4	1.18 ± 0.05
149	1.64	42.9 ± 2.6	37.9 ± 2.2	1.13 ± 0.05

[a] Uncertainties given are the SDs for 12 independent replicate measurements.

fungus in the stems, indicating inhomogeneous distribution of the mycelia over the straw stem surface. Samples taken from the tops and bottoms of these columns also displayed widely variable degradation results, indicating poor distribution of the inoculum. The methods were modified, and the uneven distribution of fungal mycelia on the straw was minimized in future experiments. These three data sets were thus not considered further in analyses of the data. The $\Delta X/\Delta G$ ratios for the preliminary tests conducted at 0.0–10.9 mg of *P. ostreatus*/g of stems and 0.40–0.77 g of H_2O/g of stems are given in Table 3, while the xylan and glucan conversions for those preliminary experiments are available elsewhere *(15)*.

Effect of Treatment Time

Treatment time is an important process variable because large process footprints such as those required for this type of treatment require large amounts of land, and thus long treatment times can have a negative influence of the economics of the process, depending on land use requirements *(16)*. In addition, depending on the sensitivity of the treatment process to initial and transient conditions, widely variable product compositions produced in time-sensitive degradation processes could have a large effect on the next step of the manufacturing process. Longer treatments gave progressively smaller gains in xylan removal and larger gains in glucan removal (Table 4). This observation is consistent with the fungus first utilizing the easily degraded hemicellulose and amorphous cellulose fractions, beginning with the hemicellulose.

In 4 wk, the maximum conversions observed were about 27% xylan and 19% glucan. At 8 wk, the maximum conversions observed were about 40% xylan and 34% glucan, while at 12 wk they were about 48% xylan and 41% glucan. At very low inoculum levels, the initial degradation (at 4 wk) was generally nonselective and thus primarily owing to indigenous organisms (Table 3). Above 10.9 mg of *P. ostreatus*/g of stems, the early degradation was much more selective for xylan vs glucan, indicating significant activity of the inoculated fungus. Maximum selectivities for xylan removal ($\Delta X/\Delta G$) for inoculum levels exceeding 10.9 mg of *P. ostreatus*/g of stems were observed earlier in the treatments, with all moisture and inoculum combinations showing similar selectivities after 12 wk of treatment.

Effect of Moisture and Inoculum

Higher conversions of xylan and glucan were seen with increases in both moisture content and inoculum size (Table 4), but no correlation was observed between the conversions and the relative amounts of inoculum and moisture (ratio of inoculum to moisture content; not shown). Thus, it is unlikely that these two parameters comprise an interaction effect that is important to the operation of the system. Lower moisture contents gave lower overall amounts of degradation, but seemingly better selectivities for xylan degradation although coefficients of variation for conversions were

higher at low moisture contents owing to the smaller changes in overall composition. Higher moisture gave better overall degradation but poorer selectivity for xylan degradation. Selective xylan degradation may not have as great an effect on the properties of straw-thermoplastic composites as may overall degradation. In the present study, selectivity for xylan removal was a convenient proxy measure of relative activity of the inoculated fungus to indigenous microbes. However, there are other uses for treated straw feedstock, such as for production of fermentable sugars for fuels and chemicals, in which selective xylan removal would be useful. If achieving high selectivity for xylan degradation is important to the final use of the feedstock, lower moisture levels would be preferred. Finally, higher inoculum was found to give faster overall degradation, which was expected.

Regression and Sensitivity Analyses of Degradation Data

Although the tests were performed in an exploratory manner and thus neither a complete factorial design nor a complete fraction of a factorial design was completed, a significant amount of revealing information was collected in the tests. Since the goal was to bracket allowable moisture and inoculum ranges, statistical analyses of the xylan and glucan degradation data were conducted by regression analysis and used to explore system sensitivity to initial moisture and inoculum contents.

Regression Analyses

The conversion data for all tests were combined into a single data set represented by 234 data points varying in inoculum amount (I, mg of *P. ostreatus*/g of stems), gravimetric moisture content (M, g of H_2O/g of stems), and treatment time (t, d). A power series expansion of the three variables through the second-order terms was fitted using linear regression; the expansion included the terms I, M, t, IM, It, Mt, I^2, M^2, and t^2, with an intercept of zero. Note that this equation has no basis in theory and was chosen simply because its shape was appropriate. The primary goal of the regression analyses was to obtain statistically valid equations for both ΔX and ΔG, and to use these relationships to estimate the sensitivity of the system to inoculum, moisture, and treatment time.

The xylan conversion (ΔX) and glucan conversion (ΔG) data were fitted separately to the power series expansion, resulting in r^2 values of 0.925 and 0.910, respectively. However, an analysis of variance indicated that the terms M, IM, M^2 in both analyses were statistically insignificant and thus unnecessary to fit the data. The data were refitted after dropping those terms, resulting in statistically valid fits with r^2 values of 0.924 and 0.909. The results of the regression analyses are presented for both fits in Table 5, and comparisons of the measured and predicted values of ΔX and ΔG are shown in Figs. 3 and 4, respectively. Relatively good fits to the data were obtained, indicating that the data were internally consistent and that the system behaved in a predictable manner. The fits were more accurate at higher values of inoculum and moisture, caused by the higher

Table 5
Regression Models for Xylan and Glucan Conversions

	Regression Results[a]	
	$\Delta X = \alpha_x I + \beta_x t + \gamma_x It + \delta_x Mt + \varepsilon_x I^2 + \phi_x t^2$	$\Delta G = \alpha_g I + \beta_g t + \gamma_g It + \delta_g Mt + \varepsilon_g I^2 + \phi_g t^2$
DOF[b]	233	233
r^2	0.924	0.909
α_i	0.106	0.0551
β_i	0.514	0.408
γ_i	1.68×10^{-3}	1.43×10^{-3}
δ_i	0.106	0.0770
ε_i	-8.19×10^{-4}	-4.45×10^{-4}
ϕ_i	-4.11×10^{-3}	-2.89×10^{-3}

[a] Variable definitions: ΔX (xylan conversion, %); ΔG (glucan conversion, %); I (inoculum amount, mg of *P. ostreatus*/g of stems); M (moisture content, g of H_2O/g of stems); t (time, d).
[b] DOF, degrees of freedom for the regression analysis.

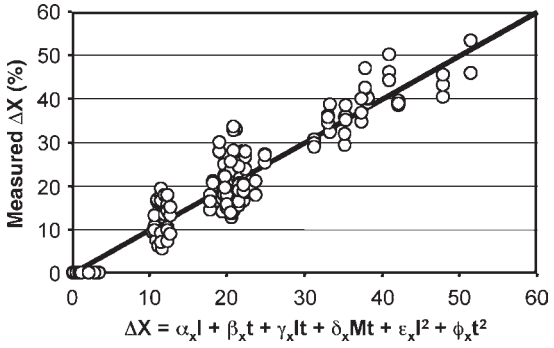

Fig. 3. Comparison of predicted and measured xylan conversions for fungal upgrading tests. The line shown has a slope of 1.0 and represents a perfect fit to the data.

amount of variability in degradation data at lower inoculum levels and moisture contents. The predicted conversions of xylan (ΔX), glucan (ΔG), and the ratio $\Delta X/\Delta G$ with time are shown for the ultimately selected treatment conditions (40 mg of *P. ostreatus*/g of stems, 1.60 g of H_2O/g of stems) in Fig. 5. The percentages of degradation for the nearest experimentally observed combination (44.0 mg of *P. ostreatus*/g of stems, 1.60 g of H_2O/g of stems) were under-predicted by 5–10% at later treatment times (not shown). It is clear from Fig. 5 that the time-rate of degradation had decreased substantially by 12 wk and thus harvesting at 10 or 14 wk would make little difference in the final composition. In addition, the selectivity for xylan degradation over glucan degradation is predicted to be initially about 2.0 and then to decrease with time to about 1.2. This suggests that shorter treatment times would be preferred with this organism if a more selective degradation is desired, although the initially high rate of decline of $\Delta X/\Delta G$ is most likely an artifact of higher measurement uncertainties in the data at lower moisture and inoculum.

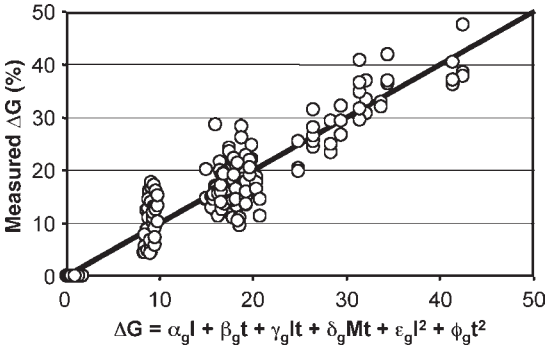

Fig. 4. Comparison of predicted and measured glucan conversions for fungal upgrading tests. The line shown has a slope of 1.0 and represents a perfect fit to the data.

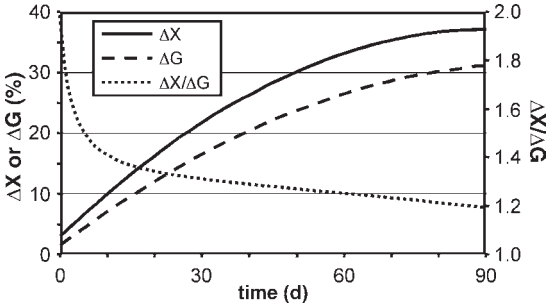

Fig. 5. Predicted time courses of xylan conversion (Δ*X*, %), glucan conversion (Δ*G*, %), and the degradation ratio (Δ*X*/Δ*G*) for 40 mg of *P. ostreatus*/g of stems and 1.60 g of H_2O/g of stems.

Sensitivity Analyses and System Stability

Sensitivity analyses were conducted using the regression models to test the sensitivity of the treatment method at 21 ± 2°C. First, the inoculum was varied ±30% in the regression model (28.0–52.0 mg of *P. ostreatus*/g of stems) at constant moisture. Second, the moisture was separately varied ±30% (1.12–2.08 g of H_2O/g of stems) at constant inoculum. The upper and lower bounds chosen represent very large variations in both inoculum and moisture. The predictions are plotted vs time in Fig. 6 for xylan degradation. The xylan degradation ranges at 12 wk for varied inoculum and moisture were 34.7–39.3 and 32.5–41.6% degraded, respectively. Similarly, the glucan degradation ranges at 12 wk for varied inoculum and moisture were 29.2–32.8 and 27.7–34.4% degraded, respectively (not shown). When varying only one parameter, the final compositions are predicted to be relatively insensitive to inoculum size, with the largest deviation of at most ±5% degradation at 12 wk. For moisture the system was predicted to be more sensitive, but it was less sensitive at shorter degradation times.

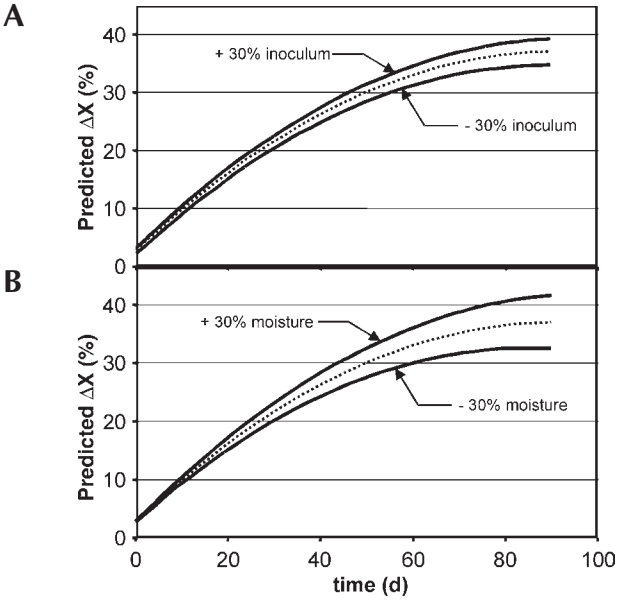

Fig. 6. Inoculum and moisture sensitivity analyses for fungal treatment of straw stems at 21 ± 2°C. **(A)** ±30% variation in inoculum at 1.6 g of H_2O/g of stems. The dotted line is the prediction for the midpoint of 40 mg of *P. ostreatus*/g of stems. **(B)** ±30% variation in gravimetric moisture content at 40 mg of *P. ostreatus*/g of stems. The dotted line is the prediction for the midpoint of 1.6 g of H_2O/g of stems.

This indicates that initial moisture is the more critical parameter to control, and also that the system is less sensitive to initial moisture at shorter treatment times. Shorter treatment times could be used without compromising final compositions by increasing initial inoculum size, depending on final costs.

Additional sensitivity analyses were conducted by simultaneously varying both inoculum amount and moisture content (±30% for each). This analysis predicted maximum ranges at 6 and 12 wk of 24.5–31.9 and 30.1–43.8% xylan degraded, and 19.4–24.7 and 25.9–36.1% glucan degraded, respectively. This corresponds to $\Delta X/\Delta G$ ranges of 1.27–1.29 and 1.16–1.21 at 6 and 12 wk, respectively, and indicates that the expected $\Delta X/\Delta G$ does not vary as widely as would be suggested by combining the individual sensitivity analyses. In addition, shorter treatment times were again favored for minimum variation in the treated straw stem compositions.

In terms of selectivity and reduced sensitivity to initial moisture and inoculum, the results indicate that shorter treatment times are preferred, especially if moisture is either not controlled or poorly controlled. The regression models were next used to generate topographic plots of ΔX, ΔG, and $\Delta X/\Delta G$ at the various combinations of inoculum and moisture.

The results are plotted in Figs. 7–9 for the regression model predictions after 6 wk of treatment. For locations of the parameter combinations used in this study on these plots, refer to Fig. 1 (which uses the same axes). Note that the parameter combinations (21.0, 0.77), (34.0, 0.90), and (41.0, 1.20) were not included in the statistical analyses because of poor distribution of the fungal inoculum onto the straw stems. The topographic plot of percentage xylan degraded after 6 wk of treatment is shown in Fig. 7. The diamond represents the conditions chosen for preparation of treated stems for the extrusion testing. The region of only 15–20% xylan degradation roughly corresponds to the region in which the inoculated *P. ostreatus* was observed to be unable to outcompete the indigenous microbes, since about 15% xylan degradation was observed to occur without inoculum. Increased xylan removal is predicted as both moisture and inoculum increase. There are, however, wide ranges of parameter combinations that will give the same amount of xylan degradation, indicating a fairly insensitive system in terms of overall xylan degradation after 6 wk of treatment. The curvature of the dividing curve between 25–30 and 30–35% xylan degradation, and above 100 mg of *P. ostreatus*/g of stems, seems odd in that it curves back toward the inoculum axis. However, this was experimentally observed by comparing the results of the (149, 1.67) and (105, 2.24) parameter combinations (*see* Fig. 1). Since these experiments were independently replicated, the behavior appears to be real.

The topographic plot of percentage glucan degraded after 6 wk of treatment is shown in Fig. 8. Again, the diamond represents the conditions chosen for preparation of treated stems for the extrusion testing. The region of only 10–15% glucan degradation closely corresponds to the experimentally observed region in which the inoculated *P. ostreatus* was unable to outcompete the indigenous microbes. Increased glucan removal is predicted as both moisture and inoculum increase. As shown for xylan, there are again wide ranges of parameter combinations that give the same amount of glucan degradation, indicating that the system is also fairly insensitive in terms of overall glucan degradation after 6 wk of treatment.

Finally, the topographic plot of $\Delta X/\Delta G$ after 6 wk of treatment is shown in Fig. 9. The diamond again represents the conditions chosen for preparation of treated stems for the extrusion testing. The region of $\Delta X/\Delta G$ of 1.20–1.25 encompasses the region in which it was experimentally observed that $\Delta X/\Delta G$ was about 1.0. A ratio of $\Delta X/\Delta G$ of 1.0 indicates nonselective polysaccharide degradation and was taken as an indication of poor competition of the inoculated fungus with the indigenous microbes. This reinforces the observations that at low moisture and inoculum, the regression model predictions are less accurate. Figure 9 also shows that $\Delta X/\Delta G$ of 1.25–1.30 is predicted after 6 wk of treatment over a very large percentage of the possible moisture and inoculum combinations. Thus, the system is very stable with respect to selectivity of polysaccharide degradation within the parameter ranges tested.

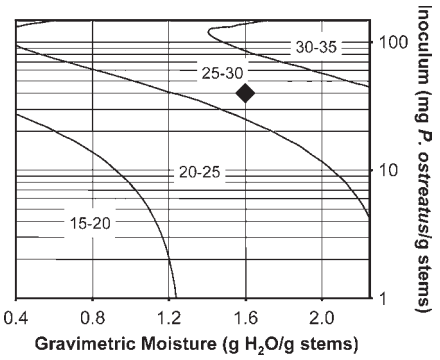

Fig. 7. Predicted topographic plot of xylan conversion (ΔX, %) with inoculum amount and moisture content. The ranges presented on the plot are ranges of xylan conversion predicted in each region. The diamond marks the conditions chosen for preparation of treated stems for the extrusion tests.

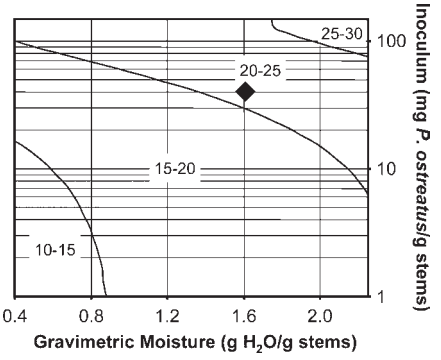

Fig. 8. Predicted topographic plot of glucan conversion (ΔG, %) with inoculum amount and moisture content. The ranges presented on the plot are ranges of glucan conversion predicted in each region. The diamond marks the conditions chosen for preparation of treated stems for the extrusion tests.

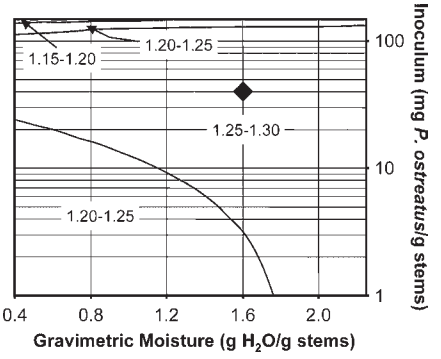

Fig. 9. Predicted topographic plot of degradation ratio ($\Delta X/\Delta G$) with inoculum amount and moisture content. The ranges presented on the plot are ranges of $\Delta X/\Delta G$ predicted in each region. The diamond marks the conditions chosen for preparation of treated stems for the extrusion tests.

Table 6
Xylan and Glucan Conversions and Degradation Ratios Estimated for Upgrading of Wheat Straw Stems Using *P. ostreatus* at 40.0 mg/g of Stems and a Moisture Content of 1.60 g of H_2O/g of Stems in Scaled-Up Columns [a]

	Percentage degraded			
	Degrade1		Degrade2	
Component degraded	Small Columns [b]	55-gal Drums	Small Columns [b]	55-gal Drums
ΔX (%)	29.8 ± 1.0	11.9 ± 0.9	28.1 ± 1.0	24.2 ± 4.9
ΔG (%)	18.3 ± 1.4	13.4 ± 1.5	18.5 ± 1.2	26.8 ± 3.4
$\Delta X/\Delta G$ [b]	1.64 ± 0.09	0.89 ± 0.03	1.52 ± 0.05	0.90 ± 0.08

[a] Uncertainties given are the SDs for eight independent replicate measurements.
[b] Columns were inoculated at the indicated concentrations of *P. ostreatus* and moisture concentration and grown for 6 wk, and the degraded stems were used to inoculate drums at a 1:10 weight ratio.

Scaled-Up Preparation of Stems for Extrusion Tests

The larger-scale columns, while necessary to produce treated straw stems for use in the preparation of composite formulations for extrusion testing, were also a good test of the sensitivity of the system to scale up to larger columns and to changes in inoculum source and inoculation method. After 6 wk of treatment in the small columns used to inoculate the drums, 28–30% xylan was degraded while about 18.5% of glucan was degraded (Table 6). This gave $\Delta X/\Delta G$ ratios of 1.52–1.64. For comparison, at 40.0 mg of *P. ostreatus*/g of stems and 1.60 g of H_2O/g of stems, the regression models predict 27.2% xylan degradation and 21.1% glucan degradation at 6 wk, for a $\Delta X/\Delta G$ of 1.29. Clearly, *P. ostreatus* was dominant in the small columns used to prepare enrichment inoculum for the barrels. However, the $\Delta X/\Delta G$ values were well outside the range predicted by the regression models. Apparently, the nitrogen-limited inoculum produced by Utah State University and shipped to INEEL for these columns was either more active or better acclimated to the nitrogen-limited conditions in the straw stems. This effect was repeatable, indicating that the history of the inoculum used may have a significant effect on $\Delta X/\Delta G$, although the actual glucan and xylan conversions were not far from the predicted values. The inoculum produced for the small columns used to inoculate the drums was produced differently than the inoculum used to inoculate the small columns in the moisture and inoculum tests—it was better acclimated to nitrogen-limited conditions. This is because the mycelia were transferred directly into the nitrogen-limited medium (C/N of 32.6) without first being grown in the carbon-limited YM broth (C/N of 7.7). Since both enrichment steps in the production of the mycelial inoculum were carried out in the nitrogen-limited medium, this likely resulted in a mycelial inoculum that was better acclimated to low-nitrogen conditions when

it was added to the straw stems, which have a C/N of about 80 *(17)*. Thus, system performance is sensitive to inoculum source and history.

The altered inoculation method also resulted in a different degradation pattern than that observed in the small-column tests. After 6 and 12 wk of treatment in the drums, only 11.9 and 24.2% of the xylan was degraded, respectively (Table 6). Glucan degradation was similarly reduced, with only 13.4 and 26.8% of the glucan degraded at 6 and 12 wk, respectively. This equates to $\Delta X/\Delta G$ values of 0.89 and 0.90 at 6 and 12 wk, respectively. Thus, selective degradation did not occur in the larger-scale columns, which indicates that *P. ostreatus* was not dominant. In fact, less degradation occurred in the barrels after 6 wk of degradation than was either observed or predicted in the small columns. It is likely that the low levels of degradation observed in the drums were owing to slower colonization of the fresh stems by the *P. ostreatus* growing in the solid enrichment inoculum. In the small-column tests, the indigenous microbes were shown to degrade about 15–20% of the polysaccharides in 12 wk in the absence of *P. ostreatus (4,15)*, which likely represents the most easily accessible glucan and xylan fractions. If *P. ostreatus* were to colonize the straw more slowly from the solid enrichment inoculum, the primary effect on the degradation system would be to extend the treatment time necessary to reach the desired levels of xylan and/or glucan degradation in the final product. Thus, inoculating the fresh stems with partially degraded stems before introduction to the drums was an ineffective inoculation method when compared with inoculating by spraying homogenized mycelia onto the stem surfaces. The nonselective degradation pattern in the drums may or may not be a detriment to the physical properties of straw-thermoplastic composites produced from Degrade1 and Degrade2 straw stems, since selectively degraded stems have not yet been compared with nonselectively degraded stems.

Preliminary Extrusion Tests

The Neat-, Degrade1-, and Degrade2-treated straw stems were run on the extruder. Measurement of several properties of the extruded composite formulations is under way (*see* Table 2). An example of the preliminary data, the data for runs 2, 31, and 32, is presented in Table 7. In these runs, composite formulations were prepared by mixing Neat, Degrade1, or Degrade2 stems at 75 wt% with 18 wt% HDPE, 4 wt% MAPE, and 3 wt% lubricant. Few statistical differences were seen in the measured values of density, modulus of elasticity (MOE), and modulus of rupture (MOR) in Table 7. This indicates that at this combination of formulation components, fungal treatment of the stems in the drums (which resulted only in nonselective degradation) may not have improved the stems for composite production. However, little can be learned by comparing only three treatments taken from such a large fractional factorial design. Thus, the data will not be compared further here but will be compared with respect to density, MOE, and MOR in the context of the complete factorial design in a future article.

Table 7
Preliminary Measurements of Density, MOE, and MOR for Neat, Degrade1, and Degrade2 Straw Stems Extruded at 75 wt% Straw Stems, 18 wt% HDPE, 4 wt% MAPE, and 3 wt% Lubricant[a]

	Straw stem source		
Property	Neat	Degrade1	Degrade2
Density (kg/m^3)	1190 ± 6	1200 ± 7	1230 ± 25
MOE (MPa)	3400 ± 35	3210 ± 24	3070 ± 19
MOR (MPa)	19.9 ± 1.7	18.0 ± 1.5	18.2 ± 2.0

[a] Uncertainties given are the SDs for five independent replicate measurements of each property.

Conclusions

Initial rates of xylan and glucan removal from wheat straw stems by *P. ostreatus* were in general higher than later in the tests. In tests in which *P. ostreatus* was inoculated to levels high enough to allow successful competition with indigenous microbes, early degradation of the xylan and glucan was nonselective, suggesting that there is a lag time before *P. ostreatus* can overtake the culture. Higher inoculum levels resulted in faster overall degradation of the stems but decreased the selectivity for xylan degradation. Increasing the moisture content also resulted in higher degradation rates of both glucan and xylan but also decreased the selectivity for xylan degradation. The regression analysis indicated that the data were internally consistent and predictable. Predictions were in general more accurate at higher values of inoculum and moisture and indicated that at 12 wk the system is insensitive to inoculum size and somewhat more sensitive to moisture content. The system is predicted to be less sensitive to moisture at 6 wk than at 12 wk. This together with decreasing selectivity of polysaccharide degradation with treatment time indicates that the system is less sensitive to initial conditions at shorter treatment times. Scale-up from the laboratory columns to drums indicated that the system is sensitive to both inoculum source/history and inoculation method. Comparative testing of straw-thermoplastic composites produced from the untreated and nonselectively degraded stems is under way.

Acknowledgments

This project was administered by the Idaho Department of Water Resources Energy Division. We thank the University of Idaho, Aberdeen Research and Extension Center for assistance in separating the straw stems used in the tests; Dr. Stephen Aust and Paul Swaner at Utah State University for maintaining and supplying the fungal cultures for inoculum pro-

duction; Peter G. Shaw at INEEL for measuring ash compositions; and Robert S. Cherry at INEEL for useful discussions regarding data analysis. This work was supported in part by the U.S. Department of Energy, Assistant Secretary for Energy Efficiency and Renewable Energy under DOE Idaho Operations Office Contract DE-AC07-99ID13727. Additional support was provided by the Idaho Wheat Commission, Grant 4-D Farms, and Energy Products of Idaho Inc.

References

1. USDA NASS. (2001), United States Department of Agriculture, National Agricultural Statistics Service, *see* Website: http://www.usda.gov/nass/.
2. Biomass Technical Advisory Committee. (2002), *Vision for Bioenergy & Biobased Products in the United States*, United States Department of Energy, Office of the Biomass Program, Washington, DC.
3. Biomass Technical Advisory Committee. (2002), *Roadmap for Biomass Technologies in the United States*, United States Department of Energy, Office of the Biomass Program, Washington, DC.
4. Thompson, D. N., Houghton T. P., Lacey, J. A., and Hess, J. R. (2003), *Appl. Biochem. Biotechnol.* **105–108,** 423–436.
5. Hess, J. R., Thompson, D. N., Hoskinson, R. L., Shaw, P. G., and Grant, D. R. (2003), *Appl. Biochem. Biotechnol.* **105–108,** 43–51.
6. Lang, E. (1997), *Bioresour. Technol.* **60,** 95–99.
7. Hadar, Y., Kerem, Z., and Gorodecki, B. (1993), *J. Biotechnol.* **30,** 133–139.
8. Lindfelser, L. A., Detroy, R. W., Ramstack, J. M., and Worden, K. A. (1979), *Dev. Ind. Microbiol.* **20,** 541–551.
9. Kirk, T. K. and Farrell, R. L. (1987), *Ann. Rev. Microbiol.* **41,** 465–505.
10. Aust, S. D. (2002), Personal communication, Biotechnology Center, Utah State University, Logan, UT.
11. Saeman, J. F., Bubl, J. L., and Harris, E. E. (1945), *Ind. Eng. Chem.* **17(1),** 35–37.
12. Thompson, D. N., Chen, H.-C., and Grethlein, H. E. (1992), *Bioresour. Technol.* **39,** 155–163.
13. ASTM (1998), *Annual Book of ASTM Standards,* ASTM Method D 790-97, American Society for Testing and Materials, Committee D20 on Plastics, Subcommittee D20.10 on Mechanical Properties, West Conshohocken, PA.
14. ASTM (1999), *Annual Book of ASTM Standards*, ASTM Method D 1037-99, American Society for Testing and Materials, Committee D7 on Wood, Subcommittee D07.03 on Panel Products, West Conshohocken, PA.
15. Thompson, D. N., Foust, T. D., Hess, J. R., Hoskinson, R. L., Houghton, T. P., Lacey, J. A., and Shaw, P. G., (2002), in: *Proceedings of Bioenergy 2002—Bioenergy for the Environment*, Omnipress, Madison, WI, paper 2013.
16. Hatakka, A. I. (1983), *Eur. J. Microbiol. Biotechnol.* **18,** 350–357.
17. Steinegger, D. H. and Janssen, D. E. (1993), *Garden Compost*, NebGuide G86-810-A, Cooperative Extension, Institute of Agriculture and Natural Resources, University of Nebraska–Lincoln, Lincoln, NE.

0273-2289/04/113/0095–0110/$25.00

Economic Analysis of Ethanol Production in California Using Traditional and Innovative Feedstock Supplies

Ellen I. Burnes,[1] John Hagen,[1] Dennis Wichelns,[*,1,2] and Kristen Callens[1]

[1]Department of Agricultural Economics, California State University, Fresno, CA 93740, E-mail: dwichelns@csufresno.edu; and
[2]California Water Institute, California State University, Fresno, CA 93740

Abstract

In this article, we estimate the costs of using alternative feedstocks to produce ethanol in a 40 million–gal facility in California's San Joaquin Valley. Feedstocks include corn imported from Midwestern states and locally grown agricultural products such as corn, grapes, raisins, oranges, and other tree fruits. The estimated feedstock costs per gallon of ethanol include $0.92 for Midwestern corn, $1.21 for locally grown corn, $6.79 for grapes, $3.36 for raisins, $3.92 for citrus, and $1.42 for other tree fruit. Adjusting for coproduct values lowers the estimated net feedstock costs to $0.67/gal of ethanol for Midwestern corn, $0.96 for locally grown corn, $6.53 for grapes, and $3.30 for raisins. We also examine the potential increases in net revenue to raisin producers, made possible by having an alternative outlet available for selling surplus raisins.

Index Entries: Biofuels; renewable energy; raisins; ethanol; feedstocks.

Introduction

Prior to the winter of 2003, the primary oxygenate added to gasoline sold in California was methyl tert-butyl ether (MTBE). Since that time, refiners in California have been discontinuing the use of MTBE, while increasing their use of ethanol as an oxygenate. As MTBE use is discontinued, most of the ethanol that will be used in its place likely will be imported from other states. An economic analysis of the potential for producing

*Author to whom all correspondence and reprint requests should be addressed.

ethanol in California is timely and appropriate, given that MTBE is being discontinued, and that California has a large agricultural industry that may benefit from increased demand for some of its products.

In the early 1980s, motivated by fuel shortages, geopolitical uncertainty, and high fuel costs, California developed the capability of producing fuel ethanol. Producers demonstrated the ability to make ethanol from local feedstocks including agricultural waste, industrial waste, and other biomass sources. Five ethanol production facilities were constructed in California during that time. Three of those facilities were closed within 10 yr, when fuel prices declined, feedstock costs rose, and subsidies for ethanol production were ended. Nonetheless, California gained valuable experience while the plants were operating. In particular, producers demonstrated that ethanol could be produced in California, provided that subsidies were available. Producers also learned that plant location and the choice of feedstocks are important firm-level decisions and that regional economics and political considerations influence the financial viability of ethanol production.

As the most productive agricultural region in the United States, it seems appropriate to reconsider the role that ethanol production might play in California. In this article, we estimate the costs of using alternative feedstocks to produce ethanol in a 40 million–gal facility in California's San Joaquin Valley. We consider seven materials that might be used as an ethanol feedstock: citrus, grapes, raisins, deciduous tree fruit (peaches, plums, and nectarines), corn, almond hulls, and whey. Any of these, except corn, can be described using one or two of the following statements: (1) it is currently produced in surplus amounts in the San Joaquin Valley (grapes and raisins), (2) it is a culled product (grapes, citrus, tree fruit), or (3) it is a byproduct (almond hulls and whey). Ethanol production from any of these sources would enhance the farm-level economics of the primary crop activity by generating new demand for culls, surplus, and byproducts that would otherwise be wasted or sold for a minimal price.

We calculate the costs of using alternative feedstocks on a per-gallon-of-ethanol basis, to enable ready comparison of the relative costs and benefits of each feedstock. We assume that ethanol producers must purchase feedstocks at the prevailing market prices of the culls, byproducts, and surplus products. Our results suggest that the cost of producing ethanol using California agricultural products or Midwestern corn is higher than the current price of ethanol. Hence, a public subsidy would be required to encourage ethanol production using any of the feedstocks we examine.

An alternative view of the ethanol question is: would crop producers be willing to sell a portion of their surplus production at a price that ethanol producers would be willing to pay in the absence of a subsidy program? That question is particularly pertinent when producers must store their surplus production for some period of time before it is sold in a primary market. The net price received by producers in those markets declines with the length of time that the surplus production is held in storage. Hence,

producers might gain by selling a portion of their surplus production to ethanol producers at a price below the primary market price. We examine this possibility for the case of raisin production and storage in California's San Joaquin Valley.

Surplus raisin production occurs often in California, and the sale of surplus raisins is restricted somewhat by a federal marketing order. The high cost of storing raisins reduces the net revenue earned by farmers, and the carryover of production from one year to the next can have a depressing impact on future raisin prices. We find that between 1992 and 2001, an ethanol industry would have generated greater revenues for raisin producers in 6 of those 10 yr. We consider only the farm-level benefits of having an alternative outlet available for selling a portion of the surplus raisin production. In particular, we examine the decision to allocate surplus raisins from storage, either to the food market or to the ethanol market. We do not consider raisin production costs, because those have already been paid. We assume that the ethanol plant exists, and that its owners would be willing to purchase raisins for use as a feedstock.

Our goals in this article are (1) to estimate the costs of using alternative feedstocks to produce ethanol in a 40 million–gal facility in California's San Joaquin Valley, and (2) to demonstrate the impact of storage costs on the decision to sell surplus crops for use in ethanol production at a price below the price available in primary markets. We describe the availability and cost of the agricultural products that might be used as feedstocks for ethanol production in California. We use that information to estimate the costs of producing ethanol and to examine the impact of storage costs on crop marketing decisions.

Feedstock Availability and Costs

We examine seven feedstocks with respect to supply, seasonality, price, and ethanol yield. In particular, we describe the price/t, the gallons of ethanol produced/t, and the feedstock cost/gal of ethanol. We examine both Midwestern corn and California-grown corn, because either crop might be used for ethanol production. In addition, the analysis for Midwestern corn provides a benchmark for comparison with corn and other feedstocks produced in California. Those alternatives include grapes, raisins, oranges, other tree fruit, almond hulls, and whey.

We describe the potential ethanol yield from almond hulls and whey, but we do not consider these materials for use in the ethanol facility. The technology exists to process almond hulls and whey for ethanol, while retaining their value as animal feed, but that activity requires an additional capital investment that is beyond the scope of this study.

Oranges

We examine oranges, rather than all citrus crops, because oranges are the primary citrus crop produced in the San Joaquin Valley. We consider

both Navel and Valencia oranges. The yield and total production of oranges can vary substantially from year to year. Considering both Navel and Valencia production removes much of the seasonality from supply consideration; Navel oranges are harvested during November through May, and Valencia oranges are harvested during June through October.

Currently, about 195,000 acres are planted in Navel and Valencia oranges in California, and most of that area is within the San Joaquin Valley. Oranges from Tulare and Fresno Counties accounted for 53.6 and 14.8%, respectively, of the value of California's production in 2001 *(1)*. California oranges are grown primarily for the fresh fruit industry. Between 1991 and 2000, the estimated average annual total pack was 110 million cartons, or 2.06 million t of oranges. On average, 515,000 t (about 25%) were culled from the total harvest during the packing process. Fruit culled from the fresh orange industry is diverted for juice. We consider this culled fruit segment a potential source of biomass for ethanol production.

The average price received by orange growers in the southern San Joaquin Valley for culled oranges diverted to processing for juice between 1991 and 2000 was $51/t. We use that price in our analysis. The estimated yield of ethanol is 13 gal/t of culled oranges *(2)*, resulting in an average feedstock cost of $3.92/gal of ethanol.

California-Grown Corn

During 1991 to 2000, field corn was planted on about 400,000 acres in California. About half of that area was harvested for silage for the dairy industry each year, while the other half was harvested for grain. The average grain yield was about 4.6 t of grain/acre. In our analysis, we assume that the grain production from 200,000 acres will be available for use in ethanol production.

Between 1991 and 2000, the average market price for California field corn was $108/t. That price is consistent with current prices and is used in our study. With current technology, 89 gal of ethanol can be produced/ton of corn *(3)*. Hence, we use an average feedstock cost of $1.21/gal of ethanol produced using California-grown corn.

Table Grapes

In 2001, there were 88,000 acres of table grapes in California and the average production was 8.07 t/acre *(1)*. The harvest season is from May through November, and table grapes can be sold as fresh fruit or for use in making juice, concentrate, or wine. Between 1991 and 2000, an average of 680,000 t of table grapes reached the fresh fruit market, each year. The average proportion of culled fruit in the fresh market is 25.5% *(4)*. Therefore, we assume that 173,400 t of culled grapes would be available for use in ethanol production.

The average price for culled grapes diverted to other uses such as in the juice and concentrate markets during 1991 to 2000 was $161.70/t. We

use that price in our analysis because it represents the value of the next-best alternative to sale in the fresh fruit market. Table grapes produced in the San Joaquin Valley and sold in California must contain a minimum sugar content of 17% *(5)*. That content implies an ethanol yield of 23.8 gal/t of grapes. This is determined by multiplying the sugar content by 100 and multiplying that result by a conversion coefficient of 1.4 gal of ethanol/t of grapes per unit of sugar (R. Murray, personal communication, 4/4/02). The estimated feedstock cost of culled table grapes becomes $6.79/gal of ethanol.

Raisins

The average annual production of raisins in California during 1991 through 2000 was 368,000 t. The Raisin Advisory Committee allocates a portion of the total production to "free tonnage" and the remainder to a "reserve pool." The reserve pool represents the potential feedstock source for ethanol production. Between 1979 and 2001, the average allocation to the reserve pool was 28% of total production. Using that proportion and the average production from 1991 through 2000 generates an expected annual reserve pool of 103,000 t of raisins. Although raisins are harvested from August through October, they can be stored for use as a feedstock in any month.

At present, there is an oversupply of raisins in California. The reserve pool for the 2000–2001 season was 203,330 t, or about 66% of total production *(6)*. Changing dynamics in international trade and market developments in the wine industry will continue to have an impact on the size of the reserve pool.

Between 1993 and 2001, growers received an average of $329/t for raisins in the reserve pool. That price fell to $250/t in 2001 *(6)*. We use the average annual price of $329/t in our analysis, while noting that raisins will be available at a lower price in the future, if the condition of excess supply continues. Hence, we consider also an alternative raisin price of $250/t. About 98 gallons of ethanol can be produced/t of raisins. Using the average reserve pool price of $32/t, the feedstock cost would be $3.36/gal of ethanol. The feedstock cost is $2.55/gal when the 2001 reserve pool price of $250/t of raisins is considered.

Deciduous Tree Fruit

We consider deciduous tree fruit production including peaches, plums, and nectarines. Between 1991 and 2000, California produced 664,000 t of tree fruit annually. The average annual cull rate is 25%, providing 166,000 t of potential ethanol feedstock. This feedstock would be available seasonally from May through October.

The prices of culled tree fruit depend on the marketing options available. Industry surveys completed in the spring of 2002 indicate that culled fruit prices range from $15 to $20/t. Hence, we use a price of $17/t in our

analysis. Ethanol yields from culled fruit vary with the fruit selected. Nectarines have the highest yield 13 gal/t; peaches yield 12 gal/t; and plums generate 11 gal/t. We use the average of these estimates (12 gal/t) in our analysis. Hence, the estimated feedstock cost for culled fruit is $1.42/gal of ethanol.

Almond Hulls and Whey

Although whey and almonds are not considered feedstocks in this study, they might be recognized as potential, alternative feedstock choices. In 2002, there were 525,000 acres of bearing almond trees in California. In 2001, these alternate-bearing trees produced 450 million tons of unprocessed almonds. Almond hulls have a high sugar and protein content. Currently, they are used as a feedstock for cattle because of the protein content. For this use, almond hulls received an average market price of $73/t between 1990 and 2000.

It may be possible to use the sugar in almond hulls for ethanol production, while leaving the protein for use by animals. Research and investments may be required to develop a suitable production process and some time and effort may be required for market development. We recommend further study of the potential use of almond hulls for ethanol production in California.

Whey is a coproduct of cheese manufacturing. In 2000, California produced an estimated 1.5 billion lb of cheese, yielding 747,000 t of dried whey. It is costly to dispose whey in municipal water systems. Hence, an alternative use for whey would enhance the economics of cheese production. Currently, whey protein is used as a food additive, a protein supplement, and an animal feed. In addition, there are a few ethanol plants in California and the Midwest that use whey as a feedstock. The current California whey production would yield approx 4.7 million gal of ethanol.

The market price of whey used as animal feed is $340/t *(7)*. As with almond hulls, it may be possible to utilize the sugar in whey for ethanol production, while enabling the protein in the byproduct to be used for animal feed. Hence, the net feedstock cost of whey in ethanol production may be less than $340/t of whey. Further research on the potential of expanding the use of whey as an ethanol feedstock would be helpful in evaluating the viability of this alternative.

Summary of Feedstock Supplies for Fuel Ethanol Production

When considering the supply and price of feedstocks, it is necessary to consider how much of each feedstock would be required to produce 40 million gal of ethanol annually, and how much of each feedstock is available throughout the year. It is not necessary that the plant use a single feedstock. In fact, further analysis could be conducted to determine optimal combinations of feedstocks based on price, seasonality, and yield. The estimated feedstock requirements and the amount of each feedstock that

Table 1
Feedstock Requirements and Availability for a 40 Million–Gal Ethanol Facility

Feedstock	Feedstock requirement (t/yr)	Feedstock available (t/yr)	Proportion of supply (%)	Ethanol (gal/t)
Culled oranges	3,076,923	515,000	17	13
Other tree fruit	3,333,333	165,916	5	12
Grapes	1,680,672	173,400	10	24
Raisins	408,163	103,000	25	98
California corn	449,438	920,000	205	89

should be available in California, given current production levels, are shown in Table 1.

Corn is the only feedstock that would be available in sufficient supply to support production of 40 million gal of ethanol, given current production levels. The current production of grain corn in California is 920,000 t, while the estimated requirement is for 449,438 t (Table 1). The proportions of supply that would be available for other feedstocks range from 5% for other tree fruit to 25% for raisins. The production, availability, and prices of feedstocks would change with farm-level and industry responses to public policies and market developments that influence the demand for ethanol production.

Ethanol Production Costs and Returns

We base our ethanol facility and production assumptions on a study conducted earlier by the California Energy Commission *(8)*. That study examined the potential for using traditional biomass sources as feedstocks for producing ethanol in California. We extend that analysis by considering nontraditional feedstock alternatives, such as California-grown corn, surplus grapes and raisins, and culled oranges and other tree fruit produced in the San Joaquin Valley. We also consider almond hulls and whey, and we use updated estimates of energy prices in our analysis.

Some of the data we use are taken from the California Energy Commission's 2001 report *(8)*. Other data sources include the California Department of Food and Agriculture; the Raisin Administrative Committee; the Renewable Fuels Association; and interviews with individuals in the tree fruit, citrus, almond, raisin, and grape industries.

We consider a new, 40 million–gal ethanol facility built in the San Joaquin Valley. Feedstocks for the facility include corn and surplus fruit products. Coproducts include dried distiller's grain (DDG), and pomace, another animal feedstock. We assume that the facility operates throughout the year, using selected combinations of feedstock materials. The seasonality of biomass availability is demonstrated in Table 2. Corn and raisins are available throughout the year, because both crops can be stored after harvest (Table 2). Oranges also are available throughout the year, because we consider two varieties that are harvested at different times of the year.

Table 2
Seasonality of Biomass Availability

Feedstock	Jan.	Feb.	Mar.	Apr.	May	June	July	Aug.	Sept.	Oct.	Nov.	Dec.
Culled oranges	•	----	----	----	----	----	----	----	----	----	----	•
Other tree fruit					•	----	----	----	----	----	•	
Grapes					•	----	----	----	----	----	•	
Raisins	•	----	----	----	----	----	----	----	----	----	----	•
California corn	•	----	----	----	----	----	----	----	----	----	----	•
Midwestern corn	•	----	----	----	----	----	----	----	----	----	----	•

Table 3
Estimated Variable Costs of Operating
a 40 Million–Gal Ethanol Facility

Item/reference	Estimated Cost in Dollars ($/gal of ethanol)
Natural gas *(11,12)* [a]	0.190
Electricity *(9)*	0.060
Water/sewage *(10)*	0.026
Maintenance *(10)*	0.003
Management and labor *(9)*	0.090
Processing materials *(10)*	0.110
Total variable costs	0.479

[a] Note that if the DG produced when using corn as a feedstock is dried, the natural gas cost rises to $0.310/gal and the total variable cost becomes $0.599/gal. The cost of natural gas was calculated using the following tariff structure for large commercial customers of the Pacific Gas & Electric Company *(11)*: summer rates (April 1–October 31): $0.77888 per therm for the first 4000 therms, $0.68719 per therm for additional therms; winter rates (November 1–March 31): $0.84189 per therm for the first 4000 therms, $0.72810 per therm for additional therms.

Other tree fruit and grapes are considered to be available only from May through October.

Fixed Costs

The estimated cost of constructing a 40 million–gal ethanol facility in the San Joaquin Valley is $55 million *(9)*. Amortizing that investment over an expected useful life of 20 yr at a discount rate of 5% generates an amortized expense of $4.41 million/yr. Dividing that cost by the expected annual production of 40 million gal generates an average amortized cost of $0.11/gal of ethanol.

Variable Costs of Plant Operation

The estimated variable costs of operating a 40 million–gal ethanol plant excluding the cost of feedstock materials are shown in Table 3. These costs were compiled using data from the California Energy Commission *(10)*, Pacific Gas and Electric *(11)*, Yancey *(9)*, and Northwestern Corporation *(12)*. The largest components of variable cost, excluding the feedstock, are the costs of natural gas and processing materials. The sum of all components is $0.479/gal of ethanol (Table 3). The estimated variable cost is $0.599/gal of ethanol if the DG is dried, when using corn as the feedstock.

Table 4
Estimated Costs of Producing Ethanol from Selected Feedstocks for a 40 Million–Gal Facility ($/gal of ethanol)

Feedstock	Feedstock cost per unit of ethanol	Credit for coproducts	Net feedstock cost	Total variable cost[a]	Total cost[b]
Culled oranges	3.92	NA[c]	3.92	4.40	4.51
Other tree fruit	1.42	NA[c]	1.42	1.90	2.01
Grapes	6.79	0.26	6.53	7.01	7.12
Raisins (high price)	3.36	0.06	3.30	3.78	3.89
Raisins (low price)	2.55	0.06	2.49	2.97	3.08
California corn	1.21	0.26	0.96	1.44[d]	1.55[d]
Midwestern corn	0.92	0.26	0.67	1.15[d]	1.26[d]

[a] Total variable cost includes the net feedstock cost plus the estimated variable cost of $0.479/gal of ethanol, from Table 3.

[b] Total cost includes the total variable cost plus the estimated fixed cost of $0.11/gal of ethanol.

[c] NA, not available.

[d] This estimate pertains to the case in which the DG is not dried. The total variable cost and the total cost will be higher by $0.12/gal if the DG is dried.

These estimates are somewhat higher than the estimated variable cost of $0.392/gal for a 40 million–gal dry-mill plant provided by Whims *(13)* and the average cash operating cost of $0.417/gal for dry mills reported in a survey of ethanol producers for 1998 *(14)*. The difference is owing primarily to the higher cost of natural gas in California at the time we prepared our estimates. The prices of natural gas we use are explained in Table 3.

The estimated feedstock costs for the materials we examine range from $0.92/gal for Midwestern corn to $6.79/gal for grapes (Table 4). We adjust these costs for the value of coproducts generated when using grapes, raisins, or corn, and we express the adjustments on a per-gallon-of-ethanol basis. The coproduct values include $0.26/gal of ethanol for grape residue sold to the concentrate market, $0.06/gal of ethanol for raisin pomace, and $0.26/gal of ethanol for DDG*. The adjusted, net feedstock costs range from $0.67/gal of ethanol for Midwestern corn to $6.53/gal for grapes (Table 4). The total variable cost of ethanol production, which includes the net feedstock cost and the nonfeedstock variable costs, ranges from $1.15/gal for Midwestern corn to $7.01/gal for grapes (Table 4). The total cost includes an additional $0.11/gal for all feedstocks. The costs shown for corn in Table 4 pertain to the case in which DG is not dried. An additional $0.12/gal of ethanol must be added to the total variable cost and total cost if the DG is dried.

* The market price for DDG has ranged between $80 and $100/t in recent years *(13,15)*. Assuming that 6.5 lb of DDG is generated per gallon of ethanol produced *(15,16)*, the estimated coproduct value is $0.26/gal of ethanol using the conservative price of $80/t of DDG.

Transportation Costs

We assume that the ethanol production facility will be located to minimize the cost of transporting feedstock materials. Studies suggest that distances greater than 40–50 miles become unprofitable for utilizing agricultural waste as biomass feedstock *(15)*. In our analysis, we assume that the cost of transportation to the ethanol facility is zero, because our goal is to compare production costs for alternative feedstock materials. The assumption regarding zero transportation costs may be realistic in cases in which small ethanol production facilities are located near a large source of a byproduct, such as an almond-processing plant. In our analysis, the price of each feedstock is based on the postharvest price at the initial point of sale, such as a packinghouse or a processing facility.

Lower transportation costs could ultimately make California-produced ethanol competitive with imported supplies. Ethanol imported from the Midwest is splash-blended at fuel distribution centers. Ethanol plants using California feedstock materials might be located near the distribution centers, to minimize the cost of transporting ethanol before it is blended with gasoline.

Ethanol Prices and Net Returns

Ethanol prices vary, over time, with changes in ethanol and corn production decisions, political statements from Washington regarding fuel policy, and expectations regarding the potential adoption of a national renewable fuels standard. These factors and others have caused moderate volatility in ethanol prices in recent years. Over the longer term, ethanol prices have been less volatile. For example, from January 1995 through May 2002, the average price of ethanol delivered to San Francisco ranged from \$0.90 to \$1.85/gal, with a mean value of \$1.20/gal *(16)*.

The net returns from producing ethanol are estimated by subtracting the adjusted production costs from the expected total revenue. We use a price of \$1.20/gal of ethanol to represent a "base-case" scenario. Given that price, the estimated net returns range from a negative \$5.92 (\$1.20–\$7.12)/gal using California grapes to a negative \$0.06 (\$1.20–\$1.26)/gal, using Midwestern corn.

Storage Cost Analysis

The negative values of the estimated net returns suggest that surplus California agricultural products may not be viable ethanol feedstocks. However, this conclusion is not satisfying when one considers that current surplus conditions generate high storage and product transformation costs. For example, the cost of storing raisins is \$11.00/t per month, and there were more than 200,000 t of raisins in storage at the end of the 2001 production season. Oranges and grapes that are either surplus or culled are stored as juice or concentrate for later use in the food and beverage industry.

Storage costs reduce the net revenue received by farmers when they sell their produce in primary markets. Hence, producers might gain net revenue by selling a portion of their surplus production in a secondary market, such as that for ethanol, rather than paying substantial storage costs while waiting for the sale of their produce in a primary market. This problem can be viewed as one of determining the net revenue maximizing strategy for allocating surplus production between storage and a secondary market. We examine this problem for the case of raisin production and marketing in California's San Joaquin Valley. We assume that surplus production can be stored for later sale in the primary market, or sold for use in ethanol production.

Raisin production and marketing in California are conducted within the framework of a federal marketing order. Each year, the Raisin Advisory Committee determines the quantity and value of raisins that are allocated for sale in the "free market," and the quantity and value of raisins held in "reserve." Approximately 240,000 t of raisins are allocated annually to the free market, while 60,000 t are targeted for the reserve (*[6]*; M. Pello, personal communication, 3/6/03). Between 1991 and 2000, total raisin production in California ranged between 240,000 and 437,000 t. The amount of raisins allocated to the free market remained consistent during those years, whereas the amount allocated to the reserve pool ranged from 0 t in 1998 to 205,000 t in 2001.

Conceptual Framework

Raisin growers receive a lower price for raisins sold from the reserve pool than from the free market, in part because storing raisins in reserve generates a storage cost. The monthly allocation of raisins from reserves is determined by the Raisin Advisory Committee. When it is possible to sell raisins for use in ethanol production, the committee might increase its net revenue by selling a portion of the reserve pool in that market. The net returns obtained from selling raisins in both the food and ethanol markets can be described as follows:

$$\text{Net returns} = \sum_{m=0}^{\tilde{m}} \left(P_F - cm\right) Q_{F_m} + P_E Q_E \tag{1}$$

in which P_F is the price of raisins in the food market ($/t), P_E is the price of raisins in the ethanol market ($/t), c is the per-unit cost of storage ($/t, per month), m is the month in storage, $\tilde{m}$ is the month in which net price in the food market equals the price in the ethanol market, Q_{F_m} is the quantity of raisins sold in the food market (t/mo), and Q_E is the quantity of raisins sold in the ethanol market (t/mo).

By construction of the model,

$$Q_E = \left(R - \sum_{m=0}^{\tilde{m}} Q_{F_m} \right) \tag{2}$$

In this model, the reserve quantity, R, is determined by the marketing order. We assume that the monthly allocation, Q_{F_m}, is determined by the Raisin Advisory Committee. Hence, neither the reserve pool nor the monthly reserve allocation to food markets is a choice variable. The per-unit cost of storage, c, also is determined outside of the model.

The Raisin Advisory Committee can maximize net revenue by storing raisins for the food market only while net price in the food market ($P_F - c\tilde{m}$) is greater than the price in the ethanol market (P_E). The net price in the food market declines as the number of months in storage increases. We use $\tilde{m}$ to represent the month in which the net price in the food market becomes equal to the price in the ethanol market (i.e., $P_F - c\tilde{m} = P_E$). The empirical value of $\tilde{m}$ is determined by the relationship of the fixed parameters P_F, P_E, and c. In particular,

$$\tilde{m} = \frac{P_F - P_E}{c} \tag{3}$$

The number of months, $\tilde{m}$, will be larger in years when P_F is relatively high, and smaller in years when P_E is relatively high.

Empirical Analysis

We have examined reserve pool prices and quantities for the years 1992 through 2001 to determine when the opportunity of selling raisins for ethanol production might have generated greater net revenues for raisin growers. We work with the assumption that 5000 t of raisins will be sold from the reserve pool every month (M. Pello, personal communication, 3/6/03). At this rate, the expected reserve pool of 60,000 t would be sold within 1 yr. The raisin marketing order requires that all raisins in the reserve pool be sold or discharged from the pool within 18 mo. This characteristic of the marketing order provides an economic incentive for developing viable market alternatives, particularly in years when production greatly exceeds the amount of raisins that can be sold in the food market. In addition, food market prices can be influenced substantially by large annual harvests and by maintaining large, nonmarketable reserve pools.

Based on an ethanol price of \$1.20/gal, the fixed and variable ethanol production costs of \$0.529/gal (this includes the credit of \$0.06/gal for the coproduct), and an ethanol yield of 98 gal/t of raisins, we determined that ethanol producers could afford to pay up to \$66/t of raisins sold for use in producing ethanol. Hence, the empirical information we use includes the following: P_F is the price of raisins in the food market[†]; P_E is the price of raisins for ethanol production, \$66/t; and c is the storage cost, \$11.00/t, per month.

[†] The average prices of raisins sold from reserves (\$/t) during the years considered in this analysis are as follows: 1991: \$238; 1992: \$281; 1993: \$192; 1994: \$152; 1995: \$432; 1996: zero; 1997: \$357; 1998: none; 1999: zero; 2000: \$250. In 1996 and 1999, farmers received no credit for raisins sold from reserves, while in 1998, the crop was reduced by weather conditions, and no raisins were held in reserve (M. Pello, personal communication, 3/6/03).

Table 5
Potential Benefits of Fuel Ethanol Production on Raisin Industry

Year	Raisins to ethanol (t)	Ethanol (million gal)	Additional revenue (thousand $)
1992	10,485	1.03	689
1993	30,535	3.00	1780
1994	47,614	4.70	3007
1996	38,094	3.73	2505
1999	45,000	4.41	2959
2000	104,165	10.21	6686

We determined the month, $\tilde{m}$, according to Eq. 3, in which c = \$11/t, per month, P_E = \$66/t, and Q_{F_m} = 5,000 t/mo. We determined the return to raisins in the ethanol market based on a price of \$1.20/gal ethanol, associated ethanol production costs of \$0.529, and an ethanol yield from raisins of 98 gal/t.

Results of Analysis

Based on the net revenue maximizing strategy, we conclude that between 1992 and 2001, the raisin industry would have benefited from an ethanol industry in 6 out of 10 yr. The additional net revenue in the beneficial years ranges from \$0.689 million dollars in 1992 to \$6.686 million in 2000 (Table 5). Preliminary market information from the 2002 harvest suggests that similar benefits might have been generated in that year.

Conclusion and Policy Implications

We have described the economic feasibility of utilizing surplus and cull citrus, grapes, raisins, tree fruit, California-grown corn, and Midwestern corn as fuel ethanol feedstocks. The cost of production exceeded the price of ethanol for all of the feedstocks we considered. However, in the case of raisins, oranges, and grapes, surplus production could generate additional storage costs. Those costs provide an incentive for considering the sale of surplus or culled production to an ethanol producer at a price less than the market price of the surplus or culled product. For example, in the case of raisins, a fuel ethanol industry might provide higher net revenues to farmers who could sell raisins from the reserve pool for ethanol production, rather than storing them until they are released for sale in the fresh market or discarded, as required by the raisin marketing order.

We estimated that the ethanol producer would be willing to pay \$66/t for raisins. That price will increase or decrease with changes in ethanol prices. At a price of \$66/t, raisin growers would not choose to grow raisins for the ethanol market. However, raisin growers could benefit from having the ethanol market as an alternative diversion when reserve pool prices are

low, or when the amount of raisins held in reserve is large. We showed that raisin producers in the San Joaquin Valley would have gained net revenue by selling raisins from storage for ethanol production in 6 of the 10 yr during 1992 and 2001.

One implication of our work is that an ethanol industry in the San Joaquin Valley might provide an economic benefit to raisin growers and producers of other agricultural products that need to be stored before they are sold. A second implication is that a broader range of potential market outlets may reduce uncertainty regarding net revenue, by alleviating some of the downside exposure to the high cost of maintaining reserve stocks.

Future work in this area might include extending our analysis to the grape concentrate and orange juice markets. That research would enhance our understanding of the potential economic impacts of developing an ethanol industry in the San Joaquin Valley. Given that the net returns from the production of ethanol are negative for all of the locally grown feedstocks we considered, private firms will not choose to produce ethanol in California without a public subsidy. The amount of public funds required to support ethanol production can be reduced if alternative marketing opportunities are identified that allow producers to obtain feedstock materials from farmers at prices that are lower than those in primary markets for surplus and culled products.

Acknowledgments

We appreciate support from the California Department of Food and Agriculture; the California Agricultural Technology Institute; and the Center for Agricultural Business at the California State University, Fresno. We appreciate also the helpful comments from two anonymous reviewers, and we retain responsibility for any oversights and omissions. This article is Contribution Number TP 03-10 of the California Water Institute.

References

1. California Department of Food and Agriculture. (2002), *Agricultural Resource Directory*, Sacramento, CA.
2. California Department of Food and Agriculture. (1980), *Ethanol Yields by Crop*, Sacramento, CA. Unpublished.
3. Urbanchuk, J. M. and Kapell, J. (2002), *Ethanol and the Local Community*, Renewable Fuels Association, Washington DC.
4. California Department of Food and Agriculture. (2001), *Agricultural Resource Directory*, Sacramento, CA.
5. California Department of Food and Agriculture. (2002), *Synopsis of Standardization Provision and Procedures*, Sacramento, CA.
6. Raisin Administrative Committee. (2002), *Analysis Report*, Fresno, CA.
7. United States Department of Agriculture (USDA). (2002), *Market News Reports*, Market News Service, AMS, Washington DC.
8. California Energy Commission. (2001), *Costs and Benefits of a Biomass-to-Ethanol Production Industry in California*, Sacramento, CA.
9. Yancey, M. (2003), Paper presented at the California Ethanol Workshop, April 14, Sacramento, CA (www.bbiothanol.com/doe/ca/Yancey_CA_DOE.pdf).

10. California Energy Commission. (1999), *Evaluation of Bio-Mass to Ethanol Fuel Potential in California: Report to the Governor*, Sacramento, CA.
11. Pacific Gas and Electric. (2003), Advice Letter No. 2471-G, issued by Karen A. Tomcala, Vice President, Regulatory Relations, San Francisco, CA.
12. Northwestern Corporation. (2002), *Northwestern Energy Signs Gas Supply Contract to Serve New South Dakota Ethanol Plant*, News Center News Display, Sioux Falls, SD.
13. Whims, J. (2002), *Corn Based Ethanol Costs and Margins: Attachment 1*. Agricultural Marketing Resource Center, Department of Agricultural Economics, Kansas State University, KA (www.agmrc.org/corn/info/ksuethl.pdf).
14. Shapouri, H., Gallagher, P., and Graboski, M. S. (2002), Agricultural Economic Report No. 808, US Department of Agriculture, Office of the Chief Economist.
15. Gabler, E., Kalter, R. J., Boisvert, R. N., Walker, L. P., Pellerin, R. A., Rao, A. M., Hang, Y. D. (1981), Cornell agricultural economics staff paper, no. 81-27.
16. Oxy Fuel News. (2002), *Oxy Fuel News Price Report, 1995–2002*, Hart Publications, Potomac, MD.

Session 1B

Enzyme Catalysis and Engineering

Session 1B

Enzyme Catalysis and Engineering

Mike Himmel[1] and David Wilson[2]

[1]National Renewable Energy Laboratory, Golden, CO; and
[2]Cornell University, Ithaca, NY

Lignocellulosic biomass is a valuable and plentiful feedstock commodity and its high cellulose and hemicellulose content (about 80% of total) provides considerable potential for inexpensive sugars production. However, enzymatic deconstruction of these polysaccharides remains a costly prospect. Strides in cellulase cost reduction have been made, yet further improvements are needed to reach the goal of $0.10/gal of EtOH expected to enable this new industry. Strategies to reach this goal will combine reduction in the cost to produce the needed enzymes as well as efforts to increase enzyme efficiency (specific activity). As this work proceeds, the more easily attained achievements will be made first, and thus the overall difficulty increases with time.

This session focused on aspects of cellulase and xylanase biochemistry needed for enhanced utilization of enzyme cocktails for bioconversion research. Fundamental studies of enzymatic action are critical to mid- and long-term success and were the subject of most presentations. Session speakers described advances in cellulase enzyme discovery, engineering, cocktail refinement, computer modeling, and active site biochemistry. Studies of enzyme production, discovery, synergism, engineering, and structure/function were also discussed. Work to select xylanases for treatment of hemicelluloses in biomass was presented as well, and these studies of relevant "accessory" enzymes are historically less well recognized than the cellulase work. Hemicellulose and lignin are now known to act as shields to cellulase action, so if hemicellulose can be degraded enzymatically, cellulase loading and pretreatment severity may be reduced. It was also concluded that we must continue to gain a better understanding of the relevant nature of biomass ultrastructure and anatomy. Such knowledge, gained primarily through application of new surface analysis tools, is necessary to design more effective pretreatments and enzyme cocktails.

The work presented by Tim Dodge (Genencor International), Elena Vlasenko (Novozymes Biotech), Brian Steer (Diversa Corporation), David Wilson (Cornell University), Tauna Rignall (Colorado School of Mines), and James Preston (University of Florida) collectively demonstrated the application of cutting-edge methodologies in biotechnology to reducing enzyme cost.

0273-2289/04/113/0115–0124/$25.00

Dynamics of Cellulase Production by Glucose Grown Cultures of *Trichoderma reesei* Rut-C30 as a Response to Addition of Cellulose

Nóra Szijártó,[1] Zsolt Szengyel,[1] Gunnar Lidén,[2] and Kati Réczey*,[1]

[1]Department of Agricultural Chemical Technology, Budapest University of Technology and Economics, H-1521 Budapest, Szent Gellért tér 4, Hungary, E-mail: kati_reczey@mkt.bme.hu; and [2]Department of Chemical Engineering, Lund University, PO Box 124, SE-221 00 Lund, Sweden

Abstract

An economic process for the enzymatic hydrolysis of cellulose would allow utilization of cellulosic biomass for the production of easily fermentable low-cost sugars. New and more efficient fermentation processes are emerging to convert this biologic currency to a variety of commodity products with a special emphasis on fuel ethanol production. Since the cost of cellulase production currently accounts for a large fraction of the estimated total production costs of bioethanol, a significantly less expensive process for cellulase enzyme production is needed. It will most likely be desirable to obtain cellulase production on different carbon sources—including both polymeric carbohydrates and monosaccharides. The relation between enzyme production and growth profile of the microorganism is key for designing such processes. We conducted a careful characterization of growth and cellulase production by the soft-rot fungus *Trichoderma reesei*. Glucose-grown cultures of *T. reesei* Rut-C30 were subjected to pulse additions of Solka-floc (delignified pine pulp), and the response was monitored in terms of CO_2 evolution and increased enzyme activity. There was an immediate and unexpectedly strong CO_2 evolution at the point of Solka-floc addition. The time profiles of induction of cellulase activity, cellulose degradation, and CO_2 evolution are analyzed and discussed herein.

Index Entries: *Trichoderma reesei*; fermentation; cellulase; growth characterization; cellulose hydrolysis.

*Author to whom all correspondence and reprint requests should be addressed.

Introduction

The accelerating accumulation of CO_2 and other greenhouse gases in the atmosphere may lead to adverse climate changes that would seriously endanger the sensitive ecologic balance of Earth *(1)*. Energy shortages in the world coupled with environmental considerations have directed applied research toward the development of novel processes to produce renewable fuels with a special emphasis on fuel ethanol production from cellulosic materials *(2)*. Even though CO_2 is released during the bioprocess of fuel ethanol production and also during its combustion, the CO_2 is reutilized to grow new biomass, replacing that harvested for ethanol production. As a result, the net produced CO_2 is small in comparison with that released by the utilization of fossil fuels, thus reducing the hazards of a global climate change *(1,3)*.

The potential for using cellulosic materials to produce fermentable sugars for biotechnological processes—including bioethanol production—is enormous *(4,5)*. Ethanol production from cellulose comprises hydrolysis of cellulosic raw materials to sugars and the subsequent anaerobic fermentation of sugar compounds by yeast to produce ethanol. Although enzymatic hydrolysis is superior, in several aspects, to acid hydrolysis, its economic realization is highly hindered by the presently too high production cost of cellulose-degrading enzymes.

Cellulases are inducible enzymes, which are synthesized by many microorganisms during their growth on cellulosic materials. Example microorganisms known to produce cellulases include bacterial species of *Clostridium* and *Bacillus* and species of filamentous fungi from *Penicillium*, *Aspergillus*, and *Trichoderma (6)*. Complete enzymatic degradation of native cellulose requires the synergistic action of three general types of cellulolytic enzymes, traditionally classified as endoglucanases, cellobiohydrolases, and β-glucosidases *(7)*. Endoglucanases preferentially hydrolyze the amorphous regions of the fibrils by randomly cleaving β-glucosidic bonds; cellobiohydrolases are exoglucanases releasing cellobiose, the repeat unit of cellulose from the chain ends; while β-glucosidases complete the degradation process by hydrolyzing cellobiose and other cellodextrins with a low degree of polymerization to glucose units. The high level of synergy among cellulase enzymes results from their different, but complementary, mode of action. This synergy increases the degree of hydrolysis by more than twofold over that achieved with individual enzymes *(8)*.

Because of its ability to produce and secrete the complete set of cellulolytic enzymes, thus making it particularly potent in hydrolyzing the cellulose polymer to glucose monomers, the soft-rot fungus *Trichoderma*, in particular *T. reesei* has been the focus of cellulase research for decades *(8)*. The preferred substrates used by most researchers for cellulase production are pure celluloses such as Avicel, Solka-floc, and cotton *(9)*. Cellulase production by *Trichoderma* is controlled by a complex metabolic regulation *(10–12)*. Cellulose acts (indirectly) as an inducer for the production of cellulases. Expression of cellulases is furthermore subject to repres-

sion by the end product of the hydrolysis—glucose. Cellulose-derived inducers, sophorose being the most potent, are likely to provide an effective induction during cultivation on cellulose, but the concentration of the end product, glucose, may negatively affect cellulase production. Glucose concentration is determined by the dynamic balance between the rates of glucose generation (by cellulose hydrolysis) and consumption (by microbial uptake). At low concentrations of cellulase and/or cellulose, glucose generation may be too slow to meet the need of active cell growth and function. On the other hand, cellulase synthesis can be halted by glucose repression when glucose generation is faster than its consumption. Glucose repression of enzyme expression is an obvious target for strain improvement. Many of the high-producing strains of *T. reesei* that have been isolated have also been shown to be partly glucose derepressed. This is the case for, e.g., the strain *T. reesei* Rut-C30 *(6)*, which is used in the present study.

The objective of the current work was to characterize carefully the dynamics of cellulase production and metabolic activity following cellulose addition in a batch cultivation of the strain *T. reesei* Rut-C30. Cells were initially grown on glucose as the carbon source, and after its depletion, cellulose was added. Since it is difficult to follow the growth directly after addition of a solid substrate, on-line measurements of CO_2 evolution were used to follow the metabolic activity of the cells. Frequent samples were also taken to measure enzyme activity and sugar concentrations.

Materials and Methods

Chemicals

All chemicals were of analytical grade and obtained from Sigma (St. Louis, MO) with the exception of bacto agar, yeast extract and peptone which were obtained from Merck (Darmstadt, Germany), and D-glucose, which was obtained from VWR. Solka-floc, a delignified pine pulp serving as the cellulosic substrate, was obtained from Fiber Sales & Development (Urbana, OH). For the preparation of solutions and media, distilled water was used.

Stock Culture

The mutant cellulase-producing strain of *T. reesei* Rut-C30 (ATCC 56765) used was obtained from the American Type Culture Collection. The culture was maintained on malt agar slants containing 20 g/L of bacto agar, 20 g/L of malt extract, 1 g/L of peptone, and 5 g/L of glucose, with regular subculturing at 30°C.

Preparation of Inoculum

Conidia were harvested from 30-d-old stock cultures, by adding 5 mL of sterile distilled water to the agar slant and then resuspending the conidia.

The spore concentration in the conidial suspension was determined by counting with a Bürker Counting Chamber. To prepare the inoculum, 1 mL of spore suspension (approx 4×10^7 spores/mL) was inoculated into a 300-mL Erlenmeyer flask containing 75 mL of growth medium similar to the basic nutrient medium of Mandels and Weber (13) with the exception that urea was omitted, a double amount of $(NH_4)_2SO_4$ was included, and the peptone content was elevated by 20%. This medium (later referred to as medium with a single set of nutrients) contained 10 g/L of glucose as the sole carbon source, which was fed separately in the form of a thick solution to the salt medium after sterilization. The initial pH of the sterilized medium was adjusted to 5.0 by adding sterile 2 *M* H_2SO_4 before inoculation, and no pH control was applied during the cultivation run. The inoculum was incubated on a rotary shaker with an agitation rate of 200 rpm at 30°C for 3 d and then was used to inoculate the fermentor.

Fermentation Experiments

Fermentations were performed in a 3-L stirred-tank laboratory fermentor (Biostat A-DCU300; B. Braun Biotech International GmbH, Germany) with a working volume of 2 L. The bioreactor was equipped with a pH electrode and a polarographic oxygen electrode (Mettler-Toledo). To 1950 mL of sterilized (121°C, 20 min) growth medium containing a double set of nutrients, 50 mL of inoculum was added; thus, the volume of the inoculum was made up to 2.5% (v/v) of the total broth volume. Fermentations were performed at 28°C with an agitation rate of 600 rpm and an aeration rate of 500 mL/min (0.25 vvm) at atmospheric pressure. A rather low airflow was used to avoid excessive foaming; however, the dissolved oxygen tension was always above 15% of the saturation value. The initial pH was adjusted to and further controlled at 5.0 by the automatic addition of 2 *M* H_2SO_4 and 2 *M* NaOH. Foaming was controlled by the manual addition of filter-sterilized antifoam agent (Sigma Antifoam 289). Fermentation was continued until the glucose was completely depleted, and then pulse addition of Solka-floc (10 g/L) was applied by adding a thick suspension of 20 g of Solka-floc in a calculated volume of distilled water, thus filling the fermentor to the original volume of 2 L. Nutrients required to support the growth on the second batch of carbon source (i.e., Solka-floc) were supplied by including a double set of nutrients in the original batch in order to avoid any coincidences of response signals that may occur from adding any component along the Solka-floc. The outlet gas composition was continuously monitored using a gas analyzer (Tandem dual gas sensor; Adaptive Biosystems, Leagrave, England). Measurement values from the gas analyzer as well as electrode signals were logged to a computer every 10 min.

Sampling

A sterile syringe was used to collect samples via the sampling tube driven to the very bottom of the fermentor. Prior to sample withdrawal,

3 mL of culture broth was taken and discharged in order to wash the remains away from the sampling tube. When taking the sample a few milliliters of fermentation broth was taken aseptically from the vessel and with the exception of an aliquot used for optical density (OD) measurement, the sample was immediately subjected to phase separation (4000 rpm, 10 min). The supernatant collected was assayed for reducing sugar content, glucose concentration, and cellulase activity.

Optical Density

OD was read at 660 nm (OD_{660}) against distilled water *(14)*.

Determination of Reducing Sugar Content

Total reducing sugar was determined by the dinitrosalicylic acid (DNS) method *(15)* using D-glucose as a standard. Appropriately diluted samples were made up to 1.5 mL with distilled water, and 3 mL of DNS reagent was added. The color obtained after boiling the mixture for 5 min and then diluting with 16 mL of distilled water was evaluated by reading the absorbance at 550 nm. Total reducing sugar generated during the assay was estimated as glucose equivalents.

Determination of Glucose

Samples were analyzed for glucose by high-performance liquid chromatography using an Aminex HPX-87H column at 65°C. The mobile phase was 5 m*M* H_2SO_4 at a flow rate of 0.5 mL/min. In addition, glucose concentrations in some samples were determined by an enzymatic glucose test (Boehringer Mannheim GmbH, Mannheim, Germany).

Enzyme Assay

Filter paper activity, which describes the overall cellulolytic activity of an enzyme preparation, was determined by the method of Mandels et al. *(16)*. A 1 × 6 cm strip of Whatman no.1 filter paper (Hillsboro, OR), which equals 50 mg of cellulose, served as the substrate and was added to the sample solution containing 0.5 mL of appropriate diluted enzyme (supernatant of culture broth) and 1.0 mL of 0.05 *M* citrate buffer (pH 4.8). After 60 min of incubation at 50°C, the hydrolysis was terminated by the addition of 3 mL of DNS solution, and the mixture was further assayed for reducing sugar content by the DNS method. One international filter paper unit (FPU) was defined as the amount of enzyme that releases 1 μmol of glucose/min under the assay conditions. Activities were reported as FPU/milliliter.

Hydrolysis Experiments

To be able to study cellulose (Solka-floc) degradation without microbial conversion of the sugars formed, separate hydrolysis experiments were carried out in stirred flasks without cells. The conditions in these experiments were the same as during the corresponding fermentation

(i.e., the same medium composition, pH 5.0, 28°C, 600 rpm). The medium composition was set according to the assumption that at the moment of Solka-floc addition, the fermentation broth would be depleted for the glucose originally present. The medium for hydrolysis experiments thus contained a single set of nutrients, 10 g/L of Solka-floc as the substrate, and added enzyme giving a desired activity. Two sources of enzyme were used: either Celluclast, a commercially available fungal cellulase preparation (a kind gift from Novozymes, Denmark) or a home-produced cellulase enzyme prepared by collecting the supernatants of Solka-floc grown in shake-flask cultures of *T. reesei* Rut-C30 (Mandels medium, 28°C, pH 5.0, 4 d) by centrifugation (5600*g*, 10 min). The enzyme-to-substrate ratio was adjusted to mimic two chosen specific points in the batch cultivation on cellulose: the point of cellulose addition and the point at which the CO_2 evolution peaked. Experiments were run in duplicate.

Results

T. reesei Rut C-30 was grown aerobically in batch cultures in two stages, using glucose in an initial phase to produce cell mass, and thereafter adding cellulose (in the form of Solka-floc) as described before. The dynamics of cellular activity and produced cellulases following the addition of Solka-floc was monitored by on-line measurements of CO_2 evolution and sampling for determination of enzyme activity and sugar concentrations.

Batch Cultivation on Glucose

A two-phase aerobic batch culture is shown in Fig. 1. The initial exponential growth phase on glucose lasted until about 26 h. The specific growth rate (determined from the logarithm of the CO_2 evolution rate [CER]) was 0.22 h^{-1}. After 25.4 h, DNS measurements of reducing sugars indicated that the glucose was exhausted from the medium (Fig. 2). Although the CO_2 evolution rapidly decreased, there was a residual CO_2 evolution, which only gradually decreased to zero. This was accompanied by a reduction in the OD (Fig. 2), indicating degradation of biomass. The measured cellulase activity remained constant after the depletion of glucose at a level of about 0.3 FPU/mL.

Second-Stage Batch Cultivation on Cellulose

After 67 h, cellulose in the form of Solka-floc was added as described above. There was an immediate increase in the CER at this point. The increase continued until $t = 73$ h, at which point there was a sharp decrease in CER. This did not coincide with complete depletion of glucose from the medium (Fig. 3). The enzyme activity increased continually up to a value of about 2.6 FPU/mL. This maximum coincided with the depletion of glucose and occurred at about $t = 100$ h. From the integrated area of the CO_2 evolution (Fig. 1), one can estimate that the CO_2 evolved on cellulose was about 80% of the value obtained from glucose.

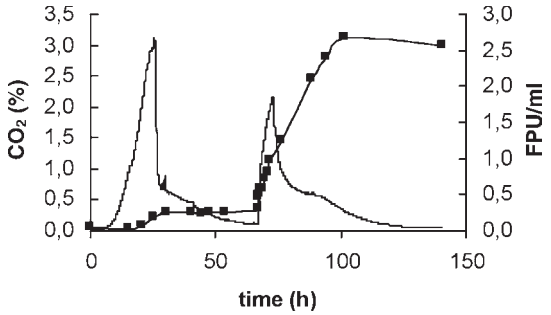

Fig. 1. CO_2 concentration in outlet gas (——) and cellulase activity (■, expressed as FPU/mL) vs time for aerobic batch cultivation of *T. reesei* Rut-C30. The initial growth medium was a Mandels medium with 10 g/L of glucose as the carbon source. At t = 67 h, Solka-floc was added to a concentration of 10 g/L.

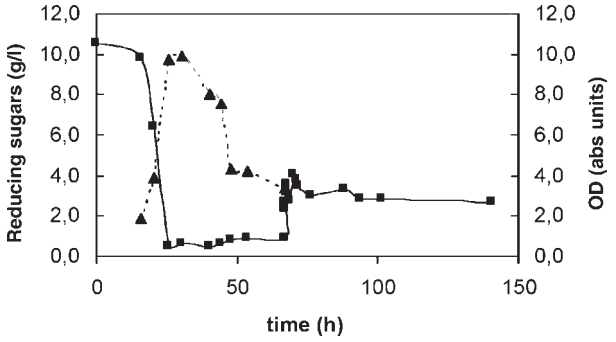

Fig. 2. Reducing sugars (■) determined by DNS method and OD (▲) vs time for aerobic batch cultivation of *T. reesei* Rut-C30. The initial growth medium was a Mandels medium with 10 g/L of glucose as the carbon source. At t = 67 h, Solka Floc was added to a concentration of 10 g/L. (There were no measurements of OD after the addition of cellulose.)

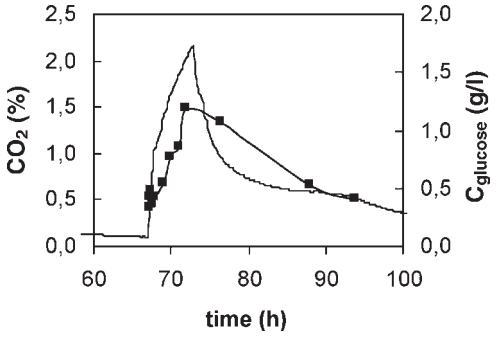

Fig. 3. CO_2 concentration in outlet gas (——) and glucose concentration (■) vs time for second aerobic batch phase in which *T. reesei* Rut-C30 grew on Solka-floc as carbon source.

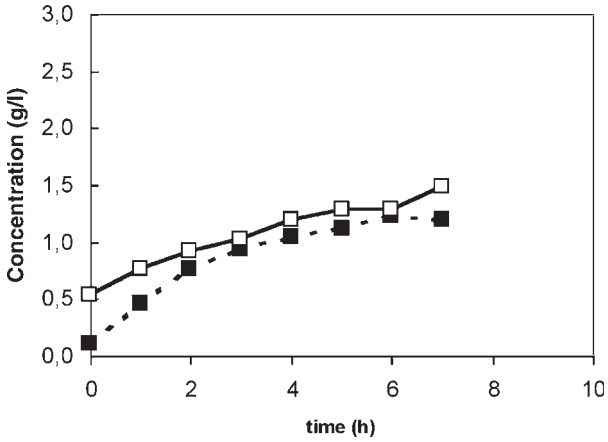

Fig. 4. Concentration of glucose (—□—) and cellobiose (– – ■ – –) during enzymatic hydrolysis of Solka-floc. The enzyme was prepared from a culture of *T. reesei* and the initial enzyme loading corresponded to 27.4 FPU/g substrate. Hydrolysis was carried out at 28°C and pH 5.0.

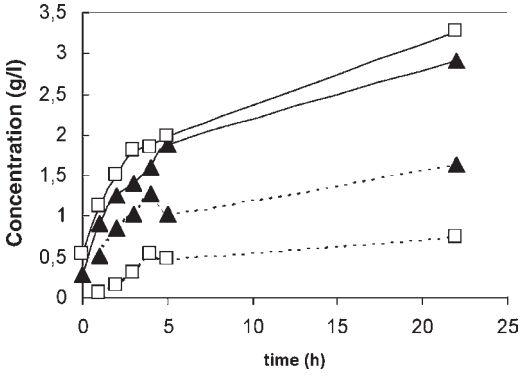

Fig 5. Concentration of glucose (——) and cellobiose (– – –) during enzymatic hydrolysis of Solka-floc. Two different enzymes were used; enzyme was prepared from a culture of *T. reesei* (□) and commercially available Celluclast (▲). Enzyme loading was 91.9 FPU/g substrate. Hydrolysis was carried out at 28°C and pH 5.0.

In Vitro Enzymatic Hydrolysis Rates

The initial, rather rapid increase in CER found in the second stage of two-phase batch cultivation was somewhat unexpected. We decided to compare this value to the initial rates of glucose and cellobiose formation in in vitro enzymatic hydrolysis experiments (Figs. 4 and 5). The enzyme loadings were chosen to represent the actual enzyme-to-substrate ratio relevant to the point of cellulose addition and the point of maximum CER.

For the enzyme solution prepared using *T. reesei*, the approximate formation rate of glucose was in the former case 0.18 g/(L·h) and in the second case 0.5 g/(L·h). The formation rate of cellobiose was 0.33 g/(L·h) in the first case and <0.2 g/(L·h) in the second case. Using Celluclast in a loading revevant to the point of maximum CER, a similar value was found for glucose, but a higher value was found for cellobiose (Fig. 5).

With a typical yield of CO_2 on sugar, Y_{sc}, of 0.4 (C-mol/C-mol), one can estimate that the sugar formation rate would give a CER of 0.018 mol of CO_2/h for a 2-L culture as in Fig. 1. This corresponds to a CO_2 concentration in the outlet gas of 1%. Within 0.5 h after addition of cellulose (Fig. 3), the measured value was in fact 1%, in good agreement with the estimated value. Calculations for the higher enzyme activity (91.9 FPU/mL) indicate that the formed glucose and cellobiose would give a CER of 0.018 mol of CO_2/h, corresponding to a CO_2 concentration in the outlet gas of 1.4%, which is a bit lower than the actual observed value.

Discussion

The final cellulase activity obtained from 10 g/L of cellulose was 2.6 FPU/mL. This is in good agreement with previously reported yields for the strain Rut-C30. For example, Persson et al. *(6)* quote a yield of 233 FPU/g of substrate in batch cultures. There was a steady increase in cellulase activity throughout the cultivation on cellulose in the current work, despite the fact that the free glucose concentration reached a value as high as 1 g/L. However, at that point of maximum glucose concentration, a sharp decrease in CO_2 evolution occurred, and the glucose concentration started to decrease after that point. The reason for this may be depletion of a medium component, or it may also be related to the regulation of enzyme expression. This is supported by the fact that the rate of activity increase changes at that point.

On depletion of glucose in the initial growth phase, there was a rapid decrease in CO_2 evolution, but it did not decrease to zero. Measurements of OD_{660} showed a decrease in biomass, suggesting that the residual CO_2 evolution is the result of endogenous metabolism. A higher volumetric enzyme productivity could therefore potentially be obtained if cellulose had been added earlier, provided that there was no remaining glucose repression effect.

The main point of making a two-stage culture was to enable the study of a pulse addition of cellulose. However, separating an initial biomass formation on glucose (or on other monosaccharides) from cellulase production with cellulose as substrate has advantages also from a process point of view. By using a two-stage process, a basal cellulase activity can be obtained before the addition of cellulose. This level allows the utilization of cellulose to commence rather quickly as shown by the CO_2 evolution. By contrast, a one-phase batch process starting directly from cellulose will initially be very slow owing to a very low hydrolysis rate. As has been pointed out previously, a key question is, to what extent will the cellulase expression be repressed by the glucose liberated in the hydrolysis.

Acknowledgment

This work was supported in part by a fellowship from the Marie Curie Training Site QCIM. We also acknowledge the National Research Fund of Hungary (OTKA T029382) and the National Research and Development Program (NKFP-OM-00231/2001) for financial support.

References

1. Wyk, J. P. H. (1999), *Biomass Bioenergy* **16,** 239–242.
2. Kheshgi, H. S., Prince, R. C., and Marland, G. (2000), *Annu. Rev. Energ. Environ.* **25,** 199–244.
3. Sun, Y. and Cheng, J. (2002), *Bioresour. Technol.* **83,** 1–11.
4. Bhat, M. K. (2000), *Biotechnol. Adv.* **18,** 355–383.
5. Himmel, M. E., Ruth, M. F., and Wyman, C. E. (1999), *Curr. Opin. Biotechnol.* **10,** 358–364.
6. Persson, I., Tjerneld, F., and Hahn-Hägerdal, B. (1991), *Process Biochem.* **26,** 65–74.
7. Beguin, P. and Aubert, J. P. (1994), *FEMS Microbiol. Rev.* **13,** 25–28.
8. Tolan, J. S. and Foody, B. (1999), in *Advances in Biochemical Engineering/Biotechnology*, vol. 65, Scheper, T., ed., Springer-Verlag, Berlin, Germany, pp. 40–67.
9. Yu, X. B., Hyun, S. Y., and Yoon-Mo, K. (1998), *J. Microbiol. Biotechnol.* **8,** 208–213.
10. Ilmén, M., Saloheimo, A., Onnela, M.-L., and Pentillä, M. E. (1997), *Appl. Environ. Microbiol.* **63,** 1298–1306.
11. Kubicek, C. P., Messner, R., Cruber, F., Mach, R. L., and Kubicek-Pranz, E. M. (1993), *Enzyme Microb. Technol.* **15,** 90–99.
12. Suto, M. and Tomita, F. (2001), *J. Biosci. Bioeng.* **92,** 305–311.
13. Mandels, M. and Weber, J. (1969), *Adv. Chem. Ser.* **95,** 391–414.
14. Bigelow, M. and Wyman, C. E. (2002), *Appl. Biochem. Biotechnol.* **98/100,** 921–934.
15. Miller, G. (1959), *Anal. Chem.* **31,** 426–28.
16. Mandels, M., Andreotti, R., and Roche, C. (1976), *Biotechnol. Bioeng. Symp.* **6,** 21–23.

0273-2289/04/113/0125–0136/$25.00

Development and Application of an Integrated System for Monitoring Ethanol Content of Fuels

Eliana M. Alhadeff, Andrea M. Salgado, Nei Pereira Jr., and Belkis Valdman*

Departamento de Engenharia Química, Escola de Química, CT/UFRJ, Ilha do Fundão, Cidade Universitária, CEP 21.949.900, Rio de Janeiro, RJ, Brasil, E-mail: belkis@eq.ufrj.br

Abstract

An automated flow injection analysis (FIA) system for quantifying ethanol was developed using alcohol oxidase, horseradish peroxidase, 4-aminophenazone, and phenol. A colorimetric detection method was developed using two different methods of analysis, with free and immobilized enzymes. The system with free enzymes permitted analysis of standard ethanol solution in a range of 0.05–1.0 g of ethanol/L without external dilution, a sampling frequency of 15 analyses/h, and relative SD of 3.5%. A new system was designed consisting of a microreactor with a 0.91-mL internal volume filled with alcohol oxidase immobilized on glass beads and an addition of free peroxidase, adapted in an FIA line, for continued reuse. This integrated biosensor-FIA system is being used for quality control of biofuels, gasohol, and hydrated ethanol. The FIA system integrated with the microreactor showed a calibration curve in the range of 0.05–1.5 g of ethanol/L, and good results were obtained compared with the ethanol content measured by high-performance liquid chromatography and gas chromatography standard methods.

Index Entries: Biosensors; gasohol; immobilized enzymes; alcohol oxidase; horseradish peroxidase.

Introduction

Since 1975, Brazil has supported a governmental program to design a new car engine technology using (95%) hydrated ethanol as biofuel.

*Author to whom all correspondence and reprint requests should be addressed.

Table 1
Enzymatic Ethanol Biosensors

Enzyme	Support	Transductor	Detection range
Alcohol dehydrogenase *(6)*	Flat glass	Amperometric	0.4–3.9 *M* ethanol in air
AOD and HRP *(8)*	poli(carbamoil)sulfonate-poliethilenimine hydrogel	Amperometric	0.02–3.75 m*M*
AODand HRP *(4)*	Not immobilized	Spectrophotometric	1.1–21.7 m*M*
AOD and HRP *(9)*	Chitosan	Spectrofluorometric	0.01–0.04 m*M*
Alcohol dehydrogenases and NAD^+/ NADH *(5)*	Not immobilized	Spectrophotometric	0.01–2.5 m*M*
AOD and catalase *(10)*	Controlled pore glass	Thermometric	1.9–3.9 *M*
Alcohol dehydrogenase and diaphorase *(11)*	Semiconductor chip	X-ray photoelectron spectroscopic	0.005–1.0 m*M*

Nowadays a worldwide focus is on renewable fuels, and ethanol has been considered an interesting option to replace petroleum derivate gasoline. It has been reported that the United States, France, Switzerland, Australia, Canada, China, Russia, India, South Africa, and the European Community are considering gasoline ethanol blends as fuel options. Recently, Brazilian government funds have been awarded to laboratories in universities and research centers in different regions of the country, and a strict control of the physicochemical characteristics of the gasohol blend and hydrated fuel alcohol for combustion machines is necessary to prevent adulteration *(1,2)*.

Among the physicochemical methodologies developed to identify chemicals, biosensors have been studied in the last 10 yr as analytical instruments that can be applied in clinical, food, and environmental analyses. Biosensors to be used as analytical instruments should present some important technical characteristics, such as low response time, high selectivity, relatively long lifetime, stability under the analytical conditions, and reproducibility of the measurements *(3)*. Biosensors, which have many advantages, can be miniaturized and/or introduced in on-line proceedings as analytical instruments to detect chemical concentrations with a very rapid response. Recently, increased applications of integrated biosensors and flow injection analysis (FIA) systems in monitoring and controlling biochemical processes have been reported *(4–6)*. Table 1 lists various enzymatic ethanol biosensors published in recent literature. Amperometric, spectrophotometric, thermometric, and X-ray photoelectron spectroscopic methods were used to detect ethanol samples using free and immobilized enzyme systems. Alcohol dehydrogenase and NAD^+/NADH, alcohol dehydrogenase and diaphorase, alcohol oxidase (AOD) and catalase, or horseradish peroxidase (HRP), have usually been applied in ethanol biosensors, as shown in Table 1.

To improve the quality control process of gasohol and hydrated ethanol, an automated FIA system was developed using AOD and HRP enzymes, and addition of 4-aminophenazone and phenol. A colorimetric detection method was used in two different methods of analysis, with free *(4)* and immobilized enzymes. Both systems have shown good results when compared with established methods such as gas chromatography (GC) and high-performance liquid chromatography (HPLC) *(4,7)*.

Materials and Methods

Chemicals

AOD, 4-aminophenazone, phenol, glutaraldehyde, dialysis sacs, and aminopropyl glass beads were from Sigma (St. Louis, MO). Toyobo of Brazil donated the HRP. All other chemicals were of analytical reagent grade.

Immobilization

AOD was immobilized on aminopropyl glass beads that were first treated with 2.5% glutaraldehyde, staying in contact with the enzyme for 24 h at 30°C in a rotatory shaker incubator at 50 rpm. The protein concentration in buffer solution was quantified before (PCBI) and after (PCAI) the immobilization proceeding, using the Lowry method. The retention efficiency was calculated using Eq. 1.

$$\text{Retention Efficiency} = \left[\frac{\text{PCBI (g/L)} - \text{PCAI (g/L)}}{\text{PCBI (g/L)}}\right] \cdot 100 \quad (1)$$

Enzymatic Reactions

Ethanol determination is based on the enzymatic reactions of AOD and HRP:

$$\text{Ethanol} + O_2 \xrightarrow{\text{AOD}} \text{Acetaldehyde} + H_2O_2$$

$$2H_2O_2 + \text{4-aminophenazone} + \text{phenol} \xrightarrow{\text{HRP}} \text{monoimino-}p\text{-benzoquinone-4-phenazone} + 4H_2O$$

The second reaction gives a colored product that can be detected in a spectrophotometer at 555 nm. The free-enzyme FIA system used an enzyme-reagent solution as described in a previous work *(4)*. The immobilized AOD (0.1 mL of AOD with 4.5 mL of phosphate buffer, pH 7.0) integrating the biosensor-FIA system worked with phosphate buffer (pH 7.0), HRP (0.5 mg/mL), and reagent solution consisting of 0.875 g/L of phenol and 0.305 g/L of 4-aminophenazone was added.

Integrated FIA System

The FIA system consisted of TMI modules (Técniques Mesura Instrumentació), a five-channel peristaltic pump, an eight-channel injection valve, an eight-channel distributed valve, and a colorimeter connected to an interface and to an IBM-PC microcomputer. A specific application software, Qcontroll®, was used for data acquisition, with a continuous historical trend, and a scheduled control program for sequential analysis. In a previous scheme as in Fig. 1, free enzymes were used and the whole system was calibrated for a linear range of 0.05–1.0 g of ethanol/L of standard ethanol solutions, and the product of the reaction was passed through the colorimeter.

As indicated in the schematic diagram in Fig. 1, AOD was mixed with HRP, 4-aminophenazone, and phenol in phosphate buffer (pH 7.0) solution, and the colored reaction occurred with the mixture flowing through a 100-cm-long coil. All tubes used had a 0.8-mm id and the 25-cm injection valve loop permitted injection of 0.185 mL of enzymes-reagents solution per analysis. After each analysis, the solution produced containing the enzymes was directed to waste.

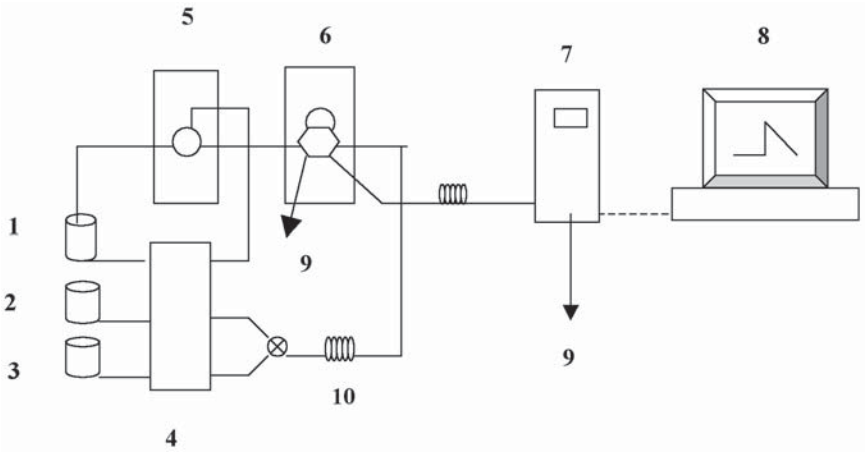

Fig. 1. Free enzymes FIA system: 1, enzymes and reagents solution; 2, sample solution; 3, buffer solution; 4, peristaltic pump; 5, three-channel valve; 6, six-channel injection valve; 7, colorimeter; 8, computer; 9, waste; 10, coil.

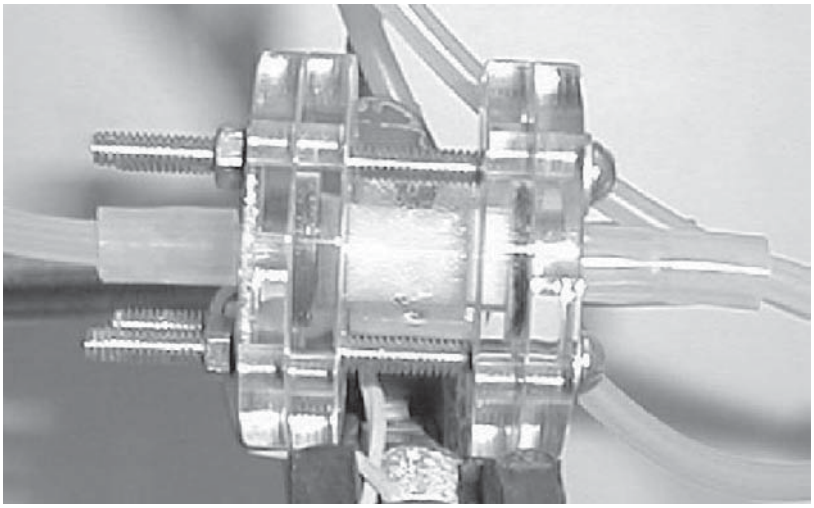

Fig. 2. Microreactor, made of acrylic packed with AOD immobilized on glass beads.

For periodic reuse of the enzymes a new project was developed including a microreactor incorporated into the FIA system. The micro-reactor shown in Fig. 2, made of acrylic acid and with a 0.91-mL void volume, and length-to-diameter ratio of 3:1, was packed with AOD immobilized on glass beads. The beads were retained in the microreactor with a 110-mesh nylon screen and two rubber O-rings with an 11.4-mm external diameter. The lids were attached to the microreactor with four stainless steel screws.

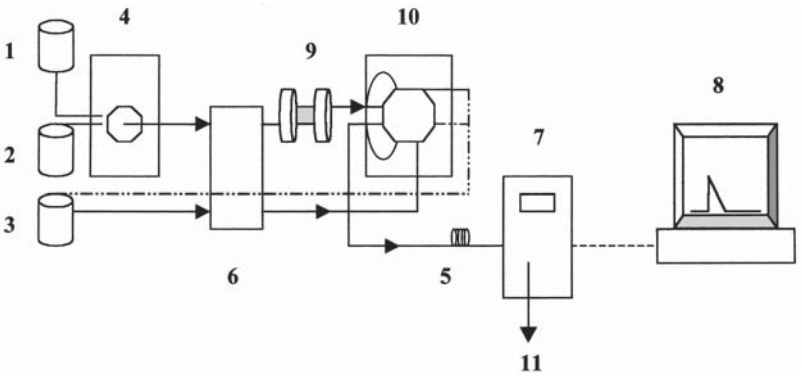

Fig. 3. Proposed integrated FIA system, with microreactor packed with immobilized AOD: 1, buffer solution; 2, sample solution; 3, horseradish peroxidase and reagents solution; 4, eight-channel distribution valve; 5, coil; 6, peristaltic pump; 7, colorimeter; 8, computer; 9, micro reactor; 10, eight-channel injection valve; 11, waste.

Flexible tubes with a 2.4-mm id were connected to each side of the microreactor as sampling lines of the integrated FIA system. In this new biosensor integrated FIA system, HRP was still used in solution with the other two reagents and injected into the FIA line after the sample reacted with the immobilized AOD. Figure 3 shows the new integrated system.

Actuator and Monitoring Equipment

In both systems studied, with free and immobilized enzymes, an automatic analysis system was coupled to the integrated biosensor-FIA system, and analysis was carried out with a specific programmed software for data acquisition and pump and valve control. The computer program controlled the analysis timing sequence, scheduling the signals to the distribution and injection valves to introduce the sample and enzymes-reagents solutions into the system. The difference between the peak heights formed and the baseline were referenced to the absorbance values detected.

Results and Discussion

Free Enzymes System

The free enzymes FIA system permitted analysis in a linear range of 0.05–1.0 g of ethanol/L, a sampling frequency of 15 analyses/h, and a relative SD of 3.5%. The total volumetric flow was 5 mL/min, and the six-channel injection valve permitted the introduction of 0.185 mL (loop volume) of enzymes-reagents solution per analysis *(4)*. Ethanol solutions of different concentrations were used to determine the linear working range and for the calibration curve construction (Fig. 4), presenting a linear relation up to 1 g of ethanol/L with a correlation factor of 0.9899 for six samples.

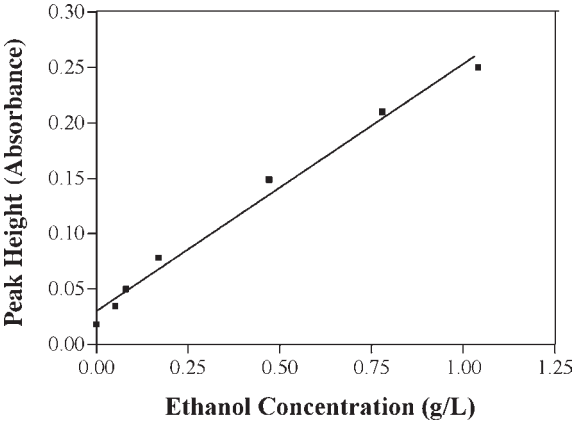

Fig. 4. Free enzymes FIA system calibration curve.

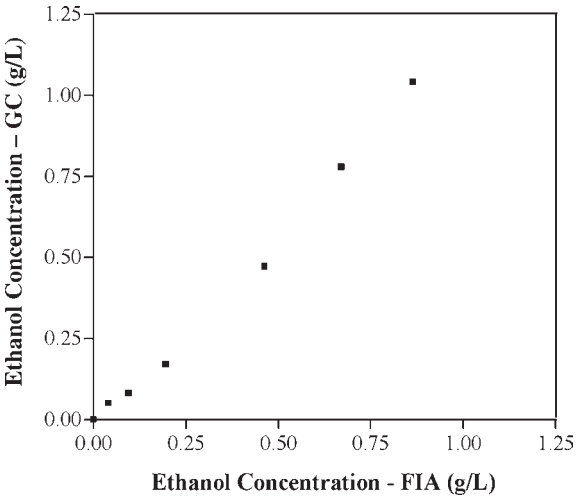

Fig. 5. Ethanol analysis by GC compared to proposed free enzymes FIA system.

The results obtained using GC for the same samples are shown in the comparative plot of Fig. 5. The curve presented a correlation factor of 0.9928, which shows the reliability of the biosensor system proposed.

Immobilization of Enzymes

AOD was successfully immobilized on aminopropyl-functionalized glass beads by covalent bonding through glutaraldehyde with an average retention efficiency of 95.14% (*see* Table 2). The method used for enzyme immobilization showed good reproducibility with a relative SD of 2.85%.

Table 2
Retention Efficiency of AOD
on Aminopropyl Glass Beads

Experiment	Retention efficiency (%)
1	92.6
2	91.9
3	96.3
4	98.8
5	96.1

Table 3
Extracted Ethanol Concentrations
from Gasohol Blends

Gasohol blend (% [v/v])	Extracted ethanol (% [v/v])
4	3.7
6	5.5
8	7.5
10	9.6
15	15.1
20	19.3

Immobilized AOD in Integrated Biosensor-FIA System

The new system was applied for standard ethanol solutions prepared in phosphate buffer solutions (pH 7.0). Extracted ethanol solutions were also used with 10% (w/v) NaCl by NBR 13992:1997 from gasohol blends *(12)* (Brazilian Association Technical Standard). Table 3 shows the concentrations of the extracted ethanol solutions measured by HPLC and respective gasohol blends. This new integrated system biosensor-FIA was used for the range of 0.05–1.5 g of ethanol/L, and good results were obtained compared with the ethanol content measured by the HPLC standard method.

Flow Adjustment of Integrated Biosensor-FIA System

Volumetric flow rate was adjusted working with three different flow rates: 0.47, 0.9, and 3.6 mL/min. Figure 6 shows the profiles obtained for the lower (0.47 mL/min, Fig. 6A) and the higher (3.6 mL/min, Fig. 6B) flow applied to the integrated biosensor-FIA system. Concerning the 0.5 g of ethanol/L sample, output signal with a short response time was achieved when the system worked with 3.6 mL/min.

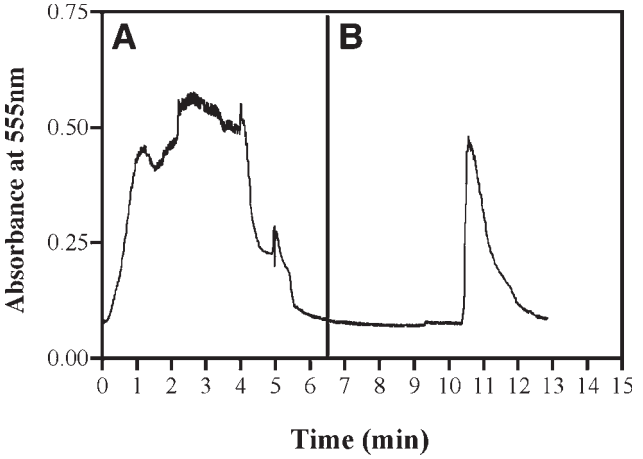

Fig. 6. Profiles registered for 0.5 g of ethanol/L: **(A)** 0.47 mL/min; **(B)** 3.6 mL/min.

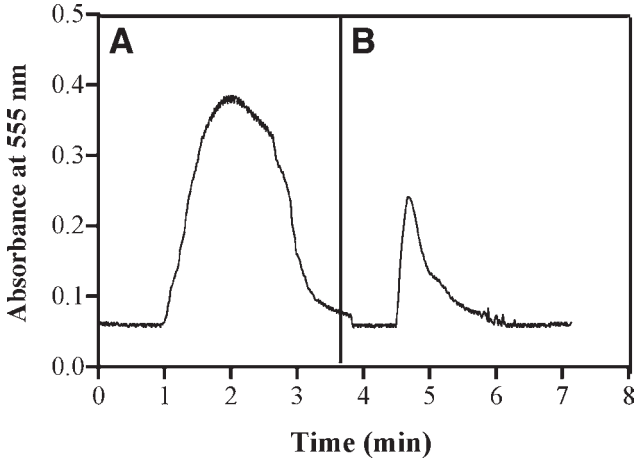

Fig. 7. Profiles registered for 0.1 g of ethanol/L: **(A)** 0.9 mL/min; **(B)** 3.6 mL/min.

Figure 7 shows the response profiles registered when 0.9 and 3.6 mL/min were applied with a 0.1 g of ethanol/L working sample. In Fig. 7A the profile was wider than that obtained when 3.6 mL/min (Fig. 7B) was used, and a maximum height of the peak (0.385) for 0.9 mL/min was observed when compared with 0.242 for 3.6 mL/min.

The measurements of extracted ethanol from gasohol and hydrated fuel alcohol, properly diluted, determined with the integrated biosensor-FIA system showed the registered signals in Fig. 8.

Good reproducibility of the registered signals was obtained with the proposed automatic analysis system. The working features used in the experiments were constant loop volume, scheduled time control program,

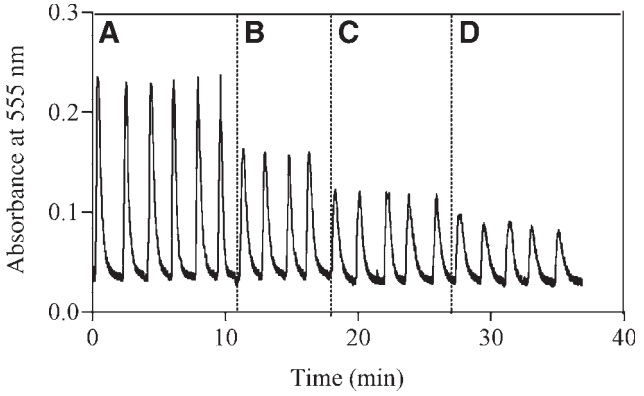

Fig. 8. Biosensor output signals for range of 0.05–1.5 g of extracted ethanol/L samples: **(A)** 1.5 g/L; **(B)** 0.3 g/L; **(C)** 0.1 g/L; **(D)** 0.05 g/L.

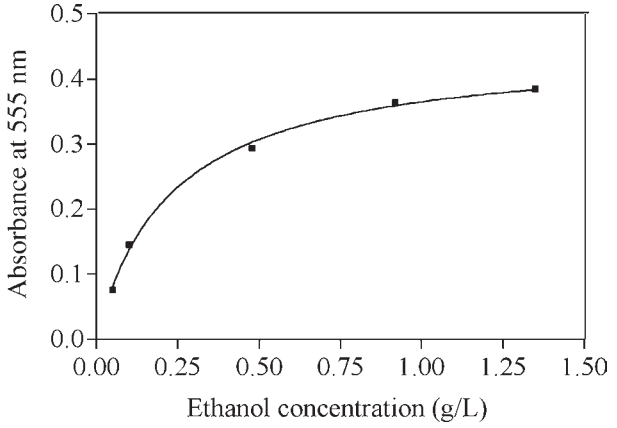

Fig. 9. Calibration curve for phosphate buffer standard ethanol solutions with integrated biosensor-FIA system.

and sample volume. The volume of free HRP mixed with 4-aminophenazone and phenol was 69.4 µL. The schedule time program controlled the timing sequence of the module's operation (cycles of 101 s), always injecting the same volume of the ethanol sample (1.0 mL) and free enzyme with reagent solution. Data were collected in real time, and the registered signal could be watched on the monitor screen as the colorimetric detector showed the absorbance signal during the measurement. The analysis response time spent only 2.0 min, between each operation cycle of the sampling line.

The calibration curves obtained with the output signals are shown in Figs. 9 and 10. Both curves were adjusted by a hyperbolic correlation with correlation coefficients of 0.9972 and 0.9909, respectively, for buffer

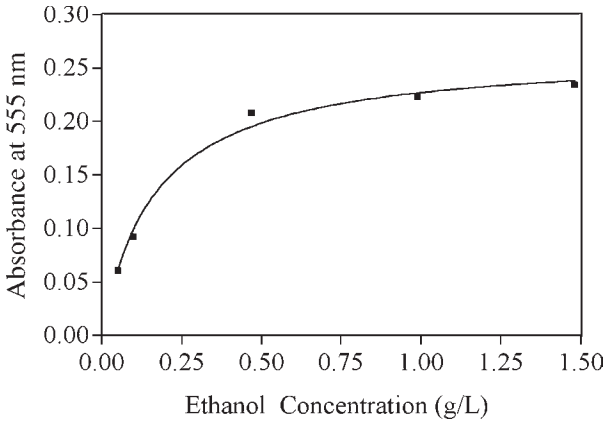

Fig. 10. Calibration curve for extracted ethanol solutions with integrated biosensor-FIA system.

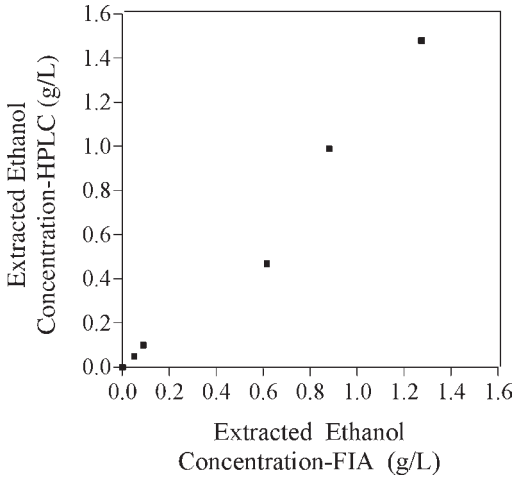

Fig. 11. Results of ethanol concentration solutions analysis by HPLC compared to proposed integrated biosensor-FIA system.

and extracted ethanol solutions. Additionally, comparison of the results obtained with the integrated biosensor-FIA system and the ethanol concentration solutions measured using HPLC is illustrated in Fig. 11.

Conclusion

The free enzyme–FIA system applied to ethanol analysis presented good results, with high reproducibility and reliability in the range of 0.05–1.0 g of ethanol/L with a relative SD of 3.5%. The methodology developed to immobilize AOD on functionalized glass beads presented high retention efficiency of the protein, about 95.14 ± 2.85%. The new, proposed,

integrated immobilized AOD biosensor-FIA system, for the reuse of this enzyme, showed excellent reproducibility and reliability for a range of 0.05–1.5 g of ethanol/L, for ethanol analysis either in buffer standard solutions or in NaCl-extracted ethanol solutions. The proposed integrated biosensor-FIA system presented a simple method, inexpensive and robust for ethanol determination in buffer or extracted ethanol solutions, with good sample frequency analysis and no significant differences compared to other analytical procedures (GC or HPLC). This system is extremely practical, giving the results of the analysis shortly after measurement, with a response time of 2.0 min. This is an advantage for a routine procedure in a quality control program, as proposed in a fuel quality control program. It was possible to perform 70 analyses in 7 d, maintaining the activity of the immobilized AOD.

Acknowledgments

We gratefully acknowledge financial support from Financiadora de Estudos e Projetos (FINEP), Project 6500018900, and valuable technical advice of Dr. Elba Bon from the Institute of Chemistry of the University of Rio de Janeiro. We also wish to thank Toyobo of Brazil for kindly donating HRP for this research and Refinaria de Petróleos Manguinhos S/A for gasoline A.

References

1. Nogueira, L. A. H. (2002), *The Evolution of Fuel Quality in Brazil, 17th World Petroleum Congress*, (Website: http://www.ANP.gov.br), retrieved November 09, 2002.
2. Szwarc, A. (2002), *Ethanol Usage in Automotive Fuels, World Fuels Conference—Latin America & the Caribbean*, (Website: http://www.chemweek.com/worldfuels/rio/pdf/1408_03.pdf), retrieved on October 11, 2002.
3. Schugerl, K.(2001), *J. Biotechnol.* **85,** 49–173.
4. Salgado, A. M., Folly, R. O. M., Valdman, B., Cós, O., and Valero, F. (2000), *Biotechnol. Lett.* **22,** 327–330.
5. Sarker, A. K., Ukeda, H., Kawana, D., and Sawamura, M. (2001), *Food Res. Int.* **34,** 393–399.
6. Setkus, A., Razumiené, J., Galdikas, A., Laurinavicius, Meskys, R., and Mironas, A. (2002), *Sens. Actuators B Chem.* **85,** 1–9.
7. Tkac, J., Vostiar, I., Gorton, L., Gemeiner, P., and Sturdik, E. (2003), *Biosens. Bioelectron.* **18,** 1125–1134.
8. Patel, N. G., Meier, S., Cammann, K., and Chemnitius, G. C. (2001), *Sens. Actuators B Chem.* **75,** 101–110.
9. Taniai, T., Sukurragawa, A., and Okitani, T. (2001), *J. AOAC Int.* **84(5),** 1475–1483.
10. Rank, M., Gram, J., and Danielsson, B. (1993), *Analytica Chimica Acta* **281,** 521–526.
11. Gué, A.-M., Tap, H., Gros, P., and Maury, F. (2002), *Sens. Actuators B Chem.* **82,** 227–232.
12. ABNT. (1997), Brazilian Association of Technical Standards, NBR 13992.

0273-2289/04/113/0137–0144/$25.00

Model Based Soft-Sensor for On-Line Determination of Substrate

Andréa M. Salgado,[1] Rossana O. M. Folly,[1] Belkis Valdman,[*,1] and Francisco Valero[2]

[1]Departamento de Engenharia Química, Escola de Química, Universidade Federal do Rio de Janeiro, CT-Bl E, sl 211, Rio de Janeiro, Brasil, E-mail: belkis@eq.ufrj.br; and [2]Departamento de D'Enginyeria Química, ETSE, Universitat Autonoma de Barcelona, 08193, Bellaterra, Spain

Abstract

A software sensor for on-line determination of substrate was developed based on a model for fed-batch alcoholic fermentation process and on-line measured signals of ethanol, biomass, and feed flow. The ethanol and biomass signals were obtained using a colorimetric biosensor and an optical sensor developed in previous works that permitted determination of ethanol at a concentration of 0–40 g/L and biomass of 0–60 g/L. The volume in the fermentor could be continuously calculated using the total measured signal of the feed flow. The results obtained show that the model used is adequate for the proposed software sensor and determines continuously the substrate concentration with efficiency and security during the fermentation process.

Index Entries: Soft-sensor; substrate; alcohol fermentation; ethanol; biomass.

Introduction

The control of a fed-batch alcoholic fermentation process can be obtained by controlling the substrate concentration in the medium by manipulation of the feed flow. The fermentation process presents complicated kinetic mechanisms. In addition, there is the absence of accurate and reliable mathematical models as well as the difficulty of obtaining direct measurements of the process variables owing to a lack of appropriate on-line analyzers and sensors. Control systems are formed by a set of instruments and control mechanisms connected through electrical signals in the

*Author to whom all correspondence and reprint requests should be addressed.

form of control loops, leading to increased efficiency and optimized process operation, reducing the costs of industrial production. A feasible way to control and monitor these processes is the use of software sensors. The software sensor uses a process model to estimate variables that neither can be directly measured nor are easily accessed through on-line available data. The limitation of currently used models is that they rarely use biologic state variable measurements *(1)*. These measurements are extremely important to providing good regulation of process performance when the physical and biochemical properties are constantly changing.

The process model can be obtained by different forms, and in bioprocesses mass balance equations can provide much information. However, in order to have efficient process models and software sensors, a previous adjustment of the model is necessary using on-line data collected from a plant under different operational conditions. This databank is important to guarantee that the model remains calibrated and represents the plant adequately. Some requisites are indispensable for the experimental implementation of models in software sensors: response speed to disturbances in the system and appropriate inference of primary variables of interest during key points of the process.

Court *(2)*, Eberhard *(3)*, and Tyagi et al. (4) have reported some applications of computers and software sensors for fermentation control in experimental research in data acquisition of bioreactors. Neural network models were used to interprete sensor signals in the control of an alcohol fed-batch fermentation *(5)* and in the detection of the individual components of a gas mixture and to measure the concentration of both gases *(6)*.

This article presents the design and implementation of a software sensor for the continuous determination of substrate concentration based on a simple model of a fed-batch fermentation process and the available signals of two other sensors—one for on-line biomass determination *(7)* and the other for on-line ethanol determination *(8)*—developed in previous works. The software sensor proposed provides a continuous signal that can be used in a control loop to manipulate the substrate feed flow in order to maintain almost constant substrate concentration and obtain an excellent level of productivity and yield during all of the process, as shown in experimental control strategy studies in previous works *(9)*.

Methods

Mathematical Model

A simple mathematical model is used for quantitative description of the process and consists of a set of equations relating inputs, outputs, and key parameters of the system. The model for an alcoholic fermentation fed-batch process developed by Mayer *(10)* and adapted with the Ghose and Tyagi *(11)* linear inhibition term by the product was used as the starting point for the development of a model-based substrate sensor with product (ethanol) and biomass on-line measurements.

To simplify study of the fed-batch alcoholic fermentation process and with the purpose of regulating the substrate concentration in the fermentation medium, the following assumptions were made: (1) the substrate concentration in the feed is constant; and (2) the volume change in the fermentor is a function of feed flow.

The following equations describe a general form of the model for the fed-batch process and total medium, having only substrate as feed flow, and include mass balances for substrate, product, biomass, and kinetic relations, respectively.

$$\frac{dV}{dt} = Fe \tag{1}$$

$$\frac{dS}{dt} = (Sa - S)\frac{Fe}{V} - X\left(\frac{\mu}{Yx/s} + \frac{\gamma}{Yp/s}\right) \tag{2}$$

$$\frac{dP}{dt} = \gamma X - \frac{Fe}{V} \tag{3}$$

$$\frac{dX}{dt} = X\left(\mu - \frac{Fe}{V}\right) \tag{4}$$

$$\mu = \mu_{max}\left(\frac{S}{Ksx + S}\right)\left(1 - \frac{P}{Kps}\right) \tag{5}$$

$$\gamma = \gamma_{max}\left(\frac{S}{Ksp + S}\right)\left(1 - \frac{P}{Kpp}\right) \tag{6}$$

To maintain optimal conditions in the fermentor, and assuming that the substrate concentration in the medium is much higher than the saturation constants (*Ksx* and *Ksp* <<< *S*), one can simplify the inhibition terms as follows:

$$\mu \approx \mu_{max}\left(1 - \frac{P}{Kpx}\right) \tag{7}$$

$$\gamma \approx \gamma_{max}\left(1 - \frac{P}{Kpp}\right) \tag{8}$$

The substrate concentration in a fed-batch fermentor can be maintained nearly constant, as shown in previous works *(9)*, and in this case one can assume that $dS/dt \approx 0$, and from Eq. 1

$$S = Sa - \left(\frac{X\,\mu\,V}{Yx/s\,Fe}\right) + \left(\frac{X\,\gamma\,V}{Yp/s\,Fe}\right) \tag{9}$$

and substituting the kinetics relations and arranging the terms one obtains

$$S(t) = Sa - \left[\frac{V(t)}{Fe(t)}\right]X(t)\left\{\left[\frac{\mu_{max}}{Yx/s}\right]\left[1 - \frac{P(t)}{Kps}\right] - \left[\frac{\gamma_{max}}{Yp/s}\right]\left[1 - \frac{P(t)}{Kpp}\right]\right\} \tag{10}$$

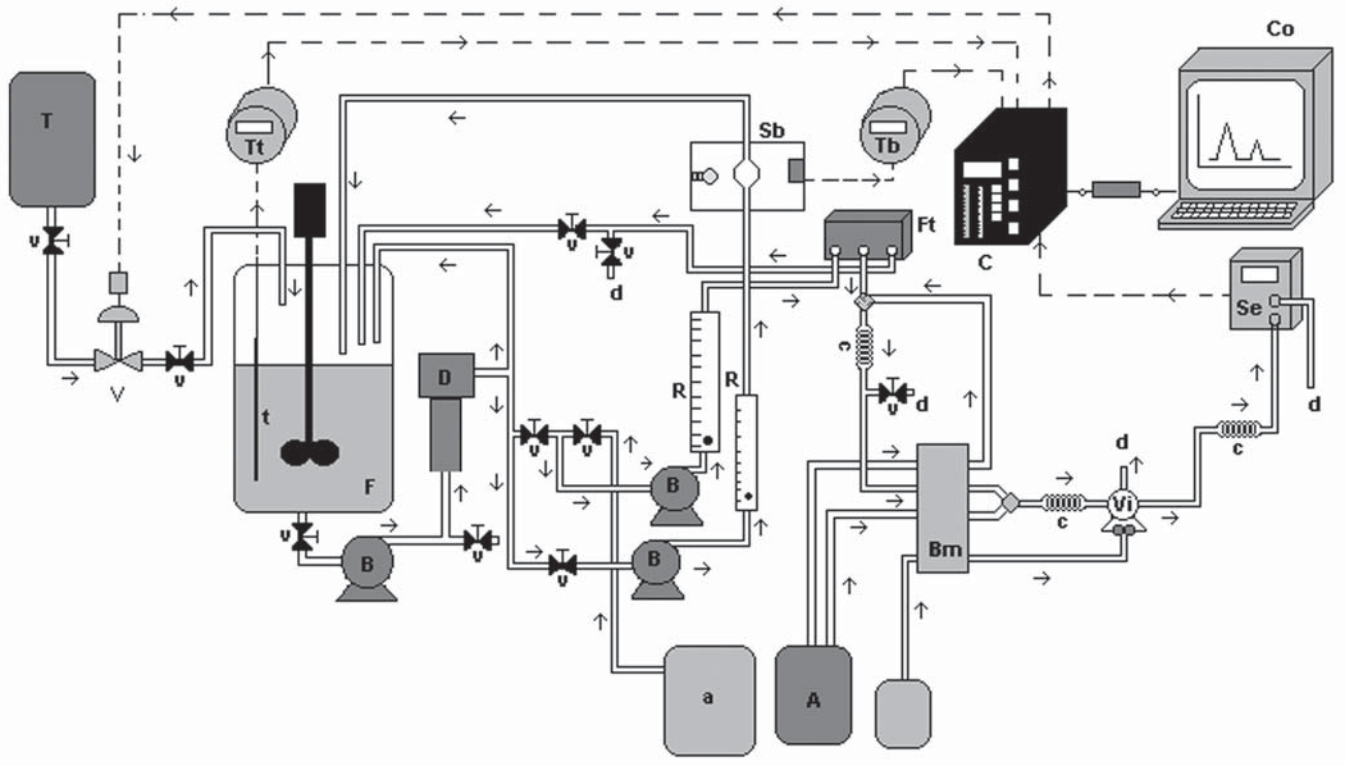

Fig. 1. Complete experimental setup for monitoring and control system for fermentor. T, feed tank; V, control valve; v, valves; F, fermentor; t, thermocouple; c, coils; A, dilutions tanks; Bm, multichannel pump; C, controller; Tt, temperature transmitter; Tb, biomass transmitter; Sb, biomass optical sensor; D, equipment to remove air bubbles; R, rotammeter; Ft, tangential filter; Co, computer; So, ethanol colorimetric sensor; Vi, injection valve; d, waste; E+R, reagents-enzymes tanks; B, pumps.

Using a new variable defined for the second term of Eq. 10 as a function of the on-line sensor signal of ethanol concentration, one obtains:

$$Pc(t) = \left[\left(\frac{\mu_{max}}{Yx/s} \right) - \left(\frac{\gamma_{max}}{Yp/s} \right) - \left(\frac{\mu_{max}}{Kps\ Yx/s} - \frac{\gamma_{max}}{Yp/s\ Kpp} \right) P(t) \right] \tag{11}$$

And using a new variable defined for biomass concentration as a function of the on-line measured biomass sensor, one obtains:

$$Xc(t) = X(t)\ Pc(t) \tag{12}$$

Finally, combining Eqs. 1, 10, 11, and 12, one obtains:

$$S(t) = Sa - \left(\frac{V_o + Fe\ (t)}{Fe} \right) Xc(t) \tag{13}$$

in which $Xc(t)$ is the combined function of the on-line measured variables; $X(t)$ is the biomass optical sensor signal, $P(t)$ is the ethanol colorimetric sensor signal, $Fe(t)$ is the feed flow signal–related control valve opening by calibration curve, and $V(t) = V_o + \int Fe\ dt$ is the volume signal calculated by the total block in the controller.

Integrated Control System for Fed-Batch Process

The complete experimental setup used as an integrated system for monitoring and control of the process variables is presented in Fig. 1. This inferred signal of substrate concentration can be continuously calculated on-line using essentially the model and combined signals of biomass and ethanol transmitters and the total of the feed flow measured signal. Implementation of this model-based sensor was carried out in a programmable digital multiloop controller combined with programmed modules in a supervisory software installed in a Pentium 200 microcomputer. The setup included on-line measurements of ethanol and biomass by sensors-transmitters adapted to appropriate sampling lines of the fed-batch fermentor, filtration equipment, feed and detecting solution tanks, pumps, and all hydraulic and electric accessories needed. Adapted equipment was used for removal of bubbles formed during the fermentation in function of the CO_2 produced in order to avoid interference in the biomass sensor signal.

The configuration of the controller was programmed to couple the signals of ethanol and biomass transmitters and infer the proposed model-based substrate sensor signal using specific calculation blocks. The controller was interfaced using an RS-232-485 interface with the microcomputer, where the supervisory software system was installed. The supervisory system software AimaxWin version 3.1 was configured, and historical trends for both direct and inferred process variables for $P(t)$, $X(t)$, $Pc(t)$, $Xc(t)$, and $V(t)$ could be incorporated directly into the previously designed screens and data sheets and tables.

Table 1
Experimental Operational Conditions and Parameters of Model

Kinetics parameters	Operational conditions
μ_{max} = 0.05 h^{-1}	V_o = 3 L
γ_{max} = 0.20 h^{-1}	P_o = 0 g/L
Yx/s = 0.18 g/g	S_o = 0 g/L
Yp/s = 0.51 g/g	t_f = 4.5 h
Ksx = 0.05 g/L	V_f = 7 L
Ksp = 0.5 g/L	X_o = 54.1 g/L (test 1) and 58.9 g/L (test 2)
Kpx = 66.57 g/L	Sa = 187 g/L (test 1) and 142 g/L (test 2)
Kpp = 78.72 g/L	Temperature = 31–34°C

Operational Conditions and Kinetic Parameters of Model

A set of alcoholic fermentations experiments was conducted in order to verify the performance of the model-based substrate sensor. Diluted molasses was used in the experiments as feed substrate and bread yeast, *Saccharomyces cerevisiae*, as inoculum. The operational conditions and kinetic parameters used are given in Table 1 for two different experiments (tests 1 and 2), and values of ethanol and biomass concentrations were also determined off-line using gas chromatography (CG) and dry cell weight standard *(7)* methods, respectively.

Results

The on-line sensors–measured values for ethanol and biomass were compared with values determined in paired analysis using off-line standard and analytical methods, shown in Fig. 2, and coincident results confirm the reliability of the two sensors. The off-line analytical methods used were GC for ethanol and dry cell weight standard for analysis of cell concentrations. The dry cell weight method was carried out using small volumes of the analyzed solutions that were centrifuged for 10 min at 800*g* and washed three times with water (for sample cells in molasses), and the cell mass obtained was transferred to a vessel weighed previously and dried at 95°C for 48 h. After this time the dry cell mass was weighed, and the sample concentration was expressed as grams of cells/liter of solution.

Figure 3 shows the experimental results of tests 1 and 2 obtained for the substrate concentration calculated using the software sensor and the filtered sensor measurements for ethanol and biomass. The differences between the two experiments are the initial biomass concentration and concentration of substrate in the feed, as shown in Table 1.

Discussion

A viable model-based software substrate sensor was developed, and the model proposed for its implementation was shown to adapt well for

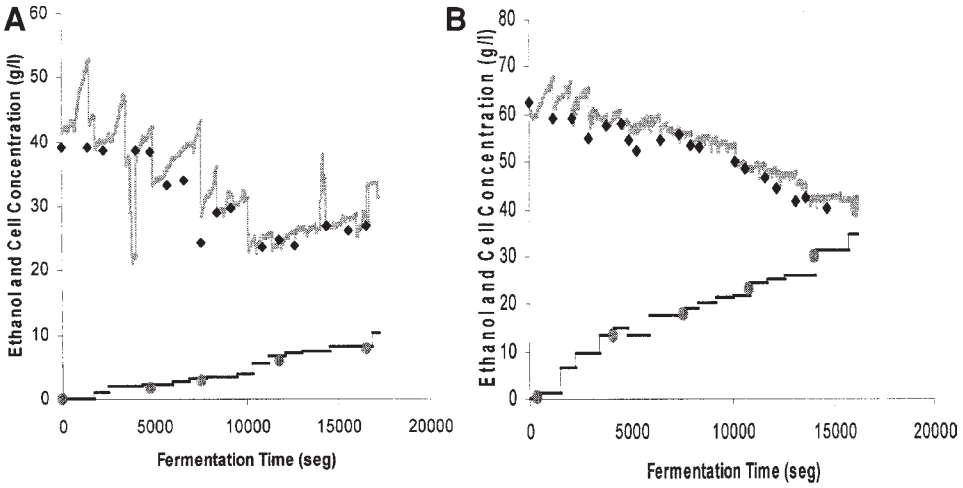

Fig. 2. Sensors on-line measurements (—— ethanol; —— biomass) compared to off-line analytical results (●, ethanol; ◆ biomass) for test 1 **(A)** and test 2 **(B)**.

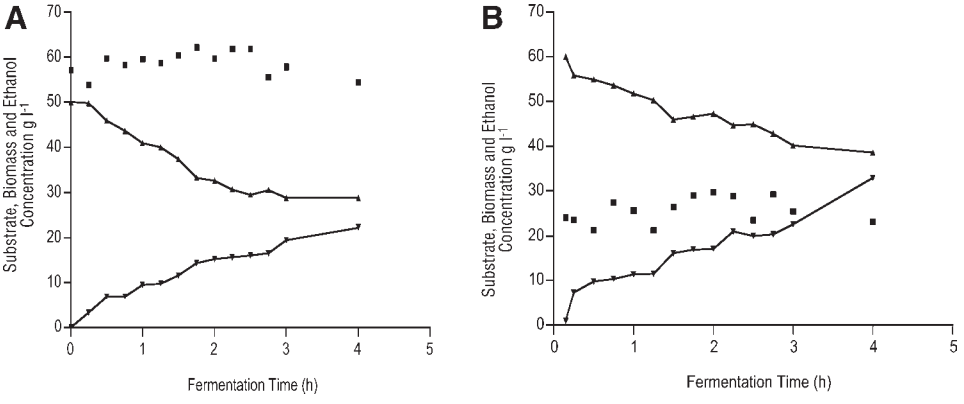

Fig. 3. Sensor filtered signals and inferred model–based substrate concentration for test 1 **(A)** and test 2 **(B)**: (▲) biomass; (▼) ethanol; (■) substrate).

fed-batch alcoholic fermentation. With on-line determinations of ethanol, biomass, and feed flow, it was possible to determine continuously the substrate concentration present in the fermentation medium during the process using this software sensor. The results of the experiments showed that the model presenting a simple, inexpensive, and robust method for substrate determination in fermentation medium, is highly efficient and reliable. In the future, this model also will allow control strategies to be implemented in order to improve the yield and efficiency of the process.

Nomenclature

ART	=	total reducing sugars (g/L)
Fe	=	feed flow to fermentor (L/h)
Kpp	=	inhibition constant of ethanol specific rate (g/L)
Kpx	=	inhibition constant of cell growth rate (g/L)
Ksp	=	saturation constant for specific ethanol production (g/L)
Ksx	=	saturation constant of substrate-microorganism (g/L)
P	=	ethanol concentration in fermentor (g/L)
S	=	substrate concentration (g/L)
Sa	=	substrate concentration in feed (g/L)
t	=	time (h)
V	=	volume of fermentor (L)
X	=	biomass concentration (g/L)
Yp/x	=	product yield coefficient based on biomass (g/g)
Yp/s	=	product yield coefficient based on substrate (g/g)
Yx/s	=	cell yield coefficient based on substrate (g /g)
μ	=	cell growth specific rate (h^{-1})
γ	=	ethanol production specific rate (g/[g·h])

Subscripts

ART	=	total reducing sugars (g/L)
o	=	initial
f	=	final
max	=	maximum value

References

1. Warnes, M. R. (1996), *Process Biochem.* **31,** 147–155.
2. Court, J. R (1988), *Progress in Industrial Microbiology*, vol. 25, Bushell, M. E., ed., Elsevier, Amsterdam, The Netherlands, p. 145.
3. Ebehard, O. V. (1992), *Biotechnol. Bioeng.* **40,** 572–582.
4. Tyagi, R. D., Du, Y. G., and Sreekrishnan, T. R (1993), *Process Biochem.* **28,** 259–267.
5. Ferreira, L. S., De Souza, M. B., and Folly, R.O.M. (2001), *Sens. Actuators B Chem.* **75(3),** 166–171.
6. Miguel Martín, A., Santos, J. P., and Agapito, J. A. (2001), *Sens. Actuators B Chem.* **77(1–2),** 468–471.
7. Salgado, A. M., Folly, R. O. M, and Valdman, B. (2001), *Sens. Actuators B Chem.* **75(1–2),** 24–28.
8. Salgado, A. M., Folly, R. O. M., Valdman, B., and Valero, F (2000), *Biotechnol. Lett.* **22,** 327–330.
9. Folly, R. O. M., Ramirez, N. I., and Valdman, B. (1994), in *Proceedings of the 5th International Symposium on Process System Engineering (PES/94)*, pp. 717–722.
10. Mayer, A. F. (1986), MS Thesis, Department of Engineering, Química EQ-UFRJ, Rio de Janeiro, Brazil.
11. Ghose, R. and Tyagi, B.(1984), *Process Biochem.* **19(4),** 136–141.

0273-2289/04/113/0145–0159/$25.00

Screening of Dowex® Anion-Exchange Resins for Invertase Immobilization

Ester Junko Tomotani and Michele Vitolo*

Department of Biochemical and Pharmaceutical Technology, Pharmaceutical Sciences School, University of São Paulo, Av. Prof. Lineu Prestes, 580, B-16, 05508-900, São Paulo, SP, Brazil, E-mail: michenzi@usp.br

Abstract

Commercial yeast invertase (Bioinvert®) was immobilized by adsorption on anion-exchange resins, collectively named Dowex® (1x8:50-400, 1x4:50-400, and 1x2:100-400). Optimal binding was obtained at pH 5.5 and 32°C. Among different polystyrene beads, the complex Dowex-1x4-200/invertase showed a yield coupling and an immobilization coefficient equal to 100%. The thermodynamic and kinetic parameters for sucrose hydrolysis for both soluble and insoluble enzyme were evaluated. The complex Dowex/invertase was stable without any desorption of enzyme from the support during the reaction, and it had thermodynamic parameters equal to the soluble form. The stability against pH presented by the soluble invertase was between 4.0 and 5.0, whereas for insoluble enzyme it was between 5.0 and 6.0. In both cases, the optimal pH values were found in the range of the stability interval. The K_m and V_{max} for the immobilized invertase were 38.2 m*M* and 0.0489 U/mL, and for the soluble enzyme were 40.3 m*M* and 0.0320 U/mL.

Index Entries: Invertase; immobilization; exchange resins; Dowex®.

Introduction

Invertase (EC 3.2.1.26) catalyzes the hydrolysis of β-fructofuranosides and has been used in analytical chemistry (biosensors), in confectionary, and in the production of inverted syrup *(1)*. Invert sugar syrup, which can be obtained by acid or enzymatic hydrolysis of sucrose, is a valuable commercial product especially in countries where the main sources of sugar are beet or cane. With acid hydrolysis, the final syrup is often contaminated with colored oxidation compounds, which arise from cyclization of hexoses at low pH and high temperatures *(2–4)*. Such a problem does not occur

*Author to whom all correspondence and reprint requests should be addressed.

when using invertase as catalyst for sucrose hydrolysis owing to the mild conditions employed (low temperature and less acidic pH) *(5,6)*.

Over the last 40 yr, an increasing number of researchers studied various methods of protein immobilization and have found widespread application for these methods in many biotechnology areas such as clinical analysis, therapeutic medicine, and the production of biomaterials *(7)*. Among these techniques, adsorption of proteins is very simple, mild, and reversible, permitting reuse of both enzyme and the support *(8)*. Applications of immobilized or adsorbed enzymes as specific catalysts have gained new routes in modern applied chemistry *(9)*.

A good carrier for immobilized enzyme must be a stable material that possesses versatile chemical properties. Among a great variety of these adsorbents, polystyrene ion-exchange resins possess some very promising properties, such as high mechanical stability, good stability against chemical agents, and a matrix structure with various possibilities of altering the mode and degree of functionalization as well as physical parameters *(8,10)*. Several types of bead derivatives of styrene-divinylbenzene (such as Dowex® 1x2, 1x4, and 1x8) are strong basic anion-exchange resins that have been used for at least 50 yr in industrial unit operations such as purification, concentration, and fractionation. They are a nontoxic material and completely inert at the conditions under which the bioconversions are carried out *(11)*. Because the literature has little information about the use of Dowex as a support for immobilizing invertase, this aspect was the aim of the present work.

Materials and Methods

Invertase and Polystyrene Ion-Exchange Resins

The commercial yeast invertase (Bioinvert®) was purchased from Quest International®. Styrene-divinylbenzene bead derivatives having different granulometry (50–400 mesh) and different degrees of crosslinking (2–8%) were purchased from Sigma (St. Louis, MO). All other chemicals were of analytical grade.

Immobilization of Invertase

Immobilization of invertase on the Dowex resin was performed as follows: The anion exchanger (100 mg dry wt) was previously equilibrated in 22 mL of deionized water (pH adjusted to 5.5 by dropping 1 *M* HCl), and the suspension was left for 24 h under agitation (100 rpm) at 32°C. Then, 3 mL of original solution of Bioinvert was added, and the system was left for 4 h under the same conditions. The complex Dowex/invertase was then centrifuged (2880*g*, 30 min), and the protein content in the supernatant was measured. The separated Dowex/invertase complex was rinsed until no protein was detectable in the supernatant, and the final suspension was stored at 4°C in deionized water (pH 5.5).

The percentage of protein retention in Dowex was calculated as follows:

$$AI = \frac{(TAP - STP)}{TAP} \times 100 \quad (1)$$

in which AI is the adsorption index, TAP is the total amount of protein before immobilization, and STP is the supernatant total protein content after 4 h under stirring (100 rpm) at 32°C.

Standard Assay for Measuring Invertase Activity

A standard assay for both forms of enzyme consisted of mixing 108 mL of sucrose solution (120 g/L in 0.010 *M* acetate buffer, pH 5.5) with 12 mL of aqueous invertase solution (diluted 1:5000 [v/v]) or 12 mL of an aqueous suspension of Dowex/invertase (100 mg of powder/mL). Hydrolysis was carried out for 6 min at 37°C under agitation (100rpm), as previously described by Vitolo et al. *(1)*. One soluble or immobilized invertase unit (U) was defined as the amount of total reducing sugar (TRS) (mg) formed per minute under the conditions of the test.

The immobilization coefficient (IC) was determined using Eq. 2:

$$IC = \frac{Activity_1}{Activity_2} \times 100 \quad (2)$$

in which IC is the immobilization coefficient, $Activity_1$ is the immobilized invertase (U), and $Activity_2$ is the soluble invertase (U).

The standard deviation (SD) and the coefficient of variation (CV) related to this method were equal to 6.20×10^{-3} mg/mL and 4.35%, respectively.

Characterization of Soluble and Immobilized Invertase

The pH, temperature, substrate concentration, and storage time of the standard reaction test related to both forms of invertase were changed one by one at the intervals cited above. In each case, the activity corresponded to the slope of the straight line attained through a plot of TRS vs time.

Effect of Temperature on Activity and Stability

The activity of soluble and immobilized invertase was determined by varying the temperature of the standard test within a range of 30–60°C (30, 35, 40, 45, 50, 55, and 60°C). A blank was prepared under the same conditions for each temperature employed. The activation energy (E_a' kJ/mol) was determined by the Arrhenius method, and the thermodynamic parameters were calculated by conventional equations (Eqs. 3–5) *(12)*. The stability of both forms of invertase (aqueous invertase solution [diluted 1:5000, v/v] or an aqueous suspension of Dowex/invertase (100 mg powder/mL]) was evaluated by maintaining the enzyme solution or suspension for 12 min in acetate buffer (0.010 M, pH 5.5) at each

temperature cited. Then, the residual activity was measured as discussed under Standard Assay for Measuring Invertase Activity.

$$\Delta G = \left(\frac{R \times T}{2.303}\right) \times \log\left(\frac{v \times h}{K \times T}\right) \quad (3)$$

$$\Delta H = E_a - R \times T \quad (4)$$

$$\Delta S = \frac{\Delta H - \Delta G}{T} \quad (5)$$

in which ΔG is the Gibb's free energy (kJ/mol), ΔH is the enthalpy (kJ/mol), ΔS is the entropy (kJ/[mol·K]), R is the gas constant (8.31 J/[mol·K]), T is the temperature (K), v is the enzyme activity, h is the Planck constant (3.978×10^{-23} J/min) and K is the Boltzman constant (1.38×10^{-23} J/K).

Thermal Inactivation of Soluble and Immobilized Invertase

Aqueous invertase solutions (soluble and immobilized enzyme) were incubated in acetate buffer (0.010 *M*, pH5.5) for 20, 40, 60, 80, and 120 min at 30, 37, 40, 45, 50, and 55°C. After incubation at each specified time, both forms were assayed for residual activity according to the standard procedure (*see* Standard Assay for Measuring Invertase Activity).

Effect of pH on Activity and Stability

The effect of pH on the activity and stability of soluble and immobilized invertase was determined always at 37°C by mixing the enzyme with buffer solutions at fixed pH. The buffers were prepared according to Bacilla et al. *(13)*. For soluble invertase, the pH values employed were 3.0, 3.5, 4.0, 4.5, 5.0, 5.5, 6.0, and 6.5, and for immobilized invertase they were 4.5, 5.0, 5.5, 6.0, and 6.5. The stability against pH was determined by measuring the residual activity of both forms of invertase after 12 min of enzyme-buffer contact.

Effect of Sucrose Concentration on Invertase Activity

The kinetic parameters (K_m and V_{max}) were determined through the conventional Lineweaver-Burk method, by varying the sucrose concentration between 10.0 and 292 m*M*.

Evaluation of Shelf Life of Immobilized Invertase

Concerning storage stability, four Dowex/invertase complexes were kept in deionized water (pH adjusted to 5.5) for 28 d at 4°C. After every 7 d the residual activity was measured.

Analytical Techniques

Determination of Protein

Protein was determined according to Segel *(14)*, by the difference between ultraviolet absorbance measured at 215 and 225 nm, using bovine serum albumin (Sigma) as a standard. The SD and the CV were 1.51 µg/mL and 3.48%, respectively.

Table 1
AI, Catalytic Activity, IC and Enzyme Retention After Hydrolysis for Invertase Adsorbed in Several Types of Dowex Anion-Exchange Resins

Dowex	AI (%)	Activity (soluble enzyme) (U/mL)	Activity (immobilized enzyme) (U/mL)	IC (%)	Retention after hydrolysis (%)
1x2-100	100	0.0214	0.0287	100	86.2
1x2-200	100	0.0214	0.0178	83.2	100
1x2-400	100	0.0214	0.0170	79.4	78.2
1x4-50	92.4	0.0214	0.0136	63.7	100
1x4-100	73.2	0.0214	0.0182	84.9	100
1x4-200	100	0.0214	0.0214	100	100
1x4-400	100	0.0214	0.0153	71.6	67.9
1x8-50	99.5	0.0214	5.00×10^{-4}	2.10	100
1x8-100	98.6	0.0214	0.0108	50.6	99.9
1x8-200	97.0	0.0214	0.0122	56.8	100
1x8-400	81.3	0.0214	0.0291	100	89.0

Measurement of TRS

TRS were measured by the method of Somogyi-Nelson *(15)* as described by Arruda and Vitolo *(16)*. The SD and the CV were 3.50×10^{-3} mg/mL and 3.86%, respectively.

Results and Discussion

Immobilization Efficiency

By applying the immobilization procedure described under Immobilization of Invertase, invertase was bound by all polystyrene beads tested, having an AI always higher than 70% (Table 1). Since the p*I* of invertase is equal to 4.0 *(17)*, its molecules in the immobilization medium (pH 5.5) had a net negative charge, which allowed it to interact strongly with the positively charged groups of the resins.

Table 1 shows that some Dowex/invertase complexes, in which the resins used were 1x2-200, 1x4-50, 1x4-100, 1x4-200, 1x8-50, and 1x8-200, retained 100% of protein molecules during sucrose hydrolysis. The absence of enzyme desorption from the support enhances the half-life of the immobilized complex when employed in repeated-batch or continuous processes *(18)*.

Furthermore, the IC for almost all Dowex/invertase complexes varied from 50.6 to 100% (Table 1), probably owing to the different mesh and crosslinking degree of the resin granules. Immobilization coefficient values of that magnitude (50.6–100%) are quite relevant when compared with other methods for invertase immobilization described in the literature *(5)*.

Table 2
Thermodynamic Parameters Calculated at 37°C[a]

Invertase	E_a (kJ/mol)	ΔG (kJ/mol)	ΔH (kJ/mol)	ΔS (kJ/[mol·K])
Soluble	37.3	–14.2	34.5	0.16
Immobilized	37.2	–14.0	34.6	0.16

[a]E_a was calculated through Arrhenius' plot.

By contrast, the Dowex-1x8-50/invertase complex had an IC of 2%, though AI and protein retention were 100%. A reasonable hypothesis for understanding this result might be related to the quite high occurrence of undesirable interactions between the active site and/or another sensitive domain of the enzyme with charged chemical groups of the resin *(11)*. Such a phenomenon, although with more or less intensity, could also have contributed to the IC variation observed for other Dowex/invertase complexes.

Undoubtedly, the best immobilized complex attained was Dowex-1X4-200/invertase, because all its immobilization efficiency parameters (AI, IC, and protein retention) were equal to 100% (Table 1). Therefore, this complex was chosen for characterization assay purposes.

Effect of Temperature

From Fig. 1 it can be seen that the highest activity for both soluble (0.0569 U/mL) and immobilized (0.0559 U/mL) invertase occurred at 55 and 50°C, respectively. As the maximal activities differed <2%, one can assume that the immobilization procedure did not significantly affect the tertiary and quarternary structures of the invertase.

By applying the conventional Arrhenius method to the data related to the activity vs temperature (Fig. 1), it was possible to establish the following equations (Fig. 2):

$$\log v = 4.61 - 1.95 \times 10^3 \left(T^{-1}\right) \quad (6)$$

$$\log v = 4.70 - 1.94 \times 10^3 \left(T^{-1}\right) \quad (7)$$

in which T is the absolute temperature (K).

The activation energy (E_a), calculated through the inclination of $\log v \times T^{-1}$ (Eqs. 6 and 7), and the thermodynamic parameters (ΔH, ΔS, and ΔG), calculated through Eqs. 3–5, for both forms of invertase are presented in Table 2. As can be seen, the values of those parameters were quite similar for both soluble and immobilized invertase. This fits very well with the previous assumption that the immobilization technique has little effect on enzyme structure. It could be speculated that the reaction catalyzed by either soluble or insoluble invertase is constituted by identical thermodynamic systems.

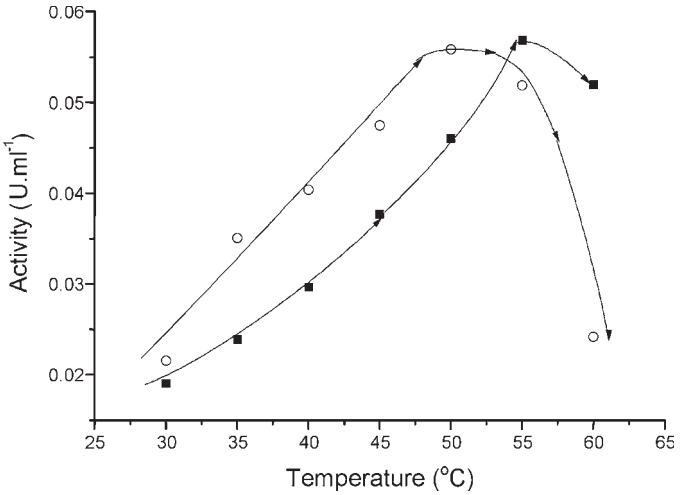

Fig. 1. Effect of temperature on activity of soluble invertase (■) and Dowex-1x4-200/invertase complex (○).

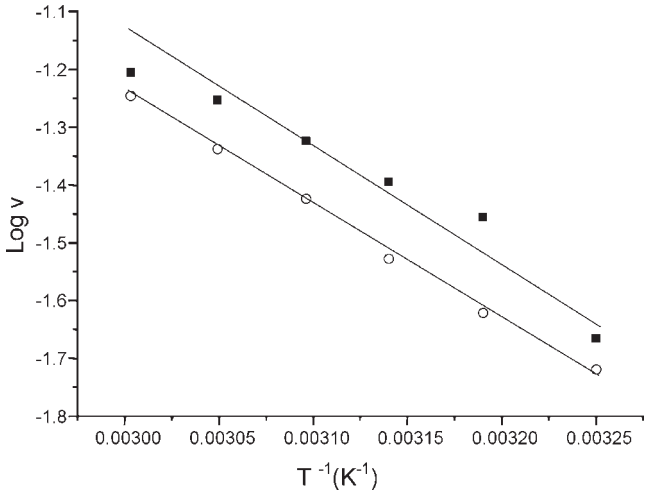

Fig. 2. Arrhenius plot for calculation of E_a for both soluble invertase (■) and Dowex-1x4-200/invertase complex (○).

The same entropy values (0.16 kJ/[mol·K]) should indicate a similar distribution of invertase molecules inside both systems. In other words, when dissolved in aqueous medium, the invertase molecules, which are natural dimers, attract each other, forming aggregates with high molecular weight (mainly hexamers and octamers) and increased hydrolytic activity *(19)*. The hexamers and octamers should be adsorbed unaltered by the pellets of Dowex-1x4-200.

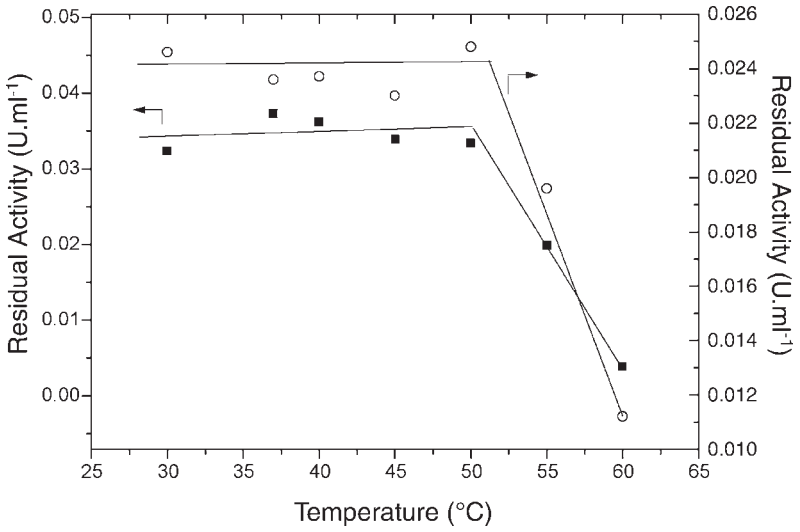

Fig. 3. Effect of temperature on stability of soluble invertase (■) and Dowex-1x4-200/invertase complex (○).

Table 3
Logarithm of Soluble Invertase Activity
Against Time at Several Temperatures

	log v				
Time (min)	(37°C)	(40°C)	(45°C)	(50°C)	(55°C)
20	–1.61	–1.62	–1.59	–1.57	–2.27
40	–1.63	–1.63	–1.62	–1.57	–2.37
60	–1.66	–1.65	–1.58	–1.61	–2.51
80	–1.66	–1.60	–1.60	–1.59	–2.62
120	–1.62	–1.62	–1.59	–1.61	–2.86

As shown in Fig. 3, both invertase forms were stable in the temperature range of 30–50°C. At 55°C the residual activity for soluble and insoluble invertase diminished about 18 and 40%, respectively, whereas at 60°C the reductions were 55 (soluble invertase) and 88% (Dowex-1x4-200/invertase).

In the range of temperatures selected for evaluation, the soluble invertase presented detectable instability only at 55°C (Table 3 and Fig. 4). Hence, the thermodynamic parameters for the heat inactivation of invertase ($\Delta G'$, $\Delta H'$, $\Delta S'$ and E_a') were not determined, because the correlation $\log k' \times T^{-1}$ might necessarily be established, as proposed by Owusu and

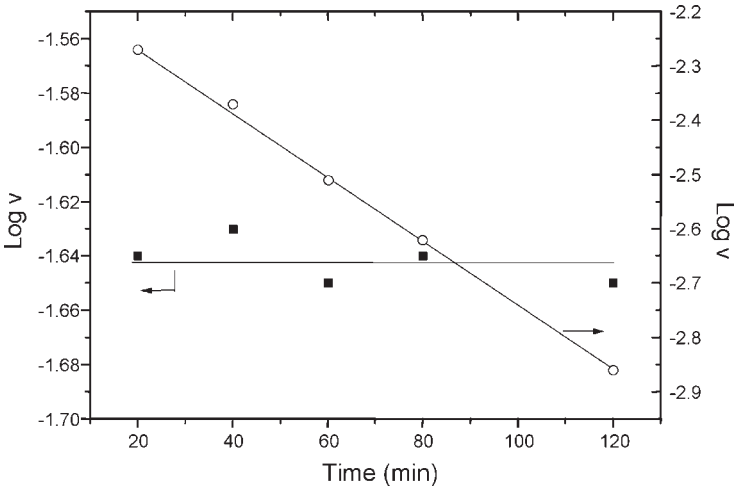

Fig. 4. Logarithm of soluble invertase activity vs time at 37°C (■) and 55°C (○).

Makhzoum *(20)*. However, the deactivation rate constant (k') at 55°C for soluble invertase was equal to 6.00×10^{-3}/min, as calculated through Eq. 8 (Fig. 4):

$$\log v = -6.00 \times 10^{-3} \cdot t - 2.14 \quad (r = 0.9998) \tag{8}$$

The relevance of the latter information lies in the fact that the activity loss (0.6%/min, in this case) can be compensated by adding an appropriate quantity of invertase, when the hydrolysis reaction is carried out at 55°C. Such a condition could apply when the reaction is carried out at a sucrose concentration higher than 150 g/L, at which viscosity should be diminished by increasing the operational temperature.

Since all ($\log v \times t$) curves were linear (Fig. 5), the following equations were established:

$$(30°C) \quad \log v = -6.00 \times 10^{-4} \cdot t - 1.57 \quad (r = 0.996) \tag{9}$$

$$(37°C) \quad \log v = -2.30 \times 10^{-3} \cdot t - 1.70 \quad (r = 0.993) \tag{10}$$

$$(45°C) \quad \log v = -1.09 \times 10^{-2} \cdot t - 2.44 \quad (r = 0.990) \tag{11}$$

$$(55°C) \quad \log v = -2.92 \times 10^{-2} \cdot t - 2.71 \quad (r = 0.997) \tag{12}$$

By plotting $\log k'$ against T^{-1}, a straight line was attained (Fig.6), the equation was as follows:

$$\log k' = 19.2 - 6.77 \times 10^{3} \cdot T^{-1} \quad (r = 0.993) \tag{13}$$

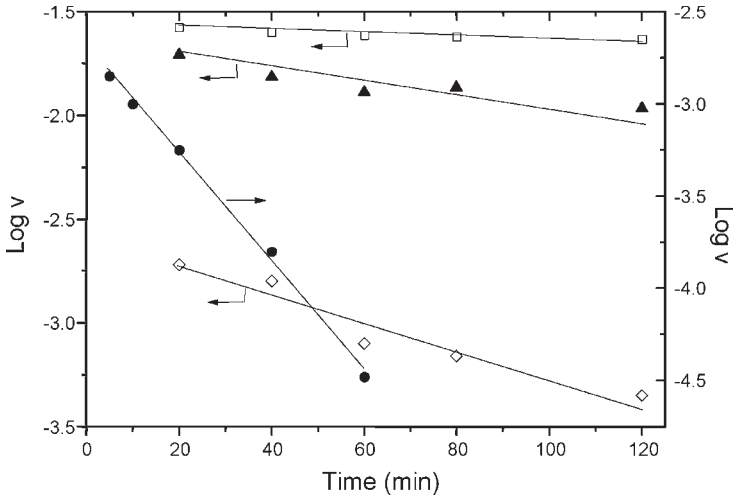

Fig. 5. Logarithm of Dowex-1x4-200/invertase complex activity vs time at 30 (□), 37 (▲), 45 (◇), and 55°C (●).

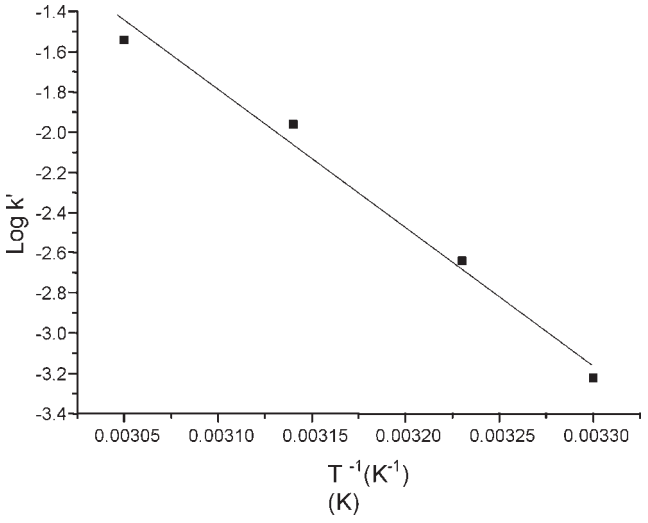

Fig. 6. Arrhenius plot for calculation of E_a related to heat inactivation of Dowex-1x4-200/invertase complex.

From Eq. 13 the activation energy (E_a') related to the heat inactivation of Dowex-1x4-200/invertase complex was calculated as 129 kJ/mol. Combining the E_a' value with the conventional thermodynamic equations *(20)*, it was possible to calculate the corresponding $\Delta G'$, $\Delta H'$ and $\Delta S'$, which were equal to –81.0 kJ/mol, 127 kJ/mol, and 0.660 kJ/(mol·K), respectively.

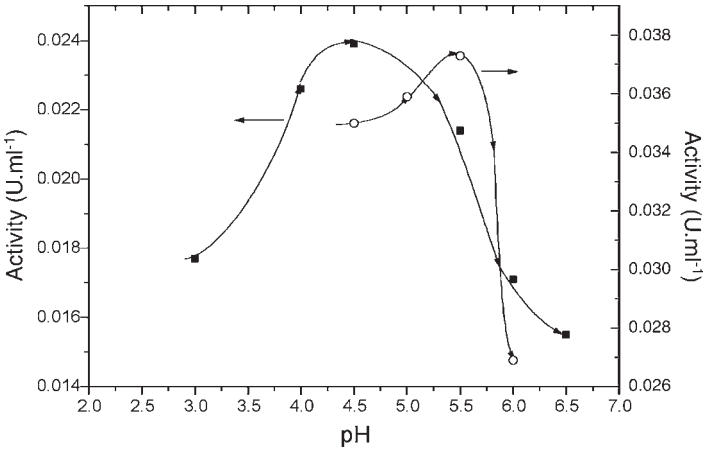

Fig. 7. Effect of pH on activity of soluble invertase (■) and Dowex-1x4-200/invertase complex (○).

According to Owusu and Makhzoum *(20)* $\Delta H'$ values of about 200–300kJ/mol would lead to unfolding of the tertiary structure of a protein. However, the Dowex-1x4-200/invertase complex had a $\Delta H'$ 37% lower than these values, indicating that the declining invertase activity vs temperature is probably owing to the breakup of the supramolecular structures of invertase rather than to the irreversible unfolding of the macromolecular tertiary structure.

At 55°C, k' was 0.006 (Eq. 8) and 0.0292 min^{-1} (Eq. 12), respectively, for soluble and insoluble invertase. As can be seen, the activity of Dowex-1x4-200/invertase complex diminished at a rate fivefold higher than the soluble enzyme, as the time increased. One possible explanation could be related to the probable different patterns of internal heat transference presented by a solution and a suspension. In a suspension, a significant portion of the thermal energy would accumulate in the resin particles in which the invertase molecules are adsorbed. As a consequence, the molecules should be submitted to a higher thermal energy than when they are homogeneously dispersed in a solution.

Effect of pH

The activity and stability of both forms of invertase against pH are presented in Figs. 7 and 8, respectively. Since the p*I* of invertase is equal to 4.0 *(17)*, the immobilized invertase was not submitted at a pH lower than 4.0 to avoid desorption of the enzyme from the support. The highest activities for soluble and immobilized invertase occurred at pH 4.5 and 5.5, respectively. Moreover, both soluble and Dowex-1x4-200/invertase were stable at a pH interval of 4.0 to 5.0 and 5.0 to 6.0, respectively. It must be pointed out that in both cases the optimum pH was within the stability interval.

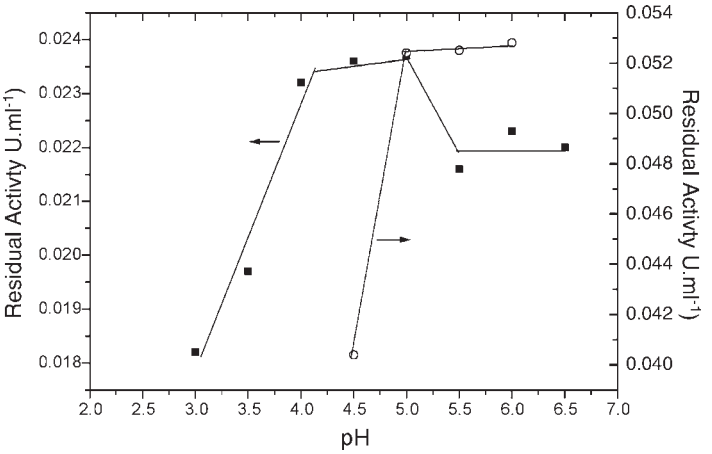

Fig. 8. Effect of pH on stability of soluble invertase (■) and Dowex-1x4-200/invertase complex (○).

By comparing the profiles of activity vs pH curves of both forms of invertase, a shifting of about one pH unit toward less acidic pH values was observed for the immobilized form (Fig. 7). According to Vitolo and Barros *(5)* such a shift could be attributed to the fact that the concentration of charged particle species (e.g., hydrogen ions) in the domain of the immobilized enzyme is different from that in the bulk solution, owing to electrostatic interactions with the fixed charges on the carrier. Unfortunately, the glass electrode effectively measures the pH in the bulk solution. Since the Dowex resins used in the present work had positively charged chemical groups, a shift toward a more acidic pH range would be expected, because the hydrogen ions should be repelled from the pellets, increasing their concentration in the bulk solution. However, exactly the opposite was observed (Fig. 7). One explanation is that the resin granules were fully covered by negatively charged invertase molecules, and as a consequence, the hydrogen ions would preferably accumulate near the particles of Dowex/invertase complex, leaving the bulk solution less acidic.

Effect of Sucrose Concentration

The activities of free and immobilized invertase for various substrate concentrations are plotted in a Lineweaver-Burk graph, from which V_{max} and K_m values were calculated (Fig. 9). The K_m of free enzyme was 40.3 m*M*, while the apparent K_m was 38.2 m*M* for the immobilized one. These similar K_m values for both forms indicate that enzyme-substract interaction is not substantially altered after immobilization. However, the V_{max} for immobilized invertase (0.0489 U/mL) was 35% higher than the V_{max} for soluble invertase (0.0320 U/mL). Such a difference could be explained by the predominance of supramolecular aggregates (hexamer, octamer forms) guaranteed under the conditions of the immobilization assay.

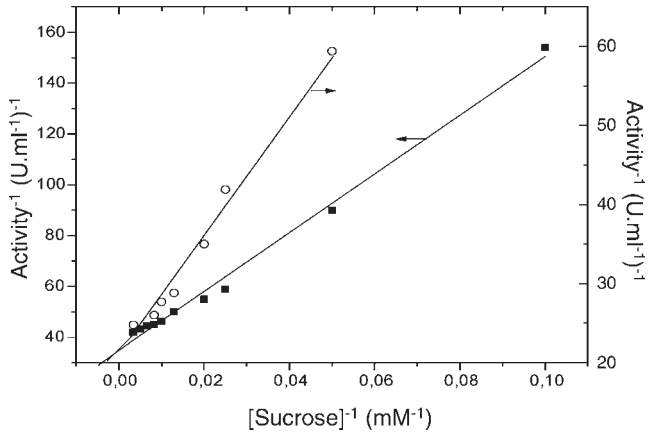

Fig. 9. Lineweaver-Burk plot for soluble invertase (■) ($V^{-1} = 1.26 \times 10^3[S] + 31.2$ [r = 0,997]) and Dowex-1x4-200/invertase complex (○) ($V^{-1} = 7.81 \times 10^2[S] + 20.5$ [r = 0,990]).

Table 4
Storage Stability of Dowex-1x4-200/Invertase
Complex Maintained in Deionized Water at 4°C for 28 d

Time (d)	AI (%)	Activity (U/mL)	IC (%)
1	100	0.0263	100
7	100	0.0325	100
14	100	0.0211	98.6
21	100	0.0246	100
28	100	0.0167	78.0

Storage Stability of Immobilized Invertase

Enzymes are not stable during storage in solution and their activities decrease gradually over time *(21)*. Immobilization technique, on the other hand, is applied considering lifetime, durability, and storage stability as important parameters. It puts the enzyme into a more stable position in comparison to free enzyme. The Dowex/invertase complexes kept at 4°C in deionized water were evaluated. Table 4 shows that after 21 d, the immobilized complexes maintained 100% of AI and retained their initial activity. These results are in accordance with the storage stability of immobilized pectinase on anionic polystyrene beads, which was stable and retained its initial activity for at least 7 wk of storage at 4°C *(22)*.

Conclusions

The data presented lead to the general conclusion that Dowex anion-exchange resins (types 1x8:50-400, 1x4:50-400, and 1x2:100-400 styrene-

divinylbenzene copolymers with different granulometry [50–400 mesh] and different degrees of crosslinking [2–8%]) are suitable for adsorbing invertase (aqueous medium at pH 5.5 and 32°C). We selected the complex Dowex-1x4-200/invertase, taking into account aspects such as high operational stability (no release of enzyme from the carrier during sucrose hydrolysis), good storage performance in deionized water (100% of the invertase activity was maintained after 21 d at 5°C), and AI and IC both equal to 100%. Since the maximal activity of soluble invertase and Dowex-1x4-200/invertase differed <2 %, it was assumed that the immobilization procedure did not significantly affect the enzyme conformation. These points make the complex Dowex-1x4-200/invertase highly suitable for use in invertase immobilization. The reutilization of Dowex/invertase complex and diminution of 5°C in the reaction temperature (less demand for energy) will lead to an overall cost reduction in the future use of the complex Dowex-1x4-200/invertase in the continuous sucrose hydrolysis process.

Acknowledgments

This work was supported by research grants from Fundação de Amparo à Pesquisa do Estado de São Paulo, Brazil.

References

1. Vitolo, M., Duranti, M. A., and Pellegrim, M. B. (1995), in *Proceedings of the 8th European Biomass Conference*, Chartier, A., Beenackers, C., and Grassi, G., eds., Pergamon, London, UK, pp. 1433–1438.
2. Monsan, P. and Combes, D. (1984), *Biotechnol. Bioeng.* **26,** 347–351.
3. Vitolo, M. and Yassuda, M. T. (1992), *Biotechnol. Lett.* **13(1),** 53–56.
4. De Queiroz, A. A., Vitolo, M., Oliveira, R. C., and Higa, Z. O. (1996), *Radiat. Phys. Chem.* **47(6),** 873–880.
5. Vitolo, M. and Barros, D. P. (1992), *Lebensm. Wiss. Technol.* **25,** 240–243.
6. Cheetam, P. S. J. (1998), *J. Biotechnol.* **66,** 3–10.
7. De Queiroz, A. A., Vargas, R. R., Higa, O. Z., Ribeiro, R. R., and Vitolo, M. (2002), *J. Appl. Polym. Sci.* **84,** 767–777.
8. Abdellah, H. A., Baker, T. M. A., Shekib, L. A., and El-Iraqi, S. M. (1992), *Food Chem.* **43,** 369–375.
9. Dabrowsky, A. (2001), *Adv. Colloid Interface Sci.* **93,** 135–224.
10. Mansfeld, J. and Schellenberger, A. (1987), *Biotechnol. Bioeng.* **29(1),** 72–78.
11. Ribeiro, R. R. and Vitolo, M. (1997), in *Proceedings of Biomass Conference of the Americas*, vol. 2, Overend, R. P. and Chornet, E., eds., Pergamon, Montreal, Quebec, Canada, pp. 1155–1162.
12. Castellan, G. W. (1976), *Físico-Química*, Livros Técnicos e Científicos, Rio de Janeiro, Brazil.
13. Bacilla, M., Villela, G. G., Tastaldi, H. (1972), *Técnicas e Experimentos de Bioquímica*, Guanabara-Koogan, Rio de Janeiro, Brazil.
14. Segel, I. H. (1979), *Bioquímica*, Livros Técnicos e Científicos, Rio de Janeiro, Brazil.
15. Somogyi, M. (1952), *J. Biol. Chem.* **195(1),** 19–23.
16. Arruda, L. M. O. and Vitolo, M. (1996), *Appl. Biochem. Biotechnol.* **81(1),** 23–33.
17. Dautzenberg, H., Koetz, J., Philipp, B., Rother, G., Schellenberger, A., and Mansfeld, J. (1991), *Biotechnol. Bioeng.* **38(9),** 1012–1019.

18. Vitolo, M. (2001), in *Biotecnologia Industrial: Engenharia Bioquímica*, vol 2, Schmidell, W., Lima, U. A., Aquarone, E., and Borzani, W., eds., Edgard Blucher, São Paulo, Brazil, pp. 373–396.
19. Reddy, A. V., Maccoll, R., and Maley, F. (1990), *Biochemistry* **29(10),** 2482–2487.
20. Owusu, R. K. and Makhzoum, M. (1992), *Food Chem.* **44,** 261–268.
21. Tümtürk, G. A., Arslan, F., Disli, A., and Tufan, Y. (2000), *Food Chem.* **69,** 5–9.
22. Demir, N., Acar, J., Sarioglu, K., and Mutlu, M. (2001), *J. Food Eng.* **47,** 275–280.

0273-2289/04/113/0161–0171/$25.00

Effects of Carbon Source on Expression of Alcohol Oxidase Activity and on Morphologic Pattern of YR-1 Strain, a Filamentous Fungus Isolated from Petroleum-Contaminated Soils

Carmen Rodríguez Robelo, Vanesa Zazueta Novoa, and Roberto Zazueta-Sandoval*

Instituto de Investigación en Biología Experimental, Facultad de Química, Universidad de Guanajuato, Noria Alta s/n, Apartado Postal 187, Guanajuato, Gto. 36000, México, E-mail: zazueta@quijote.ugto.mx

Abstract

Soluble alcohol oxidase (AO) activity was detected in the supernatant fraction of a high-speed centrifugation procedure after ballistic cellular homogenization to break the mycelium from a filamentous fungus strain named YR-1, isolated from petroleum-contaminated soils. AO activity from aerobically grown mycelium was detected in growth media containing different carbon sources, including alcohols and hydrocarbons but not in glucose. In previous work, zymogram analysis conducted with crude extracts from aerobic mycelium of YR-1 strain indicated the existence of two AO enzymes originally named AO-1 and AO-2. In the present study, we were able to separate the AO-1 band into two bands depending on culture conditions, carbon source, and polyacrylamide gel electrophoresis (PAGE) separation conditions; the enzyme activity pattern in zymograms from cell-free extracts exhibited three different bands after native PAGE. New nomenclature was used for upper bands AO-1 and AO-2 and lower band AO-3, respectively. The expression of AO activity was studied in the absence of glucose in the culture media and in the presence of hydrocarbons or petroleum as sole carbon source, suggesting that AO expression could be subjected to two regulatory possibilities: carbon catabolite regulation by glucose and induction by hydrocarbons. The possibility of catabolic inhibition of AO by glucose in the active enzyme was also tested, and the results confirm that this kind of regulatory mechanism is not present in AO activity.

*Author to whom all correspondence and reprint requests should be addressed.

Index Entries: Alcohol oxidase; filamentous fungi; hydrocarbon biodegradation; petroleum contamination; YR-1 strain.

Introduction

Hydrocarbon represents an enormous energy resource without which our actual modern lifestyle would be impossible. Principally exploited as fossilized fuels, hydrocarbons must be considered a finite resource although methane and lignin are certainly renewable. As well as being the predominant energy source in most countries, hydrocarbons are also an important feedstock for the chemical industry. Their potential impact in biotechnology processes is enormous. Unfortunately, hydrocarbon compounds are major environmental pollutants, as a result of improper disposal processes or spills of petroleum or petroleum-derived products. These facts and the continuous increase in the number of toxic compounds generated by the oil industry have emphasized the importance of the development of effective processes to eliminate these waste products *(1)*. In nature, there exist many types of microorganisms that are useful in the biodegradation processes of these hazardous materials. Because natural biodegradation rates of this kind of contaminant, principally in soils, are very low and limited by environmental factors and by adaptation difficulties of microbial populations, it is important to develop methods to increase the bioavailability of contaminants and, finally, to eliminate these compounds from soils *(1)*.

Many microorganisms are capable of using hydrocarbons as the only carbon and energy source; however, when the number of carbon atoms in the hydrocarbon chain is increased to a certain amount, only several microorganisms are capable of metabolizing the hydrocarbonated chains *(2)*. The first step in aliphatic-hydrocarbon biodegradation is catalyzed by an oxygenase named cytochrome P-450, followed by the action of an alcohol oxidase (AO) *(3)*. This enzyme is capable of using as substrates a wide range of xenobiotic compounds, and by means of many types of chemical transformations, this leads to the production of alcohols; P-450 can be found in microorganisms as well as in plants and animals *(4)*. The oxidation of alcohols to the corresponding aldehyde is catalyzed by AO; aldehyde is in turn converted to the corresponding carboxylic acid *(5)*. The reactions catalyzed by Cyt-p450 and AO are special points for bioremediation chemistry. So far most of the studies regarding the role of AO in hydrocarbon metabolism have been made on bacterial strains, and in several cases AO enzymes from eukaryotic origin with physiologic roles related to hydrocarbon metabolism have been reported *(6)*.

In the present work, we continue the studies of AO activity in the YR-1 strain. We describe some differences in morphologic development as a result of the presence of glucose or hydrocarbons present in culture media. Regarding AO activity, the results suggest the possibility that AO expression could be regulated by two mechanisms—catabolite repression by glucose and induction by hydrocarbons—and discard the inhibition of AO activity by glucose as a regulatory mechanism.

Materials and Methods

Chemical and Reagents

Phenylmethylsulfonyl fluoride (PMSF) and yeast AO were purchased from Sigma (St. Louis, MO), and the alcohol substrates were from J.T. Baker (Phillipsburg, NJ). All other reagents were of the highest purity commercially available. Protein was measured by the method of Lowry *(7)* using bovine serum albumin as standard.

Organisms and Culture Conditions

The isolation of filamentous fungi able to grow on hydrocarbons was performed using as a source petroleum-contaminated soil samples collected from the Salamanca refinery (Guanajuato, México). The primary and secondary selections were achieved using minimal medium with the addition of 1% methanol or 1% hexadecane, respectively. The isolates were named YR, and the particular strain used was named YR-1; in all cases colonial and microscopic morphologies were established as criteria for the assessment of the isolated strains as filamentous fungi. As a wild-type AO-proficient (AO^+) organism, we used strain R-25 of *Hansenula polymorpha (8)*. Yeast-peptone-glucose (YPG) complete medium *(9)*, and salts minimal medium with the addition of 0.1% peptone (named sMMP) containing the specified amounts of glucose or hydrocarbons as carbon sources, were used to cultivate the fungus. Strains were maintained in agar slant tubes, and spores were obtained after growth in YPG medium as described previously *(9)*. Liquid cultures (600 mL) were propagated in 2-L Erlenmeyer flasks inoculated with spores at a final cell density of 5×10^5/mL and incubated in a reciprocating water bath shaker at 28°C for different periods of time (*see* Fig. 3). To obtain aerobic mycelium, spores were inoculated in YPG medium, and in sMMP supplemented with glucose (0.1%), decane (1.0%), or hexadecane (1.0%), and the cultures were incubated aerobically *(9)*.

Preparation of Cell-Free Extracts

Mycelial cells were processed and broken as described by Torres-Guzmán et al. *(10)* with some modifications. Briefly, mycelial cells were washed and suspended in buffer (20 m*M* Tris-HCl [pH 8.5] containing 1 m*M* PMSF). A volume of about 20 mL of cells was mixed with an equal volume of glass beads (0.45–0.50 mm in diameter) and disrupted in a Braun Model MSK cell homogenizer (Braun, Melsungen, Germany) through four periods of 30 s each one under a stream of CO_2. The homogenate was centrifuged at 4360*g* for 10 min to remove cell walls and unbroken cells. The cell wall-free supernatant (crude extract) was centrifuged at 164,500*g* for 45 min; the resulting pellet, a mixed membrane fraction, was discarded and the 164,500*g* supernatant (cytosolic fraction) was saved for enzyme determinations.

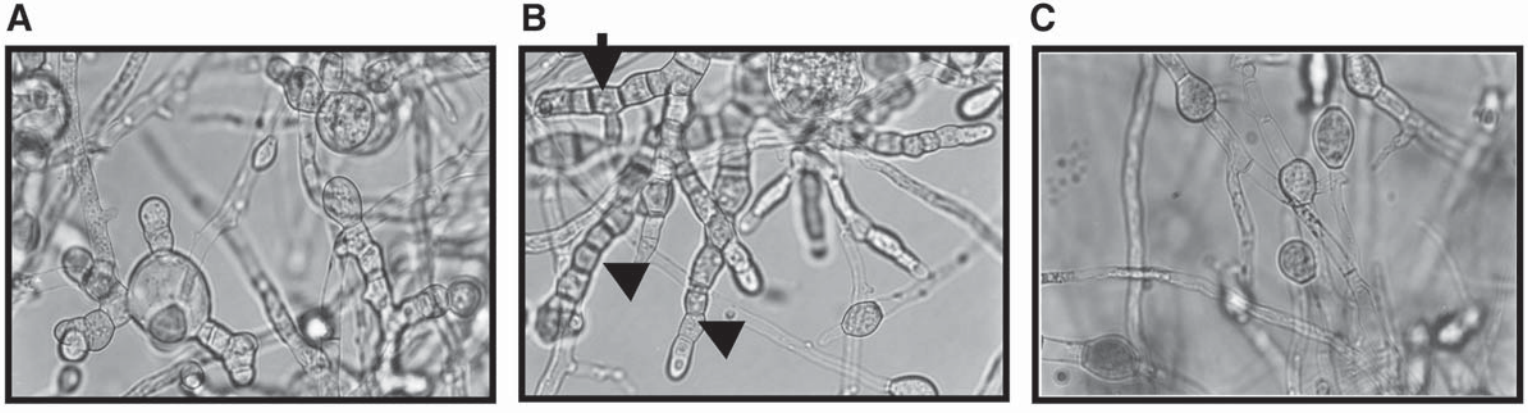

Fig. 1. Growth of YR-1 strain in different carbon sources. The microorganism was grown in sMMP with added glucose **(A)**, hexadecane **(B)**, or petroleum **(C)**. Magnification: ×400. Arrows shows specific structures formed only in medium with hexa-decane as the sole carbon source.

Enzyme Assays

AO activity was measured according to Janssen et al. *(11)*; the enzyme assays were performed at 25ºC in reaction mixtures of 1.0 mL total volume containing 780 µL of reactive A made of 1.2 mL of 0.2 *M* potassium phosphate buffer, pH 7.5; 10 µL of 1.0% *o*-dianisidine dissolved in 0.025 *M* HCl; 5 µL of 3% peroxidase (0.01% final concentration); 150 µL of 0.2 *M* potassium phosphate buffer; 15 µL of substrate (hexadecanol, decanol, or methanol); and 50 µL of cell-free extract (100–200 µg of protein). The reaction was started after adding substrate and development of color measuring the absorbance at 460 nm in a Beckman DU-650 spectrophotometer. In experiments in which the pH of the reaction was varied, phosphate (50 m*M*) and Tris-HCl (50 m*M*) buffers were employed. One unit of enzyme activity was defined as the amount of enzyme that leads to the production of 1 µmol of H_2O_2 . min at 25°C. AO specific activity was expressed as units per milligram of protein. AO activity in zymograms was detection by nondenaturing polyacrylamide gel electrophoresis (PAGE), following a variation of a spectrophotometric method *(11)*. Briefly, aftera nondenaturing 6% (w/v) PAGE, the gel was submerged in the following solution: 4 mL of 0.2 *M* potassium phosphate buffer, pH 7.5; 4 mL of 0.04% peroxidase; 0.4 mL of 0.01% *o*-dianisidine; 0.4 mL of substrate (methanol, ethanol, hexadecanol, and so on); and 31.8 mL of H_2O. After incubating at 25°C for 60 min with gentle shaking, AO electromorphs were observed as brown bands.

Electrophoresis

PAGE analysis of protein from different samples was carried out in slab gels using 6% (w/v) polyacrylamide with the buffer system of Laemmli *(12)*. After electrophoresis, proteins were visualized in the gels by Coomassie Blue R-250 staining (Sigma).

Results

Morphologic Patterns of YR-1 Strain in Different Carbon Sources

Strain YR-1 exhibited different morphologic patterns depending on the carbon source added to the sMMP culture medium. As can be seen in Fig. 1, the growth of YR-1 in glucose was typically the hyphae. However, in both hexadecane and petroleum the hyphae exhibited structures quite different from normal growth. In hexadecane, some segmented structures (Fig. 1B) were present only in this carbon source.

AO Activity in Cell-Free Extracts from Mycelial Cells

The presence of AO activity was analyzed in different cell extracts (crude extracts, 164,500*g* supernatant fractions) of aerobically grown mycelium of strain YR-1 obtained in sMMP or sMM containing 1.0% glycerol, decane, hexadecane, or glucose at different concentrations as carbon

Table 1
AO Activity of YR-1 Strain Grown in Different Culture Media[a]

	AO activity (U)[b]		
Sample	Methanol	Ethanol	Hexadecanol
SMMP	6.87×10^{-7}	1.97×10^{-5}	1.67×10^{-5}
sMMP–1% glycerol	4.25×10^{-7}	1.64×10^{-5}	1.14×10^{-6}
sMMP–1% hexadecane	0.050	0.27	0.20
sMMP–1% decane	0.053	0.28	0.25
sMM–1% hexadecane	No growth	No growth	No growth
sMM–0.2% glucose sMM–1.0% glucose sMMP–0.2% glucose sMMP–0.4% glucose	Growth and no AO detected	Growth and no AO detected	Growth and no AO detected

[a]Enzyme activity was determined in the 164,500*g* supernatant from mycelial cells grown in the indicated culture media. Mycelial cells were broken and the cytosolic fraction was obtained by centrifugation. AO was measured with methanol, ethanol, or hexadecanol as substrates, as described in Materials and Methods. The values are the means of three independent experiments with triplicate determinations in each use.

[b]One unit of activity, 1 µmol of H_2O_2 /[mg of protein (min)].

source. Table 1 shows AO activity levels when the strain was grown in different culture media, using methanol, ethanol, or hexadecanol to assay enzyme activity. AO activity was detected with methanol, ethanol, or hexadecanol as enzyme substrates only when the fungus was grown in media with the addition of peptone and without glucose. On the other hand, AO activity was only detected when the fungus was grown in minimal media containing decane or hexadecane as carbon sources. Figure 2A shows AO zymograms using hexadecanol as substrate. As can be observed in lane 1 of Fig. 2A, under these conditions it was possible to detect the presence of three bands of AO activity. This is an important point for us because in previous work *(13)*, we detected only two bands in our zymograms. We ran several experiments, but it was not possible separate the upper activity named AO-1. In the present work, it was possible to detect three activity bands (Fig. 2A, lanes 1 and 2) by means of different changes in PAGE concentration and run conditions. For the lanes in Fig. 2A corresponding to the cell-free extracts obtained when the fungus was grown in different conditions including no carbon source, glucose, or glycerol (lane 3, 4, and 5, respectively), in these cases the activity bands are absent. Figure 2B shows the protein pattern stained by Coomassie blue, which is similar in all cases. In all lanes, 100 µg of protein was loaded.

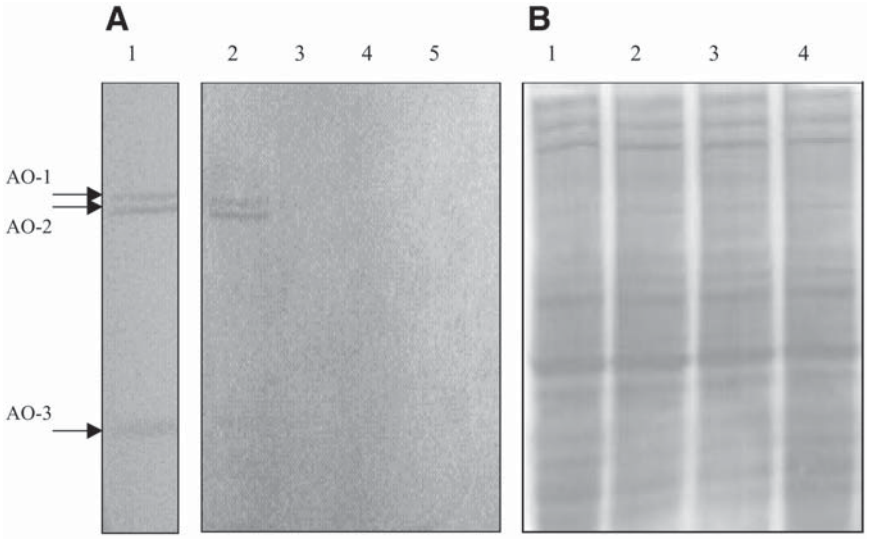

Fig. 2. AO activity zymograms from mycelium cells of YR-1. The 164,500*g* supernatant of mycelium cells grown aerobically for 22 h in sMMP media with added different carbon sources was electrophoresed using 6% acrylamide. AO activity was developed in the gel with hexadecanol as substrate. **(A)** Lane 1, sMMP-hexadecane; lane 2, sMMP-hexadecane; lane 3, sMMP without carbon source; lane 4, sMMP-glucose; lane 5, sMMP-glycerol. In all cases 300 (g of protein was loaded in each lane. **(B)** Protein patterns of samples stained by Coomassie blue R-250. Lane 1, sMMP-hexadecane; lane 2, sMMP without carbon source; lane 3, sMMP-Glucose; lane 4, sMMP-glycerol. One hundred micrograms of protein was loaded in each lane. Arrows show the bands of AO activity.

Specific Growth Rate and Generation Time

The appearance of AO activity as a function of incubation time in growth medium with hexadecane or glucose was estimated. Figure 3 shows that in the case of hexadecane as sole carbon source, the enzyme production reached its maximum after 22 h and then declined; this decrease in enzyme activity coincided with the onset of the stationary phase of growth. Meanwhile, in glucose there was no activity during the incubation period. The kinetic growth parameters specific growth rate (μ) and generation time (T_g) were calculated. Table 2 shows that the microorganism presents a value of T_g for growth in hexadecane twice that obtained for glucose and a value of μ for hexadecane half that of the glucose value, indicating that glucose is a much better substrate for growth than hexadecane, but hexadecane is a possible inducer of AO activity and glucose could be a repressor or possibly an activity inhibitor; the latter observation can not be disregarded.

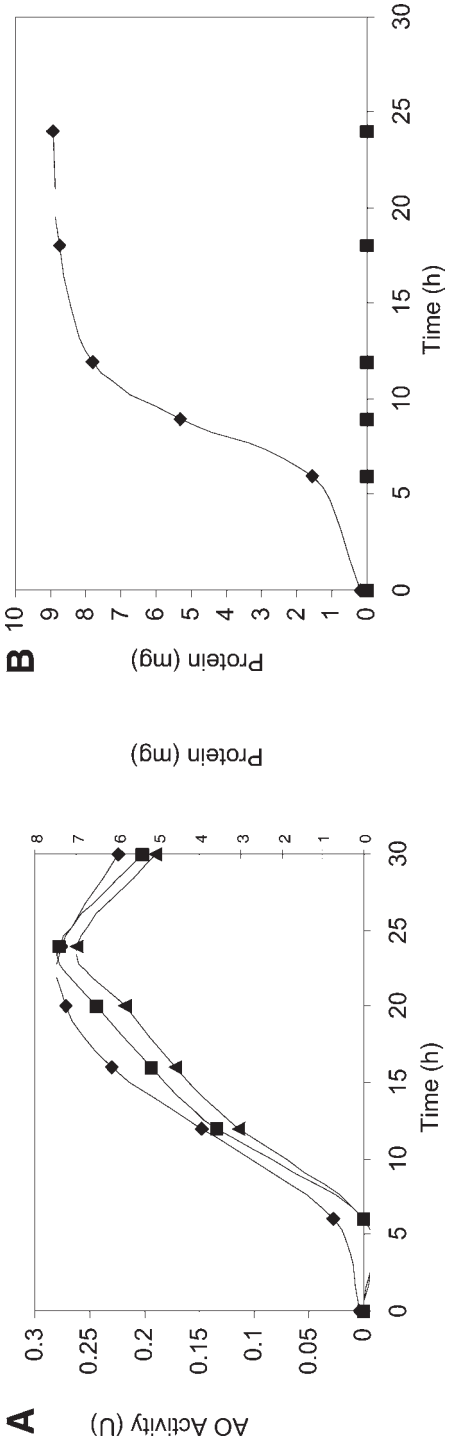

Fig. 3. Growth kinetics of YR-1 strain and appearance of AO activity as function of incubation time in different carbon sources. The 164,500*g* supernatant of samples from different incubation times from mycelium cells grown aerobically in sMMP supplemented with 1% hexadecane **(A)** or glucose **(B)**, was used to measure the AO activity using decanol (■)or hexadecanol (▲) as substrates. Protein (◆) indicates fungus growth measure. One unit of activity, µmol of H_2O_2 /(mg of protein (min); protein, $A_{280\ nm}$.

Table 2
Specific Growth Rate (μ) and Generation Time (T_g) of YR-1 Strain Grown in Different Carbon Sources[a]

	μ (h^{-1})	T_g (h)
SMMP–1% Glucose	0.536	1.19
SMMP–1% Hexadecane	0.330	2.10

[a]The values given are the mean of two independent experiments with triplicate determinations in each case.

Table 3
AO Activity in Strain YR-1 with Various Alcohols as Substrates in Experiments of Mycelium Transfer[a]

	AO activity (U)[b]		
Transfer from glucose to	Methanol	Ethanol	Decanol
sMMP–0.5% Decane	0.0870	0.0570	0.58
sMMP–0.5% Hexadecane	0.0690	0.0480	0.67
sMMP–1% Methanol	0.0027	0.0023	0.35
sMMP	7×10^{-5}	4.5×10^{-5}	8×10^{-6}
sMMP–1% Glycerol	2.2×10^{-5}	2.6×10^{-5}	3.6×10^{-5}
sMMP–1% Glucose	ND	ND	ND

[a]The microorganism was grown for 8 h in YPG medium. The mycelium was then exhaustively washed and transferred to minimal salts media (sMMP) supplemented with different carbon sources. AO was assayed as described in Materials and Methods, the substrates listed were used at different concentrations: 127 m*M* methanol; ethanol and decanol were at 60 m*M* final concentration. Activities are expressed as units of activity. The values given are the mean of two independent experiments with triplicate determinations in each case. ND, not detected.

[b]One unit of activity, 1 μmol of H_2O_2 /[mg of protein (min)].

Induction of AO Activity

All previous results of the present study strongly suggest that AO activity is negatively affected by the presence of glucose and also that the presence of a hydrocarbon as a possible inducer is necessary. To obtain more information about the inducible mechanism of AO synthesis, we conducted some experiments transferring mycelia grown in minimal medium with the addition of 1.0% glucose for 8 h. After this incubation period, the mycelium was exhaustively washed in sterile conditions and transferred into fresh minimal medium with the addition of different carbon sources—glucose, glycerol, methanol, and hydrocarbons—and, finally, a flask with the minimal medium but without carbon source. It is clear from the data in Table 3 that the transference of mycelium grown in the presence of glucose (not induced) to an induction medium (hydrocarbon present) was able to permit AO expression. By contrast, in cases when the fresh medium contained glucose, glycerol (a nonfermentable carbon source), or methanol, no AO activity was detected, suggesting that the induction mechanism is present in the expression of AO enzyme.

Table 4
Effect of Presence of Glucose on AO Activity[a]

Sample	AO activity (U) in decanol
Control (no glucose added)	0.0368
0.1% Glucose	0.0239
0.5% Glucose	0.0339
1.0% Glucose	0.0323
2.0% Glucose	0.0280

[a]Glucose at different concentrations was added to the reaction mixture to determine AO activity. The activity of AO from strain YR-1 using 0.5 m*M* decanol (final concentration) as substrate was assayed as described in Materials and Methods. The values given are the mean of two independent experiments with triplicate determinations in each case.

Inhibition of AO Activity by Glucose

To explore whether the presence of glucose in the reaction mixture of the AO activity measure could negatively affect the enzymatic activity of AO by means of an inhibitory effect, we conducted several experiments in which we added different amounts of glucose to the reaction mixture in order to determine enzyme activity. The results, shown in Table 4, clearly demonstrate that the presence of glucose at any concentration had no effect on AO activity.

Discussion

Figure 1 clearly shows the differences in the morphologic pattern of growth of the fungi when it was growing in glucose or hexadecane. Interesting, in hexadecane there was a formation of "septa-like" structures that could be similar to the structures formed when the fungi were in the late stationary phase of growth and the nutrients in the culture medium are exhausted.

AO activity in aerobically grown mycelial cells of strain YR-1 obtained under different nutritional conditions was measured in the 164,500*g* supernatant of each growth condition. Activity was present only when glucose in the culture medium was absent. This result could suggest that AO synthesis is subjected to catabolic repression, but more experiments investigating the amount of mRNA synthesized by cells growing in glucose or hydrocarbon are necessary to establish whether there is an effect of catabolite repression by glucose in the synthesis of the mRNA. A complementary experiment was conducted to prove the inhibitory effect of glucose over AO activity. In this case, the enzyme activity was not under the mechanism of glucose inhibition.

The previous finding of two different AO activities in the 164,500*g* supernatant *(13)* and the actual result of three activity bands in zymo-

grams are not unexpected; for instance, in the methylotrophic yeast *Candida boidinii*, the presence of two AO enzymes has been reported *(14)*. It is very important to be extremely sure about the exact number of AO activities present in the YR-1 strain and which one is the most important for hydrocarbon metabolism. To date, we are studing the purification of the three activity bands, and by means of double dimension PAGE, we will be able to determine whether these bands correspond to different enzymes, and whether they are isozymes or could be the same enzyme with different aggregation states. In filamentous fungi, the presence of AO enzymes has been reported in a limited number of cases, such as *Penicillium simplisimum*, which has a vanillyl alcohol oxidase *(15)*. The principal difference between AOs of strain YR-1 and the AO of methylotrophic organisms is the capacity of the former to use complex alcohols as well as methanol as substrates.

When the microorganism was transferred from growth in glucose to different carbon sources, the results in the presence of glucose indicate the possible effect of catabolite repression, but more important, was the transference from glucose to glycerol in which no activity was detected, because this result strongly suggests that the presence of a hydrocarbon is necessary to induce the synthesis of AO activity. Further studies will indicate the relationship of AO-1 and AO-2 to each other as well as to AO enzymes from other microorganisms. In addition, these studies will be important in establishing the role of these enzymes in hydrocarbon metabolism in the YR-1 strain. Finally, we are conducting molecular experiments to identify taxonomically the YR-1 strain.

References

1. Atlas, R. M. (1995), *Chem. Eng. News* **73(14),** 32–42.
2. Alper, J.(1993), *Biotechnology* **11,** 973–975.
3. Guenguerich, F. P. and Macdonald, T. L. (1990), *FASEB J.* **4,** 2453–2459.
4. Kellner, D. G., Maves, S. A., and Sligar, S. P. (1997), *Curr. Opin. Biotechnol.* **8,** 274–278.
5. Jones, J. G. and Bellion, E. (1991), *Biochem. J.* **280,** 475–481.
6. Evers, M. E., Titorenko, V., Harder, W., ven der Hlei, Y., and Veehhuis, M. (1996), *Yeast* **12,** 917–923.
7. Lowry, O. H., Rosebrough, N. J., Farr, A. L., and Randall, R. J. (1951), *J. Biol. Chem.* **193,** 265–275.
8. Gleason, M. A., Ortori, S., and Sudberry, P. E. (1986), *J. Gen. Microbiol.* **132,** 3459–3465.
9. Bartnicki-Garcia, S. and Nickerson, W. J. (1962), *J. Bacteriol.* **84,** 841–858.
10. Torres-Guzman, J. C., Arreola-Garcia, G. A., Zazueta-Sandoval, R., Carrillo-Rayas, T., Martínez-Cadena, G., and Gutiérrez-Corona F. (1994), *Curr. Genet.* **26,** 166–171.
11. Janssen, F. W., Kerwin, R. M., and Ruelius, H. W. (1975), in *Methods in Enzymology*, vol. XLI, Academic, London, UK, pp. 364–369.
12. Laemmli, U. K. (1971), *Nature* **227,** 680–685.
13. Alvarado-Caudillo, Y., Bravo-Torres, J. C., Zazueta-Novoa, V., Silva-Jiménez, H., Torres-Guzmán, J. C., Gutiérrez-Corona, J. F., and Zazueta-Sandoval, R. (2002), *Appl. Biochem. Biotechnol.* **98–100,** 243–255.
14. Sakai, Y. and Tani, Y. (1992), *Gene* **114,** 67–73.
15. Benen, J. A. E., Sánchez-Torres, P., Wagemaker, M. J. M., Fraaije, M. W., van Berkel, W. J. H., and Visser, J. (1998), *J. Biol. Chem.* **273,** 7865–7872.

0273-2289/04/113/0173–0180/$25.00

Effect of Temperature, Moisture, and Carbon Supplementation on Lipase Production by Solid-State Fermentation of Soy Cake by *Penicillium simplicissimum*

Marco Di Luccio,[*,1] Fernando Capra,[1] Najara P. Ribeiro,[1] Gean D. L. P. Vargas,[1] Denise M. G. Freire,[2] and Débora de Oliveira[1]

[1]Department of Food Engineering, URI–Campus de Erechim, Av. Sete de Setembro 1621, Erechim, 99700-000, RS, Brazil, E-mail: diluccio@uricer.edu.br; and
[2]Department of Biochemistry–IQ/UFRJ, Centro de Tecnologia, Bl. A, Sala 549-2, Rio de Janeiro, 21945-900, RJ, Brazil

Abstract

The production of lipases by *Penicillium simplicissimum* using solid-state fermentation and soy cake as substrate was investigated. The effects of temperature, cake moisture, and carbon supplementation on lipase production were studied using a two-level experimental plan. Moisture, pH, and lipase activity were followed during fermentation. Statistical analysis of the results was performed to evaluate the effect of the studied variables on the maximum lipase activity. Incubation temperature was the variable that most affected enzyme activity, showing a negative effect. Moisture and carbon supplementation presented a positive effect on activity. It was possible to obtain lipase activity as high as 21 U/g of dry cake in the studied range of process variables.

Index Entries: Solid-state fermentation; lipase; *Penicillium*, soy cake; olive oil; moisture.

Introduction

The use of lipases in wastewater treatment in the food industry has been proposed to improve process efficiency *(1,2)*. However, economical feasibility depends on low-cost enzyme preparations. Lipase production

*Author to whom all correspondence and reprint requests should be addressed.

by solid-state fermentation (SSF) may be suitable because this kind of fermentation process presents many advantages over the submerged process, including higher productivity, higher product concentrations, and the use of simpler equipment and low-cost substrate such as agroindustry wastes. In addition, industrial plants for production of enzymes by SSF require low investment and operation costs *(3,4)*.

In a recent study, Castilho et al. *(3)* presented an economical evaluation of lipase production by *Penicillium restrictum* using both submerged fermentation and SSF. They demonstrated that the total investment required for a plant based on submerged fermentation was 78% higher than the investment necessary for installation of an SSF plant. The final enzyme cost in the submerged fermentation process was 68% higher than the cost of a commercial lipase *(3)*. SSF proved to be a highly attractive alternative from an economical point of view. The use of a low-cost raw material (babassu oil extraction waste) coupled with a low investment decreased the final enzyme cost up to 47% lower than the cost of the commercial enzyme *(3)*. The return of the investment was only 1.5 yr and the return rate was 62%, considering a 5-yr lifetime for the project. These aspects, make the production of lipase by SSF extremely promising. In this context, the aim of the present work was to study the effect of some cultivation parameters on lipase production by *Penicillium simplicissimum* using soy cake as substrate for application in wastewater treatment in the food industry.

Materials and Methods

Microorganism

The microorganism used was *P. simplicissimum*, previously isolated by Freire *(5,6)*, using samples of babassu nuts, which were naturally fermented at a babassu oil plant.

Production of Inoculum

The medium used for inoculum production consisted of soluble starch (2% [w/v]), olive oil (1% [w/v]), yeast extract (0.1% [w/v]), $MgSO_4 \cdot 7H_2O$ (0.025% [w/v]), KH_2PO_4 (0.05% [w/v]), $CaCO_3$ (0.5% [w/v]), and agar (1.5% [w/v]). The constituents of the medium were dissolved in deionized water, transferred to a 500-mL Erlenmeyer flask, and then sterilized at 111°C for 30 min. The medium was inoculated with a spore suspension obtained previously from a stock agar slant and incubated at 30°C for 7 d. Spores were collected by adding 10 mL of an aqueous solution of Tween-80 (0.1% vol) and glass beads to the Erlenmeyer flask containing the fermented medium.

Cultivation Medium

The substrate used in all experiments consisted of soy cake, which is the byproduct of soybean oil extraction. The cake was milled and classified (Tyler 35-60) and then stored at –10°C in vacuum packs. Fermentation was

Table 1
Experimental Design and Results of Maximum Lipase Activity

Experiment	Temperature (°C)	Olive oil (%)	Initial moisture (%)	Maximum activity (U/g dry cake)	Time (h)[a]
1	27	0	50	11.1 ± 1.7	64.2
2	27	4	50	16.3 ± 2.4	59.3
3	27	0	70	16.3 ± 2.4	93.4
4	27	4	70	21.5 ± 3.2	94.0
5	33	0	70	9.6 ± 1.4	43.7
6	33	4	70	13.9 ± 2.1	168.0
7	33	0	50	10.9 ± 1.6	85.4
8	33	4	50	10.9 ± 1.6	45.8
9	30	2	60	12.7 ± 1.9	49.9

[a]Time necessary to reach maximum lipase activity.

carried out in 600-mL polypropylene beakers covered with sheets of acrylic fabric. Each experimental point consisted of one beaker with 10 g of cake (dry basis) supplemented with the amount of olive oil and water following a two-level full factorial experimental design (Table 1). The water added with the inoculum was also considered in moisture correction. The beakers with the substrate were sterilized at 111°C for 30 min. The medium was inoculated with the stock spore suspension collected as already described. The final spore concentration in the cake was 10^8 spores/g of dry cake. Spore concentrations were determined using a hematocytometer after appropriate dilution. The beakers were incubated for 7 d in a climatic chamber at different temperatures, with humid air injection. Relative humidity of the air inside the chamber was kept at about 99%. Samples were taken periodically to monitor pH, cake moisture, and lipase activity.

Experimental Procedure

The effect of incubation temperature, initial cake moisture, and olive oil supplementation on lipase production was evaluated following a two-level experimental plan. The range of study of the variables was chosen based on previous results of the our group *(2,7,10)*.

Analytical Methods

Two 0.5-g samples were taken from each beaker for moisture and pH determination. Moisture content was measured by gravimetry, and pH was measured after adding 5 mL of deionized water to the sample, using a pH meter. The enzyme was extracted from the remaining fermented cake by adding 45 mL of sodium phosphate buffer (100 mmol/L, pH 7.0) following incubation at 35°C and 200 rpm for 30 min. After filtration the liquid phase was used for determination of lipase activity.

Lipase activity was determined by adding 2 mL of the extract to an emulsion of olive oil (10% olive oil, 5% Arabic gum in 100 mmol/L of phosphate buffer, pH 7.0.) and incubating at 37°C and 200 rpm for 15 min. The reaction was stopped with the addition of a solution of ethanol and acetone (1:1). The fatty acids released in the hydrolysis were titrated with a solution of 0.04 *N* NaOH *(5)*. Blank tests were performed by titration of a sample of emulsion without incubation, adding the enzyme extract sample just before the beginning of titration. One unit of lipase activity corresponds to the amount of enzyme that produces 1 μmol of fatty acids/min in the reaction conditions just described.

The total nitrogen of the substrate was determined following the standard Kjeldahl method *(8)*. The oil content of the cake was determined by gravimetry after extraction of the samples with *n*-hexane using a Soxhlet extraction apparatus *(8)*.

Results and Discussion

The mean content of oil and grease and of nitrogen of the cake, after milling and classification, was 13.0 and 5.4 wt%, respectively. The C/N ratio of the cake was estimated using the average triglyceride content of the soybean and olive oil *(9)*, considering that the microorganism consumes preferentially the carbon of the oil, which is promptly available in the medium. The estimated C/N ratios for the nonsupplemented and for the 2 and 4 wt% supplemented cake were 1.87, 2.15, and 2.44, respectively. The results show that the cake is rich in oil. This explains the good lipase yields obtained even when the substrate is not supplemented with oil. The mean moisture of the cake was 7.6 wt%. This value was considered for moisture correction of the substrate.

An experimental plan was designed with nine experiments, which were performed in duplicate to estimate experimental errors. The plan is presented in Table 1, as well as the results of maximum lipase activity and necessary fermentation time to reach the maximum activity in each experiment.

It is known that the moisture content in the substrate is essential for good development of the microorganism in SSF *(4)*. Therefore, the moisture of the cake during the fermentation was monitored in all experiments. In most of the studied conditions, the moisture was quite constant with time until 100 h of fermentation, considering an experimental error of 6%. The only exception to this behavior occurred at low initial moisture conditions. In such experiments, there was a strong decrease in moisture of the cake during the course of fermentation. The increase in incubation temperature caused a stronger decrease in cake moisture, probably owing to the higher water uptake rate by the microorganism and the increase in water vapor pressure in the system at higher temperatures.

Figure 1 presents the kinetics of lipase activity for the different studied conditions. In all cases, a maximum in lipase activity could be observed,

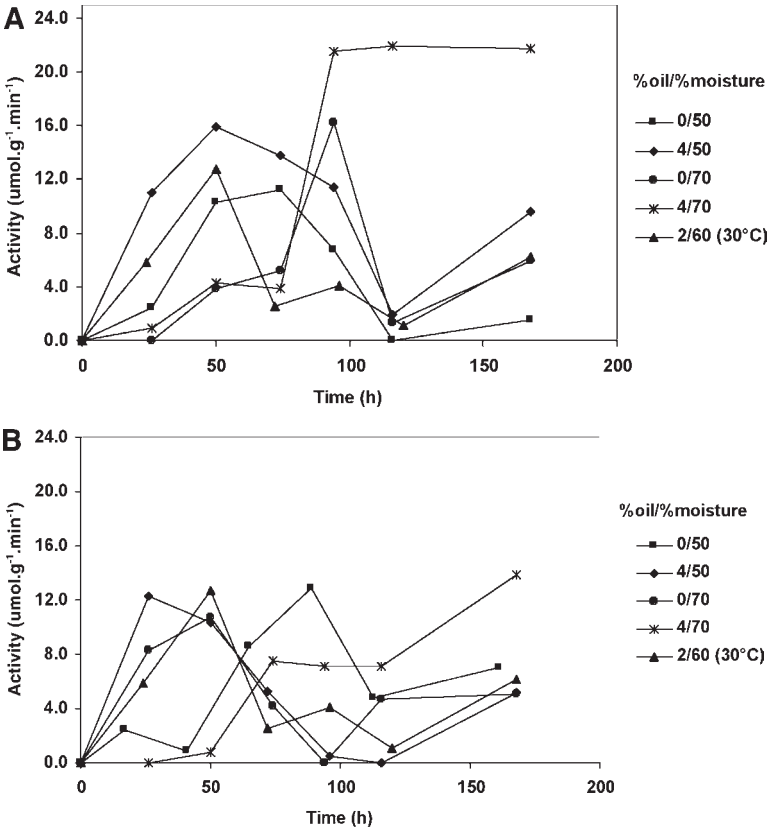

Fig. 1. Lipase production at different conditions of moisture and supplementation: **(A)** 27°C and **(B)** 33°C.

often followed by a new increase by the end of fermentation. The decrease in lipase activity may be related to the effect of pH; temperature; or, still, the protease production by the microorganism, as shown by Gombert et al. *(10)* and Palma et al. *(11)* in previous studies with *P. restrictum*. The presence of proteases in the medium may cause deactivation of the lipase and even the complete loss of lipase activity. The increase in lipase activity at the end of fermentation may be related to the production of a new lipase or decrease in the protease activity. However, new experiments, in which protease activity should be determined, are necessary for confirmation of such a hypothesis. The mean experimental error of lipase activity, calculated based on duplicates, was 14%.

In a preliminary analysis, we noted that the production of lipase was higher at lower temperature (27°C). This result was later confirmed by statistical analysis, which is discussed in the next section. The negative effect of temperature may be related to the increase in the protease activity at higher temperatures.

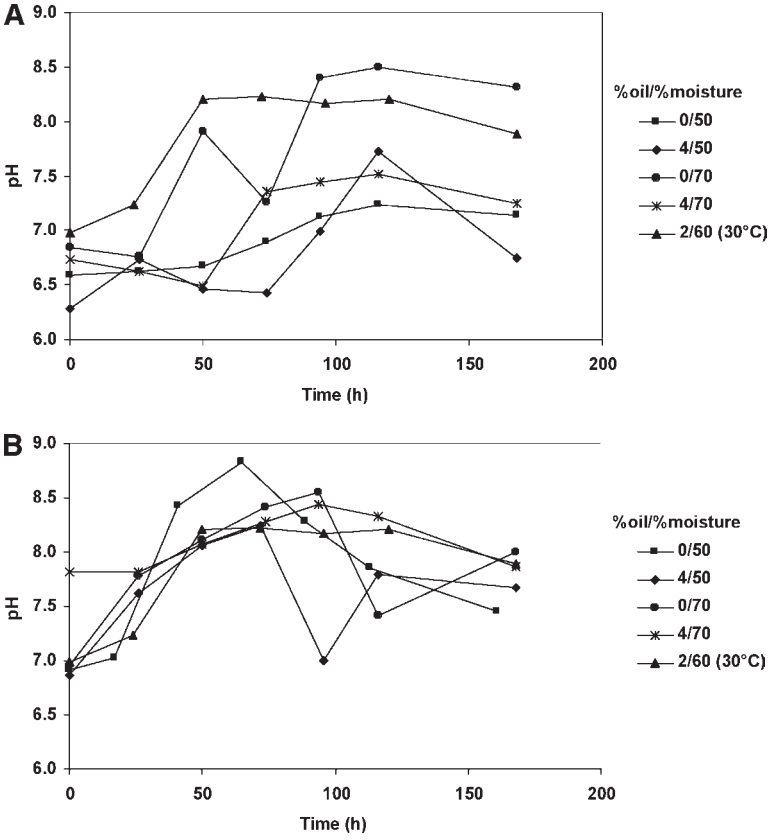

Fig. 2. Evolution of pH during fermentation at different conditions of moisture and supplementation: **(A)** 27°C and **(B)** 33°C.

Supplementation of the substrate with oil led to an increase in lipase activity and a reduction in the time required to reach the maximum activity. This might be owing to acceleration of the metabolism of the microorganism. However, the time to reach the maximum must be analyzed carefully, since factors such as inoculum age and physiologic state may directly affect this result.

Figure 2 shows pH evolution during fermentations. The mean experimental error of pH was 2.2%. pH increased after 24 h of fermentation, and in some experiments it reached 8.5 after 70 h of fermentation. In all experiments the increase in pH may be correlated to the decrease in lipase activity. This behavior is probably owing to the proteolysis, which yields ammonia to the culture medium, increasing pH *(6)*. A decreasing pH trend could also be noted after 100 h of fermentation, matching the new increase in lipase activity. This behavior suggests a reduction in the protease activity in the medium.

Table 2
Best Fit for Maximum Lipase Activity in Function of Temperature, Moisture, and Olive Oil Content [a]

Model: $AT = a_0 + a_1 \times T + a_2 \times OO + a_3 \times M + a_4 \times T \times M + a_5 \times T \times OO$
Dependent variable: AT Loss function: $([OBS\text{-}PRED]^2)/S^2_{experim}$
Final value of loss function: 0.117 R^2: 0.97

Parameter [b]	a_0	a_1	a_2	a_3	a_4	a_5
Estimate	2.76	–0.487	0.371	0.338	–0.256	–0.156
SE	0.07	0.065	0.079	0.076	0.078	0.080

[a] AT, maximum lipase activity; T, temperature; M, moisture; OO, % olive oil; a_0, a_1, a_2, a_3, a_4, and a_5, model parameters; $S^2_{experim}$, experimental variance.
[b] Confidence level >95%.

Statistical Analysis

Statistical analysis of the results was performed using the software Statistica 5.5 (Stat Soft). Maximum lipase activities and time to reach the maximum were calculated through fitting of kinetic curves. The maximum was estimated by derivation of the fits. Empirical models were built to fit maximum lipase activity in the function of incubation temperature (T), moisture of the cake (%M), and supplementation (%OO). The experimental error estimated from the duplicates was considered in the parameter estimation. The choice of the best model to describe the influence of the variables on lipase activity was based on the correlation coefficient (r^2) and on the χ^2 test. The model that best fits the experimental data is presented in Table 2.

Note that the three variables present quite the same effect on maximum lipase activity. Nevertheless, temperature presented a negative effect, which was unexpected, since the metabolism of mesophyllic microorganisms tends to increase with temperature in the range investigated. In this situation, the negative influence might be related to the strong correlation between temperature and substrate moisture. The increase in temperature may lead to the decrease in cake moisture, owing to the increase in vapor pressure of the water. An indication of such an effect may be observed by the strong correlation between moisture and temperature effects (parameter a_4). This correlation also negatively influences the activity to the same degree as the other isolated variables. Other possibilities may be related to a higher level of denaturation of the produced lipase induced by the increase in temperature or to the increase in the proteolytic activity, so that the balance for lipase favors deactivation rather than production.

The concentration of olive oil and moisture content showed positive effects in the range investigated. The increase in olive oil content may favor lipase production by the microorganism owing to accelerated metabolism.

The increase in water content in the medium also increased the metabolic activity of the mold, resulting in a higher lipase production. These results were also observed by Gombert et al. *(10)* for lipase production using *P. restrictum* in babassu cake.

The time to reach the maximum lipase activity did not show any satisfactory correlation with the studied variables. This behavior is probably owing to the high error associated with this variable or with other factors, such as inoculum age and concentration, which were not considered in the statistical analysis and may be influencing this response, although inoculum standardization procedures were used in all the experiments. Fermentation time was not found to be a determinant factor. However, this may be important on an industrial scale, since it can directly compromise enzyme productivity and production costs.

Conclusions

Our study showed that incubation temperature is the variable that most influences lipase production by *P. simplicissimum* using soy cake as substrate, even though it shows a negative effect. To maximize lipase production, fermentation should be carried out at low temperature levels, high moisture in the substrate, and higher concentration of oil. However, good results may also be obtained at lower temperatures without cake supplementation, owing to its high oil content.

The use of soy cake is a promising substrate for lipase production. Even without optimization it is possible to achieve lipase activity as high as 21 U/g of dry cake, comparable with lipase activity obtained with other microorganisms and substrates.

References

1. Jung, F., Cammarota, M. C., and Freire, D. M. G. (2002), *Biotechnol. Lett.* **24,** 1797–1802.
2. Cammarota, M. C., Teixeira, G. A., and Freire, D. M. G. (2001), *Biotechnol. Lett.* **23,** 1591–1595.
3. Castilho, L. R, Polato, C. M. S., Baruque, E. A., and Sant´Anna, G. L., Jr. (2000), *Biochem. Eng. J.* **4,** 239–247.
4. Del Bianchi, V. L., Moraes, I. O., and Capalbo, D. M. F. (2001), in *Biotecnologia Industrial: Engenharia Bioquímica*, vol. 3, Schmidell, W., Lima, U.A., Aquarone, E., and Borzani, W., eds., Edgard Blücher, São Paulo, Brazil.
5. Freire, D. M. G. (1996), PhD thesis, PEQ/COPPE/UFRJ, Rio de Janeiro, Brazil.
6. Freire, D. M. G., Gomes, P. M., Bon, E. P. S., and Sant´Anna, G. L., Jr. (1997), *Revista Microbiologia* **28(1),** 6–12.
7. Leal, M. C. M. R., (2000), MS thesis, PEQ/COPPE/UFRJ, Rio de Janeiro, Brazil.
8. Pregnolatto, W., Pregnolatto, N. P. (coord.), and Rebocho, D. D. E. (ed.) (1985), *Normas analíticas do Instituto Adolfo Lutz: vol.1. Métodos químicos e físicos para análise de alimentos*, 3rd Ed., Instituto Adolfo Lutz, São Paulo, Brazil.
9. MCT, Ministério da Ciência e Tecnologia (Ministry of Science and Technology) (1985), Technical Report on Vegetable Oils, MCT.
10. Gombert, A. K., Pinto, A. L., Castilho, L. R., and Freire, D. M. G. (1999), *Process Biochem.* **35,** 85–90.
11. Palma, M. B., Pinto, A. L., Gombert, A. K., Seitz, K. H., Kivatinitz, S. C., Castilho, L. R., and Freire, D. M. G. (2000), *Appl. Biochem. Biotechnol.* **84–86,** 1137–1145.

0273-2289/04/113/0181–0187/$25.00

The Effect of Temperature, Pressure, Exposure Time, and Depressurization Rate on Lipase Activity in $SCCO_2$

Marcelo Lanza, Wagner Luís Priamo, José Vladimir Oliveira, Cláudio Dariva, and Débora de Oliveira*

Department of Food Engineering, URI–Campus de Erechim, Av. Sete de Setembro, 1621-Erechim-RS, 99700-000, Brazil, E-mail: odebora@uricer.edu.br

Abstract

We investigated the influence of temperature, pressure, exposure time, and decompression rate on lipase activity in high-pressure CO_2 medium. A high-pressure, variable-volume view cell was employed in the experiments, varying the temperature from 30 to 70°C in the pressure range of 70–250 bar at various high-pressure exposure times (60–360 min) and adopting several decompression rates (10–200 kg/[m^3·min]). The results obtained show that an increase in temperature and density led to an enhancement of enzyme activity losses while the decompression rates had a weak influence on enzyme inactivation.

Index Entries: Lipase activity; high pressure; decompression rate; CO_2; $SCCO_2$; exposure time.

Introduction

Bioconversion of vegetable oils through the use of enzymes as catalysts in supercritical medium is undoubtedly a matter of great scientific and technological interest. The possibility of using a much less pollutant fuel (biodiesel) compared to diesel from petroleum and producing many chemical raw materials for food, pharmaceutical and cosmetic industries has motivated research efforts in the biotransformation of vegetable oils with the desired end result of high-value-added products or drastic reduction in environmental investments *(1)*.

*Author to whom all correspondence and reprint requests should be addressed.

Enzyme-catalyzed reactions of vegetable oils in $SCCO_2$ seems to be a promising technique toward obtaining high-grade products—fatty acid ethyl esters, mono- and diglycerides—with very satisfactory reaction rates. Because biocatalysts have high specific activity and a low impact on the environment, they have become increasingly important for industry. For example, immobilized lipases are used as catalysts for reactions involving biomodification of triglycerides *(2)*. In this case, supercritical fluids, particularly CO_2, have currently received widespread attention as a possible medium for enzymatic reactions *(3)*. The main advantage of supercritical fluids over liquid solvents, such as *n*-hexane, is that the high diffusivity, low viscosity, and low surface tension of supercritical fluids can speed up mass transfer–limited enzymatic reactions *(4)*.

To conduct such reactions at high pressures, the enzyme behavior in $SCCO_2$ is of primary importance since the loss of enzyme activity may lead to undesirable poor reaction rates and reduction of desired product production. With respect to the stability of lipases, the high pressure and kind of medium are both interesting parameters from a theoretical and practical point of view *(5)*. Changes in protein structure may occur under extreme conditions, and the spatial structure of many proteins may be significantly altered, causing denaturation and consequent loss of activity. If conditions are less adverse, protein structure may largely be retained. Minor structural changes may induce an alternative active protein state, which may possess altered activity, specificity, and stability *(6)*.

Many enzymes are stable and catalyze reactions in supercritical fluids, just as they do in other non- or microaqueous environments *(7)*. Enzyme stability and activity may depend on the enzyme species, supercritical fluid, water content of the enzyme/support/reaction mixture, decompression rates, exposure times, and pressure and temperature of the reaction system.

To understand the potential of pressure application to enzyme processes and to help elucidate the reaction mechanism as well as a rational design of alcoholysis reactors for future scale-up, we investigated the influence of temperature, pressure, exposure times, and decompression rates on the activity of a commercial immobilized lipase (Novozym 435) activity in high-pressure CO_2 medium.

Materials and Methods

Chemicals

Lauric acid, ethanol, acetone, and other chemicals (analytical grade) were from Merck. CO_2 with a purity >99.99% was used as solvent in the high-pressure experiments.

Enzyme

The commercial lipase *Candida antarctica* (Novozym 435), immobilized on a macroporous anionic resin (0.12 U/g, 1.4% water, and diameter

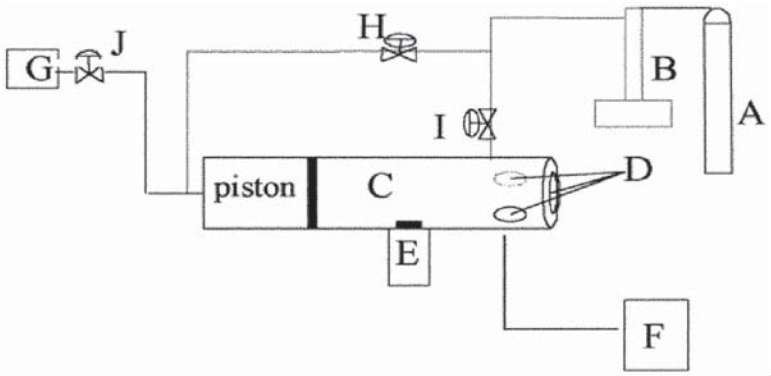

Fig. 1. Schematic diagram of high-pressure apparatus for enzyme activity tests. A, CO_2 cylinder; B, syringe pump; C, equilibrium cell; D, sapphire windows; E, magnetic stirrer; F, white light source; G, pressure transducer; H, ball valve; I, micrometering valve; J, relief valve.

in the range of 0.3–0.9 mm), was kindly supplied by Novozymes Brazil (Araucária, PR, Brazil).

Lipase Activity

Enzyme activity was determined as the initial rates in esterification reactions between lauric acid and propanol at a molar ratio of 1:3, a temperature of 60°C, and an enzyme concentration of 5 wt% in relation to the substrates. At the beginning of the reaction, samples containing the mixture of lauric acid and propanol were collected and the lauric acid content was determined by titration with 0.04 *N* NaOH. After the addition of the enzyme to the substrates, the mixture was kept at 60°C for 15 min. Then, lauric acid consumption was determined.

Apparatus and Experimental Procedure

The equipment used in all experiments consisted basically of a CO_2 cylinder, a 20-mL view cell with three sapphire windows for visual observations, an absolute pressure transducer (Smar LD 301) with a precision of ±0.012 MPa, a portable programmer (Smar HT 201) for pressure data acquisition, and a syringe pump (ISCO 260D). The equilibrium cell contained a movable piston, which permitted pressure control inside the cell. Figure 1 presents schematic diagram of the experimental unit.

Lipase (approx 1.0 g) was charged into the cell, and the temperature established in the experimental design was reached. Afterward, the system was pressurized and maintained at a constant temperature and pressure for a preestablished exposure time. Typically, the pressure elevation time was <0.5 min and was not included in the pressure holding time because of its comparatively short duration. Then, at the decompression rates (10–200 kg/[m^3·min]) defined, the system was depressurized and the lipase activity was measured. The loss of lipase activity was defined as the difference between the activity at the beginning and at the end of the process.

Table 1
Taguchi Experimental Plan Conditions

Run	Temperature (T) (°C)	Initial pressure (bar)	Exposure time (t) (min)	Decompression rate (R) (kg/[m^3·min])	Reduced density (RD)
1	40	80.0	60	10	0.60
2	40	130.7	60	200	1.60
3	40	130.7	360	10	1.60
4	40	80.0	360	200	0.60
5	70	255.5	60	10	1.60
6	70	107.2	60	200	0.60
7	70	107.2	360	10	0.60
8	70	255.5	360	200	1.60
9	55	132.0	210	105	1.10

Experimental Design

A Taguchi experimental plan with two levels and four variables (temperature, exposure time, decompression rate, and reduced density) was adopted. The experimental plan, covering the variable ranges commonly used for transesterification reactions *(1)*, is presented in Table 1. The experiments were accomplished randomly, and duplicate runs were carried out for all experimental conditions leading to an average reproducibility better than 5%. The activity loss was then modeled empirically in order to determine the influence of the process variables on main and cross-interaction parameters.

Results and Discussion

The experimental results obtained are presented in Fig. 2. One can observe from Fig. 2 that temperature, reduced density, and exposure time influenced positively the activity loss whereas decompression rate had a weak negative effect.

The influence of temperature; exposure time; decompression rate; and reduced density; as well as the cross-interaction variables exposure time–decompression rate and temperature–exposure time were investigated. To allow a direct comparison of each variable effect, the independent variables were normalized in the range of –1 to +1. The –1 level represents the inferior limit, while the +1 level represents the superior limit of each variable. A statistical modeling technique was used to obtain an empirical model able to represent the experimental data. Empirical models were built by assuming that all variable interactions were significant, estimating the parameters related to each variable interaction and main variable effects, and discarding the meaningless parameters considering a confidence level of 95%, by using the student's t-test.

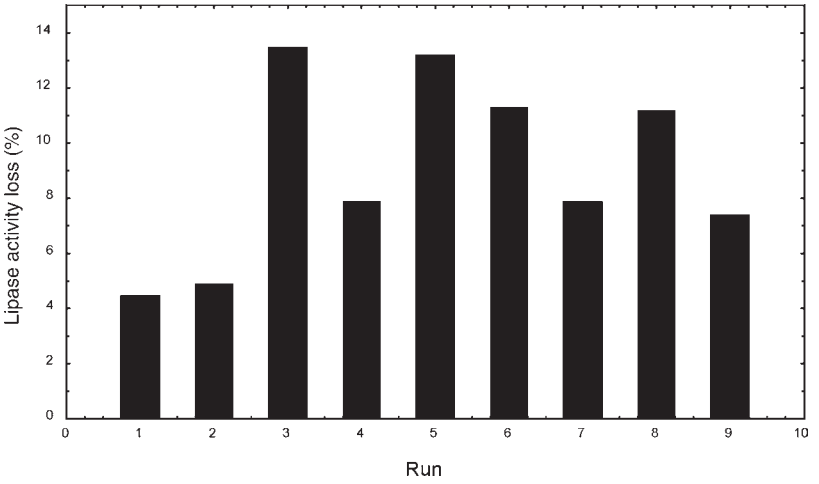

Fig. 2. Loss of enzyme activity obtained in experimental planning.

Table 2
Regression Results for Novozym 435–$SCCO_2$

Model:
Activity loss = $a_0 + a_1 \times T + a_2 \times t + a_3 \times R + a_4 \times RD + a_5 \times T \times R + a_6 \times T \times t + a_7 \times T \times T$
$R = 0.99957$

Parameter	a_0	a_1	a_2	a_3	a_4	a_5	a_6	a_7
	7.36	1.590	0.830	–0.480	1.390	0.860	–2.180	1.940
SD	0.28	0.099	0.099	0.099	0.099	0.099	0.099	0.295

a_0, a_1, a_2, a_3, a_4, a_5, a_6, a_7, model parameters.

Table 2 presents the results obtained in the statistical modeling. Temperature and reduced density had a pronounced effect on enzyme activity loss, both showing a positive effect. At this point, it is important to mention that the cross-interaction temperature–exposure time had a significant negative effect. In the range investigated (10–200 kg/[m^3·min]), the decompression rate had a weak negative effect on loss of enzyme activity. The same effect was observed with the exposure time (60–360 min).

The results show that in all experimental conditions the enzyme activity loss was lower than 15%. When compared to the work presented by Habulin and Knez *(8)*, this activity loss is considered low. Some works available in the literature point to the use of $SCCO_2$ as a satisfactory medium to inactivate some enzymes *(8,9)*. It is important to mention that all these works used enzymes in native form, and the results presented herein are related to an immobilized enzyme (Novozym 435). On the other hand, our results are in perfect agreement with those obtained by Castellari et al. *(9)* for the system containing a polyphenoloxidase present in grape musts.

In that work, at pressures from 300 to 900 MPa, the residual activity after the high-pressure treatment for 10 min was approx 90%.

A series of enzyme-catalyzed reactions recently conducted in both conventional and supercritical fluid medium has shown that while no loss of enzyme activity was experimentally observed for the conventional medium, the same was no longer valid for supercritical CO_2 systems *(1,4,10,11)*. For instance, Steinberger and Marr *(12)* have pointed out that the stability of an enzyme in supercritical CO_2 depends on both its tertiary structure and several parameters during exposure to high-pressure fluid. They argued that high temperatures, the water content in CO_2 and pressurization/depressurization steps might cause enzyme inactivation.

Another interesting aspect verified by Oliveira and Oliveira *(1,4)* and by Cernia et al. *(13)* is that the reaction rate generally exhibits an unusual behavior in the range of 6–25 MPa. A rise in pressure leads to an increase in the reaction rate, and then a dramatic decrease occurs after a certain pressure limit inducing modifications in both structure and function of enzyme.

Conclusion

We conclude that a commercial immobilized lipase from *C. antarctica* (Novozym 435) was stable in $SCCO_2$ for all experimental conditions investigated. Based on the results obtained here and comparison of them with the results obtained by other investigators, it can be concluded that the magnitude of pressure, temperature, decompression rate, and exposure time needed to inactivate the enzyme strongly depends on the nature and the source of enzyme and, primarily, whether the enzyme is in its native or immobilized form. For the purpose of using this enzyme to catalyze the transesterification reaction of vegetable oils in order to produce esters, the results obtained herein are relevant, because the immobilized lipase can be used with low activity loss at typical conditions of temperature and pressure employed in many biotransformations of raw materials.

Acknowledgments

We thank Conselho Nacional de Desenvolvimento Científico e Tecnológico (CNPq), FAPERGS, and ANP/FINEP/PETROBRAS for financial support and scholarships.

References

1. Oliveira, D. and Oliveira, J. V. (2001), *J. Supercritical Fluids* **19,** 141–148.
2. Basri, M., Yunus, W. M. W., Razak, C. N. A., Salleh, A. B., and Yoong, W. S. (1996), *J. Chem. Technol. Biotechnol.* **66,** 169–173.
3. Habulin, M., Krmelj, V. and Knez, Z. (1999), *Proceedings of the 5th Conference on Supercritical Fluids and Their Applications*, Verona, Italy, pp. 331–338.
4. Oliveira, J. V. and Oliveira, D. (2000), *Ind. Eng. Chem. Res.* **39,** 4450–4458.

5. De Cordt, S., Ludikhuyze, L., Weemaes, C., Hendrickx, M., Heremans, K., and Tolback, P. (1996), *High Pressure Biosci. Biotechnol.* **1,** 203–209.
6. Mozhaev, V. V., Kudryashova, E. V., and Bec, N. (1996), *High Pressure Biosci. Biotechnol.* **1,** 221–227.
7. Aaltonen, O. (1999), *Chem. Synthesis Using Supercritical Fluids* **1,** 414–419.
8. Habulin, M. and Knez, Z. (2001), *J. Chem. Technol. Biotechnol.* **76,** 1260–1265.
9. Castellari, M., Matricardi, L., Arfelli, G., Rovere, P., and Amati, A. (1997), *Food Chem.* **60,** 647–651.
10. Oliveira, D. and Alves, T. L. M. (1999), *Appl. Biochem. Biotechnol.* **77,** 835–844.
11. Oliveira, D. and Alves, T. L. M. (2000), *Appl. Biochem. Biotechnol.* **84,** 59–68.
12. Steinberger, D. J. and Marr, T. G. R. (1999), in *Proceedings of the 5th Conference on Supercritical Fluids and Their Applications*, pp. 339–346.
13. Cernia, E., Palocci, C., Celia, E.C. and Soro, S. (1999), in *Proceedings of the 5th Conference on Supercritical Fluids and Their Applications*, pp. 325–330.

0273-2289/04/113/0189–0199/$25.00

Ester Synthesis Catalyzed by *Mucor miehei* Lipase Immobilized on Magnetic Polysiloxane–Polyvinyl Alcohol Particles

Laura M. Bruno,[1] José L. de Lima Filho,[2] Eduardo H. de M. Melo,[2] and Heizir F. de Castro,[*,3]

[1]Embrapa Agroindústria Tropical, Rua Dra. Sara Mesquita, 2270, Pici, 60511-110, FORTALEZA-CE, Brazil;
[2]Departmento de Bioquímica, Laboratório de Imunopatologia Keizo Assami, Universidade Federal de Pernambuco, 50670-420, RECIFE-PE, Brazil; and
[3]Departmento de Engenharia Química, Faculdade de Engenharia Química de Lorena, PO Box 116, 12600-970, Lorena-SP, Brazil, E-mail: heizir@dequi.faenquil.br

Abstract

Mucor miehei lipase was immobilized on magnetic polysiloxane–polyvinyl alcohol particles by covalent binding with high activity recovered. The performance of the resulting immobilized biocatalyst was evaluated in the synthesis of flavor esters using heptane as solvent. The impact on reaction rate was determined for enzyme concentration, molar ratio of the reactants, carbon chain length of the reactants, and alcohol structure. Ester synthesis was maximized for substrates containing excess acyl donor and lipase loading of 25 mg/mL. The biocatalyst selectivity for the carbon chain length was found to be different concerning the organic acids and alcohols. High reaction rates were achieved for organic acids with 8 or 10 carbons, whereas increasing the alcohol carbon chain length from 4 to 8 carbons gave much lower esterification yields. Optimal reaction rate was determined for the synthesis of butyl caprylate (12 carbons). Esterification performance was also dependent on the alcohol structure, with maximum activity occurring for primary alcohol. Secondary and tertiary alcohols decreased the reaction rates by more than 40%.

Index Entries: Lipase; sol-gel matrix; polysiloxane–polyvinyl alcohol; esterification; activity.

*Author to whom all correspondence and reprint requests should be addressed.

Introduction

The use of lipases in organic media is now of major commercial importance, and this interest is expected to grow over the coming years as a wider range of lipase catalysts becomes available *(1–4)*. For example, a range of fatty acid esters is now being synthesized on a commercial scale using lipases in essentially nonaqueous media *(1,2)*. To expand further their synthetic utility, efficient methods for immobilizing lipases are needed because immobilization allows enzyme reuse and thus reduces overall process costs *(2,5)*. Several methods have been reported, such as deposition on solid supports *(6,7)*, covalent binding *(8,9)* and entrapment within a polymer matrix or hydrophobic sol-gel material *(10,11)*. The latter method can be applied to a variety of lipases, yielding immobilized systems with 80-fold esterification activity compared with the free enzyme *(11)*.

The sol-gel process involves the transition of a system from a liquid "sol" (mostly colloidal) into a solid "gel" phase *(11)*. By applying this methodology, it is possible to fabricate ceramic or glass materials in a wide variety of forms: ultrafine or spherical-shaped powders, thin film coatings, ceramic fibers, microporous inorganic membranes, monolithic ceramics and glasses, or extremely porous aerogel materials.

The sol-gel technique is also an excellent method to prepare hybrid material. The low temperature synthesis enables organic or inorganic species to be incorporated into rigid silicon oxide matrices without degradation. The resulting composite combines the chemical and physical properties of the guest with the excellent optic, thermal, and chemical stability of the host silicon oxide matrices *(12)*. Recently we reported a novel procedure for covalent immobilization of antigens from *Yersinia pestis* for antibody detection onto small disks of a polysiloxane–polyvinyl alcohol (POS-PVA) composite prepared by the sol-gel technique *(12)*. This simple but effective procedure gave an immobilized antigen preparation with greatly improved activity and stability *(12)*. The procedure used tetraethoxysilane (TEOS) and PVA for the matrix formation followed by activation with glutaraldeyde to render a more biocompatible surface for covalent immobilization *(12,13)*.

Here, we report the application of this procedure for immobilizing *Mucor miehei* lipase. A catalytic test was aimed at producing esters by direct esterification reactions with a large range of carboxylic acids (from C4 to C16), and a diversity of alcohols (from C4 to C8). Several reaction model systems are analyzed in order to illustrate the kind of products that can be made by using an experimental preparation of lipase immobilized on POS-PVA particles.

Materials and Methods

Chemicals

Mucor miehei lipase (4.79 ± 0.21 U/mg of protein) was kindly donated by Novozymes (Araucaria, PR, Brazil). TEOS was from Aldrich (Milwau-

kee, WI). Glutaraldehyde (25% [w/v]), HCl (minimum 36%), ethanol (minimum 99%), and PVA (MW mol wt. = 72,000) were supplied by Reagen (Rio de Janeiro, RJ, Brazil). Alcohols (*n*-butanol, *sec*-butanol, *tert*-butanol, pentanol, hexanol, and octanol) and organic acids (butyric, octanoic, lauric, palmitic) were purchased from Merck (Darmstadt, Germany). Solvents were standard laboratory grade. Heptane was dried with metallic sodium and used as the solvent for all experiments. Substrates for esterification reactions were dehydrated with 0.32 molecular sieves (aluminum sodium silicate, type 13X; BHD Chemicals, Toronto, Canada) previously activated in an oven at 350°C for 6 h.

POS-PVA Synthesis

A POS-PVA hybrid composite was prepared by the hydrolysis and polycondensation of TEOS as described by Lima Barros et al. *(12)*. The reagents TEOS (5 mL), ethanol (5 mL), and PVA solution 2% (w/v) (6 mL) were carefully mixed and stirred for 5 min at 60°C, followed by addition of two or three drops of concentrated HCl in order to catalyze the reaction. After an incubation period of 40 min, the material was transferred to microwells of tissue culture plates and kept at 25°C until complete gel solidification (formation of the interpenetrated network of POS-PVA). Then the spheres were ground in a ball mill to attain with 37-µm-diameter particles, which was magnetized according to the methodology described by Carneiro-Leão et al. *(8)* based on the coprecipitation from a solution of $FeCl_3 \cdot 6H_2O$ and $FeCl_2 \cdot 4H_2O$. Activation of POS-PVA particles was carried out with 2.5% (w/v) glutaraldehyde at pH 7.0 for 1 h at room temperature, and the particles were thoroughly washed with distilled water.

Lipase Immobilization onto Magnetic POS-PVA Particles

Magnetic POS-PVA particles were incubated with lipase solution containing 0.05 U/mg of protein in phosphate buffer (0.1 *M*, pH 7.0) under low stirring for 16 h at room temperature. The immobilized lipase derivative was recovered by applying a magnetic field (6000 Oe), washed with 1 *M* NaCl, and maintained in 50 m*M* Tris-HCl buffer (pH 8.0) at 4°C. Immediately before the esterification reaction, the immobilized derivative was washed with hexane and vacuum dried to remove water. The resulting preparation had a specific activity of 3.31 U/(mg protein·g of dry support) using *p*-nitrophenol as substrate, and the degree of lipase immobilization was 70% *(13)*.

Esterification Reactions

Esterification reactions were carried out in a closed reactor with 10 mL of dried n-heptane containing suitable amounts of alcohol and acid. A molecular sieve (aluminum sodium silicate, type 13X; BHD Chemicals) was used to removal water. The mixture was incubated at 37°C for 24 h with continuous shaking at 150 rpm. The effects of concentration of immobilized lipase (5–50 mg/mL); molar ratio of reactants (0.5–2.0), acid chain length

(C4–C16), alcohol chain length (C4–C8), and alcohol structure (e.g., primary or secondary) were studied.

Analytical Methods

Water concentrations in liquid and solid phases were measured by the Karl Fisher method using the Karl Fisher Titrator (Mettler DL 18). Butanol and butyl butyrate were determined by gas chromatography using a 6-ft, 5% DEGS on a Chromosorb WHP, 80/10 mesh column (Hewlett Packard, Palo Alto, CA) and hexanol as internal standard. Acid consumption was monitored by volumetric titration of samples diluted in ethanol employing 0.02 *M* KOH alcoholic solution and phenolphthalein as pH indicator. Esterification was expressed as molar percent of consumed reactant, according to Eq. 1:

$$\text{Molar conversion \%} = \frac{C_o - C}{C_o} \times 100 \quad (1)$$

in which C_o is the initial molar concentration of reactant, and C is the reactant molar concentration at a given time.

Estimation of Partition Coefficients

The partition coefficients (POS-PVA/ external organic solvent) of butanol and butyric acid were estimated according to Eq. 2 as previously described by Dias et al. *(14)*.

$$\text{Partition coefficient} = \frac{C_o - C}{C} \times \frac{V_o}{V - V_o} \quad (2)$$

in which P is the reactant partition coefficient, C_o is the reactant concentration of organic phase, C is the reactant concentration after contact with support, V_o is the total volume (organic phase + support), and V is the organic-phase volume.

Partition experiments were conducted under the same conditions as their reaction counterparts. To estimate the support volume ($V - V_o$) a calibration curve of volume vs support mass was established (matrix volume [cm^3] = 1.72 × support mass [g] – 0.07; $R^2 = 0.999$). The equilibrium concentrations were attained 2 h after the immobilized lipase was added to the organic medium.

Results and Discussion

Influence of Immobilized Lipase Concentration

Butanol conversion to butyl butyrate employing different concentrations of immobilized lipase was examined in the presence of butyric acid and n-butanol at a 1.25:1 molar ratio. Syntheses were performed at 37°C, and immobilized lipase concentration varied from 5 to 50 mg/mL. As expected, completion of the reaction was very dependent on the enzyme

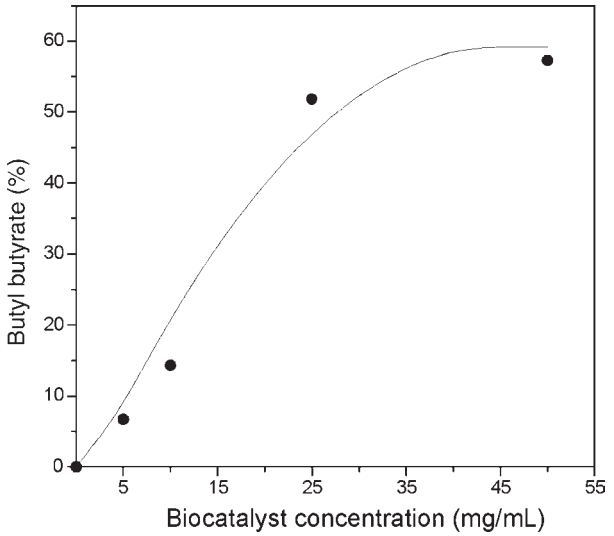

Fig. 1. Effect of immobilized lipase contents on the butyl butyrate synthesis at 37°C for 24 h. A molar ratio between butyric acid and butanol of 1.25 was used for enzyme contents of 5, 10, 25, and 50 mg/mL.

concentration (Fig. 1). Molar conversions > 50% were achieved in 24 h when high enzyme concentrations were used (25 and 50 mg/mL). Reactions carried out with lower enzyme concentrations (5 and 10 mg/mL) achieved lower molar conversions (6.7 and 14.7%, respectively). Such performance could be improved by modifying other variables that also affect the reaction yield, such as increasing the incubation temperature up to the optimum (45°C) for this lipase preparation *(13)* or using a higher butyric acid:*n*-butanol ratio. Acid in excess allows acyl group complex formation, leading to ester formation and reducing the competition between acceptors, an important parameter for esterification reaction kinetics *(15)*.

Effect of Substrate Molar Ratio

Lipase is known to catalyze esterification through an acyl-intermediate formed between the fatty acid substrate and the enzyme. Free enzyme can bind fatty acid to produce either this intermediate or the ester product. With a high concentration of alcohol, the acyl-intermediate will be consumed, and the enzyme may then start to bind product and catalyze its hydrolysis, thereby reversing the reaction. When present in an excess of fatty acid, however, most of the enzyme is found in the acylated form, preventing it from binding the product *(15,16)*.

Table 1
Partition Coefficients Matrix/Heptane of Reactants Estimated According to Eq. 2 at Initial Bulk Concentration of 100 m*M* in Heptane at 37°C and 150 rpm

	Partition coefficients	
Reactants	POS-PVA lipase	STY-DVB lipase[a]
n-Butanol	2.68	2.32
Butyric acid	1.28	1.66

[a]From ref. *7*.

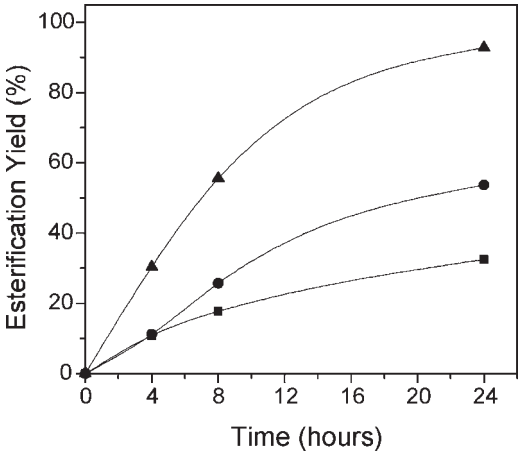

Fig. 2. Influence of butyric acid:butanol molar ratio on butyl butyrate yield. Molar ratios of 2:1 (▲), 1:1 (●), and 0.5:1 (■) were used at 37°C and 50 mg/mL of POS-PVA lipase.

For immobilized lipase preparations, a more complex mechanism is expected to occur since esterification efficiency is also highly dependent on the hydration state of the enzyme preparation, which can be greatly modified by the nature of the substrate and the support *(1,4)*. In the case of butyl butyrate synthesis, analysis of substrate polarity measured as partition coefficient (Table 1) showed a higher value for butanol than for butyric acid, favoring butanol migration to the solid phase (immobilized lipase). Thus, there should be more alcohol than acid at the active site of the immobilized lipase, requiring an excess of acid in the reaction medium to provide equimolar amounts of reactants and satisfactory yields *(7)*.

This expectation was confirmed by running a set of experiments in which the effect of the butyric acid (BA): butanol (ButOH) molar ratio on the esterification catalyzed by POS-PVA lipase was investigated in the range of 0.5–2.0. As shown in Fig. 2, no inhibition of enzyme activity was

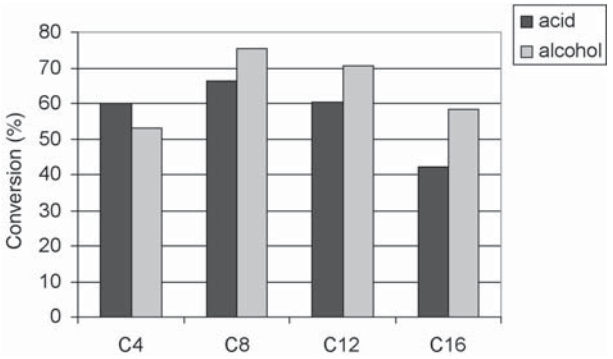

Fig. 3. Effect of acid chain length on ester synthesis catalyzed by POS-PVA lipase Reactions were carried out at 37°C for 24 h using *n*-butanol. C4, Butyric acid; C8, caprylic acid; C12, lauric acid; C16, palmitic acid.

detected when butyric acid was used in excess. Actually, progress of the esterification was limited by the availability of butyric acid in the reactor vessel. When the molar ratio was 0.5 a low esterification yield (33%) was obtained. This percentage increased with the rise in butyric acid concentration, reaching 93% yield, when the acid:alcohol molar ratio was 2.0. At an equimolar ratio, the yield was approximately half that attained when butyric acid was used in excess. The results suggest that the POS-PVA lipase, like other preparations, is greatly influenced by substrate molar ratio in the formation of the product. For example, studying the same reaction system with *Candida rugosa* lipase immobilized on styrene-divinylbenzene copolymer (STY-DVB) as catalyst, Oliveira et al. *(7)* verified that the molar ratio between butanol and butyric acid was a critical factor for attaining a high yield of butyl butyrate, requiring an amount of butyric acid on the order of 1.5 times that of butanol. This similarity can be attributed to the hydrophobic character of the supports and partition coefficient values attained for these immobilized derivatives: POS-PVA lipase and STY-DVB lipase (Table 1).

Effect of Acid Chain Length

It has been clearly demonstrated in the literature that in the case of direct esterification, the chain length of acid and alcohol affects the ester yield *(16–19)*. In the present work, we investigated the reactivity of acyl donors of various chain lengths, ranging from butyric (C4) to palmitic acid (C16) in the esterification of butanol. The reaction medium consisted of amounts of the required acid and butanol at a fixed molar ratio (1.5) and 25 mg/mL of POS-PVA lipase. The molar conversion of butanol was calculated after 24 h of reaction, and the values attained for each acyl donor tested are displayed in Fig. 3.

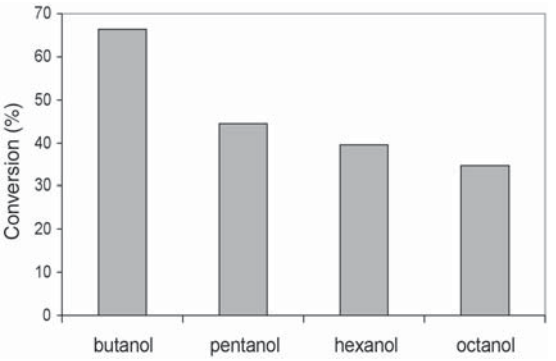

Fig. 4. Effect of alcohol chain length on ester synthesis catalyzed by POS-PVA lipase. Reactions were performed at 37°C for 24 h using caprylic acid as acyl donor.

Reaction rates by POS-PVA lipase gradually increased from C4 to C8, reached a plateau between C8 and C12, and then an activity decrease was observed, probably owing to a substrate-size feature limitation. From this set of results, caprylic acid (C8) may be considered the best acyl donor for the synthesis of butyl esters in heptane by POS-PVA lipase.

Similar results from Langrand et al. *(18)* showed that lipase from *M. miehei* was more active in synthesizing geranyl esters by esterification in the presence of acids with carbon atom numbers 4 to 6. Other researchers *(19)* have demonstrated that for esterification of octanol, this enzyme was most active in the presence of an acid with a carbon atom number of 7. According to these researchers, this effect seems to be related to the fitting of both substrates into the active site of the enzyme: an optimum value of 15 for the sum of carbon chain length of the two substrates was deduced from those results *(19)*. Selmi et al. *(20)* reported a different behavior in triglyceride synthesis catalyzed by a commercial immobilized *M. miehei* lipase: high rates and equilibrium yields were obtained with long chain fatty acids, mainly hexadecanoic and octadecanoic acids. These differences probably can be explained by the diversity among enzyme sources; the type of support; and the methods of immobilization employed in each investigation, since immobilization technique can change fatty acid specificity *(17,21,22)*.

Effect of Alcohol Chain Length

The influence of alcohol chain length was studied by using substrate containing caprylic acid and the required alcohol (C4 to C6 and C8) at a fixed molar ratio (1.5) and 50 mg/mL of POS-PVA lipase. The results of acid molar conversion after 24 h are displayed in Fig. 4. The carbon chain significantly influenced esterification performance. As the length of the alcohol carbonic chain increased, lower molar conversion was detected. The highest value (70%) was attained for butanol and the lowest (40%) for octanol.

Table 2
Influence of Butanol Structure on Ester Synthesis Performed at 37°C for 24 h

Butanol structure	Reaction time (h)	Butyric acid (mg/mL)	Water content (ppm)	Molar conversion (%)
n-Butanol	0	21.25	317	0
	24	8.57	302	59.63
sec-Butanol	0	21.82	343	0
	24	16.51	302	24.33
tert-Butanol	0	22.61	392	0
	24	17.81	423	21.27

Pereira et al. *(17)* did not observe differences on acid conversion with alcohol varying between C4 and C10 in reactions performed with *C. rugosa* lipase immobilized on chitosan. However, Manjon et al. *(23)* working with *M. miehei* lipase immobilized on Celite verified that esterification yields decreased as the chain length of the acid or alcohol increased, with the alcohol length having a higher influence than the acid.

Comparison of Figs. 3 and 4 reveals that alcohol chain length exerted more influence on ester yield than the acid carbon size. For alcohol size varying from C5 to C8, conversion was lower than 40%, and for acid size from C4 to C16, similar esterification yields (60–80%) were found. These results may reflect both the intrinsic selectivity of the enzyme and different accessibility of substrates to enzyme active site *(22)*.

Effect of Alcohol Structure

In addition to the chain length, the effect of branching of the carbon chain was studied. Specificity of POS-PVA lipase was studied by monitoring esterification reactions of *n*-butanol, *sec*-butanol, and *tert*-butanol with butyric acid, as shown in Table 2. The highest rate of conversion to ester (60%) occurred in the presence of *n*-butanol, compared with *sec*-butanol and *tert*-butanol. The branching was found to decrease significantly the esterification yield by a factor of 0.4 for sec-butanol and 0.65 for tert-butanol. Antczak et al. *(24)* reported a similar conversion pattern.

Note that control and maintenance of low water contents during esterification progress was a difficult task only for reactions carried out with *tert*-butanol (Table 2). Besides affecting reaction yields, high water contents favors the reverse reaction (ester hydrolysis) by decreasing even more the amount of ester formed *(1,4)*.

Conclusions

The alkoxysilane sol-gel process is an efficient method to prepare silica glass by the hydrolysis of alkoxysilane precursors and by subsequent con-

densation of the remaining silanols, followed by aging and drying under ambient atmospheres and sintering. The hydrolysis and polycondensation of TEOS is as follows:

Si (OEt)e → Hydrolysis → n(EtO)x Si (OH)y-x → Polycondensation → (SiO_2)n

In our work, particles of POS-PVA were utilized to immobilize *M. miehei* lipase, and the performance of the immobilized derivative was investigated for ester synthesis in organic media. POS-PVA lipase was able to catalyze ester synthesis by proper selection of the environmental parameters enzyme concentration, molar ratio of the reactants, substrate size, and chemical structure. Higher yields were achieved for substrates containing acyl donor in excess and using high loading of immobilized lipase (25 mg/mL). A close relationship between reactant polarity and ester formation was verified. Acid containing eight carbons and primary alcohol with four carbons were considered to be suitable reactants resulting in high esterification rates. Other reaction parameters, such as temperature, could be investigated to improve esterification yields.

Acknowledgments

We gratefully acknowledge Embrapa and Conselho Nacional de Desenvolvimento Científico e Tecnológico (CNPq) for financial support.

References

1. Yahya, A. R. M., Anderson, W. A., and Moo-Young, M. (1998), *Enzyme Microb. Technol.* **23,** 438–450.
2. Balcao, V. M., Paiva, A. L., and Malcata, F. X. (1996), *Enzyme Microb. Technol.* **18,** 392–416.
3. Pandey, A., Benjamin, S., Soccol, C. R., Nigam, P., Krieger, N., and Soccol, V. T. (1999), *Biotechnol. Appl. Biochem.* **29,** 119–131
4. Castro, H. F. and Anderson, W. A. (1995), *Quim Nova* **18,** 544–554.
5. Villeneuve, P., Muderhwa, J. M., Graille, J., and Hass, M. J. (2000), *J. Mol. Cat. B Enzymatic* **9(4–6),** 113–148.
6. Gitlesen, T., Baucer, M., and Adlercreutz, P. (1997), *Biochim. Biophys. Acta* **1345,** 188–196.
7. Oliveira, P. C., Alves, G. M., and de Castro, H. F. (2000), *Quim Nova* **23,** 632–636.
8. Carneiro-Leão, A. M. A., Oliveira, E. A., and Carvalho, Jr., L. B. (1991), *Appl. Biochem. Biotechnol.* **31,** 53–58.
9. Soares, C. M. F., de Castro, H. F., Moraes, F. F., and Zanin, G. M. (1999), *Appl. Biochem. Biotechnol.* **77–79,** 745–757.
10. Keeling-Tucker, T., Rakic, M., Spong, C., and Brennan, J. D. (2000), *Chem. Mater.* **12,** 3695–3704.
11. Reetz, M. T., Zonta, A., and Simpelkamp, J. (1996), *Biotechnol. Bioeng.* **49,** 527–534
12. Lima Barros, A. E., Almeida, A. M. P., Carvalho, Jr., L. B., and Azevedo, W. M. (2002), *Braz. J. Med. Biol. Res.* **35,** 459–463.
13. Bruno, L. M. (2003), PhD thesis, Universidade Federal de Pernambuco, Av. Prof. Moraes Rego, 1235; Cidade Universitária, Recife, PE, CEP, Brazil.
14. Dias, S. F., Vilas-Boas, L., Cabral, J. M. S., and Fonseca, N. M. R. (1991), *Biocatalysis* **5,** 21–34.
15. de Castro, H. F., Pereira, E. B., and Anderson, W. A. (1996), *J. Brazi. Chem. Soc.* **7,** 219–224.

16. de Castro, H. F., Oliveira, P. C., and Soares, C. M. F. (1997), *Cienc. Tecnol. Aliment.* **17,** 237–241.
17. Pereira, E. B., de Castro, H. F., Moraes, F. F., and Zanin, G. M. (2002), *Appl. Biochem. Biotechnol.* **98–100,** 977–986.
18. Langrand, G., Rondon, N., Triantaphylides, C., and Baratti, J. (1990), *Biotechnol. Lett.* **12,** 581–596.
19. Miller, C., Austin, H., Posorske, L., and Gonzlez, J. (1988), *JAOCS* **65,** 927–931.
20. Selmi, B., Gontier, E., Ergan, F., and Thomas, D. (1998), *Enzyme Microb. Technol.* **23,** 182–186.
21. Aguiar, C. L., Moreira, M. R. V., and de Castro, H. F. (2001), *Cienc. Tecnol. Aliment.* **3,** 134–139.
22. Sinestra, J. V. (1996), in *Engineering of/with Lipases*. Malcata, F. X., ed., Kluwer Academic Publishers, Dordrecht, The Netherlands, pp. 73–101.
23. Manjon, A., Iborra, J. L., and Arocas, A. (1991), *Biotechnol. Lett.* **13,** 339–344.
24. Antczak, T., Mrowiec-Bialon, J., Bielecki, S., Jarrzebski, A. I., and Galas, I. (1997), *Biotechnol. Techniques* **11,** 9–11.

0273-2289/04/113/0201–0211/$25.00

Effect of pH on Cellulase Production of *Trichoderma reesei* RUT C30

Tamás Juhász, Zsolt Szengyel,* Nóra Szijártó, and Kati Réczey

Department of Agricultural Chemical Technology, Budapest University of Technology and Economics, Szent Gellért tér 4., Budapest, 1521 Hungary

Abstract

Currently, the high market price of cellulases prohibits commercialization of the lignocellulosics-to-fuel ethanol process, which utilizes enzymes for saccharification of cellulose. For this reason research aimed at understanding and improving cellulase production is still a hot topic in cellulase research. *Trichoderma reesei* RUT C30 is known to be one of the best hyper producing cellulolytic fungi, which makes it an ideal test organism for research. New findings could be adopted for industrial strains in the hope of improving enzyme yields, which in turn may result in lower market price of cellulases, thus making fuel ethanol more cost competitive with fossil fuels. Being one of the factors affecting the growth and cellulase production of *T. reesei*, the pH of cultivation is of major interest. In the present work, numerous pH-controlling strategies were compared both in shake-flask cultures and in a fermentor. Application of various buffer systems in shake-flask experiments was also tested. Although application of buffers resulted in slightly lower cellulase activity than that obtained in non-buffered medium, β-glucosidase production was increased greatly.

Index Entries: Cellulase production; *Trichoderma reesei* RUT C30; pH profiling; β-glucosidase; shake flask; fermentor.

Introduction

Because of the environmental considerations that has emerged during the past two decades, biomass-originated alternative fuels have gained remarkable attention. Ethanol, owing to its advantageous physical properties, seems to be a potential substitute for gasoline in internal combustion engines in the near future. The obvious choice of raw material that could support large-scale fuel ethanol production would be lignocellulo-

*Author to whom all correspondence and reprint requests should be addressed.

sics because of their widespread availability. One of the process alternatives suggested for the production of fuel ethanol from lignocellulosic materials is based on the enzymatic saccharification of cellulose. For efficient conversion of the cellulose fraction, a large enzyme dosage per unit of raw material must be applied, which, owing to the high market price of cellulases, significantly increases the overall production cost of ethanol.

Trichoderma reesei RUT C30 is known to be one of the best hyperproducing cellulolytic fungi. Several factors, such as the amount and quality of carbon source, temperature and pH of the cultivation, and aeration, influence enzyme production of this strain. It has been indicated in previous studies that pH and the pH-controlling strategy have a great effect on the amount of cellulase produced *(1–9)*.

It has been shown that depending on the nature of the carbon source used to induce the cellulase production of *Trichoderma* strains, different initial pH values of the cultivation may be optimal for maximum cellulase yield. Ryu and Mandels *(1)* have reported that a pH range of 3.0 to 4.0 was optimal for pure cellulose carbon source, but a higher initial pH was recommended for lignocelluloses. For medium containing sugarcane bagasse (free of water-soluble sugars), a pH between 5.0 and 6.0 was observed to be optimal using *T. reesei* QM 9123 (NRRL 3653) *(2)*. In other studies, maximum yield of cellulases was obtained in the range of pH 3.0–5.0 *(3–5)*.

Tangnu et al. *(6)* studied the influence of pH on cellulase production of *T. reesei* RUT C30 in a pH-controlled fermentor. In the pH range of 4.0–6.0, no significant effect on the production rate and final cellulase yield was observed, but β-glucosidase production was affected to a large extent. At pH 4.0 and 5.0, β-glucosidase activity gradually increased until it reached its maximum value by d 8 of cultivation. Controlling the pH in the fermentor to 6.0 increased the production rate of β-glucosidase considerably, and an approx 30% higher enzyme yield was achieved by d 4 than at lower pH values. However, during the final stage of the fermentation the level of β-glucosidase activity decreased to the same value as measured at lower pH levels. Hendy et al. *(7)* reported that performing the fermentation above pH 5.0 resulted in a significant loss of cellulase activity. Instead of keeping the pH at a constant value during the whole fermentation process, Doppelbauer et al. *(8)* recommended using pH profiling. For the growth phase of *T. reesei*, the pH of cultivation was suggested to be maintained at 4.0, while in the later stage of production and secretion of cellulases, an elevated pH level of 5.0 was recommended. In another study, pH cycling coupled with temperature profiling increased the amount of cellulases by 13% compared to the control case during which the pH was maintained at a constant value *(9)*.

In shake-flask cultures, pH control is usually limited to either addition of buffering salts such as phosphates, or periodic manual pH adjustment, which is obviously tedious and less effective. The use of ammonium sulfate as the major nitrogen source in Mandels' medium *(10)* requires a more compelling buffering system. Without buffering, the pH drops quickly

during the first stage of the fermentation owing to the depletion of ammonia and liberation of protons *(11–13)*. Application of a KH_2PO_4-K_2HPO_4 buffer system for controlling the pH in shake flasks proved to be inefficient in compensating acidification. However, higher cellulase activity was obtained in the buffered system than in the basal Mandels' medium *(14)*. Kadam and Keutzer *(5)* investigated several organic acid buffer systems—acetate, succinate, phthalate, and citrate; unfortunately, they did not report the efficiency of the various buffer systems.

In the present study, pH-controlling strategies were executed in both shake-flask cultures and a fermentor. Furthermore, various organic acid buffer systems were studied and their efficiency was evaluated in shake-flask cultures.

Materials and Methods

Inoculum Preparation

Freeze-dried conidia of *Trichoderma reesei* RUT C30 (ATCC 56765) were obtained from the American Type Culture Collection (ATCC). The stock culture of the fungus was maintained on agar slants containing 20 g/L of malt extract, 5 g/L of glucose, 1 g/L of proteose peptone, and 20 g/L of bacto agar. After 14 d at 30°C, the greenish conidia were suspended in 5 mL of sterile water, and 1 mL of this suspension was transferred aseptically to a 750-mL Erlenmeyer flask containing 150 mL of sterile and pH-adjusted (5.5) Mandels' medium in which the concentrations of nutrients were as follows: 0.3 g/L of urea, 1.4 g/L of $(NH_4)_2SO_4$, 2.0 g/L of KH_2PO_4, 0.3 g/L of $CaCl_2$, 0.3 g/L of $MgSO_4$, 0.25 g/L of yeast extract, 0.75 g/L of proteose peptone and 7.5 g/L of Solka Floc 200 (International Fiber, New York, NY) cellulose powder. Furthermore, the medium was supplemented with the following trace elements: 5 mg/L of $FeSO_4 \cdot 7H_2O$, 20 mg/L of $CoCl_2$, 1.6 mg/L of $MnSO_4$, 1.4 mg/L of $ZnSO_4$. Preparation of the inoculum was completed by 4 d of cultivation at 30°C on an orbital shaker (350 rpm) *(10)*.

Enzyme Production in Shake Flasks

A 15-mL mycelium suspension obtained from the inoculum cultures was used to initiate growth in a 750-mL Erlenmeyer flask containing 150 mL of a modified Mandels' medium in which the concentration of the carbon source (i.e. Solka Floc 200), was increased to 10.0 g/L. After inoculation, the Erlenmeyer flasks were incubated on an orbital shaker at 30°C and 350 rpm for 7 d. Samples were withdrawn daily at the same hour of the day, and when necessary, the pH in the flasks was manually adjusted using sterile, 10 wt% solutions of NaOH or H_2SO_4. Aseptically taken samples were centrifuged at 3400*g* for 5 min. The collected supernatants were analyzed for enzyme activities. In shake-flask cultures, basically three pH-controlling strategies were applied: (1) the pH was adjusted to its initial value (5.0 or 6.0), thereby obtaining a sawtooth-like pH profile; (2) starting from pH values of 5.0 or 6.0, the adjustment was restricted to

those cases when the pH dropped below 4.0; (3) by applying various buffers in the production medium, the pH was kept at a constant value of 5.0 or 6.0. Each experimental condition was performed in triplicate, and the average of measured parameters (pH, enzyme activities) was calculated.

Enzyme Production in Laboratory-Scale Fermentor

Upscale enzyme production experiments were performed in a 31-L double-walled stainless steel laboratory fermentor (Biostat CDCU-3; B Braun Biotech, Germany). Fermentation of *T. reesei* RUT C30 was performed in modified Mandels' medium as described in the previous section. Prior to sterilization at 121°C for 20 min, the nutrients, carbon source, and trace elements required for 20 L of production medium were dissolved in 19.5 L of tap water. During sterilization, vapor equivalent to about 500 mL of water was bled through the gas exhaust system in order to achieve sterile conditions. After sterilization, the temperature of the fermentor was decreased to 30°C and 1 L of starter culture was aseptically added to initiate growth and enzyme production. Cultivation of *T. reesei* RUT C30 was carried out with an agitation rate of 250 rpm for 72 h. Samples were withdrawn regularly and centrifuged at 3400*g* for 5 min. Supernatants were collected and enzyme activities were measured. Four different experimental conditions were performed applying two pH-controlling strategies: (1) from the initial pH (5.0 or 6.0), the pH was allowed to drop to 3.5, after which it was adjusted to and further controlled at the starting pH; (2) no pH shift was allowed and the pH was continuously set to the starting pH of 5.0 or 6.0. In both strategies the pH was controlled by automatic addition of sterile, 10 wt% solutions of either H_2SO_4 or NaOH. The dissolved oxygen (DO) level in the production medium was kept at 30% of saturation value for the medium throughout the fermentation by controlling the flow rate of the air supply. To avoid the formation of foam, silicon oil–based Sigma-Aldrich Antifoam A (Munsch, Germany) in 30% ionic emulsion was added manually four times a day at about 6-hour intervals.

Analysis

Cellulase activity of the samples was determined as filter paper activity (FPA) expressed in filter paper units (FPU) using Mandels' procedure *(15)*, and β-glucosidase activity was assayed using 4-nitrophenyl-β-D-glucopyranoside substrate according to Berghem and Petterson's *(16)* method. All samples were analyzed in triplicate and the mean values were calculated. The relative standard deviation of enzyme activity measurements was always below 5%.

Prior to high-performance liquid chromatography (HPLC), samples were filtered through a 0.2-μm pore size mixed cellulose ester filter (Schleicher & Schuell, Dassel, Germany). Buffer components such as acetic acid, citric acid, maleic acid, and succinic acid were separated on an Aminex HPX-87H (Bio-Rad, Hercules, CA) organic acid column at 65°C using a

Table 1
Application of Organic Acid Buffer Systems in Shake-Flask Cultures

Buffer system	Cellulase	β-Glucosidase	pH stability
0.1 *M* Citric acid–citrate, pH 5.0	Poor	Poor	Poor
0.1 *M* Acetic acid–acetate, pH 5.0	—	—	Very good
0.1 *M* Succinic acid–NaOH, pH 5.0	High	High	Poor
0.1 *M* Tris–maleic acid, pH 6.0	Good	Good	Very good
0.1 *M* Maleic acid, pH 6.0	Good	High	Very good

5 m*M* H_2SO_4 mobile phase at a flow rate of 0.5 mL/min. The analytical column was protected with a Cation-H (Bio-Rad) precolumn. For detection of organic acids separated on the analytical column, a Shimadzu RID-10A refractive index detector (Kyoto, Japan) was used.

Results and Discussion

Shake-Flask Cultivations

The aim of the first set of experiments performed in shake-flask cultures was to develop a buffer system with a sufficiently high buffering capacity to compensate the rapid pH drop typically observed on Mandels' medium during the first stage of the cultivation process. Inorganic phosphate salts were excluded during the selection of potential buffer systems, because they have already been proved to be insufficient *(14)*. The choice of organic acid buffer systems seemed to be promising for two reasons: (1) organic acids were believed not to be utilizable by the microorganism, and, therefore, they could be applied in relatively small concentrations compared to phosphate salts; and (2) most of the organic acid buffer systems are capable of controlling the pH in the range of our interest. Although citric acid and acetic acid have already been examined in a previous study, the pH range in which they were applied was much lower than our primary interest *(5)*. Thus, these organic acids were also tested in our experimental series along with Tris–maleic acid, maleate, and succinate as shown in Table 1. All buffer systems were applied in a 0.1*M* concentration. The concentration of various organic acids in fermentation samples was determined using HPLC. The acetic acid–acetate buffer system applied at pH 5.0 kept the pH constant throughout the fermentation. No changes in acetic acid concentration could be observed in the medium. However, no enzyme activities were detected after 7 d of cultivation. Inhibition of microbial growth by weak acids in pH intervals below or close to the pK_A of the acid used (4.8 in this case) could be a reasonable explanation for the poor performance of *T. reesei* RUT C30. Although employing succinic acid in the fermentation medium at pH 5.0 resulted in rather high enzyme activities compared to the other buffer systems used,

Table 2
pH-Controlling Strategies Followed in Shake-Flask Cultivation of *T. reesei* RUT C30

Condition	pH-controlling strategy
A	Daily pH adjustment to 5.0
B	pH adjustment in case pH drops below 4.0, starting pH: 5.0
C	Daily pH adjustment to 6.0
D	pH adjustment in case pH drops below 4.0, starting pH: 6.0
E	0.1 *M*, Tris–maleic acid buffer, pH 6.0, no manual adjustment necessary
F	0.1 *M*, Maleic acid–NaOH buffer, pH 6.0, no manual adjustment necessary

the pH fluctuated over a wide range. At the beginning of the cultivation, buffering capacity was not high enough to prevent acidification caused by ammonia depletion, whereas in the final stage, succinic acid was taken up by the fungus and a dramatic pH shift to the alkaline region was observed. In contrast to previous results reported by Kadam and Keutzer *(5)*, citric acid buffer could not control the pH at 5.0. Similarly to the succinic acid buffer system, citric acid was also consumed by *T. reesei* RUT C30, and an extensive basification of the medium was observed. In this case, cellulases and β-glucosidase enzymes were produced in moderate amounts. Cultivation of *T. reesei* RUT C30 in Tris–maleic acid, and maleic acid–NaOH buffer systems was quite promising. Both FPA and β-glucosidase activities were considerably high in the fermentation broth using these systems. Furthermore, these buffer systems managed to maintain the pH around the desired value with great stability.

In another set of shake-flask experiments, Tris–maleic acid and maleic acid–NaOH buffer systems were quantitatively compared with two other pH-controlling strategies. All together six experimental setups were tested against each other, as shown in Table 2. No significant difference was observed when final FPA activities were compared. Cellulase activites of about 1.2–1.4 FPU/mL were measured on the d 7 of cultivation in each condition. In conditions A and B, the cellulase activity increased gradually, reaching a maximum value of 1.4 FPU/mL on the last day of cultivation. However, when the initial pH of the cultivation was 6.0 without buffer addition (conditions C and D), the cellulase activity reached its maximum of 1.5 FPU/mL on d 4, while was followed by a steady decrease until the end of fermentation. As for the two sets of buffered conditions, a cellulase activity of 1.3 FPU/mL was achieved by the d 4. Moreover, the cellulase activity remained at this level for the rest of the cultivation. In terms of enzyme production rates (*see* Table 3), the highest value of 15.8 FPU/(L·h) was reached with non-buffered conditions C and D, whereas the value was slightly lower, 13.4 FPU/(L·h), for the buffered conditions E and F. It seems

Table 3
Cellulase Activities and Cellulase Formation Rates (r_c) in Shake-Flask Experiments by d 4 of Cultivation

Condition	FPA (FPU/mL)	r_c (FPU/[L·h])
A	1.034	10.8
B	1.054	11.0
C	1.520	15.8
D	1.520	15.8
E	1.282	13.4
F	1.282	13.4

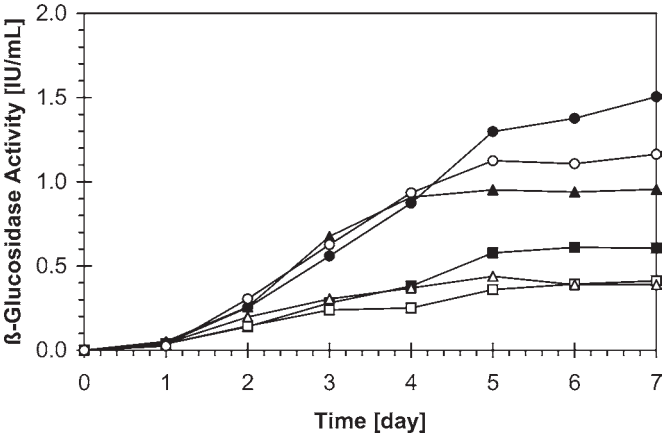

Fig. 1. β-Glucosidase activity vs time for shake-flask cultivations using different pH-controlling strategies. (—■—), Condition A; (—□ —), condition B; (—▲ —), condition C; (—△—), condition D; (—● —), condition E; (—○—), condition F.

that in non-buffered conditions it is only the starting pH that influences cellulase production with *T. reesei* RUT C30, since similar results were obtained with two different pH-controlling strategies (A, B or C, D).

Both the starting pH of cultivation and pH-controlling strategy followed during the fermentation process had a synergistic effect on the amount of produced β-glucosidase enzyme. To obtain some exact data for the pH representative for a certain pH-controlling strategy, time-averaged pH values were calculated from the daily measured pH values for each condition. These averaged pH values were the highest, pH 6.0, for the buffered conditions E and F. The best β-glucosidase activities, 1.5 and 1.2 IU/mL, were also obtained for condition E and F, respectively (Fig. 1).

Table 4
pH-Controlling Strategies Followed in Fermentor

Condition	pH-controlling strategy
I	pH continuously controlled to 5.0
II	pH allowed to drop down to 3.5 from initial 5.0, and further controlled to 5.0
III	pH continuously controlled to 6.0
IV	pH allowed to drop down to 3.5 from initial 6.0, and further controlled to 6.0

An approximate β-glucosidase activity of 1.0 IU/mL was reached when condition C was applied. In this case, the time-averaged pH was calculated to be 5.7. With daily pH adjustment to 5.0 (condition A), a β-glucosidase level as low as 0.6 IU/mL was reached. On the other hand, the time-averaged pH of cultivation, 4.7, was much lower than in previously mentioned cases. The lowest β-glucosidase activities of about 0.4 IU/mL were obtained with conditions B and D, in which cases the time-averaged pH values were also the lowest, 4.1 and 4.6, respectively. In most cases, except for conditions, B and D, in which the β-glucosidase activity was steadily increasing throughout the whole fermentation, maximum β-glucosidase activities were obtained on d 5 of cultivation.

Cellulase Production in Laboratory-Scale Fermentor

Four different pH-controlling strategies were subjected for further investigation in a laboratory-scale fermentor. Based on the results of the shake-flask trials, it seemed that keeping the pH at a constant value could be advantageous for both cellulase and β-glucosidase production. Although slightly faster cellulase production was observed in nonbuffered cultures with the pH-adjusted daily to 6.0, the 50% higher β-glucosidase activity obtained applying the Tris–maleic acid buffer system was appealing for constant pH regulation strategy. Table 4 summarizes the pH-controlling strategies followed in the fermentor. Hereafter these conditions are referred to by roman numerals.

Andreotti et al. *(17)* reported that the growth of *T. reesei* was more rapid at high pH ranges, while the optimum pH interval for enzyme production was between 3.0 and 4.0 *(1,17)*. Cultivation of *T. reesei* RUT C30 using control strategies I and II is summarized in Fig. 2. Throughout the fermentation process, the DO was kept at a constant value of 30% of saturation for the medium; therefore, the airflow rate could be used as a representative measure of microbial growth (Fig. 2B). Although the growth of *T. reesei* RUT C30 was faster when the pH was regulated to 5.0 (Fig. 2B), the formation of cellulases was slower than for condition II (Fig. 2A), as we had expected based on literature data. However, in the case of condition II,

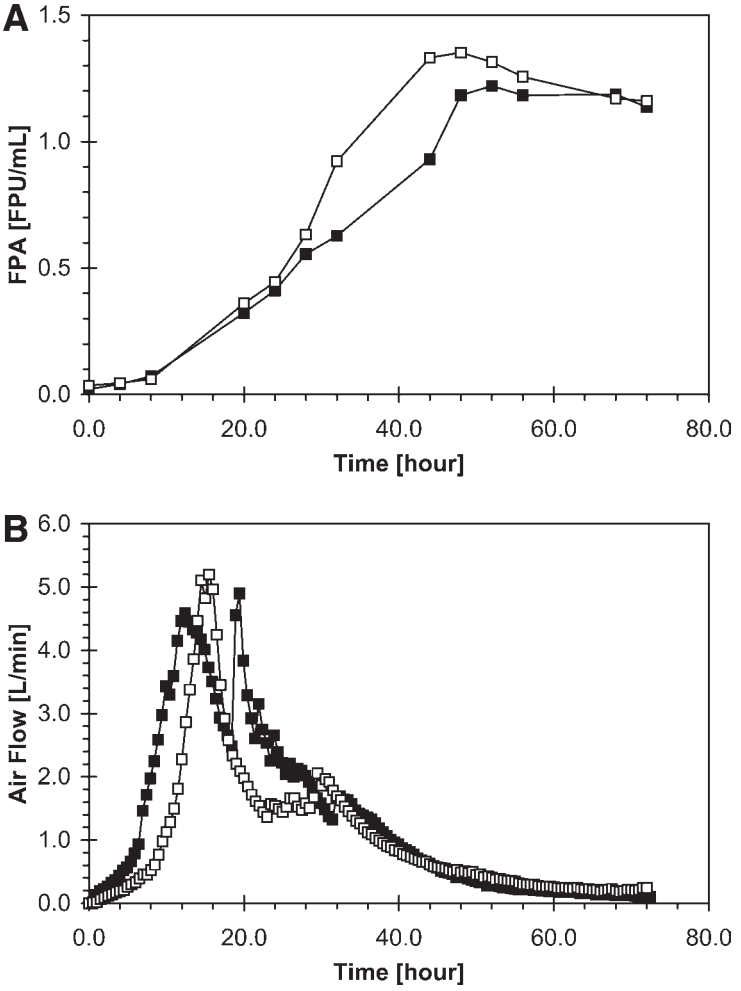

Fig. 2. Cultivation of *T. reesei* RUT C30 in laboratory fermentor using pH-controlling strategies I and II: **(A)** cellulase activity; **(B)** air flow rate. (—■ —), Condition I; (—□ —), condition II.

in which the pH was allowed to drop to 3.5, contrary to our expectation, the cellulase production rate was similar to that of condition I, until the pH was shifted back and regulated to 5.0 for the rest of the fermentation. For cellulase production, an immediate response to the pH shift was observed. About 40% higher cellulase activity was achieved by h 44 of the fermentation, when compared with that obtained with constant pH (condition I). Unfortunately, during the later phase of the fermentation, deactivation of cellulases was observed.

In the case of pH strategies III and IV, no remarkable differences in the growth and production rate of cellulases were seen up to h 52 of fermentation (data not shown), after which deactivation of cellulases was detected.

At a constant pH of 6.0 (condition III), this deactivation occurred to a greater extent than for that seen in the case of pH shift applied (condition IV).

The amounts of β-glucosidase were below the expected values and an activity of about 0.4 IU/mL was achieved in all cases. In each experiment, the amount of β-glucosidase increased steadily throughout the whole fermentation, reaching a maximum at h 60. No noteworthy differences in the production rates were seen.

Conclusions

Six pH-controlling strategies were compared in shake-flask experiments using *T. reesei* RUT C30. The initial pH of the cultivation did not influence the final cellulase activity remarkably, but the cellulase production rates and β-glucosidase activities were affected to a great extent. Regardless of the pH-controlling strategy applied, at pH 6.0, a maximum cellulase activity was achieved by d 4 of cultivation; however, during the final stage of the fermentation, deactivation of cellulases was observed. At pH 5.0, cellulase activity gradually increased throughout the whole fermentation process. A correlation between time-averaged pH values of the cultivations and the β-glucosidase activity was observed. Higher pH is favorable for β-glucosidase production of *T. reesei* RUT C30. Organic acid buffer systems were evaluated for their potential to keep the pH of the cultivation constant. Most of the buffer systems tested could not regulate the pH throughout the fermentation because they were possibly metabolized by the fungus. Tris–maleic acid and maleic acid–NaOH systems performed very well in shake-flask cultures, and a noteworthy improvement in β-glucosidase production was achieved. It was assumed that regulating the pH at a constant level would be favorable for β-glucosidase production. However, laboratory-scale fermentor experiments performed in non-buffered but pH-regulated medium did not confirm this theory. In fact, significantly lower β-glucosidase production was seen in the fermentor, which may suggest that one of the buffer components affected the cellulase production. However, based on these results, it would be a rather premature conclusion to claim any of the buffer components responsible for the higher cellulase and β-glucosidase activities obtained in the shake-flask experiments. A sudden pH shift after allowing acidification of the production medium during the initial phase of the cultivation increased the rate and titer of the cellulases at pH 5.0. However, at pH 6.0 no difference was observed.

Acknowledgments

This work was supported by EC "TIME" project (ENK6-CT-2002-00604). We also gratefully acknowledge the Hungarian Ministry of Education for its financial contribution (NKFP-OM 00231/2001).

References

1. Ryu, D. D. Y. and Mandels, M. (1980), *Enzyme Microb. Technol.* **2,** 91–102.
2. Kanson, A. L., Essam, S. A., and Zeinat, A. N. (1999), *Polym. Degrad. Stabil.* **63,** 273–278.

3. Mukhopadhyay, S. and Nandi, B. (1999), *J. Sci. Ind. Res*. **58,** 107–111.
4. Wayman, M. and Chen, S. (1992), *Enzyme Microb. Technol*. **14,** 825–831.
5. Kadam, K. L. and Keutzer, W. J. (1995), *Biotechnol. Lett*. **17,** 1111–1114.
6. Tangnu, S. K., Blanch, H. W., and Wilke, C. R. (1981), *Biotechnol. Bioeng*. **23,** 1837–1849.
7. Hendy, N. A., Wilke, C. R., and Blanch, H. W. (1984), *Enzyme Microb. Technol*. **6,** 73–77.
8. Doppelbauer, R., Esterbauer, H., Steiner, W., Lafferty, R. M., and Steinmüller, H. (1987), *Appl. Microbiol. Biotechnol*. **26,** 485–494.
9. Mukhopadhyay, S. N. and Malik, R. K. (1980), *Biotechnol. Bioeng*. **22,** 2237–2250.
10. Mandels, M. and Weber, J. (1969), *Adv. Chem. Ser*. **95,** 391–414.
11. Sternberg, D. (1976), *Biotechnol. Bioeng. Symp*. **6(6),** 35–53.
12. Chahal, D. S., McGuire, S., Pikor, H., and Noble, G. (1982), *Biomass* **2(2),** 127–137.
13. Duff, S. J. B., Cooper, D. G., and Fuller, O. M. (1987), *Enzyme Microb. Technol*. **9,** 47–51.
14. Yu, X.-B., Hyun S. Y., and Yoon-Mo, K. (1998), *J. Microbiol. Biotechnol*. **8,** 208–213.
15. Mandels, M., Andreotti, R., and Roche, C. (1976), *Biotechnol. Bioeng. Symp*. **6(6),** 21–33.
16. Berghem, L. E. E. and Petterson, L. G. (1976), *Eur. J. Biochem*. **46,** 295–305.
17. Andreotti, R. E., Mandels, M., and Roche, C. (1977), in *Bioconversion of Cellulosic Substrates into Energy, Chemicals and Microbial Protein: Proceedings of Bioconversion Symposium*, Ghose, T. K., ed., Indian Institute of Technology, Delhi, pp. 249–267.

0273-2289/04/113/0213–0231/$25.00

Quantitative Analysis of Cellulose-Reducing Ends

Sasithorn Kongruang, Myung Joo Han, Claudia Isela Gil Breton, and Michael H. Penner*

Department of Food Science and Technology, Oregon State University, Corvallis, OR 97331-6602, E-mail: Mike.Penner@oregonstate.edu

Abstract

Methods for the quantification of total and accessible reducing ends on traditional cellulose substrates have been evaluated because of their relevance to enzyme-catalyzed cellulose saccharificaion. For example, quantification of accessible reducing ends is likely to be the most direct measure of substrate concentration for the exo-acting, reducing end-preferring cellobiohydrolases. Two colorimetric assays (dinitrosalicylic acid [DNS] and bicinchoninic acid [BCA] assay) and a radioisotope approach (NaB^3H_4 labeling) were evaluated for this application. Cellulose substrates included microcrystalline celluloses, bacterial celluloses, and filter paper. Estimates of the number of reducing ends per unit mass cellulose were found to be dependent on the assay system (i.e. the DNS and BCA assays gave strikingly different results). DNS-based values were several-fold higher than those obtained using the BCA assay, with fold-differences being substrate specific. Sodium borohydride reduction of celluloses, using cold or radiolabeled reagent under relatively mild conditions, was used to assess the number of surface (solvent-accessible) reducing ends. The results indicate that 30–40% of the reducing ends on traditional cellulose substrates are not solvent accessible; that is, they are buried in the interior of cellulose structures and thus not available to exo-acting enzymes.

Index Entries: Cellulose; cellobiohydrolase; reducing sugar assays; insoluble reducing ends; solvent-accessible reducing ends.

Introduction

Typical kinetic analyses of enzyme-substrate systems are based on observed rates of enzyme-catalyzed reactions over a range of enzyme and substrate concentrations. Analyses of this type are commonplace for soluble enzyme-soluble substrate systems in which measures of substrate and

*Author to whom all correspondence and reprint requests should be addressed.

enzyme concentrations are rather straightforward. However, the biological world is replete with soluble enzyme-insoluble substrate systems for which measurements of substrate concentration can be rather ambiguous. Systems of this type include lipases, proteases, and many of the glycosyl hydrolases that act on polysaccharides. In this article, we address the concern of how to best measure the substrate concentration in cellulase-cellulose systems. More specifically, we focus on the substrate parameters that are of most relevance to the activity of exo-acting cellulases, hereafter referred to as cellobiohydrolases (CBHs).

Fungal cellulase enzyme systems capable of efficiently catalyzing the hydrolytic degradation of crystalline cellulose are typically composed of endo-acting cellulases (EGs), exo-acting cellulases (CBHs), and at least one cellobiase *(1–6)*. The CBHs are typically the predominant enzymes, on a mole fraction basis, in such systems *(7)*. Consequently, the CBHs have been the focus of many studies *(8)*. The three-dimensional structure of prototypical CBHs is known *(9–12)* and their specificities are, in general, well characterized *(13,14)*. However, mechanism-based kinetic analyses of CBH-catalyzed cellulose saccharification are rather limited *(15,16)*. Studies of this latter type are particularly difficult owing to the inherent complexity of native cellulose substrates.

A fundamental dilemma that must be addressed when analyzing CBH-cellulose reaction mixtures is how to express substrate concentrations. Substrate concentrations for cellulase-cellulose reaction mixtures in general are most commonly expressed in units of mass (such as milligrams of cellulose per reaction mixture) or enzyme-accessible surface area *(17)*. The latter values are typically obtained from solute exclusion experiments *(17–19)*. Expressing substrate concentrations in terms of surface area is theoretically appealing in that it seems to better represent the amount of substrate actually available to the enzymes *(20,21)*. The same reasoning suggests that it would be beneficial, at least for some analyses, if measures of substrate concentration for reaction mixtures containing only exo-acting cellulases were based on cellulose chain ends.

In this article, we address the issue of determining substrate concentrations based on cellulose chain ends. Typical insoluble cellulose substrates were evaluated. Our study focused on the analysis of reducing ends, rather than non reducing ends, because of the relative ease with which reducing ends can be detected and because of their importance with respect to reducing end-specific CBHs. The results are expected to be of relevance to those considering factors that dictate rates of CBH activity on typical cellulose substrates.

Materials and Methods

Preparation of Cellulose Substrate

Microcrystalline cellulose (MCC) was obtained commercially (Avicel, PH 101, FMC, Philadelphia, PA). Amorphous microcrystalline cellulose

(AMCC) was produced from MCC by the method of Isogai and Atalla *(22)* using an SO_2-diethylamine-dimethylsulfoxide (DMSO) solvent for cellulose dissolution. Phosphoric acid swollen cellulose (PSC) was prepared according to Ståhlberg et al. *(23)*. Bacterial microcrystalline cellulose (BMCC) was prepared from cultures of *Acetobacter xylinum* (ATCC #23769). Cultures were incubated in nutrient medium–containing trays for 10 d at 30°C without shaking *(24)*. Surface layers of cellulose were harvested and purified by the method of Gilkes et al. *(25)*. Amorphous bacterial microcrystalline cellulose (ABMCC) was prepared by first soaking BMCC in DMSO for 2 h, followed by centrifugation and then two additional washes with DMSO. The BMCC was then treated as in the preparation of amorphous MCC, first being dissolved in the SO_2-diethylamine-DMSO solvent *(22)* and then precipitated, and subsequently washed, with cold water. The AMCC, BMCC, and ABMCC preparations were kept in water containing 0.02% sodium azide until used. Amorphous celluloses, including PSC, were prepared on a minimum of two occasions to ensure reproducibility. Filter paper, obtained commercially (Whatman no. 1; Maidstone, England), was added to reaction mixtures as 7 = mm diameter, 3.5-mg disks.

Colorimetric Reducing End Assays

All samples were analyzed in triplicate on at least two separate occasions.

Soluble-Phase Reducing Groups

The DNS (DNS and DNS_{sg}) were performed as described by Ghose *(26)*. Assays including "supplemental glucose," 100 µg, are herein referred to as DNS_{sg}. The Nelson-Somogyi copper-based assays were performed as described by Nelson *(27)* and Robyt and Whelan *(28)*. The traditional assay results in a final reaction mixture volume, prior to measuring absorbance, of 10 mL. We also included a series of assays for which final reaction mixture volumes were 5 mL ($Nelson_{5mL}$). The *p*-hydroxybenzoic acid (PAHBAH) assay was done according to Lever *(29)*. The assay based on BCA chelation of cuprous ions (BCA assay) was conducted as described by Garcia et al. *(30)*.

Insoluble-Phase Reducing Groups

The BCA assay, as applied to the quantification of insoluble reducing ends, was taken from Johnston et al. *(31)*. One milliliter of BCA "working reagent," (prepared as in Garcia et al., *[30]*) was added to glass tubes containing 1 mL of test cellulose suspension. The tubes were mixed, capped with glass marbles, and incubated at 80°C for 30 min. Tubes were then cooled to room temperature by standing in water, mixed, and transferred to 2-mL microcentrifuge tubes, and the cellulose was pelleted by centrifuging at 3000 rpm for 5 min. The absorbance, at 560 nm, of the cellulose-free supernatants was then determined. Nanomoles of reducing groups per milligram of cellulose was calculated from measured color yields for standard glucose samples (0–55 µ*M*) treated per the aforementioned protocol.

The DNS assay, as applied to the quantification of insoluble reducing ends, was taken from Irwin et al. *(32)*. DNS reagent, 1 mL, was added to 0.4 mL of cellulose suspension containing 200 nmol of cellobiose (cellobiose addition being analogous to using supplemental glucose in the DNS_{sg} assay). Reaction mixtures were then mixed, capped with glass marbles, and incubated in boiling water for 15 min. Following heating, the tubes were cooled to room temperature, again mixed, transferred to 2-mL microcentrifuge tubes, and centrifuged at 3000 rpm for 5 min. The absorbance of the resulting cellulose-free supernatants was measured at 600 nm. Nanomoles of reducing groups per milligrams of cellulose were calculated from measured color yields for standard cellobiose solutions (0–800 nmol/assay).

Solvent Accessible Reducing Ends

All samples were analyzed in triplicate on at least two separate occasions. Sodium borohydride solutions were prepared just prior to initiating experiments.

Sodium Borohydride Reduction

The "mild" $NaBH_4$ reduction was done at 22°C (room temperature) and pH 8.0 The slightly alkaline conditions were necessary to maintain reasonable stability for the $NaBH_4$ reagent. Sodium borohydride, 0.1 mL of 0.25 *M* $NaBH_4$ in 0.1 *M* NaOH, was added to test solutions containing 1 mg of cellulose suspended in 0.785 mL of 0.1 *M* sodium phosphate, pH 8.0 Reaction mixtures were mixed and allowed to react for up to 90 min at room temperature. Reactions were terminated at selected times by the addition of 20 µL of 37% (w/v) HCl. Terminated reaction mixtures were typically allowed to stand for 30 min prior to neutralization by the addition of 95 µL of 2 *N* NaOH. Separate experiments showed that residual sodium borohydride could not be detected following the low-pH 30-min incubation period.

Sequential Sodium Borohydride Treatments

MCC was used as a representative cellulose. Cellulose was initially reduced as described above. The terminated, neutralized reaction mixture was then centrifuged at 3000 rpm for 5 min and the supernatant removed. To the resulting cellulose pellet was added 0.785 mL of reaction buffer and 0.1 mL of fresh sodium borohydride (all concentrations as given above). The cellulose was suspended by mixing and the reaction allowed to proceed for another 90 min, at which time the reaction was terminated, and neutralized, and the cellulose was again separated via centrifugation. The same cycle was repeated a third time. In total, test celluloses received three sequential $NaBH_4$ treatments, each treatment using fresh reagents.

The "mild" reduction protocol, see previous section, was modified to simulate reaction conditions used in the colorimetric assays for reducing ends. This test included three treatments: (1) the "mild" protocol in 0.1 *M* sodium phosphate, pH 8.0, and 22°C; (2) the "high pH" treatment in 0.25 *M*

sodium carbonate/bicarbonate, pH 10.0, and 22°C; and (3) the "high-pH/high-temperature" treatment in 0.25 *M* sodium carbonate/bicarbonate, pH 10.0, and 80°C. As in the previous section, reactions were initiated by adding 0.1 mL of 0.25 *M* $NaBH_4$ in 0.1 *M* NaOH to 0.785 mL of cellulose suspension (containing 1 mg of cellulose). Reactions were allowed to continue for 90 min. The cellulose was then separated from the soluble phase, as just described, and the treatment was repeated. Samples received a maximum of five sequential $NaBH_4$ treatments (up to 450 min). Following the last treatment, reactions were terminated by the addition of HCl and subsequently neutralized with NaOH.

Reductions with Sodium Borotritiide

All reductions and subsequent treatments involving tritium, up to the scintillation counting, were done in a hood using 20-mL scintillation vials as reaction vessels. The NaB^3H_4-containing reducing solution was 0.2505 *M* $NaBH_4/NaB^3H_4$ in 0.1 *M* NaOH with a specific activity of 0.738 mCi/mmol of sodium borohydride. Thus, 100 µL of reducing solution contained 50 nmole of original NaB^3H_4 preparation (specific activity of 370 mCi/mmol; obtained from ICN, Irvine, CA) and 25 µmol of cold $NaBH_4$. Reductions were initiated by adding a 100-µL aliquot of NaB^3H_4-containing reducing solution to a 20-mL scintillation vial containing cellulose (0.1–1.0 mg of cellulose) suspended in 0.88 mL of 0.1 *M* sodium phosphate buffer, pH 8.0 Initiated reaction mixtures were mixed and allowed to proceed at 22°C for the desired reaction time. Reactions were terminated by the addition of 20 µL of 37% HCl. The acidified reaction mixture was allowed to stand open for a minimum of 30 min. Reaction mixtures were then evaporated to dryness on a hot plate at 50°C (approx 1 h). The evaporation step was necessary to drive off residual labeled $^3H_2$ gas *(33)*. The solid residue remaining was then resuspended in 1 mL of phosphate buffer and to that suspension was added 10 mL of scintillation cocktail (Scintisafe Gel; Fisher, Pittsburgh, PA). Samples were counted in a Beckman LS 6500 Scintillation System (Fullerton, CA) at 20 min per vial. Blanks containing no reducing sugar and "zero-time" samples to which the acid was added prior to the addition of reducing agent were included in all experiments. Corrected counts per minute were converted to micromoles of reducing ends per gram of cellulose using calibration curves, 0–40 nmol, with glucose as the calibration standard (tests showed that results based on cellobiose as the calibration standard gave equivalent results). As for previous experiments, all samples were done in triplicate on a minimum of two occasions.

Quantification of Reducing Ends on $NaBH_4$-Treated Celluloses

Reduced and neutralized cellulose preparations were assayed using the BCA assay as described for insoluble reducing ends using glucose as the calibration standard.

Table 1
Detection Limit, Linear Range and Working Range for DNS, DNS_{sg}, Nelson-Somogyi (Nelson 10 mL), Modified Nelson-Somogyi (Nelson 5 mL), PAHBAH,[a] and BCA Assays

Assay	Detection limit (µg glu)	Associated SE	Linear range upper limit (µg glu)	Working range (µg glu) [b]
DNS	55.0	0.058	>4000	80–257
DNS_{sg}	1.9	0.157	>4000	25–187
Nelson 10 mL	1.1	0.050	~400	22–170
Nelson 5 mL	0.66	0.024	~200	12–86
PAHBAH	0.22	0.024	>20 [a]	2–16
BCA	0.12	0.007	~10	1–8

[a] The PAHBAH calibration curve is not linear over a wide range, but for small ranges appears linear (with slope changes). The range reported here was used for determination of sensitivity and detection limit.

[b] Based on linear regression parameters, slope and intercept.

Results and Discussion

The present study was initiated in response to the desire to know the number of chain ends available to exo-acting enzymes in typical cellulose/cellulase reaction mixtures. Several laboratories have published relevant data. In each case the number of reducing ends associated with a particular cellulose preparation was estimated by adapting a colorimetric reducing sugar assay traditionally used with aqueous solutions. Colorimetric assays adapted in this way include those based on DNS *(32)*, PAHBAH *(34)*, Cu-arsenomolybdate (Nelson-Somogyi; *[23]*), and Cu-BCA *(31)*. Published studies give little indication of how results obtained with the different assays compare, making assay selection and data comparisons difficult. Thus, an objective of the present study was to provide such information, along with estimates of the number of reducing ends associated with traditional cellulose substrates.

Soluble-Phase Reducing Ends

Initial experiments were designed to obtain analytical parameters for common colorimetric reducing sugar assays when used to quantify soluble reducing sugars generated as a consequence of cellulose saccharification. The assays were run as published, with the exception of the more concentrated Nelson (5 mL) assay. The results are presented in Tables 1–3. Detection limits for all of the assays are near 1 µg (although values in this range differ by nearly 16-fold), with the exception of the traditional DNS assay, which is known to consume a fixed amount of analyte *(26)*.

Table 2
Calibration Sensitivity, Analytical Sensitivity, and SEs for DNS, DNS_{sg}, Nelson-Somogyi (Nelson 10mL), Modified Nelson-Somogyi (Nelson 5mL), PAHBAH, and BCA assays

	Calibration sensitivity (Abs/μg glu)		Analytical sensitivity (DAbs/μg glu)[a]			
Assay	Calibration sensitivity ($\times10^{-3}$)	Associated SE ($\times10^{-3}$)	Analytical sensitivity	Associated SE ($\times10^{-2}$)	SD ($\times10^{-3}$)[b]	Reference concentration[c]
DNS	3.95	0.042	1.780	1.91	2.22	90
DNS_{sg}	4.31	0.067	0.896	1.60	4.81	90
Nelson 10 ml	4.73	0.023	0.783	1.12	6.04	90
Nelson 5 mL	9.37	0.030	1.770	3.03	5.33	50
PAHBAH	50.40	0.880	3.880	7.38	13.40	12
BCA	106.00	1.070	15.400	40.33	6.87	5

[a] Signal change is defined as absorbance change for the assays.
[b] Pooled SD from different experiments.
[c] The concentration at which replicate measurements were analyzed to obtain pooled SDs.

Table 3
Cellodextrin Reponses for DNS, Nelson-Somogyi (Nelson), and BCA Assays

Assay [a]	Similar response of equimolar amounts of G, G2, G3	G		G2		G3	
		m_{ratio} [b]	b_{ratio} [c]	m_{ratio}	b_{ratio}	m_{ratio}	b_{ratio}
DNS	No	1.0	1.0	1.5	1.0	1.8	0.9
Nelson	Yes	1.0	1.0	1.0	1.0	1.0	1.0
BCA	Yes	1.0	1.0	1.0	1.0	1.0	1.0

[a] Not determined for PAHBAH assay.

[b] Calculated as the ratio of the calibration sensitivities (or slope m) of the different cellodextrin standard curves to the glucose standard curve. Thus, a ratio of 1 is expected, theoretically, for a true reducing sugar assay, which has the same molar color yield for a series of saccharides.

[c] Calculated as the ratio of the intercepts of the different cellodextrin standard curves to the glucose standard curve. Thus, a ratio of 1 indicates agreement in the intercepts between the cellodextrin and the glucose calibration curves.

The combined data provide a ready means by which to compare and select appropriate assays for application in cellulase-catalyzed cellulose saccharification experiments. Products in such experiments are expected to include glucose; cellobiose; and, potentially, some cellooligosaccharides. Optimum reducing sugar assays would have equivalent molar color yields for these soluble products. As shown in Table 3, this optimum situation only applies to the two copper-based assays (Nelson, BCA). Because of their importance with respect to the analysis of insoluble cellulose (discussed next), calibration curves reflecting the molar color yields for the DNS and BCA assays are presented in Fig. 1.

Insoluble-Phase Reducing Ends

The DNS- and BCA-based assays are frequently used for the quantification of insoluble reducing ends in cellulose/cellulase systems *(31, 32, 35–40)*. The relative merit of using the assays for this determination was evaluated by applying the assays, as published, to traditional cellulose substrates (Table 4). The results from both assays had relative errors of approx 3%. Figures 2–5, from which the values in Table 4 were calculated, illustrate the linear relationship between mass of cellulose and number of reducing ends for both assays. The linear relationships suggest that either method may be used to determine relative numbers of reducing ends for a given cellulose preparation (e.g., relative values for MCC-derived substrates). The similar values obtained for MCC, AMCC, and PSC, and for BMCC and ABMCC, further support this conclusion. The similarity in the results for the MCCs and the corresponding amorphous preparations demonstrates that the solid-state structure of the cellulose, typically expressed in terms of relative crystallinity *(41)*, had little effect on color yield. This conclusion is based on the premise that the method used for the prepa-

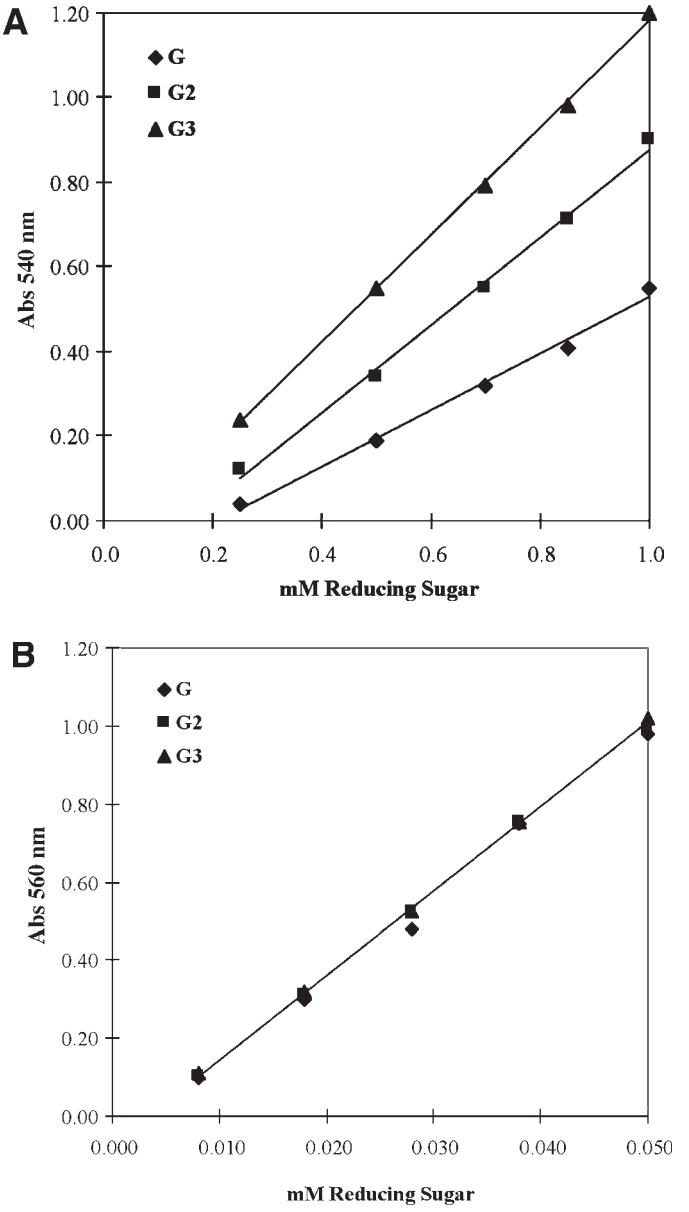

Fig. 1. Absorbance response of equimolar amounts of soluble cellulose saccharification products glucose (G), cellobiose (G2), and cellotriose (G3) by **(A)** DNS assay and **(B)** BCA assay.

ration of the amorphous celluloses did not result in significant depolymerization and concomitant production of new reducing ends (as shown by Isogai and Attala *[22]*). The ordinates of the BCA- and DNS-based plots in Figs. 2–5 are in units of glucose and cellobiose equivalents, respectively, owing to the use of the different sugars for the preparation of standard curves (*see* Materials and Methods).

Table 4
Reducing Ends Per Amount Cellulose as Determined by BCA and DNS Assays

Cellulose preparation	Amount (mg)	Reducing ends (μmol/g) SE	
		BCA[a]	DNS[b]
MCC	0.1 – 1.0	32.13 (0.38)	188.36 (3.27)
AMCC	0.1 – 1.0	30.40 (0.68)	197.39 (8.80)
PSC	0.1 – 1.0	30.02 (0.77)	179.27 (5.80)
BMCC	0.1 – 1.0	18.26 (0.25)	60.98 (1.00)
ABMCC	0.1 – 1.0	20.51 (1.93)	67.73 (1.12)
Filter Paper	3.5 – 17.50	1.25 (0.03)	10.50 (0.43)

[a] Glucose equivalents.
[b] Cellobiose equivalents.

An obvious conclusion from the data in Table 4 is that the DNS assay, compared with the BCA assay, consistently gives higher values for equivalent cellulose preparations. The fold-difference between the two assays was dependent on the source of the cellulose. Values for the MCC-based substrates (MCC, PSC, and AMCC) differed approximately six-fold. Those for filter paper differed approx eight-fold. The DNS values for the bacterial cellulose–based preparations (BMCC, ABMCC) were just over three-fold higher than the corresponding BCA values. The high DNS-obtained values, relative to the BCA-obtained values, are likely attributable to overconsumption of the DNS reagent as a result of the generation of reactive side products during the assay *(42)*. These reactive side products are likely to be a result of cellulose degradation under the relatively harsh conditions used for the DNS assay (100°C, pH 13.0, 15 min). The conditions for the BCA assay, by comparison, were relatively mild (80°C, pH 10.0, 30 min).

It is not clear why the fold-differences between the DNS- and BCA-obtained values vary to the extent they do for the different celluloses. As already discussed, the fold-differences are not likely attributable to differences in the crystallinity of the substrates—or to properties thought to be associated with crystallinity, such as porosity and surface area. The differences appear to be attributable to characteristics originating with the starting material, since MCC-based substrates have similar values, BMCC-based substrates have similar values, and so on. This suggests that the substrate-specific fold-differences between the DNS and BCA assays are related to the degree of polymerization (DP) of the substrates. The average DP of the filter paper (~1640) is clearly greater than that of the microcrystalline substrates (~220) *(43)*. The average DP for the different MCC- and BMCC-derived substrates is expected to be similar, and yet the corresponding fold-differences for these substrates differ nearly twofold. This apparent discrepancy may be explained by the DP profiles of the different substrates.

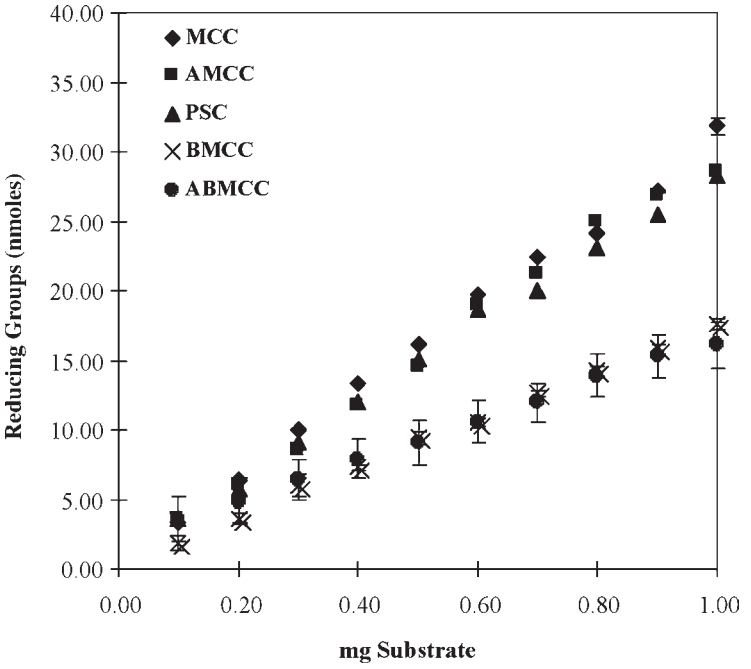

Fig. 2. Reducing groups per amount of cellulose determined by BCA assay for MCC (◆), AMCC (■), PSC (▲), BMCC, (×), and ABMCC, (●). Values represent the mean of triplicate determinations; error bars represent ± the SE. When not shown, the error bars fall within the symbols.

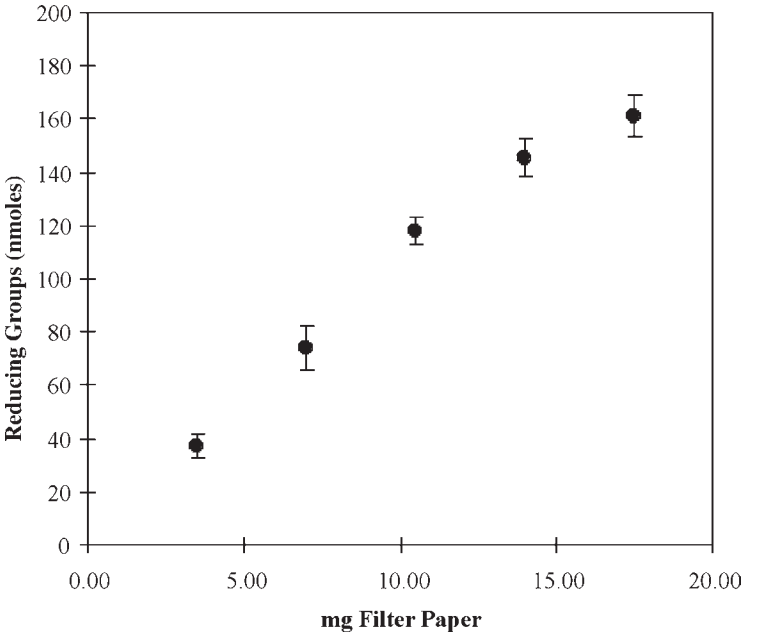

Fig. 3. Reducing groups per amount of filter paper determined by BCA assay. The statistical parameters are as in Fig. 2.

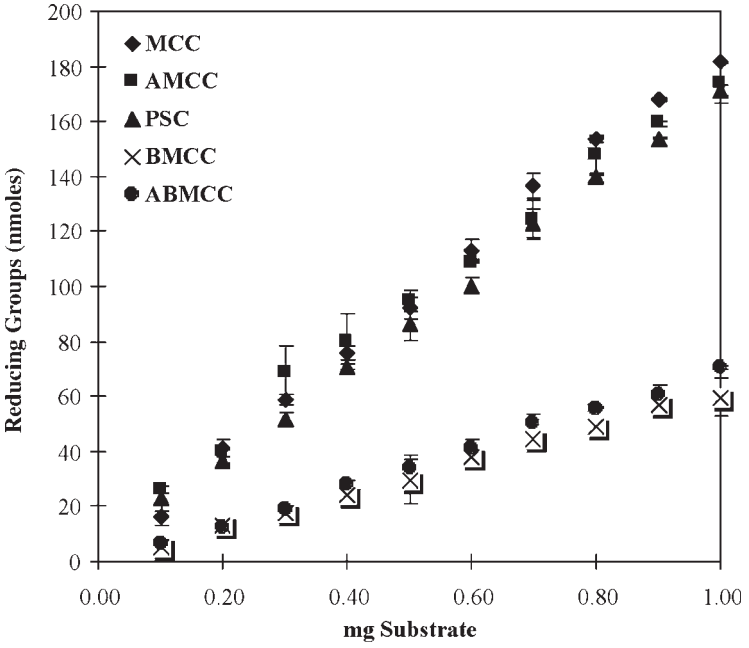

Fig. 4. Reducing groups per amount of cellulose determined by DNS assay for MCC, (◆), AMCC, (■), PSC, (▲), BMCC, (×), ABMCC, (●). The statistical parameters are as in Fig. 2.

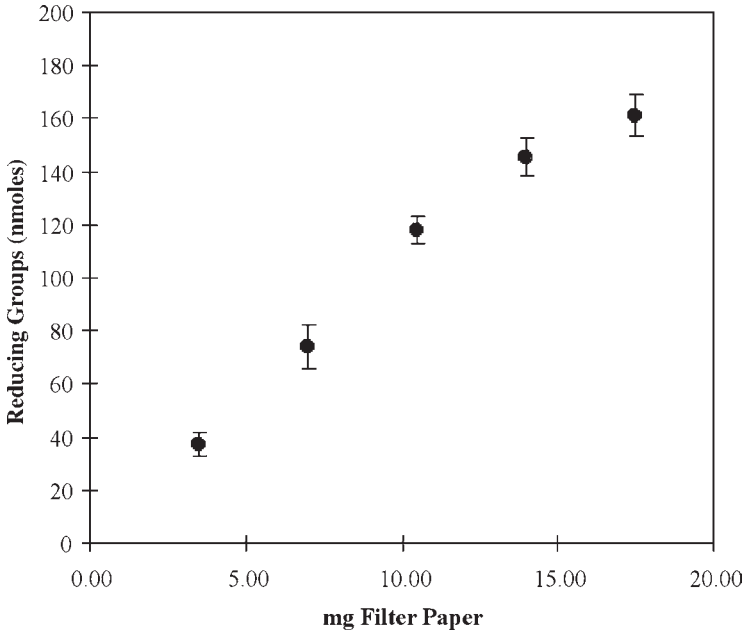

Fig. 5. Reducing groups per amount of filter paper determined. The statistical parameters are as in Fig. 2.

Stålbrand et al. *(44)* have shown that although the average DP values for an MCC- and a BMCC-derived substrate were similar, their DP profiles were significantly different. The BMCC substrate was shown to have a higher mole fraction of its constituent molecules in the low DP range. As discussed with relation to Fig. 1, the DNS assay is DP sensitive when working with cellooligosaccharides and, presumably, also with cellulose, whereas the BCA assay is not. Hence, it seems that if the observed substrate-specific fold-differences are a function of the cellulose preparations' DP, as is suspected, then that function is best considered in terms of the overall DP profiles of the substrates rather than simply average DP values.

The BCA assay results presented here for the MCC substrates are comparable with those obtained by Ståhlberg et al. *(23)* using the Nelson-Somogyi method. They reported ~37 µmol of reducing ends/g of cellulose for their microcrystalline (MCC) and phosphoric acid–regenerated cellulose (PSC) preparations. Similarly, Johnston et al. *(31)*, using the BCA assay, reported 30–35 µmol of reducing ends/g of phosphoric acid–regenerated cellulose. (The similar results for the Nelson-Somogyi and the BCA assays are expected since both are based on quantification of the cupric-to-cuprous reduction.) The DNS results for the filter paper substrate are in general agreement with those reported by Irwin et al. *(32)*. The similarity of the values obtained in our laboratory to those scattered in the literature indicates that the interlaboratory reproducibility of the assays, at least when applied to substrates for which we can make a comparison, is good.

Insoluble-Phase/Solvent-Accessible Reducing Ends

Values obtained using the DNS and BCA assays are presumably a function of the total number of reducing ends per unit weight cellulose. This is an important number for many purposes, but it may not be the most relevant value when considering enzyme-accessible reducing ends. The latter value is important when asking questions related to effective substrate concentrations for reducing end-specific exo-acting cellulases, a prototypical enzyme in this category being *Trichoderma reesei* CBH I *(10)*. An approach to obtaining these enzyme-applicable values is to determine the fraction of reducing ends exposed to solvent under conditions more conducive to enzyme activity. In the DNS and BCA assays, the cellulose is in a highly alkaline solution (pH ≥ 10.0) at elevated temperatures ($T \geq 80°C$). These conditions are conducive to cellulose swelling and thus increase solvent accessibility *(45)*, and they are clearly well outside those compatible with typical enzyme systems. The "enzyme-applicable" approach just suggested was implemented in this present work by first reducing the cellulose with $NaBH_4$ under relatively mild conditions ($NaBH_{4,\,mild}$), and then assaying the $NaBH_{4,\,mild}$-treated cellulose for remaining reducing ends (using the BCA assay as described for insoluble cellulose. The number of solvent-accessible reducing ends could then be calculated by taking the difference in the number of reducing ends associated with the $NaBH_{4,\,mild}$-treated and the untreated substrates. Results from such assays applied to the test

Table 5
Solvent-Accessible Reducing Ends per Amount of Cellulose as Determined by Combined $NaBH_4$-BCA and NaB^3H_4-Tritium Uptake Assays

Cellulose preparation[a]	Solvent-accessible reducing ends (mmol/g) $NaBH_4$-BCA[b]	NaB^3H_4-tritium uptake[b]	Solvent accessibility (% of total)[b,c]
Glucose	—	—	100
Cellobiose	—	—	100
MCC	17.12 ± 0.55	13.85 ± 0.50	60.00 ± 3.59
AMCC	23.63 ± 0.28	22.50 ± 0.64	72.37 ± 0.66
PSC	24.08 ± 0.99	20.93 ± 0.73	72.36 ± 2.03
BMCC	8.64 ± 0.46	14.55 ± 0.26	45.32 ± 2.34
ABMCC	10.29 ± 0.21	15.71 ± 0.73	49.04 ± 1.52
Filter Paper	0.773 ± 0.06	1.33 ± 0.08	59.22 ± 4.49

[a] As in Fig. 4
[b] ± SE.
[c] Calculated from BCA-obtained values in Table 4 and $NaBH_4$-BCA values in this table.

celluloses are presented in Table 5. While these values are not optimum for assessing the number of CBH-accessible reducing ends—the optimum would be an "enzyme-accessible" value rather than a "solvent-accessible" value—they are a significant improvement over the "total" reducing end values obtained by traditional colorimetric assays. A second assay was developed for our study in order to check the validity of the values obtained using the combined $NaBH_4$-BCA assay. In this second approach, the initial reduction was done using sodium borotritiide, and then the number of solvent-accessible reducing ends was determined by the extent of tritium incorporation into cellulose (*see* Materials and Methods for details). It can be seen that the results obtained using this isotope uptake approach are in general agreement with those obtained using the $NaBH_4$-BCA colorimetric approach (Table 5). The similarity in the values lends credibility to the numbers obtained from either assay.

A comparison of the relative accessibility of the different substrates' reducing ends, as determined by the combined $NaBH_4$-BCA assay, is also included in Table 5. The tabulated values were taken from the plateau region of the progress curves presented in Fig. 6. The time courses for reduction of the soluble substrates (glucose and cellobiose) show that all reducing ends are readily susceptible to $NaBH_4$ reduction under the chosen "mild" conditions. By contrast, the insoluble substrates all show a minimum of two classes of reducing ends; for simplicity, the two classes are heretofore referred to as those that are generally susceptible to $NaBH_4$ reduction and those that aren't. The percentages of reducing ends susceptible to $NaBH_4$ reduction were found to be similar for all of the celluloses, ranging from 45 (BMCC) to 72% (AMCC, PSC).

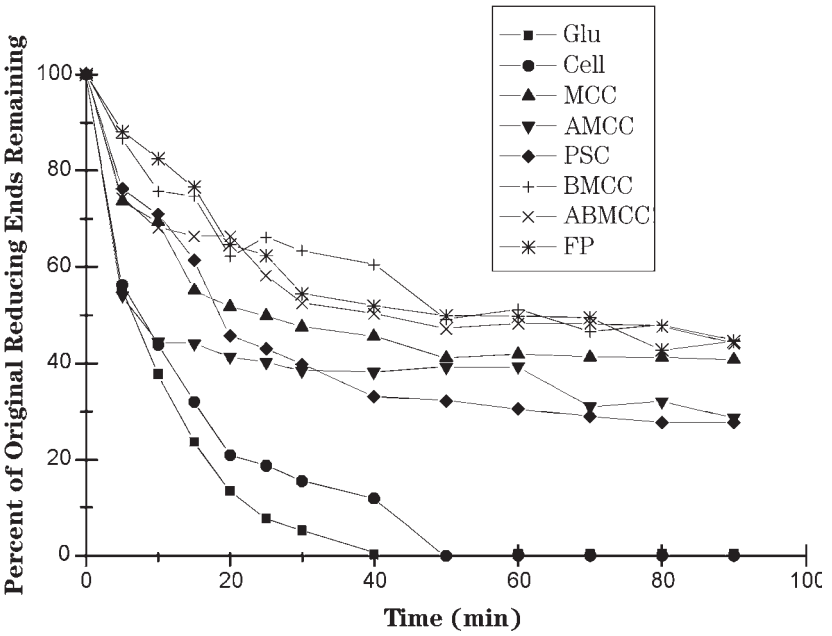

Fig. 6. Time courses of reduction of celluloses by $NaBH_4$ at pH 8.0, 22°C. Unreacted reducing ends were determined by BCA assay. The celluloses are as in Table 4. FP, filter paper.

A small increase (~20%) in solvent-accessible reducing ends was observed for the amorphous MCC-based preparations (AMCC and PSC) compared with the MCC starting material. This result can be rationalized based on the documented enhanced reactivity, presumably corresponding to a more open structure, of amorphous vs crystalline cellulose *(21,46)*. The fact that 30% of the reducing ends of the AMCC preparation are not susceptible to $NaBH_4$ reduction shows that, even with amorphous substrates, a significant fraction of the "total" reducing ends (as measured by traditional colorimetric assays) are not available as sites for initiation of reducing end–specific saccharification. The two BMCC-based substrates had essentially the same percentage of total reducing ends unavailable for reaction with $NaBH_4$. This result was not anticipated based on the presumed higher surface area associated with amorphous, vs crystalline, substrates. The somewhat unexpected lower accessibility of the reducing ends in the amorphous preparation (vs BMCC) suggests that amorphous aggregates formed during ABMCC preparation are not particularly solvent ($NaBH_4$) permeable; interestingly, they are less so than those in the analogous AMCC substrate preparation. The difference in the aggregation states of the two amorphous cellulose preparations (ABMCC and AMCC) detected, as a difference in the percentage of $NaBH_4$-susceptible reducing ends, is likely a result of complex aggregation events that occur during cellulose regeneration. The percent-

age of reducing ends accessible in the filter paper substrate was in line with that observed for the MCC and BMCC substrates.

Several experiments were conducted to evaluate the effect of reaction conditions on $NaBH_4$-accessible reducing ends. An initial concern in the pH 8.0/22°C reductions was that the observed plateaus in reduction time courses (Fig. 6) were the result of reagent decomposition. If this were the case, then the observed plateaus would reflect a lack of reagent rather than inaccessible reducing groups. The experiment depicted in Fig. 7 illustrates that this is not the case. In this experiment, the MCC preparation underwent the mild $NaBH_4$ treatment, as did the preparations depicted in Fig. 6, but at the completion of the typical time course the cellulose was washed and then again treated with fresh $NaBH_4$ reagent. Subsequent to this second $NaBH_4$ treatment the cellulose was again washed and $NaBH_4$ treated. The consequence of the three sequential $NaBH_4$ treatments was only a minimal decrease in residual BCA-detectable reducing ends when compared to the celluloses that had received only the single treatment (as in Fig. 6). This result provides strong support for the notion that the plateaus observed in Fig. 6 are owing to the $NaBH_4$-inaccessible nature of a significant fraction of the reducing ends associated with these cellulose preparations.

Time courses of $NaBH_4$ reduction of the MCC substrate under different pH/temperature conditions were compared to test the hypothesis that reaction conditions corresponding to those of the colorimetric assays are consistent with measuring "total" reducing ends (Fig. 8). Three reaction conditions were compared: (1) the "mild" conditions as employed above, (2) those analogous to the BCA assay (i.e., pH 10.0 and 80°C), and (3) those of intermediate severity. A plateau in the extent of reduction is evident in the time courses corresponding to the two milder conditions. By contrast, reductions under the more severe conditions resulted in complete depletion of BCA-detectable reducing ends. This result supports the contention that conditions commonly used for traditional colorimetric assays are consistent with measuring "total" numbers of reducing ends. The results from this experiment also demonstrate that the color generated in the BCA assay is dependent on the presence of reducing ends, since no reducing ends could be detected after exhaustive $NaBH_4$ reduction. This was also shown to be the case for color generation in the DNS assay (data not shown). This is significant in that it indicates that potentially color-yielding side products generated during the course of reducing sugar assays (as suggested above for the DNS assay) are a result of the presence of reducing ends *per se*—and not owing to side reactions occurring at sites away from the reducing end termini.

Conclusion

The colorimetric assays discussed herein are most commonly used in cellulose/cellulase studies to quantify the number of reducing sugars associated with the soluble phase (glucose, cellobiose, low-DP cellooli-

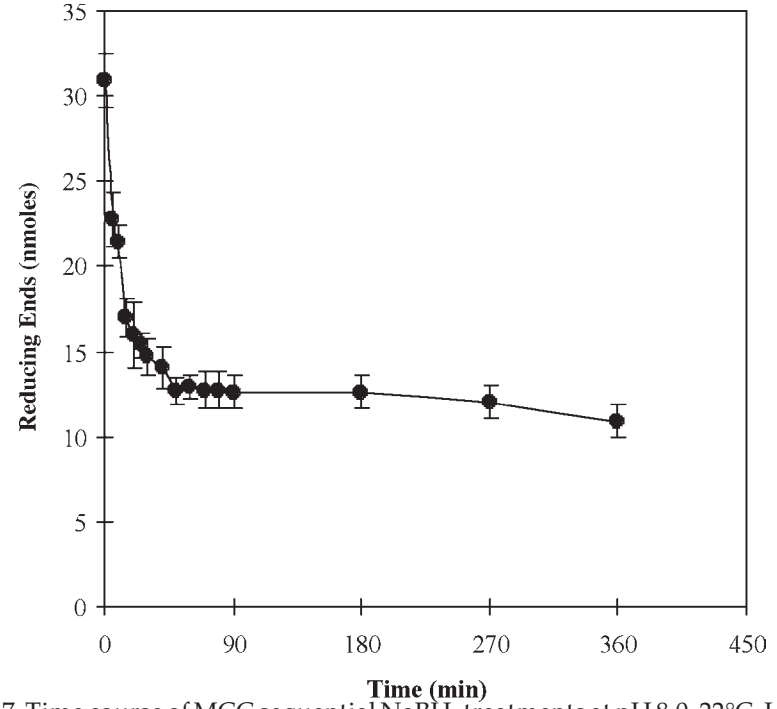

Fig. 7. Time course of MCC sequential $NaBH_4$ treatments at pH 8.0, 22°C. Unreacted reducing ends were determined by BCA assay.

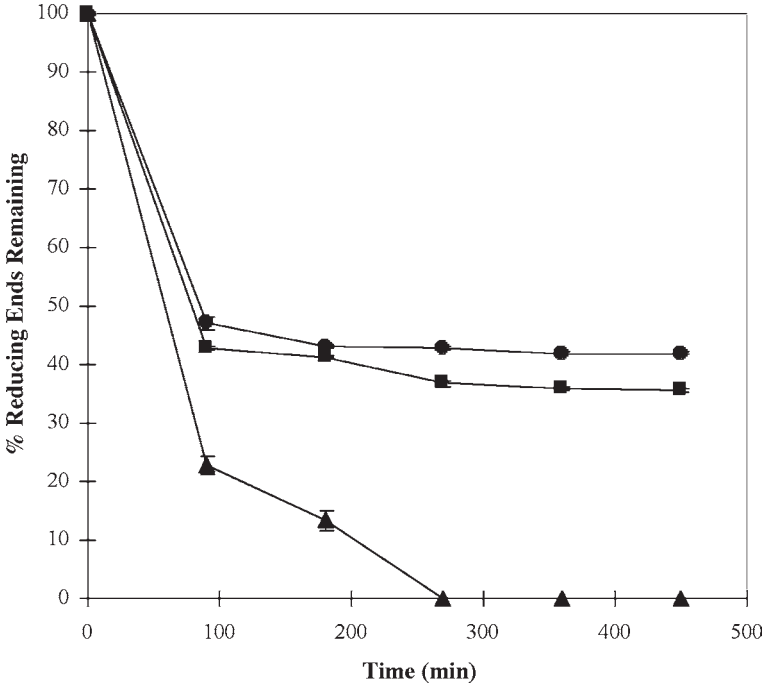

Fig. 8. Time courses of MCC reduction by $NaBH_4$ at different reaction conditions: (●), pH = 8.0, *T* = 22°C; (■), pH = 10.0, *T* = 22°C; (▲), pH = 10.0, *T* = 80°C.

gosaccharides). However, they are increasingly being used to determine the number of reducing ends associated with the insoluble phase, cellulose. The combined results from this study show the merits of the different reducing sugar assays when used with either the soluble or the insoluble substrates (detection limits, sensitivities, and so on) and suggest that the limitations of these assays regarding the analysis of celluloses *per se* should be considered. The DNS assay tends to overestimate absolute numbers of reducing ends per unit mass cellulose, and it appears likely that the degree of overestimation is a function of the cellulose's DP profile. Hence, the BCA assay apprears to be the more appropriate assay for obtaining absolute values for cellulose reducing ends. Both the BCA and the DNS assays are shown to relate to the "total" number of cellulose-associated reducing ends. One can obtain reasonable estimates of the absolute number of solvent-accessible reducing ends by using either the combined $NaBH_4$/BCA assay or the sodium borotritiide/tritium uptake assay as presented herein. Values obtained with the latter two assays will be particularly relevant in studies concerned with the number of available catalytic sites for exo-acting cellulases and for those studies examining general changes in the surface properties and/or accessibility of cellulose substrates.

References

1. Gilkes, N. R., Henrissat, B., Kilburn, D. G., Miller, R. C. Jr., and Warren, R. A. J. (1991), *Microbiol. Rev*. **55,** 303–315.
2. Henrissat, B. (1991), *Biochem. J.* **280,** 309–316.
3. Goyal, A., Ghosh, B., and Eveleigh, D. (1991), *Bioresour. Technol*. **36,** 37–50.
4. Tomme, P., Warren, R. A. J., and Gilkes, N.R. (1995), *Adv. Microb. Physiol*. **37,** 1–81.
5. Davies, G. and Henrissat, B. (1995), *Structure* **3,** 853–859.
6. Henrissat, B., Callebaut, I., Faberega, S., Lehn, P., Mormon, J. P., and Davies, G. (1995), *Proc. Natl. Acad. Sci. USA* **92,** 7090–7094.
7. Teeri, T. T. (1997), *Trends Biotechnol*. **160,** 155–195.
8. Schulein, M. (2000), *Biochimg Biophys Acta* **1543,** 239–252.
9. Henrissat, B. and Davies, G. (1997), *Curr. Opin. Struct. Biol*. **7,** 637–644.
10. Divne, C., Stahlberg, J., Teeri, T. T., and Jones, T.A. (1998), *J. Mol. Biol.* **275,** 309–325.
11. Zou, J. Y., Kleywegt, G. J., Stahlberg, J., Driguez, H., Nerinckx, W., Claeyssens, M., Koivula, A., Teeri, T. T., and Jones, T. A. (1999), *Structure* **7,** 1035–1045.
12. Koivula, A., Laura, R., Gerd, W., et al. (2002), *J. Am. Chem. Soc*. **124,** 10,015–10,024.
13. White, A. and Rose, D. R. (1997), *Curr. Opin. Struct. Biol*. *7*, 645–651.
14. Bayer, E.A., Chanzy, H., Lamed, R., and Shoham, Y. (1998), *Curr. Opin. Struct. Biol.* **8,** 548–557.
15. Medve J., Karlsson, J., Lee, D., and Tjerneld, F. (1998), *Biotechnol. Bioeng*. **59,** 621–634.
16. Nidetzky, B., Steiner, W., and Claeyssens, M. (1995), in *Enzymatic Degradation of Insoluble Carbohydrate.* Saddler, J. N. and Penner, M. H. , eds., American Chemical Society, Washington, DC, pp. 90–112.
17. Gama, F. M, Teixeira, J. A., and Mota, M. (1994), *Biotechnol. Bioeng*. **43,** 381–387.
18. Lin, J. K., Ladisch, M. R., Patterson, J. A., and Noller, C. H. (1987), *Biotechnol. Bioeng*. **24,** 976–981.
19. Neuman, R. P. and Walker, L. P. (1992), *Biotechnol. Bioeng*. **40,** 218–225.
20. Walker, L. P., Wilson, D. B., Irwin, D. C., McQuire, C., and Price, M. (1992), *Biotechnol. Bioeng.* **40,** 1019–1026.
21. Grethlein, H. E. (1978), *Biotechnol. Bioeng*. **20,** 503–525.
22. Isogai, A. and Atalla, R. H. (1991), *J. Polyma Sci.: Part A. Polyma Chem*. **29,** 113–119.

23. Ståhlberg, J., Johasson, G., and Peterson, G. (1993), *Biochim. Biophys. Acta* **1157,** 107–113.
24. Hestrin, S. (1963), *Methods Carbohydr. Chem.* **3,** 4–9.
25. Gilkes, N. R., Jervis, E., Henrissat, B., Tekant, B., Miller, R. C. Jr., Warren, R. A. J., and Kilburn, D. G. (1992), *J. Biol. Chem.* **267,** 6743–6749.
26. Ghose, T. K. (1987), *Pure Appl. Chem.* **59,** 257–268.
27. Nelson, N. J. (1944), *J. Biol. Chem.* **153,** 375–380.
28. Robyt, J. F. and Whelan, W. J. (1972), *Anal. Biochem.* **45,** 510–516.
29. Lever, M. (1972), *Anal. Biochem.* **47,** 273–279.
30. Garcia, E., Johnston, D., Whitaker, J., and Shoemaker, S. (1993), *J. Food Biochem.* **17,** 135–145.
31. Johnston, D. B., Shoemaker, S. P., Smith, G. M., and Whitaker, J. R. (1998), *J. Food Biochem.* **22,** 301–319.
32. Irwin, D. C., Spezio, M., Walker, L. P, and Wilson, D. B. (1993), *Biotechnol. Bioeng.* **42,** 1002–1013.
33. Conrad, H. E., Bamburg, J. R., Epley, J. D., and Kindt, T. J. (1966), *Biochemistry* **5,** 2808–2817.
34. Boraston, A. B., Creagh, A. L., Alam, M. M., Kormos, J. M., Tomme, P., Haynes, C. A., Warren, R. A. J., and Kilburn, D. G. (2001), *Biochemistry* **40,** 6240–6247.
35. Kruus, K., Wang, W. K., Ching, J. and Wu, J. H. D. (1995), *J. Bacteriol.* **177,** 1641–1644.
36. Irwin, D., Shin, D. H., Zhang, S., Barr, B. K., Sakon, J., Karplus, P. A., and Wilson, D. B. (1998), *J. Bacteriol.* **180,** 1709–1714.
37. Kim, E., Irwin, D. C., Walker, L. P., and Wilson, D. B. (1998), *Biotechnol. Bioeng.* **58,** 494–501.
38. Zhang, S., Wolfgang, D. E., and Wilson, D. B. (1999), *Biotechnol. Bioeng.* **66,** 35–41.
39. Zhang, S., Barrt, B. K., and Wilson, D. B. (2000), *Eur. J. Biochem.* **267,** 244–252.
40. Zhang, S., Irwin, D. C., and Wilson, D. B. (2000), *Eur. J. Biochem.* **267,** 3101–3115.
41. Kulshreshtha, A. K. and Dweltz, N. E. (1973), *J. Polym. Sci. Polym. Phys. Ed.* **11,** 487–497.
42. Brooks, R. D. and Thompson, N. S. (1966), *TAPPI. J.* **49,** 362–366.
43. Liaw, E. T. (1994), PhD thesis, Oregon State University, Corvallis, OR.
44. Stalbrånd, H., Mansfield, S. D, Saddler, J. N., Kilburn, D. G., Warren, R. A. J., and Gilkes, N. R. (1998), *Appl. Environ. Microbiol.* **64,** 2374–2379.
45. Michell, A. J. (1993), *Cell. Chem. Technol.* **27,** 3–15.
46. Fan, L. T., Lee, Y. H, and David, H. B. (1980), *Biotechnol. Bioeng.* **22,** 177–199.

0273-2289/04/113/0233–0250/$25.00

Properties of a Recombinant β-Glucosidase from Polycentric Anaerobic Fungus *Orpinomyces* PC-2 and Its Application for Cellulose Hydrolysis

Xin-Liang Li,[*,1] Lars G. Ljungdahl,[2] Eduardo A. Ximenes,[3] Huizhong Chen,[4] Carlos R. Felix,[3] Michael A. Cotta,[1] and Bruce S. Dien[1]

[1]Fermentation Biotechnology Research Unit, National Center for Agricultural Utilization Research, USDA/ARS,[†] 1815 N. University Street, Peoria, IL 61604-3902, E-mail: lix@ncaur.usda.gov; [2]Department of Biochemistry & Molecular Biology and Center for Biological Resource Recovery, Life Science Building, University of Georgia, Athens, GA 30602; [3]Laboratorio de Enzimlogia, Departamento de Biologia Celular, Universidade de Brasilia, Asa Norte, Brasilia-DF, Brazil 70910-900; and [4]Division of Microbiology, National Center for Toxicological Research, US Food and Drug Administration, 3900 NCTR Road, Jefferson, AR 72079-9501

Abstract

A β-glucosidase (BglA, EC 3.2.1.21) gene from the polycentric anaerobic fungus *Orpinomyces* PC-2 was cloned and sequenced. The enzyme containing 657 amino acid residues was homologous to certain animal, plant, and bacterial β-glucosidases but lacked significant similarity to those from aerobic fungi. Neither cellulose- nor protein-binding domains were found in BglA. When expressed in *Saccharomyces cerevisiae*, the enzyme was secreted in two forms with masses of about 110 kDa and also found in two forms associated with the yeast cells. K_m and V_{max} values of the secreted BglA were 0.762 m*M* and 8.20 μmol/(min·mg), respectively, with *p*-nitrophenyl-β-D-glucopyranoside (pNPG) as the substrate and 0.310 m*M* and 6.45 μmol/(min·mg), respectively,

[†]Names are necessary to report factually on available data; however, the USDA neither guarantees nor warrants the standard of the product, and the use of the name by USDA implies no approval of the product to the exclusion of others that may be suitable.

*Author to whom all correspondence and reprint requests should be addressed.

for the hydrolysis of cellobiose. Glucose competitively inhibited the hydrolysis of pNPG with a K_i of 3.6 m*M*. β-Glucosidase significantly enhanced the conversion of cellulosic materials into glucose by *Trichoderma reesei* cellulase preparations, demonstrating its potential for use in biofuel and feedstock chemical production.

Index Entries: Cellulose; cellulase; β-glucosidase; *Orpinomyces*; cellobiase.

Introduction

Cellulosic biomass photosynthesized by solar energy from CO_2 and H_2O is one of the most important renewable energy resources on Earth. Its effective utilization through biologic processes might be an important way to overcome the shortage of foods, feeds, and fuels, which will inevitably be seen in the near future as a consequence of the explosive increase in the human population *(1)*. Degradation of cellulose is accomplished through the synergistic action of endoglucanase (EC 3.2.1.4), exoglucanase or cello-biohydrolase (CBH) (EC 3.2.1.91), and β-glucosidase (EC 3.2.1.21) *(2)*. β-Glucosidase is common among animals, plants, fungi, and bacteria. The enzyme plays an important role in the process of saccharification, catalyzing hydrolysis of β-D-glucosidic linkages of cellobiose and cellooligosac-charides. It alleviates the inhibitory effect of the sugars on exo- and endoglucanases *(2,3)*.

Anaerobic fungi have been isolated from the alimentary tracts of herbivores and other environments *(4)*. These fungi are active in the degradation of plant cell wall polysaccharides and represent a potential source of enzymes against cellulose and hemicelluloses. Among the isolated fungi, *Orpinomyces* PC-2, a polycentric fungus, produces high levels of cell wall–degrading enzymes *(4)*. Genes coding for several cellulases *(5–8)*, a xylanase *(5)*, a 1,3-1,4-β-D-glucanase *(9)*, and an acetylxylan esterase *(10)* have been cloned and sequenced. An 85-kDa extracellular β-glucosidase produced by *Orpinomyces* PC-2 has been purified and characterized *(3)*, but a gene coding for such an enzyme of the fungus has not been described.

In this article, we report the cloning in *Escherichia coli* and sequencing of an *Orpinomyces* β-glucosidase cDNA. The enzyme was overexpressed in and secreted from the yeast *Saccharomyces cerevisiae*. Physiochemical properties of the secreted enzyme were determined after it was purified. Its applicability for cellulose saccharification was also assessed.

Materials and Methods

Strains, Plasmids, and Genes

E. coli TOP10, *S. cerevisiae* INSC1 (MAT α his 3-D 1 *El* 2 *trp*1-289 *ura*3-52), and the plasmid pYES2 were purchased from Invitrogen (San Diego, CA). pYES2 possesses ampicillin and tetracycline resistance genes for selection in *E. coli*, a *URA3* gene for high-copy-number maintenance and selection in *S. cerevisiae* INSC1, and a GAL 1 promoter sequence. The *bgl*A

cDNA of *Orpinomyces* sp. PC-2 was cloned and identified by screening a cDNA library *(11)* as described next.

Screening of Orpinomyces cDNA Library Using Antibodies

The production of antibodies against the different regions of *Orpinomyces* xylanase A has been described previously *(5)*. Immunoscreening was done following the procedure of a Pico Blue™ Immunoscreening kit (Stratagene). Pure positive plaques were obtained after a secondary screening. λ phages were converted into pBluescript SK– by *in vivo* excision, and the pBluescript DNA was purified from cultures grown overnight in Luria-Bertani (LB) medium containing 50 µg/mL of ampicillin using a plasmid purification system purchased from Qiagen (Valencia, CA). DNA sequences were determined by automated polymerase chain reaction (PCR) sequencing *(5)*.

DNA Hybridization Screening

A 400-bp DNA fragment of the partial *bgl*A gene sequence obtained by antibody screening was amplified by PCR and labeled with digoxigenin. The labeled fragment was utilized as a hybridization probe and using a Genius kit, the same cDNA library was screened according to the manufacturer's instructions (Roche, Indianapolis, IN). Positive plaques were converted to pBluescripts, and their inserted DNA sequences were determined as previously described *(5)*.

Construction of Plasmid Cassette

Plasmid pYES2 was digested with *Sac*I and *Xba*I overnight. The digested plasmid was purified using the Geneclean II kit (Bio 101, La Jolla, CA). On the basis of the nucleotide sequence of the cloned gene, forward (PFBgl, 5'GCCGAGCTCGATGAAGACTCTTACTGTTTTC3') and reverse (PRBg1, 5'GCTCTAGAGTTAGTTTTGTTCAACATTTTC3') primers were synthesized. PFBgl corresponded to the first seven amino acids of the open reading frame (ORF) and had a *Sac*I site attached, whereas PRBgl corresponded to the last six amino acids plus a stop codon and had an *Xba*I site attached. Using PFBgl and PRBgl as primers and plasmid PBgl13 as template, the whole ORF was amplified by PCR. PCR was carried out for 30 cycles of denaturation (1 min at 94°C), annealing (1.5 min at 42°C), and extension (3.5 min at 72°C) on a 480 Thermocycler (Perkin-Elmer, Norwalk, CT). PCR products were purified using a Geneclean kit and digested with *Sac*I and *Xba*I. Digested DNA fragments were purified and concentrated before they were ligated to the digested pYES2 with T4 ligase.

Transformation of E. coli *and Propagation of Plasmids*

Ligation reactions were performed using a rapid ligation kit (Roche). *E. coli* TOP10 transformants were plated onto LB plates containing ampicillin (50 µg/mL). Colonies were picked and grown overnight in LB liquid

medium containing ampicillin. Plasmids were purified with a spin column kit from Qiagen. Restriction digestion and nucleotide sequencing were done to verify the presence, orientation, and sequence of the insert.

Transformation of S. cerevisiae

A single colony of yeast strain INVSc1 was grown to an OD_{600} of 1.3 in YPD medium, pH 6.5, containing 1% (w/v) yeast extract, 1% (w/v) bactopeptone, and 1% (w/v) dextrose. Cells were harvested by centrifuging (4000g, 5 min) at 4°C and washed twice with ice-cold sterile H_2O and twice with ice-cold 1 M sterile sorbitol. Then, the cells were resuspended in 0.5 mL of 1 M sorbitol. Approximately 5 µg of plasmid was used to transform 40 µL of prepared yeast cells utilizing an electroporator (Bio-Rad, Hercules, CA). Transformants were grown on DOB medium containing 0.17% (w/v) yeast nitrogen base without amino acids and NH_2SO_4, 2.0% (w/v) dextrose, 0.08% (w/v) drop-out supplements lacking uracil (Bio101), 2% (w/v) agarose, and 1 M sorbitol. The plates were incubated at 30°C for 3–5 d.

Induction of Gene Expression

Ten putative transformants were chosen for induction experiments. They were cultivated in 10 mL of DOB medium containing 4% (w/v) raffinose. After the OD_{600} reached 1.0, galactose was added to a final concentration of 2% (w/v). Samples were collected before and periodically after the addition of galactose. Transformant no. 7, which produced the highest level of β-glucosidase activity, was chosen for induction experiments in YPD medium. A single colony of the transformant was used for inoculating 2 mL of DOB medium. After the OD_{600} reached 0.8, 1.0 mL of the culture was added to 100 mL of YPD-raffinose (4% w/v) medium, and the culture was shaken (250 rpm) at 30°C. Sterile galactose (2.0% w/v) was added to the culture after the OD_{600} reached 1.0. Samples were collected before and periodically after the addition of galactose. Cells were harvested by centrifuging (5000*g*, 5 min) at 4°C. All samples were kept at –20°C until analyzed.

Enzyme Assay

β-glucosidase (*p*-nitrophenyl-β-D-glucosidase) and cellobiase activities were determined by the following standard procedures. With *p*-nitrophenyl-β-D-glucopyranoside (pNPG) as the substrate, the reaction mixture of 1.2 mL contained 0.3 mL of appropriately diluted enzyme solution; 0.6 mL of 50 m*M* sodium phosphate buffer, pH 6.0; and 0.3 mL of 12 m*M* pNPG. The reaction was carried out for 10 min at 40°C and stopped by the addition of 2.4 mL of 1 *M* Na_2CO_3. The liberated *p*-nitrophenol was measured spectrophotometrically at 405 nm *(12)*. Cellobiase activity was determined by using a reaction mixture of 2 mL containing 1 mL of appropriately diluted enzyme solution in 50 m*M* sodium phosphate buffer, pH 6.0, and 1 mL of 2 m*M* cellobiose. The reaction was carried out at 40°C for

30 min and was stopped by placing the assay tubes in boiling water for 5 min. Liberated glucose was measured with a glucose determination kit (Sigma, St. Louis, MO) as described in the manufacturer's instructions. One unit of β-glucosidase or cellobiase activity was defined as the amount of enzyme required to hydrolyze 1 μmol of substrate/min. Specific activity was expressed as units per milligram of protein.

Hydrolysis of Avicel cellulose (Sigma) was set up in test tubes with 3.0 mL of solution containing 30 mg of cellulose and 0.25 filter paper activity units of *T. reesei* cellulase *(13)*. The buffer was 50 m*M* sodium citrate, pH 5.5. The *Orpinomyces* β-glucosidase (0.25 U) was added to some of the tubes. The tubes were sealed and shaken (200 rpm) at 37°C for 16 h. Following incubation, insoluble materials were removed by centrifuging (5000*g*, 15 min), and sugars in the supernatant were separated and quantified using a high-performance liquid chromatography (HPLC) system equipped with a Bio-Rad HPX-87P column and a 1047A RI detector.

Purification of Enzyme

S. cerevisiae culture (7.5 L) harboring pBgl13 was grown in YPD-raffinose medium for 24 h at 30°C. The supernatant was obtained by centrifugation (4000*g*, 20 min) and concentrated to a volume of approx 155 mL by using an ultrafiltration cell (Amicon, Beverly, MA) equipped with a PM 10 membrane. The buffer was changed to 50 m*M* sodium phosphate, pH 6.0, and then ammonium sulfate was added to a concentration of 0.8 *M*. The solution was centrifuged (20,000*g*, 10 min) at 4°C to remove precipitated material. More than 80% of the activity was found in the supernatant that was loaded on a Phenyl Superose 10/10 (Pharmacia, Piscataway, NJ) column equilibrated with 50 m*M* sodium phosphate buffer, pH 6.0, containing 0.8 *M* ammonium sulfate. The major β-glucosidase fraction did not bind to the column. This sample was then concentrated, and the buffer was changed to 20 m*M* piperazine-HCl, pH 6.0. The solution was applied to a Mono Q 5/5 (Pharmacia) column equilibrated with 20 m*M* piperazine-HCl, pH 6.0. The enzyme bound to the column. Two peaks of activity were eluted with a linear gradient of NaCl (0 to 1 *M*). The major fraction was concentrated and changed to 20 m*M* formic acid buffer, pH 4.0. The sample was applied to a Resource S column (Pharmacia). The enzyme did not adsorb to the column. Final purification was achieved by gel filtration in a Superdex 200 26/60 column (Pharmacia) equilibrated with 20 m*M* sodium phosphate buffer, pH 6.0, containing 100 m*M* NaCl. Fractions containing β-glucosidase were stored at –20°C until further analyzed. Procedures for partial purification of the cell-associated β-glucosidases were basically identical to those for the secreted BglA.

N-Terminal Amino Acid Sequencing of Proteins

Proteins were separated on sodium dodecyl sulfate polyacrylamide gel electrophoresis (SDS-PAGE) *(14)* and transferred to polyvinylidine

difluoride membranes in a Mini Trans-Blot cell (Bio-Rad). Protein bands on the membranes were visualized by Coomassie Blue R-250 staining and excised using a razor blade. N-terminal amino acid sequencing of the protein bands was performed on an Applied Biosystems Model 477A gas-phase sequencer equipped with an automatic on-line phenylthiohydantoin analyzer.

Analytical Methods

SDS-PAGE (7.5 and 10%) was carried out in Laemmli's buffer *(14)*. High-molecular-weight protein standards (Bio-Rad) were used as markers. Electrophoresis was performed in a Mini-Protein II cell and gels were stained with Coomassie brilliant blue R-250 *(15)*. β-Glucosidase activity bands in native gels were visualized by the method of Rutenburg et al. *(16)* with 6-bromo-naphthyl-β-d-glucopyranoside as substrate.

Characterization of Expressed β-Glucosidases

The carbohydrate content of the purified enzyme was determined using the phenol-sulfuric method of Dubois et al. *(17)* with mannose as standard. Protein content was measured by the method of Lowry et al. *(18)* with bovine albumin as standard.

The pH optimum was determined by performing an assay with either pNPG or cellobiose as substrate at 40°C in the following buffer systems: 0.1 *M* sodium acetate (pH 3.8 to 5.6), 0.1 *M* sodium phosphate (pH 5.8–7.6), and 0.1 *M* HEPES-NaOH (pH 8.0–8.6). Enzyme stability at different pH values was determined by measuring the residual activity after incubating the enzyme for 24 h at 4°C with these buffers plus glycine-HCl for pH 3.0–3.4 and piperazine-HCl for pH 9.0–10.2. The effect of temperature on β-glucosidase activity was determined by assaying the enzyme at temperatures from 30 to 65°C. To assess the stability of the glycosylated and deglycosylated BglA at various temperatures, enzyme preparations were incubated in 50 m*M* sodium phosphate buffer, pH 6.0, from 10 min to 8 h at temperatures from 40 to 60°C. During the time course, aliquots were withdrawn and kept on ice. Remaining activity in the samples was determined under standard assay conditions.

Several α- and β-glucosides (1 m*M*) and polysaccharides (0.5% [w/v]) were tested as substrates for the purified enzyme. *p*-Nitrophenol *(12)* and glucose were determined as described by HPLC (*see* Enzyme Assay). Reducing sugars were determined following the procedure of Miller *(19)*.

To measure kinetic parameters, hydrolysis rates were determined by varying the concentrations of pNPG (0.05–10 m*M*) and cellobiose (0.04–16 m*M*). The inhibition by glucose was evaluated with only pNPG (10 m*M*) as substrate, whereas the inhibitory effect of glucono-1,5-lactone was verified with both pNPG (10 m*M*) and cellobiose (1.0 m*M*) as substrates. K_m, V_{max}, and K_i values were calculated from Lineweaver-Burk plots.

Results and Discussion

Isolation of a BglA cDNA

Previous work *(4)* revealed that *Orpinomyces* sp. strain PC-2, a polycentric anaerobic fungus isolated from the rumen of a cow, produces high levels of β-glucosidase in addition to endoglucanase, CBH, and xylanase. A β-glucosidase produced in the culture supernatant of the fungus has been purified and characterized *(3)*. Different hydrolytic enzymes produced by this fungus can function individually or in high-molecular-weight enzyme complexes such as cellulosomes *(5–9)*. The fungal cellulosomes purified from residual solid substrate of the fungal culture contained β-glucosidase activity *(20)*, indicating that β-glucosidases may be components of the cellulosomes produced by the fungus. More recently, the gene coding for a cellulosomal β-glucosidase of the monocentric anaerobic fungus *Piromyces* E2 was cloned and sequenced *(21)*.

Many of the hydrolytic enzymes of anaerobic fungi sequenced to date contain, in addition to catalytic domains, a noncatalytic docking domain (NCDD) *(22)*, which functions in a fashion similar to dockerins in the cellulosomes of anaerobic bacteria *(23)*, but no sequence similarity has been identified between the fungal NCDDs and the bacterial dockerins *(5,24)*. Polyclonal antibodies raised against the NCDD of *Orpinomyces* XynA crossreacted with a number of different other polypeptides in the culture media of *Orpinomyces* and *Neocallimastix* grown on cellulose *(5)*, suggesting that a number of NCDD-containing enzymes remain to be isolated. To isolate cDNAs coding for NCDD-containing polypeptides, we used the XynA NCDD-specific antibodies to screen an *Orpinomyces* expression cDNA library *(11)*. Twenty-five positive plaques were isolated after screening 1.0×10^5 plaque-forming units. Sequencing of the inserted cDNAs in the pBluescipts, after being excised from pure positive λ plaques, revealed that several represented different lengths of cDNAs coding for, in addition to *xyn*A *(5)*, *cel*A *(6)*, *cel*B *(5)*, *cel*C *(6)*, and *cel*E *(7)*, three new sequences were isolated. One of the new sequences had 800 bp (pBgl6) and its deduced amino acid sequence was homologous to certain β-glucosidases. Using the cDNA fragment in pBgl6 as a hybridization probe, plaques containing cDNAs (pBgl13) with a complete ORF encoding a putative β-glucosidase (*bgl*A) were isolated from the same cDNA library.

Nucleotide and Deduced Amino Acid Sequences of Orpinomyces *sp. Strain PC-2* bgl1

The complete nucleotide sequence of *bgl*1 cDNA was determined and deposited in GenBank with accession no. AF016864 (submitted on July 31, 1997). The total length of the cDNA is 2435 bp. It contains an ORF of 1974 bp encoding a polypeptide of 657 amino acids with a molecular mass of 75,227 Daltons (BglA). Like cellulase B *(5)* and cellulase F *(8)* isolated from the same fungus, a long 3' noncoding A-T-rich end (423 bp) was observed after the ORF, but no typical long poly (A) stretch was found.

The putative translation start codon (ATG) for *bgl*1 was assigned based on the fact that there were stop codons in all three frames preceding the ORF and there was no ATG codon upstream of the proposed ORF. In addition, the proposed N-terminal region of BglA contains the properties of signal peptides of fungi *(25)*. Furthermore, close examination of the complete amino acid sequence of BglA failed to detect an NCDD sequence, indicating that BglA lacks a dockerin and there is not a component of the *Orpinomyces* cellulosome. Its cDNA was isolated owing to nonspecific crossreaction between the partial BglA protein and the NCDD-specific antibodies.

The G+C content of the entire cDNA and the ORF of *bgl*1 were 36 and 42.3%, respectively, and that of the 5' and 3' noncoding region was only 9.1%. Low G+C contents have also been found in other cDNAs of *Orpinomyces (5–9)*.

Homology of BglA with Other β*-Glucosidases*

The deduced amino acid sequence of BglA was compared with other protein sequences in the SWISS PROT and GP databanks. Comparison using the Bestfit program revealed that BglA had significant levels of identity with β-glucosidases from *Piromyces* E2 (Cel1A, 72.0%) *(26)*, *Cavia porcellus* (pig, 41.2%) *(27)*, *Costus speciosus* (40%) *(28)*, *Clostridium thermocellum* (40.2%) *(29)*, *Bacillus circulans* (41.7%) *(30)*, *Thermoanaerobacter* sp. (40.6%) *(31)*, and *Thermotoga maritima* (40.7%) *(32)*. According to Henrissat and Bairoch (*33*) and http://afmb.cnrs-mrs.fr/~cazy/CAZY, these enzymes belong to family 1 glycosyl hydrolases. No significant identity (<20%) was found with the family 3 β-glucosidases from *T. reesei* and *Aspergillus aculeatus*. Comparison of the homologous β-glucosidases of the family revealed that the β-glucosidases of *Orpinomyces* and *Piromyces* have about 50 more amino acid residues after their signal peptides than those of the other organisms. These 50 amino acid regions are probably not critical for catalysis because the recombinant polypeptides of *Orpinomyces* BglA with this region partially truncated remained catalytically active. These regions between the *Orpinomyces* and *Piromyces* enzymes are the least homologous to each other (Fig. 1). Furthermore, the short repeated sequences within the region of the *Piromyces* enzyme *(26)* are absent in the *Orpinomyces* enzyme. Glu-250 and Glu-523 of the *Orpinomyces* BglA are conserved between all the enzymes, and these two residues in the *Bacillus polymyxa* β-glucosidase were found to be directly involved in catalysis *(34)*. Gln82, His 260, Tyr 433, Glu-523, and Tyr 607, which are also conserved, have been identified as determinant residues for the recognition of substrates *(34)*.

Expression of bgl1 *in and Secretion of BglA from* S. cerevisiae

No β-glucosidase activity was detected in *E. coli* culture harboring the complete *bgl*A cDNA. This finding is in agreement with no positive colo-

```
Orpinomyces    1 MKTLTVFSALLAVTAAKKCIVK..SDAAVASEAE.EVTAELTAPEDSGVE 47
                 ||||.:|. ||||.|||||:|:  .|.|  .: .  || :: .  :. |
Piromyces      1 MKTLSIFTTLLAVSAAKKCVVRNPTDSAKTNDVKAPVTDDIPSDNETPVN 50

Orpinomyces   48 SGEDDEL..LDLSTIDYGDDVDMSTVK...KLPADFKWGAATAAYQVEGA 92
                   |.  |   : | |:   |:: |  |   ||||||||||||||||||
Piromyces     51 VDENTPLDKEEDSGIE.NSDIENSEDKPKGKLPADFKWGAATAAYQVEGA 99
```

Fig.1. Comparison of the amino-terminal regions of *Orpinomyces* BglA (AF016864) and *Piromyces* CelA1 *(26)* β-glucosidases. Vertical lines indicate identical matches, and single and double dots indicate different levels of conservation.

nies detected when using 4-methylumbelliferyl-β-D-glucoside, a fluorescent substrate of β-glucosidases, as a screening substrate. Lack of functional expression in *E. coli* might be related to differences between anaerobic fungi and *E. coli* with respect to posttranslational modifications such as glycosylation and folding. We attempted to express the gene in *S. cerevisiae*, since several heterologous genes coding for hydrolytic enzymes have been expressed in various strains of the yeast. These include genes coding for two endoglucanases *(35)*, two CBHs *(36)*, and one β-glucosidase from *T. reesei (37)*; a xylanase from *Aureobasidium pullulans (38)*; an α-amylase from wheat *(39)*; and others. Recently, a cellulase gene cassette encoding the *Butyrivibrio fibrisolvens* endo-β-1,4-glucanase (END1), the *Phanerochaete chrysosporium* CBH (CBH1), the *Ruminococcus flavefaciens* cellodextrinase (CEL1), and the *Endomyces fibrilizer* cellobiase (Bgl1) was successfully expressed in a laboratory strain of *S. cerevisiae (40)*.

After transformation, 10 transformants were grown in synthetic dropout supplemented medium without uracil, using raffinose as growth substrate and galactose as inducer (*see* Materials and Methods). β-Glucosidase activity was determined for the cells and in culture medium. All activity was found to be associated with cells, and no activity was found in the culture medium for all the transformants. It has been reported that culture conditions can strongly affect the secretion of enzymes from *S. cerevisiae*. For example, the secretion of a wheat α-amylase from *S. cerevisiae* into the medium was efficient only in a rich medium but barely detectable in a minimal medium *(39)*. The secretion of the *Orpinomyces* BglA from *S. cerevisiae* was similar (Fig. 2). A substantial percentage (40%) of the total β-glucosidase activity was found in the culture medium after 24 h of growth in rich medium. The levels of activity in cell-associated and culture medium fractions stayed almost constant during the cultivation period (96 h). The growth rates between the transformants using plasmids with and without *bgl*1 inserted were almost identical, indicating that BglA and its gene did not affect the physiology of the yeast. A higher percentage of a *T. reesei* β-glucosidase, when expressed in *S. cerevisiae*, was found in the culture medium *(37)*.

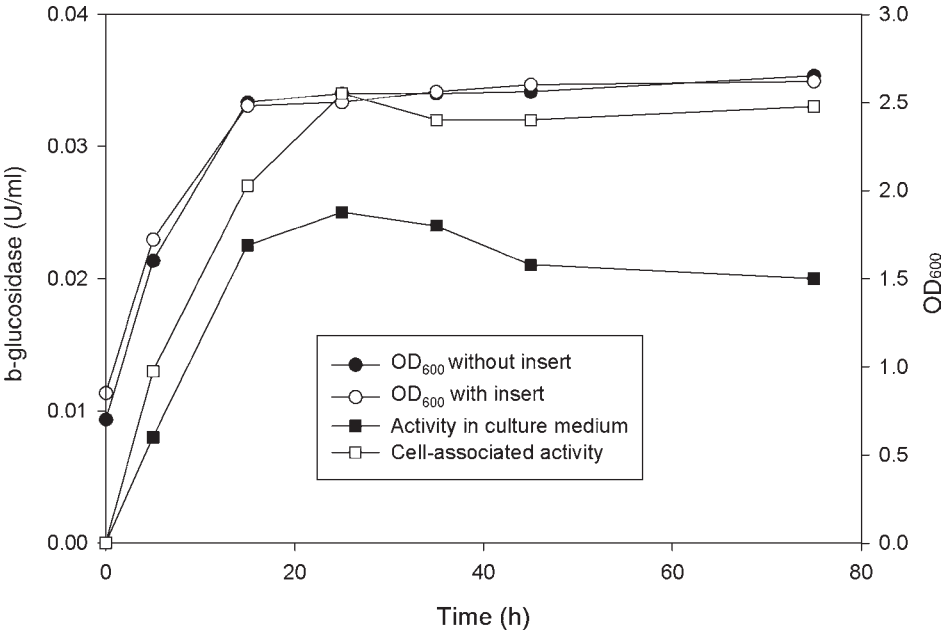

Fig 2. β-glucosidase production of *S. cerevisiae* cultures grown in raffinose-YPD medium after galactose induction. An aliquot of an overnight culture grown in DOB medium was used to inoculate raffinose-YPD medium. After growth to an OD_{600} of 1.0, sterile galactose was added. Samples were withdrawn at the time points shown. The OD_{600} of control culture (●), OD_{600} (○), and β-glucosidase activity of cell extract (□) and culture medium (■) of transformant no. 7 were determined. Culture conditions, preparation of the samples, and enzyme assays were described in Materials and Methods. The control culture corresponded to the yeast containing the pYES2 without any insert.

Purification and N-Terminal Processing of BglA Produced by S. cerevisiae

A summary of purification of the *Orpinomyces* BglA secreted by *S. cerevisiae* culture is given in Table 1. The enzyme was purified about 28-fold to homogeneity with a specific activity of 18.8 U/mg and a yield of about 1%. Multiple peaks of activity were observed during the purification steps, but only the major activity peak was used for further purification, indicating that BglA may be secreted into culture medium with multiple forms owing to proteolysis or different levels of glycosylation.

Two cell-associated forms (BglA1 and BglA2) of BglA were also partially purified from the cell-free extract of yeast cells using Phenyl Sepharose, Mono Q, and Superdex 200. The sizes of BglA1 (first band in lanes 4 and 7 of Fig. 3) and BglA2 (first band in lanes 5 and 8 of Fig. 3) were estimated to be about 65 kDa on SDS-PAGE/zymogram analysis (Fig. 3).

Table 1
Summary of Purification of Recombinant BglA
from Culture Medium of *S. cerevisiae*

Purification step	Total protein (mg)	Total units (μmol/min)[a]	Specific activity (μmol/[min·mg])	Yield (%)
Culture filtrate	480.00	326.8	0.68	100.0
Concentrated supernatant	165.30	319.7	1.93	97.8
Phenyl Sepharose	17.10	101.4	5.90	31.0
Mono Q	5.20	66.0	12.80	20.2
Resource S	2.23	38.3	17.20	11.7
Superdex 200	0.17	3.2	18.80	1.0

[a]Activities were measured with pNPG as substrate.

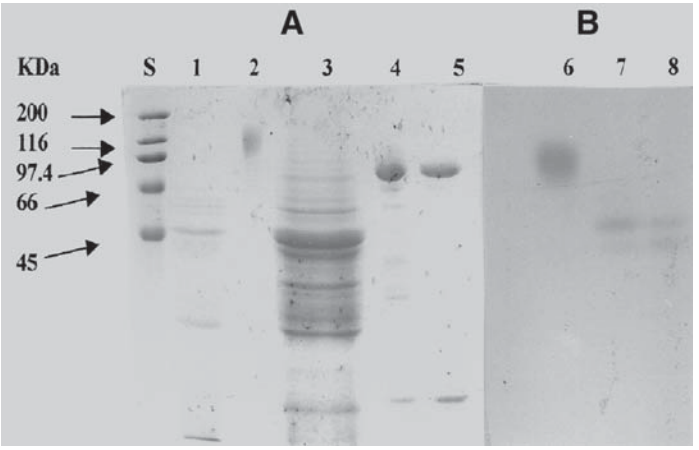

Fig. 3. SDS-PAGE (10%)/zymogram analysis of secreted and cell-associated forms of BglA. **(A)** SDS-PAGE stained with Coomassie brilliant blue R-250; **(B)** β-glucosidase zymogram gel. Lane S, protein molecular mass standards; lane 1, crude culture supernatant (10 μg); lane 2, purified secreted BglA (2 μg); lane 3, crude cell extract (60 μg); lane 4, partially purified BglA1 (2 μg); lane 5, partially purified BglA2 (2 μg); lane 6, purified secreted BglA (2 μg); lane 7, BglA1 (2 μg); lane 8, BglA2 (2 μg).

The purified BglA, BglA1, and BglA2 were all subjected to N-terminal amino acid sequencing. The secreted BglA had an N-terminal sequence of KKCIVKSDAA, which matched amino acid residues 17–26 (Fig. 1), demonstrating that amino acid residues 1–16 were cleaved during secretion. Thus, the first 16 amino acid residues might serve as a signal peptide in both *Orpinomyces* and *S. cerevisiae*. Removal of 16 amino acid residues at the N-terminus resulted in 641 amino acid residues with a calculated mass of 73,608 Daltons for the mature BglA. The signal peptide had a basic amino acid (Lys) as the second N-terminal residue, followed by a hydrophobic amino acid region containing in some points nonhydrophobic residues.

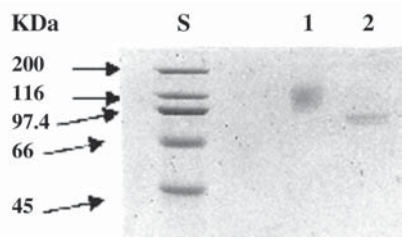

Fig. 4. SDS-PAGE analysis of BglA treated with N-glycosidase F. Lane S, protein molecular mass standards; lane 1, purified secreted BglA (2.4 μg); lane 2, purified secreted BglA (2.4 μg) treated with N-glycosidase F.

This is in agreement with the work of Ngsee et al. *(41)*, who, using site-directed mutagenesis of the signal sequence of yeast invertase gene, *suc* 2, demonstrated that the essential feature of a signal peptide for yeast is a hydrophobic core of 6–15 amino acids. The core region can be interrupted to a certain extent by nonhydrophobic residues. The purified recombinant BglA yielded a broad band with an average size of about 110 kDa on SDS-PAGE (Fig. 3), which was larger than that calculated for the deduced mature enzyme. According to Orlean et al. *(42)*, only one *N*-glycosylation site, Asn-X-Ser/Thr, corresponding to amino acid residues 280–282 was found on the entire BglA sequence. However, the size of the purified enzyme after treatment with *N*-glycosidase F, an enzyme specifically removing N-glycosylation, shifted to two sharp bands with very similar sizes (87 and 92 kDa) on SDS-PAGE (Fig. 4). N-terminal amino acid sequencing revealed that these two bands had amino acid sequences at their N-termini identical to those of the secreted BglA. These results indicate that about 20% (w/w) of *N*-glycosylation is added to BglA during secretion from *S. cerevisiae* and that the size difference between the two similar bands after the *N*-glycosidase F treatment is probably owing to *O*-glyco-sylation. The β-glucosidase purified from the culture supernatant of the same fungus had a mass of 85 kDa including 8.5% (w/w) carbohydrate *(3)*. Assuming that the native β-glucosidase *(3)* and the secreted BglA reported here are products of the same gene, *bgl*1 of *Orpinomyces* PC-2, glycosylation (hyperglycosylation) by *S. cerevisiae* is much greater than by *Orpinomyces*. Hyperglycosylation was also found for *T. reesei* endoglucanases *(35)*, CBHs *(36)*, and β-glucosidase *(37)* expressed in and secreted from *S. cerevisiae.*

The N-terminal sequence for BglA1 was APEDSGVES, which matched amino acid residues 40–48 (Fig. 1), and that of BglA2, GEDDELLDLS, corresponded to amino acid residues 49–58 (Fig. 1). Thus, the cleavages resulted in two truncated forms (BglA1 and BglA2) of BglA (Fig 3). These results suggest that BglA1 and BglA2 were cleaved at the wrong sites and subsequently trapped during transport in the secretory pathway. The fact

Table 2
Some Properties of Purified Recombinant BglA of *Orpinomyces* Produced in *S. cerevisiae*

Molecular mass	
Deduced	75,227 Daltons
Before deglycosylation	110,000 Daltons
After glycosidase F treatment	87 and 97 kDa
Optimum pH at 40°C	5.5–7.5
Optimum Temperature at pH 6.0	55°C
K_m	
pNPG	0.762 m*M*
Cellobiose	0.310 m*M*
V_{max}	
pNPG	8.20 μmol/(min·mg)
Cellobiose	6.20 μmol/(min·mg)
K_i of glucose	3.6 m*M*

that these two truncated forms retained catalytic function indicates that the sequences of the *Orpinomyces* BglA and the *Piromyces* Cel1A up to amino acid residue 48 are not critical for catalysis. This may be why this region is absent in the homologous bacterial β-glucosidases.

Catalytic Properties

The activity of the purified secreted BglA against pNPG and cellobiose was determined from pH 3.8 to 8.6 at 40°C. The optimum pH with both substrates was found to be between 5.5 and 7.5 (Table 2) with detectable levels of activity from pH 4.0 to 8.0. The enzyme was stable for at least 24 h between pH 3.4 and 10.2 at 4°C. Hydrolysis of pNPG and cellobiose by BglA, determined in 50 m*M* sodium phosphate buffer (pH 6.0), was most active at 50°C (Table 2) when assayed for 10 min. Enzyme activity decreased rapidly above 55°C and the enzyme lost its activity at 65°C. The enzyme maintained 100% of its activity for 8 h at 40 and 50°C. Inactivation of BglA occurred slowly at 55°C, with 50% of the enzyme activity remaining after 8 h of incubation. At 60°C the enzyme was quickly inactivated. The optimum pH and temperature ranges of the recombinant BglA are similar to those reported for the native β-glucosidases of *Orpinomyces* sp. strain PC-2 *(3)*, *Neocallimastix frontalis (43)*, and *Piromyces* sp. strain E2 *(44)*.

K_m, K_i, and V_{max} values for the secreted BglA were obtained from Lineweaver-Burk plots (Table 2). The K_m value with pNPG as substrate at 40°C and pH 6.0 was 0.762 m*M*, higher than that (0.35 m*M*; *[3]*) reported for the native β-glucosidase of the same fungus. However, the K_m value with cellobiose as substrate in the range of 0.04–1.0 m*M* was 0.31 m*M*,

Table 3
Substrate Specificity of *Orpinomyces* BglA Purified from *S. cerevisiae*[a]

Substrate (1 m*M*)	Specific activity (μmol/[min·mg])[b]
p-Nitrophenyl-β-glucopyranoside	2.10
Cellobiose (β-1,4)	1.87
o-Nitrophenyl-β-glucopyranoside	2.99
Sophorose (β-1,2)	4.53
Laminaribiose (β-1,3)	6.10

[a] Conditions were 40°C and pH 6.0.

[b] Activity on gentibiose (β-1,6-glucoside), methyl-β-glucoside, *p*-nitrophenyl-β-xyloside, salicin, maltose, sucrose, lactose, xylan (1.0% [w/v]), Avicel (1.0% [w/v]), or carboxymethylcellulose (1.0% [w/v]) was <1.0% of that on pNPG.

which is very similar to the K_m (0.25 m*M*) for the native β-glucosidase. These values are within the range of K_m values reported for several β-glucosidases of anaerobic fungi *(43–46)*. Comparison of the K_m values for β-glucosidases from various sources indicates that those from anaerobic fungi have lower K_m values than those from bacteria or aerobic fungi. The differences in K_m values between the *Orpinomyces* native β-glucosidase and the recombinant BglA could be owing to the different levels of glycosylation. Ward *(47)* has reported that when a site for *N*-glycosylation was introduced, chymosin had resulted in lower specific activity. The effect on specific activity was considered to be probably a consequence of active site change by the glycosylation *(47,48)*.

Hydrolysis rate decreased as cellobiose concentration was increased higher than 2.0 m*M* (Fig. 5). This phenomenon is caused by substrate inhibition by cellobiose and transglycosylation for the formation of cellooligosaccharides, as described for a cellobiase of *N. frontalis (46)*. A close comparison of the same plots between the *Orpinomyces* BglA (Fig. 5) and the *Neocallimastix* cellobiase (Fig. 4, of ref. *46*) shows that the *Orpinomyces* and the *Neocallimastix* enzymes had their highest activity when cellobiose concentrations were 1.0 and 0.25 m*M*, respectively, suggesting that the former tolerates higher cellobiose concentrations.

Glucose and glucono-1,5-lactone competitively inhibited BglA with a K_i of 3.6 and 0.05 m*M*, respectively. These numbers are lower than those for the native *Orpinomyces* β-glucosidase, and the reason for this could be again owing to difference in glycosylation.

BglA is specific for aryl-β-glucoside bonds and was not able to hydrolyze alkyl-β-glucoside bonds or α-1,4-glucoside bonds. The enzyme rapidly hydrolyzed sophorose (β-1,2-glucobiose), laminaribiose (β-1,3-glucobiose), and cellobiose (β-1,4-glucobiose) but lacked activity on gentibiose (β-1,6-

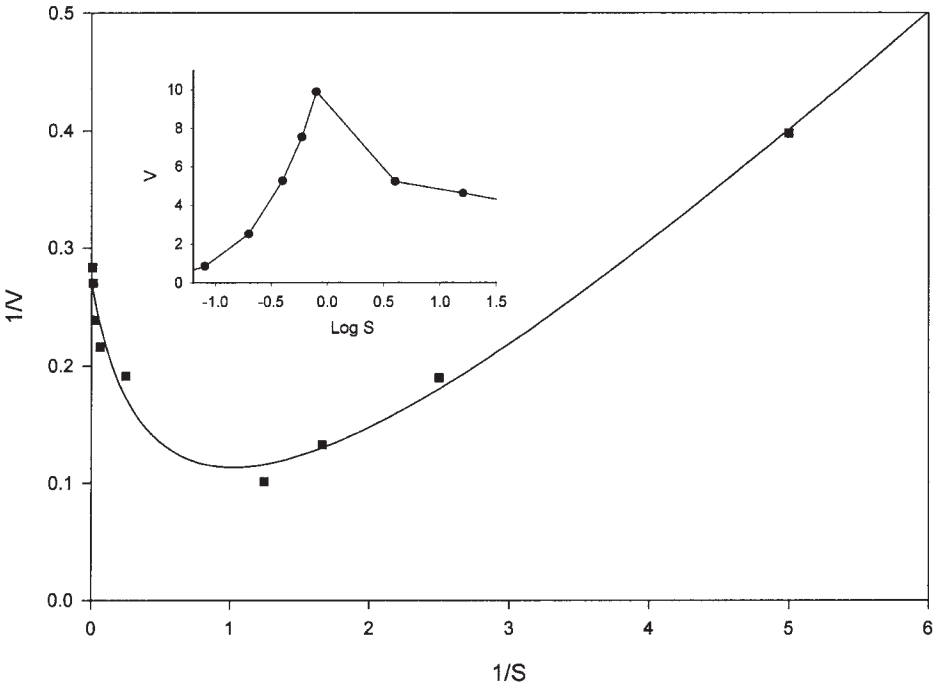

Fig. 5. Lineweaver-Burk plot of the *Orpinomyces* BglA on hydrolysis of cellobiose (0.04–16 m*M*). The release of glucose was measured. Reciprocal initial velocities (mg/U) are plotted against the reciprocal concentrations of substrates (1 m*M*). The inset is a plot of initial velocities (U/mg) against the log cellobiose concentrations (m*M*).

glucobiose), methyl-β-glucoside, *p*-nitrophenyl-β-xyloside (pNPX), salicin, maltose, sucrose, lactose, xylan, microcrystalline cellulose, or carboxymethyl cellulose. A low level of activity was found against pNPX when the enzyme level in the assays was increased 20 times. BglA reported here and the native β-glucosidase *(3)* had almost identical substrate specificity. Interestingly, such substrate specificity is very similar to that of a β-glucosidase purified from the anaerobic rumen bacterium *Ruminococcus albus (49)*.

To assess the ability of BglA to convert cellooligosaccharides to glucose, we added BglA to the saccharification reaction of Avicel by *T. reesei* cellulase since it is well known that *T. reesei* secretes insufficient levels of β-glucosidase activity. Glucose, cellobiose, and cellotriose generated by the cellulase mixtures were measured (Fig. 6). In the presence of BglA under the test conditions, cellobiose and cellotriose disappeared almost completely and glucose increased more than sixfold. The amount of glucose in the presence of BglA was more than the total amount of glucose, cellobiose, and cellotriose without the addition of BglA, indicating that the conversion of the oligosaccharides to glucose removed inhibition of the sugars on both endoglucanases and CBHs of *T. reesei*.

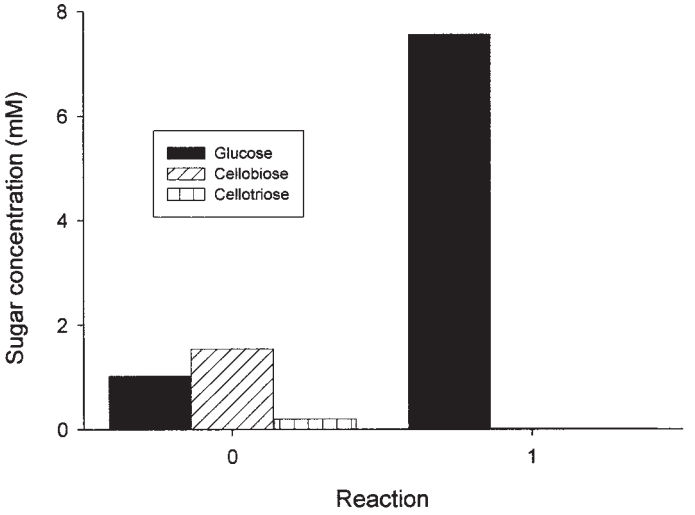

Fig. 6. Saccharification of Avicel cellulose by *T. reesei* cellulase without (panel 0) and with (panel 1) *Orpinomyces* BglA. Concentrations of sugars were measured using an HPLC system (*see* Materials and Methods) after 16 h of reaction.

Acknowledgments

We wish to thank Patrick Kane for excellent technical input in the kinetic analysis. This work was supported by grants from the US Department of Energy (DE-FG02-93ER20127), the Consortium for Plant Biotechnology Research (OR220 72-64), Aureozyme, and Georgia Research Alliance (TDP98.001-UGA). L. G. L. received a distinguished professorship from Georgia Power and E. A. X. received a scholarship from the Conselho Nacional de Desenvolvimento Científico e Tecnológico (CNPq).

References

1. Ohmiya, K., Sakka, K., Karita, S., and Kimura, T. (1997), *Gen. Eng. Rev*. **14,** 365–414.
2. Filho, E. X. F. (1996), *Can. J. Microbiol*. **42,** 1–5.
3. Chen, H., Li, X.-L., and Ljungdahl, L. G. (1994), *Appl. Environ. Microbiol*. **60,** 64–70.
4. Borneman, W. S., Akin, D. E., and Ljungdahl, L. G. (1989), *Appl. Environ. Microbiol.* **55,** 1066–1073.
5. Li, X.-L., Chen, H., and Ljungdahl, L. G. (1997), *Appl. Environ. Microbiol*. **63,** 628–635.
6. Li, X.-L., Chen, H., and Ljungdahl, L. G. (1997), *Appl. Environ. Microbiol*. **63,** 4721–4728.
7. Chen, H., Li, X.-L., Blum, D. L., and Ljungdahl, L. G. (1998), *FEMS Microbiol. Lett.* **159,** 63–68.
8. Chen, H., Li, X.-L., Blum, D. L., Ximenes, E. A., and Ljungdahl, L. G. (2003), *Appl. Biochem. Biotechnol*. **105–108,** 775–785.
9. Chen, H., Li, X.-L., and Ljungdahl, L. G. (1997), *J. Bacteriol*. **179,** 6028–6034.
10. Blum, D. L., Li, X.-L., Chen, H., and Ljungdahl, L. G. (1999), *Appl. Environ. Microbiol.* **65,** 3990–3995.
11. Chen, H., Li, X.-L., and Ljungdahl, L. G. (1995), *Proc. Natl. Acad. Sci. USA* **9,** 2587–2591.
12. Herr, D., Baumer, F., and Dellweg, H. (1978), *Appl. Microbiol. Biotechnol.* **5,** 29–36.

13. Chen, H., Ximenes, E. A., Li, X.-L., and Ljungdahl, L. G. (1999), in *Cellulose Degradation*, Ohmiya, K., Hayashi, K., Sakka, K., Kobayashi, Y., Karita, S., and Kimura, T., eds., Uni Publishers, Tokyo, Japan, pp. 173–181.
14. Laemmli, U. K. (1970), *Nature (Lond.)* **227,** 680–685.
15. Fairbanks, G., Steak, T. S., and Wallach, D. F. H. (1971), *Biochemistry* **10,** 2606–2616.
16. Rutenburg, A. M, Goldbarg, J. A., Rutenburg, S. H., and Lang, R. T. (1960), *J. Histochem. Cytochem.* **8,** 268–272.
17. Dubois, M., Gilles, K. A., Hamilton, J. K., Rebers, P. A., and Smith, F. (1956), *Anal. Chem*. **28,** 350–356.
18. Lowry, O. H., Rosebrough, N. J., Farr, A. L., and Randall, R. J. (1951), *J. Biol. Chem*. **193,** 265–273.
19. Miller, G. L. (1959), *Anal. Chem*. **31,** 426–428.
20. Li, X.-L., Chen, H., He, Y., Blum, D. L., and Ljungdahl, L. G. (1997), in *Abstracts of 97th General Meeting of the American Society for Microbiology,* American Society for Microbiology, Washington, DC, p. 424.
21. Steenbakkers, P. J. M., Harhangi, H. R., Bosscher, M. W., van der Hooft, M. M. C., Keltjens, J. T., van der Drift, C., Vogels, G. D., and Op den Camp, H. J. M. (2003), *Biochem. J.* **370,** 963–970.
22. Steenbakkers, P. J. M., Li, X.-L., Ximenes, E. A., Arts, J. G., Chen, H., Ljungdahl, G. L., and Op den Camp, H. J. M. (2001), *J. Bacteriol*. **183,** 5325–5333.
23. Béguin, P. and Lemaire, M. (1996), *Crit. Rev. Biochem. Mol. Biol*. **31,** 201–236.
24. Fannuti, G., Ponyi, T., Black, G. W., Hazlewood, G. P., and Gilbert, H. J. (1995), *J. Biol. Chem.* **270,** 29,314–29,322.
25. von Heijne, G. (1986), *Nucleic Acids Res*. **14,** 4683–4690.
26. Harhangi, H. R., Steenbakkers, P. J. M., Akmanova, A., Jetten, M. S. M., van der Drift, C., and Op den Camp, H. J. M. (2002), *Biochem. Biophys. Acta* **1574,** 293–303.
27. Hays, W. S., Jenison, S. A., Yamada, T., Pastuszyn, A., and Glew, R. H. (1996), *Biochem. J.* **319,** 829–837.
28. Inoue, M., Shibuya, M., Yamamoto, K., and Ebizuka, Y. (1996), *FEBS Lett.* **389,** 273–277.
29. Gräbnitz, F., Seiss, M., Rücknagel, K. P., and Staudenbauer, W. L. (1991), *Eur. J. Biochem.* **200,** 301–309.
30. Paavilainen, S., Hellman, J., and Korpela, T. (1993), *Appl. Environ. Microbiol*. **59,** 927–932.
31. Breves, R., Bronnenmeier, K., Wild, N., Lottspeich, F., Staudenbauer, W. L., and Hofemeister, J. (1997), *Appl. Environ. Microbiol*. **63,** 3902–3910.
32. Liebl, W., Gabelsberger, J., and Schleifer, K.-H. (1994), *Mol. Gen. Genet*. **242,** 111–115.
33. Henrissat, B. and Bairoch, A. (1993), *Biochem. J.* **293,** 781–788.
34. Sanz-Aparicio, J., Hermoso, J. A., Martinez-Ripoll, M., Lequerica, J. L., and Polaina, J. (1998), *J. Mol. Biol*. **275,** 491–502.
35. Penttilä , M. E., André, L., Saloheimo, M., Lehtovaara, P., and Knowles, J. K. C. (1987), *Yeast* **3,** 175–185.
36. Penttilä, M. E., André, L., Lehtovaara, P., Bailey, M., Teeri, T. T., and Knowles, J. K. C. (1988), *Gene* **63,** 103–112.
37. Cummings, C. and Fowler, T. (1996), *Curr. Genet.* **29,** 227–233.
38. Li, X.-L. and Ljungdahl, L. G. (1996), *Appl. Environ. Microbiol*. **62,** 209–213.
39. Rothstein, S. J., Lanhners, K. N., Lazarus, C. M., Baulcombe, D. C., and Gatenby, A. A. (1987), *Gene* **55,** 353–356.
40. van Rensburg, P., Van Zyl, W. H., and Pretorius, I. S. (1998), *Yeast* **14,** 67–76.
41. Ngsee, J. K., Hansen, W., Walter, P., and Smith, M. (1989), *Mol. Cell. Biol*. **9,** 3400–3410.
42. Orlean, P., Kuranda, M. J., and Albright, C. F. (1991), *Methods Enzymol*. **194,** 682–696.
43. Herbaud, M. and Fevre, M. (1990), *Appl. Environ. Microbiol*. **56,** 3164–3169.
44. Teunissen, M. J., Lahaye, D. H. T. P., Huis In't Veld, J. H. J., and Vogels, G. D. (1992), *Arch. Microbiol*. **158,** 276–281.
45. Li, X.-L. and Calza, R. E. (1991), *Enzyme Microb. Technol.* **13,** 622–628.
46. Li, X.-L. and Calza, R. E. (1991), *Biochem. Biophys. Acta* **1080,** 148–154.

47. Ward, M. (1989), in *EMBO-ALKO Workshop on Molecular Biology of Filamentous Fungi*, Nevalainen, H. and Pentillä, M., eds., Foundation for Biotechnical and Industrial Fermentation Research, Espoo, Finland, pp. 119–128.
48. Archer, D. B. and Peberdy, J. F. (1997), *Crit. Rev. Biotechnol*. **17,** 273–306.
49. Ohmiya, K., Shirai, M., Kurachi, Y., and Shimizi, S. (1985), *J. Bacteriol*. **161,** 432–434.

0273-2289/04/113/0251–0259/$25.00

Characterization and Performance of Immobilized Amylase and Cellulase

Bradley A. Saville,* Mikhail Khavkine, Gayathri Seetharam, Behzad Marandi, and Yong-Li Zuo

Department of Chemical Engineering and Applied Chemistry, University of Toronto, 200 College Street, Toronto, Ontario, Canada M5S 3E5, E-mail: saville@chem-eng.utoronto.ca

Abstract

The performance of cellulase and amylase immobilized on siliceous supports was investigated. Enzyme uptake onto the support depended on the enzyme source and immobilization conditions. For amylase, the uptake ranged between 20 and 60%, and for cellulase, 7–10%. Immobilized amylase performance was assessed by batch kinetics in 100–300 g/L of corn flour at 65°C. Depending on the substrate and enzyme loading, between 40 and 60% starch conversion was obtained. Immobilized amylase was more stable than soluble amylase. Enzyme samples were preincubated in a water bath at various temperatures, then tested for activity. At 105°C, soluble amylase lost ~55% of its activity, compared with ~30% loss for immobilized amylase. The performance of immobilized cellulase was evaluated from batch kinetics in 10 g/L of substrate (shredded wastepaper) at 55°C. Significant hydrolysis of the wastepaper was also observed, indicating that immobilization does not preclude access to and hydrolysis of insoluble cellulose.

Index Entries: Amylase; cellulase; immobilization; inactivation; wastepaper.

Introduction

Enzymes such as "cellulases" and α-amylases are currently used by several industries to hydrolyze cellulose or starch to products such as dextrins, syrups, and sugars. Such reactions represent the key first step toward the production of a variety of useful chemicals and sweeteners and are also useful in the pulp and paper industry for fiber modification and de-inking.

*Author to whom all correspondence and reprint requests should be addressed.

α-Amylases hydrolyze starch by cleaving the internal α-1,4-glucosidic bonds, producing polysaccharides that may be further converted by glucoamylases to produce sugars that can be utilized during fermentations. The conventional enzymatic starch hydrolysis process consists of two steps—liquefaction and saccharification—both of which are carried out at high temperatures. However, soluble α-amylases are easily inactivated at higher temperatures and longer reaction durations. Furthermore, these enzymes are inhibited by products generated during hydrolysis.

Enzyme immobilization has been reported to improve the thermal stability of enzymes *(1,2)* and may also affect binding of substrates and inhibitors to the enzyme, thereby affecting the Michaelis constant and enzyme inhibition. Several previous studies have considered the advantages of immobilized enzymes with soluble substrates, and a few studies have also investigated the properties of immobilized enzymes with insoluble substrates. The main objective of the present work was to establish the effect of immobilization on the thermal stability of these enzymes, so that they may be used at elevated temperatures without significant activity loss. The immobilization conditions were varied, and their effect on the performance of the immobilized enzymes was analyzed with reference to their physiochemical and structural properties.

Materials and Methods

Immobilization

Enzymes were immobilized onto silica gel by covalent crosslinking with glutaraldehyde in a procedure similar to that of Kondo et al. (3). Briefly, 1–4 g of silica gel was incubated in 1–13 wt% glutaraldehyde and in 100–1000 mL of enzyme solution for up to 48 h. The immobilized enzyme was recovered by filtration and washed to remove loosely bound enzyme. Samples of the soluble enzyme were collected before and after immobilization and assayed for activity, to provide an estimate of enzyme uptake onto the support. The α-amylases studied were Spezyme Fred® (Genencor), Allyzme® (Alltech), and Liquozyme® (Novozymes). The cellulases studied were Spezyme CP® and Spezyme CE® (Genencor).

Enzyme Uptake

For enzyme uptake studies, 0.1 g of substrate (corn flour or carboxymethylcellulose) and 24 mL of buffer were added to a 40-mL jacketed reactor. The temperature was maintained at 52 ± 2°C using a water bath. A 1.5-mL "blank" sample was collected from the reaction mixture and added to 3 mL of the dinitrosalicylic acid (DNS) reagent. Then 500 µL of the soluble enzyme was added to the reactor to initiate the reaction. Samples were collected every 3 min, and the DNS assay *(4)* was performed for all the samples. One unit of enzyme releases 1 µmol of reducing groups/min, the absorbance of which can be measured at 540 nm. Thus, the amount of activity transferred to the support can be determined from the sugar pro-

duction rates observed with enzyme solutions collected before (t = 0 h) and after the immobilization step. The fraction of residual enzyme (R) is defined as follows:

$$R = \frac{\text{µmol of glucosidic linkages hydrolyzed/min from sample after immobilization}}{\text{µmol of glucosidic linkages hydrolyzed/min from sample after 0 h}}$$

Therefore, the immobilization yield, or fraction of enzyme activity that was transferred to the support, Y_i, would equal $(1 - R)$. For these experiments, the uptake was determined via a point-by-point comparison of absorbance values from the "before" and "after" samples.

Amylase Assay

Kinetics studies were conducted at 65 ± 1°C in a jacketed batch reactor. Five hundred milliliters or 1 L of buffer was added to the reactor and heated to the assay temperature. The buffer pH was chosen according to the optima specified by the enzyme manufacturers. Corn flour (100–300 g/L) was then added to the reactor, along with a specified quantity of either soluble or immobilized amylase to initiate hydrolysis. Samples were collected at regular intervals over 30–60 min, and centrifuged to separate solids. The supernatant was analyzed for sugar content by measuring the %Brix with an optical refractometer.

Cellulase Assay

Kinetics studies were conducted at 55°C in a jacketed batch reactor. Shredded wastepaper (10 g/L) was added to 500 mL or 1 L of citrate buffer, pH 4.8, and heated to the assay temperature. A specified quantity of either soluble or immobilized cellulase was added to the reactor to initiate hydrolysis. Samples were collected at regular intervals over 30–60 min, and centrifuged to separate solids. The DNS assay (4) was used to detect sugars formed during hydrolysis experiments. The supernatant from the centrifuge tube and the DNS solution were mixed and cooked for exactly 5 min in boiling water. Finally, the sample was transferred to a methacrylate cuvet, and its absorbance was measured at 540 nm.

Thermal Stability of Amylase

Enzyme samples were added to test tubes and heated at a controlled temperature before conducting a standard activity assay. Samples were incubated either in boiling water for 15 min, or in a constant-temperature bath at 65, 85, or 105°C for 15 min. Samples were then cooled to room temperature and tested for activity at 65°C using the standard assay outlined above. To determine whether the substrate offered protection against thermoinactivation, another set of trials was conducted in which 0.5 g of corn was added to the enzyme during the preincubation period. The enzyme was then cooled and assayed for activity at 65°C, as outlined above. In these experiments, samples were incubated in a silicone oil bath at either 85, 105, or 125°C.

Modeling of Amylase Kinetics

%Brix values were converted to product concentrations (g/L) using maltose as a standard. Although it is extremely likely that we had a distribution of mono-, di-, and polysaccharides, we simply used a total sugars concentration for kinetics modeling at this point. Various mathematical forms were tested in an effort to represent the inhibitory effect of product on reaction rate; however, the form recommended by Lim et al. (2) (Eq. 1) provided the best overall fit to the data.

Product concentrations at each time point during the kinetics experiment were estimated by numerical integration of the following equations:

$$dP/dt = \left[V_{\max} S/\left(S + K_m\right)\right]\left[e^{\left(-K_I \cdot P\right)}\right] \quad (1)$$

$$S = S_0 - P \cdot n \quad (2)$$

in which S_0 is the initial substrate concentration (g/L), P is the product concentration (g/L), $V_{\max}$ is the maximum reaction velocity (g/[L·min]), K_m is the Michaelis constant (g/L), K_I is a constant that accounts for product-mediated inhibition (L/g), and n is the fraction of starch in the corn flour. Values of the unknown parameters ($V_{\max}$, K_m, and K_I) were estimated by nonlinear regression of the predicted product concentrations vs experimental data, using E-Z Solve software. Because of cross-correlation between parameters, and the fact that experiments were not conducted over a wide range of substrate concentrations, the model fit was relatively insensitive to K_m values.

Results and Discussion

The enzyme uptake varied significantly according to the enzyme source, type, loading, and incubation time. The typical uptake for amylase ranged between 20 and 60%, whereas for cellulase, only 7–10% uptake was obtained. Since these uptake measurements simply reflect losses in soluble enzyme activity from the immobilization solution, they set a maximum on the activity that may be expressed by the immobilized enzyme. The actual activity is expected to be less, once losses resulting from shear, conformational changes, and nonproductive binding are taken into account. Direct measurements of immobilized enzyme activity therefore provide the best measure of the effectiveness of a particular immobilization technique.

A typical profile for starch hydrolysis using soluble amylase is shown in Fig. 1. The profile predicted by the kinetics model is also shown. Clearly, the model describes the experimental concentration profiles very well. The model curves also show the insensitivity of the model fit to K_m; there is very little difference in the quality of the model predictions with K_m = 5 g/L and K_m = 50 g/L. Similarly, a typical profile for starch hydrolysis using immobilized amylase is shown in Fig. 2. The model also predicts these data very well, with little sensitivity to the K_m value.

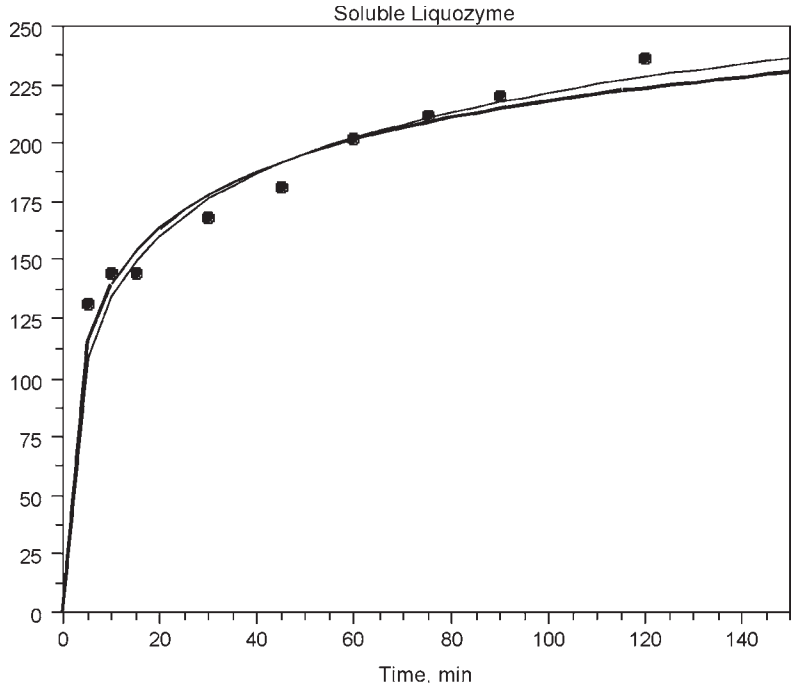

Fig. 1. Kinetics of starch hydrolysis with soluble liquozyme. V_{max} = 122 g/(L·min); K_I = 0.026 L/g; (—) K_m = 50; (– – –) K_m = 5; (●) experimental data.

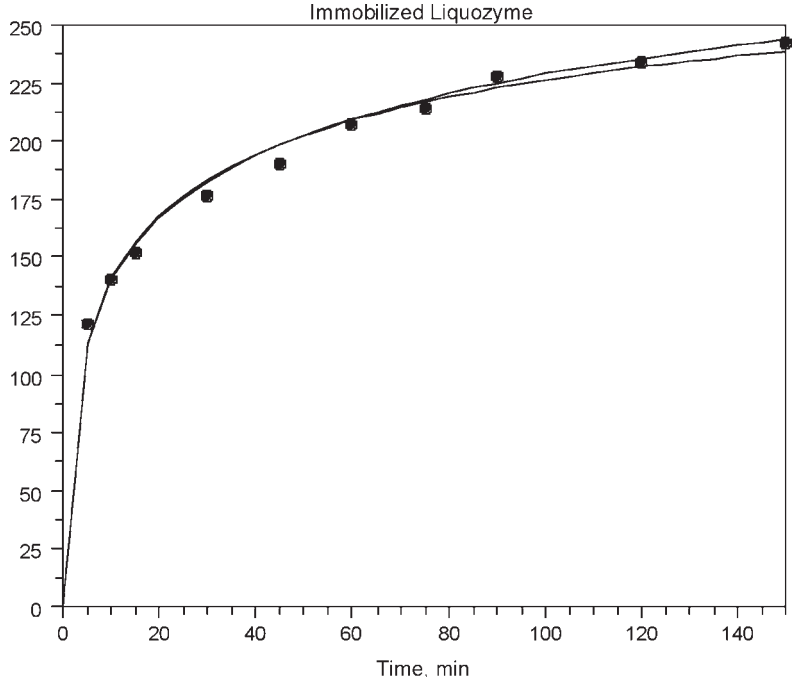

Fig. 2. Kinetics of starch hydrolysis with immobilized liquozyme. V_{max} = 144 g/(L·min); K_I = 0.023 L/g; (—) K_m = 50; (– – –) K_m = 5; (●) experimental data.

Table 1
Kinetics Parameters for Soluble and Immobilized Amylases

Enzyme	Quantity	pH	T (°C)	V_m	K_m	K_I
Soluble Allzyme	334.0 µL	5.5	65	93.0	50	0.026
Immobilized Allzyme	6.1 g	5.5	65	72.0	50	0.021
Soluble Spezyme Fred	334.0 µL	6.8	65	279.0	50	0.043
Immobilized Spezyme Fred	6.0 g	6.8	65	46.8	50	0.031
Immobilized Spezyme Fred	6.0 g	6.8	67	47.1	50	0.030
Immobilized Spezyme Fred	8.0 g	6.9	66	53.1	50	0.032
Soluble Liquozyme	334.0 µL	5.5	66	168.0	50	0.027
Immobilized Liquozyme	4.5 g	5.5	66	86.1	50	0.023
Immobilized Liquozyme	3.0 g	5.5	65	60.6	50	0.024
Immobilized Liquozyme	6.0 g	5.6	66	118.0	50	0.024

Table 1 summarizes the parameters obtained from the kinetics modeling. The modeling results indicate that soluble Spezyme Fred is more active than soluble Allzyme or Liquozyme, but Allzyme and Liquozyme are less sensitive to product inhibition. The V_{max} values for immobilized Liquozyme are greater than those for immobilized Fred or Allzyme, indicating that Liquozyme is more amenable to immobilization and provides better performance. Furthermore, the immobilized forms of enzyme, particularly Spezyme Fred, are less subject to product inhibition than the soluble forms, as demonstrated by a reduction in K_I. It is also useful to note that for immobilized Liquozyme, values of V_{max} are approximately proportional to the enzyme loading. Such scaling was not observed with immobilized Spezyme Fred, possibly indicating limitations in substrate access to this form of the enzyme.

The relative activities of the soluble and immobilized amylases were compared based on the values of V_{max}, accounting for the enzyme uptake and loading onto the support. Depending on the immobilization conditions and source of amylase, the immobilized enzyme possessed from 1 to 4% of the activity of its soluble counterpart.

It is difficult to compare directly the immobilized amylase activities (i.e., V_{max} and K_m) observed in these studies with values obtained by other researchers, owing to the fact that we used industrial corn flour as the substrate, whereas others used an activity assay based on soluble starch *(5–9)*. Moreover, the substrate concentrations used in our studies (100–300 g/L) are high enough to facilitate gelatinization, and the reaction takes place with the substrate present as a slurry. By contrast, the starch assays are typically based on a substrate concentration of ~10–20 g/L *(5–7,9)*, low enough to completely dissolve the substrate.

Aksoy et al. *(9)* did observe a 12-fold increase in K_m on immobilization to polymethacrylic acid microspheres and noted that the immobilized

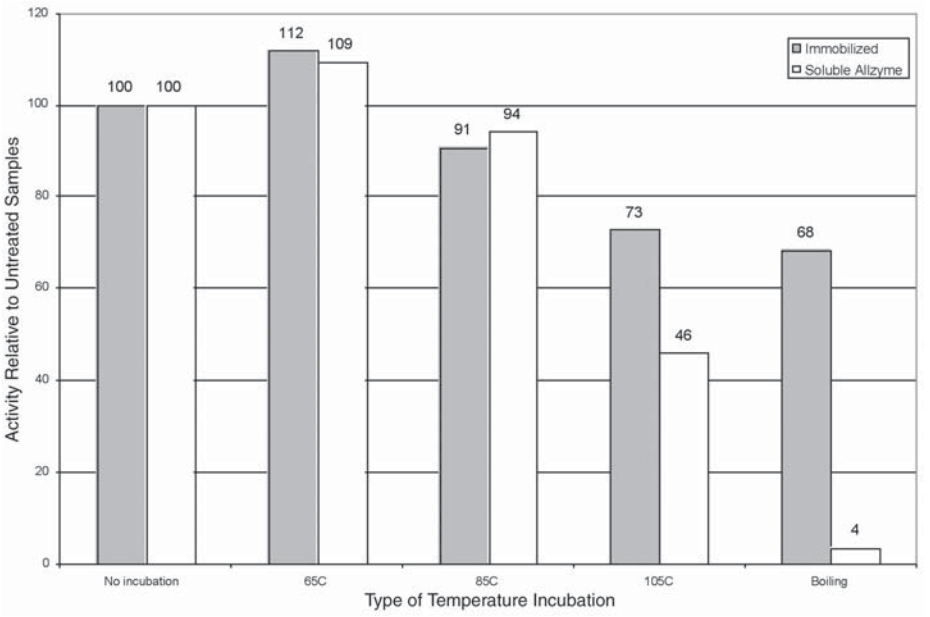

Fig. 3. Effect of temperature on activity of soluble and immobilized Allzyme®.

forms possessed between 68 and 80% of the activity of the soluble enzyme, depending on the coupling method used. Ju et al. *(7)* observed a 5% activity yield for α-amylase immobilized onto cellulose-based hollow fibers.

Figure 3 illustrates that immobilized amylase is more thermostable than its soluble counterpart. There was little difference between soluble and immobilized Allzyme following preincubation at either 65 or 85°C. However, after incubation for 15 min at 105°C, immobilized Allzyme lost ~30% of its activity, compared with ~55% activity loss for soluble Allzyme. Furthermore, after boiling for 15 min., immobilized Allzyme retained about 70% of its activity, whereas the soluble form was almost completely deactivated.

For comparison, Arasaratnam and Balasubramanian *(8)* showed that coupling praline with α-amylase during immobilization to Sepharose 4-B could increase the thermal stability of the enzyme without adversely affecting the activity of amylase (based on comparison of amylase activity following immobilization without proline). Sadhukhan et al. *(6)* observed that immobilization of α-amylase onto Sepharose, alginate beads, and polyacrylamide gels could increase the optimum reaction temperature to about 70°C, compared with about 60°C for the soluble form. In thermal stability studies analogous to ours, they observed improved thermal stability on immobilization but still observed about a 40% loss of activity following incubation of the immobilized enzyme for 15 min at 80°C. By contrast, in our studies, only a 5–10% activity loss was observed following incubation at 85°C (Fig. 3).

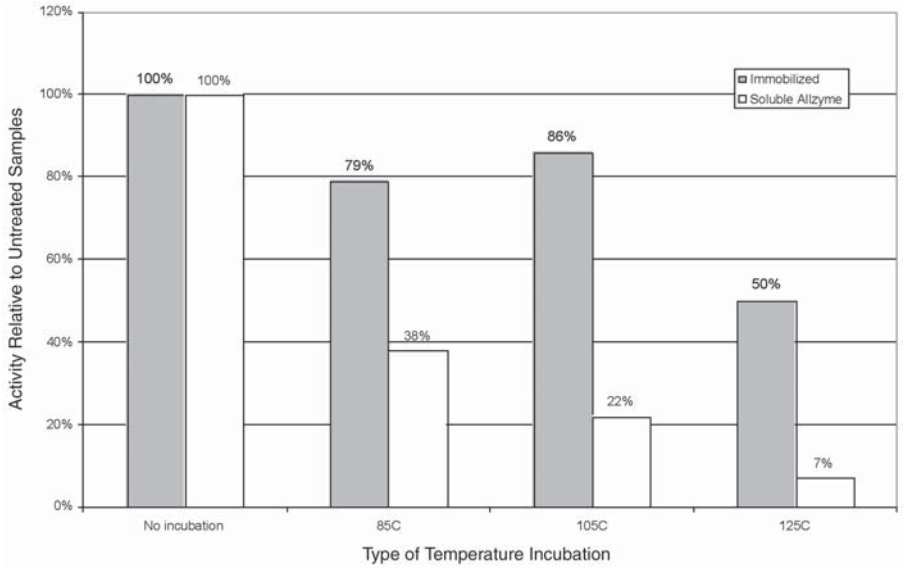

Fig. 4. Effect of substrate preincubation on activity of soluble and immobilized Allzyme®.

Figure 4 illustrates the impact of the substrate on thermal stability. Typically, the substrate is expected to have a protective effect on the enzyme, because the active site is occupied. However, Fig. 4 shows that the substrate can have both positive and negative effects. At all temperatures, incubation of the soluble enzyme with substrate decreased the retained activity of the soluble enzyme. For example, at 85°C, 94% of the original enzyme activity was retained following incubation in buffer (Fig. 3), but only 38% of the original activity was retained when the enzyme was incubated in the presence of substrate (Figure 4). This observation is in contrast to that of Ju et al. *(7)*, who suggested that starch has a stabilizing effect on α-amylase. Perhaps this is owing to differences in the source of the enzyme.

The substrate had little effect on the immobilized enzyme, perhaps a slight deleterious effect at 85°C and a slight protective effect at 105°C. Regardless, the immobilized enzyme was more stable than the soluble form, with or without substrate. This protective effect of immobilization is not surprising, since immobilization can help to distribute the thermal energy imposed on the protein at higher temperatures.

Figure 5 illustrates the performance of immobilized cellulase in comparison with that of soluble cellulase. The small difference between the "crude" and "used" Spezyme CP profiles illustrates the very low uptake of soluble cellulase onto the support. Furthermore, soluble cellulase is much more active; the dose of soluble enzyme is approx one-twentieth that of immobilized cellulase, once enzyme uptake is taken into account. Nonetheless, it is important to note that the immobilized enzyme is able to hydrolyze this insoluble substrate, albeit at a much lower rate.

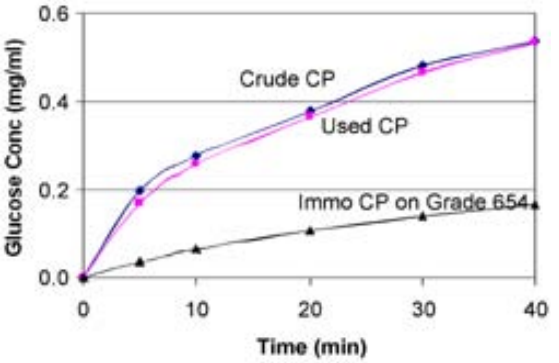

Fig. 5. Comparison of cellulose hydrolysis with soluble and immobilized cellulase. "Crude" and "Used" designations refer to the soluble enzyme collected before and after immobilization, respectively. CP, Spezyme CP.

Conclusions

Immobilized cellulase and amylase are able to hydrolyze cellulose and starch. However, the immobilized enzymes possess only about 1–6% of the activity of the soluble forms. In addition, immobilization clearly enhanced the thermal stability of amylase. Immobilized amylase retained more than half of its activity, even after incubation at 125°C. By comparison, soluble amylase was almost completely inactivated under these conditions. Furthermore, kinetics modeling indicates that the susceptibility to product inhibition is dependent on the amylase source. Finally, immobilization can reduce the susceptibility to product inhibition; K_I was less for each of the immobilized forms, compared with their soluble counterparts.

Acknowledgments

We thank Alltech, Genencor, and Novozymes for provision of enzyme samples. We also gratefully acknowledge funding from Advanced Biochemical and the University of Toronto (fellowship to Y.-L. Z.).

References

1. Wiseman, A. (1994), *Chem BR* **30(7),** 571–573.
2. Lim, L. H., Macdonald, D. G., and Hill, G. A. (2003), *J. Biochem. Eng*. **13,** 53–62.
3. Kondo, A., Urabe, T., and Higashitani, K. (1994), *J. Ferment. Bioeng*. **77(6),** 700–703.
4. Miller, G. (1959), *Anal. Chem*. **31,** 426–428.
5. Yang, Y. and Chase, H. A. (1998), *Biotechnol. Appl. Biochem*. **28,** 145–154.
6. Sadhukhan, R., Roy, S. K., and Chakrabarty, S. L. (1993), *Enzyme Microb. Technol*. **15,** 801–804.
7. Ju, Y-H., Chen, W-J, and Lee, C-K. (1995), *Enzyme Microb. Technol*. **17,** 685–688.
8. Arasaratnam, V. and Balasubramanian, K. (1995), *Proc. Biochem*. **30(4),** 299–303.
9. Aksoy, S., Tumturk, H., and Hasirci, N. (1998), *J. Biotechnol*. **60,** 37–46.

0273-2289/04/113/0261–0272/$25.00

Immobilized Enzyme Studies in a Microscale Bioreactor

Francis Jones,[1] Scott Forrest,[2] Jim Palmer,[2] Zonghuan Lu,[2] John Elmore,[2] and Bill B. Elmore*,[2]

[1]Chemical and Environmental Engineering, The University of Tennessee at Chattanooga, 615 MacCallie Avenue, Chattanooga, TN 37403-2598; and [2]Department of Chemical Engineering, Louisiana Tech University, 600 W. Arizona Avenue, Ruston, LA 71272, E-mail: belmore@coes.latech.edu

Abstract

Novel microreactors with immobilized enzymes were fabricated using both silicon and polymer-based microfabrication techniques. The effectiveness of these reactors was examined along with their behavior over time. Urease enzyme was successfully incorporated into microchannels of a polymeric matrix of polydimethylsiloxane and through layer-bylayer self-assembly techniques onto silicon. The fabricated microchannels had cross-sectional dimensions ranging from tens to hundreds of micrometers in width and height. The experimental results for continuous-flow microreactors are reported for the conversion of urea to ammonia by urease enzyme. Urea conversions of >90% were observed.

Index Entries: Microscale bioreactor; polydimethylsiloxane microreactor; immobilized enzymes; urease enzyme; silicon wafer.

Introduction

The field of chemical process miniaturization is growing at a rapid pace with promising improvements in process control, product quality, and safety, *(1,2)*. Microreactors typically have fluidic conduits or channels on the order of tens to hundreds of micrometers. With large surface area–to–volume ratios, rapid heat and mass transfer can be accomplished with accompanying improvements in yield and selectivity in reactive systems. Microscale devices are also being examined as a platform for traditional unit operations such as membrane reactors in which a rapid removal of reaction-inhibiting products can significantly boost product yields *(3–6)*.

*Author to whom all correspondence and reprint requests should be addressed.

While microscale devices and systems are typically fabricated from silicon, alternative materials are being examined as suitable supports. Microsystem features as small as 1 μm may be fabricated precisely by using a variety of etching, molding, and milling techniques. Since enzymatic reactions typically occur at moderate operating conditions (moderate pressures and ambient temperatures), plastics may be considered an inexpensive alternative to silicon for use as microreactor fabrication material.

In this article, we report on the fabrication and performance of microreactors constructed of silicon and polydimethylsiloxane (PDMS). The resulting structures contain immobilized enzymes for converting biochemical substrates to useful products or for breaking down organics into waste streams.

Materials and Methods

Materials Used

Urease (EC 3.5.1.5 Type IX, Sigma-Aldrich: from Jack Beans) was used throughout the experiments. Before immobilizing urease onto the microreactor systems, the enzyme was evaluated for activity in the chosen buffer system (Tris[hydroxymethyl]aminomethane [THAM]). Free enzyme tests of the urease showed an approximate activity of 44,800 U/g of solid.

Batch studies for evaluating immobilized enzyme activity and properties of the "bioplastic" (urease entrapped in PDMS) material were conducted in 250-mL shake flasks in an environmentally controlled shaker/incubator.

Continuous studies were performed in specially prepared microreactors molded from PDMS, designated PDMS (Sylgard™ 184 silicone elastomer; Dow Corning) poured onto silicon wafer molds. The microreactor molds were prepared using 4-in. silicon wafers of Type P, crystal orientation of <1-0-0>, resistivity of 1 to 2 Ω, and thickness of 457–575 μm from Silicon Quest (Santa Clara, CA). After preparation, mixtures of urease enzyme and PDMS (designated PDMS-E) were poured onto the microreactor mold and allowed to cure at ambient conditions.

A negative photoresist, SU-8 (Microchem), was used in the microreactor mold process for preparing the PDSM-E microreactors. When exposed to ultraviolet light, material may be removed via a wet etching process leaving high-definition features in micrometer dimensions. Additionally, a microreactor has been constructed in silicon onto which layer-bylayer self-assembled polyelectrolytes and enzymes are deposited. This system is being used for comparison with the PDMS-E system performance.

Scanning electron microscopy (SEM) images were taken with an AMRAY, 1800 series scanning electron microscope having a resolution of 0.2 μm. All objects in this work, except the silicon wafer microreactor, were first sputtered with a nickel layer a few nanometers thick in order to obtain an SEM image.

Preparation of Biomaterial and Layer-by-Layer Self-Assembly

The combination of PDMS and urease enzyme to form a microreactor from the resulting "bioplastic" material (PDMS-E) has been reported previously *(7)*. When enzyme concentrations were maintained at 2.5% (w/w) or less, the resulting microreactor cured with good structural integrity and high definition (e.g., well-formed microchannels and >90% retention of triangular transverse packing features in the microchannels).

For enzyme attachment to the silicon microreactor tested, a layer-by-layer technique was employed to build a multilayer system of polyions and enzyme. Deposition of multilayers was accomplished by alternating positively and negatively charged layers of polydimethyldiallyl ammonium chloride (PDDA) and polystyrene sulfonate (PSS), respectively, to which was attached urease enzyme. After depositing in succession three layers of PDDA, PSS, and PDDA, three layers of urease enzyme were alternately deposited with three layers of PDDA. The resulting architecture is described as follows:

$$PDDA/PSS/PDDA + (UR/PDDA)_3$$

Batch Studies for Evaluating Enzyme Immobilization and Pdms-E Characteristics

To assess the enzymatic activity of the PDMS-E complex, "nonstructural" PDMS preparations with various enzyme fractions were prepared and cured in glass petri dishes. On curing, these preparations were removed and cut into cubes nominally 3 mm on a side. Equal weights of these cubes (~10 g/reactor) were placed in 250-mL shake flasks. A 150-mL preparation of 0.1 mol/L THAM buffer solution containing 0.1 mol/L of urea was placed in each of three flasks. The pH of the buffer/urea medium was adjusted to 7.5 by the addition of HCl. Shake flasks were placed on a shaker incubator at 25°C and 200 rpm. Sample volumes of 2 mL were removed periodically for ammonia analysis. Additionally, swelling studies were conducted by periodically removing PDMS-E cubes from the urea solution, removing surface water, and weighing to assess the degree of water adsorption by the biopolymer *(8)*.

Microreactor Fabrication

PDMS-E microreactor

The devices employed in this work were fabricated using silicon wafers as either microreactors or molds for the PDMS-E. The silicon wafers were treated by standard photolithographic techniques to form the desired features. Process steps to fabricate micromolds have been presented elsewhere *(8)*. Figure 1 depicts a PDMS-E microreactor after curing on a silicon wafer mold. Figure 2 shows an SEM micrograph of a portion of the microchannel with triangular features fixed within the channel. PDMS-E microreactors were fabricated in 50-, 500-, and 1000-mm lengths to study

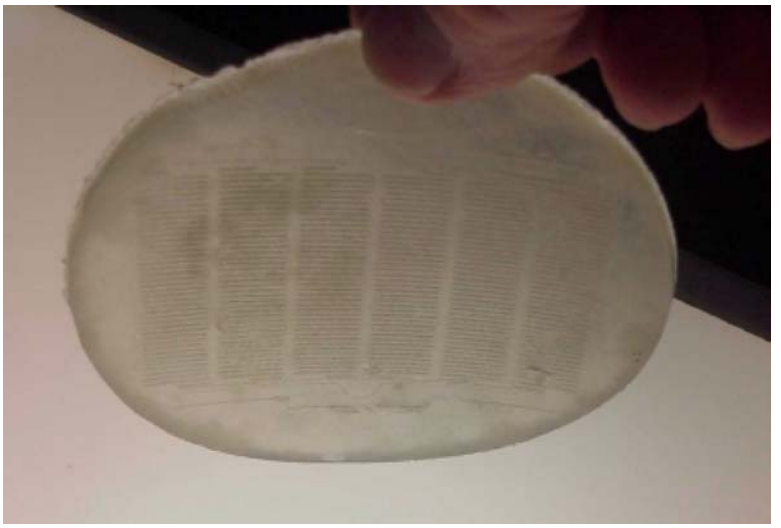

Fig. 1. PDMS-E microreactor containing 1.7 wt% urease.

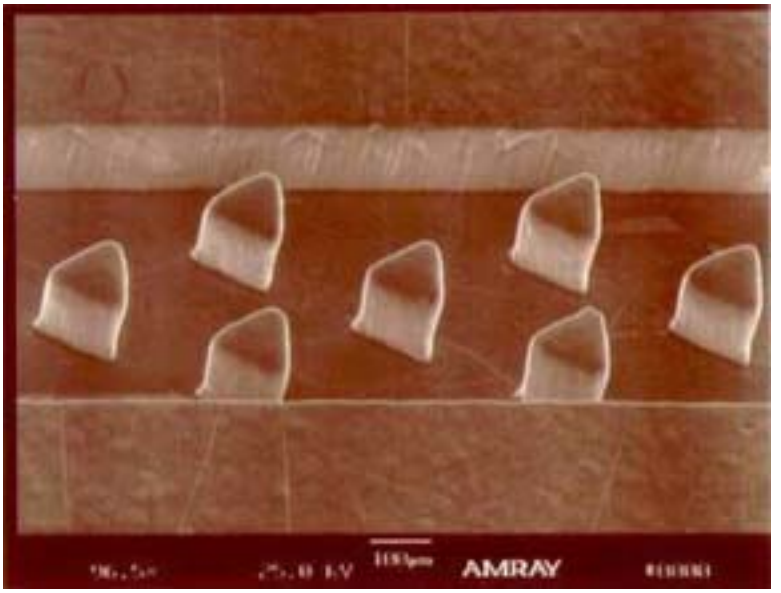

Fig. 2. SEM micrograph of portion of the microchannel with triangular features.

performance characteristics. Table 1 gives the various dimensions and operating conditions under study. Each microreactor enzyme loading was tested at various flow rates. Mean residence times were calculated taking into account the volume occupied by the triangular mixing features.

Table 1
Dimensions and Operating Conditions of PDMS-E Microreactor

Reactor Description	Channel width (μm)/length (mm)	Per channel volume (mm^3)/surface area (mm^2)	Enzyme "loading" g"E"/g PDMS	Urea Feed Solution	
				Flow rate (mL/min)	Mean residence time (min)
1a Six channels (with triangular transverse features)	500/50	2.67/48.3	0.25	0.060	0.27
			0.50	0.006	2.67
			0.75	0.001	16.01
2a Six channels (with triangular transverse features)	500/500	27.7/484.8	0.25	0.060	2.77
			0.25	0.023	7.28
			0.50	0.006	27.65
			0.50	0.001	165.56
3a Six channels (with triangular transverse features)	500/1000	55.4/970	0.25	0.048	6.92
			0.50	0.023	14.56
			0.75	0.006	27.65

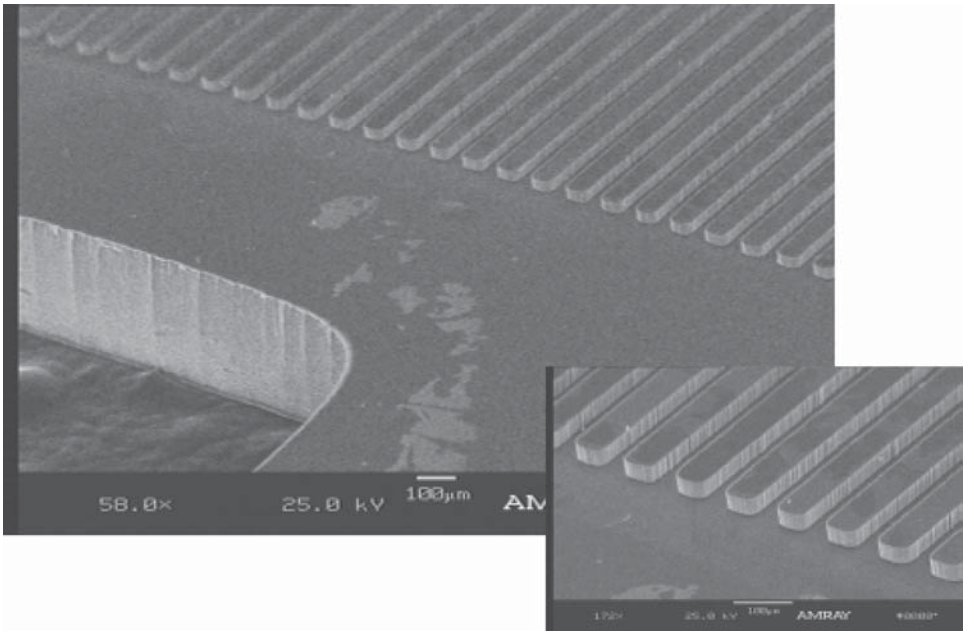

Fig. 3. Silicon wafer microreactor.

Silicon Wafer–Based Microreactor

For comparison of performance, a microreactor was constructed by directly etching microchannels into a silicon wafer using standard lithographic processes. An emulsion mask of the design template was produced using a high-resolution printer and transferred to a chrome mask for alignment and exposure steps. The design was transferred to a <1,0,0> silicon wafer using positive photoresist. The channels were then etched via inductive coupled plasma utilizing the Bosch process that allows microscale perpendicular walls to be fabricated with high aspect ratios (i.e., height/width ratios). Figure 3 shows a portion of the silicon wafer microreactor, and the dimensions for the microreactor are given in Table 2. The experimental system is shown in Fig. 4. Syringe pumps are used to create a precise, slow, and repeatable flow. Direct comparison of this microreactor configuration with the PDMS-E microreactor is the emerging focus of this project for both reactor performance and process economics.

Biochemical Reaction and Microreactor Testing Systems

Urease converts urea to ammonia and carbon dioxide by the following reaction:

$$NH_2CONH_2 + H_2O \text{ g } 2NH_3 + CO_2$$

For the urease enzyme system, a reactant solution of 0.1 mol/L of urea was fed to the microreactors by Cole Parmer Series 74900 Syringe pumps.

Table 2
Characteristics of Silicon Wafer Microreactor

Length	2.7 cm
Width	0.5 cm
Channel width	50.0 µm
Channel depth	100.0 µm
Number of channels	98

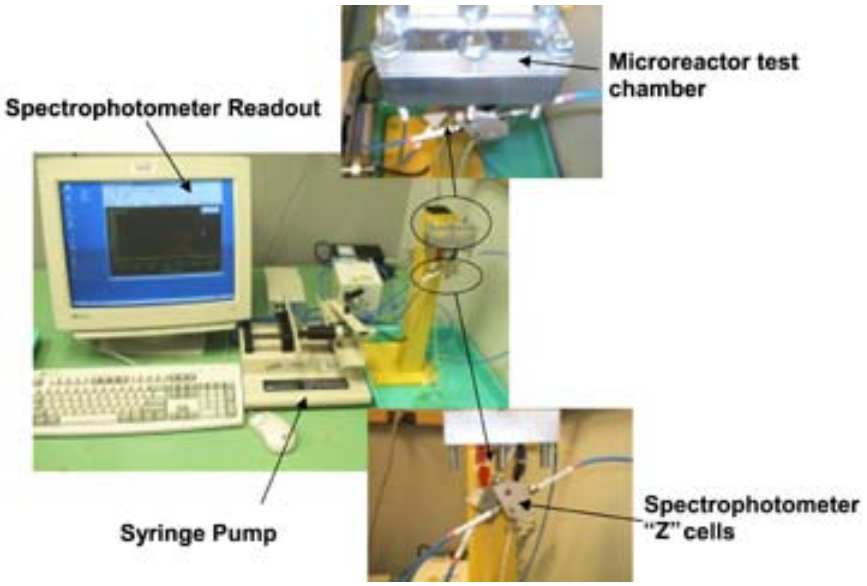

Fig. 4. Experimental setup for testing silicon wafer microreactors.

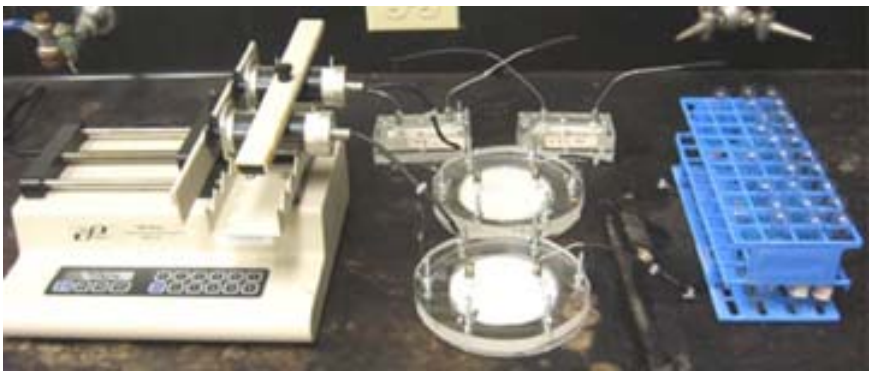

Fig. 5. Experimental setup for testing PDMS-E microreactors.

The experimental setup for the PDMS-E microreactor system is shown in Fig. 5. Reactor effluent was analyzed by a Hewlett Packard 1100 HPLC (UV-Vis detector) and an Ocean Optics SD 2000 UV-Vis Spectrometer with fiberoptic flow analysis "Z" cells (FIA Lab).

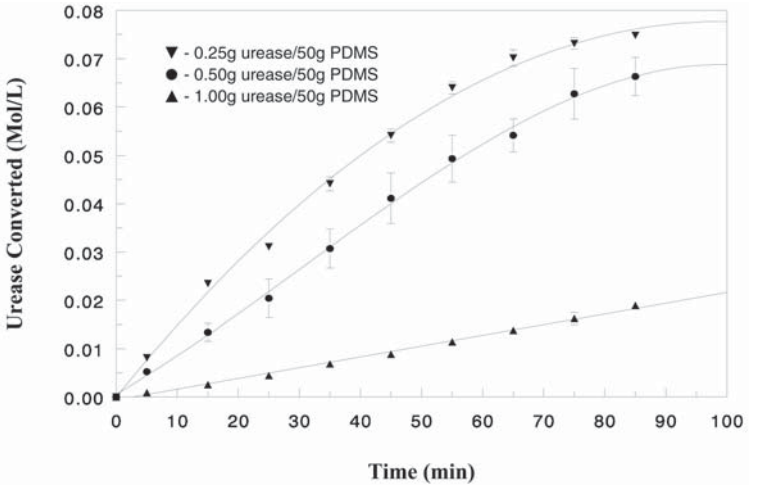

Fig. 6. Urea conversions for various enzyme loadings in PDMS in batch reactors.

Results and Discussion

Batch Studies

A series of batch studies was run to test the biomaterial made from urease entrapped in PDMS. Quantities of urease (0.25, 0.50, and 1.00 g, respectively) were each mixed with separate 50-g quantities of PDMS elastomer. Once cured at ambient conditions (25°C, atmospheric pressure), the resulting bioplastic was cut into sections (nominal 3-mm cubes) and added in 10-g quantities to separate 250-mL flasks containing 0.01 *M* urea solution (in THAM buffer at pH ~7.4). Urea conversion and pH were monitored with time. Figure 6 shows initial rates of urea conversion as a function of time. For each data set, flasks were run in triplicate and results were averaged. Error bars are shown for 1 SD from the mean. For the higher enzyme concentration, the pH approached a value of 9.0 in approx 55 min, at which level urease enzyme activity has been shown to be inhibited *(8–9)*. Here, as our batch systems approached this pH value (9.0), a noticeable decrease in reaction rate was observed. Thus, the decline in activity is most likely attributable to pH effects. The increase in the rate of urea conversion was observed to be significant for increased enzyme loadings. The initial reaction rates were calculated to be 0.2, 0.8, and 0.9 mmol/(L·min) for the 0.25-, 0.50-, and 1.00-g enzyme loading, respectively. These rates are in the range of those reported for various urease immobilization techniques *(10–12)*.

Continuous-Flow Studies

The PDMS-E described in the batch studies was used to mold reactors. These microreactors were fed the same 0.1 *M* urea solution as used in batch experiments. Reactors were operated for approx 1 h before acquiring operational data to reduce the effects of any loosely bound enzymes that may wash out from the surfaces of the microchannel walls.

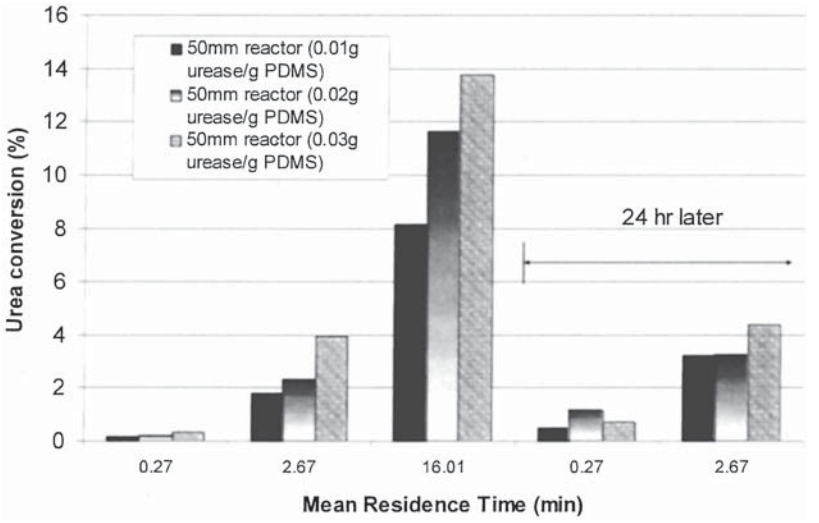

Fig. 7. Effect of enzyme loading on conversion in 50-mm PDMS-E continuous-flow reactors.

The shallow depth of the channels (125 μm in the PDMS-E microreactors and 100 μm in the silicon wafer microreactor) provides for very short reactant diffusion lengths. This is one of the great advantages of microscale reactors. Small cross-channel dimensions also induce laminar flow. All experimental flows in this study had Reynolds numbers below 1.0.

Residence Time and Enzyme Loading

Figures 7 and 8 show conversions in PDMS-E microreactors having 50- and 500-mm channel lengths. In Fig. 7, microreactors with a 50-mm channel length and three different enzyme loadings (0.01, 0.02, and 0.03 g of urease/g of PDMS, respectively) were operated with three different flow rates each (shown as residence time on the *x*-axis) during a 48-h period. In the first 24 h, the microreactor systems showed an increase in urease conversion both with higher residence times and with higher enzyme loadings, supporting the idea of increased enzyme availability in the cured polymeric microstructure. However, during a second 24-h period a significant decline in enzyme activity was noted. While inconclusive, the relative comparison among the three enzyme loadings during the second 24-h period points to a combination of enzyme inactivation and possible detachment of the additional enzyme initially incorporated into the PDMS polymer matrix accompanying the observed decline in enzyme activity. Additional testing is under way to ascertain the potential for enzyme detachment and residual activity in the microreactor effluent. Figure 8 shows a comparison of 50- and 500-mm channel length microreactors for an enzyme loading of 0.01 g of urease/g of PDMS elastomer. To highlight

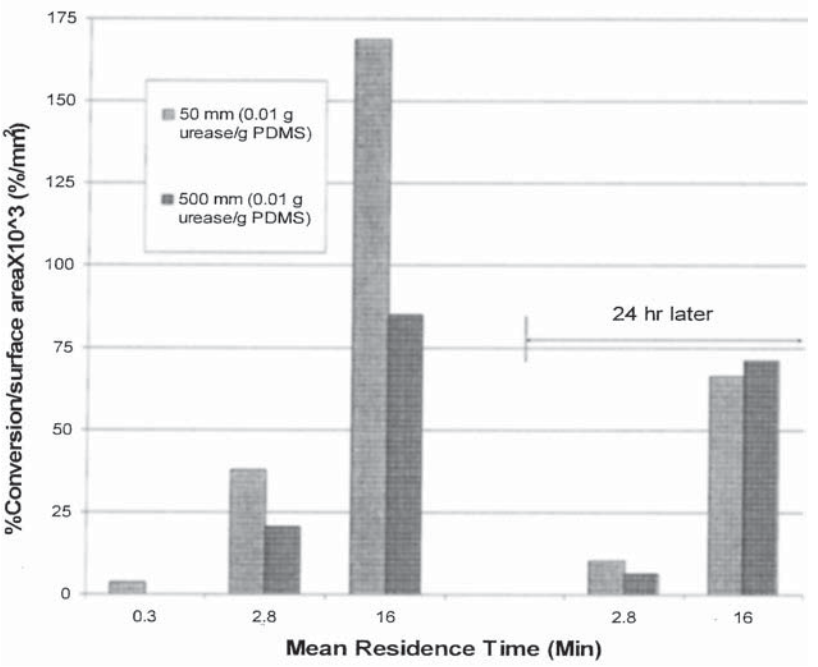

Fig. 8. Effect of residence time on conversion in PDMS-E continuous-flow reactors.

reactor efficiency, conversion per unit of reactor surface area (% conversion/mm2) is plotted vs mean residence time. The relative efficiency of both the 50- and 500-mm microchannel reactors is comparable. For a residence time of 16 min, there is an apparently significant increase in the 50-mm microreactor over the 500-mm microreactor. However, at this residence time, the 500-mm microreactor achieved nearly 100% urea conversion, pointing to the possibility that it may have been "underutilized," thereby exhibiting the comparative inefficiency. As in the previous experiment, a decline in reactor performance was observed during the second 24-h period.

Figure 9 illustrates the operation of 1000-mm microchannel length reactors at enzyme loadings of 0.01 and 0.03 g of urease/g of PDMS and at various volumetric flow rates. Flow rates of 0.023 and 0.073 mL/min correspond to mean residence times of 14.55 and 4.55 min, respectively. Data sets are averages for three runs at each condition. Error bars depict 1 SD from the mean. In all cases, a significant decline in reactor activity was observed after initial startup. However, in the case of the microreactor with a loading of 0.03 g of urease/g of PDMS and a flow rate of 0.073 mL/min, virtually 100% conversion was maintained for 6 h with a gradual decline and leveling off at approx 55%. Generally, activity seems to level off at about 50% after about 24 h. This behavior is similar to the decline in enzyme reactivity for other immobilized enzyme systems (*see* e.g. ref *13*).

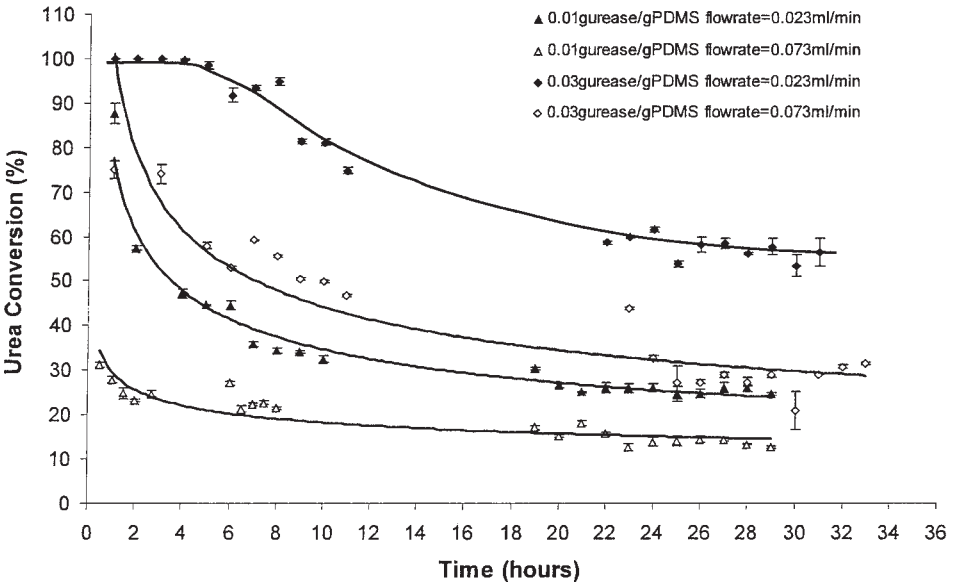

Fig. 9. Effect of time on conversions for 1000-mm PDMS-E continuous-flow reactor with various enzyme loadings.

Silicon Microreactor

While per-unit cost for a silicon wafer microreactor is higher than the PDMS-E microreactor system, silicon-based devices may have significant advantages. Since PDMS is extremely inert, it would be very difficult to attach enzymes to its surface. The layer-by-layer selfassembly techniques to apply enzymes to silicon surfaces allow for a higher population of enzymes on the surface than entrapment can provide. Assuming a cubic array of perfectly mixed enzymes in a PDMS matrix, there are approx 10^{10} enzymes/cm^2 on the surface. For enzymes of about 10 nm in diameter, complete surface coverage is 10^{12} enzymes/cm^2. Enzymes immobilized by self-assembly may also display a greater stability than those entrapped in PDMS. For comparison to the PDMS-E system, an additional study is under way to examine the performance of a silicon wafer–based microreactor to examine both reaction efficiency and longevity of performance. In this system, a technique of layer-by-layer self-assembly *(14–17)* is used for attaching enzymes to the microchannel surface. Preliminary data show high urea conversions after a significant "shelf life." For example, silicon microreactors >1 mo old (stored at 4°C) have exhibited significant enzyme activity. Future reports will describe this work in detail.

Conclusion

Continuous-flow microreactors were successfully fabricated from PDMS and entrapped urease. Conversions increased almost proportion-

ally with an increase in residence time. Conversions increased significantly with enzyme loading. Over a 30-h period of continuous operation, conversions decreased by about half and then leveled off.

Continuous-flow microreactors were successfully fabricated by etching channels in silicon and immobilizing urease onto channel surfaces by a layer-by-layer self-assembly technique. Preliminary results show urea conversion. The potential advantages of this surface-coating technique in microreactors warrant continued investigation.

Acknowledgments

We acknowledge Dr. Yuri Lvov at Louisiana Tech's Institute for Micromanufacturing for assistance in applying layer-by-layer self-assembly techniques. We also wish to thank the Department of Defense (DAAH04-96-1-0200) and the Louisiana Board of Regents (LEQSF [1999-02]-RD-A-24) for their support of this work.

References

1. Srinivasan, R., Hsing, I.-M., Berger, P. E., Jensen, K. F., Firebaugh, S. L., Schmidt, M. A., Harold, M. P., Lerou, J. J., and Ryley, J. (1997), *AIChE J.* **43(11),** 3059–3069.
2. Wegeng, R., Call, C., and Drost, K. (1996), *Chemical System Miniaturization*, PNNL-SA-27317, Pacific Northwest National Laboratory, Richland, WA.
3. Schuth, F. (1995), *Crystallographically Defined Pore Systems: Reaction Vessels with Molecular Dimensions*, Microsystem Technology for Chemical and Biological Microreactors, Max Planc Institute, Mainz, Germany.
4. Zheng, A.-P., Jones, F., Fang, J., and Cui, T. (2000), in *Proceedings of the 4th International Conference on Microreaction Technology (IMRET IV)*, Atlanta, GA, pp. 284–292.
5. Palmer, J., Ramprasad, S., and Forrest, S. (2003), *TexMEMS V*.
6. Palmer, J., Ramprasad, S., and Forrest, S. (2003), in *Proceedings for the AIChE Spring 2003 National Conference*, New Orleans, LA.
7. Laidler, K. J. and Hoare, J. P. J. (1950), *Amer. Chem. Soc.* **72,** 2487–2494.
8. Jones, F., Lu, Z., and Elmore, B. B. (2002), *Appl. Biochem. Biotechnol.* **98–100,** 627–640.
9. Ramachandran, K. B. and Perlmutter, D. D. (1976), *Biotechnol. Bioeng.* **18,** 685–699.
10. Dumitriu, S., Popa, M., Artenie, V., and Dan, F. (1989), *Biotechnol. Bioengin.* **34,** 283–290.
11. Moynihan, H. J., Lee, C. K., Clark, W., and Wang, N. H. L. (1989), *Biotechnol. Bioengin.* **34,** 951–963.
12. Schussel, L. J. and Atwater, J. E. (1995), *Chemosphere* **30(5),** 985–994.
13. Subramanian, A., Kennel, S. J., Oden, P. I., Jacobson, K. B., Woodward, J., and Doktycz, M. J. (1999), *Enzyme Microb. Technol.* **24,** 26–34.
14. Hua, F., Shi, J., Lvov, Y., and Cui, T. (2002), *Nano Lett.* **2,** 1219–1222.
15. Chang-Yen, D., Lvov, Y., McShane, M., and Gale, B. (2002), *Sens. Actuators B* **87,** 336–345.
16. Fang, M., Grant, P., McShane, M., Sukhorukov, G., Golub, V., and Lvov, Y. (2002), *Langmuir* **18,** 6338–6344.
17. Hua, F., Lvov, Y., and Cui, T. (2002), *Nanosci. Nanotechnol.* **2,** 257–361.

0273-2289/04/113/0273–0285/$25.00

Performance of Chloroperoxidase Stabilization in Mesoporous Sol-Gel Glass Using *In Situ* Glucose Oxidase Peroxide Generation

Abhijeet Borole,* Sheng Dai, Catherine L. Cheng, Miguel Rodriguez Jr., and Brian H. Davison

Oak Ridge National Laboratory,
PO Box 2008, Oak Ridge, TN 37831-6226,
E-mail: borolea@ornl.gov

Abstract

A unique mesoporous sol-gel glass possessing a highly ordered porous structure (with three pore sizes of about 50, 150, and 200 Å diameter) was used as a support material for immobilization of the enzyme chloroperoxidase (CPO). CPO was bound onto the glass via a bifunctional ligand, trimethoxysilylpropanal. *In situ* production of the cosubstrate, H_2O_2, was achieved using glucose oxidase. Solvent stability in acetonitrile mixtures was enhanced when a pore size larger than the size of CPO was used (i.e., 200 Å). From these results, it appears that the glass-enzyme complex developed through the present work can be used as high-performance biocatalysts for various chemical-processing applications, particularly in harsh conditions.

Index Entries: Sol-gel glass; chloroperoxidase; glucose oxidase; acetonitrile; horseradish peroxidase; thermostability.

Introduction

Chloroperoxidase (CPO) is a very versatile enzyme capable of carrying out a number of reactions including epoxidation *(1,2)*, sulfoxidation, alcohol oxidation, N-dealkylation, *(3)* and hydroxylation in the presence of a suitable reductant *(4–7)*. Most of these hydrophobic molecules require the use of an organic solvent in the reaction medium to enhance solubility. However, the enzyme has very low activity in organic solvents *(8)*, reducing its potential for industrial application.

*Author to whom all correspondence and reprint requests should be addressed.

Factors that affect the activity of enzymes, in general, in an organic medium are structural denaturation, substrate desolvation, degree of hydration, and diffusional limitations (owing to the insolubility of native enzymes) *(9)*. For redox enzymes, another complication is the requirement that cosubstrates be provided (e.g., H_2O_2 or other cofactors). Various activation and stabilization methodologies for enzymes have been reported. These include covalently modifying enzymes with chemical groups *(10–13)*, complexation with surfactants *(14,15)* or polymers *(16)*, freeze-drying with inorganic salts *(17)*, and incorporation of enzymes into polymeric supports *(18–20)*. In particular, the covalent binding of enzymes to solid supports can effectively extend the lifetime of biocatalysts by protecting the native three-dimensional structure of enzyme molecules. Traditional enzyme immobilization technologies have been developed mostly based on consideration of the reuse of biocatalysts *(21,22)*, but the detrimental mass transfer effect usually leads to very low apparent enzyme activity and thus considerably limits the effectiveness of the biocatalysts. By contrast, attachment of enzyme to solid supports may result in enhanced enzyme activity in organic solvents as compared with that of the native enzyme in the same reaction medium. It has been demonstrated that the incorporation of enzymes into synthetic polymers, especially those via multiple covalent bonds, can significantly improve their activities in a nonaqueous environment *(18–20,23,24)*. Particularly, the plastic enzymes showed activities that were comparable or even higher than those of enzymes solubilized via ion pairing with surfactant in organic solvents *(18)*.

The *in situ* incorporation of enzymes into inorganic materials, as compared with organic materials, is rather difficult. Nevertheless, sol-gel silica materials have been investigated by different groups as an alternative to organic matrices *(25,26)*. The requirement for cosolvent to overcome the low aqueous solubility of alkyl silicate precursors and the formation of alcohols during the gelation reaction process, however, can adversely affect enzyme activity. Even though different precursors (such as poly-[glyceryl silicate]) have been examined in an effort to generate milder sol-gel conditions *(27)*, *in situ* sol-gel incorporation has been mostly applied in the development of enzyme-coated electrodes for analytical applications, in which enzyme is entrapped in a sol-gel thin film attached to electrodes *(26,28,29)*. In most of these applications, the effective enzyme loading is not as critical as in other bioprocessing applications.

Immobilization onto inorganic surfaces generally severely limits the possible enzyme loading. Recent breakthroughs, *(30–33)* in catalyst synthesis have resulted in a novel methodology for preparing mesoporous inorganic materials with extremely high surface areas and ordered mesostructure. Mesoporous silicon, aluminum, and transition metal oxides have been prepared. The essence of this new methodology is the use of molecular assemblies of surfactants or related substances as structure templates during the formation of oxides. The surfactants used in synthesis can be cationic, anionic, or neutral, depending on the charge of

the inorganic precursors. Unlike microporous materials, which can only interact with enzyme molecules on outer surfaces, mesoporous materials have larger pore openings that allow access to the inner pore surfaces. In a recently published article, mesoporous silica materials (pore diameter ranged from 27 to 92 Å) were used to physically absorb horseradish peroxidase (HRP), and improved enzyme activity in organic solvents and enhanced thermostability in aqueous solutions were demonstrated *(34)*. The use of highly porous glass may allow the enzyme to be hosted inside the microchannel via multiple point attachment, which is expected to improve enzyme structural stability *(35)*. In addition, the mass transfer of organic chemicals in these materials is far more efficient than in conventional microporous catalysts, such as zeolites, because of their unique mesoporous pore diameters (20–250 Å). Immobilization of other peroxidases into sol-gel material has been shown to improve their operational stability *(33,36,37)*. An HRP–sol-gel catalyst was shown to be recyclable for multiple reactions without loss of activity. These considerations prompted us to investigate immobilization of industrially useful enzymes in ordered mesoporous hosts. We recently reported immobilization of α-chymotrypsin into mesoporous silica *(38)*. Here, we extend that work to immobilize CPO into sol-gel and evaluate its thermostability and solvent stability.

A second hurdle in industrial applications of CPO is its sensitivity to H_2O_2, a required cosubstrate. The enzyme undergoes a mechanism-based inactivation in the presence of primary olefins and peroxide *(39)*. Small amounts of allylbenzene can result in formation of *N*-alkylporphyrin resulting in deactivation. This problem can be solved in two ways: first, by controlled addition or *in situ* generation of H_2O_2 and second, by modifying the enzyme (genetically) to prevent inactivation. Use of *glucose oxidase* (Go_x) allows *in situ* generation of H_2O_2. This is a convenient although more expensive, way of providing H_2O_2 compared to a pump-based continuous addition. A mutant enzyme that does not denature in the presence of excess peroxide has also been produced *(40)*. Another way to protect the enzymes from oxidation by peroxide is sol-gel immobilization *(41)*. The activity was reported to be unchanged apparently owing to preservation of the protein structure in the sol-gel matrix. We therefore were interested in evaluating the effect of sol-gel immobilization on CPO and report the results here.

Materials and Methods

CPO Assay

The standard chlorination assay for measuring CPO activity is as follows: 100 m*M* potassium phosphate buffer, pH 2.75; 0.16 m*M* monochlorodimedone (MCD); 0.3 mg/L of CPO, 10 m*M* KCl. The typical H_2O_2 concentration was 2 m*M*. The peroxide stability was studied by varying the concentration of H_2O_2 and by using *in situ* produced peroxide.

The assay procedure was modified to study the effect of solvent concentration and use of CPO with *in situ* H_2O_2. To produce H_2O_2 *in situ*, 24 µmol of glucose and 20 µg GOx were added in a 3 mL reaction mixture. The disappearance of MCD was monitored spectrophotometrically at 278 nm with an extinction coefficient of 12,200 M^{-1} cm^{-1}. The various enzymatic reactions are as follows:

CPO Standard Assay

$$MCD + Cl^- + H_2O_2 \rightarrow CPO \rightarrow Dichlorodimedone + H_2O + OH^-$$

GOx Standard Assay

$$\beta\text{-D-Glucose} + O_2 + H_2O \rightarrow GOx \rightarrow D\text{-Glucose-1,5-lactone} + H_2O_2$$

$$H_2O_2 + o\text{-Dianisidine (reduced)} \rightarrow HRP \rightarrow o\text{-Dianisidine (oxidized)}$$

Combined *in situ* H_2O_2 CPO-GOx Reaction

$$\beta\text{-D-Glucose} + O_2 + H_2O \rightarrow GOx \rightarrow D\text{-Glucose-1,5-lactone} + H_2O_2$$

$$MCD + Cl^- + H_2O_2 \rightarrow CPO \rightarrow Dichlorodimedone + H_2O + OH^-$$

The peroxidase activity of CPO was measured using other assays that utilize other substrates such as 2,2'-azino-bis 3-ethylbenzthiazoline-6-sulfonic acid (ABTS) and *o*-dianisidine. A typical assay consisted of 1 m*M* substrate in 100 m*M* potassium phosphate, pH 5.0, and 2 m*M* H_2O_2. The absorbance for ABTS was measured at 414 nm using an extinction coefficient of 3.6×10^4 M^{-1} cm^{-1}, and that for *o*-dianisidine was measured at nm using 11,600 M^{-1} cm^{-1}. Preliminary experiments with solvents indicated loss of activity at higher solvent concentrations and were therefore repeated using alternate substrates, in order to confirm that the loss of activity was not owing to substrate desolvation.

Solvent Stability

Acetonitrile (MeCN) was used as a model solvent to measure the stability of CPO in a solvent environment. Enzyme assays were performed as just described with the addition of MeCN. The experimental problem of salt precipitation was minimized by using citric acid (7.5 *M*) for pH adjustment and reducing the phosphate buffer concentration to 10m*M*. The concentration of the remaining reagents in the CPO assay remained the same.

Thermostability

The enzyme was incubated for a given amount of time at different temperatures, after which the activity was measured by the standard assay at 30, 40, and 50°C using MCD as the substrate. GOx was used for *in situ* production of H_2O_2.

CPO Immobilization in Sol-Gel

Preparation of Ordered Mesoporous Silica Support

The typical procedure *(42)* involved mixing 4 g of nonionic triblock copolymer L123 (BASF), 20 g of water, and 80 g of 2 *M* HCl. To this solution, 8 g of tetraethylorthosilicate was added at room temperature. The mixture was then stirred at room temperature for 24 h. The solid product was recovered by filtration. The polymer template was removed by calcination at 500°C for 5 h.

Ligand Synthesis

Trimethoxysilylpropanal was synthesized via a method similar to the one reported by Takeuchi and Soto (43). A solution of 20.0 g (135 mmol) of vinyltrimethoxysilane, 92 mg (0.01 mmol) of $RhH(CO)(PPh_3)$, and 0.21 g (0.8 mmol) of PPh_3 in 100 mL of toluene was placed in a 300-mL autoclave. The vessel was loaded with 600 psi of CO and stirred for 10 min followed by the addition of H_2 to 1200 psi total pressure ($CO/H_2 = 1/1$). It was then heated at 80°C for 4 h under stirring (70 rpm). The products (90%) were isolated by distillation under vacuum (0.5 torr, 45–50°C) and consisted of the mixture of two isomers (normal and iso) at a ratio of normal:iso of 95:5 (38).

CPO Immobilization

In a typical immobilization procedure, 0.5 g of porous silica glass was added to 5 mL of ethanol at 40°C. The mixture was stirred for 1 h to wet the glass thoroughly, and 0.2 g of the trimethoxysilylpropanal ligand and 0.5 mL of water were added to the mixture. One hour later, the mixture was centrifuged and the supernatant solution was then removed. The reagent-coated gel was then washed extensively with ethanol, then water, to remove residual reagent. The washed sol-gel was mixed with CPO (2.0 mL of 7.6 mg/mL solution in water) and stirred at 4°C for 48 h. The mixture was centrifuged, and the protein loading was determined by a difference between the enzyme activity of the supernatant solution and that of the initial enzyme solution. The enzyme-bound glass was washed five times with 25 mL of deionized water until no absorbance at 280 nm was observed in the washing solution and then dried by purging with N_2 gas. The enzyme activity of all washes was measured. The CPO was immobilized on sol-gels with three different pore sizes: 50, 150, and 200Å.

CPO Sol-Gel Activity Measurements

Sacrificial sampling was used to assess the activity of sol-gel–immobilized CPO over a 3-h period. H_2O_2 was provided via the *in situ* reaction with GOx. Experiments were conducted in by preparing solutions of sol-gel enzyme preparations in assay buffer in a centrifugal filter unit. About 10 mg of sol-gel enzyme was used for each assay. The purpose of the filter was to allow easy separation of the solid-phase enzyme for measurement

of changes in substrate concentration by spectrometry at the time of assay (5-min period). These mixtures were incubated for 30, 60, 100, and 180 min at 40 and 50°C, followed by the standard activity assay. Sample was centrifuged to separate the sol-gel from the supernatant, and the concentration of the substrate in the supernatant was measured every minute for 5 min. After absorbance measurement, the solution was returned to the centrifuge tube containing the sol-gel for another minute of incubation. The stability of the sol-gel enzyme in solvents was measured in a similar manner.

Results and Discussion

Effect of Peroxide

Experiments were conducted to evaluate two modes of supplying peroxide for the CPO reaction. In one reaction, it was supplied as an H_2O_2 solution, and in the second it was produced *in situ*. Figure 1 shows the progress of the reactions in the two modes. In the presence of 2 m*M* H_2O_2 (added externally), the enzyme lost than 50% of its activity in (Fig. 1A). This drop in activity was determined by taking the first derivative of the polynomial equation and then calculating the rate at time (x) = 1 and 60. The substrate:peroxide ratio under these conditions is 1:25. The use of 20 m*M* peroxide resulted in similar substrate disappearance curves (data not shown). Lloyd and Eyring *(41)*, who studied the stability of HRP, reported that a ratio of peroxide to substrate of 50 resulted in 90% loss of enzyme activity, whereas a ratio of 5 resulted in no loss of activity. To prevent enzyme inactivation, the alternate method of *in situ* peroxide production was tested. This would allow better control of both the peroxide substrate ratio and the excess peroxide concentration. The results (Fig. 1B) show that *in situ* production of the peroxide at a controlled rate did not result in enzyme deactivation. These results demonstrate the utility of the GOx method for supplying peroxide. We also studied the peroxide stability of HRP and found the results to be very similar (data not shown). The rate of H_2O_2 production was determined separately using an assay coupled with HRP. The rate under the conditions studied (0.013 mg/mL of GOx, 0.067 m*M* glucose, 3-mL reaction volume) was found to be 0.16 µmole/min. Under similar conditions, the substrate:peroxide ratio would not reach 1:25 for at least 30 min.

Effect of Solvent Concentration on Free CPO Reaction

The solvent stability of CPO was measured by varying the MeCN concentration. The enzyme ceased to be active above 40% MeCN (Fig. 2). The stability of GOx was also under question in the solutions with 40% MeCN or higher. This was verified by using HRP in place of CPO (Fig. 3B) along with GOx. The results indicate that GOx was active up to 70% MeCN. This proves that the drop in the rates at 40% and higher MeCN concentrations is owing to inactivation of CPO. Assays measuring peroxidase activity using the alternate substrates *o*-dianisidine and ABTS (Figs. 3A, and 4)

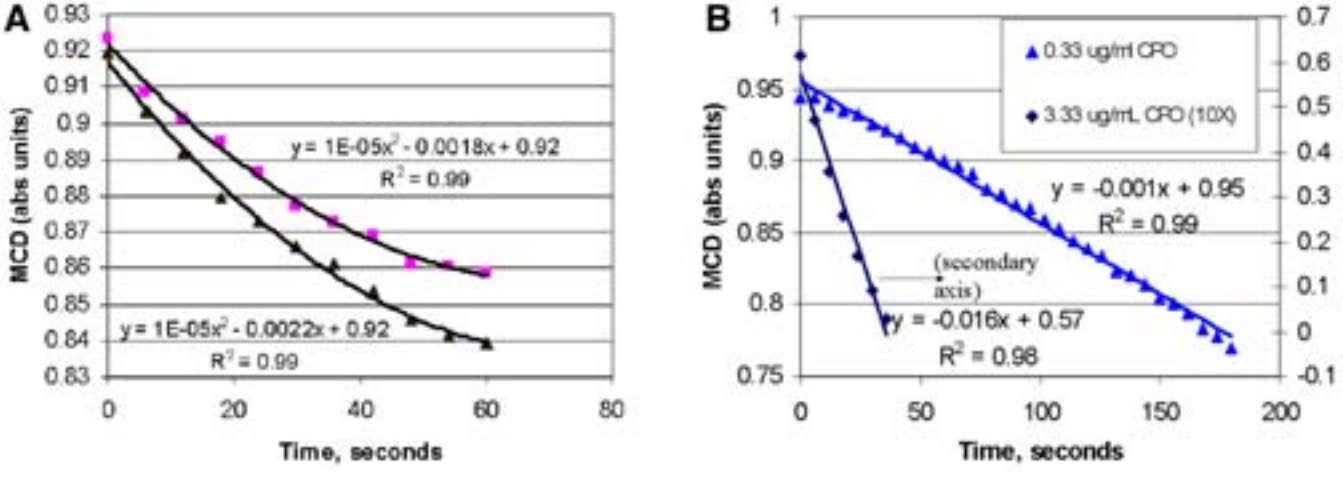

Fig. 1. Conversion of MCD in two different H_2O_2 supply modes: **(A)** direct addition of H_2O_2 to reaction solution in two replicate experiments (CPO concentration = 0.33 µg/mL); **(B)** *in situ* H_2O_2 production using GOx.

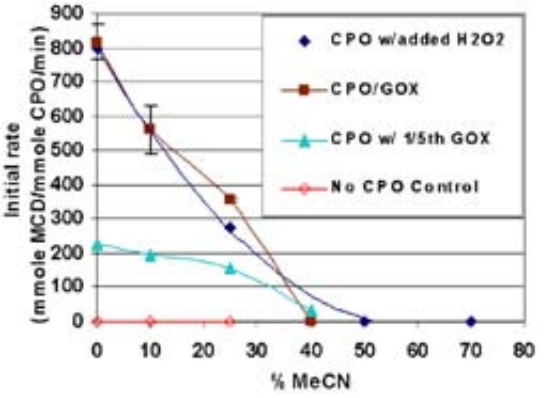

Fig. 2. Conversion of MCD by CPO in MeCN.

in MeCN also demonstrated that CPO was the enzyme that was inactivated at and above 40% MeCN.

CPO assays with added H_2O_2 and combined CPO/GOx assays in 100% aqueous buffer showed a rate of conversion similar to that of MCD. Note that the rates reported in Fig. 2 are initial rates. Similar initial rates for *in situ* and added H_2O_2 suggest that the amount of peroxide generated by GOx was at least equal to the stoichiometric amounts required for reaction with CPO. To verify this, an experiment was conducted with a lower amount of GOx. Reducing the amount of GOx to one-fifth reduced the rates of the CPO reaction proportionately, indicating that the rate was controlled by the rate of peroxide production. This also implies that the peroxide produced would be immediately consumed, and no significant accumulation would occur.

Sol-Gel CPO Immobilization

The extent of CPO immobilized on the sol-gel was determined by the difference between the activity of the initial enzyme solution and that measured in cumulative washes. Based on the cumulative activity lost in six washes, a second preparation of the CPO-bound sol-gel contained 10, 24, and 55 mg of CPO/g of sol-gel for the 50-, 150-, and 200-Å CPO sol-gels, respectively. In prior experiments, the total activity was measured and an estimated 80% of the bound CPO was active. The sol-gel immobilization is expected to limit the unfolding of the protein bound inside pores of the sol-gel. Thus, immobilization is expected to affect solvent stability and thermostability. Immobilization would probably not impact peroxide stability, since the mechanism of peroxide inactivation is associated with changes in the redox properties and oxidation state of the heme iron and the active center, which cannot be protected by immobilization. Experimental studies of immobilized CPO were therefore limited to temperature and solvent stability.

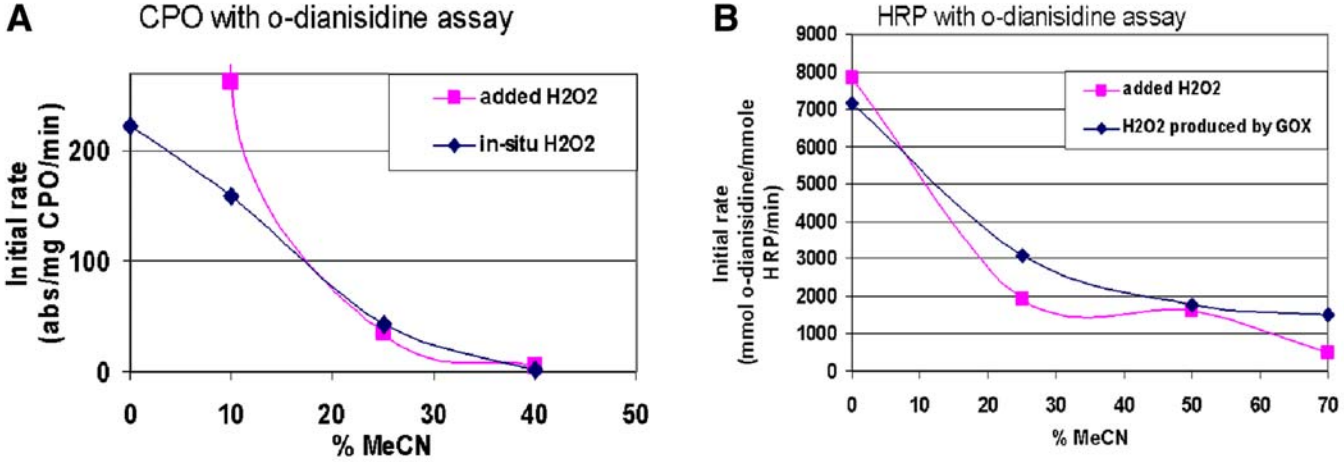

Fig. 3. Conversion of *o*-dianisidine by **(A)** CPO and **(B)** HRP in % MeCN.

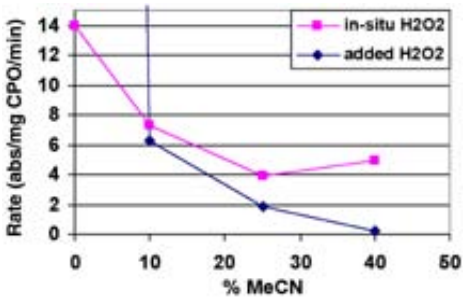

Fig. 4. Conversion of ABTS by CPO at various MeCN concentrations. The maximum activity of CPO was 260 abs units/(mg of CPO·min) and was observed in the absence of MeCN but in the presence of added peroxide.

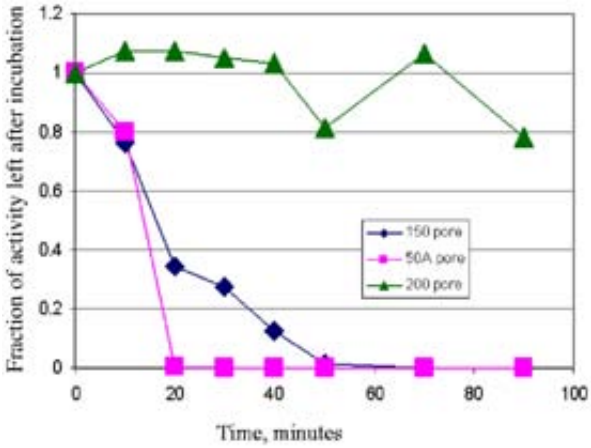

Fig. 5. Effect of solvent on stability of sol-gel–immobilized CPO. The highest stability displayed in 200-Å pore sol-gel may be owing to immobilization of the enzyme within the pores of the sol-gel, whereas it may have been immobilized effectively only on the surface in the case of the other pore sizes.

Effect of Pore Size on Solvent Stability

The 50-Å sol-gel CPO showed no protective effect from immobilization to MeCN. Both free and sol-gel CPO had no activity above 40% MeCN. This is not surprising given that the size of CPO (59×71×92 Å) is larger than the pore size of this sol-gel and the CPO must be bound to the outer gel surface. The largest stabilization was observed with 200-Å sol-gel (Fig. 5). This must be owing to immobilization of the enzyme within the pores of the sol-gel as compared to just surface immobilization, as must be the case with the 50-Å sol-gel. Partial stabilization was observed with the 150-Å sol-gel enzyme. The stabilization of the enzyme within the larger pores is probably owing to multipoint attachment of the enzyme to the glass surface. A convex surface such as in a pore provides several points of attachment as compared to a flat glass surface, where typically a single bond is realized *(38)*.

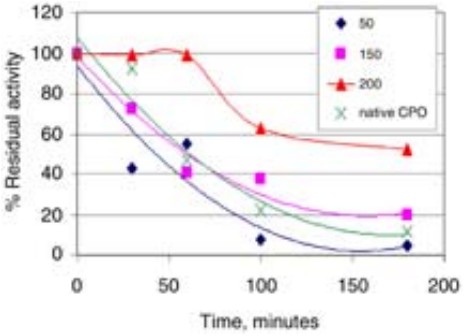

Fig. 6. Thermostability of CPO immobilized on sol-gel material of different pore sizes.

Thermostability

Free CPO lost 95% activity within 3 h when incubated at 40ϒC, whereas sol-gel CPO lost only 50% activity under this condition (Fig. 6). At an incubation temperature of 50ϒC, no protection was observed by sol-gel immobilization for CPO. Only the CPO immobilized in 200-Å sol-gel retained activity over 3 h at 40ÀöC.

Conclusions

Nonaqueous enzymatic redox reactions have been limited by stability owing to solvents and highly reactive substrates (H_2O_2). Here we have shown evidence of methods to alleviate these concerns for reactions with CPO. In experimental systems, the *in situ* production of H_2O_2 by GOx was shown to function equally well and more reproducibly than added H_2O_2. *In situ* production is experimentally easier and prevents enzyme deactivation owing to high peroxide levels. GOx was more solvent stable than CPO; therefore, the GOx system may be useful for this and other redox systems.

Immobilization has also been shown to stabilize against solvent denaturation of enzymes. However, here we presented suggestive data on the mechanisms of this stabilization. Only the CPO immobilized in 200-Å sol-gel showed any solvent or temperature stabilization. CPO bound to matrices with pores smaller than the protein showed little or no stabilization effect owing to surface immobilization alone. This supports the concept that steric hindrance to protein unfolding within a pore is part of the stabilization mechanism. An unresolved question for the future applications of this research is to increase the overall enzyme activity or loading.

Acknowledgments

We wish to acknowledge Dr. J. Dordick and D. Clark for helpful discussions and Ping Wang of the Department of Chemical Engineering, The University of Akron, Akron, OH for advice. Oak Ridge National Laboratory is

operated by UT-Battelle, LLC for the Department of Energy under contract DE-AC05-00OR22725. This research was funded by the US Department of Energy, Office of Energy Efficiency and Renewable Energy. This article has been authored by a contractor of the US government under contract DE-AC05-00OR22725. Accordingly, the US government retains a nonexclusive, royalty-free license to publish or reproduce the published form of this contribution, or allow others to do so, for US government purposes.

References

1. Hu, S. H. and Hager, L. P. (1999), *Tetrahedron Lett*. **40(9),** 1641–1644.
2. Santhanam, L. and Dordick, J. S. (2002), *Biocatalysis and Biotransformation*. **20(4),** 265–274.
3. Hager, L. P., Lakner, F. J., and Basavapathruni, A. (1998), *J Mol. Catal. B Enzymat*. **5(1–4),** 95–101.
4. van de Velde, F., van Rantwijk, F., and Sheldon, R. A. (1999), *J. Mol. Catal. B Enzymat*. **6(5),** 453–461.
5. Lakner, F. J. and Hager, L. P. (1997), *FASEB J*. **11(9),** p. 9.
6. Manoj, K. M., Lakner, F. J., and Hager, L. P. (2000), *J. Mol. Catal. B Enzymat*. 2000. **9(1–3),** 107–111.
7. van de Velde, F., Bakker, M., van Rantwijk, F., Sheldon, R. A. (2001), *Biotechnol. Bioeng*. **72(5),** 523–529.
8. Loughlin, W. A. and Hawkes, D. B. (2000), *Bioresour. Technol*. **71(2),** 167–172.
9. Klibanov, A. M. (1997), *Trends Biotechnol*. **15(3),** 97–101.
10. Takahashi, K., et al. (1985), *J. Org. Chem*. **50(18),** 3414–3415.
11. Vazquez-Duhalt, R., Fedorak, P. M., and Westlake, D. W. S. U. A. (1992), *Enzyme Microb. Technol*. **14,** 837–841.
12. Wang, P., Woodward, C. A., and Kaufman, E. N. (1999), *Biotechnol. Bioeng*. **64(3),** 290–297.
13. Pina, C., Clark, D., and Blanch, H. U. B. (1989), *Biotechnol. Biotechniques*. **3(5),** 333–338.
14. Powers, M. E., et al. (1993), *Biopolymers*. **33,** 927–932.
15. Paradkar, V. M. and Dordick, J. S. (1994), *J. Am. Chem. Soc*. **116,** 5009–5010.
16. Secundo, F., et al. (1999), *Biotechnol. Bioeng*. **64(5),** 624–629.
17. Ru, M. T., et al. (1998), *Biotechnol. Bioeng*. **63(2),** 233–241.
18. Wang, P., et al. (1997), *Nat. Biotechnol*. **15(8),** 789–793.
19. Yang, Z., Williams, D., and Russell A. J. U. P. (1995), *Biotechnol. Bioeng*. **45,** 10–17.
20. Yang, Z. U. P., et al. (1995), *J. Am. Chem. Soc*. **117,** 4843–4850.
21. Tischer, W. and Wedekind, F. (1999), *Topics Curr. Chem*. **200,** 95–126.
22. Malcata, F. X., et al. (1990), *JAOCS*. **67(12),** 890–910.
23. Miyanaga, M., et al. (1999), *J. Biosci Bioeng*. **87(4)** 463–472.
24. Dordick, J. S. (1992), *Biotechnol. Prog*. **8,** 259–267.
25. Greaves, M. D. and Rotello, V. M. (1997), *J. Am. Chem. Soc*. **119(44),** 10,569–10,572.
26. Li, J., Tan, S. N. and Oh, J. T. J. (1988), *Electroanal. Chem*. **448(1),** 69–77.
27. Gill, I. and Ballesteros, A. (1998), *J. Am. Chem. Soc*. **120(34),** 8587–8598.
28. Ogura, K., et al. (1999), *Anal. Chim. Acta*. **384(2),** 219–225.
29. Subramanian, A., et al. (1999), *Enzyme Microb. Technol*. **24(1–2),** 26–34.
30. Tian, Z. R., et al. (1997), *Science*. **276(5314),** 926–930.
31. Bhatia, R. B., et al. (2000), *Chem. Materi*. **12(8),** 2434–2441.
32. Park, C. B. and Clark, D. S. (2002), *Biotechnol. Bioeng*. **78(2),** 229–235.
33. Smith, K., et al. (2002), *J. Am. Chem. Soc*. **124(16),** 4247–4252.
34. Takahashi, H., et al. (2000), *Chem. Materi*. **12(11),** 3301–3305.
35. Martinek, K., et al. (1977), *Biochimi. Biophys. Acta*. **485(1),** 1–12.
36. Ferrer, M. L., et al. (2003), *J. Sol-Gel Sci. Technol*. **26(1–3),** 1169–1172.
37. Kadnikova, E. N. and Kostic, N. M. (2003), *J. Org. Chem*. **68(7),** 2600–2608.
38. Wang, P., et al. (2001), *Biotechnol. Bioeng*. **74(3),** 249–255.

39. Lee, H. I., et al. (1997), *J. Am. Chem. Soc*. **119(17)**, 4059–4069.
40. Rai, G. P., Zong, Q., and Hager, L. P. (2000), *Isr. J. Chem*. **40(1),** 63–70.
41. Lloyd, C. R. and Eyring, E. M. (2000), *Langmuir*. **16(23),** 9092–9094.
42. Zhao, D. Y., et al. (1998), *J. Am. Chem. Soc*. **120(24),** 6024–6036.
43. Takeuchi, R. and Sato, N. (1990), *J. Organometallic Chem*. **393(1),** 1–10.

0273-2289/04/113/0287–0297/$25.00

Integration of Computer Modeling and Initial Studies of Site-Directed Mutagenesis to Improve Cellulase Activity on Cel9A from *Thermobifida fusca*

José M. Escovar-Kousen,*[,1] David Wilson,[2] and Diana Irwin,[2]

[1]Martek Biosciences, 555 Rolling Hills Lane, Winchester, KY 40391, E-mail: jescovar@martekbio.com; and [2]Department of Biochemistry, Cornell University, Ithaca, NY 14853, E-mail: dbw3@cornell.edu

Abstract

Cellulases are a complex group of enzymes that are fundamental for the degradation of amorphous and crystalline cellulose in lignocellulosic material. Unfortunately, cellulases have a low catalytic efficiency on their substrates when compared to similar enzymes such as amylases, which has led to a strong interest in improving their activities. *Thermobifida fusca* secretes six cellulose degrading enzymes: two exo- and three endocellulases and an endo/exocellulase Cel9A (formerly called E4). Cel9A shows unique properties because of its endo- and exocellulase characteristics, strong activity on crystalline cellulose, and good synergistic properties. Therefore, it is an excellent target for mutagenesis techniques to improve crystalline cellulose degradation. In this article, we describe research conducted to improve Cel9A catalytic efficiency using a rational design and computer modeling. A computer model of Cel9A was created using the program CHARMM plus its PDB structure and a cellohexose molecule attached to the catalytic site as a starting model. Initially molecular graphics and energy minimization were used to extend the cellulose chain to 18 glucose residues spanning the catalytic domain and cellulose-binding domain (CBD). The interaction between this cellulose chain and conserved CBD residues was determined in the model, and mutations likely to improve the binding properties of the CBD were selected. Site-directed mutations were carried out using the pET vector pET26b, *Escherichia coli* DH5-α, and the QuickChange mutagenesis method. *E. coli* BL21-DE3 was used for protein production and expression. The puri-

*Author to whom all correspondence and reprint requests should be addressed.

fied proteins were assayed for enzymatic activity on filter paper, swollen cellulose, bacterial microcrystalline cellulose, and carboxymethylcellulose (CMC). Mutation of the conserved residue F476 to Y476 gave a 40% improved activity in assays with soluble and amorphous cellulose such as CMC and swollen cellulose.

Index Entries: *Thermonospora fusca*; Cel9A; cellulases; protein engineering; computer modeling.

Introduction

Cellulose is the most widespread biologic material on Earth. It has been realistically estimated that 3.3×10^{11} tons of CO_2/yr is fixed on the world's surface and that approx 6.6% of this (e.g., 22,000 million t/yr will be cellulose (almost 4 t per person per year) *(1)*. Pure cellulose can be hydrolyzed by chemical or enzymatic methods to soluble sugars, which in turn may be used as the raw material for many different bioprocesses. Therefore, cellulose from both agriculture and forestry sources has the potential to become a major source of feedstock for the production of chemicals, single cell protein, and biofuels such as ethanol *(1)*.

However, cellulose is a complex biopolymer and invariably occurs in nature in close association with lignin, and to a lesser degree with hemicellulose, starch, proteins, and salts. The ability of lignocellulose to withstand degradative forces is witnessed by the longevity of trees and by the expensive energy-consuming pretreatment processes required to open up this complex structure to bioconversion. The high cost of converting cellulose into an easily metabolized raw material for industrial bioprocesses makes the use of cellulosic materials unattractive when compared with other sources of fermentable sugars such as corn starch or sugarcane. Therefore, important technological developments have to be achieved before economic use may be made of this plentiful compound *(2)*.

The enzymes responsible for cellulose degradation are a complex group of cellulases consisting of at least three classes: endo-1,4-β-glucanase (EC 3.2.1.4), also called endocellulases; exo-1,4-β-glucanase (EC 3.2.1.91), also called exocellulases; and β-1,4-glucosidase (EC 3.2.1.21) or cellobiase *(2–5)*. More than 200 different cellulase genes have been sequenced, and all cellulases and similar enzymes such as xylanases have been classified within 11 families that are sometimes referred to as cellulase families, with 7 of those families considered to contain true cellulases *(6–9)*. Structural studies show that the majority of cellulases are multidomain proteins and their structure resembles a tadpole *(7)* consisting of a catalytically competent core structure linked to a carbohydrate-binding domain (CBD) also known as a cellulose-binding domain (CBD) via a flexible, often highly glycosylated linker region *(6)*. Even though all of these structures share a similar acid/base catalytic mechanism involving two or more aspartate or glutamate residues, the structures of the cellulases from each family may be totally different.

Many microorganisms, particularly fungi and thermophilic bacteria, possess cellulolytic enzymes of different kinds *(10–21)*. Because of their

strong cellulose-degrading enzymes, extensive research has been performed on the cellulases of the following microorganisms: *Trichoderma reesei (11,17,18)*, *Clostridium thermocellum (8,22)*, *Thermomonospora fusca (2,4,5,19–21)*, *Cellulomonas fimi (23)*, and *Humicola insolens (9,12,14)*. *T. reesei* cellulases are particularly well known, degrade cellulose in a cooperative manner, and consist of cellobiohydrolases (CBH-I and CBH-II) releasing cellobiose from the reducing end and nonreducing end, respectively, of the cellulose chain and two endoglucanases (EG-I and EG-III) cleaving internal glucosidic bonds *(11)*. *T. reesei*'s cellulolytic mixture, coming from selected strains in industrial fermentation processes, has the strongest cellulose-degrading activity of all known microorganisms. However, the hydrolysis of cellulose using these microbial enzymes—or for that matter any other hydrolysis procedure—is a long and inefficient process.

The actinomycete *T. fusca*, a thermophilic, filamentous soil bacterium, produces six structurally and functionally distinct cellulases: two exocellulases—Cel48A (ex-E6), which attacks the cellulose chain from the reducing end, and Cel6B (ex-E3), which attacks from the nonreducing end; three endocellulases—Cel5A (ex-E5), Cel6A (ex-E2), and Cel9B (ex-E1); and an endo/exo cellulase—Cel9A or ex-E4 *(2,4,5)*. All are moderately heat stable and have a broad pH optimum centered at 6.5.

The enzyme Cel9A, the subject of this article, is a unique cellulase because it has characteristics of both an exocellulase and an endocellulase *(20,21)*. It is endocellulase-like in that it can hydrolyze and reduce the viscosity of carboxymethylcellulose (CMC), and it is exocellulase-like in that it produces mostly soluble oligosaccharides (87%) from insoluble cellulose *(20,21)*. Cel9A is also of interest because it possesses very high activity on bacterial microcrystalline cellulose (BMCC) and an unusual synergistic activity in cellulase mixtures. It is unique in that it shows synergism with endocellulases and both types of exocellulases *(20,21)*. It also retains more than 70% of its activity from pH 4.7 to 10.1.

Structurally, Cel9A consists of a catalytic domain (CD) and an adjacent CBD (CBM or CBD) (family IIIc), a linker, and another CBM (family II) (*see* Fig. 1). Cel9A CD is homologous to celD from *C. thermocellum* while the adjacent CBM is homologous to one in a scaffoldin from the same microorganism. Cel9A-68 (also E4-68) is generated by limited proteolysis and contains the CD and the adjacent CBM. Constructs containing the CD alone (Cel9A-51), and the CD plus the fibronectin linker and family II CBM (Cel9A-74), were also produced. The activities of all these enzymes were measured on BMCC, filter paper, swollen cellulose, and CMC. Removal of the internal CBD decreased activity substantially on every substrate. Cel9A-74 did bind to BMCC but had almost no hydrolytic activity, while Cel9A-68 retained 32% of the activity on BMCC even though it did not bind. Cel9A-68 maintains most of the activity toward all soluble substrates, suggesting that the family IIIc CBD is important for processivity while the second CBD is important for insoluble substrate binding *(20,21)*. This article focuses on Cel9A-68 in general and the adjacent CBM in particular.

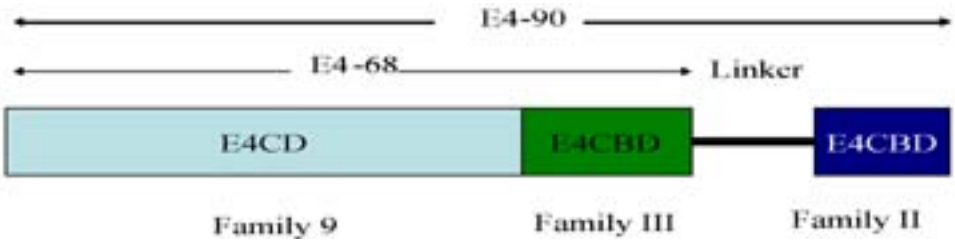

Fig. 1. Cel9A (E4) domain structure.

The crystal structure of Cel9A-68 has been determined by X-ray diffraction at 1.9 Å *(20)*. The structure reveals a CD from family 9 with an $(\alpha/\alpha)_6$ barrel fold directly linked to a CBD with an antiparallel β-sandwich fold. A model of the active-site configuration suggests that a water molecule is bound to Asp55 and Asp58, which are believed to function as the catalytic base, while Glu424 appears to be the catalytic acid. The observed cleavage product clearly shows the α configuration of the anomeric carbon, a fact expected from family 9 cellulases that cleave cellulose with inversion. Next to the active center there are six glucosyl-binding sites numbered for the nonreducing end, –4 to +2. Cel9A seems to processively cleave cellotetraose molecules from the nonreducing end of the cellulose chain until either they are completely hydrolyzed or it dissociates. The active-site cleft is blocked by a loop at the nonreducing end, and after each cleavage, the cellotetraose unit is expected to dissociate while the fragment that is bound to the catalytic site +1 and +2 and the family IIIc CBM is fed into the active site in a processive manner *(20,21)*.

To make biomass conversion more efficient, it will be necessary to either improve the catalytic activity of the enzymes (mainly cellulases) already known, discover new cellulases or cellulose-modifying proteins, increase the amount of protein secreted, modify the process, or combine these approaches. Cellulases show relatively low catalytic activity when compared with other hydrolases, and the low activities have called into question whether the genes encoding for the enzymes are under selection pressure to increase their catalytic efficiency *(24)*. Cellulase performance may be enhanced by the use of random mutagenesis techniques such as directed evolution *(25–29)* or rational protein design *(6,24,30)*. A major difficulty in making predictions for site-directed mutations for rational design in macromolecules is the lack of understanding of the forces that operate within proteins and between the protein and its substrate. Molecular mechanics calculations allow the theoretical positioning of substrate molecules into active sites through computer modeling and examination of the range of structural fluctuations that is possible for a protein-substrate complex *(31,32)*. Hence, computational studies usually facilitate the analysis of known protein structures as well as the design of proteins with novel

functional properties, reducing the cumbersome task of creating and studying countless mutants. Therefore, a good alternative for rational design is the use of computer modeling to determine individual changes followed by construction of the desired molecule by site-directed mutagenesis *(6,24,30)*. For our purposes, we concentrated on understanding the relationships among the structure of Cel9A-68, its catalytic activity, and particularly the interaction between the family IIIc CBM and cellulose. A molecular mechanics software and visualization programs *(31)* were used in combination with site-directed mutagenesis techniques.

Materials and Methods

Computer Modeling

All of the calculations were done using the CHARMM molecular mechanics program and the CHARMM22 parameter set for protein atoms *(33)*. All atoms from the glucose residues in the cellulose chain (initially a cellohexose) were modeled using parameters specifically developed for carbohydrates *(34)*. In all calculations, the lengths of chemical bonds to hydrogen atoms were kept fixed using the constraint algorithm SHAKE *(35)*.

A computer model of Cel9A-68 was created using the PDB file from the crystal structure published by Sakon et al. *(20)*. The protein structure plus the cellohexose molecule directly bound to the catalytic site were used as the starting point for all calculations. In the initial phase, molecular graphics visualization programs such as QUANTA and energy minimization calculations were used to place 12 additional glucose residues to extend the cellulose chain to 18 glucose residues spanning the CD and CBD. A number of possible conformations were evaluated using different starting positions and energy minimization-driven conformational refinement. The interactions between the cellulose chain and the conserved CBM residues (F476, D513, Y520, Q561, D513) *(36)* were determined in the model. Computational studies were conducted to determine the mutations most likely to create improved activity and were selected for site-directed mutagenesis.

Mutagenesis Procedure, Hosts, and Plasmids

The cloning and expression of recombinant proteins in *Escherichia coli* was done using the pET System developed by Novagen. The target gene from Cel9A-68 was ligated into pET26b to create plasmid pJE2 and transformed into *E. coli* DH5-α for mutagenesis. Plasmid pJE2 was constructed by ligating four DNA fragments: (1) a 4.3-kb *Sph*I-*Apa*I fragment from the pet vector, (2) a 1.15-kb *Apa*I-*Not*I fragment from pEJ containing the E2 signal peptide *(5)*, (3) a 1.0-kb *Not*I-*Acc*I polymerase chain reaction (PCR) fragment containing the mature Cel9A N-terminus plus a part of the gene obtained from pEJ2 (pD568) *(20)*, (4) a 0.7-kb *Acc*I-*Sph*I fragment containing the remaining part of Cel9A plus the C-terminus from pSZ46 (or pD687) *(21)*.

Plasmid pJE2 was used to construct the mutant plasmids (F476Y) using the QuickChange method for site-directed mutation. The forward and reverse primers were designed using the program DNAStar-Primer Select. The primers containing a silent mutation for threonine that created a unique restriction site for *Xma*I and *Sma*I, plus the desired codon change (underlined) for Tyr (TAC) instead of Phe (TTC), were as follows: Je1476tyr: TCA AC**ACC**CCGGGCACCACGTACACCGAGATC (forward); Je2476tyrrev: GATCTCGGTGTACGTGGTGCCCGG**GGT**GTTGA (reverse). The resulting PCR fragment was cloned into pET26b to produce pJE9. All coding regions in the new plasmids were sequenced by the Cornell Biotechnology Facility and only the desired mutations were found. All plasmids were transformed into *E. coli* BL21-DE3 for protein production and expression, and the modified enzymes were purified and characterized.

Protein Purification

Protein expression and production was scaled up to 2-L fermentors and a combination of hydrophobic interaction chromatography and ion-exchange chromatography proved very effective for purifying the enzymes *(20,21)*.

Enzyme Assays

The purified proteins were assayed for enzyme activity on filter paper, swollen cellulose, BMCC, and CMC following the procedures stated by Irwin et al *(5)*.

Results

Computer Modeling

Figures 2–4 indicate the CHARMM predictions for the structure and position of the cellulose chain (green) with respect to Cel9A (white and red) and the sequential manner in which the model was predicted by the program (one glucose residue at a time), starting from the original structure with 6 glucose residues *(20)* to 8 (*see* Fig. 2) to 12 (Fig. 3) and 16 (Fig. 4) with the CBD conserved residues in blue. Figure 5 shows the coordinates for the catalytic residues (yellow and red); the substrate (green); and the CBM conserved residues D513, R563, Y520, Q561, and F476 *(36)* (blue). As predicted in previous articles, based on the planar structure of the Cel9A-68 CBM, the cellodextrin chain is directly linked to the catalytic region through the CBD.

An important part of the present study was determining whether the residues suggested by Sakon et al. *(20)* (N470, CEL9A78, K480, R557, E559, Q561, and R563) and Bayer et al. *(36)* (D513, R563, Y520, Q561, and F476) interact with the cellulose substrate. The computational results indicate that all of these amino acids are well aligned and interact with the cellulose

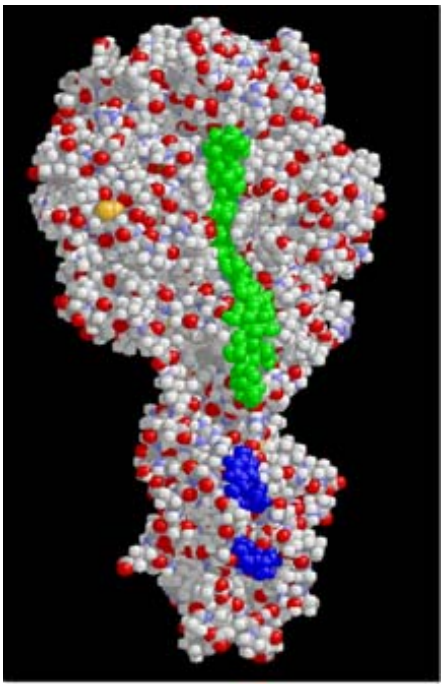

Fig. 2. CHARM progressive prediction for interaction between Cel9A and a cellulose chain with eight glucose residues.

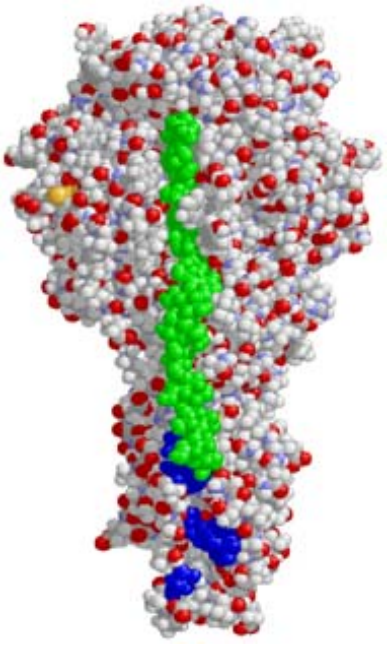

Fig. 3. CHARM progressive prediction for interaction between Cel9A and a cellulose chain with 12 glucose residues.

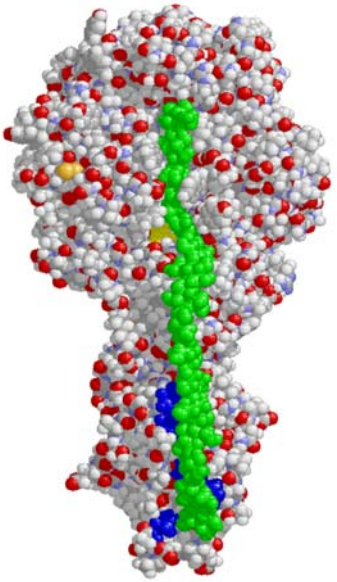

Fig. 4. CHARM progressive prediction for interaction between Cel9A and a cellulose chain with 16 glucose residues.

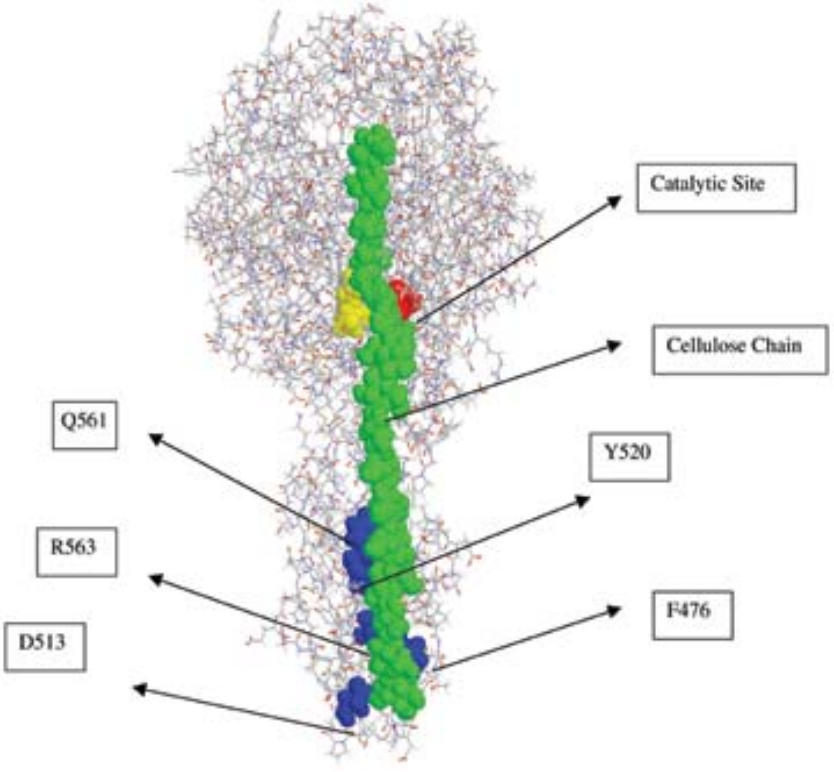

Fig. 5. CHARM predicted interaction between a 16 glucose cellulose chain and the CBM conserved residues.

Table 1
Cel9A-68 F476Y Activity [a]

Substrate	CMC (%)	Swollen cellulose (%)	Filter Paper (%)	BMCC (%)
Cel9A-68 F476Y	139	138	101	100

[a] With Cel9A-68 wild-type activity as 100%.

chain, with most of them forming hydrogen bonds or other interactions, i.e., a salt bridge and a planar interaction with the aromatic residue Y520 that are anchoring the surface of the CBM to the surface of the substrate.

The novel, conserved aromatic residue F476, which is characteristic of subfamily IIIc CBMs, was particularly interesting in the sense that it did not form a hydrogen bond with the cellodextrin chain, and as a consequence its interaction with the substrate seems to be weak. Therefore, computational studies were conducted on this residue, and the results indicated that mutation of F476 to Y created a hydrogen bond between the CBM and the cellulose chain. This was likely to improve binding, and thus it was selected for site-directed mutagenesis.

Mutagenesis

The enzyme from the F476Y mutant was purified and assayed on CMC, BMCC, filter paper, and swollen cellulose; the results are given in Table 1 as percentages of Cel9A-68 wild-type activity. An improvement in enzyme activity close to 40% was observed in soluble and amorphous cellulose (CMC and swollen cellulose), and no change or very small in crystalline cellulose (filter paper and BMCC). It has been found that the family IIIc CBM is important for processivity *(21)*. Processivity, as measured by the ratio of soluble reducing sugar ends to insoluble sugar ends, was found to be almost identical for the two enzymes: 3.1 for the wild type and 3.0 for the mutant.

Discussion

The combination of computational studies and site-directed mutagenesis was found to be an effective way to reduce the number of mutants to be tested. The enzyme activity assays of Cel9A-68 F476Y indicate an improvement of 40% in activity on CMC and swollen cellulose and no modification in activity on crystalline substrates (filter paper and BMCC). This result seems to confirm the computer model prediction that a new hydrogen bond would be the result of mutating the phenylalanine residue F476 to a tyrosine. This novel hydrogen bond in F476Y improved activity on soluble and amorphous cellulose probably owing to better binding properties that are important for placing the cellulose chain in the CBD for the mentioned substrates. The fact that no improvement was found for crystalline cellulose indicates a different kind of interaction between the CBD and crystalline cellulose, on one hand, and amorphous and soluble cellulose, on the other.

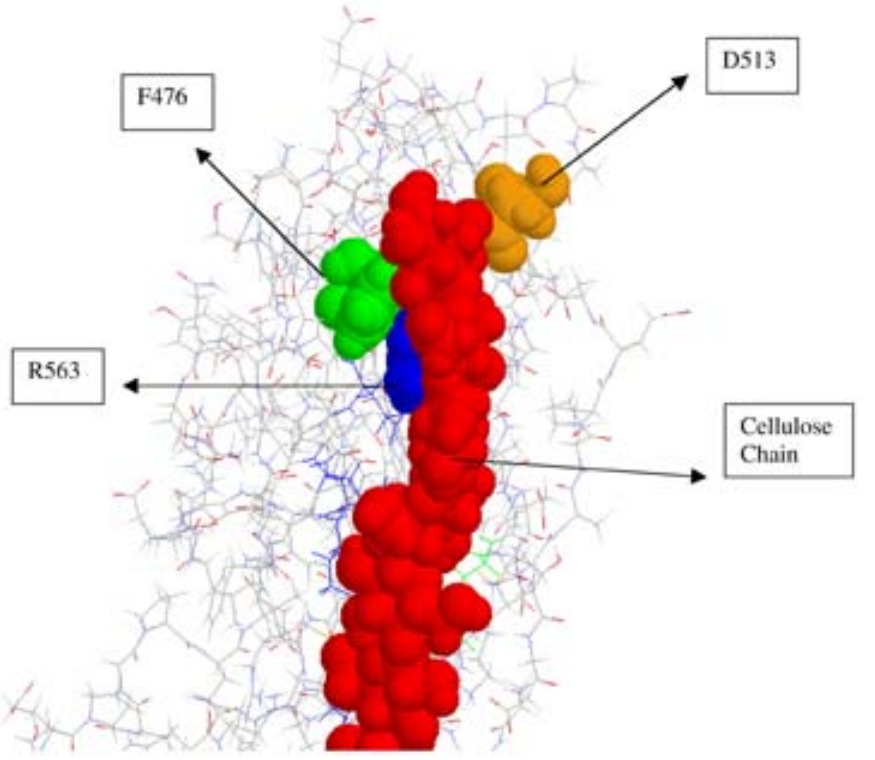

Fig. 6. Interaction between CBM residues R563, F476, and D513 with cellulose chain.

A possible explanation might be found in previous suggestions that Cel9A's CBD from family IIIc seems to bind transiently to only a single cellulose chain *(36)*, a factor that favors the interaction between the CBM and soluble and amorphous cellulose rather than crystalline cellulose.

Computer calculations indicate that the residues D513 and Y520 interact directly with the cellulose chain, a fact that is contrary to previous observations *(36)*. This result should be confirmed by future mutagenesis studies.

Because of the particular location at the end of the CBM (*see* Fig. 6) of residues D513 (orange), R563 (blue), and F476 (green), they seem to play an important role in the initial binding of the cellulose chain. By improving the binding properties of F476Y, the cellulose chain most likely binds faster to Cel9A, and as a result, there is an increase in the activity of the mutated enzyme. Future experiments will include other changes in these residues to prove or disprove the previous hypothesis.

Acknowledgment

We are indebted to Dr. John Brady at the Food Science Department at Cornell University for his invaluable collaboration and initial financial support.

References

1. Smith, J. E. (1996), in *Biotechnology*, Cambridge University Press, Cambridge, MA, pp. 22–23.
2. Walker, L. P., et al. (1993) *Biotech. Bioeng.* **42,** 1019–1028.
3. Teeri, T. T. (1997), *Trends Biotech.* **15,** 160.
4. Walker, L. P., et al. (1992), *Biotech. Bioeng.* **40,** 1019–1026.
5. Irwin, D. C., Spezio, M., Walker, L. P., and Wilson, D. B. (1993), *Biotech. Bioeng.* **42,** 1002–1013.
6. Davies, G. J., et al. (1996), *Acta Crystallographica* **D52,** 7–17.
7. Henrissat, B., et al. (1989), *Gene (Amst.)* **81,** 83–95.
8. Juy, M., et al. (1992), *Nature* **357,** 89–91.
9. Davies, G. J., et al. (1993), *Nature* **365,** 362–364.
10. Takashima, S., Nakamura, A., Masaki, H., and Uozumi, T. (1996), *Biosci. Biotech. Biochem.* **60(1),** 77–82.
11. Kraulis, P. J., et al. (1989), *Biochemistry* **28,** 7241–7257.
12. Dalbøge, H. and Heldt-Hansen, H. P. (1994), *Mol. Gen. Genet.* **243,** 253–260.
13. Azevedo, Mde O., et al. (1990), *J. Gen. Microbiol.* **136,** 120–123.
14. Cui, Z., et al. (1992), *Biosci. Biotechnol. Biochem.* **56,** 1230–1235.
15. Huang, J., et al. (1992), *J. Bacteriol.* **174,** 1314–1323.
16. Ong, E., et al. (1989), *Trends Biotechnol.* **7,** 239–243.
17. Divne, C., et al. (1994), *Science* **265,** 524–528.
18. Rouvinen, J., et al. (1990), *Science* **249,** 380–386.
19. Spezio, M., et al. (1993), *Biochemistry* **32,** 9906–9916.
20. Sakon, J., Irwin, D., Wilson, D. B., and Karplus, P.,A. (1997), *Nat. Struct. Biol.* **4,** 810–818
21. Irwin, D. C., et al. (1998), *J. Bacteriol*. **180(7),** 1709–1714.
22. Sacco, M., Millet, J., and Aubert, J. P. (1984), *Ann. Microbiol. (Inst. Pasteur)* **135A,** 485–488.
23. Curry, C., et al. (1988), *Appl. Environ. Microbiol.* **54,** 476–484.
24. Konstantinidis, A. K., et al. (1993), *Biochem. J.* **291,** 883.
25. Stemmer, W. P. C. (1994), *Nature* **370,** 389–391.
26. Stemmer, W. P. C. (1996), *Nat. Biotechnol*. **14,** 315–319.
27. Stemmer, W. P. C. (1995), *Biotechnology* **13,** 549–553.
28. Matsumura, I. and Ellington, A. D. (1996), *Nat. Biotechnol.* **14,** 366.
29. Zhang, J. H., Dawes, G., and Stemmer, W. P. C (1997), *Proc. Natl. Acad. Sci. USA* **94,** 4504–4509.
30. Cleland, J. L. and Craik, C. (1996), in *Protein Engineering Principles and Practice*, Wyley-Liss, New York, NY, pp. 22.
31. Taylor, J. S., Teo, B., Wilson, D. B., and Brady, J. W. (1988), *Prot. Eng*. **8(11)**, 1145–1152.
32. Brooks, C. L., Karplus, M. and Pettit, B. M. (1988), in *Proteins: A Theoretical Perspective of Dynamics, Structure and Thermodynamics*, *Adv. Chem. Phys.*, Vol. 71, Wiley-Interscience, New York, NY.
33. MacKerell, A. D., Bashford, D., et al (1998), *J. Physi. Chem.* **102,** 3586–3616.
34. Palma, R., Zuccato, P., et al. (2000), in *Glycosyl Hydrolases in Biomass Conversion*. Himmel, M. E., ed., American Chemical Society, Washington, DC.
35. Van Gunsteren, W. F., and Berendsen, H. J. C. (1977) *Mol. Physiol.* **34(5),** 1311–1327.
36. Bayer, A. E., et al. (1998) in *Carhohydrases from* Trichoderma reesei *and Other Microorganisms*. Claeyssens, M., Nerinckx, W., and Piens, K., eds., The Royal Society of Chemistry, pp. 39–65.

0273-2289/04/113/0299–0305/$25.00

Kinetics of Asparaginase II Fermentation in *Saccharomyces cerevisiae ure2dal80* Mutant

Effect of Nitrogen Nutrition and pH

Maria Antonieta Ferrara,*[,1] Josiane M. V. Mattoso,[2] Elba P. S. Bon,[2] and Nei Pereira Jr.[3]

[1]Far-Manguinhos, FIOCRUZ, Av. Sizenando Nabuco, 100, 21041-250, Rio de Janeiro, RJ, Brazil, E-mail: ferrara@far.fiocruz.br; and [2]Departamento de Bioquímica, Instituto de Química, Universidade Federal do Rio de Janeiro, RJ 22949-900, Brazil; and [3]Escola de Química, Universidade Federal do Rio de Janeiro, CT Bloco E, Rio de Janeiro, RJ 22945-900, Brazil

Abstract

Although the quality of nitrogen source affects fermentation product formation, it has been managed empirically, to a large extent, in industrial scale. Laboratory-scale experiments successfully use the high-cost proline as a nonrepressive source. We evaluated urea as a substitute for proline in *Saccharomyces cerevisiae ure2dal80* fermentations for asparaginase II production as a model system for nitrogen-regulated external enzymes. Maximum asparaginase II levels of 265 IU/L were observed in early stationary-phase cells grown on either proline or urea, whereas in ammonium cells, the maximum enzyme level was 157 IU/L. In all cases, enzyme stability was higher in buffered cultures with an initial pH of 6.5.

Index Entries: *Saccharomyces cerevisiae; ure2dal80* mutants; nitrogen sources; asparaginase II; fermentation kinetics.

Introduction

The quality of nitrogen source in a growth medium regulates a variety of bacteria, yeast, and fungus genes. This phenomenon, known as nitrogen regulation *(1)*, besides affecting the synthesis of permeases and metabolic enzymes, plays an important role in the fermentation of industrial bioproducts such as enzymes *(2)*.

Nitrogen regulation is also important for the production of a range of products derived from the secondary metabolism since it regulates the

*Author to whom all correspondence and reprint requests should be addressed.

induction or repression of the genes responsible for enzymes involved in the relevant metabolic pathways. Although medium optimization, including the quality and concentration of nitrogen source, has been of paramount importance in industrial fermentations, it has been managed empirically, to a large extent, with only a few studies on product formation by changing the nitrogen source. The knowledge that has been accumulated so far on nitrogen regulation allows the use, in laboratory-scale experiments, of proline as a nonrepressive source. However, its high cost precludes its use in industrial scale. Therefore, in light of its nonrepressive role stepwise studies to better characterize other less expensive sources are relevant to process yields and economical viability. Within this framework, we have been studying nitrogen regulation of asparaginase II in *Saccharomyces cerevisiae* as a model system aiming at the acquisition of valuable information to be used in the optimization of medium composition for external enzyme production *(3–5)*.

The synthesis of the *S. cerevisiae* periplasmic asparaginase II, encoded by the gene *ASP3*, is not repressed by carbon or induced by asparagine, being solely regulated by nitrogen *(6)*. Preferred sources, such as ammonium, glutamine and asparagine, repress its production, whereas nonpreferred sources, such as proline, or nitrogen starvation allow higher enzyme levels. Nitrogen regulation of asparaginase II synthesis operates via the GATA activators Gln3p and Nil1p and the GATA repressors Nil2p and Dal80p. The protein Ure2p, which is involved in the signaling pathway in response to preferential nitrogen sources, down-regulates Gln3p and Nil1p *(3,4,5,7,8)*. Nitrogen regulation studies of this enzyme using *S. cerevisiae* mutant strains have shown that fresh mid-log *ure2dal80* cells present enzyme levels 4-fold higher when grown in ammonium and 16-fold higher when grown in proline, in comparison with their wild-type counterparts. The $mRNA_{ASP3}$ levels were in accordance with the enzyme activity data *(5)*. Reported data have also shown that enzyme levels are affected by the pH of the growth medium and the cell's growth phase *(9,10)*.

In the present work, we studied the effect of repressive and nonrepressive nitrogen sources and different pH conditions on the kinetics of asparaginase II fermentations using an *S. cerevisiae ure2dal80* mutant strain. The profiles of cell growth, substrate consumption, asparaginase II accumulation, and changes in pH were monitored in cultures having glucose as carbon source and proline, urea, or ammonium sulfate as nitrogen source. Cultures were carried out under buffered and nonbuffered conditions in the pH range of 4.5–6.5.

Materials and Methods

Microorganism and Fermentation Conditions

S. cerevisiae ure2dal80 mutant strain YAE3R-D12 *(5)* was used. Fermentations were carried out in 1000-mL flasks containing 100 mL of growth medium (20 g/L of glucose; 1.6 g/L of ammonium sulfate, 2.0 g/L of pro-

line, or 0.5 g/L of urea; plus 2.0 g/L of yeast nitrogen base without amino acids and ammonium sulfate).

All media were supplemented with 0.1 g/L of adenine, 0.2 g/L of uracil, 0.1 g/L of histidine, and 0.1 g/L of leucine and presented a C/N ratio of 37. Whenever necessary, the initial pH of the medium was adjusted using an NaOH solution. Potassium phosphate buffer (20 m*M*) was used in buffered cultures. Fermentations were carried out at 29°C and 180 rpm in an Innova 4340 incubator shaker (New Brunswick Scientific).

Analytical Procedures

The culture supernatant was used for determination of glucose concentration by the dinitrosalicylic acid method *(11)* and pH measurement. Cell growth was monitored by the determination of optical density (OD) at 600 nm in a spectrophotometer (Shimadzu-UV 1601). One OD_{600} unity was found to be equivalent to 0.46 mg dry cell weight (DCW). Asparaginase II activity was assayed using fresh cells as previously described *(3,4)*.

Results and Discussion

The effect of initial pH values of 4.5 (pH of the medium without adjustment), 5.5, and 6.5 was evaluated in a first round of proline fermentations using nonbuffered medium. According to the data presented in Fig. 1, irrespective of the medium initial pH, a specific growth rate of 0.32 h^{-1} was measured. After a short lag phase, exponential growth was observed for 7 h, followed by a subsequent decline in the growth rate. Fermentations were completed within 18 h on glucose depletion (data not shown). Asparaginase was detected in late exponential phase cells and peaked (100–120 IU/g of DCW) within 11 to 12 h of fermentation. Although enzyme production per unit of dry cell weight decreased sharply in the cultures with an initial pH of 4.5 and 5.5, in cultures with an initial pH of 6.5 half of the peak enzyme level was still present after 20 h of fermentation. Different from the other cultures, the minimum pH value in this case did not fall bellow 3.3, protecting the enzyme from full inactivation. In accordance with these results, Kim and Roon *(12)* reported a correlation between asparaginase II inactivation and the culture pH: when the pH was maintained at 3.4 or above, a significant retention of asparaginase II activity was observed, whereas when the pH fell below 3.2, the enzyme became inactivated.

Considering the detrimental effects of low pH on the periplasmic asparaginase, phosphate buffer (pH 4.5, 5.5, and 6.5) was used in the subsequent proline fermentations. In these fermentations, the measured minimum pH values were higher than the threshold inactivating pH of 3.2 (Fig. 2). Although maximum enzyme levels were similar to the ones observed in the nonbuffered cultures, the use of buffer reflected positively on the enzyme stability, since a plateau rather than a peak of maximum levels was observed. The use of an initial pH of 6.5 resulted in the highest enzyme level (106 IU/g of DCW) and also in the highest volumetric enzyme concentra-

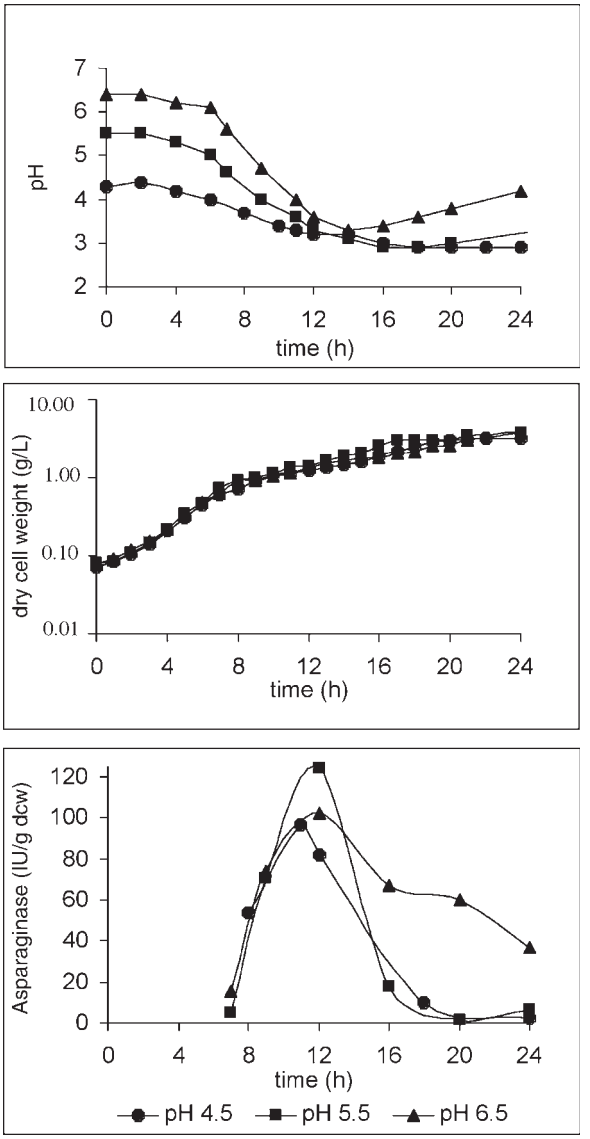

Fig. 1. Time course of *S. cerevisiae ure2dal80* mutant strain culture in nonbuffered medium containing proline as nitrogen source as function of initial pH.

tion (265 IU/L) within 15 h of culture. As such, enzyme levels increased 2.5-fold in comparison to the nonbuffered proline culture with an initial pH of 4.5. Cell growth rates (0.31 h^{-1}) and glucose consumption profiles (data not shown) were not significantly affected by the differences in the initial pH values of the culture nor by the use of buffer.

Accordingly, the subsequent urea and ammonium fermentations were carried out in buffered medium, pH 6.5. Figure 3 compares the cell growth,

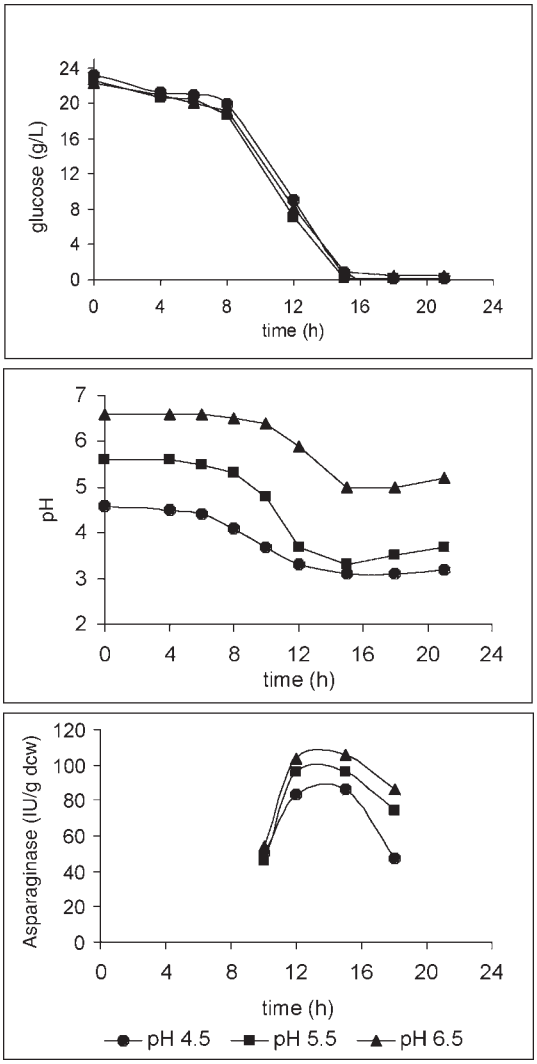

Fig. 2. Time course of *S. cerevisiae ure2dal80* mutant strain culture in buffered medium containing proline as nitrogen source as function of initial pH.

asparaginase production, glucose consumption, and change in pH for these fermentations. The already discussed proline data were included for comparison. Equivalent and somewhat higher specific cell growth rates of 0.35 and 0.34 h^{-1} were respectively observed for the ammonium and the urea medium, compared with the proline medium (0.31 h^{-1}). These results are in agreement with the literature, since according to Magasanik and Kaiser *(1)*, the differences in growth rate supported by very different nitrogen sources are often small. A different pattern of response, though, was observed for enzyme production regarding the nitrogen substrates.

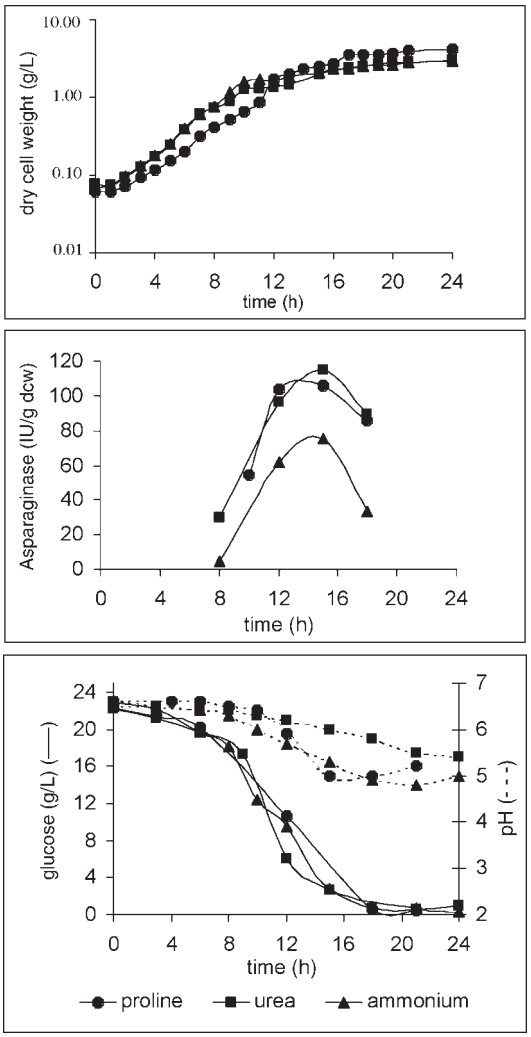

Fig. 3. Time course of *S. cerevisiae ure2dal80* mutant strain culture in pH 6.5 buffered medium containing proline, urea, or ammonium sulfate as nitrogen source.

Equivalent peak enzyme levels of 115 IU/g of DCW (265 IU/L) and 106 IU/g of DCW (265 IU/L) were observed, within 15 h, in the nonrepressive nitrogen sources urea and proline, respectively, and a lower enzyme level of 75 IU/g of DCW (157 IU/L) was measured in the ammonium medium. Therefore, the effect of the nitrogen sources on the general cell metabolism, as evaluated by cell growth, and on the regulation of *ASP3* expression were quite dissociated. This result was expected since in this *S. cerevisiae ure2dal80* mutant strain, *ASP3* expression in the ammonium culture would be repressed by the GATA factor Nil2p *(5)*. According to the data presented in Fig. 3, in all fermentations glucose depletion occurred within 16 h and a similar pattern for glucose consumption was observed.

At peak asparaginase concentration, the urea medium showed a higher pH value (6.0) in comparison with the proline (5.0) and ammonium (5.3) media.

All in all, the study of the effect of nitrogen nutrition and pH of the medium on the kinetics of cell growth, substrate consumption, and periplasmic asparaginase II accumulation using a nitrogen partially derepressed *S. cerevisiae ure2dal80* mutant strain showed that the conditions studied did not significantly affect cell growth. Enzyme production, however, was affected by both nitrogen source and pH of the medium: the use of buffer protected the periplasmic enzyme from inactivation, and the nitrogen nonrepressive urea or proline substrates allowed 50% higher enzyme levels in comparison to the repressive source ammonium. Since urea, a low-cost source, showed to be as derepressive as proline in the asparaginase II fermentations, this source is a valuable option to study nitrogen regulation in a range of other nitrogen-repressed enzymes and metabolites of industrial interest. Moreover, the use of urea is also advantageous, because its metabolism did not result in a sharp pH decline during the fermentation, preventing the inactivation of external enzymes.

Acknowledgments

This work was supported by the Brazilian Research Council (RHAE/Conselho Nacional de Desenvolvimento Científico e Tecnológico [CNPq]), Far-Manguinhos/FIOCRUZ, and Quiral Química do Brasil.

References

1. Magasanik, B. and Kaiser, C. A. (2002), *Gene* **290,** 1–18.
2. Bon, E. P. S. and Webb, C. (1993), *Appl. Biochem. Biotechnol*. **39–40,** 349–369.
3. Bon, E. P. S., Carvajal, E., Stambrough, M., and Magasanik, B. (1997), *Appl. Biochem. Biotechnol*. **63–65,** 203–212.
4. Oliveira, E. M. M., Carvajal, E., and Bon, E. P. S. (1999), *Appl. Biochem. Biotechnol*. **77–79,** 311–316.
5. Oliveira, E. M. M., Carvajal, E., Martins, A. S., and Bon, E. P. S. (2003), *Yeast* **20,** 31–37.
6. Dunlop, P. C., Meyer, G. M., and Roon, R. J. (1980), *J. Bacteriol*. **143,** 422–426.
7. Coffman, J. A. and Cooper, T. G. (1997), *J. Bacteriol*. **179,** 5609–5613.
8. Rowen, D. W., Esiobu, N., and Magasanik, B. (1997), *J. Bacteriol*. **179,** 3761–3766.
9. Roon, R. J., Murdockh, M., Kunze, B., and Dunlop, P. C. (1982), *Arch. Biochem. Biophys.* **219,** 101–109.
10. Pauling, K. D. and Jones, G. E. (1980), *J. Gen. Microbiol*. **117,** 423–430.
11. Miller, G. L. (1959), *Anal. Chem.* **31,** 426–428.
12. Kim, K. W. and Roon, R. J. (1983), *Biochemistry* **22,** 2704–2707.

0273-2289/04/113/0307–0319/$25.00

Studies on Immobilized Lipase in Hydrophobic Sol-Gel

Cleide M. F. Soares,[1] Onelia A. dos Santos,[1] Heizir F. de Castro,[2] Flavio F. de Moraes,[1] and Gisella M. Zanin*,[1]

[1]State University of Maringa, Department of Chemical Engineering, Av. Colombo 5790, Bloco D-90, 87020-900, Maringa-PR, Brazil, E-mail: gisellazanin@maringa.com.br; and [2]Faculdade de Engenharia Quimica de Lorena, Department of Chemical Engineering, PO Box 116, 12606-970, Lorena-SP, Brazil.

Abstract

The hydrolysis of tetraethoxysilane using the sol-gel process was used to produce silica matrices, and these were tested for the immobilization of lipase from *Candida rugosa* by three methods: physical adsorption, covalent binding, and gel entrapment in the presence and absence of polyethylene glycol (PEG-1450). The silica matrices and their derivatives were characterized regarding particle size distribution, specific surface area, pore size distribution (Brunauer, Emmett, and Teller [B.E.T.] method), yield of grafting (thermogravimetric analyzer [TGA]), and chemical composition (Fourier transform infrared). Immobilization yields based on recovered lipase activity varied from 3.0 to 32.0%, and the highest efficiency was attained when lipase was encapsulated in the presence of PEG.

Index Entries: Silica matrices; immobilization; lipase; additive; sol-gel.

Introduction

The sol-gel process is the name given to a number of processes in which a solution, or sol, undergoes a sol-gel transition. In this broadest sense, the term *sol-gel* refers to the preparation of inorganic oxides by wet chemical methods, irrespective of final form product—monolith, crystalline, or amorphous *(1)*. Using sol-gel materials for mechanical entrapment of enzymes permitted stabilization of the proteins, tertiary structure owing to the tight gel network *(2)*. Moreover, the easy insertion of substituent groups into

*Author to whom all correspondence and reprint requests should be addressed.

silicate matrix may provide the entrapped enzymes with a beneficial microenvironment *(3)*. Therefore, it is not surprising that a great effort has been dedicated to the development of encapsulating processes for increasing the enzyme activity, especially those like lipases (EC 3.1.1.3) with potential application in a number of industrial processes. Lipases are used as additives to detergents, in the manufacture of food ingredients, in pitch control in the pulp industry, and as biocatalyst of stereoselective transformations *(4,5)*. The works of several research groups *(2–5)* are good examples of how this new technology has been successfully applied to these enzymes.

In the sol-gel methodology, it is essential to prepare a homogeneous solution containing the catalytic precursor in order to uniformly coagulate the solution. Since the rate of polymerization of different precursors varies considerably, it is necessary to test them with respect to their reactive levels in polar solvents to form the matrix, or to increase their condensation rate, with the addition of an acid or base. Systems already tested for lipases from either microbial or animal sources include the utilization of different precursors (tetramethoxysila, methyltrimethoxyla, ethyltrimethoxysila, polydimethysiloxa, and others), stabilizing additives (alcohol polyvinyl, albumin, gelatin, and others), and solvents such as methanol and ethanol. The drying conditions vary as follows: xerogels are dried by evaporation of the liquid, and aerogels are usually obtained by removing solvents in hypercritical conditions *(6)*.

Chemical derivatization of silica particles, which enables covalent linkage of various compounds (either biologic or not), leads to considerable changes in their physical and chemical properties. Indeed, reacting the silica hydroxyl groups with selected silane compounds can produce specific silica carriers for immobilization reactions. Since the reactions take place at the support surfaces, knowledge of the texture of the carriers is of crucial importance. It has been recognized that the particle surface area and, especially, the pore size distribution greatly control the final behavior of the supports. The smaller the pore diameter, the higher the surface area, but small-diameter pores may limit biologic compound immobilization as well as diffusion of substrates and reaction products. Therefore, an extensive knowledge of the support properties is essential for better understanding the carrier's performance *(7,8)*.

Here we report on the sol-gel immobilization of commercial *Candida rugosa* lipase (CRL) and analyze the effect of different immobilizing techniques on its activity, by modifying a procedure previously established for a chemical catalyst *(9)*. Hydrophobic silica gels were prepared according to Dutoit et al. *(9)*, in a procedure consisting of dissolving tetraethoxysilane (TEOS) in ethanol followed by condensation with ammonium solution. The matrix obtained was used to immobilize the lipase from *C. rugosa* by three methods: physical adsorption (ADS), covalent binding (CB and CB1), and gel entrapment in the absence (EN1) or presence (EN2) of polyethylene glycol (PEG-1450). The materials obtained were characterized with respect to their morphologic properties—particle size, surface area, and pore size

distribution—and for the biocatalyst samples obtained after lipase immobilization, the immobilization yield was also determined.

Materials and Methods

Lipase, Chemicals, and Reagents

Commercial CRL (Type VII) was purchased from Sigma (St. Louis, MO). The lipase was a crude preparation with a nominal activity of 104.94 U/mg. The silane γ-aminopropyltriethoxysilane (γ-APTS) and glutaraldehyde (25% solution) were from Sigma. PEG 1450 (Sigma) was used as stabilizing agent. The silano precursor TEOS was from Aldrich (Milwaukee, WI). Ethanol (minimum of 99%), ammonia (minimum of 28%), HCl (minimum of 36%), and gum Arabic were from Synth (São Paulo, Brazil). Olive oil (low acidity) was purchased at a local market. Solvents were standard laboratory grade and other reagents were purchased from either Aldrich or Sigma.

Preparation of Sol-Gel

Method 1: Without Addition of Enzyme

The methodology previously established by Dutoit et al. *(9)* was used with some modifications as follows: Thirty milliliters of TEOS was dissolved in 36 mL of absolute ethanol under inert nitrogen atmosphere. To this, 0.22 mL of HCl dissolved in 5 mL of ultrapure water was slowly added, and the mixture was agitated (200 rpm) for 90 min at 35°C. Then, 1 mL of ammonium hydroxide dissolved in 6 mL of ethanol was added (hydrolysis solution), and the mixture was maintained under static conditions for 24 h to complete the condensation. The material was collected and dried by evaporation, which leads to the formation of xerogels *(6)*. The support obtained was used for immobilizing commercial CRL by ADS and covalent binding (CB).

Immobilization of Lipase by ADS

Lipase was immobilized by ADS on the support following the methodology of Pereira et al. *(10)* with slight modifications. Pure silica (1 g dry wt) was soaked previously in hexane under agitation (100 rpm) for 1 h. Excess hexane was then removed with a 10 mL pipet, and 0.3 g of powdered lipase dissolved in 10 mL of distilled water was added. The fixation of lipase onto the support was performed under agitation for 3 h at room temperature and followed by an additional period of 18 h under static conditions at 4°C. The derivative was filtered (Whatman filter paper no. 41) and thoroughly rinsed with hexane.

Immobilization of Lipase by CB

Silica gel was silanized with γ-APTS followed by reaction with glutaraldehyde solution, and then lipase was immobilized by CB according to the procedure described by Soares et al. *(11)*. The enzyme (0.3 g) was

dissolved in 10 mL of distilled water and mixed with the support (1 g dry wt) under slow agitation for 2 h at room temperature. To observe the influence of an additive, PEG was added together with the enzyme solution (5 mg/g of support, 200 μL of aqueous solution containing 50 mg of PEG/mL). Then, 10 mL of hexane was added and the mixtures enzyme-support (CB1) and enzyme-support-additive (CB2) were incubated overnight at 4°C. The immobilized lipase derivatives were filtered (Whatman filter paper no. 41) and thoroughly rinsed with hexane.

Method 2: With Addition of Lipase During Gel Formation

For the preparation of lipase-encapsulated derivatives, a procedure was adopted similar to that described for Method 1, except, in this case, the lipase solution (2.70 g of enzyme diluted in 15 mL of ultrapure water) was added simultaneously with the hydrolysis solution (NH_4OH). The encapsulation of CRL in the hydrophobic silica gels was performed in the absence and presence of PEG-1450, resulting in the EN1 and EN2 derivatives, respectively.

Activity-Coupling Yield

Hydrolytic activities of free and immobilized lipase were assayed by the olive oil emulsion method according to the modification proposed by Soares et al. *(11).* One unit of enzyme activity was defined as the amount of enzyme that liberated 1 μmol of free fatty acid/min under the assay conditions (37°C, pH 7.0, 150 rpm). Analyses of hydrolytic activities carried out on the lipase loading solution and immobilized preparations were used to determine the activity-coupling yield (η%), which measures the recovered enzymatic activity according to Eq. 1:

$$\eta(\%) = \frac{Us}{Uo} \times 100 \tag{1}$$

in which *Us* is the enzyme activity recovered on the support, and *Uo* is the total enzyme units offered for immobilization.

Assessment of Grafted Material

The amount of grafted material resulting from the lipase immobilization experiments was determined by weight loss in a TGA apparatus (TGA-50 Shimadzu Thermogravimetric Analyzer) over the range of 25–1000°C, with a heating rate of 20°C/min, using air as the purge gas. To eliminate error sources that could arise from the presence of residual reactants, the weight loss was only considered for temperatures above 130°C. The percentage of the grafted material was calculated using Eq. 2:

$$\text{Grafted material}\,(\%) = 100\left(w_i - w_f\right)/w_f \tag{2}$$

in which w_i and w_f are the initial and final weight of samples, respectively, the first taken at 130°C and the latter at 1000°C.

Table 1
Hydrolytic Activities and Activity-Coupling Yield
of Original Silica Gel Matrix and Immobilized Derivatives

Experiment	Hydrolytic activities (μmol/mg·min)	Activity-coupling yield (η%)[a]
ADS	41.5	12.04
CB1	27.3	7.93
CB2	24.8	7.20
EN1	66.4	13.92
EN2	128.9	31.98

[a]Calculated using Eq. 1.

Determination of Surface Area

The surface area measurements were performed by adsorption, using nitrogen as the adsorbate. The samples were previously degassed to below 50 mmHg at room temperature and the analyses were performed at 77 K, using liquid nitrogen. The equilibrium interval was 5 s. The surface area was calculated using the Brunauer, Emmett, and Teller (B.E.T.) method. Pore volume and area distributions based on BJH calculation (*8*) were evaluated by the B.E.T. apparatus software (NOVA 1200-Quantachrome).

Fourier Transform Infrared Spectroscopy

The samples of free lipase, pure silica (PS), silanized and activated silica, and immobilized derivatives were submitted to the Fourier Transform Infrared Spectroscopy (FTIR) analysis (Spectrophotometer FTIR BOMEM MB-100). The spectra were obtained in the wavelength range of 400–4000 cm^{-1} for evaluation of the immobilization procedures.

Results and Discussion

The support obtained by the sol-gel technique was used to immobilize commercial CRL following three procedures. In the first, the lipase was immobilized on PS by ADS; in the second, the enzyme was covalently bonded on the support previously silanized and activated with glutaraldehyde (SPS) in the absence (CB1) and presence of an additive (CB2); and, in the third, the enzyme was encapsulated in the absence (EN1) and presence of an additive (EN2).

Table 1 shows the activity-coupling yield (η%) results for the immobilization of lipase on hydrophobic silica gels. As expected, the activity-coupling yield for the lipase immobilized by ADS was very poor (η = 12.04%), probably owing to the inefficiency of this methodology for the silica support used. Similarly, experiments performed by covalent binding (CB1 and CB2) also gave low activity-coupling yield (η < 8.0%).

Table 2
Characterization of Original Silica Gel Matrix and Immobilized Derivatives

Experiment	Surface area (m^2/g)[a]	Mean pore diameter (Å)[a]	Pore volume (cm^3/g)[a]	w_i (mg)[b]	w_f (mg)[b]	Grafted material (%)[c]
PS	607.17	18.23	0.37	557	479	16.29
SPS	468.72	36.51	0.46	543	488	11.27
ADS	556.30	14.30	0.46	410	374	9.62
CB1	560.10	14.46	0.49	417	375	10.07
CB2	531.10	14.39	0.43	451	409	9.31
EN1	382.32	49.99	0.48	518	430	16.99
EN2	300.22	56.59	0.43	403	329	18.36

[a] Evaluated from B. E. T
[b] w_i and w_f are the initial and final weight of samples, respectively.
[c] Calculated using Eq. 2;

It is possible that the silanization and activation of the PS might induce conformational changes in the enzyme chains on its adhesion on the support surface leading to the low activity-coupling yields observed. These changes in structure may cause steric hindrance, which makes certain areas of the enzyme molecule inaccessible to the substrate (olive oil). In this case, the addition of an additive (PEG-1450) did not produce a beneficial effect. However, the positive effect of the PEG was noticed for the derivatives obtained by the encapsulation technique (EN2). The highest coupling yield (31.98%) was observed for the immobilized derivative obtained by lipase encapsulation in the presence of PEG-1450, confirming the effectiveness of this kind of additive *(12,13)*.

Concerning the physical characteristics (*see* Table 2), EN1 and EN2 derivatives showed the largest mean pore diameter, 49.99 and 56.58 Å, respectively. These values are greater than the mean pore diameter obtained by the traditional immobilization techniques: ADS, CB1, and CB2 (14.30, 14.46, and 14.39 Å, respectively), which gave very close results.

Figure 1 shows the pore size distribution of primary supports and the immobilized derivatives in silica matrix on an incremental (derivative) basis, dV/d Log (D), to highlight the differences among the immobilized derivatives in silica gels. The computation of pore size distribution, from gas adsorption, was based on the BJH method using the desorption branch. From these plots it was observed that all solid samples (PS, SPS, ADS, CB1, CB2, EN1, and EN2) exhibit a unimodal distribution of pores, and the smaller mean pore diameters were observed with the samples PS, ADS, CB1, and CB2 (Table 2).

Pore volume, surface area, and mean pore diameter were influenced by the methodology of producing the silica derivatives, and the greatest

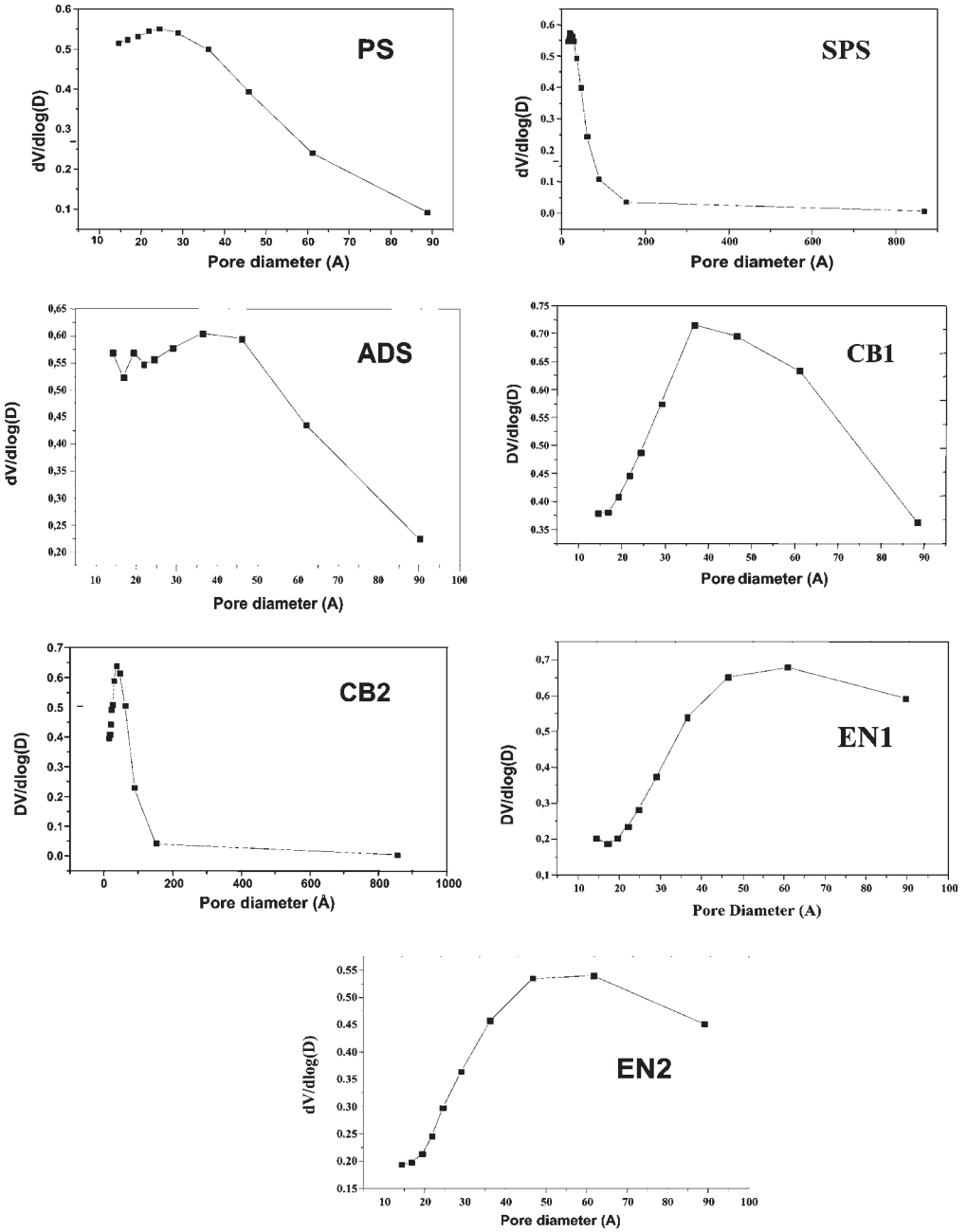

Fig. 1. Pore size distributions (dV/d Log [D]) of pure silica gel (PS), silanized and activated silica (SPS), and immobilized derivatives in silica gels (ADS, silica with lipase physically adsorbed; CB1, silica with lipase covalently bonded; CB2, silica with lipase covalently bonded in the presence of PEG; EN1, silica with entrapped lipase; EN2, silica with lipase entrapped in presence of PEG).

deviations of the mean behavior were observed with the biocatalysts produced by the encapsulation technique. Lipase encapsulated in the presence of the additive PEG showed the largest mean pore size (56.59 Å), and an increase of about 6.6 Å in relation to the mean pore size of the lipase encapsulated in the absence of PEG (Table 2 and Fig. 1). Results described by Keeling-Tucker et al. *(14)* also showed an increase in the pore size with the addition of organic macromolecules, and this was associated mainly with the encapsulation of those macromolecules that inhibit gel contraction during the synthesis of the support.

Several works have explained the occurrence of a step change in adsorption isotherms by the structural orientation of the adsorbed species and also by the manner in which the adsorption occurred *(15)*. However, none related the activity-coupling yield observed with different techniques of lipase immobilization in hydrophobic sol-gels to the adsorption isotherms of the supports.

Similar adsorption isotherms were obtained for samples PS and SPS, and for the lipase immobilized derivatives of silica gels (ADS, CB1, CB2, EN1, and EN2). Typical examples are shown in Fig. 2. We observed hysteresis loops in the adsorption-desorption isotherms, denoting materials with well-defined ordered structures, and the presence of mesopores, with hysteresis loops between isotherms types H1 and H2 *(8,16)*. Primarily on the mesopores of silica, a multilayer of adsorbate is formed, increasing the relative pressure, and depending on the mean pore diameter, at $P/P_0 \approx 0.4$, capillary condensation takes place on the multilayer, resulting in a further increase in pore volume *(1)*.

The parameters of the pore structure, such as surface area, pore volume, and mean pore diameter, can generally be used for a formal description of the porous systems, irrespective of their chemical composition and their origin, and for a more detailed study of the pore formation mechanism, the geometric aspects of pore structure are important. This picture, however, oversimplifies the situation because it provides a pore uniformity that is far from reality. Thorough attempts have been made to achieve the mathematical description of porous matter. Researchers discussed the cause of porosity in various materials and concluded that there are two main types of material based on pore structure that can be classified as corpuscular and spongy systems. In the case of the silica matrices obtained with TEOS and other precursors, the porous structure seems to be of the corpuscular type, in which the pores consist of the interstices between discrete particles of the solid material. In such a system, the pore structure depends on the pores mutual arrangements, and the dimensions of the pores are controlled by the size of the interparticle volumes *(1)*.

The stepped intrusion curves clearly denote different pore size ranges. In the case of experiments EN1 and EN2, this is possibly the reason for the mean pore diameter and activity-coupling yield being the highest. The specific surface areas obtained for all experiments are listed in Table 2.

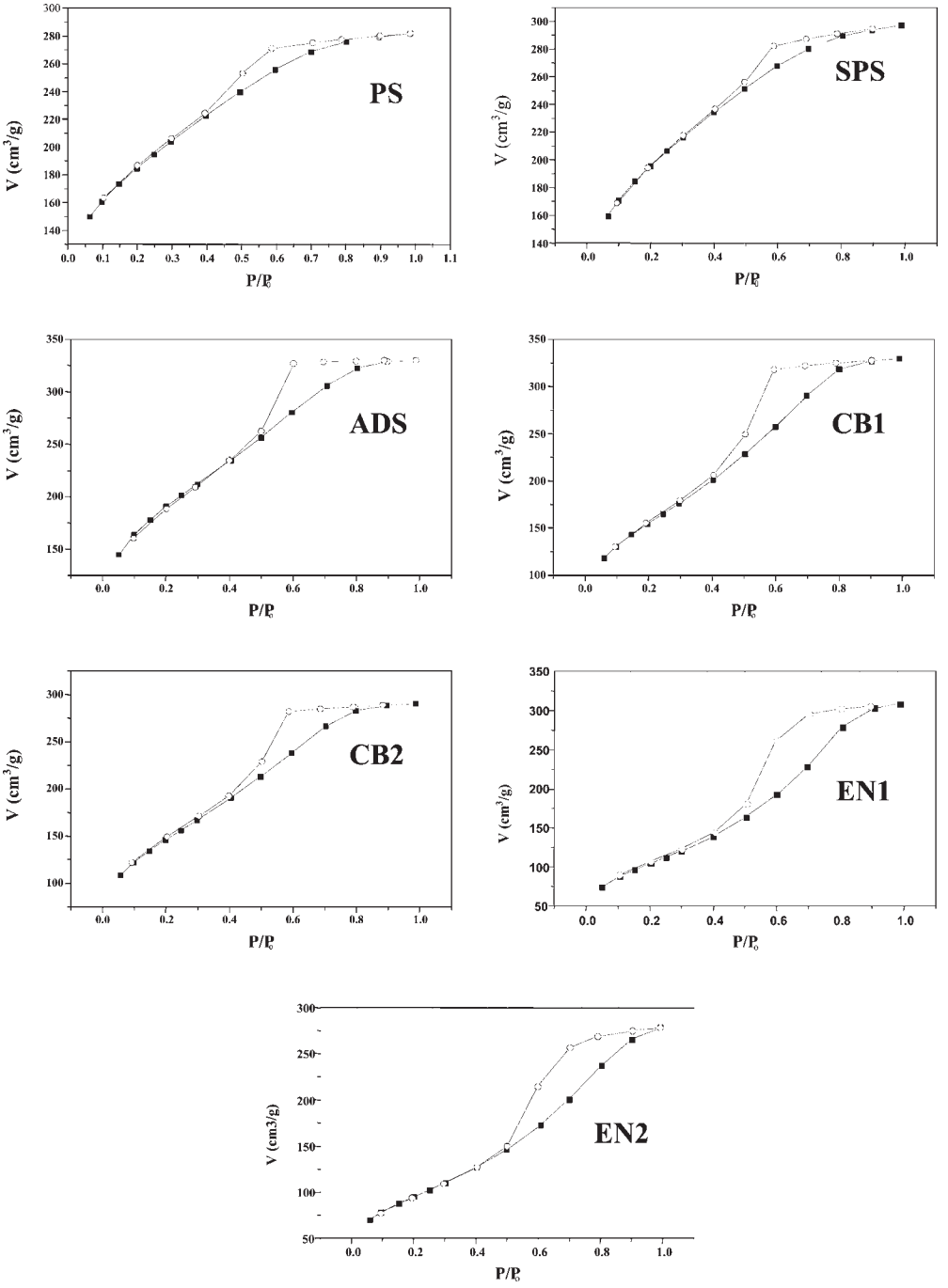

Fig. 2. Gas adsorption/desorption isotherms obtained for pure silica gel (PS), silanized and activated silica (SPS), and immobilized derivatives in silica gels (ADS, silica with lipase physically adsorbed; CB1, silica with lipase covalently bonded; CB2, silica with lipase covalently bonded in presence of PEG; EN1, silica with entrapped lipase; EN2, silica with lipase entrapped in presence of PEG). (○),Adsorption; (■), desorption.

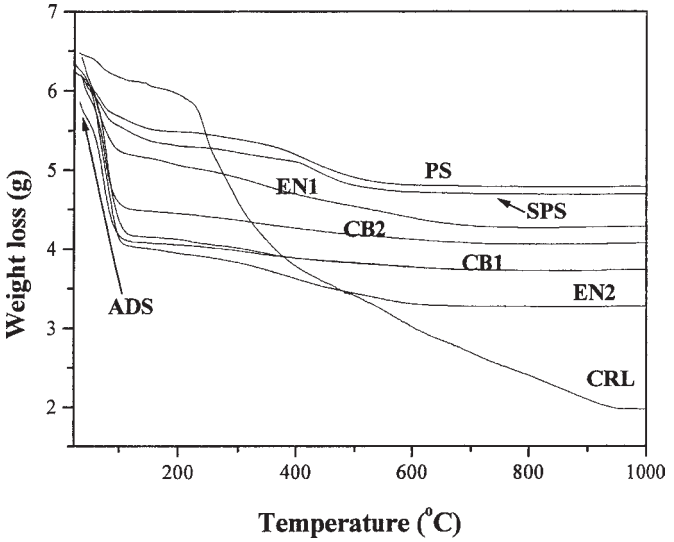

Fig. 3. Loss of grafted mass by heating of immobilized lipase samples. TGA profiles are shown for the free lipase (CRL), original silica (PS), silanized derivative (SPS), and immobilized derivatives (ADS, silica with lipase physically adsorbed; CB1, silica with lipase covalently bonded; CB2, silica with lipase covalently bonded in presence of PEG; EN1, silica with entrapped lipase; EN2, silica with lipase entrapped in presence of PEG).

Although the knowledge of the sample surface area is important, as already pointed out, the pore size distribution is even more critical, since it greatly affects the activity-coupling yield of the biologic immobilization because of the diffusion-controlled phenomena.

From the results presented in Tables 1 and 2, it can be observed that in general the greater the mean pore diameter, the higher the percentage of grafted material (calculated using Eq. 2 and taking into consideration the weight loss as a function of temperature, as shown in Fig. 3). The percentage of grafted material can also be correlated with the activity-coupling yield, as displayed in Fig. 4. In this set of experiments, the highest values for the activity-coupling yield and for the percentage of grafted material were observed for the derivatives obtained by encapsulation in the presence of an additive (EN2).

To verify the efficiency of the methodology in relation to the incorporation of lipase in silica gel matrices, infrared spectroscopy was used. Figure 5 shows the spectra of the free lipase (CRL), pure silica gel (PS), silanized and activated silica (SPS), and immobilized derivatives in silica gels (ADS, CB1, CB2, EN1, and EN2).

The immobilized lipase derivatives have shown the same characteristic bands—950 (Si-O-Si stretching), 810 (Si-O-Si- stretching), and 600 (Si-O-Si bending) cm^{-1} bands *(7,17)*, as the supports (PS and SPS). The

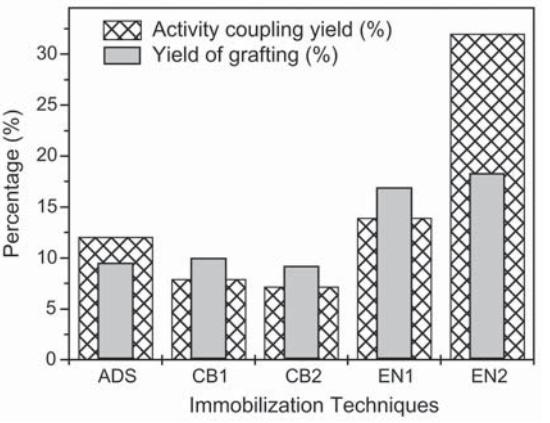

Fig. 4. Comparison of activity-coupling yield (η%) and yield of grafting for samples of CRL immobilized on silica hydrophobic matrices by different methodologies.

negative effect in the recovered activity yield of the silane used to activate the support for covalent binding can be observed in the considerable differences in the percentage of –OH groups (3400 cm^{-1} bands) exhibited in the spectra of the PS and SPS samples (Fig. 5A,B).

As described in the literature *(7,17)*, the lipase enzyme has two characteristic bands at 1650 and 1600 cm^{-1} (primary and secondary amino groups), and these are clearly shown in Fig. 5A,B. These bands are also displayed in the spectra for the immobilized derivatives (ADS, CB1, CB2, EN1, and EN2), revealing, owing to the greater peak height, a higher efficiency for the encapsulation technique in the presence of PEG (EN2), when compared with the other tested methods. Further information on the catalytic activity was obtained by testing the derivatives according to our method for synthetic applications—i.e., the esterification of *n*-butanol with butyric acid *(10–12)*. This reaction was selected because it gave measurable results with great accuracy in a short span of time and with a minimum amount of lipase *(11,12)*. In addition, this reaction system has been used by our group as a standard reaction system for testing lipases immobilized in several supports *(10,11,18)*.

Conclusion

Various lipase immobilization methods were tested with different silica matrices, and the immobilized enzyme samples were examined by morphologic, physicochemical, and biochemical characterization methods. The results allowed correlation of the activity-coupling yield of different immobilization methods in relation to the incorporation of lipase in the silica gels and showed that the most active biocatalyst resulted from the encapsulation of commercial CRL in the presence of PEG.

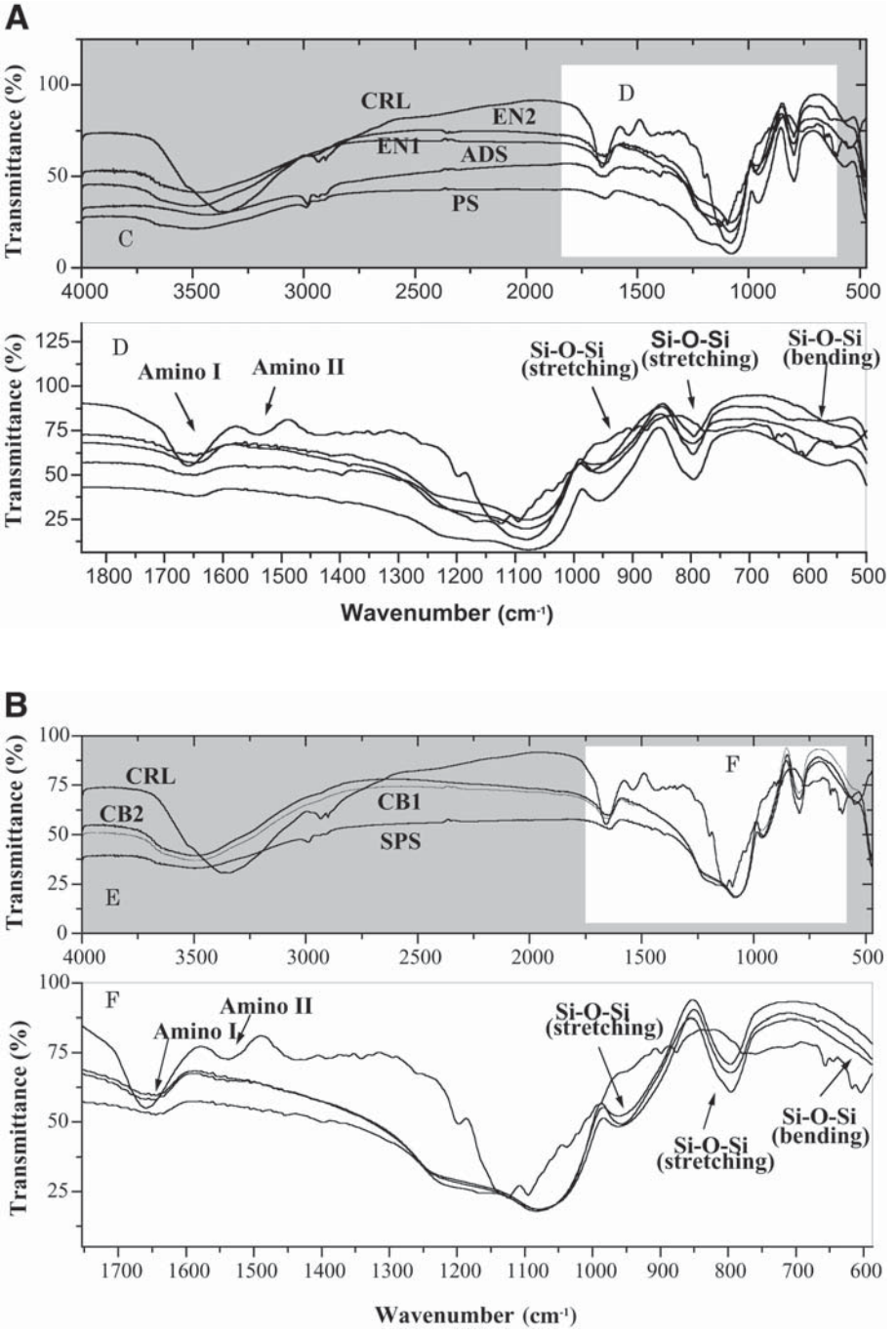

Fig. 5. **(A)** FTIR spectra for free lipase (CRL), original silica (PS), and immobilized derivatives (ADS, silica with lipase physically adsorbed; EN1, silica with entrapped lipase; EN2, silica with entrapped lipase in presence of PEG). **(B)** FTIR spectra for free lipase (CRL), silanized derivative (SPS), and immobilized derivatives (CB1, silica with lipase covalently bonded; CB2, silica with lipase covalently bonded in presence of PEG).

Acknowledgments

We acknowledge financial assistance from Coordenação de Aperfeiçoamento de Pessoal de Nível Superior and Conselho Nacional de Desenvolvimento Científico e Tecnológico.

References

1. Unger, K. K. (1979), *Porous Silica: Its Properties and Use as Support in Column Liquid Chromatography*, Elsevier, New York, NY.
2. Kauffmann, C. and Mandelbaum, R. T. (1998), *J. Biotechnol.* **62,** 169–176.
3. Reetz, M. T., Zonta, A., and Simpelkamp, J. (1996), *Biotechnol. Bioeng.* **49,** 527–534.
4. Pierre, A. and Buisson, P. (2001), *J. Mol. Catal. B: Enzymatic* **11,** 639–647.
5. Buisson, P., Hernandez, C., Pierre, M., and Pierre, A. C. (2001), *J. Non-Crystalline Solids* **285,** 295–302.
6. Siouffi, A. M. (2003), *J. Chromatogr.* **1000,** 801–818.
7. Bosley, J. A. and Peilow, A. D. (1997), *J. Amer. Oil Chem. Soc.* **74(2),** 107–111.
8. Ramos, M. A., Gil, M. H., Schact, E., Matthys, G., Mondelaers, W., and Figueiredo, M. M. (1998), *Powder Technol.* **99,** 79–85.
9. Dutoit, D.C. M., Schneider, M., Fabrizioli, P., and Baiker, A. (1996), *Chem. Mater.* **8,** 734–743.
10. Pereira, E. B. (1999) MS thesis, Chemical Engineering Department, State University of Maringa, Maringa-PR, Brazil.
11. Soares, C. M. F., Castro, H. F., Moraes, F. F., and Zanin, G. M. (1999), *Appl. Biochem. Biotechnol.* **77–79,** 745–758.
12. Soares, C. M. F., Castro, H. F., Santana, M. H., and Zanin, G. M. (2001), *Appl. Biochem. Biotechnol.* **91–93,** 715–719.
13. Soares, C. M. F., Castro, H. F., Santana, M. H., and Zanin, G. M. (2002), *Appl. Biochem. Biotechnol.* **98–100,** 703–718.
14. Keeling-Tucker, T., Rakic, M., Spong, C., and Brennan, J. D. (2000), *Chem. Mater.* **12,** 3695–4704.
15. Al-Duri, B. and Yong, Y. P. (2000), *Biochem.l Eng. J.* **4,** 207–215.
16. Ravikovitch, P. I. and Neimark, A. V. (2000), *Langmuir* **18,** 9830–9837.
17. Assis, O. B. G. (2003), *Braz. J. Chem. Eng.* **20(3),** 339–342.
18. De Castro, H. F., Oliveira, P. C., Soares, C. M. F., and Zanin, G. M. (1999), *J. Amer. Oil Chem. Soc.* **76(1),** 125–131.

Volume 114

Session 2

Introduction to Microbial Catalysis and Engineering

Session 2

Introduction to Microbial Catalysis and Engineering

Thomas W. Jeffries[1] and Lee R. Lynd[2]

[1]USDA, Forest Service, Forest Products Laboratory, Madison, WI; and [2]Thayer School of Engineering and Department of Biological Sciences, Dartmouth College, Hanover, NH

The development of microbial catalysts has been an integral part of this symposium series since its inception. The first symposium on biotechnology in energy production and conservation, which was held in Gatlinburg, TN, on May 10–12, 1978, included presentations on large-scale algal production, improved cellulase-producing strains of *Trichoderma reesei*, simultaneous cellulose hydrolysis and ethanol production by *Clostridium thermocellum*, and improved microbial strains for commercial nitrogen fixation. In this most recent symposium, we have seen a continuing interest in biologic hydrogen production, cellulases, and saccharification, but, at the same time, the field has become increasingly diverse as new methodologies and process concepts have emerged.

This year's lecture and poster sessions on microbial catalysts and engineering were among the biggest ever, and the range of research topics was very broad. There were 6 oral presentations and 50 published abstracts. Keeping with the trend in recent years, many of the presentations dealt with genetically engineered microbial strains, but the target products ranged widely. Ethanol, polyhydroxyalkanoates, organic acids, xylitol, hydrogen, biosurfactants, cellulases, and xylanases were all well represented. Producing organisms included yeasts, bacteria, fungi, and algae.

Genomics and genomewide expression analyses have strongly affected strain development and were well represented in this year's symposium. In contemporary biocatalyst development, it is common to start with a total genome, predict the optimal path through models, and change the organism toward a desired end. At least six of the presentations made use of genomics, microarray, or other high-throughput screening technologies in the development and characterization of biocatalyst. The Department of Energy has been very active in sponsoring genome sequencing for microbes that have significant or potential roles in bioconversion, so this trend is certain to increase in coming years.

Many novel bioengineering approaches were also presented. These ranged from the bioelectrosynthesis of chemicals and fuels to the biocon-

version of syngas to ethanol. Over the years, international symposium participants often have offered diverse, stimulating perspectives and processes, and this was much in evidence at this year's meeting. Almost half of all the submissions were from scientists outside of the United States, and many of these were on topics that do not receive as much domestic attention as they deserve.

The development of microbial catalyst remains a highly vibrant, challenging, and rapidly expanding part of the symposium, and we expect that it will continue to play an important role in future years.

0273-2289/04/114/0325–0334/$25.00

Polykaryon Formation Using a Swollen Conidium of *Trichoderma reesei*

Hideo Toyama,* Makiko Yano, and Takeshi Hotta

Department of Health and Nutrition, Minamikyushu University, Kirishima 5-1-2, Miyazaki 880-0032, Japan, E-mail: gaf00771@nifty.com

Abstract

The cellulolytic fungus, *Trichoderma* has oval and mononucleate conidia. When these conidia are incubated in a liquid medium, they begin to swell and their shape becomes spherical followed by an increase in inner space. In such swollen conidia, it is possible to produce a larger autopolyploid nucleus using a mitotic arrester compared with the case of the original conidia. In this study, polykaryon formation was attempted using these swollen conidia. Dried mature green conidia of *Trichoderma reesei* QM6a (IFO 31326) were incubated in Mandel's medium in order to swell. The swollen conidia were treated with a mitotic arrester, colchicine, for autopolyploidization. After autopolyploidization, polykaryon formation was carried out using the swollen conidia. After the treatment, multiple smaller nuclei whose diameter was almost the same as that of the original strain were generated from an autopolyploid nucleus in a swollen conidium. A cellulase hyperproducer without decrease in growth rate could be selected using such swollen conidia.

Index Entries: *Trichoderma reesei*; polykaryon; cellulase; colchicines; polyploid.

Introduction

We attempt to develop a new breeding system for *Trichoderma reesei* without gene-engineering techniques for the safety of food. As a result, we previously reported the new breeding techniques using colchicine and benomyl for this fungus *(1)*. A mitotic arrester, colchicine, causes autopolyploidization and benomyl causes deletion and recombination of chromosomes in an autopolyploid nucleus of this fungus *(2,3)*. When the new techniques were applied on this fungus, the cellulase productivity per mycelia increased but the growth rate tended to decrease *(1)*. The growth rate of such a low-growing strain of this fungus could be recovered by additional autopolyploidization, but it took substantial time *(4)*.

*Author to whom all correspondence and reprint requests should be addressed.

We examined new conditions of these techniques in order to construct strains whose cellulase productivity increases and the growth rate does not decrease without additional autopolyploidization. At first, it was considered that cellulase genes are amplified in an autopolyploid nucleus of this fungus. However, the cellulase productivity of an autopolyploid strain did not increase (data not shown). In other words, the cellulase productivity of an autopolyploid strain seemed not to be directly related to the amplified cellulase genes. Thus, we investigated the change in cellulase productivity by altering the nuclear nature of an autopolyploid nucleus. For that purpose, we tried to produce smaller nuclei whose diameter is almost the same as that of the original strain from an autopolyploid nucleus in a swollen conidium of this fungus by polykaryon formation technique.

Materials and Methods

Microorganism and Medium

T. reesei QM6a (IFO 31326) was used as a model strain. This fungus was cultivated on potato dextrose agar (PDA) medium (Wako, Osaka, Japan) at 28°C and preserved at 4°C. For swelling of conidia, Mandels' medium containing 0.5% (w/v) peptone (Wako) and 1.0% (w/v) glucose (Wako) (pH 6.0) was used. Mandels' medium was composed of 1.4 g of $(NH_4)_2SO_4$, 2.0 g of KH_2PO_4, 0.3 g of urea, 0.3 g of $CaCl_2$, 0.3 g of $MgSO_4 \cdot 7H_2O$, 0.005 g of $FeSO_4 \cdot 7H_2O$, 0.0016 g of $MnSO_4 \cdot H_2O$, 0.0014 g of $ZnSO_4 \cdot H_2O$, 0.0020 g of $CoCl_2$ (all from Wako), and 1000 mL of distilled water: (pH 6.0) *(5)*.

As the medium for autopolyploidization, Mandels' medium containing 0.5% (w/v) peptone, 1.0% (w/v) glucose, and 0.1% (w/v) colchicine (Wako) was used (pH 6.0). As the medium for polykaryon formation, Mandels' medium containing 0.5% (w/v) peptone, 1.0% (w/v) glucose, and 0.5% or 2.0% (w/v) colchicine was used (pH 6.0).

For the selection medium, 96 mL of the Mandels' medium containing 1.0 g of Avicel (Funakoshi, Tokyo, Japan), 0.5 g of peptone, 1.0 g of wood powder (*Fagus crenata*), 0.1 mL of polyoxyethyleneoctylphenylether (Triton X-100) (Wako), 1.5 g of agar (Difco, Detroit, MI), and conidia (the bottom layer medium) was added to a deep glass plate (150-mm diameter and 60-mm depth) and left at 4°C in order to harden the agar *(6)*. After the agar hardened, 196 mL of Mandels' medium containing 1.0 g of Avicel, 0.5 g of peptone, 1.0 g of wood powder, 0.1 mL of Triton X-100, and 1.5 g of agar (the upper layer medium) was added to the bottom layer of medium and the agar was hardened at 4°C.

For the solid medium for the estimation of cellulase productivity, Mandels' medium containing 1.0% (w/v) carboxymethylcellulose sodium salt (CMC-Na) (degree of substitution [D.S.] 0.7) (Wako), 0.5% peptone, 1.5% (w/v) agar, and 0.1% (v/v) Triton X-100 was used (pH 6.0). For measurement of cellulose hydrolyzing activity, 7.5 g of wheat bran was added to 7.5 mL of Mandels' medium in a 100-mL Erlenmeyer flask.

Preparation of Dried Mature Green Conidia

A mycelial mat (3×3 mm) was put on the PDA medium and incubated for 2 wk at 28°C in order to generate mature green conidia. Conidia generated on the PDA medium were added to 50 mL of sterilized distilled water in a 100-mL Erlenmeyer flask and suspended well. The conidial suspension was filtrated with a glass filter 3G-2 in order to remove hyphae. Conidia were collected by centrifugating at 5510*g*. The collected conidia were dried in a desiccator containing silica gel (Wako). These conidia were used for experiments as dried mature green conidia *(7)*.

Nuclear Staining of Conidia

Conidia were fixed on a slide glass by heating and treated with 5 *N* HCl (Wako) for 40 min followed by washing with tap water. After washing, the treated conidia were immersed in Giemsa solution (Merck, Darmstadt, Germany) for 30 min followed by washing with tap water for observation with a microscope (BH-2; Olympus, Tokyo, Japan) *(8)*. The HCl-treated conidia were also stained with 0.1 µg/mL 4.6'-diamidino-2-phenylindole (DAPI) (Sigma, St. Louis, MO) solution followed by observation using a fluorescent microscope (BX-50; Olympus) *(9)*. Photomicrographs were taken using a microscope with an automatic exposure meter (PM-CBAD; Olympus) and a camera (C35AD; Olympus), and the photographs were then enlarged. The diameter and number of conidia were measured using a digital caliper (Mitsutoyo, Koshigaya, Japan) on enlarged photographs.

Preparation of Swollen Conidia

Dried mature green conidia were added to 50 mL of the medium for swelling in a 100-mL Erlenmeyer flask and incubated for 6 h at 28°C using a rotary shaker (TAITEC R-30 mini; Taitec, Koshigaya, Japan) (160 rpm). The changes in conidium and nucleus were then observed using a microscope (BH-2, BX-50; Olympus) with or without nuclear staining.

Autopolyploidization

Swollen conidia were added to 25 mL of the medium for autopolyploidization in a 50-mL Erlenmeyer flask and incubated statically for 7 d at 28°C. The nuclear changes were then observed by nuclear staining using microscopes.

Polykaryon Formation

The swollen conidia containing autopolyploid nuclei were added to 25 mL of the medium for polykaryon formation in a 50-mL Erlenmeyer flask and incubated statically for 3 or 7 d at 28°C. The nuclear changes were then observed by nuclear staining using microscopes.

Selection of Cellulase Hyperproducer

After polykaryon formation, the treated swollen conidia containing multiple smaller nuclei were added to the bottom layer of selection medium and left for 60 min at 4°C to harden the agar. The upper layer selection medium was then overlayed and left for 60 min at 4°C in order to harden the agar, and the conidia were incubated at 28°C.

Comparison of Cellulase Productivity on Solid Medium

A mycelial mat (2 × 2 mm) was put on the center of the solid medium for estimation of cellulase productivity and incubated for 6 d at 28°C. Then, 0.1% (w/v) Congo red solution (Wako) was added to the plate and left for 1 h, followed by washing with 1 *M* NaCl (Wako). The diameter of a clear zone around a colony and the diameter of the colony were measured using a digital caliper (Mitsutoyo).

Measurement of Cellulose Hydrolyzing Activity

A mycelial mat (2 × 2 mm) was added to the medium for the measurement of cellulose hydrolyzing activity in a 100-mL Erlenmeyer flask and incubated at 28°C for 5 d. Three flasks were used for one strain and shaken once a day. After incubation, 15 mL of 0.1 *M* acetate buffer (pH 5.0) was added, stirred using a glass rod, and left to stand for 1 h. The enzyme solution was then extracted from the wheat bran culture using a nylon cloth. The extracts were centrifuged at 5510*g*, and the top clear portion was used as the enzyme solution. As the substrates of enzyme reaction, 1.0 g of Avicel (Funakoshi), CM-cellulose (Wako), or Salicin (Wako) was added to 99 mL of 0.1 *M* acetate buffer (pH 5.0). Then 0.2 mL of enzyme solution and 4.0 mL of substrate were mixed and incubated for 120 min at 40°C using a reciprocal shaker (Thomastat T-22S; Thomaskagaku, Tokyo, Japan). The agitation speed was 125 strokes/min. The reaction mixture was filtrated with filter paper (no. 2; Whatman, Maidstone, UK). The amount of reducing sugar in the reaction mixture was measured using dinitrosalicylic acid (DNS) (Wako) *(10)*. One unit (IU) was defined as the amount of enzyme-producing reducing sugar equivalent to 1 μmol of glucose/min.

Results

Formation of Swollen Conidia

Dried mature green conidia, which are mononucleate, were incubated in the medium for swelling of conidia for 6 h at 28°C using a rotary shaker. After incubation, the conidia became spherical and the inner volume increased. However, the mononucleate nature of *Trichoderma* was maintained and the diameter was unchanged *(7)*. Such conidia, called swollen conidia, were used for the experiments.

Autopolyploidization

Swollen conidia were incubated statically in the medium for autopolyploidization for 7 d at 28°C. After incubation, it appeared that a larger

Table 1
Changes in Number and Diameter of Nucleus in Swollen Conidia

Nuclear number	Proportion (%)	Nuclear diameter (μm)	Proportion (%)
Swollen conidia containing autopolyploid nuclei			
1	100	0.10–0.49	0
2	0	0.50–0.89[a]	0
3	0	0.90–1.29	0
4	0	1.30–1.69	0
5	0	1.70–2.09	4
6	0	2.10–2.49[b]	96
Swollen conidia treated with 0.5% colchicine for 3 d			
1	18	0.10–0.49	0
2	26	0.50–0.89[a]	0
3	44	0.90–1.29	5
4	12	1.30–1.69	10
5	0	1.70–2.09	12
6	0	2.10–2.49[b]	73
Swollen conidia treated with 2.0% colchicine for 3 d			
1	63	0.10–0.49	2
2	21	0.50–0.89[a]	33
3	12	0.90–1.29	5
4	4	1.30–1.69	10
5	0	1.70–2.09	8
6	0	2.10–2.49[b]	42
Swollen conidia treated with 0.5% colchicine for 7 d			
1	0	0.10–0.49	0
2	8	0.50–0.89[a]	15
3	34	0.90–1.29	49
4	41	1.30–1.69	36
5	17	1.70–2.09	0
6	0	2.10–2.49[b]	0

[a] Nuclear diameter of original strain.
[b] Diameter of autopolyploid nucleus.

nucleus was produced in one swollen conidium by nuclear staining using Giemsa solution or DAPI solution, as shown in Table 1 and Fig. 1. This larger nucleus was regarded as an autopolyploid nucleus.

Polykaryon Formation

The swollen conidia containing autopolyploid nuclei were incubated statically in the medium for polykaryon formation containing 0.5 or 2.0% (w/v) colchicine for 3 or 7 d at 28°C. When these swollen conidia were treated with 2.0% colchicine for 3 d, micronucleation occurred, as shown

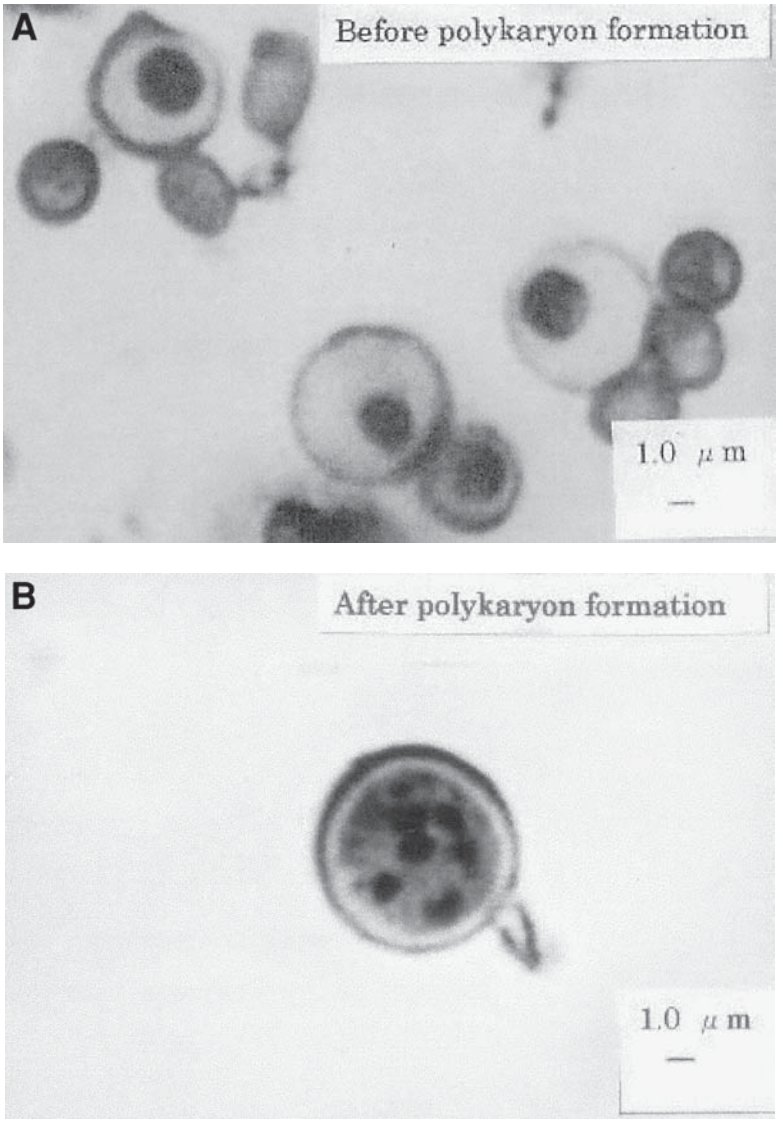

Fig. 1. **(A)** Autopolyploid nuclei produced with 0.1% (w/v) colchicine solution. **(B)** Nuclei after treatment with 0.5% (w/v) colchicine.

in Table 1. This phenomenon was also seen when the swollen conidia were treated with 2.0% colchicine for 7 d (data not shown). However, when the swollen conidia were treated with 0.5% colchicine for 7 d, multiple smaller nuclei whose diameter was almost the same as that of the original nucleus were generated from one autopolyploid nucleus, and the autopolyploid nucleus disappeared, as shown in Table 1 and Fig. 1. Thus, we used 0.5% colchicine in order to cause polykaryon formation.

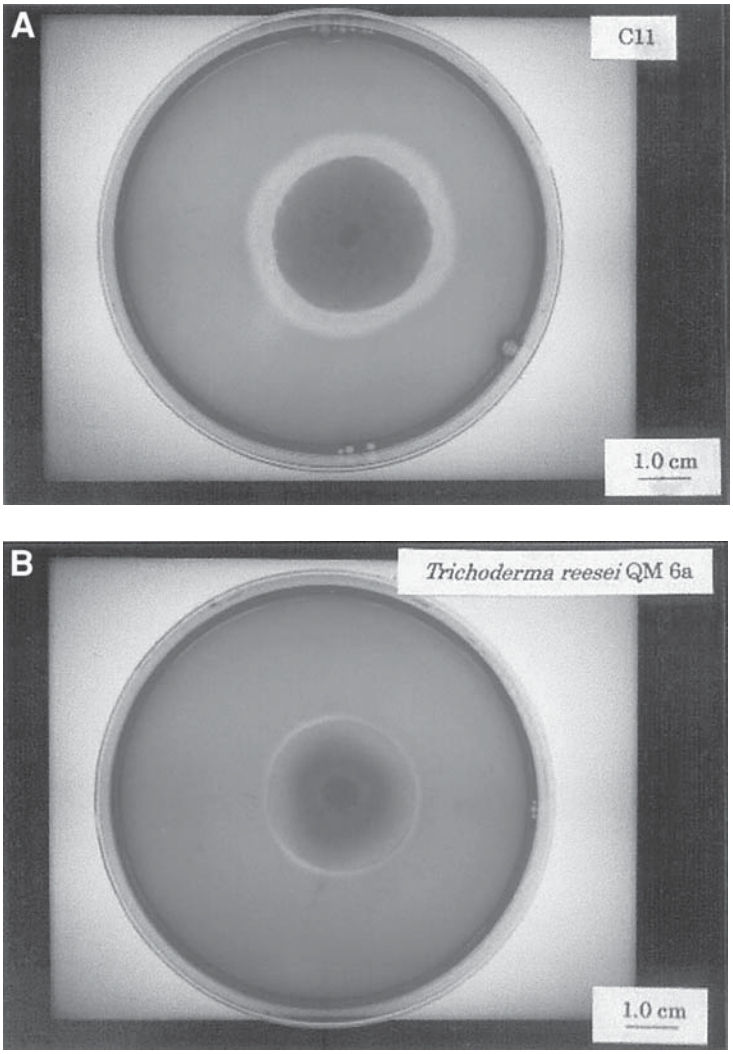

Fig. 2. Cellulase production of *T. reesei* QM6a and strain C11. A mycelial mat (2 × 2 mm) was incubated on the medium to estimate cellulase productivity for 6 d at 28°C. After incubation, 0.1% (w/v) Congo red solution was added to the plate and left for 1 h, followed by washing with 1 *M* NaCl. After washing, the diameter of a clear zone around a colony and the diameter of the colony were measured using a digital caliper.

Selection of Cellulase Hyperproducer

The swollen conidia treated with 0.5% colchicine for 7 d after auto-polyploidization were incubated in the double layer selection medium for 10 d at 28°C in order to select cellulase hyperproducers. After incubation, 35 colonies appeared on the surface of the selection medium. Those colonies were used for estimation of cellulase productivity on the solid medium.

Table 2
Cellulase Productivity of *T. reesei* QM6a and Strain C11 on Solid Medium[a]

Strain	Diameter of clear zone	Diameter of colony (mm)
T. reesei QM6a	32.54 ± 0.81	30.76 ± 0.64
C11	42.32 ± 0.95	32.65 ± 1.01

[a]A mycelial mat (2 × 2 mm) was incubated on the medium for estimation of cellulase productivity for 6 d at 28°C. After incubation, the diameter of a clear zone and the diameter of a colony were measured with a digital caliper. Those values are average of nine plates in each strain.

Estimation of Cellulase Productivity on Solid Medium

Mycelial mats of the selected 35 strains and the original strain were incubated on the medium for estimation of cellulase productivity for 6 d at 28°C in order to compare cellulase productivity. After Congo red staining, strain C11, showed the highest cellulase productivity. Moreover, the cellulase productivity of strain C11 was compared with that of the original strain using 18 agar plates of the medium for estimation of cellulase productivity. After incubation, strain C11 showed superior cellulase productivity, as shown in Fig. 2 and Table 2. Thus, strain C11 was selected as a cellulase hyperproducer.

Nuclear Characteristics in Conidium of Strain C11

The nuclear nature of the conidia of strain C11 was observed. For this purpose, a mycelial mat of strain C11 was incubated on a PDA plates for 7 d at 28°C in order to generate green conidia. After nuclear staining of these conidia using Giemsa solution or DAPI solution, it appeared the number of nuclei in the conidia of strain C11 ranged from one to four although the original conidia were mononucleate, as shown in Table 3. Furthermore, the mycelia of strain C11 were observed by nuclear staining. As a result, a larger number of nuclei were observed in the mycelia of strain C11 compared with that of the original strain (data not shown). Thus, the genetic conditions of the mycelia of strain C11 were regarded as polykaryon.

Measurement of Cellulose Hydrolyzing Activity

The cellulose hydrolyzing activity of strain C11 and the original strain was compared using the medium for measurement of cellulose hydrolyzing activity. As a result, the Avicel and CMC hydrolyzing activity of strain C11 was increased more than that of the original strain, as shown in Table 4. The Salicin hydrolyzing activity of strain C11 was almost the same as that of the original strain.

Table 3
Nuclear Diameter and Number of Conidia of Strain C11 Derived from Swollen Conidia Treated with 0.5% Colchicine for 7 d

Nuclear number	Proportion (%)	Nuclear diameter (μm)	Proportion (%)
1	11	0.10–0.49	17
2	55	0.50–0.89[a]	47
3	32	0.90–1.29	36
4	2	1.30–1.69	0
5	0	1.70–2.09	0
6	0	2.10–2.49[b]	0

[a] Nuclear diameter of original strain.
[b] Diameter of autopolyploid nucleus.

Table 4
Cellulose Hydrolyzing Activity in *T. reesei* QM6a and Strain C11[a]

	Hydrolyzing activity		
Strain	Avicel	CMC	Salicin (IU/mL)
T. reesei QM6a	46 ± 7	46 ± 0	37 ± 6
C11	53 ± 6	70 ± 6	38 ± 8

[a] A mycelial mat (2 × 2 mm) was incubated in wheat bran medium for 6 d at 28°C. Three Erlenmeyer flasks were used for estimation of one strain. The enzyme solution and the substrate were incubated for 2 h at 4°C using a reciprocal shaker (125 strokes/min). The amount of reducing sugar was measured using DNS.

Discussion

The question arises: Why does this polykaryon formation occur? In animal cells, the phenomenon of micronucleation is known to occur *(11)*. It is suspected that this is owing to abnormal nuclear division. We previously reported that micronucleation occurs in the fungus *T. reesei* when this fungus is treated with higher concentrations of colchicine, although autopolyploidization occurs when this fungus is treated with 0.1% (w/v) colchicine *(12,13)*. In the present study, it was suspected that 2.0% (w/v) colchicine (higher concentration) caused abnormal nuclear division followed by micronucleation from one autopolyploid nucleus in a swollen conidium. However, 0.5% (w/v) colchicine could produce multiple smaller nuclei whose diameter was almost the same as that of the original nucleus from an autopolyploid nucleus. Such smaller nuclei matched with our experimental purpose. This phenomenon also seems to be owing to abnormal nuclear division.

We discussed how the multinucleate conidia were produced. In the original conidia of this fungus, nuclear division was carried out in the first conidium and only one nucleus was distributed into one conidium correctly *(7)*. However, there were an excessive number of nucleus in the swollen conidium after polykaryon formation, and there were a larger number of nuclei in the mycelial mat derived from such a swollen conidium (data not shown). When many nuclei began to divide in a swollen conidium and to distribute into conidia through mycelia, an excessive number of nuclei seemed to be transported into a conidium by the nuclear transfer mechanism of this fungus. The genetic stability of such polykaryons will be the next target of investigation.

Finally, we discussed why cellulase productivity increased. The cellulase productivity of the autopolyploid strain was almost the same as that of the original strain or decreased (data not shown). However cellulase productivity increased after polykaryon formation. Thus, it is likely that the changes in nuclear nature are related to the changes in cellulase productivity. Changes in the nature of autopolyploid nucleus might cause the expression of amplified genes in an autopolyploid nucleus. But, further investigation is necessary to elucidate this phenomenon clearly.

Based on our study's results, we believe that the discussed techniques can be used to increase cellulase productivity in cellulase hyperproducers produced by chemical mutation, genetic engineering, and protein engineering.

References

1. Toyama, H. and Toyama, N. (2000), *Appl. Biochem. Biotech* **84–86,** 419–429.
2. Wolff, J. and Knipling, L. (1995), *J. Biol. Chem*. **270(28),** 16,809–16,812
3. Zelesco, P. A., Barbieri, I., and Graves, J. A. M. (1990), *Mutat. Res.* **242,** 329–335.
4. Toyama, H. and Toyama, N. (2001), *Appl. Biochem. Biotech*. **91–93,** 787–790.
5. Mandels, M. and Sternberg, D. (1976), *J. Ferment. Technol*. **54,** 267–286.
6. Toyama, H., Yamagishi, N., and Toyama, N. (2002), *Appl. Biochem. Biotech.* **98–100,** 257–263.
7. Rosen, D., Edelman, M., Galun, E., and Danon, D. (1974), *J. Gen. Mirobiol.* **83,** 31–49.
8. Friend, K., Chen, S., and Ruddle, F. (1976), *Somatic Cell Genet.* **2,** 183–188.
9. Yamada, M., Matsumoto, Y., Hamada, S., Fujita, S., and Yoshida, Y. (1986), *Zbl. Bakt. Hyg.* **86,** 6503–6507.
10. Miller, G. L. (1959), *Anal. Chem.* **31,** 426–428.
11. Kallio, M., Sjoeblom, T., and Laehdetie, J. (1995), *Environ. Mol. Mutagen.* **25,** 2, 106–117.
12. Toyama, H. and Toyama, N. (1995), *World J. Microbiol. Biotechnol.* **11,** 326–329.
13. Toyama, H. and Toyama, N. (1991), *Agric. Biol. Chem.* **55,** 2393–2394.

0273-2289/04/114/0335–0346/$25.00

Biosynthesis of Poly(3-hydroxybutyrate-*co*-3-hydroxyalkanoates) by Metabolically Engineered *Escherichia coli* Strains

Si Jae Park[†,1] and Sang Yup Lee[*,1,2]

[1]Metabolic and Biomolecular Engineering National Research Laboratory, Department of Chemical & Biomolecular Engineering, BioProcess Engineering Research Center, and [2]Department of BioSystems and Bioinformatics Research Center, Korea Advanced Institute of Science and Technology, 373-1 Guseong-dong, Yuseong-gu, Daejeon 305-701, Republic of Korea, E-mail: leesy@kaist.ac.kr

Abstract

Biosynthesis of polyhydroxyalkanoates (PHAs) consisting of 3-hydroxyalkanoates (3HAs) of 4 to 10 carbon atoms was examined in metabolically engineered *Escherichia coli* strains. When the *fadA* and/or *fadB* mutant *E. coli* strains harboring the plasmid containing the *Pseudomonas* sp. 61-3 *phaC2* gene and the *Ralstonia eutropha phaAB* genes were cultured in Luria-Bertani (LB) medium supplemented with 2 g/L of sodium decanoate, all the recombinant *E. coli* strains synthesized PHAs consisting of C4, C6, C8, and C10 monomer units. The monomer composition of PHA was dependent on the *E. coli* strain used. When the *fadA* mutant *E. coli* was employed, PHA containing up to 63 mol% of 3-hydroyhexanoate was produced. In *fadB* and *fadAB* mutant *E. coli* strains, 3-hydroxybutyrate (3HB) was efficiently incorporated into PHA up to 86 mol%. Cultivation of recombinant *fadA* and/or *fadB* mutant *E. coli* strains in LB medium containing 10 g/L of sodium gluconate and 2 g/L of sodium decanoate resulted in the production of PHA copolymer containing a very high fraction of 3HB up to 95 mol%. Since the material properties of PHA copolymer consisting of a large fraction of 3HB and a small fraction of medium-chain-length 3HA are similar to those of low-density polyethylene, recombinant *E. coli* strains constructed in this study should be useful for the production of PHAs suitable for various commercial applications.

Index Entries: Polyhydroxyalkanoates; *Escherichia coli*; β-oxidation; sodium decanoate; copolymer.

[†]Present address: LG Chem, Ltd./Research Park 104-1, Moonji-dong, Yuseong-gu, Daejeon, 305-380, Republic of Korea.

*Author to whom all correspondence and reprint requests should be addressed.

Introduction

Polyhydroxyalkanoates (PHAs) are accumulated in numerous Gram-positive and Gram-negative bacteria as a carbon/energy storage material under the nutrient-limiting condition in the presence of excess carbon source *(1–5)*. PHAs have been drawing much attention as a family of completely biodegradable plastics and elastomers *(4,6)*. More than 150 kinds of (*R*)-hydroxyalkanoic acid monomers have been found to be assimilated into bacterial PHAs *(7)*. The monomer composition of PHAs highly depends on the metabolic capability of host microorganism and on the substrate specificity of PHA synthase *(8)*.

Bacterial PHAs have been generally classified into two groups depending on the number of carbon atoms in the monomer units: short-chain-length (SCL) PHAs consisting of monomers having C3–C5 atoms, and medium-chain-length (MCL) PHAs consisting of monomers having C6–C14 atoms *(3,5)*. Recently, PHAs containing both SCL and MCL monomer units have also been found in several bacteria *(9–15)*. Poly(3-hydroxybutyrate) (P[3HB]) is the most extensively studied member of SCL-PHAs, and it is rather stiff and crystalline, thus making it difficult to process and be commercially utilized. On the other hand, MCL-PHAs possess low crystallinity and high elasticity, which makes them good candidates for biodegradable rubber and elastomer. The copolymer of randomly incorporated 3-hydroxybutyrate (3HB) and 3-hydroxyhexanoate (3HHx), P(3HB-*co*-3HHx), was recently found to be accumulated in several aeromonads cultured on oils and fatty acids *(13,14)*. The material properties of this copolymer were dependent on the 3HHx mole fraction; the copolymer containing 20 mol% of 3HHx shows properties similar to low-density polyethylene (LDPE) *(16)*. Therefore, the incorporation of MCL monomer unit into the P(3HB) polymer backbone improves the ductility and processibility suitable for commercial applications *(16)*. Furthermore, copolymers consisting of 3HB and a small amount of MCL monomers (e.g., 95 mol% 3HB and 5 mol% MCL monomers) were shown to be more flexible material than P(3HB-co-3HHx), having material properties similar to those of LDPE *(17)*.

Recently, the PHA biosynthesis genes were cloned from *Pseudomonas* sp. 61-3, which is able to produce a random PHA copolymer consisting of 3HAs having C4–C12 carbon atoms *(18)*. The heterologous expression of the *Pseudomonas* sp. 61-3 PHA synthase gene ($phaC1_{Ps}$ or $PhaC2_{Ps}$) in recombinant *Ralstonia eutropha* PHB^{-4} and *Pseudomonas putida* GPp104 resulted in the accumulation of copolymer consisting of C4–C12 monomers from fatty acids, but the 3HB monomer fraction in coplymers was lower than 50 mol% *(18)*. The additional introduction of the *R. eutropha* $phaAB_{Re}$ genes along with the $phaC1_{Ps}$ gene allowed production of copolymer having a high 3HB fraction up to 85 mol% *(19)*. In addition, a copolymer having a very high 3HB fraction of 94 mol% could be produced from glucose by expressing the $phaC1_{Ps}$ and $phaAB_{Re}$ genes in *Pseudomonas* sp. 61-3 deficient in P(3HB) synthase gene ($phbC_{ps}$) *(17)*.

This kind of copolymer consisting of C4–C12 monomers could also be produced in recombinant *Escherichia coli* by the introduction of the $phaC1_{Ps}$ gene and one of the *P. aeruginosa* (*R*)-specific enoyl-CoA hydratase genes ($phaJ1_{Pa}$ or $phaJ2_{Pa}$). However, the mole fraction of 3HB in the copolymer was lower than 10 mol%, resulting in a material property quite similar to that of MCL-PHA *(20)*. In principle, the intermediates of fatty acid metabolism can be converted to 3-hydroxyacyl-CoAs (3HA-CoAs) of different carbon numbers depending on the supplied fatty acids *(4)*. Recently, it has been reported that the *fad* mutant *E. coli* strains could supply various MCL monomers, the number of carbon atoms of which were the same and reduced by two or four compared with those of supplied fatty acids *(21–26)*. This means that *E. coli* impaired in the β-oxidation pathway can supply acetyl-CoAs, the major precursors for 3HB, along with MCL monomers from fatty acids. Therefore, in the present study, we investigated the biosynthesis of copolymers composed of 3HB and a small amount of MCL monomers in *fadA* and/or *fadB* mutant *E. coli* strains by the coexpression of the *Pseudomonas* sp. 61-3 $phaC2_{Ps}$ gene and the *R. eutropha* $phaAB_{Re}$ genes.

Materials and Methods

Bacterial Strains and Plasmids

The strains used are provided in Table 1. All cloning was carried out using *E. coli* XL1-Blue as a host strain. The *E. coli* strains defective in fatty acid β-oxidation pathway were previously described (21,26) and used for the production of PHA: WA101 (W3110 *fadA::Km*), WB101 (W3110 *fadB::Km*), and WAB101 (W3110 *fadBA::Km*).

Plasmid Construction

The plasmids used are also provided in Table 1. All DNA manipulations including restriction digestion, ligation, and agarose gel electrophoresis were carried out by standard procedures *(27)*. The sequences of the primers used in polymerase chain reaction (PCR) are given in Table 2. PCR was performed by a PCR Thermal Cycler MP (Takara Shuzo, Shiga, Japan) using an Expand™ High Fidelity PCR System (Roche, Mannheim, Germany). DNA sequencing was carried out using a Bigdye terminator cycle sequencing kit (Perkin-Elmer, Boston, MA) and *Taq* polymerase using ABI Prism™ 377 DNA sequencer (Perkin-Elmer). The procedures for constructing the plasmids are illustrated in Fig. 1. pBlueReAB was constructed by the ligation of *Pst*I-digested fragment containing the *R. eutropha* $phaAB_{Re}$ genes from pSYL107 *(28)* with *Pst*I-digested pBluescript SK(–). The *gntT104* promoter, which can transcribe the genes constitutively owing to the substitutional mutation in the internal operator of *gntT* promoter, was used for the constitutive expression of genes *(21,26,29)*. The PCR product of the *gntT104* promoter containing the *E. coli* ribosomal binding site was amplified using *E. coli* W3110 chromosomal DNA as a template. The *Pseudomonas* sp. 61-3 $phaC2_{Ps}$ gene was amplified using pBSEB50 *(18)* as a template.

Table 1
Bacterial Strains and Plasmids Used

Strains or plasmids	Relevant characteristics	References or source
E. coli strains		
XL1-Blue	*recA1*, *endA1*, *gyrA96*, *thi*, *hsdR17*, *suppE44*, *relA1*, *l*$^{-}$, *lac*$^{-}$, *F'[proAB lacl*^{q} *lacZ*DM15, *Tn10 (tet)r]*	Stratagene [a]
W3110	*F*$^{-}$ *mcrA mcrB IN(rrnD*$^{-}$*rrnE)1*l^{-}	KCTC [b]
WA101	W3110 (*fadA::Km*)	*21,26*
WB101	W3110 (*fadB::Km*)	*26*
WAB101	W3110 (*fadBA::Km*)	*26*
Plasmids		
pBluescript SK(–)	Ap^{r}; *lacZ*; cloning vehicle	Stratagene
pBSEB50	pBluescript II KS(+) derivative; *Pseudomonas* sp. 61-3 PHA biosynthesis genes ($phaC1_{Ps}$, $phaZ_{Ps}$, $phaC2_{Ps}$)	*18*
pSYL107	pBluescript KS(–) derivative; *R. eutropha* PHA biosynthesis genes ($phaCAB_{Re}$), *parB*, *E. coli ftsZ* gene	*28*
pJC4	pGEM-7Zf(+) derivative; *Alcaligenes latus* PHA biosynthesis genes, *parB* (*hok/sok*) locus of plasmid R1	*30*
pBlueReAB	pBlueScript SK (–) derivative; $phaAB_{Re}$	This study
pUCstb	pUC19 derivative; *parB* (*hok/sok*) locus of plasmid R1	This study
p104613C2ReABstb	pBlueScript SK (–) derivative; *gntT104* promoter, $phaC2_{Ps}$, $phaAB_{Re}$, *parB*	This study

[a] Stratagene Cloning System, La Jolla, CA.
[b] Korean Collection for Type Cultures, Daejeon, Republic of Korea.

Table 2
Primers Used in PCR Experiments[a]

Primer	Primer sequence	Gene	Template
1	5-CGC**GGATCC**AATAAGGAGATA**TCTAGA**TGAGAGAGAAACCAACGCCG	*phaC2*$_{Ps}$	pBSEB50
2	5-C**GGATCC**CCGGGTACCGAGCTCGAATTCTCAGCGCACGCGCACGTAGGTA	*phaC2*$_{Ps}$	pBSEB50
3	5-G**ACTAGT**TGAAAGGTGTGCGCGATCTCAC	*gntT104* promoter	*E. coli* W3110 chromosome
4	5-GC**GGATCC**CATTTGTTATGGGCGACGTCAATTT	*gntT104* promoter	*E. coli* W3110 chromosome

[a] Restriction enzyme sites are shown in bold. The ribosome binding site is underlined.

Gene fragment containing *gntT104* promoter and *Pseudomonas* sp. 61-3 $phaC2_{Ps}$ gene was cloned into pBlueReAB to make p104613C2ReAB, as shown in Fig. 1. Finally, to increase plasmid stability, the *parB* (*hok/sok*) locus of plasmid R1 from pJC4 *(30)* was introduced into p104613C2ReAB to make p104613C2ReABstb (Fig. 1).

Culture Conditions

E. coli XL1-Blue was grown at 37°C in Luria-Bertani (LB) medium (containing 10 g/L of tryptone, 5 g/L of yeast extract, and 5 g/L of NaCl). Recombinant *E. coli* strains for the PHA production were cultivated at 30°C for 72 h in LB medium containing two different carbon sources: (1) 2 g/L of sodium decanoate (Sigma, St. Louis, MO); and (2) 10 g/L of sodium gluconate (Junsei, Tokyo, Japan) plus 2 g/L of sodium decanoate. All the flask cultures were carried out in triplicate in a rotary shaker at 250 rpm. For the cultivation of recombinant *E. coli* strains, ampicillin (50 mg/L) was added to the medium.

Analytical Procedures

Cell growth was monitored by measuring the absorbance at 600 nm (OD_{600} (DU Series 600 Spectrophotometer; Beckman, Fullerton, CA). PHA concentration and monomer composition were determined by gas chromatography (Donam, Seoul, Korea) equipped with a fused silica capillary column (Supelco SPB™-5, 30 m × 0.32 mm id, 0.25 μm film; Bellefonte, PA) using benzoic acid as an internal standard *(31)*. Cell concentration, defined as dry cell weight per liter of culture broth, was determined as previously described *(14)*. The residual cell concentration was defined as the cell concentration minus PHA concentration. The PHA content (wt%) was defined as the percentage of the ratio of PHA concentration to cell concentration.

Results

PHA Production in Flask Cultures

Recombinant *E. coli* strains WA101, WB101, and WAB101 harboring p104613C2ReABstb were cultured in LB medium containing 2 g/L of sodium decanoate at 30°C. These recombinant *E. coli* strains were also cultured in LB medium containing 2 g/L of sodium decanoate plus 10 g/L of sodium gluconate. The results of flask cultures are summarized in Table 3. When sodium decanoate was used as a sole carbon source, all the recombinant *E. coli* strains accumulated poly(3-hydroxybutyrate-*co*-3-hydroxyalkanoates) (P[3HB-*co*-3HAs]) consisting of various monomers including 3HB, 3HHx, 3-hydroxyoctanoate (3HO), and 3-hydroxydecanoate (3HD). The mole fraction of 3HB and 3HHx in copolymer varied considerably depending on the host strain and the kind of mutation. When the *fadB* mutant *E. coli* strain was employed, PHA containing a high 3HB fraction up to 86 mol% was obtained. When the *fadA* mutant *E. coli* strain was used,

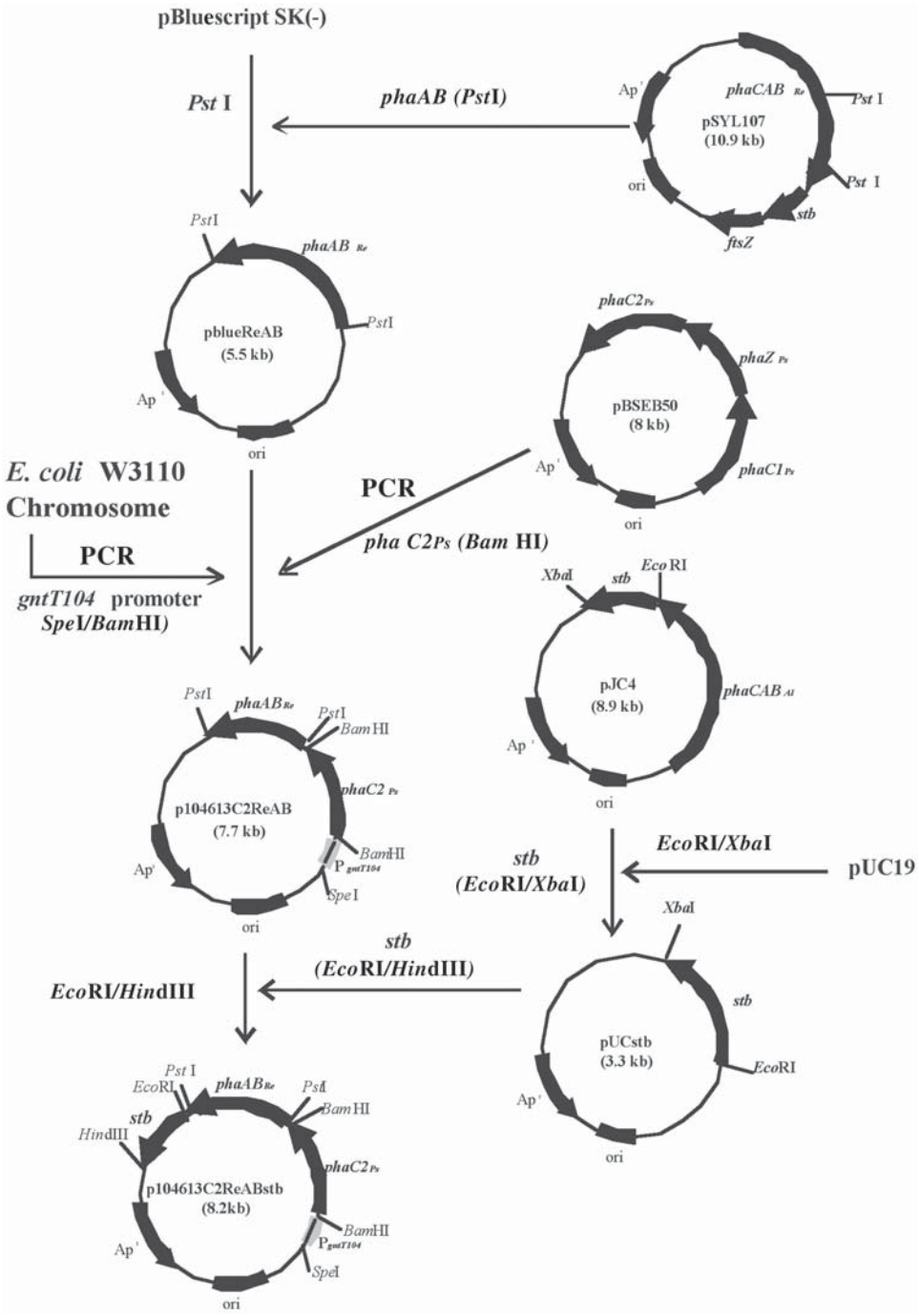

Fig. 1. Construction of plasmid p104613C2ReABstb, which is used to transform *fad* mutant *E. coli* strains for production of SCL-MCL PHA copolymers.

Table 3
Results of Flask Cultures of Recombinant *E. coli* Strains Harboring p104613C2ReABstb[a]

Strain	Carbon source[b]	Dry cell weight (g/L)	PHA concentration (g/L)	PHA content (wt%)	Composition (mol %)			
					3HB	3HHx	3HO	3HD
WA101	Decanoate	1.90 ± 0.02	0.60 ± 0.02	31.4 ± 2.0	34 ± 2	63 ± 2	3 ± 2	0
	Gluconate + decanoate	3.92 ± 0.08	1.90 ± 0.04	48.4 ± 2.0	89 ± 2	8 ± 2	2 ± 2	1 ± 2
WB101	Decanoate	1.20 ± 0.03	0.30 ± 0.02	25.5 ± 2.0	86 ± 2	10 ± 2	4 ± 2	0
	Gluconate + decanoate	3.48 ± 0.04	0.88 ± 0.02	25.3 ± 2.3	87 ± 2	11 ± 2	1 ± 2	1 ± 2
WAB101	Decanoate	1.25 ± 0.02	0.31 ± 0.03	25.0 ± 2.6	70 ± 2	26 ± 2	3 ± 2	1 ± 2
	Gluconate + decanoate	4.15 ± 0.05	1.34 ± 0.05	32.3 ± 1.6	95 ± 2	2 ± 2	2 ± 2	1 ± 2

[a] Cells were cultivated for 72 h in LB medium supplemented with different carbon sources. All experiments were carried out in triplicate.
[b] Sodium decanoate and sodium gluconate were added to concentrations of 2 g/L and 10 g/L, respectively.

PHA containing a high mole fraction of 3HHx up to 63 mol% was produced. Unexpectedly, only a very small amount of 3HD was incorporated into the copolymer, even though the *Pseudomonas* sp. 61-3 PHA synthase has a wide range of substrate specificity to monomers having C4–C12 atoms *(18)*.

To increase further the 3HB fraction in the copolymer, sodium gluconate (10 g/L) was added to supply more acetyl-CoAs. By supplementing sodium gluconate, the 3HB fraction in the copolymer significantly increased. The effect of supplementing sodium gluconate was much more significant in the *fadAB* mutant *E. coli* strain; this resulted in a striking increase in the 3HB monomer fraction up to 95 mol% at the expense of the 3HHx monomer fraction. In addition, only a small amount of 3HD was incorporated into PHA by the addition of sodium gluconate in all the *fad* mutant *E. coli* strains.

Discussion

Recent studies suggest that the monomer composition of PHA is highly dependent on the metabolic capability of the host microorganism and substrate specificity of PHA synthase. In the present study, we developed recombinant *fad* mutant *E. coli* strains for the biosynthesis of PHA copolymer consisting of a high mole fraction of 3HB and a low mole fraction of MCL monomers. PHA has been routinely produced from the intermediates of the fatty acid metabolism by natural or recombinant bacteria using related or unrelated carbon sources such as glucose and fatty acid *(4)*. In *E. coli*, 3HB monomers have been efficiently generated by the expression of *phaAB* genes from acetyl-CoA *(26)*. It has been reported that recombinant *E. coli* expressing the MCL-PHA synthase gene could accumulate MCL-PHA from MCL fatty acids by the coexpression of the enoyl-CoA hydratase *(20)* or ketoacyl-ACP reductase gene *(21,25,32)*, or by inhibition of the β-oxidation pathway *(21–26)*. We have developed *E. coli* strains defective in the β-oxidation pathway for the production of SCL-MCL PHA copolymers. The *fad* mutant *E. coli* strains have been reported to be able to generate 3HA-CoAs, whose carbon numbers are reduced by two, four, six, or more, from the supplied fatty acids *(21–26)*. This means that acetyl-CoA, the starting metabolite for 3HB monomers, can also be generated by the *fad* mutant *E. coli* strain by supplying fatty acids. Recently, it has been reported that various enzymes homologous to Fad enzymes, such as YfcY and YfcX, are involved in the generation of 3HA-CoAs in the *fad* mutant *E. coli* strain *(24,33)*. Furthermore, *E. coli* MaoC has been revealed to have enoyl-CoA hydratase activity, which allows generation of (*R*)-3HA-CoAs in *fadB* mutant *E. coli* strain *(34)*.

The inherent substrate specificities of *Pseudomonas* sp. 61-3 PHA synthases ($PhaC1_{Ps}$ and $PhaC2_{Ps}$) are rather low toward 3HB monomer *(17,18)*, and the *fad* mutant *E. coli* strain used in our study cannot generate enough 3HB monomers from the β-oxidation pathway *(21,26)*. Therefore, we introduced the *R. eutropha* $phaAB_{Re}$ genes to generate enough more 3HB

monomers to increase the 3HB fraction in the copolymer. In addition, gluconate was provided as an auxiliary carbon source to supply more acetyl-CoAs, which are in turn converted into 3HB monomers in two reaction steps catalyzed by PhaA and PhaB. The metabolic pathways for PHA biosynthesis in several different *fad* mutant *E. coli* strains are shown in Fig. 2.

Previously, coexpression of the $phaAB_{Re}$ genes with the $phaC1_{Ps}$ gene in recombinant *R. eutropha* and pseudomonads resulted in the P(3HB-*co*-3HA) having a high mole fraction of 3HB, the material properties of which are tougher and flexible, thus making it suitable for a wide range of commercial applications *(17,19)*. As expected, when the $phaAB_{Re}$ and $phaC2_{Ps}$ genes were coexpressed in *fad* mutant *E. coli* strains and gluconate was added, copolymers consisting of a high mole fraction of 3HB were produced (Table 3), which have been suggested to have ductile material property similar to that of LDPE *(17)*. The mole fractions of monomer were dependent on the kind of *fad* mutation and host strain. The 3HHx fraction of the copolymer produced in the *fadA* mutant *E. coli* WA101 was much higher than that produced in the *fadB* and *fadAB* mutant *E. coli* strains. Previously, we reported that *E. coli* WA101 harboring only the $phaC2_{Ps}$ gene was able to produce MCL-PHA consisting of 3HHx, 3HO, and 3HD from sodium decanoate, in which 3HO and 3HD were the major components and 3HHx was a minor component *(21)*. The striking increase in the 3HHx mole fraction in the copolymer seems to be owing to the coexpression of the $phaB_{Re}$ gene because more 3HHx monomers can be generated by the reduction of 3-ketohexanoyl-CoA in *fadA* mutant *E. coli*, as previously reported by Ren et al. *(35)*. In the *fadB* and *fadAB* mutant *E. coli* strains, similar monomer compositions were observed with a slight increase in 3HHx fraction in *fadAB* mutant *E. coli*.

Conclusion

We developed several recombinant *E. coli* strains for the production of P(3HB-*co*-3HA) having various monomer compositions. By blocking the β-oxidation pathway and coexpressing the *phaAB* genes, various PHA monomers could be efficiently supplied. In addition, the monomer composition in the copolymer could be altered by supplying different carbon sources. The recombinant *E. coli* system that we developed should be useful for the production of copolymers consisting mainly of 3HB monomer and a small amount of MCL monomers, which can be used in a wide range of applications owing to their tougher and flexible material properties.

Acknowledgment

We thank Professor Y. Doi (RIKEN, Saitama, Japan) for kindly providing the *Pseudomonas* sp. 61-3 *phaC2* gene. This work was supported by a Korea Systems Biology Research Grant (M10309020000-03B5002-00000) and the National Research Laboratory Program (2000-N-NL-01-C-237) of the

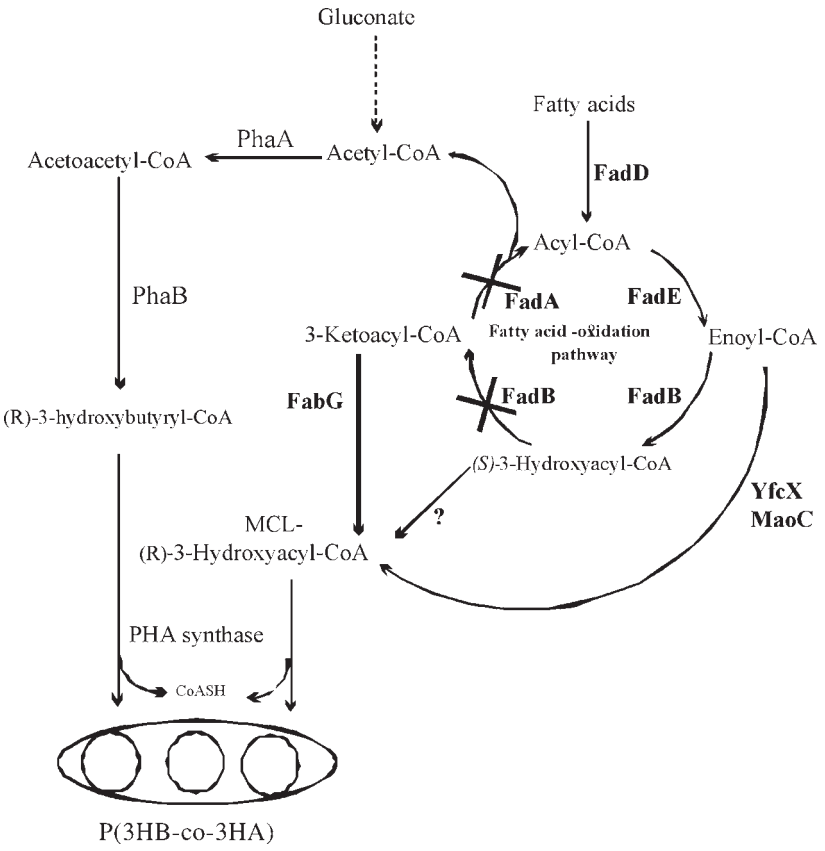

Fig. 2. Metabolic pathways for PHA biosyntheis in *fad* mutant *E. coli* strains used in this study. Enoyl-CoA hydratase, epimerase, and 3-ketoacyl-CoA or ACP reductase have been suggested to supply PHA precursors from inhibited b-oxidation pathway. The crosses indicate inactivation of corresponding enzymes. The question mark represents uncharacterized enzyme. Enzymes involved in the metabolic pathways shown have been described previously: FabG *(21,32)*, YfcX *(24,33)*, MaoC *(34)*, PhaA *(36)*, and PhaB *(36)*.

Ministry of Science and Technology, Center for Ultramicrochemical Process Systems; and by the BK21 project from the Ministry of Education. Hardware for computational analysis during primer design and other bioinformatics studies was supported by the IBM SUR Program.

References

1. Anderson, A. J. and Dawes, E. A. (1990), *Microbiol. Rev.* **54,** 450–472.
2. Doi, Y. (1990), *Microbial Polyesters*, VCH, New York, NY.
3. Lee, S. Y. (1996), *Biotechnol. Bioeng.* **49,** 1–14.
4. Madison, L. L. and Huisman, G. W. (1999), *Microbiol. Mol. Biol. Rev.* **63,** 21–53.
5. Steinbüchel, A. and Füchtenbusch, B. (1998), *Trends Biotechnol.* **16,** 419–427.
6. Lee, S. Y. (1996), *Trends Biotechnol*. **14,** 431–438.

7. Steinbüchel, A. and Valentin, H. E. (1995), *FEMS Microbiol. Lett*. **128,** 219–228.
8. Liebergesell, M., Mayer, F., and Steinbüchel, A. (1993), *Appl. Microbiol. Biotechnol.* **40,** 292–300.
9. Brandl, H., Knee, E. J., Fuller, R. C., Gross, R. A., and Renz, R. W. (1989), *Int. J. Biol. Macromol*. **11,** 49–55.
10. Liebergesell, M., Hustede, E., Timm, A., Steinbüchel, A., Fuller, R. C., Lenz, R. W., and Schlegel, H. G. (1991), *Arch. Microbiol*. **155,** 415–421.
11. Haywood, G. W., Anderson, A. J., Williams, G. A., Dawes, E. A., and Ewing, D. F. (1991), *Int. J. Biol. Macromol*. **13,** 83–87.
12. Kato, M., Bao, H. J., Kang, C. K., Fukui, T., and Doi, Y. (1996), *Appl. Microbiol. Biotechnol*. **45,** 363–370.
13. Kobayashi, G., Shiotani, T., Shima, Y., and Doi, Y. (1994), in *Biodegradable Plastics and Polymers*, Doi, Y. and Fukuda, K., eds., Elsevier Science, Amsterdam, The Netherlands, pp. 410–416.
14. Lee, S. H., Oh, D. H., Ahn, W. S., Lee, Y., Choi, J., and Lee, S. Y. (2000), *Biotechnol. Bioeng*. **67,** 240–244.
15. Steinbüchel, A. and Wiese, S. (1992), *Appl. Microbiol. Biotechnol.* **37,** 601–697.
16. Doi, Y., Kitamura, S., and Abe, H. (1995), *Macromolecules* **28,** 4822–4828.
17. Matsusaki, H., Abe, H., and Doi, Y. (2000), *Biomacromoles* **1,** 17–22.
18. Matsusaki, H., Manji, S., Taguchi, K., Kato, M., Fukui, T., Doi, Y. (1998), *J. Bacteriol*. **180,** 6459–6467.
19. Matsusaki, H., Abe, H., Taguchi, K., Fukui, T., and Doi, Y. (2000), *Appl. Microbiol. Biotechnol*. **53,** 401–419.
20. Tsuge, T., Fukui, T., Matsusaki, H., Taguchi, S., Kobayashi, G., Ishizaki, A., and Doi, Y. (2000), *FEMS Microbiol. Lett*. **184,** 193–198.
21. Park, S. J., Park, J. P., and Lee, S. Y. (2002), *FEMS Microbiol. Lett*. **214,** 217–222.
22. Langenbach, S., Rehm, B. H. A., and Steinbüchel, A. (1997), *FEMS Microbiol. Lett.* **150,** 303–309.
23. Qi, Q., Steinbüchel, A., and Rehm, B. H. A. (1998), *FEMS Microbiol. Lett.* **167,** 89–94.
24. Snell, K. D., Feng, F., Zhong, L., Martin, D., and Madison, L. L. (2002), *J. Bacteriol*. **184,** 5696–5705.
25. Ren, Q., Sierro, N., Witholt, B., and Kessler, B. (2000), *J. Bacteriol.* **182,** 2978–2981.
26. Park, S. J., Park, J. P., Lee, S. Y., and Doi, Y. (2003), *Enzyme Microb. Technol.* **33,** 62–70.
27. Sambrook, J., Fritsch, E. F., and Maniatis, T. (1989), *Molecular Cloning: A Laboratory Manual*, 2nd Ed., Cold Spring Harbor Laboratory Press, Cold Spring Harbor, NY.
28. Lee, S. Y. (1994), *Biotechnol. Lett.* **16,** 1247–1252.
29. Peekhaus, N. and Conway, T. (1998), *J. Bacteriol*. **180,** 1777–1785.
30. Choi, J., Lee, S. Y., and Han, K. (1998), *Appl. Environ. Microbiol.* **64,** 4897–4903.
31. Braunegg, G., Sonnleitner, B., and Lafferty, R. M. (1978), *Eur. J. Appl. Microbiol. Biotechnol.* **6,** 29–37.
32. Taguchi, K., Aoyagi, Y., Matsusaki, H., Fukui, T., and Doi, Y. (1999), *FEMS Microbiol. Lett.* **176,** 183–190.
33. Campbell, J. W., Morgan-Kiss, R. M., and Cronan, J. E. Jr. (2003), *Mol. Microbiol.* **47,** 793–805.
34. Park, S. J. and Lee, S. Y. (2003), *J. Bacteriol*. **185,** 5391–5397.
35. Ren, Q., Sierro, N., Kellerhals, M., Kessler, B., and Witholt, B. (2000), *Appl. Environ. Microbiol*. **66,** 1311–1320.
36. Schubert, P., Steinbüchel, A., and Schlegel, H. G. (1988), *J. Bacteriol.* **170,** 5837–5847.

0273-2289/04/114/0347–0360/$25.00

Effect of Corn Stover Concentration on Rheological Characteristics

Natalia V. Pimenova[1] and Thomas R. Hanley*[,2]

[1]Department of Chemical Engineering, University of Louisville, Louisville, KY 40292; and [2]Auburn University, Auburn, AL 36899, Email: hanley@auburn.edu

Abstract

Corn stover, a well-known example of lignocellulosic biomass, is a potential renewable feed for bioethanol production. Dilute sulfuric acid pretreatment removes hemicellulose and makes the cellulose more susceptible to bacterial digestion. The rheologic properties of corn stover pretreated in such a manner were studied. The Power Law parameters were sensitive to corn stover suspension concentration becoming more non-Newtonian with slope n, ranging from 0.92 to 0.05 between 5 and 30% solids. The Casson and the Power Law models described the experimental data with correlation coefficients ranging from 0.90 to 0.99 and 0.85 to 0.99, respectively. The yield stress predicted by direct data extrapolation and by the Herschel-Bulkley model was similar for each concentration of corn stover tested.

Index Entries: Corn stover; rheological measurement; shear stress; shear rate; non-Newtonian fluids; Power Law parameters.

Introduction

The production of fuel ethanol from renewable lignocellulosic material ("bioethanol") has the potential to reduce world dependence on petroleum and to decrease net emissions of carbon dioxide. The lignin-hemicellulose network of biomass retards cellulose biodegradation by cellulolytic enzymes. To remove the protecting shield of lignin-hemicellulose and make the cellulose more readily available for enzymatic hydrolysis, biomass must be pretreated *(1)*.

Thermochemical treatment, such as with steam and dilute sulfuric acid, is a popular pretreatment process. This treatment opens the lignocellulosic pore structure and increases the susceptibility of biomass to enzymatic attack *(2)*. This pretreatment step effectively hydrolyzes the biomass,

*Author to whom all correspondence and reprint requests should be addressed.

yielding liquor typically rich in pentose sugars and generating a cellulose-rich solid with greater porosity and improved enzymatic digestibility *(2)*.

Stirred tanks are typically used for the thermochemical pretreatment. To simulate flow of corn stover slurries in stirred tanks, the rheologic properties of these suspensions must be known. The corn stover slurries in stirred tank reactors typically range from 10 to 40% solids *(3)*.

In systems with suspended solids, rheologic measurements are difficult to perform owing to settling in the measurement devices. Conventional methods for measuring rheologic properties (cone-and-plate, concentric cylinder, and rotating-bob viscometers) do not produce accurate and reliable data for some solid suspensions.

To avoid the apparent complications with absolute rheologic measurement techniques, a number of investigators *(4,5)*. have used relative measurement systems to make rheologic measurements. The major difference between the relative and absolute measurement techniques is that the fluid mechanics in the relative systems are complex. The constitutive equations needed to find the fundamental rheologic variables cannot be readily solved. Relative measurement systems require the use of Newtonian and non-Newtonian calibrations fluids with known properties to relate torque and rotational speed to the shear rate and shear stress *(6)*.

Research on the impeller method using the helical ribbon impeller is well documented *(7,8)*. The impeller method is often employed to measure the rheology of suspensions. Previous researchers assumed that the effective shear rate of such a device is related to the impeller speed by a fluid-independent constant, but this assumption may not be accurate for all impellers *(8,9)*. It has been suggested that a properly designed helical ribbon impeller might be more appropriate for this technique.

Yield stress can be determined by indirect and direct methods. The indirect method consists of curve fitting the experimental shear stress–shear rate data to rheologic models with a yield stress term. Accurate data are essential at lower shear rates to obtain reliable results. A direct method, such as the stress growth method, relates the yield stress to the maximum torque registered in a shear stress–time response. The goal of the present investigation was to determine the rheologic properties of dilute-acid-pretreated corn stover suspensions using the impeller method and to determine the yield stress of these suspensions using the indirect and direct methods.

Data Analysis for Impeller Viscometer Technique

The complex flow field created by the impeller does not allow the direct calculation of shear rate *(6,8)*. It is assumed that the dimensionless power number (p_{No}) is inversely proportional to the impeller Reynolds number (Re_i) for Newtonian fluids in a laminar flow regime in which the RE_i is <10:

$$p_{No} = c/Re_i = \frac{2\pi M}{\rho N^2 D_i^5} \text{ for } Re < 10 \quad (1)$$

$$Re_i = \frac{\rho N D_i^2}{\mu} \tag{2}$$

in which c is an empirically determined constant, M is the torque, D_i is the diameter of the helical impeller, and ρ is the density of the fluid.

For a given impeller, the torque is directly proportional to the impeller speed and the apparent viscosity:

$$M = \frac{cD_i^3}{2\pi} \mu N \tag{3}$$

If the torque is measured as a function of the impeller speed for a known-viscosity Newtonian fluid, the constant, c, can be determined. The apparent viscosity for a non-Newtonian fluid can then be determined from measurements of the impeller torque as a function of impeller speed from Eq. 3 *(7)*.

Replacing the viscosity, μ, in the Re_i with the apparent viscosity of the non-Newtonian fluid, η_a, at the average shear rate, and solving Eq. 2 for the apparent viscosity produces

$$\eta_a = \frac{2\pi M}{cND_i^3} \tag{4}$$

The "average" shear rate in the measuring vessel, γ_{avg}, is assumed to be proportional to the impeller speed, N, and independent of the rheology of the fluid in the vessel. The shear rate constant, k, is used as a fluid-independent constant:

$$\gamma_{avg} = kN \tag{5}$$

If this approach is valid, the shear rate constant can be determined from experimental measurements of torque vs impeller speed for non-Newtonian fluids of known properties *(10)*.

The apparent viscosity is determined from Eq. 4. The value of shear rate that corresponds to this viscosity is obtained from the known viscosity vs shear rate rheogram for the non-Newtonian fluids generated using the cone-and-plate method. The value of k is determined from Eq. 5.

Yield Stress

Yield stress is defined as the shear stress that has to be applied before the material starts to flow. Nguen and Boger *(11)*. indicated that the yield stress can be measured by either indirect or direct methods. Indirect methods consist of either using rheologic models to fit the shear stress–shear rate experimental data or extrapolating the shear stress–shear rate data to zero shear rate. Direct methods involve shearing a fluid in a rotational viscometer at a low and constant shear rate and measuring the shear stress as a function of time. The stress-vs-time (or shear strain) response typically consists of an initially linear portion indicating elastic solid behavior, followed by a nonlinear region, a stress overshoot, and a stress decay region *(11)*.

Indirect determination of the yield stress simply involves extrapolation of the experimental shear stress–shear rate data to obtain the yield value as the shear stress limit at zero rate of shear. The extrapolation is performed numerically on the available data, or the latter can be fitted to a suitable rheologic model representing the fluid, and the yield stress parameter in the model is determined.

A more convenient extrapolation technique is to approximate the experimental data with a viscosity model. The Power Law, shown in Eq. 6, is the most commonly used two-parameter model. The Bingham model, shown in Eq. 7, postulates a linear relationship between τ and γ but can lead to overprediction of the yield stress. Extrapolation of the nonlinear Casson model (1954), shown in Eq. 8, is straightforward from a linear plot of $\tau^{0.5}$ vs $\gamma^{0.5}$. Application of the Herschel-Bulkley model (1926), shown in Eq. 9, is more tedious and less certain although systematic procedures for determining the yield value and the other model parameters are available *(11)*:

$$\tau = K_{pl}(\gamma)^n \tag{6}$$

$$\tau - \tau_y^B = \eta_p \gamma \tag{7}$$

$$\tau^{0.5} = \left(\tau_y^c\right)^{0.5} + \eta^c (\gamma)^{0.5} \tag{8}$$

$$\tau = \tau_y^{HB} + K^{HB}\gamma^{n_{HB}} \tag{9}$$

Materials and Methods

Equipment

Two Brookfield rheometers with full-scale spring torques of 7178 and 57,496 dyne-cm were used: a digital RV-DV III cone-and-plate instrument and a digital HB-DV III, respectively. The uncertainty specified by the manufacturer for these devices is 1% of the full-scale range. Therefore, no data were taken unless the torque displayed was >5% of the maximum value for a given instrument. A cone/plate attachment (RV-DV III viscometer) was used to characterize the rheology of the Newtonian and non-Newtonian calibration fluids used (Brookfield spindle cp-42). The temperature was maintained at 25.0 ± 0.1°C for all tests using a circulating water bath.

The helical impeller was fashioned from nylon using selective laser sintering technology and is shown in Fig. 1. It had a diameter of 0.04 m and a pitch of 0.02 m. The impeller featured two helices, an ascending outer flight and a descending inner flight. The length of the impeller was 0.055 m, and it was located at an off-bottom clearance of 0.025 m.

The use of Newtonian and non-Newtonian calibration fluids allows the determination of constants relating the measured torque and speed to viscosity and shear rate. Silicone oil and glycerin (Newtonian) with viscosities of 1.024 and 0.912 Pa·s, respectively, were used to determine the impeller constant, *c*, while xanthan and guar gum solutions (non-Newtonian) were used to determine the shear rate constant, *k*.

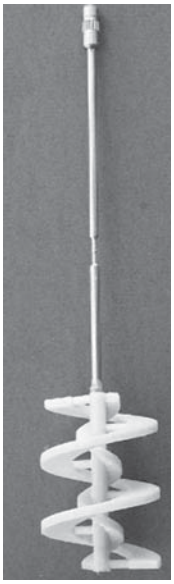

Fig. 1. Helical impeller.

Corn Stover Suspensions

The corn stover suspensions used were composed of various concentrations of corn stover particles (average fiber length = 120 μm) suspended in water. The National Renewable Energy Laboratory (NREL) provided the pretreated corn stover used to prepare the corn stover suspensions. This corn stover was pretreated in a 1.4% sulfuric acid solution for 3–12 min and then dewatered. It contained byproducts of the pretreatment process including lignocellulosic sugars, sulfuric acid, and acetic acid. To prepare samples for viscosity testing, the pretreated corn stover was dried and then reconstituted to the desired concentration by adding deionized water.

Rheologic Measurements

Rheologic measurements were performed at 25oC with the cone-and-plate and helical impeller viscometers. Impeller viscometer measurements were performed in a 1000-mL beaker with a diameter of 0.115 m. A liquid height of 0.115 m was used for all tests.

For the impeller ribbon viscometer technique, the power number of an impeller is inversely proportional to the impeller Reynolds number (Eq. 1). As the impeller rotational speed increases, the flow will gradually change from laminar to turbulent, passing through a transition region. Parameter c can be obtained from the calibration fluids. If the same value for c is assumed to apply to a non-Newtonian fluid, then Eq. 4 can be used to calculate the apparent viscosity of that fluid. The range of the impeller method is determined by the minimum and maximum torques that can be measured *(5)*.

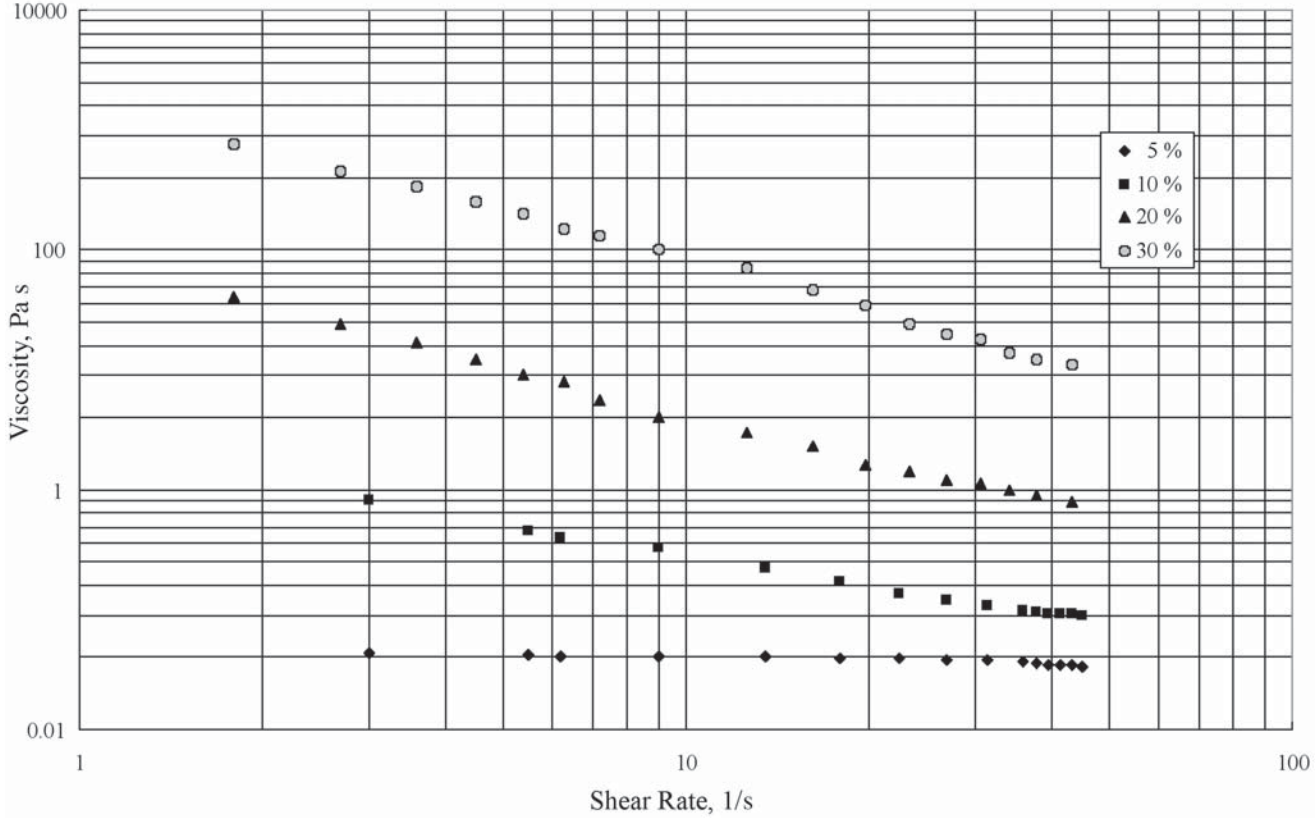

Fig. 2. Viscosity vs shear rate for corn stover suspensions between 5 and 30 wt%.

Table 1
Power Law Parameters for Corn Stover Suspensions

Corn stover concentration (%)	K_{pl} (Pa·s)	n	R^2
5%	0.05	0.91	0.90
10%	1.87	0.08	0.99
20%	71.82	0.06	0.99
30%	1684.5	0.05	0.99

Yield Stress

The indirect method can be employed by extrapolating the rheologic models or the shear stress–shear rate data to zero shear rate. The computer software Table Curve 1.12 was used to fit the shear stress–shear rate data to the different rheologic models. This software uses the Simplex method for a nonlinear regression curve fit.

Results

Determination of Viscosity

Using Newtonian calibration fluids the value for the constant, c, was determined to be 135 *(12)*. The deviation in the value of c between Reynolds numbers from 1 to 10 was <5%.

The value of the shear rate constant, k, was determined for solutions of xanthan gum and guar gum with concentrations of 0.5, 1.0, and 1.5%. The shear rate constant k obtained from the cone-and-plate and helical impeller was 10.9. A similar value of k was obtained for 1.0 and 1.5% of xanthan and guar gum solutions. The same value of k was reported for this type of impeller in earlier investigations *(7,9)*.

The results of the rheologic measurements for the corn stover suspensions of 5, 10, 20, and 30% are presented in Fig. 2. The viscosity of the suspension increased as the fiber loading increased.

Power Law Parameters

The consistency index constant, K_{pl}, and the consistency index number, n, were calculated for all corn stover suspensions, using linear regression. The results are presented in Table 1. All of the regression coefficients are above 0.99. The parameters are independent of the method of measuring rheologic data and dependent on the fluid.

Yield Stress

Indirect Methods

Four models (Power Law, Herschel-Bulkley, Casson, and Bingham) were used to fit the experimental data and to determine the yield stress of

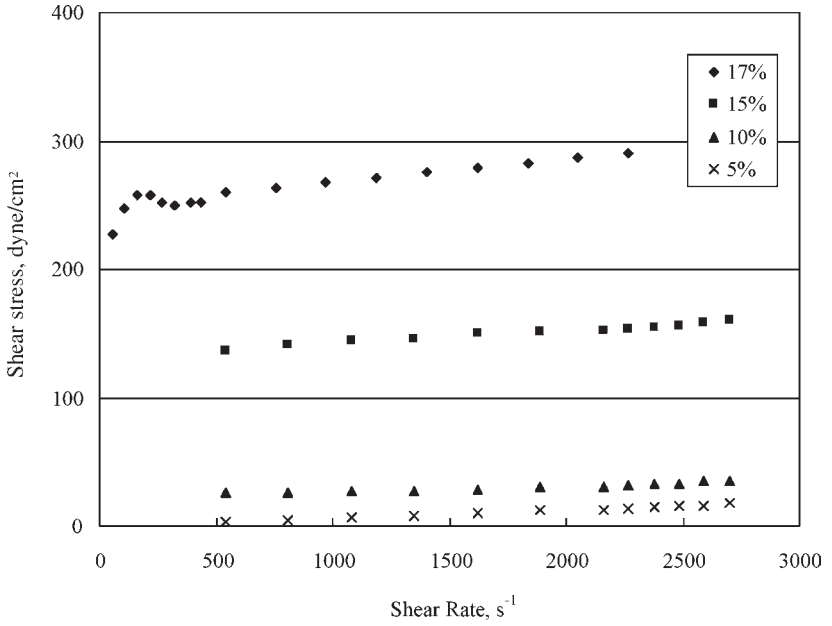

Fig. 3. Shear stress vs shear rate for 5, 10, 15 and 17% corn stover suspensions.

the solution. Figure 3 illustrates shear stress vs shear rate data for 5, 10, 15, and 17% corn stover suspensions; Table 2 lists the yield stress values determined by extrapolation of the shear stress vs shear rate data. Figure 4 shows the experimental data and the four rheologic models used to fit the data; Table 3 lists the fitted parameters for the corn stover suspensions at the various concentrations.

Direct Methods

Yield stress measurements were performed with corn stover suspensions in mass concentrations ranging from 5 to 17 wt%. Less concentrated suspensions did not draw sufficient torque to permit reliable yield stress measurements. To demonstrate the difficulty of obtaining meaningful rheologic data using conventional rotational viscometers, the stress growth method was applied to directly measure the yield stress of 5% corn stover suspension. The stress growth method is not suited for measuring yield stress for filamentous suspensions because of particle settlement. Conventional viscometers are not able to cope with the filamentous nature of the suspensions. The long filaments tend to block the gap between the cone and the plate. Furthermore, using the cone- and-plate viscometer in the stress growth method requires 1- or 2-mL fluid samples depending on the spindle used. Because of the filamentous nature of the solution, it is difficult to be sure that the sample placed in the cup contains the correct concentration of fibers. Solid particles would tend to separate out of the suspension, causing a lower concentration of the solid in the test fluid.

Table 2
Yield Stress Values for Corn Stover Suspensions
Determined with Shear Stress vs Shear Rate Data Extrapolation

	wt%			
	5	10	15	17
Yield stress (Pa)	0.26	2.57	12.7	22.9

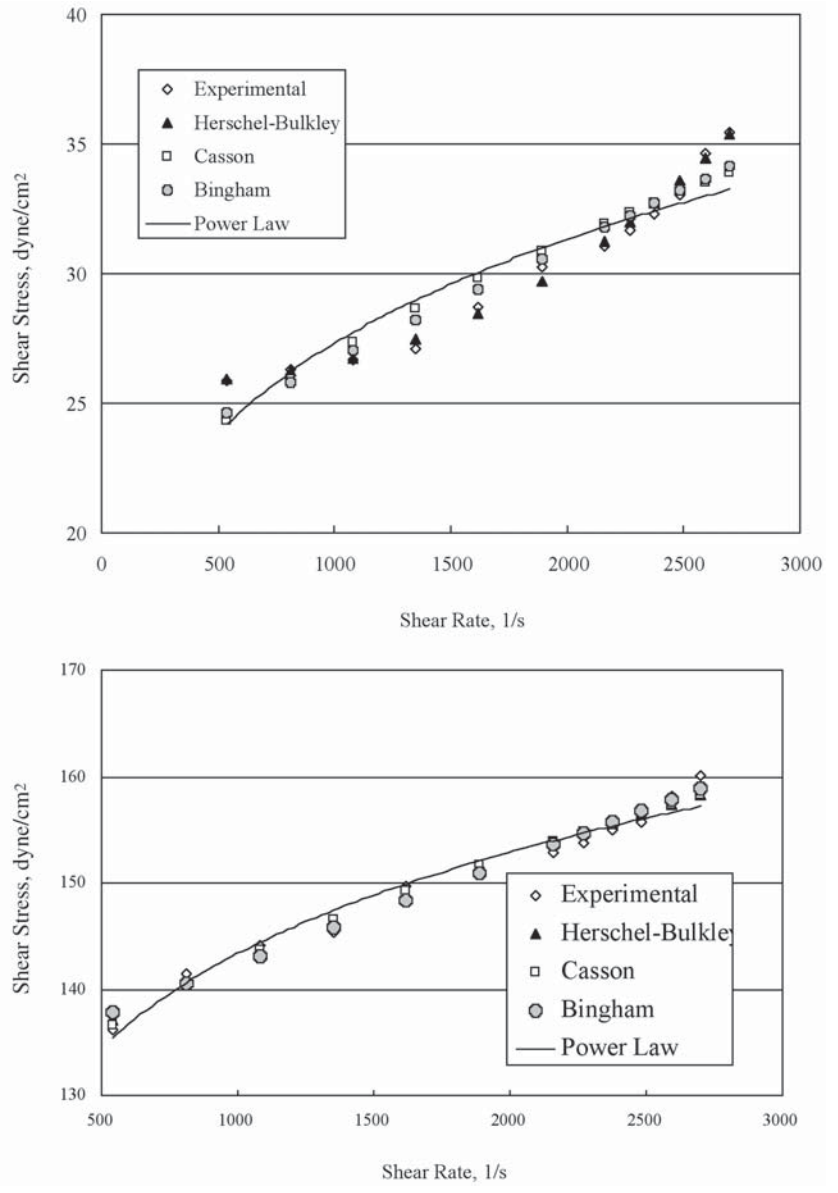

Fig. 4. Rheologic models used to fit shear stress vs shear rate data calculated from impeller method for 10 and 15% corn stover suspensions.

Table 3
Results for Indirect Yield Stress Determination for Corn Stover Suspensions in 1.0-L Beaker (Helical Impeller Method)

wt%	Model fitted	τ (Pa)	K (Pa·s^n)	n	R^2
5	Herschel-Bulkley	τ_y^{HB}: 0.152	K^{HB}: 0.001	n_{HB}: 1.13	0.985
	Casson	τ_y^{c}: 0	η_c: 0.081	0.50	0.993
	Bingham	τ_y^{B}: 0.089	η_P: 0.006	—	0.992
10	Herschel-Bulkley	τ_y^{HB}: 2.42	K^{HB}: 2.5×10^{-8}	n_{HB}: 0.87	0.991
	Casson	τ_y^{c}: 2.08	η_c: 0.031	0.50	0.900
	Bingham	τ_y^{B}: 2.23	η_P: 0.004	—	0.938
15	Herschel-Bulkley	τ_y^{HB}: 12.77	K^{HB}: 0.0912	n_{HB}: 0.736	0.982
	Casson	τ_y^{c}: 12.03	η_c: 0.031	0.50	0.981
	Bingham	τ_y^{B}: 13.26	η_P: 0.0097	—	0.979
17	Herschel-Bulkley	τ_y^{HB}: 22.9	K^{HB}: 1.573	n_{HB}: 0.722	0.917
	Casson	τ_y^{c}: 23.196	η_c: 0.037	0.50	0.917
	Bingham	τ_y^{B}: 24.553	η_P: 0.02045	—	0.891

Finally, the distribution of solid particles across the gap may not be uniform if the fibers separated out of the suspension. Therefore, based on the previous reasoning, it is concluded that the stress method does not offer a reliable and accurate way to measure yield stress in filamentous suspensions. Figure 5 shows the typical torque-time relationship obtained with the helical impeller method for corn stover suspensions.

Discussion

Calibration Procedure

The basic assumption of the impeller viscometer approach is that the shear rate constant is independent of the rheologic properties of the fluid. This assumption allows the helical impeller viscometer to be calibrated using Newtonian and non-Newtonian fluids. The calibration results for guar and xanthan gum solutions ranging in concentration from 0.5 to 1.5% produced a single value of k = 10.8, which is sufficient to represent all the data.

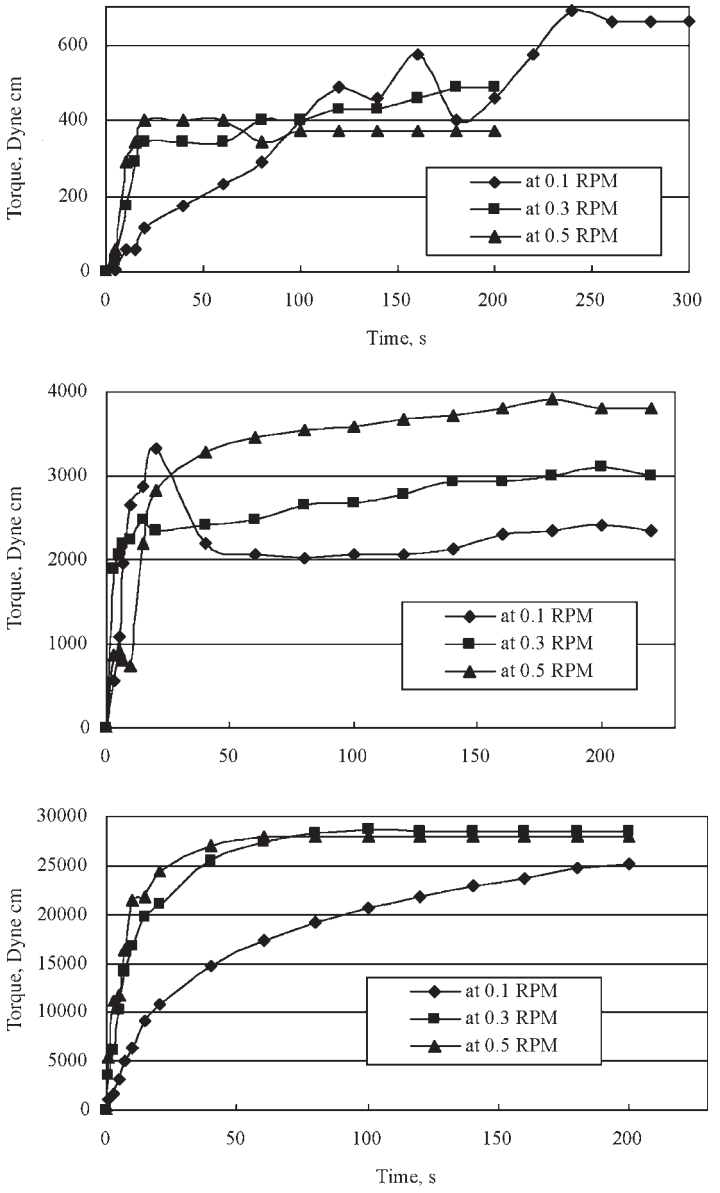

Fig. 5. Torque vs time for 5, 10, and 15% corn stover suspensions.

Corn Stover Suspensions

The viscosity of the corn stover suspensions was determined for concentrations up to 30%. The helical impeller method was ineffective above corn stover concentrations of 32%.

The Power Law parameters for the corn stover suspensions could not be located in previous studies. Dronawat *(13)*. studied a similar system using filamentous particles (Solka-Floc with a fiber length 215 µm in

a 0.5% xanthan gum water solution). Comparison of the Power Law parameters indicates that the suspensions studied here were less viscous and less shear thinning than the suspensions Dronawat studied. The difference can be attributed to the fact that the present study used water rather than a 0.5% of xanthan gum solution. In both studies the increase in the consistency index as the Power Law index increased was moderate.

Shear Stress vs Shear Rate

The relationship between shear stress and shear rate is also an indication of the degree of Newtonian behavior that a fluid exhibits. The linearity of the relationship is a direct indication of Newtonian behavior. The 5% corn stover suspension exhibited Newtonian behavior; the remaining corn stover suspensions exhibited non-Newtonian behavior. At the other concentrations (>5%), the degree of linearity decreased with increasing mass concentration. Figure 4 illustrates the non-Newtonian characteristics of the remaining corn stover suspensions.

Yield Stress

Various techniques have been devised for measuring the yield stress directly and independently of the basic shear stress–shear rate data. Although the general principle of the yield stress as the stress limit between flow and nonflow conditions is often used, the specific criterion employed for defining the yield stress seems to vary among these techniques. Furthermore, each technique appears to have its own limitations and sensitivity so that no single one can be considered versatile or accurate enough to cover the whole range of yield stress and fluid characteristics.

Cone- and-plate stress growth experiments are sensitive to torque deflections in the measuring spring. This effect was more pronounced at higher guar gum concentrations owing to the high viscosity of the solutions. The stress growth method can be ineffective in measuring yield stress for filamentous suspensions, such as corn stover suspensions. The solid particles can block the gap between the cone and plate, hampering any reliable rheologic measurement. Nguen *(11)* wrote that determination of yield stress from the stress growth method is doubtful since lower and upper yield stress values may be obtained. As reported by Joch *(14)*, the values determined herein correspond to the upper, or overshoot, yield stress. The lower yield stress is reported to be the point where the fluid changes from elastic to plastic behavior; the upper yield stress is where the fluid changes from plastic to viscous behavior. When the structure of the fluid has been broken, the fluid has made the transition from plastic to viscous behavior.

The helical impeller technique is better suited to measure yield stress in a greater variety of fluids, including filamentous suspensions. The helical impeller technique is also less sensitive to initial undesired torque deflections in the measuring spring. The undesired initial torque, introduced at the moment the helical impeller is submerged into the liquid, can easily be

minimized by slowly and gently rotating the vessel in the proper direction to compensate for the initial torque. This procedure worked best in moderate to very viscous solutions, since rotation of the vessel for more dilute solutions did not exert enough drag on the helical impeller.

Comparison of the curves in Fig. 5 gives a clear indication of the difficulty involved in working with corn stover suspensions. At some concentrations and rotational rates, the curves show a well-defined maximum followed by a region where torque became independent of time. At other concentrations and rotational rates, the curves show a well-defined global maximum followed by various local maxims. These local peaks can be a consequence of particle settling during the experiment. The experiments using the helical impeller method were 400 s in duration to allow sufficient time for a change in the extent of dispersion of the solids throughout the vessel.

The yield stress values given in Table 3 demonstrate that the yield stresses determined with the Herschel-Bulkley model were lower than the yield stresses determined with all the other methods at equal concentrations. The yield stress predicted by direct data extrapolation and by the Herschel-Bulkley model was similar for each concentration of corn stover.

Conclusions

The parameter *c* was found to be a linear function of Reynolds number with regression coefficients between 0.98 and 1.00. The shear rate constant, *k*, was within 10% of the values found by Donnelly *(15)* and Rieth *(16)* for a double-helical ribbon impeller. Furthermore, the Power Law could be used to describe corn stover suspension viscosity with correlation coefficients above 0.99 for all four concentrations tested. Finally, the yield stress predicted by direct data extrapolation and by the Herschel-Bulkley model was similar for each concentration of corn stover.

Acknowledgment

Funding for this project was provided by the National Renewable Energy Laboratory, Golden, CO (subcontract no. XCO-1-31016-01).

References

1. Esteghlalian, A., Hashimoto, A. G., Fenske, J. J., and Penner, M. (1997), *Bioresour. Technol.* **59,** 129–136.
2. McMillan, J. D. (1997), *Renewable Energy* **10(2/3),** 295–302.
3. Ranatunga, T. D., Jervis, J., Helm, R. F., McMillan, J. D., and Wooley, R. J. (2000), *Enzyme Microb. Technol.* **27,** 240–247.
4. Kemblowski, L. and Kristiansen, B. (1986), *Biotechnol. Eng.* **28,** 1474–1483.
5. Metz, B., Kossen, N. W. F., and Van Suijdam, J. C. (1979), *Adv. Biochem. Eng.* **11,** 103–155.
6. Charles, M. (1978), *Adv. Biochem. Eng.* **8,** 1–62.
7. Svihla, C. K., Dronawat, S. N., and Hanley, T. R. (1995), *Appl. Biochem. Biotechnol.* **51/52,** 355–366.
8. Allen, D. G. and Robinson, C. W. (1990), *Chem. Eng. Sci.* **45(1),** 37–48.

9. Dronawat, S. N., Rieth, T. C., Svihla, C. K., and Hanley, T. R. (1996), in *Proceedings of the 5th World Congress of Chemical Engineering*, vol. 1, American Institute of Chemical Engineers, New York, NY, p. 629 .
10. Svihla, C. K., Dronawat, S. N., Donnelly, J. A., Rieth T. C., and Hanley, T. R. (1997) *Appl. Biochem. Biotechnol.* **63/65,** 375–385.
11. Nguen, Q.D. and Boger, D.V. (1992), *Annu. Rev. Fluid Mech.* **24,** 47–88.
12. Pimenova, N.V. and Hanley, T.R. (2003), *Appl. Biochem. Biotechnol.* **105/108,** 383–392.
13. Dronawat, S. N. (1996), PhD thesis, University of Louisville, Louisville, KY.
14. Joch, R. E. C. (1993), MS thesis, University of Louisville, Louisville, KY.
15. Donnelly, J. A. (1995) MS thesis, University of Louisville, Louisville, KY.
16. Rieth, T. C. (1997) MS thesis, University of Louisville, Louisville, KY.

0273-2289/04/114/0361–0372/$25.00

Construction of Recombinant *Escherichia coli* Strains for Production of Poly-(3-hydroxybutyrate-*co*-3-hydroxyvalerate)

Kin-Ho Law,[1] Pui-Ling Chan,[1] Wai-Sum Lau,[1] Yin-Chung Cheng,[1] Yun-Chung Leung,[1] Wai-Hung Lo,[1] Hugh Lawford,[2] and Hoi-Fu Yu*,[1]

[1]Open Laboratory of Chirotechnology of the Institute of Molecular Technology for Drug Discovery & Synthesis, Applied Biology and Chemical Technology, Hong Kong Polytechnic University, Hong Kong, China, E-mail: bcpyu@polyu.edu.hk; and [2]Bioengineering Laboratory, Department of Biochemistry, University of Toronto, Canada M5S 1A8

Abstract

Plastic wastes constitute a worldwide environmental problem, and the demand for biodegradable plastics has become high. One of the most important characteristics of microbial polyesters is that they are thermoplastic with environmentally degradable properties. In this study, pUC19/PHA was cloned and transformed into three different *Escherichia coli* strains. Among the three strains that were successfully expressed in the production of polyhydroxyalkanoates (PHA), *E. coli* HMS174 had the highest yield in the production of poly-(3-hydroxybutyrate-co-3-hydroxyvalerate) (P[HB-HV]). The cell dry weight and PHA content of recombinant HMS174 reached as high as 10.27 g/L and 43% (w/w), respectively, in fed-batch fermentor culture. The copolymer of PHA, P(HB-HV), was found in the cells, and the biopolymers accumulated were identified and analyzed by gas chromatography, proton nuclear magnetic resonance spectroscopy, and differential scanning calorimetry. We demonstrated clearly that the *E. coli* host for PHA production has to be carefully selected to obtain a high yield. The results obtained indicated that a superior *E. coli* with high PHA production can be constructed with a desirable ratio of P(HB-HV), which has potential applications in industry and medicine.

Index Entries: *Escherichia coli*; polyhydroxyalkanoates; fed-batch fermentation; nuclear magnetic resonance; differential scanning calorimetry.

*Author to whom all correspondence and reprint requests should be addressed.

Table 1
Thermal and Mechanical Properties of Different Polymer Samples *(6,7)*[a]

Sample	T_m (°C)	T_g (°C)	Tensile strength (Mpa)	Elongation to break (%)
P(3HB)	177	4	43	5
P(HB-HV) 10% HV	150	ND	25	20
P(HB-HV) 20% HV	135	ND	20	100

[a]ND, not determined; T_g, glass transition temperature; T_m, melting temperature

Introduction

Plastics have become integral to our lives, and the generation of plastic wastes has increased dramatically. From 1986 to 1998, about 15% of the total domestic, commercial, and industrial waste in Hong Kong was plastic *(1)*. The most immediate advantage of making biodegradable plastics is to address the problems of litter and marine pollution resulting from plastics disposal, which are difficult to solve any other way.

Polyhydroxyalkanoate (PHA) is a polyester of hydroxyalkanoates synthesized by numerous bacteria as an intracellular carbon and energy storage compound and accumulated as granules in the cytoplasm of cells *(2)*. PHA has been attracting much attention because it is a biodegradable, biocompatible, microbial thermoplastic that is regarded as a potentially useful polyester to replace petroleum-derived thermoplastics *(3)*.

The copolymer poly-(3-hydroxybutyrate-co-3-hydroxyvalerate) (PHB-co-PHV) produced by *A. eutrophus* has generated more interest than poly-(R)-3-hydroxybutyrate (PHB) homopolymer. Since these bacterial polyesters are biodegradable thermoplastics, their mechanical and physical properties have received much attention. PHB is a relatively stiff and brittle material because of its high crystallinity. However, the physiochemical and mechanical properties of [P(HB-HV)] vary widely and depend on the molar percentage of 3-hydroxyvalerate (HV) in the copolymer *(4,5)* as shown in Table 1. Propionic acid is converted by a synthetase to propionyl-CoA, and the biosynthetic β-ketothiolase catalyzes the condensation of propionyl-CoA with acetyl-CoA to 3-ketovaleryl-CoA by the acetoacetyl-CoA reductase. The hydroxyvaleryl moiety is finally covalently linked to the polyester by the PHA synthase *(6)*.

However, the price of PHB-co-PHV exceeds US $10/kg, which is much higher than the cost of conventional oil-derived plastic *(7)*. PHA yield is another major factor of the economic production of PHA. The bacterium *Escherichia coli* has proven to be a powerful microbial species in the microbial synthesis of bioproducts using molecular biology techniques.

One of the major factors affecting the overall production cost is bioreactor productivity, which can be defined as the amount of PHA accumulated per unit volume per unit time. To increase PHA productivity, not

Table 2
E. coli Strains and Plasmids

	Relevant characteristics	Reference or source
E. coli strain		
XL1-Blue	*supE44 hsdR17 recA1 endA1 gyrA46 thi relA1 lac–*	Stratagene
HMS174	*recA1 hsdR rif* r	*E. coli* Genetic Stock Center at Yale University
DH5α	*supE44 ΔlacU169 (Φ80 lacZΔM15) hsdR17 recA1 endA1 gyrA96 thi-1 relA1*	Gibco
Plasmid		
pUC19	2.68 kb, Amp^r (80 μg/mL)	New England Biolabs
pKS-/PHA	8.2 kb, Amp^r (80 μg/mL)	Ref. *8*
pUC19/PHA	7.9 kb, Amp^r (80 μg/mL)	This study
pJM9131	8.55 kb, Kan^r (50 μg/mL), its own σ^{70} promoter	Dr. Douglas D. Dennies

only must the cultivation time be reduced, but the cell density and PHA (% dry cell mass) must be increased *(8)*. Fed-batch cultivation is a popular fermentation process design for improving yield and productivity.

In the present experiment, the yield of copolymer production was optimized on a molecular basis using a fermentation strategy.

Materials and Methods

Bacterial Strains and Plasmids

The bacterial strains and plasmids used are given in Table 2. Cells were maintained in 15% (v/v) glycerol stock at –80°C after growing in Luria-Bertan (LB)i medium (10 g/L of tryptone, 5 g/L of yeast extract, 10 g/L of NaCl) at 37°C overnight. Ampicillin (80 μg/mL) was added for *E. coli* strains with pKS-/PHA, pUC19, and pUC19/PHA, and 50 μg/mL of kanamycin was added for *E. coli* with pJM9131.

Construction of Recombinant E. coli *Strains*

Plasmids were isolated using the Wizard Plus SV Minipreps DNA Purification System (Promega, Madison, WI). Plasmid DNA was analyzed by electrophoresis in a 0.8% (w/v) agarose horizontal slab gel, and a 1-kb DNA ladder (Promega) was used as marker. DNA fragments were isolated from the agarose gel using the Concert Rapid Gel Extraction System (Pharmacia). Restriction enzymes and T4 DNA ligase (Pharmacia) were used according to the instructions provided by the supplier. A 5.2-kb *Eco*RI and *Hind*III restriction fragment comprising the entire *pha* operon was cut out from plasmid pJM9131, and these three genes form an operon in the order *phaC*, *phaA*, and *phaB* coding for PHA synthase, β-ketothiolase,

and reductase, respectively. The *pha* operon was used as an insert, and pUC19 carrying the *lac* promoter was employed as vector. The ligation product was transformed into *E. coli* cells XL1-Blue, DH5α, and HMS174 (recA1 hsdR; Rifr). Its capacity for PHA accumulation and composition was analyzed by gas chromatography (GC) and ^{1}H-nuclear magnetic resonance (NMR), respectively.

Medium and Cultivation

Preparation of Food Wastes Medium

Malt waste, mostly semisolids of spent barley and millet refuse, was obtained from Carlsberg Company, a Hong Kong beer brewery. Soy waste, chiefly semisolid cellular residues of soy beans, was collected from Vitasoy International Holdings Ltd, a Hong Kong soy milk company.

The malt and soy wastes were prepared with 80 g of waste that was hydrolyzed with 1 L of 0.6 *M* HCl, which broke down various oligosaccharides into simple sugars such as glucose. The mixture was allowed to reach 121°C and was incubated for 30 min at evaluated pressure (1 kgf/cm^2). The resultant mixture was neutralized by the NaOH pellet, centrifuged, and filtered. The hydrolyzed malt waste was diluted with a third volume of distilled water.

Fermentation

A glycerol stock of cells was used directly as an inoculum in all experiments. It was first inoculated into 5 mL of LB broth in universal bottles. One percent inoculum was added to a 1-L conical flask containing 200 mL of flask fermentation medium that was grown on a rotary shaker at 250 rpm and 37°C. Antibiotic ampicillin was added in a final concentration of 80 μg/mL.

Fed-batch fermentation was performed in a computer-controlled 15-L Biostat C fermentor (B. Braun Biotech, Melsungen, Germany) with 8 L of culture medium with the conditions of 20% dissolved oxygen that was controlled based on both airflow (1 to 2 vvm) and stir rate (300–1000 rpm). The temperature was maintained at 37°C, and the pH was maintained at 7.0 by 2 *M* NaOH only. The basic medium for fed-batch fermentation was the same as for the seed flask (medium A: 10 g/L of glucose, 7 g/L of KH_2PO_4, 1 g/L of $MgSO_4$, 1.5 g/L of citrate, 2 g/L of tryptone, 2 g/L of yeast extract, and 1 g/L of propionate; pH 7.0) except 15 g/L of glucose, 6 g/L of tryptone, and 1.5 g/L of propionate were used. Medium B (750 g/L of glucose and 15 g/L of $MgSO_4 \cdot 7H_2O$, and 75 g/L of propionate) was used as the fed medium.

The medium in the fermentor was inoculated with 1% (v/v) inoculum, and feeding was started when the glucose in the medium was completely consumed with a rise in pH since the medium's pH increased as a result of glucose depletion and the use of organic acid as the carbon source. When the pH rose, the base pump was turned off and the fed rate of the fed medium was controlled by an acid pump. When the glucose feed in, the

acid formation from cells was able to lower the pH and the pH rose again when the glucose was used up again.

In shake-flask fermentation, the food wastes were placed in a 1-L flask with 250 mL of waste medium. To maintain the lowest production cost, no other chemicals were added.

Extraction of Biopolymers

After fermentation, the culture was centrifuged at 14333*g* for 25 min at 4°C, washed with ddH_2O, and freeze dried. One gram of the freeze-dried cell powder was treated with a dispersion containing 15 mL of chloroform and 30% NaOCl solution. The mixture was incubated at 37°C with 250 rpm of agitation for 1.5 h, then centrifuged at 2610*g* for 15 min, resulting in three phases. The upper phase was a hypochlorite solution, the middle phase contained the non-PHA cell material and undisrupted cells, and the bottom phase was chloroform-containing PHA.

The bottom chloroform layer was filtered and allowed to concentrate to a final volume of 5 mL. Pure PHA was obtained by nonsolvent precipitation (chloroform:methanol in a ratio of 1:9). Finally, the white precipitate was dried and weighted.

Analytical Methods

Analysis of Total Organic Carbon

The fermentation medium was analyzed with an Astro 2000 TOC Analyzer according to the APHA (4500-Norg) method *(9)*.

Analysis of Total Kjeldahl Nitrogen

The fermentation medium was analyzed with a Kjeltec Auto 1030 Analyzer according to the APHA (5310C) method *(9)*.

GC Analysis

Freeze-dried cells or extract polymer was added to 1 mL esterification solution (3 mL of 95–98% H_2SO_4, 0.29 g of benzoate, and 97 mL of methanol), and 1 mL of chloroform. The mixture was heated at 100°C for 4 h. ddH_2O (1 mL) was added to the cooled mixture, which was vortexed for phase separation. The lower organic phase portion (1 µL) was subjected to GC analysis, which was performed on a Hewlett Packard 5890 Series II gas chromatograph with a flame ionization detector using a Supelco (10% Carbowax 20 M with 80/100 mesh size Chromosorb WAW) packed column 6 ft in length. Nitrogen was chosen as the carrier gas at a flow rate of 20 mL/min. The working temperature of the column, injector, and the flame ionization detector was 135, 260, and 300°C, respectively. The temperature was kept stable for 10 min to determine both the content and composition of the polymer.

Analysis by ^{1}H NMR

^{1}H NMR analysis was carried out on a Bruker DPX-400 spectrometer. ^{1}H NMR spectra were recorded at room temperature. Ten to 20 mg of

extracted biopolymer sample was put into the NMR tube, and 1 mL of deuterated chloroform ($CDCl_3$) solution was added to dissolve the sample. ^1H NMR spectra (400 MHz) were recorded, and tetramethylsilane was used as an internal reference *(10)*.

Analysis by Differential Scanning Calorimetry

Three to 4 mg of extracted biopolymers was encapsulated in aluminum pans for the measurements. Each sample was first annealed at 200°C for 3 min. The melting point was determined using a Mettler DSC 30 Thermal Analysis System. Dry nitrogen was used as the flow gas with a flow rate of 30 mL/min, calibrated with indium and mercury.

Results and Discussion

Construction of Recombinant Strains

A 5.2-kb *Eco*RI/*Hind*III restriction fragment comprising the entire *pha* operon obtained from plasmid pJM9131 was used as an insert, as well as plasmid pUC19 possessing *lac* promoter. The copy number of plasmid pJM9131 was lower than pUC19, and the effect of *lac* promoter on PHA production was investigated. Three *E. coli* strains were chosen. *E. coli* XL1-Blue and DH5α and typical *E. coli* expression host cells, which were recombinant-deficient strains, were extensively used. The HMS174 strain of *E. coli* was chosen because it contains a lactose utilization system and is recombinant deficient so that a plasmid containing lactose genetic regions will not recombine and make the construct unstable. The lactose utilization system present in *E. coli* HMS174 may be allowed better utilization of food wastes as a carbon source for the production of PHB *(11)*.

Cloning was confirmed by restriction digestions and agarose gel electrophoresis. It demonstrated that the newly cloned plasmid was successfully transformed into the *E. coli* XL1-Blue, HMS174, DH5α and demonstrated that the construction of the recombinant *E. coli* with plasmid pUC19 containing the entire *pha* operon was successful.

Comparison of PHA Production in Different Recombinant E. coli *Strains*

Comparison of the yield of PHA produced by the three new strains revealed that the *E. coli* HMS174 harboring plasmid pUC19/PHA accumulated the highest amount of PHA. The absorbance of the strains during flask cultivation at 600 nm is shown in Fig. 1.

Excess propionate is not taken up and metabolized by the cells, and the toxicity of propionate can inhibit cell growth. Figure 1 shows that the recombinant *E. coli* HMS174/PHA experienced better cell growth than the *E. coli* XL1-Blue/PHA and *E. coli* DH5α. It represents better resistance to the growth inhibition effect of the propionic acid. Hence, *E. coli* HMS174/PHA was chosen to be the target subjected to the high-cell-density fed-batch fermentation in the fermentor.

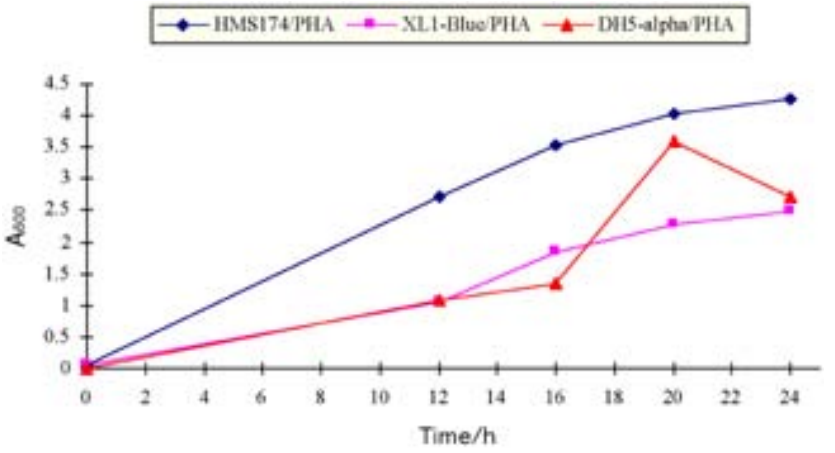

Fig. 1. Time profile of absorbance at 600 nm of *E. coli* strains during flask cultivation.

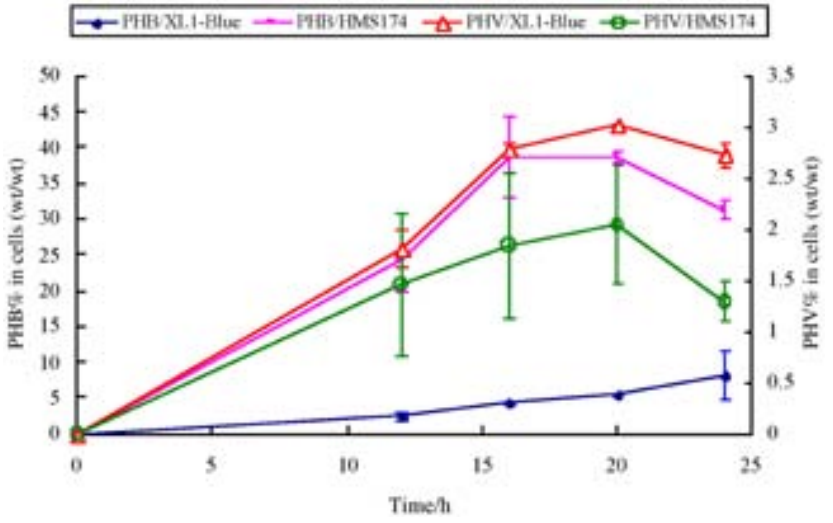

Fig. 2. Percentages of PHB and PHV in CDW of *E. coli* strains during flask cultivation.

The composition and percentage yield of biopolymer within the cells were analyzed by GC, and the GC spectra show that the biopolymer accumulated was P(HB-HV). The percentage yield of copolymer of dry cell weight (DCW) at different times is shown in Fig. 2. It shows that most biopolymer accumulated in the cells was PHB and its yield was much higher using *E. coli* HMS174/PHA compared with *E. coli* XL1-Blue/PHA. A higher PHV yield was also obtained using *E. coli* HMS174/PHA. The PHA percentage yield was as high as 41% (w/w) of its CDW in flask culture, which was higher than the recombinant *E. coli* previously cloned *(12)*.

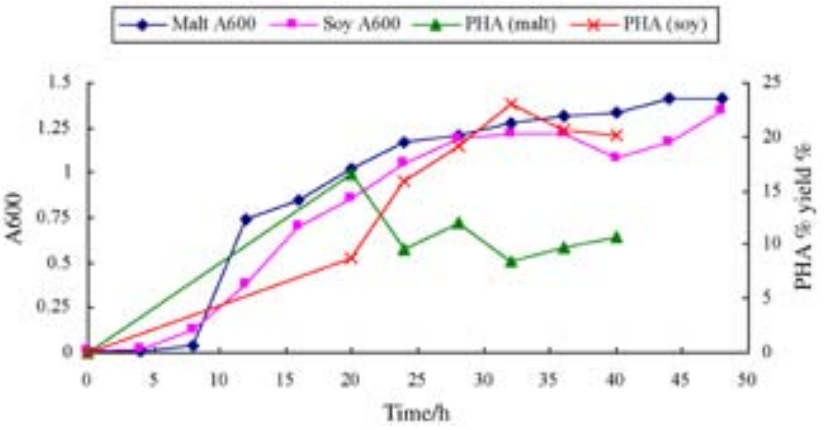

Fig. 3. Time profile of absorbance (A_{600}) of recombinant *E. coli* in malt and soy wastes.

There are two possible reasons for these differences in yield. First, the pUC19 might be a better expression vector for *pha* operon in this case, and therefore a higher amount of PHA accumulated. Second, the capacity of PHA synthesis in different *E. coli* strains was different because the metabolite may be different in *E. coli* HMS174 and *E. coli* XL1-Blue.

Production of P(HB-HV) Using a Recombinant Strain of E. coli *DH5α (pUC19/PHA) in Different Food Wastes*

The carbon source should be inexpensive because it is the major contributor to the total substrate cost (up to 50% of the total operating cost) *(13)*. The ratios of the C and N contents of the hydrolyzed malt and soy wastes were 9:1 and 7.5:1, respectively, as determined by total organic carbon *(4)* and total Kjeldahl nitrogen (TKN) *(4)*.

We cultivated the *E. coli* DH5α (pUC19/PHA) in malt and soy wastes and compared it to PHA production to determine its ability to utilize food wastes. The absorbance at 600 nm of the recombinant *E. coli* in the food wastes is shown in Fig. 4.

The results in Fig. 3 show that the recombinant *E. coli* had better growth in 1:3 malt waste medium than in the soy waste medium. The efficient utilization of the food waste medium can greatly reduce the cost of PHA production. The PHA accumulation of the recombinant *E. coli* in malt and soy wastes medium was 16 and 23% of the CDW, respectively.

Production of P(HB-HV) Using Recombinant Strain of E. coli *HMS174 (pUC19/PHA) in a 15-L Fermentor*

Because the *E. coli* HMS174/PHA exhibited good growth in the presence of propionate and also had a high yield of P(HB-HV) accumulation in flask fermentation, *E. coli* HMS174/PHA was subjected to a fed-batch culture in which the cells were fed by glucose and propionic acid. The A_{600}

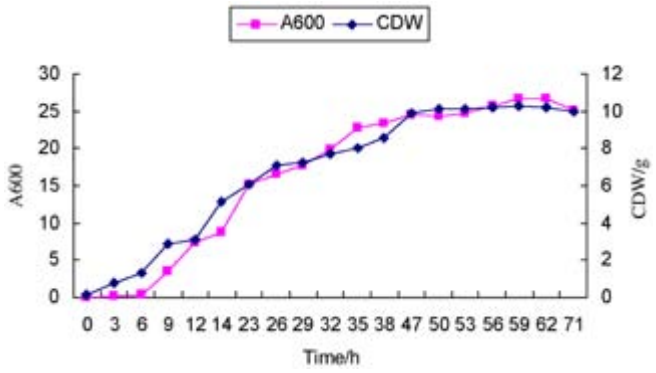

Fig. 4. Time profile of absorbance at 600 nm and CDW of *E. coli* HMS174 with plasmid pUC19/PHA during 15-L fermentor cultivation.

Table 3
Effect of Ampicillin on PHA Production
in *E. coli* HMS174 with Plasmid pUC19/CAB

	Culture Time (h)				
Strain	0	12	16	20	24
HMS 174 pUC19/CAB with ampicillin					
PHB% (w/w)	0	11.69	18.36	17.92	26.74
PHV% (w/w)	0	0.29	0.43	0.92	1.77
Total PHA% (w/w)	0	11.99	18.78	18.83	28.51
A600	0.022	1.99	3.08	3.98	5.19
HMS 174 pUC19/CAB without ampicillin					
PHB% (w/w)	0	12.26	16.78	24.48	29.80
PHV% (w/w)	0	0.30	0.61	0.69	0.91
Total PHA% (w/w)	0	12.56	17.40	25.17	30.71
A_{600}	0.018	1.88	2.93	4.08	4.69

and its CDW were recorded at different time points throughout the fermentation, and the A_{600} and CDW reached as high as 26.7 and 10.27 g/L, respectively, at 59 h of cultivation in the fed-batch culture. The results are shown in Fig. 4.

The use of antibiotics in large-scale fermentation is not desirable because of the high production cost. *E. coli* HMS174 with plasmid pUC19/CAB showed relatively low instability problems during PHA production in the absence of antibiotic selective pressure when in the flask culture (Table 3). The percentage yield of PHA in cell culture with or without ampicillin was similar. Therefore, it was desirable to subject this strain to a fermentor experiment.

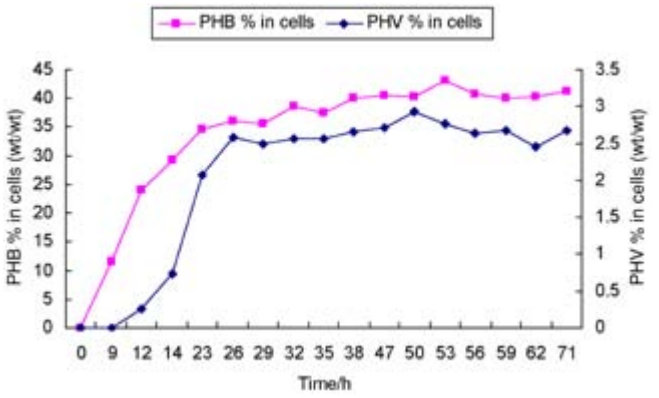

Fig. 5. Percentages of PHB and PHV in CDW of *E. coli* HMS174 with plasmid pUC19/PHA during 15-L fermentor cultivation.

A fed-batch culture was grown in which the cells were fed glucose and propionic acid. The PHA content of the culture was analyzed by GC, and the percentage yield of PHB and PHV in the cells is shown in Fig. 5. The cell concentration increased to 10 g/L CDW when 1% inoculation was used, and the PHB content was maintained at about 40% of CDW throughout the culture and reached as high as 43.2%. However, the PHV content was maintained at about 2% of CDW.

Physical Properties of Extracted Biopolymer from Fermentor

The composition of the hydroxyalkanoates units in extracted products were determined by analyzing the NMR spectra. The ^{1}H-NMR spectrum (Fig. 6) shows the presence of five groups of characteristic signals of the P(HB-HV). The signals with different chemical shifts are attributed to the different groups coupled to different numbers of protons and are labeled in Fig. 6. The spectra showed the presence of CH-, CH_2-, and CH_3- groups in the molecule as labeled in Fig. 6, but no -COOH and -OH groups. Thus, the compound should be a polymer, not a monomer. The magnitudes of the CH_3- and CH_2- groups of PHV in Fig. 6 are lower than those of the PHB that represented the lower percentage of PHV content in the biopolymer when compared with PHB content.

The melting temperature (T_m) of the biopolymer was determined from differential scanning calorimetry thermograms. The T_m value of the P (3HB) homopolymer was about 177°C and P (3HB) with 10% P(3HV) was about 150°C (Table 1), but the T_m values of biopolymer extracted from *E. coli* HMS174 were about 166°C. The T_m of the sample was lower than that of the P (3HB) homopolymer, but higher than that of the P (3HB) with 10% P (3HV), because the P (3HV) content in the sample is only about 4.5% of the biopolymer produced. The PHV content in extracted biopolymer was low, the flexibility of extracted biopolymer was low, and different fermentation conditions should be investigated.

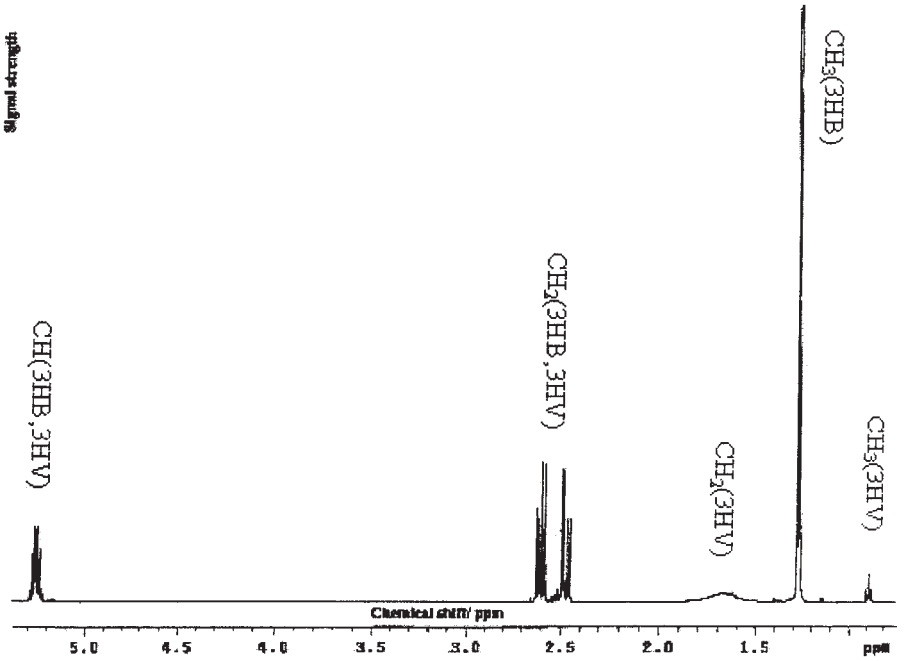

Fig. 6. ^{1}H NMR spectrum of biopolymer produced by *E. coli* HMS174 with plasmid pUC19/PHA in fermentation.

Conclusion

The construction of recombinant *E. coli* harboring *pha* operon from *R. eutrophus* was successful. The plasmids in XL1-Blue, HMS174, and DH5α strains were successfully expressed in the production of PHA, but *E. coli* HMS174 was superior for the production of [P(HB-HV)], whose levels could reach as high as 41% of its dry weight in shake-flask culture and could reach relatively high cell density. The CDW and PHA content of recombinant HMS174 could reach as high as 10.27 g/L and 43% (w/w), respectively, in fed-batch fermentor culture. The strains were also successfully expressed in hydrolyzed soy and malt wastes, which have the potential to lower the cost of production.

Acknowledgments

We wish to express our gratitude to the Hong Kong Polytechnic University and the University Grant Council of Hong Kong for their support (PolyU 5205/00M and PolyU 5272/01M) of this research. We also wish to thank the *E. coli* Genetic Stock Center at Yale University, which kindly contributed the *E. coli* HMS174; and Dr. Dennis Douglas (Department of Biology, James Madison University, Harrisonburg, VA), who kindly contributed the plasmid pJM9131.

References

1. Hong Kong Environmental Protection Department (1999), in *Environment Hong Kong 1999*, Hong Kong Government Press, China.
2. Lee, S. Y. (1996), *Biotechnol. Bioeng.* **49,** 1–14.
3. Chang, Y. K., Hahn, S. K., Kim, B. S., and Chang, H. N. (1994), *Biotechnol. Bioeng.* **44,** 256–261.
4. Doi, Y., Kitamura, S., and Abe, H. (1995), *Macromolecules* **23,** 4822–4828.
5. Porier, Y., Nawrath, C., and Somerville, C. (1995), *Biotechnology* **13,** 142–151.
6. Steinbuchel, A. (1991), in *Biomaterials: Novel Materials from Biological Sources*, Byrom, D., ed., Macmillan, New York, NY, pp 123–213.
7. Steinbuchel, A. (1995), in *Degradable Polymers: Recycling and Plastic Waste Management*, Albertsson, C. and Huang, J., eds., Marcel Dekker, New York, NY, pp. 61–68.
8. Yamane, T., Fukunaga, M., and Lee, Y. W. (1996), *Biotechnol. Bioeng.* **50,** 197–202.
9. Greenberg, A. E., Clesceri, L. S., and Eton, A. D. (1992), *Standard Methods for the Examination of Water and Wastewater*, 18th Ed., APHA, Washington, DC.
10. Yu, H. F., Chua, H., Huang, A. L., Lo, W. H., and Ho, K. P. (1999), *Water Sci Technol.* **40(1),** 365–370.
11. Dennis, D. (1990), US patent no. 5334520.
12. Slater., S., Gallaher, T., and Dennis, D. (1992), *Appl. Environ. Microbial.* **58(4),** 1089–1094.
13. Lee, S. Y. (1998). *Bioprocess Eng.* **18,** 397–399.

0273-2289/04/114/0373–0379/$25.00

Biosynthesis of (*R*)-3-Hydroxyalkanoic Acids by Metabolically Engineered *Escherichia coli*

Si Jae Park,[†,1] Sang Yup Lee,[*,1,2] and Young Lee[1,3]

[1]Metabolic and Biomolecular Engineering National Research Laboratory, Department of Chemical & Biomolecular Engineering, BioProcess Engineering Research Center and [2]Department of BioSystems and Bioinformatics Research Center, Korea Advanced Institute of Science and Technology, 373-1 Guseong-dong, Yuseong-gu, Daejeon 305-701, Republic of Korea, E-mail: leesy@kaist.ac.kr; and [3]ChiroBio Inc., #6102-6103, KAIST Alumni Venture Hall, 400 Guseong-dong, Yuseong-gu, Daejeon 305-338, Republic of Korea

Abstract

An efficient system for the production of (*R*)-hydroxyalkanoic acids (RHAs) was developed in natural polyhydroxyalkanoate (PHA)-producing bacteria and recombinant *Escherichia coli*. Acidic alcoholysis of purified PHA and in vivo depolymerization of PHA accumulated in the cells allowed the production of RHAs. In recombinant *E. coli*, RHA production was achieved by removing CoA from (*R*)-3-hydroxyacyl-CoA and by in vivo depolymerization of PHA. When the recombinant *E. coli* harboring the *Ralstonia eutropha* PHA biosynthesis genes and the depolymerase gene was cultured in a complex or a chemically defined medium containing glucose, (*R*)-3-hydroxybutyric acid (R3HB) was produced as monomers and dimers. R3HB dimers could be efficiently converted to monomers by mild alkaline heat treatment. A stable recombinant *E. coli* strain in which the *R. eutropha* PHA biosynthesis genes were integrated into the chromosome disrupting the *pta* gene was constructed and examined for the production of R3HB. When the *R. eutropha* intracellular depolymerase gene was expressed by using a stable plasmid containing the *hok/sok* locus of plasmid R1, R3HB could be efficiently produced.

Index Entries: (*R*)-Hydroxyalkanoic acids; polyhydroxyalkanoate; *Escherichia coli*; poly-(*R*)-3-hydroxybutyrate; (*R*)-3-hydroxybutyric acid.

[†]Present address: LG Chem, Ltd., 104-1, Moonji-dong, Yuseong-gu, Daejeon, 305-380 Republic of Korea.

*Author to whom all correspondence and reprint requests should be addressed.

Introduction

Polyhydroxyalkanoates (PHAs) are a group of completely biodegradable polyesters that are synthesized in many bacteria under unfavorable growth conditions in the presence of excess carbon source *(1–4)*. More than 150 types of alkanoic acids hydroxylated at the 3-, 4-, 5-, or 6-position, all in (*R*)-configuration if they possess an asymmetric center at the carbon position linked to the hydroxyl group, can be incorporated into PHAs *(5)*. These (*R*)-hydroxyalkanoic acids (RHAs) contain two functional groups that can easily be modified to produce many chiral compounds, especially fine chemicals such as antibiotics, vitamins, perfumes, and pheromones *(6–8)*. For example, (*R*)-3-hydroxybutyric acid (R3HB) is an important precursor of 4-acetoxyazetidinone, which is used for the synthesis of the antibiotics-carbapenem, which has a market worth of almost $1 billion. Methods for producing RHAs by chemical digestion of PHAs have been reported *(8–11)*. However, large amounts of organic solvents were used, and the production efficiency was rather low owing to complex processes.

Poly-(*R*)-3-hydroxybutyrate (PHB) is the most ubiquitous member of PHAs. The metabolism for the synthesis and degradation of PHB plays an important role in many bacteria for the reservation and reutilization of excess carbon/energy source and reducing power *(1)*. In short-chain-length PHA-producing bacteria, PHB is synthesized from acetyl-CoA by three sequential enzymatic reactions catalyzed by β-ketothiolase, acetoacetyl-CoA reductase, and PHA synthase *(12–14)* (Fig. 1). PHB is known to be depolymerized to R3HB by intracellular PHA depolymerase and oligomer hydrolase *(1,2)*. R3HB is further converted to acetoacetate by R3HB dehydrogenase. By employing this cyclic nature of PHB synthesis and degradation, we have recently demonstrated that R3HB could be efficiently produced in the natural PHA-producing bacteria *Alcaligenes latus* by lowering the fermentation pH, under which high activity of intracellular PHA depolymerase was observed, but no activity of R3HB dehydrogenase was found *(15)*.

Recombinant *Escherichia coli* strains harboring the heterologous PHA biosynthesis genes have been shown to be suitable for the high-level production of PHAs. In addition, several engineered metabolic pathways for the synthesis of various RHAs have recently been established in recombinant *E. coli (16–18)*.

In this article, we review the development of processes for the production of RHAs in natural PHA-producing bacteria and metabolically engineered *E. coli* strains.

Bioconversion

Conventional methods for the production of R3HB by bioconversion include chiral oxidation of 1,3-butanediol by bacteria *(19)*, microbial hydroxylation of butyric acid, and microbial or enzymatic reduction of alkyl-3-ketobutyrate *(20,21)*. However, all of these methods have the problem of low productivity and are therefore difficult to industrialize.

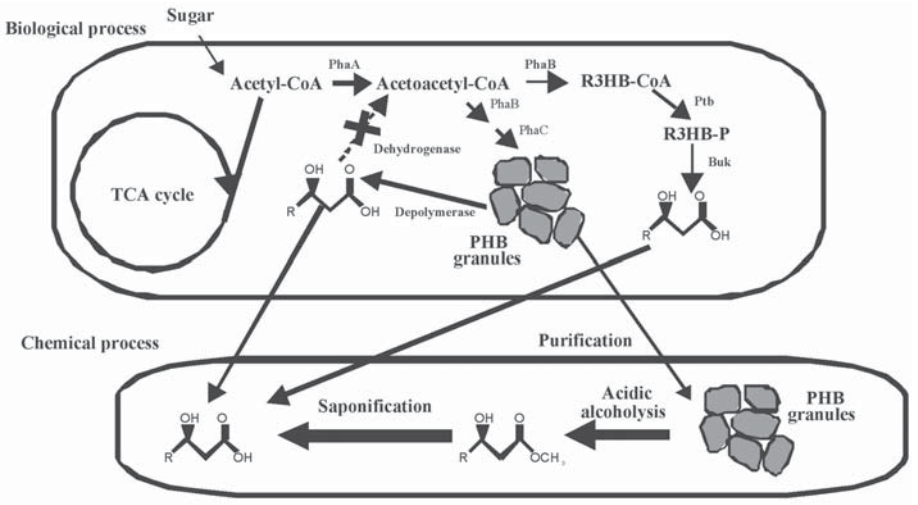

Fig.1. Biologic and chemical processes for production of R3HB in natural and recombinant bacteria. PhaA, β-ketothiolase; PhaB, acetoacetyl-CoA reductase; PhaC, PHA synthase; Ptb, phosphotransbutyrylase; Buk, butyratekinase; TCA, tricarboxylic acid.

Chemical Process of PHA Degradation

Chemical processes for the production of RHAs and RHA alkyl esters are composed of two steps *(9,22)* (Fig. 1). First, PHA is synthesized in natural or recombinant bacteria and then purified. Cells containing PHA can also be used. Second, purified PHA (or cells containing PHA) is depolymerized by acidic alcoholysis using sulfuric acid or hydrochloric acid as an acidic catalyst to produce RHA alkylesters. Subsequent saponification of the purified RHA alkylesters yields corresponding RHAs.

PHB produced by recombinant *E. coli* harboring the *R. eutropha* PHA biosynthesis genes was subjected to acidic alcoholysis, resulting in the production of R3HB methylester *(9)*. One of the disadvantages of acidic alcoholysis is that the purity of PHA should be high enough to support good yield, and, therefore, the production cost is rather high owing to the expensive polymer purification procedure. Recombinant *E. coli* seems to be suitable for the development of processes for the economical production of R3HB because it allows production of a large amount of PHB and economical purification of PHB by a simple NaOH digestion method *(23)*.

Medium-chain-length (MCL) (*R*)-3-hydroxyalkanoic acid (R3HA) methylesters having carbon numbers of 6–12 were produced by acidic methanolysis of MCL-PHA purified from *Pseudomonas putida (22)*. Because MCL-PHA is composed of several monomers, the produced R3HA methylester mixtures were further seperated using distillation. Distillation yield decreased with increasing carbon numbers of MCL-R3HA methylesters, resulting in 99.9, 99.8, 88.4, and 56.8% for 3-hydroxyhexanoic, 3-hydroxyoctanoic, 3-hydroxydecanoic, and 3-hydroxydodecanoic acid

methylester, respectively. MCL-R3HA methylesters could be easily converted into R3HAs by saponification *(22)*.

Biologic Process of PHA Degradation

Construction of Pathways for Production of RHAs Without PHA Synthesis

When two of the PHA biosynthesis genes coding for β-ketothiolase and reductase are expressed without PHA synthase gene, (*R*)-hydroxyacyl-CoAs (R3HA-CoAs) should be accumulated in the cytoplasm. The key challenge of this process toward R3HA production is how to efficiently remove CoA from R3HA-CoA. Recently, it was found that *E. coli* possesses unknown enzymes that are able to remove the CoA moiety from R3HA-CoA *(16,17)*. The pathways for the production of R3HB and MCL-R3HA were constructed in recombinant *E. coli*. When the recombinant *E. coli* DH5α harboring the *R. eutropha phaAB* genes was cultured on glucose, R3HB was produced and excreted into the medium up to 0.66 g/L. In addition, the expression of the *P. putida phaG* gene encoding 3-hydroxydecanoyl-ACP:CoA transacylase in recombinant *E. coli* DH5α resulted in production of the mixtures of 3-hydroxyoctanoic acid and 3-hydroxydecanoic acid up to 0.19 g/L *(16)*.

A more efficient pathway for the production of R3HB was constructed by the coexpression of the *R. eutropha phaAB* genes, and the phosphotransbutyrylase (*ptb*) and butyrate kinase (*buk*) genes in *E. coli* (Fig. 1). CoA was efficiently removed from R3HB-CoA by conversion of R3HB-CoA to R3HB-P, and finally to R3HB by butyrate kinase. Up to 1.4 g/L of R3HB was produced by culturing this recombinant *E. coli* DH5α on glucose. In addition, fed-batch culture of this recombinant *E. coli* yielded 12 g/L of 3HB in 48 h *(17)*.

Construction of Pathways for Production of RHAs with PHA Synthesis

Using Natural PHA-Producing Bacteria

The key concept consists of PHA biosynthesis and subsequent depolymerization of produced PHA in cells; therefore, it can be called an in vivo PHA depolymerization process *(15)*. RHAs produced by the depolymerization of PHAs can be excreted into the medium when the further intracellular metabolism of RHAs is inhibited. Because all the PHA-producing bacteria also possess PHA degradation pathways, in vivo depolymerization of PHA can be achieved by natural PHA-producing bacteria when the proper conditions are met.

We have recently reported the development of a process for the in vivo depolymerization of PHA in several natural PHA producing bacteria including *A. latus*, *R. eutropha*, and pseudomonads *(15)*. Metabolic pathways involved in the synthesis and degradation of PHB are shown in Fig. 1.

As seen from the metabolic pathways, it is important to maintain the highest activity of depolymerase with the lowest or no R3HB dehydrogenase activity for the successful production of R3HB. Because PHA is first accumulated and subsequently depolymerized into monomers, the initial amount of accumulated PHA is important to achieve efficient monomer production. Different concentrations (10.1 g/L and 135.6 g/L) of *A. latus* cells containing PHB were examined for the production of R3HB *(15)*. When these cells were incubated at pH 4.0, which supports highest depolymerase and lowest R3HB dehydrogenase activities, 8.7 and 117.8 g/L of R3HB, respectively, were obtained. Other RHAs such as (*R*)-3-hydroxyvaleric acid (R3HV) and MCL-R3HAs could also be produced by in vivo depolymerization of corresponding PHAs accumulated in *R. eutropha* and pseudomonads *(15)*. These results suggest that more than 150 different types of R3HA can be produced by accumulating and depolymerizing PHA in cells having PHA metabolism using the strategy described *(5)*.

Using Metabolically Engineered *E. coli*

It has previously been demonstrated that recombinant *E. coli* strains harboring the *R. eutropha* PHA biosynthesis genes *(12–14)* are able to accumulate a large amount of PHB, up to 90% of dry cell weight *(24)*. Recently, the intracellular PHB depolymerase gene was cloned from *R. eutropha (25)*. It was therefore reasoned that R3HB and other RHAs may be efficiently produced by establishing a heterologous PHA biosynthesis and degradation pathway in *E. coli*. It is advantageous that *E. coli* does not possess a metabolic pathway consuming R3HB. For the construction of a R3HB production system employing recombinant *E. coli*, a plasmid containing the *R. eutropha* PHA biosynthesis genes and the PHA depolymerase gene was constructed and transformed into *E. coli (18)*. When this metabolically engineered *E. coli* was cultured in complex or chemically defined medium containing glucose, R3HB was produced as monomers and dimers. R3HB dimers could be efficiently converted to monomers by mild alkaline heat treatment. Additionally, R3HV could be produced by culturing recombinant *E. coli* on glucose and propionic acid as carbon sources *(18)*.

During the batch culture of recombinant *E. coli* for the production of R3HB, it was found that the concentration of R3HB dimers increased at the expense of R3HB monomer concentration (Table 1; *[18]*). This result suggests that some of the R3HB monomers excreted are esterified to form R3HB dimers. Generally, the carboxylic acid group of R3HB can readily be esterified with alcohol groups to form esters *(26,27)*. Since R3HB molecules possess both alcohol and carboxylic acid functional groups, the produced R3HB monomers can serve as reactants for reversible intermolecular esterification to form R3HB dimers. When R3HB was excreted mainly as monomers by the depolymerization of PHB during the exponential growth phase, the ratio of R3HB monomer to its dimer was high enough to proceed with the esterification reaction. Nonetheless, R3HB could be successfully obtained by mild alkaline heat treatment *(18)*.

Table 1
Summary of Batch Cultivation of Recombinant *E. coli* XL1-Blue for the Production of R3HB[a]

Plasmid	Cultivation time (h)	Cell mass (g/L)	Concentration (g/L)			Monomer yield (%)
			PHB	R3HB[b]	R3HB[c]	
Single plasmid[d]	30	1.29	1.29	2.38	9.60	48.1
Two plasmids[e]	30	0.46	ND[f]	1.67	9.89	49.5

[a] Data are taken from ref. *18*.
[b] R3HB concentration produced in monomeric form.
[c] R3HB concentration obtained after alkaline heat treatment.
[d] Plasmid pSYL105Red containing *R. eutropha* PHA biosynthesis genes and depolymerase gene was used.
[e] Plasmids p5184 containing *R. eutropha* PHA biosynthesis genes and pUC19Red containing *R. eutropha* depolymerase gene were used.
[f] Not detected.

To solve the problem that some PHB was left over in recombinant *E. coli*, the two-plasmid system, in which depolymerase gene was cloned into a high-copy-number plasmid, pUC19, and the PHA biosynthesis genes into a low-copy-number plasmid, pACYC184, was developed. Using this two-plasmid system, R3HB could be efficiently produced with a negligible amount of PHB left over (Table 1; *[18]*).

Conclusion

As indicated, R3HA could be efficiently produced by employing natural PHA producers or metabolically engineered *E. coli* harboring the genes involved in the biosynthesis and degradation of PHA. Since more than 150 different monomer units (RHAs) have been found to be incorporated into PHAs *(5)*, these RHAs can be produced by employing the same strategy. The biosynthesis described here is a good example of "green chemistry" since high-value fine chemicals and enantiomerically pure hydrocarboxylic acids are produced from renewable resources such as glucose and fatty acids.

Acknowledgments

This work was supported by the Ministry of Commerce, Industry and Energy, the Brain Korea 21 program of the Ministry of Education, and by the National Research Laboratory Program (2000-N-NL-01-C-237) of the Korean Ministry of Science and Technology (MOST).

References

1. Anderson, A. J. and Dawes, E. A. (1990), *Microbiol. Rev.* **54,** 450–472.
2. Doi, Y. (1990), *Microbial Polyesters*, VCH, New York, NY.

3. Lee, S. Y. (1996), *Biotechnol. Bioeng.* **49,** 1–14.
4. Steinbüchel, A. and Fuchtenbusch, B. (1998), *Trends Biotechnol.* **16,** 419–427.
5. Steinbüchel, A. and Valentin, H. E. (1995), *FEMS Microbiol. Lett.* **128,** 219–228.
6. Chiba, T. and Nakai, T. (1985), *Chem. Lett.,* 651–654.
7. Schnurrenberger, P., Hungerbühler, E., and Seebach, D. (1987), *Liebigs Ann. Chem.,* 733–744.
8. Yu, D., Ellis, H. M., Lee, E.-C., Jenkins, N. A., Copeland, N. G., and Court, D. L. (2000), *Proc. Natl. Acad. Sci. USA* **97,** 5978–5983.
9. Lee, Y., Park, S. H., Lim, I. T., Han, K., and Lee, S. Y. (2000), *Enzyme Microb. Technol.* **27,** 33–36.
10. Seebach, D., Beck, A. K., Breitschuh, R., and Job, K. (1992), *Org. Synth.* **71,** 39–47.
11. Seebach, D. and Zuger, M. F. (1982), *Helvetica Chim. Acta.* **65,** 495–503.
12. Peoples, O. P. and Sinskey, A. J. (1989), *J. Biol. Chem.* **264,** 15,298–15,303.
13. Schubert, P., Steinbüchel, A., and Schlegel, H. G. (1988), *J. Bacteriol.* **170,** 5837–5847.
14. Slater, S. C., Voige, W. H., and Dennis, D. (1988), *J. Bacteriol.* **170,** 4431–4436.
15. Lee, S. Y., Lee, Y., and Wang, F. (1999), *Biotechnol. Bioeng.* **65,** 363–368.
16. Gao, H. J., Wu, Q., and Chen, G. Q. (2002), *FEMS Microbiol. Lett.* **213,** 59–65.
17. Zhao, K., Tian, G., Zheng, Z., Chen, J. C., and Chen, G. Q. (2003), *FEMS Microbiol. Lett.* **218,** 59–64.
18. Lee, S. Y. and Lee, Y. (2003), *Appl. Environ. Microbiol.* **69,** 3421–3426.
19. Hasegawa, J., Ogura, M., Kanama, H., Noda, N., Kawaharada, H., and Watanabe, K. (1982), *J. Ferment. Technol.* **60,** 501–508.
20. Deol, B. S., Ridley, D. D., and Simpson, G. W. (1976), *Aust. J. Chem.* **29,** 2459–2467.
21. Mochizuki, N., Sugai, T., and Ohta, H. (1994), *Biosci. Biotech. Biochem.* **58,** 1666–1670.
22. de Roo, G., Kellerhals, M. B., Ren, Q., Witholt, B., and Kessler, B. (2002), *Biotechnol. Bioeng.* **77,** 717–722.
23. Choi, J., and Lee, S. Y. (1999), *Biotechnol. Bioeng.* **62,** 546–553.
24. Madison, L. L. and Huisman, G. W. (1999), *Microbiol. Mol. Biol. Rev.* **63,** 21–53.
25. Saegusa, H., Shiraki, M., Kanai, C., and Saito, T. (2001), *J. Bacteriol.* **183,** 94–100.
26. Miltenberger, K. and Aktiengesellschaft, H. (1985–1996), in *Ullmann's Encyclopedia of Industrial Chemistry*, 5th Ed., Arpe, H.-J. et al., eds., Wiley-VCH, Weinheim, Berlin, Germany, pp. 507–517.
27. Gerdes, K. (1988), *Bio/Technology* **6,** 1402–1405.

0273-2289/04/114/0381–0388/$25.00

Gibberellic Acid Production by Free and Immobilized Cells in Different Culture Systems

Enrique Durán-Páramo,* Héctor Molina-Jiménez, Marco A. Brito-Arias, and Fabián Robles-Martínez

Bioprocess Department, Unit of Biotechnology (UPIBI), National Polytechnic Institute, Ave. Acueducto s/n, La Laguna, Ticomán, 07340 Mexico, D.F., E-mail: eduran@acei.upibi.ipn.mx

Abstract

Gibberellic acid production was studied in different fermentation systems. Free and immobilized cells of *Gibberella fujikuroi* cultures in shake-flask, stirred and fixed-bed reactors were evaluated for the production of gibberellic acid (GA_3). Gibberellic acid production with free cells cultured in a stirred reactor reached 0.206 g/L and a yield of 0.078 g of GA_3/g biomass.

Index Entries: Cell immobilization; gibberellic acid; *Gibberella fujikuroi*; shake flasks; free cells; immobilized cells.

Introduction

Gibberellic acid represents one of the most important plant growth regulators produced from microorganisms owing to its extensive practical uses in agriculture. At present, the production of gibberellic acid by submerged fermentation with the filamentous fungi *Gibberella fujikuroi* can be a practical alternative to increase the production of vegetal biomass for the production of more and better foods, fuels, and chemicals. Gibberellic acid production has been widely studied with different strains of *G. fujikuroi* in different fermentation systems *(1–8)*. In the present work, we studied gibberellic acid production using free and immobilized cells of *G. fujikuroi* NRRL-2278 in order to select the most suitable fermentation system using this particular strain.

*Author to whom all correspondence and reprint requests should be addressed.

Materials and Methods

Microorganism

G. fujikuroi NRRL-2278 obtained from the US Department of Agriculture, maintained on potato dextrose agar (PDA) slants, and stored at 4°C.

Growth Medium and Inoculum

The culture medium proposed by González et al. *(4)* with a slight modification was used. The composition was glucose (25.0 g/L), KH_2PO_4 (5.0 g/L), NH_4NO_3 (1.33 g/L), and $MgSO_4$ (1.0 g/L). The culture medium was sterilized at 121°C for 20 min. The pH of the culture medium was about 4.0 after sterilization. Inoculum (200 mL) for submerged fermentations was obtained from a 48-h shake-flask culture (120 rpm) at 30°C. The seed medium was inoculated with mycelium grown 5 d in PDA slants.

Fermentation

The microorganism was grown at 38°C within agitation of 200 rpm and a 0.3-vvm aeration in a 5-L laboratory fermentor with a working volume of 3.5-L (Bioflo II; New Brunswick Scientific). For free-cell cultures, 0.7 L of preinoculum was grown in Erlenmeyer flasks for 12 h at 38°C in a rotary shaker and used to inoculate 3.5 L of medium in the fermentor.

Immobilization

The mycelium biomass recovered from 200 mL of the seed culture was mixed with 200 mL of sterile 2% (w/v) κ-carrageenan (E407; Ceca, Paris, France) at 42°C. The mycelium-carrageenan suspension was then pumped through a couple of needles and dropped into sterile KCl solution (0.3 *M*) to form gel beads with an average diameter of 3 mm. Gel beads were soaked for 30 min in the same KCl solution. All immobilization experiments were carried out under aseptic conditions.

Dissolution of Beads

To quantify the immobilized biomass, gel beads were dissolved by the addition of 0.1 *M* sodium citrate *(9)*.

Analysis

Reducing sugars were determined using the dinitrosalicylic acid reagent *(10)*. The biomass was determined by mycelial dry weight. Ammonia was determined by the phenol-hipochlorite reaction *(11)*. Quantification of gibberellic acid was performed by the spectrophotometric method of Holbrook et al. *(12)*, and the purity of gibberellic acid was verified by thin-layer chromatography.

Results and Discussion

The objective of the present study was to compare gibberellic acid production with free and immobilized cells of *G. fujikuroi* in different

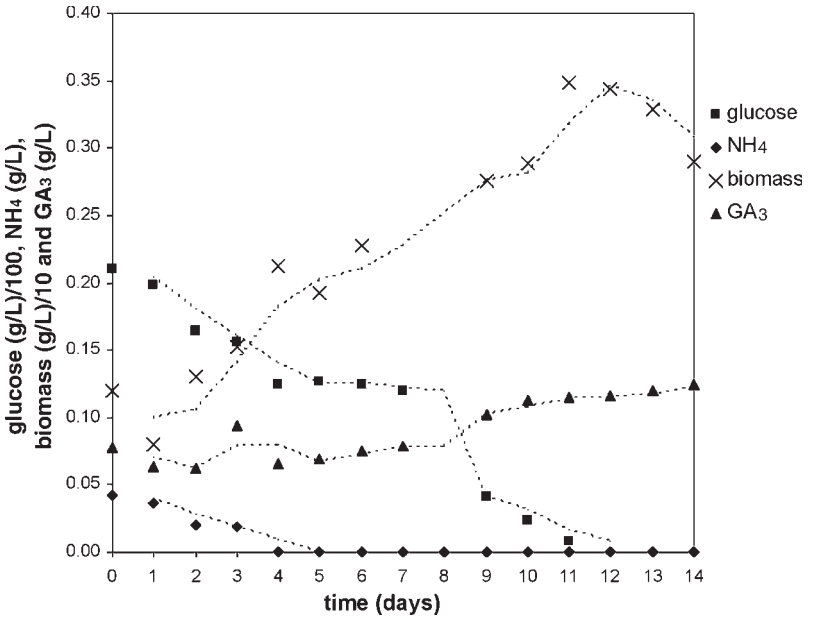

Fig. 1. Gibberellic acid production with free cells of *G. fujikuroi* cultured in Erlenmeyer flasks.

fermentation systems. All experiments were carried out three times, and average results are presented in Figs. 1–5.

Fermentation of Free Cells in Shake Flasks

Figure 1 shows the gibberellic acid production with free cells in shake flasks. Fermentation was carried out at 31° C with an initial pH of 4.5 and agitation of 120 rpm. As can be observed, the nitrogen source was exhausted after 5 d of fermentation. Under nitrogen limitation, gibberellic acid production was effective. Gibberellic acid concentration at the beginning of the fermentation seems to be related to that of the seed inoculum. On d 14, 0.12 g/L of gibberellic acid was produced. Glucose was exhausted after 12 d of fermentation, and at the same time, exponential growth plateaud and then fell. The pH fell because of the production of gibberellic acid. The fermentation of free cells in shake flasks presented a behavior according to that described by Borrow et al. *(13,14)*, in which two phases are presented: producing and nonproducing. The nonproducing phase was characterized by uptake of carbon and nitrogen sources. Under nitrogen limitations, the metabolism of *G. fujikuroi* switches to the production of gibberellic acid and storage compounds such as lipids and polyols, as described by Brückner and Blechschmidt *(15,16)*.

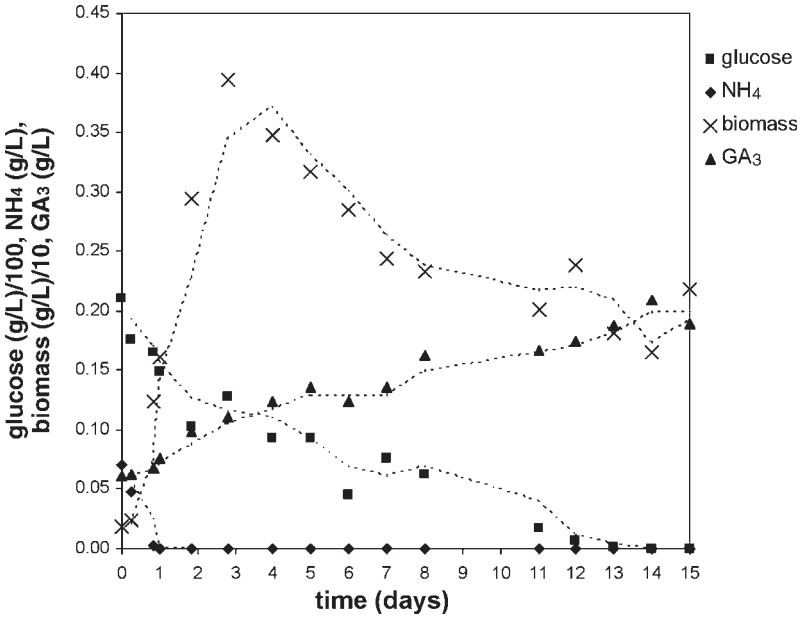

Fig. 2. Gibberellic acid production with free cells of *G. fujikuroi* cultured in stirred reactor.

Fermentation of Free Cells in Stirred Reactor

Figure 2 shows gibberellic acid production by free *G. fujikuroi* cells cultured in a stirred reactor. Some kinetic differences in the stirred reactor regarding shake flasks cultures are observed. The aeration (0.3 vvm) and agitation (200 rpm) in the stirred reactor may be implied in these kinetic differences. As reported by Borrow et al. *(13,14)*, exponential growth ceases when assimilable nitrogenous nutrients are exhausted. However, glucose was exhausted only after 13 d of fermentation. Gibberellic acid production reached a concentration of 0.206 g/L and was almost twice that obtained with free cells in shake flasks.

Fermentation of Immobilized Cells in Erlenmeyer Flasks and in Stirred Reactor

The growth of immobilized cells ceased once the nitrogen source was exhausted, as reported by Nava et al. *(17)* (Fig. 3). After that, immobilized cells were released from the immobilization support and became free cells. Gibberellic acid production (0.160 g/L) was effective once the ammonia was exhausted, and it continued until total glucose consumption. In the case of immobilized cells cultured in a stirred reactor, Fig. 4 shows the fermentation kinetics. One can observe some differences related to the immobilized biomass production, and the uptake in nitrogen and carbon sources. However,

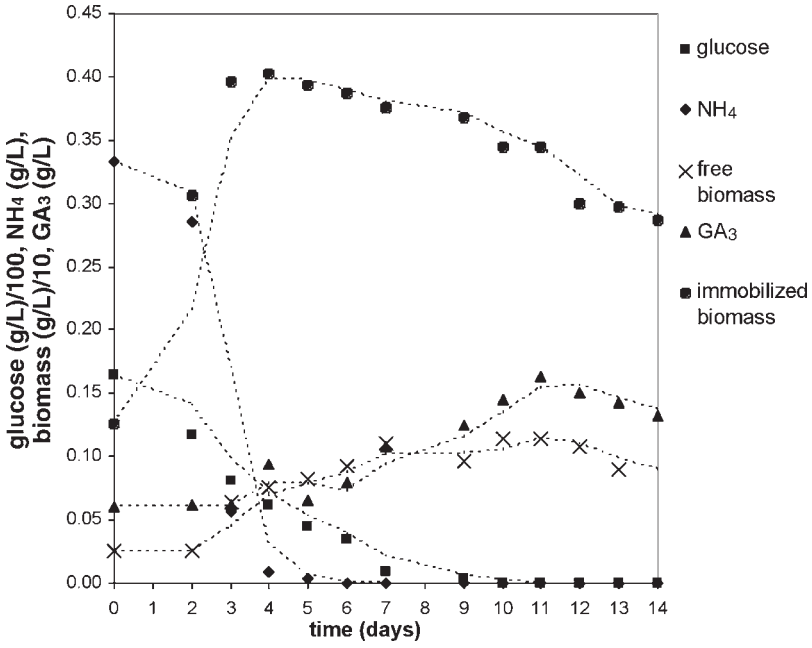

Fig. 3. Gibberellic acid production with immobilized cells of *G. fujikuroi* cultured in Erlenmeyer flasks.

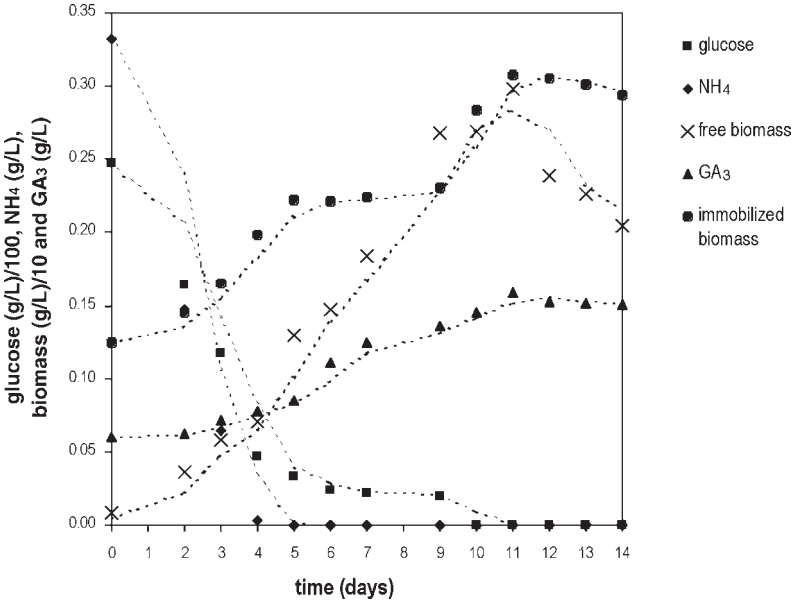

Fig. 4. Gibberellic acid production with immobilized cells of *G. fujikuroi* cultured in stirred reactor.

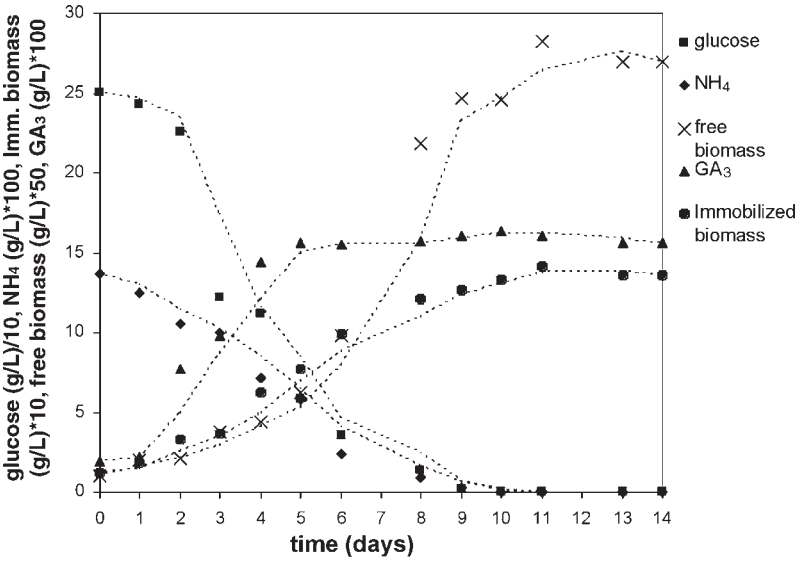

Fig. 5. Gibberellic acid production with immobilized cells of *G. fujikuroi* cultured in fixed-bed reactor.

gibberellic acid concentration (0.163 g/L) had no significant difference regarding the fermentation of immobilized cells in shake flasks. The differences found in the fermentation kinetics seem to be related to the agitation (200 rpm) and aeration (0.3 vvm) in the stirred reactor.

Fermentation of Immobilized Cells in Fixed-Bed Reactor

Figure 5 shows gibberellic acid production by immobilized cells of *G. fujikuroi* in a fixed-bed reactor. Gibberellic acid production after d 4 was effective even under conditions of no nitrogen limitations. Carbon and nitrogen sources were exhausted on d 10, when released and immobilized biomass reached a maximum. The differences observed in that culture may be related to the diffusional limitations imposed by the immobilization support. Cell immobilization allows high biomass concentration and gradient formation inside the immobilization support by diffusional limitations. Diffusional limitations give rise to different microenvironments inside the carrier where fungi cells can develop under nitrogen limitations. Thus, the concentrations dosed into the immobilization support may be different from those dosed in the bulk solution *(9)*.

Gibberellic acid production was almost the same regarding the other immobilized cell fermentation systems (0.164 g/L). There was no significant difference among all immobilized cell systems tested. Further optimization studies should be carried out with immobilized cell systems for the production of gibberellic acid.

Table 1
Production and Yields of Gibberellic Acid by Free and Immobilized Cells of *G. fujikuroi* in Different Culture Systems

	GA_3 (g/L)		$Y_{P/X}$ (g GA_3/g biomass)	
Fermentation system	Free cells	Immobilized cells	Free cells	Immobilized cells
Shake flasks	0.120	0.160	0.052	0.054
Stirred reactor	0.206	0.163	0.078	0.036
Fixed-bed reactor	—	0.164	—	0.027

Conclusion

Table 1 summarizes the results of the fermentations performed in the present study with free and immobilized cells of *G. fujikuroi*. Under the tested culture conditions, no significant differences were found among the immobilized cell systems for gibberellic acid production. However, gibberellic acid production with free cells cultured in the stirred reactor was higher than that obtained in Erlenmeyer flasks or in any other fermentation system assessed. Specific production of gibberellic acid was also the most important in the fermentation of free cells in stirred reactor compared with the other systems evaluated (Table 1). The culture medium and conditions should be further optimized in order to increase gibberellic acid production with immobilized cell culture systems. At present, we trying to meet this goal by using an orthogonal experimental design. In addition, we are working on optimizing the immobilization technique and its use with fixed-bed reactors for the production of gibberellic acid.

Acknowledgments

We wish to thank the Consejo Nacional de Ciencia y Tecnología of Mexico (CONACYT) and the Instituto Politécnico Nacional (CGPI and COFAA), Mexico, for their help and financial support (CONACYT-30206 and CGPI-20010709).

References

1. Bandelier, S., Renaud, R., and Durand, A. (1997), *Process Biochem.* **32,** 141–145.
2. Escamilla, E. M., Dendooven, L., Magaña, I. P., Parra, R. S., and De la torre, M. (2000), *J. Biotech.* **76,** 147–155.
3. Gelmi, C., Pérez-Correa, R., González, M., and Agosin, E. (2000), *Process Biochem.* **35,** 1227–1233.
4. González, P., Delgado, G., Antigua, M., Rodríguez, J., Larralde, P., Viniegra, G., Pozo, L., and Pérez, M. (1994), in *Advances in Bioprocess Engineering*, Galindo, E. and Ramirez, O. T., eds., Kluwer Academic, Dordrecht, The Netherlands, pp. 425–430.

5. Lu, Z. X., Xie, Z. C., and Kumakura, M. (1995), *Process Biochem.* **30,** 661–665.
6. Pastrana, L. M., Gonzalez, M. P., Pintado, J., and Murado, M. A. (1995), *Enzyme Microb. Technol.* **17,** 784–790.
7. Qian, X. M., du Perez, J. C., and Kilian, S. G. (1994), *World J. Microbiol. Biotechnol.* **10,** 93–99.
8. *Tomasini, A., Fajardo, C., and Barrios-González, J. (1997),* World J. Microbiol. Biotechnol. *13, 203–206.*
9. Durán-Páramo, E. (1997), PhD thesis, Université de Technologie de Compiègne, Compiègne, France.
10. Miller, G. L. (1959), *Anal. Chem.* **31,** 426–428.
11. Weatherburn, M. W. (1967), *Anal. Chem.* **39,** 971–974.
12. Holbrook, A. A., Edge, W. J. W., and Baily, F. (1961), *Adv. Chem. Ser.* **28,** 159–167.
13. Borrow, A., Brown, S., Jefferys, E. G., Kerssell, R. H. J., Lloyd, E., Lloyd, P. B., Rothwell, A., Rothwell, B. and Swait, J. C. (1964), *Can. J. Microbiol.* **10,** 407–444.
14. Borrow, A., Jefferys, E. G., Kerssell, R. H. J., Lloyd, E., Lloyd, P. B., and Nixon, I. S. (1961), *Can. J. Microbiol.* **7,** 227–276.
15. Brückner, B. and Blechschmidt, D. (1991), *Appl. Microbiol. Biotechnol.* **35,** 646–650.
16. Brückner, B. and Blechschmidt, D. (1991), *Crit. Rev. Biotechnol.* **11,** 163–192.
17. Nava Saucedo, J. E., Barbotin, J. N., and Thomas, D. (1989), *Appl. Environ. Microbiol.* **55,** 2377–2384.

0273-2289/04/114/0389–0401/$25.00

Screening Genus *Penicillium* for Producers of Cellulolytic and Xylanolytic Enzymes

Kristian B. R. Krogh, Astrid Mørkeberg, Henning Jørgensen,[†] Jens C. Frisvad, and Lisbeth Olsson[*]

Center for Process Biotechnology, BioCentrum-DTU, Technical University of Denmark, Building 223, DK-2800 Lyngby, Denmark, E-mail: lo@biocentrum.dtu.dk.

Abstract

For enzymatic hydrolysis of lignocellulosic material, cellulolytic enzymes from *Trichoderma reesei* are most commenly used, but, there is a need for more efficient enzyme cocktails. In this study, the production of cellulolytic and xylanolytic enzymes was investigated in 12 filamentous fungi from genus *Penicillium* and compared with that of *T. reesei*. Either Solka-Floc cellulose or oat spelt xylan was used as carbon source in shake flask cultivations. All the fungi investigated showed coinduction of cellulolytic and xylanolytic enzymes during growth on cellulose as well as on xylan. The highest filter paper activity was measured after cultivation of *Penicillium brasilianum* IBT 20888 on cellulose.

Index Entries: Cellulolytic enzymes; hemicellulolytic enzymes; enzymatic hydrolysis; coinduction.

Introduction

Today, an international awareness of the increasing CO_2 concentration in the atmosphere has resulted in the formation of the Kyoto Protocol, which has led many countries to make the commitment to decrease the emission of CO_2. One way of decreasing CO_2 emissions could be substitution of fossil fuels with renewable energy sources. The net production of CO_2 is significantly lower when bioethanol produced from plant materials is used as transportation fuel instead of fossil fuels, since CO_2 is assimilated

[†]Present address: Plant Fibre Laboratory, Department of Agricultural Sciences, The Royal Veterinary and Agricultural University, Højbakkegård Alle 1, DK-2630 Taastrup, Denmark.

*Author to whom all correspondence and reprint requests should be addressed.

during photosynthesis *(1)*. To meet the future demand for bioethanol, not only starch but also lignocellulosic materials need to be used as substrate.

The polysaccharides in the raw materials need to be hydrolyzed before the sugar monomers can be fermented to ethanol. Today, enzymatic hydrolysis is regarded as a method with great potential. One major obstacle to overcome is the high cost of cellulolytic enzymes. In 2001, the United States Department of Energy formed a contract with two commercial producers of cellulolytic enzymes in an attempt to achieve a 10-fold decrease in the cost of the cellulolytic enzymes (www.ott.doe.gov/biofuels/research_partnerships.html).

The decay of plant material in nature is partly owing to the production of cellulolytic and hemicellulolytic enzymes in microorganisms. Filamentous fungi, such as *Trichoderma reesei*, *Penicillium pinophilum*, and *Humicola insolens* have demonstrated the capability of secreting large amounts of cellulolytic enzymes *(2)*. The most extensively studied microorganism producing cellulolytic enzymes is the filamentous fungus *T. reesei* which is the preferred microorganism for industrial production of cellulolytic enzymes. One of the main limitations of the cellulolytic system from *T. reesei* is the low amount of β-glucosidase (BG) *(3)*. Low BG activity leads to a buildup of cellobiose during hydrolysis, which inhibits the activity of the cellobiohydrolases (CBHs) to a larger extent than glucose does *(4)*. Therefore extra BG needs to be added for an efficient hydrolysis of cellulosic materials *(5)*.

Microorganisms grow in various habitats in nature, and they have therefore adapted to various physical and chemical conditions. In the search for microorganisms that efficiently can degrade lignocellulose, several species from genus *Penicillium* were tested. In forest soil, where large amounts of plant materials are degraded, an abundance of *Penicillium* species is present *(6)*. Because of this fact and that enzyme mixtures from various *Penicillium* species have been shown to perform well in the hydrolysis of different kinds of lignocellulosic material *(7–9)*, we screened 12 different *Penicillium* species for their production of cellulolytic and xylanolytic enzymes.

Materials and Methods

Strains

The filamentous fungi screened were all from the genus *Penicillium* (Table 1) and were selected from the culture collection at BioCentrum-DTU, Technical University of Denmark. The filamentous fungi *T. reesei* Rut C30 was used as reference strain.

Preparation of Inoculum

Each strain was received on a Czapek yeast autolysate agar plate from the culture collection. Spores were transferred to a potato dextrose agar (PDA) (Difco, Detroit, MI) plate and the PDA plates were kept at the optimal temperature for growth (Table 1). After 2 wk the strains on the PDA

Table 1
Subgenus, Optimal Growth Temperature, and Origin for 12 *Penicillium* Strains Investigated

Strain	Subgenus	Temperature (°C)	Isolated from
P. allii IBT 3803	*Penicillium*	25	Garlic, Denmark
P. persicinum IBT 13226	*Furcatum*	25	Soil, USA
P. simplicissimum IBT 13237	*Furcatum*	30	Flannel bag, South Africa
P. simplicissimum IBT 15303	*Furcatum*	30	Feed, Norway
P. brasilianum IBT 20888	*Furcatum*	30	Seaweed, Denmark
P. pinophilum IBT 4186	*Biverticillium*	30	Maize, India
P. funiculosum IBT 5816	*Biverticillium*	30	Citric acid (10 %), Australia
P. pinophilum IBT 10872	*Biverticillium*	30	Maize, India
P. rubicundum IBT 10943	*Biverticillium*	30	Cultivated soil, United States
P. aculeatum IBT 18363	*Biverticillium*	30	Rhizosphere of bamboo, Taiwan
P. verruculosum IBT 18366	*Biverticillium*	30	Soybeen seed, Taiwan
P. minioluteum IBT 21486	*Biverticillium*	25	Fruit, Denmark

plates had produced spores, which were suspended in 0.1% (v/v) Tween-80 (P-1754; Sigma, St. Louis, MO).

Shake Flask Cultivations

An amount of each spore suspension was transferred to a 500-mL shake flask in order to obtain a spore concentration of 10^6 spores/mL. The medium was a modified Mandels and Weber medium *(10)*, in which the concentration of KH_2PO_4 was increased by 50% to improve buffer capacity. The initial volume in the shake flask was 150 mL. The carbon sources were either 2% (w/v) Solka-Floc cellulose (FCC200; Fiber Sales & Development) or 2% (w/v) oat spelt xylan (X-0627; Sigma). Cultivations were carried out aerobically at 150 rpm and at the optimal growth temperature for each strain (Table 1) and *T. reesei* Rut C30 was cultivated at 30°C. Samples were taken at regular time intervals during the cultivations, filtered through a 0.22-µm low-protein-binding filter (Cameo 25 GSS; Osmonics), and the filtrates were stored at –20°C.

Enzymatic Assays

Filter Paper Activity

Total cellulolytic activity was measured using the filter paper assay (FPA) according to Ghose *(11)* based on an estimation of the released reducing sugars by dinitrosalicylic (DNS) acid *(12)*.

Xylanase Activity

Xylanase (XA) activity was measured through the degradation of birch-wood xylan (7500.1; Roth, Karlsruhe, Germany) according to Bailey et al. *(13)* based on an estimation of the released reducing sugars by DNS acid *(12)*.

Endoglucanase and Endoxylanase Activities

Endoglucanase (EG) and endoxylanase (EX) activities were measured using azo-carboxymethyl cellulose (Megazyme, Bray, Ireland) and azo-xylan (Megazyme), respectively, as substrate as described by Jørgensen et al. *(14)*.

BG, β-Xylosidase, and α-L -Arabinofuranosidase Activities

BG, β-xylosidase (BX), α-L -arabinofuranosidase (AF), and β-galactosidase activities were measured using *p*-nitrophenyl-β-D-glucopyranoside (73676; Fluka), *p*-nitrophenyl-β-D-xylopyranoside (Sigma N-2132), and *p*-nitrophenyl-α-L-arabinofuranoside (N-3641; Sigma), respectively, as substrate as described by Jørgensen et al. *(14)*.

CBH Activity

CBH activity was measured in a 1 m*M* *p*-nitrophenyl-β-D-cellobioside (N-5759; Sigma) substrate solution at pH 4.8 with 50 m*M* sodium citrate. The substrate solution also contained 1.3 m*M* D-glucono-1,5-δ-lactone in

order to inhibit BG from hydrolyzing the substrate and thereby overestimating the CBH activity *(15)*. Otherwise, the procedure was as described for BG, BX, and AF activity.

Determination of Protein

Intracellular Protein

Mycelium was washed twice with 0.9% (w/v) NaCl followed by three extraction steps. In each extraction step the mycelium was boiled for 10 min with 1 *M* NaOH and the supernatant was collected after centrifugation *(16)*. The amount of protein in the pooled supernatant was measured based on the biuret method *(17)*.

Extracellular Protein

The concentration of extracellular protein was quantified using the "Bio-rad total protein" assay based on the Bradford *(18)* method with γ-globulin (G-7516; Sigma) as standard. The assay was performed using an analytical robot (Cobas Mira; Roche, Rotkreutz, Switzerland).

Results and Discussion

Production of cellulolytic and xylanolytic enzymes was investigated in 12 *Penicillium* species isolated from different habitats (Table 1), as well as in the well-characterized fungus *T. reesei* Rut C30. These filamentous fungi were cultivated aerobically for 220–240 h in shake flasks with 20 g/L of cellulose (Solka-Floc) or 20 g/L of xylan from oat spelts as carbon source. The cell mass concentration was estimated through measurements of intracellular protein. Cellulolytic enzyme production was characterized through measurements of BG, EG, and CBH activity, and total cellulolytic activity was determined as FPA. Xylanolytic enzyme production was investigated by measuring BX, EX, and AF activity, and the total XA activity was determined through the degradation of birchwood xylan.

Growth

To keep the production time as short as possible, it is important that the microorganism grows relatively fast. In samples containing insoluble substrates, the amount of cell mass cannot be determined by measurement of dry matter. The general trend in cell mass concentration, estimated indirectly from the amount of intracellular protein, was a faster initial growth on xylan compared to cellulose, but a higher final cell mass concentration when cellulose was used as carbon source compared to xylan (data not shown). Xylan is less ordered and has fewer hydrogen bonds than cellulose, and the higher initial growth rate on xylan may be owing to the structure of xylan, which is more accessible for the enzymes than cellulose. *P. verruculosum* IBT 18366, *P. brasilianum* IBT 20888, and *T. reesei* RUT C30 reached the highest cell mass concentration after cultivation on cellulose, and after cultivation on xylan, *P. persicinum* IBT 13226 and *P. verruculosum* IBT 18366 reached the highest cell mass concentration.

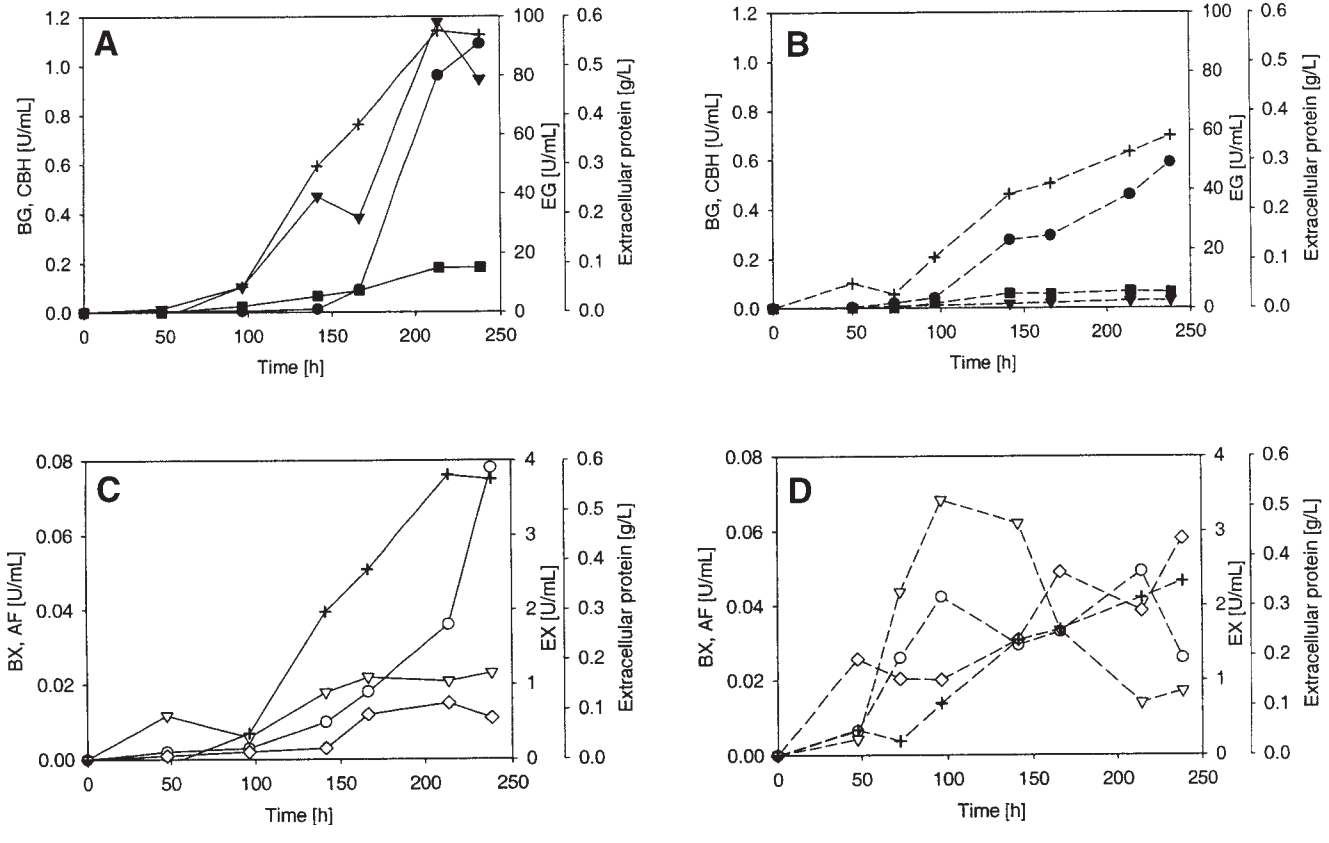

Fig. 1. Cellulolytic and xylanolytic activities and extracellular protein during time course of the cultivation of *P. brasilianum* IBT 20888. **(A)** Cellulolytic activities on cellulose; **(B)** cellulolytic activities on xylan; **(C)** xylanase activities on cellulose; and **(D)** xylanolytic activities on xylan. (●) BG; (■) CBH; (▼) EG; (○) BX; (◇) AF; (▽) EX; (+) extracellular protein; (—) cultivation on cellulose; and (- - -) cultivation on xylan.

Enzyme Production

In all cultivations, the general trend was a steady increase in cellulolytic and xylanolytic enzyme activities in the cultivation broth during the time course, as previously demonstrated by Schulz and Hirte *(19)* in a screening experiment of different *Penicillium* species cultivated on a plant hydrolysate. The same trend was observed during both cultivation on cellulose and on xylan (as exemplified in Fig. 1 A–D). Even though each measured enzyme activity increased during the time course of the cultivation, the specific activity of all enzymes was not constant in all cultivations. During cultivation of *P. brasilianum* IBT 20888 on cellulose, BG activity increased 10 times from 170 to 240 h, but CBH and EG activity only doubled (Fig. 1A). Increasing xylanolytic activity throughout cultivation on cellulose has been observed in *T. reesei (20)*, and increasing cellulolytic activity throughout cultivation on xylan has been demonstrated for an *Aspergillus* species *(21)*. Activities of cellulolytic enzymes in the supernatant were generally higher during growth on cellulose than during growth on xylan (Fig. 1A, 1B), whereas the activities of xylanolytic enzymes were higher during growth on xylan than during growth on cellulose (Fig. 1C, 1D). Our study demonstrated that there was a coinduction between cellulolytic and xylanolytic activities whether the substrate for cultivation of the fungus was cellulose or xylan. Furthermore, EX activity decreased in some cultivations when the substrate was xylan (data not shown).

Cellulolytic Enzymes

Cultivation of the different filamentous fungi for 230 h on cellulose resulted in different concentrations of extracellular protein and FPA, ranging from 0.01 to 0.78 g/L and from 0.02 up to 0.68 filter paper units (FPU)/mL, respectively. A relatively high protein concentration was shown to be correlated with a high FPA during growth on cellulose (Fig. 2). The specific FPA was found to be 0.77 FPU/mg of protein through linear regression with a regression coefficient of 0.77. A similar specific activity has been shown to result from a cultivation of *P. pinophilum (22)* on a substrate containing both cellulose and hemicellulose. Comparison of the specific FPA resulting from the growth of *P. occitanis* and *T. reesei* QM9414 on cellulose showed that the specific FPA was higher for the *Penicillium* species than for *T. reesei (23)*, as observed for *P. brasilianum* IBT 20888 and *T. reesei* Rut C30 in the present study. The *Penicillium* species with the highest FPA after growth on cellulose were *P. brasilianum* IBT 20888, *P. verruculosum* IBT 18366, *P. pinophilum* IBT 10872, and *P. minioluteum* IBT 21486. The highest FPA (0.68 FPU/mL) was measured after cultivation of *P. brasilianum* IBT 20888; this FPA was even higher than the 0.54 FPU/mL resulting from growth of *T. reesei* Rut C30 (Table 2). Fungi with low FPA might contain specific enzymes with interesting properties, such as higher specific activity for single enzymes or a lower product inhibition; thus, it might be interesting to also investigate these strains in further detail. If a fungus produces

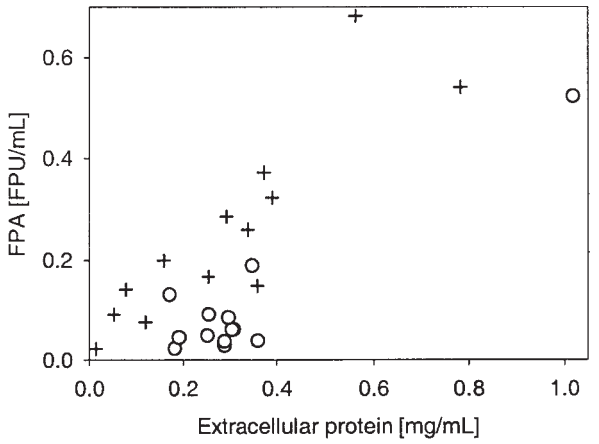

Fig. 2. FPA vs protein concentration in cultivation broth after cultivation of fungi on cellulose (+) and xylan (○). Each point in the plot represents the final protein concentration and the corresponding measured FPA in the cultivation broth for each fungus on each substrate.

Table 2
Cellulolytic Activities for *T. reesei* Rut C30 and for Four *Penicillium* Species with Highest FPA After Cultivation in Shake Flasks[a]

	BG (U/mL)	EG (U/mL)	CBH (U/mL)	FPA (FPU/mL)
T. reesei Rut C30	0.03 (0.31)	87 (44)	0.16 (0.07)	0.54 (0.52)
P. brasilianum IBT 20888	1.09 (0.59)	98 (2.6)	0.18 (0.07)	0.68 (0.19)
P. verruculosum IBT 18366	0.97 (0.33)	12 (0.5)	0.08 (0.02)	0.37 (0.13)
P. pinophilum IBT 10872	2.45 (0.80)	6 (1.3)	0.07 (0.07)	0.32 (0.06)
P. minioluteum IBT 21486	1.70 (0.78)	9 (1.2)	0.11 (0.06)	0.29 (0.05)

[a]Numbers not in parenthesis are activities after cultivation on cellulose, and numbers in parenthesis are activities after cultivation on xylan. Owing to assay limitations, the measured CBH activity should be seen as a quantitative indication.

a single enzyme with a desirable property, it is possible to increase the secretion of this enzyme through mutagenesis. It has been demonstrated that FPA in a *P. pinophilum* strain can be increased four times through three rounds of mutation and selection of the best-producing strain *(24)*.

BG activity was more than one order of magnitude higher for the four *Penicillium* species than BG activity resulting from cultivating *T. reesei* Rut C30. EG activity was one order of magnitude higher for *T. reesei* Rut C30 and *P. brasilianum* IBT 20888 than for the other three *Penicillium* species, which may provide an explanation for the lower FPA obtained from *P. verruculosum* IBT 18366, *P. pinophilum* IBT 10872, and *P. minioluteum* IBT 21486.

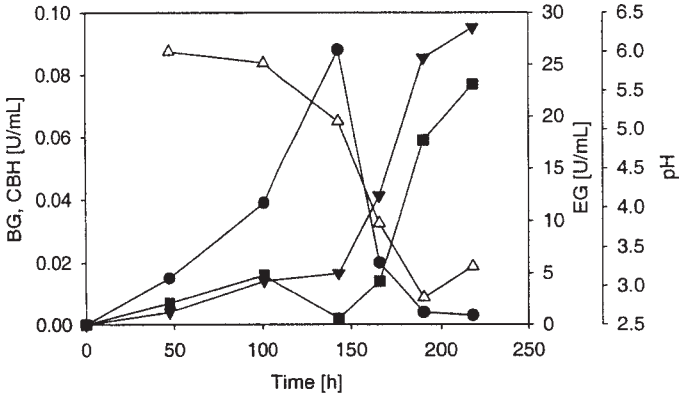

Fig. 3. Cellulolytic activities and pH during cultivation of *P. persicinum* IBT 13226 on cellulose (●) BG; (■) CBH; (▼) EG; and (△) pH.

When considering the results for FPA after cultivation of the fungi on xylan, the filter paper activity showed less correlation to the concentration of extracellular protein than when the fungi were grown on cellulose (Fig. 2). *T. reesei* Rut C30 had a much higher FPA, 0.52 FPU/mL, than any of the other fungi when grown on xylan (Table 2). The FPA for *T. reesei* Rut C30 was one order of magnitude higher than the FPA for *P. pinophilum* IBT 10872, although the only activity that was higher for *T. reesei* Rut C30 was the EG activity. The FPA could not be fully explained by the measured cellulolytic activities, for instance after growth on xylan, the cellulolytic activities were all lower for *P. verruculosum* IBT 18366 than for *P. pinophilum* IBT 10872, and yet *P. verruculosum* IBT 18366 yielded higher FPA (Table 2).

BG activity seemed to deviate from the general trend in that the activity of the individual cellulolytic enzymes increased throughout the cultivation (Fig. 1). In some cultivations, the measured BG activity decreased in the middle or toward the end of the cultivation, as exemplified in Fig. 3. After growing *P. persicinum* IBT 13226 on cellulose for 140 h, BG activity started to decrease, and after 191 h no BG activity could be measured in the cultivation broth. In this time period, the pH dropped concurrently to a value of 2.85. For *T. reesei* Rut C30 and *P. minioluteum* IBT 21486, BG activity also decreased as the pH dropped to a value of 3.0. The pH instability of BG has been reported for other microorganisms: several species of *Aspergillus (25)*, *Thermomyces lanuginosus (26)*, and also *Trichoderma harzianum (27)*. Other experiments (data not shown) have demonstrated that during cultivation of *P. persicinum* IBT 13226 on cellulose in well-controlled bioreactors with pH control, BG activity reached a significantly higher value, 1.3 U/mL, compared to the present experiments, in which no activity was detected.

Table 3
Xylanase Activities for *T. reesei* Rut C30 and Four *Penicillium* Species with Highest Xylanase Activity After Cultivation in Shake Flasks[a]

	BX (U/mL)	EX (U/mL)	AF (U/mL)	XA (U/mL)
T. reesei Rut C30	1.67 (0.07)	3.9 (59)	0.17 (0.42)	16 (176)
P. persicinum IBT13226	ND (0.19)	3.8 (30)	ND (0.15)	2 (105)
P. funiculosum IBT 5816	0.08 (0.33)	0.39 (10)	0.02 (0.20)	2 (42)
P. simplicissimum IBT 13237	ND (ND)	0.30 (1.6)	0.01 (0.21)	7 (31)
P. simplicissimum IBT 15303	ND (ND)	3.4 (2.7)	ND (0.21)	19 (23)

[a]ND, not detected. Numbers not in parenthesis are activities after cultivation on cellulose, and numbers in parenthesis are activities after cultivation on xylan.

Xylanolytic Enzymes

Cultivation of filamentous fungi on xylan resulted in extracellular protein concentrations for the *Penicillium* species in the range of 0.17–0.36 mg/mL and 1.02 mg/mL for *T. reesei* Rut C30. The XA activity was measured to be between 1.5 and 105 U/mL for the *Penicillium* species and 176 U/mL for *T. reesei* Rut C30. No linear correlation was observed between the XA activity and the amount of secreted protein, although the highest XA activities were measured in cultivation broths with relatively high protein concentrations (data not shown). Among the *Penicillium* species examined, *P. persicinum* IBT 13226 had the highest XA activity (105 U/mL) after growth on xylan. *P. funiculosum* IBT 5816 had the second highest XA activity of 42 U/mL (Table 3). XA activity was in the range of 1.5–19 U/mL after the fungi were grown on cellulose, and like on xylan, no linear correlation between XA activity and the amount of secreted protein was observed (data not shown). A possible explanation for the missing linear correlation could be the heterogeneity of hemicellulose. Owing to adaptation to the habitat, each fungus may have changed the regulation of individual hemicellulolytic enzymes to the given conditions, but during growth on xylan from oat spelts in the present experiment, the fungus might still produce enzymes needed to hydrolyze the "original" substrate. Therefore, the best producers found in a screening experiment heavily depend on the chosen substrate.

The highest EX and AF activities were measured after cultivation of *T. reesei* Rut C30 on xylan, (59 and 0.42 U/mL, respectively) (Table 3). These activities were with a few exceptions almost twice as high as any of the activities obtained after cultivation of the *Penicillium* species. BX activity reached by far the highest activity after cultivation of *T. reesei* Rut C30 on cellulose. This was not the case for the *Penicillium* species that had the highest BX activity when they were cultivated on xylan. XA activity could not, like FPA, be fully explained by the individual xylanolytic enzymes, as demonstrated in a comparison of *T. reesei* Rut C30 and *P. simplicissimum* IBT 15303 after growth on cellulose.

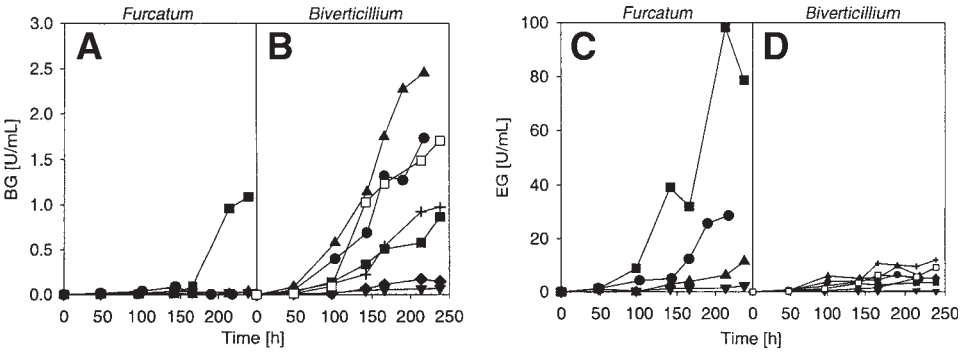

Fig. 4 BG activity during cultivation on cellulose for **(A)** subgenus *Furcatum* and **(B)** subgenus *Biverticillium*; and EG activity during cultivation on cellulose for **(C)** subgenus *Furcatum* and **(D)** subgenus *Biverticillium*. Subgenus *Furcatum*: (●) *P. persicinum* IBT 13226; (▼) *P. simplicissimum* IBT 13237; (▲) *P. simplicissimum* IBT 15303; (■) *P. brasilianum* IBT 20888. Subgenus *Biverticillium*: (●) *P. pinophilum* IBT 4186; (■) *P. funiculosum* IBT 5816; (▲) *P. pinophilum* IBT 10872; (▼) *P. rubicundum* IBT 10943; (◆) *P. aculeatum* IBT 18363; (+) *P. verruculosum* IBT 18366; (□) *P. minioluteum* IBT 21486.

Comparison of Enzyme Profiles in Subgenera Within Genus Penicillium

The genus *Penicillium* can be classified into different subgenera according to differences in morphology, physiology, and secondary metabolite production (Table 1). The *Penicillium* subgenus *Biverticillium* often occurs on wood, paper, and textile-related plant products *(28)*. By contrast, *P. brasilianum*, *P. simplicissimum*, and related species belong to the subgenus *Furcatum*, which often occurs in grassland soils *(6)*.

Comparisons of the cellulolytic activities resulting from growth on cellulose and xylanolytic activities resulting from growth on xylan for each subgenus showed that BG activity was higher for the subgenus *Biverticillium* than for the subgenus *Furcatum* during cultivation on cellulose (Fig. 4A, B). EG activity tended to be highest for the subgenus *Furcatum* during growth on cellulose (Fig. 4C, D). An investigation of the xylanolytic activities showed that six of seven fungi from the subgenus *Biverticillium* reached a higher BX activity than the maximum BX activity for the subgenus *Furcatum*. EX activity did not reveal any difference between the two subgenera (data not shown).

In the future, when a larger number of filamentous fungi in each subgenus have been screened for their production of cellulolytic and xylanolytic enzymes, a powerful tool to search for characteristics in the subgenera will be multivariate data analysis. In the search for an enzyme mixture with desirable properties for a given application, knowledge of enzyme activities characterizing each subgenus during growth on a given substrate can be valuable.

Other Screening Experiments

In the present study, the fungi were cultivated in submerged cultures, which can be habitats that are far from the conditions that each fungus has adapted to during evolution. Solid-state fermentation could very well be another interesting way to cultivate the microorganisms of interest for cellulase and hemicellulase production. It has earlier been shown that when *P. citrinum* was grown on rice husks, cellulolytic activity was three times higher in the solid-state fermentation than in the submerged culture *(29)*.

Conclusion

The filamentous fungi investigated showed coinduction of cellulolytic and xylanolytic enzymes. During growth on cellulose, products from the hydrolysis of cellulose also induced production of xylanolytic enzymes, and during growth on xylan, products from the hydrolysis of xylan also induced the production of cellulolytic enzymes.

FPA was used to evaluate how well suited filamentous fungi could be as a producer of cellulolytic enzymes. *P. brasilianum* IBT 20888 cultivated on cellulose resulted in the highest FPA, an activity that was even higher than the FPA resulting from growth of *T. reesei* Rut C30. *P. brasilianum* IBT 20888 was different from the other *Penicillium* species in the way that it produced almost an order of magnitude higher EG activity than any of the other species. Even though differences in single cellulolytic activities among the fungi were found, a linear correlation was observed between the amount of extracellular protein and the FPA measured after cultivation of each fungus on cellulose. The screening among the different filamentous fungi belonging to *Penicillium* showed that many species are interesting as producers of cellulolytic and xylanolytic enzymes, but further cultivation experiments need to be performed under more controlled conditions. Cultivations in shake flasks can be used as a relatively fast approach when screening many microorganisms for their production of cellulolytic and xylanolytic enzymes, but certain characteristics may not be apparent owing to the nature of shake flask cultivations.

References

1. Kheshgi, H. S., Prince, R. G., and Marland, G. (2000), *Annu. Rev. Energy Environ.* **25,** 199–244.
2. Wood, T. M. (1985), *Biochem. Soc. Trans.* **13,** 407–410.
3. Ryu, D. D. Y. and Mandels, M. (1980), *Enzyme Microb. Technol.* **2,** 91–102.
4. Holtzapple, M., Cognata, M., Shu, Y., and Hendrickson, C. (1990), *Biotechnol. Bioeng.* **36,** 275–287.
5. Tengborg, C., Galbe, M., and Zacchi, G. (2001), *Enzyme Microb. Technol.* **28,** 835–844.
6. Christensen, M., Frisvad, J. C., and Tuthill, D. E. (2000), in *Integration of Modern Taxonomic Methods for Penicillium and Aspergillus Classification*, Samson, R. A. and Pitt, J. I., eds., Harwood Academic Publishers, London, UK, pp. 309–320.
7. van Wyk, J. P. H. (1999), *Biomass Bioenergy* **16,** 239–242.
8. Thygesen, A., Thomsen, A. B., Schmidt, A. S., Jørgensen, H., Ahring, B. K., and Olsson, L. (2003), *Enzyme Microb. Technol.* **32,** 606–615.

9. Castellanos, O. F., Sinitsyn, A. P., and Vlasenko, E.Y. (1995), *Bioresour. Technol.* **52,** 119–124.
10. Mandels, M. and Weber, J. (1969), *Adv. Chem. Ser*. **95,** 394–414.
11. Ghose, T. (1984), in *Measurement of Cellulase Activities*, Commission on Biotechnology, International Union of Pure and Applied Chemistry, Delhi, India, pp. 1–13.
12. Miller, G. L. (1959), *Anal. Chem.* **31,** 426–428.
13. Bailey, M. J., Biely, P., and Poutanen, K. (1992), *J. Biotechnol.* **23,** 257–270.
14. Jørgensen, H., Eriksson, T., Börjesson, J., Tjerneld, F., and Olsson, L. (2003), *Enzyme Microb. Technol.* **32,** 851–861.
15. Deshpande, M. V., Eriksson, K.-E., and Pettersson, L. G. (1984), *Anal. Biochem.* **138,** 481–487.
16. Herbert, D., Phipps, P. J., and Strange, R. E. (1971), in *Methods in Microbiology*, vol. 5B, Norris, J.R. and Ribbons, D.W., eds., Academic Press, London, UK, pp 242–248.
17. Gronall, A. G., Bardawill, D. J., and David, M. M. (1949), *J. Biol. Chem.* **177,** 751–766.
18. Bradford, M. M. (1976), *Anal. Biochem.* **72,** 248–254.
19. Schulz, G. and Hirte, W. F. (1989), *Zentralbl. Mikrobiol.* **144,** 81–96.
20. Margolles-Clark, E., Ilmén, M., and Penttilä, M. (1997), *J. Biotechnol.* **57,** 167–179.
21. van Peij, N. N. M. E., Gielkens, M. M. C., de Vries, R. P., Visser, J., and de Graaff, L. H. (1998), *Appl. Environ. Microbiol.* **64,** 3615–3619.
22. Brown, J. A., Collin, S. A., and Wood, T. M. (1987), *Enzyme Microb. Technol.* **9,** 176–180.
23. Chaabouni, S. E., Hadj-Taieb, N., Mosrati, R., and Ellouz, R. (1994), *Enzyme Microb. Technol.* **16,** 538–542.
24. Brown, J. A., Falconer, D. J., and Wood, T. M. (1987), *Enzyme Microb. Technol.* **9,** 169–175.
25. Decker, C. H., Visser, J., and Schreier, P. (2000), *J. Agric. Food. Chem.* **48,** 4929–4936.
26. Lin, J., Pillay, B., and Singh, S. (1999), *Biotechnol. Appl. Biochem*. **30,** 81–87.
27. Yun, S. I., Jeong, C. S., Chung, D. K., and Choi, H. S. (2001), *Biosci. Biotechnol. Biochem.* **65,** 2028–2032.
28. Pitt, J. I. (1979), *The genus* Penicillium *and its teleomorphic states* Eupenicillium *and* Talaromyces, Academic Press, London, UK.
29. Kuhad, R. C. and Singh, A. (1993), *World J. Microbiol. Biotechnol.* **1,** 100–101.

0273-2289/04/114/0403–0416/$25.00

Production of Ethanol from Cellulosic Biomass Hydrolysates Using Genetically Engineered *Saccharomyces* Yeast Capable of Cofermenting Glucose and Xylose

Miroslav Sedlak and Nancy W. Y. Ho*

Laboratory of Renewable Resources Engineering (LORRE), Purdue University, 500 Central Drive, West Lafayette, IN 47907, E-mail: nwyho@ecn.purdue.edu

Abstract

Recent studies have proven ethanol to be the ideal liquid fuel for transportation, and renewable lignocellulosic materials to be the attractive feedstocks for ethanol fuel production by fermentation. The major fermentable sugars from hydrolysis of most cellulosic biomass are D-glucose and D-xylose. The naturally occurring *Saccharomyces* yeasts that are used by industry to produce ethanol from starches and cane sugar cannot metabolize xylose. Our group at Purdue University succeeded in developing genetically engineered *Saccharomyces* yeasts capable of effectively cofermenting glucose and xylose to ethanol, which was accomplished by cloning three xylose-metabolizing genes into the yeast. In this study, we demonstrated that our stable recombinant *Saccharomyces* yeast, 424A(LNH-ST), which contains the cloned xylose-metabolizing genes stably integrated into the yeast chromosome in high copy numbers, can efficiently ferment glucose and xylose present in hydrolysates from different cellulosic biomass to ethanol.

Index Entries: Ethanol; *Saccharomyces* yeasts; hydrolysate; corn stover; corn fiber; xylose; glucose; glycerol; xylitol.

Introduction

Recent studies have proven ethanol to be an ideal liquid fuel for transportation and renewable lignocellulosic biomass to be an attractive feedstock for ethanol fuel production by fermentation *(1,2)*. The major fermentable sugars from hydrolysis of lignocellulosic biomass, such as rice and wheat straw, sugarcane bagasse, corn stover, corn fiber, softwood, hardwood, and grasses, are D-glucose and D-xylose except that softwood

*Author to whom all correspondence and reprint requests should be addressed.

also contains substantial amounts of mannose. Economically, it is essential that both glucose and xylose present in lignocellulosic biomass can be fermented to ethanol in order for these renewable resources to be used as feedstock for ethanol fuel production.

The naturally occurring *Saccharomyces* yeasts have been proven to be safe, effective, and user-friendly microorganisms for the large-scale production of industrial ethanol from various traditional feedstocks such as starch and cane sugar. The fermentable sugars present in those feedstocks are glucose and fructose. However, these yeasts cannot metabolize xylose. We successfully developed genetically engineered recombinant *Saccharomyces* yeasts that can effectively coferment glucose and xylose to ethanol *(3,4)*. This was accomplished by the cloning and overexpression of three xylose-metabolizing genes: xylose reductase (XR), xylitol dehydrogenase (XD), and xylulokinase (XK) genes in yeast. Subsequently, we further developed stable *Saccharomyces* yeasts that contain multiple copies of XR, XD, and XK stably integrated into the yeast chromosomes *(5,6)*. Even more important, we developed a convenient system for testing and converting virtually any *Saccharomyces* yeast, wide type or mutants, to glucose/xylose cofer-menting yeast. As such, we can screen the best yeast for cofermentation of sugars from lignocellulosic biomass to ethanol. In recent years, we have tested more than 10 different strains of yeast for glucose/xylose cofermentation and converted three of the best ones to stable recombinant yeasts with high efficiencies in cofermenting glucose and xylose to ethanol. They are 1400 (LNH-ST) *(5)*, 259 (LNH-ST) *(7)*, and 424A (LNH-ST) *(8)*. These three yeasts can all fer-ment 8% glucose and 4% xylose to nearly 6% ethanol in 30–40hrs *(5,7,8)*.

However, the cost-effective conversion of various types of lignocellulosic biomass to fermentable sugars with as little toxic inhibitory byproducts as possible remains a challenge for the production of cellulosic ethanol (ethanol produced from lignocellulosic biomass). Furthermore, the ability of individual recombinant yeast to tolerate the inhibitors present in the hydrolysates is also an important factor for cost-effective production of cellulosic ethanol. The effective production of cellulosic ethanol from hydrolysates of various lignocelluloses with our 1400 (LNH-32) or 1400 (LNH-ST) yeast has previously been reported *(6,7,9,10)*. In this article, we examine the effectiveness of our stable recombinant *Saccharomyces* yeast 424A (LNH-ST) in cofermenting cellulosic sugars (glucose and xylose from hydrolysates) derived from different lignocellulosic biomass to ethanol. We also compare the effectiveness of 424A(LNH-ST) with those recombinant yeasts developed by others in converting sugars from cellulosic hydrolysates to ethanol.

Materials and Methods

Microorganisms and Growing Conditions

The genetically engineered *Saccharomyces cerevisiae* 424A (LNH-ST) was used for fermentation of lignocellulosic hydrolysates to ethanol. *S. cerevisiae* 424A (LNH-ST) was constructed by integrating multiple copies of XD, XR, and XK into the chromosomes of *S. cerevisiae* ATCC 4124 accord-

ing to the technology reported by Ho and colleagues *(3–6)*. The 424A (LNH-ST) strain was maintained in liquid YEPX medium (20 g/L of Difco peptone; Becton Dickinson, St. Louis, MO), 10 g/L of Difco yeast extract (Becton Dickinson), and 20 g/L of xylose (Sigma, St. Louis, MO). Fresh seed cultures were prepared by inoculating the respective seed cultures in 100 mL of YEPX (for 424A [LNH-ST]) in 300-mL baffled Erlenmeyer flask equipped with a sidearm (Bellco). The cultures were incubated in a shaker at 30°C and 200 rpm and grown aerobically overnight. The following morning, when the cultures reached OD 350–400 Klett unit (KU) (OD 400 KU corresponds to a cell mass concentration of 9 g dry wt/L), the flasks containing the seed cultures were stored in a refrigerator at 4°C.

Lignocellulosic Hydrolysates

The corn fiber– and corn stover–based hydrolysates (hydrolysates A and B, respectively) were prepared by the following procedure. Two hundred grams of corn fiber or 100 g of corn stover was mixed with 800 mL of 1% sulfuric acid. The mixture was divided into four 2-L flasks and hydrolyzed for 1 h in an autoclave (SG-120 Scientific Gravity Sterilizer; Amsco Century) at 121°C. The hydrolysate was filtered (Whatman No. 1, 125-mm diameter). The filtrate was adjusted to pH 10.0 using $Ca(OH)_2$ and kept at room temperature overnight, followed by adjusting the pH to 6.0 using H_3PO_4. The precipitation that appeared was removed by centrifugation and the supernatant in some cases was concentrated (two- to three-fold) using a vacuum evaporator. The resulting liquid was used for fermentation.

Hydrolysates C–G were supplied by others as follows: hydrolysates C and D from Laboratory Renewable Resources Engineering, Purdue University; hydrolysate E from Department of Chemical Engineering, Purdue University; hydrolysates F and G from Tennessee Valley Authority, Public Power Institute, Muscle Shoals, AL.

Fermentation

For ethanol production, 8 mL of seed cultures was used to inoculate 100 mL of YEPD (YEP plus 2% glucose, for ethanol fermentation) in a 300-mL baffled Erlenmeyer flask equipped with a sidearm. The cultures were incubated in a shaker at 30°C and 200 rpm and grown aerobically overnight. By the next morning, they reached OD 350–400 KU. The yeast was harvested by centrifugating (J-21 Beckman) at 5000 rpm for 5 min at room temperature. The supernatant was discarded, and the cells were transferred into a 300-mL baffled Erlenmeyer flask containing 100 mL of lignocellulosic hydrolysate supplemented with 10 mL of 10% yeast extract. The initial cell mass concentration prior to fermentation in each experiment was 8.5–9.0 g dry wt/L. The flasks were then sealed with Saran Wrap to allow fermentation to be carried out under largely anaerobic conditions. The cultures were placed in a shaker and incubated as just described. One milliliter of the fermentation mixture was removed at proper intervals to serve as a sample for monitoring fermentation.

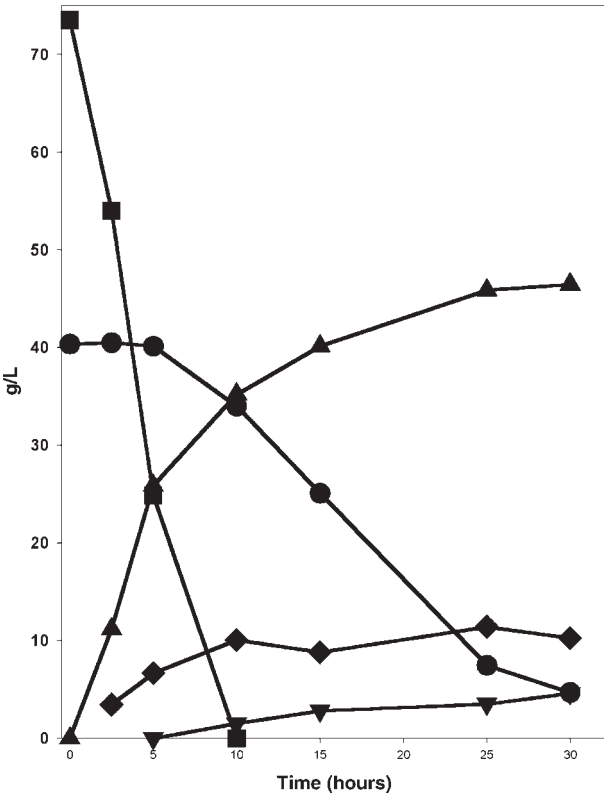

Fig. 1. Fermentation of standard sugar mixture (glucose and xylose) by *S. cerevisiae* 424A(LNH-ST). (■) Glucose; (●) D-xylose; (▲) ethanol; (◆) glycerol; (▼) xylitol.

Analysis of Sugars and Fermentation Products

Xylose, glucose, acetic acid and their fermentation products such as xylitol, glycerol, ethanol, and lactic acid were analyzed as we reported previously *(3)* by high-performance liquid chromatography using an HPX-87H (8×300 mm; Bio-Rad, Hercules, CA) equipped with an autoinjector (Hitashi model AS-4000), an isocratic liquid pump (Hitashi model L-6000), an RI detector (Hitashi model L-3350), and a computing integrator (Hitashi model D-2500). One-milliliter samples were centrifuged and the supernatant was collected. Ten microliters of the 10-fold diluted sample was used for analysis.

Results

Fermentation of Standard Sugar Mixture

Our standard sugar mixture (Std. Mix) for fermentation contained YEP, and 70 g/L of pure glucose and 40 g/L of pure D-xylose. Glucose in Std. Mix was completely fermented in 10 h. Higher rates of xylose fermentation started when glucose concentration dropped below 2.5%. Of the xylose 88.5% was fermented in 30 h (Fig. 1). The production of xylitol dur-

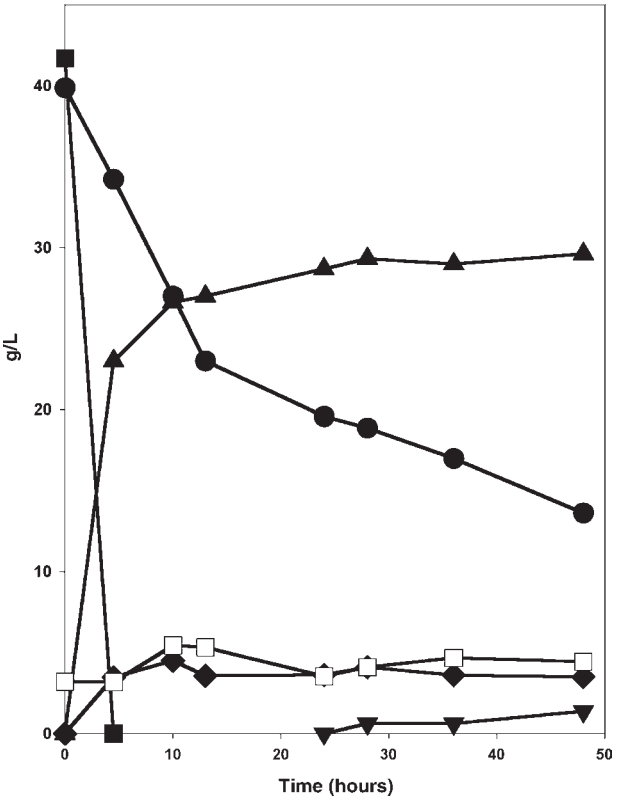

Fig. 2. Fermentation of hydrolysate A (corn fiber–based hydrolysate) by *S. cerevisiae* 424A(LNH-ST). (■) Glucose; (●) D-xylose; (▲) ethanol; (◆) glycerol; (▼) xylitol; (□) acetic acid.

ing fermentation was very low, only 4.6 g/L (Table 1). The maximum glycerol concentration reached approx 11 g/L (Fig. 1). The amount of ethanol produced was 46.5 g/L, and the ethanol yield from consumed sugar was 0.43 g/g (Table 1).

Fermentation of Lignocellulosic Hydrolysates Method

Hydrolysate A prepared from corn fiber as described earlier contained 41.7 g/L of glucose, 39.9 g/L of xylose, 21 g/L of arabinose, and 3.2 g/L of acetic acid. The glucose in hydrolysate A was fermented completely in 4.5 h. Of the xylose 42.3% was fermented in 13 h. Afterward only 23.6% of the remaining xylose was fermented in 35 h. One hundred percent of the glucose and 65.9% of the xylose was fermented in 48 h (Fig. 2). The production of ethanol was 29.6 g/L in 48 h. The yield of ethanol from consumed sugars reached 85% of the theoretical yield. The yeast did not consume arabinose or acetic acid. The production of xylitol was very low; only 5.3% (1.4 g/L) of the consumed xylose was converted to xylitol (Table 1).

Table 1
Fermentability of Different Lignocellulosic Hydrolysates by *S. cerevisiae* 424A(LNH-ST)[a]

Hydrolysate	G (g/L)	X (g/L)	T (g/L)	CX (%)	Xyl (g/L)	E (g/L)	$Y_{E/CS}$ (g/g)	$Y_{E/T}$ (g/g)	$TY_{E/CS}$ (%)	$TY_{E/TS}$ (%)
A	41.7	39.9	81.6	65.9	1.4	29.6	0.44	0.36	85.4	36.3
B	4.0	17.9	21.9	83.2	0.0	9.0	0.48	0.41	93.4	80.6
C	37.2	39.8	77.0	70.9	0.5	29.8	0.46	0.39	89.5	76.0
D	32.0	18.1	50.1	69.4	0.0	22.0	0.49	0.44	96.7	86.1
E	4.0	26.7	30.7	98.5	0.0	12.8	0.42	0.42	82.8	81.6
F	6.9	26.9	33.8	72.7	0.0	9.8	0.37	0.29	72.6	56.5
G	25.5	17.0	42.5	80.0	0.0	15.1	0.39	0.36	75.7	69.6
Std. Mix	73.5	40.4	113.9	88.5	4.6	46.5	0.43	0.41	83.5	80.0

[a]G, glucose; X, xylose; T, total fermentable sugar; CX, consumed xylose; Xyl, xylitol; E, ethanol; $Y_{E/CS}$, g of ethanol/g of consumed sugars; $Y_{E/T}$, g of ethanol/g of initial total fermentable sugars; $TY_{E/CS}$, theoretical ethanol yield of consumed sugar; $TY_{E/TS}$, theoretical ethanol yield of initial total fermentable sugar; Std. Mix, a mixture of pure glucose (7%) and xylose (4%). The fermentation time for hydrolysates A, and C–G was 48 h. The fermentation time for hydrolysate B was 24 h and for Std. Mix was 30 h. The initial cell mass concentration was 8.5–9 g dry wt/L.

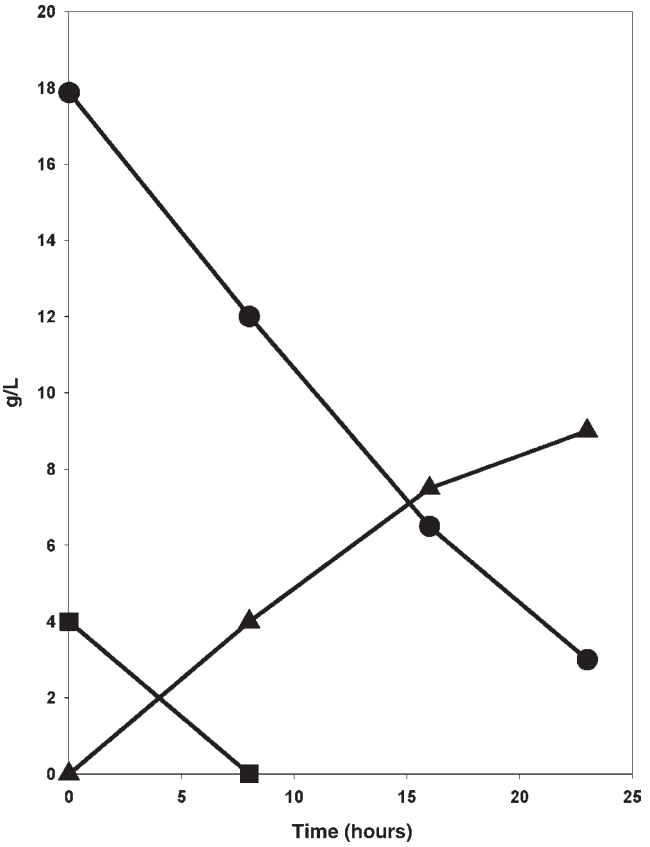

Fig. 3. Fermentation of hydrolysate B (corn stover based hydrolysate) by *S. cerevisiae* 424A(LNH-ST). (■) Glucose; (●) D-xylose; (▲) ethanol.

Hydrolysate B from corn stover contained 4 g/L of glucose, 17.9 g/L of xylose, 5 g/L of arabinose, and 2.5 g/L of acetic acid. Glucose was readily fermented; eighty-three percent of xylose was fermented in 23 h. The production of ethanol by fermentation of the corn stover hydrolysate was 9 g/L (Fig. 3). The yield of ethanol from consumed sugars reached 93% of theoretical yield. We did not observe xylitol production and acetic acid consumption.

Hydrolysates C contained 37.2 g/L of glucose, 5.5 g/L of xylose, 15.3 g/L glycerol of, and 11.5 g/L of lactic acid. This hydrolysate was not optimized for xylose recovery although there is a possibility for higher xylose recovery from the original feedstock (R. Hendrickson, personal communication). For this reason, we added xylose to a final concentration of 39.8 g/L to evaluate how effectively our yeast ferments the hydrolysate in case the process will be optimized for xylose recovery. Glucose was fermented

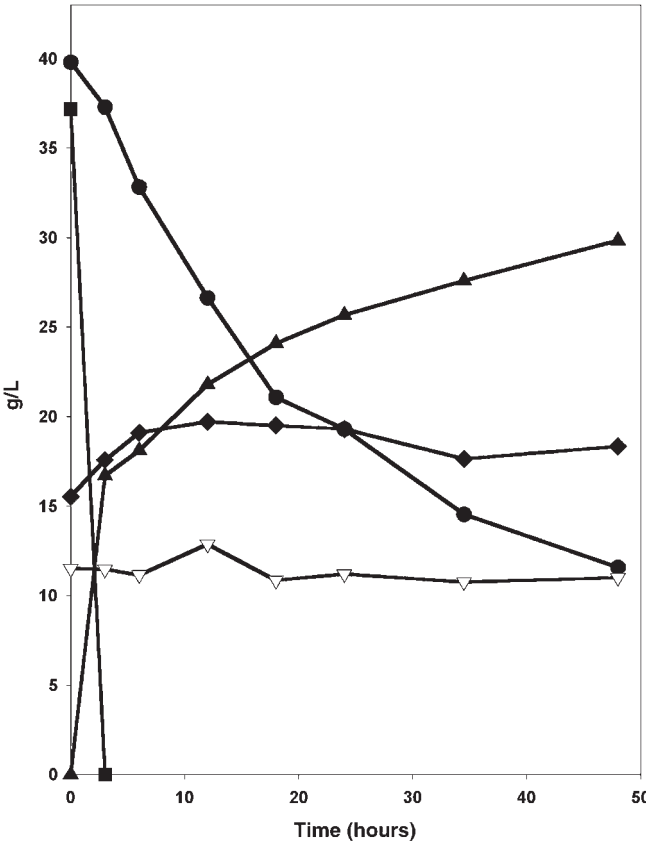

Fig. 4. Fermentation of hydrolysate C (corn fiber based hydrolysate) by *S. cerevisiae* 424A(LNH-ST). (■) Glucose; (●) D-xylose; (▲) ethanol; (◆), glycerol; (▽), lactic acid.

in 3 h. Of the xylose 70.9% was fermented in 48 h (Fig. 4). The ethanol produced during 48 h of fermentation of this hydrolysate was 29.8 g/L. The yield of ethanol from consumed sugars reached 89.5% of the theoretical yield, and xylitol production was below 0.5 g/L (not shown).

Hydrolysates D contained 32 g/L of glucose, 18.11 g/L of xylose, 6.5 g/L of arabinose, and 1.5 g/L of acetic acid. Glucose was readily fermented; in addition, 69.4% of the xylose was fermented in 48 h. The ethanol was produced from fermentation of this hydrolysate was 22 g/L (Fig. 5). The yield of ethanol from consumed sugars reached 96.7% of the theoretical yield. Xylitol production was not detected in this fermentation.

Hydrolysates E contained 4 g/L of glucose, 26.7 g/L of xylose, and 3.4 g/L of arabinose. Glucose was completely consumed in 3 h, and 98.5% of xylose was fermented in 48 h. The ethanol produced by fermentation of this hydrolysate in 48 h was 12.8 g/L (Fig. 6). The yield of ethanol from con-

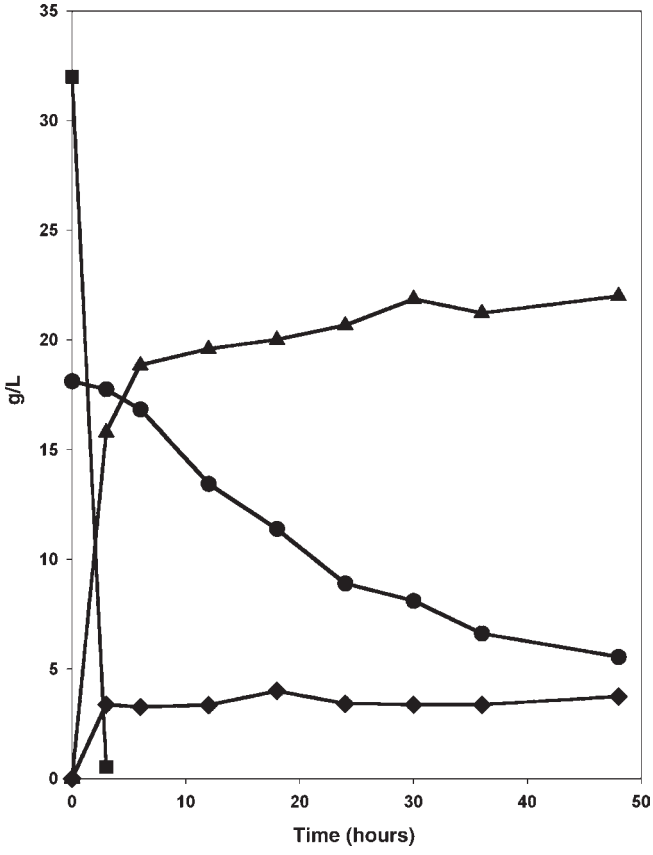

Fig. 5. Fermentation of hydrolysate D (corn stover based hydrolysate) by *S. cerevisiae* 424A(LNH-ST). (■) Glucose; (●) D-xylose; (▲) ethanol; (◆), glycerol.

sumed sugars reached 82.8% of the theoretical yield. There was no xylitol production. Arabinose was partially converted into arabitol (not shown).

Hydrolysate F contained 6.9 g/L of glucose, 26.9 g/L of xylose, 1 g/L of arabinose, and 3 g/L of acetic acid. One hundred percent glucose and 72.7% xylose were consumed during fermentation of this hydrolysate. Ethanol production in 48 h was 9.8 g/L (Fig. 7), and the yield of ethanol from consumed sugars reached 72.6% of the theoretical yield. Arabinose and acetic acid were not utilized during fermentation (not shown), and no xylitol production was detected. Hydrolysate G contained 25.5 g/L of glucose, 17 g/L of xylose, and 2.5 g/L of acetic acid. The glucose was fermented in 3 h and 80% of xylose was consumed in 48 h (Fig. 8). During fermentation of this hydrolysate,15.1 g/L of ethanol was produced. The yield of ethanol from consumed sugar reached 75.7% of the theoretical yield. Acetic acid was not utilized during fermentation (not shown), and no xylitol production was detected.

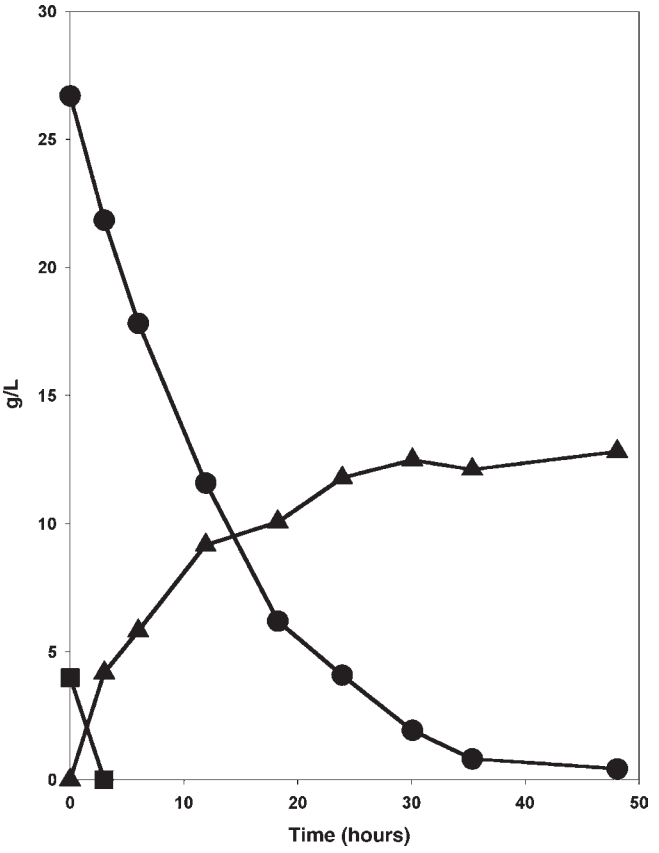

Fig. 6. Fermentation of hydrolysate E by *S. cerevisiae* 424A(LNH-ST). (■) Glucose; (●) D-xylose; (▲) ethanol.

Discussion

We have confirmed that our strain 424A(LNH-ST), recombinant glucose/xylose cofermenting yeast carrying multiple copies of XD, XR, and XK integrated into its chromosomes, is capable of effectively fermenting not only mixtures of pure glucose and xylose (Fig. 1) but also glucose and xylose present in lignocellulosic hydrolysates to ethanol. In fermentation of a mixture of pure glucose (7%) and xylose (4%), 424A(LNH-ST) fermented 100% glucose and 88.5% xylose in 30 hours with an ethanol yield of 0.41 g/g of initial total sugar and 80% of the ethanol theoretical yield of initial total sugar (Fig. 1 and Table 1). This strain also had very low production of xylitol; only 14% of consumed xylose was converted into xylitol. These results are comparable with data obtained previously using our recombinant *Saccharomyces* strain 1400 (pLNH32) *(3)*.

However, the efficiency of fermentation of hydrolysates by 424A(LNH-ST) was also largely dependent on how the hydrolysates were prepared.

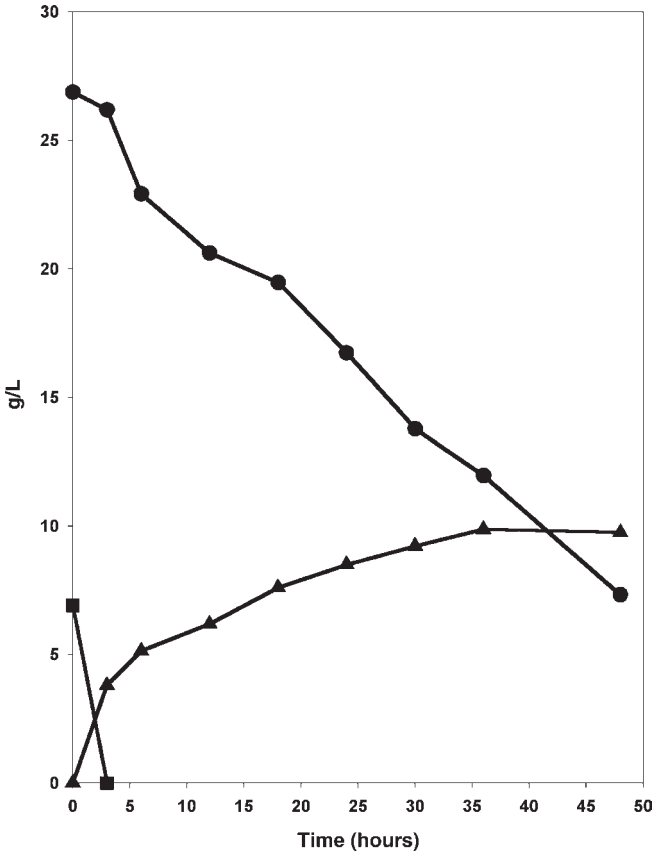

Fig. 7. Fermentation of hydrolysate F by *S. cerevisiae* 424A(LNH-ST). (■) Glucose; (●) D-xylose; (▲) ethanol.

Nevertheless, in all cases, all glucose was fermented within the first 3 h and >65% of xylose was consumed in 48 h (Figs. 1–9 and Table 1). The ethanol yield was >75% of the theoretical yield of consumed sugar (Table 1). In addition, the percentage of theoretical ethanol yield of initial total sugar was high with the exception of hydrolysate A from corn fiber, which was prepared in our laboratory as described in Materials and Methods. This demonstrates that our process for preparing hydrolysates from corn fiber needs to be improved. We observed that fermentation of most hydrolysates by our yeast produced very little xylitol except in the fermentation of the corn fiber based hydrolysates, which was still no more than 2–5% of consumed xylose (Table 1). One possible explanation might be that xylose in the hydrolysates was metabolized slower, so xylitol could be completely converted to ethanol.

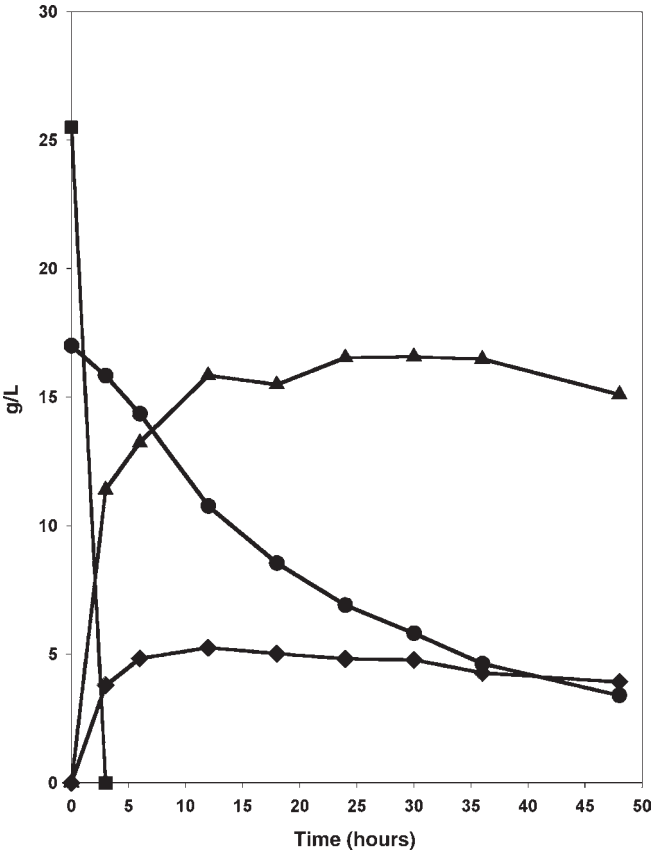

Fig. 8. Fermentation of hydrolysate G by *S. cerevisiae* 424A(LNH-ST). (■) Glucose; (●) D-xylose; (▲) ethanol; (◆), glycerol.

Now others have used our approaches (i.e., by cloning three genes, XR, XD, and XK, into the yeast rather than just XR and XD) to develop their recombinant *Saccharomyces* yeast for cofermenting glucose and xylose to ethanol. Our recombinant yeasts are still far more effective in cofermenting glucose and xylose to ethanol. For example, Johansson et al. *(11)* used their recombinant *Saccharomyces* strains to ferment their standard sugar mixture (39 g/L of xylose, 5.7 g/L of glucose 3.5 g/L of mannose, 3.1 g/L of galactose 1.7 g /L of arabinose, 0.16 g/L of hydroxymethylfurfural, and 0.7 g/L of furfural) and sugars present in lignocellulosic hydrolysate. One strain was able to metabolize xylose but it converted xylose mostly to xylitol; approx 78% (estimated from the published figures, designated as est.) of xylose was converted to xylitol and the percentage of theoretical ethanol yield of initial total sugar was just 19% (est.) with an estimated ethanol yield of 0.1 g/g of initial total sugar. Another of their strains produced lower

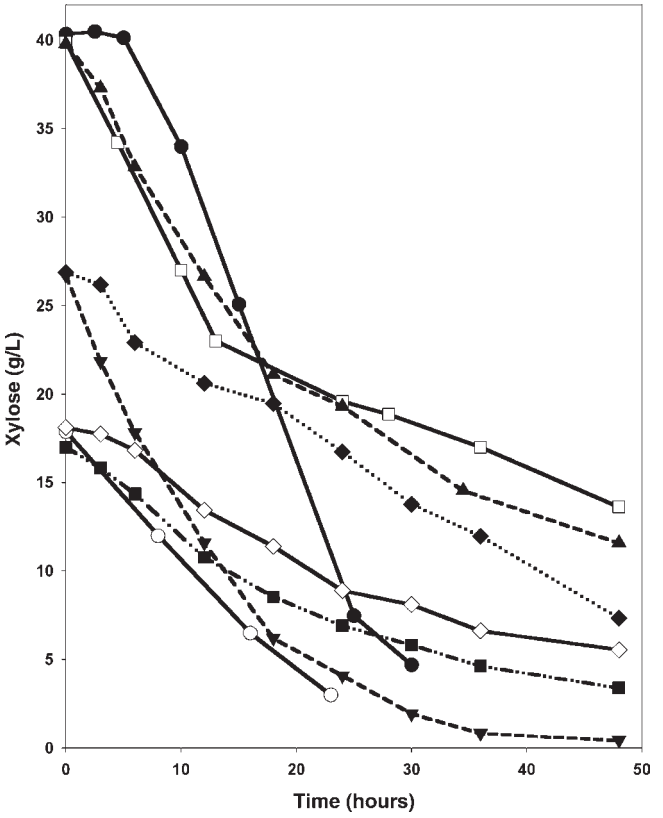

Fig. 9. Xylose consumption by *S. cerevisiae* 424A(LNH-ST) during fermentation the different hydrolysates. (●——●) Std. mixture; (□——□) hydrolysate A; (○——○) hydrolysate B; (▲– – –▲) hydrolysate C; (◇——◇) hydrolysate D; (▼– – –▼) hydrolysate E; (◆• • •◆) hydrolysate F; (■• •—• •■) hydrolysate G.

amounts of xylitol; just 6% (est.) of xylose was converted to xylitol, but the strain consumed only 23% of xylose in 65 h with an initial concentration of xylose of 39 g/L. The percentage of theoretical ethanol yield of the initial total sugar was 25% (est.) with an estimated ethanol yield of 0.13 g/g of initial total sugar. In addition, the fermentation time was 65 h or more. The sugar consumption was even slower during fermentation of their birch wood hydrolysate *(11)* with the same sugar concentration as for their standard sugar mixture.

Zadivar et al. *(12)* reported fermentation of a pure glucose/xylose mixture using their xylose-fermenting *S. cerevisiae*, but xylose mainly converted to xylitol with ethanol only as a minor product *(12)*. Furthermore, the time needed for completion of the fermentation exceeded 100 h with an initial xylose concentration of 50 g/L.

Martin et al. *(13,14)* used their genetically engineered *S. cerevisiae (11)* for fermentation of sugars presented in sugarcane bagasse hydrolysates, but very little xylose utilization was observed *(13,14)*. It is now generally acknowledged *(15–17)* that cloning three genes, the XR, XD, and XK, is needed to make the *Saccharomyces* yeast ferment xylose, as we recommended nearly a decade ago *(3)*.

Why our recombinant yeasts are superior to those developed by others using the same principles of construction is most likely owing to a combination of factors, including how our genes were modified, how our genes were integrated into the yeast chromosomes, and how our host yeast strain for cloning was selection.

Reference

1. Chandrakant, P. and Bisaria V. S. (1998), *Crit. Rev. Biotechnol.* **18,** 259–331
2. Bothast R. J., Nichols N. N., and Dien B. S. (1999), *Biotechnol. Prog.* **15,** 867–875
3. Ho, N. W. Y., Chen, Z., and Brainard, A. (1998), *Appl. Environ. Microbiol.* **64,** 1852–1859
4. Ho, N. W. Y. and Tsao, G. T. (1998), US patent application #08/148, 581; patent no. 5,789, 210.
5. Ho, N. W. Y. and Chen Z. D., (1997), PCT patent no. WO97/42307.
6. Ho, N. W. Y., Chen, Z., Brainard, A. P., and Sedlak, M. (1999), in *Advances in Biochemical Engineering/Biotechnology*, vol. 65, Tsao, G. T., ed., Springer-Verlag, Berlin Heiderberg, Germany, pp. 163–192.
7. Ho, N. W. Y., Chen, Z., Brainard, A. P., and Sedlak, M. (2000), in *ACS Symposium Series 767*, Anastas, P. T., Heine G. H., and Williamson, T. C., eds., American Chemical Society, Washington, DC, pp. 142–159.
8. Sedlak, M., Edenberg, H., and Ho, N. W. Y. (2003), *Enzyme. Microb. Technol.* **33,** 19–28
9. Toon, S. T., Philippidis, G. P. , Ho, N. W. Y., Chen, Z., Brainard, A., Lumpkin, R. E., and Riley, C. J. (1997), *Appl. Biochem. Biotechnol.* **63/65,** 243–255,
10. Moniruzzaman, M., Dien, B. S., Skory, C. D., Chen, Z. D., Hespell, R. B., Ho, N. W. Y., Dale, B. E., and Bothast, R. J. (1997), *World J. Microbiol. Biotech.* **13,** 341–346.
11. Johansson, B., Christensson, C., Hobley, T., and Hahn-Hagerdal, B. (2001), *Appl. Environ. Microbiol.* **67,** 4249–4255.
12. Zadivar, J., Borges, A., Johansson, B., Smits, H. P., Villas-Boas, S. G., Nielsen, J., and Olsson, L. (2002), *Appl. Microbiol. Biotechnol.* **59,** 436–442.
13. Martin, C., Gable, M., Wahlbom, C. F., Hahn-Hagerdal, B., and Jonsson, L. J. (2002), *Enzyme Microb. Technol.* **31,** 274–282
14. Martin, C., Gable, M., Nilvebrant, N.-O., and Jonsson, L. J. (2002), *Appl. Biochem. Biotechnol.* **98–100,** 699–716.
15. Eliasson, A., Christensson, C., Wahlbom, C. F., and Hahn-Hagerdal, B. (2000), *Appl. Environ. Microbiol.* **66,** 3381–3386.
16. Toivari, M. H., Aristidou A., Rhuohonen, L., and Penttila, M. (2001), *Metab. Eng.* **3,** 236–249.
17. Jin, Y-S., Ni, H., Laplaza J. M., and Jeffries, T. M. (2003), *Appl. Environ. Microbiol.* **69,** 495–503.

0273-2289/04/114/0417–0432/$25.00

Secondary Membranes for Flux Optimization in Membrane Filtration of Biologic Suspensions

Parag R. Nemade and Robert H. Davis*

Department of Chemical and Biological Engineering, University of Colorado, Boulder, CO 80309-0424, E-mail: robert.davis@colorado.edu

Abstract

We employ in situ deposited secondary membranes of yeast (SMYs) to optimize permeate flux during microfiltration and ultrafiltration of protein solutions. The deposited secondary membrane was periodically removed by backflushing, and a new cake layer was deposited at the start of the next cycle. The effects of backflushing time, backflushing strength, wall shear rate, and amount of secondary membrane deposited on the permeate flux were examined. Secondary membranes were found to increase the permeate flux in microfiltration by severalfold. Protein transmission was also enhanced owing to the presence of the secondary membrane, and the amount of protein recovered was more than twice that obtained during filtration of protein-only solutions under otherwise identical conditions. In ultrafiltration, the flux enhancement owing to the secondary membrane was only 50% or less. In addition, the flux for ultrafiltration was relatively insensitive to changes in the concentration of yeast used during deposition of SMY and to the backflushing strength used to periodically remove the secondary membrane.

Index Entries: Secondary membrane; backflushing; microfiltration; ultrafiltration; direct visual observation; fouling.

Introduction

Membrane filtration, with gentle conditions, no phase change, and low energy expenditure, has great potential for separations in biotechnology and other fields. However, fouling has hindered the adoption of membrane technology for separations *(1)*. Membrane fouling during filtration of biotechnological fluids with cells, proteins, cell debris, colloidal particulate matter, and dissolved solutes is quite complex *(2)*. Fouling in this case can be broadly divided into two types: external fouling and internal fouling.

*Author to whom all correspondence and reprint requests should be addressed.

External fouling is caused by the formation of a cake layer of cells or other materials on the membrane surface, leading to a reduction in permeate flux (defined as the volume of permeate produced per time and membrane area). Internal fouling is caused mainly by proteins and particles smaller than membrane pores. Proteins and protein aggregates can adsorb or deposit at the pore entrance or inside the pores and cause pore blockage or narrowing, leading to increased hydraulic resistance *(2)*.

Fouling can often be minimized by using backflushing, which involves periodic reversal of flow for a few seconds after several minutes of forward filtration. Redkar and Davis *(3)* achieved a 30-fold increase in permeate flux using more rapid backpulsing conditions of 0.5 s of backpulse after every 5 s of forward filtration. Backflushing or backpulsing has also been applied to ultrafiltration to improve separation performance. Rodgers and Sparks *(4)* observed that the permeate flux could be increased as much as two orders in magnitude in crossflow ultrafiltration of protein solutions when transmembrane pressure pulsing was applied. Although some studies show that backflushing is not always effective in increasing the permeate flux for crossflow ultrafiltration *(5)*, other studies have demonstrated flux improvement and optimization, using backflushing or backpulsing for microfiltration *(6–9)* and ultrafiltration *(10–12)*.

Backflushing and backpulsing are least effective in tackling irreversible or internal fouling, such as when proteins adhere to the membrane surface or inside the membrane pores. Kuberkar and Davis *(13)* carried out backflushing during microfiltration of mixtures of yeast and bovine serum albumin (BSA). They observed that backflushing is only partially effective in removing the internal foulants. The flux decreased with increased internal fouling and finally appeared to reach a nearly steady value as low as 5% of the clean membrane flux. However, the permeate flux for filtration of the protein-cell mixture with backflushing showed a marked improvement over that of a protein-only solution. This finding is related to the concept of dynamic secondary membranes. The yeast cake layer formed simultaneously with membrane separation during filtration of yeast-BSA acts as a selective barrier, screening the primary membrane from fouling by protein aggregates, while allowing individual protein molecules to pass through the cake layer and primary membrane. Protein aggregates are notorious for depositing at the entrance of and inside the membrane pores and acting as nuclei for further protein deposition *(14,15)* leading to pore narrowing or blockage. This type of fouling is, to a large extent, irreversible and is the primary cause of lower fluxes and lower protein transmission.

Marcinkowsky et al. *(16)* were the first to use dynamic secondary membranes in reverse osmosis for rejection of salts. Güell et al. *(17)* later investigated protein transmission and permeate fluxes in microfiltration of protein mixtures using yeast to form a predeposited secondary membrane, and they observed higher flux and protein transmission in the presence of the secondary layer. Kuberkar and Davis *(18)* also observed higher flux and transmission of BSA in the presence of a cake layer of yeast,

showing that the separation is improved by using the secondary membrane. At low yeast concentrations (<1g/L), BSA transmission was 50–100% and a high BSA recovery was achieved; at higher yeast concentrations, the transmission was higher but recovery was lower owing to low fluxes. Even with a secondary membrane, the flux gradually decreased owing to slow fouling of the secondary membrane. Periodic removal of the secondary membrane can temporarily recover the flux, but then irreversible fouling of the primary membrane occurs due to its temporary exposure to the feed solution after each time the secondary membrane is removed *(13)*.

In the current work, we employed a modified approach, with predeposition of a secondary membrane of yeast (SMY) before starting the filtration of protein. Backflushing was employed periodically to remove the deposited secondary membrane to recover the flux, and a new secondary membrane was deposited subsequently with the start of each new cycle, prior to restarting the filtration of protein. Microfiltration experiments were performed with yeast as the secondary membrane and BSA-only solutions and yeast-BSA mixtures as the feed. Ultrafiltration experiments were performed with yeast as the secondary membrane deposition medium and cellulase enzyme solutions, used in the conversion of biomass into ethanol, as the feed. In this article, we also present direct visual observation images *(19)* of the formation of the secondary membrane and its subsequent removal.

Materials and Methods

Secondary Membrane Experiments

The membrane filtration experiments were carried out using the setup shown in Fig. 1. The primary feed reservoir, the backflush reservoir, and the secondary feed reservoir (model DIV. WT 304, 1 gal; Alloy Products, Waukesha, WI) used for depositing the secondary layer of yeast were pressurized using high-pressure nitrogen. In the microfiltration experiments, the feed was pumped using a peristaltic pump (model no. XX 800 000 000; Millipore, Bedford, MA) and passed over a flat-sheet membrane module fabricated previously *(19)*. The membrane had an effective area of 5.5 cm^2. The module had a single channel 2.35 cm long, 2.35 cm wide, and 0.4 mm high. Permeate was collected and its mass is measured using an electronic balance (PG 5002; Mettler Toledo, Columbus, OH) interfaced to a personal computer using a serial port. The retentate from the feed was returned to the feed reservoir, and the retentate from the secondary feed was returned to the secondary feed reservoir. Three-way solenoid valves (model no. 453239F 3/2; Burkert, Irvine, CA) interfaced to the computer were used to switch between primary feed and secondary feed (valves A and B) and between forward filtration and reverse filtration (valve C). The valves were controlled using a QuickBasic program via a data acquisition card (DT 2805; Data Translation, Marlboro, MA). The amount of fluid lost during reverse

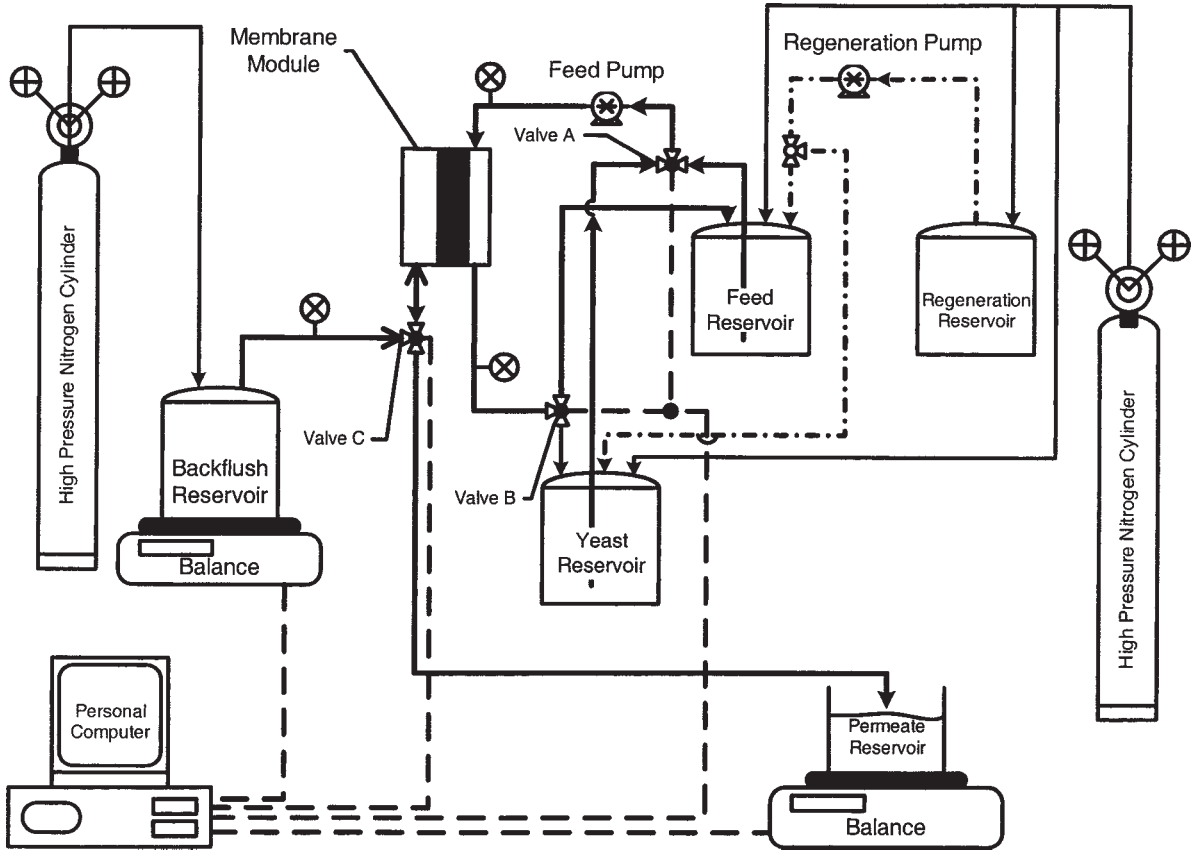

Fig. 1. Schematic of experimental setup for membrane filtration.

filtration or backflushing was measured using another balance (PM-11; Mettler Toledo, Columbus, OH), also interfaced to the computer.

Flat-sheet cellulose-acetate membranes (Acetate plus, 0.22 µ, plain, supported, catalog no. A02SP04700, batch no. 166421; GE Osmonics, Minnetonka, MN) were used in the microfiltration experiments. The membranes were hydrophilic and symmetric and had an approximate thickness of 85 µ. Each membrane was used once and then discarded. Washed yeast (*Saccharomyces cerevisiae*, commercially available Fleischmann's Active Dry Yeast) was used in preparing the yeast-only suspensions for depositing the secondary membrane. BSA (heat-shocked fractionate, fraction V powder, catalog no. A7906; Sigma, St. Louis, MO) was used for the protein-only feed suspensions. Mixtures of yeast and BSA were used as feed in a few experiments. Commercial dry yeast contains solutes and cell debris, which are removed during the process of washing. The weight of dry washed yeast remaining is found to be 68% of the weight of dry unwashed yeast. Washed yeast was prepared by adding the appropriate amount of yeast to 250 mL of deionized water and then centrifuging (Beckman GPR Centrifuge) at 1500*g* for 10 min, the supernatant was discarded, and the pellet was resuspended. This procedure was repeated three times. Feed consisted of BSA solutions (2.0–4.0 g/L) and yeast-BSA mixtures (0.68–1.34 g/L of washed yeast, 2.0–4.0 g/L of BSA).

The secondary feed used for deposition of the secondary membrane consisted entirely of yeast suspensions with concentrations ranging from 1.34 to 4.0 g/L. Yeast concentrations are reported as dry weight after washing. An average transmembrane pressure (TMP) of 7.5 psi was maintained during forward as well as reverse filtration (1 psi = 6894.7 Pa). A recirculation flow rate of 5.2–6.2 mL/s was used, with corresponding wall shear rate of 2100–2500 s^{-1}. The clean membrane steady flux was found to be $J_o = 3000 \pm 200$ L/(m^2·h) at a forward transmembrane pressure of P_f = 7.5 psi, and it was found to vary almost linearly with TMP. This flux value is reported as average ±1 SD for 25–30 repeats. The filtration cycle started with deposition of the SMY for t_{sf} = 5–25 s, followed by forward filtration for 275–300 s, and finally removing the SMY by backflushing with a reverse TMP of P_b = 7.5 psi for t_b = 0.1–10 s. The cycle was then repeated. The experiments were carried out at room temperature (22°C). Protein transmission was measured by analyzing samples of permeate for the total protein content using a Coomassie® Plus Protein Assay (no. 23236; Pierce, Rockford, IL,) at 595 nm on a Perkin-Elmer Lambda 40 UV/VIS spectrometer. The Coomassie Plus Protein Assay uses a Coomassie dye-protein-binding colorimetric method based on modification of the Bradford method for total protein quantization.

Ultrafiltration experiments were carried using the same setup, except the flat-sheet membrane module had a filtration area 38 mm long, 29 mm wide, and 1.6 mm high, with a surface area of 11 cm^2. The permeate side had 11 grooved channels that supported the membrane, leaving an effective filtration area of 6.4 cm^2. However, the total membrane area including the supports was used in calculating the fluxes. The feed consisted of cellulase enzyme solution (5.0 g/L of supplied cellulase, unless noted otherwise).

The cellulase enzyme was a commercial preparation made specifically for the National Renewable Energy Laboratory by Iogen (Ottawa, Ontario, Canada). It is supplied as a liquid solution, reported to contain 205 g/L of total soluble protein, of which 158 g/L is high molecular weight proteins retained by a 30,000-Dalton mol wt cutoff ultrafiltration membrane *(20)*.

The secondary feed used for deposition of the secondary membrane consisted entirely of yeast suspensions with concentrations ranging from 1.34 to 6.8 g/L. Ultrafiltration experiments were carried out using a flat-sheet, asymmetric polysulfone membrane (lot no. 0589702311M11 3355-04P; Millipore) with a 30,000-Dalton mol wt molecular weight cutoff. The membranes were used once and then discarded after each experiment. The feed was circulated at 5.0-16.2 mL/s, corresponding to a wall shear rate of 100–1300 s^{-1}. The steady flux of deionized water for clean membrane was found to be J_o = 375 ± 40 L/(m^2·h), independent of the wall shear rate. Ultrafiltration experiments employed a filtration cycle similarity to that of the microfiltration experiments, with a forward filtration time of t_f = 300 s and an SMY deposition time of t_{sf} = 5–30 s. Average TMPs of P_f = 15–30 psi and P_b = 5–15 psi were maintained during forward and reverse filtration, respectively, with a fixed backflushing time of t_b = 2 to 3 s.

Direct Visual Observation

Fouling of the cellulose-acetate microfiltration membranes was observed using a Nikon Labophot microscope in a direct visual observation setup described elsewhere *(19)*. The membrane was observed from above using a glass cover slip for the top of the channel. The images were captured with a color digital camera (JVC TK-1270; Victor, Yokohama, Japan) connected to a PowerMac G4 containing an LG-3 framegrabber card (Scion, Frederick, MD). The real-time images were displayed on the screen of a PowerMac monitor using NIH Image (US National Institutes of Health, http://rsb.info.nih.gov/nih-image/). Cellulose-acetate membranes were viewed at a magnification of ×350 using a Nikon E-10 ×10 objective. Scanning electron microscopy (SEM) images were also taken to observe the surface of fouled membrane more precisely.

Results and Discussion

Direct Visual Observation of Membrane Fouling

Figure 2A depicts pictures of the microfiltration membrane surface for various stages of deposition of yeast. The concentration of yeast in the secondary feed was 2.0 g/L, with the primary feed containing 2.0 g/L of BSA. A complete cycle consists of t_{sf} = 15 s of SMY, followed by t_f = 275 s of forward filtration, and ending with t_b = 10 s of reverse filtration, all at a TMP of $P_f = P_b$ = 7.5 psi. The pictures become progressively darker with increasing yeast deposition during the first cycle. After 9 to 10 s of yeast deposition, the images of the membrane surface are completely dark, an indication that multiple layers of yeast were deposited over the membrane surface.

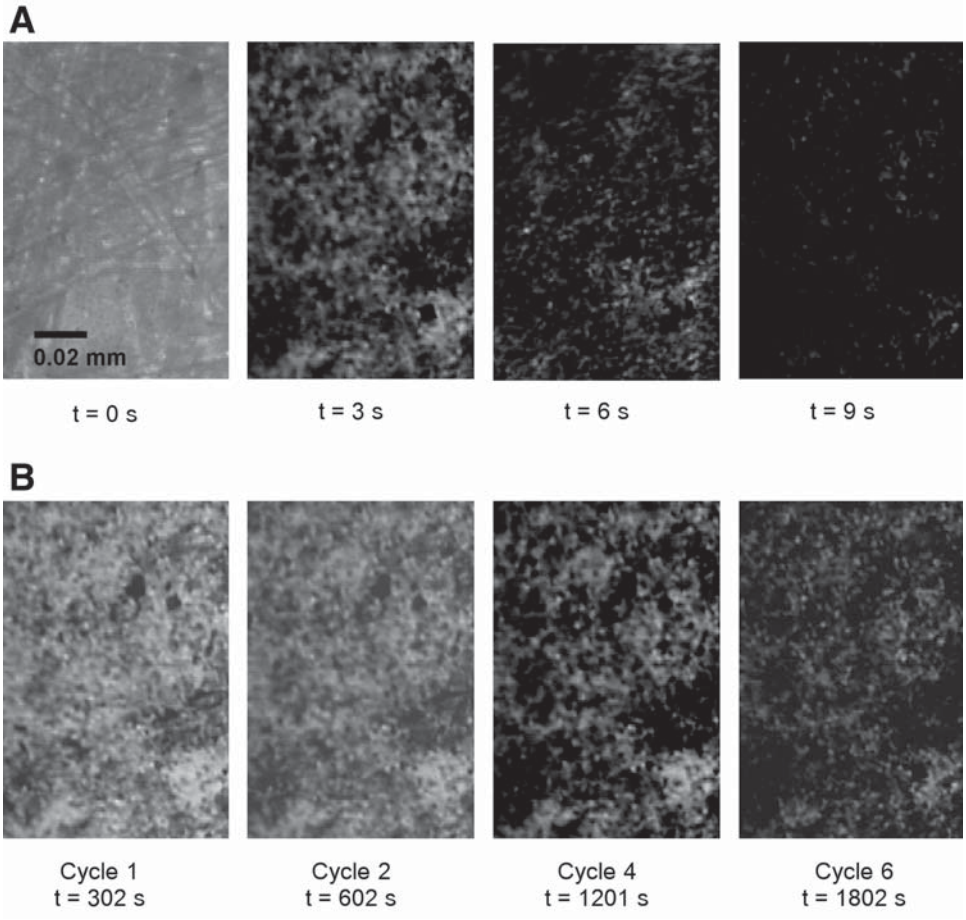

Fig. 2. Direct visual observation pictures of surface of membrane **(A)** during first cycle of deposition of SMY, and **(B)** at end of several cycles of yeast-BSA microfiltration with a secondary membrane, with the pictures taken just after backflushing portion at end of indicated cycle.

Images of the membrane surface taken just after completion of backflushing for several cycles are shown in Fig. 2B. It is apparent that backflushing is partially effective in removing the deposited SMY. The images of the membrane become progressively darker as the number of cycles increases. Therefore, backflushing becomes less and less effective over time, owing to irreversible fouling of the membrane. Apparently, the BSA in the primary feed gradually foul the primary membrane and caused yeast cells to adhere to the membrane.

Figure 3A is an SEM image of a CA microfiltration membrane with a nominal pore size of 0.22 m, fouled by BSA. The image is taken after 3100 s of filtration of 2.0 g/L of BSA at a TMP of 7.5 psi without an SMY. The image is characterized by heavy fouling of the membrane owing to deposition of BSA, leading to pore narrowing and blockage seen in the image.

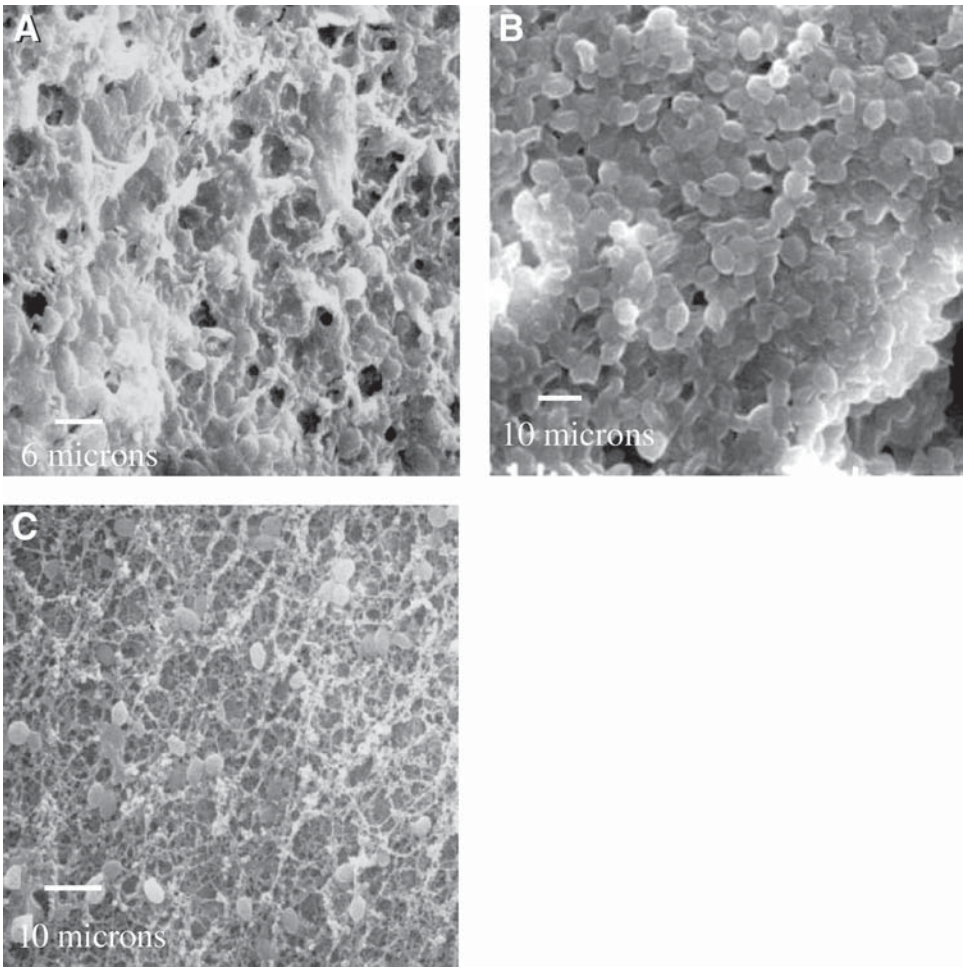

Fig. 3. SEM micrograph of a CA microfiltration membrane fouled **(A)** after filtration of BSA only for 3100 s, **(B)** after completion of SMY deposition portion of cycle 11, and **(C)** after completion of backflushing portion of cycle 11. The primary feed contained 2.0 g/L of BSA, and the secondary feed contained 1.34 g/L of yeast. The cycle conditions were t_f = 300 s, t_{sf} = 15 s, and t_b = 3, with an average TMP of 7.5 psi maintained during forward as well as reverse filtration.

Figure 3B is a representative SEM image of another CA microfiltration membrane taken immediately after the SMY deposition portion of cycle 11, for an SMY experiment with 2.0 g/L of BSA in the primary feed, 1.34 g/L of yeast in the secondary feed, and $P_f = P_b$ = 7.5 psi. In this image, the primary membrane is completely covered by multiple layers of yeast. These layers will shield the primary membrane from internal fouling by BSA. Figure 3C is a representative SEM image of another CA microfiltration membrane taken immediately after the backflushing portion of cycle 11. Here, the membrane is relatively clean with most of the SMY removed, but there is evidence of internal fouling owing to BSA in a few places.

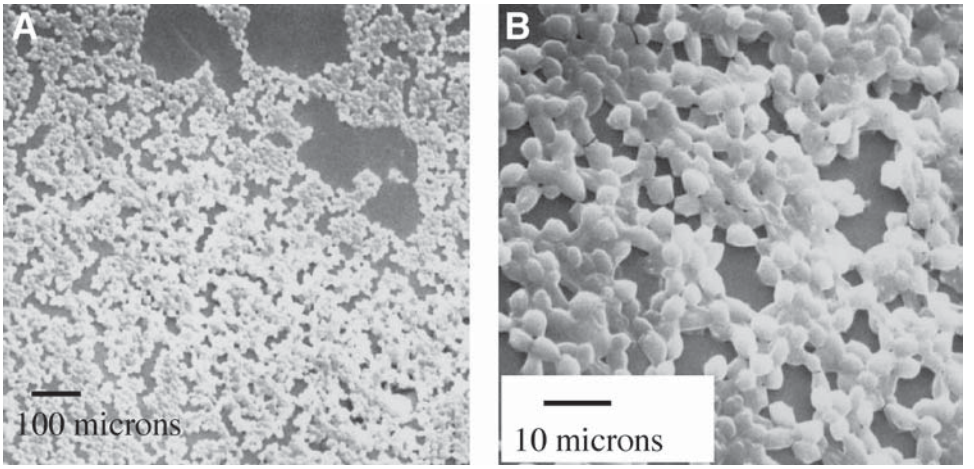

Fig. 4. SEM images of a SMY deposited over a polysulfone ultrafiltration membrane at **(A)** low magnification (↔200) and **(B)** high magnification (↔700). The image is captured during the protein filtration portion of cycle 10. The primary feed contained 5 g/L of cellulase, and the secondary feed contained 5.36 g/L of yeast. The cycle conditions were $t_f = 300$ s, $t_{sf} = 30$ s, and $t_b = 2$, with an average TMP of 15 psi maintained during forward as well as reverse filtration and a wall shear rate of 100 s^{-1}.

Figures 4A and 4B are scanning electron micrographs of a an ultrafilitration polysulfone membrane with a 30,000-Dalton mol wt cutoff at low and high magnification, respectively. The image was taken during the protein-filtration portion of cycle 10 (~3100 s), for an SMY experiment with 5.0 g/L of cellulase in the primary feed, 5.36 of g/L yeast in the secondary feed, and $P_f = P_b = 15$ psi. The majority of the membrane is covered by an SMY, but in a few places the SMY is absent or has been eroded. Note that the SMY is mostly monolayered, compared with the multilayered SMY seen during microfilitration. This difference is apparently due to the lower flux in ultrafiltration.

Microfiltration Experiments with Secondary Membranes and Backflushing

The goal of microfiltration of protein solutions is to remove particulate matter and protein aggregates while passing individual protein molecules through the membrane. Figure 5 shows a comparison of the permeate flux, *J*, vs time obtained during microfiltration in various configurations, including microfiltration of a 2.0 g/L BSA solution with backflushing and SMY deposition, with backflushing but without predeposited SMY, and without backflushing or SMY deposition. Also shown are results for microfiltration of a mixture of 1.34 g/L of yeast and 2.0 g/L of BSA with and without backflushing. A steep decline in permeate flux was observed during microfiltration of the yeast-protein mixture without backflushing,

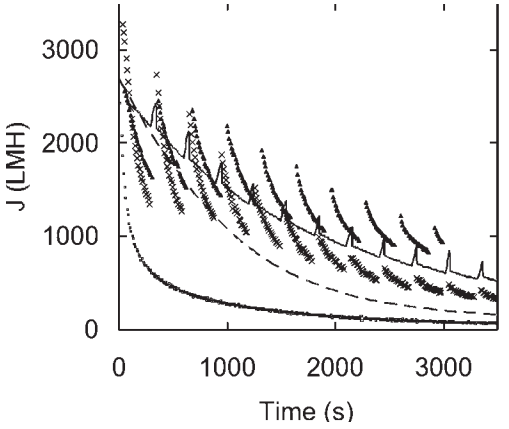

Fig. 5. Permeate flux during microfiltration of mixture of 2.0 g/L of BSA and 1.34 g/L of yeast with deposition of SMY and with backflushing (▲), without SMY but with backflushing (×), and without deposition of SMY and without backflushing (□); permeate flux for filtration of BSA without deposition of SMY and with backflushing (——), and without SMY and without backflushing (– – –). The feed for the SMY contained 0.68 g/L of yeast. The cycle conditions were t_f = 280 s, t_{sf} = 10 s, and t_b = 10 s, with $P_f = P_b$ = 7.5 psi. LMH = L(m²·h).

and it appeared to reach a nearly steady value of 60 L/(m²·h) or only 2% of the clean membrane flux. A slightly higher flux was obtained during filtration of the BSA-only solution, but a rapid decline in permeate flux was again observed and reached a nearly steady value of 90 L/(m²·h) after 5000 s. The permeate fluxes obtained during filtration of the BSA-only solution and the yeast-BSA mixture accompanied by periodic backflushing showed improvement; however, the fluxes continued to decline steadily. The best performance was obtained during filtration of the BSA-solution with periodic deposition and removal of the secondary membrane of yeast. Apparently, the secondary membrane was effective in partially shielding the primary membrane from irreversible fouling by protein aggregates and monomers. After 3000 s, a fivefold enhancement in permeate flux was obtained owing to use of secondary membranes and backflushing over BSA-only filtration without backflushing. However, when a secondary membrane was not redeposited after each backflush, the primary membrane was exposed to fouling by BSA in the feed, and a lower flux enhancement was obtained.

Average permeate fluxes (normalized by the clean membrane water flux, J_o) for yeast-BSA mixtures are plotted vs time in Fig. 6 for different concentrations of yeast in the primary and secondary feed reservoirs. The average flux, $\langle J \rangle$, was calculated by dividing the amount of net permeate collected by the time required to complete one cycle of yeast deposition, feed filtration, and backflushing ($t_{sf} + t_f + t_b$); the net permeate collected is

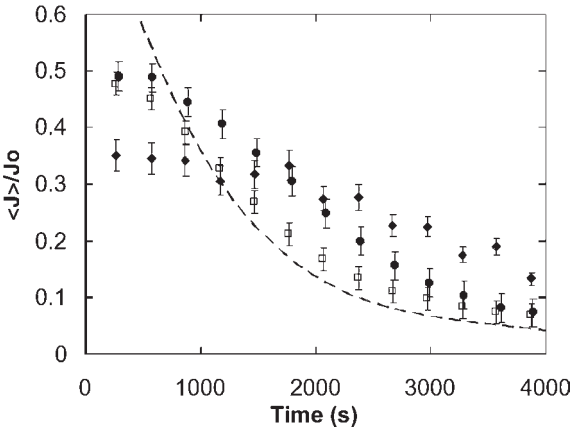

Fig. 6. Normalized microfiltration permeate flux vs time for different concentrations of yeast in secondary feed reservoir: (◆) 1.36 g/L; (●) 0.68 g/L; (□) 0.34 g/L. The cycle conditions were $t_f = 280$ s, $t_{sf} = 10$ s, and $t_b = 10$ s, with $P_f = P_b = 7.5$ psi. The primary feed contained a mixture of yeast (with the same concentration of yeast as in the secondary feed) and 2.0 g/L of BSA. The dashed line represents the normalized permeate flux during filtration of protein alone without deposition of SMY and without backflushing. Error bars represent ± SD for two to three repeats.

the difference between the mass of permeate collected during filtration of primary feed and the mass lost during backflushing. The permeate flux for the highest yeast concentration (1.36 g/L) was low initially, owing to the resistance of the thicker secondary membrane formed, but the flux tended to remain steady for longer times. By contrast, with lower yeast concentrations (0.34 and 0.68 g/L), the flux decreased more rapidly. After only 1800 s of filtration, the permeate fluxes for the lower yeast concentrations fell below that obtained for the higher yeast concentration. With a higher yeast concentration in the secondary feed reservoir, the secondary membrane of yeast formed was thicker and did a better job of shielding the primary membrane from protein foulants. By comparison, the flux for the forward filtration of BSA only started at a higher level, owing to a lack of yeast cake with added resistance, but it dropped below those with SMY after about 1000 s, as a result of protein fouling of the unprotected primary membrane.

The normalized average flux is plotted in Fig. 7 vs the duration of backflushing at the end of cycles 2, 3, and 4 for filtration of a BSA solution with an SMY. It is seen that the recovered permeate values decreased with each cycle, owing to gradual irreversible fouling. More significantly, the average flux obtained for each cycle is a maximum at a backflushing time of about 1.0 s. For lower backflushing durations, the removal of cake from the primary membrane was incomplete, and thus the flux declined owing to external foulant buildup. For higher backflushing times, there was sig-

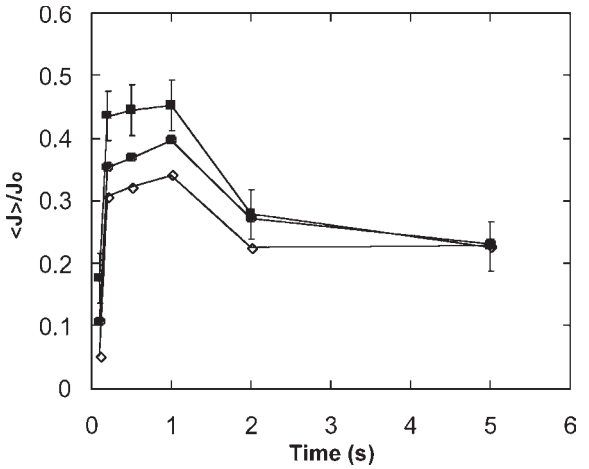

Fig. 7. Normalized recovered flux plotted after 600 s (■, cycle 2), 900 s (●, cycle 3), and 1200 s (◇, cycle 4) of microfiltration with deposition of SMY. The SMY was deposited for t_{sf} = 25 s, followed by forward feed filtration of 2.0 g/L of BSA for t_f = 275 s and then t_b = 0.1, 0.2, 0.5, 1.0, 2.0, or 5.0 s of backflushing. The points are joined by straight lines for clarity. The error bars represent ± SD for three repeats.

nificant loss of permeate through the membrane in the reverse direction without additional cleaning, which reduced the net flux from the maximum values.

Protein transmission data (Fig. 8) indicate nearly 100% transmission of protein initially, but the fraction of protein transmitted decreased rapidly for forward filtration of a BSA-only solution and appeared to reach a steady value of only 35% transmission after 10,000 s. When a secondary membrane of yeast was deposited at the beginning of each cycle, and then filtration of a BSA solution was carried out, the protein transmission values remained at nearly 100% for about 4000 s and subsequently decreased gradually to about 60% after 18,000 s of filtration. With SMY, the amount of protein recovered in the permeate is more than two times that recovered after filtration of the BSA-only solution after 18,000 s.

Ultrafiltration Experiments with Secondary Membranes and Backflushing

The goal of ultrafiltration, in contrast to microfiltration, is to retain protein molecules by the membrane while passing smaller solutes through the membrane with the permeate. Ultrafiltration experiments were performed with polysulfone membranes (30,000-Dalton mol wt cutoff). Figure 9 shows a comparison of the permeate flux vs time obtained during ultrafiltration of cellulase in the presence and absence of SMY that was periodically removed by backflushing and then replaced with a new SMY.

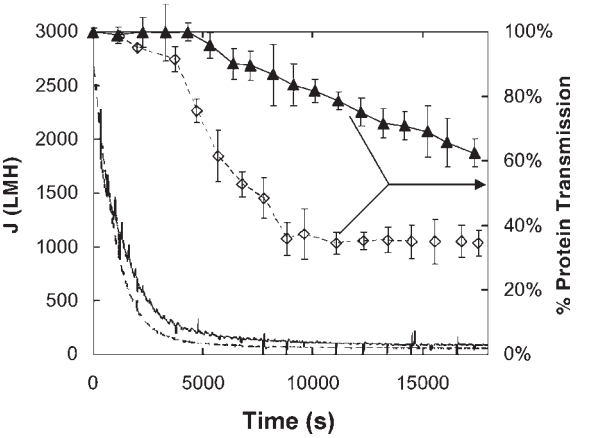

Fig. 8. Protein transmission during microfiltration of 2.0 g/L BSA only (◇) and 2.0 g/L of BSA in presence of SMY and backflushing (▲), and permeate flux vs time for microfiltration of BSA only (– – –) and for microfiltration of BSA with deposition of SMY and backflushing (——). The cycle conditions were t_f = 300 s, t_{sf} = 15 s, and t_b = 2 s, with P_f = P_b = 7.5 psi, and the yeast concentration in the secondary feed was 1.34 g/L. The error bars represents ± SD for two to three repeats. LMH = L(m²·h).

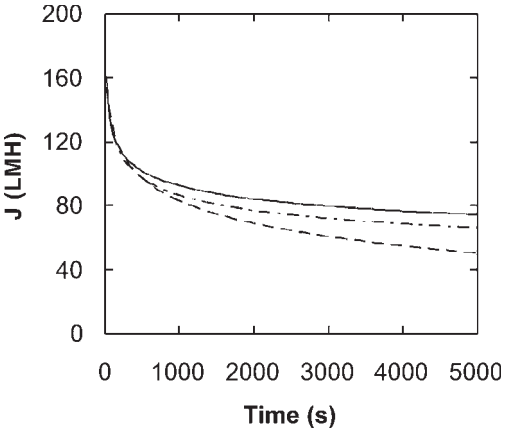

Fig. 9. Permeate flux vs time during ultrafiltration of 5.0 g/L of cellulase. The solid line represents SMY and backflushing with P_f = 30 psi, P_b = 15 psi, t_f = 300 s, t_{sf} = 5 s, and t_b = 2 s; the line with short and long dashes represents SMY and backflushing under the same conditions but with t_{sf} = 10 s. The yeast concentration in the secondary feed was 4.0 g/L. The dashed line is the permeate flux obtained without deposition of a secondary membrane or backflushing. A wall shear rate of 1300 s^{-1} was used. LMH = L(m²·h).

For the conditions in Fig. 9, improvements of 35–50% in the permeate flux were observed when a secondary membrane was used, owing to a reduction in the protein fouling of the primary membrane. Little or no flux recovery was observed with each backpulse, as might be expected from the relatively low resistance of the yeast layer and the irreversible nature of the protein fouling. The flux continuously declined with time owing to irreversible fouling, though the rate of decline was reduced by the SMY.

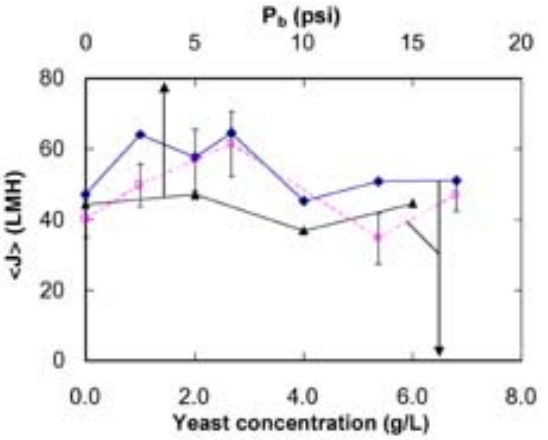

Fig. 10. Average permeate flux after 6000 s of ultrafiltration of 5.0 g/L of cellulase for different concentrations of yeast in secondary feed for wall shear rates of 400 s^{-1} (—◆—) and 100 s^{-1} (– –□– –), with $P_f = P_b = 7.5$ psi, $t_f = 300$ s, $t_b = 3$ s, and $t_{sf} = 30$ s. Also shown is the average permeate flux after 6000 s of ultrafiltration of 5.0 g/L of cellulase for varying reverse TMP (—▲—), with $P_f = 30$ psi, $t_f = 300$ s, $t_b = 2$ s, $t_{sf} = 5$ s, a wall shear rate of 1300 s^{-1}, and a concentration of yeast in the secondary feed of 4.0 g/L. The error bars represent ± SD for two to three repeats. LMH L(m^2·h).

In Fig. 10, the average permeate flux after 6000 s of ultrafiltration is plotted vs the concentration of yeast in the secondary feed, for two shear rates of 100 and 400 s^{-1}. Without any secondary membrane or backflushing, the average permeate fluxes are 48 ± 3 and 40 ± 6 L/(m^2·h) at the high and low shear rates, respectively. When an SMY was employed, the average permeate flux increased by about 20%, to maxima of 65 and 61 L/(m^2·h) for high and low shear rates, respectively. These maxima occur at an intermediate yeast concentration in the secondary feed of about 2.7 g/L. At even higher yeast concentrations, there was no longer an improvement in the average flux. Apparently, the increased resistance of the thicker SMY at higher yeast concentrations offset the reduced protein deposition on the primary membrane.

Also depicted in Fig. 10 is the variation in the average permeate flux after 6000 s of ultrafiltration vs the reverse TMP. The average permeate flux do not appear to vary significantly with the reverse TMP in the range investigated (0–15 psi). This finding may reflect the trade-off between better removal of the yeast layer and protein foulants at higher reverse TMP and less loss of the permeate in the reverse direction across the membrane at lower reverse TMP. The lower reverse TMP is therefore recommended, because it is less likely to cause membrane damage. A comparison of the average permeate flux obtained with SMY and backflushing and that obtained without SMY or backflushing (Fig. 9) indicates that the improvement flux with SMY for ultrafiltration is small, if any. Previously, Knutsen and Davis *(21)* demonstrated an improve-

ment in performance of cellulase ultrafiltration by the addition of lignocellulosic solids, but this was attributed to cellulase binding to the solids (which were removed by sedimentation prior to ultrafiltration) rather than the secondary membrane effect. They also demonstrated that there is essentially no transmission of cellulase enzyme through the 30,000-Dalton ultrafiltration membrane, as desired.

Conclusion

An increase in overall permeate flux was observed when microfiltration of protein solutions was carried out in the presence of secondary membranes. This increase was observed in microfiltration of both protein-only and yeast-protein mixtures. The backflushing time and the concentration of yeast used during deposition of the secondary membrane are the principal parameters governing the permeate flux for microfiltration. A higher yeast concentration led to a lower flux at shorter times, owing to increased resistance, but higher flux at long times, owing to increased protection of the primary membrane. There is an optimum backflushing duration for the removal of the secondary membrane, owing to a trade-off between cleaning the membrane and losing permeate during reverse filtration. The protein transmission during filtration of protein solutions with secondary membranes is higher than that obtained during filtration of protein solutions alone, leading to improved protein recovery. The use of secondary membranes may also increase the permeate flux in ultrafiltration, but the improvement is much smaller than in microfiltration. In microfiltration, protein aggregates were the primary cause of the fouling of the primary membrane, and these aggregates are effectively removed by the secondary membrane. In ultrafiltration, individual protein molecules were the primary cause of fouling of the primary membrane, and these individual protein molecules were less effectively removed by the secondary membrane. Thus, the primary application of the current work is microfiltration of biologic suspensions, in which the combination of increased permeate flux and increased protein transmission with the use of secondary membranes leads to high protein recovery.

Acknowledgments

We wish to thank Wendy Mores and Jeffrey Knutsen for assistance. This work was supported by the US Department of Energy and National Renewable Energy Laboratory.

References

1. Lonsdale, H. K. (1982), *J. Membr. Sci.* **10,** 81–181.
2. Belfort, G., Davis, R. H., and Zydney, A. L. (1994), *J. Membr. Sci.* **96,** 1–58.
3. Redkar, S. G. and Davis, R. H. (1995), *AIChE J.* **41,** 501–508.
4. Rodgers, V. G. J. and Sparks, R. E. (1991), *AIChE J.* **37**, 1517–1528.
5. Sondhi, R., Lin, Y. S., and Alvarez, F. (2000), *J. Membr. Sci.* **174,** 111–122.

6. Kuberkar, V. T., Czekaj, P., and Davis, R. H. (1998), *Biotechnol. Bioeng*. **60,** 77–87.
7. Jones, W. F., Valentine, R. L., and Rodgers, V. G. J. (1999), *J. Membr. Sci*. **15**7, 199–210.
8. Wilharm, C. and Rodgers, V. G. J. (1996), *J. Membr. Sci*. **121,** 217–228.
9. Mores, W. D., Bowman, C. N., and Davis, R. H. (2000), *J. Membr. Sci*. **165,** 229–240.
10. Srijaroonrat, P., Julien, E., and Aurelle, Y. (1999), *J. Membr. Sci*. **159,** 11–20.
11. Meacle, F., Aunins, A., Thornton, R., and Lee, A. (1999), *J. Membr. Sci.* **161,** 171–184.
12. Laitinen, N., Michaud, D., Piquet, C., Teilleria, N., Luonsi, A., Levanen, E., and Nystrom, M. (2001), *Sep. Purif. Technol*. **24,** 319–328.
13. Kuberkar, V. T. and Davis, R. H. (2001), *J. Membr. Sci*. **183,** 1–14.
14. Kelly, S. T., Opong, W. S., and Zydney, A. L. (1993), *J. Membr. Sci*. **80,** 175–187.
15. Tracey, E. M. and Davis, R. H. (1994), *J. Colloid Interface Sci.* **167,** 104–116.
16. Marcinkowsky, A. E., Krauss, K. A., Phillips, H. O., Johnson, J. S., and Shor, A. J. (1966), *J. Am. Chem. Soc*. **88,** 5744–5766.
17. Güell, C., Czekaj, P., and Davis, R. H. (1999), *J. Membr. Sci*. **155,** 113–122.
18. Kuberkar, V. T. and Davis, R. H. (1999), *Biotechnol. Prog*. **15,** 472–479.
19. Mores, W. D. and Davis, R. H. (2001), *J. Membr. Sci*. **189,** 217–230.
20. Knutsen, J. S. and Davis, R. H. (2002), *Appl. Biochem. Biotechnol*. **98–100,** 1161–1172.

0273-2289/04/114/0433–0445/$25.00

Enzymatic Synthesis of Monolaurin

Carla C. B. Pereira,[1] Mônica A. P. da Silva,[1] and Marta A. P. Langone*,[2]

[1]Escola de Química, Universidade Federal do Rio de Janeiro, Centro de Tecnologia, Bloco E, Lab I 221, Cidade Universitária, CEP: 21949-900, RJ, RJ, Brazil; and [2]Instituto de Química, Universidade do Estado do Rio de Janeiro, Rua São Francisco Xavier 524, PHLC, sl 310/lab.427, CEP: 20550-013, RJ, RJ, Brazil, E-mail: langonem@uerj.br.

Abstract

The aim of this study was to produce monolaurin utilizing a commercial immobilized lipase (Lipozyme IM-20; Novo Nordisk, Bagsvaerd, Denmark) through the direct esterification of lauric acid and glycerol in a solvent-free system. The influence of fatty acid/glycerol molar ratio, temperature, and Lipozyme (IM-20) concentration on the molar fraction of monolaurin were determined using an experimental design. The best conditions employed were 55°C, lauric acid/glycerol molar ratio of 1.0, and 3.0% (w/w) enzyme concentration. The final product, obtained after 6 h of reaction, was 45.5% monolaurin, 26.8% dilaurin, 3.1% trilaurin, and 24.6% lauric acid. The reusability of the enzyme was also studied.

Index Entries: Monolaurin; immobilized lipase; esterification; experimental design; solvent-free medium.

Introduction

Monolaurin, a monoglyceride resulting from the reaction between lauric acid and glycerol, is a nonionic surfactant with important applications in pharmaceutics, food, and cosmetics production *(1,2)*. Recently, the potential of monolaurin and other monoglycerides to inhibit the growth of bacterial spores and vegetative cells was demonstrated, including that of *Clostridium botulinum* and *Bacillus cereus (2–4)*. Chemical preservation is widely used to extend food shelf life and to delay or inhibit the growth of pathogenic microorganisms. However, the questionable safety of some chemical food preservatives has stimulated efforts to develop alternatives based on natural substances.

*Author to whom all correspondence and reprint requests should be addressed.

Monolaurin has also been studied for its bactericidal activity against *Helicobacter pylori*, which is responsible for chronic gastritis and duodenal ulceration, also a known risk factor in gastric cancer owing to inflammatory mechanisms *(5)*. The best available treatments with combinations of drugs result in between 70 and 100% eradication of the bacterium, but adverse reactions, side effects, and the developing resistance of bacterium to available antibiotics are continuing problems *(6)*. Therefore, new methods to prevent and treat gastrointestinal infections caused by *H. pylori* have been studied. In studies on antibacterial activity of monoglycerides, Bergsson et al. *(5)* found monocaprin and monolaurin to be the most active agents against *H. pylori* for short incubation times.

Monolaurin has demonstrated a large spectrum of activity against fungi and viruses. Beyond the antiviral activity, monolaurin increases an organism's defenses against virus attack, potentializing immunologic reactions initiated by agents such as antigens.

Presently, monoglycerides are manufactured on an industrial scale by continuous chemical glycerolysis of fats and oils at high temperatures (220–250°C), employing inorganic alkaline catalysts under a nitrogen gas atmosphere. The product obtained by this route has several drawbacks such as low yield, dark color, and burnt taste. In addition, the process is not very selective toward monolaurin and is intensive on energy consumption. Recently, some studies involving alternative heterogeneous catalytic routes have been reported, such as glycerol esterification with fatty acids using different catalysts: cationic resins, zeolitic molecular sieves, functionalized mesoporous materials, and oxides such as MgO and ZnO *(1)*. Alternative methods have been developed as substitutes for conventional chemical processes. In the last decade, many approaches have been investigated for the enzymatic synthesis of monoglycerides using lipase *(7)*. The advantages of enzymatic synthesis are mild reaction conditions, resulting in products of higher quality and lower energy consumption; the selectivity of lipases; and fewer environmental problems *(8)*.

The objective of the present work was to study the synthesis of monolaurin by direct lipase-catalyzed esterification between glycerol and lauric acid without any solvent or surfactant. The effects of lauric acid/glycerol molar ratio, enzyme concentration, and temperature were studied using an experimental design. The reuse of the commercial immobilized lipase, to reduce the process cost, was also investigated.

Materials and Methods

Chemicals

Lypozyme IM-20 (*Mucor miehei* lipase immobilized on a weak anion-exchange resin) was kindly supplied by Novo Nordisk (Bagsvaerd, Denmark). The gas chromatography (GC) standards (mono-, di-, and trilaurin) were obtained from Sigma (St. Louis, MO). Analytical-grade glycerol, lauric acid (99.9%), *n*-hexane, ethyl acetate, acetone, and ethanol were purchased from Merck (Darmstadt, Germany).

Measurement of Lipase Activity

The esterification activity of Lipozyme IM-20 was measured according to the method described by Langone and Sant'Anna *(9)*, which determines the consumption rate of fatty acid at 60°C in a reaction system containing glycerol, lauric acid, and a given amount of the commercial enzyme preparation. One international unit of esterification activity is the quantity of enzyme that consumes 1 µmol of lauric acid/min under the reaction conditions. The enzyme used has an esterification activity of 20 IU/g.

Nonpolar-Phase Analysis

Lauric acid and mono-, di-, and trilaurin were analyzed by capillary GC according to the method described by Langone and Sant'Anna *(9)*. All concentrations were calculated as molar fractions from the peak area using calibration curves.

Esterification Experiments

All experiments were performed in a 20-mL open batch reactor with constant stirring and temperature control. The reaction system contained a mixture of lauric acid and glycerol and the biocatalyst Lipozyme IM-20. The reaction's progress was followed by withdrawing 20-µL aliquots at various time intervals and analyzing them by GC, as previously described.

Experimental Design

The effects of different variables on a process can be determined using experimental design methodology, which employs a reduced, but meaningful, number of experiments *(10)*. The statistical analysis of monolaurin molar fraction (Y_{mon}) was made by means of a two-level-three-factors central composite design with six star points and six central points. The experimental data were analyzed using STATISTICA® for Windows, release 5.5, produced by Statsoft.

Recovery of Immobilized Enzyme

After completion of each esterification reaction, the medium was centrifuged, and the solid phase (immobilized enzyme) was recovered according to the method described by Langone and Sant'Anna *(11)*. Then, the experiments were performed reusing the enzyme recovered after each batch reaction assay.

Results and Discussion

Experimental Design

An experimental design technique was used to identify the best conditions to produce monolaurin. The basic idea was to devise a small set of

Table 1
Coded Levels and Corresponding Actual Values Employed

Variables	Code	Actual factor level at coded factor levels of				
		–1.682	–1	0	+1	1.682
Acid/glycerol molar ratio	*R*	0.5	0.7	1.0	1.3	1.5
Temperature (°C)	*T*	48	51	55	59	62
Enzyme Concentration(%w/w)	*E*	0.5	1.5	3.0	4.5	5.5

experiments accounting for all pertinent factors *(10)*. The subsequent analysis of data identified optimal conditions, factors that most influenced the results as well as those that did not, and the presence of significant interactions. A model relating the dominating factors to the response variable (monolaurin molar fraction Y_{mon} %) was obtained.

A central composite design for three factors was used to generate 20 combinations. The effects of independent variables—acid/glycerol molar ratio (*R*), temperature (*T*), and enzyme concentration (*E*)—on the response (i.e., the monolaurin molar fraction at 4 h) were investigated. The upper and lower limits of each variable were chosen based on published data and preliminary studies *(12,13)*. Actual independent variables or factors and their corresponding coded levels are presented in Table 1.

The enzymatic synthesis of monolaurin was quantified in terms of molar fraction of each component in the nonpolar phase (lauric acid, mono-, di-, and trilaurin), and monolaurin molar fraction was chosen to define the best reaction conditions. The selectivity parameter, defined as the ratio between concentrations of monolaurin and total concentration of reaction products (mono-, di-, and trilaurin), was also evaluated.

The full factorial central composite design includes factorial points, star points, and center points. The corresponding model is the complete quadratic surface between the response and the factors, as given by Eq. 1:

$$Y_{pred} = b_0 + b_1x_1 + b_2x_2 + b_3x_3 + b_{11}x_1^2 + b_{22}x_2^2 + b_{33}x_3^2 + b_{12}x_{12} + b_{13}x_{13} + b_{23}x_{23} \quad (1)$$

in which Y_{pred} is the predicted response (monolaurin molar fraction), $x_1 = R$, $x_2 = T$, $x_3 = E$, $x_{12} = RT$, $x_{13} = RE$, $x_{23} = TE$, b_1 through b_{23} are the respective coefficients of variables and interactions, and b_0 is the mean.

Table 2 presents the analysis of the main effects and interactions of the factors (linear and quadratic) for the chosen response and their statistical significance (*p* value). It can be observed that the main factor *E* (linear and quadratic) and two main factors (*R* and *T* quadratic) are the important ones with a statistically significant effect on the response of monolaurin molar fraction ($p < 0.05$).

Substituting the coefficients b_i in Eq. 1 by their values from Table 2 on obtains:

$$Y_{mon} = 40.1 - 0.2R + 0.9T + 7.6E - 1.2R^2 - 3.2T^2 - 4.5E^2 + 0.2RT + 0.4RE - 0.1TE \quad (2)$$

Table 2
Estimated Factor and Interaction Effects, Coefficients for Predictive Mathematical Models, and *p* Values

Variable	Coefficient	SEC [a]	Effect	SEE [b]	*t*-test	*p* Value
Mean	40.10 (b_0)	0.52	40.1	0.52	76.87	0.0000
R—linear (x_1)	–0.20 (b_1)	0.35	–0.4	0.69	–0.59	0.5775
R—quadratic (x_1^2)	–1.19 (b_{11})	0.34	–2.58	0.68	–3.48	0.0177
T—linear (x_2)	0.93 (b_2)	0.34	1.86	0.68	2.73	0.0411
T—quadratic (x_2^2)	–3.20 (b_{22})	0.31	–6.40	0.63	–10.16	0.0001
E—linear (x_2)	7.61 (b_3)	0.35	15.21	0.69	21.92	0.0000
E—quadratic (x_3^2)	–4.50 (b_{33})	0.34	–9.00	0.68	–13.18	0.0000
RT (x_{12})	0.22 (b_{12})	0.45	0.45	0.90	0.50	0.6395
RE (x_{13})	0.44 (b_{13})	0.45	0.88	0.87	0.98	0.3722
TE (x_{23})	–0.12 (b_{23})	0.45	–0.24	0.90	–0.27	0.7970

[a] SEC, standard error of coefficient.
[b] SEE, standard error of effect.

After estimating the factors' main effects, other significant factors affecting the monolaurin molar fraction were established by analysis of variance (ANOVA), as shown in Table 3. From the *p* values, defined as the smallest level of significance leading to rejection of the null hypothesis, it appears that the main effect of each factor (linear and quadratic) and the interaction effects are statistically significant when $p < 0.05$. The effects of E and E^2, and T^2 were of higher statistical significance. The effects statistically not significant were *R*, *RT*, *RE*, *TE*.

A useful plot for identifying factors that are important is a Pareto chart. The graph in Fig. 1 shows the *t*-test values in the horizontal axis and also includes a vertical line to indicate the *p* value (an effect that exceeds the vertical line may be considered significant). As observed in the Pareto chart, enzyme concentration is the most significant variable influencing monolaurin molar fraction.

Based on *F*-test and student's *t*-test, some effects were discarded, because they did not exhibit any statistical significance. The resultant model can be represented by

$$Y_{mon} = 40.1 + 0.9T + 7.6E - 1.2R^2 - 3.2T^2 - 4.5E^2 \quad (3)$$

Figure 2 shows the three-dimensional plot for the response of monolaurin molar fraction vs temperature ratio and enzyme concentration at a molar ratio of 1.0 and reaction time of 4 h. The highest Y_{mon} values were reached at temperatures between 54 and 56°C and an enzyme concentra-

Table 3
Analysis of Variance[a]

Factor	Sum of squares	Degree of freedom	Mean of squares (MS)	F_0	p Value
R	0.578	1	0.578	0.3545	0.577516
R^2	19.727	1	19.727	12.0903	0.017714
T	12.187	1	12.187	7.4689	0.041136
T^2	168.332	1	168.332	103.1681	0.000159
E	784.152	1	784.152	480.5950	0.000004
E^2	283.391	1	283.391	173.6861	0.000045
RT	0.405	1	0.405	0.2482	0.639470
RE	1.566	1	1.566	0.9601	0.372172
TE	0.120	1	0.120	0.0736	0.797041
Lack of fit	36.939	5	7.388	4.5279	0.061487
Pure Error	8.158	5	1.632	—	—
Total sum of squares	1255.291				

[a]$F_0 = MS_{FACTOR}/MS_{ERROR}$; $R^2 = 0.9641$; R^2 adj. = 0.9317.

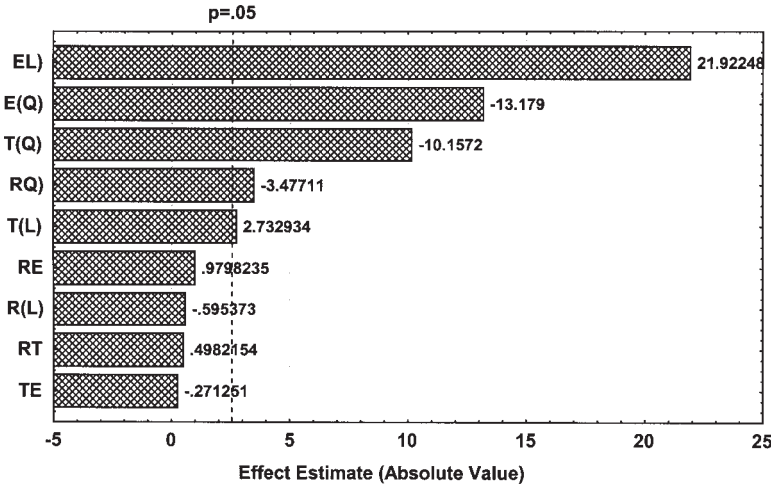

Fig. 1. Pareto chart of effects.

tion in the range of 4.0 to 5.0% (w/w). These observations are consistent with the experimental data in Fig. 3. The best measured results in terms of molar fraction of monolaurin were obtained at 55°C, with a reagent molar ratio of 1 and an enzyme concentration of 3% (w/w).

Data analysis led to the optimal conditions: 55.5°C, molar ratio of 1.0, and enzyme concentration of 4.3% (w/w) corresponding to monolaurin molar fraction (43.3%). The best measured values are closer than those obtained from the statistical analysis. ANOVA demonstrated that modeling was successful with a coefficient of determination (R^2) of 0.964. The plot

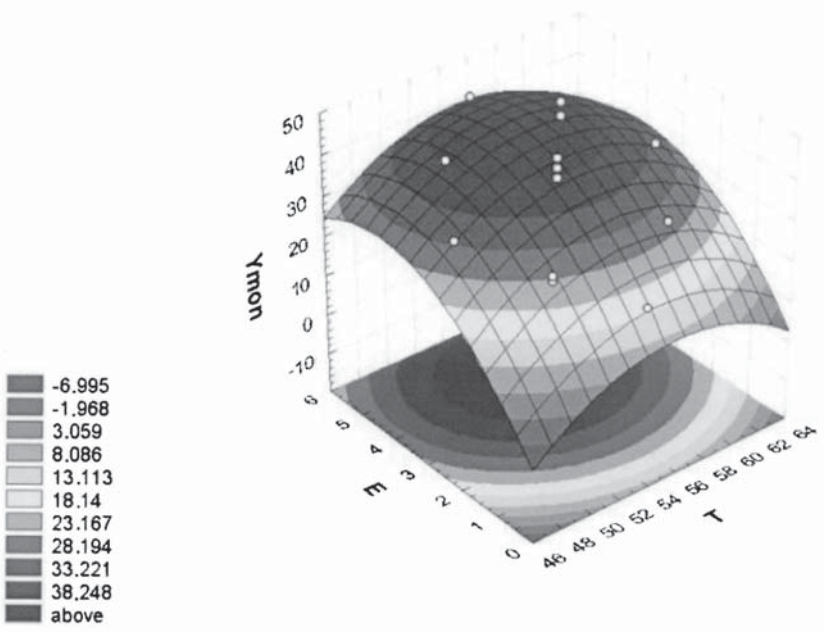

Fig. 2. Response surface for monolaurin molar fraction.

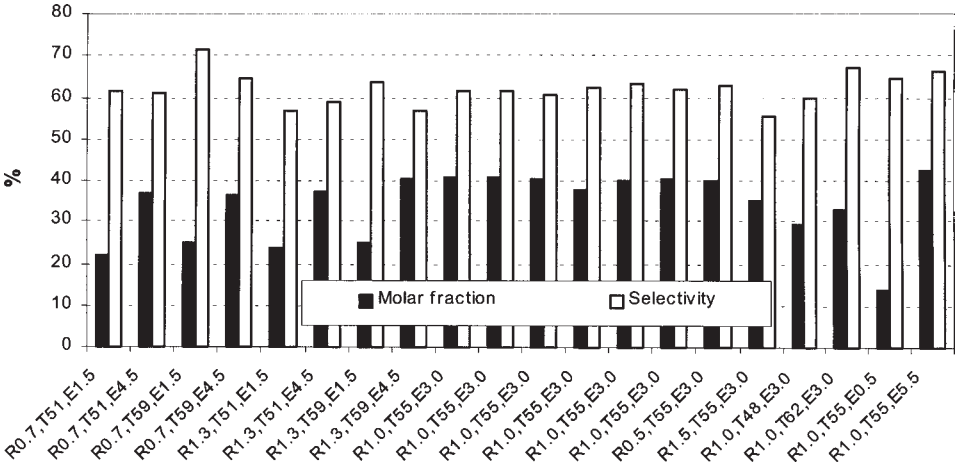

Fig. 3. Influence of variables (*R*, *T*, and *E*) on monolaurin molar fraction and monolaurin selectivity after 4-h reaction.

of experimental vs predicted values is shown in Fig. 4. Clearly the model represents the experimental range of studied variables adequately.

Effects of Enzyme Concentration

According to Fig. 1, the enzyme concentration is the variable presenting higher statistical importance on monolaurin synthesis. Therefore,

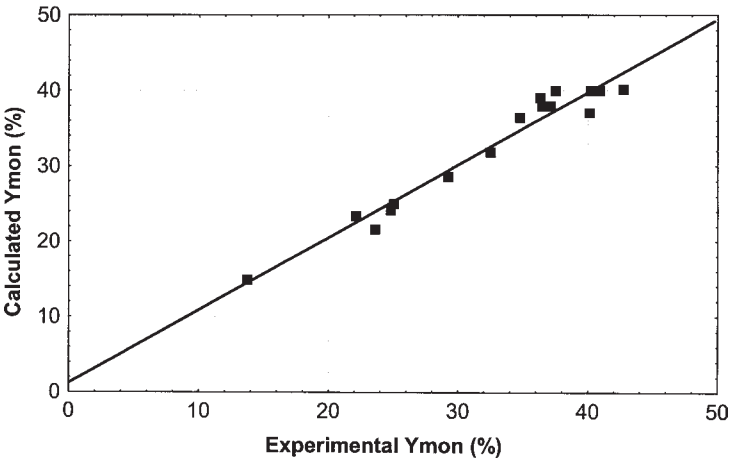

Fig. 4. Comparison of experimental and calculated values of monolaurin molar fraction.

experiments with different concentrations were proposed, keeping the stoichiometric molar ratio of reagents and temperature of 55°C; results are presented in Fig. 5. The best measured results were obtained with Lipozyme IM-20 at 3.0–5.8 % (w/w). Enzyme concentration affected the initial reaction rate but did not significantly affect the final (after 6 h) molar fraction. Figure 5 confirms the data in Fig. 3 and in the response surface (Fig. 2). Considering the advantages of reduced operating costs, the best concentration of enzyme preparation was 3.0% (w/w).

Wong et al. *(14)* also studied the effect of the amount of enzyme (lipase from *Candida rugosa*; Sigma) on monocaprin synthesis in isooctane at 37°C. They observed that monocaprin molar fraction increased when the amount of lipase was increased, but no significant increase in monocaprin yield (conversion of capric acid equal to 35%) was observed for a lipase loading of more than 100.0 mg (corresponding to 16.4% [w/w]).

Ferreira-Dias et al. *(15)* tested Lipozyme IM-20 for the glycerolysis of olive oil residue in *n*-hexane aimed at the production of monoglycerides and diglycerides. The highest monoglyceride production was in the range of 43–45% (w/w), on the basis of total fat, with about 26% Lipozyme IM-20.

It can be concluded that in the system used in our work (without solvent, open reactor, at 55°C), it is possible to obtain better conversions (up to 70%) using lower enzyme concentration.

Effect of Temperature

The effect of temperature on monolaurin synthesis was also statistically significant. The best temperature tested was 55°C. Figure 6 shows the effect of temperature on monolaurin molar fraction during 6 h of reaction using a concentration of enzyme preparation of 3.0% (w/w) and substrate molar ratio of 1.0. An increase in temperature (above 55°C) did not favor

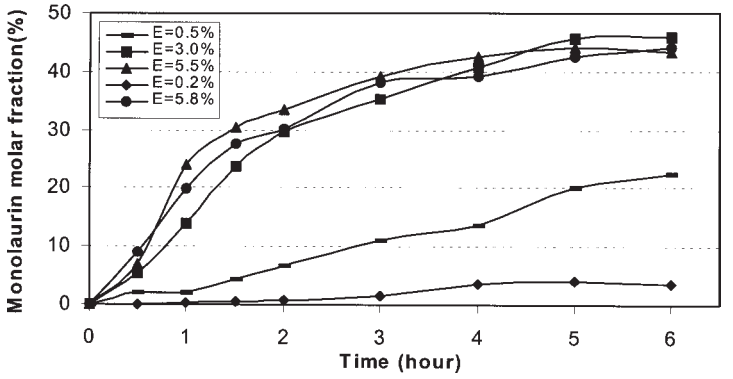

Fig. 5. Effect of Lipozyme IM-20 concentration on molar fraction in monolaurin for synthesis performed at 55°C using R = 1.0.

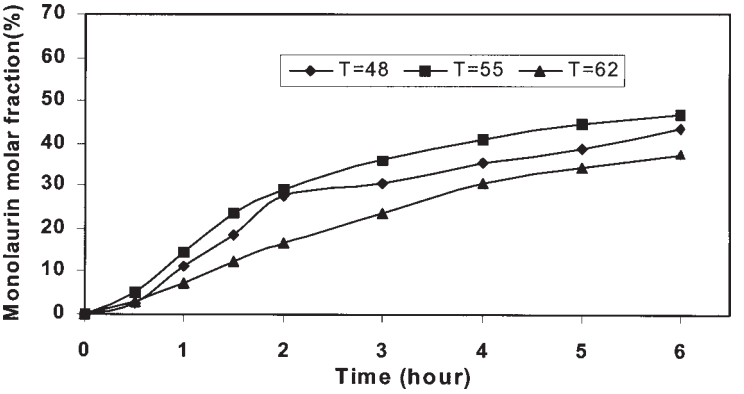

Fig. 6. Effect of temperature on monolaurin synthesis (molar fraction) carried out for 6 h with lauric acid/glycerol molar ratio of 1 and 3.0% (w/w) Lipozyme IM-20.

monolaurin synthesis. This can be confirmed by the lesser values of monolaurin molar fraction during the reaction course at 62°C (Fig. 6).

Langone et al. *(13)* observed a lower thermal stability of Lipozyme IM-20 in the synthesis of monoglycerides (monomiristin and monolaurin) compared with the synthesis of the respective triglycerides. The synthesis of triglycerides (direct esterification between an excess of fatty acid and glycerol: R = 5.0) in a solvent-free system was possible at temperatures near 100°C, allowing a triglyceride selectivity of 100% after 24 h. For the synthesis of monoglycerides (using R = 1.0), Langone et al. *(13)* showed that an increase in temperature from 60 to 90°C resulted in a decrease in monolaurin molar fraction of 30%. Thus, temperature itself is not the unique factor affecting lipase denaturation; the higher glycerol concentration required for the synthesis of monolaurin seems to reduce the enzyme activity.

Effect of Molar Ratio of Reagents

As shown in Fig. 3, using an excess of glycerol corresponding to the lauric acid/glycerol molar ratio of 0.5 and 0.7 did not result in a significant increase in monolaurin molar fraction. Wong et al. *(14)* also investigated the effect of substrate molar ratio on monocaprin synthesis catalyzed by a lipase from *C. rugosa*. They concluded that an excess of glycerol on the reaction mixture inhibited enzyme activity. This can be explained by the fact that glycerol is a polar substance and in excess can be adsorbed by the immobilized enzyme support, removing the catalyst water layer that is necessary for lipase stabilization causing enzyme inactivation. On the other hand, an increase in lauric acid concentration (R = 1.3; R = 1.5) enhanced the synthesis of di- and trilaurin. Therefore, the best lauric acid/glycerol molar ratio tested for the monolaurin synthesis was the stoichiometric molar ratio (R = 1).

Time Course on Best Condition

Considering the results presented, the best experimental conditions used for monolaurin synthesis were 55°C, an enzyme concentration of 3% (w/w), and use of the stoichiometric molar ratio of reagents. Figure 7 shows the nonpolar phase for monolaurin synthesis under these conditions. The final product, obtained after 6 h of reaction, was 45.5% monolaurin, 26.8% dilaurin, 3.1% trilaurin, and 24.6% lauric acid.

Bellot et al. *(16)* investigated monoglyceride synthesis by *Rhyzomucor miehei* lipase (Lipozyme) via direct esterification between glycerol and oleic acid in organic solvents. In pure *n*-hexane, the monoglyceride represented only 6 molar % of the total products at the thermodynamic equilibrium (34 and 60% for di- and triglyceride, respectively). The use of a mixture of *n*-hexane/2-methyl-2-butanol enables a product mixture to be obtained containing 94% monoglycerides at equilibrium. However, this positive effect is counterbalanced by a decrease in both initial velocities and substrate conversion at thermodynamic equilibrium.

Again, it can be concluded that the system used in our work, without solvent, is a less costly and more selective process to produce mono- and diglycerides by direct esterification of glycerol and fatty acid. Such a system avoids the problems of separation, toxicity, and flammability of organic solvents, permitting recovery of product without further complex purification or evaporation steps and lowering the cost of the final product.

The results presented here are close to those obtained by chemical glycerolysis of fat and oils at high temperatures, employing inorganic alkaline catalysts. The product is a mixture that contains 35–60% monoglycerides, 35–50% diglycerides, 1–20% triglycerides, and 1–10% free fatty acids and their alkali metal salts *(8)*.

Machado et al. *(1)* studied the synthesis of monolaurin from lauric acid and glycerol employing commercial Beta, Y, and Mordenite zeolites as catalysts. The optimized conditions for the monolaurin synthesis

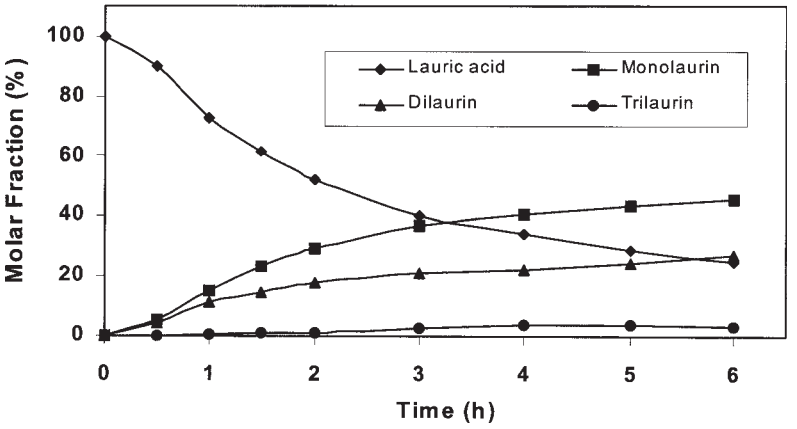

Fig. 7. Time course for monolaurin synthesis carried out at 60°C with lauric acid/glycerol molar ratio of 1 and 3.0% (w/w) Lipozyme IM-20.

were 110°C, stoichiometric ratio of reagents, catalyst concentration of 5.0% (w/w), and reaction time of 24 h. The best results were obtained by using zeolite Beta as catalyst, and monolaurin yields of 20% with selectivities higher than 65% were achieved.

A comparison of these methods shows that the development of monoglyceride production by enzymatic method could be considered as compared to the chemical process, since milder reaction conditions are utilized and less energy is consumed in a shorter time.

Reusability of Enzyme

The results of the production of monolaurin at 55°C with an enzyme concentration of 3.0 (w/w) and substrate molar ratio of 1.0, in several sequential experiments performing enzyme recover and reuse are shown in Fig. 8. The test was realized in triplicate (medium 1, 2, and 3). The enzyme could be reused, keeping its performance, two times for the synthesis of monolaurin. Langone and Sant'Anna *(11)* investigated the reutilization of immobilized lipase in triglyceride synthesis. They observed that the enzyme remained stable even when reused 16 times. The small number of enzyme reuses obtained in monolaurin synthesis can be explained considering the greater amount of glycerol in the reaction medium, which, as previously described, can inactivate the enzyme.

Conclusion

A fully central composite design was applied to optimize monolaurin synthesis. A three factorial design was proven effective to establish the influence of the variables on the monolaurin synthesis. The central composite design procedure was adopted to optimize variables affecting the monolaurin molar fraction.

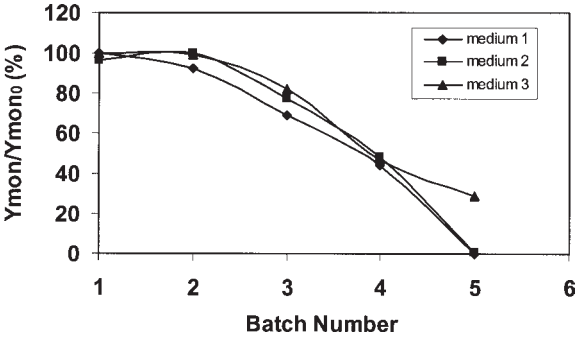

Fig. 8. Effect of enzyme reutilization—Lipozyme IM-20 3.0% (w/w)—on monolaurin synthesis (molar fraction). Successive 6-h batches were performed using a lauric acid/glycerol molar ratio of 1 at 55°C.

Statistical analysis showed that within the experimental range considered, the most important factor was enzyme concentration. The temperature also affected the monolaurin molar fraction. This factor had a negative influence. According to these results, the maximum monolaurin molar fraction (43.3%) was achieved at 55°C, a molar ratio of 1.0, and an enzyme concentration of 4.3% (w/w) within the range studied.

The results of our work illustrate the technical feasibility of producing monoglycerides in a solvent-free medium, although conversions (defined as the percentage of consumed lauric acid) near 70% were attained, with monolaurin being the main product. Such a system avoids problems of separation, toxicity, and flammability of organic solvents, lowering the cost of the final product and permitting recovery of product without further purification or evaporation steps. Furthermore, the results obtained are in accordance with the directives of the World Health Organization. The requirements for utilization of these mixtures as food emulsifiers are (1) to have at least 70% mono- and diglycerides, (2) to have a minimum of 30% monoglycerides, and (3) to present concentrations of both glycerol and triglycerides below 10% *(17)*. Therefore, the results indicate that direct esterification of lauric acid and glycerol under catalysis by immobilized lipase (Lipozyme IM-20) is a very efficient method, allowing production of an appreciable amount of monolaurin with good selectivity.

The possibility of immobilized enzyme reuse was confirmed for monolaurin synthesis. This aspect, not often investigated, certainly increases the economical viability of the process.

Acknowledgments

This work was partially financed by Fundação de Amparo à Pesquisa do Estado do Rio de Janeiro (FAPERJ) (projects E-20/170.731/2000 and E-26/150.356/2002).

References

1. Machado, M. S., Perez-Pariente, J., Sastre, E., Cardoso, D., and Guerenu, A. M. (2000), *Appl. Catalysis. A* **203,** 321–328.
2. Cotton, L. and Marshall, D. (1997), *Lebensm. Wiss. U. Technol.* **30,** 830–833.
3. Chaibi, A., Ababouch, L., and Busta, F. (1996a), *J. Food Protection* **59(8),** 832–837.
4. Chaibi, A., Ababouch, L., and Busta, F. (1996b), *J. Food Protection* **59(7),** 716–722.
5. Bergsson, G., Steingrímsson, O., and Thormar, H. (2002), *Int. J. Antimicrob. Agents* **20,** 258–262.
6. Sun, C., O'Connor, C., and Roberton, A. (2003), *Immun. Med. Microbiol.* **1496,** 1–9.
7. Bornscheuer, U. T. (1995), *Enzyme Microb. Technol.* **17,** 578–586.
8. Rosu, R., Uozaki, Y., Iwasaki, Y., and Yamane, T. (1997), *J. Am. Oil Chem. Soc.* **74,** 445–450.
9. Langone, M. A. P. and Sant'Anna, G. L. P. (1999), *Appl. Biochem. Biotechnol.* **77–79,** 759–770.
10. Montgomery, D. C. (1997), *Design and Analysis of Experiments*, 4th Ed., John Wiley & Sons, New York, NY.
11. Langone, M. A. P. and Sant'Anna, G. L. P. (2002), *Appl. Biochem. Biotechnol.* **98–100,** 997–1008.
12. Da Silva, M. A. M, Medeiros, V. C., Langone, M. A. P., and Freire, D. M. G. (2003), *Appl. Biochem. Biotechnol.* **105–108**, 757–768.
13. Langone, M. A. P., Abreu, M. E, Rezende, M. J. C., and Sant'Anna, G. L. P. (2002), *Appl. Biochem. Biotechnol.* **98–100,** 987–996
14. Wong, W.C., Basri, M., Razak, C.N.A. and Salleh, A.B. (2000), J. Am. Oil Chem. Soc., 77(1), 85–88.
15. Ferreira-Dias, S., Correia, A. C., Baptista, F. O., and Fonseca, M. M. R. (2001), *J. Mol. Cat. B-Enzym.* **11,** 699–711.
16. Bellot, J. C., Choisnard, L., Castillo, E., and Marty, A. (2001), *Enzyme Microb. Technol.* **28,** 362–369.
17. Arcos, J. A. and Otero, C. (1996), *J. Am. Oil Chem. Soc.* **74(6),** 673–682.

Session 3

Bioprocessing, Including Separations

Session 3

Bioprocessing, Including Separations

Dale A. Monceaux[1] and David R. Short[2]

[1]Katzen International, Inc., Cincinnati, OH; and
[2]E. I. DuPont de Nemours, Wilmington, DE

Bioprocessing addresses the phases, developments, and process unit operations required to take a technology from the conceptual or bench-scale stages of development to the pilot, demonstration, and commercial development stages. These critical steps in technology development o ften stand between the invention and the ultimate goal of commercial success.

This session strived to address several perspectives on this broad subject. In consideration of the fact that this was the 25th anniversary of the first symposium on biotechnology for fuels and chemicals, a program was developed to provide a perspective on advancements in bioprocessing that have occurred during that time. As is the case with many such endeavors, the process proved to be very challenging. The basic criteria utilized while reviewing the abstracts considered for oral presentations at Session 3 included the following concepts:

1. Subject matter diversity: The program assembled for Session 3 attempted to emulate the "real world" of technology development over the course of the session. The presentations for Session 3 began with modeling techniques, proceeded to pilot and demonstration programs and ended with commercial applications.
2. Geographic diversity: One goal of Session 3 was to deliver distinguished technical content while simultaneously providing a perspective on the international nature of today's research programs. Speakers represented a cross section of nationalities and cultures working in the field of biotechnology for fuels and chemicals.
3. Research program diversity: Session 3 introduced presentations and speakers from outside the more established centers of research. The presenters were a mix of academia, research laboratories, and industry. This served to provide additional evidence of the breadth of the research that is occurring in the field of biotechnology-based fuels and chemicals.

To deliver the diverse program proposed, we decided that the number of presentations delivered in Session 3 would be expanded. Therefore,

seven papers were selected for oral presentation consistent with the outlined criteria.

The first paper of the session, "Development and Application of Computational Fluid Dynamics Models for Scale-up of Biocommodity Processes," presented by Xiongjun Shao of Dartmouth College, provided insight into a new CFD model for bioprocess scale-up that includes dynamic treatment of enzyme adsorption, and discrete as well as continuous feeding. The second paper, "Identification of Microbial Inhibitory Functional Groups in Corn Stover Hydrolysate by ^{13}C NMR," presented by Foster Agblevor of Virginia Polytechnic Institute and State University, detailed the use of ^{13}C NMR techniques to elucidate the mechanism by which overliming reduces microbial inhibition in hydrolysates and identified key hydrolysate components involved in this inhibition.

The third paper, "Nisin and Lactic Acid Simultaneous Production from Cheese Industry Byproducts: Optimization of Fermentation Conditions Through Statistically Based Experimental Designs," presented by Chaunbin Liu of Washington State University, described a novel fermentation process for coproduction of the aforementioned products optimized and validated through the use of the SDOE approach. The fourth paper, "High-Rate Thermophilic Methane Fermentations on Short-Chain Fatty Acids," presented by Masahiro Tatara of the Kajima Technical Research Institute, Tokyo, provided insight into a novel two-stage anaerobic digestor for hydrogen and methane production from organic wastes for power generation.

The fifth paper, "A Separative Bioreactor: Direct Product Capture and pH Control," presented by Seth Snyder of the Argonne National Laboratory, reviewed development and performance of a novel bioreactor incorporating electrodeionization to simultaneously produce and separate products from both enzymatic and microbially mediated reactions. The sixth paper, " Optimization of Xylose Fermentation in Spent Sulfite Liquor by *Saccharomyces cerevisiae* 259ST," presented by Steven Helle of the University of British Columbia, provided an overview of an approach to fermentation optimization utilized to identify key process variables limiting use of the SSL for commercial ethanol production.

The seventh and final paper, "Development of a Fermentation-Based Process for 1,3-Propanediol: Highlights of a Successful Path from Corn to Textile Fiber," by Tyler Ames of DuPont, reviewed the multiyear effort by DuPont and its development partners (Genecor International and Tate & Lyle) to commercialize a new biocatalytic process for the production of 1,3-propanediol (PDO), a key ingredient in DuPont's new Sorona™ advanced polymer platform. PDO is currently being produced at pilot scale at Tate & Lyle's Decatur, IL, site, and construction of a commercial-scale facility is expected to begin soon.

The session cochairmen wish to thank the authors for their contributions to a timely and well-received session. The seven oral presentations

and more than 70 poster presentations in this session served to demonstrate the diverse nature of the research and development that has occurred in the area of bioprocessing and separations since the first symposium was held in 1978.

0273-2289/04/114/0453–0468/$25.00

Evaluation of Recombinant Green Fluorescent Protein, Under Various Culture Conditions and Purification with HiTrap Hydrophobic Interaction Chromatography Resins

Thereza Christina Vessoni Penna,*[,1] Marina Ishii,[1] Adalberto Pessoa Junior,[1] Laura de Oliveira Nascimento,[1] Luciana Cambricoli de Souza,[1] and Olivia Cholewa[2]

[1]Department of Biochemical and Pharmaceutical Technology, School of Pharmaceutical Science, University of São Paulo, Rua Antonio de Macedo Soares, 452, 04607-000, São Paulo/SP, Brazil, E-mail: tcvpenna@usp.br, and
[2]Molecular Probes Incorporated, 4849 Pitchford Avenue, Eugene, OR 97402

Abstract

To determine the influence of various culture conditions, transformed cells of *Escherichia coli* expressing recombinant green fluorescent protein (GFPuv) were grown in nine cultures with four variable conditions (storage of inoculated broth at 4°C prior to incubation, agitation speed, isopropyl-β-D-thiogalactopyranoside [IPTG] concentration, and induction time). The pelleted cells were resuspended in extraction buffer and subjected to the three-phase partitioning (TPP) extraction method. To determine the most appropriate purification resin, protein extracts were eluted through one of four types of HiTrap hydrophobic interaction chromatography (HIC) columns prepacked with methyl, butyl, octyl, or phenyl resins and analyzed further on a 12% sodium dodecylsulfate polyacrylamide gel. With Coomassie staining, a single band between 27 (standard GFPuv) and 29 kDa (molecular weight standard) was visualized for every HIC column sample. TPP extraction with HIC elution provided about 90% of the GFPuv recovered and eight-fold GFPuv enrichment related to the specific mass. Rotary speed and IPTG concentration showed, respectively, greater negative and positive influences on GFPuv expression at the beginning of the logarithmic phase for the set culture conditions (37°C, 24-h incubation).

*Author to whom all correspondence and reprint requests should be addressed.

Index Entries: Recombinant green fluorescent protein; GFPuv; hydrophobic interaction chromatography; sodium dodecylsulfate polyacrylamide gel electrophoresis; three-phase partitioning extraction.

Introduction

The recombinant green fluorescent protein, GFPuv, expressed by *Escherichia coli* DH5-α, exhibits fluorescence intensity 18 times greater than the wild-type GFP protein of the jellyfish *Aequorea victoria*. GFPuv is a compact, globular, acidic protein monomer (p*I* 4.6–5.4) consisting of 238 amino acids, with a mol wt between 27 and 29 kDa, that has a propensity to dimerize *(1)*. The fluorescence of GFPuv requires no cofactor, and GFPuv is a widely utilized genetic marker because it can be easily monitored in a variety of applications.

Because GFPuv exhibits stability to extreme conditions such as exposure to heat and chemical denaturants (disinfectants) in a wide pH range, its expression by prokaryotes, followed by extraction and purification, should be studied for its potential utility as a marker in validation procedures. In addition, the protein extracted from *E. coli* and further purified by hydrophobic interaction chromatography (HIC) resins should be analyzed qualitatively *(2)* by sodium dodecylsulfate polyacrylamide gel (SDS-PAGE) to define the best purification method. SDS-PAGE with Coomassie or silver staining provides a sensitive method to determine the most appropriate HIC support for the purification of GFPuv.

The aims of the present work were (1) to determine what culture conditions influence the expression of GFPuv by *E. coli*, and (2) to select the most appropriate HIC medium for the separation of three-phase partitioning (TPP)–extracted GFPuv from total cell extract by analyzing the purity of GFPuv. The HIC column was selected by using comparative qualitative analysis with SDS-PAGE and postelectrophoresis staining with either Coomassie or silver stain.

Material and Methods

Transformation of E. coli

Transformation of *Escherichia coli* DH5-α with a high copy plasmid, *pGFPuv* (Clontech Laboratories, Palo Alto, CA), was performed using the standard calcium chloride method *(3,4)*.

Experimental Design

To evaluate the effectiveness of different parameters to improve the expression of GFPuv by *E. coli*, nine culture conditions were set up using a fractional factorial (2^{4-1}) design at two levels. The varibles were as follows:

1. Effect of storing the starting culture in Luria Bertani (LB) broth (USB, Cleveland, OH) supplemented with 100 µg/mL of ampicillin (amp) (Boehringer, Mannheim, Germany) at 4°C for 24, 36, and 48 h ("storage") prior to incubation at 37°C.

Table 1
Expression of GFPuv by *E. coli*
from Nine Cultures (Groups)
Set Up Using a Factional Factorial (2^{4-1})
Design at Two Levels [a]

Culture Group	x_1	x_2	x_3	x_4
1	–	–	–	–
2	+	–	–	+
3	–	+	–	+
4	+	+	–	+
5	–	–	+	+
6	+	–	+	–
7	–	+	+	–
8	+	+	+	+
9	0	0	0	0

Independent Variables	(–)	0	(+)
x_1 Storage 4°C (h)	24	36	48
x_2 Agitation speed (rpm)	100	150	200
x_3 OD_{660}nm [b]	0.01	0.40	0.80
x_4 IPTG (m*M*) [c]	0.050	0.275	0.500

[a] The cultures were incubated at 37°C on a rotary shaker for 8 (x_5 = –1) and 24 h (x_5 = +1).
[b] The addition of IPTG at different cell densities.
[c] The final concentration of IPTG added.

2. Effect of rotary speed (100, 150, and 200 rpm).
3. Effect of the addition of isopropyl-β-D-thiogalactopyranoside (IPTG) (USB) at set cell densities (OD_{660} between 0.01 and 0.8) corresponding to cultures at 10^3–10^7 CFU/mL.
4. Concentration of IPTG with final concentrations of 0.05, 0.275, and 0.5 m*M*.
5. Incubation of the culture at 37°C for 8 and 24 h (Table 1).

Inoculum

A 24-h culture of transformed *E. coli* (LB/amp broth; 37°C, 100 rpm) was transferred onto the surface of LB/amp/IPTG agar and incubated at 37°C for 24 h. Isolated green fluorescent colonies (illuminated with a handheld long UV lamp, 360–395 nm; Model UVL 4; UVP, Upland, CA) were picked and transferred to 25 mL of LB/amp broth in 250-mL Erlenmeyer flasks (starter cultures). The starter cultures were incubated at 37°C and 100 rpm) until a cell density of 0.0054–0.026 absorbance units (10^4–10^5 CFU/mL) was obtained as measured by OD_{660} with a spectrophotometer (Beckman DU-600; Beckman Coulter, Fullerton, CA). An inoculum of

1.0 mL was transferred to each of 32 Erlenmeyer flasks (250 mL) containing 25 mL of LB/amp broth. The flasks of inoculated broth (expression cultures) were stored at 4°C prior to being incubated on a rotary shaker at 37°C (Tecnal model TE 240; SP, Brazil).

Induction by IPTG

The expression cultures were incubated at 37°C until the broth cultures attained a set OD_{660} for the addition of IPTG (Table 1). Expression cultures from corresponding flasks (two flasks/h) were assayed every hour for cell density: (1) OD_{660} with LB/amp broth in the reference cell; (2) dried biomass related to GFPuv expression (µg of GFPuv/mg of dry cell weight [DCW]); from cells retained on the surface of a 0.22-µm membrane (Millipore, SP, Brazil) and dried at 105°C for approx 24 h to attain steady weight.

Extraction of GFPuv by TPP Method (5–7)

The TPP method was applied to induced *E. coli* cultures overexpressing GFPuv. Through the TPP extraction, proteins (other than GFPuv) and other molecules were precipitated and separated from GFPuv. At the end of 24 h of incubation, the cultures were centrifuged at 1000*g* for 30 min at 4°C and the pellets resuspended in 4 mL of cold extraction buffer (XE: 25 m*M* Tris-HCl, pH 8.0, Trizma® Base [Sigma, St. Louis, MO] 1.0 m*M* β-mercaptoethanol [β-ME] [Amersham Biosciences, Uppsala, Sweden]; 0.1 m*M* phenylmethylsulfonyl fluoride [PMSF] [USB]). From every suspension in XE, each of eight 450-µL aliquots was subjected to one-step extraction by the TPP method. To each 450 µL of cell suspension, 300 µL of 4 *M* $(NH_4)_2SO_4$ (1.6 *M* final concentration) and 750 µL of *t*-butanol (ratio 1:1) were added. The mixtures were vortexed for 1.0 min and centrifuged at 6,000*g* for 10 min. The three phases formed were collected. After the *t*-butanol upper layer and the white interfacial precipitate were removed, another equal volume of *t*-butanol was mixed with the lower aqueous layer and centrifuged. The upper layer was discarded. The interfacial green layer was collected and dissolved in 1.0 mL of XE buffer. Every eight TPP-extracted aliquots from the same pellet cell culture were pooled. The final concentration of GFPuv into TPP extraction aliquots varied up to 42.60 µg of GFPuv/mL (Table 2), for a mean specific productivity of 27.39 µg of GFPuv/mg of DCW.

Purification of GFPuv Through HIC Columns

Protein extracts were eluted through HiTrap 1-mL columns, prepacked with one of four HIC resins: methyl support (Macro-Prep HIC supports; Bio-Rad, Hercules, CA); HiTrap HIC fast flow (FF) columns (Amersham Biosciences, Piscataway, NJ) butyl 4 FF; octyl 4 FF; phenyl 6 FF (low sub) sepharose. From every pelleted cell culture, 250-µL aliquots TPP extract were mixed with 250 µL of 4 *M* $(NH_4)_2SO_4$ and transferred to the top of each of the four FF support columns. The columns were previously

Table 2
Enrichment and Recovery of TPP-Extracted GFPuv Aliquots in Eluted Samples from Methyl HIC Columns[a]

TPP-extracted GFPuv aliquot[b]			Eluted samples from methyl HIC columns									
			First group					Second group				
GFPuv (μg/mL)	BSA (mg/mL)	SM (μg/mg)	GFPuv (μg/mL)	BSA (mg/mL)	SM (μg/mg)	GFPuv (times)	GFPuv (%)	GFPuv (μg/mL)	BSA (mg/mL)	SM (μg/mg)	GFPuv (times)	GFPuv (%)
1.15	4.79	0.24	1.10	0.29	3.84	16.02	95.52	1.19	0.20	5.91	24.67	103.40
1.21	0.89	1.37	1.13	0.15	7.57	5.54	92.88	1.21	0.48	2.51	1.84	99.70
2.03	1.74	1.16	1.47	0.41	3.60	3.09	72.72	1.62	0.53	3.04	2.61	80.05
3.65	3.72	0.98	3.29	0.71	4.65	4.75	90.27	3.67	0.54	6.83	6.98	100.57
5.33	0.81	6.56	4.51	0.34	13.46	2.05	84.63	5.03	0.65	7.70	1.17	94.38
6.86	0.77	8.89	6.68	0.20	33.67	3.79	97.50	6.82	0.36	18.90	2.12	99.43
8.18	1.89	4.33	8.28	0.24	35.12	8.11	101.22	8.71	0.43	20.39	4.71	106.50
10.17	3.40	2.99	9.82	0.53	18.51	6.20	96.60	10.27	0.45	22.89	7.66	100.97
11.30	2.91	3.89	10.99	0.40	27.75	7.14	97.29	10.94	0.33	33.40	8.59	96.88
12.56	0.90	13.97	14.33	0.36	40.32	2.89	108.36	12.82	0.51	24.91	1.78	102.05
15.50	5.56	2.79	11.43	0.24	46.72	16.77	73.73	11.53	0.29	39.81	14.29	74.40
17.35	1.79	9.72	18.59	0.31	59.22	6.10	107.13	11.93	0.49	24.28	2.50	68.77
19.79	4.70	4.21	15.98	0.29	55.91	13.28	72.67	15.08	0.60	25.21	5.99	76.20
20.09	3.49	5.75	20.41	0.62	32.82	5.71	101.61	16.96	0.36	47.55	8.27	84.41
20.80	4.83	4.30	16.48	0.31	52.54	12.21	79.26	15.69	0.45	34.55	8.03	75.46
21.31	2.22	9.58	22.33	0.58	38.27	3.99	99.56	17.60	0.50	35.22	3.67	82.60
22.13	7.92	2.79	17.27	0.70	24.70	8.84	74.16	17.66	0.47	37.36	13.38	75.79

(Continued on next page)

Table 2 *(Continued)*
Enrichment and Recovery of TPP-Extracted GFPuv Aliquots in Eluted Samples from Methyl HIC Columns[a]

TPP-extracted GFPuv aliquot[b]			Eluted samples from methyl HIC columns									
			First group					Second group				
GFPuv (μg/mL)	BSA (mg/mL)	SM (μg/mg)	GFPuv (μg/mL)	BSA (mg/mL)	SM (μg/mg)	GFPuv (times)	GFPuv (%)	GFPuv (μg/mL)	BSA (mg/mL)	SM (μg/mg)	GFPuv (times)	GFPuv (%)
22.14	9.53	2.32	17.86	0.27	65.88	28.36	80.67	16.26	0.53	30.40	13.09	73.45
23.76	2.49	9.55	18.83	0.36	53.00	5.55	79.25	19.58	0.32	61.89	6.48	82.43
26.66	4.43	6.02	21.36	0.49	43.64	7.25	80.13	21.18	0.56	37.77	6.28	79.43
27.07	5.70	4.75	27.06	0.28	95.82	20.17	89.96	38.83	0.45	85.45	17.99	136.25
27.83	4.32	6.44	29.52	0.35	84.87	13.18	100.78	25.67	0.24	105.86	16.43	92.24
28.51	2.07	13.80	26.35	0.48	54.35	3.94	92.43	22.72	0.42	54.58	3.96	79.69
28.82	1.99	14.47	25.53	0.55	46.12	3.19	79.74	24.68	0.67	36.96	2.55	85.67
29.26	1.34	21.86	27.30	0.37	74.74	3.42	93.31	27.15	0.44	61.75	2.82	92.81
29.81	2.41	12.35	27.01	0.32	84.48	6.84	90.64	24.01	0.39	62.10	5.03	80.56
31.49	6.16	5.11	31.17	0.38	81.39	15.91	99.00	27.95	0.36	78.66	15.38	88.75
31.90	8.23	3.88	28.90	0.44	65.78	16.97	90.57	27.59	0.47	58.76	15.16	86.49
32.85	1.62	20.25	30.31	0.37	82.80	4.09	92.27	28.01	0.35	79.81	3.94	85.27
34.13	4.28	7.97	31.66	0.55	57.33	7.19	88.12	29.14	0.60	48.66	6.10	85.36
38.34	2.85	13.47	39.46	0.74	53.33	3.96	102.92	37.28	0.39	95.39	7.08	97.23
42.60	1.56	27.39	43.97	0.37	119.72	4.37	103.23	38.83	0.54	71.95	2.63	91.16

[a] SM, Specific mass (μg of GFPuv/mg of BSA); GFPuv (%) = Recovery (%), (eluted GFPuv sample/TPP-extracted GFPuv aliquot) × 100; GFPuv (times) = Enrichment (E), (specific mass of eluted GFPuv sample/specific mass of TPP-extracted GFPuv aliquot).
[b] TPP-extracted GFPuv aliquot before HIC fast flow.

equilibrated with 2 *M* $(NH_4)_2SO_4$. After the columns were loaded, GFPuv was retained near the top of the columns by affinity binding to the HIC resin. The loaded columns were washed first with 250 µL of 1.3 *M* $(NH_4)_2SO_4$ to elute proteins other than GFPuv that bind with low affinity. GFPuv was eluted with 750 µL of buffer solution (10 m*M* Tris-HCl; 10 m*M* EDTA, pH 8.0) and stored at 4°C. The progress of GFPuv through the column was observed with a handheld UV light, as well by the analysis of the eluted material. The fluorescence intensity (excitation/emission maxima at 394/509 nm) of eluted samples was related to µg of GFPuv/mL by the standard curve (Eq. 1).

$$\mu g \text{ of GFPuv/mL} = 0.0256 \times \left(\text{fluorescence intensity}\right) + 0.8576;\ R^2 = 0.99 \qquad (1)$$

Electrophoresis (7,8)

The eluted GFPuv samples were run on a 12% SDS-PAGE gel along with samples of TPP-extracted GFPuv. The first 30 min was performed at a fixed voltage of 50 V, which was increased to 200 V for the last 40 min. The protein bands were visualized with Coomassie Brilliant Blue. The same samples were run on another 12% SDS polyacrylamide gel at a fixed voltage of 350 V (approx 1 h) and stained with silver nitrate solution, using the PhastSystem (Amersham Biosciences).

Measurement of Fluorescence Intensity

The fluorescence intensity of GFPuv was measured in the eluted samples in a spectrofluorophotometer (RF-5301 PC; Shimadzu, Kyoto, Japan), with an excitation filter of 394 nm and an emission filter of 509 nm. Known amounts of purified recombinant GFPuv (standard GFPuv; Clontech) diluted in buffer (10 m*M* Tris-HCl, pH 8.0; 1.0 m*M* βME; 0.1 m*M* PMSF) were used to generate a standard curve (Eq. 1) in order to relate the protein concentration with fluorescence intensity of the TPP-extracted/HIC-purified aliquots.

Total Protein Concentration

The total protein concentration released *(4,7)* in the eluted samples was compared relative to purified bovine serum albumin (BSA) (mol wt 66 kDa; Sigma) in buffer solution at A_{280} in a spectrophotometer and was expressed in mg of BSA/mL. The total protein concentrations in the buffer solution ranged from 100 to 1000 µg/mL with the maximum $A_{280} = 0.615$. The relationship between total proteins and BSA was made through the standard curve (µg of BSA/mL = $1727.2 \times [A_{280}] - 26.86$; $R^2 = 0.99$). The specific GFPuv mass was expressed as µg of GFPuv/mg of BSA.

Statistical Growth Variables

The effects of the culturing variables, interaction coefficients (95%), correlation matrix for estimated parameters, respective confidence inter-

Table 3
Extracted Concentrations of GFPuv and Effects of Expression Derived from *E. coli* Cells Cultivated at Set Conditions for Standard Period of 8 h ($x_5 = -1$) of Incubation at 37°C

Assay [a]	Group [b]	Storage x_1	RPM x_2	IPTG (m*M*) x_3	OD_{660} IPTG x_4	Incubation (h) x_5	DCW (mg/mL)	Concentration (µg GFPuv/mL) (mean ± CI)[c]	Specific productivity (µg GFPuv/mg DCW) (mean ± CI)[c]
1	1	-1	–1	-1	–0.99	–1	0.24	1.16 ± –0.11	4.85 ± 0.47
2	2	1	–1	1	–0.98	–1	0.43	1.42 ± 0.19	3.18 ± 0.51
3	2	1	–1	1	–0.98	–1	0.43	1.68 ± 0.22	3.91 ± 0.52
4	2	1	–1	1	–0.98	–1	0.47	1.16 ± 0.07	2.44 ± 0.16
5	3	1	1	–1	–0.98	–1	1.76	15.24 ± 3.28	9.20 ± 1.54
6	7	–1	1	–1	0.99	–1	1.68	3.98 ± 0.57	2.36 ± 0.34
7	7	–1	1	–1	0.99	–1	1.68	3.98 ± 0.57	2.36 ± 0.34

[a] The order in which the experiments were carried out.
[b] The set of conditions for every experiment carried out.
[c] $p < 0.05$; $n = 10$ observations.

vals (CIs), significance levels ($p < 0.05$) and regression variance analysis (analysis of variance [ANOVA]) *(8)* were calculated using the SGWIN program (Statgraphics Plus for Windows version 3; Statistical Graphics, Rockville, MD). The four variables (x) considered in regression analysis were taken as dimensionless values over the same (–1) to (+1) range. The maximum (+1), intermediate (0), and minimum (–1) codified ranges for each independent variable, shown in Table 1, were as follows: x_1 = storage at 4°C (24, 36, 48 h); x_2 = rotary speed (100, 150, and 200 rpm); x_3 = effect of IPTG added at set OD_{660} (0.01, 0.40, and 0.80); x_4 = final concentrations of IPTG (0.05, 0.275, and 0.5 m*M*); x_5 = incubation time at 37°C for 8 h (x_5 = –1) and 24 h (x_5 = +1). The intermediate levels in code units were given by the following equation: codified variable (x_n) = {[(effect studied) – (maximum level + minimum level)/2]/[(maximum level – minimum level)/2]}.

Results

Optimal Conditions for Expression of GFPuv During Growth of E. coli

The expression of GFPuv, which is under tight control of the *lacZ* protein β-galactosidase promoter/repressor *(1)*, was continuously induced with a concentration varying from 0.05 to 0.5 m*M* (w/v) IPTG added to the transformed *E. coli* culture at different growth phases, when no lag phase was exhibited. Independent of the growth phase for the IPTG addition, the remaining stationary phase (for 24 h of incubation) was long enough for the overexpression of GFPuv by *E. coli*. On the other hand, for 8 h of incubation, the expression of GFPuv by *E. coli* was dependent on the timing of the addition of IPTG at the beginning of the log phase (Tables 3 and 4).

The influence of the set culture conditions (variables) on the expression of GFPuv (Tables 3 and 4) was analyzed by applying a multiple linear regression to the data related to the concentrations of expressed, extracted, and purified GFPuv obtained from the induced *E. coli* cultures. ANOVA analysis outlines the results by fitting a multiple linear regression model to describe the relationship between μg of GFPuv/mL and the independent variables. Since $p < 0.01$ in the ANOVA, there is a statistically significant relationship between the variables at the 99% confidence levels. The attained quadratic polynomial model is Eq. 2:

$$\mu\text{g of GFPuv/mL} = 10.28 - 1.13x_1 - 5.65x_3 + 8.28x_5 - 1.76x_1x_5 - 5.38x_2x_5 + 1.21x_4x_5 \quad (2)$$

for the independent variables x_1 = period (h) of storage at 4°C, x_2= rotary speed (rpm), x_3 = cell densities (OD_{660}) on the addition of IPTG, x_4 = concentration of IPTG (m*M*) added, and x_5= culture incubation at 37°C set at 8 h and 24 h.

With 8 h of incubation at 37°C (x_5 = –1), the expressed GFPuv is proportional to the positive coefficient related to rotary speed (x_2 = +1) and to the negative coefficient of the culture cell density (OD_{660}, x_3 = –1) at which IPTG is added to the cultures of *E. coli*. This observation can be confirmed

Table 4
Extracted Concentrations of GFPuv and Effects of Expression Derived from *E. coli* Cells Cultivated at Set Conditions for Standard Period of 24 h (x_5 = +1) of Incubation at 37°C

Assay [a]	Group [b]	Storage x_1	RPM x_2	IPTG (m*M*) x_3	OD_{660} IPTG x_4	Incubation (h) x_5	DCW (mg/mL)	Concentration (µg GFPuv/mL) (mean ± CI)[c]	Specific productivity (µg GFPuv/mg DCW) (mean ± CI)[c]
1	1	–1	–1	–1	–0.98	1	1.98	33.54 ± 1.07	16.97 ± 0.54
2	1	–1	–1	–1	–0.99	1	2.03	30.92 ± 1.57	15.24 ± 0.77
3	2	1	–1	1	–1.00	1	2.14	25.64 ± 1.84	12.00 ± 0.86
4	2	1	–1	1	–0.99	1	2.19	29.12 ± 1.80	13.30 ± 0.82
5	3	1	1	–1	–0.99	1	2.06	14.54 ± 0.82	7.05 ± 0.40
6	3	1	1	–1	–0.99	1	2.12	16.32 ± 1.11	7.68 ± 0.52
7	4	–1	1	1	–0.99	1	2.16	22.73 ± 1.29	10.52 ± 0.60
8	4	–1	1	1	–0.98	1	1.95	23.46 ± 1.30	10.86 ± 0.56
9	5	1	–1	–1	0.12	1	2.05	19.24 ± 2.20	9.38 ± 1.08
10	5	1	–1	–1	0.31	1	2.09	21.76 ± 0.58	10.43 ± 0.28
11	5	1	–1	–1	–0.35	1	2.14	22.20 ± 1.38	10.28 ± 0.65
12	5	1	–1	–1	–0.096	1	2.16	17.32 ± 0.44	8.03 ± 0.20
13	6	–1	–1	1	–0.56	1	1.98	31.98 ± 2.02	16.19 ± 1.02
14	6	–1	–1	1	–0.53	1	2.02	30.64 ± 1.46	15.17 ± 0.73
15	6	–1	–1	1	0.37	1	2.07	24.78 ± 1.88	11.97 ± 0.91
16	7	–1	1	–1	1.00	1	2.15	11.47 ± 0.82	5.33 ± 0.38
17	7	–1	1	–1	0.69	1	2.09	9.84 ± 2.74	4.71 ± 1.31
18	7	–1	1	–1	0.73	1	2.15	7.26 ± 0.47	3.38 ± 0.22
19	8	1	1	1	0.75	1	2.22	9.57 ± 0.51	4.30 ± 0.23
20	8	1	1	1	0.026	1	2.10	9.67 ± 0.33	4.61 ± 0.23
21	9	0	0	0	0.49	1	2.41	12.76 ± 0.91	5.29 ± 0.38
22	9	0	0	0	0.13	1	2.19	20.16 ± 1.45	9.19 ± 0.66
23	9	0	0	0	0.013	1	2.31	18.71 ± 1.00	8.11 ± 0.43

[a] The order in which the experiments were carried out.
[b] The set of conditions for every experiment carried out.
[c] $p < 0.05$; $n = 10$ observations.

when storage is kept at 4°C for a maximum of 48 h ($x_1 = +1$), the final IPTG concentration added at a minimum concentration of 0.05 m*M* ($x_4 = -1$), and the GFPuv concentration is calculated through the fitted Eq. 3:

$$\mu g \text{ of GFPuv/mL} = 3.84 + 5.39x_2 - 5.65x_3 \quad (3)$$

By analyses of the extreme conditions, the highest concentration of GFPuv extracted (15.24 µg of GFPuv/mL, Table 3) related to maximum 200-rpm rotary speed ($x_2 = +1$), minimum cell densities ($OD_{660} = 0.01$, $x_3 = -1$) on the addition of IPTG; the worst condition that provided no expression of GFPuv was evident with the minimum 100-rpm rotary speed ($x_2 = -1$) with the addition of IPTG at the highest OD_{660} of 0.8 ($x_3 = +1$); and the equivalent effect on the expression of ~4 µg of GFPuv/mL was verified for both x_2 and x_3 at minimum levels (100 rpm and OD_{660} of 0.01) or at maximum levels (200 rpm and OD_{660} of 0.8).

For 24 h incubation at 37°C ($x_5 = +1$), setting the storage at 4°C to a minimum of 24 h ($x_1 = -1$) and the maximum IPTG concentration of 0.5 m*M* ($x_4 = +1$), we observe through the fitted Eq. 4:

$$\mu g \text{ GFPuv/mL} = 22.65 - 5.38x_2 - 5.65x_3 \quad (4)$$

that the influence of both negative coefficients for rotary speed ($x_2 = -1$) and cell OD_{660} density ($x_3 = -1$) on GFPuv expression resulted in the highest concentration of 33.54 µg of GFPuv/mL (Table 4) when rotary speed (100 rpm, $x_2 = -1$) and OD_{660} cell density (0.01 OD_{660}, $x_3 = -1$) were kept at minimum levels. Otherwise, at maximum levels for both variables, 200-rpm rotary speed ($x_2 = +1$) and 0.8 OD_{660} ($x_3 = +1$) cell densities for the addition of IPTG to the culture, the expression of GFPuv by *E. coli* decreased three times between 9.57 and 9.67 µg of GFPuv/mL (Table 4).

Comparing the highest expression of GFPuv by *E. coli* after incubation at 8 h ($x_5 = -1$) and 24 h ($x_5 = +1$) at 37°C, we observed that although GFPuv expression began following the addition of IPTG (maximum and minimum concentrations), the rotary speed was shown to exhibit a remarkable influence on the increase in cell density at the minimum level of 0.01 OD_{660} at the beginning of the logarithmic phase, when the newly divided cells are induced by IPTG to express GFPuv. Maximum rotary speed of 200 rpm ($x_2 = +1$) for a shorter incubation, 8 h ($x_5 = -1$), almost compensated, without success, the minimum speed at 100 rpm ($x_2 = -1$) for a longer incubation, 24 h, at 37°C ($x_5 = +1$), unless the 8 h ($x_5 = -1$) incubation provided half the concentration of GFPuv obtained for 24 h of incubation.

Another remarkable positive effect on GFPuv expression was the storage of the starter culture at 4°C for 24 ($x_1 = -1$) and 48 h ($x_1 = +1$). Expression of the highest concentrations of GFPuv was shown to be independent of the time in storage.

Separation Efficiency of HIC on GFPuv Purification

The selected HIC supports present similar hydrophobic characteristics, appropriate for purification of intermediate to weakly hydrophobic

Fig. 1. Polyacrylamide gel run by SDS-PAGE. Protein was stained with Coomassie Brilliant Blue. The eluted samples from HIC columns applied to the wells were as follows: lane 1, mass molecular weight markers 18–200 kDa (Gibco); lane 2, standard GFPuv (20 µg/mL); lane 3, sample eluted from methyl column (0.32 µg); lane 4, sample eluted from butyl column (0.30 µg); lane 5, sample eluted from octyl column (0.29 µg); lane 6, sample eluted from phenyl cloumn (0.26 µg).

proteins *(9)*. The selection of these various resins allowed screening of the most appropriate HIC support for the purification of the TPP-extracted GFPuv from a complex mixture of proteins typically found in cell extracts. HIC is ideally suitable after salt precipitation of the TPP-extracted GFPuv from the pelleted cells, since HIC uses a decreasing salt gradient as the mobile phase, preserving the conformation of GFPuv and, hence, its fluorescence *(2,6,9)*.

TPP-extracted GFPuv from pelleted cells of *E. coli* was eluted through four HiTrap FF HIC columns: methyl, butyl, octyl, phenyl Sepharose. The fluorescence intensity (excitation/emission maxima at 394/509 nm) of eluted samples was related to µg of GFPuv/mL, and then the same samples were run on a 12% SDS-PAGE gel (Figs. 1 and 2).

A single band between 27 (standard GFPuv) and 29 kDa (standard molecular weight) for every HIC column sample (Fig. 1) was visualized by Coomassie staining. As seen in every lane in Fig. 1, the gels proved the effectiveness of TPP extraction for GFPuv, and the bands observed were similar for every sample eluted through a column. With SDS-PAGE, it was not possible to distinguish which HIC column improved the purity of the extracted GFPuv. However, using the more sensitive silver staining, the butyl HIC eluted samples showed some bands >29 kDa (Fig. 2).

Table 5 shows that the amount of BSA eluted with GFPuv from the methyl and butyl HIC columns was half that recovered in the samples eluted from the octyl and phenyl columns, for a range of respective mean concentrations of GFPuv from 27.92 (methyl column) to 28.66 µg/mL (phenyl support), corresponding to a total average of 28.25 ± 0.36 µg of GFPuv/mL.

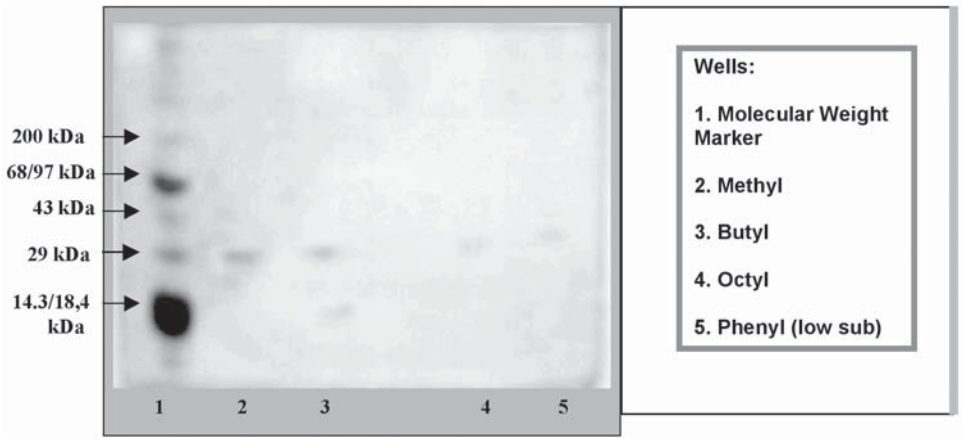

Fig. 2. Polyacrylamide gel run by SDS-PAGE (PhastSystem). Protein was stained with silver nitrate. Gel visualization was altered by nitrate oxidation. The eluted samples from HIC columns applied to the wells were as follows: lane 1, mass molecular weight markers, 18–200 kDa (Gibco); lane 2, sample eluted from methyl column (0.085 µg); lane 3, sample eluted from butyl column (0.080 µg); lane 4, sample eluted from octyl column (0.077 µg); lane 5, sample eluted from phenyl column (0.069 µg).

Table 5
Protein Concentration in Eluted Samples
from HIC Columns Expressed in Terms of GFPuv (µg GFPuv/mL),
BSA (mg BSA/mL), and Specific Mass (µg GFPuv/mg BSA)[a]

		Eluted Samples				
HIC Column		1	2	3	4	5
Methyl						
	GFPuv (µg/mL)	28.33	27.13	26.58	28.27	29.31
	BSA (mg/mL)	1.65	0.45	0.49	0.20	0.37
	SM (µg/mg)	17.12	59.98	54.60	138.35	78.95
Butyl						
	GFPuv (µg/mL)	27.72	23.78	29.89	29.06	31.85
	BSA (mg/mL)	0.87	0.25	0.33	0.26	1.09
	SM (µg/mg)	31.85	96.00	90.30	110.69	29.12
Octyl						
	GFPuv (µg/mL)	27.56	25.37	29.05	29.62	28.27
	BSA (mg/mL)	2.63	0.27	1.01	0.60	0.43
	SM (µg/mg)	10.50	95.52	28.78	49.00	65.34
Phenyl						
	GFPuv (µg/mL)	22.92	25.93	30.50	31.07	32.88
	BSA (mg/mL)	3.18	0.39	0.76	1.05	0.44
	SM (µg/mg)	7.22	65.87	40.05	29.46	74.01

[a]The range of GFPuv concentration analyzed was about 20–30 µg/mL. SM, specific mass.

The same HIC column was used five times with five different samples from the same TPP-extracted 4-mL aliquot. The GFPuv concentration, eluted from the four columns and from five runs through each of the columns, was shown to be equivalent for all four HIC supports. In relation to the removal of BSA from the eluted sample, for the first, second and third runs, the butyl column provided the higher specific masses; for the fourth and fifth runs the methyl support increased the specific mass up to 138.35–78.95 μg of GFPuv/mg of BSA. The use of the same HIC columns after five elutions of the TPP-extracted aliquot did not interfere with the evaluation of their performance.

For further work, the methyl HIC column was chosen for the purification of the TPP-extracted GFPuv samples. GFPuv recovery and enrichment from the eluted samples were also determined (Table 2).

Enrichment and Recovery of GFPuv in Eluted Samples from Methyl Columns

The number of hydrophobic groups covering the surface of the methyl matrix is higher than the other matrices, resulting in a higher capacity for protein retention. Although the protein may contain a large percentage of hydrophobic residues throughout its structure, only residues at the surface contribute to the hydrophobic character of the native protein.

The purification efficiency of GFPuv eluted from the methyl HIC columns was evaluated through (1) the enrichment (E, times) and (2) recovery (%) indices *(7,9)*:

Enrichment (E):

$$\text{Enrichment} = \frac{\text{Specific mass of eluted purified GFPuv sample}}{\text{Specific mass of TPP-extracted GFPuv aliquot}} \quad (5)$$

The enrichment index measures the level of purity of the GFPuv samples by the increase in specific mass (μg of GFPuv/mg of BSA) owing to the removal of proteins (quantified as BSA) other than GFPuv *(5,8)*. Enrichment is expressed in terms of number of times (E) the specific mass of the eluted purified GFPuv sample (μg of GFPuv/mg of BSA) is greater than the corresponding specific mass of the TPP-extracted GFPuv aliquot (μg of GFPuv/mg of BSA) before HIC, by the reduction of BSA concentration and maintaining the initial concentration of GFPuv.

Recovery (%):

$$\text{Recovery} = \frac{\text{Eluted GFPuv sample (μg of GFPuv/mL)}}{{}^{1}\text{TPP-extracted GFPuv aliquot}} \quad (6)$$

in which, ^{1} is a 1-mL aliquot of TPP-extracted GFPuv loaded onto the HIC column. The recovery index measures the percentage (%) of the amount of TPP-extracted GFPuv that was present in the purified GFPuv sample after passage through the HIC columns.

Each TPP-extracted aliquot was divided into two samples that were independently loaded onto the methyl support (Table 2), providing a total

of 64 eluted samples in duplication: the first group of 32 samples plus the second group of 32 samples.

The recovery index varied from 72.67 to 107.13%, and the methyl support showed a very high efficiency in the recovery of GFPuv. From 64 assays, seven samples of the first group and seven samples of the second group presented recovery of GFPuv between 70 and 80%. The majority of the samples (about 78%) showed a recovery index >80% of GFPuv in the eluted samples. Therefore, the range for GFPuv recovery index from the eluted samples was from 90.88 ± 3.62% for the first group to 89.32 ± 4.60% for the second group. Even for samples with concentrations lower than 10 μg of GFPuv/mL (from 1.15 to 8.18 μg of GFPuv/mL, in seven TPP-extracted aliquots), the recovery was confirmed to be higher than 80%.

The enrichment index varied from (1) 1.17 – 2.05 times for a 5.33 μg of GFPuv/mL aliquot corresponding to (2) 24.67 – 28.36 times for 1.15 and 22.14 μg of GFPuv/mL TPP-extracted aliquots, respectively. The specific mass of each 25 eluted samples of the first plus the second groups was enriched up to 9.5-fold. Otherwise, a total of 12 eluted samples belonging to the first group (6 samples) and the second group (6 samples) provided GFPuv enrichment between 10- and 20-fold, and one sample of each group showed 28- and 24-fold enrichment, respectively. Therefore, the average index of enrichment provided by the methyl HIC support over TPP-extracted aliquots ranged from an 8.46 ± 2.13 increase (first group) to a 7.60 ± 2.00 increase (second group). Taking into consideration the total proteins in the samples, expressed in mg of BSA/mL, three and four eluted samples of the first and second groups, respectively, contained concentrations >0.5 mg of BSA/mL, and three samples of the first group had up to 0.7 mg of BSA/mL, independent of the initial specific mass of the TPP aliquot eluted through the methyl HIC medium.

Discussion

The present work verified that the influence of the range of IPTG, from 0.05 to 0.5 m*M*, added to the cultures was independent of cell density (OD_{660} between 0.01 and 0.8); however, the induction timing and the addition of IPTG at the beginning of exponential phase of growth favored the expression of GFPuv by *E. coli*. Shi and Su *(10)* examined the highest IPTG concentration and optimal induction time on the expression of GFP on the extracellular surface of *E. coli* JMIO9 (pUMC101) cells. They verified that the timing of induction showed a significant effect on cell growth when the culture was induced at a density lower than OD_{660} <1.0 for concentrations >0.05 m*M* IPTG.

The effectiveness of the TPP extraction of GFPuv from *E. coli* was analyzed by electrophoresis and confirmed to be the same in every lane for samples eluted from all HIC columns. The performance of the HIC columns was not affected after five elutions per column.

The enrichment in GFPuv in the eluted samples was dependent on the amount of total proteins (expressed in mg of BSA/mL). After elution

through the methyl HIC columns, the recovery and enrichment of GFPuv in the eluted samples exhibited very high indices, about 90.10 ± 4.11% of GFPuv recovery and 8.03 ± 2.07-fold enrichment of GFPuv related to the specific mass. Therefore, the HIC procedure did improve the effectiveness of TPP extraction on GFPuv purification, confirming Sharma and Gupta's *(6)* and Yakhnin et al.'s *(11)* observations.

Acknowledgments

We thank our personal assistants for providing technical support for biologist Irene A. Machoshvili. This work was made possible by financial support provided by the Brazilian Committees for Scientific Technology Research (Conselho Nacional de Desenvolvimento Científico e Tecnológico and Fundação de Amparo à Pesquisa do Estado de São Paulo).

References

1. Chalfie, M. and Kain, S. (1998), in *Green Fluorescent Protein Properties: Applications and Protocols*. Chalfie, M. and Kain, S. , eds., Wiley-Liss, New York, NY, pp. 3–75.
2. Wheelwright, S. M. (1991), *Protein Purification, Design and Scale Up of Downstream Processing*. Wheelwright, S. M., ed., John Wiley & Sons, New York, NY, pp. 154–162.
3. Sambrook, J., Fritsch, E. F., and Maniatis, T. (1989), in *Molecular Cloning: A Laboratory Manual*. 2nd Ed., Nolan, C., ed., Cold Spring Harbor Laboratory, Cold Spring Harbor, New York, pp. 1.74–1.84.
4. Vessoni Penna, T. C., Chiarini, E., Machoshvili, I. A., Ishii, M., and Pessoa Jr., A. (2002), *Appl. Biochem. Biotechnol.* **98–100**, 791–802.
5. Denninson, C., and Lovrien, R. (1997), *Protein Expr. Purif.* **11,** 149–161.
6. Sharma, A. and Gupta, M. N. (2001), *Process Biochem.* **37,** 193–196.
7. Vessoni Penna, T. C., Chiarini, E., and Pessoa Jr., A. (2003), *Appl. Biochem. Biotechnol.* **105–108,** 481–491.
8. Drapper, N. and Smith, H. (1981), *Applied Regression Analysis*. John Wiley, New York, NY.
9. Scopes, R. K. (1993), in *Protein Purification: Principles and Practice*. 3rd Ed., Cantor, C. R., ed., Springer-Verlag, New York, NY, pp. 39–89,324–325.
10. Shi, H. and Su, W. W. (2001), *Enzyme Microb. Technol.* **28,** 25–34.
11. Yakhnin, A. V., Vinokurov, L. M., Surin, A. K., and Alalhov, Y. B. (1998), *Protein Expr. Purif.* **14,** 382–386.

0273-2289/04/114/0469–0483/$25.00

Thermal Stability of Recombinant Green Fluorescent Protein (GFPuv) at Various pH Values

Thereza Christina Vessoni Penna,[*,1] Marina Ishii,[1] Adalberto Pessoa Junior,[1] and Olivia Cholewa[2]

[1]Department of Biochemical and Pharmaceutical Technology, School of Pharmaceutical Science, University of São Paulo, Rua Antonio de Macedo Soares, 452, 04607-000, São Paulo/SP, Brazil, E-mail: tcvpenna@usp.br; and [2]Molecular Probes Incorporated, 4849 Pitchford Avenue, Eugene, OR 97402

Abstract

The thermal stability of the recombinant green fluorescent protein (GFPuv) expressed by *Escherichia coli* cells and isolated by three-phase partitioning extraction with hydrophobic interaction chromatography was studied. The GFPuv (3.5–9.0 μg of GFPuv/mL) was exposed to various pH conditions (4.91–9.03) and temperatures (75–95°C) in the 10 m*M* buffers: acetate (pH 5.0–7.0), phosphate (pH 5.5–8.0), and Tris-HCl (pH 7.0–9.0). The extent of protein denaturation (loss of fluorescence intensity) was expressed in decimal reduction time (*D*-value), the time exposure required to reduce 90% of the initial fluorescence intensity of GFPuv. For pH 7.0 to 8.0, the thermostability of GFPuv was slightly greater in phosphate buffer than in Tris-HCl. At 85°C, the *D*-values (pH 7.1–7.5) ranged from 7.24 (Tris-HCl) to 13.88 min (phosphate). The stability of GFPuv in Tris-HCl (pH > 8.0) was constant at 90 and 95°C, and the *D*-values were 7.93 (pH 8.38–8.92) and 6.0 min (pH 8.05–8.97), respectively. The thermostability of GFPuv provides the basis for its potential utility as a fluorescent biologic indicator to assay the efficacy of moist-heat treatments at temperatures lower than 100°C.

Index Entries: Green fluorescent protein; thermal stability; decimal reduction time; three-phase partitioning; fluorescence intensity; acetate; phosphate.

*Author to whom all correspondence and reprint requests should be addressed.

Introduction

The biotechnological application of proteins to monitor the preservation of manufactured and processed products has expanded rapidly. Moist-heat treatments using steam at low temperatures ($T \leq 100°C$; pasteurization, blanching, and disinfection) have been applied to food and pharmaceuticals to hinder microbial growth and inactivate endogenous enzymes to preserve and expand product shelf life. Moist-heat disinfection is also utilized for the preservation of low-acid products (pH > 4.5) such as milk and other dairy products. Blanching efficiency is evaluated through the enzyme activity of the most thermostable enzyme present in the product and this enzyme is usually selected and employed as the biologic indicator (BI) to evaluate the immediate efficacy of thermal procedures, as well as to ensure the satisfactory preservation and shelf life of the product. These endogenous thermostable enzymes have been observed to exhibit greater thermal resistance than intact bacteria and yeast cells present in the product.

The high thermostability of lysozyme, an antimicrobial enzyme with considerable potential as a natural food preservative in vegetables, fresh fruits, seafood, and wine, makes it attractive for use in pasteurization processes, reducing nutritional and esthetic quality loss *(1)*. Alkaline phosphatase, lactoperoxidase, and other enzymes have been used for many years as an index of adequate pasteurization of milk *(2)*. Pasteurization associated with the blanching processing of fruit juices is necessary to prevent microbiologic spoilage and to inactivate endogenous enzymes *(3)*. The pectinesterases are an example of endogenous enzymes that also have an important influence on the quality and stability of processed products *(4)*. The dependence of the conditions of the protein inactivation thermal process (time and temperature) varies with pH *(5)* and the heating medium.

Because of the importance of validating the moist-heat treatments and related processes, it is necessary to develop a BI that can efficiently assess the success of the treatment. The use of a fluorescent marker designed for a quick and reliable assay, detectable by microscopy, spectrofluorometry, or a handheld UV lamp, is examined herein. GFPuv provides the basis for its potential utility as a fluorescent BI, to monitor moist-heat treatments ($T < 100°C$). GFPuv is a compact, globular acidic protein (p*I* 4.6–5.4) with one fluorophore consisting of a cyclic tripeptide in the primary protein sequence, a chain of 238 amino acids. It has been shown to be resistant to heat ($T > 70°C$) and alkaline pH (between 5.5 and 12.0; optimum = 8.0).

The term *thermal stability* (also *thermostability*) refers to the resistance of a protein to adverse intrinsic and extrinsic environmental influences, i.e., the thermal characteristic of the protein to remain steady against the denaturation of its molecular integrity and inactivation of its biologic activity on facing high temperatures or other deleterious agents *(6)*. One of the most important indices to measure protein stability is the decimal reduction time, or *D*-value, the time required to reduce 90% of the initial protein concentration exposed to the reference temperature. The *D*-value was used

as the main kinetic parameter to compare the influence of environmental conditions on the thermal behavior of GFPuv.

The purpose of the present work was to determine the thermal stability of the three-phase partitioning (TPP)–extracted recombinant protein, GFPuv, in different buffers, as well as to verify its utility as a quick, accurate, and economical BI for moist-heat treatments ($T < 100°C$) in different pH conditions.

Materials and Methods

Transformation and Expression

Escherichia coli DH5-α cells *(7)* transformed (pGFPuv; Clontech, Palo Alto, CA) by the standard calcium chloride method *(8,9)* to express GFPuv (excitation/emission maxima at 394 /509 nm) were grown (37°C, 100 rpm) in Luria-Bertani broth (USB, Cleveland, OH) supplemented with 100 µg/mL of ampicillin (amp) (Boehringer, Mannheim, Germany) until the broth culture attained $OD_{660} = 0.8$ (10^7 CFU/mL). Isopropyl-β-D-thiogalactopyranoside (USB) was then added to a final concentration of 0.5 m*M*. After 24 h of incubation, brightly green fluorescent cells were harvested by centrifugating at 6.000*g* for 30 min at 4°C. The supernatant was decanted and the cell pellet was resuspended in 4 mL of chilled (4°C) extraction buffer XE (25.0 m*M* Tris-HCl, pH 8.0; 1.0 m*M* β-mercaptoethanol [Pharmacia Biotech, Uppsala, Sweden]; 0.1 m*M* phenylmethylsulfonyl fluoride, [USB]) prior to subjecting the cells to the TPP extraction method.

TPP Extraction Method (10,11) *and Hydrophobic Interaction Chromatography Column Purification*

In a 2-mL microcentrifuge tube, to each 450-µL aliquot of resuspended cells, 300 µL of 4 *M* $(NH_4)_2SO_4$ and 750 µL of *t*-butanol were added. The mixture was stirred for 2 min at 25°C, centrifuged, and then the three phases formed were collected separately. The upper phase of *t*-butanol and the white interfacial precipitate were removed and discarded. A second aliquot of 750 µL of *t*-butanol was mixed into the lower aqueous phase. The mixture was allowed to settle to visible phase separation and centrifuged. At the separation of the three phases, the upper phase was discarded. The interfacial green phase was collected and dissolved in 500 µL of XE. While the lower phase was still fluorescent, it was subjected to repeated TPP extraction. A 1.0-mL aliquot of protein extract was mixed with 1.0 mL of 4 *M* $(NH_4)_2SO_4$, and this mixture was transferred to the top of a methyl support hydrophobic interaction chromatography (HIC) column, fast flow, for final purification. The HIC column was previously equilibrated with 2 *M* $(NH_4)_2SO_4$. The loaded column was first washed with 250 µL of 1.3 *M* $(NH_4)_2SO_4$ to elute proteins that bind with low affinity to the methylated resin of the column packing. GFPuv was eluted with 1.0 mL of buffer solution (10 m*M* Tris-HCl; 10 m*M* EDTA, pH 8.0) and stored at 4°C.

Measurement of Fluorescence Intensity

The fluorescence intensity (±0.005) of GFPuv was measured in the eluted samples in a spectrofluorometer (excitation/emission maxima, 394/509-nm filters, RF 5301 PC; Shimadzu, Kyoto, Japan). Purified recombinant GFPuv (standard GFPuv; Clontech) was used to generate a standard curve to determine TPP-extracted GFPuv concentration and provide an experimental comparison for thermal stability. The fluorescence intensity (*I*) of the TPP-extracted samples was compared with the standard calibration curve Eq. 1:

$$I = -33.078 + 38.943 \times (\text{GFPuv } \mu\text{g/mL})$$
$$R^2 = 0.997 \quad (1)$$

To determine the concentration of the TPP-extracted GFPuv, fluorescence intensity was correlated to the concentration of native GFPuv, since denatured GFPuv cannot fluoresce, and the loss in fluorescence intensity was a measure of denatured GFPuv concentration.

Moist-Heat Treatment of Extracted GFPuv Under Different pH Conditions

Samples of purified GFPuv were exposed (24 h, 4°C) to different pH conditions (5.0 ± 0.2 to 9.0 ± 0.2) in 10 m*M* buffer solutions before heating: (1) acetate (pH 5.0–7.0), (2) phosphate (pH 5.5–8.0), and (3) Tris-HCl (pH 7.0–9.0). To each 3900 µL of buffer solution, 100 µL of TPP-extracted sample (at an initial concentration of about 420 µg of GFPuv/mL) was added. The mixture (4000 µL) was stored at 4°C overnight and centrifuged (6000*g* for 30 min). Precipitation was not observed. The pH values of the buffer solutions were also measured and correlated with the correspondent µg of GFPuv/mL by the standard calibration curve (Eq. 1). A pHmeter AR-20 (Fisher) was previously adjusted with standard buffers (Synth, Saõ Paulo, Brazil) of known pH values: 4.0, 7.0 and 9.0. One-milliliter samples were transferred to quartz cuvets ([3 × 10 mm] light path length × 45 mm height) and sealed with plastic covers. Each cuvet was inserted into the adapter assembly and adjusted in the cell holder. The cell holder was connected to a constant-temperature bath and the circulating water stabilized at the assay temperature. A constant-temperature water-circulating device (Thermo-bath TB-85 P/N 200-65022; Shimadzu), was used to heat and control the temperature of the cell holder. The temperature of the water bath was maintained within ±0.05°C and provided constant temperature by continuous circulation of water from the water bath to the cell holder and the sample in the cuvet via a circulation pump. From the moment the sample-filled cuvets were placed in the cell holder and the heat treatment was initiated, a fluorescence reading was taken at defined exposure intervals at different temperatures (75, 80, 85, 90, and 95°C). The variation in fluorescence intensity (±0.005) was measured by

a spectro-fluorometer every 20 s and converted to native GFPuv concentrations by the standard calibration curve (Eq. 1).

Analysis of Thermal Kinetic Parameters

The GFPuv inactivation curves were considered first-order models represented by

$$\mathrm{Log}_{10} C_f = \mathrm{Log}_{10} C_0 - (1/D) \times t = \mathrm{Log}_{10} C_0 - (k/2.303) \times t \quad (2)$$

in which C_0 is the initial concentration of native GFPuv (from 3.5 to 9.0 µg of GFPuv/mL); and C_f is the final concentration of GFPuv (from 1.00 to 1.55 µg of GFPuv/mL), after exposure to heating time (t, min), D-value (h or min), and inactivation rate constant (k, h^{-1}, min^{-1}). The D-value, the interval of time required to reduce one decimal logarithm of the initial fluorescence intensity of GFPuv at reference temperature, was determined from the negative reciprocal of the slopes of the regression lines, using the linear portions of the inactivation curves (Log_{10} µg of GFPuv/mL vs time of exposure at a constant temperature). The temperature coefficient, Q_{10}, was calculated to evaluate the dependence of the D-value on an increase of 10°C in the heating temperature (T, °C), by the following relation:

$$Q_{10} = \left| D_T / D_{(T+10)} \right| = \left(10^{10/z} \right) \quad (3)$$

The z-value, expressed as the number of degrees (°C) required for one Log_{10} change in the D-value (D = 2.303/k), was determined by plotting the relation between Log_{10} D-value and corresponding temperatures. The z-value may be related to the coefficient Q_{10} of the process by $Q_{10} = (10^{10/z})$. Activation energy (E_a, kcal/mol) was estimated by using the Arrhenius equation, which was applied to evaluate the dependence of the inactivation rate constant, k, on the heating temperature:

$$\mathrm{Log}_{10} k_1 = \mathrm{Log}_{10} k_2 - \left\{ \left(E_a / 2.303 \times R \right) \left[\left(1/T_1 \right) - \left(1/T_2 \right) \right] \right\} \quad (4)$$

in which T_1 and T_2 are the heating temperatures in degrees Kelvin (K), and R is the universal gas constant (1.987 calories × mol^{-1} K^{-1}).

Results

Stability in Buffers

GFPuv, expressed by *E. coli*, isolated by the TPP-extraction method and eluted from a methyl HIC column (extracted GFPuv), was diluted in buffers and stored at 4°C to stabilize the solution pH values before heating. After 24 h at 4°C, the concentration of GFPuv varied in accordance with buffer solution and respective pH values. In acetate buffer, the lower GFPuv concentration ranged from 1.34 to 5.87 µg of GFPuv/mL at pH between 4.91 and 5.72, and the higher GFPuv concentration ranged from 6.20 to 9.20 µg of GFPuv/mL at pH between 6.13 and 7.03. In phosphate buffer, the lower GFPuv concentration ranged from 4.89 to 5.96 µg of GFPuv/mL at pH

between 5.67 and 5.97, and the higher GFPuv concentration ranged from 5.31 to 9.08 μg of GFPuv/mL at pH between 6.19 and 8.00. In Tris-HCl buffer, the GFPuv concentration ranged from 5.52 to 9.33 μg of GFPuv/mL at pH between 6.67 and 9.03. The greater loss of fluorescence intensity for GFPuv in acetate buffer was about 74% at pH 4.92, lowering the loss to 49% at pH 5.32, decreasing to 10% of loss at pH 5.66 and to 2.0% at pH > 6.0. The stability of fluorescence intensity was verified for GFPuv in phosphate and Tris-HCl buffers at pH ≥ 6.40, and the maximum losses of fluorescence intensity in both buffers occurred at about 15.0 ± 5.0%. The effect of pH on the standard and TPP-extracted/purified GFPuv was previously studied and confirmed that a quite good, stable fluorescence intensity for GFPuv was characterized in the pH range of 6.0–9.8, declining abruptly between pH 5.5 and 4.5, with a minimum fluorescence intensity at pH < 4.5 *(9)*. Bokman and Ward *(12)* verified that native GFPuv maintains stable fluorescence in the pH range of 5.5–12.0; however, fluorescence intensity decreases between pH 5.5 and 4.4 and drops sharply above 12.0.

Thermal Treatments

The variation in fluorescence intensity was measured by a spectrofluorometer and converted to the concentration of native GFPuv. After heating and repeated exposure to light during the assay, the GFPuv samples were stored for 24 h at 4°C, and fluorescence intensity was again measured and compared to final heat-treatment intensity. No increase in fluorescence inten-sity was observed that may be related to the recovery of the native conformation of the protein. Postheating, the pH did not change and the samples remained clear, without any protein precipitating out of the solution.

D-*Value*

The denaturation of GFPuv in buffer solutions at various pH values was measured by the loss of fluorescence intensity and expressed in the decimal logarithm of the decrease in native GFPuv concentration vs the time of exposure at constant temperature (Fig. 1). To estimate *D*-values at constant heating temperatures and pH values (Table 1), the interval of GFPuv concentrations considered was between 3.5 (acetate, pH 5.18) and 9.0 μg/mL (Tris, pH > 8.0, for initial concentration [C_o]) and ranged from 1.00 to 1.55 μg/mL for final concentration (C_f), which corresponded to the linear portion of the inactivation curves (Log_{10} μg of GFPuv/mL vs time of exposure at a constant temperature and pH value; Fig. 1).

Fig. 1. *(opposite page)* Inactivation curves for GFPuv in **(A)** acetate buffer at pH 6.0, **(B)** phosphate buffer at 85°C and different pH values, **(C)**Tris-HCl at pH 8.5. The *D*-values were determined from the reciprocal of the slope of the linear portion of the GFPuv inactivation curves, considered first-order models.

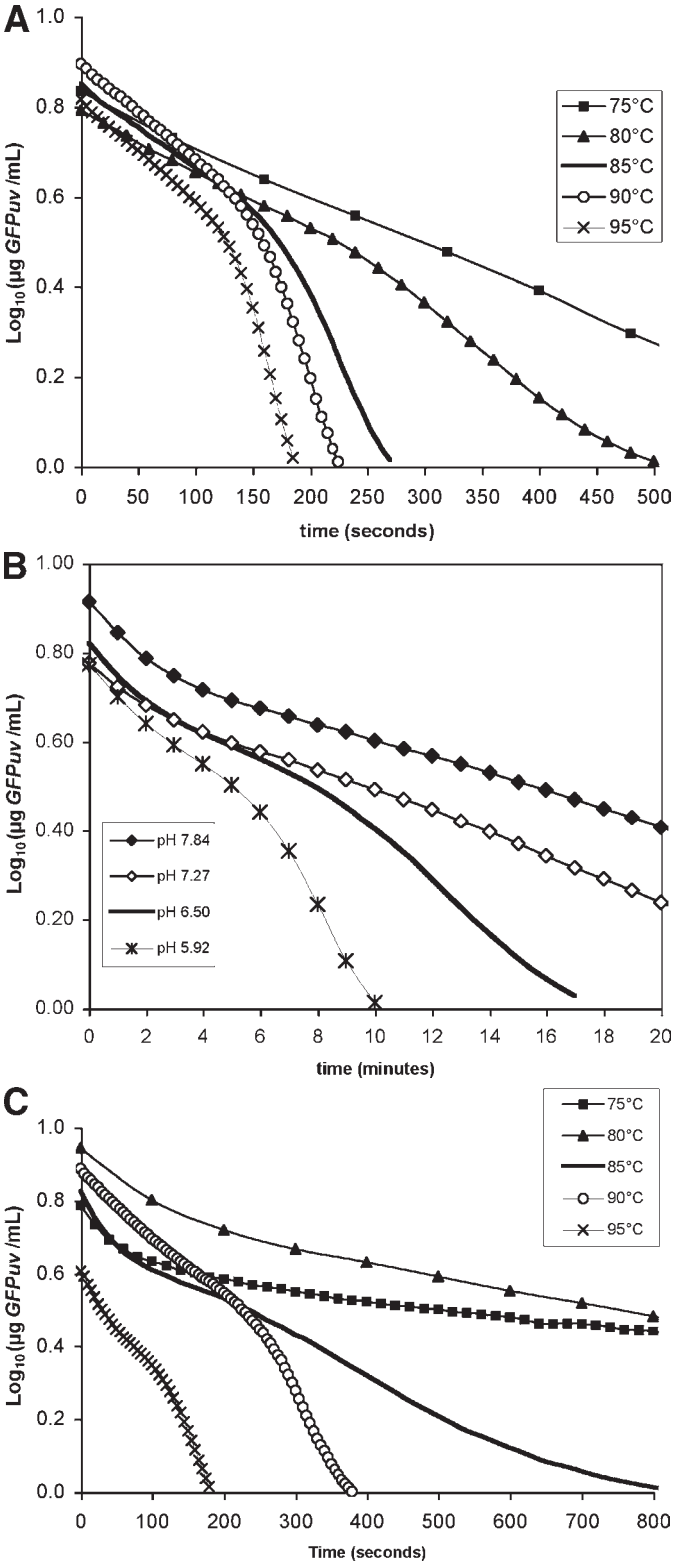
A
1.0
0.8
0.6
0.4
0.2
0.0
Log10 (µg GFPuv /mL)
0 50 100 150 200 250 300 350 400 450 500
time (seconds)
75°C
80°C
85°C
90°C
95°C
B
1.00
0.80
0.60
0.40
0.20
0.00
Log10 (µg GFPuv /mL)
0 2 4 6 8 10 12 14 16 18 20
time (minutes)
pH 7.84
pH 7.27
pH 6.50
pH 5.92
C
1.0
0.8
0.6
0.4
0.2
0.0
Log10 (µg GFPuv /mL)
0 100 200 300 400 500 600 700 800
Time (seconds)
75°C
80°C
85°C
90°C
95°C

Table 1
D-values at Reference Temperatures and pH Intervals[a]

Temperature (°C)	Buffer solution (10 m*M*)	*D*-value (min)[b]							
		5.0–5.5	5.6–6.0	6.1–6.5	6.6–7.0	7.1–7.5	7.6–8.0	8.1–8.5	8.6–9.0
75	Acetate	7.60 ± 2.39	7.93 ± 2.40	21.40 ± 7.13	41.60 ± 0.48				
	Phosphate		12.89 ± 1.12	11.54 ± 3.94	58.33 ± 28.29	76.38 ± 13.61	104.16 ± 40.83		
	Tris-HCl				25.7 ± 22.04	30.52 ± 3.19	69.44 ± 15.72	125.00 ± 47.15	52.08 ± 35.36
80	Acetate	5.74 ± 1.12	7.24 ± 1.20	10.14 ± 1.50	17.95 ± 3.23	20.80 ± 2.20			
	Phosphate			9.72 ± 0.55	23.80 ± 0.62	55.55 ± 0.73	84.15 ± 0.96		
	Tris-HCl					23.83 ± 0.75		55.55 ± 0.64	55.55 ± 0.42
85	Acetate	3.71 ± 0.80	4.76 ± 0.15	5.55 ± 0.23	7.09 ± 0.17	8.33 ± 0.10			
	Phosphate		4.38 ± 0.36	6.40 ± 0.96	13.88 ± 0.15	13.88 ± 0.05	17.67 ± 1.65		
	Tris-HCl					7.24 ± 1.20	10.57 ± 1.50	18.51 ± 1.10	27.75 ± 0.06
90	Acetate	3.26 ± 0.80	3.96 ± 0.45	4.62 ± 0.10	5.13 ± 0.08	5.05 ± 0.13			
	Phosphate			4.38 ± 0.09	5.74 ± 0.07	6.66 ± 0.05	6.94 ± 0.09		
	Tris-HCl					3.56 ± 0.73	4.91 ± 0.16	6.25 ± 1.29	5.5 ± 2.62
95	Acetate	3.74 ± 0.58	4.06 ± 0.47	4.38 ± 0.32	4.70 ± 0.23	4.9 ± 0.26			
	Phosphate		3.78 ± 0.05	4.44 ± 0.07	5.96 ± 0.24	5.95 ± 0.33	6.08 ± 0.38	5.42 ± 0.06	
	Tris-HCl			2.92 ± 0.72		2.46 ± 0.69	3.35 ± 0.79	5.17 ± 2.51	5.48 ± 2.05

[a] $n = 10$ observations; $p < 0.05$.
[b] ($D \pm$ CI) min.

At 90°C and 95°C, a slight drop in fluorescence intensity was observed (Fig. 1) without interfering with the determination of *D*-value. For lower temperatures, the loss of fluorescence intensity decreased gradually. For the same temperatures, the thermal stability of GFPuv was observed to gradually increase proportionally with pH and was shown to be dependent on the buffer used.

At 75°C, the mean *D*-values for GFPuv attained their maximum in acetate at pH 6.6–7.0 (D = 41.60 min), doubled in phosphate at pH 7.6–8.0 (D = 104.16 min), and increased threefold in Tris-HCl at pH 8.1–8.5 (D = 125.00 min). The phosphate buffer system was shown to provide greater thermal stability to the protein between pH 6.6 and 8.0. However, at pH 6.1–6.5, the *D*-values for GFPuv in acetate were double those for GFPuv in phosphate, and at 6.6–7.0 the thermal behavior of GFPuv was equivalent for both buffers.

At 80 and 85°C, respectively, the *D*-values for GFPuv in acetate (D = 20.80 and 8.33 min) and in Tris-HCl (D = 23.83 and 7.24 min) at pH 7.1–7.5 were very close and half the *D*-values (D = 55.55 and 13.88 min) observed in phosphate. Therefore, the phosphate buffer provided the optimal buffering system to maintain the thermal GFPuv stability in an important range of pH 6.0–8.0. At ≥85°C, *D*-values dropped at least twice for every buffer system. The *D*-values were similar for GFPuv in phosphate and acetate buffers at 90–95°C, pH 5.5–7.0. The thermal stability of GFPuv was the highest in the phosphate buffer at pH 7.6–8.0 and Tris-HCl at pH > 8.0. At pH 7.6–8.0 in phosphate and pH > 8.0 in Tris-HCl buffer, the highest thermal stability of GFPuv was shown to be equivalently maintained.

Correlation of D*-Value with pH and Buffer Systems*

A good stability of the GFPuv molecule was observed *(9)* to start at pH about 5.0–5.2. This corresponds to our findings on the minimum thermal GFPuv stability that was shown at pH 4.91, referent to acetate buffer and treatment at 85°C, very close to the p*I* of the protein, which was verified *(13)* between pH 4.7 and 5.1, corresponding to our finding on GFPuv extraction efficiency.

The fluorescence intensity of GFPuv demonstrated thermal stability at pH > 6.0. However, at pH 8.5–9.0, the fluorescence intensity was variable at 75°C in Tris-HCl and was kept constant for the higher temperatures, considering the same buffer system. Therefore, the range of pH for different buffers and treatments was linear correlated to *D*-values, which proportionally to the increase in pH followed higher thermal GFPuv stability.

The linear correlation between extreme pH intervals and *D*-values was shown to be dependent on buffer systems and heating temperatures, as shown in Table 2, from (1) pH 4.91 (85°C) to 7.03 (85°C) for acetate, (2) pH 5.63 (85°C) to 7.91 (80°C) for phosphate, and (3) pH 6.91 (75°C) to 9.03 (90°C) for Tris-HCl solutions.

Table 2
Equations to Determine *D*-values for GFPuv in Various Buffers Exposed to Different Conditions of Temperature and pH

Buffer solution	Temperature (°C)	pH range	*D*-value equation	R^2
Acetate	75	5.5–7.01	–138.09 + 25.677 × pH	0.97
	80	5.18–7.01	–41.644 + 8.8106 × pH	0.94
	85	4.91–7.03	–12.1 + 2.8747 × pH	0.94
	90	5.19–7.01	–1.9854 + 1.0318 × pH	0.97
	95	5.46–7.01	–0.9143 + 0.8296 × pH	0.91
Phosphate	75	6.19–7.20	–392.14 + 64.603 × pH	0.92
	80	5.97–7.91	–271.76 + 45.632 × pH	0.96
	85	5.63–7.84	–35.676 + 6.8552 × pH	0.94
	90	6.03–7.80	–5.6922 + 1.6322 × pH	0.93
	95	5.89–7.82	–3.6824 + 1.3041 × pH	0.97
Tris-HCl	75	6.91 – 8.50	–636.99 + 92.299 × pH	0.89
	80	7.50–8.84	–182.68 + 27.510 × pH	0.91
	85	7.41–8.90	–91.089 + 13.097 × pH	0.94
	90	7.27–9.03	–14.998 + 2.5629 × pH	0.77
	95	7.08–8.92	–30.48 + 4.5551 × pH	0.98

Kinetic Parameters Z-Value, Q_{10} Coefficients, and E_a

The kinetic parameters *z*-value and the related Q_{10} coefficient ($Q_{10} = 10^{10/z}$) reflect the temperature dependence of the denaturation phenomenon (decrease in fluorescence intensity). The *z*-value is the interval of temperature required to change the *D*-value by a factor of 10.

For every temperature and buffer, the corresponding *D*-values at pH between 6.0 and 8.5 were calculated from the set equations shown in Table 2. The respective *z*-values (°C), were determined from the negative reciprocal of the slopes of the regression lines of the relations between Log_{10} *D*-value and corresponding temperatures. The Q_{10} coefficients were estimated through the relation to *z*-values ($Q_{10} = 10^{(10/z)}$); those parameters are given in Table 3.

The thermal stability of GFPuv was closely maintained at pH > 6.0 in the buffers: (1) acetate at pH 6.5 (z = 23.42°C) and pH 7.0 (z = 20.45°C); (2) phosphate at pH 7.0 (z = 16.64°C), pH 7.5 (z = 14.01°C), and pH 8.0 (z = 13.75°C); (3) Tris-HCl at pH 7.5 (z = 15.41°C), pH 8.0 (z = 15.60°C), and pH 8.5 (z = 14.95°C). At pH 6.0, the *z*-value of 30.96°C for GFPuv in acetate led to the highest thermal stability of the protein for the temperature interval between 75 and 95°C. The *z*-values dropped about 25% at pH 7.0 and 7.5, from z = 23.42°C (acetate) and 22.42°C (phosphate) to z = 20.45°C (acetate) and 20.79°C (Tris-HCl), respectively. At pH 8.0, the *z*-values dropped by half, between 13.75 and 15.60°C considering phosphate and Tris-HCl buffers, respectively.

Table 3
z-value, Q_{10} Coefficients, and E_a of Thermal Stability for GFPuv

	Acetate			Phosphate			Tris-HCl		
pH	z-value (°C)	Q_{10}	E_a (kcal/mol)	z-value (°C)	Q_{10}	E_a (kcal/mol)	z-value (°C)	Q_{10}	E_a (kcal/mol)
6.0	30.96	2.10	19.27						
6.5	23.42	2.67	25.15	22.42	2.79	26.18			
7.0	20.45	3.08	28.76	16.64	3.99	35.28	20.79	3.03	28.19
7.5				14.01	5.17	42.63	15.41	4.46	38.15
8.0				13.75	5.34	42.67	15.6	4.38	38.2
8.5							14.95	4.67	39.9

Meanwhile, the process coefficient Q_{10} ($Q_{10} = 10^{10/z}$) of about 3.0 suggested that acetate and Tris-HCl buffers at pH 7.0 provided similar stabilization for the protein's thermal characteristics greater than phosphate ($Q_{10} = 3.99$), whose system exposed GFPuv to more dependence on temperature change. At pH 8.0, the protein in Tris-HCl was confirmed to exhibit greater stability than in phosphate, when the *D*-values decreased, respectively, four and five times for every 10°C increase in heating temperature.

The rate of inactivation dependent on treatment temperatures can also be described by either activation energy (E_a) or the Arrhenius equation. E_a, which relates the intrinsic energy of the system, indicates the stability of the system during heat treatment. Therefore, stable systems possess lower energy than unstable ones. E_a and *z*-value are related: inactivation reactions that exhibit large *z*-value and small E_a are less influenced by temperature; however, systems that have small *z*-value and high E_a have greater temperature susceptibility (Table 3).

The stability of GFPuv was greater in acetate at pH 6.0 ($E_a = 19.27$ kcal/mol), and equivalent ($E_a \sim 26.50$ kcal/mol) at pH 6.5 in acetate and phosphate and at pH 7.0 in acetate and Tris-HCl. For the same buffers, on the increase in pH to 7.5–8.5, the thermal vulnerability of GFPuv incremented 30% in the E_a range from 38.15 to 39.9 kcal/mol. Otherwise, the solutions of GFPuv in phosphate at pH 7.5 and 8.0 (E_a = 42.63 and 42.67 kcal/mol, respectively) established the lowest thermal stability for GFPuv.

For pH > 7.0, the $Q_{10} > 5.0$ coefficient showed *D*-values 13% more vulnerable for GFPuv in phosphate than in Tris-HCl and acetate buffers, confirming its role in the improved maintenance of GFPuv conformation and fluorophore emission output.

The thermal stability of GFPuv was similar for the following systems: (1) acetate solutions at pH interval of 6.5–7.0 and respective *z*-values of 23.42 and 20.45°C; (2) phosphate solutions between pH of 7.0 and 8.0 and respective *z*-values of 16.64, 14.01, and 13.75°C; (3) Tris-HCl at pH interval of 7.5–8.5 and respective *z*-values of 15.41, 15.60, and 14.95°C.

The thermal stability of GFPuv was (1) higher when heated in acetate solution pH 6.0 (E_a = 19.27 kcal/mol), and (2) equivalent for the systems provided by acetate solutions at the pH interval of 6.5–7.0 (E_a = 25.15 and 28.76 kcal/mol), phosphate at pH 6.5 (E_a = 26.18 kcal/mol), and Tris-HCl at pH 7.0 (E_a = 28.19 kcal/mol).

The data confirmed the previous *(14)* thermal stability of standard GFPuv in Tris-HCl buffer at pH 8.5, when the *z*-value was about 12.9°C (Q_{10}= 6.0, E_a = 45.54 kcal/mol), comparable with an average of z = 13.75°C (Q_{10}= 5.34) observed for the extracted protein heated in phosphate buffer at pH 8.0, and the system corresponded to an average E_a = 42.67 kcal/mol, for the same interval of temperature, between 75 and 95°C.

Discussion

Laratta et al. *(15)* studied five tomato varieties and all varieties showed the same thermal performance: the thermal pectin methyl esterase resis-

tance was higher at higher pH. All pectin methyl esterase varieties showed a typical biphasic performance, characterized by a lower thermal resistance at temperatures lower than 74°C and a higher thermal resistance above that temperature. The temperature range between 90 and 115°C is generally employed in the food industry to microbiologically and enzymatically stabilize these products. The *z*-values for the five varieties of tomatoes varied from 18.9 to 36.0°C related to a pH range of 3.9–4.9, which was responsible, in our point of view, for a low interval of *D*-values, between 0.16 and 0.18 min. The variation in thermal stability of GFPuv verified in the present work related to the three buffers was similar considering the *z*-value range from 13.75°C in phosphate (pH 8.0) to 30.96°C for acetate (pH 6.0) solutions, corresponding to an interval of *D*-value between 4.06 (pH 5.6–6.0) and 6.08 min (pH 7.6–8.0) at 95°C.

Forsyth et al. *(16)* studied the thermal performance of peroxidase at 75°C and obtained a *D*-value range from 0.01 to 7.38 min for the native enzyme and between 0.096 and 18.96 min for the partially inactivated enzyme.

Griffiths *(2)* studied the thermal stability of the naturally occurring enzymes in milk at temperatures between 65 and 80°C, in order to choose an enzymatic index of adequate pasteurization of milk. For the acid phosphatase, the *D*-values of 7.38 min at 75°C and 7.87 min at 80°C corresponded to a *z*-value of 6.6°C; for the inactivation of lactoperoxidase, *D*-values of 0.80 min at 75°C and 0.075 min at 80°C corresponded to a *z*-value of 5.4°C; for amylase (saccharifying activity), *D*-values of 0.85 min at 75°C and 0.45 min at 80°C corresponded to a *z*-value of 16.2°C. The naturally occurring enzymes in milk showed lower *D*-values than those found for GFPuv in the three buffers. However, a *z*-value of 16.64°C characterized for GFPuv in phosphate buffer solutions at pH 7.0 was similar to that obtained for amylase in milk.

The thermal kinetics for lysozyme in beer *(1)* was characterized for systems containing 15% glucose at pH 5.20 and 7.20, corresponding respectively to *z*-values of 13.8 and 14.1°C, and to E_a values of 42.0 and 41.1 kcal/mol. For systems containing 1.0 *M* NaCl at pH 7.20, the obtained parameters were a *z*-value of 13.9°C and a E_a value of 41.8 kcal/mol. For both systems, the kinetic parameters were similar to those verified for GFPuv in phosphate solutions at pH 7.5 and 8.0.

Thermal inactivation of *Bacillus cereus* spores was confirmed to be affected by the solutes used to control water activity (A_w) of the heating medium. For the spores of *B. cereus* ATCC 7004 subjected to a heating interval between 92 and 106°C, Mazas et al. *(17)* determined the following parameters: (1) *z*-value of 8.3°C for spores in water (A_w = 1.0) at pH 7.60, as a medium control; (2) *z*-value of 10.3°C for spores in 5.6 *M* NaCl solution at pH 8.35 and A_w = 0.75. For both extreme systems, the spores of *B. cereus* exhibited lower thermal stability than even the system of GFPuv in phosphate solution (*z*-value minimum of 13.75°C). Among the environmental conditions that affect spore thermoresistance, Vessoni Penna et al. *(18)*

stated that pH value is a major intrinsic factor in microbial destruction, as well as in the recovery medium of the injured spores.

Since the direct estimation of microbial numbers by conventional culturing methods is time-consuming and well affected by environmental conditions *(18)*, a simple test for the most resistant enzyme activity is appropriate on a routine basis. If enzyme activity is detected, it can be assumed that the heat treatment was inadequate *(4,15)*. Appropriately, GFPuv can be employed as a BI in thermal processes (blanching, pasteurization, disinfection) at temperatures ≥75°C for products at pH > 5.5, with the inactivation of GFPuv shown to be directly related to the time of exposure to moist heat and pH.

Conclusion

The thermal stability of GFPuv provides the basis for its potential utility as a fluorescent BI to assay the efficacy of processes at temperatures lower than 100°C at an interval of pH between 5.5 and 8.5 and dissolved in various buffers.

Acknowledgments

We thank our personal assistants for providing technical support for biologist Irene A. Machoshvili. This study was made possible by financial support provided by the Brazilian Committees for Scientific Technology Research (Coordenacão de Aperfeiçoamento de Pessoal de Nível Superior, Conselho Nacional de Desenvolvimento Científico e Tecnológico, and Fundação de Amparo à Pesquisa do Estado de São Paulo).

References

1. Makki, T. F. and Durance, T. D. (1996), *Food Res. Int.* **29,** 635–645.
2. Griffiths, M. W. (1986), *J. Food Protect.* **49,** 696–705.
3. Labib, A. A. S., El-Ashwah, F. A., Omhan, H. T., and Askar, A. (1995), *Food Chem.* **53,** 137–142.
4. Fayyaz, A., Asbi, B. A., Ghazali, H. M., Che Man, Y. B., and Jinap, S. (1995), *Food Chem.* **53,** 129–135.
5. Eargerman, B. A. and Rouse, A. H. (1976), *J. Food Sci.* 41, 1396–1397.
6. Fagain, C. Ó. (1995), *Biochim. Biophys. Acta* **1252,** 1–14.
7. Chalfie, M., Tu, Y., Euskirchen, G., Ward, W. W., and Prasher, D. C. (1994), *Science* **263,** 802–805
8. Sambrook, J., Fritsch, E. F., and Maniatis, T.(1989), *Molecular Cloning: A Laboratory Manual*, Cold Spring Harbor Laboratory, Cold Spring Harbor, NY.
9. Vessoni Penna, T. C., Chiarini, E., Machoshvili, I. A.. Ishii, M., and Pessoa, A., Jr. (2002), *Appl. Biochem. Biotechnol.* **98–100,** 791–802.
10. Dennison, C. and Lovrien, R. (1997), *Protein Expr. Purif.* **11,** 149–161.
11. Vessoni Penna, T. C. and Ishii, M. (2002), *BMC Biotechnol.* **2,** 7. (Website: http://www.biomedcentral.com/1472-6750/2/7).
12. Bokman, S. H. and Ward, W.W. (1981), *Biochem. Biophys. Res. Commun.* **101,** 1372–1380.
13. Ward, W. W. (1998), in *Green Fluorescent Protein, Properties, Applications and Protocols*, Chalfie, M. and Kain, S., eds., Wiley-Liss, New York, NY, pp. 45–75.

14. Vessoni Penna, T. C. , Ishii, M., and Nascimento, L. O. (2002), *24th Symposium on Biotechnology for Fuels and Chemicals,* Gatlinburg, TN. Poster presentation 3-49. (Website: www.ct.ornl.gov/symposium/24th/ index_files/poster03_49.htm)
15. Laratta, B., Fasarano, G., De Sio, F., Castaldo, D., Palmieri, A., Giovane, A., and Servillo, L. (1995), *Process Biochem.* **30,** 251–259.
16. Forsyth, J. L., Owusu Apeten, R. K., and Robinson, D. S. (1999), *Food Chem.* **65,** 99–109.
17. Mazas, T. F., Martínez, S., López, M., Alvarez, A. B., Martin, R. (1999), *J. Food Microbiol.* **53,** 61–67.
18. Vessoni Penna, T. C, Ishii M., Machoshvili, I. A., and Marques, M. (2002), *Appl. Biochem. Biotechnol.* **98–100,** 525–538.

0273-2289/04/114/0485–0496/$25.00

Evaluation of Optimization Techniques for an Extractive Alcoholic Fermentation Process

Aline C. da Costa* **and Rubens Maciel Filho**

DPQ/FEQ/UNICAMP,
Cx. Postal 6066,
Campinas, SP, 13081-970 Brazil,
E-mail:accosta@feq.unicamp.br

Abstract

The mathematical optimization of a continuous alcoholic fermentation process combined with a flash column under vacuum was studied. The objective was to maximize % yield and productivity in the fermentor. The results using surface response analysis combined with modeling and simulation were compared withy those obtained when the problem was written as a nonlinear programming problem and was solved with a successive quadratic programming (SQP) technique. Two process models were evaluated when the process was optimized using the SQP technique. The first one is a deterministic model, whose kinetic parameters were experimentally determined as functions of the temperature, and the second is a statistical model obtained using the factorial design technique combined with simulation. Although the best result was the one obtained using the rigorous model, the values for productivity and % yield obtained using the simplified model are acceptable, and these models can be used when the development of a rigorous model is excessively difficult, slow, or expensive.

Index Entries: Extractive alcoholic fermentation; optimization; successive quadratic programming; factorial design; response surface methodology; productivity.

Introduction

Despite many advantages of using ethanol produced from biomass as a fuel (it is a high-energy, clean-burning, and totally renewable liquid fuel), it will only substitute gasoline if it is economically competitive. Thus, there is an increased interest in the optimization of all the steps of ethanol production.

*Author to whom all correspondence and reprint requests should be addressed.

Many aspects related to optimization of the ethanol production process have been addressed in previous works. A key to the optimization of a process is a thorough understanding of the system's dynamics, which can be obtained using an accurate model of the process. Atala et al. *(1)* developed a mathematical model for the alcoholic fermentation based on fundamental mass balances. The kinetic parameters were determined from experimental data and were described as functions of the temperature. The experiments were conducted with high biomass concentration and sugarcane molasses as substrate to simulate the real conditions in industrial units.

Although deterministic models are important to enhance the knowledge of the process, for many bioprocesses they are only valid in specific conditions. Changes in medium composition, process disturbances, or the use of different strains may nullify the modeling predictions. All these changes happen commonly in an industrial unit, and frequent reestimation of the model parameters is usually difficult and time-consuming. Hybrid neural models are a good alternative to deal with this problem. Harada et al. *(2)* proposed a hybrid model for the alcoholic fermentation combining mass balance equations with neural networks that described the kinetics. They proposed the use of functional link networks (FLNs) and obtained an accurate model that can be updated frequently without much effort. Because estimation of the FLN parameters is a linear problem, the training of these neural networks is rapid, requires low computational effort, and the convergence is guaranteed. These characteristics give the FLN a significant potential to be used for on-line control and optimization implementation.

Because ethanol fermentation is inhibited by product, the selective extraction of ethanol during fermentation is also important to improve process performance. Silva et al. *(3)* have reported that the scheme that combines a fermentor with a vacuum flash vessel presents many positive features and good performance when compared to a conventional process *(4)*.

Another important consideration is the development of an efficient control strategy, because this minimizes the costs by maintaining the process in its optimal conditions. Costa et al. *(5)* determined the best control structures and studied the control of the process proposed by Silva et al. *(3)* using a linear predictive controller. Later, a nonlinear predictive controller using FLNs as the internal model was developed and implemented with the same process with promising results *(6)*.

The main objective of the present work was to verify the potential of one of the proposed approaches to optimization: the use of a successive quadratic programming (SQP) technique combined with a statistical model instead of a rigorous model. The results were compared with those obtained by Costa et al. *(5)* using response surface methodology (RSM). In the present work the optimization of the extractive fermentation process proposed by Silva et al. *(3)* is addressed. The objective is to maximize productivity while maintaining high yield. Costa et al. *(5)* optimized the same process using response surface analysis combined with modeling and simulation.

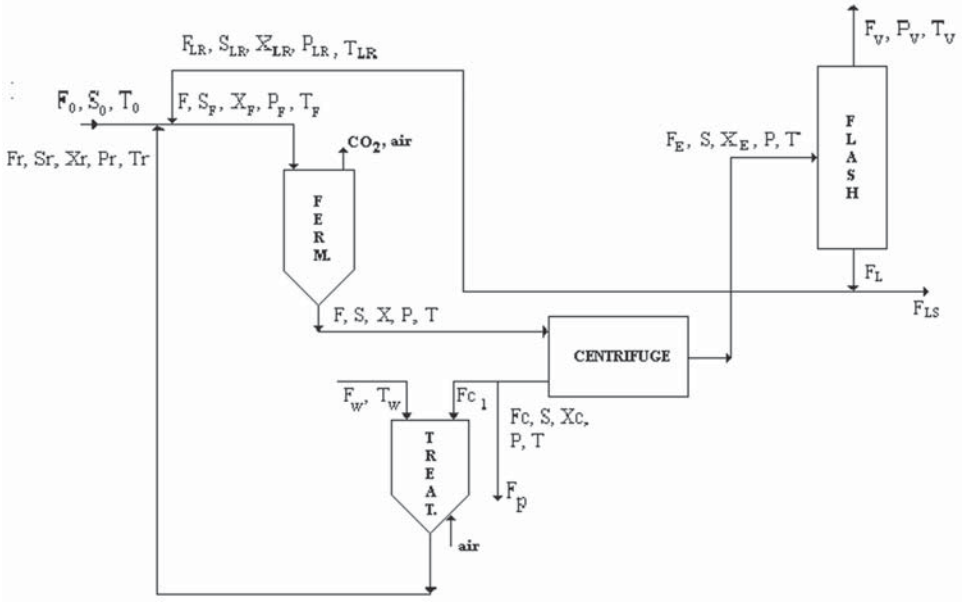

Fig. 1. Extractive alcoholic fermentation.

Although this methodology has the advantage of not requiring model simplifications, it is extremely time-consuming and cannot be used in a real-time optimization scheme.

In the present study, the problem is written as a nonlinear programming problem and is solved with SQP technique. Two process models are evaluated when the process is optimized using the SQP technique. The first one is a deterministic model with the kinetic parameters determined by Atala et al. *(1)*, and the second one is a statistical model obtained using the factorial design technique combined with simulation.

Material and Methods

Extractive Alcoholic Fermentation

A general scheme of the extractive alcoholic fermentation proposed by Silva et al. *(3)* is shown in Fig. 1. The process consists of four interlinked units: the fermentor (ethanol production unit), the centrifuge (cell separation unit), the cell treatment unit, and the vacuum flash vessel (ethanol-water separation unit). A detailed description of the process and mathematical model can be found in ref. *5*.

Assuming constant volume, the mass and energy balance equations for the fermentor using the intrinsic model *(7,8)* are as follows:

Viable cells:
$$\frac{dX_v}{dt} = r_x - r_d - \frac{F}{V}\left(X_v - X_{vF}\right) \quad (1)$$

Dead cells:
$$\frac{dX_d}{dt} = r_d - \frac{F}{V}\left(X_d - X_{dF}\right) \tag{2}$$

Substrate:
$$\frac{d\left[\left(1 - \frac{X_t}{\rho}\right) SV\right]}{dt} = F\left(S_F - S\right) - Vr_s \tag{3}$$

Product:
$$\frac{d\left[\left(1 - \frac{X_t}{\rho}\right) PV + \frac{X_t}{\rho}\gamma PV\right]}{dt} = Vr_p + F\left(P_F - P\right) \tag{4}$$

$$\frac{dT}{dt} = D\left(T_F - T\right) + \frac{\Delta H r_s}{\rho_m Cp} \tag{5}$$

ρ and γ in Eqs. 3 and 4 are the ratio of dry cell weight to wet cell volume and the ratio of concentration of intracellular to extracellular ethanol, respectively.

The values of the constants in the energy balance equation (Eq. 5) are given by *(3)*: ΔH = 51.76 kcal/(kg of total reducing sugars [TRS]); ρ_m =1000 kg/m^3, and Cp = 1 kcal/(kg·°C).

The kinetic rates of growth, death, ethanol formation and substrate consumption are as follows:

$$r_x = \mu_{\max} \frac{S}{K_s + S} \exp\left(-K_i S\right) \left(1 - \frac{X_t}{X_{\max}}\right)^m \left(1 - \frac{P}{P_{\max}}\right)^n X_v \tag{6}$$

$$r_d = \left[K_{dT} \exp\left(-K_{dP} P\right)\right] X_v \tag{7}$$

$$r_p = Y_{px} r_x + m_p X_v \tag{8}$$

$$r_s = \frac{r_x}{Y_x} + m_x X_v \tag{9}$$

The parameters were adjusted as functions of the temperature from the experimental data and are given in Table 1. The proposed model described the dynamic behavior of the alcoholic fermentation *(1)*.

Results

The variables considered for optimization were the same as those used in the work of Costa et al. *(5)*: inlet substrate concentration (S_0), cell recycle rate (R), residence time (t_r), and flash recycle rate (r). They were determined by Silva et al. *(3)* as the relevant variables.

The objective of the optimization problem is to maximize productivity while maintaining a high yield. Productivity and % yield were defined as follows:

$$\text{Prod} = \frac{F_v \cdot P_v + F_{LS} \cdot P_{LR}}{V} \tag{10}$$

Table 1
Kinetic Parameters as Functions of Temperature (°C)

Parameter	Expression or value
μ_{max}	$1.57 \exp\left(\frac{41.47}{T}\right) - 1.29 \cdot 10^{4} \exp\left(\frac{-431.4}{T}\right)$
X_{max}	$-0.3279 \cdot T^2 + 18.484 \cdot T - 191.06$
P_{max}	$-0.4421\, T^2 + 26.41 \cdot T - 279.75$
Y_x	$2.704 \exp(-0.1225 \cdot T)$
Y_{px}	$0.2556 \exp(0.1086 \cdot T)$
K_s	4.1
K_i	$1.393 \cdot 10^{-4} \exp(0.1004 \cdot T)$
m_p	0.1
m_x	0.2
m	1.0
n	1.5
K_{dP}	$7.421 \cdot 10^{-3} \cdot T^2 - 0.4654 \cdot T + 7.69$
K_{dT}	$4 \cdot 10^{13} \exp\left[\frac{41947}{1.987 \cdot (T + 273.15)}\right]$
ρ	390
γ	0.78

$$\%\text{Yield} = \frac{F_v \cdot P_v + F_{LS} \cdot P_{LR}}{S_0 \cdot S_0 \cdot 0.511} \tag{11}$$

Conversion was defined as follows:

$$\text{Conv} = \frac{S_0 - S}{S_0} \tag{12}$$

Optimization Using SQP Technique and Deterministic Model

Optimization was conducted with the deterministic steady-state model of the process. It consists of the steady-state mass and energy balances for the fermentor and all the other process units (*see* Fig. 1).

The optimization problem can be written as follows:

$$\text{Maximize Prod} \tag{13}$$

subject to the equality constraints described by the steady-state mass and energy balances for the fermentor and to the following inequality constraints:

$$\%\ \text{Yield} > 0.82 \tag{14}$$

$$28 < T < 40°\text{C} \tag{15}$$

$$80 < S_0 < 280\ \text{kg/m}^3 \tag{16}$$

$$0.2 < R < 0.5 \tag{17}$$

$$1.0 < t_r < 2.5\ \text{h} \tag{18}$$

$$0.2 < r < 0.6 \tag{19}$$

Productivity and % yield are calculated by Eqs. 10 and 11. The constraints for the optimization variables are the same as those used by Costa et al. *(5)*. The balance equations for the other process units were not considered explicitly as constraints but were used to calculate the flow rate and concentrations at the input of the fermentor. The optimization problem was solved by SQP implementation using the routine DNCONF of the IMSL math library of FORTRAN.

When the optimization problem is solved using the SQP technique and the deterministic model, the values of temperature and concentrations in the fermentor have to be considered as optimization variables, so the number of the optimization variables is higher than using RSM. The optimization variables are concentrations of viable cells (X_v), dead cells (X_d), substrate (S), product (P), temperature (T); as well as the variables used by Costa et al. *(5)*: S_0, R, t_r, and r.

The values of the optimization variables calculated by Costa et al. *(5)* were $S_0 = 130$ kg/m^3, $t_r = 1.3$ h, $R = 0.3$, and $r = 0.25$, which leads to productivity of 21 kg/(m^3·h), % yield of 0.82, and conversion of 0.96. Costa et al. *(5)* analyzed 16 surfaces to determine the values of the four optimization variables and they cited that it was difficult to determine the best combination of optimization variable values without taking advantage of previous knowledge of the process.

Using the SQP method, solving the optimization problem was straightforward. The calculated values were $S_0 = 180$ kg/m^3, $t_r = 1$ h, $R = 0.35$, and $r = 0.4$. The values of productivity, % yield, and conversion were 22.7 kg/(m^3·h), 0.82, and 0.96, respectively.

The productivity for the same % yield calculated by the SQP technique was higher than that calculated using the RSM. The RSM calculates the ranges of the optimization variables and not exact values, so it is difficult to determine the exact global maximum point. In addition, the RSM uses statistical models for productivity and % yield and these are simplified models, while the SQP technique uses a rigorous process model.

The conversion values corresponding to optimal conditions calculated may be considered low for industrial units. If one includes a constraint in conversion (conversion > 0.99) and solves the optimization problem using the SQP technique again, the following values are calculated: $S_0 = 180$ kg/m^3, $t_r = 1$ h, $R = 0.42$, and $r = 0.52$. Productivity is 13 kg/(m^3·h), conversion is 0.99, and % yield is 0.89. In this case, the extractive process has productivity only a little higher than the optimized conventional process. Kalil et al. *(9)* optimized the conventional process of Andrietta and Maugeri *(4)* and obtained productivity of 12 kg/(m^3·h), conversion of 0.99, and % yield of 0.86.

Although the productivity calculated using the SQP technique was higher and the result seemed easier to be obtained than using RSM, the results obtained using the SQP technique are highly dependent on the initial guess. For some values of the initial guess, the SQP technique may reach a local maximum or does not converge. In the present work, the initial guess used was $X_v = 30$ kg/m^3, $X_d = 0$ kg/m^3, $S = 2$ kg/m^3, $P = 40$ kg/m^3, $T = 30$°C, $S_0 = 120$ kg/m^3, $t_r = 1.3$ h, $R = 0.3$, and $r = 0.6$. However, when the initial guess $X_v = 30$ kg/m^3, $X_d = 0$ kg/m^3, $S = 2$ kg/m^3, $P = 40$ kg/m^3, $T = 30$°C, $S_0 = 120$ kg/m^3, $t_r = 1$ h, $R = 0.2$, and $r = 0.2$, was used, there was no convergence.

Another point to be discussed is the use of the rigorous model compared with the use of simplified models as the statistical models determined by factorial design and used with RSM. Although rigorous models are more realistic and probably lead to better results, for many processes they can be excessively complex, which hinders determination of the optimal result.

Optimization Using SQP Technique and a Simplified Model of the Process

The statistical models determined by factorial design can be used as simplified models with the SQP technique. In this work the results obtained through this approach are compared with the results obtained using a rigorous model of the process. Costa et al. *(5)* determined quadratic models for productivity and % yield as functions of the significant input variables. These equations evaluated productivity and % yield and the SQP technique to determine the optimal values for S_0, t_r, R, and r. The optimization problem is postulated as follows:

$$\text{Maximum Prod} \tag{20}$$

$$\%\ \text{Yield} > 0.82 \tag{21}$$

$$28 < T < 40°\text{C} \tag{22}$$

$$80 < S_0 < 280\ \text{kg/m}^3 \tag{23}$$

$$0.2 < R < 0.5 \tag{24}$$

$$1.0 < t_r < 2.5\ \text{h} \tag{25}$$

$$0.2 < r < 0.6 \tag{26}$$

Productivity and % yield are described by the statistical models, which are written as functions of the optimization variables (S_0, t_r, R, and r).

The optimization variables values are $S_0 = 118.3$ kg/m^3, $t_r = 1$ h, $R = 0.2$, and $r = 0.2$. The values for % yield and productivity calculated by the statistical models are 0.82 and 26.73 kg/(m^3·h), respectively. Using the values calculated for S_0, t_r, R, and r in the rigorous model, however, the % yield calculated was 0.69 and productivity was 26.39 kg/(m^3·h). Note that although the statistical model for yield developed by Costa et al. (5) has a high correlation coefficient and passed the *F*-test with 99% confidence, at the calculated optimal conditions, it presents a great deviation from the rigorous model.

We also tested the influence of the initial guess on the optimal values calculated. The results shown above were obtained with the following initial guess: $S_0 = 130$ kg/m^3, $t_r = 2$ h, $R = 0.2$, and $r = 0.6$. Many other values were tested and the optimal result was almost always obtained. The exception was when we used a high initial value for S_0. For example, the initial guess $S_0 = 230$ kg/m^3, $t_r = 2$ h, $R = 0.2$, and $r = 0.6$ led to the following values calculated for the optimization variables: $S_0 = 280$ kg/m^3, $t_r = 2.5$ h, $R = 0.2$, and $r = 0.597$. Yield and productivity calculated by the statistical models are 0.82 and 20.63 kg/(m^3·h), respectively. These results show one of the disadvantages of the SQP technique: the optimization algorithm can reach a local maximum. The values for % yield and productivity calculated using the rigorous model are 0.77 and 16.20 kg/(m^3·h), respectively. In this case, the statistical model for productivity also presents a high deviation from the result calculated from the rigorous model.

The statistical models developed by Costa et al. *(5)* were functions only of the inputs considered statistically significant by a test performed with the software Statistica (Statsoft, v. 5.0). Since the results obtained by these models presented deviations from the rigorous model, complete models were tested. The following models were developed using the software Statistica:

$$\begin{aligned}\text{Rend} = \\ 72.10 - 0.40S_0 - 6.56\cdot 10^{-4}S_0^2 + 23.83t_r - 4.76t_r^2 + 53.55R - 47.73R^2 + 33.49r - 38.83r^2 \\ + 7.09\cdot 10^{-2}S_0t_r + 0.42S_0R + 0.59S_0r - 11.42t_rR - 22.64t_rr - 64.85Rr\end{aligned} \quad (27)$$

$$\begin{aligned}\text{Prod} = \\ 27.44 + 0.14S_0 - 2.84\cdot 10^{-4}S_0^2 - 23.04t_r + 3.77t_r^2 + 20.50R - 48.18R^2 + 13.63r - 41.61r^2 \\ - 7.75\cdot 10^{-3}S_0t_r + 9.58\cdot 10^{-4}S_0R + 9.44\cdot 10^{-2}S_0r + 7.34t_rR + 3.22t_rr - 78.49Rr\end{aligned} \quad (28)$$

Table 2 depicts the analysis of variance for % yield and productivity. Both responses present a high correlation coefficient, and the model can be considered statistically significant according to the *F*-test with 99% confidence. As a practical rule, a model has statistical significance if the calculated *F* value is at least three to five times greater than the listed value *(9)*.

Table 2
Analysis of Variance

Source of variation	Sum of squares		Mean square		Degrees of freedom	*F*-value	
	Rend	Prod	Rend	Prod		Rend	Prod
Regression	2326.5	726.3	166.2	51.9	14	35.8	28.1
Residual	46.4	18.5	4.64	1.85	10		
Total	2372.9	744.8			24		
Correlation coefffecient	0.980	0.975					
F listed value					$4.56 < F_{14,10} = 4.71$ (99%)		

Table 3
Results Using RSM, SQP Technique + Rigorous Model, and SQP Technique + Simplified Model

	RSM	SQP + rigorous model	SQP + simplified model
S_0 (kg/m^3)	130.00	180.00	103.00
t_r (h)	1.30	1.00	1.00
R	0.30	0.35	0.34
r	0.25	0.40	0.20
Prod (kg/[m^3·h])	21.00[a]	22.70	21.60[a]
% yield	0.82[a]	0.82	0.83[a]

[a]Calculated using the rigorous model.

The optimization problem described by Eqs. 20–26 was solved using Eqs. 27 and 28 to calculate % yield and productivity. At the low S_0 initial guess (S_0 = 130 kg/m^3, t_r = 2 h, R = 0.2, and r = 0.6) the optimal values calculated are S_0 = 103 kg/m^3, t_r = 1 h, R = 0.344, and r = 0.2. Yield and productivity calculated by the statistical models are 0.82 and 21.63 kg/(m^3·h), respectively, and calculated using the rigorous model are 0.83 and 21.62 kg/(m^3·h), respectively. If the high S_0 initial guess is used (S_0 = 230 kg/m^3, t_r = 2 h, R = 0.2, and r = 0.6), the optimization variables calculated are S_0 = 186 kg/m^3, t_r = 1 h, R = 0.247, and r = 0.6, resulting in % yield and productivity of 0.82 and 21.57 kg/(m^3·h), respectively, calculated by the statistical model, and 0.82 and 21.01 kg/(m^3·h), respectively, calculated by the rigorous model. Note that when the complete statistical models were used, the results for % yield and productivity are very close to those calculated by the rigorous model. It can also be observed that different initial guesses can lead to different results. A comparison of the optimization variables and responses calculated by the three approaches is shown in Table 3.

Discussion

Comparison of the performance of the three approaches (RSM, SQP + rigorous model, and SQP + statistical model) shows that the SQP + rigorous model approach led to the highest productivity (22.7 kg/[m^3·h]), while maintaining a high % yield (at least 0.82). Comparison of the two approaches with the simplified model demonstrates that the one using the SQP technique led to the highest productivity value (21.6 kg/[m^3·h]). Using the RSM, the productivity was 21 kg/m^3·h. In this case, many surfaces are analyzed at the same time and the determination of the global maximum is more difficult.

Note that although the productivity and % yield values are similar using the three approaches, the optimization variables values calculated are different, which shows that there are many combinations of values of the optimization variables that lead to high productivity and % yield. This conclusion had already been drawn in the work of Costa et al. *(5)* by analysis of the response surfaces. One of the advantages of the RSM is that it is possible to picture the behavior of the optimization variables in the region of interest.

Although the best result was the one obtained using the rigorous model, the values for productivity and % yield obtained using the simplified model are acceptable, and these models can be used when the development of a rigorous model is excessively difficult, slow, or expensive. Several simulations were carried out with the SPQ optimizer, which was shown to be very robust despite some initial condition dependence.

Another situation when the use of the statistical model can be a good choice over the RSM is when the deterministic model is excessively complex. For example, when the process is described by a distributed parameters model, the steady-state mass and energy balances are differential equations. The use of differential equations as constraints in an optimization problem makes its solution difficult and increases the incidence of convergence problems. In this case, solving the optimization problem using the statistical model is much simpler. The statistical model can also be used when the computational effort to solve the optimization problem using the deterministic model is too high, as can be the case for real-time optimization problems.

The simulations were performed using a mathematical model validated experimentally *(5)*, and their results can be said to have physical meaning. The next step is to perform experiments using the optimal conditions determined using the three methods shown in Table 3. In fact, a simulation study and analysis is a good tool to discriminate among possible techniques as well as to determine the possible operating range to be tested in an experimental apparatus.

Nomenclature

Cp = heat capacity (kcal/[kg·°C])
$D = F/V$ = dilution rate, (h^{-1})

F = feed stream flow rate (m^3/h)
F_0 = fresh medium flow rate (m^3/h)
F_L = liquid outflow from vacuum flash tank (m^3/h)
F_{LR} = liquid phase recycling flow rate (m^3/h)
F_{LS} = liquid phase flow to rectification column (m^3/h)
F_r = cell recycling flow rate (m^3/h)
F_V = vapor outflow from the vacuum flash tank (m^3/h)
K_{dP} = coefficient of death by ethanol (m^3/kg)
K_{dT} = coefficient of death by temperature (h^{-1})
K_{ei} = equilibrium constant
K_i = substrate inhibition constant (m^3/kg)
K_s = substrate saturation constant (kg/m^3)
m = constant in Eq. 6
m_p = ethanol production associated to growth (kg/[kg·h])
m_x = maintenance coefficient (kg/[kg·h])
n = constant in Eq. 6
P = product concentration in fermentor (kg/m^3)
P_F = feed product concentration (kg/m^3)
P_{LR} = product concentration in light phase from centrifuge (kg/m^3)
P_{max} = product concentration when cell growth ceases (kg/m^3)
P_V = product concentration in vapor phase from flash tank (kg/m^3)
$r = F_{LR}/F_L$ = flash recycle rate
r_d = kinetic rate of death ($kg/[m^3 \cdot h]$)
r_p = kinetic rate of product formation ($kg/[m^3 \cdot h]$)
r_s = kinetic rate of substrate consumption ($kg/[m^3 \cdot h]$)
r_x = kinetic rate of growth ($kg/[m^3 \cdot h]$)
$R = Fr/F$ = cells recycle rate
S = substrate concentration in fermentor (kg/m^3)
S_0 = inlet substrate concentration (kg/m^3)
S_F = feed substrate concentration (kg/m^3)
T = temperature in fermentor (°C)
T_F = feed temperature (°C)
t_r = residence time (h)
V = reactor volume (m^3)
X_d = dead biomass concentration in fermentor (kg/m^3)
X_{dF} = dead biomass concentration in feed stream (kg/m^3)
X_F = feed biomass concentration (kg/m^3)
X_{max} = biomass concentration when cell growth ceases (kg/m^3)
$X_t = X_v + X_d$ = total biomass concentration in fermentor (kg/m^3)
X_v = viable biomass concentration in fermentor (kg/m^3)
X_{vF} = viable biomass concentration in feed stream (kg/m^3)
Y_{px} = % yield of product based on cell growth (kg/kg)
Y_x = limit cellular yield (kg/kg)
ΔH = reaction heat (kcal/[kg TRS])

γ = ratio of concentration of intracellular to extracellular ethanol (kg/m^3)
μ_{max} = maximum specific growth rate (h^{-1})
ρ = ratio of dry cell weight per wet cell volume (kg/m^3)
ρ_m = density (kg/m^3)

References

1. Atala, D. I. P., Costa, A. C., Maciel, R., and Maugeri, F. (2001), *Appl. Biochem. Biotechnol.* **91(3),** 353–365.
2. Harada, L.H.P., Costa, A. C., Maciel Filho, R. (2002), *Appl. Biochem. Biotechnol.* **98(1–3),** 1009–1024.
3. Silva, F. L. H., Rodrigues, M. I., and Maugeri, F. (1999), *J. Chem. Tech. Biotechnol.* **74,** 176–182.
4. Andrietta, S. R. and Maugeri, F.(1994), *Adv. Bioprocess Eng.,* 47–52.
5. Costa, A. C., Atala, D. I. P., Maciel Filho, R., and Maugeri Filho, F. (2001), *Process Biochem.* **37(2),** 125–137.
6. Costa, A. C., Meleiro, L. A. C., and Maciel Filho, R. (2002), *Process Biochem.* **38(5),** 743–750.
7. Monbouquette, H. G. (1987), *Biotechnol Bioeng.* **29,** 1075–1080.
8. Monbouquette, H. G. (1992), *Biotechnol Bioeng.* **39,** 498–503.
9. Kalil, S. J., Maugeri, F., and Rodrigues, M. I. (2000), *Process Biochem.* **35,** 539–550.

0273-2289/04/114/0497–0508/$25.00

Yields from Glucose, Xylose, and Paper Sludge Hydrolysate During Hydrogen Production by the Extreme Thermophile *Caldicellulosiruptor saccharolyticus*

Zsófia Kádár,[1,2] Truus de Vrije,[1] Giel E. van Noorden,[1] Miriam A. W. Budde,[1] Zsolt Szengyel,[2] Kati Réczey,[2] and Pieternel A. M. Claassen*[,1]

[1]Agrotechnology & Food Innovations, PO Box 17, 6700 AA Wageningen, The Netherlands, E-mail: pieternel.claassen@wur.nl; and [2]Budapest University of Technology and Economics, Department of Agricultural Chemical Technology, Szent Gellért tér 4., H-1521 Budapest, Hungary

Abstract

This study addressed the utilization of an industrial waste stream, paper sludge, as a renewable cheap feedstock for the fermentative production of hydrogen by the extreme thermophile *Caldicellulosiruptor saccharolyticus*. Hydrogen, acetate, and lactate were produced in medium in which paper sludge hydrolysate was added as the sole carbon and energy source and in control medium with the same concentration of analytical grade glucose and xylose. The hydrogen yield was dependent on lactate formation and varied between 50 and 94% of the theoretical maximum. The carbon balance in the medium with glucose and xylose was virtually 100%. The carbon balance was not complete in the paper sludge medium because the measurement of biomass was impaired owing to interfering components in the paper sludge hydrolysate. Nevertheless, >85% of the carbon could be accounted for in the products acetate and lactate. The maximal volumetric hydrogen production rate was 5 to 6 mmol/(L·h), which was lower than the production rate in media with glucose, xylose, or a combination of these sugars (9–11 mmol/[L·h]). The reduced hydrogen production rate suggests the presence of inhibiting components in paper sludge hydrolysate.

Index Entries: Hydrogen production; paper sludge hydrolysate; extreme thermophile; *Caldicellulosiruptor saccharolyticus*, glucose; xylose; carbon balances.

*Author to whom all correspondence and reprint requests should be addressed.

Introduction

Hydrogen has been recognized as one of the potential energy carriers for a sustainable energy economy in the future providing the feedstock for fuel cells. Hydrogen made from local renewable energy resources provides a clean, CO_2-neutral energy source with the additional benefit of decreasing foreign fuel dependency. During the energy crisis of the 1970s, enormous efforts were put into work exploring possible resources for production and applications of hydrogen. Unfortunately, after the decrease in crude oil price on the world market, alternative fuels were no longer of interest *(1)*. However, new concerns about greenhouse effects owing to the utilization of fossil fuel resources have brought research and development activities targeting production of biofuels from renewable resources back to life since the early 1990s. At present more than 96% of hydrogen produced worldwide depends on fossil energy resources. Alternative routes that are cost-effective and CO_2 neutral are required. The production of hydrogen from renewable resources could be a promising alternative to the present situation *(2,3)*.

Among the sustainable alternatives—electrochemical production using renewable resources, and thermochemical or biologic conversion of biomass or photobiologic hydrogen production—the biologic production of hydrogen from biomass seems to be a very attractive technology *(1,4)*. Advantages of the anaerobic fermentative route have been pointed out since several carbohydrates containing residues and byproducts can be utilized. Various waste streams, such as sugarcane juice, corn pulp, tofu-manufacturing residues, rice straw, and bean- and curd-manufacturing waste, have been investigated for hydrogen production *(5,6)*. Woodward et al. *(7)* have estimated that in the United States alone about 7.26 million t of cellulose ends up in waste newspapers annually. Utilization of this huge amount of cellulose would yield 10.6 million m^3 of hydrogen, which could provide energy for 37 cities each with a population of 27,000 *(7)*.

Already in the late 1800s, fundamental research had established that algae and bacteria could produce hydrogen. Microbiologic hydrogen production can be carried out by various bacteria including anaerobic, facultatively anaerobic, methylotrophic, and photosynthetic species in different processes *(8)*. Anaerobic thermophilic microorganisms, such as *Thermotogales* and *Caldicellulosiruptor* species, are able to convert glucose and sucrose to hydrogen, with yields close to the theoretical stoichiometry of 4 mol of hydrogen/mol of hexose. Two moles of acetic acid and CO_2 are maximally generated as byproducts *(9,10)*. Van Ooteghem et al. *(11)* have reported that most members of *Thermotogales* tolerate moderate amounts of oxygen with no apparent decrease in hydrogen production.

Thermophilic microorganisms are able to utilize a wide range of organic wastes, such as residues from the food-processing industry *(12)*. Paper sludge is another industrial waste with relatively high cellulose content, which could provide for an interesting feedstock after, e.g., enzymatic

hydrolysis. As raw material, paper sludge is very attractive in terms of economy, because presently it is deposited in areas such as landfills. For this reason the contribution of raw material cost to the overall hydrogen production cost will become very small. However, to judge whether the process economy using paper sludge is favorable, detailed economic analysis is required especially in view of the cost deposition of inorganic residues present in the paper sludge. In addition, utilization of the fermentation byproduct acetic acid is another issue that needs to be taken into account. This could be done by integration of a photofermentation involving photosynthetic bacteria capable of producing hydrogen from organic acids *(13)*. This way an economically advantageous process can be established in which material losses are minimized *(14)*. In a previously published work, nutritional requirements of two hydrogen-producing bacteria, *Thermotoga elfii* and *Caldicellulosiruptor saccharolyticus* were investigated in small-scale experiments using paper sludge hydrolysate. It was shown that the halophilic *T. elfii* needed sodium chloride in a concentration as high as 1% in order to produce hydrogen. Furthermore, a considerable amount of yeast extract was necessary to achieve good hydrogen yields. On the other hand, *C. saccharolyticus* was much less affected by nutrient supplementation, and hydrogen production was not greatly influenced by the addition of yeast extract, salts, or trace elements *(15)*.

In this article, we present our findings on hydrogen production by the extreme thermophilic *C. saccharolyticus* using paper sludge hydrolysate in a controlled laboratory fermentor, which allowed accurate determinations of hydrogen yields and production rates.

Materials and Methods

Preparation of Inoculum

A culture of *C. saccharolyticus* was grown in 100-mL sealed anaerobe serum flasks containing 30 mL of culture medium consisting of 0.9 g/L of NH_4Cl, 1.5 g/L of K_2HPO_4, 0.75 g/L of KH_2PO_4, 0.4 g/L of $MgCl_2{\cdot}6H_2O$, 0.9 g/L of NaCl, 2.5 mg of $FeCl_3{\cdot}6H_2O$, 1 g/L of yeast extract, 0.75 g/L of cysteine-HCl, and 0.5 mg of resazurin. Prior to sterilization at 120°C for 20 min, the medium was flushed with nitrogen gas for 15 min. After sterilization, 0.4 mL of sterile 300 g/L glucose or xylose—when the fermentation was on xylose—solution was aseptically added. The medium was also supplemented with 1 mL of sterile trace element solution containing 1.5 g/L of $FeCl_2{\cdot}4H_2O$, 70 mg/L of $ZnCl_2$, 100 mg/L of $MnCl_2{\cdot}4H_2O$, 6 mg/L of H_3BO_3, 190 mg/L of $CoCl_2{\cdot}6H_2O$, 2 mg/L of $CuCl_2{\cdot}2H_2O$, 24 mg/L of $NiCl_2{\cdot}6H_2O$, 36 mg/L of $Na_2MoO_4{\cdot}2H_2O$, 15 mg/L of Na_2WO, 15 mg/L of $Na_2SeO_3{\cdot}5H_2O$, and 10 mL/L of 25% HCl. The pH of the medium was adjusted to 7.2 by adding a sterile solution of either 1 *M* KOH or 1 *M* HCl. After 1 d of incubation at 70°C, the culture of *C. saccharolyticus* was used for fermentations.

Table 1
Cultivation Conditions for Hydrogen Production by *C. saccharolyticus* Using Various Carbon Sources[a]

Condition	Description
A	10 g/L glucose as carbon source, 10% inoculum
B	10 g/L xylose as carbon source, 10% inoculum
C	6.6 g/L glucose and 1.8 g/L xylose as carbon source, 10% inoculum
D1	PS hydrolysate as carbon source, 20% inoculum
D2	PS hydrolysate as carbon source, 20% inoculum
E	PS hydrolysate as carbon source, 20% inoculum, only yeast extract added

[a] PS, paper sludge.

Preparation of Paper Sludge Hydrolysate

Paper sludge containing about 45% carbohydrates (cellulose and xylan) based on dry matter was obtained from Dunapack Paper and Packaging, Budapest, Hungary. Hydrolysis of paper sludge was performed as described previously *(15)*. The pH of the hydrolysate, containing 12.8 g/L of glucose and 2.4 g/L of xylose, was set to 7.2 by the addition of phosphate buffer containing 1.5 g/L of K_2HPO_4 and 0.75 g/L of KH_2PO_4. The neutralized hydrolysate was cleared from precipitated inorganic salts by centrifuging at 13,200*g* for 10 min. Because of the dilution resulting from the pH adjustment, inoculation, and addition of medium components, the initial concentration of glucose and xylose in the bioreactor was reduced to 6.6 and 1.8 g/L, respectively.

Hydrogen Production in a Bioreactor

Batchwise anaerobic hydrogen production by *C. saccharolyticus* was performed in a 2-L bioreactor using the medium already described. For control experiments nutrients, trace elements and carbon source (glucose, xylose, or mixture of these two) were dissolved in 1 L of deionized water (Table 1). Prior to the addition of starter culture, the production medium was heated to 70°C and sparged with nitrogen gas for 30 min in order to remove any traces of oxygen and ensure anaerobic conditions. The inoculum volume was 10% (v/v). The temperature was controlled at 70°C and the pH was maintained at neutral with 1 *M* KOH corresponding to pH 6.4 at the temperature of the fermentation. *C. saccharolyticus* was cultivated with an agitation rate of 350 rpm. Hydrogen was continuously removed by sparging with nitrogen at a flow rate of 7 L/h. Hydrogen production from the previously neutralized paper sludge hydrolysate was performed similarly to control cultivations except that nutrients and trace elements were directly added to the hydrolysate and the volume of starter culture was

Table 2
Sugar Consumption and Product Formation
for Various Cultivation Conditions Using *C. saccharolyticus*[a]

Condition	Glucose (m*M*)	Xylose (m*M*)	H_2 (m*M*)	Acetate (m*M*)	CO_2 (m*M*)	Lactate (m*M*)	Biomass (g/L)
A	51.1	—	129.5	73.8	70.7	4.0	1.7
B	—	61.7	138.1	72.7	79.3	5.6	1.6
C	34.3	14.5	113.3	63.2	64.8	15.0	1.0
D1	29.0	7.9	132.1	57.7	ND	2.7	ND
D2	37.2	6.1	84.7	49.9	ND	24.5	ND
E	37.2	6.2	87.3	41.0	ND	41.9	ND

[a]ND, not determined.

doubled (*see* Table 1). Samples were withdrawn regularly and analyzed for concentrations of biomass, glucose, xylose, and various organic acids. Calculations presented in Tables 2–4 were based on data obtained at the point at which no additional hydrogen production was achieved.

Analytical Procedures

Changes in biomass concentration throughout the fermentation process were followed by optical density (OD) measurement at 580 nm using an Ultrospec 2000 Spectrophotometer. Quantitative biomass concentration was assayed applying microbiuret cell protein determination *(16)*. Biomass concentration was expressed in grams of dry matter per liter of fermentation broth by assuming a twofold multiplication constant for microbial protein to cell mass. For carbon balance calculations, the elemental composition of *C. saccharolyticus* was assumed to be $CH_{1.8}O_{0.5}N_{0.2}$ (24.6 mg/mmol).

Prior to high performance liquid chromatography (HPLC) samples were centrifuged at 9000*g* for 5 min. Each sample was diluted 1:1 with 1 *M* sulfuric acid containing 250 m*M* propionic acid as internal standard and then passed through a 0.45-µm-pore-size filter. Glucose, xylose, lactic acid, and acetic acid were separated on an Shodex Ionpack KC811 column at 80°C using a 3 m*M* sulfuric acid mobile phase at a flow rate of 1 mL/min. For the detection of various compounds separated on the analytical column, a refractive index detector was used.

Production of hydrogen and CO_2 was monitored on-line using a CP 4900 micro Gas Chromatograph (Varian, Middelburg, The Netherlands) equipped with a thermal conductivity detector and nitrogen as the carrier gas. Hydrogen was determined on a MolSieve MSA^{HI}BF module at constant injector (60°C) and column (80°C) temperature. Analysis of CO_2 was carried out using a Pora Plot Q PPQ^{HI}BF module. The temperature of the injector and the column was kept at 80°C. For some experiments, hydro-

Table 3
Carbon Balances for Various Cultivation Conditions Using *C. saccharolyticus*

Condition	Glucose (m*M* C)	Xylose (m*M* C)	Acetate (m*M* C)	CO_2 (m*M* C)	Lactate (m*M* C)	Biomass (m*M* C)[a]	C-balance (%)[b]
A	306.6	—	147.6	70.7	12.0	68.3	97
B	—	308.5	145.4	79.3	16.8	66.7	99
C	205.8	72.5	126.4	64.8	45.0	39.0	99
D1	174.0	37.0	115.4	57.7	8.1	ND	86
D2	223.2	30.5	99.8	49.9	73.5	ND	88
E	223.2	31.0	82.0	41.0	125.7	ND	98

[a]ND, not determined.
[b]C-balance is shown as m*M* C in products as percentage of m*M* C in substrate.

gen was determined on a second gas chromatograph with an RVS MolSieve 5A (60/80 mesh, 3 m × 1/8 in.) column at 50°C. The temperature of the detector and the injector was 100 and 80°C, respectively. N_2 was used as carrier gas.

Results

Hydrogen Production on Pure Sugars

Prior to utilization of paper sludge hydrolysate for growth and hydrogen production of *C. saccharolyticus*, a set of experiments was carried out using the standard production medium described previously supplemented with analytical-grade sugars as carbon and energy source. Glucose, xylose, and a mixture of these two were applied in various concentrations as described in Table 1. The concentrations of glucose and xylose in the mixture were at the same level as found in the paper sludge hydrolysate (*see* Table 1). As shown in Fig. 1, glucose, xylose, and a mixture of these sugars supported the growth of *C. saccharolyticus*. Sugars were completely utilized by the bacterium. When xylose (condition B) was the sole carbon source present in the medium, consumption of this sugar was somewhat slower than consumption of glucose (condition A). When a mixture of sugars was used as carbon source (condition C), xylose and glucose were taken up simultaneously (Fig. 1). Utilization of sugars resulted in the formation of hydrogen, CO_2, and acetic acid, as expected (Table 2). A low amount of lactate was also produced. The molar lactate yield appeared to be higher on the sugar mixture. Biomass production was higher on single sugars compared with that on the sugar mixture. Of the available carbon source, about 22% of the consumed sugars was used for biomass production in the case of conditions A and B, while only 14% of the sugars was assimilated in cell mass for condition C (Table 3).

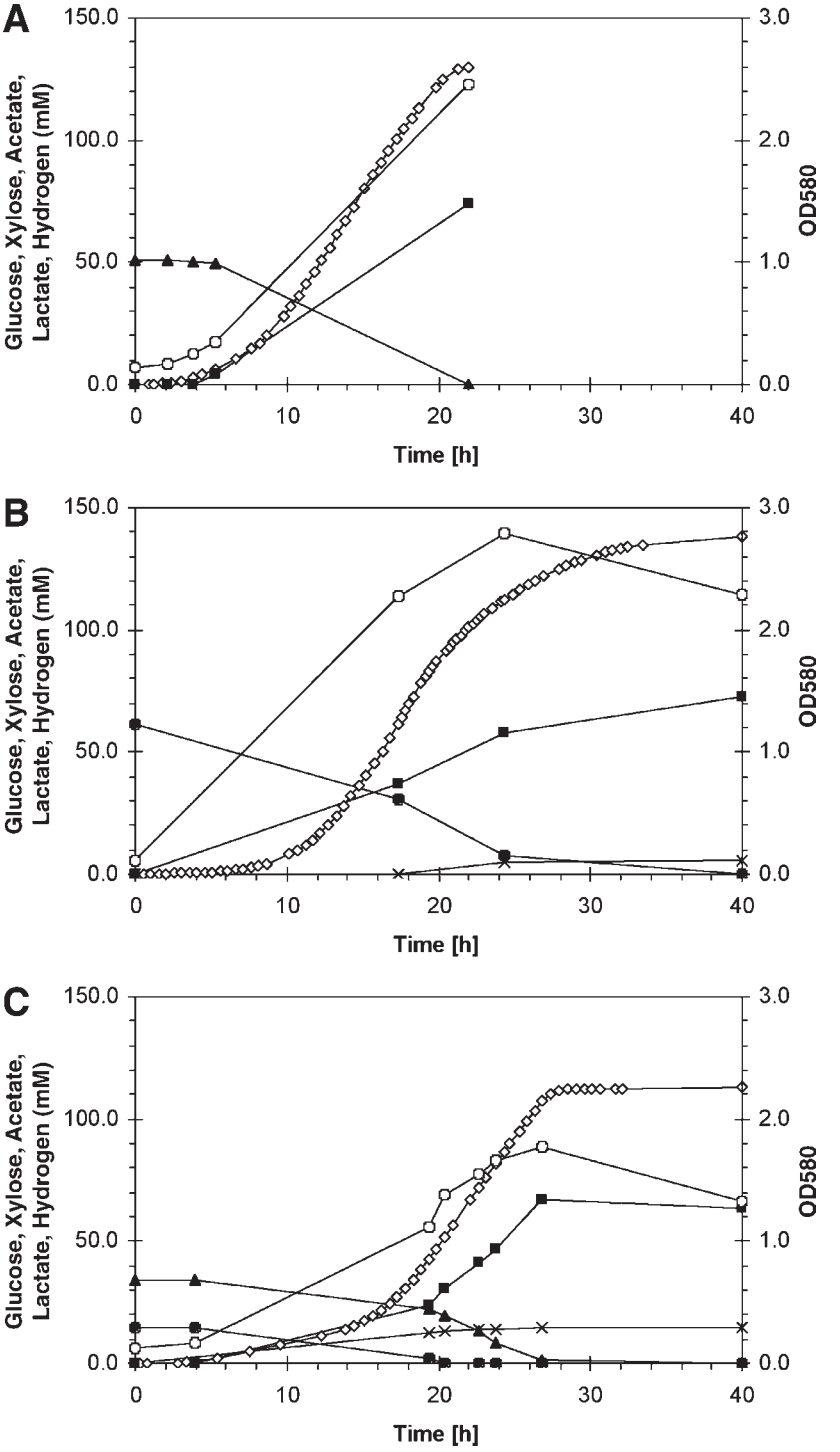

Fig. 1. Hydrogen production by *C. saccharolyticus* using: **(A)** glucose medium; **(B)** xylose medium; and **(C)** glucose and xylose medium. (—◇—), Hydrogen; (—■—), acetate; (—×—), lactate; (—▲—), glucose; (—●—), xylose; (—○—), OD580nm.

Table 4
Hydrogen and Acetate Yields as Percentage of Theoretical Maximum Yield and Maximum Hydrogen Production Rates

Condition	H_2 Yield (%)	Acetate Yield (%)	$r_{H2,max}$ (mmol/[L·h])
A	63	72	10.7
B	67	71	11.3
C	61	68	9.2
D1	94	82	5.3
D2	50	59	6.0
E	52	48	5.3

The carbon balances determined after complete consumption of the sugars are shown in Table 3. All three balances (A, B, and C) could be completed, which shows that no other products were formed from these sugars. The stoichiometry of the glucose fermentation (A) was 2.5 mol of hydrogen and 1.4 mol of acetate/mol of consumed glucose. The xylose fermentation (B) showed a stoichiometry of 2.2 mol of hydrogen and 1.2 mol of acetate/mol of xylose. Taking into account the xylose part, which was used for lactate and biomass production, since no hydrogen is produced during lactate and biomass production , 1 mol of xylose was fermented to 3.1 mol of hydrogen and 1.6 mol of acetate. These yields are close to the theoretical stoichiometry according to the following reaction:

$$3C_5H_{10}O_5 + 5H_2O \rightarrow 5CH_3COOH + 5CO_2 + 10H_2$$

In Table 4 the molar yields of hydrogen and acetic acid are presented as the percentage of the maximum theoretical yields. For conditions A and B, no major differences were observed in yields of hydrogen and acetate. The hydrogen yield was approx 65%. In the case of condition C, hydrogen and acetate yields were only slightly lower. Here, higher lactate formation was compensated by the lower biomass production. Maximal hydrogen production rates were determined for each condition. The rates were in the range of 9.2–11.3 mmol/(L·h) (Table 4).

Hydrogen Production on Paper Sludge Hydrolysate

Fermentation experiments utilizing sugars present in paper sludge hydrolysate were first carried out on complete medium as presented in Materials and Methods. Results on carbohydrate consumption and hydrogen production of two typical fermentations are shown in Table 2 (conditions D1 and D2). Acetate and lactate were the main byproducts.

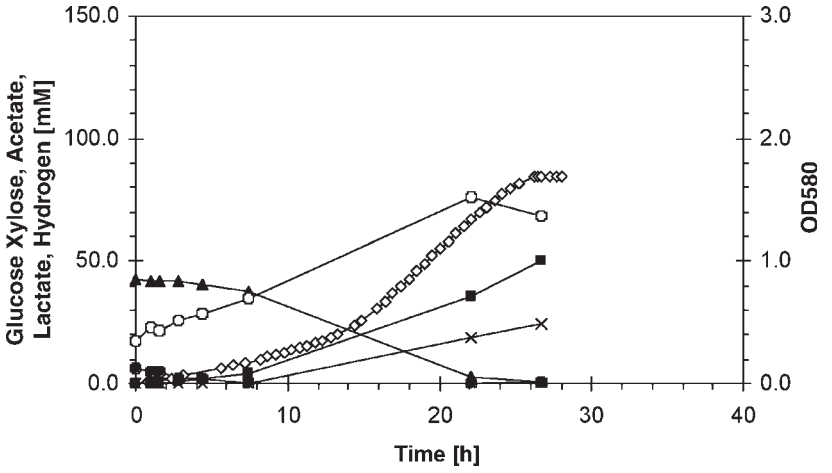

Fig. 2. Hydrogen production by *C. saccharolyticus* using paper sludge hydrolysate. (—◇—), Hydrogen; (—■—), acetate; (—×—), lactate; (—▲—), glucose; (—●—), xylose; (—○—), OD580nm.

Lactic acid formation occurred to a different extent when paper sludge hydrolysate was used. Although the same batch of hydrolysate was used for all experiments under identical conditions, lactate production was observed from the early stage (Fig. 2, condition D2) of the fermentation or lactate was only found in the fermentation broth in the very late phase of the process (condition D1).

Utilization of sugars for hydrogen production was primarily dependent on the pretreatment of the paper sludge hydrolysate. It was observed that insufficient removal of calcium ions originally present in the hydrolysate disturbed the hydrogen production of *C. saccharolyticus*. If calcium ions were not completely removed during pretreatment with phosphate buffer, precipitation of calcium salts occurred at the point of starter culture addition, thereby entirely preventing growth and hydrogen production.

Results on the carbon balances for these fermentation experiments with paper sludge hydrolysate are presented in Table 3. Interference of unidentified components in the hydrolysate with the protein content determination disallowed accurate biomass content determination, resulting in an incomplete mass balance. However, similar OD was measured as observed for the mixture of pure sugars (condition C).

Hydrogen and acetate yields on paper sludge hydrolysate were considerably higher than on pure sugars (Table 4, condition D1). When a shift in metabolism toward lactic acid production occurred (condition D2), acetate and hydrogen yields became significantly lower.

Previous experiments showed that *C. saccharolyticus* did not depend on nutrients for hydrogen production from paper sludge hydrolysate *(15)*.

Therefore, in the next experiments with paper sludge hydrolysate, all nutrients, except yeast extract and cysteine, were omitted from the production medium (condition E). Carbohydrate consumption and hydrogen and acetate production were comparable to the values found on complete medium (condition D2), where also a significant amount of the sugars was converted to lactate (Table 2). In addition, similar hydrogen and acetate yields were found and the maximum hydrogen production rate was comparable (Table 4). However, the molar carbon balance, without the contribution of the biomass, was nearly complete (Table 3), suggesting that in this case other carbon sources in the paper sludge hydrolysate were used.

Discussion

Hydrogen made from renewable energy resources provides a clean, CO_2-neutral energy source. In addition, its use would reduce fossil fuel dependency. Biologic production of hydrogen seems to be a very attractive technology for decentral hydrogen production from wet biomass *(1,4)*. Various waste streams, such as cane juice, corn pulp, tofu-manufacturing residues, rice straw, and bean- and curd-manufacturing waste, are already under investigation for hydrogen production *(5,6)*.

Small-scale fermentation experiments in sealed anaerobic serum flasks carried out with *C. saccharolyticus* have already shown that hydrogen production could be based on enzymatically hydrolyzed paper sludge *(15)*. In the present study, the potential of this hydrolysate for hydrogen production using *C. saccharolyticus* was investigated in controlled bioreactors applying nitrogen sparging to prevent product inhibition by accumulation of hydrogen in the bioreactor. Prior to using paper sludge hydrolysate as carbon source, reference fermentation experiments with pure sugars typically present in such hydrolysates were carried out for comparison (Fig. 1). This way potential inhibition by components present in organic wastes could be demonstrated *(5)*.

On glucose- and xylose-containing culture media, equal amounts of hydrogen, acetate, lactate, and biomass were produced. The yield of hydrogen based on sugars was approx 65% of the theoretical, which was found to be slightly lower than reported for sucrose (74%) *(10)*. A slightly lower yield, 61% of the theoretical was achieved, when a mixture of glucose and xylose was added to the production medium. Maximum production rates of hydrogen obtained were in the range of 9–11 mmol/(L·h) using glucose- and xylose-containing media (Fig. 1). On the other hand, a drastically reduced hydrogen production rate of approx 5.5 mmol/(L·h) was observed for fermentation on paper sludge hydrolysate, possibly owing to unidentified components in the paper sludge. For *C. saccharolyticus* cultivated on sucrose-containing medium, a maximum hydrogen production rate of 8.4 mmol/(L·h) was published in the literature *(16)*, which is very close to the rates observed in our study. *C. saccharolyticus* was able to grow directly on paper sludge hydrolysate supplemented with yeast extract and cysteine

alone. Results were comparable with those of fermentations on complete medium, showing that the requirements for other salts and trace elements is low. Analysis of the consumption of the different sugars showed that preference for xylose utilization was not as obvious as previously reported *(15)*. This may have occurred owing to the lower initial xylose concentration applied in the present study, but this theory needs further research (H. Goorissen, personal communication, 6-11-02).

On paper sludge hydrolysate the formation of lactate occurred inconsistently (Table 2). It is not clear yet what triggered the shift in the metabolism of the cells. Perego et al. *(17)* have found that at high substrate concentrations another metabolic pathway becomes active, which reduces the rates of glucose consumption and hydrogen production in *Enterobacter aerogenes*. According to van Niel et al. *(18)*, lactate and other reduced organic compounds such as ethanol or alanine were produced when reducing equivalents accumulated in the cell.

The aim of the present study was to achieve high hydrogen yields and production rates on paper sludge hydrolysate. Hydrogen production was comparable with production from pure sugars. On paper sludge hydrolysate, higher yields were achieved than on control medium. This is possibly owing to the presence of water-soluble oligosaccharides in the paper sludge hydrolysate, which were not taken into account during our calculations, but which may have been metabolized to hydrogen. The hydrogen production rate on paper sludge hydrolysate was less than observed on pure sugars. From an industrial point of view, higher volumetric production rates are advantageous. Therefore, volumetric productivity needs to be addressed in future studies. Furthermore, future research needs to address the regulation of lactate production during thermophilic hydrogen fermentation.

Acknowledgments

This study was financially supported by the Commission of the European Communities, Quality of Life and Management of Living Resources (project no. QLK5-1999-01267); the Netherlands Organization for International Cooperation in Higher Education (Huygens Program); the Dutch EET Program; and the Fellowship Program of The Netherlands Ministry of Agriculture, Nature Management and Fisheries.

References

1. Benemann, J. (1996), *Nat. Biotechnol.* **14,** 1101–1103.
2. Wünschiers, R. and Lindblad., P. (2002), *Int. J. Hydrogen Energy* **27,** 1131–1140.
3. Gosselink, J. W. (2002), *Int. J. Hydrogen Energy* **27,** 1125–1129.
4. Claassen, P. A. M., van Lier, J. B., Lopez Contreras, A. M., van Niel, E. W. J., Sijtsma, L., Stams, A. J. M., de Vries, S. S., and Weusthuis, R. A. (1999), *Appl. Microbiol. Biotechnol.* **52,** 741–755.
5. Noike, T., Takabatake, H., Mizuno, O., and Ohba, M. (2002), *Int. J. Hydrogen Energy* **27,** 1367–1371.

6. Mizuno, O., Dinsdale, R., Hawkes, F. R., Hawkes, D. L., and Noike, T. (2000), *Bioresour. Technol.* **73,** 59–65.
7. Woodward, J., Mattingly, S. M., Danson, M., Hough, D., Ward, N., and Adams, M. (1996), *Nat. Biotechnol.* **14,** 872–874.
8. Nandi, R. and Sengupta, S. (1998), *Crit. Rev. Microbiol.* **24(1),** 61–84.
9. Schröder, C., Selig, M., and Schönheit, P. (1994), *Arch. Microbiol.* **161,** 460–470.
10. van Niel, E. W. J., Budde, M. A. W., de Haas, G. G., van der Wal, F. J., Claassen, P. A. M., and Stams, A. J. M. (2002), *Int. J. Hydrogen Energy* **27,** 1391–1398.
11. van Ooteghem, S. A., Beer S. K., and Yue P. C. (2002), *Appl. Biochem. Biotechnol.* **98,** 177–189.
12. Noike, T. and Mizuno O. (2000), *Water Sci. Tech.* **42,** 155–162.
13. Claassen, P.A.M., van Groenestijn, J.W., Janssen, A.J.H. van Niel, E.W.J., and Wijffels, R.H. (2000), in *Proceeding of 1st World Conference and Exhibition on Biomass for Energy, Industry and Climate Change Protection*, Palz, W., Spitzer, J., Maniatis, K., Kwant, K., Helm, P., and Grassi, A., eds., ETA-Florance, Italy; WIP-Munich, Germany, pp. 529–532
14. Hallenbeck, P. C. and Benemann, J. R. (2002), *Int. J. Hydrogen Energy* **27,** 1185–1193.
15. Kádár, Z., de Vrije, T., Budde, M., Szengyel, Z., Réczey, K., and Claassen, P. A. M. (2003), *Appl. Biochem. Biotechnol.* **105,** 557–566.
16. Goa, J. (1953), *Scand. J. Clin. Lab. Invest.* **5,** 218–222.
17. Perego, P., Fabiano, B., Ponzano, G. P., and Palazzi, E. (1998), *Bioprocess Eng.* **19,** 205–211.
18. van Niel, E., Claassen, P. A. M., and Stams, A. J. M. (2003), *Biotechnol. Bioeng.* **81,** 255–262.

0273-2289/04/114/0509–0523/$25.00

Optimization of Steam Pretreatment of Corn Stover to Enhance Enzymatic Digestibility

Enikő Varga,[1] Kati Réczey,*[,1] and Guido Zacchi[2]

[1]Department of Agricultural Chemical Technology, Budapest University of Technology and Economics, H-1521 Budapest, Szt. Gellért tér 4, Hungary, E-mail: kati_reczey@mkt.bme.hu; and [2]Department of Chemical Engineering 1, Lund University, PO Box 124, SE-221 00 Lund, Sweden

Abstract

Among the available agricultural byproducts, corn stover, with its yearly production of 10 million t (dry basis), is the most abundant promising raw material for fuel ethanol production in Hungary. In the United States, more than 216 million t of corn stover is produced annually, of which a portion also could possibly be collected for conversion to ethanol. However, a network of lignin and hemicellulose protects cellulose, which is the major source of fermentable sugars in corn stover (approx 40% of the dry matter [DM]). Steam pretreatment removes the major part of the hemicellulose from the solid material and makes the cellulose more susceptible to enzymatic digestion. We studied 12 different combinations of reaction temperature, time, and pH during steam pretreatment. The best conditions (200°C, 5 min, 2% H_2SO_4) increased the enzymatic conversion (from cellulose to glucose) of corn stover more then four times, compared to untreated material. However, steam pretreatment at 190ºC for 5 min with 2% sulfuric acid resulted in the highest overall yield of sugars, 56.1 g from 100 g of untreated material (DM), corresponding to 73% of the theoretical. The liquor following steam explosion was fermented using *Saccharomyces cerevisiae* to investigate the inhibitory effect of the pretreatment. The achieved ethanol yield was slightly higher than that obtained with a reference sugar solution. This demonstrates that baker's yeast could adapt to the pretreated liquor and ferment the glucose to ethanol efficiently.

Index Entries: Corn stover; pretreatment; steam explosion; hydrolysis; bioethanol.

*Author to whom all correspondence and reprint requests should be addressed.

Introduction

The inevitable depletion of the world's fossil energy supply and the increasing greenhouse effect have resulted in an increasing worldwide interest in alternative nonfossil-based sources of energy, including bioethanol. Bioethanol is currently made by large-scale yeast fermentation of glucose or sucrose that is mainly extracted or prepared from sugars or starch-containing crops *(1)*. The world-wide bioethanol production in 2001 was approx 22 billion L *(2)*; however, bioethanol will remain uncompetitive compared with fossil fuels unless a significant reduction in the production cost is achieved.

A potential source for cost-effective ethanol production is lignocellulosic feedstock, because it is available in bulk quantities at a relatively low cost *(3)*. During corn harvesting, the amount of byproducts, such as corn stover and corncobs, is two times higher than the amount of crop *(4)*. This, together with the fact that nearly half of the world's bioethanol production is based on corn, makes corn stover one of the most important agricultural byproducts in every corn-growing country. In the US, more than 216 million tons of corn stover (dry basis) is produced annually *(5)*; its heat value could replace about 40% of the energy content of the US gasoline market *(6)*.

Corn stover, like lignocellulosic materials in general, is resistant to enzymatic hydrolysis, because of both the tight network in the lignocellulose complex and the crystalline structure of the native cellulose. These difficulties can be overcome by employing a suitable pretreatment *(7)*.

Steam pretreatment is an extensively investigated method that is especially used for treatment of several types of wood *(8,9)*. However, the literature on the treatment of herbaceous materials is scarce *(10,11)*. Steam pretreatment effectively enhances the conversion of carbohydrates to ethanol using combined enzymatic hydrolysis and fermentation *(12)*. Several previous studies have shown that impregnation prior to steam pretreatment improves the enzymatic saccharification of both lignocellulosic biomass and softwood *(12)*. However, the addition of external catalyst could be omitted in the case of herbaceous plants, such as rice straw *(13,14)*. The three most important pretreating parameters, which affect the total sugar yields, are the amount of the impregnating agent, such as SO_2 or H_2SO_4; the temperature; and the residence time *(15)*. During steam pretreatment, sugars and other degradation products can be formed from the xylan and the lignin fraction, which may be inhibitory to microorganisms used in the downstream processing *(16–18)*.

The aim of the present study was to apply steam pretreatment to corn stover and investigate the influence of different pretreatment conditions—temperature, residence time, and concentration of H_2SO_4—on sugar yield and the effect of inhibitors on subsequent ethanol yield.

Materials and Method

Experimental Procedure

Figure 1 is a schematic of the experimental procedure used. The ground corn stover was impregnated with H_2SO_4 (0.5 or 2%) and then pretreated

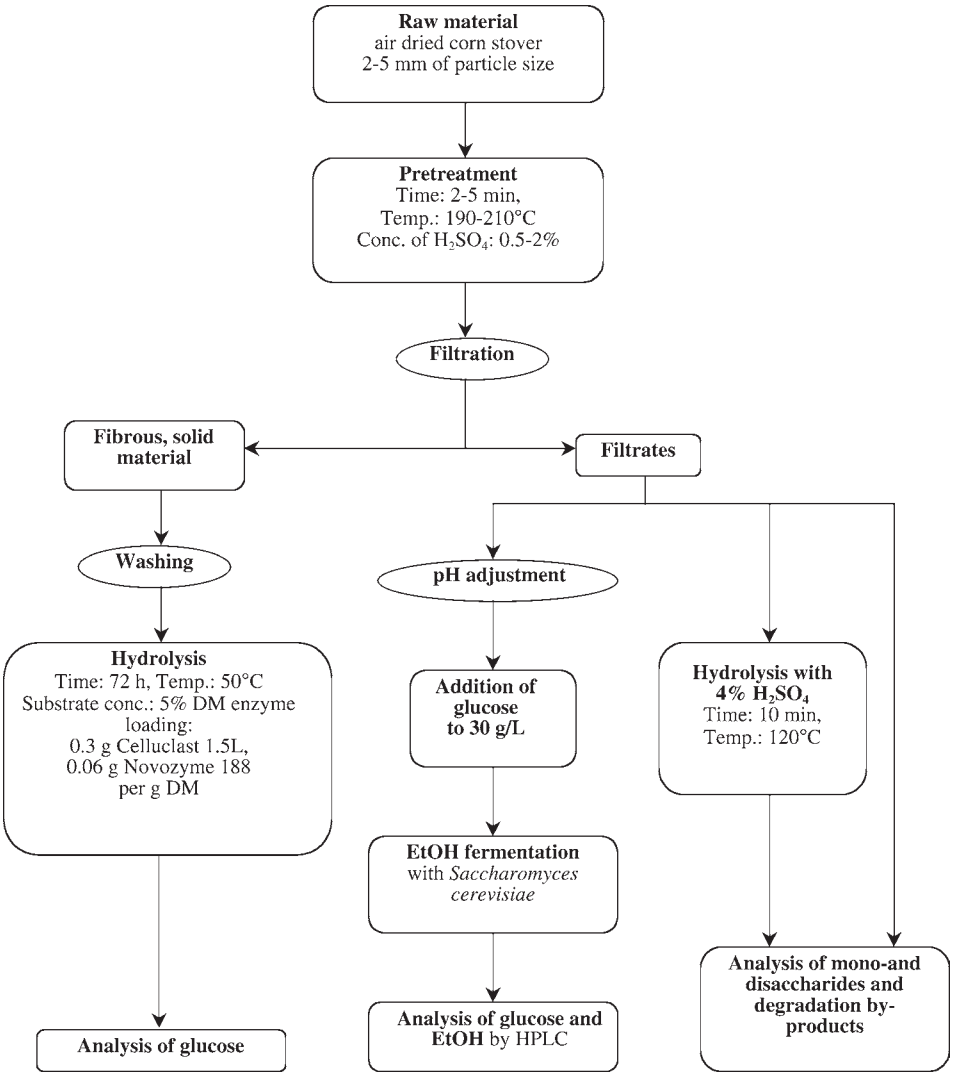

Fig. 1. Schematic procedure for assessment of pretreatment.

with steam at various temperatures (190, 200, and 210°C) and residence times (2 and 5 min). The pretreated material was separated into a solid fibrous fraction and filtrate. The solid residue was washed with distilled water to remove water-soluble components and the insoluble fiber fraction was enzymatically hydrolyzed. A portion of the filtrate was hydrolyzed with H_2SO_4 to determine the amount of released sugars in oligomer form during the pretreatment. Another portion of the filtrate was complemented with glucose and used in a fermentability test with *Saccharomyces cerevisiae* in the form of compressed baker's yeast. Sugar yield and fermentability were used to estimate the optimal pretreatment conditions.

Raw Material

Corn stover was harvested from south Hungary in the fall of 2001. The selected and washed straw was air-dried to an average 90% dry matter (DM) content. The air-dried material was ground and sieved, and the fraction with a particle size of 2–5 mm was used. The composition of this material and also the washed, solid fibrous fraction remaining after pretreatment was determined using Kaar's *(19)* method. To measure the total ash content, approx 0.5 g of dried sample was placed in a crucible, ignited at 550°C for 3 h, cooled in a desiccator, and weighed.

Steam Pretreatment

Corn stover (180 g [DM]) was mixed with 1720 mL of diluted H_2SO_4 or with distilled water and was swollen for one night. Then the material was steam treated in an equipment previously described *(20)*. The pretreatment vessel (2-L volume) was preheated with steam prior to loading the impregnated corn stover. The corn stover was heated by steam to the desired temperature, and when the preset pretreatment time had elapsed, the material was discharged into a flash drum. The material was then separated, by filtration, into a solid fraction and a filtrate. Three variable factors were investigated: the concentration of the H_2SO_4 (0.5 and 2%), the reaction temperature (190, 200, and 210°C), and the reaction time (2 and 5 min). Each experiment was performed in duplicate and the order of experiments was randomized. After the pretreatments, the samples were separated into a liquid and a solid fraction, and both fractions were analyzed. Both the filtrates and the separated solid fraction were stored frozen (–20°C) for further analysis, including enzymatic hydrolysis and fermentability testing.

Determination of Poly- and Monosaccharides (High-Performance Liquid Chromatography)

The sugars in the liquid after pretreatment are partly obtained in oligomer form. To convert the residual oligosaccharides to mono- and disaccharides, the samples were hydrolyzed with 4% H_2SO_4 at 121°C for 10 min. To determine the potential sugar degradation during the acid hydrolysis, the experiments were carried out in triplicate, and known amounts of monosaccharides were added to one of the hydrolysate samples.

The amount of mono- and disaccharides released (glucose, xylose, cellobiose, and arabinose) by pretreatment utilizing acid and enzymatic hydrolysis was analyzed by high-performance liquid chromatography (HPLC) (Shimadzu, Kyoto, Japan), using an Aminex HPX-87H column with a matching precolumn (Bio-Rad, Hercules, CA) at 65°C. The eluent was 5 m*M* H_2SO_4 at a flow rate of 0.5 mL/min with detection by refractive index.

For yield calculations, the measured amount of xylose and arabinose was used as a measure of the hemicellulose fraction, while the cellulose fraction was calculated from the amount of glucose and cellobiose.

Enzymatic Hydrolysis

The pretreated, washed, solid materials were enzymatically hydrolyzed to determine the efficiency of cellulose conversion. The fibrous material was diluted to 5% (DM) using 0.5 *M* acetate buffer (pH 4.8). Hydrolysis was performed in 250-mL shake flasks using a total working weight of 150 g. Hydrolysis was carried out in duplicate at 50°C for 72 h, and the flasks were agitated at 300 rpm in a shaker incubator (LAB-Therm; Kühner, Birsfeldon, Switzerland). Commercially available enzyme solution, Celluclast 1.5L (cellulase from *Trichoderma reesei*) and Novozym 188 (β-glucosidase; Novozymes A/S, Bagsværd, Denmark), were applied in the enzymatic hydrolysis. The enzyme activity of Celluclast 1.5L was 82 filter paper units (FPU)/g, the β-glucosidase activity of Novozyme 188 was 450 IU/g, and the enzyme loading applied was 0.3 and 0.06 g/g of DM, respectively.

To determine the time required for total hydrolysis, the samples were hydrolyzed for 72 h. Samples were taken after 0, 1, 2, 3, 4, 5, 6, 7, 8, 12, 24, 48, and 72 h. The samples were centrifuged at 1400*g* for 10 min, and the composition of monosaccharides was analyzed by HPLC. The percentage of cellulose enzymatically converted to glucose (ECC) was calculated as a quotient of liberated glucose (g) during the hydrolysis and weight of cellulose (g) before enzymatic hydrolysis. The ECC value based on the glucose concentration measured by HPLC was calculated as follows:

$$\mathrm{ECC} = \frac{c \cdot V}{m \cdot 1.11} \cdot 100\% \qquad (1)$$

in which c is the concentration of D-glucose after enzymatic hydrolysis (g/L), V is the total volume (L), and m is the weight of cellulose before enzymatic hydrolysis (g). The factor 1.11 converts the cellulose concentration to the equivalent glucose concentration.

Measurement of Enzyme Activity

The activity of the cellulytic enzymes was measured as filter paper activity units. A 1 × 6 cm strip of Whatman No. 1 filter paper was added to a total volume of 1.5 mL of enzyme solution containing 0.05 *M* citrate buffer, pH 4.8. All enzyme activity measurements were carried out in triplicate. The samples were incubated for 1 h at 50°C. Reducing sugars were determined after stopping the hydrolysis by adding 3 mL of dinitrosalicylic acid solution followed by boiling for 5 min. After cooling, 20.0 mL of distilled water was added and the absorbance was read at 540 nm *(21)*.

β-Glucosidase activity was measured by incubating the enzyme solution with 10 μ*M* *p*-nitrophenyl-β-D-glucopyranoside and 0.05 *M* citrate buffer, pH 4.5, at 50°C for 10 min. The reaction was stopped by adding 0.1 *M* Na_2CO_3, and the liberated *p*-nitrophenol was measured spectrophotometrically at 400 nm. One unit of activity was defined as the release of 1 μmol of *p*-nitrophenol/min *(22)*.

Table 1
Amount of Solids and Yield of Various Components in Solid Fraction
After Steam Pretreatment, Expressed as g/100 g of Dry, Untreated Corn Stover

Pretreatment conditions			Components in solid fraction[b]					
Temperature (°C)	Acid conc.[a] (%)	Time (min)	Total amount of solid	Lignin	Glucose	Xylose	Arabinose	Ash
Raw material			100.0	20.2 ± 0.2	41.6 ± 0.3	27.7 ± 0.4	3.6 ± 0.0	4.6 ± 0.0
190	0.5	2	69.4 ± 2.3	18.5 ± 0.5	33.3 ± 0.5	14.3 ± 0.7	1.0	1.7
		5	62.5 ± 2.1	17.4 ± 0.3	29.6 ± 0.5	11.9 ± 0.6	0.3	1.7
	2	2	48.4 ± 2.8	16.6 ± 0.6	24.3 ± 0.4	3.8 ± 0.8	0.1	2.1
		5	49.1 ± 1.3	19.1 ± 0.2	24.2 ± 0.3	1.4 ± 0.5	0.0	2.2
200	0.5	2	67.7 ± 1.7	19.5 ± 0.1	32.9 ± 0.2	9.4 ± 0.4	0.0	2.7
		5	65.3 ± 0.7	19.5 ± 0.4	32.6 ± 0.3	8.5 ± 0.5	0.0	3.9
	2	2	50.1 ± 1.1	17.9 ± 0.2	24.1 ± 0.4	4.5 ± 0.3	0.1	2.8
		5	41.1 ± 0.4	19.1 ± 0.3	20.0 ± 0.1	1.1 ± 0.4	0.0	2.2
210	0.5	2	61.4 ± 1.4	19.2 ± 0.4	30.7 ± 0.3	6.4 ± 1.1	0.0	2.4
		5	58.2 ± 0.7	18.8 ± 0.2	30.2 ± 0.2	5.7 ± 0.6	0.1	2.6
	2	2	41.2 ± 0.9	18.4 ± 0.2	17.4 ± 0.3	2.3 ± 0.2	0.0	2.8
		5	36.9 ± 0.7	19.4 ± 0.1	13.9 ± 0.1	0.7 ± 0.1	0.0	2.2
210	—	5	85.4 ± 1.5	19.7 ± 0.5	38.6 ± 0.2	21.6 ± 0.4	2.7	2.2

[a] Conc., concentration.
[b] Main value ± errors.

Fermentation

The liquid fractions after pretreatment were fermented using baker's yeast (Jästbolaget AB, Rotebro, Sweden) to determine the toxicity of the samples. Fermentation was carried out in 25-cm^3 glass flasks, sealed with rubber stoppers and equipped with cannulas for removal of produced broth CO_2. The volume of the fermentation broth was 20 cm^3 (18.5 cm^3 of filtrate, 0.5 cm^3 of nutrients, and 1 cm^3 of inoculum).

The filtrates were adjusted to pH 5.5 with 10 *M* NaOH solution and supplemented with glucose to a total concentration of 30 g/L, and with nutrients to a final concentration of 2.5 g/L of yeast extract, 0.25 g/L of $(NH_4)_2HPO4$, 0.025 g/L of $MgSO_4 \cdot 7H_2O$, and 0.1 g/L of NaH_2PO_4. Glucose was added, since the purpose of the fermentation was to investigate the effect of inhibitors on fermentation. The filtrates were inoculated with compressed baker's yeast to a cell concentration of 3 g of DM/L, incubated at 30°C, and stirred with a magnetic stirrer. Reference fermentations, using a pure sugar solution containing 30 g/L of glucose, nutrients, and cells, were run for comparison. Samples were withdrawn from the fermentation broth at the start; before the addition of yeast; and after 1, 2, 4, 6, 8, and 10 h, and a final sample was taken after 20 h. All samples were analyzed for glucose and ethanol by HPLC.

Results and Discussion

Pretreatment

After steam pretreatment the yield of solid material ranged from 37 to 85.4 g/100 g and decreased with increased acid concentration at the same temperature (*see* Table 1). The reduction in solid material was owing to the solubilization and/or degradation of hemicellulose and extractives. However, under more severe conditions, a part of the cellulose was also solubilized.

Table 1 summarizes the composition of the solid fibrous fractions after pretreatment, and Table 2 provides the amount of dissolved compounds in the filtrate from 100 g of untreated corn stover. As expected, steam pretreatment preferentially attacked the hemicellulose fraction; the harsher the pretreatment conditions, the higher amount of hemicellulose was solubilized. Under the harshest conditions (210°C, 2% [w/w] H_2SO_4, 5 min), almost all hemicellulose was removed from the solid fraction, its amount decreased from 31.3 to 0.7 g. However, the solubilization of hemicellulose was significant, about 85%, also at the lowest temperature (190°C) using 2% H_2SO_4. The concentration of H_2SO_4 had a greater effect on the decrease in the hemicellulose fraction in the solid residues than the temperature (Tables 1 and 2). Without the addition of H_2SO_4, even at 210°C for 5 min, the pretreatment solubilized only 20% of the hemicellulose, while 0.5% H_2SO_4 decreased the hemicellulose content by 82%. It seems that acid hydrolysis is the main mechanism involved, which was also supported by our previous work, in which corn stover was pretreated with 1% H_2SO_4 at

Table 2
Sugar Yields in Liquid After Steam Pretreatment, Expressed as g/100 g of Dry, Untreated Corn Stover and Concentration of Byproducts (g/L)

Pretreatment conditions			Components in solid fraction						
							Concentration (g/L)		
Temperature (°C)	Acid conc. (%)[a]	Time (min)	Cellobiose	Glucose	Xylose	Arabinose	Acetic acid	HMF	Furfural
190	0.5	2	0.3	3.3 ± 0.0	9.2 ± 0.2	1.7 ± 0.0	0.7	0.1	0.4
		5	0.6	6.2 ± 0.2	12.5 ± 0.2	1.9 ± 0.0	1.0	0.1	0.7
	2	2	0.2	9.9 ± 0.2	16.6 ± 0.3	3.2 ± 0.1	2.4	0.2	2.7
		5	0.5	12.8 ± 0.3	18.3 ± 0.4	3.0 ± 0.1	1.8	0.1	1.5
200	0.5	2	0.5	3.9 ± 0.0	11.8 ± 0.2	1.8 ± 0.0	1.1	0.1	0.9
		5	0.4	2.5 ± 0.0	10.7 ± 0.2	1.6 ± 0.0	1.5	0.1	0.8
	2	2	0.5	7.4 ± 0.1	13.8 ± 0.3	2.3 ± 0.0	1.6	0.2	1.5
		5	0.3	12.9 ± 0.2	16.3 ± 0.3	2.7 ± 0.0	2.1	0.3	2.6
210	0.5	2	0.3	3.6 ± 0.0	12.7 ± 0.2	1.7 ± 0.0	1.2	0.1	1.0
		5	0.4	4.5 ± 0.1	13.8 ± 0.3	2.1 ± 0.0	1.7	0.2	1.7
	2	2	0.3	12.8 ± 0.2	13.3 ± 0.2	2.6 ± 0.1	2.2	0.3	2.6
		5	0.3	16.2 ± 0.2	13.7 ± 0.2	3.1 ± 0.1	3.4	0.5	4.6
210	—	5	0.3	1.0 ± 0.05	5.5 ± 0.1	1.1 ± 0.0	0.7	0.1	0.2

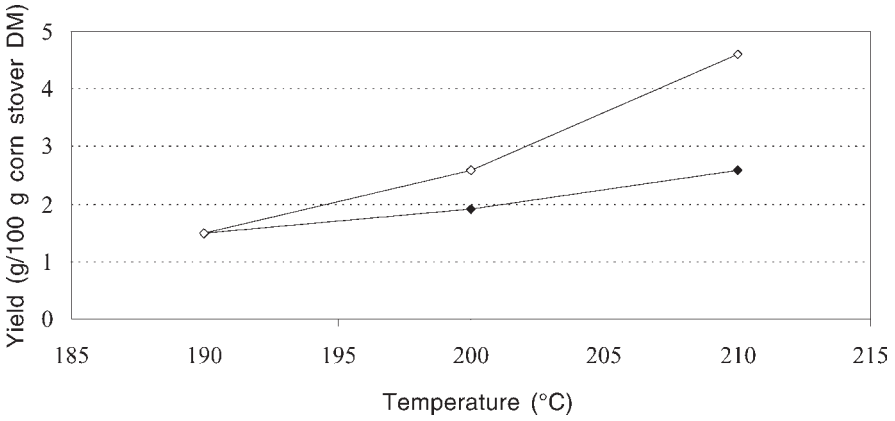

Fig. 2. Amount of formed furfural during pretreatment as a function of reaction temperature and time (2 [◆] and 5 min. [◇] using 2% H_2SO_4).

120ºC and the hemicellulose content decreased by 76% *(23)*. For calculation of the amount of hemicellulose, the amount of mono- and disaccharides (xylose and arabinose) in the liquid was measured by HPLC following the strong acid hydrolysis by Hägglund.

Two percent H_2SO_4 was also effective in solubilizing cellulose from the solid material. Even at the lowest temperature (190°C), the cellulose content in the solid fraction decreased by 50%, from 41.6 to 24.3 g. Solubilization and/or degradation of the lignin during steam pretreatment was not significant. The amount of lignin decreased only slightly from 20.2 to 18.4 g, even under the harshest conditions (210°C, 5 min, 2% H_2SO_4).

The amount of the formed byproducts (acetic acid, furfural, and hydroxymethylfurfural [HMF]) during pretreatment increased with increased temperature and reaction time. Figure 2 shows the formation of furfural as a function of temperature at different pretreatment times. The tendency was similar for all byproducts.

The recovery of both hemicellulose and cellulose sugars is an important point for a suitable pretreatment. The recovery of cellulose and hemicellulose was calculated to estimate their losses during steam pretreatment at different conditions (Table 3). Calculation according to the following equations was based on the mass balance (Tables 1 and 2).

Recovery of cellulose (%) =

$$\frac{\left[\text{cellulose in solid residue (g)} + \left(\text{released glucose in filtrate (g)}/1.11\right)\right]}{\text{cellulose in untreated corn stover (g)}} \quad (2)$$

Table 3
Recovery (%) of Cellulose and Hemicellulose

Pretreatment conditions			Recovery %		
Temperature (°C)	Acid concentration (%)	Time (min)	Cellulose	Hemicellulose	All sugars
190	0.5	2	88.8	83.8	86.6
		5	83.4	80.6	86.5
	2	2	89.7	75.7	79.7
		5	83.1	72.4	82.5
200	0.5	2	89.7	73.5	82.8
		5	85.3	66.5	77.2
	2	2	76.9	65.9	72.2
		5	74.2	64.1	69.9
210	0.5	2	83.2	66.5	76.1
		5	84.2	69.2	77.7
	2	2	73.5	58.0	66.8
		5	73.1	55.9	65.7
210	—	5	95.9	93.8	97.2

$$\text{Recovery of HC (\%)} = \frac{\left[\text{HC in solid residue (g)} + \left(\text{released xylose + arabinose in filtrate (g)}/1.14\right)\right]}{\text{HC in untreated corn stover (g)}} \quad (3)$$

in which HC is hemicellulose. The amount of HC in the solid residue was calculated from the amount of xylose and arabinose in the filtrate following Hägglund's hydrolysis.

Table 3 shows that mainly the hemicellulose was converted and/or degraded in the steam pretreatment. About 60% of the original hemicellulose could be recovered, except when 2% H_2SO_4 was combined with high reaction temperature (210°C). In this case, the hemicellulose recovery was only 55.9%. This relatively low recovery could be explained by the hemicellulose degradation to other byproducts during steam pretreatment.

The maximal recovery of hemicellulose (83.8%) was obtained following the mildest pretreatment at 190°C for 2 min using 0.5% H_2SO_4. The harsher the conditions, the lower the hemicellulose recovery was reached. The maximum cellulose recovery was 89.7%, following steam pretreatment at 200°C, but the recovery was sufficient, about 75%, even at 210°C. Cellulose and hemicellulose exhibited maximum recovery at different conditions, which was also found in other studies *(24,25)*. However, in the case of softwood, the hemicellulose solubilization needed harsher pretreatment conditions than corn stover, and the maximum mannose yield from wood was obtained at between 200 and 210°C *(26)*.

The concentration of H_2SO_4 affected the recovery of cellulose significantly. Using less concentrated H_2SO_4 (0.5%), the recovery of cellulose was approx 10% higher than using 2% H_2SO_4 at the same temperature and time.

The overall recovery of all sugars varied from 79 to 86% at 190°C and from 65 to 77% at 210°C, which was a bit lower than achieved with corn stover using wet oxidation *(27)*.

Enzymatic Hydrolysis

The pretreated solid residue was enzymatically hydrolyzed to determine the degree of cellulose conversion to glucose (ECC%), which is valuable information about the effectiveness of the pretreatment. Hydrolysis at 50°C with the applied relative high enzyme loading was completed after 24 h, as was also found in a previous study *(27)*. The achieved conversion after 48 h of enzymatic hydrolysis is presented in Table 4. The enzymatic conversion of pretreated cellulose was between 31 and 83% compared with 27% obtained with enzymatic hydrolysis of untreated corn stover. To verify the pretreatment effect of the freezing-thawing period, a portion of the raw material was also frozen and then hydrolyzed. The achieved enzymatic conversion was not signficantly higher (29.2%) in this case.

Considering that the pretreatment without addition of H_2SO_4 only slightly modified the composition of corn stover (Table 1), it is not sur-

Table 4
ECC% Conversion After 48 h of Enzymatic Hydrolysis and Amounts of Released Glucose (g) from 100 g of Untreated Material (DM) During Pretreatment and Hydrolysis

Pretreatment conditions			During the hydrolysis			During hydrolysis and pretreatment	
Temperature (°C)	Acid conc. (%)[a]	Time (min)	ECC (%)	Released glucose (g)	Released xylose (g)	Total released glucose (g)	Total sugars (g)
Raw material			27.3	12.5	0.2	12.5	12.7
Freezed raw material			29.2	13.4	0.2	13.5	13.9
190	0.5	2	47.4	17.4	0.3	20.7	31.9
		5	52.2	17.0	0.2	23.2	35.8
	2	2	71.8	19.2	0.2	29.1	49.1
		5	81.1	21.6	0.5	34.3	56.1
200	0.5	2	58.4	21.1	0.5	25.0	39.2
		5	65.7	23.6	0.5	26.0	38.8
	2	2	65.8	17.4	0.5	24.9	41.4
		5	83.6	18.4	0.3	31.3	50.5
210	0.5	2	67.2	22.7	0.3	26.3	41.0
		5	74.8	24.8	0.4	29.3	45.6
	2	2	74.0	14.2	0.3	27.0	43.3
		5	78.8	12.0	0.3	28.3	45.3
210	—	5	31.1	13.2	0.4	14.2	21.2

[a] Conc., concentration.

prising that the ECC after this pretreatment was quite poor (31.1%). The highest conversion (83.6%) was achieved with a pretreatment at 200°C for 5 min with 2% H_2SO_4. The ECC conversions in general were higher following pretreatment using 2% H_2SO_4, than 0.5% H_2SO_4, but the amounts of released glucose by enzymatic hydrolysis were still higher using less concentrated H_2SO_4. This could be explained by the higher solubilization of cellulose during pretreatment. The highest amount of total released glucose (34.3 g/100 g of DM) was achieved following pretreatment at 190°C for 5 min with 2% H_2SO_4.

Although most cellulase enzyme complexes, including Celluclast, contain xylanase activity (data not shown), the amount of released xylose after enzymatic hydrolysis was negligible, especially compared with the amount of released xylose after pretreatment.

The highest overall sugar yield after both pretreatment and enzymatic hydrolysis, 56.1 g/100 g of DM, was also obtained at 190ºC, for 5 min with 2% H_2SO_4.

Fermentability Test

Ethanol production depends not only on the sugar yield, but also on the fermentability of the solution. To investigate the fermentability of the pretreated corn stover, fermentations were performed with baker's yeast. Baker's yeast has often been proposed as the best organism for the fermentation of lignocellulosic hydrolysates *(28,29)* and has the advantages that it is quite robust and was found to be less sensitive to inhibitors than cultivated yeast *(30,31)*.

Table 5 shows the achieved ethanol concentrations after 24 h of fermentation and the calculated ethanol yield as percent of theoretical. After 1 d of fermentation the ethanol concentrations varied from 12.1 to 13.8 g/L, corresponding to 78.4 and 90.3% of the theoretical yield. Glucose was totally consumed after 6 h of fermentation following pretreatment with 0.5% H_2SO_4. The maximum ethanol concentration was also reached after 6 h in these cases, but when 2% H_2SO_4 was used in pretreatment, glucose was consumed more slowly and the formation of ethanol needed more time. However, even in these cases the achieved ethanol yield was about 85% of the theoretical. These results are quite similar to those achieved after fermentation of wet oxidized wheat straw in a previous study *(17)*.

Conclusion

This study shows that steam pretreatment is an efficient method to increase the enzymatic accessibility of the water-insoluble, cellulose-rich component in corn stover. After pretreatment, the enzymatic conversion from cellulose to glucose increased nearly four times, compared to the untreated corn stover.

The best pretreatment conditions for obtaining high conversion of cellulose to glucose were 200°C for 5 min after swelling the fibers with 2%

Table 5
Ethanol Yield (%) of Theoretical and Achieved Ethanol Concentration (g/L) After 24 h of Fermentation at 30°C with Baker's Yeast from 30 g/L of Glucose Solution

Pretreatment Conditions				
Temperature (°C)	Acid concentration (%)	Time (min)	EtOH concentration (g/L)	Ethanol yield (%)
Control			12.9	84.0
190	0.5	2	13.2	86.0
		5	13.4	87.5
	2	2	13.3	87.3
		5	12.1	78.4
200	0.5	2	13.4	87.8
		5	13.7	89.7
	2	2	13.0	85.2
		5	13.7	89.4
210	0.5	2	13.8	90.3
		5	13.8	90.1
	2	2	13.5	88.4
		5	13.1	85.6
210	—	5	13.6	89.2

H_2SO_4. Most of the hemicellulose was dissolved during the pretreatment, and approx 60% of the original hemicellulose could be recovered. Enzymatic hydrolysis at 50°C was completed after 24 h, and the highest enzymatic conversion from cellulose to glucose was above 80%, corresponding to 18 g of glucose/100 g of untreated solid material. However, the highest overall yield of sugars was 56.1 g from 100 g of untreated material DM, corresponding to 73% of the theoretical, which was achieved following steam pretreatment at 190°C for 5 min with 2% H_2SO_4.

The fermentability of the solution gave good results. The achieved ethanol yields were about 90%, slightly above those obtained with a reference sugar solution, showing that baker's yeast could adapt to the pretreated liquor and ferment the glucose to ethanol without problems.

References

1. Lyons, T. P., Kelsall, D., and Murtagh, J., eds. (1995), *The Alcohol Textbook*, Nottingham University Press, Nothingam, UK.
2. Mielenz, J.R. (2001), *Curr. Opin. Microbiol* **4,** 324–329.
3. Von Sivers, M. and Zacchi, G., (1996), *Bioresour. Technol.* **56,** 131–140.
4. Hungarian Central Statistical Office. (2001), *Statistical Annual Reviews of the Hungarian Agriculture*, Hungarian Central Statistical Office, Budapest, Hungary.
5. Sokhansanj, S., Turhollow, A., Cushman, J., and Cundi, J., (2002), *Biomass Bioenergy* **23,** 347–355.

6. Sun, Y. and Cheng, J., (2002), *Bioresour. Technol.* **83,** 1–11.
7. Elshafei, A. M., Vega, J. L., Klasson, K. T., Clausen, E. C., and Gaddy, J. L. (1991), *Bioresour. Technol.* **35,** 73–80.
8. Brownell, H. H. and Saddler, J. N. (1984), *Biotechnol. Bioeng. Symp.* **14,** 55–68.
9. Clark, T. A. and Mackie, K. L. (1987), *J. Wood Chem. Technol.* **7(3),** 373–403.
10. Schmidt, A. S., Puls, J., and Bjerre, A.B., (1996), in *Biomass for Energy and Environment Proceedings of the 9th European Bioenergy Conference*, vol. 3, Chartier, P., Ferrero, G. L., Henius, U. M., Hultberg, S., Sachau, J. and Wiinbland, M., eds. Pergamon, Oxford, UK, pp. 1510–1515.
11. Esteghlalian, A., Hashimoto, A. G., Fenske, J. J., and Penner, M. H. (1997), *Bioresour. Technol.* **59,** 129–136.
12. Saddler, J. N., Ramos, L. P., and Breuil, C. (1993), in *Bioconversion of Forest and Agricultural Plant Residues*. C.A.B. International, Wallingford, UK, pp. 73–91.
13. Ballesteros, I., Oliva, J. M., Negro, M. J., Manzanares, P., and Ballesteros, M. (2002), *Process Biochem.* **38,** 187–192.
14. Vlasenko, E. Y., Ding, H., Labavitch, J. M., and Shoemaker S. P. (1997), *Bioresour. Technol.* **59,** 109–119.
15. Stenberg, K., Tenborg, C., Galbe, M., and Zacchi G. (1998), *Appl. Biochem. Biotechnol.* **71,** 299–308.
16. Delgenes, J. P., Moletta, R., and Navarro, J. M. (1996), *Enzyme Microb. Technol.* **19(3),** 220–225.
17. Klinke, H. B., Ahring, B. K., Schmidt, A. S., and Thomsen, A. B. (2002), *Bioresour. Technol.* **82(1),** 15–26.
18. Palmqvist, E., Hahn-Hägerdal, B., Galbe, M., and Zacchi, G. (1999), *Enzyme Microb. Technol.*, **19(6),** 470–476.
19. Karr, W. E., Cool, L. G., Marriman, M. M., and Brink, D. L. (1991), *J. Wood Chem. Technol*. **11,** 447–463.
20. Eklund, R., Galbe, M., and Zacchi, G. (1988), *J. Wood Chem. Technol.* **8(3),** 379–392.
21. Mandels, M., Andreotti, R., and Roche, C. (1976), *Biotechnol. Bioeng. Symp.* **6,** 21–33.
22. Berghem, L. E. R. and Petterson, L. G. (1974), *Eur. J. Biochem.* **46,** 295–305.
23. Varga, E., Szengyel, Z., and Réczey, K. (2002), *Appl. Biochem. Biotechnol.* **98–100,** pp. 73–87.
24. Garrote, G., Dominguez, H., and Parajó, J. C. (2002), *Process Biochem.* **37,** 1067–1073.
25. Tenborg, C., Stenberg, K., Galbe, M., Zacchi, G., Larsson, S., Palmquist, E., and Hahn-Hägerdal, B. (1998), *Appl. Biochem. Biotechnol.* **70–72,** 3–15.
26. Larsson, S., Palmquist, E., Hahn-Hägerdal, B., Tenborg, C., Stenberg, K., Zacchi, G., and Nilvebrant, N. O. (1999), *Enzyme Microb. Technol.* **24,** 151–158.
27. Varga, E., Schmidt, A. S., Réczey, K., and Thomsen, A. B. (2002), *Appl. Biochem. Biotechnol.* **104,** 37–49.
28. Olsson, L. and Hahn-Hägerdal, B. (1993), *Proc. Biochem.* **28,** 249–257.
29. Hahn-Hägerdal, B., Lindén, T., Senac, T., and Skoong, K. (1991), *Appl. Biochem. Biotechnol.* **28/29,** 131–134.
30. Stenberg, K., Bollók, M., Réczey, K., Galbe, M., and Zacchi, G. (2000), *Biotechnol. Bioeng.* **68,** 204–210.
31. Stenberg, K., Galbe, M., and Zacchi, G. (2000), *Enzyme Microb. Technol.* **26,** 71–79.

0273-2289/04/114/0525–0538/$25.00

Selection of Anion Exchangers for Detoxification of Dilute-Acid Hydrolysates from Spruce

Ilona Sárvári Horváth,[1,2] Anders Sjöde,[3] Nils-Olof Nilvebrant,[3] Andrei Zagorodni,[4] and Leif J. Jönsson[*,1]

[1]Biochemistry, Division for Chemistry, Karlstad University, SE-651 88 Karlstad, Sweden, E-mail: Leif.Jonsson@kau.se; [2]Institute of Chemical Engineering and Environmental Sciences, Department of Chemical Reaction Engineering, Chalmers University of Technology, SE-412 96 Göteborg, Sweden; [3]STFI AB, Swedish Pulp and Paper Research Institute, PO Box 5604, SE-114 86 Stockholm, Sweden; and [4]Department of Material Science and Engineering, Royal Institute of Technology, KTH, SE-100 44 Stockholm, Sweden

Abstract

Six anion-exchange resins with different properties were compared with respect to detoxification of a dilute-acid hydrolysate of spruce prior to ethanolic fermentation with *Saccharomyces cerevisiae*. The six resins encompassed strong and weak functional groups as well as styrene-, phenol-, and acrylic-based matrices. In an analytical experimental series, fractions from columns packed with the different resins were analyzed regarding pH, glucose, furfural, hydroxymethylfurfural, phenolic compounds, levulinic acid, acetic acid, formic acid, and sulfate. An initial adsorption of glucose occurred in the strong alkaline environment and led to glucose accumulation at a later stage. Acetic and levulinic acid passed through the column before formic acid, whereas sulfate had the strongest affinity. In a preparative experimental series, one fraction from each of six columns packed with the different resins was collected for assay of the fermentability and analysis of glucose, mannose, and fermentation inhibitors. The fractions collected from strong anion-exchange resins with styrene-based matrices displayed the best fermentability: a sevenfold enhancement of ethanol productivity compared with untreated hydrolysate. Fractions from a strong anion exchanger with acrylic-based matrix and a weak exchanger with phenol-based resin dis-

*Author to whom all correspondence and reprint requests should be addressed.

played an intermediate improvement in fermentability, a four- to fivefold increase in ethanol productivity. The fractions from two weak exchangers with styrene- and acrylic-based matrices displayed a twofold increase in ethanol productivity. Phenolic compounds were more efficiently removed by resins with styrene- and phenol-based matrices than by resins with acrylic-based matrices.

Index Entries: *Saccharomyces cerevisiae*; anion-exchange resins; hydrolysate; fermentability.

Introduction

Dilute-acid hydrolysis is the oldest technology for converting lignocellulose-based biomass to ethanol *(1)*. After many years of research and development, the dilute-acid process has evolved into a general concept in which hydrolysis occurs in two stages to maximize sugar yields from the hemicellulose and cellulose fractions of the biomass *(2,3)*. The liquid hydrolysates from each stage are recovered and then fermented to ethanol. Because of the complex structure of lignocellulose, high temperature and/or addition of acid is used to liberate the monosaccharides. Under these conditions, other compounds will be formed in addition to the fermentable sugars. Several of these byproducts are known to inhibit the following fermentation step.

The fermentation inhibitors include furan aldehydes, aliphatic acids, and phenolic compounds. The furan aldehydes, furfural, and hydroxymethyl furfural (HMF), are formed from pentoses and hexoses, respectively *(4,5)*. Several studies indicate that furfural inhibits *Saccharomyces cerevisiae*, at least when present in high concentrations *(6–10)*. HMF has a similar effect *(11,12)*.

The breakdown of furan aldehydes leads to the formation of formic and levulinic acid. Moreover, acetic acid is formed during the degradation of hemicellulose. Partial breakdown of lignin can generate a variety of phenolic compounds *(13)*, which also inhibit *S. cerevisiae (14,15)*. In contrast to furan aldehydes and aliphatic acids, the toxic effect of specific phenolic compounds is highly variable *(15)*. Different raw materials and different approaches to prepare lignocellulose hydrolysates will result in different concentrations of the fermentation inhibitors *(16,17)*.

The most powerful approach to improve the fermentability of a hydrolysate is to perform a detoxification prior to ethanolic fermentation. Chemical, biologic, and physical methods have been used to increase fermentability *(18,19)*. In a previous study, 12 detoxification methods were compared with respect to the effect on the chemical composition of a spruce hydrolysate and the fermentability using *S. cerevisiae (20)*. The results showed that treatment with anion-exchange resin was one of the most efficient detoxification methods. Furthermore, a comparison of three different resins—an anion exchanger, a cation exchanger, and a resin without charged groups *(21)*—showed that treatment of a spruce hydrolysate with anion exchanger

increased the fermentability most efficiently. The mechanisms of detoxification were found to be complex and dependent on both the functional groups and the properties of the polymer matrix.

In the present study, six different anion-exchange resins with different properties were selected for detoxification of a dilute-acid hydrolysate from spruce. The anion-exchange resins tested have styrene-, phenol-, and acrylic-based matrices and strong as well as weak functional groups. In previous studies *(20,21)*, detoxification was performed using a batch procedure, which is useful when the method is studied from an analytical point of view. However, although the batch approach is simple, its applicability to practical separation is limited owing to inconvenience, inefficient use of the resin, and the large amounts of regeneration agents required. In our study, a column treatment was used instead. In an analytical experiment, fractions of a spruce dilute-acid hydrolysate were collected and analyzed for fermentable sugars and inhibitors. A preparative treatment was also performed, and the effect on the fermentability was assayed using *S. cerevisiae*. The aim was to select the most efficient anion exchanger for detoxification.

Materials and Methods

Dilute-Acid Hydrolysate from Spruce

Chipped Norway spruce, *Picea abies*, was used in a two-step hydrolysis process in which H_2SO_4 was used as catalyst. The conditions and procedures were as previously reported *(22)*. The solid fraction was removed by filtration after hydrolysis, and the liquid fraction, hereafter referred to as the hydrolysate, had a pH of 1.9.

The hydrolysate contained: 15.7 g/L of glucose, 12.8 g/L of mannose, 1.4 g/L of HMF, 0.4 g/L of furfural, 1.4 g/L of levulinic acid, 3.2 g/L of acetic acid, 1.1 g/L of formic acid, and 2.4 g/L of phenolic compounds, (based on Folin and Ciocalteu's reagent [Sigma, Steinheim, Germany] and vanillin as the standard).

Detoxification by Anion-Exchange Resins

Six different anion-exchange resins were used representing both strong (Dowex 1x4 [Carl Roth KG, Chemische Fabrik, Karlsruhe], Dowex 2x8 [J.T. Baker, Phillipsburg, NJ], and Amberlite IRA 458 [Polyscience, Warrington, PA]) and weak (Amberlite IRA 67 [Fluka Chemie Gmbh, Buchs, Switzerland], Amberlite IRA 92 [Supelco, Bellefonte, PA], and Duolite A7 [Sigma-Aldrich]) anion exchangers (Table 1).

Five grams of dry anion exchanger were used. The amount of each anion exchanger was calculated using the dry content (Table 1). All anion exchangers were swollen in a saturated aqueous solution of NaCl, then converted to OH form with a 1 *M* solution of NaOH, and finally washed with Milli-Q® water (Millipore, Billerica, MA) until the pH was neutral.

All column experiments were performed with 1-cm id columns. The pumping rate was 0.5 mL/min, corresponding to a velocity of 0.4 m/h.

Table 1
Anion-Exchange Resins Used for Detoxification

Resin	Matrix	Type	Physical structure	Capacity (meq/mL)	Dry wt (%)[a]
Dowex 1x4	Styrene-DVB[b]	Strong base, type I	Gel	1.0	67
Dowex 2x8	Styrene-DVB	Strong base, type II	Gel	1.4	71
IRA 458	Acrylic-DVB	Strong base	Gel	1.25	53
IRA 67	Acrylic-DVB	Weak base	Gel	1.6	58
IRA 92	Styrene-DVB	Weak base	Macroporous	1.6	75
Duolite A7	Phenolic	Weak anion	Macroporous	2.1	58

[a] The dry weight was determined by using an MA-40 moisture analyzer (Sartorius AG, Geottingen, Germany).
[b] DVB, divinylbenzene.

In an analytical experimental series (Fig. 1), the effluent was collected in fractions. These fractions were analyzed with respect to pH, fermentable sugars, furan aldehydes, phenolic compounds, aliphatic acids, sulfate, and ultraviolet (UV) absorption at 280 nm.

In a preparative experimental series (Table 2, Fig. 2), 100-mL fractions were collected from columns with each of the different anion exchangers starting from the appearance of glucose in the effluent. These six fractions, obtained with different resins, were used for the fermentation experiments and analyzed as just described.

Analysis of Composition of Hydrolysate

The glucose, mannose, and xylose concentrations were determined by high-performance anion-exchange chromatography (HPAEC) using a DX 500 high-performance liquid chromatography (HPLC) system (Dionex, Sunnyvale, CA) equipped with a CarboPac PA-1 column (Dionex). The column was initially activated with a mixture of 200 m*M* NaOH and 170 m*M* sodium acetate for 5 min. The eluent was then changed to Milli-Q water (1 mL/min), and after 7 min the sample was injected. The injection was followed by an isocratic elution (1 mL/min) with Milli-Q water and a postcolumn addition of 300 m*M* NaOH. The sugar concentrations were determined by external calibration using a pulsed amperometric detector (Dionex ED 40).

The furan aldehydes HMF and furfural were determined by HPLC using a Waters 2690 separation module, with a binary pump, an autoinjector, and a diode array detector at 282 nm. The furan aldehydes were separated on a YMC ODS-AL column (50×3 mm, 120 Å, and 5-µm particles) (Waters, Milford, MA). The flow rate was 0.8 mL/min. Elution was performed with a gradient composed of Milli-Q water and acetonitrile containing 0.016% (v/v) trifluoroacetic acid. The gradient was formed in four steps over 17 min. In the first step, 10% acetonitrile was added for 3 min.

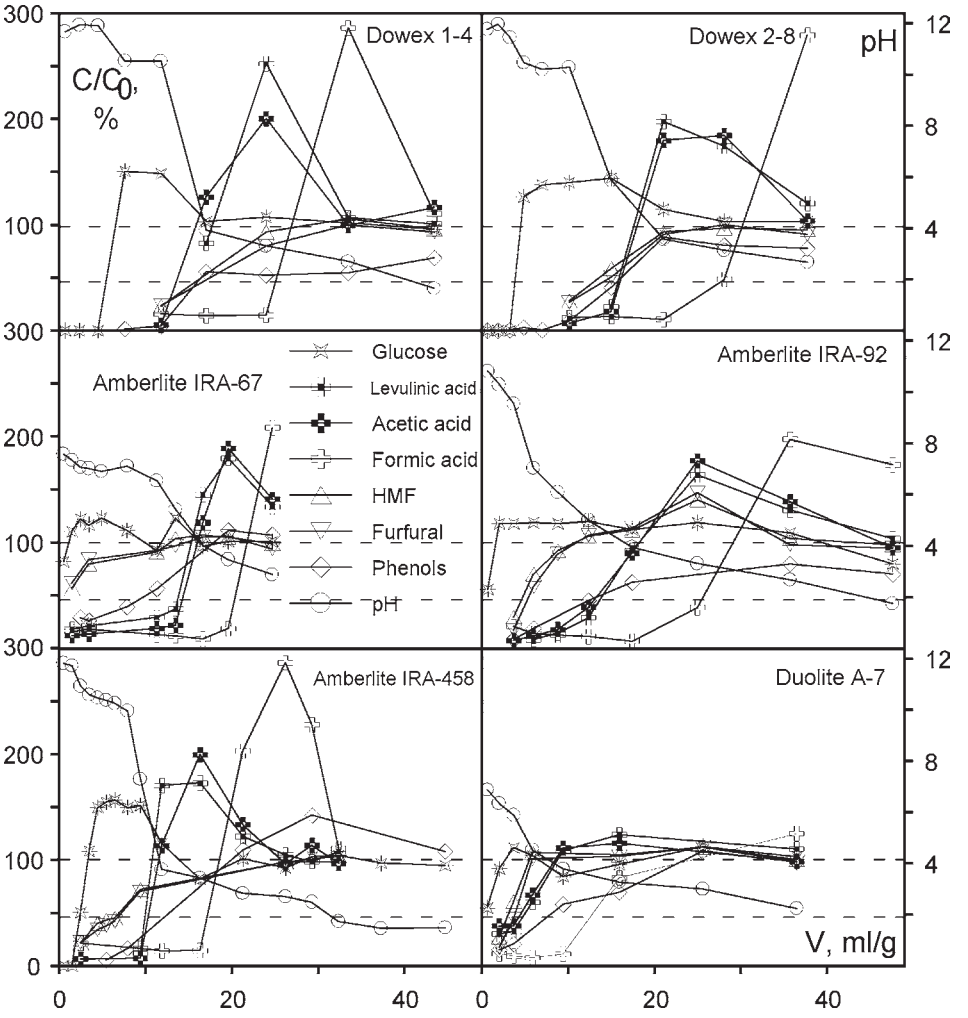

Fig. 1. Relative concentrations of glucose, levulinic acid, acetic acid, formic acid, HMF, furfural, and phenolic compounds compared with the initial concentration (100%, upper dashed lines) in fractions obtained from dilute-acid hydrolysate of spruce allowed to pass through columns with six different anion-exchange resins. The sulfate concentration was also determined but was zero in the fractions shown. The right axis shows the pH (the initial pH, 1.9, is indicated by the lower dashed lines).

Then, the gradient of acetonitrile was increased linearly to 100% in 7 min, was maintained for 5 min, and finally was decreased to 10% in 2 min. For quantification, syringic acid was used as an internal standard. The UV absorbance at 280 nm was also determined for all samples. The values followed approximately the concentrations of furfural and HMF, but the phenols also contributed to the absorbance. As a result, the UV measurements were used only as a convenient way to monitor the process.

Table 2
Effect of Anion-Exchange Treatments
on Concentrations of Fermentable Sugars and Inhibitors[a]

	Fermentable sugars							Total phenolics	
Method	Glucose	Mannose	Levulinic acid	Acetic acid	Formic acid	Furfural	HMF	Folin	HPLC[b]
Hydrolysate	100	100	100	100	100	100	100	100	100
Dowex 1x4	107	111	10	28	27	68	71	7	8
Dowex 2x8	101	102	98	96	28	62	71	40	24
IRA 458	103	106	124	108	33	91	94	65	79
IRA 67	93	92	18	93	23	117	136	57	39
IRA 92	99	100	51	50	26	109	137	21	17
Duolite A7	98	100	65	68	21	117	129	31	24

[a] The concentrations are given in percent of initial values.
[b] See ref. *21*.

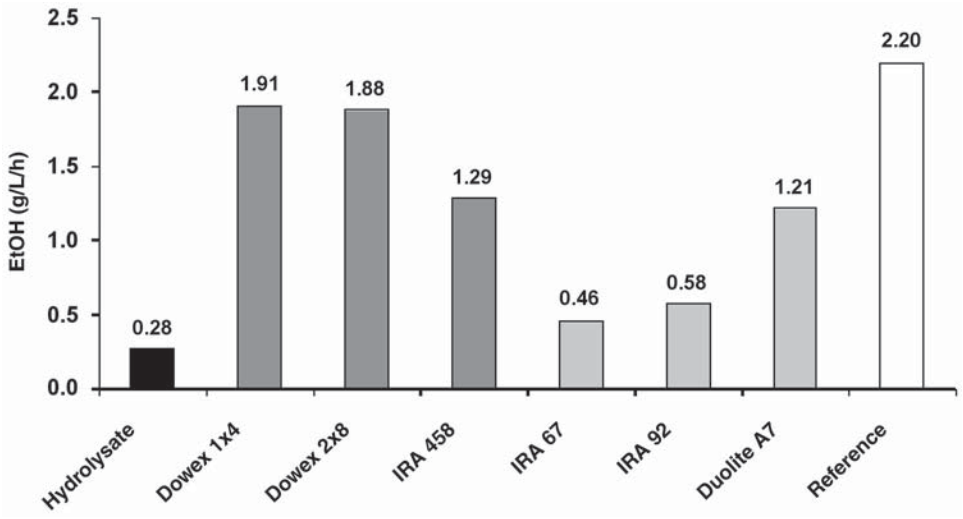

Fig. 2. Ethanol productivity for untreated hydrolysate (black bar), fractions from strong anion-exchange resins (dark gray bars), fractions from weak anion-exchange resins (light gray bars), and reference fermentation (glucose added but no hydrolysate) (white bar). The maximum mean volumetric productivity of ethanol (Q_{EtOH}) in g/(L·h) is indicated above each bar.

The concentrations of phenolic compounds were determined by HPLC (Waters) using a method described previously by Nilvebrant et al. *(21)*. The total concentration of phenols was also estimated by a spectrophotometric method *(23)* based on the Folin and Ciocalteu's reagent (Sigma).

Sulfate was determined using the DX 500-series ion chromatograph (Dionex) equipped with a conductivity detector (ED-40). An IonPac AS4A-SC anion-exchange column (250 × 4 mm id), equipped with an AG4A-SC guard column, was used for separation. A membrane suppressor (ASRS-I) was used to convert the eluent and the separated anions to their respective acid forms and to lower the conductivity of the eluent relative to that of the ions of interest. The eluent used consisted of a mixture of 1.7 m*M* $NaHCO_3$ and 1.8 m*M* Na_2CO_3. For all analyses, a flow rate of 2.0 mL/min was used.

The analysis of aliphatic acids was performed using a P/ACE MDQ capillary electrophoresis instrument equipped with a 60 cm × 50 µm id fused silica capillary (Beckman Coulter, Fullerton, CA). The samples were filtered through a 0.45-µm cellulose acetate filter (Whatman, Maidstone, UK) prior to hydrodynamic injection at 15 psi for 4 s. The voltage was set to 20 kV at reversed polarity. The electrolyte, composed of 5.0 m*M* trimellitic acid, 50 m*M* tris(hydroxymethyl)-aminomethane, 1.0 m*M* tetradecyltrimethylammoniumbromide, and 0.5 m*M* calcium chloride, had a pH of 9.8. Before use, it was filtered through a 0.2-µm cellulose nitrate filter and degassed with helium. Detection was performed by indirect UV absorption at 220 nm. Succinic acid was used as internal standard.

Yeast Strain and Growth Conditions

The fermenting microorganism was baker's yeast, *S. cerevisiae*, kindly provided by Jästbolaget AB (Rotebro, Sweden). Agar plates with YEPD medium (2% yeast extract, 1% peptone, 2% D-glucose, 2% agar) were used to maintain the strain. Cultures for inoculum were grown aerobically in 2000-mL cotton-plugged conical flasks with 500 mL of YEPD medium at 30°C using a rotary shaker. Cells were harvested in the exponential growth phase by centrifugating at 1500*g* for 5 min at 4°C and washed using a solution of NaCl (9 g/L).

Fermentations

Prior to the fermentations, the pH of the different hydrolysate samples was adjusted to 5.5 with NaOH (5 *M*). All fermentations were carried out under oxygen-limited conditions in 55-mL glass vessels containing 50 mL of medium of which 47.5 mL was hydrolysate (or, alternatively, an aqueous glucose solution for reference fermentations). The vessels were sealed with rubber stoppers and equipped with cannulas for outlet of CO_2. The hydrolysates were supplemented with nutrients as previously described *(20)*. Fermentations of 35 g/L of glucose and nutrients but no hydrolysate were used for reference. The flasks were inoculated to an initial cell mass concentration of 2.0 g/L dry wt and incubated at 30°C with stirring. The fermentations were run for 36 h. Samples of 200 µL were taken after 0, 2, 4, 6, 8, 10, 24, and 36 h.

Analysis of Fermentation Products

Samples taken from the different fermentations were diluted and filtered with 0.45-µm GHP Acrodisc syringe filters (Pall Gelman Laboratory, Ann Arbor, MI) prior to analysis.

The glucose and mannose concentrations were determined by HPAEC as described before. The ethanol concentration was measured using an HP 5890 gas chromatograph (Hewlett-Packard, Palo Alto, CA) equipped with a BP-20 column with a film thickness of 1.0 µm (SGE, Austin, TX) and a flame ionization detector. The temperature was maintained at 30°C for 5 min followed by heating to 180°C with a heating rate of 15°C/min. Acetonitrile was used as internal standard.

The biomass concentration was determined from dry wt measurements. Three-milliliter samples were taken in duplicate at the beginning and the end of the fermentations. The samples were then centrifuged (1500*g*, 5 min), and the pellets were washed once with distilled water and dried at 103°C for 24 h.

Calculations

All peaks obtained in the chemical analysis were integrated and the concentrations were calculated using the EZChrom Elite software (Scientific Software, Pleasanton, CA).

The maximum mean volumetric productivity of ethanol was obtained after 4 h in the reference fermentations. Therefore, the fermentability was evaluated by comparing the volumetric productivity, Q_{EtOH} (g/[L·h]), of the different fermentations. Q_{EtOH} was calculated as the produced ethanol within the first 4 h of the fermentations divided by 4.

The ethanol yield, Y_{EtOH} (g/g), was calculated as the produced ethanol after the depletion of glucose and mannose divided by the amount of consumed fermentable sugar (glucose and mannose). The anaerobic growth yield, Y_x (g/g), hereafter referred to as the biomass yield, was calculated as the produced biomass in 36 h divided by the amount of fermentable sugars initially present.

Results

Six different detoxification treatments were performed using both weak and strong anion-exchange resins (Table 1) in an analytical experiment (Fig. 1) and a preparative experiment (Table 2, Fig. 2), in which the fermentability of the fractions was assayed. Figure 1 shows how the pH and the concentrations of glucose, furan aldehydes, phenols, aliphatic acids, and sulfate varied in hydrolysate fractions collected from columns packed with the six different resins in the analytical anion-exchange experiment.

Considerably higher (~50%) glucose concentrations than in the untreated hydrolysate were observed for Dowex 1x4, Dowex 2x8, and IRA 458 (Fig. 1). The fractions containing the highest concentration of glucose appeared after about 10 mL/g of resin. In addition, the weak anion exchangers, IRA 92, IRA 67, and Duolite A7, gave rise to fractions with higher glucose concentrations than the untreated hydrolysate, although the increase was more modest (~20%).

All resins initially adsorbed furan aldehydes and phenols (Fig. 1). In some cases, a subsequent release of adsorbed furan aldehydes and phenols was observed, resulting in concentrations slightly over the concentrations in untreated hydrolysate (Fig. 1). Levulinic, acetic, and formic acid initially adsorbed well to all resins. The trapped levulinic and acetic acid were released before formic acid.

Sulfate was trapped very efficiently, as expected, by all anion-exchange resins. All sulfate was removed from the hydrolysate fractions used for fermentation. The sulfate ions remained adsorbed to the anion exchangers, displacing previously trapped aliphatic acids.

Chemical analyses of the fermentable sugars and different inhibitory compounds in the preparative anion-exchange experiment were done before and after detoxification (Table 2). Relatively limited decreases (≤8%) or increases (≤11%) in the concentration of the fermentable sugars, glucose and mannose, were observed in the fractions collected for fermentation. As already evident from the analytical anion-exchange experiment, the strong anion exchangers initially trapped the monosaccharides, which were then released when the adsorbed sugars were replaced by compounds with higher affinity toward the resin. This resulted in increases in

the concentration of glucose and mannose in the fractions collected from the strong anion exchangers. The increases ranged from 1 to 11% compared with the untreated hydrolysate.

The furan aldehydes were also affected differently by the resins. The fractions from the strong anion exchangers showed decreased concentrations of furan aldehydes, whereas the weak anion exchangers showed increased concentrations of furan aldehydes in the fractions used for fermentation. The lowest concentrations of furan aldehydes were observed in fractions from the strong anion exchangers with styrene-based matrices, Dowex 1x4 and Dowex 2x8, which displayed a decrease in the concentrations of furfural and HMF to approx 60–70%.

All treatments decreased the concentration of phenolic compounds in the hydrolysate (Table 2). The two different methods used to estimate the phenolic content, based on Folin-Ciocalteu's reagent and HPLC, indicated the same order for the treated hydrolysates regarding the concentration of phenolic compounds: IRA 458 > IRA 67 > Dowex 2x8 ≥ Duolite A7 > IRA 92 > Dowex 1x4. However, the concentrations of remaining phenolic compounds after the treatments did not always agree perfectly when the results from the two different methods for determination of phenols were compared (Table 2). The reason is that HPLC quantification is based on UV absorbance from the individual phenols and the Folin-Ciocalteu's reagent reacts with the phenolic groups. The fraction obtained with the strong anion-exchange resin Dowex 1x4 showed a decrease in the total amount of phenols by as much as 93 to 94%. The anion exchangers with styrene- and phenolic-based matrices (Dowex 1x4, Dowex 2x8, IRA 92, and Duolite A7) gave larger decreases (60–90%) than the acrylic-based matrices (20–60%).

The concentration of aliphatic acids was affected differently depending on the selectivity of the resins used for the treatment (Table 2). The treatment with Dowex 1x4 resulted in a removal of 90% of the levulinic acid and about 70% of the acetic and formic acid. By contrast, the fraction collected from IRA 458 was enriched in acetic and levulinic acid (about 110–120%), while the concentration of formic acid was decreased by two thirds. Acetic and levulinic acid separated only partly, and the relative concentrations in the accumulated fractions thus partly differed depending on when the fractions were collected.

Volumetric productivity and ethanol yield increased after treatment with all six resins. The volumetric productivity in the reference fermentation, 2.20 g/(L·h), was eight times higher than in the untreated hydrolysate (Fig. 2). The volumetric productivity in the anion-exchange-treated samples was two to seven times higher than in the untreated hydrolysate. The lowest ethanol productivities among the anion-exchange-treated samples, 0.46 and 0.58 g/(L·h), about twice as high as that for the untreated hydrolysate (0.28 g/[L·h]), were observed for the fractions from the weak anion exchangers IRA 67 and IRA 92, respectively (Fig. 2). The fractions from Duolite A7 and IRA 458 showed an intermediate improvement in productivity, four to five times higher than for the untreated hydrolysate.

The highest ethanol productivities, seven times higher than the untreated hydrolysate, were achieved using the strong anion exchangers Dowex 1x4 and Dowex 2x8. The fractions from the strong anion exchangers showed a larger improvement in productivity (five to seven times) than the fractions from the weak ones (two to four times).

The ethanol yield was 0.4–0.5 g/g of consumed glucose and mannose for all anion-exchange-treated samples, although the time required to achieve depletion of glucose and mannose differed greatly (8–24 h) owing to the large difference in productivity. At the end of the experiment, only about 20% of the fermentable sugar had been consumed in the untreated hydrolysate. The biomass yield increased (0.05–0.1 g/g) in the samples treated with anion exchangers compared with the untreated hydrolysate (0.015 g/g), which also indicates that a detoxification had been achieved for all anion-exchange-treated samples.

Discussion

Treatment with anion exchangers affected the inhibitors as well as the fermentable sugars in the hydrolysate (Fig. 1). The anion-exchange resins can act by substitution of anions in the hydrolysate for hydroxyl ions leading toward neutralization. Furthermore, the strong alkaline surfaces of the anion exchanger lead to ionization and entrapment of uncharged compounds. The results suggest that monosaccharides as well as furan aldehydes are involved in such interactions, considering the initial decrease in the concentrations of these compounds. This was followed by a relatively rapid increase to higher concentrations than in untreated hydrolysate. The pH profile could be used to monitor the process. For instance, the displacement of glucose from the column occurred simultaneously as a slower decrease in pH in the effluent was observed.

Another type of interaction is represented by hydrophobic interactions between the matrix and some of the components in the hydrolysate. When these interactions occur, the removal of a compound is dependent on the matrix polymer, rather than on the type of the functional groups. The results indicate that styrene- and phenol-based matrices (here represented by Dowex 1x4, Dowex 2x8, IRA 92, and Duolite A7) have an excellent ability to trap phenols, whereas acrylic-based matrices (represented by IRA 67 and IRA 458) have poorer ability. Nevertheless, the concentration of phenolic compounds decreased by more than 20% after all treatments.

Both ethanol productivity and ethanol yield were improved after treatment. However, treatment with the strong anion exchangers resulted in a larger improvement than treatment with weak exchangers. The improvement in fermentability was clearly indicated by comparisons of the volumetric ethanol productivity data (Fig. 2), although the yields did not differ dramatically. Comparison of the different resins revealed that the best result was obtained after treatment with Dowex 1x4, which increased the fermentability by nearly seven times, whereas treatment with IRA 67 resulted in an increase of only two times. Treatment with

Dowex 1x4 resulted in the largest decrease of all inhibitors determined, which is in agreement with the high increase in fermentability.

Different types of anion-exchange resins have previously been used for detoxification of lignocellulose hydrolysates. Watson et al. *(24)* used a weak anion-exchange resin for detoxification of a bagasse hemicellulose hydrolysate. Dominguez et al. *(25)* used a weak anion-exchange resin for detoxification of corncob hemicellulose hydrolysates. We have previously used a strong anion-exchange resin with a styrene-based matrix for detoxification of spruce hydrolysates *(20,21)*. The results of the present study suggest that the use of a strong anion exchanger with styrene-based matrix is a good alternative for dilute-acid hydrolysates of softwood.

The concentration of furan aldehydes was relatively low (0.4 g/L of furfural and 1.4 g/L of HMF) in the untreated hydrolysate used in the present study. The concentration of furfural and HMF in spruce hydolysates prepared under different conditions varied between 0.2–1.4 and 1.5–8.4 g/L, respectively *(17)*. Although the concentration of furan aldehydes increased in some fractions in the preparative experiment (Table 2), the fermentability was improved compared with the untreated hydrolysate (Fig. 2). This observation agrees with the low initial concentrations and suggests that furan aldehydes were not important inhibitors in the present hydrolysate. However, it is well known that high concentrations of furan aldehydes will prolong the lag phase of cell growth and ethanol formation *(26)*. The fractions collected from strong anion exchangers generally contained less furan aldehydes, but also other factors could possibly affect the interaction with furan aldehydes.

It is well known that phenolic compounds are important inhibitors in hydrolysates prepared from hardwood *(27)* as well as softwood *(20)*. The hydrophobicity of the matrix is likely to be an important property that contributes to the ability of an ion-exchange resin to remove phenols. Although the knowledge regarding the suitability of different methods to determine phenolics in lignocellulose hydrolysates has increased *(28)*, the quantification of phenolics and the correlation with the inhibitory effect is still a challenging task, because hydrolysates contain a wide variety of phenolic compounds that have very different toxic effects.

Although the resins adsorbed levulinic, acetic, as well as formic acid, formic acid was released later than acetic and levulinic acid, which typically were eluted similarly. This can be explained by the fact that the pK_a of formic acid (3.75) is considerably lower than that of acetic (4.74) and levulinic (4.5) acid. The initial concentrations of levulinic, acetic, and formic acid in untreated hydrolysate were 12, 53, and 24 m*M*, respectively. The total concentration of the three aliphatic acids, 89 m*M*, is relatively modest considering that previous results indicate that concentrations below 100 m*M* lead to an increase rather than a decrease in the ethanol yield *(11)*. The effect of the acids is pH dependent, and under anaerobic conditions, the concentration of the undissociated form of acetic acid in the medium should not exceed 5 g/L (80 m*M*) for growth to occur *(29)*. The low concentration

of aliphatic acids in the untreated hydrolysate in the present study strongly suggests that they do not play any significant role as inhibitors. Notably, the highest ethanol yield (0.48 g/g) was determined for the IRA 458–treated sample, which contained the highest concentration of aliphatic acid among the anion-exchange-treated samples.

In agreement with previous findings *(20)*, it can be concluded that treatment with anion-exchange resin is a very effective way to detoxify dilute-acid hydrolysates of spruce. Treatment with strong anion exchangers leads to higher ethanol productivity than treatment with weak ones. Furthermore, styrene- and phenol-based resins are more efficient than acrylic-based resins in trapping phenolic inhibitors. Finally, detoxification using anion-exchange resins can result in removal of inhibitors as well as in accumulation of sugars in the treated hydrolysate.

Acknowledgments

We gratefully acknowledge the support of the Swedish National Energy Administration.

References

1. Faith, W. L. (1945), *Ind. Eng. Chem.* **37,** 9–11.
2. Lee, Y. Y., Iyer, P., and Torget, R. W. (1999), *Adv. Biochem. Eng./Biotechnol.* **65,** 93–115.
3. Harris, J. F., Baker, A. J., and Zerbe, J. R. (1984), *Energy Biomass Wastes* **8,** 1151–1170.
4. Banerjee, N., Bhatnagar, R., and Vishwanathan, L. (1981), *Enzyme Microb. Technol.* **3,** 24–28.
5. Sjöström, E. (1993), *Wood Chemistry: Fundamental and Applications*. Academic, San Diego, CA.
6. Soboleva, G. A. and Vitrinskaja, A. M. (1975), *Prikl. Biokhim. Mikrobiol.* **11,** 649–652.
7. Taherzadeh, M. J., Gustafsson, L., Niklasson, C., and Lidén, G. (1999), *J. Biosci. Bioeng.* **87,** 169–174.
8. Palmqvist, E., Almeida, J. S., and Hahn-Hägerdal, B. (1999), *Biotechnol. Bioeng.* **62,** 447–454.
9. Sárvári Horváth, I., Taherzadeh, M. J., Niklasson, C., and Lidén, G. (2001), *Biotechnol. Bioeng.* **75,** 540–549.
10. Sárvári Horváth, I., Franzén, C. J., Taherzadeh, M. J., Niklasson, C., and Lidén, G. (2003), *Appl. Environ. Microbiol.* **69,** 4076–4086.
11. Larsson, S., Palmqvist, E., Hahn-Hägerdal, B., Tengborg, C., Stenberg, K., Zacchi, G., and Nilvebrant, N.-O. (1999), *Enzyme Microb. Technol.* **24,** 151–159.
12. Taherzadeh, M. J., Gustafsson, L., Niklasson, C., and Lidén, G. (2000), *Appl. Microbiol. Biotechnol.* **53,** 701–703.
13. Clark, T. and Mackie, K. (1984), *J. Chem. Tech. Biotechnol.* **34B,** 101–110.
14. Ando, S., Arai, I., Kiyoto, K., and Hanai, S. (1986), *J. Ferment. Technol.* **64,** 567–570.
15. Larsson, S., Quintana-Sáinz, A., Reimann, A., Nilvebrant, N.-O., and Jönsson, L. J. (2000), *Appl. Biochem. Biotechnol.* **84–86,** 617–632.
16. Martín, C., Galbe, M., Nilvebrant, N.-O., and Jönsson, L. J. (2002), *Appl. Biochem. Biotechnol.* **98–100,** 699–716.
17. Taherzadeh, M. J., Eklund, R., Gustafsson, L., Niklasson, C., and Lidén, G. (1997), *Ind. Eng. Chem. Res.* **36,** 4659–4665.
18. Olsson, L. and Hahn-Hägerdal, B. (1996), *Enzyme Microb. Technol.* **18,** 312–331.
19. Palmqvist, E. and Hahn-Hägerdal, B. (2000), *Bioresour. Technol.* **74,** 17–24.
20. Larsson, S., Reimann, A., Nilvebrant, N.-O., and Jönsson, L. J. (1999), *Appl. Biochem. Biotechnol.* **77–79,** 91–103.

21. Nilvebrant, N.-O., Reimann, A., Larsson, S., and Jönsson, L. J. (2001), *Appl. Biochem. Biotechnol.* **91–93,** 35–49.
22. Nilvebrant, N.-O., Persson, P., Reimann, A., de Sousa, F., Gorton, L., and Jönsson, L. J. (2003), *Appl. Biochem. Biotechnol.* **105–108,** 615–628.
23. Singleton, V. L., Orthofer, R., and Lamuela-Raventós, R. M. (1999), *Methods Enzymol.* **299,** 152–178.
24. Watson, N. E., Prior, B. A., Lategan, P. M., and Lussi, M. (1984), *Enzyme Microb. Technol.* **6,** 451–456.
25. Dominguez, J. M., Ningjun, C., Gong, C. S., and Tsao, G. T. (1997), *Bioresour. Technol.* **61,** 85–90.
26. Chung, I. S. and Lee, Y. Y. (1985), *Biotechnol. Bioeng.* **27,** 308–315.
27. Jönsson, L. J., Palmqvist, E., Nilvebrant, N.-O., and Hahn-Hägerdal, B. (1998), *Appl. Microbiol. Biotechnol.* **49,** 691–697.
28. Persson, P., Larsson, S., Jönsson, L. J., Nilvebrant, N.-O., Sivik, B., Munteanu, F., Thörneby, L., and Gorton, L. (2002), *Biotechnol. Bioeng.* **79,** 694–700.
29. Taherzadeh, M. J., Niklasson, C., and Lidén, G. (1997), *Chem. Eng. Sci.* **52,** 2653–2659.

0273-2289/04/114/0539–0557/$25.00

Ethanol Production in Immobilized-Cell Bioreactors from Mixed Sugar Syrups and Enzymatic Hydrolysates of Steam-Exploded Biomass

Isabella De Bari,* Daniela Cuna, Francesco Nanna, and Giacobbe Braccio

ENEA CR TRISAIA, SS 106 Jonica, km 419+500, 75025 Policoro (MT), Italy, E-mail: de_bari@trisaia.enea.it

Abstract

We investigated ethanol production from mixed sugar syrups. Hydrolysates were prepared from enzymatic saccharification of steam-pretreated aspen chips. Syrups containing 45 g/L of glucose and 12 g/L of xylose were detoxified through two ion-exchange resins and then fermented with *Pichia stipitis* and *Saccharomyces cerevisiae* immobilized in Ca-alginate gel beads. Combinations of different gel fractions in the fermentation volume, amount of yeast cells, and ratios of *P. stipitis* vs *S. cerevisiae* within each bead were compared. In the best conditions, by using a total beads volume corresponding to 25% of the working volume, we obtained a yield of 0.39 $g_{ethanol}/g_{initial\ sugars}$. This amount of gel entrapped an initial cell concentration of 6×10^{12}cells/L with ratio of *S. cerevisiae*/*P. stipitis* of 0.25 g/g. Modified stirred-tank reactors were obtained either by adding marbles or by inserting a perforated metal cylinder, which reduced considerably the rupture of beads while visibly improving oxygenation of the medium.

Index Entries: Biomass; ethanol; coimmobilization; Ca-alginate; *Pichia stipitis*; steam explosion.

Introduction

The simultaneous bioconversion of mixed sugar syrups is one of the most ambitious challenges in the field of bioethanol production. Different productivities and ethanol-tolerance of the yeasts used in the fermentation of glucose and xylose (the most abundant biomass sugars) have led

*Author to whom all correspondence and reprint requests should be addressed.

investigators to prefer process schemes in which hydrolysis and fermentation of cellulose and hemicellulose streams occur separately *(1)*. However, when the percentage of glucose in the feed biomass is much higher than xylose, cofermentation could be a more efficient approach since the cost of separate processes would be high.

The use of recombinant microorganisms for cofermentation is one of the most promising approaches in the field of bioethanol production, though their use for large-scale industrial processes still requires fine-tuning of the reliability of the entire process *(2)*. The technical hurdles of cofermentation increase when real biomass hydrolysates have to be fermented. In fact, whatever the biomass pretreatment, the formation of degradation byproducts that could inhibit the fermentation usually requires the addition of a further detoxification step. Therefore, the production of ethanol from hydrolysates should be considered in its entirety, from the optimal pretreatment to the choice of the proper fermentation process.

Among the most common hexose- and pentose-fermenting yeasts, *Saccharomyces cerevisiae* and *Pichia stipitis* are by far the most used *(3)*. However, cocultures of both yeasts do not always ensure the xylose conversion because of the diauxic behavior of *P. stipitis* (i.e., the preferential use of glucose when both substrates are available) *(4)*. To favor xylose consumption by *P. stipitis*, some researchers have proposed the use of a respiratory-deficient strain of *S. cerevisiae* while maintaining a specific oxygen uptake per cell during the fermentation process *(5)*. Nevertheless, the feasibility of this approach depends on the development of a system able to monitor and automatically adjust the oxygen level throughout the process.

Immobilization of yeasts into Ca-alginate beads is regarded as a valuable alternative to overcome the limitations of *P. stipitis (6)*. Using computer simulations, Grootjen et al *(6)* investigated the cofermentation of glucose and xylose mixtures with bead-immobilized *P. stipitis* in combination with either suspended or coimmobilized *S. cerevisiae*. They demonstrated that *P. stipitis* was not able to grow when it was coimmobilized with *S. cerevisiae*. It was also concluded that to make the process feasible, higher initial *P. stipitis* concentrations in the beads and/or a higher beads fraction relative to the fermentation volume would be required.

Although a preindustrial project of ethanol production with immobilized cells goes back to the 1980s *(8)*, its application is still limited because of technical problems related to the gel stability and even more to the mass-transfer resistance of the gel membrane *(9)*. Specifically, both substrate and product counterdiffusion (in addition to the presence of cells inside the beads) could reduce the diffusion coefficients of glucose and ethanol up to 13.7 and 28.1%, respectively *(10)*.

In a conventional stirred-tank bioreactor (STR) equipped with air bubbling, an increase in the agitation of the medium could improve oxygenation and circumvent the diffusion limitations. Conversely, the shearing effect of the impeller could somehow damage the beads, especially at high stirring rates. Alternatively, fluidized-bed bioreactors (FBR) allow

continuous movement of the beads, which ensures an efficient mass transfer. However, some design optimization is required to achieve the fluidization while preventing the cells from sloughing off the beads.

In the present study, the fermentation of glucose and xylose model solutions and hydrolysate samples from steam-pretreated aspen was investigated. After the steam explosion, the obtained slurry was suspended in water to a solid-to-liquid ratio of 200 g/L of dry matter (DM) and enzymatically hydrolyzed with a mixture of cellulolytic and hemicellulolytic enzymes. Subsequently, the hydrolysate was detoxified using a two-step treatment through cationic and anionic resins.

The fermentation tests were carried out in shake flasks, STR and FBR. The effect of the following parameters was investigated: the amount of gel and the total cell concentration in the bioreactor; the addition of hydrogen acceptor (acetone), instead of air, to activate the electron transport in the respiratory chain; and the use of Teflon-made filters as air diffusers to reduce air bubble dimension and increase oxygen solubility.

Furthermore, design modifications to the STR were also considered: equipping the STR with marbles to ensure a larger distribution of the gel beads inside the reactor while damping down the shearing effect of the Rushton impeller; and equipping the STR with a perforated stainless still cylinder that confines the beads in the external cavity between the reactor walls and the impeller zone. A description of the explained configurations is shown in Fig. 1.

The obtained results are intended to provide a preliminary assessment of the incidence of the investigated parameters on the process yields.

Materials and Methods

Pretreatment of Biomass

Steam explosion pretreatment was carried out in a continuous Staketech digester processing 150 kg/h of DM. Water was added to the chips to raise the intrinsic humidity to 50%. The severity of the steam explosion pretreatment was expressed through the logarithm of the semiempirical relation described in Eq. 1 *(11)*:

$$R_0 = t \times \exp\left(\frac{T - 100}{14.75}\right) \quad (1)$$

in which T is the steaming temperature (°C) and t is the residence time (min).

A mild severity parameter was chosen to reduce the hemicellulose degradation while ensuring an adequate cellulose fiberization. The steam pretreatment was therefore carried out at 215°C for 3 min corresponding to Log R_0 3.86.

Biomass was analyzed for carbohydrate, lignin, and ash content by the following standard procedures: carbohydrates and lignin by the Klason procedure (modified TAPPI T-13 m-54 and ASTM D1106), and ash by ASTM D1102. Details of the procedures adopted in our laboratory

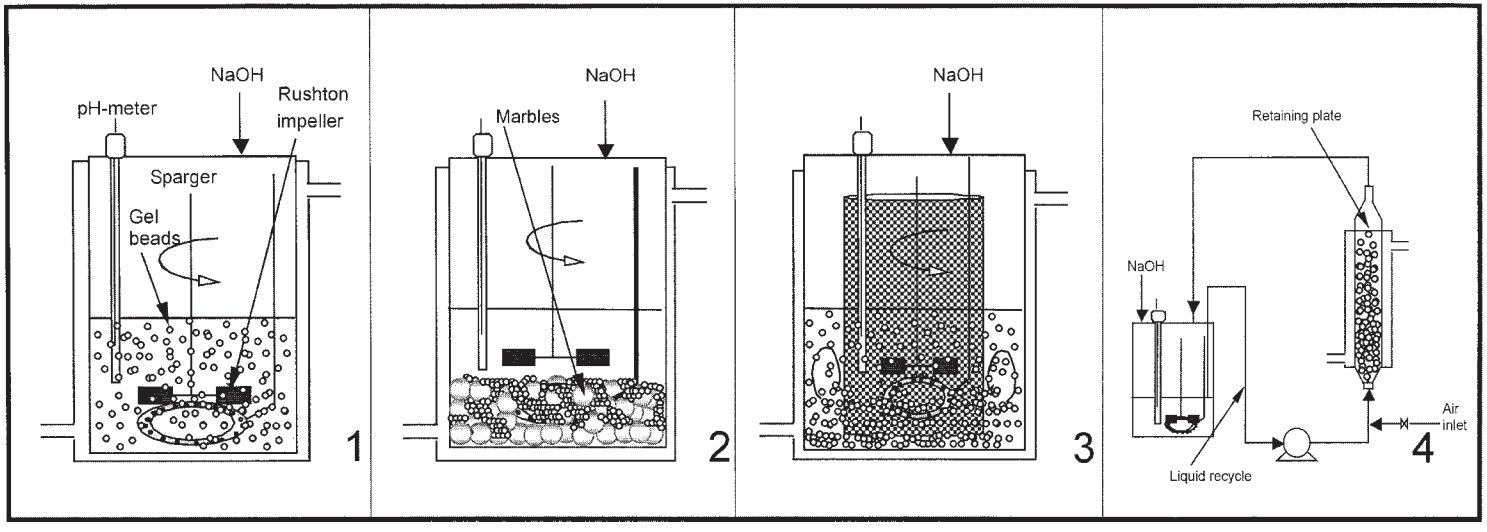

Fig. 1. Description of studied bioreactor configurations: 1, STR; 2) STR modified through addition of marbles; 3, STR modified through insertion of a metal perforated cylinder; 4, FBR.

are provided elsewhere *(12,13)*. The results reported here are the means of six values (two replicates for three samples).

Analysis of hydroxymethylfurfural (HMF), furfural, acetic acid, and formic acid was performed using the HP1100 system equipped with a diode array detector. Aliquots of a few milliliters were filtered (0.2 μm) and eluted through a Dionex AS1 column with a flow rate of 0.8 mL/min. A gradient of HCl and CH_3CN from 0.3 m*M* HCl and 1% (v/v) CH_3CN to 4 m*M* HCl and 15% (v/v) CH_3CN was used as the eluent. Quantification was carried out at two different wavelengths, 205 and 280 nm, for acids and aldehydes, respectively. The analytical method was tested over five calibration standards in the range of 3–140 ppm for HMF and furfural and 5-380 ppm for acetic and formic acid. The detector sensibility to HMF and furfural was 100-fold higher than that to acetic acid. Nevertheless, the analytical procedure showed a good linearity also for acetic acid.

Microorganisms and Maintenance

S. cerevisiae was Bakers Yeast Type II from Sigma. *P. stipitis* NRRL Y-11544 was obtained from DSMZ (Germany). The culture was maintained at 4°C on agar slants containing 20 g/L of D-xylose, 3 g/L of yeast extract, 3 g/L of malt extract, 5 g/L of peptone, and 15 g/L of agar. The culture medium contained 50 g/L of D-xylose, 5 g/L of D-glucose, 3 g/L of yeast extract, 3 g/L of malt extract, 5 g/L of peptone (pH 5 ± 0.2). According to the procedure reported by Nigam *(14)*, the nutrients were sterilized by autoclaving at 120°C for 15 min, and D-xylose and D-glucose were sterilized at 110°C for 10 min.

To prepare the inoculum, 1000-mL Erlenmeyer flasks containing 200 mL of medium were inoculated from a fresh agar slant and incubated at 30 ± 2°C in a rotary shaker at 200 rpm. After 65 h, yeast cells were harvested by centrifuging at 2000 rpm for 15 min. The cells were washed twice and resuspended in saline solution (0.85% NaCl). The obtained suspensions were used for preparation of the gel beads.

To evaluate the cell mass concentration, a few milliliters of the suspension was filtered through 0.45-μm filters and dried at 60°C overnight until there was no weight change. The number of live cells was determined by counting in the samples the number of cells capable of forming colonies (CFU) on agar slants maintained at 30 ± 2°C. Cell viability was determined by using methylene blue.

Cell Immobilization

Cell suspensions containing one or both yeasts were mixed with alginate solution containing 2% (w/v) sodium alginate *(15)*. The suspension was pumped through a peristaltic pump in 0.2 *M* $CaCl_2$ solution. The alginate gel beads had diameters of 2 to 3 mm. After 30 min the beads were replaced with medium, washed twice, and stored in saline solution at 4°C.

The cell concentration was determined by microscopic counting (Olympus B-201) in a Bürker-type chamber on five beads dissolved in 10 mL of 1% sodium citrate solution and shaken for 10 min at 30°C. Although this method gives the total number of cells (dead and live), methylene blue dyeing revealed that most of the cells were alive.

The dosage of the yeasts during preparation of the beads was based on cell dry mass. However, the ratio by weight did not coincide with the ratio between *S. cerevisiae* and *P. stipitis* cell numbers; that is, 1 g of *P. stipitis* was roughly 10^{11} cells whereas 1 g of *S. cerevisiae* was approx 3×10^6 cells. Under the microscope, neither yeast showed appreciable difference in shape or dimension. Therefore, when referring to coimmobilized yeasts, the overall number of cells is reported. Details on the specific conditions of each test are provided when necessary.

Fermentation

The composition of the fermentation medium was 2 g/L of yeast extract, 5 g/L of KH_2PO_4, 0.4 g/L of $MgSO_4$, 2 g/L of $(NH_4)_2SO_4$, and 0.04 g/L of $CaCl_2$. $CaCl_2$ was added to prevent the alginate beads from dissolving owing to the phosphates. Before fermentation, the hydrolysate was sterilized by membrane filtration. The pH was adjusted to 5.5 and the temperature was kept at 30°C.

Batch fermentations with immobilized cells were carried out both in 500-mL Erlenmeyer flasks and in the 2-L Biostat B from BBInternational. All results are the mean of two duplicate experiments. For the shake-flask experiments, 100 mL of the culture medium supplemented with glucose and xylose or aspen hydrolysates was used. pH corrections were done discontinuously every 10 h.

The STR was equipped with temperature, pH, and P_{O_2} control units. Only one Rushton impeller was used to homogenize the system. Almost 1 L of the culture medium supplemented with the carbon sources was used during the test runs. In the configuration with marbles, the total volume occupied by marbles (average diameter of 16 mm) was roughly 350 mL. In the configuration with the metal cylinder around the stirrer axle, the volume available in the external cavity was 565 mL.

For FBR configuration, a column (73 × 3.2 cm) was packed with a volume of beads corresponding to half the volume of the column. A water jacket kept the temperature stable at 30°C. The culture medium was continuously pumped through a peristaltic pump from the reservoir into the packed column with a flow rate of 3–3.5 mL/min. pH adjustment was carried out in the reservoir tank.

Preparation of Hydrolysate Samples

Three enzymatic mixtures with predominantly cellulase and xylanase activity were used for the saccharification tests. To hydrolyse the cellulose, the mixtures Celluclast 1.5L and Novozym 188 from Novo Nordisk were

Table 1
Chemical Composition of Aspen Chips
Steam Exploded at Log R_0 3.86

Compound	Chemical composition (%)
Glucan	46 ± 2
Xylan	7.8 ± 0.3
Arabinan	0.48 ± 0.04
Glactan	0.30 ± 0.02
Ash	2.01 ± 0.01
Lignin	31 ± 1

added by using the internal dosage previously optimized *(13)*. The xylanase mixture, Multieffect xylanase, kindly provided by Genencor, was used to hydrolyze the hemicellulose fraction. From the data in the literature, the xylanase activity was 400 IU/mL *(16)*. Dosages of this enzyme mixture were based on the xylanase activity reported in the literature. Preliminary evaluations were carried out in shake flasks thermostated at 45°C and stirred at 180 rpm. The hydrolysate used in the detoxification and cofermentation tests was prepared in a 10-L bioreactor.

Detoxification of hydrolysates was accomplished in a continuous ion-exchange bench-scale unit. The resins used were Dowex 1 (50/100 mesh, density: 0.71 g/cm^3), weak basic anion exchanging, and Dowex-50W (50/100 mesh, density: 0.80 g/cm^3), strong acidic cation exchanging.

Results and Discussion

Hydrolysis

The steam-exploded aspen had an average DM of 63.5%; the chemical composition is described in Table 1. Poplar has been one of the most investigated biomass sources for ethanol production. The xylose/glucose ratio in the raw material is almost 0.3; that is, glucose is the most abundant component. After steam explosion, the residual xylose in the biomass could be recovered by posthydrolysis of the water-extracted hemicellulose or by enzymatic hydrolysis of the entire slurry. Through the former route, the maximum xylose concentration that we recovered by using an extracting ratio of 130 g/L (DM) was 6.94 g/L (68% of the xylose in the biomass). The solution also extracted degradation byproducts whose total amount was 3.6 g/L. Under these conditions, to ferment this stream a subsequent step of concentration in addition to an effective detoxification treatment would be required. A further optimization of the pretreatment (e.g., by adding acid catalysts) is likely to enhance the water-extracted hemicellulose, but this topic is beyond the scope of this article.

Preliminary evaluations of the enzymatic hydrolysis yields of the entire slurry (cellulose and hemicellulose) were carried out in shake flasks in order to evaluate the effect of concentrated slurries on the process yields. High contents of enzymatic proteins were used in order to overcome the inhibition of byproducts already ascertained in concentrated and nondetoxified suspensions *(13)*; the results are summarized in Table 2. The percentages of the recovered xylose ranged between 72 and 95%, higher than those obtained by the posthydrolysis of the water-extracted hemicellulose. The effect of doubling the biomass loading was remarkable, as shown by the decrease in both glucose and xylose hydrolysis yields. By contrast, no significant improvement could be observed by increasing the IU of xylanase. Therefore, hydrolysate samples used in the detoxification and cofermentation tests were prepared in a 10-L STR according to the conditions regarding the third case listed in Table 2. The obtained yields were comparable with those obtained in shake flasks. These results do not presume to be conclusive on the optimization of the enzymatic hydrolysis of nondetoxified slurries; they are simply a way to produce concentrated syrups containing 45 g/L of glucose and 12 g/L of xylose. Obviously, this approach could become more valuable depending on the research progresses concerning the production of more effective enzyme mixtures *(17)*.

Detoxification of Hydrolysate by Treatment with Cation- and Anion-Exchange Resins

To optimize the operating conditions for the detoxification of the hydrolysates with resins, experiments were carried out with synthetic solutions. Table 3 shows how the detoxifying efficiency of the anionic resin Dowex 1 diminished with increasing treated volume. Aliquots of the solution eluted through the column were sampled after 120, 230, and 250 mL. As a whole, after the early 600 mL, the column still had a fair cleaning efficiency for acids but a reduced removal efficiency toward the furan compounds: the data show that the cleaning efficiency of the column was 99% for formic acid, 87% for acetic acid, 40% for HMF, and 46% for furfural. An optimized resin/solution ratio of 0.14 g/g was thus extrapolated. The addition of a subsequent detoxification step with the cationic resin Dowex-50W left the concentrations of the acids almost unchanged whereas it further reduced those of HMF and furfural by 14 and 26%, respectively. The detoxification of the hydrolysate was performed on the basis of this optimized detoxification setup.

Table 4 summarizes the concentrations of the steam-exploded degradation byproducts and the most abundant monosaccharides released from the chips during hydrolysis. No meaningful differences in the concentrations of the byproducts were observed after 48 h. Only the concentrations at 24 h appeared slightly higher than they were later. This trend could be owing to a partial adsorption through the hydrolysis time of these mol-

Table 2
Monosaccharide Yields (%DM) from Bench-Scale Enzymatic Hydrolysis of Steam-Exploded Aspen Chips[a]

Xylanase (IU/g)	Biomass loading (DM) (g/L)	Glucose	Xylose
63	100	53 ± 4	95 ± 3
100	100	55 ± 6	92 ± 2
63	200	42 ± 3	72 ± 6
100	200	45 ± 1	79 ± 5

[a]The cellulase and β-glucosidase activities were 30 filter paper units/g of DM substrate and 47 IU/g of DM substrate, respectively.

Table 3
Variation of Detoxifying Efficiency of Anionic Resin DOWEX 1 at Increasing Eluted Volume: After 120 mL (I), After 230 mL (II), and After 250 mL (III)[a]

		Percentage of removed inhibitors		
Compound	Initial concentration (ppm)	I	II	III
Formic acid	1285	100.0	99.8	98.1
Acetic acid	10302	99.6	100.0	63.4
5HMF	56	100.0	100.0	6.9
Furfural	1178	76.5	36.3	19.6

[a]The column bed was made with 90.13 g of DM resin. The elution flow rate was 3 mL/min.

ecules onto the insoluble lignin fraction. Although not quantitative, the hydrolysis was already completed at 48 h and the syrup composition did not change after the stage of thermal deactivation of the enzyme. Through the use of the two ion-exchange columns arranged as described under Subheading "Detoxification of Hydrolysate by Treatment with Cation- and Anion-Exchange Resins," almost all the detected inhibitors were efficiently removed. The sugars composition remained unaffected in agreement with data reviewed by Parajó et al. *(18)* on the retention of carbohydrates of ion-exchange resins. Other aromatic compounds (e.g., lignin-derived compounds) were likely to be removed from this treatment since the treated solution appeared pale yellow while the hydrolysate was brown .

Fermentation of Standard Model Solutions of Glucose and Xylose

The fermentative performance of *P. stipitis* immobilized in Ca-alginate beads was first investigated using concentrated solutions of xylose. The higher ethanol yield and productivity obtained from the fermentation of 60 g/L of xylose working with a cell concentration of 2.34×10^9 cells/L were 0.46 $g_{ethanol}/g_{initial\ sugars}$ (g_e/g_s) and 0.40 g/(L·h), respectively. Only traces of secondary metabolites were detected.

Table 4
Concentrations (g/L) of Main Degradation Byproducts and Monosaccharides Obtained During Enzymatic Hydrolysis and After Detoxification with Ion-Exchange Resins

Compounds	Concentrations during hydrolysis			Concentrations after thermal deactivation of enzymes	Concentrations after detoxification
	24 h	48 h	72 h		
Formic acid	1.60 ± 0.06	1.30 ± 0.03	1.4 ± 0.04	1.39 ± 0.05	0.049 ± 0.008
Acetic acid	8.1 ± 0.4	7.26 ± 0.16	7.8 ± 0.4	8.0 ± 0.3	0.553 ± 0.041
5HMF	0.160 ± 0.001	0.146 ± 0.001	0.148 ± 0.008	0.139 ± 0.004	0.008 ± 0.001
Furfural	0.420 ± 0.003	0.356 ± 0.001	0.345 ± 0.001	0.337 ± 0.001	0.0160 ± 0.0005
Glucose	34 ± 3	49 ± 4	45 ± 4	43 ± 3	43 ± 3
Xylose	12 ± 1.0	12.2 ± 1.1	11 ± 1.0	12.0 ± 1.1	11.2 ± 1.0

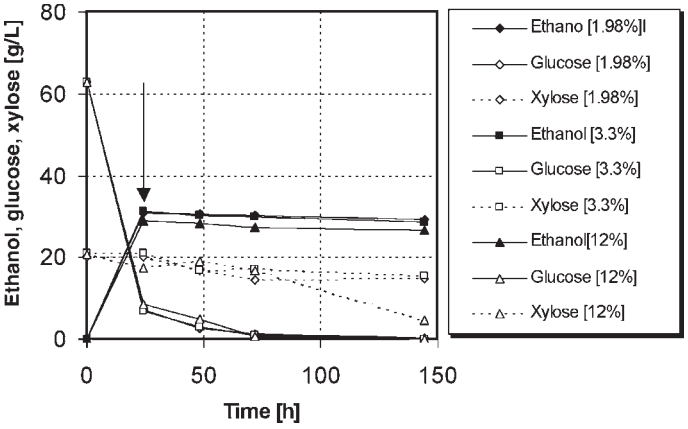

Fig. 2. Sequential fermentation of model solutions of glucose (60 g/L) and xylose (20 g/L) in shake flasks containing same amount of suspended *S. cerevisiae* (3 g/L) and different gel fractions (percentages in parenthesis) of immobilized *P. stipitis*. The initial cell concentrations of *P. stipitis* were (◆), 7.02×10^9; (■), 1.17×10^{10}; (▲), 4.10×10^{10} cells/L.

Several strategies were investigated to achieve the cofermentation of mixed sugar syrups containing glucose and xylose in concentrations similar to those recoverable from the hydrolysis of steam-exploded aspen chips. Since glucose causes the so-called xylose catabolism repression, beads of *P. stipitis* were introduced into the flasks after the glucose consumption from *S. cerevisiae* was almost completed. This approach is not exactly a cofermentation scheme but rather a sequential fermentation. The pH was not adjusted. Figure 2 shows the trend of ethanol production and sugar consumption obtained by varying the gel fractions. During the early 24 h almost all the glucose in the medium was converted into ethanol. At that time (arrow in Fig. 2) different fractions of beads containing *P. stipitis* were introduced into the three systems in order to convert the residual xylose. However, from that point the ethanol yield leveled off, and the diminution of the xylose concentration in the system was owing to the formation of xylitol. The nonregulation of the pH and/or the relatively high ethanol concentration (30 g/L) during the lag phase of *P. stipitis* could have inhibited the production of ethanol from this yeast. To ascertain the influence of pH, mixed sugar syrups were fermented using the same approach but with regular adjustment of the pH to the initial value of 5.5. Higher concentrations of *P. stipitis* were also loaded; Fig. 3 summarizes the results. The trends show that even when the pH was adjusted to 5.5, the xylose consumption did not correspond to the ethanol increase and that already 15 g/L could inhibit the fermentation from *P. stipitis* in a sequential fermentation approach. Isolated strains of ethanol-adapted *P. stipitis* could be necessary in this process scheme. Moreover, this result also confirms that the immobilization somehow stabilizes the fermentation capacity of yeasts in a wide range of pH values *(19)*.

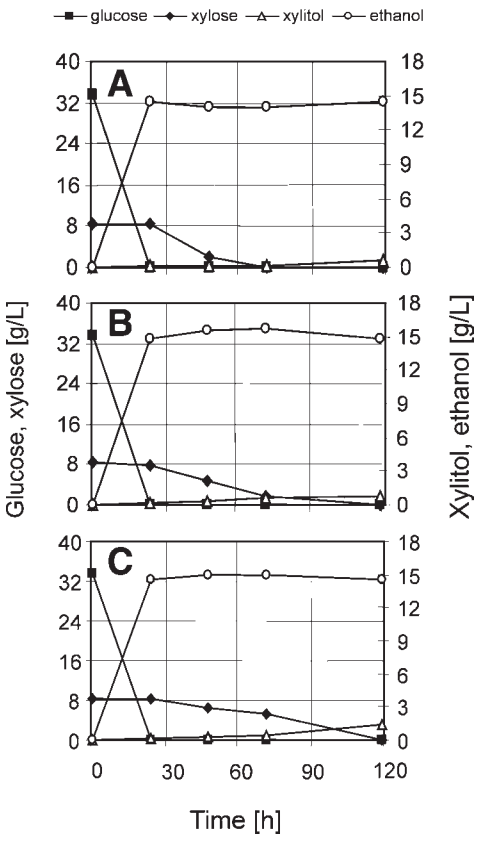

Fig. 3. Sequential fermentation of model solutions of glucose and xylose in shake flasks. Systems A, B, and C contained suspended *S. cerevisiae* and immobilized *P. stipitis* with a loading ratio of *P. stipitis*/*S. cerevisiae* of 1.4 g/g dry wt. The gel fractions were as follows: system A, 0.36; system B, 0.18; and system C, 0.09 g/g. The concentrations of *P. stipitis* cells were as follows: system A, 2.83×10^{12}; system B, 1.41×10^{12}; and system C 7.31×10^{11} cells/L.

The coimmobilization of both yeasts was therefore investigated. Taking into account the results from Grootjen et al. *(6,7)*, the amounts of *P. stipitis* loaded into the beads were higher than those of *S. cerevisiae*. Usually the internal ratio was fixed at 1:4 *S. cerevisiae*/*P. stipitis* dry cell mass.

Figure 4 presents data on the cofermentation of glucose and xylose. The production of ethanol still appeared to be at the expense of glucose consumption. Note that systems E and F did not show significant differences whereas the amount of ethanol in system D was roughly 25% higher. This could imply that a threshold cell concentration is necessary.

To ascertain whether different process configurations could have any effect on the process yields, the same cell loading of system D in Fig. 4 was

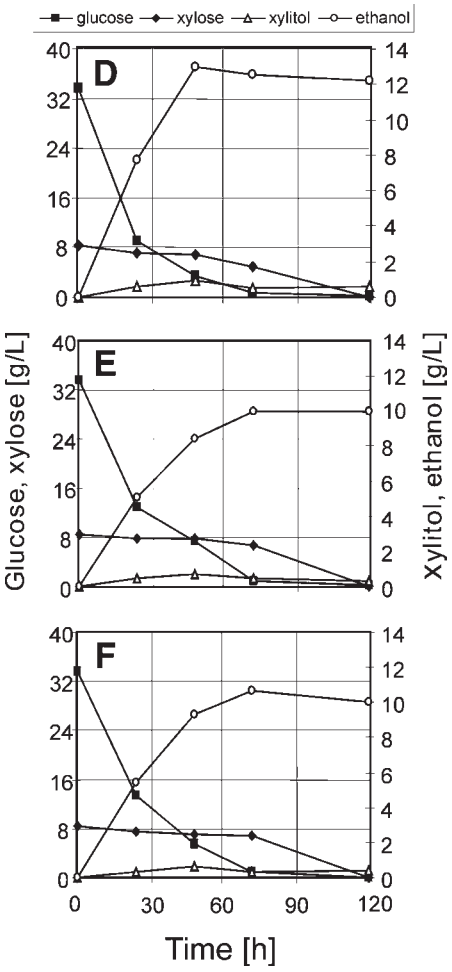

Fig. 4. Cofermentation of model solutions of glucose and xylose. Systems D, E, and F contained beads of *S. cerevisiae* and *P. stipitis* coimmobilized with a loading ratio of *P. stipitis*/*S. cerevisiae* of 4 g/g. The gel fractions were as follows: system D, 0.10; system E, 0.05; and system F, 0.025 g/g. The total cells concentrations were as follows: system D, 4.80×10^{11}; system E, 2.40×10^{11}; and system F, 1.20×10^{11} cells/L.

used in the FBR and STR. Moreover, to avoid rupture of the beads owing to the impeller agitation in the STR, experiments were conducted using modified STR configurations. An early attempt to achieve this purpose was made by adding marbles to the bioreactor volume. The resulting effect was a broader distribution of the gel beads throughout the bioreactor and the formation of a low shear environment. Specifically, the marbles protected the beads from shear and allowed them to overcome the diffusion limitations by settling at higher stirring rates.

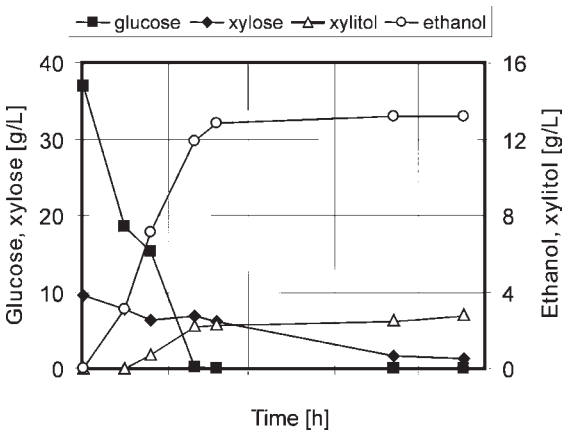

Fig. 5. Cofermentation of model solutions of glucose and xylose in FBR. The total initial cell concentration was 6.57×10^{11}cells/L and the gel fraction was 0.1 g/g. The ration of *P. stipitis*/*S. cerevisiae* was 4 g/g. The number of beads inside the column was 3286. The airflow in the column and inside the reservoir was 0.030 vvm.

Figure 5 shows the experimental results of the continuous glucose and xylose cofermentation in the FBR. The aeration conditions were chosen on the basis of the ranges reported in the literature for free-cell cultures *(5,20)*. The maximum amount of ethanol produced is comparable with that of system D in Fig. 4, and the xylose consumption is evidently the result of the formation of xylitol. Despite the air bubbled into the medium reservoir and at the bottom of the column, the oxygen concentration in the medium continuously dropped during the fermentation, reaching zero after 24 h. When the concentration of ethanol leveled off, the process was stopped, and the beads were washed with saline solution before being used in a second fermentation run with a fresh solution of sugars. After 24 h, the glucose concentration was almost zero while only 47% of xylose was consumed. In other words, the ethanol productivity in the second cycle was 49% higher than in the first cycle, whereas the rate of xylose consumption was still lower than that of glucose.

It is already known that under anaerobic conditions the xylose-fermenting yeasts do not produce ethanol because the electron transport in the respiratory chain is not activated *(20)*. Since either aeration or oxidizing compounds, such as acetone, could increase the ethanol yield, the effect of improving the oxygenation of the medium or adding oxidizers was investigated using an STR partially filled with marbles.

Perego et al. *(20)* found that during the fermentation of hemicellulose hydrolysates by *Candida shehatae*, the addition of 50 m*M* acetone resulted in ethanol yields comparable with those obtained under microaerophilic conditions. Thus, the addition of 50 m*M* acetone to the culture

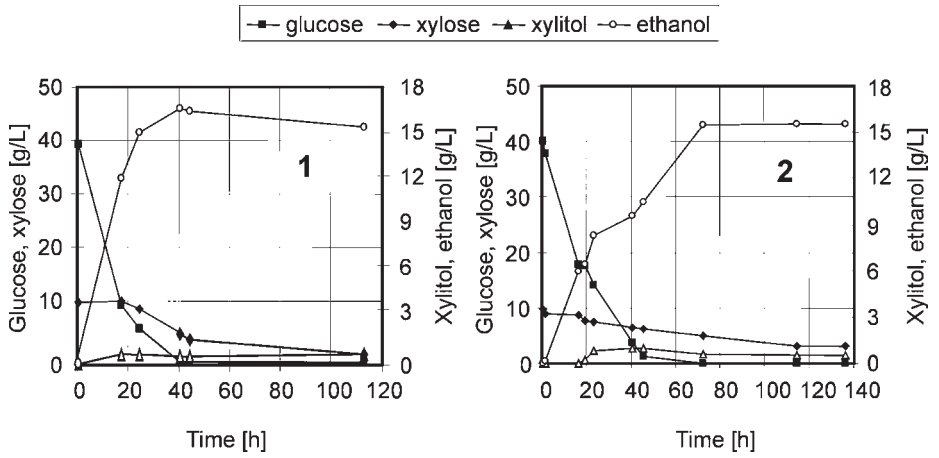

Fig. 6. Effect of aeration (0.030 vvm) through Teflon-made diffusers (system 1) and acetone addition (50 m*M*) (system 2) on cofermentation of synthetic solutions of glucose and xylose in STR containing marbles. In both cases, the beads were prepared with an internal ratio of *P. stipitis*/*S. cerevisiae* of 4 g/g, and the gel fraction was almost 0.1 g/g. The initial cell concentration in system 1 was 8.6×10^{11} cells/L while that in system 2 was 8.42×10^{11} cells/L.

broth was considered in place of aeration during the fermentation of synthetic solutions.

On the other hand, to improve oxygenation of the medium, two Teflon-made high-performance liquid chromatography filters were used as air diffusers. The dimension of the bubbles was then visibly smaller than that obtained with the metallic annular sparger and a slightly better dispersion of bubbles was possible with the Rushton impeller. The results obtained by improving the oxygenation and adding acetone are shown in Fig. 6 (system 1) and (system 2), respectively. Both trends show an increase in ethanol production, though in both cases a significant xylose consumption never started before 24 h, and the ethanol production appeared still dependent mainly on the glucose metabolism. In addition, the presence of acetone even slowed down the glucose consumption and therefore the ethanol productivity.

Based on the results discussed so far, it appears that under similar cell-loading conditions neither the reactor configuration nor the aeration conditions had a remarkable effect on the xylose conversion into ethanol, although they could affect the yield of ethanol from glucose and the concentration of secondary metabolites (xylitol and lactic acid). As a result, higher initial cell concentrations were considered. However, when beads were loaded with high amounts of yeast, the cells counted inside the beads after all the sugars were consumed did not differ significantly from the initial number.

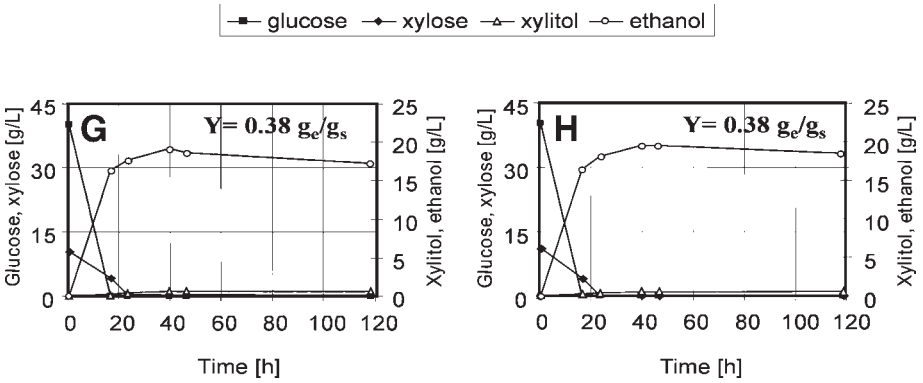

Fig. 7. Cofermentation of model solutions of glucose and xylose with *P. stipitis* and *S. cerevisiae* separately immobilized (system G) and coimmobilized (system H) in Ca-alginate beads. The gel fraction in system G was made of 0.20 g/g of beads containing *P. stipitis* and 0.05 g/g of beads containing *S. cerevisiae*. The initial concentrations of *P. stipitis* and *S. cerevisiae* cells were 5.64×10^{12} and 1.89×10^{11} cells/L, respectively. The gel fraction in system H was made of 0.25 g/g of beads containing *P. stipitis* and *S. cerevisiae* coimmobilized with a loading ratio of *P. stipitis*/*S. cerevisiae* of 4 g/g of dry cells. The total cells concentration was 6.01×10^{12} cells/L.

Moreover, it would seem that whatever the amount of yeast suspended in the alginate mixture before its gelling in the $CaCl_2$ solution, the beads would not entrap more than 6 to 7 $\times$ 10^8 cells/bead. On the whole, it could be inferred that the microenvironment of the beads has a saturating uptake and that an excessive yeast loading could produce a rapid diffusion of the cells out of the beads. In light of these results, higher initial cell concentrations were realized by loading a higher fraction of beads instead of higher cell concentrations inside the gel matrix. The maximum number of yeast cells that could be entrapped within the beads might be critical when yeasts with different growing rates are coimmobilized. In fact, the faster-growing yeast could reduce the available bead volume. To ascertain whether a different distribution of the yeasts in the gel phase could affect the process yield, cofermentation tests were conducted with two different gel phases: (1) a gel phase made of 80% beads entrapping *P. stipitis* and 20% beads entrapping *S. cerevisiae*; and (2) a gel phase made of beads coimmo-bilizing *P. stipitis* and *S. cerevisiae* with an internal ratio of 4:1 g/g, respectively. In the former case, the same yeast DM per gel was used for the preparation of the two stocks of beads; the results are displayed in Fig. 7. In both cases, glucose and xylose were consumed simultaneously. The ethanol yields after 40 h were very similar (0.38 g_e/g_s). This means that the cell concentration affected the process yields more than the way that the yeasts were distributed in the gel phase.

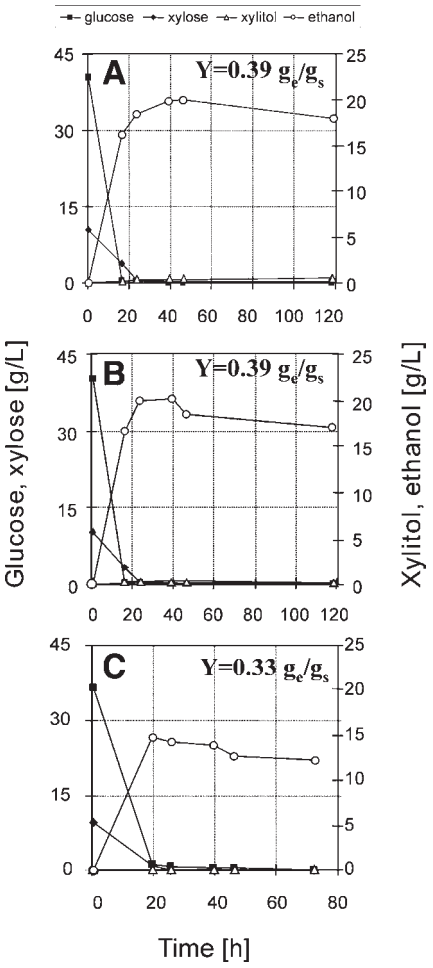

Fig. 8. Cofermentation of detoxified hydrolysates in shake flasks (A and B) and in STR modified with perforated cylinder. For the experimental conditions of graph A, refer to graph G in Fig. 7, and for those of graphs B and C refer to graph H in Fig. 7.

Fermentation of Hydrolysates

Considering the results obtained in the test runs of synthetic solutions, the cofermentation of detoxified hydrolysates was carried out at flask scale using the same experimental conditions as described in Fig. 7; the results are presented in Fig. 8. The ethanol yields were slightly higher than those obtained working with synthetic solutions, but they were still comparable with respect to the composition of the sugar syrup used (0.39 g_e/g_s). It is likely that in the absence of furfural, the residual amount of acetic acid in the detoxified hydrolysate could have enhanced ethanol production *(21,22)*.

Figure 8C illustrates the experimental results of the cofermentation of the hydrolysate in the STR modified with a perforated cylinder. The function of this cylinder was the same as previously discussed for marbles. The cylinder confined the beads in the cavity between the bioreactor and the impeller, thereby preventing the beads from knocking against the impeller. This allows higher stirring rates (up to 300 rpm) to be settled. Moreover, the radial agitation of the Rushton impeller, combined with the presence of the pierced cylinder, made the beads flow in a circular bottom-up direction. Glucose and xylose were consumed simultaneously and even faster than in shake flasks under similar experimental conditions. Nevertheless, the ethanol yield was $0.33 g_e/g_s$, lower than that obtained in shake flasks and a diminution of ethanol was observed soon after 20 h. This result was probably owing to nonoptimized aeration conditions.

Conclusion

The main purpose of this study was to investigate one of the possible process schemes for ethanol production from glucose and xylose of steam-exploded aspen chips. The process strategy provided the simultaneous hydrolysis of cellulose and hemicellulose followed by detoxification through resins and cofermentation with immobilized cells. In the best conditions, the cofermentation of 40 g/L of glucose and 10 g/L of xylose with coimmobilized *S. cerevisiae* and *P. stipitis* yielded 0.396 $g_{ethanol}/g_{sugars\ consumed}$ and a conversion of 0.995 $g_{consumed}/g_{initial}$. In other words, the process produced 77% of the theoretical ethanol yield. Attention was devoted to improvement of the performances of the STR by making some modifications in the original design. Although preliminary, our results suggest that insertion of marbles at the bottom of the reactor enables a high stirring rate (up to 300 rpm) without affecting the beads' lifetime. The same effect was observed using a perforated metal cylinder placed around the stirrer axle. In the latter case, a larger fluidization can be achieved. These results are not intended to be conclusive. Further investigations are still in progress to define the fermentation scheme and bioreactor configuration that will ensure higher productivities and yields without reducing the catalyst stability inside the gel carrier.

Acknowledgments

We gratefully acknowledge Dr. Ugo De Corato for helpful discussions about the biochemistry of yeasts, G. Cardinale for preparation of the steam-exploded aspen, and C. Gargaglione and A. Manfredi for their skilled and encouraging assistance in the realization of some mechanical components of the bioreactors. The work was carried out within programmatic agreement between ENEA-MIUR (Italian Ministry of University and Scientific Research) and cofinanced by the European Union, Framework Program V (project NNE5-1999-00272, contract ERK6-CT-1999-0012).

References

1. Delgenes, J. P., Laplace, J. M., Moletta, R., and Navarro, J. M. (1996), *Biomass Bioenergy* **11(4),** 353–360.
2. Bothast, R. J., Nichols, N. N., and Dien, B. S. (1999), *Biotechnol. Prog.* **15,** 867–875.
3. du Prez, J. C., Bosch, M., and Prior, B. A. (1986), *Enzyme Microb. Technol.* **8,** 360–364.
4. Nakamura, Y., Sawada, T., and Inoue, E. (2001), *J. Chem. Technol. Biotechnol.* **76,** 586–592.
5. Taniguchi, M., Tohma, T., Itaya, T., and Fujii, M. (1997), *J. Ferment. Bioeng.* **83(4),** 364–370.
6. Grootjen, D. R. J., Meijlink, L. H. H. M., Vleesenbeek, R., van der Lans, R. G. J. M., and Luyben, K. C. A. M. (1991), *Enzyme Microb. Technol.* **13,** 530–536.
7. Grootjen, D. R. J., Meijlink, L. H. H. M., van der Lans, R. G. J. M., and Luyben, K. C. A. M. (1991), *Enzyme Microb. Technol.* **12,** 860–862.
8. Nagaschima, M., Azuma, M., and Noguchi, S. (1983), *Ann. NY Acad. Sci.* **413,** 457–468.
9. Sajc, L., Grubisic, D., and Vunjak-Novakovic, G. (2000), *Biochem. Eng. J.* **4,** 89–99.
10. Estapé, D., Gòdia, F., and Solà, C. (1992), *Enzyme Microb. Technol.* **14,** 396–401.
11. Abatzoglou, N., Chornet, E., and Belkacemi, K. (1992), *Chem. Eng. Sci.* **47,** 1109–1122.
12. Zimbardi, F., Viggiano, D., Nanna, F., Demichele, M., Cuna, D., and Cardinale, G. (1999), *Appl. Biochem. Biotechnol.* **117,** 77–79.
13. De Bari, I., Viola, E., Barisano, D., Cardinale, M., Nanna, F., Zimbardi, F., Cardinale, G., and Braccio, G. (2002), *Ind. Eng. Chem. Res.* **41(7),** 1745–1753.
14. Nigam, J. N. (2002), *J. Biotechnol.* **97,** 107–116.
15. Walsh, P. K., Isdell, F. V., Noone, S. M., O'Donovan, M. G., and Malone, D. M. (1996), *Enzyme Microb. Technol.* **18,** 366–372.
16. Haltrich, D., Nidetzky, B., Kulbe, K. D., Steiner, W., and Zupancic, S. (1996), *Bioresour. Technol.* **58,** 137–161.
17. Sun, Y. and Cheng, J. (2002), *Bioresour. Technol.* **83,** 1–11.
18. Parajó, J. C., Domínguez, H., and Domínguez, J. M. (1998), *Bioresour. Technol.* **66,** 25–40.
19. Jirku, V. (1999), *Process Biochem.* **34,** 193–196.
20. Perego, P., Converti, A., Palazzi, E., del Borghi, M., and Ferraiolo, G. (1990), *J. Ind. Microbiol.* **6,** 157–164.
21. Palmqvist, E., Grage, H., Meinander, N. Q., and Hahn-Hägerdal, B. (1998), *Biotechnol. Bioeng.* **63(1),** 46–55.
22. Pampulha, M. E. and Loureiro-Dias, M. C. (2000), *FEMS Microbiol. Lett.* **184,** 69–72.

0273-2289/04/114/0559–0568/$25.00

Silymarin Extraction from Milk Thistle Using Hot Water

Lijun Duan,[1] Danielle Julie Carrier,[2] and Edgar C. Clausen*,[1]

[1]Department of Chemical Engineering, University of Arkansas, 3202 Bell Engineering Center, Fayetteville, AR 72701, E-mail: eclause@engr.uark.edu; and [2]Department of Biological and Agricultural Engineering, University of Arkansas, 203 Engineering Hall, Fayetteville, AR 72701

Abstract

Hot water is attracting attention as an extraction solvent in the recovery of compounds from plant material as the search for milder and "greener" solvents intensifies. The use of hot water as an extraction solvent for milk thistle at temperatures above 100°C was explored. The maximum extraction yield of each of the silymarin compounds and taxifolin did not increase with temperature, most likely because significant compound degradation occurred. However, the time required for the yields of the compounds to reach their maxima was reduced from 200 to 55 min when the extraction temperature was increased from 100 to 140°C. Severe degradation of unprotected (plant matrix not present) silymarin compounds was observed and first-order degradation kinetics were obtained at 140°C.

Index Entries: Milk thistle; extraction; silymarin; hot water; silybinin; taxifolin; silychristin.

Introduction

Milk thistle (*Silybum marianum*) is an annual or biennial plant native to the Mediterranean that now grows wild throughout Europe, America, and Australia. The active ingredients in milk thistle seeds are the dihydroquercitin taxifolin, and the flavanolignans silybinin (present as silybinin A and B), isosilybinin, silydianin, and silychristin. The structures of these compounds are shown in Fig. 1. The flavanolignans, also referred to as silymarin, are found throughout the entire milk thistle plant but are concentrated in the fruits and seeds *(1)*.

*Author to whom all correspondence and reprint requests should be addressed.

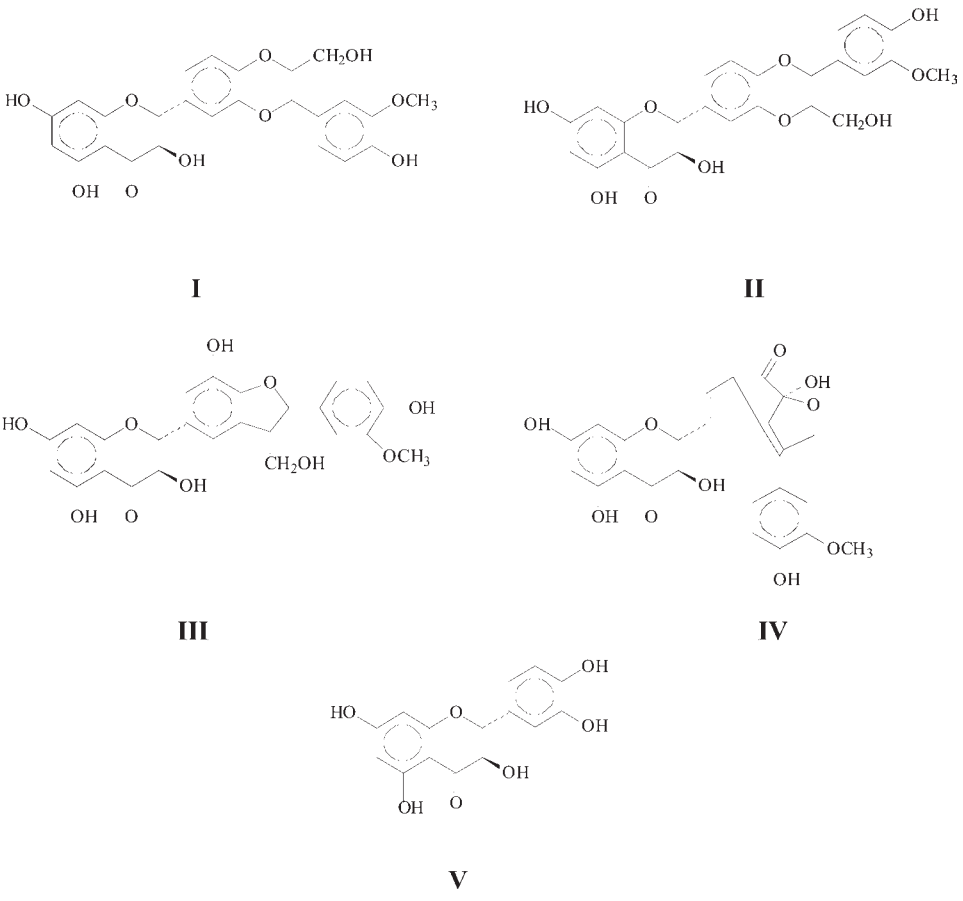

Fig. 1. Structures of dihydroflavanol and flavanolignan compounds found in milk thistle seeds: (I) Silybinin; (II) isosilybinin; (III) silychristin; (IV) silydianin; (V) taxifolin.

Silymarin has been used to prevent and treat a variety of liver diseases and to protect the liver against toxicity. Double-blind studies of 57 patients with acute hepatitis showed that therapy with silymarin deceased complications, hastened recovery, and shortened hospitalization *(2)*. Silymarin has also proved to be effective in treating chronic hepatitis and cirrhosis *(1,3)*, and more recent studies have shown that silymarin has potential in treating many other human diseases such as skin cancer, prostate cancer, and damaged kidneys *(4–8)*. Milk thistle extracts containing silymarin as the active ingredient have become increasingly popular worldwide. In 2001, sales of milk thistle in the United States increased 13% and now exceed $7 million *(9)*. Annual sales of milk thistle extract in Germany exceed $180 million *(2)*.

Although organic solvents such as hexane, methanol, and ethanol are traditionally used in extracting compounds from plants, water has

recently received special attention as an extraction solvent owing to its "greenness" and comparatively low purchase and disposal costs. Water has been reported to solubilize environmentally aggressive compounds at increased temperatures using elevated pressure to keep the water in the liquid state *(10)*. The dielectric constant, surface tension, and viscosity of water are so dependent on temperature *(10,11)* that with a mere adjustment of temperature and pressure, water can be made to have properties approaching those of organic solvents. Similarly, temperature adjustment enables water to extract both polar and nonpolar compounds from plant matrices. Alvarez Barreto et al. *(12)* studied the batch extraction of silymarin from ground milk thistle seeds using water at 50–100°C. Their results showed that higher yields were obtained at increased temperature, and that the more polar compounds (taxifolin and silychristin) were preferentially extracted at 85°C, while the less polar silybinin was favored at 100°C. Unlike organic solvents, which require defatting of the milk thistle prior to extraction, water extraction did not require defatting.

The present study focused on using hot water as the extraction solvent at 100–140°C to extract silymarin compounds from milk thistle seed meal without prior defatting in a batch dynamic mode. A laboratory apparatus was constructed and used to obtain silymarin compound concentrations as a function of time. Because compound degradation is possible at elevated temperatures, degradation kinetics were also investigated at 140°C using commercial preparations of silymarin.

Materials and Methods

Milk Thistle Seeds and Compounds

Milk thistle seeds were purchased from Frontier Herbs (Norway, IA). Water for extraction was treated in a Milli-Q TM Water System from Millipore (Bedford, MA), and high-performance liquid chromatography (HPLC)–grade methanol was obtained from Honeywell (Muskegon, MI). Silymarin (also known as silybin) was purchased from Sigma (St. Louis, MO) and used in compound degradation studies. Taxifolin standard was obtained from Extrasynthese (Lyon, France). Among the silymarin compound standards, silybinin was obtained from Sigma, and silychristin from PhytoLab (Hamburg, Germany). No standard was available for isosilybinin.

Extraction Apparatus

A hot water dynamic extraction device was constructed using the solubilization apparatus of Miller and Hawthorne *(10)* as a model and was used for pressurized extraction of milk thistle seed meal. Figure 2 shows a schematic diagram of the apparatus. Water, the extraction solvent, was pressurized and pumped using a Bio-Rad 2800 HPLC solvent delivery system (Hercules, CA) to an extraction cell housed in the oven of a Hewlett-Packard 5890 gas chromatography (GC) oven (Wilmington, DE). Before

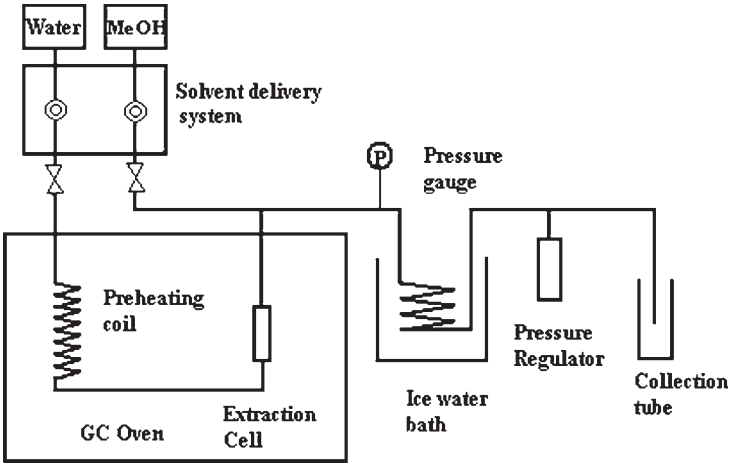

Fig. 2. Diagram of pressurized hot/liquid water extraction apparatus.

entering the extraction cell, the water was fed through a 3-m stainless steel (1.6-mm id) preheating coil. The preheating coil is necessary to ensure that water is at the required operating temperature prior to entering the extraction cell. The stainless steel extraction cell (6.4-mm id, 9.5-mm od, 67.1-mm length) held the ground milk thistle seed meal, along with a layer of washed sea sand, placed just before the cell outlet to prevent seed meal solids from clogging the system. To prevent deposition of the extracted compounds on leaving the oven, methanol was added to the aqueous solution using a Bio-Rad HPLC solvent delivery system through a tee, placed in the oven between the cell and the pressure gage. The pressure gage indicated the pressure under which the extraction is carried out. A 1-m cooling coil, immersed in ice water, was used to cool the water/extracts/methanol mixture to room temperature prior to collection. The mixture was collected in tubes as a function of time and stored for subsequent analysis.

Extraction Procedures

To prepare the solids for extraction, an aliquot of milk thistle seeds was ground to an average particle size of 0.4 mm using a Braun KSM 2B coffee grinder. Approximately 0.5 g of the milk thistle seed meal was packed into the extraction cell along with about 2 g of washed sea sand (40–50 mesh) at the extraction cell outlet to prevent plugging of the cell frit. After the loaded extraction cell was installed in the GC oven, water was pumped through the cell at a constant flow rate via the preheating coil. When water was observed at the collection exit, methanol flow was initiated. The pressure regulator was adjusted to keep the pressure above the saturation pressure of water at the desired temperature selected in the GC oven. When the desired temperature was reached, continuous sample

collection began using preset time intervals for each sample tube. After collection, 1 mL of each sample was evaporated to dryness in a self-constructed evaporator while sparging with compressed nitrogen. The solids were redissolved in 1 mL of methanol, filtered (0.45-µm filter), and analyzed by HPLC.

Compound Degradation Procedures

Silymarin compound degradation studies were carried out at 140°C in stainless steel tubes (2.0-mm id, 3.2-mm od, 152-mm length) completely filled with the silymarin solution so as to exclude air and sealed with end caps on both sides. pH was not monitored in these initial experiments aimed at determining whether degradation was indeed likely present. At the beginning of a degradation experiment, all of the tubes were placed in the GC oven at the desired temperature. Six tubes were removed simultaneously every 10 min and quickly placed in ice water. The liquid was collected and analyzed by HPLC as described below.

Analytical Methods

The concentrations of the individual silymarin compounds and taxifolin were determined by HPLC using a Waters system (Milford, MA) composed of an Alliance 2690 separations module and a 996 Photodiode Array detector controlled with Millennium[32] chromatography software. The HPLC procedure was previously described by Wallace et al. *(13)*. Calibration curves were prepared from standard solutions of taxifolin, silychristin and silymarin. The silybinin standard from Sigma contained two distinct peaks, which are further referred to as silybinin A (the first peak) and silybinin B (the second peak).

Results and Discussion

Extraction

Milk thistle seed extraction experiments were carried out with hot water at 100, 120, and 140°C using the same water flow rate (0.30 mL/min) and seed meal particle size (0.4 mm). The pressures employed in the experiments at these temperatures were approx 1, 4, and 5 atm, respectively. Figure 3 shows results from typical runs at 100, 120, and 140°C, where the compound concentrations from the collected water (methanol added for solubilization is subtracted out) in each sample aliquot from the continuous flow apparatus are plotted as a function of time. Thus, the concentrations presented represent the average concentrations of the four main extracted compounds in an aliquot. As noted in Fig. 3, the concentrations of each of the compounds reached a maximum after a few minutes of extraction time and then fell exponentially with time as the extracted material was removed from the solid sample. The time for obtaining the maximum compound concentration decreased with temperature.

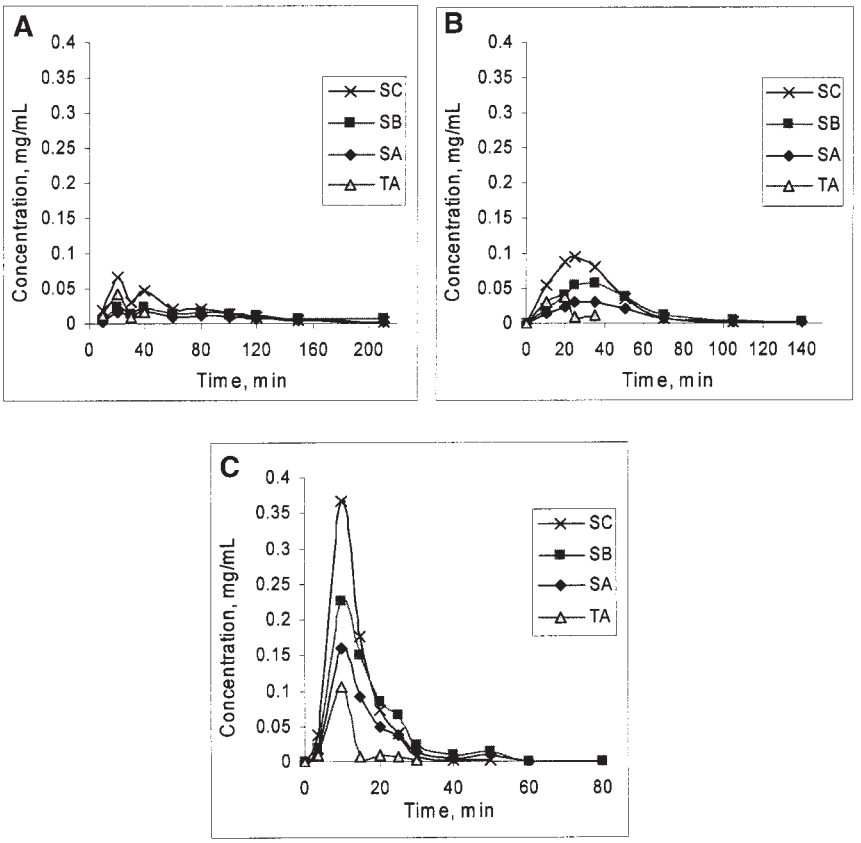

Fig. 3. Concentrations of silymarin compounds and taxifolin at outlet of extraction cell as function of time with extraction temperature at **(A)** 100°C, **(B)** 120°C, and **(C)** 140°C. SC, Silychristin; SB, silybinin B; SA, silybinin A; TA, taxifolin).

The data in Fig. 3 were used to prepare cumulative yield plots as a function of time and each extraction temperature, as noted in Fig. 4. The cumulative yield is defined as the cumulative quantity of extracted compound per mass of seed. These plots are useful in comparing the quantities of each of the compounds extracted but are limited in that they do not show any information about compound degradation. In analyzing the results in Fig. 4, a short, rapid extraction period at the beginning of the extraction was followed by a longer, slow extraction period, shown as a leveling off of the compound yields. Each of the curves for the extracted compounds presented similar shapes at the three different temperatures, reaching essentially the same yield maxima regardless of the experimental condition. This observation was unexpected, since elevated temperatures should result in the extraction of more nonpolar compounds (silybinin A and B), while lower temperatures should favor the extraction of more polar compounds (such as silychristin). In fact, Alvarez Baretto et al. *(12)* saw this preferential extraction effect in studying the extraction

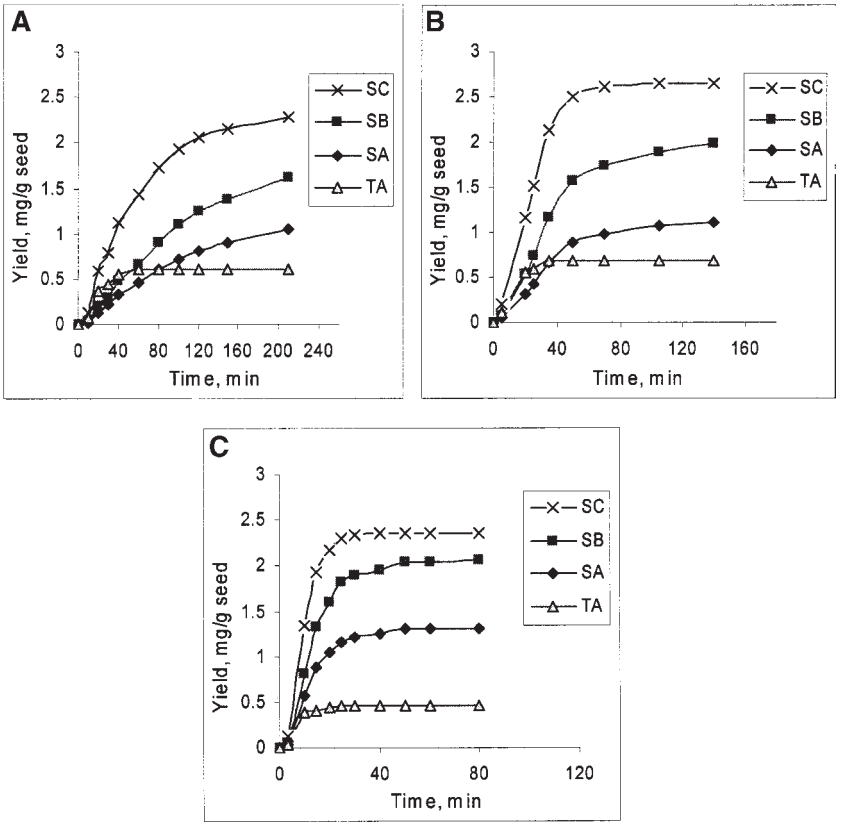

Fig. 4. Extraction yields of silymarin compounds and taxifolin as function of time at **(A)** 100°C, **(B)**120°C, and **(C)**140°C. SC, Silychristin; SB, silybinin B; SA, silybinin A; TA, taxifolin.

of silymarin compounds and taxifolin over a temperature range of 50–100°C. As expected, the maxima were reached faster as the temperature was increased and pseudo equilibrium was approached.

Further comparisons of the extraction data at the three temperatures are shown in Tables 1 and 2. As noted in Table 1, the maximum yields of the silymarin compounds at the three extraction temperatures essentially did not vary, with the yields of silymarin compounds at 120°C being just slightly higher than those at 100 and 140°C. It is known that extraction efficiency increases with temperature. Richter et al. *(11)* theorized that this is owing to enhanced solubilization, higher diffusivity of solutes, and disruption of the strong solute-matrix interaction caused by Van der Waals forces, hydrogen bonding, and dipole forces of solute molecules and active sites on the matrix at increased temperature. According to these theories, the yields of the silymarin compounds and taxifolin should have increased with temperature. Thus, temperature had a positive effect on extraction yield, however, it was perhaps circumvented by a temperature-induced degradation.

Table 1
Yields of Silymarin Compounds and Taxifolin at 100, 120, and 140°C

	Maximum yield (mg/g seed)			
Temperature (°C)	Taxifolin	Silychristin	Silybinin A	Silybinin B
100	0.6	2.3	1.0	1.6
120	0.7	2.5	1.2	2.2
140	0.5	2.4	1.2	2.0

Table 2
Times for Yields of Silymarin Compounds and Taxifolin
to Reach Their Maximum Concentrations at 100, 120 and 140°C

	Time to reach maximum yield (min)			
Temperature (°C)	Taxifolin	Silychristin	Silybinin A	Silybinin B
100	60	200+	200+	200+
120	40	140+	140+	140+
140	30	55	55	55

Wallace et al. *(13)* observed potential thermal degradation of silymarin compounds when extracting milk thistle seed meal with ethanol in a Soxhlet apparatus at 78°C, they noted that the yield of silymarin decreased at long extraction times and that the yields were higher at 60°C. The times for the yields of the silymarin compounds to reach a maximum, shown in Table 2, significantly decreased with increasing temperature. For example, the time for the yield of silychristin to reach its maximum at 140°C was about one-fourth the time at 100°C, with close yields at both temperatures.

Compound Degradation

Preliminary compound degradation studies were performed with solutions of the silymarin compounds, and thus the compounds were unprotected by the plant matrix during heating. The results of the experiment, performed at 140°C, confirm the existence of significant compound degradation. More extensive degradation studies (additional temperatures, degradation product identification) will be performed later. Exponential decay of silybinin A and silybinin B was observed, as demonstrated in Fig. 5. After 10 min of incubation of the silymarin solution at 140°C, no silychristin was detected by HPLC.

Thermal degradation can be modeled as a first-order irreversible reaction, which can be described by Eq. 1:

$$\frac{dC_C}{dt} = -kC_C \tag{1}$$

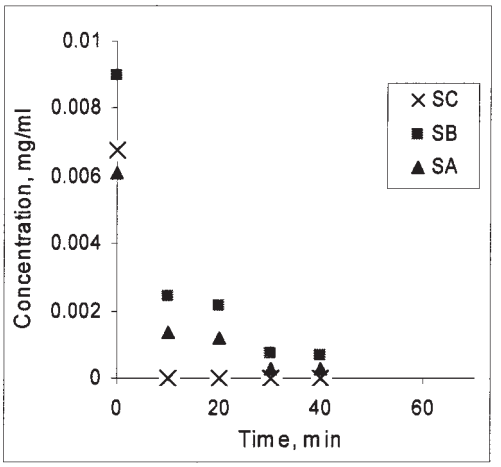

Fig. 5. Concentrations of silybinin A, silybinin B and taxifolin at 140°C as function of time during compound degradation studies. SC, Silychristin; SB, silybinin B; SA, silybinin A.

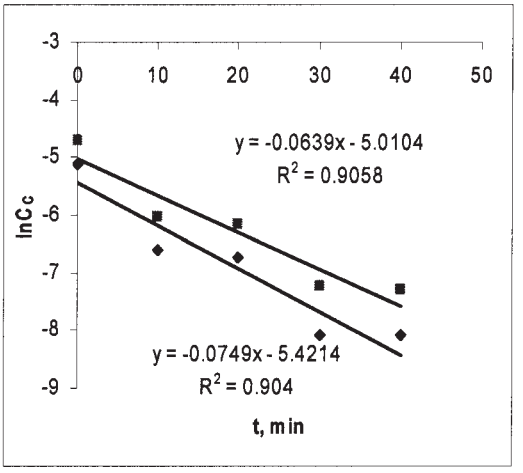

Fig. 6. Degradation kinetics for silybinin A (◆) and silybinin B (■) at 140°C as function of time.

where C_C is the concentration of the compound (g/L), t is the reaction time (min), and k is degradation reaction constant (min^{-1}). The degradation constants obtained for silybinin A and silybinin B at 140°C were 0.064 and 0.075 min^{-1}, respectively, as shown in Fig. 6. The degradation constant for silychristin is at least an order of magnitude higher, assuming nearly complete conversion in 10 min. Thus, the yields of compounds in extracting compounds at elevated temperatures are indeed compromised by compound degradation.

Conclusion

The extraction of silymarin compounds and taxifolin from milk thistle seed meal using hot water at 100–140°C was investigated. The maximum extraction yield of each of the silymarin compounds did not increase with temperature, most likely because compound degradation occurred. In addition, preferential extraction of nonpolar compounds over polar compounds was not observed at elevated temperature, as previously observed by Alvarez Baretto et al. *(12)*. However, the time required for the yields of the compounds to reach their maxima was reduced from 200 to 55 min when the extraction temperature was increased from 100 to 140°C. Significant degradation of unprotected (cell matrix not present to slow degradation) silymarin compounds was observed and first-order degradation kinetics were obtained at 140°C. Future work needs to focus on obtaining true equilibrium data as well as additional extraction and degradation data.

References

1. Luper, S. (1998), *Altern. Med. Rev.* **3(6),** 410–421.
2. Flora, K., Hahn, M., Rosen, H., and Benner, K. (1998), *Am. J. Gastroenterol.* **93,** 139–143.
3. Wang, M., Grange, L. L.m and Tao, J. (1996), *Fitoterapia. LXVII* **2,** 166–171.
4. Zi, X. and Agarwal, R. (1999), *Med. Sci.* **96,** 7490–7495.
5. Zhao, J. and Agarwal, R. (1999), *Carcinogenesis* **20(11),** 2101–2108.
6. Chatterjee, M. L., Katiyar, S. K., Mohan, R. R., and Agarwal, R. (1999), *Cancer Res.* **59,** 622–632
7. Zi, X., Mukhtar, H., and Agarwal, R (1997), *Biochem. Biophys. Res. Commun.* **239,** 334–339.
8. Sonnenbichler, J., Scalera, F., Sonnenbichiler, I., and Weyhenmeyer, R. (1999), *J. Pharmacology and Experimental Therapeutics* **290(3),** 1375–1383.
9. Blumenthal, M. (2002), *J. American Botanical Council* **55,** 60.
10. Miller, D. and Hawthorne, S. (1998), *Anal. Chem*. **70,** 1618–1621.
11. Richter, B. E., Jones B. A., Ezzell, J. L., and Porter, N. L. (1996), *Anal. Chem*. **68,** 1033–1039.
12. Alvarez Barreto, J. F., Wallace, S. N., Carrier, D. J., and Clausen, E.C. (2003), *Appl. Biochem. Biotechnol.* **105–108,** 881–889.
13. Wallace, S., Carrier, D. J., and Clausen, E. C. (2003), *Appl. Biochem. Biotechnol.* **105–108,** 891–903.

0273-2289/04/114/0569–0583/$25.00

Extraction of Antioxidant Compounds from Energy Crops

Ching S. Lau,[1] Danielle Julie Carrier,[2] Luke R. Howard,[3] Jackson O. Lay Jr.,[4] Jean A. Archambault,[5] and Edgar C. Clausen*,[1]

[1]Department of Chemical Engineering, University of Arkansas, 3202 Bell Engineering Center, Fayetteville, AR 72701, E-mail: eclause@engr.uark.edu; [2]Department of Biological and Agricultural Engineering, University of Arkansas, 203 Engineering Hall, Fayetteville, AR 72701; [3]Department of Food Science, University of Arkansas, 2650 N. Young Avenue, Fayetteville, AR 72704; [4]Department of Chemistry and Biochemistry, University of Arkansas, 115 Chemistry Building, Fayetteville, AR 72701; and [5]Phytobiotech Inc., 525 des Prairies Boulevard, Laval, Québec, Canada, H7V 1B7

Abstract

Energy crops offer enormous opportunities for increasing the sustain ability of agriculture and energy production in the United States. Nevertheless, opportunities for sustaining biomass energy production may well hinge on producing energy and extracting high-value products from the same crop. Seven potential energy crops (mimosa, sericea, kudzu, arunzo, switchgrass, velvet bean, and castor) were extracted and assayed for the presence of potentially high-value antioxidant compounds. Of these crops, mimosa and sericea had the highest antioxidant potential and were selected for further study. High-performance liquid chromatography (ultraviolet) and liquid chromatography/mass spectrometry techniques were then utilized to help identify the compounds with high antioxidant potential using extract fractionation, and total phenolics and oxygen radical absorbance capability assays as a guide. These analyses indicate that methanol extracts of mimosa foliage most likely contain quercetin, a flavonol that has been associated with cardioprotection. Future work will concentrate on quantifying the quercetin content of mimosa (likely parts-per-million levels), as well as identifying and quantifying other antioxidants found in energy crops.

Index Entries: Mimosa; sericea; energy crops; quercetin; antioxidant.

*Author to whom all correspondence and reprint requests should be addressed.

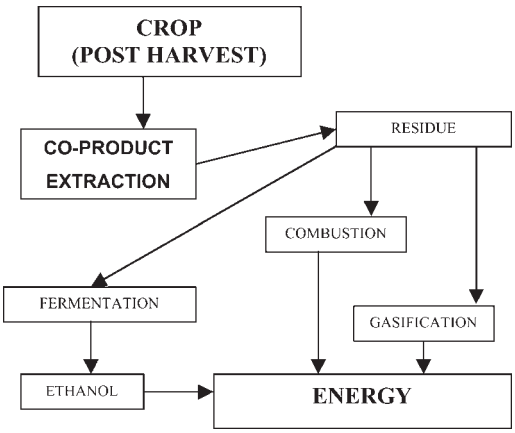

Fig. 1. Possible scenario for coupling extraction of coproducts and energy production.

Introduction

Energy crops offer enormous opportunities for increasing the sustainability of agriculture and energy production in the United States. This is particularly true in the Southeast, where 1.59 quads of biomass is used in energy production, or 56% of the total used nationally. To date, energy crops have not been economically competitive with fossil fuels. At $50/t of biomass, energy crops cost $3.57 per million BTU, whereas coal typically costs only $1.50–$1.80 per million BTU. However, provisions in the pending energy bill will help to change this situation by providing incentives for incorporating biomass into energy production.

Although these developments will certainly launch the commercialization of energy crops, opportunities for sustaining biomass energy production for power and liquid fuel production may well hinge on producing energy and extracting high-value-products from the same crop. In this scenario, shown diagrammatically in Fig. 1, high-value products such as antioxidants and antimicrobials are first extracted from the biomass using water or other solvents. Depending on the extraction technique employed, extraction may either replace or enhance pretreatment prior to enzymatic hydrolysis and fermentation during liquid fuel production. Because the concentrations of the extractables are likely to be at parts-per-million levels, the extracted biomass is available for combustion, gasification, or hydrolysis/fermentation without a detectable decrease in energy yield. A further benefit of extraction coupled with energy production is the potential increase in income to the limited resource farmer who grows the biomass. Since the total value of products obtained from biomass increases, the income per acre for the farmer will likely increase as well.

David Bransby (personal communication, October, 2002) recommended seven potential energy crops (mimosa, sericea, kudzu, arunzo, switchgrass, velvet bean, and castor) as candidates for the extraction of high-value products based on crop yields and largely anecdotal medicinal information.

Of these crops, mimosa and sericea showed the most promise based on preliminary analysis of antioxidant potential and thus were the focus of the present study. Mimosa (*Albizia juribrissin*) and sericea (*Sericea lespedeza*) are two leguminous species that have shown high potential as energy crops in the Auburn University energy crop research program over the last 10 yr *(1)*. Mimosa shows high forage yields (4.7 dry t/acre over a 5-yr test); high forage quality that decreases very little with age; a long growing season; no need for nitrogen (since it is a legume), potassium, and phosphorus fertilizer; extremely good drought tolerance; a relatively low-cost establishment by seed; no need for treatment with insecticides; and excellent longevity. Sericea is a leguminous forage that has undergone genetic improvement at Auburn University for more than three decades. It is a low-cost perennial plant that is better adapted to acidic soils than most legumes; is established from seed; and, in energy crop tests conducted in Alabama, has recorded yields (5–10 t/acre·yr) similar to those obtained from switchgrass (*Panicum virgatum*).

In addition to using mimosa and sericea as energy crops, it is possible that they could yield valuable compounds that could be used in the health arena. From a health benefit perspective, living cells are constantly battling free-radical invasions. However, the cell fights off this invasion by internal antioxidant mechanisms. Detoxification occurs by converting the invaders into electrophilic water-soluble compounds, which will then be conjugated to molecules, such as glutathione or uridine 5'-diphosphate-glucoronosyl, before being excreted. Mimosa has documented medicinal uses in the Orient (David Bransby; personal communication, October, 2002). Kinjo et al. *(2)* reported isolation of the saponins julibrosides A_1, A_2, A_3, A_4, B_1, and C_1 from the dried stem bark of mimosa, which would have uterotinic activity. Flavonoids and saponins have been documented to have antimicrobial activity against, among others, *Pseudomonas*, *Xanthomonas*, *Staphylococcus*, and *Streptococcus* strains *(3)*. Sericea and mimosa most likely contain flavonoids and saponins.

In this article, we present results from the extraction of potentially high-value antioxidant compounds from energy crops. Extract fractions were examined for antioxidant activity, and the results from high-value compound identification efforts are presented. These identification studies are a major first step in making these energy crops economically sustainable.

Materials and Methods

Extraction Experiments

Samples of dried and ground (0.3 mm) energy crops (mimosa, sericea, kudzu, arunzo, switchgrass, velvet bean, and castor) were kindly supplied by Dr. David Bransby of the Department of Agronomy and Soils at Auburn University. To perform an extraction, 2 g of the selected energy crop was mixed with 60 mL of solvent (either water, 60% methanol in water, or 60% ethanol in water) and blended in a standard household blender for 1 min

at 40ºC. The resulting mixture of solvent and solids was centrifuged at 12,000*g* for 30 min to separate the supernatant from the solids. The supernatant was then filtered through a 0.45-µm syringe filter. The solids-free crude extracts were collected and stored at 4°C for subsequent fractionation and analysis. These extractions should not have removed significant quantities of sugars or protein to hinder subsequent biomass conversion, but this assumption needs to be demonstrated in later biomass hydrolysis studies.

Compound Fractionation

Fractionation of the crude extracts was done in 2-mL disposable Symmetry® (Waters, Milford, MA) C_{18} Sep-Pak columns. The columns were preconditioned by first injecting 10 mL of methanol through the column, followed by the injection of 10 mL of HCl at pH 2.0. To produce fractions from the crude extracts, 0.25 mL of filtered crude extract was injected into the column. Then, 2 mL of 20% methanol (or ethanol) solution was injected and collected as the first fraction. This was followed by the sequential injection of first 60% and then 100% methanol (or ethanol) solutions, and the collection of the second and third fractions. The three fractions were dried using a speed vacuum (Savant, Holbrook, NY) without heat. After drying, the samples were dissolved in 2 mL of methanol.

Antioxidant Analysis

Preliminary assessments of the antioxidant potential of each of the energy crop extracts, fractionated crude extracts and high-performance liquid chromatography (HPLC) fractions (described later) were obtained by two different methods: (1) a modified Folin-Ciocalteu (FC) assay, which yields the concentration of the total phenolic compounds *(4)*, and (2) a modified oxygen radical absorbance capability (ORAC) assay, which measures the degree to which a sample inhibits the action of an oxidizing agent and how long it takes to do so *(5)*.

Dilutions of a 400-ppm chlorogenic acid solution were used to obtain a calibration curve for the FC assay. One milliliter of 0.25 *N* Folin reagent was added to 1 mL of the diluted chlorogenic acid solution. After mixing, the solution was allowed to stand for 3 min. One milliliter of sodium carbonate (1 *N*) was then added, mixed, and allowed to stand for another 7 min. Subsequently, 7 mL of deionized water was added, mixed, and allowed to stand for 2 h. The absorbance of the mixture was read on a spectrophotometer (HP 8452A Diode Array) at a wavelength of 726 nm and plotted as a function of the chlorogenic acid concentration. Samples of crude and fractionated plant extracts were analyzed in a similar manner.

Fluorescein (FL) (3',6'-dihydroxyspiro[isobenzofuran-1[3H], 9'[9H]-xanthen]-3-one) was used for the ORAC assay. Excitation and emission filters of 490 and 520 nm, respectively, were used. A stock solution of 1.2 m*M* FL was diluted to a working solution of 94 n*M* made up in 0.75 m*M* phosphate buffer (pH 7.4). Two pipettors, which were part of the microplate

reader (FLUORstar Optima; BMG, Durham, NC), added FL solution (400 µL) on cycle 2 and AAPH (150 µL of 0.137 g/16 mL of phosphate buffer) on cycle 4. The assay was run at 37ºC with a total of 28 reading cycles of 197 s duration. The duration of the reading cycle could vary depending on the number of wells assayed. Trolox (40 µL of 6.25, 12.5, 25, and 50 µ*M* solutions) was used as standard.

HPLC Analyses for Separation of Antioxidant Compounds

Initial separation of compounds for subsequent identification was performed with a Symmetry (Waters) C_{18} column (250 × 4.6 mm). A 100-mL sample volume was injected. Solvent A contained 5% formic acid in water, and solvent B consisted of HPLC-grade methanol. The gradient program was initiated with 98:2 solvent A:solvent B and linearly decreased to 40:60 solvent A:solvent B over 60 min. Compounds were monitored at 280, 320, 360, and 510 nm.

Crude extract was also separated and collected on another Waters system, which consisted of a 600 pump, a 2996 Photodiode Array Detector, and a 2767 fraction collector. The detection wavelength was set in the ultraviolet (UV) between 190 and 400 nm. The column used was a 150 × 21 mm long ACE AQ with 10-mm particles (Advanced Chromatography Technologies, Aberdeen, UK). The system was operated at room temperature. The injection volume was 1500 µL. The mobile phase consisted of 1:3 acetonitrile:water with 0.01% trifluoroacetic acid, which was flowing at a rate of 10 mL/min. The system was operated in the isocratic mode. Fractions of 1.25 mL were collected every 7.5 s.

Identification of Compound

The Sep-Pak fractionated compounds were analyzed using liquid chromatography/mass spectrometry (LC/MS) with a quadrupole ion-trap MS (Bruker Esquire LC/MS, Billerica, MA). The column used was a Symmetry (Waters) C_{18} column (250 × 4.6 mm). A 25-mL sample volume was injected using the system's autosampler. Solvent A contained 5% formic acid in water, and solvent B consisted of HPLC-grade methanol. The gradient program was initiated immediately by starting with a ratio of 98:2 A:B, and B was increased to 60% over 60 min. The flow rate was set to 0.7 mL/min. The UV response during LC/MS was monitored at 360 nm, the highest absorbance wavelength for each set of components as determined from prior HPLC studies. The LC/MS was operated in the positive-ion mode using the electrospray ionization (ESI) source and the manufacturer's recommended operating conditions.

Results and Discussion

Extraction Experiments

Extraction experiments were performed to evaluate the antioxidant capacity of selected energy crops. Table 1 presents the total phenolics con-

Table 1
Total Phenolics and ORAC Values
of Crude Methanol/Water Extracts

Energy crop	Phenolics value [a]	ORAC value [b]
Mimosa foliage	68,000	470
Sericea	65,000	330
Velvet bean foliage	63,000	300
Mimosa seed	1200	16
Kudzu	17,000	190
Arunzo	25,000	170
Switchgrass	11,000	110
Spinach	6300	16
Castor foliage	48,000	150

[a] Milligrams of chlorogenic acid equivalents per gram of dry weight.
[b] Micromoles of Trolox equivalents per gram of dry weight.

Table 2
Total Phenolics Values of Crude Extracts in Different Solvents

	Total phenolics value [a]		
Energy crop	Methanol:water (60:40)	Ethanol:water (60:40)	Water
Mimosa foliage	68,000	60,000	9400
Sericea	65,000	65,000	3600

[a] Milligrams of chlorogenic acid equivalents per gram of dry weight.

tent and ORAC values of crude extracts of selected energy crops in 60% methanol. Also shown for comparison are values for spinach, a crop with known antioxidant properties. As is noted, mimosa foliage, sericea, and velvet bean foliage showed the highest antioxidant potential of the selected energy crops, even exceeding the total phenolics and ORAC values of spinach. Although a high antioxidant potential does not ensure the presence of useful antioxidants for commercial use owing to possible toxicity, high antioxidant potential does indicate that compounds with high antioxidant content are present. The presence of total phenolics also implies the presence of flavonoid compounds, of which antimicrobial properties have been documented *(3)*. Mimosa foliage and sericea were also extracted in 60% ethanol and water (*see* Table 2). The alcohol solutions were found to be better extracting solvents than water.

Fractionation of Compound

LC/MS analyses of both crude extracts showed the presence of many peaks, making identification of compounds very difficult. See, e.g., Figs. 2 and 3, where crude sericea extracts prepared in 60% methanol and water

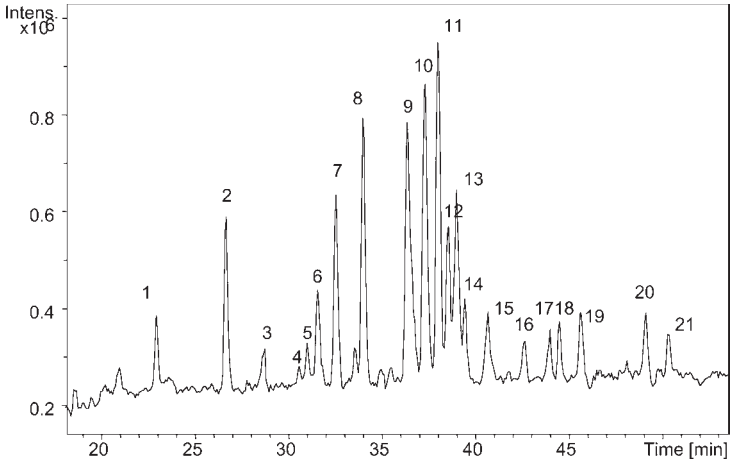

Fig. 2. LC/MS (total ion current [TIC]) analysis of crude sericea extracted with 100% water.

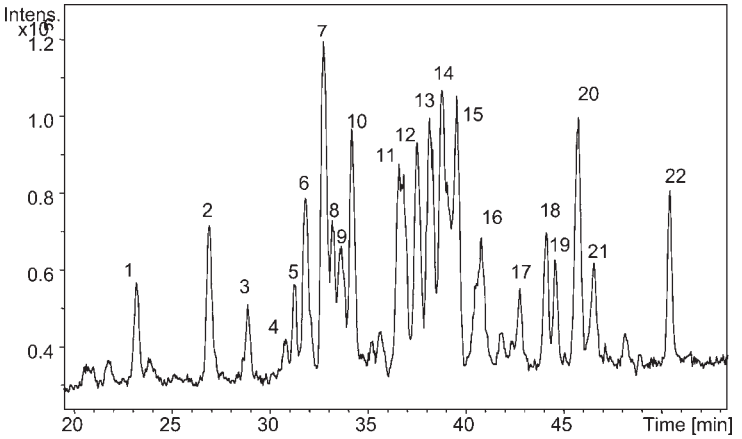

Fig. 3. LC/MS (TIC) analysis of crude sericea extracted with 60% methanol.

are presented. Each of the peaks may represent one or more compounds present in the crude extract. Typically chromatographically separated peaks would contain a single major component by ESI giving two ionmasses corresponding to the protonated molecules for a substituted flavonoid (e.g., sugar attached) and the aglycone component (parent flavonoid). All of the peaks have molecular masses >490 (data not shown), which indicates that the flavonoids present are most likely conjugated with carbohydrate or phenolic acid moieties. Although the flavonoid and substituent masses give some indication of the specific compound, identification of a specific flavonoid required a reference standard and tandem MS as noted later. At a retention time of about 40 min, the two chromatograms differ somewhat, with the methanol extract showing the presence of a few additional compounds.

Table 3
Phenolic and ORAC Values for Sep-Pak Fractionation of Crude Methanol Extracts

	Total phenolics[a]			
Energy crop	20% Methanol in water	60% Methanol in water	100% Methanol	Total phenolics value[b]
Mimosa foliage	23,000 (140)	31,000 (290)	14,000 (92)	68,000
Sericea	11,000 (71)	26,000 (224)	11,000 (60)	48,000

[a] Milligrams of chlorogenic acid equivalents per gram of dry weight. ORAC value, micromoles of Trolox equivalents per gram of dry weight, are given in parenthesis.
[b] Sum of the three fractionates' phenolics value.

Sep-Pak fractionation of the crude extracts prior to analysis helped to reduce the number of peaks per sample, thus aiding LC/MS analysis. In performing total phenolics and ORAC tests on the three fractions, the 60% methanol fraction was found to yield the highest antioxidant values for both crops, as shown in Table 3. As expected, HPLC analyses of the 60% methanol fractions at wavelengths of 280, 320, 360 and 510 nm showed tremendously reduced and more distinct peaks (*see* Figs. 4A, 5A). Neither mimosa foliage nor sericea showed much evidence of the presence of anthocyanins, based on their low absorbances at 510 nm. However, both of the extracts showed high absorbance at 360 nm, a wavelength characteristic of the presence of flavonols.

The 60% methanol sep-pak fractions from the mimosa foliage and sericea extracts were analyzed by LC/MS. The mimosa foliage fraction had nearly the same profiles by both LC/MS (Fig. 4B) and HPLC (Fig. 4A), as indicated by the three major peaks. The LC/MS profile showed that the mimosa foliage fraction had major peaks at 42.5 (significant ions at m/z 303 and 633), 49.0 (m/z 303 and 487), and 53.5 (m/z 303 and 471), min. The molecular weights of compounds were inferred from the positive-ion mass spectra (results not shown). On the other hand, the chromatograms for the sericea extracts (Fig. 5A, 5B) are quite different. The LC/MS profile for sericea in Fig. 5B shows major peaks at 47.0 (major ions at m/z 433 and 545) and 48.5 (m/z 517 only) min.

The same 60% methanol Sep-Pak fraction from the mimosa foliage extract was fractionated into 10 subfractions by HPLC (a different HPLC was used from the Fig. 4 results) and collected for subsequent analysis (*see* Fig. 6). In analyzing the ORAC value of these sub-fractions, it was found that the sixth sub-fraction contained nearly 90% of the total ORAC value (*see* Table 4). Initial HPLC and LC/MS tests on this sixth subfraction indicated the presence of a single peak giving strong ions at m/z 303 and 487 (*see* Fig. 7A, 7B). The m/z 303 ion in this component was subsequently confirmed as protonated quercetin (*see* Fig. 8 for the structure of querce-

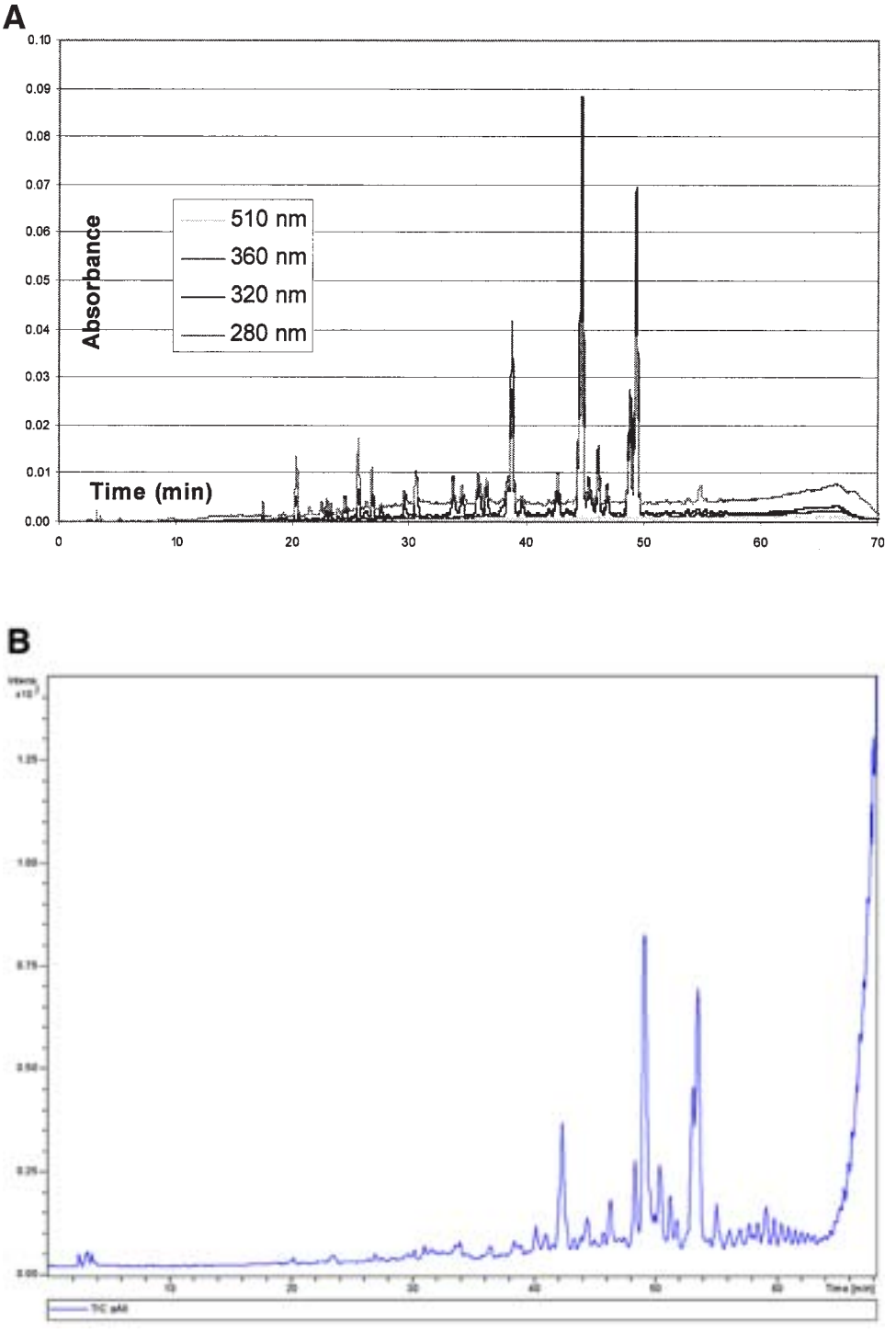

Fig. 4. Analyses of mimosa foliage crude extract fractionated with 60% methanol in Sep-Pak column. **(A)** HPLC (UV); **(B)** LC/MS.

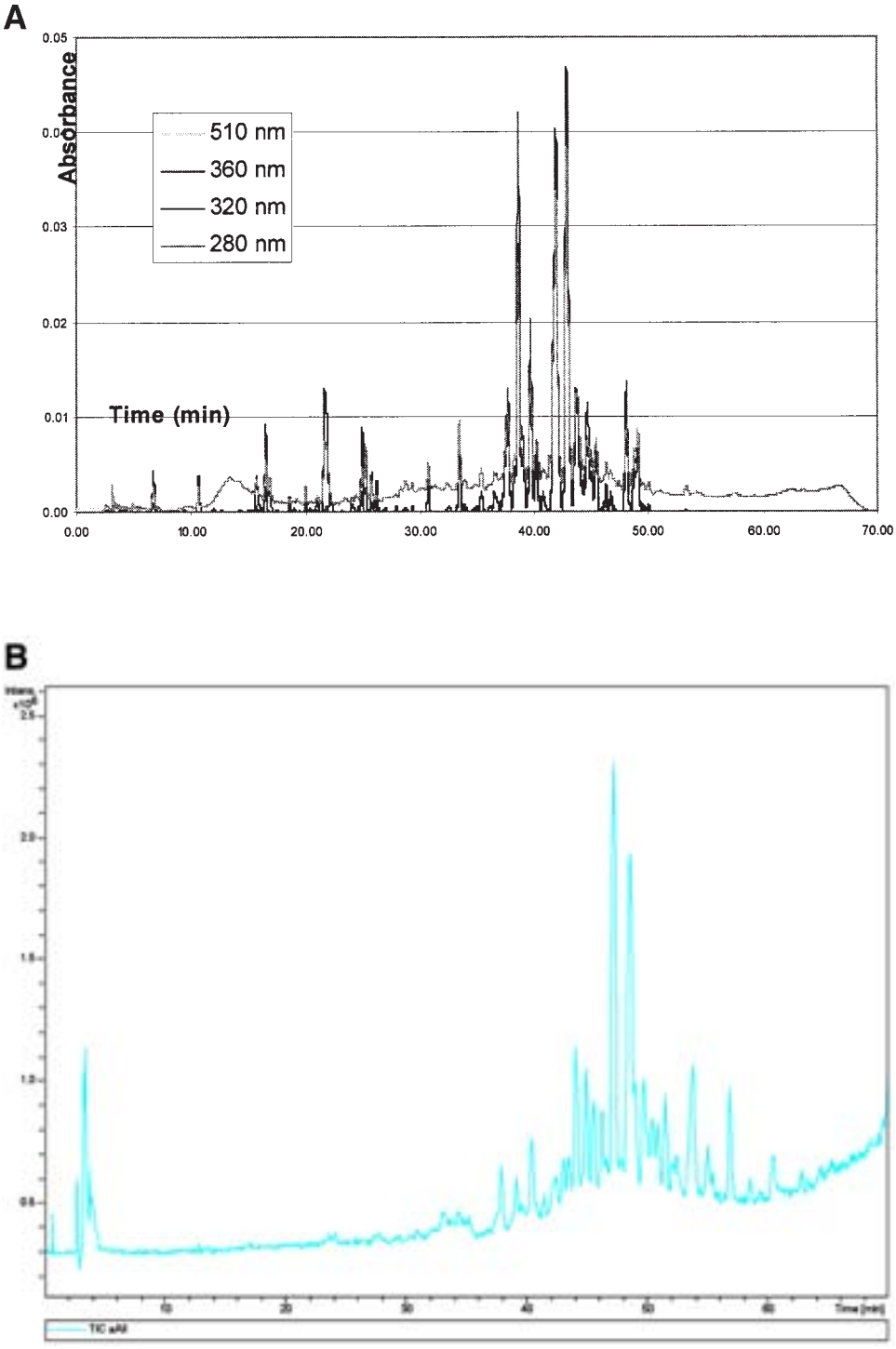

Fig. 5. Analyses of crude sericea extract, fractionated with 60% methanol in Sep-Pak column. **(A)** HPLC (UV); **(B)** LC/MS.

Table 4
ORAC Values of 10 Subfractions from 60% Methanol Extract of Mimosa Foliage

Subfraction	ORAC value [a]
1	0.22
2	0.55
3	0.78
4	1.58
5	0.02
6	38.41
7	0.55
8	0.39
9	0.40
10	0.00
Total	42.90

[a] Micromoles of Trolox equivalents per gram of dry weight.

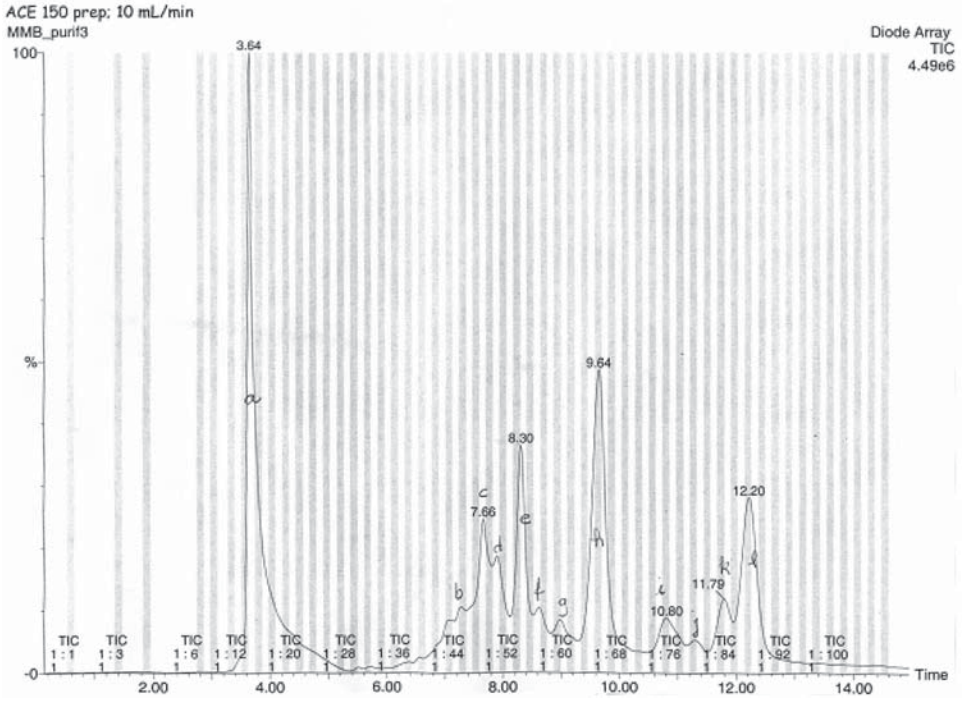

Fig. 6. Second HPLC analysis of mimosa foliage extract, fractionated with 60% methanol in Sep-Pak column.

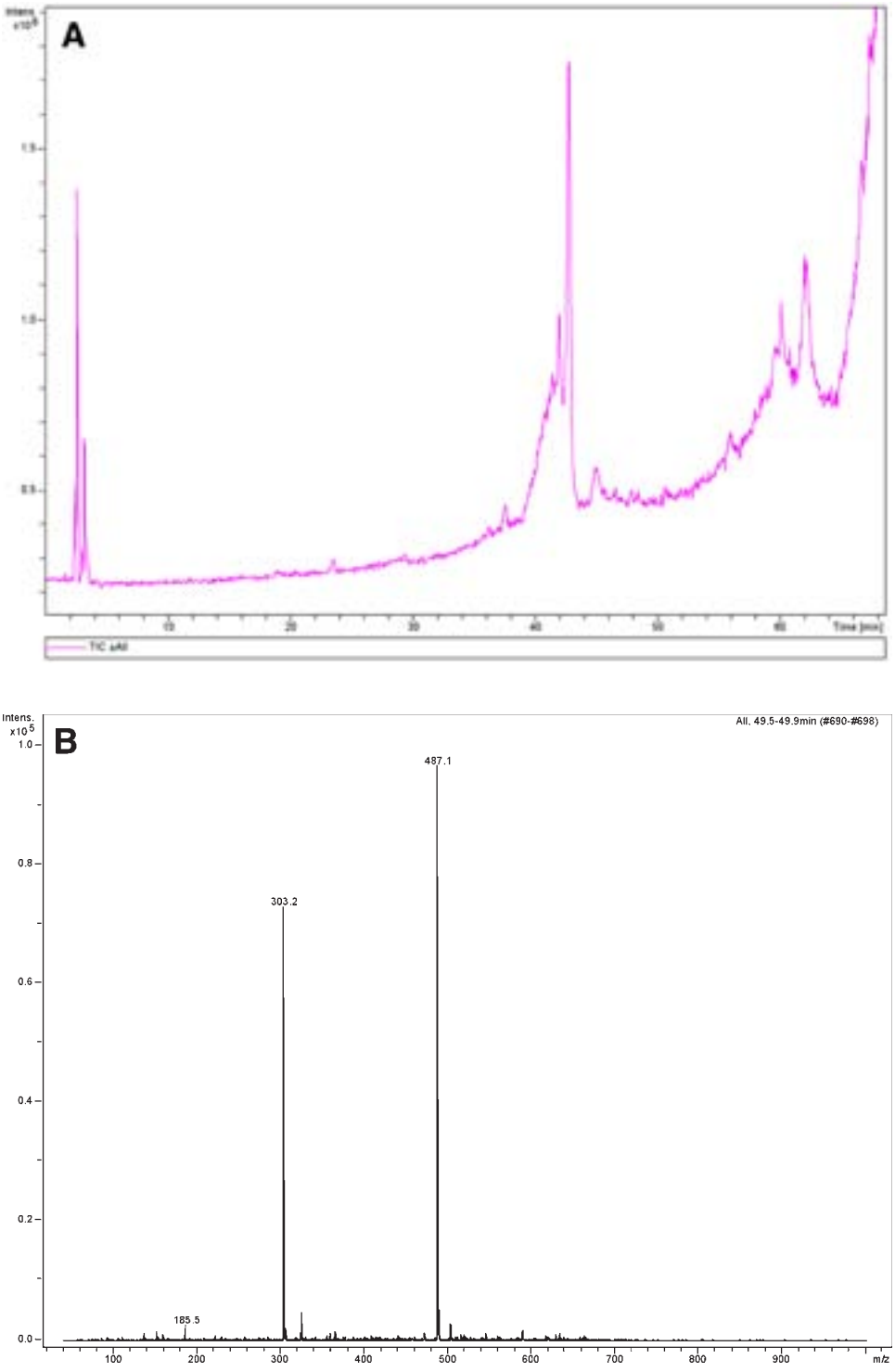

Fig. 7. HPLC/UV analyses of fraction 6 from 60 % methanol mimosa foliage extract. **(A)** HPLC (UV); **(B)** LC/MS.

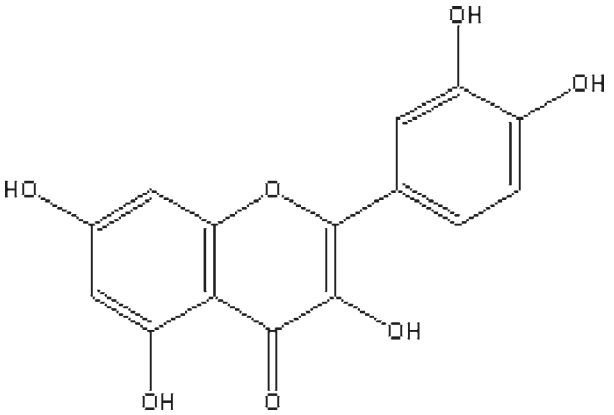

Fig. 8. Molecular structure of quercetin ($C_{15}H_{10}O_7$), mol wt = 302.

tin) based on a comparison between the MS/MS product-ion spectrum obtained during the HPLC separation and a reference spectrum from reagent-grade quercetin (*see* Fig. 9A, 9B). The difference in mass between m/z 487 and 303 in the full-scan spectrum for this component indicated the presence of a sugar or other moiety attached to the quercetin. Fragmentation and loss of this moiety to yield the parent flavonol protonated molecule is typical in positive-ion ESI analyses of this class of compounds. The position and identification of this substitutent are currently under investigation. However, it can be inferred that its mass is about 184 Daltons.

Quercetin is a flavonol, which belongs to a group of naturally occurring compounds that are usually present in the plant as glycosides and are colorless or light yellow *(6)*. It is found in plants such as onions, apples, and berries, as well as many seeds, nuts, flowers, bark, and leaves. It is also found in medicinal botanicals including *Ginkgo biloba*, *Hypericum perforatum* (St. John's Wort), and *Sambucus canadensis* (elder). Quercetin has been associated with cardioprotective phenomenon *(7–10)*. The mechanism of protection has been speculated to involve the action of the quercetin as an antioxidant, which attenuates tissue injury that results from the production of proinflammatory oxidants such as hypochlorous acid (HOCl). HOCl is generated by neutrophils through the enzyme myeloperoxidase (MPO), which catalyzes the oxidation of chloride anion (Cl^-) by H_2O_2 to yield HOCl. The production of HOCl is an integral part of the nonspecific host defense mechanism triggered by opsonized bacteria or activated complement components, but under certain conditions it can also destroy healthy tissues. The ability of quercetin to effectively inhibit MPO activity as well as directly scavenge HOCl may limit the vascular injury associated with inflammatory reactions *(9)*.

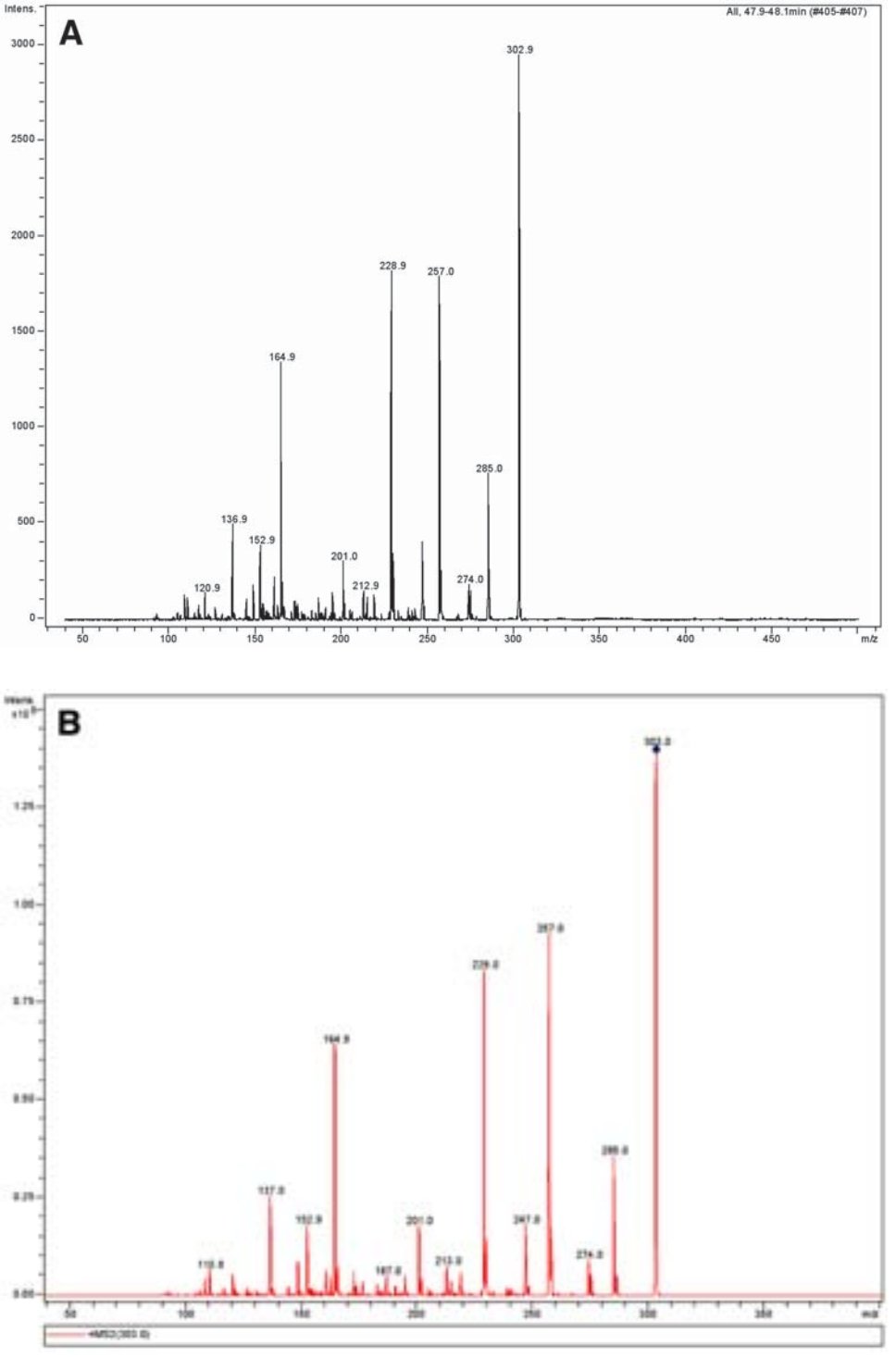

Fig. 9. MS/MS spectrum of m/z 303 of **(A)** fraction 6 from a 60 % methanol mimosa foliage extract and **(B)** protonated quercetin.

Conclusion

Seven possible energy crops (mimosa, sericea, kudzu, arunzo, switchgrass, velvet bean, and castor) were extracted and assayed for the presence of potentially high-value antioxidant compounds. Of these crops, mimosa foliage and sericea showed the highest antioxidant potential. HPLC (UV) and LC/MS techniques were utilized to help identify the compounds with high antioxidant potential using extract fractionation, and total phenolics and ORAC assays as a guide. These analyses indicate that methanol extracts of mimosa foliage most likely contain parts-per-million levels of quercetin, a flavonol that has been associated with cardioprotection. Future work will concentrate on quantifying the quercetin content of mimosa, as well as identifying and quantifying other antioxidants found in energy crops.

Acknowledgment

This project was supported by the Southeastern Regional Biomass Energy Program and administered by the Southern States Energy Board for the United States Department of Energy.

References

1. Sladden, S., Bransby, B., Aiken, G., and Rose, P. (1992), *Highlights Agric. Res*. **39,** 4.
2. Kinjo J., Araki, K., Fujui, K., Higuchi, H., Ikeda, T., Nohara, T., Ida, Y., Takemoto, N., Miyakoshi, M., and Shoji, J. (1992), *Chem. Pharm. Bull.* **40**, 3269–3273.
3. Naidu A. (2000), *Natural Food Antimicrobial Systems*, CRC Press, Boca Raton, FL.
4. Singleton, V. L. and Rossi, J. A. (1965), *Am. J. Enol. Vitic.* **16,** 144–158.
5. Cao, G. H. and Prior, R. L. (1999), *Methods Enzymol.* **299,** 49–62.
6. Van der Sluis, A. A., Dekker, M., Skrede, G., and Jongen, W. M. F. (2002), *J. Agric. Food Chem.* **50,** 7211–7219.
7. Meyer, A. S., Heinonen, M., and Frankel, E. N. (1998), *Food Chem.* **61,** 71–75.
8. Chan, M. M-Y., Mattiacci, J. A., Hwang, H. S., Shah, A., and Fong, D. (2000), *Biochem. Pharmacol*. **60,** 1539–1548.
9. Binsack, R., Boersma, B. J., Patel, R. P., Kirk, M., White, C. R., Darley-Usmar, V., Barnes, S., Zhou, F., and Parks, D. A. (2001). *Alcohol. Clin. Exp. Res. Online* **25,** 434–443 (Website: http://fn.cfs.purdue.edu/bot/Downloads/Publications/Binsack_quercetin_ACER_2001.pdf).
10. Careri, M., Corradini, C., Elviri, L., Nicoletti, I., and Zagnoni, I. (2003), *J. Agric. Food Chem.* **51,** 5226–5231.

0273-2289/04/114/0585–0599/$25.00

Cellulase Retention and Sugar Removal by Membrane Ultrafiltration During Lignocellulosic Biomass Hydrolysis

Jeffrey S. Knutsen and Robert H. Davis*

Department of Chemical and Biological Engineering, University of Colorado, Boulder, CO 80309-0424, E-mail: robert.davis@colorado.edu

Abstract

Technologies suitable for the separation and reuse of cellulase enzymes during the enzymatic saccharification of pretreated corn stover are investigated to examine the economic and technical viability of processes that promote cellulase reuse while removing inhibitory reaction products such as glucose and cellobiose. The simplest and most suitable separation is a filter with relatively large pores on the order of 20-25 mm that retains residual corn stover solids while passing reaction products such as glucose and cellobiose to form a sugar stream for a variety of end uses. Such a simple separation is effective because cellulase remains bound to the residual solids. Ultrafiltration using 50-kDa polyethersulfone membranes to recover cellulase enzymes in solution was shown not to enhance further the saccharification rate or overall conversion. Instead, it appears that the necessary cellulase enzymes, including β-glucosidase, are tightly bound to the substrate; when fresh corn stover is contacted with highly washed residual solids, without the addition of fresh enzymes, glucose is generated at a high rate. When filtration was applied multiple times, the concentration of inhibitory reaction products such as glucose and cellobiose was reduced from 70 to 10 g/L. However, an enhanced saccharification performance was not observed, most likely because the concentration of the inhibitory products remained too high. Further reduction in the product concentration was not investigated, because it would make the reaction unnecessarily complex and result in a product stream that is much too dilute to be useful. Finally, an economic analysis shows that reuse of cellulase can reduce glucose production costs, especially when the enzyme price is high. The most economic performance is shown to occur when the cellulase enzyme is reused and a small amount of fresh enzyme is added after each separation step to replace lost or deactivated enzyme.

Index Entries: Saccharification; corn stover; cellulase; glucose; ultrafiltration; vacuum filtration.

*Author to whom all correspondence and reprint requests should be addressed.

Introduction

Alternative energy sources are being investigated owing to limited reserves of nonrenewable petroleum-based fuels. One such alternative is ethanol derived from agricultural or industrial lignocellulosic biomass. However, economic considerations have so far hindered the construction of lignocellulosic biomass-to-ethanol conversion facilities on a large scale. One way to reduce the cost of these processes is to reuse the expensive cellulase enzyme, which was estimated in 1999 to comprise 20% of the total cost of ethanol production *(1)*. While a more recent economic model *(2)* suggests that the price of cellulase may now be as low as 9% of the total ethanol production cost, significant cellulase activity still remains after saccharification. Recovery and reuse of this remaining enzyme may prove profitable.

Previously, we reported a method of recovering and reusing cellulase enzyme during the hydrolysis of ground yellow poplar using a two-part separation *(3–4)*. First, inclined sedimentation was used to remove most of the solid particles from the 2.5–10% (w/w) yellow poplar suspension. Second, an ultrafiltration unit was used to retain and concentrate the relatively large cellulase enzymes while water, sugars, and other small molecules passed through the membrane. While this separation strategy works reasonably well for ground yellow poplar at low solids concentrations, inclined settling does not effectively remove liquids from a suspension of pretreated corn stover at more realistic solids concentrations of about 15% (w/w). At these concentrations, pretreated corn stover has a mudlike consistency, and it does not settle effectively.

Many reseachers have previously studied the use of ultrafiltration to recycle cellulase during saccharification *(5–22)*. However, much of this previous work involved either purified cellulosic substrates, such as Solka-Floc, which are not representative of feedstocks in large-scale operations, or lignocellulosic substrates at concentrations that would be much too low to be economical in a full-scale process.

In the present study, we explored enzyme reuse and sugar production at reagent concentrations typical of a full-scale biomass-to-ethanol design *(2)*, using pretreated corn stover as the lignocellulosic substrate. We investigated the advantages of using technologies such as vacuum filtration and ultrafiltration to recover and reuse cellulase enzymes in a saccharification process. Because it is known that a significant fraction of cellulase enzymes remains bound to the spent hydrolysate *(23)*, we used vacuum filtration to extract inhibitory reaction products such as glucose and cellobiose, while retaining solid particles and bound enzymes. This vacuum filter cake was then contacted with fresh pretreated corn stover, encouraging additional saccharification without the use of additional enzymes. Such a separation also creates a sugar stream that can be processed for a variety of end uses. Because some cellulase enzymes such as β-glucosidase may remain in solution and pass through the vacuum filter, we also investigated whether it is necessary to recover these enzymes using ultrafiltration as an additional

processing step. Finally, an economic model of a large-scale saccharification process was developed using data measured in the laboratory. Such a model can be used to consider the reuse of cellulase across a range of enzyme prices, especially useful since the cost of cellulase continues to decline.

Materials and Methods

Pretreated Corn Stover and Cellulase Enzyme

Pretreated corn stover containing approx 59% cellulose and 41% lignin by dry weight was obtained from a pilot facility at the National Renewable Energy Laboratory (NREL) in Golden, CO. Because of the pretreatment process, the corn stover contains sulfuric acid, which must be removed prior to saccharification experiments. Hence, the corn stover was washed with deionized water and centrifuged six times. The supernatant was discarded after each washing. The resulting corn stover slurry had an insoluble solids concentration of 15±1% (w/w), measured by drying samples in an oven. Washed corn stover was stored frozen until use. Cellulase used in these experiments is from a commercial preparation made specifically for NREL by Iogen (Ottawa, Ontario, Canada). It is supplied as a liquid solution reported to contain a filter paper activity of 55 filter paper units (FPU)/mL *(24)*.

Saccharification

Saccharification took place in 250-mL Erlenmeyer flasks incubated at 45°C in a shaker. Each flask was initially charged with 50 g of washed corn stover slurry. Citrate buffer (50 m*M*) was used to maintain a pH of 4.7. Sodium azide (0.1% [w/v]) was used to inhibit microbial growth. Cellulase was loaded at 10 or 20 FPU/g of cellulose. The contents of each flask were then mixed with a spatula, and a sample was taken to measure background glucose concentrations. Samples were taken using the top end of a Pasteur pipet and were then centrifuged. Glucose concentrations in the supernatants were determined using a YSI 2700 Select Biochemistry Analyzer (Yellow Springs Instrument, Yellow Springs, OH). Cellobiose concentrations in samples taken at the beginning and end of selected saccharification experiments were determined by high-performance liquid chromatography using a Hewlett Packard model HP1090 high-performance liquid chromatograph and a standard methodology based on the use of Bio-Rad HPX-87H and HPX-87P columns. Cellulose is converted to these sugars with the following stoichiometries:

$$(\text{Glucan})_n + n\,\text{H}_2\text{O} \rightarrow n\,\text{Glucose} \quad (1)$$

$$2\,(\text{Glucan})_n + n\,\text{H}_2\text{O} \rightarrow n\,\text{Cellobiose} \quad (2)$$

in which the glucan monomers of cellulose are converted into glucose and cellobiose. Cellulose conversion to glucose (moles of glucose produced per mole of initial glucan) is calculated based on the measured amounts of glucose generated from the glucan originally present in each flask, with additional conversion to cellobiose included in selected experiments.

The original mass of glucan is calculated based on the measured 15% (w/w) total insoluble solids fraction and the reported 59% (w/w) of these solids consisting of cellulose.

Vacuum Filtration and Ultrafiltration

Vacuum filtration was used to remove liquids containing glucose, cellobiose, and other dissolved solutes from the saccharification flask, while retaining spent hydrolysate solids and the associated bound enzymes. Whatman no. 41 filter paper (pore size: 20–25 μm) was used because of its relatively large pores and high permeability. Vacuum filtration was run until filtrate was no longer being collected (about 5 min), and the resulting filter cake was scraped off and returned to the saccharification flask. In a few experiments, ultrafiltration was used to recover any soluble enzymes (such as β-G) present in the vacuum filtrate. In these experiments, 3.8-cm-diameter polyethersulfone Biomax membrane disks from Millipore (Bedford, MA) with a 50-kDa molecular weight cutoff were used in a stirred-cell apparatus. In all cases, the stirred cell was pressurized with nitrogen to its maximum rated pressure of 70 psi (4.8 bar). Ultrafiltration was run until about 7 mL of retentate remained in the stirred cell. The retentate was then returned to the saccharification flask. Protein transmission during vacuum filtration and protein rejection during ultrafiltration were measured by spectrophotometry using a Coomassie Blue protein assay (Pierce, Rockford, IL). Glucose concentrations were measured between all steps of the separation.

Batch and Semibatch Saccharification

Saccharification experiments were divided into three types: control, semibatch, and diafiltration. During the control experiments, saccharification progress was monitored as already described over 15 d. No attempt was made to remove glucose using filtration.

During the semibatch experiments, vacuum filtration was applied at 4 d and 8 d after the start of saccharification, to remove the sugar product as filtrate. In selected semibatch experiments, ultrafiltration was applied to the vacuum filtrate to recover soluble enzymes. In other semibatch experiments, the vacuum filter cake was washed extensively with deionized water to remove any enzymes not bound to the solids. After filtration, pretreated corn stover slurry and 7 mL of solution (the ultrafiltration filtrate, or citrate buffer when ultrafiltration was not used) were added to the residual solids and bound enzymes, to replace the volume removed as filtrate during the ultrafiltration step. The additional substrate promotes further saccharification by reusing the cellulase enzymes. To promote further saccharification in a final set of semibatch experiments, additional cellulase at a specific activity of 5 FPU/g of fresh cellulose was added along with the fresh corn stover after vacuum filtration.

Diafiltration experiments were conducted to determine whether enough inhibitory reaction products could be removed by filtration to enhance the saccharification rate. During these experiments, vacuum fil-

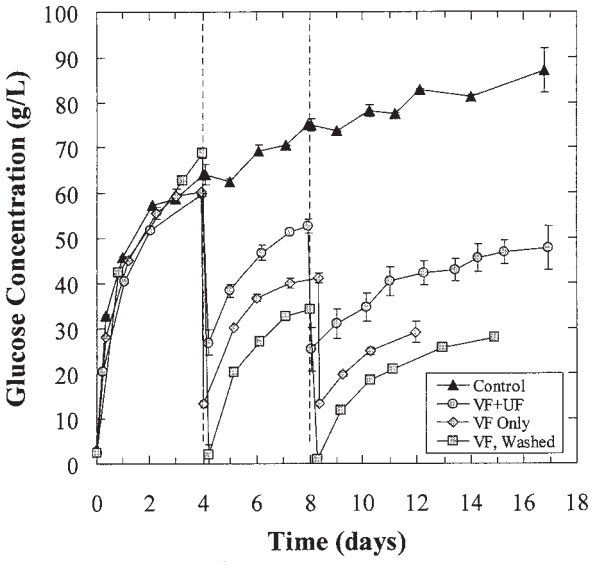

Fig. 1. Glucose concentration over time for semibatch saccharification experiments at 15% (w/w) initial insoluble solids concentration and 20 FPU/g of cellulose enzyme loading. Filtration was applied at two different times to remove glucose (vertical dashed lines). VF Only: vacuum filtration was applied alone; VF+UF: ultrafiltration was also applied following vacuum filtration; VF, Washed: Vacuum filtration was applied and the filter cake was washed with water. Error bars represent averages ± 1 SD for two repeated experiments.

tration followed by ultrafiltration was applied at 4 h, 12 h, 24 h, and 4 d after the start of saccharification, as described in the previous section. Buffer was added to the flasks after each of the four separations, to restore the liquid volume removed as permeate. Filtration applied in this manner is expected to remove inhibitory products such as glucose and cellobiose, while retaining corn stover and cellulase enzymes.

Results and Discussion

Semibatch Saccharification

Glucose concentrations measured during the semibatch saccharification experiments at a cellulase loading of 20 FPU/g of cellulose are shown in Fig. 1. Removal of sugar in the vacuum filtrate resulted in glucose concentrations lower than in the control experiment, as expected. Concentrations in semibatch experiments with ultrafiltration tended to be higher because of glucose returned in the retentate. By contrast, glucose was nearly absent just after filtration in the semibatch experiments with washed filter cakes owing to the washing away of the supernatant. To determine the effectiveness of cellulase reuse, the total amount of glucose generated per liter of initial reactants was calculated for all semibatch experiments.

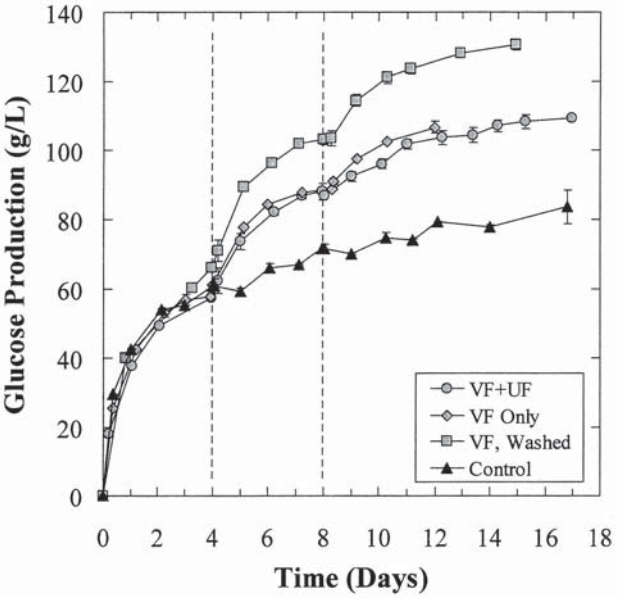

Fig. 2. Glucose production per liter of reactants over time for same experiment as shown in Fig. 1. (definitions of symbols and vertical dashed lines are the same). Error bars represent averages ± 1 SD for two repeated experiments.

Results at a cellulase loading of 20 FPU/g of cellulose are shown in Fig. 2. Immediately apparent is that additional glucose was generated using recycled cellulase and fresh cellulose, though the rate of glucose production declined after each filtration and addition step. In the economic analysis presented later, we examine the trade-off between the savings generated by reusing cellulase enzymes and the costs of adding fresh cellulose.

It is also important to note from Figs. 1 and 2 that the use of ultrafiltration did not result in the generation of any additional glucose over the case in which vacuum filtration was applied alone. Moreover, the experiments in which the corn stover was washed during vacuum filtration generated as much or more glucose than observed for the other experiments. These results suggest that sufficient β-glucosidase activity is adsorbed onto corn stover particles, so that hydrolysis continues when fresh corn stover is added even without recovering soluble enzymes in the supernatant. This hypothesis is supported by the work of Kadam and Knutsen *(23)*, who reported a strong β-glucosidase adsorption affinity toward pretreated corn stover. Furthermore, it should be noted that glucose production was accelerated shortly after the addition of fresh pretreated corn stover at 4 and 8 d after the start of saccharification. This effect is probably owing to the abundance of amorphous cellulose present in the fresh pretreated corn stover, which is more easily converted than is the remaining cellulose from the original charge.

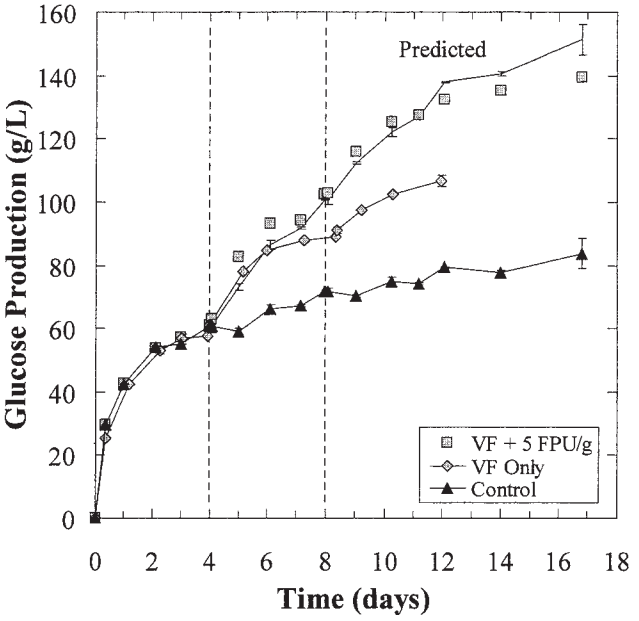

Fig. 3. Glucose production per liter of reactants over time for semibatch saccharification experiments at 15% (w/w) initial insoluble solids concentration and initial enzyme loading of 20 FPU/g of cellulose. Vacuum filtration was applied at two different times to remove glucose (vertical dashed lines). Fresh pretreated corn stover was added to replenish the volume removed by filtration. Additional enzyme was loaded at 5 FPU/g of fresh cellulose. The predicted curve was calculated by summing the amount of glucose generated by additional control experiments at 20 and 5 FPU/g of cellulose. Error bars represent averages ± 1 SD for two repeated experiments.

Irreversible binding of enzymes to lignin or recalcitrant cellulose may limit the production of glucose, and it may be the cause of the reduced production rate observed in each successive step in Fig. 1. In an attempt to increase the production of glucose, additional cellulase at 5 FPU/g of cellulose was added along with fresh corn stover after vacuum filtration. Glucose production during this experiment is shown in Fig. 3. The additional cellulase results in a marked increase in glucose production over the original batch and semibatch experiments. The improved performance occurs because both the residual and new cellulosic solid are converted to sugars by the combined action of the initial and added enzyme during the second and third 4-d periods. The trade-off between the extra value of higher glucose production and the increased cost of using additional enzyme is examined in our economic analysis. The predicted curve is based on the total amount of glucose generated from control experiments at 20 and 5 FPU/g of cellulose. This curve is the total

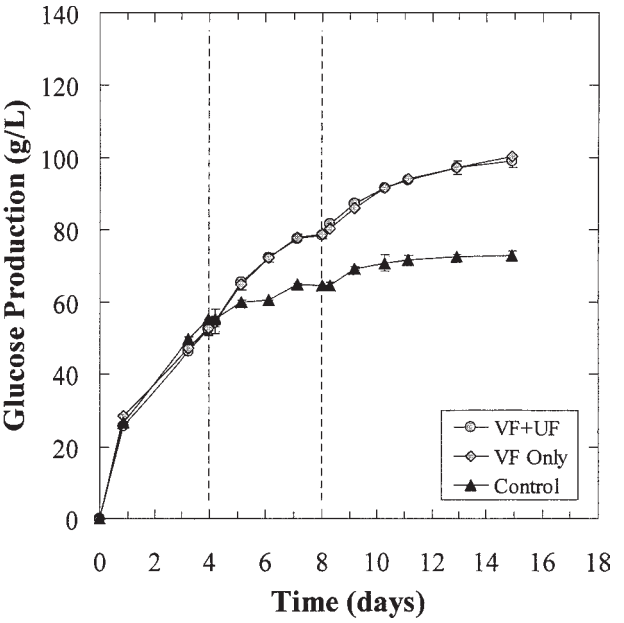

Fig. 4. Glucose production per liter of reactants over time for similar semibatch experiment as shown in Fig. 2, but at a lower enzyme loading of 10 FPU/g of cellulose (definitions of symbols and vertical dashed lines are the same). Error bars represent averages ± 1 SD for two repeated experiments.

amount of glucose that would be generated if the semibatch experiment were divided into three separate control experiments, with 50 g in control flask 1 and a mass in control flasks 2 and 3 equal to the amount of fresh corn stover added after each filtration in the semibatch experiment. Semibatch glucose production lower than this predicted curve might be attributed to cellulase deactivation. Fortunately, it appears that cellulase is only minimally deactivated by filtration, since the semibatch data closely match the predicted curve up to 11 d of saccharification and are only slightly lower thereafter.

To determine whether similar trends would be observed at lower enzyme loadings, semibatch experiments were conducted at an initial cellulase concentration of 10 FPU/g of cellulose, with glucose productions shown in Fig. 4. The use of ultrafiltration to recover β-glucosidase again appears unnecessary. Additionally, glucose productions after 12 d of saccharification at the lower enzyme loading were only slightly lower than those reported at the higher enzyme loading, suggesting that the use of cellulase beyond 10 FPU/g of cellulose might be unnecessary if long-term cellulose conversion is the process goal.

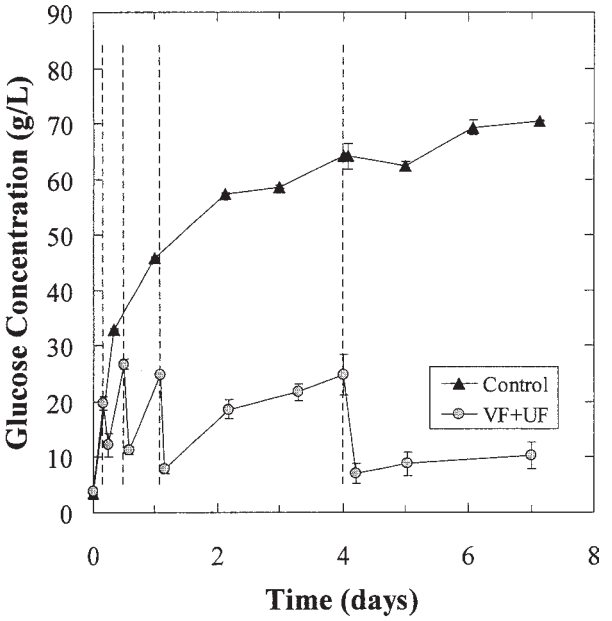

Fig. 5. Glucose concentration over time for diafiltration saccharification experiments at 15% (w/w) initial insoluble solids concentration and 20 FPU/g of cellulose enzyme loading. Vacuum filtration and ultrafiltration were applied at four different times to remove glucose (vertical dashed lines). Filtration was not applied to the control flasks. Error bars represent averages ± 1 SD for three repeated experiments.

Saccharification with Diafiltration

Glucose concentrations measured during diafiltration saccharification experiments at a cellulase loading of 20 FPU/g of cellulose are shown in Fig. 5. Removal of sugar as permeate resulted in glucose concentrations that are much lower than for the control experiments, as expected. Cellulose conversions to glucose were calculated using these concentrations, and the glucose removed as permeate was also included. It was anticipated that the lower glucose concentrations might result in an increased cellulose conversion, because saccharification kinetics are known to be product inhibited *(5,6)*. However, as shown in Fig. 6, the lower glucose concentration did not result in a higher conversion-both the diafiltration and control experiments show just over 60% conversion to glucose after 7 d. When cellobiose production is also considered, the conversion in both experiments after 7 d is increased to about 65%. It is possible that the glucose concentrations after filtration, which never fell below 10 g/L without washing, were still too high to result in a significant increase in the rate of conversion. Lower glucose concentrations could be obtained with more frequent filtration or washing, but the resulting product sugar stream would then be too dilute for economic use.

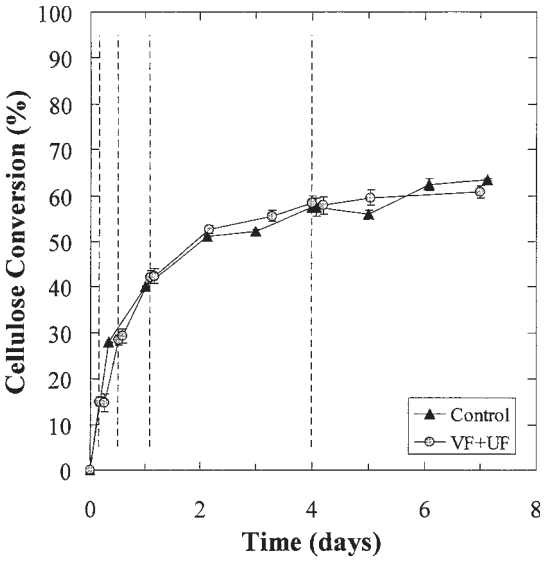

Fig. 6. Cellulose conversion over time for the same experiments as shown in Fig. 5. The data represent cellulose conversions based on glucose production alone. Cellobiose measurements taken at the end of the experiments account for an additional conversion of about 4%. Error bars represent averages ± 1 SD for three repeated experiments.

Economic Analysis

An economic analysis of a hypothetical full-scale lignocellulosic saccharification process was carried out to determine possible cost savings owing to enzyme reuse. The production cost of glucose is compared in three different operating configurations: batch, semibatch, and semibatch with additional cellulase. In this section, the batch-operating configuration is similar to the "control" experiments discussed in previous sections. These designs are based on the 2002 Lignocellulosic Biomass to Ethanol Process Design report from NREL *(2)*, which uses a continuous operation. However, to simulate the experiments in our laboratory, the present economic analysis uses only batch or semibatch operation. Hence, the production costs reported here are expected to be higher than in a large-scale continuous operation and were calculated primarily as a means of comparing the relative production costs across the three operating configurations.

The initial steps for all three configurations are the same. Raw corn stover enters the plant at a rate of nearly 100,000 kg/h and is washed, milled, and sent to the pretreatment unit. During pretreatment, the milled corn stover is exposed to high-pressure sulfuric acid, converting most of the hemicellulose into soluble sugars by hydrolysis reactions. In addition, these conditions "expose" the cellulose for the subsequent enzymatic saccharification. Following pretreatment, the stover is conditioned and the pH is adjusted to 4.5. In all configurations, an average of 430,000 kg/h of pretreated corn stover is sent to the saccharification vessels. Capital costs for these three initial processes are shown in Table 1.

Table 1
Economic Model Parameters and Glucose Production Costs for Batch and Semibatch Saccharification Processes

	20 FPU/g Batch	20 FPU/g Semibatch	20+5 FPU/g Semibatch	10 FPU/g Batch	10 FPU/g Semibatch
Biomass flow (kg/h)	98,000	98,000	98,000	98,000	98,000
Average hydrolysate flow (kg/h)	429,000	429,000	429,000	429,000	429,000
Average cellulose flow (kg/h)	28,400	28,400	28,400	28,400	28,400
Average cellulase flow (L/h)	11,400	4200	6000	5700	2100
Average cellulase loading (FPU/g)	20.0	7.4	10.5	10.0	3.7
Reactor volume (L)	48,000,000	55,000,000	56,000,000	48,000,000	55,000,000
No. of saccharification vessels	14	16	16	14	16
No. of filtration Units	6	7	7	6	7
Capital costs					
Feed handling	$7,500,000	$7,500,000	$7,500,000	$7,500,000	$7,500,000
Pretreatment	$19,000,000	$19,000,000	$19,000,000	$19,000,000	$19,000,000
Neutralization/conditioning	$7,800,000	$7,800,000	$7,800,000	$7,800,000	$7,800,000
Saccharification cost	$9,100,000	$10,400,000	$10,400,000	$9,100,000	$10,400,000
Filtration cost	$12,700,000	$14,800,000	$14,800,000	$12,700,000	$14,800,000
Total capital investment	$56,100,000	$59,500,000	$59,500,000	$56,100,000	$59,500,000
Annual expenses					
Biomass feedstock	$23,200,000	$23,200,000	$23,200,000	$23,200,000	$23,200,000
Cellulase	$12,100,000	$4,500,000	$6,400,000	$6,000,000	$2,200,000
Labor	$2,150,000	$2,150,000	$2,150,000	$2,150,000	$2,150,000
Amortized capital payment	$6,600,000	$7,000,000	$7,000,000	$6,600,000	$7,000,000
Total expenses	$44,050,000	$36,850,000	$38,750,000	$37,950,000	$34,550,000
Cellulose conversion to glucose	58 ± 4%	48 ± 4%	62 ± 4%	52 ± 4%	49 ± 3%
Cycle time (d)	5	15	15	5	15
Glucose production (g/[L·cycle])	45 ± 3	98 ± 7	129 ± 6	40 ± 3	101 ± 6
Annual glucose production (kg)	$1.50 \pm 0.08 \times 10^8$	$1.26 \pm 0.08 \times 10^8$	$1.6 \pm 0.1 \times 10^8$	$1.34 \pm 0.08 \times 10^8$	$1.30 \pm 0.08 \times 10^8$
Glucose production cost (¢/kg)	29 ± 2	29 ± 2	24 ± 2	28 ± 2	27 ± 2

During saccharification, pretreated corn stover is sent to several 950,000-gal (3600-m^3) vessels, with an associated capital cost of $650,000 per vessel. Cellulase is then added at 10 or 20 FPU/g of cellulose, and the reaction proceeds. The number of required vessels is calculated based on the total volume required to process 430,000 kg/h of pretreated corn stover over the reaction cycle, which is 5 d for batch operation and 15 d for semibatch operation. The total volume for the semibatch processes is slightly higher than the batch processes owing to inert solids that build up during the 15-d processing time.

Every 4 d, the reactor's contents are sent to a series of pressure filters to remove residual solids from the product sugar stream. In the batch configurations, the filter cake is discarded and the saccharification vessels are charged with fresh pretreated corn stover and enzyme. In the semibatch configuration, the filter cake is returned to the saccharification vessels, and fresh corn stover (either with or without additional cellulase at 5 FPU/g of cellulose) is added to restore the mass of products removed as filtrate. After every third filtration, the filter cake is discarded and the saccharification vessels are loaded with fresh pretreated corn stover and enzyme.

Each filtration unit can process about 100,000 kg/h of slurry, and the effluent is to be processed in 1 d. To economize on the number of filters, saccharification is divided into four staggered batches so that the filters are operating nearly continuously. The number of required filtration units for each operating condition is shown in Table 1. The capital cost associated with each filtration unit is $2,110,000.

The total capital investment associated with feed handling, pretreatment, neutralization/conditioning, saccharification, and filtration is amortized over the 20-yr design life of the plant at a fractional interest rate of 10%. Annual labor costs are estimated by NREL to be $2,150,000 *(2)*. These costs were estimated using data from similar ethanol plants.

The production of glucose from each reaction cycle is calculated from cellulose conversions measured in the laboratory, assuming that cellulose conversion remains independent of reactor size. The model also assumes that cellulose conversion remains independent of the initial glucan concentration, because corn stover tested in the laboratory had a solids fraction of 15 ± 1% (w/w), while the design report specifies a lower initial solids fraction of 11.2% (w/w). The amount of glucose generated in one reaction cycle is calculated by multiplying the molar flow rate of glucan into the reactor by the cellulose conversion measured in the laboratory. Conversions measured at 4 d and 12 d are used in the batch and semibatch process models, respectively. The cycle times of 5 d and 15 d are longer for the two process models because filtration will require 1 day after every 4 d of saccharification. The glucose productions listed in Table 1 are lower than those measured experimentally in the laboratory because of the lower initial solids fraction. The annual glucose production is calculated by assuming that the processes are operated 350 d/yr.

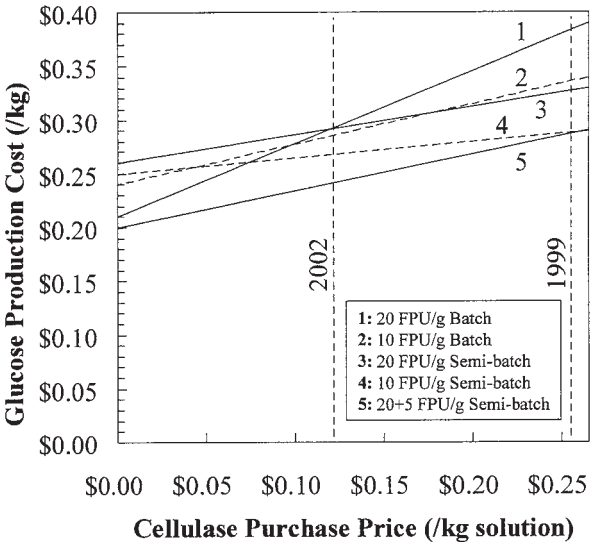

Fig. 7. Glucose production cost as a function of cellulase purchase price for three process configurations: batch, semibatch, and semibatch with additional cellulase. Vertical dashed lines are cellulase purchase prices in 1999 (26.6¢/kg) and in 2002 (12.2¢/kg).

The only chemical expenses considered are from the biomass feedstock and cellulase enzyme; all other chemical costs are small and essentially the same for the batch and semibatch models. NREL estimates the annual cost of corn stover to be $23,200,000 *(2)*. The annual cellulase flow rate is calculated based on the enzyme loading in the saccharification vessels and the specific activity in the cellulase solution of 50,000 FPU/L. The rate of cellulase consumption in all operating configurations is shown in Table 1. The price of cellulase solution has dropped rapidly in the past several years. In 1999, the price of cellulase solution was 25.6¢/kg *(1)*. In 2002, however, the price fell to only 12.2¢/kg, and it is expected to continue to decline *(2)*. Because of this variability, the glucose production costs were calculated for a range of cellulase prices and are shown in Fig. 7 for enzyme loadings of 10 and 20 FPU/g of cellulose. Glucose production costs listed in Table 1 are based on the price of enzyme in 2002. The uncertainties in glucose production and, hence, cost shown in Table 1 are primarily owing to the uncertainties in the solids concentrations used in the laboratory experiments.

From Table 1 and Fig. 7, there are several trends worth noting. First, using the lower enzyme concentration of 10 FPU/g of cellulose is economical only at high enzyme costs. Second, when the enzyme price declines below about 10¢/kg, the use of 20 FPU/g of cellulose becomes more economical for the batch case, because the higher conversion of substrate is more important than the reduced enzyme use. Third, enzyme reuse by employing the semibatch process is economically attractive only for

enzyme prices of 5 and 12¢/kg for 10 and 20 FPU/g of cellulose, respectively. Finally, the most economical process appears to be that for which a small concentration of new enzyme is added after each filtration step in the semibatch case. In this process, the enzyme costs are relatively low and yet high conversion of the relatively expensive cellulose feedstock is obtained. The cost savings are only modest (about 5¢/kg of glucose produced) at current enzyme prices, because the total biomass feedstock cost dominates over the total enzyme costs (*see* Table 1).

Conclusion

The results that we have presented show that a simple solid/liquid separation using a large-pore vacuum filtration unit is a viable method for recovering significant quantities of active cellulase enzymes bound to the solid substrate, and that these enzymes may be reused by simply mixing fresh substrate with the spent hydrolysate. Our work has also shown that reducing the concentration of inhibitory reaction products to levels low enough to enhance the saccharification rate is unproductive-the benefits of an enhanced saccharification rate are more than offset by the expenses owing to frequent filtration and the associated dilute product stream. The use of ultrafiltration to recover enzymes in solution was also shown to be unnecessary, since enzymes appear to be tightly bound to the residual solids; even when the filter cake is thoroughly washed with water and then mixed with fresh substrate, glucose continues to be generated. Thus, vacuum filtration alone can be used to retain solids and enzymes in the retentate, with the filtrate then representing a sugar stream that may be used for additional processing. Finally, an economic model suggests that the reuse of cellulase is potentially favorable using current cellulase prices. However, as cellulase prices continue to decline, future biomass conversion facilities will likely use the enzyme in only one round of saccharification.

Acknowledgments

We thank Jim McMillan and Bob Wooley of the National Renewable Energy Laboratory (NREL) for providing advice and materials, and undergraduate research assistant Ingrid Leth for providing laboratory assistance. We also gratefully acknowledge the US Department of Energy, Colorado Institute for Research in Biotechnology, and NREL for funding this project. Jeffrey Knutsen was also supported by the Department of Education's Graduate Assistantships in Areas of National Need program, and by the National Institutes of Health.

References

1. Wooley, R., Ruth, M., Sheehan, J., Ibsen, K., Majdeski, H., and Galvez, A. (1999), *Lignocellulosic Biomass to Ethanol Process Design and Economics Utilizing Co-Current Dilute Acid Prehydrolysis and Enzymatic Hydrolysis Current and Futuristic Scenarios*, NREL/TP-580-26157, National Renewable Energy Laboratory, Golden, CO.

2. Aden, A., Ruth, M., Ibsen, K., Jechura, J., Neeves, K., Sheehan, J., Wallace, B., Montague, L., Slayton, A., and Lukas, J. (2002), *Lignocellulosic Biomass to Ethanol Process Design and Economics Utilizing Co-Current Dilute Acid Prehydrolysis and Enzymatic Hydrolysis for Corn Stover*, NREL/TP-510-32438, National Renewable Energy Laboratory, Golden, CO.
3. Mores, W. D., Knutsen, J. S., and Davis, R. H. (2001), *Appl. Biochem. Biotechnol.* **91–93,** 297–309.
4. Knutsen, J. S. and Davis, R. H. (2002), *Appl. Biochem. Biotechnol.* **98,** 1161–1172.
5. Ghose, T. K. and Kostick, J. A. (1970), *Biotechnol. Bioengr.* **12,** 921–946.
6. Howell, J. A. and Stuck, J. D. (1975), *Biotechnol. Bioengr.* **17,** 873–893.
7. Berghem, L. E. R., Pettersson, L. G., and Axiöfredriksson, U. B. (1975), *Eur. J. Biochem.* **53,** 55–62.
8. Henley, R. G., Yang, R. Y. K., and Greenfield, P. F. (1980), *Enzyme Microb. Technol.* **2,** 206–208.
9. Hägerdal, B., López-Leiva, M., and Mattiasson, B. (1980), *Desalination* **35,** 365–373.
10. Klei, H. E., Sundstrom, D. W., Coughlin, R. W., and Ziolkowski, K. (1981), *Biotechnol. Bioeng.* **23,** 593–601.
11. Alfani, F., Albanesi, D., Cantarella, M., Scardi, V., and Vetromile, A. (1982), *Biomass* **2,** 245–253.
12. Alfani, F., Cantarella, M., and Scardi, V. (1983), *J. Membr. Sci.* **16,** 407–416.
13. Ohlson, I., Trägårdh, G., and Hahn-Hägerdal, B. (1984), *Biotechnol. Bioeng.* **26,** 647–653.
14. Kinoshita, S., Chua, J. W., Kato, N., Yoshida, T., and Taguchi, H. (1986), *Enzyme Microb. Technol.* **8,** 691–695.
15. Tan, L. U. L., Yu, E. K. C., Campbell, N., and Saddler, J. N. (1986), *Appl. Microbiol. Biotechnol.* **25,** 250–255.
16. Tanaka, M., Fukui, M., and Matsuno, R. (1988), *Biotechnol. Bioeng.* **32,** 897–902.
17. Ishihara, M., Uemura, S., Hayashi, N., and Shimizu, K. (1991), *Biotechnol. Bioeng.* **37,** 948–954.
18. Roseiro, J. C., Conceicao, A. C., and Amaralcollaco, M. T. (1993), *Bioresour. Technol.* **43,** 155–160.
19. Cheryan, M. and Escobar, J. (1993), *Improving Ethanol Production by Membrane Technology: The Continuous Saccharification Reactor*, National Renewable Energy Laboratory, Golden, CO.
20. Lee, S. G. and Kim, H. S. (1993), *Biotechnol. Bioeng.* **42,** 737–746.
21. Singh, N. and Cheryan, M. (1998), *Starch-Stärke* **50,** 16–23.
22. Lu, Y. P., Yang, B., Gregg, D., Saddler, J. N., and Mansfield, S. D. (2002), *Appl. Biochem. Biotechnol.* **98,** 641-654.
23. Kadam, K. and Knutsen, J. (2001), *Saccharification Experiments #6-9: Characterization of Cellulase Adsorption onto Pretreated Corn Stover*, National Renewable Energy Laboratory, Golden, CO.
24. McMillan, J. D., Dowe, N., Mohagheghi, A., and Newman, M. (1999), *Reducing the Cost of Saccharification and Fermentation by Decreasing the Cellulase Enzyme Loading Required for Cellulose Conversion*, National Renewable Energy Laboratory, Golden, CO.

0273-2289/04/114/0601–0617/$25.00

Controlled Fed-Batch Fermentations of Dilute-Acid Hydrolysate in Pilot Development Unit Scale

Andreas Rudolf,* Mats Galbe, and Gunnar Lidén

Chemical Engineering, Lund University,
Box 124, SE-221 00 Lund, Sweden,
E-mail: andreas.rudolf@chemeng.lth.se

Abstract

Inhibitors formed during wood hydrolysis constitute a major problem in fermenting dilute-acid hydrolysates. By applying a fed-batch technique, the levels of inhibitory compounds may be held low, enabling high ethanol productivity. In this study, a previously developed fed-batch strategy was modified and implemented for use in pilot development unit (PDU) scale. The rate of total gas formation, measured with a mass flow meter, was used as input variable in the control algorithm. The feed rate in the PDU-scale experiments could be properly controlled based on the gas evolution from the reactor. In fed-batch experiments utilizing TMB 3000, an inhibitor-tolerant strain of *Saccharomyces cerevisiae*, close to 100% of the hexoses in the hydrolysate was converted.

Index Entries: Pilot development unit scale; dilute-acid hydrolysate; fed-batch fermentation; feed rate; carbon dioxide evolution rate.

Introduction

Hydrolysis of lignocellulose is necessary to enable its use for ethanol production. However, when lignocellulosic materials are hydrolyzed with acid, compounds toxic to the yeast cells are released. The inhibitors are of three main types: aldehydes, organic acids, and phenolic compounds. Among the aldehydes, furfural and hydroxymethylfurfural (HMF) are typically found in high concentrations—particularly in dilute-acid hydrolysates *(1,2)*. These compounds have been shown to inhibit certain enzymes in the catabolism necessary for cell growth *(3–9)*.

The amount of inhibitory compounds can be decreased by detoxification. Several methods have been suggested, of which overliming is probably the most well studied *(10,11)*. One major drawback with

*Author to whom all correspondence and reprint requests should be addressed.

overliming is the necessity of handling the precipitates formed in the process. The potential loss of fermentable sugars is another important drawback *(10,11)*. An alternative strategy is to use the capacity of the yeast itself to convert the inhibitors, and thereby obtain in vivo detoxification. However, this only works if the concentrations of inhibitors are rather low. In a batch process, it is likely that the concentrations of inhibitors will be so high that cellular metabolism will completely stop *(12–14)*. High concentrations of inhibitors may be avoided if a fed-batch procedure is applied provided that there is an accurate control of the feed rate in order to keep the level of inhibitors low *(12–14)*.

Feed rate control based on the carbon dioxide evolution rate (CER) has been shown to be an efficient method. Taherzadeh et al. *(14)* increased the feed rate stepwise as long as the relative increase in CER was at least 50% of the relative increase in feed rate. Nilsson et al. *(13)* developed the method further and used the derivative of the CER to control the feed rate. This control principle was very successful in keeping the hexoses at low levels and preventing inhibition from toxic compounds and was the chosen control algorithm in the present work.

In small-scale fermentations, the most common way to measure the CER is to have a controlled flow of nitrogen through the reactor and monitor the outlet gas concentration with a gas analyzer. Nitrogen flushing is obviously not an option in large-scale operation, but the total gas evolution is still a measurable quantity.

In the present work, the objective was to develop and implement a control algorithm for addition of hydrolysate, based on the total gas flow from a pilot development unit (PDU)-scale reactor. The control algorithm was tested in fed-batch fermentations of dilute-acid hydrolysate made with two different yeast strains.

Controlling the addition of hydrolysate from the total exhaust gas flow proved successful. With one of the strains tested (TMB 3000), complete conversion of the hexoses present in a strongly inhibiting hydrolysate was obtained.

Material and Methods

Wood Hydrolysate

The hydrolysate used was a dilute-acid hydrolysate produced in Rundvik, Sweden, by a two-stage hydrolysis process performed in a 350-L rebuilt Masonite gun-batch reactor *(1)*. In the first process stage, about 10 kg of dry wood splinter was impregnated with H_2SO_4 and water to obtain an acid concentration of 5 g/L and a solids concentration of 30%. After impregnation the wood was loaded into the reactor and the reaction was started by direct steam injection. After a heat-up period of 50 s, a pressure of 12 bars was held for 10 min, followed by a rapid decompression. The solid material was separated from the liquid by filtration. Further hydrolysis of the remaining solid was carried out at a pressure of 21 bars for 7 min. The hydrolysates from

Table 1
Compositions of Dilute-Acid
Hydrolysates Used in PDU Experiments

Components	Hydrolysate A Concentration (g/L)	Hydrolysate B Concentration (g/L)
Glucose	24.3	19.9
Mannose	11.8	15.9
Xylose	5.7	7.4
Galactose	3.4	4.0
Arabinose	1.5	1.7
Acetate	1.7	1.7
HMF	2.1	1.8
Furfural	0.4	0.5

the two stages were mixed together. Two different batches of hydrolysate were used (Table 1).

Yeast Strains and Medium

Two different strains of *Saccharomyces cerevisiae* were used: CBS 8066 (Centralbureau voor Schimmelcultures, Delft, The Netherlands) and TMB 3000 (Division of Applied Microbiology, Lund University, Sweden). TMB 3000 is a strain originally isolated from spent sulfite liquor, and therefore it has a high tolerance to inhibitors. The strains were maintained on agar plates (20 g/L of agar, 20 g/L of soya peptone, 20 g/L of glucose, and 10 g/L of yeast extract). Before the fermentations, inoculum cultures were grown in 250-mL conical E-flasks. The flasks were placed in a shaker bath (30°C, 140 rpm) for 24 h.

Cultivation Procedures

Fed-Batch Fermentations

The fed-batch fermentations in PDU scale were performed in a 22-L reactor (NLF 22; Bioengineering AG, Wald, Switzerland). The pH was maintained at 5.0 by the addition of 2 *M* NaOH. The stirrer speed was 600 rpm and the fermentation temperature was 30°C. The fed-batch phase was preceded by a batch phase for production of cell mass. The initial glucose concentration in the medium was 64 or 45 g/L. To the medium was added 28.5 g/L of $(NH_4)_2SO_4$, 12.1 g/L of KH_2PO_4, and 2.6 g/L of $MgSO_4$ as sources for nitrogen, phosphorus, magnesium, and sulfur. Trace metal solution, Ergosterol/Tween-80, and vitamin solution were also added in accordance with Taherzadeh et al. *(15)*. The outlet gas flow was measured with a mass flow meter calibrated for CO_2 at a flow of 10–500 mL/min (F 111C; Bronkhorst High-Tech B.V., Ruurlo, The Netherlands). After consumption of the glucose in the batch medium, feeding of the hydrolysate was started.

In total, about 15 L of dilute-acid hydrolysate was pumped into the reactor using a peristaltic pump (U1-M; Alitea AB, Stockholm, Sweden). Before addition the pH of the hydrolysate was increased from 1.8 to 3.0 by the addition of about 22 mL of 2 *M* NaOH/L of hydrolysate. The reason for the pH adjustment was to avoid disturbance of the CO_2 signal owing to large base additions during the fed-batch fermentation.

Batch Fermentations

Batch fermentations of dilute-acid hydrolysate were done to compare the performance between batch and fed-batch procedures. Since the amount of hydrolysate available from each hydrolysis batch was limited, the batch fermentations were made in a 2.5-L fermentor (Biostat A, B. Braun Biotech, Melsungen, Germany). Scaling effects could potentially affect the comparison between batch and fed-batch fermentations. However, comparisons between batch and fed-batch fermentation of dilute-acid hydrolysates have been made repeated times, and our results were in good agreement with previous findings, showing a strong inhibition in batch fermentation *(12,13)*.

The pH was maintained at 5.0 by the addition of 2 *M* NaOH (Micro DCU-300; B. Braun Biotech). The fermentation temperature was 30°C and the stirrer speed was 500 rpm (MCU-200; B. Braun Biotech). Cell mass was produced in an initial batch phase using a glucose concentration of 64 g/L. The concentrations of mineral salts, trace metals, vitamins, and Ergosterol/Tween-80 were the same as in the fed-batch experiments. When the glucose in the batch medium was completely consumed, 1.9 L of dilute-acid hydrolysate was pumped into the reactor at maximum pump speed, by using a peristaltic pump (U1-M; Alitea AB). The ratio between batch volume and the final volume (i.e., after all the hydrolysate had been added) was similar to the ratio in the PDU fed-batch experiments, approx 1:4. The reactor medium was sparged with nitrogen (600 mL/min). The CO_2 content in the exhaust gas was measured with a gas analyzer (TanDem; Adaptive Biosystems, Luton, UK).

Analytical Methods

Metabolite Analysis

During the batch experiments, samples were withdrawn every hour. Samples were taken less frequently during the fed-batch experiments to avoid disturbances in the CO_2 signal. The samples were centrifuged in Eppendorf tubes at 12,000*g* for 5 min (Z 160 M; Hermle Labortechnik, Wehingen, Germany). Afterward, the supernatant was filtered with 0.2-µm sterile filters and the filtered samples were stored in a freezer. Analysis of the most common metabolites was done using high-performance liquid chromatography. The concentrations of glucose, mannose, xylose, and galactose were determined using a polymer column (Aminex HPX-87P; Bio-Rad, München, Germany) at 85°C. Ethanol, glycerol, acetate, HMF, and furfural were analyzed using an Aminex HPX-87H column (Bio-Rad) at

60°C. The compounds of interest were detected with a refractive index detector (Waters 2410; Milford, MA).

Biomass

Dry weight was determined from duplicate 10-mL samples. The samples were centrifuged for 4 min at 1000*g* (Z 200 A, Hermle). The supernatant was then discarded and the pellet washed. After a second centrifugation the pellet was dried at 105°C for 24 h.

CO_2 Evolution

The analog signals from the mass flow meter (during the fed-batch fermentations) and from the gas analyzer (during the batch fermentations) were transformed to digital signals by 12-bit data acquisition cards (PCI-6024E; National Instruments, Austin, TX). Labview 5.1 software from National Instruments was used for data logging and feed rate control.

Cell Viability

Samples for cell viability tests were taken three times during the different batch and fed-batch fermentations. A sample of 1 mL was diluted 10^4–10^5 times and 0.1 mL of diluted sample was applied to an agar plate. Five to six plates were prepared for every sample, and the plates were incubated for 24 h at 30°C. The total cell concentration in the reactor sample was determined with microscopy using a Bürker counting chamber. The viability, expressed as the fraction of cells able to form colonies, was calculated by dividing the concentration of colony-forming cells by the total cell concentration.

Theory

Feed Rate Optimization

Measuring the CO_2 evolution, CER, is an excellent way to monitor the ethanol production since the dominant source of CO_2 production in anaerobic fermentations is directly linked to ethanol formation *(13)*. One of the main goals of the present project was to maximize ethanol production. The feed rate, $F(t)$, which maximizes the overall ethanol production, $I(F)$ (Eq. 1), for a given time, t, should therefore be found *(16)*:

$$I(F) = \int_t R_p\left[F(t)\right] dt \tag{1}$$

The productivity, R_p (g/h), is composed of three factors (Eq. 2):

$$R_p = q_p(t)X(t)V(t) \tag{2}$$

in which q_p (g/g·h) is the specific productivity, X (g/L) is the biomass concentration, and V (L) is the volume (Eq. 3):

$$V(t) = \int_t F(t)dt + V_0 \tag{3}$$

The composition of the hydrolysate will affect growth rate, specific substrate uptake rates, and yield coefficients in a not easily predictable way *(14)*. It is thus not possible to use a predetermined feed profile, but instead a closed-loop procedure should be used. One approach is to maximize the productivity at every point in time, and this can relatively easily be implemented in a closed-loop control. This approach was used by Taherzadeh et al. *(14)*, who applied step changes in the feed rate and gradually increased the feed rate as long as there was a relative response in CER corresponding to at least include 50% of the relative increase in feed rate. The major drawbacks of this control were that the increase in feed rate was fixed and that the CER-response ratio was somewhat sensitive to measurement errors.

Control Strategy

The control algorithm in the present work was based on using the derivative of the CER (Eqs. 4 and 5) as the variable on which to base the control *(13)*:

$$\nu = \frac{d\,\mathrm{CER}}{dt} \tag{4}$$

ν expressed in a discretized form is given in Eq. 5:

$$\nu = \frac{\left(\mathrm{CER}_t - \mathrm{CER}_{t-1}\right)}{\left(t_t - t_{t-1}\right)} \tag{5}$$

The derivative of the CER was continuously calculated during the length of a step, and the maximal value of ν, denoted ν^{max}, was the basis for determining the increase in feed rate, ΔF. The increase in feed rate was determined by the ratio between the maximal value of the CER derivative following a step change, ν^{max}, and the maximal CER derivative obtained after the first step, ν_0^{max}. In the beginning of the fed-batch fermentation, the levels of inhibitors are low and the response to the first increase in feed rate thus represents a noninhibited system. During the fed-batch fermentation, if the cell growth is strongly inhibited, there will be a dilution of the cells resulting in a lower *X* (cell mass concentration). Nilsson et al. *(13)* showed that a decreasing *X* will lead to a lower ν. This fact was taken into consideration in the control program by introducing a correction factor, $V/\Delta F$ (Eq. 6). This factor compensates for the dilution of biomass, as well as the magnitude of the increase in feed rate in the preceding step. The expression of ΔF as a function of the corresponding ν^{max} is given by Eq. 6:

$$\Delta F_i = \frac{\left(\nu_{i-1}^{max} \times \frac{V_{i-1}}{\Delta F_{i-1}}\right)}{\left(\nu_0^{max} \times \frac{V_0}{\Delta F_{max}}\right)} \tag{6}$$

If the concentration of inhibitors increases to such levels that the yeast metabolism is affected, the numerator in Eq. 6 will decrease. In case the ratio on the right-hand side of Eq. 6 decreases below a threshold value, no further increase in feed rate will be made.

Disturbances in the measured signal of only a few percent can affect the CER derivative (ν) considerably. Therefore, ν must be calculated from an average value of the CER, obtained within a certain time span.

Results

Fed-batch fermentations in PDU scale were made with two different *S. cerevisiae* strains, CBS 8066 and TMB 3000. Batch fermentations in a 2.5-L scale were done to compare the performance of batch and fed-batch procedures.

Comparison of Strain Performance

Fed-Batch Fermentations

There was a significant difference in the ability of the two strains to ferment the hydrolysates in fed-batch cultivation, as seen in the measured CER profiles of the two strains (Fig. 1). This is in accordance with observations made by A. Nilsson, (Chemical Engineering, Lund University, personal communication). During fed-batch fermentations with TMB 3000, there was a clear and significant response to the steps in feed rate throughout the whole fed-batch phase (Fig. 1A). This was in contrast to fed-batch fermentations with CBS 8066, in which responses to the changes in feed rate decreased after 1.30 h and ceased completely at 2 h (Fig. 1B). Even though the feed rate remained constant the CER continued to decrease. When CBS 8066 was used, only 75% of the hexoses (glucose plus mannose) was fermented whereas close to 100% of the hexoses in the hydrolysate was fermented when TMB 3000 was used. In addition, very significant differences in cell viability after the fed-batch phase were observed. The cell viability of CBS 8066 at the end of feeding was merely 15%, whereas it was close to 100% for TMB 3000 (Table 2).

Batch Fermentations

After a 500-mL batch phase with an initial glucose concentration of 64 g/L, 1.9 L of dilute-acid hydrolysate was added using the maximum pump speed. Batch experiments with both TMB 3000 and CBS 8066 were concluded (Figs. 2 and 3). In addition, TMB 3000 was tested with two different batches of dilute-acid hydrolysate (Table 1).

Compared with the fed-batch fermentations the performance of the batch fermentations was poor. Only a small fraction of the hexoses was fermented (Table 3), compared with almost 100% during the fed-batch fermentations with TMB 3000. As a consequence, the specific ethanol productivity was very low in the batch experiments. The levels of HMF did not decrease significantly during the batch fermentations. On the other hand, furfural was completely converted. The cell viability was close to 0% at the end of all three batch fermentations.

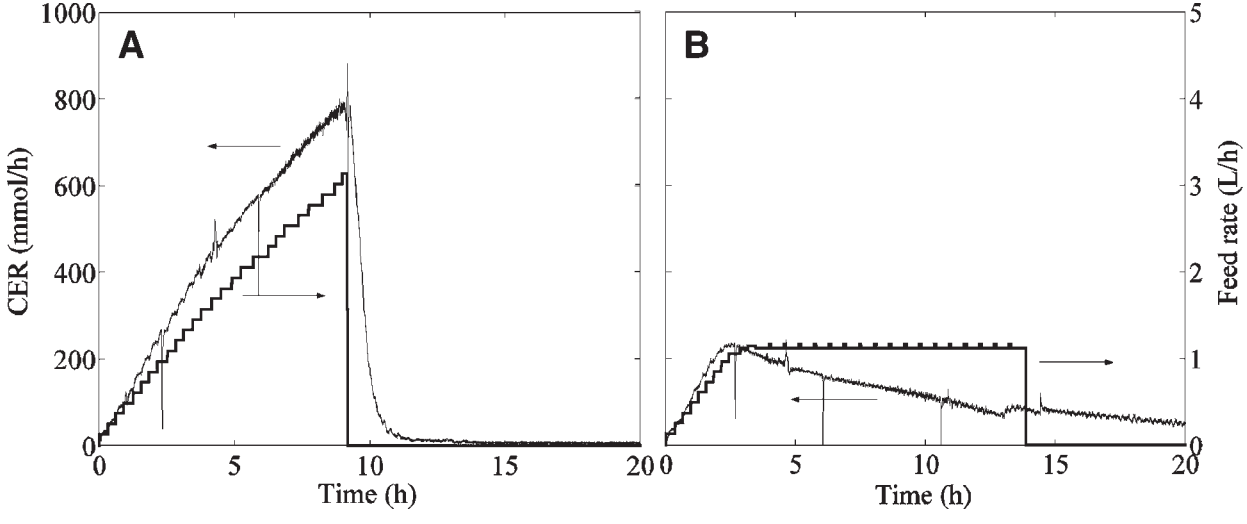

Fig. 1. CER and feed rate during fed-batch fermentations in PDU-scale. After 2 h the CBS 8066 culture was severely inhibited and the increase in feed rate was stopped. Dilute-acid hydrolysate B was used. **(A)** TMB 3000; **(B)** CBS 8066.

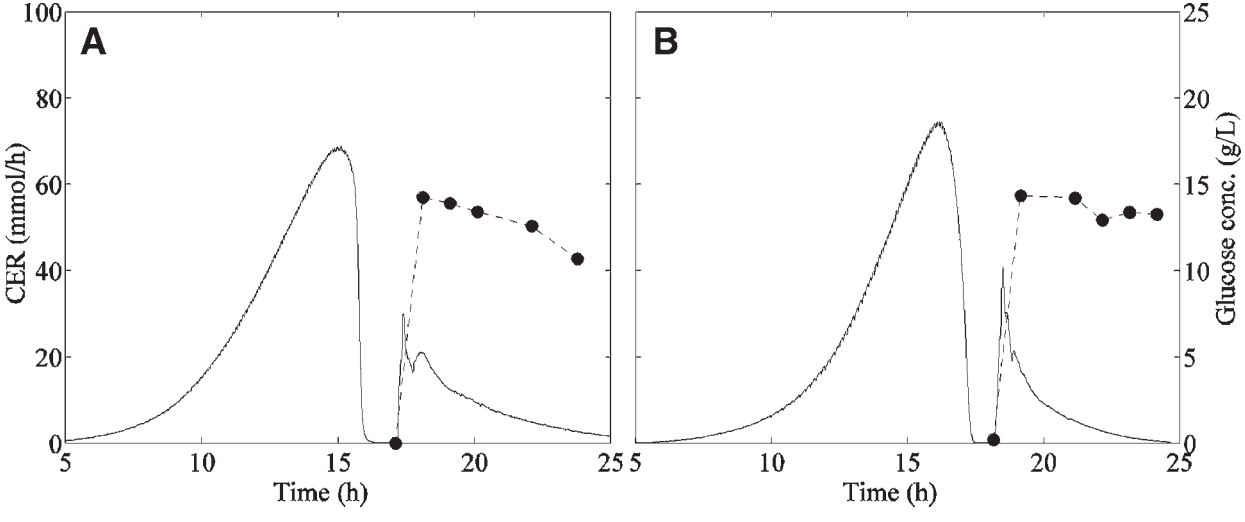

Fig. 2. CER (—) and glucose concentration (– –●– –) during batch fermentations with dilute-acid hydrolysate B. Batch fermentations (0.5 L) on glucose were made during the first 15–17 h to produce cell mass. **(A)** TMB 3000; **(B)** CBS 8066.

Table 2
Cell Viability After Fed-Batch Phase

Strain	Hydrolysate	Viability at end of fed-batch phase (%)
CBS 8066	B	15
TMB 3000	B	~100
TMB 3000	A	93
TMB 3000	A	95

Table 3
Conversion of Glucose and Mannose in Small-Scale Batch Fermentations

Strain	Hydrolysate	Conversion of mannose (%)	Conversion of glucose (%)
CBS 8066	B	9	8
TMB 3000	B	28	30
TMB 3000	A	20	20

Productivity and Yields

The productivity of the strain TMB 3000 was clearly superior to that of CBS 8066, and therefore strain TMB 3000 was analyzed further. Two fed-batch fermentations with dilute-acid hydrolysate A (Table 1) were run using two different glucose concentrations in the batch phase.

The overall specific ethanol productivity, calculated on the whole fed-batch fermentation, was 0.72 g/(g·h) when the glucose concentration in the batch phase was 45 g/L and 0.58 g/(g·h) when the glucose concentration in the batch phase was 64 g/L. The specific ethanol productivity in fact reached a value as high as 0.9 g/(g·h) at the end of the fed-batch fermentations (Fig. 4). The levels of HMF were low during the fed-batch experiments (Fig. 5), and the levels of furfural were too low to be detected, indicating a successful *in situ* detoxification. The total cell mass was doubled (Fig. 6) during the two fed-batch fermentations with TMB 3000, but since the volume during the same time increased fivefold, the cell mass concentration decreased substantially. The ethanol yield on hexoses (glucose and mannose) was 0.45 g/g in the two fed-batch fermentations. The biomass yield on hexoses in the mentioned fed-batch fermentations was about 0.05 g/g (Table 4). This value can be compared with the value of 0.10 g/g obtained for growth on glucose in synthetic medium (i.e., the value obtained in the anaerobic batch phases preceding the fed-batch phases). A cell yield of 0.05 g/g is rather low, but it is well known that inhibitors in the dilute-acid hydrolysate affect cell growth negatively *(1,3,4,6–8,17)*.

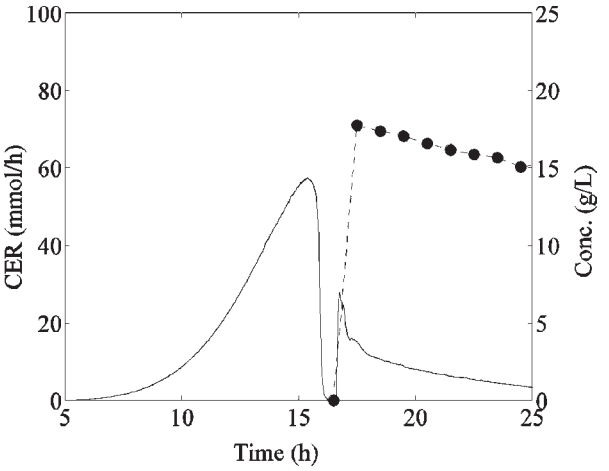

Fig. 3. CER (—) and glucose concentration (– – ● – –) during batch fermentation with dilute-acid hydrolysate A. The strain used was TMB 3000. Batch fermentations (0.5 L) on glucose were made during the first 15–17 h to produce cell mass.

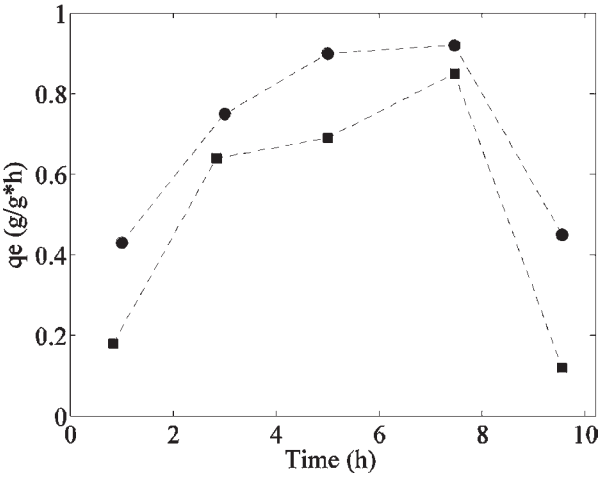

Fig. 4. Specific ethanol productivity in two fed-batch fermentations with TMB 3000. Dilute-acid hydrolysate A was used. (– – ● – –) *qe* for the fed-batch fermentation with 45 g/L of glucose in the batch phase; (– – ■ – –) *qe* for the fed-batch fermentation with 64 g/L of glucose in the batch phase.

Performance of Control

There was initially a fast and significant response in CER after a step change in the feed rate. During the first 3 h, the stepwise increases in feed rate gave sharp and smooth peaks in ν. However, during the last 5 h, the noise in the input signal created a more irregularly shaped ν profile (Fig. 7A).

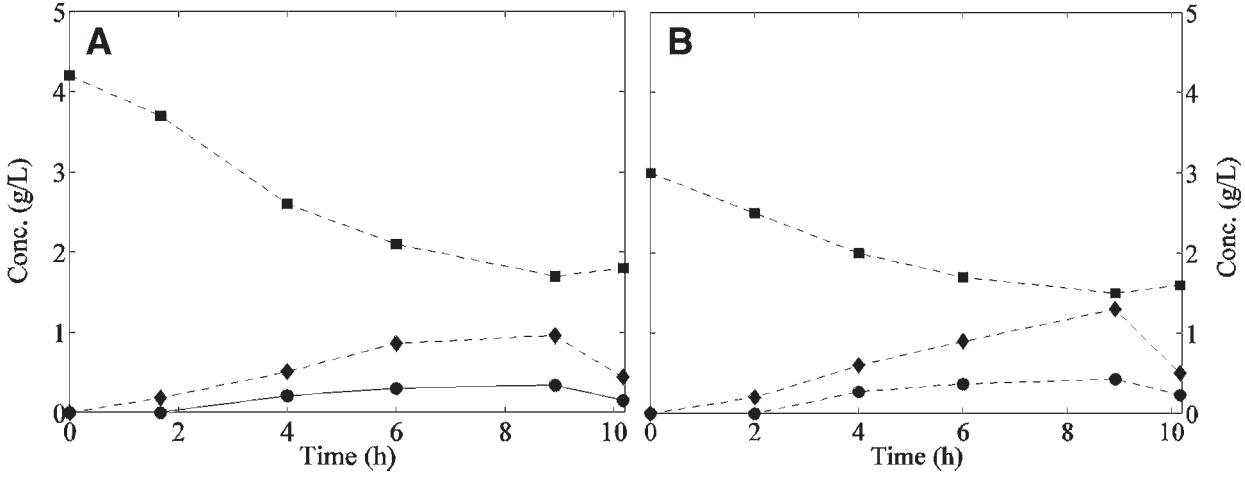

Fig. 5. Concentrations of glycerol (--■--), glucose (--◆--), and HMF (--●--) during two fed-batch fermentations with TMB 3000. Dilute-acid hydrolysate A was used. **(A)** 64 g/L of glucose in the batch phase; **(B)** 45 g/L of glucose in the batch phase.

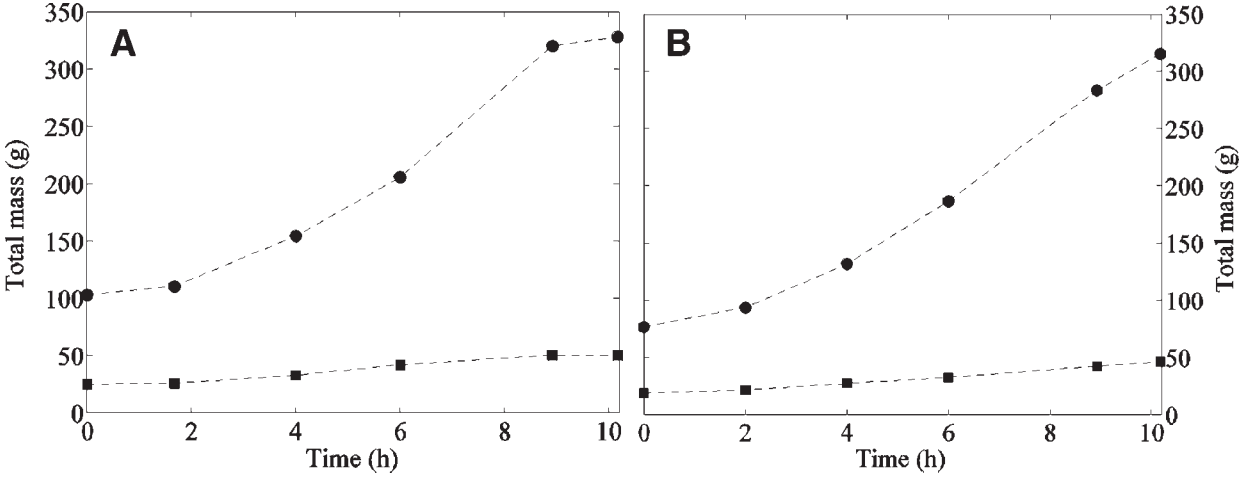

Fig. 6. Total amount of ethanol (– – ● – –) and cells (– – ■ – –) produced during two fed-batch fermentations with TMB 3000. Dilute-acid hydrolysate A was used. **(A)** 64 g/L of glucose in the batch phase; **(B)** 45 g/L of glucose in the batch phase.

Table 4
Yield Coefficients from Fed-Batch Fermentation with TMB 3000 and Dilute-Acid Hydrolysate A[a]

		Batch phase		Fed-batch phase	
Yield coefficients	Explanation	(C-mol/C-mol)	(g/g)	(C-mol/C-mol)	(g/g)
Y_{SE}	Yield of ethanol on glucose and mannose	0.47	0.36	0.57	0.45
Y_{SX}	Yield of cell mass on glucose and mannose	0.12	0.10	0.064	0.053
Y_{SG}	Yield of glycerol on glucose and mannose	0.066	0.068	0.036	0.037
Y_{SC}	Yield of CO_2 on glucose and mannose	—	—	0.27	0.40

[a]The initial glucose concentration in the batch phase was 64 g/L. Y_{SC} could not be calculated during the batch phase because the gas bulk in the fermentor initially consisted of air and not CO_2, as when the fed-batch was started.

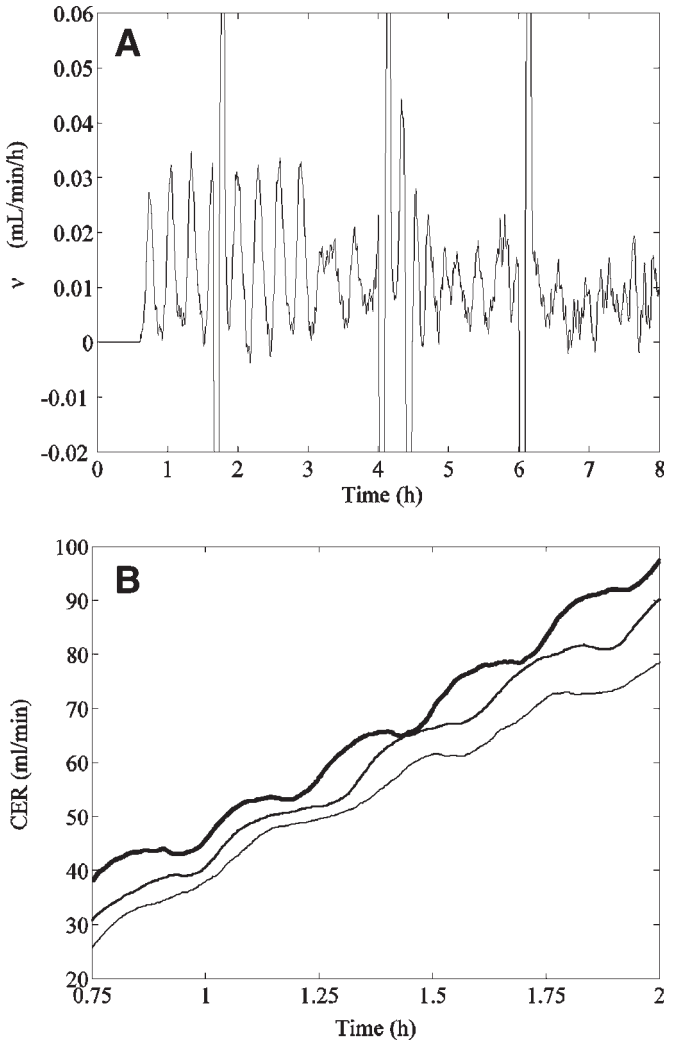

Fig. 7. Dynamics of CER responses during fed-batch fermentations in PDU scale. **(A)** CER derivative, ν, plotted during fed-batch fermentation with TMB 3000. The peaks at 1.45, 4, and 6 h are disturbances owing to sampling. **(B)** Comparison of step responses in CER: (▬)CBS 8066, 35 g/L of glucose solution; (—) TMB 3000, dilute-acid hydrolysate B; (—) CBS 8066, dilute-acid hydrolysate B.

The step length was important for a successful control. It was found that the dynamics of CER was different depending on which carbon source was used. When a 35 g/L glucose solution was used as feed, a step length of 15 min was enough for the CER to stabilize again within the pulse length (Fig. 7B). However, when dilute-acid hydrolysate was used as a substrate, a step length of 18 min had to be applied for both TMB 3000 and CBS 8066 (Fig. 7B) in order to get a $\nu < 37\%$ of ν^{max} (no increases in feed rate were made before $\nu < 37\%$ of ν^{max}).

Discussion

Problem of Measurement Noise

Using the total mass flow from the reactor as input signal in the control algorithm was overall found to work quite satisfactorily. The main improvement to be made relates to handling measurement noise. The measurement noise was not much of a problem during the first hours of the fed-batch fermentations, but it increased continuously and became problematic in the end of the fed-batch fermentations. The reason for this increased noise was not quite clear. As expected, the base addition, necessary for the pH control, contributed to the noise somewhat but was not the sole explanation. Possibly, the noise level can be explained by the changed headspace volume. With increasing liquid volumes, the headspace volume decreased. The pressure changes caused by a changed CER thereby progressively increased, taking away the "buffering capacity" of the headspace to CER fluctuations.

The used control algorithm should be modified to improve the performance in the presence of measurement noise. The time span during which the average CER is calculated could be further prolonged. This has been tested and it has a great impact on the ν profile. However, if the time span is too long, the delay time will demand increased pulse lengths in order to allow ν to decrease below 37% of ν_{max}. Another approach to moderate the effects of the noise could be to implement some kind of signal filter into the algorithm. However, the frequency and amplitude of the noise seems to be very irregular, which would probably hamper signal filtering.

Advantage of Comparing Strains in Batch and Fed-Batch Fermentations

No major difference in performance of the strains was found in the batch cultivations, but the performance was quite different during fed-batch operation. This shows the importance of using not just batch cultivations for comparing strains. Presumably, the toxicity levels in the batch case were so high that both strains were completely inhibited. However, at intermediate levels, as obtained in fed-batch cultures, the strain performances were quite different.

Acknowledgments

This work was financially supported by the Swedish National Energy Administration.

References

1. Taherzadeh, M. J., Eklund, R., Gustafsson, L., Niklasson, C., and Lidén, G. (1997), *Ind. Eng. Chem. Res.* **36,** 4659–4665.
2. Larsson, S., Palmqvist, E., Hahn-Hägerdal, B., Tengborg, C., Stenberg, K., Zacchi, G., and Nilvebrant, N.O. (1999), *Enzyme Microb. Technol.* **24,** 151–159.

3. Banerjee, N. and Viswanthan, L. (1976), *Proc. Annu. Conv. Sugar Technol. Assoc. India* **41,** G75–G80.
4. Sanchez, B. and Bautista, J. (1988), *Enzyme Microb. Technol.* **10,** 315–318.
5. Taherzadeh, M. J., Gustafsson, L., Niklasson, C., and Lidén, G. (2000), *J. Biosci. Bioeng.* **90,** 374–380.
6. Taherzadeh, M. J., Gustafsson, L., Niklasson, C., and Lidén, G. (2000), *Appl. Microbiol. Biotechnol.* **53,** 701–708.
7. Sárvári Horváth, I., Taherzadeh, M. J., Niklasson, C., and Lidén, G. (2001), *Biotechnol. Bioeng.* **75,** 540–549.
8. Palmqvist, E., Almeida, J. S., and Hahn-Hägerdal, B. (1999), *Biotechnol. Bioeng.* **62,** 447–457.
9. Modig, T., Lidén, G., and Taherzadeh, M. J. (2002), *Biochem. J.* **363,** 769–776.
10. Nilvebrant, N.-O., Persson, P., Reimann, A., de Sousa, F., Gorton, L., and Jönsson, L. J. (2003), *Appl. Biochem. Biotechnol.* **105,** 615–628.
11. Millati, R., Niklasson, C., and Taherzadeh, M. J. (2002), *Process Biochem.* **38,** 515–522.
12. Nilsson, A., Taherzadeh, M. J., and Lidén, G. (2002), *Bioprocess Biosyst. Eng.* **25,** 183–191.
13. Nilsson, A., Taherzadeh, M. J., and Lidén, G. (2001), *J. Biotechnol.* **89,** 41–53.
14. Taherzadeh, M. J., Niklasson, C., and Lidén, G. (2000), *Biotechnol. Bioeng.* **69,** 330–338.
15. Taherzadeh, M. J., Lidén, G., Gustafsson, L., and Niklasson, C. (1996), *Appl. Microbiol. Biotechnol.* **46,** 176–182.
16. Lidén, G. (2001), *Bioprocess Biosyst. Eng.* **24,** 273–279.
17. Chung, I. S. and Lee, Y. Y. (1985), *Biotechnol. Bioeng.* **27,** 308–315.

0273-2289/04/114/0619–0625/$25.00

Degeneration of β-Glucosidase Activity in a Foam Fractionation Process

Vorakan Burapatana, Ales Prokop, and Robert D. Tanner*

Department of Chemical Engineering,
Vanderbilt University,
Station B, PO Box 351604,
Nashville, TN 37235,
E-mail: rtanner@vuse.vanderbilt.edu

Abstract

Foam fractionation is a promising technique for concentrating proteins because of its simplicity and low operating cost. One such protein that can be foamed is the enzyme cellulase. The use of inexpensively purified cellulase may be a key step in the economical production of ethanol from biomass. We conducted foam fractionation experiments at total reflux using the cellulase component β-glucosidase to study how continuous shear affects β-glucosidase in a foam such as a fermentation or foam fractionation process. The experiments were conducted at pH 2.4, 5.4, and 11.6 and airflow rates of 3, 6, 15, 20, and 32 cc/min to determine how β-glucosidase activity changes in time at these different conditions. This is apparently a novel and simple way of testing for changes in enzyme activity within a protein foam. The activity did not degenerate during 5 min of reflux at pH 5.4 at an airflow rate of 10 cc/min. It was established that at 10 min of refluxing, the β-glucosidase denatured more as the flow rate increased. At pH 2.4 and a flow rate of 10 cc/min, the activity remained constant for at least 15 min.

Index Entries: β-Glucosidase; foam fractionation; cellulase; reflux time; airflow rate.

Introduction

Cellulase is a collection of enzymes that together can hydrolyze cellulose to glucose, a key step in the low-cost conversion of biomass to ethanol. Such a process would be useful for three reasons. First, in large scale it could contribute to the substitution of the renewable fuel ethanol for petroleum-based gasoline. Second, it is known that the addition of 5% ethanol to

*Author to whom all correspondence and reprint requests should be addressed.

present-day gasoline can reduce carbon monoxide, carbon dioxide, and hydrocarbon emissions from automobiles. Third, at the 5% addition level, no engine modification is needed. Unfortunately, the use of ethanol for a fuel addition from a waste crop source for biomass is not financially feasible at present *(1)*. Without a significant decrease in the production cost, the petroleum-sparing and environmental benefits of this "bioethanol" will likely not be achieved.

Foam fractionation can be used as a low-cost concentration and/or separation process for surface-active materials such as proteins *(2–5)*. It is possible to recover the protein cellulase via a foam fractionation process *(2)*, thereby possibly lowering the cost of ethanol derived from biomass. This lowering in cost follows because the production cost of bioethanol is heavily dependent on the cost of cellulase. However, foaming is thought to denature proteins such as enzymes and thus lower enzymatic activity. Surface denaturation, shear stress, and oxidation are three important factors known to denature proteins in a foam fractionation process *(6,7)*. A protein can denature at a gas-liquid interface owing to a change in folding of its structure. Generally, the hydrophobic parts of a protein will orient themselves toward the gas phase and the hydrophilic parts toward the liquid water phase. This orientation becomes important in an air-water system such as a fermentation process producing cellulase and in a foam recovery process of that fermentation broth since it can also change the shape of the cellulase molecule. The resulting degree of denaturation depends on the ability of a protein to refold back to its original structure following foaming. Shear stress caused by rising and bursting air bubbles can also damage proteins such as cellulase. In addition, it is suspected that an interaction between oxygen and enzymes may cause enzymes to denature. Changes in pH and temperature can denature proteins as well.

The loss of cellulase activity in a foam fractionation process has been observed previously *(2)*. Since cellulase is a collection of enzymes, and different proteins denature differently, it is not obvious which foam fractionation strategy (such as the best pH and temperature conditions to use) is best to invoke to minimize the loss in cellulase activity in each of the individual primary components of cellulase during a foam fractionation process. In particular, if recovery of the "combined" cellulase directly from a fungal fermentation process as it is being produced is desired, which single condition should be followed to maximize the activity of the cellulase grouping? Cellulase has three main components: endo-β-glucanase, exo-β-glucanase, and β-glucosidase.*(8)* In this article, we focus on the loss of activity of β-glucosidase caused by different pH values, airflow rates, and reflux times during a foam fractionation process. In previous experiments, it was shown that the relatively hydrophilic β-glucosidase can be recovered from a water solution via foam fractionation with a modest amount of foaming *(9)*. We studied β-glucosidase as a key component for characterizing activity degeneration in the "combined" cellulase because of the three cellulase components it is the one that is commercially avail-

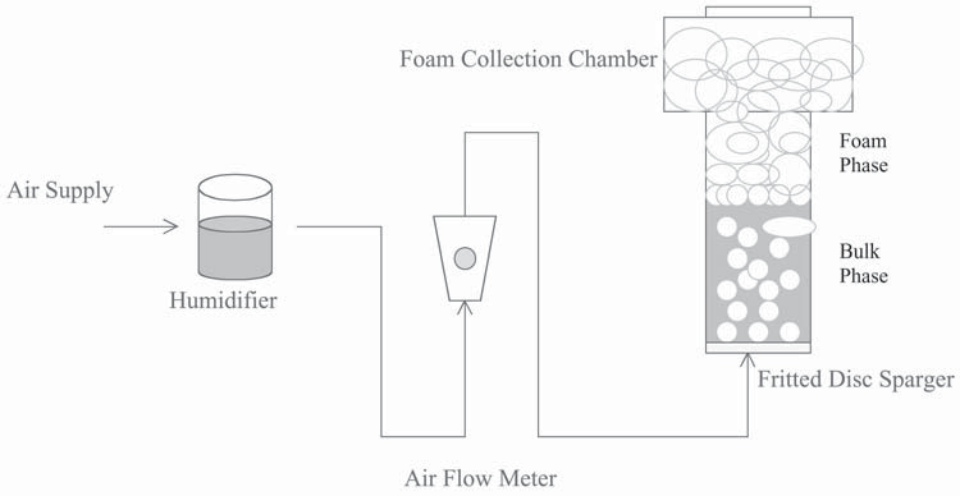

Fig. 1. Schematic of apparatus for foam fractionation of β-glucosidase at total reflux.

able. Herein, we define the amount of activity recovered as the relative activity (RA):

$$RA = \frac{\text{Activity}}{\text{Activity}_{\text{base case (pH 5.4)}}} \quad (1)$$

The base case is set at pH 5.4, the initial activity. RA is the ratio of the activity after the foam experiment to the activity before the foam experiment (referred to as time zero).

Materials and Methods

Effect of Airflow Rate

Twenty milligrams of glucosidase (containing both α and β glucosidase) derived from *Aspergillus niger* purchased from Fluka (catalog no. 49291) was dissolved and mixed well in 200-mL of deionized water to make a 100 mg/L solution. Ten milliliters of this glucosidase solution was poured into the foam fractionation column depicted in Fig. 1. This small column of 2-cm diameter and 9-cm length was used because the high cost of purified glucosidase prohibited multiple runs in a larger column. The semibatch (continuous in air) column was operated at total reflux at different air velocities for 10 min for each run. One- milliliter samples were taken from the liquid phase at airflow rates of 3, 6, 15, 20, and 32 cc/min. The concentration of β-glucosidase remained relatively constant throughout the experiment because we did not collect the foamate.

Effect of Reflux Time

A 100-mg/L glucosidase solution was used throughout this part of the experiment. Ten milliliters of this solution was poured into the foam fractionation column. The air velocity was then set at 10 cc/min and the pH at 5.4 (the unadjusted solution pH). A 1-mL sample was taken from the liquid phase at several different times: 0, 1, 1.5, 2, 3, 4, 5, 7, and 10 min. The experiment was repeated with 100-mg/L of glucosidase solution for more acidic and basic conditions, at pH 2.4 and 11.6, respectively.

Activity Assay

One hundred microliters of each sample from the foam fractionation column was mixed with 100 µL of 15 m*M* glucosidase substrate solution in a 1.5-mL microcentrifuge tube. The samples were incubated at 50°C for 30 min. After incubation, the samples in the microcentrifuge tubes were put in boiling water for 5 min. Then, the tubes were cooled down in an ice bath for 10 min. After cooling, 10 µL of solution from each tube was added, along with 90 µL of deionized water, into a selected well in a 96-well microplate. Next, 100 µL of glucose oxidase reagent (catalog no. G3660; Sigma Aldrich; the assay is included as part of the assay kit) was added to each filled well. After 15 min, 100 µL of 12 N H_2SO_4 was added to each filled well to stop the glucose reaction. The microplate was scanned at 540 nm using a µQuant Plate Reader from Biotek.

Results and Discussion

Bubbling air into a foam fractionation column containing a glucosidase water solution can cause damage to the glucosidase molecules. Figure 2 shows that at pH 5.4, as the airflow rate increased, the glucosidase activity decreased in a decaying, exponential manner. It is seen that the change in activity was rapid for airflow rates in the range of 0–6 cc/min. Then, the rate of change in relative activity decreased as the airflow rate increased. Even at the relatively slow flow rate of 3 cc/min (held for 10 min), the activity dropped to 93% of the original β-glucosidase activity. The degradation of activity owing to air shear can be crudely estimated as $0.92e^{-kF}$, in which $k = 0.0086$ min/cc and F = airflow rate (cc/min). Here, the R^2 of the fit is 0.72.

The effect of reflux time at pH 5.4 (holding the airflow rate at 10 cc/min) is shown in Fig. 3. It is observed that the activity held at about 95% of the initial activity until about 6 min of refluxing, at which time the activity dropped to about 80% of the initial activity. This means that with comparable aeration shear, experienced in a fermentor or a foam fractionation column, the activity of this cellulase component remains relatively intact for up to 6 min. At pH 3.5 and 4.0, when the activities were measured, following foaming for 6–8 min, the activities decreased only slightly (to about 95%). This low airflow rate usually led to foamate (recovered solution at the top of the foam) that was highly enriched.

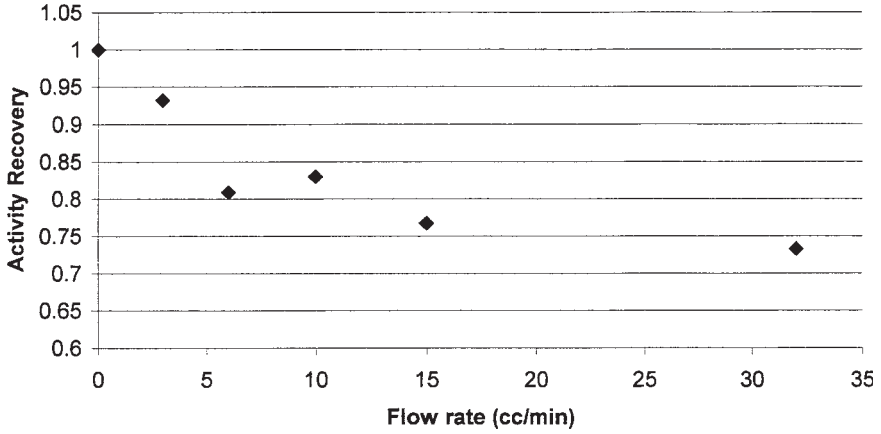

Fig. 2. Shearing effect of air on β-glucosidase activity at pH 5.4 and 10 min of refluxing.

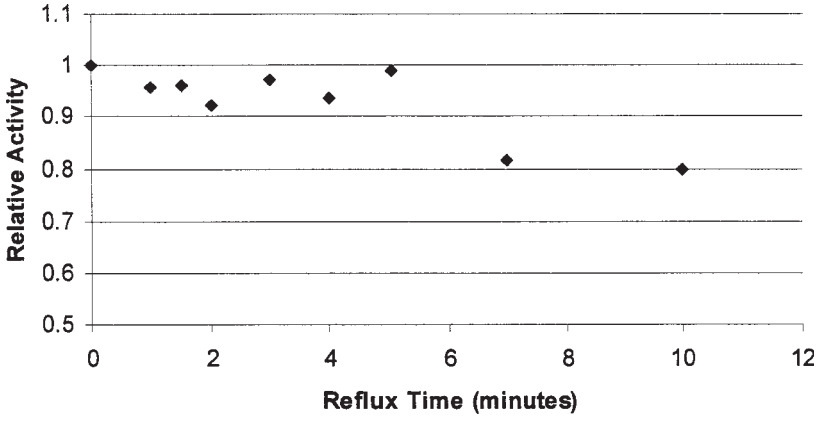

Fig. 3. Effect of reflux time on β-glucosidase activity at pH 5.4. The airflow rate was set at 10 cc/min.

The effect of aeration on glucosidase activity can be dependent on the reflux time, as seen in Fig. 3. A short time period of foaming apparently does minor (about 5% activity loss) damage to glucosidase. Figure 3 shows that the relative activity of glucosidase fluctuated between 0.9 and 1 for the first 5 min of foaming. Then the activity dropped to 80% by about 7 min of foaming and remained at that level for the next 3 min. The data indicate that glucosidase molecules can withstand the air bubble shear quite well for up to about 6 min of foaming at pH 5.4 and an airflow rate of 10 cc/min in the small reflux foam fractionation column.

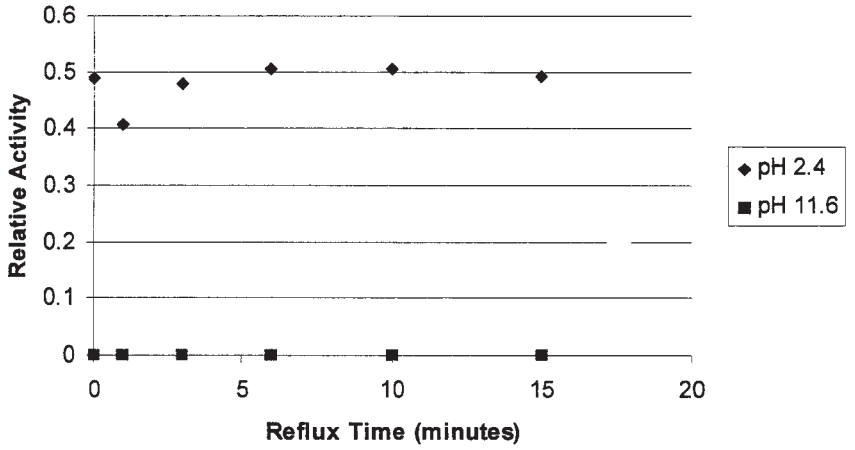

Fig. 4. Effect of reflux time (at two extremes pH values) on β-glucosidase activity. The airflow rate was set at 10 cc/min.

The glucosidase molecules appear to behave like an elastic spring. Like a spring losing some of its elasticity after being stretched for a significant time period, glucosidase loses some of its activity after being sheared by air bubbles over a given time. At an air-liquid interface (such as at the surface of an air bubble), a protein molecule such as glucosidase can be oriented so that the hydrophilic part stays in the liquid while the hydrophobic part tends to point toward the air (within the gas bubble). This orientation is thought to cause enzymes (such as glucosidase) to denature at air-water interfaces like those found in bubbles of a foam fractionation column. Such enzymes can also refold back to their original structure following temporary denaturation in an air shear environment like refluxing in a foam fractionation column. The ability to refold might be lost, however, because the molecules remain under shear at the interface over long time periods. In most foam fractionation experiments, the entire separation of concentrated foam in the foamate phase is completed well before the 3–7 min refluxing times noted here. The data presented here indicate that foam fractionation over shorter periods of time (less than 3–7 min) does not significantly denature glucosidase.

Foaming experiments were also conducted at pH 2.4 and 11.6 to determine how glucosidase is affected at very acidic and very basic environments; the findings are shown in Fig. 4. At pH 2.4, the activity dropped to 47% of that present initially (essentially at zero time) but then remained constant at this level throughout the subsequent 15 min of foaming. At pH 11.6, the activity was essentially all lost on the addition of base and did not recover on refluxing.

Conclusion

Glucosidase activity is best retained in a moderately acidic environment during refluxing in a foam fractionation column. Activity retention is also dependent on the airflow rate. The greater the airflow rate (the greater the bubble shear stress on glucosidase), the greater the reduction in glucosidase activity. Foaming time is another important factor: keeping the foaming time below a certain time threshold (i.e., 6 min) at pH 5.4 and an airflow rate of 10 cc/min minimizes loss of glucosidase activity. This means that glucosidase in a foam fractionation column experiences minimal loss of activity with a typical foaming time (residence time) of less than 1 min.

Acknowledgments

We are pleased to thank Prof. R. Robert Balcarcel for allowing us to use the μQuant Plate Reader (Biotek). We also greatly appreciate financial support from the US Department of Agriculture (grant no. 2001-52104-11476).

References

1. Sheehan, J. and Himmel, M. (1999), *Biotechnol. Prog.* **75,** 817–827.
2. Loha, V., Prokop, A., and Tanner, R. D. (1999), *Appl. Biochem. Biotechnol.* **77–79,** 701–712.
3. Varley, J. and Ball, S. (1994), *Separat. Biotechnol.* **158,** 525–531.
4. Uraizee, F. and Narsimhan, G. (1990), *Microbiol. Technol.* **12(4),** 315–316.
5. Lockwood, C., Bummer P., and Jay, M. (1997), *Pharma. Res.* **14(11),** 1511–1515.
6. Clarkson, J. R., Cui, Z. F., and Darton, R. C. (1999), *J. Colloid Interface Sci.* **215,** 323–332.
7. Clarkson, J. R., Cui, Z. F., and Darton, R. C. (1999), *J. Colloid Interface Sci.* **215,** 333–338
8. Bhat, M. K. and Bhat, S. (1997), *Biotechnol. Adv.* **15,** 583–620.
9. Lambert, W. D., Du, L., Ma, Y., Loha., V., Burapatana, V., Prokop, A., Tanner, R. D., and Pamment, N. B. (2003), *Bioresour. Technol.* **87,** 247–253.

0273-2289/04/114/0627–0638/$25.00

Simultaneous Production of Nisin and Lactic Acid from Cheese Whey

Optimization of Fermentation Conditions Through Statistically Based Experimental Designs

Chuanbin Liu, Yan Liu, Wei Liao, Zhiyou Wen, and Shulin Chen*

Department of Biological Systems Engineering, Washington State University, Pullman, WA 99164-6120, E-mail: chens@wsu.edu

Abstract

A biorefinery process that utilizes cheese whey as substrate to simultaneously produce nisin, a natural food preservative, and lactic acid, a raw material for biopolymer production, was studied. The conditions for nisin biosynthesis and lactic acid coproduction by *Lactococcus lactis* subsp. *lactis* (ATCC 11454) in a whey-based medium were optimized using statistically based experimental designs. A Plackett-Burman design was applied to screen seven parameters for significant factors for the production of nisin and lactic acid. Nutrient supplements, including yeast extract, $MgSO_4$, and KH_2PO_4, were found to be the significant factors affecting nisin and lactic acid formation. As a follow-up, a central-composite design was applied to optimize these factors. Second-order polynomial models were developed to quantify the relationship between nisin and lactic acid production and the variables. The optimal values of these variables were also determined. Finally, a verification experiment was performed to confirm the optimal values that were predicted by the models. The experimented results agreed well with the model prediction, giving a similar production of 19.3 g/L of lactic acid and 92.9 mg/L of nisin.

Index Entries: Nisin; whey; fermentation; optimization; experimental design.

Introduction

Cheese whey is a byproduct of the dairy industry obtained by separating the coagulum from whole milk, cream, or skim milk. About 30 million t of liquid whey is produced annually in the United States alone.

*Author to whom all correspondence and reprint requests should be addressed.

Cheese whey represents about 85–90% of the milk volume and retains 55% of the milk nutrients. Among the most abundant of these nutrients are lactose (4.5–5.0% [w/v]), soluble proteins (0.6–0.8% [w/v]), and mineral salts (0.5–0.7% [w/v]) *(1)*. Unfortunately, this byproduct and its associated nutritional quality have traditionally been treated as a waste because of its low value, low concentration, and limited market *(2)*. As a waste stream, though, cheese whey represents a major disposal and pollution problem because of its high biological oxygen demand (BOD) and chemical oxygen demand (COD) levels (BOD_5 = 30,000 – 50,000 and COD = 60,000 – 80,000) *(1)*. Thus, finding an environmentally friendly and economically advantageous method of disposal for whey is of great interest to the dairy industry, and using microbial cultures on cheese whey to produce value-added products is now considered the most profitable solution to the present disposal dilemma *(3)*.

Nisin is an antimicrobial peptide produced by certain *Lactococcus* species *(4)*. The peptide has strong antimicrobial activity against almost all Gram-positive bacteria and their spores, especially several food-borne pathogens such as *Listeria monocytogenes*, *Staphylococcus aureus*, and psychotrophic enterotoxigenic *Bacillus cereus (5–7)*. As a result of its antimicrobial properties, nisin has been accepted as a safe and natural preservative in more than 50 countries and is widely used in the food industry *(8)*. The Food and Drug Administration views nisin derived from *Lactococcus lactis* subsp. *lactis* to be a generally recognized as safe substance for use as an antimicrobial agent *(9)*, and, therefore, direct addition of nisin to various types of foods, such as cheese, margarine, flavored milk, and canned foods, is permitted *(10)*. In addition, nisin is also being considered for use in health and cosmetic products *(11)*.

In the current industrial process, nisin is manufactured by fermentation of *L. lactis* subsp. *lactis* in a milk-based medium. Biosynthesis of nisin is coupled with the growth of lactic acid bacteria and the production of a significant amount of lactic acid *(7)*. Lactic acid is an important chemical for food processing. It can also be used as a raw material in the production of the biodegradable polymer poly(lactic) acid *(12)*. Unfortunately, lactic acid is not recovered in the current nisin process.

Several studies *(13,14)* have indicated that cheese whey could also be used as feedstock for the production of nisin given supplementation of some essential nutrients. However, the systematic investigation of lactic acid formation accompanied by nisin biosynthesis, and the possibility of the simultaneous production of nisin and lactic acid, have not been reported.

In the present work, the major variables that have significant effects on nisin biosynthesis and lactic acid coproduction from whey were identified, and the optimal conditions for the production of nisin and lactic acid were determined respectively using statistically based experimental designs. In this article, we also discussed the feasibility of simultaneous production of nisin and lactic acid from cheese whey.

Materials and Methods

Microorganisms, Media, and Cultivation

L. lactis subsp. *lactis* (ATCC 11454) was the nisin-producing microorganism used in this work. *Micrococcus luteus* (ATCC 9341) was used as an indicating microorganism in the bioassay of nisin concentrations. The compositions of media used for the growth of microorganisms are summarized as follows. Medium I, used for seed culture of *L. lactis* (pH 7.0), contained 5 g/L of glucose, 5 g/L of polypeptone, and 5 g/L of yeast extract. Medium II, used for bioassay of nisin (pH 7.0), contained 10 g/L of glucose, 5 g/L of polypeptone, 5 g/L of yeast extract, and 5 g/L of NaCl. Medium III, used for the main fermentation, contained 50 g/L of sweet whey powder (provided by WesternFarm Food, Seattle, WA) and a predetermined amount of other nutrients shown in the experimental designs. $CaCO_3$ powder (30 g/L) was added in medium III in order to maintain a stable pH during fermentation.

Seed culture of *L. lactis* was conducted in 125-mL Erlenmeyer flasks placed on an orbital shaker at 160 rpm and 30°C for 8 h. Main fermentations were performed in 250-mL Erlenmeyer flasks containing 100 mL of medium III and 5 mL of the seed medium.

Analysis

Nisin concentration was measured using a bioassay procedure based on the method of Shimizu et al. *(15)*. A high-performance anion-exchange chromatography method *(16)* was used for lactic acid analysis.

Plackett-Burman Experimental Design

The Plackett-Burman (PB) design has proven very effective and has been widely used to identify significant variables from a larger number of potential variables (>5) with a minimum of testing *(17,18)*. A 12-run PB design was used to identify which variables have significant effects on nisin and lactic acid production by *L. lactis*. The design matrix shown in Table 1 was developed according to Greasham and Herber *(17)*. Seven variables (A–G)—i.e., yeast extract, polypeptone, KH_2PO_4, $MgSO_4$, surfactant (Tween-80), pH, and temperature—were chosen as the candidate factors based on Parente and Ricciardi's review *(7)*. D_1 to D_4 in Table 1 are dummy factors employed to evaluate the standard errors of the experiment. Low levels (–1) and high levels (+1) were assigned for each factor. Two flasks in parallel were performed for each condition. The average value of nisin and lactic acid concentrations after 24 h of fermentation were used as the responses in this design.

Greasham and Herber *(17)* described in detail the statistical analyses used to identify the significance of the variables. The significance of variables was determined by student's *t*-test. Variables with p values < 0.2 were considered significant.

Table 1
PB Design of Variables with Nisin and Lactic Acid Concentration as Response

	Variable											Response	
Run	A	B	C	D	E	F	G	D_1	D_2	D_3	D_4	Nisin (mg/L)	Lactic acid (g/L)
1	+1	+1	–1	+1	+1	+1	–1	–1	–1	+1	–1	80.2	19.0
2	–1	+1	+1	–1	+1	+1	+1	–1	–1	–1	+1	14.6	7.8
3	+1	–1	+1	+1	–1	+1	+1	+1	–1	–1	–1	87.7	19.1
4	–1	+1	–1	+1	+1	–1	+1	+1	+1	–1	–1	85.9	18.1
5	–1	–1	+1	–1	+1	+1	–1	+1	+1	+1	–1	11.5	7.9
6	–1	–1	–1	+1	–1	+1	+1	–1	+1	+1	+1	88.2	18.3
7	+1	–1	–1	–1	+1	–1	+1	+1	–1	+1	+1	11.2	6.7
8	+1	+1	–1	–1	–1	+1	–1	+1	+1	–1	+1	10.7	7.3
9	+1	+1	+1	–1	–1	–1	+1	–1	+1	+1	–1	13.1	6.4
10	–1	+1	+1	+1	–1	–1	–1	+1	–1	+1	+1	79.0	11.1
11	+1	–1	+1	+1	+1	–1	–1	–1	+1	–1	+1	84.3	17.8
12	–1	–1	–1	–1	–1	–1	–1	–1	–1	–1	–1	6.4	6.1

Table 2
Central Composite Design of Factors in Coded Levels with Nisin and Lactic Acid Concentration as Response

Run	Type	*A*	*B*	*C*	Nisin (mg/L)	Lactic acid (g/L)
1	Center	0	0	0	87.7	18.8
2	Center	0	0	0	87.0	19.0
3	Center	0	0	0	87.4	18.8
4	Center	0	0	0	87.1	18.9
5	Center	0	0	0	87.5	18.9
6	Center	0	0	0	86.8	18.9
7	Axial	0	0	–1.68	78.3	19.0
8	Axial	0	0	1.68	86.8	19.0
9	Axial	–1.68	0	0	63.5	17.3
10	Axial	0	–1.68	0	80.6	18.2
11	Axial	0	1.68	0	87.6	19.1
12	Axial	1.68	0	0	89.0	19.1
13	Fact	1	–1	1	88.1	18.6
14	Fact	1	1	–1	88.0	18.8
15	Fact	–1	1	1	64.9	17.5
16	Fact	–1	–1	–1	60.9	16.9
17	Fact	–1	1	–1	63.4	17.5
18	Fact	1	1	1	88.9	19.1
19	Fact	–1	–1	1	62.1	16.9
20	Fact	1	–1	–1	85.1	18.2

Table 3
Coded and Actual Values of Factors in Central Composite Design

Factor	Name	Units	Axial (–1.68)	Low (–1)	Central (0)	High (+1)	Axial (+1.68)
A	Yeast extract	g/L	6.64	8.00	10.00	12.00	13.36
B	KH_2PO_4	g/L	0.08	0.25	0.50	0.75	0.92
C	$MgSO_4$	g/L	0.08	0.25	0.50	0.75	0.92

Central Composite Experimental Design

Once the variables having the greatest influence on the responses were identified, a 20-run central composite design was used to optimize the levels of these variables *(18)*. A design matrix was developed (Table 2) and the true values for the variables were determined (Table 3).

After the responses were obtained, they were subjected to multiple nonlinear regression and optimization using the software Design-Expert (V6.0; Stat-Ease, Minneapolis, MN). Second-order polynomial models were applied to correlate these variables. Only the estimates of coefficients with significant levels higher than 90% (i.e., $p < 0.10$) were included in the final model. An *F*-test was used to evaluate the significance of the models.

Table 4
Variables Screened in PB Design and Their Real Values

	Variable						
	A (pH)	B (Temperature) (°C)	C (Tween-80) (g/L)	D (Yeast extract) (g/L)	E (Polypeptone) (g/L)	F (KH_2PO_4) (g/L)	G ($MgSO_4$) (g/L)
Low level (–1)	5.5	30	0	0	0	0	0
High level (+1)	6.5	37	1	1	10	1	1

Table 5
Effects of Variables in PB Design on Nisin and Lactic Acid Production and Associated Statistical Tests[a]

	Nisin			Lactic acid		
Variables	Effects (mg/L)	*t* value	*p* value	Effects (g/L)	*t* value	*p* value
pH	1.6	0.20	0.85	7.0	1.08	0.34
Temperature	–5.8	–0.71	0.52	–6.2	–0.76	0.49
Tween-80	7.6	0.93	0.41	–5.4	–0.66	0.55
Yeast extract	437.8	53.78	0.00	61.2	7.49	0.00
Polypeptone	2.6	0.32	0.77	9.0	1.10	0.33
KH_2PO_4	13.0	1.60	0.18	13.2	1.62	0.18
$MgSO_4$	28.6	3.51	0.02	7.2	0.88	0.43

[a] Significant values are underlined.

Results and Discussion

Screening Experiment

Table 4 gives the seven variables chosen as candidate factors with their assigned low and high levels. Table 1 provides the 12-run PB design used to identify which variables have significant effects on nisin and lactic acid production by *L. lactis*. Table 5 shows the resulting effects of the variables on the responses and the associated *t*-values and significant levels.

The results showed that yeast extract, KH_2PO_4, and $MgSO_4$, in the tested range, had significant effects on nisin biosynthesis while the significant factors for lactic acid coproduction were yeast extract and KH_2PO_4. The results in Table 5 clearly show that nisin biosynthesis and lactic acid production were dramatically influenced by the composition of the medium. This is because the nisin-producing strain *L. lactis* is a well-known nutritionally fastidious microorganism *(19)*, and, therefore, an abundance of nutrients is required for cell growth and metabolism.

De Vuyst *(20)* found that the amino acids serine, threonine, and cysteine highly stimulated nisin production, indicating their precursor role during nisin biosynthesis. In the present work, the significant effect of yeast extract in the tested concentration range supported the De Vuyst's findings. The significant effects of inorganic phosphate and magnesium sulfate on nisin biosynthesis revealed in our work are also consistent with the results of De Vuyst and Vandamme *(21)* and Meghrous et al. *(22)*.

The significance of yeast extract and KH_2PO_4 for lactic acid formation indicates the important role of protein and inorganic phosphate in the metabolism of *L. lactis*. The lesser influence of polypeptone compared with yeast extract proves that yeast extract is a good nitrogen source for nisin and lactic acid production. The influences of pH and temperature were not significant in this screening experiment, because this test was carried out close to the optimal conditions of these two variables *(16)*.

Optimization Using Surface Response Methodology

In the second optimization step, the exact values of the three variables that were identified to have significant effects on nisin and/or lactic acid production were determined using a central composite design (Table 2). The coded and actual values of each variable are given in Table 3. The fermentation media (pH 6.5) were composed of 50 g/L of whey, 5 g/L of polypeptone, 1 g/L of Tween-80, and 30 g/L of $CaCO_3$, and the predetermined amount of the three variables was assigned by the central composite design. The content of nisin and lactic acid after 24 h of fermentation at 30°C was measured and are presented as responses in Table 2.

The responses of nisin and lactic acid were correlated by nonlinear regression using the following full quadratic polynomial model:

$$Y = b_0 + b_1A + b_2B + b_3C + b_{12}AB + b_{13}AC + b_{23}BC + b_{11}A^2 + b_{22}B^2 + b_{33}C^2 \quad (1)$$

Table 6
Estimate of Coefficient of Factors and Associated Significant Levels[a]

	Nisin		Lactic acid	
Factor	Coefficient estimate	*p* value	Coefficient estimate	*p* value
Intercept	87.28	0.00	18.90	0.00
A	10.38	0.00	0.66	0.00
B	1.52	0.18	0.27	0.00
C	1.52	0.18	0.05	0.45
A^2	–5.07	0.00	–0.39	0.00
B^2	–2.30	0.05	–0.24	0.01
C^2	–2.86	0.02	–0.11	0.13
AB	–0.21	0.88	0.00	1.00
BC	–0.23	0.91	0.00	0.98
AC	0.16	0.87	0.07	0.43

[a]Significant values are underlined.

in which *Y* is the desired response; b_i are the coefficients; and *A*, *B*, and *C* are the three factors. Table 6 provides the results of coefficient estimates and the associated significance levels obtained from the Design-Expert software. The estimates with significance levels higher than 90% ($p < 0.10$) were included in the final model. The models that describe the responses of nisin and lactic acid as functions of the most significant variables are as follows:

$$\text{Nisin}\,(\text{mg/L}) = 87.28 + 10.38 \times [\text{Yeast extract}] - 5.07 \times [\text{Yeast extract}]^2 - 2.30 \times [\text{KH}_2\text{PO}_4]^2 - 2.86 \times [\text{MgSO}_4]^2 \quad (2)$$

$$\text{Lactic acid}\,(\text{g/L}) = 18.90 + 0.66 \times [\text{Yeast extract}] + 0.27 \times [\text{KH}_2\text{PO}_4] - 0.39 \times [\text{Yeast extract}]^2 - 0.24 \times [\text{KH}_2\text{PO}_4]^2 \quad (3)$$

in which [Yeast extract], [KH_2PO_4], and [$MgSO_4$] represent the coded values of yeast extract, KH_2PO_4, and $MgSO_4$, respectively. *F*-test showed that the models were reliable because the significance levels were >99%.

The three-dimensional surface plots presented in Figs. 1 to 4 demonstrate the effects of yeast extract, KH_2PO_4, and $MgSO_4$ on nisin and lactic acid production. The optimal value of each factor is also clearly shown in the plots. Figure 1 shows the function of yeast extract and KH_2PO_4 on nisin production when $MgSO_4$ was kept at the central point. Nisin concentration reached a maximum level with about 12 g/L of yeast extract and 0.6 g/L of KH_2PO_4. Figure 2 shows nisin biosynthesis as the function of yeast extract and $MgSO_4$ (KH_2PO_4 was kept at the central point). The optimal value of $MgSO_4$ for nisin biosynthesis was close to the central point. Figures 3 and 4 also show that the optimal conditions of lactic acid production were about 12 g/L of yeast extract, 0.6 g/L of KH_2PO_4, and 0.6 g/L of $MgSO_4$.

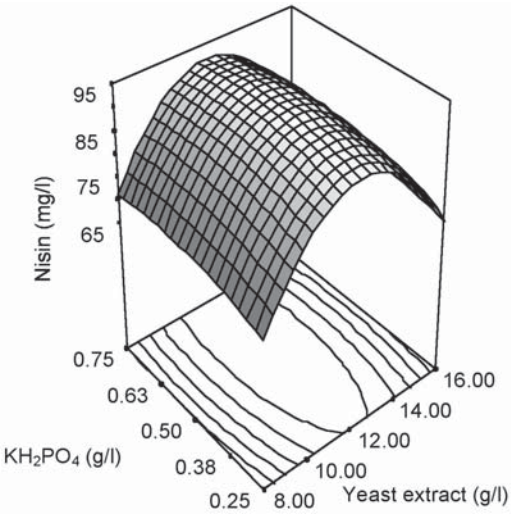

Fig. 1. Three-dimensional surface plot of nisin production as function of yeast extract and KH_2PO_4 ($MgSO_4$ was kept at central point).

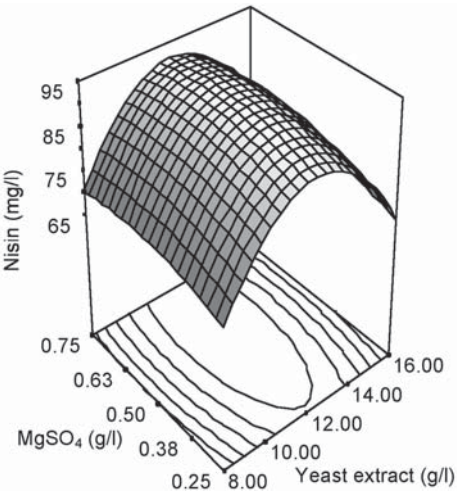

Fig. 2. Three-dimensional surface plot of nisin production as function of yeast extract and $MgSO_4$ (KH_2PO_4 was kept at central point).

The optimal conditions for nisin biosynthesis and lactic acid formation were obtained by further numerical analysis of the response surface using Design-Expert software and are presented in Table 7. The solution to the maximal nisin biosynthesis was 12.04 g/L for yeast extract, 0.57 g/L for KH_2PO_4, and 0.57 g/L for $MgSO_4$. The solution to the maximal lactic acid production was 11.78 g/L for yeast extract, 0.64 g/L for KH_2PO_4, and 0.63

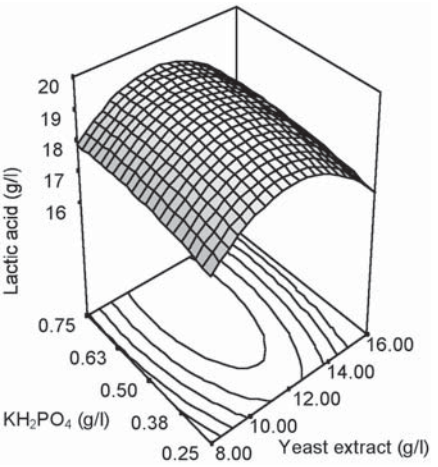

Fig. 3. Three-dimensional surface plot of lactic acid production as function of yeast extract and KH_2PO_4 ($MgSO_4$ was kept at central point).

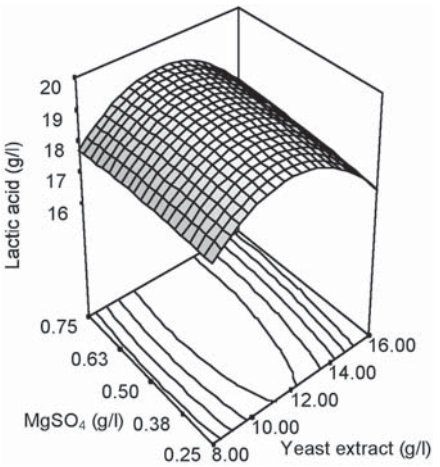

Fig. 4. Three-dimensional surface plot of nisin production as function of yeast extract and $MgSO_4$ (KH_2PO_4 was kept at central point).

g/L for $MgSO_4$. Finally, the solution to the simultaneous maximal production of nisin and lactic acid was 11.89 g/L for yeast extract, 0.61 g/L for KH_2PO_4, and 0.59 g/L for $MgSO_4$. The data in Table 7 also reveal that the predicated values of nisin and lactic acid under these three conditions have no significant difference. Thus, simultaneous production of nisin and lactic acid is feasible, since the optimal conditions for nisin biosynthesis and lactic acid formation by *L. lactis* using whey as feedstock are almost the same.

Table 7
Optimal Conditions for Nisin and Lactic Acid Production from Whey Obtained from Response Surface Analyse

Criteria		Optimal values			Predicated results	
Nisin	Lactic acid	Yeast extract	KH_2PO_4	$MgSO_4$	Nisin	Lactic acid
—	Maximum	11.78	0.64	0.63	92.5	19.3
Maximum	—	12.04	0.57	0.57	93.0	19.2
Maximum	Maximum	11.89	0.61	0.59	92.9	19.3

Verification

A verification experiment under the conditions of 12 g/L for yeast extract, 0.6 g/L for KH_2PO_4, and 0.6 g/L for $MgSO_4$ was conducted separately in order to confirm the optimal conditions obtained from the statistically based experimental designs. After 24 h of fermentation, 92.1 mg/L of nisin and 19.3 g/L of lactic acid were obtained. This result was very close to the predicted value of 92.9 mg/L of nisin and 19.3 g/L of lactic acid. In addition, the nisin result also agreed well with the "ceiling concentration" of nisin previously reported by Kim et al. *(23)*. Therefore, the optimal conditions predicted from the statistically based experimental designs were valid.

Conclusion

We aimed at optimizing lactic acid and nisin coproduction by *L. lactis* from cheese whey using statistically based experimental designs. The significant factors for nisin and lactic acid formation were screened and then quantitatively optimized using only 32 shake-flask trials. Compared with the conventional and time-consuming one-variable-at-a-time approach, the statistically based experimental designs proved to be efficient tools in this optimization process. However, considering industrial application, this work is only the very first step needed for bioprocess development. In particular, 19.3 g/L of lactic acid is too low for practical application, with this value of lactic acid not even able to compensate for separation costs. Therefore, further research on the improvement of nisin and lactic acid production and the associated development of effective product recovery methods is required.

Acknowledgments

Special thanks are given to Western Farm Food (Seattle, WA) for providing cheese whey for the experiments. This work was carried out under a grant from the Washington State Dairy Product Commission.

References

1. Gonzalez, S. M. I. (1996), *Bioresour. Technol.* **57,** 1–11.
2. Yang, S. T. and Silva, E. M. (1995), *J. Dairy Sci*. **78,** 2541–2562.
3. Warwaha, S. S. and Kennedy, J. F. (1988), *Int. J. Food Sci. Technol.* **23,** 323–336.
4. Broughton, J. B. (1990), *Food Technol*. **44,** 100–117.
5. Montville, T. J. and Chen, Y. (1998), *Appl. Microbio. Biotechnol.* **50,** 511–519.
6. Cleveland, J., Thomas, J., Montville, J. T., Nes, F. I., and Chikindas, L. M. (2001), *Int. J. Food Microbiol.* **71,** 1–20.
7. Parente, E. and Ricciardi, A. (1999), *Appl. Microbiol. Biotechnol.* **52,** 628–638.
8. Sablon, E., Contreras, B., and Vandamme, E. (2000), *Adv. Biochem. Eng./Biotechnol.* **68,** 21–59.
9. Food and Drug Administration. (2001), GRAS Notice No. GRN 000065.
10. Sloan, A. E. (1998), *Food Technol.* **52,** 37–44.
11. Jack, R. W., Tagg, J. R., and Ray, B. (1995), *Microbiol. Rev.* **59,** 171–200.
12. Datta, R. and Tsai, S. P. (1997), In: *Fuels and Chemicals from Biomass* (ACS Symposium Series 666), Saha, B. C. and Woodward, J., eds., American Chhemical Society, Washington, DC, pp. 224–236.
13. Nelson, P. G. and Lorenzo, P. (2001), *Biotechnol. Lett.* **23,** 609–612.
14. Penna, T. C. V. and Moraes, D. A. (2002), *Appl. Biochem. Biotechnol.* **98–100,** 775–789.
15. Shimizu, H., Mizuguchi, T., Tanaka, E., and Shioya, S. (1999), *Appl. Environ. Microbiol.* **65,** 3134–3141.
16. Saccani, G., Gherardi, S., Trifirò, A., Soresi, B. C., Calza, M., and Freddi, C. (1995), *J. Chromatogr. A* **706,** 395–403.
17. Greasham, L. R. and Herber, K. W. (1997), in *Applied Microbial Physiology*, 1st Ed., Rhodes, P. M. and Stanbury, P. F., eds., Oxford University Press, New York, NY, 53–74.
18. Montgomery, D. C. (1997), *Design and Analysis of Experiments*, 4th Ed. John Wiley & Sons, New York, NY.
19. Kim, W. S., Hall, R. J., and Dunn, N. W. (1997), *Appl. Microbiol. Biotechnol*. **48,** 449–453.
20. De Vuyst, L. (1995), *J Appl. Bacteriol.* **78,** 28-33.
21. De Vuyst, L. and Vandamme, E. J. (1993), *Appl.Microbiol. Biotechnol.*, **40,** 17–22.
22. Meghrous, J., Huo, M., Quittelier, M., and Petitdemange, H. (1992), *Res. Microbiol*. **143,** 879–890.
23. Kim, W. S., Hall, R. J., and Dunn, N. W. (1998), *Appl. Microbiol. Biotechnol.* **50,** 429–433.

0273-2289/04/114/0639-0652/$25.00

Effect of Process Parameters on Production of a Biopolymer by *Rhizobium* sp.

Flávia Pereira Duta,[1] Francisca Pessôa De França,[*,1] Eliana Flávia Camporese Sérvulo,[1] Léa Maria De Almeida Lopes,[2] Antonio Carlos Augusto Da Costa,[3] and Ana Barros[4]

[1]Universidade Federal do Rio de Janeiro Departamento de Engenharia Bioquímica, Bloco E, Ilha do Fundão, Rio de Janeiro, RJ CEP: 21949-900 Brazil, and [2]Instituto de Macromoléculas Professora Eloisa Mano, Rio de Janeiro-RJ, Brazil, E-mail: fpfranca@eq.ufrj.br and [3]Universidade do Estado do Rio de Janeiro, Departamento de Tecnologia de Processos Bioquímicos, and [4]Universidade de Aveiro, Portugal

Abstract

The production of biopolymers by a *Rhizobium* strain was studied under batch and bioreactor conditions. The best viscosity levels were obtained under low mannitol concentrations as well as low agitation and aeration conditions. Infrared spectra indicated the presence of chemical groups characteristic of microbially produced biopolymers, including C = O and O-acetyl groups. Thermogravimetric analysis showed the characteristic degradation profiles of the exopolysaccharide produced (T_{onset} = 290°C). The experimental design showed that a low substrate concentration (10.0 g/L), and low aeration (0.2 vvm) and agitation (200 rpm) levels should be used. The maximum yield of the process was a Yp/s (g/g) of 0.19 ± 0.1, obtained under optimized conditions.

Index Entries: Biopolymer; exopolysaccharides; *Rhizobium* sp; viscosity; conversion factor.

Introduction

Polysaccharides constitute an important class of natural macromolecules present in all living organisms, with a wide range of functions, some

*Author to whom all correspondence and reprint requests should be addressed.

of them still under investigation. Polysaccharides are formed by the condensation of monosaccharides or their derivatives through glucosidic bonds. They are usually substances with a high molecular weight, reaching values up to 1 million. Polysaccharides differ from high molecular weight oligosaccharides, not only by the size of the molecule, but also by their common ability to combine during biosynthesis; this property contributes to the formation of chains with different species of monosaccharides, linked through glucosidic bonds under distinct configurations. Those polysaccharides can have linear, branched, or cyclic chains *(1,2)*.

Microbial polysaccharides constitute a specific class of biopolymers. These biopolymers are formed during the growth of the living organisms, and are thus, called natural polymers. Their synthesis usually involves enzymatic catalysis and an increase in the chain through polymerization reactions of the monomers, typically inside the cells, mediated by complete metabolic processes *(3,4)*.

Because of the diversity of their structural and physical properties, microbial polysaccharides are widely used in the food, pharmaceutical, chemical, and petroleum industries. These microbial gums can act as emulsifying agents, stabilization and ligand agents, gelifying agents, flocculating agents, and film-forming and lubrifying compounds *(1,5)*. The structure and composition of the microbial polysaccharides depend on several factors, such as the composition of the culture medium, carbon source, type of strain, and fermentation conditions (pH, temperature, oxygen concentration) *(6)*.

Most of the research on bacteria from the genus *Rhizobium* is conducted in the field of genetics and bacteria-host plant simbiotic interactions. Little is known about the production of extracellular polysaccharides produced by *Rhizobium* as well as their properties in solution; in particular, no studies have been conducted on the effect of substrate concentration, agitation, and aeration as relevant parameters to monitor in the process of exopolysaccharide (EPS) production. The present work aimed to determine the extent to which some variables affect the production of polysaccharides by *Rhizobium* sp.

Materials and Methods

Microorganism

The strain *Rhizobium* EQ1 was used. This strain was isolated from culture of the beans variety "Caupi" from an arid region of the northeast of Brazil. This strain was kept in agar-mannitol-yeast extract (YMA) for several months, and, after its characterization was cataloged, at the culture bank of the School of Chemistry from Federal University of Rio de Janeiro, under the code EQ1.

Culture Media

All culture media were autoclaved at 121°C for 20 min.

Medium for Maintenance of Culture

The microorganism was kept in modified YMA with the following composition: 10–50 g/L of mannitol, with the concentration changed according to the experimental design; 0.1 g/L of K_2HPO_4; 0.4 g/L of KH_2PO_4; 0.2 g/L of $MgSO_4 \cdot 7H_2O$; 0.1 g/L of NaCl; 0.4 g/L of yeast extract; 15 g/L of agar. The pH of the medium was adjusted to 7.0 *(7)*.

Medium for Preparation of Inoculum

For preparation of the inoculum, the YMA medium was used without the addition of agar.

Medium for Production of Polysaccharide

The production of extracellular polysaccharides was done using a culture medium similar to YMA, supplemented with manganese ions (0.12 g/L of $MnCl_2 \cdot 4H_2O$) and omitting agar. The pH of this medium was adjusted to 7.0 by the addition of NaOH (50%, w/v).

Maintenance of Microorganisms

The microorganism was cultivated in laboratory tubes containing YMA medium at 30 ± 1ºC for 48 h. After growth, the cultures were stored at 5 ± 1ºC.

Preparation of Inoculum

The inoculum was prepared from the stock culture in 500-mL Erlenmeyer flasks containing 100 mL of the corresponding medium. Incubation was performed in a rotary shaker at 200 rpm and 30 ± 1ºC for 48 h with the cells in the exponential phase of growth.

Production of EPS in Bioreactors

The experiments were conducted in a fermentor (Model BioFlow IV); New Brunswick Scientific, with a 20-L capacity. All process parameters were monitored on-line, with the help of the software AFS 3.0 (Advanced Fermentation Software, New Brunswick Scientific). The temperature (30 ± 1ºC) and pH value (7.0) were kept constant during the experiments. The parameters of substrate concentration, aeration, and agitation were chosen as the most significant ones for the experimental design. After selecting these parameters, experiments were conducted in duplicate for superior (+) and lower (–) levels of the experimental design, and triplicate for the central point (0). The inoculum was added at 1% of the initial working volume (10 L); thus, 1000 mL of the grown inoculum was used. The process was conducted for 48 h.

Qualitative and Quantitative Determinations During Fermentation Process

The determinations were made during the fermentation process and immediately after in the broth.

Purity of Culture

During the process, microscopic examinations were performed in laboratory preparations (with the addition of dyes) through the method of Gram, in order to detect possible contaminations in the medium.

Absolute Viscosity of Broth

Measurements of viscosity of the fermented broth were done in a Brookfield Synchro-Lectric, model LVT rheometer with the accessory Small Sample Adapter. Absolute viscosity was determined at various shear rates. The temperature was kept constant at 20°C.

Determination of Mannitol

For the quantitative determination of mannitol, the fermented broth was initially filtered through 0.2-µm Millipore membranes in order to remove the cells. In the filtrate, the substrate was analyzed through high-performance liquid chromatography in a Waters chromatograph equipped with SHODEX SC1011 ion-exchange columns at 75°C. Milli-Q water was used as the eluent and the elution rate was 0.8 mL/min. The final result was obtained through a detector-type Waters 410 model differential refractometer, and Waters 746 integrator-registrator (data module).

Extraction and Purification of EPS

The quantity of EPS produced after fermentation was determined through dry weight measurements. The fermentation broth was heated at 80° ± 1°C for 10 min, to ensure microbial inactivation. A filtration was then conducted to remove the cells. To precipitate the EPS, ethanol P.A. (3:1) was added to the fermented broth. After total precipitation of the EPS present in the medium, the mixture (broth plus ethanol) was filtered through a 0.2-µm Millipore membrane using a Gouche crucible previously weighed. The obtained product was dried at 80 ± 1°C until constant weight. All determinations were done in triplicate.

The biopolymer extracted from the fermented broth was purified through successive washings with 70, 80, and 90% (v/v) ethanol P.A., respectively. The biopolymer was dried by introducing nitrogen gas under controlled heating.

Molecular Characterization

Infrared Spectrometry

Infrared-spectrometry (IR) was used for the investigation of substituent acetyl groups in the molecules of the polysaccharides. A Fourier transform IR Perkin-Elmer spectrometer, Model 1720-X, was used. The

presence of the substituent acetyl groups is observed in 1700- and 1200-cm^{-1} peaks, owing to axial deformation of the carbonyl groups of esters and to assymetric axial deformation of the C-O-C bonds, respectively. KBr pastilles were prepared in a proportion of 2 mg of polysaccharide/200 mg of KBr.

Thermal Analysis Through Thermogravimetry

Thermogravimetric analysis can measure the amount and ratio of changes of mass in a material, as a function of temperature or time, in a controlled atmosphere. The measurements are used to determine the composition and thermal stability of a material. This technique is used to determine the purity, humidity, volatile content, and residues in polymeric materials *(8)*. To determine the thermal stability and humidity levels of the biopolymer synthesized by *Rhizobium* sp. EQ1 in a specific experimental condition, thermogravimetric analysis was conducted using DSC 2910 TA instruments. The loss of weight was registered from 25 to 700°C at a heating rate of 10°C/min. The analysis of the sample was conducted in a nitrogen atmosphere at a flow rate of 20 cm^3/min.

Experimental Design

This experimental design technique is widely used as a tool to verify the efficiency of several processes. In the present work, it was used for the purpose of obtaining information from the EPS production process; consequently, a reduction in the variability, as well as in operational costs can be expected. The choice of the variables (factors that affect the process), as well as the superior (+), lower (–), and central (0) levels used in the design, was defined from preliminary studies that defined the parameters as the most significant for the production of EPS. The selected variables were aeration, agitation, and initial substrate concentration (*see* Table 1).

This way, a factorial 2^k design is thus obtained, with a central point, in which k is the number of factors and 2 is the number of levels, resulting in $2^3 = 8$; the central point 1 is, done in duplicate, in a total of 11 experiments, according to Table 1.

The data obtained were processed using the software Statistica™,'99 for Windows, Version 5.5, produced by StatSoft. From the software, the values of the effects of each parameter were determined as well as their interactions.

Results

Viscosity Analysis

Table 1 presents the results obtained from the fermented broth in the different experimental conditions selected after 48 h. Determination of the viscosities indicated that at conditions below the control factors, higher viscosity values were obtained for the fermented broth; low values of substrate concentration, aeration, and agitation promoted higher viscosity values in the cultivation broth after 48 h of process.

Table 1
Control Factors and Levels Used in Matrix for Experimental Design 2^3 with Central Point, Viscosity Values for Fermented Broth, and Substrate/Product Yield ($Y_{P/S}$) at Distinct Conditions after 48 h at 20°C

	Factor			Apparent viscosity (cP)			
				Shear rate (s^{-1})			$Y_{P/S}$
Expt	X_1 (substrate, g/L)	X_2 (aeration, vvm)	X_3 (agitation, rpm)	20,400	10,200	4080	(g/g)
1	10 (–)	0.2 (–)	200 (–)	56.5 ± 1.2	42.5 ± 1.0	28.5 ± 1.2	0.19 ± 0.10
2	10 (–)	0.2 (–)	800 (+)	28.0 ± 1.0	***	***	0.13 ± 0.10
3	10 (–)	1.3 (+)	200 (–)	47.5 ± 0.8	3.5 ± 0.8	***	0.18 ± 0.10
4	10 (–)	1.3 (+)	800 (+)	35.0 ± 0.5	***	***	0.16 ± 0.10
5	50 (+)	0.2 (–)	200 (–)	25.0 ± 1.1	***	***	0.06 ± 0.10
6	50 (+)	0.2 (–)	800 (+)	25.0 ± 0.2	***	***	0.07 ± 0.11
7	50 (+)	1.3 (+)	200 (–)	7.5 ± 0.4	***	***	0.03 ± 0.30
8	50 (+)	1.3 (+)	800 (+)	8.5 ± 1.2	***	***	0.03 ± 0.22
9	30 (0)	0.8 (0)	500 (0)	31.5	***	***	0.06
10	30 (0)	0.8 (0)	500 (0)	32.0	***	***	0.06
11	30 (0)	0.8 (0)	500 (0)	32.5	***	***	0.06

***Not detected

On-line Monitoring

pH

During the on-line monitoring of the pH of the medium, no significant changes in the values of pH were observed in the time course of the process.

Concentration of Dissolved Oxygen

Monitoring of dissolved oxygen concentration indicated that in the first 12 h of the process, the concentration remained constant. Afterwards between 12 and 24 h of the process, a slight decrease in the concentration of oxygen was observed, which was kept constant up to 48 hours of monitoring.

Molecular Characterization

IR Spectrometry

Figure 1 presents the IR spectra of different samples of the EPS obtained at different conditions of the process. The polysaccharides produced in the fermented broth presented the same chemical composition. These spectra did not show significant differences in relation to the characteristic bands.

Around 3400 cm^{-1} a band could be observed characteristic of axial deformation of hydroxyl groups that participate in interactions of bridge-type hydrogen bonds. Close to 2900 cm^{-1} another band appeared characteristic of axial deformation of a C-H bond. At 1246 cm^{-1}, a band indicating an axial deformation of ester C-O bonds could also be detected *(9)*.

The characteristic bond for axial deformation of ester carbonyl (C=O), around 1730 cm^{-1}, was observed in the three samples of the biopolymer. The absorption of that band demonstrates the presence of substituent O-acetyl groups in the molecule of the biopolymer. In the 400- to 1400-cm^{-1} region, the differences between the biopolymers synthesized by *Rhizobium* sp could be clearly observed *(9)*.

Thermal Analysis Through Thermogravimetry

The variation in the total mass of the polymer registered between 25 and 700 °C is presented in Fig. 2. The thermogravimetric analysis of the EPSs produced are presented for both purified and nonpurified EPS from *Rhizobium* sp. EQ1.

Experimental Design

Table 1 presents the matrix from the experimental design and the results obtained for substrate/product yield ($Y_{P/S}$). After 48 h of process the maximum value for $Y_{P/S}$ was 0.19 (g/g), relatively low, considering biochemical processes involving polymerization reactions.

A direct analysis of the results in Table 1 cannot be made; the data presented do not enable verification of the significance of the parameters studied. The use of a Pareto chart is necessary. From the results of the conversion factor ($Y_{P/S}$), the main effects of the interactions were calculated

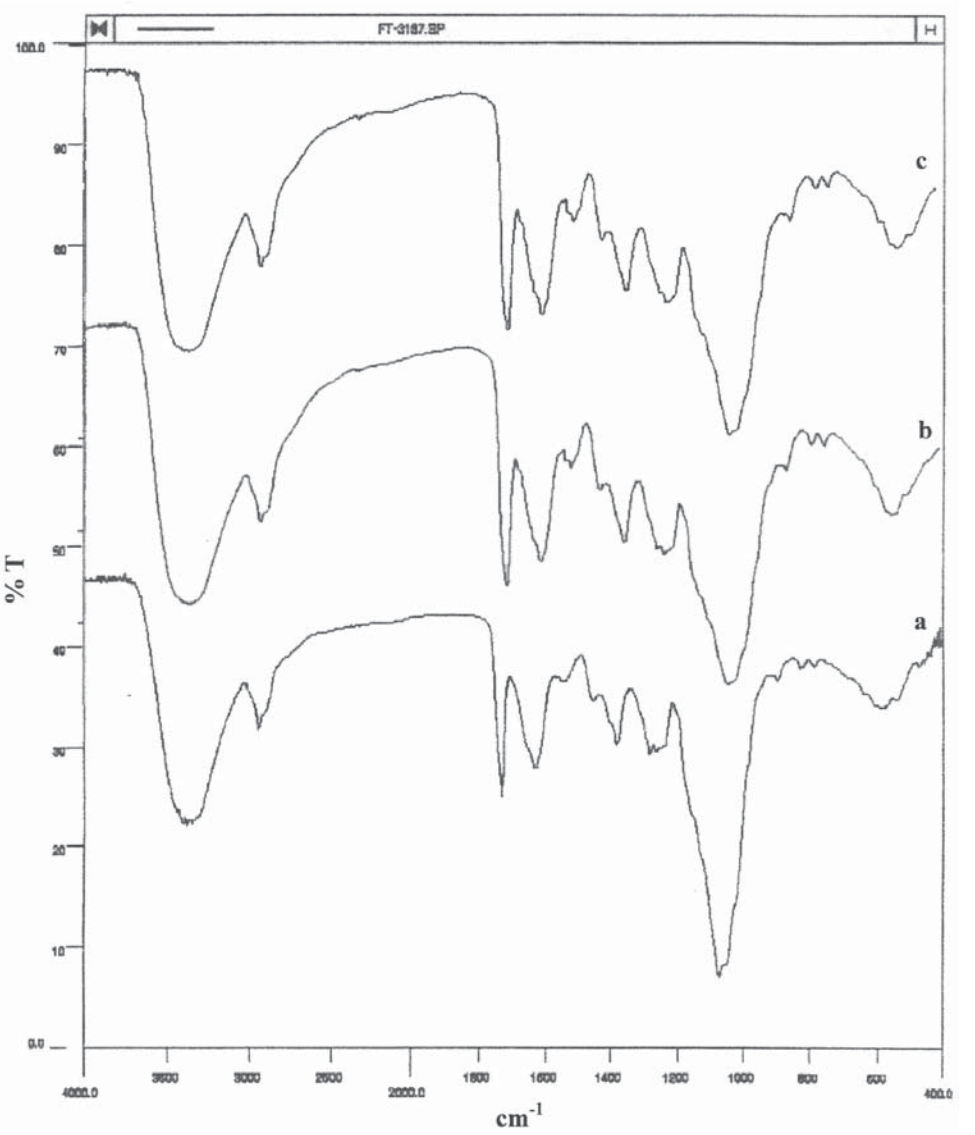

Fig. 1. IR spectra of samples of EPS produced by *Rhizobium* sp. EQ1 at different conditions: **(A)** expt. 1; **(B)** expt. 2; **(C)** expt. 4.

through use of the matrix from Table 1. Analysis of the main effects and interactions was done through a Pareto chart (*see* Fig. 3) from data obtained from analysis of variance, and surface graphs (Figs. 4 and 5).

The stippled line in the Pareto chart in Fig. 3 indicates the minimal magnitude of the statistically significant effect for a 95% confidence level. Values presented in the horizontal columns correspond to the values of the student's *t*-test for each factor studied. Figures 4 and 5 present a better visualization of the effect of the factors studied on $Y_{P/S}$. Analogously,

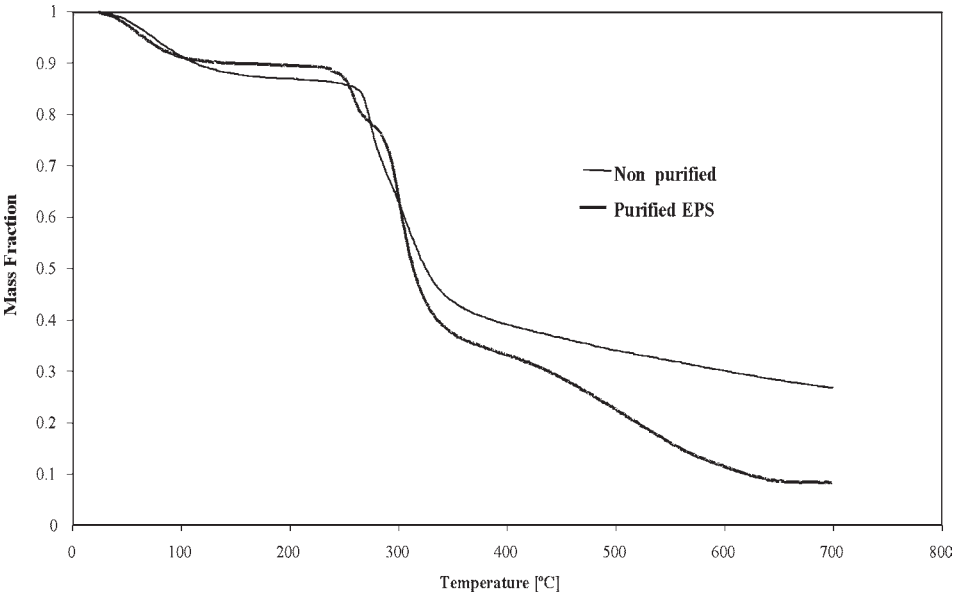

Fig. 2. Thermogravimetric curves obtained for purified and nonpurified EPS produced by *Rhizobium* sp. EQ1 (experiment 1).

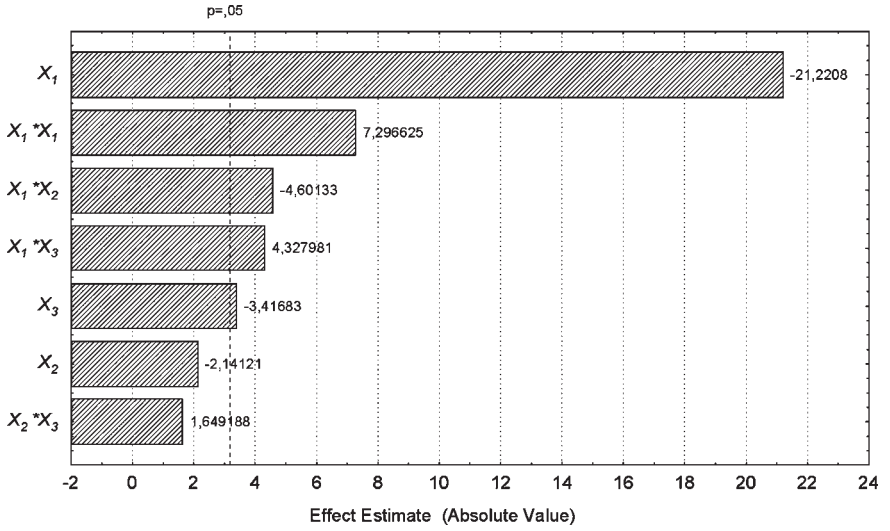

Fig. 3. Pareto chart: X_1, concentration of substrate; X_2, aeration; X_3, agitation.

Fig. 5 shows the effect of substrate concentration and agitation on substrate/EPS factor, $Y_{P/S}$. Figure 6 shows the correlation between experimental results and values predicted by the mathematical model generated by *Statistica*, indicating a good correlation between experimental and predicted values.

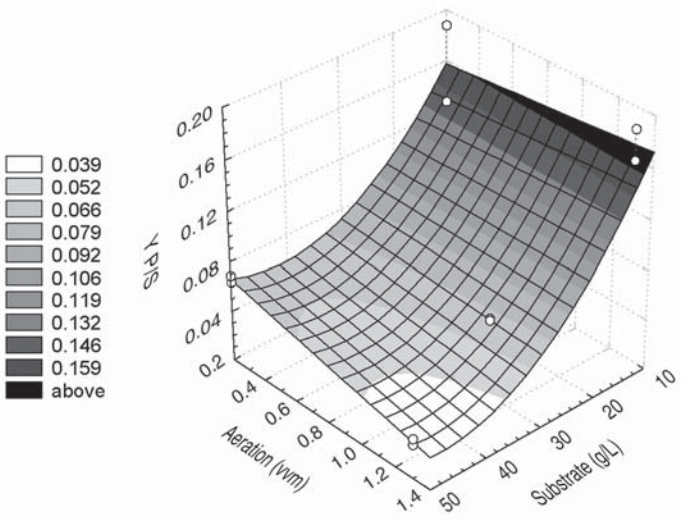

Fig. 4. Effect of X_1 and X_2 on substrate/EPS factor, $Y_{P/S.}$

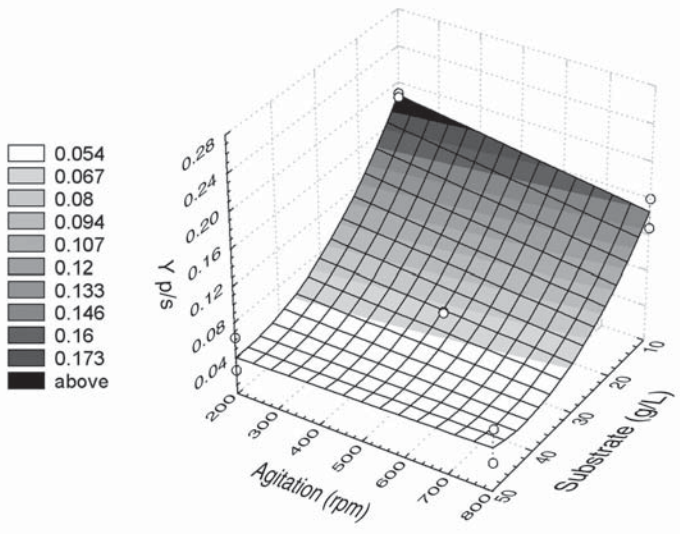

Fig. 5. Effect of X_1 and X_3 on substrate/EPS factor, $Y_{P/S.}$

Discussion

As described, production of the biopolymer was accompanied by the determination of the viscosity of the fermented broth. Viscosity measurements under different conditions described in the experimental design were done as a function of shear rate. In order to obtain suitable conditions that

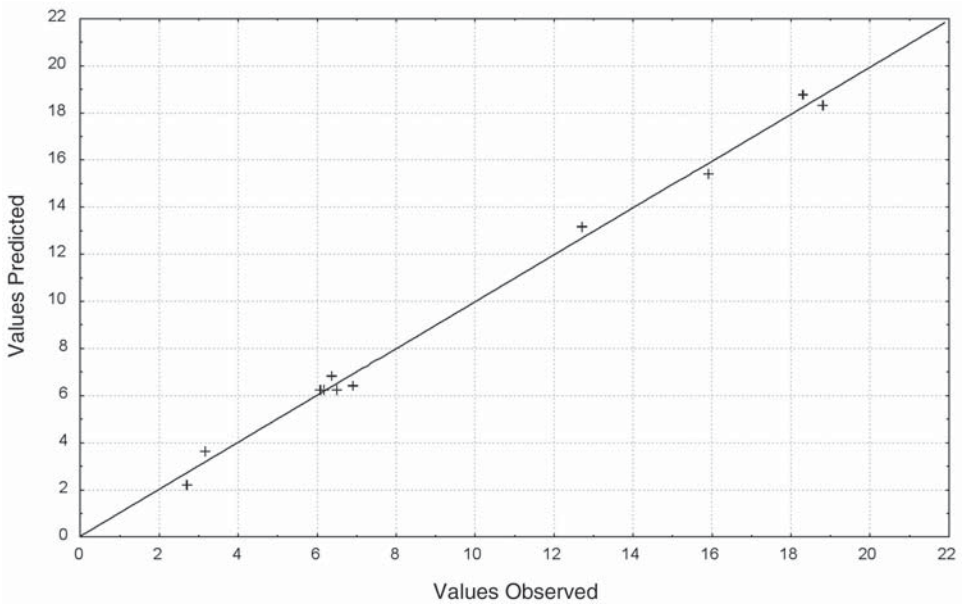

Fig. 6. Correlation between experimental values and values predicted by mathematical model.

could enhance the apparent viscosity of the medium corresponding to a higher production of extracellular polysaccharides. In some cases, the low values of viscosity found suggest that the production medium must be improved, in order to improve its nutrition value, thus enhancing EPS production by the strain.

pH was constant during the process, probably owing to the formation of phosphate-buffering substances. The results indicate that the product synthesized was neutral.

It is widely known that oxygen dissolution in a medium is highly dependent on the medium's viscosity. The decrease observed in the dissolved oxygen concentration is probably associated with the increase in the viscosity observed along the process. The two observations, the decrease in oxygen concentration and the increase in viscosity, were simultaneously observed during the production of EPS by *Rhizobium* sp. EQ1.

Zevenhuizen and Scholten-Koerselman *(10)* studied the carbohydrates on the surface of *Rhizobium* (β-1,2-glucans) and determined the nature of the glucosidic bonds by IR spectrometry in KBr pastilles based on the methodology proposed by Barker et al. *(11)*. This methodology distinguishes among various types of polymers, indicating the predominating type of bond present, as well as the existence of side chains in the molecule. The authors *(10)* observed that in the region between 960 and 730 cm^{-1}, IR spectra of several derivatives of pyranosidic rings could be related to some stereochemical characteristics of the molecule.

D-Glucopiranose derivatives presenting α-type bonds absorbed at 844 cm^{-1}. This characteristic band, named 2a type, was attributed to the deformation of equatorial $C_{(1)}$-H. D-Glucopiranose derivatives containing β bonds present an absorption band (2b type) at 891 ± 7 cm^{-1}, attributed to the deformation of equatorial $C_{(1)}$-H bond. Derivatives of α-D-galactopiranose and α-D-manopiranose present absorption bands (2a type) at 825 ± 11 and 833 ± 8 cm^{-1}, respectively.

Absorption from 2b type was observed at 895 ± 9 and 893 ± 6 cm^{-1} in α-D-galactopiranose and β-D-manopiranose derivatives, respectively. An absorption band (type 1) related to the vibration of a piranose ring in α-D-glucopiranose was observed (peak with a strong to moderate intensity at 917 ± 13 cm^{-1}). On the other hand, for β-D-glucopiranose a peak was generated at 920 ± 5 cm^{-1}.

A band close to 880 cm^{-1}, can be attributed to a β-glycosidic bond. Another band in the region of 846 cm^{-1} could indicate the presence of an α type involving galactose and/or mannose units. The principles of the method proposed by Barker et al. *(11)* proved to be a useful tool for the interpretation of IR spectra obtained from EPS from *Rhizobium* sp. EQ1.

The curves presented in Fig. 2 show the thermal degradation of the polysaccharide; a decomposition stage for both samples tested, with the initial temperature of degradation (T_{onset}) of 290°C, can be clearly observed. This fact implies that the material should not be submitted to temperature ranges close to 290°C, in order not to compromise the physical integrity of the material evaluated. Regarding the purified sample, there was a less intense decrease, probably associated with some degree of heterogeneity. This means that it is possible for aggregate and disperse types to exist, considering that the material contains only polymers.

The results showed that for the nonpurified sample, humidity levels were 14% and final residue was 27%, whereas for the purified sample those values were 10 and 8.5%, respectively.

The Pareto chart (*see* Fig. 3) showed that the substrate concentration was the most significant parameter affecting the process. The interaction $X_1 \cdot X_2$ and $X_1 \cdot X_3$ also presented a significant effect over the process, although less marked than the one caused by the substrate concentration. The effect of agitation on the conversion factor substrate/EPS ($Y_{P/S}$) showed a less significant action over the process, whereas the effect of aeration and agitation was clearly negligible.

From the analysis of surface graphs, it can be observed that the conversion factor substrate/EPS ($Y_{P/S}$) changed from 3.9 to 15.9%, representing an increase of 24.5% in the efficiency of the process. Smaller values of substrate concentration (X_1) increased in the conversion factor, $Y_{P/S}$, whereas aeration did not represent a significant effect.

From Fig. 6, it can be concluded that small values of X_1 and X_2 produced an increase in the conversion factor, changing from 5.4 to 17.3%, representing an increase of 31.2% in the efficiency of the process.

Considering the conversion factor as the response variable, the mathematical regression obtained indicated that 99.49% of the total variation around the mean could be explained by the regression at a 95% significance level; this demonstrates a good agreement between the mathematical model generated by *Statistica* indicating a good fitting of experimental data to the model.

The decrease in the conversion factor with the increase in substrate concentration was also observed by Stredansky et al. *(3)*, who compared the EPS production through solid-state fermentation with *Xanthomonas campestris, Rhizobium hedysari* and *Agrobacterium tumefaciens*. A comparison of submerged and solid-state fermentation indicated that the yield obtained in solid-state conditions was 2 to 4.7 times higher than for submerged fermentation. The polymer yields obtained from solid-state fermentation, as referred to impregnating liquid volumes, were as follows: 38.8 g/L of xanthan from *X. campestris*, 21.8 g/L of succinoglycan from *R. hedysar* and 20.3 g/L of succinoglycan from *A. tumefaciens* PT45.

Selbmann et al. *(12)* used starch as the source of carbon for the production of EPS with the fungal species *Sclerotium glucanicum* and *Botryosphaeria rhodina*. They observed a maximum EPS production of 30.6 (*B. rhodina*) and 19.8 g/L (*S. glucanicum*).

Further characterization of the EPS produced by *Rhizobium* sp. EQ1 is necessary in order to determine its specific application. The use of *Rhizobium* cells for the production of EPS relies on their easy manipulation, cultivation, and the previous knowledge about their potential ability to produce EPS. This work makes the unique contribution of the knowledge of the metabolic activity of these nitrogen-fixing bacteria for the production of EPS, which is still incipient in the published literature.

Acknowledgments

We wish to thank National Council for Scientific and Technological Development and CAPES Foundation (ICCTI 049/00) for financial support.

References

1. Rinaudo, M. (2001), *Food Hydrocolloids* **22,** 433–440.
2. Bobbio, F. O. and Bobbio, P. A. (1992), *Introdução à Química de Alimentos,* 2nd Ed. Livraria Varela, São Paulo, Brazil.
3. Stredansky, M., Conti, E., Navarini, L., and Bertocchi, C. (1999), *Process Biochem*. **34,** 11–16.
4. Guentas, L., Pheulpin, P., Heyraud, A., Gey, C., Courtois, B., and Courtois, J. (2000), *Int. J. Biol. Macromol*. **27,** 269–277.
5. Copetti, G., Grassi, M., Lapasin, R., and Pricl, S. (1997), *Glycoconj. J*. **14,** 951–961.
6. Margaritis, A. and Pace, G. W. (1985), *Compr. Biotechnol*. **49(3),** 1004–1005.
7. Jordan, D. C. (1984), *Bergey's Manual of Systematic Bacteriology*, Williams & Wilkins, Baltimore.
8. Sepe, M. P. (1997), *Rev. Rep. 8(11)*, 3–40.
9. Silverstein, R. M., Bassler, G. C., and Morrill, T. C. (1979), *Identificação Espectrométrica de Compostos Orgânicos*, 3rd Ed., Guanabara dois S.A.

10. Zevenhuizen, L. P. T. M. and Scholten-Koerselman, H. J. (1979), *Antonie van Leeuwenhoek* **45,** 165–175.
11. Barker, S. A., Bourne, E. J., and Whiffen, D. H. (1956), *Methods Biochem. Anal.* **3,** 213–245.
12. Selbmann, L., Crognale, S., and Petruccioli, M. (2002), *Lett. Appl. Microbiol.* **34(1),** 51–58.

0273-2289/04/114/0653–0669/$25.00

Succinic Acid Adsorption from Fermentation Broth and Regeneration

Brian H. Davison,* Nhuan P. Nghiem, and Gerald L. Richardson

Oak Ridge National Laboratory,
PO Box 2008, Oak Ridge, TN 37831-6226,
E-mail: davisonbh@ornl.gov

Abstract

More than 25 sorbents were tested for uptake of succinic acid from aqueous solutions. The best resins were then tested for successive loading and regeneration using hot water. The key desired properties for an ideal sorbent are high capacity, complete stable regenerability, and specificity for the product. The best resins have a stable capacity of about 0.06 g of succinic acid/g of resin at moderate concentrations (1–5 g/L) of succinic acid. Several sorbents were tested more exhaustively for uptake of succinic acid and for successive loading and regeneration using hot water. One resin, XUS 40285, has a good stable isotherm capacity, prefers succinate over glucose, and has good capacities at both acidic and neutral pH. Succinic acid was removed from simulated media containing salts, succinic acid, acetic acid, and sugar using a packed column of sorbent resin, XUS 40285. The fermentation byproduct, acetate, was completely separated from succinate. A simple hot water regeneration successfully concentrated succinate from 10 g/L (inlet) to 40–110 g/L in the effluent. If successful, this would lower separation costs by reducing the need for chemicals for the initial purification step. Despite promising initial results of good capacity (0.06 g of succinic/g of sorbent), 70% recovery using hot water, and a recovered concentration of >100 g/L, this regeneration was not stable over 10 cycles in the column. Alternative regeneration schemes using acid and base were examined. Two (XUS 40285 and XFS-40422) showed both good stable capacities for succinic acid over 10 cycles and >95% recovery in a batch operation using a modified extraction procedure combining acid and hot water washes. These resins showed comparable results with actual broth.

Index Entries: Succinic acid; sorbent; adsorption; hot water regeneration; glucose; fermentation broth.

*Author to whom all correspondence and reprint requests should be addressed.

Introduction

Many industrial organic acids can be produced by fermentation, such as acetic, citric, and lactic acids. Succinic acid is a dicarboxylic acid of potential industrial interest as a platform chemical (1–3). Separation and purification of succinic acid by adsorption was tested to replace current precipitation methods and their associated waste disposal problems. Succinic acid is a valuable intermediate value chemical with a moderate market. For succinic acid to have an economic and energy impact, it will need to become a commodity chemical intermediate with a much lower price. This target price has been estimated to be between $0.22 and $0.30/lb ($0.48–$0.66/kg) and is potentially achievable with advanced technology *(1)*. At this price, succinic acid can be catalytically upgraded into other higher valued chemicals such as tetrahydrofuran, 1,4-butanediol, γ-butyrolactone, 2-pyrrolidinone, and *N*-methylpyrrolidinone.

There is no current commercial biologic process for the production of succinic acid. In past laboratory systems, when succinic acid has been produced by fermentation, lime is added to the fermentation medium to neutralize the acid, yielding calcium succinate *(2)*. The calcium succinate salt then precipitates out of the solution. Subsequently, sulfuric acid is added to the salt to produce the free soluble succinic acid and solid calcium sulfate (gypsum). The acid is then purified with several washings over a sorbent to remove impurities. The disposal of the solid waste is both a directly economic and an environmental concern, as is the cost of the raw materials. Some key process-related problems have been identified as follows: (1) the separation of dilute product streams and the related costs of recovery, (2) the elimination of the salt waste from the current purification process, and (3) the reduction of inhibition to the product succinic acid on the fermentation itself. Acetic acid is also a byproduct of the fermentation of glucose by *Anaerobiospirillium succiniciproducens*; almost 1 mol of acetate will be produced for every 2 mol of succinate *(3)*. Under certain cultivation conditions by a mutant *Escherichia coli,* lesser amounts of acetate can be produced *(4,5)*. This byproduct will also need to be separated.

Adsorption has shown good potential and some data have been gathered for the distribution properties of other carboxylic acids, including acetic, lactic, and citric acids. These sorbents were tested with succinic acid. The key desired properties for an ideal sorbent are high capacity, complete low-cost stable regenerability, and specificity for the product. The economics of the adsorption process have not been evaluated in detail; however, as a stand-alone primary separation, an ultimate goal of a final concentration of >100 g of succinic acid/L was chosen as likely to be economically feasible if achieved.

Solid sorbents have been used and studied for subsequent product recovery from fermentation broth *(6)*. Sorbents were used in a subsequent fluidized-bed contactor for product recovery from fermentation broths *(7)*. Kaufman et al. *(8)* tested a variety of sorbents for lactic acid. Garcia *(6)*

and Garcia and King *(9)* have reviewed the use of some polymeric adsorbents for acetic acid. Many of these sorbents are weak base resins such as poly(4-vinylpyridine) (PVP). PVP showed good capacities for a variety of carboxylic acids *(10)*; succinic acid was not tested. King and colleagues *(9,11–15)* have shown that the sorption is very pH dependent owing to different binding of dissociated and undissociated carboxylic acids. The resins work best at pH less than the pK_a of the acid where the organic acid is primarily in the undissociated or protonated form. The pK_a values of succinic acid are 4.2 and 5.6. Sorption data for succinic acid have been reported *(11,13–15)* with strong pH effects and maximum capacities of 0.2–0.45 g of succinic acid / g of sorbent at acidic pH. Unfortunately, the pH that is typically required for the fermentation (i.e., pH 5.0–7.0) is above the acidic pH that is optimal for most adsorbents. Following King, we use the generic terms *sorption* and *sorbent* to indicate our observational approach and not to presume whether the mechanism is strictly absorption or adsorption.

Competition from other solutes may also be important. In particular, glucose in the fermentation broth has been shown to be sorbed *(16,17)*. This may decrease the total capacity available and the product purity. Solute anions, such as phosphate and sulfate, can also compete for binding sites on basic resins *(11)*.

It may also be economical to remove the inhibitory product directly from the ongoing fermentation by extraction, membranes, or sorption. The use of sorption with simultaneous fermentation and separation for succinic acid has not been investigated. Separation has been used to enhance other organic acid fermentations through *in situ* separation or separation from a recycled side stream. Solid sorbents have been added directly to batch fermentations *(18,19)*. Seevarantnam et al. *(20)* tested a sorbent in the solvent phase to enhance recovery of lactic acid from free cell batch culture. A sorption column was also used to remove lactate from a recycled side stream in a free-cell continuously stirred tank reactor *(21)*. Continuous sorption for *in situ* separation in a biparticle fermentor was successful in enhancing the production of lactic acid *(16,22)*. Recovery in this system was tested with hot water *(16)*.

The extraction of the desired product from the sorbent and the stable regeneration of the resin for further use are essential. The regeneration of some of these sorbents by methanol has also been tested *(23)*. Hot water regeneration has been proposed as well *(24)*. Back extraction with trimethylamine has been tested for succinic acid with consideration of formation of a succinate ester *(13,25)*.

In the present study, various sorbents were tested for the critical properties of capacity for succinic acid, regenerability of the sorbent, and coadsorption of substrates. These criteria were evaluated in order to choose a suitable sorbent for use with either a primary purification step or an *in situ* separation and fermentation. Other factors that were considered were the pH, temperature, and potential ability to concentrate the product.

Table 1
Initial Screening of Sorbents for Uptake of Succinic Acid with First Loading Cycle Capacity Values at 25ºC [a]

Sorbent	Source [b]	Type	Equilibrium (g succinic acid/L)	Capacity (g/g)
XUS 40285	Dow	Weak base polymer	2.53	0.06
XUS 40091	Dow	Weak base	3.98	0.04
XUS 40323	Dow	Strong base	3.78	0.04
XUS 40283	Dow	Strong base	1.98	0.06
XUS 43432	Dow	Weak base	2.81	0.03
XUS 40196	Dow	Strong base	4.88	0.02
XUS 40189	Dow	Strong base	2.03	0.05
XFS-40422	Dow	Polymer	1.50	0.07
IRA-93	RH	Weak base macroreticular	1.03	0.07
IRA-35	RH	Weak base macroreticular	0.79	0.11
XAD-4	RH	Weak base polymer	3.53	0.04
XAD-7 [c]	RH	Weak base polymer	4.80	0.04
Dow-11 MXBD	Dow	Strong base	5.01	0.01
Dowex 1x2	Dow	Weak base	2.77	0.06
Marathon WBA	Dow	Strong base macroreticular	2.04	0.04
MSA-1	Dow	Strong acid PVP	3.98	0.04
MSA-2	Dow	Strong acid PVP	3.99	0.02
Reillex 425	Reilly	PVP	1.74	0.05
Reillex 425	Reilly	PVP	4.8	0.08
Reillex HPQ	Reilly	Hydrophobic molecular sieve	1.03	0.06
Reillex 402 [c]	Reilly	Polymer	3.90	0.02
Silicalite powder [c]	Linde	Hydrophobic molecular sieve	3.68	0.07
Silicalite pellet [c]	Linde	Hydrophobic molecular sieve	4.01	0.05
		with binder	4.01	0.05
AG-3 [c]	Bio-Rad	Styrene	4.10	0.02
AG-1 [c]	Bio-Rad	Styrene quaternary amine	3.99	0.03
MWA-1	Dow	Tertiary amine macroreticular	4.81	0.02

[a] Fifty-milliliters of a solution of acidic succinic acid (~5 g/L) was equilibrated overnight with a known amount of sorbent (~5 grams wet wt). Initial and final concentrations were measured. Calculated capacities are based on the dry weights calculated from dried samples. Most sorbents were preconditioned by washing in 0.01 *M* HCl and triple washing in 50 mL of water at 90ºC. The wash pH was 6.5–7.8.

[b] RH, Rohm & Haas; Linde, Union Carbide.

[c] These sorbents were not preconditioned.

Materials and Methods

Resins

Sorbents were selected from a variety of sources: sorbents previously studied for lactic acids at Oak Ridge National Laboratory; the literature; and sorbents provided by interested industries such as Rohm & Haas, Dow, Union Carbide, and Reilly. The sources are listed in Table 1.

Batch Screening

The initial screening was performed in batch tests. In each test, a known amount (usually 5 g wet wt) of sorbent was contacted with a known volume (usually 50 mL) of an aqueous solution containing the organic acid made from succinic acid crystals. The initial concentration varied between 1 and 50 g/L, with a typical value of approx 5 g/L. The mixture was agitated and allowed to equilibrate overnight and analyzed with the resin's capacity being determined by the difference between the measured initial and equilibrium concentrations. A separate sample of the sorbent was also dried at 90°C; this measured wet/dry ratio of each sorbent was used to calculate the true dry weight, which was used in all capacity calculations. Dried samples were unsuitable for tests themselves owing to greatly reduced wettability. The first tests were performed at ambient 25°C at acidic pH (approx 2.0); later tests were performed at neutral pH (6.0) in a simulated fermentation medium. The simulated medium contained: 1–50 g/L succinic acid as stated; 5 g/L of yeast extract (Difco; Detroit, MI); 0.3 g/L of $MgSO_4$; 0.5 g/L of $(NH_4)_2SO_4$; 0.2 K_2HPO_4; 0.2 g/L of KH_2PO_4; and 0, 5, or 40 g/L of glucose.

All chemicals were laboratory grade and dissolved in distilled water. The medium was sterilized by autoclaving, and sorption experiments were performed in sealed 150-mL serum bottles. Subsequent tests for *in situ* use may need to be performed at mesophilic fermentation temperatures. In a similar manner, the sorbents were also tested for their capacity for the substrate of the possible fermentation, glucose, at a concentration of about 5 g/L. Frequently the glucose was included in the fermentation medium for competitive sorption.

Regeneration with Hot Water

The best resins were then tested for successive loading and regeneration. Acid and bases are conventionally used to extract and regenerate sorbents. However, the standard regeneration technique was hot water. Hot water regeneration was considered to avoid environmental and raw material costs associated with solvent stripping or acid regeneration. The resins were loaded as already described, except that actual medium containing salts and nutrients was used. After loading with succinic acid and determining the capacity, the bulk medium was removed and replaced with a known amount (20–40 mL) of pure water. The resin was then shaken for more than 4 h at 90°C, and the amount extracted was determined by analyzing the bulk solution. The final pH was near 5.0. This cycle was repeated several times with the results calculated at intervals of either 3, 5, or 10 cycles. In later tests, acid regeneration of certain sorbents was studied using 1 *M* HCl. In a few limited tests, a sequential combination of dilute base (0.01 *M* NaOH) and hot water was used; *see* Results for details.

Column Tests

Some resins were tested for in-process removal of succinic acid. Industrial-scale sorption is performed in columns. A packed column (1-cm id,

30-cm length) of the sorbent was contacted with a stream of succinic acid in simulated medium. The total column volume including connections was measured as 75 mL. Samples were taken with a fraction collector and analyzed to create a breakthrough curve. The feed was continued until the column was fully loaded with the succinic acid. The column was then heated to 90°C and stripped with hot water while collecting samples with the fraction collector. This allowed estimation of the concentration factor possible and the fraction recovered. A process scheme would use sorbent columns in series. As breakthrough occurs in the first column, the effluent would be introduced into the second column. Once the first column is fully loaded, the feed stream would be diverted to the second column directly and the first column would be regenerated while the second column continues to be loaded. Depending on the regeneration time, an additional column might be needed in the series.

Analytical Methods

Succinic acid concentrations were analyzed using a Dionex 4500i ion chromatograph. Some effort was spent on developing an accurate, reproducible method using an Ion-Pax AS-10 column, a suppressor module, and a PED electroconductivity detector. A carbonate trap is required to prevent interference from the carbonate peak. This technique can also measure other organic acids and anions such as phosphate. Care must be taken to maintain standards and to store samples. An alternative analytic method was developed using gas chromatography for the fermentation experiments and to confirm the analysis. This method also allows the detection of alcohols such as ethanol and butanol and other organic acids such as lactic and acetic. The method uses a packed column of Chromosorb 101 at 200°C with a helium carrier and an FID detector after sample preparation with metaphosphoric acid. The glucose and l-lactate were measured with a Yellow Springs Instruments glucose analyzer.

Results

Batch Screening

Twenty-five sorbents were screened for uptake of succinic acid. Table 1 lists the initial capacity for each of the sorbents as well as the type and manufacturer of the sorbents.

The capacities ranged from 0.02 to 0.11 g succinic acid/g of dry sorbent at the measured equilibrium succinic acid concentration. In order to have complete removal, a high binding affinity and capacity at low concentration is desired. This screen was performed at moderate concentrations in order to quickly identify sorbents with good capacities at lower concentrations. These are not maximum capacities reported elsewhere. Isotherms were measured for several sorbents that agreed with the literature and followed Langmuir isotherms (data not shown). For example, Reillex 425 has a good capacity (0.08 g/g at 5 g/L) and very good binding affinity

Table 2
Repetitive Sorption of Succinic Acid in Media Capacities After Successive Loading and Regeneration with Hot Water[a]

Sorbent	Loading cycle	Equilibrium concentration (g/L)	Capacity (g/g)
Reillex 425	1	3.56	0.050
	5	2.67	0.040
XUS 40091	1	0.51	0.080
	3	2.74	0.050
XUS 40285	1	1.20	0.079
	3	2.41	0.062
XAD-4	1	4.20	0.040
	3	5.34	0.020
IRA-35	1	0.13	0.305
	3	3.56	0.010
Silicalite powder	1	3.68	0.075
	3	4.11	0.015
IRA-93	1	0.19	0.320
	3	4.45	0.010
Dowex 1x2,16-100	1	2.77	0.060
	5	3.98	0.030
Reillex HPQ	1	1.03	0.060
	5	4.03	0.020
XUS 40283	1	1.98	0.060
	5	3.55	0.040
XFS-40422	1	1.50	0.070
	5	2.70	0.050

[a]Fifty milliliters of a solution of succinic acid in medium was equilibrated overnight with a known amount of sorbent (~5 g) in a manner similar to that in Table 1. Resins were regenerated in hot water at 90°C and capacities calculated using dry weights.

(*K* approx 0.8 g/L). The requirement for a high binding affinity and capacity at low concentration can be partially addressed by use in a packed column as discussed later. Total capacity and regenerability then are critical factors. Since the possibility of *in situ* separation was being considered, the effect of the substrate glucose was also used to screen sorbents.

Approximately half of the better resins were then tested for successive loading of succinic acid in simulated medium and regeneration using hot water. The final pH was near pH 5.0 This cycle was repeated for multiple cycles. Some of the hot water regeneration results are excerpted in Table 2. The best resins (Reillex 425, XUS 40285, and XUS 40091) have a stable capacity of about 0.06 g of succinic acid/g of resin. MWA-1 was not included in these tests because of its lower capacity; however, it was reexamined in later

tests for stability. These capacities were measured at moderate to low equilibrium concentration of succinic acid; and , thus these capacities are not the maximum loadings for these resins, which have been reported by other investigators. The use of a lower succinic acid concentration for the screening gave a measurement of the specificity as well as the capacity without performing a complete isotherm for each sorbent. Because nearly complete recovery is required for most commercial separation, the capacity at the lower concentrations will be important. Other resins had initially higher capacities (e.g., IRA-35), but the capacities were unstable and their capacity rapidly fell to 0.01 g/g. In these cases, it was unclear whether the resin itself was unstable at 90°C or whether the binding sites never released the sorbate (incomplete regeneration). About 50–80% of the succinic acid was removed in each of these cycles. Some of the resins with the highest initial capacity were unstable under the regeneration temperatures; other resins (e.g., Silicalite) did not release the acid under this procedure.

In a similar manner, the sorbents were tested for their capacity for the substrate of the planned fermentation, glucose. Glucose was found to adsorb with all tested resins (data not shown). Maximum glucose capacities ranged from 0.01 to 0.04 g/g. However, the resin preferred succinic acid at a ratio near 4:1 for Reillex 425, 4:1 for XUS 40091, and 8:1 for XUS 40285. Sorbents that preferentially sorbed glucose over succinic acid were eliminated from further testing.

The possible impact of solution pH was also examined by testing two resins more exhaustively for uptake of succinic acid and successive loading and regeneration using hot water. One resin, XUS 40285, has a good stable isotherm capacity, prefers succinate over glucose, and has good capacities at both acidic and neutral pH. Sorption isotherms were constructed for the Dow resin XUS 40285 for uptake of succinic acid after three cycles of loading and regeneration with hot water. These tests were performed at both acidic and neutral pH. The resin has a stable capacity of approx 0.06 g of succinic acid/g of resin at moderate succinic acid concentrations.

Tests were performed in a simulated medium, containing salts and nutrients, as described earlier at an ambient temperature of 25°C, and at both acidic pH (approx 2.0) and neutral pH (approx 6.0). The final pH value was adjusted to the desired value with HCl and allowed to reequilibrate. After loading with succinic acid and determining the capacity, the bulk medium was removed and replaced with a known amount of hot water. The resin was then shaken for more than 4 h at 90Ÿ°C, and the amount extracted was determined by analyzing the bulk solution. The final pH of the aqueous wash was near 5.0. This load/wash cycle was repeated three times. About 70–80% of the succinic acid was removed in each of these cycles. In a similar manner, the sorbents were tested for their regenerated capacity for the fermentation substrate, glucose (*see* Table 3). The resin prefers succinic acid despite an excess of glucose under these conditions. The ion chromatograph analyses indicated that phosphate and sulfate from the medium were adsorbed. This agrees with the findings of Tung and King *(11)*.

Table 3
Repetitive Competitive Sorption of Succinic Acid in Medium with Glucose at pH 2.0 and 6.0[a]

pH	Succinate (g/L)	Capacity (g succinate/g)	Capacity (g glucose/g)
Resin XUS 40285			
pH 2.0	1.44	0.041	0.013
	2.34	0.053	0.015
	3.88	0.061	0.020
pH 6.0	1.44	0.048	0.011
	2.66	0.059	0.013
	3.48	0.066	0.022
Resin MWA-1			
pH 2.0	1.28	0.043	0.023
	3.55	0.047	0.022
	4.81	0.060	0.021
pH 6.0	1.21	0.046	0.024
	2.70	0.053	0.024
	4.14	0.060	0.025

[a]Fifty milliliters of a solution of acidic succinic acid (~5 g/L) was equilibrated overnight with a known amount of sorbent (~5 grams wet wt). Initial and final concentrations were measured at each cycle. Between cycles the sorbent was regenerated with hot water. Calculated capacities are based on the dry weights estimated from separate dried samples. The reported capacities are from the third successive loading and are based on the direct measured sorption in that cycle, not on the cumulative capacity.

Sorption isotherms were also constructed for another resin, MWA-1, for uptake of succinic acid and regeneration with hot water. The isotherms of the final capacities of MWA-1 were similar to those of the XUS 40285, with a maximum capacity of about 0.05 at both 2.0 and 6.0. About 70% of the succinic acid was removed in each of these cycles. In a similar manner, the sorbent was tested for its regenerated capacity for the fermentation substrate, glucose, (Table 3). Glucose was also found to competitively adsorb; however, MWA-1 prefers succinic acid despite an excess of glucose under these conditions. In comparison with the XUS 40285 resin, MWA-1 has a very comparable succinic acid sorption isotherm in terms of capacity and pH; it has a somewhat less regenerability in hot water. MWA-1 also has about twice the affinity for glucose, which would disqualify it for optimal use in simultaneous fermentation and separation. In a batch fermentation, the glucose could desorb as its concentration falls and the conversion could proceed to completion; however, in an extractive fermentation, the continuous removal of the resin would also remove a significant amount of the substrate.

Packed Column Tests

The sorption results from the batch tests just reported indicated good potential for the separation and purification of succinic acid. The key desired properties for an ideal sorbent are high capacity, complete stable regenerability, and specificity for the product. Two of the best sorbents identified by our screening and provided by industry were tested more exhaustively for uptake of succinic acid and for successive loading and regeneration using hot water. These resins, MWA-1 and XUS 40285, had capacities of approx 0.06 g of succinic acid/g of resin over three cycles. They have good capacities at both acidic and neutral pH. This should allow efficient removal of succinic acid from the fermentation broth. Both prefer to adsorb succinate over glucose. This will have no impact on sorption when used as a primary purification step but is necessary if *in situ* separation is to be used.

Two resins were tested for the removal of succinic acid from simulated medium on a packed column of sorbent to simulate an actual process on a small scale. It is important to test the sorption with medium, because salts and other nutrients can interfere with the sorption. Table 4 presents the results for XUS 40285; MWA-1 was comparable. This indicates that either sorbent can remove succinic acid efficiently from the fermentation broth without direct loss of product. Both columns were then stripped or regenerated with hot water. Stripping with hot water recovered 70–80% of the succinic acid from the XUS 40285 resin whereas less (50–60%) was recovered from the MWA-1. The XUS 40285 column was stripped with 2 column volumes of hot water with eluent concentrations up to 49 g/L. Succinic acid was concentrated on average to 40 g/L in the XUS resin by this operation and to 30 g/L by the MWA-1. The 10-fold concentration factor bodes well for the use of sorbents to purify the fermentation broth.

Subsequent tests used streams containing 10, 5, and 2 g/L of succinic acid and acetic acid. Acetic acid is a byproduct of the fermentation and should be in the broth at less than a 1/4 weight ratio. Here, we used an equal concentration of acetic acid and succinic acid as a more stringent screen. Figure 1A shows the contacting that resulted for 10 g/L on XUS 40285. Breakthrough of succinic acid occurred after more than 20 column volumes were passed through. The column was fully loaded with succinic acid, then heated to 90°C and stripped with hot water (Fig. 1B). The regeneration was almost finished in the first 2 column volumes with a maximum concentration of 133 g/L and 70% of total recovery. The consistent recovery at more than 10-fold concentration bodes well for the use of sorbents to purify the fermentation broth. Concentrations of >100 g/L are needed from the primary separation step before subsequent concentration. It can be noted that acetic acid was minimally adsorbed and thus almost completely separated from succinic acid. The acetic acid concentration in the regenerant was always <1 g/L. Succinic acid was also partially purified from the salts by this procedure. This purification will decrease the load on subsequent secondary purification methods such as ion exchange. Methods to concentrate and use the dilute acetic acid or recycle the tailings have not been considered to date.

Table 4
Succinic Acid Sorption on Columns of XUS 40285

	Loading at breakthrough		Loading at saturation		Regeneration with hot water			
Feed (g/L)	Column vol	Capacity (g/g) average	Column vol	Capacity (g/g)	Column vol	Recovery on first cycle (%)	Maximum concentration (g/L)	Average concentration (g/L)
2	31.0	0.11	37	0.12	3.1	60%	41	18
5	16.0	0.13	34	0.20	2.8	71%	59	28
10	9.3	0.16	34	0.36	3.3	71%	133	43

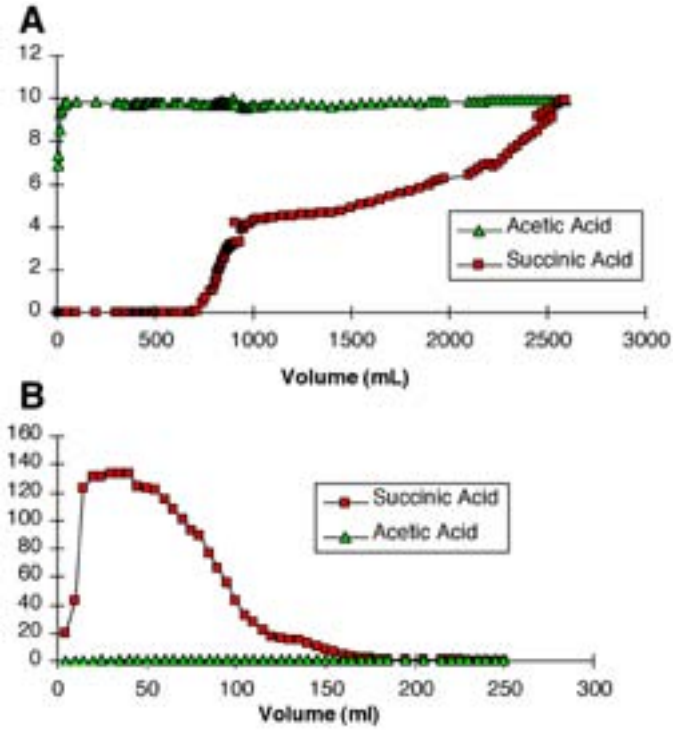

Fig. 1. **(A)** Loading and breakthrough profile for packed column of sorbent (XUS 40285) exposed to 10 g/L of succinic acid and 10 g/L of acetic acid in simulated media. The column volume was 75 mL and the pH of the feed was 6.0. The pH fell to 5.2 during the breakthrough and slowly rose as the bed loaded. **(B)** Elution profile of same column with water at 90°C.

These tests will need to be repeated at higher concentration and for multiple loading and regeneration cycles. At the *n*th cycle, the recovery per cycle needs to be near 100%, even if the capacity is lower. The stability of this resin to this procedure must be confirmed as well. Regeneration also was tested by the use of acid. We wished to minimize this because acid regeneration will require subsequent neutralization. The next experiments extended long-term tests of the use in a packed absorber column of the best resin from the previous screening, a Dow polymeric sorbent, XUS 40285. This resin was tested in a packed column with simulated medium containing salts, 40 g/L of succinic acid, acetic acid, and sugar. The column was loaded with succinic acid and then extracted with hot water at 90°C. The results using a hot water regeneration step were very promising, comparable to those in Fig. 1; however, succinic acid was no longer extracted after 10 repeated cycles of loading and hot water regeneration.

This resin has the characteristics of a capacity of 0.06 g of succinic acid/g of sorbent. With extraction using only hot water, 70–80% of the succinic

acid was recovered per run in the first cycles and concentrated more than fivefold. The long-term regenerability of this hot water method is in question. There are several possible explanations for this. It may be that the hot water regeneration step is not sufficient to remove all of the succinic acid. This residual succinic acid slowly builds up and blocks the binding sites. It may also be that the heat allows the succinic acid to bind more tightly to the resin.

More traditional acid and base regeneration steps were tested for this high-capacity resin. The column of sorbent XUS 40285 was loaded with succinic acid at 35 g/L and extracted with 1 *M* HCl. Eighty-one percent of the succinic acid was recovered; however, there was no increased concentration of the succinic acid in the final product stream. The recovered product stream must be at least as concentrated as the fermentation broth and should be significantly concentrated.

Batch Acid Regeneration

Despite promising initial results of good capacity (0.06 g of succinic acid/ g of sorbent), 70% recovery using hot water, and a recovered concentration of >100 g/L, the hot water regeneration was not stable over 10 cycles in a packed column. Therefore, alternative regeneration schemes using acid and base were examined for the best resins and more sorbents were reexamined at this time.

Tests were performed with both simulated broth containing succinic acid at various concentrations and actual broth provided by MBI. Seven resins were tested for regenerability and stability with acid; XUS 40285, Dowex 1x2, XUS 40283, XUS 440323, XFS-40422, IRA-35, and IRA-93. Previous results had shown a decrease in capacity with repeated hot water regeneration. It is essential for economical operation that the organic acid recovery be >90% and that the sorbents be stable for at least 20 cycles (based on industrial comments). Several resins were tested for stability with a single-step dilute-acid regeneration. The resins were either low capacity after five cycles or had incomplete recovery of the succinic acid (data not shown). Therefore, we modified the procedure to extract the succinic acid first with dilute base, then hot water.

Combined Base/Hot Water Regenration

In the modified procedure, dilute base was used followed by three hot water washes. The resins were preconditioned in 0.01 *M* HCl overnight and then rinsed three times in water. Dry and wet weights of representative samples were measured to allow the capacities to be calculated with estimated dry weights. The resins were contacted overnight with 5 g/L of succinic acid in simulated medium also containing 5 g/L of glucose. Glucose was added to check for interference as well as for possible use in an *in situ* separation from the ongoing fermentation. The extraction procedure was with 0.01 *M* NaOH for 3 h at 40°C followed by three washes

of 90°C water. To determine the total percentage recovered, the succinate from these four steps were combined. This was followed by another cycle of loading. The samples from the first, fifth, and tenth cycles were analyzed. The capacities of four sorbents remained above 0.04 g of succinic acid/g of dry sorbent for the 10 cycles (*see* Table 5). Two of the resins (XUS 40285 and XFS 40422) had both good stability and recovery of succinic acid of >95%. However, the first extraction step would release the organic acid as an aqueous salt, sodium succinate. Based on this and earlier data, the XUS 40285 and the XFS 40422 resins appear to be the most promising for further column process testing. Proper operation of sorbent columns for extraction can concentrate the product and, therefore, simplify further purification steps.

Discussion

More than 25 sorbents were tested for uptake of succinic acid. The best resins were then tested for successive loading and regeneration using hot water. The key desired properties for an ideal sorbent are high capacity, complete stable regenerability, and specificity for the product. The best resins have a stable capacity of approx 0.06 g of succinic acid/g of resin at moderate concentrations (1–5 g/L) of succinic acid. Tung and King *(11)* reported first-cycle maximum capacities at pH 6.0 between 0.0 and 0.08 g/g for weak base resins and 0.22 and 0.25 g/g for strong base resins. The strong base resins needed reactive regeneration. From discussions with individuals in the industry, we estimate that the final resin will need a capacity of >0.05 g/g; however, the regenerability and stability as well as the concentration factor are more important.

Several sorbents were tested more exhaustively for uptake of succinic acid and for successive loading and regeneration using hot water. One resin, XUS 40285, has a good stable isotherm capacity, prefers succinate over glucose, and has good capacities at both acidic and neutral pH.

Succinic acid was removed from medium on a packed column of sorbent. The resin XUS 40285 was tested in a packed column with simulated medium containing salts, succinic acid, acetic acid, and sugar. The packed column completely separated the fermentation byproduct, acetate, from succinate. A simple hot water regeneration successfully concentrated succinate from 10 g/L (inlet) to 40–110 g/L in the effluent with a pH of about 5.0. The end pH indicates that succinate salt was sorbed from the "medium" and released in a partially acidic form by the hot water regeneration. If successful, this would lower separation costs by reducing the need for chemicals for the initial purification step.

Despite promising initial results of good capacity (0.06 g of succinic acid/ g of sorbent), 70% recovery using hot water, and a recovered concentration of >100 g/L, this regeneration was not stable over 10 cycles. Alternative regeneration schemes using acid and base were examined and more sorbents screened. Tests were performed with simulated broth containing succinic acid at various concentrations.

Table 5
Successive Cycles of Batch Loading of Succinic Acid
and Regeneration with Both Dilute Base and Hot Water[a]

Resin	Capacity (cycle 5) (g succinic acid/g resin)	Capacity (cycle 10) (g succinic acid/g resin)	Glucose capacity (g/g resin)	Recovery (% succinic acid after 10 successive cycles of loading and regeneration)	
				Recovered in first step of base	Combined recovery from base and hot water steps
XUS 40285	0.05	0.04	0.025	81	97
Dowex 1x2	0.05	0.05	0.038	38	74
XUS 40283	0.05	0.03	0.03	59	90
IRA-35	0.08	0.03	0.042	44	90
IRA-93	0.06	0.05	0.032	60	78
XUS 40323	0.03	0.02	0.031	8	81
XFS-40422	0.06	0.05	0.034	85	97

[a] NaOH 0.01 *M* followed by three steps of hot water.

Seven of the most promising resins were tested for regenerability and stability using a modified extraction procedure combining acid and hot water washes. Two (XUS 40285 and XFS-40422) showed both good stable capacities for succinic acid over 10 cycles and >95% recovery in a batch operation.

These results show that sorption is a technical possibility for succinic acid separation. In particular, sorption remains an excellent candidate for *in situ* separation. However, targets for capacity, regeneration, and concentration were not met in these preliminary studies. Additional process tests focusing on regeneration and succinic acid concentration will be required. Therefore, these and other economic considerations not reported here have favored membrane or crystallization methods such as described in the referenced patents *(3,26–28)*; these approaches were continued in the larger succinic acid fermentation project *(29,30)*. The sorption data are presented as a baseline for other researchers in the examination of organic acid separation schemes.

Acknowledgments

Funding was provided by the US Department of Energy—EERE—Office of Industrial Technologies. ORNL is operated by UT Battelle under contract with the US Department of Energy. Actual succinic acid fermentation broth was kindly provided by Michigan Biotechnology Institute.

References

1. Bozell, J. J. and Landucci, R. (1993), NREL Report #TP4305565, National Renewable Energy Laboratory, Golden, CO.
2. Datta, R. (1992), US patent no. 5,143,833.
3. Glassner, D. A. and Datta, R. (1992), US patent no. 5,143,834.
4. Donnelly, M., Millard, C. S., and Stols, L. (2001), US patent no. RE37, 393, reissue of US patent no. 5,770,435.
5. Donnelly, M. I., Sanville-Millard, C., and Chatterjee, R. (2001), US patent no. 6,159,738.
6. Garcia, A. A. (1991), *Biotechnol. Prog*. **7,** 33–42.
7. Gaillot, F. P., Gleason, C., Wilson, J. J., and Zwarick, J. (1990), *Biotechnol. Prog*. **6,** 370–375.
8. Kaufman, E. N., Cooper, S. P., and Davison, B. H. (1994), *Appl. Biochem. Biotech*. **45/46,** 545–554.
9. Garcia, A. A. and King, C. J. (1988), Report no. LBL-24543, Lawrence Berkeley Laboratory, Berkeley, CA.
10. Kawabata, N., Yoshida, J., and Tanigawa, Y. (1981), *Ind. Eng. Chem. Prod. Res. Dev*. **20,** 386–390.
11. Tung, L. A. and King, C. J. (1994), *Ind. Eng. Chem. Res*. **33,** 3217–3223.
12. Garcia, A. A. and King, C. J. (1989), *Ind. Eng. Chem. Res*. **28,** 204–212.
13. Tung, L. A. and King, C. J. (1995), *Ind. Eng. Chem. Res*. **28,** 3224–3229.
14. King, C. J. and Tung, L. A. (1992), US patent no. 5,132,456.
15. Husson, S. M. and King, C. J. (1999), *Ind. Eng. Chem. Res*. **38,** 502–511.
16. Kaufman, E. N., Cooper, S. P., Budner, M. K., and Richardson, G. (1996), *Appl. Biochem. Biotechnol*. **57/58,** 503–515.
17. Evangelista, R. L., Mangold, A. J., and Nikolov, Z. L. (1994), *Appl. Biochem. Biotechnol*. **45/46,** 131–144.

18. Wang, H. Y., Robinson, F. M., and Lee, S. S. (1981), *Biotech. Bioeng. Symp. Ser*. **11,** 555–565.
19. Wang, H. Y. and Sobnosky, K. (1985), *ACS Symp. Ser*. **271,** 123–131.
20. Seevarantnam, J., Holst, O., Hjorleifsdottir, S., and Mattiasson, B. (1991), *Bioprocess Eng*. **6,** 35–41.
21. Srivastava, A., Roychoudhury, P. K., and Sahai, V. (1992), *Biotechnol. Bioeng*. *39,* 607–613.
22. Davison, B. H. and Thompson, J. E. (1992), *Appl. Biochem. Biotechnol*. **34/35,** 431–439.
23. Ng, M. and King, C. J. (1988), MS thesis, report no. LBL-25542, Lawrence Berkeley Laboratory, Berkeley, CA.
24. Ernset, E. E. and McQuigg, D. M. (1992), Paper presented at AIChE National Meeting, Miami Beach, FL.
25. Husson, S. M. and King, C. J. (1998), *Ind. Eng. Chem. Res*. **37,** 2996–3005.
26. Berglund, K., Yedur, S., and Dunuwila, D. D. (1999), US patent no. 5,958,744.
27. Yedur, S., Berglund, K. A., and Dunuwila, D. D. (2001), US patent no. 6,265,190.
28. Nghiem, N. P., Donnelly, M., Millard, C. S., and Stols, L. (1999), US patent no. 5,869,301.
29. Davison, B., Nghiem, J., Donnelly, M., Tsai, S., Frye, J., Landducci, R., and Griffin, M. (2002), CRADA Final Report no. 96-0407, Oak Ridge National Laboratory, Oak Ridge, TN.
30. Davison, B., Nghiem, J., Donnelly, M., and Peabody, M. (2003), CRADA Final Report no. C/ORNL/99-0552, Oak Ridge National Laboratory, Oak Ridge, TN.

0273-2289/04/114/0671–0688/$25.00

A Hollow-Fiber Membrane Extraction Process for Recovery and Separation of Lactic Acid from Aqueous Solution

Hanjing Huang,[1,2] Shang-Tian Yang,[*,1] and David E. Ramey[2]

[1]Department of Chemical Engineering, The Ohio State University, 140 West 19th Avenue, Columbus, OH 43210, E-mail: yangst@che.eng.ohio-state.edu; and [2]Environmental Energy Inc., PO Box 15, 1253 N. Waggoner Road, Blacklick, OH 43004

Abstract

An energy-efficient hollow-fiber membrane extraction process was successfully developed to separate and recover lactic acid produced in fermentation. Although many fermentation processes have been developed for lactic acid production, an economical method for lactic acid recovery from the fermentation broth is still needed. Continuous extraction of lactic acid from a simulated aqueous stream was achieved by using Alamine 336 in 2-octanol contained in a hollow-fiber membrane extractor. In this process, the extractant was simultaneously regenerated by stripping with NaOH in a second membrane extractor, and the final product is a concentrated lactate salt solution. The extraction rate increased linearly with an increase in the Alamine 336 content in the solvent (from 5 to 40%). Increasing the concentration of the undissociated lactic acid in the feed solution by either increasing the lactate concentration (from 5 to 40 g/L) or decreasing the solution pH (from 5.0 to 4.0) also increased the extraction rate. Based on these observations, a reactive extraction model with a first-order reaction mechanism for both lactic acid and amine concentrations was proposed. The extraction rate also increased with an increase in the feed flow rate, but not the flow rates of solvent and the stripping solution, suggesting that the process was not limited by diffusion in the liquid films or membrane pores. A mathematical model considering both diffusion and chemical reaction in the extractor and back extractor was developed to simulate the process. The model fits the experimental data well and can be used in scale up design of the process.

Index Entries: Reactive extraction; hollow-fiber membrane; lactic acid; mass transfer; Alamine 336.

*Author to whom all correspondence and reprint requests should be addressed.

Introduction

Lactic acid is an important chemical that has wide applications in food, pharmaceutical, cosmetic, and chemical industries. There are increasing interests in production of lactate esters and biodegradable polylactic acid (PLA) from lactic acid. Lactate esters are a relatively new family of solvents with specific properties. They are considered safe and are biodegradable *(1)*. In many situations they can replace toxic solvents. Their functions vary from that of intermediates in chemical reactions to solvents in ink formulations and cleaning applications *(2)*. PLA has been widely used in medical implants, sutures, and drug-delivery systems because of its capacity to dissolve over time *(3–5)*. PLA also can be used in products such as plant pots, disposable diapers, and textile fabrics.

Lactic acid can be produced from a petrochemical route or from fermentation *(6,7)*. The petrochemical route can only produce racemic mixtures of lactic acid, whereas fermentation can produce optically pure isomer. D(–)-Lactic acid is toxic and must be limited in animal feeds *(8)*, and an optically pure lactic acid is required to produce a specific PLA *(9)*. In addition, fermentation utilizes renewable resources that make fermentation more attractive than the petrochemical route. Extractive fermentation, which couples fermentation with on-line product removal, can eliminate end product inhibition and increase product yield, final product concentration, and reactor productivity. A number of extractive fermentation methods have been reported in the literature, including solvent extraction *(10–12)*, precipitation *(13)*, electrodialysis *(14,15)*, adsorption by ion-exchange resin *(16–18)*, and an aqueous two-phase system *(19–20)*.

Reactive extraction is a promising technology for the recovery of lactic acid because it provides a high distribution coefficient and the extractant can be readily regenerated by back extraction with an alkaline solution *(10,11)*. Aliphatic amines are effective and relatively inexpensive extractants that have been used successfully to extract carboxylic acids *(21)*. Primary amines are too soluble in water to be used with aqueous solutions. Quaternary amines such as Aliquat 336 and secondary amines such as Adogen 283 are more toxic to microorganisms than tertiary amine such as Alamine 336, which is an ideal extractant for use in extractive lactic acid fermentation *(12)*. Emulsion has been a problem in the solvent extractive fermentation process because emulsion causes toxicity to cells *(22)*. To overcome this problem, a solvent extraction approach called hollow-fiber membrane-based extraction has been proposed that can provide nondispersive phase contact. With the membrane-immobilized-phase contact, cells can be protected from direct contact with solvents, and the emulsions, which would otherwise be produced in most cases, can be avoided. The additional advantages of hollow-fiber membranes are ease of separation of two phases and high efficiency owing to high specific surface area per unit reactor volume.

In the present work, continuous extraction of lactic acid from an aqueous solution with a solvent consisting of Alamine 336 and 2-octanol in a hollow-fiber membrane extractor was studied. The lactic acid in the solvent

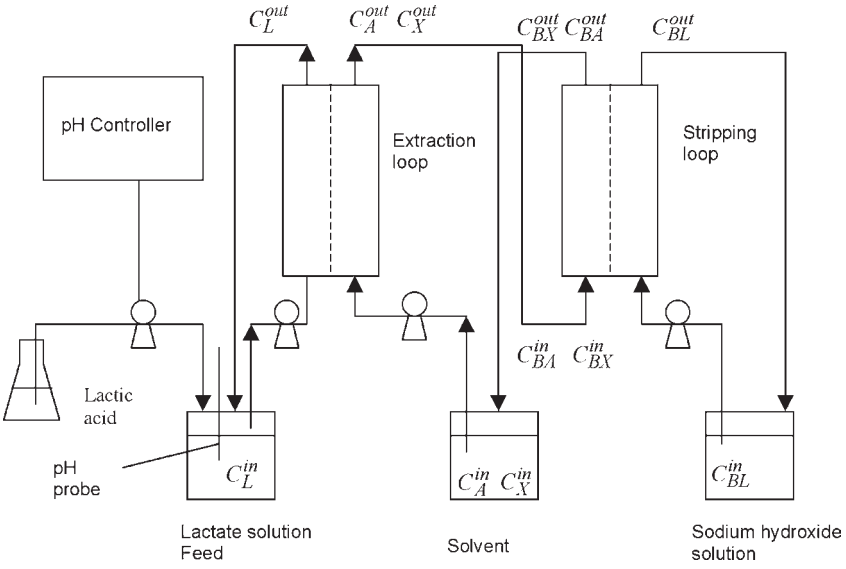

Fig. 1. Experimental setup for extraction and stripping using two hollow-fiber membrane modules.

was then stripped or back extracted with an alkaline solution in a second membrane extractor, which simultaneously regenerated the solvent extractant. The effects of operational variables, including concentrations of lactic acid in the aqueous feed solution and Alamine 336 in the solvent; pH; and flow rates of the feed, solvent, and stripping solution, on the extraction rate were studied. In addition, a theoretical model considering both diffusion and chemical reaction was developed. The model simulated the data well and can be used for optimal design and scale up of the extraction process.

Materials and Methods

Experimental Setup

Figure 1 shows the experimental setup for the simultaneous extraction and stripping process using two hollow-fiber membrane modules. Each hollow fiber membrane extractor (Liqui-Cel Extra Flow, 2.5 in. × 8 in., Celgard, Hoest Celanese) contained about 10,200 polypropylene hollow fibers (15-cm length, 240-µm id, 300 µm o od, 30-µm wall thickness, 0.03-µm membrane pore size, 40% membrane porosity) with an effective membrane surface area of 1.4 m^2. The priming volume of the tube side was 145 mL, and that of the shell side was 195 mL. The feed solution was prepared from 85% lactic acid (pharmaceutical grade; Sigma, St. Louis, MO) diluted with distilled water to a desirable concentration (5–40 g/L). The pH of the feed lactic acid solution was adjusted to the set point (4.0, 4.5, and 5.0) by adding NaOH pellets to the solution. The organic solvent was Alamine 336

(straight-chain tertiary amine containing C_8-C_{10} alkyl groups, with a mol wt of 363.3 and a density of 0.81; Henkel) in 2-octanol (mol wt of 130.23 and a density of 0.822) as a diluent. The Alamine content in the solvent varied from 5 to 40% (v/v). The stripping solution was a 6 *N* NaOH solution.

In the experiments, the lactic acid solution (500 mL) was circulated through the shell side of the extractor, the organic solvent (500 mL) was circulated through the tube side of the extractor and back extractor, and the base solution (500 mL) was circulated through the shell side of the back extractor. The pressure difference across the membrane was adjusted by partially closing a valve at the outlet of the aqueous phase. The pressure difference across the hollow-fiber membrane was kept at ~4 psi, with the aqueous-phase (shell) side being higher than the organic-phase (tube) side to prevent solvent breakthrough. The pH and the concentration of lactic acid in the feed solution were maintained at constant values by automatically adding a concentrated lactic acid solution to the feed reservoir, as lactic acid was being extracted, through the use of a pH controller and a feed pump. The concentration of lactic acid in the stripping base solution was monitored to evaluate the extraction rate. Unless otherwise noted, the experiments were carried out at the same flow rate of 80 mL/min for all three streams (the lactic acid solution, solvent, and stripping solution), at pH 4.5 and ambient temperature (~25°C), with 40 g/L of lactic acid solution and 30% (v/v) Alamine 336 in 2-octanol as the solvent. The effects of amine content in the organic solvent (from 5 to 40%), lactic acid concentration (from 5 to 40 g/L) and pH (4.0, 4.5, and 5.0) of the feed solution, and liquid flow rates (from 20 to 120 mL/min) on the extraction process performance were studied.

Analytical Methods

A high-performance liquid chromatograph (HPLC) was used to analyze the concentration of lactic acid in the base solution. The HPLC system consisted of an automatic injector (Shimadzu SIL-10Ai), a pump (Shimadzu LC-10Ai), an organic acid analysis column (HPX-87H; Bio-Rad, Hercules, CA), a column oven at 45°C (Shimadzu CTO-10A), and a refractive index detector (Shimadzu RID-10A). The eluent was 0.01 *N* H_2SO_4 at a flow rate of 0.6 mL/min. The viscosity of the organic phase was measured using a digital viscometer (Brookfield Model DV.II).

Mathematical Model

Extraction

The reactive extraction of lactic acid by the amine solvent follows a reversible reaction and can be represented by the following reaction mechanism:

$$\text{Lactic Acid} + \text{Amine} \underset{k_{-1}}{\overset{k_1}{\leftrightarrow}} \left[\text{Lactic acid} - \text{Amine}\right]$$

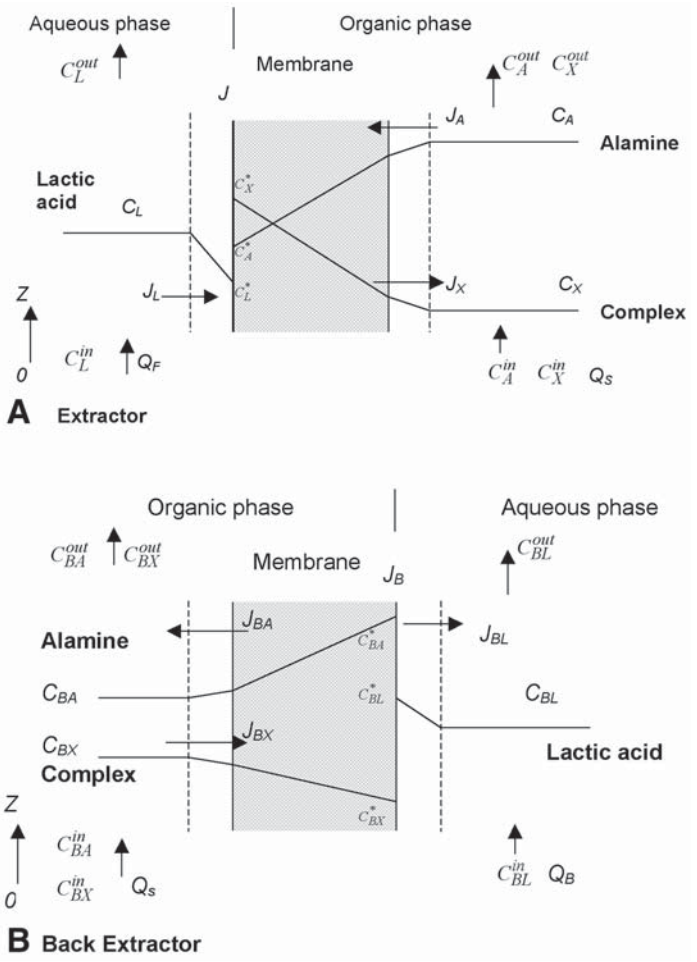

Fig. 2. Concentration profiles of various species in aqueous and organic phases and membrane: **(A)** extractor, **(B)** back extractor.

Figure 2 illustrates the concentration profiles of various species (lactic acid, amine, and lactic acid–amine complex) in the extraction system. Both reactive and physical extractions of lactic acid take place at the interface between the aqueous and organic phases or at the outer membrane surface of the hollow fiber, and the solute flux owing to the extraction, *J*, can be described by Eq. 1:

$$J = k_1 C_L^* C_A^* - k_{-1} C_X^* + k_2 C_L^* \quad (1)$$

In Eq. 1, a first-order reaction kinetics between lactic acid and amine is assumed. The second term is the reverse reaction and the last term is attributed to physical extraction.

The fluxes for lactic acid (J_L) through the aqueous-phase liquid film, and amine (J_A) and the complex (J_X) through the organic-phase liquid film and the membrane, can be expressed, respectively, as follows:

$$J_L = k_L\left(C_L - C_L^*\right) \tag{2}$$

$$J_A = k_{AO}\left(C_A - C_A^*\right) \tag{3}$$

$$J_X = k_{XO}\left(C_X^* - C_X\right) \tag{4}$$

At steady state, all fluxes are equal and $J = J_L = J_A = J_X$. After substituting for C_L^*, C_A^*, and C_X^* using the expressions given in Eqs. 2–4, Eq. 1 becomes

$$J = k_1\left(C_L - J/k_L\right)\left(C_A - J/k_{AO}\right) - k_{-1}\left(J/k_X + C_X\right) + k_2\left(C_L - J/k_L\right) \tag{5}$$

Back Extraction

Back extraction with a strong alkaline (NaOH) solution is an irreversible reaction that simultaneously regenerates the amine and produces sodium lactate and water:

$$\left[\text{Lactic Acid} + \text{Amine}\right] + \text{NaOH} \overset{k_{-1}}{\leftrightarrow} \text{Na} \cdot \text{Lactate} + \text{water} + \text{Amine}$$

The flux of the stripping reaction, J_B, can be described by the following equation when there is an excessive amount of NaOH in the stripping solution (pH >> 10.0):

$$J_B = k_{-1} C_{BX}^* \tag{6}$$

The fluxes for lactic acid (J_{BL}) to move across the aqueous-phase film to the stripping solution, and amine (J_{BA}) and the complex (J_{BX}) through the organic-phase liquid film and the membrane, are, respectively, as follows:

$$J_{BL} = k_L\left(C_{BL}^* - C_{BL}\right) \tag{7}$$

$$J_{BA} = k_{AO}\left(C_{BA}^* - C_{BA}\right) \tag{8}$$

$$J_{BX} = k_{XO}\left(C_{BX} - C_{BX}^*\right) \tag{9}$$

At steady state, all fluxes are equal and thus

$$J_B = J_{BX} = J_{BA} = J_{BL} = k_{-1} k_{XO} C_{BX} / \left(k_{-1} + k_{XO}\right) \tag{10}$$

Concentrations of Solutes

The local concentrations of lactic acid in the aqueous feed and stripping solutions inside the extractor and back extractor, respectively, can be obtained from the following equations:

$$-Q_F \int_{C_L^{in}} dC_L = \pi d_o N \int_0 J dz \tag{11}$$

$$Q_B \int_{C_{BL}^{in}} dC_{BL} = \pi d_o N \int_0 J_B dz \tag{12}$$

Similarly, the concentrations of amine and the complex in the organic solvent inside the extractor and back extractor, respectively, can be obtained from the following equations:

$$-Q_S \int_{C_A^{in}} dC_A = \pi d_o N \int_0 J_A dz \tag{13}$$

$$Q_S \int_{C_{BA}^{in}} dC_{BA} = \pi d_o N \int_0 J_{BA} dz \tag{14}$$

$$Q_S \int_{C_X^{in}} dC_X = \pi d_o N \int_0 J_X dz \tag{15}$$

$$-Q_S \int_{C_{BX}^{in}} dC_{BX} = \pi d_o N \int_0 J_{BX} dz \tag{16}$$

However, both C_A and C_X can be found from C_L in the extractor, and C_{BA} and C_{BX} from C_{BL} in the back extractor, by using material balance as follows:

$$Q_S\left(C_A^{in} - C_A\right) = Q_S\left(C_X - C_X^{in}\right) = Q_F\left(C_L^{in} - C_L\right)$$

$$Q_S\left(C_{BA}^{in} - C_{BA}\right) = Q_S\left(C_{BX} - C_{BX}^{in}\right) = Q_B\left(C_{BL}^{in} - C_{BL}\right)$$

The unsteady-state concentrations of lactic acid in the feed reservoir (C_L^{in}), lactic acid in the stripping solution reservoir (C_{BL}^{in}), and amine (C_A^{in}) and the complex (C_X^{in}) in the organic solvent reservoir can be found from the following equations, respectively:

$$V_F \int_{C_{L0}} dC_L^{in} = Q_F \int_0 \left(C_L^{out} - C_L^{in}\right) dt \tag{17}$$

$$V_B \int_0 dC_{BL}^{in} = Q_B \int_0 \left(C_{BL}^{out} - C_{BL}^{in}\right) dt \tag{18}$$

$$V_S \int_{C_{A0}} dC_A^{in} = Q_S \int_0 \left(C_A^{out} - C_{BA}^{in}\right) dt \tag{19}$$

$$V_S \int_0 dC_X^{in} = Q_S \int_0 \left(C_X^{out} - C_{BX}^{in}\right) dt \tag{20}$$

As can be seen in Fig. 1, $C_A^{out} = C_{BA}^{in}$ and $C_X^{out} = C_{BX}^{in}$. In the experiment, the concentration of lactic acid in the feed reservoir was maintained at a constant initial level, C_{L0}. At steady state, the extraction rate in the extractor should be equal to the stripping rate in the back extractor, which can be

determined from the changes in the amount of lactate in the stripping solution reservoir with respect to time using Eq. 18.

Mass Transfer Coefficients

The mass transfer coefficients k_{AO} and k_{XO} in Eqs. 3, 4, 8, and 9 can be calculated from the following equations:

$$k_{AO} = 1/\left(d_o/k_A d_i + d_o/k_M d_m\right) \tag{21}$$

$$k_{XO} = 1/\left(d_o/k_X d_i + d_o/k_M d_m\right) \tag{22}$$

in which d_o and d_i are the outer and inner diameter, respectively; and d_m is the log mean diameter of the hollow-fiber tube.

The mass transfer coefficient in the aqueous phase, $k_{L,}$ can be determined from the liquid velocity, $\nu_{aq,}$ and the diffusivity of lactic acid, $D_{aq} = 8.24 \times 10^{-6}$ cm^2/s, in the aqueous phase as follows *(23)*:

$$\frac{k_L d_o}{D_{aq}} = 1.4\left(\frac{d_o \nu_{aq}}{D_{aq}}\right)^{1/3} \tag{23}$$

For the mass transfer coefficients in the organic liquid film (k_A and k_X) and the porous membrane (k_M), they can be estimated using the following correlations *(23)*:

$$\frac{k_j d_i}{D_{org,j}} = 1.62\left(\frac{d_i^2 \nu_{org}}{L D_{org,j}}\right)^{1/3} \tag{24}$$

$$k_M = \frac{D_{org,j}\varepsilon}{\delta\tau} \tag{25}$$

in which the subscript j indicates either subscript A (for amine) or subscript X (for the complex), and the diffusivity of the amine and the complex in the organic phase can be determined as follows *(24)*:

$$D_{org,j} = 8.2 \times 10^{-8}\left[1 + \left(\frac{3V_o}{V_j}\right)^{0.66}\right] T/\left(\mu_o V_j^{0.33}\right) \tag{26}$$

The estimated mass transfer coefficients for solvents containing various amounts of Alamine 336 are listed in Table 1.

Model Calculation and Parameter Estimation

Numerical integration was applied to the model. The local fluxes in the extractor and back extractor were first calculated from Eqs. 5 and 10, respectively. The solute flux J in Eq. 5 was determined using Fortran IMSL subroutine NEQNJ. The concentrations of lactic acid, amine, and the complex in the extractor and back extractor were then calculated from Eqs. 11–16, which were solved by using the Runge-Kutta method. Equations 17–20

Table 1
Values of μ_O, V_O, $D_{org,A}$, k_A, k_M and k_{AO} for Solvents with Various Alamine 336 Contents

Alamine 336 content (%)	μ_O (10^{-3} Pa·s)	V_O (cm^3/mol)	$D_{org,A}$ (cm^2/s)	k_A (m/s)	k_M (m/s)	k_{AO} (m/s)
5	6.70	163.7	10.0×10^{-7}	1.20×10^{-6}	5.30×10^{-7}	3.1×10^{-7}
10	7.00	169.4	9.7×10^{-7}	1.15×10^{-6}	5.20×10^{-7}	3.1×10^{-7}
20	7.25	182.0	9.6×10^{-7}	1.14×10^{-6}	5.10×10^{-7}	3.0×10^{-7}
30	7.50	196.6	9.6×10^{-7}	1.13×10^{-6}	5.09×10^{-7}	3.0×10^{-7}
40	8.00	213.7	9.2×10^{-7}	1.10×10^{-6}	4.90×10^{-7}	2.9×10^{-7}

were then used to find the concentrations of lactic acid in the feed reservoir and stripping solution reservoir, and amine and the complex in the solvent reservoir. The calculated values for lactic acid concentration in the stripping solution (C_{BL}^{in}) were then compared with the data to adjust the model parameters. The best values for k_1, k_{-1}, and k_2 in the model were obtained using the Simplex subroutine. In the model calculation, it was assumed that there was no significant change in the liquid volume in all three reservoirs (feed solution, solvent, and stripping solution) and that the system was at steady state. The pk_a value (=3.86) for lactic acid at 25°C and 1 atm was used in estimating the undissociated lactic acid concentration.

Results and Discussion

Effects of Alamine 336 Content

The content of Alamine 336 in the solvent extractant is known to greatly affect lactic acid extraction. San-Martin et al. *(25)* reported that the equilibrium concentration of lactic acid in the solvent increased with an increase in the Alamine 336 content but remained unchanged when the amine content was >40%. Therefore, the amine content in 2-octanol was varied from 5 to 40% (v/v) to study the effect of Alamine 336 content on the extraction rate. As shown in Fig. 3, the lactate concentration in the base solution increased linearly with time, and the extraction rate, as determined from the slope of the linear regression, increased linearly with the Alamine 336 content in the solvent. As can be seen in Fig. 3B, the extraction rate would be greater than zero at 0% Alamine 336 content, indicating physical extraction of lactic acid by 2-octanol. This finding is consistent with the proposed mechanism for the reactive extraction with amine and physical extraction with 2-octanol, as depicted by Eq. 1. It is noted that increasing the amine content had only a minimal effect on the mass transfer coefficients in the organic phase (*see* Table 1), although the viscosity of the organic solvent increased significantly with an increase in the Alamine 336 content, from 6.7×10^{-3} Pa·s at 5% to 8.0×10^{-3} Pa·s at 40%. Table 1 only

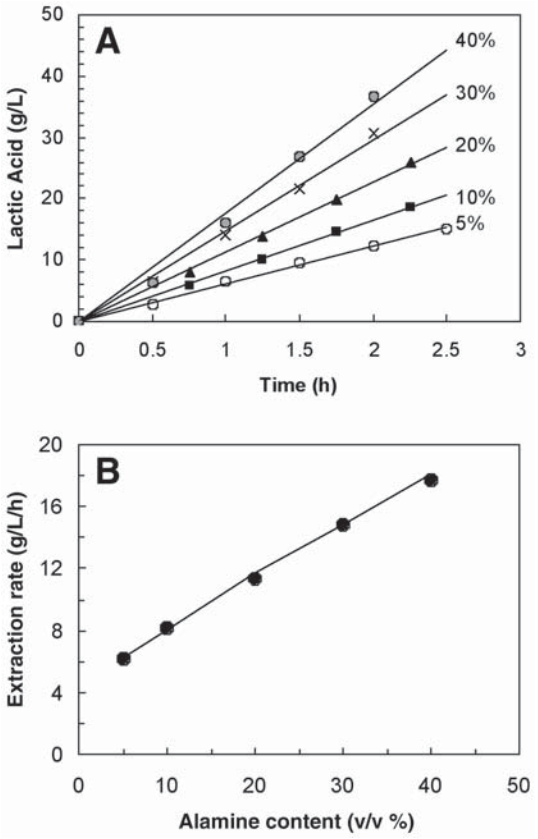

Fig. 3. Effect of Alamine 336 content in solvent on extraction of lactic acid (40 g/L) at pH 4.5 and 80 mL/min flow rate: **(A)** time course of lactate concentration in stripping base solution; **(B)** extraction rate as affected by amine content (the line is the model fit).

lists the values of mass transfer coefficients for amine in the organic phase because the effect on the mass transfer coefficient for the complex is similar. The mass transfer coefficient for the complex is about 10% lower than that for amine because of its larger molecular weight.

Effects of Lactic Acid Concentration and pH

The extraction rate increased with an increase in the lactic acid concentration (Fig. 4) and a decrease in the solution pH (Fig. 5). It is well known that Alamine 336 can only extract the undissociated acid *(26)*. The observed effects of pH and lactic acid were mainly attributed to the undissociated lactic acid concentration in the solution, as illustrated in Fig. 6 with combined data from Figs. 4 and 5. At low acid concentrations, the extraction rate was proportional to the lactic acid concentration, indicating that the reaction was first order with lactic acid concentration. However, at higher acid

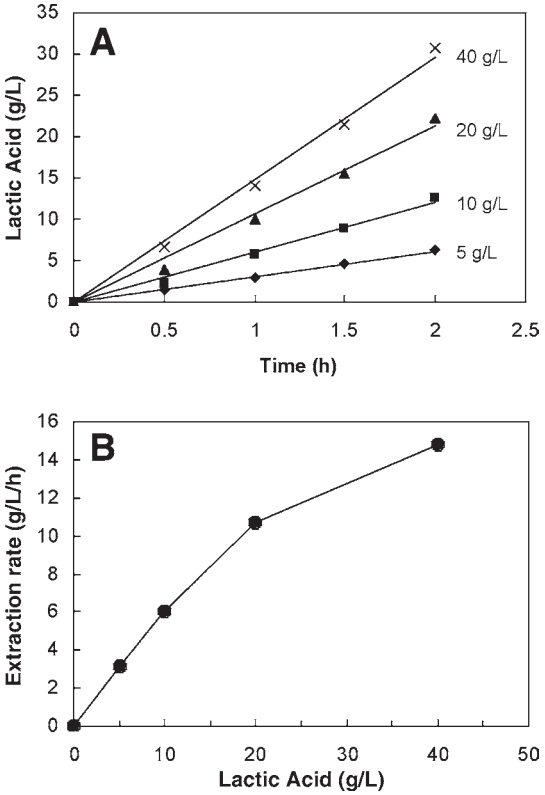

Fig. 4. Effect of lactate concentration on extraction of lactic acid by Alamine 336 (30% [v/v] in 2-octanol) at pH 4.5 and 80 mL/min flow rate: **(A)** time course of lactate concentration in base reservoir; **(B)** extraction rate as affected by concentration of lactic acid in feed solution.

concentrations, the increase in the extraction rate was less than proportional, indicating that the reactive extraction was also affected by the amine concentration at the interface. With more acid molecules in the solution, more amine molecules would be reacted to form the complex, resulting in fewer free amine molecules at the interface. Consequently, the increase in extraction rate would level off at a high lactic acid concentration owing to reduced amine concentration.

Effects of Flow Rate

The liquid velocity in the hollow-fiber membrane extractor affects the thickness of the liquid film on the membrane surface and, thus, may affect the mass transfer rates in the extractor and back extractor. In the present study, one flow rate was varied from 20 to 120 mL/min, whereas the other two flow rates were kept at 80 mL/min. As shown in Fig. 7,

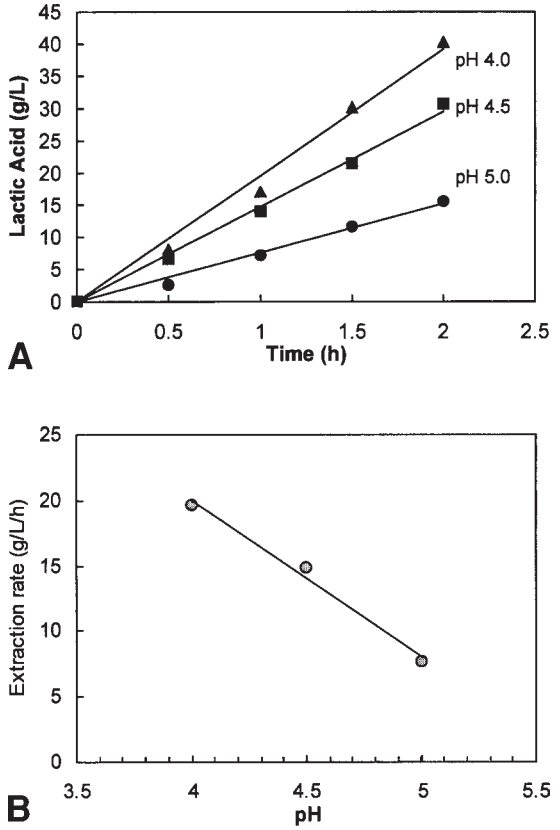

Fig. 5. Effect of pH on extraction of lactic acid (40 g/L) by Alamine 336 (30% [v/v] in 2-octanol) at 80 mL/min flow rate: **(A)** time course of lactate concentration in base reservoir; **(B)** extraction rate as affected by pH of feed solution.

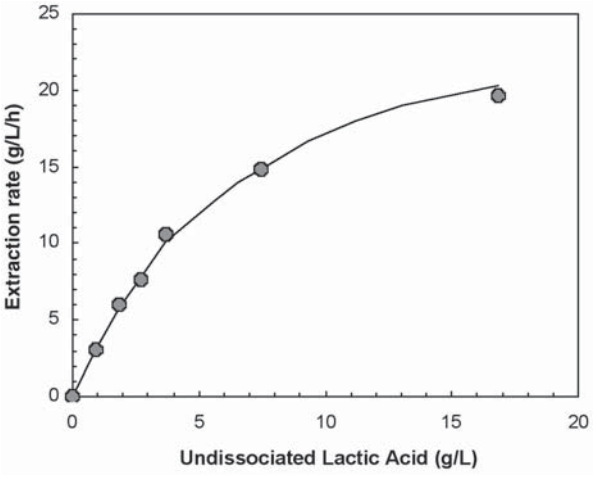

Fig. 6. Effect of undissociated lactic acid concentration on extraction rate with Alamine 336 (30% [v/v] in 2-octanol) at pH 4.5 and 80 mL/min flow rate. The curve is from the model simulation.

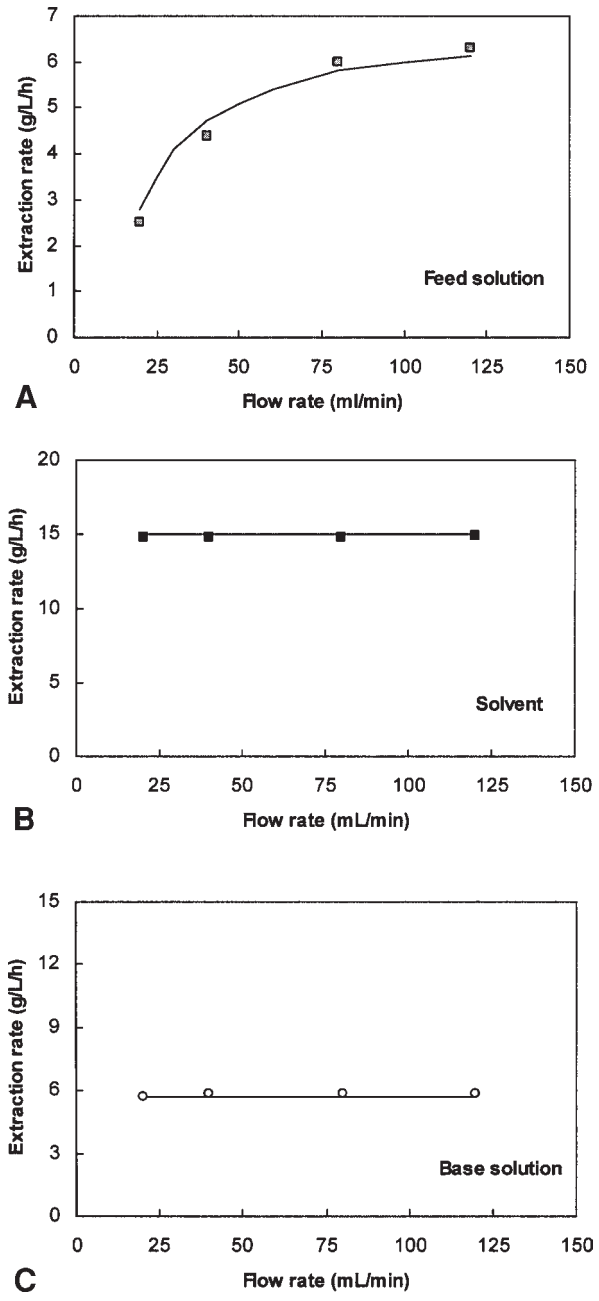

Fig. 7. Effects of flow rates of **(A)** feed solution, **(B)** organic solvent, and **(C)** stripping base solution on extraction of lactic acid by Alamine 336 (30% [v/v] in 2-octanol) at pH 4.5. Only one flow rate was varied in the range studied whereas the other two flow rates were kept at 80 mL/min. The feed contained 10 g/L of lactic acid in (A) and (C), and 40 g/L of lactic acid in (B). The curve and horizontal lines are from the model simulation.

the extraction rate increased with an increase in the flow rate of the feed solution but was not significantly affected by the flow rates of solvent and stripping base solution. The mass transfer coefficient (k_i) in the liquid film should increase with the liquid velocity (v) since k_i is proportional to $v^{1/3}$. However, mass transfer in the system was mainly limited by the membrane resistance since it had a much lower mass transfer coefficient (k_M) than the one in the solvent-phase liquid film (k_A). The overall mass transfer coefficient in the organic phase for amine increased from 2.5×10^{-7} m/s at 20 mL/min to 3.2×10^{-7} m/s at 120 mL/min. However, the increase was not significant and did not affect the overall extraction rate.

The mass transfer coefficient for lactic acid in the aqueous phase was much higher—1.71×10^{-5} m/s at 20 mL/min and 3.1×10^{-5} m/s at 120 mL/min, and thus should not pose any significant resistance to mass transfer in the extraction process. The observed effect of feed flow rate was mainly attributed to the effect of concentration. At a lower feed rate, the lactic acid concentration in the feed solution passing through the extractor would be lowered significantly owing to a longer contact time with the solvent, resulting in a lower mean lactic acid concentration in the extractor and thus a lower extraction rate since the reactive extraction rate is proportional to the lactic acid concentration at the interface. As the feed flow rate continued to increase, the mean concentration of lactic acid in the extractor would approach the feed concentration, and the effect would thus be diminished.

Model

The time course data shown in Fig. 3A were used to determine the model parameters (k_1, k_{-1}, k_2) by fitting the model to the data. The best values for the model parameters are listed in Table 2 and gave excellent fits with the data (*see* Fig. 3B). The model was then used to simulate the remaining data shown in Figs. 6 and 7. As can be seen in Figs. 6 and 7, the model predictions also fit these experimental data very well. Based on the proposed model and experimental observations, the chemical reaction between lactic acid and amine at the interface is the rate-limiting step in the extraction process. For example, in the extraction with 40 g/L of lactic acid at pH 4.5 and 30% Alamine 336, 71.5% of the total resistance is attributed to chemical reaction, whereas mass transfer resistance in the organic phase contributes 26.2% and diffusion resistance in the aqueous phase accounts for only 2.3%. In the back extractor, the reaction resistance is 94.1%, the mass transfer resistance in the organic phase is 5.9%, and there is no significant resistance (0%) in the aqueous phase. It thus can be concluded that the reaction resistance dominates in the reactive extraction carried out in the hollow-fiber membrane extractor. Since the reaction occurs on the interface between the two phases on the membrane surface, the overall reaction or extraction rate is also dependent on the total membrane surface area, as is predicated in Eqs. 11 and 12. Therefore, the extraction process can be scaled up based on the membrane surface area.

Table 2
Best Values for Model Parameters
Determined from Experimental Data

Parameter	Value
k_1 (m^4/mol·s)	9.5×10^{-10}
k_{-1} (m/s)	1.9×10^{-8}
k_2 (m/s)	2.5×10^{-7}

Basu and Sirkar *(27)* modeled the extraction of citric acid from an aqueous solution with tri-*n*-octylamine (TOA) in methyl isobutyl ketone in hollow-fiber membranes. They assumed that the reaction between TOA and citric acid occurring at the interface was rapid compared to membrane resistance and organic-phase diffusion resistance. In the case of back extraction, they concluded that the interfacial reaction rate was much lower than the extraction rate and cannot be neglected and should be considered in series with the diffusion resistances. However, they did not show the simulation result for back extraction. Coelhoso et al. *(28)* studied the extraction of lactic acid with Aliquat 336, a quaternary amine used as an ion-exchange carrier, in a hollow-fiber membrane and concluded that membrane resistance was the limiting step. They used an equilibrium equation, instead of a constant distribution coefficient, to describe the concentration relationship at interface because the distribution coefficient can vary with the solute concentration. Juang et al. *(29)* studied the extraction of lactic acid from an aqueous solution with TOA in a hollow-fiber membrane and proposed an interfacial chemical reaction mechanism in their model. However, they did not study the simultaneous extraction and stripping of lactate using two hollow-fiber membrane modules. The apparent differences in the extraction mechanism and model proposed between the present study and the aforementioned previous studies may be owing to the different amine solvents used in these studies.

It should be noted that the extraction rate shown in Figs. 3–7 is based on the concentration change in the stripping solution, which can be converted to the extraction rate per unit membrane area commonly used in process scale-up design. With 500 mL of the stripping solution and 1.4 m^2 of the membrane area in the extractor, 1 g/(L·h) is equivalent to 0.357 g/(m^2·h). Thus, the extraction rate at pH 4.0 with 40 g/L of lactic acid and 30% Alamine 336 was ~7.1 g/(m^2·h). A higher extraction rate can be achieved with a more reactive extractant such as Adogen 283, which is a secondary amine.

Conclusion

Simultaneous extraction with solvent containing Alamine 336 and stripping with NaOH in two hollow-fiber membrane extractors from an

aqueous feed of lactic acid solution was demonstrated. The extraction process is effective to continuously recover lactic acid from the aqueous feed containing lactic acid at a concentration as low as 5 g/L and pH between 4.0 and 5.0, which is in the range appropriate for lactic acid fermentation. The process thus can be used to recover and separate lactic acid produced from fermentation. Since the solvent extractant is contained in the hollow fibers and continuously regenerated on-line, the extraction process can be readily integrated with a fermentor for continuous production of lactic acid from sugars. Such an extractive fermentation process will have many advantages over conventional fermentation processes and has been previously demonstrated with propionic acid and butyric acid fermentations *(10,11)*. The process can be used to produce sodium lactate at a high concentration of >30% *(12)* and is more energy efficient compared with other separation methods. The extraction rate increased with an increase in the amine content, the undissociated lactic acid concentration, and the feed flow rate. The proposed reactive extraction model based on a first-order reaction mechanism between lactic acid and amine simulates the experimental data well and can be used in the scale-up design of the process.

Nomenclature

C = solute concentration in bulk solution (mol/m^3)
C^* = solute concentration at interface (mol/m^3)
d_i = inner diameter of hollow fiber, $=2.4 \times 10^{-4}$ (m)
d_m = Log mean diameter of hollow fiber (m)
d_o = outer diameter of hollow fiber, $=3.0 \times 10^{-4}$ (m)
D_{aq} = diffusion coefficient of lactic acid in aqueous phase (cm^2/s)
D_{org} = diffusion coefficient of amine or complex in organic phase (cm^2/s)
J = solute flux (mol/[m^2·s])
k = mass transfer coefficient (m/s)
k_1 = forward reaction rate constant (m^4/mol·s)
k_{-1} = backward reaction rate constant (m/s)
k_2 = physical extraction rate constant (m/s)
N = number of hollow fiber tubes in membrane extractor module, =10,200
Q = volumetric flow rate (m^3/s)
t = time (s)
T = absolute temperature (K)
V = volume of solution in reservoir, $=5 \times 10^{-4}$ (m^3)
V_A = molar volume of amine, =363.3/0.81 (cm^3/mol)
V_O = molar volume of organic solvent (cm^3/mol)
V_X = molar volume of complex, =453.3/0.81 (cm^3/mol)
z = hollow-fiber length coordinate (m)
δ = membrane thickness, $=3.0 \times 10^{-5}$ (m)
ε = membrane porosity, =0.4
μ_O = organic phase viscosity (cP)
ν = liquid velocity (m/s)
τ = tortuosity, =2.5

Subscripts

A = amine
B = back extractor
F = feed
L = lactic acid
M = membrane
O = organic phase
S = solvent
X = complex
0 = initial condition

Superscripts

in = inlet to hollow-fiber module
out = outlet from hollow-fiber module

Acknowledgment

This work was supported in part by the US Department of Agriculture (grant no. 2002-00389).

References

1. Clary, J. J., Feron, V. J., and van Velthuijsen, J. A. (1998), *Regul. Toxicol. Pharm.* **27,** 88–97.
2. Nikles, S. M., Piao, M., Lane, A. M., and Nikles, D. E. (2001), *Green Chem.* **3,** 109–113.
3. Datta, R., Tsai, S. P., Bonsignore, P., Moon, S. H., and Frank, J. R. (1995), *FEMS Microbiol. Rev.* **16,** 221–231.
4. Drumright, R. E., Gruber, P. R., and Henton, D. E. (2000), *Adv. Mater.* **12,** 1841–1846.
5. Wasewar, K. L., Heesink, A. B. M., Versteeg, G. F., and Pangarkar, V. G. (2002), *J. Chem. Technol. Biot.* **77,** 1068–1075.
6. Holten, C. H. (1971), *Lactic Acid*, Verlag Chemie GmbH, Weinheim, Germany.
7. Tay, A. and Yang, S. T. (2002), *Biotechnol. Bioeng.* **80,** 1–12.
8. Mulligan, C. N., Safi, B. F., and Grolea, U. D. (1991), *Biotechnol. Bioeng.* **38,** 1173–1181.
9. Tsai, S. P. and Moon, S. H. (1998), *Appl. Biochem. Biotechnol.* **70,** 417–428.
10. Jin, Z. W. and Yang, S. T. (1998), *Biotechnol. Prog.* **14,** 457–465.
11. Wu, Z. T., and Yang, S. T. (2003), *Biotechnol. Bioeng.* **82,** 93–102.
12. Tay, A. (2000), PhD thesis, Ohio State University, Columbus, OH.
13. Yang, C. W., Lu, Z. J., and Tsao, G. T. (1995), *Appl. Biochem. Biotechnol.* **51,** 57–71.
14. Vonktaveesuk, P., Tonokawa, M., and Ishizaki, A. (1994), *J. Ferment. Bioeng.* **77,** 508–512.
15. Xuemei, L., Jianping, L., Mo'e, L., and Peilin, C. (1999), *Bioprocess Eng.* **20,** 231–237.
16. Srivastava, A., Roychoudhury, P. K., and Sahai, V. (1992), *Biotechnol. Bioeng.* **39,** 607–613.
17. Wang, J. L., Wen, X. H., and Zhou, D. (2000), *Bioresour. Technol.* **75,** 231–234.
18. Wang, J. L., Liu, P., and Zhou, D. (1994), *Biotechnol. Tech.* **8,** 905–908.
19. Planas, J., Radstrom, P., Tjerneld, F., and HahnHagerdal, B. (1996), *Appl. Microbiol. Biotechnol.* **45,** 737–743.
20. Kwon, Y. J., Kaul, R., and Mattiasson, B. (1996), *Biotechnol. Bioeng.* **50,** 280–290.
21. Kertes, A. S., and King, C. J. (1986), *Biotechnol. Bioeng.* **28,** 269–282.
22. Lewis, V. P. and Yang, S. T. (1992), *Biotechnol. Prog.* **8,** 104–110.
23. Lazarova, Z., Syska, B., and Schugerl K. (2002), *J. Membr. Sci.* **202,** 151–164.
24. Reid, R. C., Prausnitz, J. M., and Sherwood, T. K. (1987), *The Properties of Gases and Liquids*, 4th Ed., McGraw-Hill, New York, NY.

25. San-Martin, M., Pazos, C., and Coca, J. (1992), *J. Chem. Technol. Biotechnol.* **54,** 1–6.
26. Yang, S. T., White, S. A., and Hsu, S. T. (1991), *Ind. Eng. Chem. Res.* **30,** 1335–1342.
27. Basu, R. and Sirkar, K. K. (1992), *Solvent Extr. Ion Exch.* **10,** 119–142.
28. Coelhoso, I. M., Silvestre, P., Viegas, R. M. C., Crespo, J. P. S. G., and Carrondo, M. J. T. (1997), *J. Membr. Sci.* **134,** 19–32.
29. Juang, R. S., Chen, J. D., and Huang, H. C. (2000), *J. Membr. Sci.* **165,** 59–73.

0273-2289/04/114/0689–0711/$25.00

Evaluation of Tocopherol Recovery Through Simulation of Molecular Distillation Process

E. B. Moraes, C. B. Batistella, M. E. Torres Alvarez, Rubens Maciel Filho, and M. R. Wolf Maciel*

Separation Process Development Laboratory (LDPS),
Faculty of Chemical Engineering,
State University of Campinas (UNICAMP),
CP 6066, 13081-970, Campinas-SP, Brazil,
E-mail: wolf@feq.unicamp.br

Abstract

DISMOL simulator was used to determine the best possible operating conditions to guide, in future studies, experimental works. This simulator needs several physical-chemical properties and often it is very difficult to determine them because of the complexity of the involved components. Their determinations must be made through correlations and/or predictions, in order to characterize the system and calculate it. The first try is to have simulation results of a system that later can be validated with experimental data. To implement, in the simulator, the necessary parameters of complex systems is a difficult task. In this work, we aimed to determe these properties in order to evaluate the tocopherol (vitamin E) recovery using a DISMOL simulator. The raw material used was the crude deodorizer distillate of soya oil. With this procedure, it is possible to determine the best operating conditions for experimental works and to evaluate the process in the separation of new systems, analyzing the profiles obtained from these simulations for the falling film molecular distillator.

Index Entries: Molecular distillation; vitamin E; deodorizer distillate of soya oil; DISMOL; property estimation.

Introduction

Molecular distillation is characterized by short exposure of the distilled liquid to elevated temperatures, high vacuum in the distillation space, and a small distance between the evaporator and the condenser. The short residence time of the liquid on the evaporating cylinder, in the order of a

*Author to whom all correspondence and reprint requests should be addressed.

few seconds to 1 min, is guaranteed by distributing the liquid in the form of a uniform thin film *(1)*. By reducing the pressure of noncondensable gas in the evaporator to lower than 10^{-1} mbar, a reduction in distillation temperature can be obtained. A molecular distillation process is useful in the separation and purification of materials of high molecular weight, as well as for those that are thermally sensitive, such as the vitamins *(2–4)*, by minimizing losses through thermal decomposition. The combination of a small distance between the evaporator and the condenser (about 2 cm) and a high vacuum in the distillation gap results in a specific mass transfer mechanism with evaporation outputs as high as 20–40 $g/(m^{-2} \cdot s)$. Under these conditions (e.g., short residence time and low temperature), distillation of heat-sensitive materials is accompanied by only negligible, thermal decomposition and at flow rates that make the process technologically viable *(1)*. This means that in relation to conventional or even vacuum distillation, in the case of molecular distillation, the materials in some cases remain unaltered but in others small decomposition can occur (e.g., 3% in the case of tocopherols). The decomposition is a direct function of the residence time and an exponential function of the temperature. On the other hand, the productivity of the process is high, considering the treatment of high-added-value compounds.

During molecular distillation, small variations in process conditions can lead to considerable changes in the characteristics of product streams *(5–7)*. Thus, it is very important to have robust simulation results in order to evaluate the process and even to guide the experimental work. The objective of the present work was to incorporate in the Dismol simulator the data to simulate the process. The complex systems typical of the application of molecular distillation must be well characterized.

Molecular distillation shows promise in the separation, purification, and/or concentration of natural products, usually constituted by complex and thermally sensitive molecules. Furthermore, this process has advantages over other techniques that use solvents as the separating agent, avoiding problems with toxicity. Molecular distillation has also been used for heavy petroleum characterization, demonstrating the potential of this separation process in other situations *(8)*.

Tocopherols are extensively used as antioxidants in a growing trend of consumer preference for natural antioxidants. Natural tocopherols are recovered from vegetable oil deodorizer distillate, a byproduct of the vegetable oil–refining process. Deodorizer distillate is composed of fatty acids, sterols, tocopherols, sterol esters, hydrocarbons, breakdown products of fatty acids, aldehydes, ketones, and acyl glycerol species. This byproduct is sold on the basis of tocopherol content, which is valued for both its vitamin E activity and antioxidant property *(9)*. Sterols are used as starting materials or as intermediates for the manufacture of pharmaceutical drugs, and steroids are used for medicinal purposes. Fatty acids constitute 25–75% of the distillate depending on the raw material being refined, the type of refining process, and the conditions employed. Deodorizer distillate can

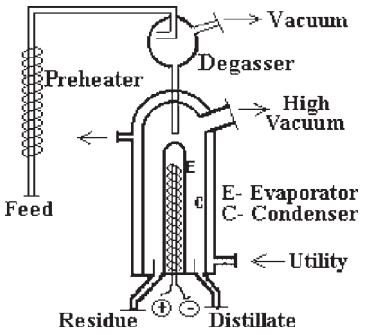

Fig. 1. Falling film molecular distillation.

have significantly different characteristics, uses, and values. When derived from soybean or other unsaturated vegetable oils, it can be a good raw material for the production of vitamin E and sterols. From other fats and oils, the distillate may be useful only for fatty acid production *(10)*. Deodorizer distillates are used in nonfood and low-cost applications, because they are contaminated with fatty acids *(11)*.

Taking all of these concerns into consideration, in the present work, we propose a molecular distillation process for tocopherol (vitamin E) recovery using as a raw material the crude deodorizer distillate of soya oil (DDSO). The determination of several physical-chemical properties must be made through correlations and/or predictions, in order to have a better characterization of the system that will be studied. Then, the DISMOL simulator can be used to evaluate tocopherol recovery from crude DDSO, in order to determine the feasibility of the process and the best experimental conditions for the falling film molecular distillation. The simulator used was a DISMOL, which was developed by Batistella *(12)*. Tocopherols need to present a low acidity level (< 2%) and purity according to their application (from 30 to 90%). The price varies according to this concentration. Squalene is tolerable in tocopherol concentration, but fatty acids must be eliminated during the process.

DISMOL Simulator: Falling Film Distillation

A schematic of the falling film molecular distillator is shown in Fig. 1. The main part of the installation consists of a cylindrical evaporator surrounded by a condenser jacket. The liquid to be distilled is transported from a storage tank through a preheater to the surface of the unheated evaporator. It is also possible to heat the evaporator internally. In the case of a heated evaporator, the distillation rate is faster, but the separation factor decreases at higher temperatures. The velocity is that of a laminar and isothermal film with a smooth surface. In the first stage, tocopherols are recovered in the residue stream (according to Fig. 1) and in the second processing stage in the distillate stream.

The simulator used was a DISMOL, described previously by Batistella and Maciel *(2)*. All explanations of the equations used, the solution methods, and the routine of solution are described in Batistella and Maciel *(5)*. DISMOL is a simulator that permits changes in feed composition, feed temperaturethe evaporation rate, as well as feed flow rate. The effective rate of surface evaporation is obtained from the kinetic theory of gases. The liquid film thickness is obtained by mass balance and geometry of the evaporator. The temperature in the liquid obeys the Fourier-Kirchhoff equation. The solution of the velocity profile requires knowledge of the viscosity and the liquid film thickness over the evaporator. The solution for the temperature and the concentration profiles requires knowledge of the velocity profiles, which determine the convective heat and mass fluxes.

The solution is accomplished by a numerical technique using a finite-difference method. The procedure involves the following steps:

1. Solution of the rate equation of the distillation components.
2. Solution of the thickness equation of the liquid film over the evaporator.
3. Solution of the velocity profile equation in the liquid film flowing over the evaporator.
4. Solution of the temperature profile equation in the liquid film.
5. Solution of the concentration profile equation in the liquid film.

These equations are solved in each segment of the evaporator, from the feed point to the exit points of the components, and depend on the process conditions and the properties of the system to be studied including the vapor pressure, vaporization enthalpy, molecular weight, mass diffusivity, mean free path, and composition of the involved components; and the density, thermal conductivity, heat capacity, and viscosity of the mixture. Regarding the equipment, it is necessary to know the dimensions (evaporator diameter and length), and as characteristic of the process, the feed flow rate, feed temperature, and heating temperature. The simulator also allows comparative analyses between the centrifugal flJd falling-film processes *(2)*.

Calculation and Estimation of Physical, Thermodynamic, and Transport Properties

Table 1 gives the components present in the crude DDSO and their properties: critical pressure (P_c), critical temperature (T_c), critical volume (V_c) and acentric factor (ω). These properties were obtained from hypothetical components (a tool of the commercial simulator HYSYS) that are created through the UNIFAC group contribution. The developed DISMOL simulator requires these properties (mean free path; enthalpy of vaporization; mass diffusivity; vapor pressure; liquid density; heat capacity; thermal conductivity; viscosity; and equipment, process, and system characteristics that are simulation inputs) in calculating other properties of the system, such as evaporation rate, temperature and concentration profiles, residence time, stream compositions, and flow rates (output from the simulation). Furthermore, film thickness and liquid velocity profile on the evaporator are also calculated.

Table 1
Properties Obtained from HYSYS Commercial Simulator

Components	X_i	P_c (bar)	T_c (K)	V_c (cm^3/mol)	ω	M (g/mol)
Palmitic acid	0.1271	14.0801	887.34	955.50	0.9744	256.43
Stearic acid	0.0283	12.2512	935.12	1067.50	0.9678	284.48
Linoleic acid	0.3295	13.1943	950.98	1027.50	0.9656	280.45
Oleic acid	0.1438	12.7097	942.86	1047.50	0.9683	282.47
Lauric acid	0.0221	19.2198	797.43	731.50	0.9047	200.31
Araquidic acid	0.0496	10.7569	985.41	1179.50	0.9290	312.52
Campesterol	0.0417	9.1661	1128.81	1461.50	0.8130	400.69
β-Sitosterol	0.0933	8.6556	1159.21	1517.50	0.7465	414.72
Stigmasterol	0.0355	8.9267	1162.70	1497.50	0.7850	412.70
α-Tocopherol	0.0114	2.9222	1075.61	5355.74	1.8001	430.71
γ-Tocopherol	0.0462	3.3819	1058.62	4624.61	1.7325	416.69
Δ-Tocopherol	0.0275	3.9136	1041.13	3994.35	1.6621	402.66
Squalene	0.0440	6.3845	978.38	2447.09	1.4036	410.70

We do not discuss equilibrium because the molecular distillation is a nonequilibrium process. Molecular distillation belongs to the class of processes that uses the technique of separation under high vacuum, operation at reduced temperatures, and low exposition of the material at the operating temperature. It is a process in which vapor molecules escape from the evaporator in the direction of the condenser, where condensation occurs. Then, it is necessary that the vapor molecules generated find a free path between the evaporator and the condenser, the pressure be low, and the condenser be separated from the evaporator by a smaller distance than the mean free path of the evaporating molecules. In these conditions, theoretically, the return of the molecules of the vapor phase to the liquid phase should not occur, and the evaporation rate should only be governed by the rate of molecules that escape from the liquid surface; therefore, phase equilibrium does not exist.

Equipment, Process, and System Characteristics

The equipment, process, and stystem characteristics are as follows:

1. Equipment characteristics: evaporator diameter = 10 cm; evaporator length = 0.25 m.
2. Process characteristics: feed temperature = 60°C; heat temperature = 120–180°C (evaporator); feed flow rate = 0.5–1.0 kg/h.
3. System characteristics—crude DDSO *(13)*: properties of the components and of the mixture calculated from the properties obtained from HYSYS (*see* Table 1) through the equations presented. Note that all errors mentioned, one for correlation, were suggested by the authors of the equations.

Table 2 illustrates the simulation procedure.

Table 2
Simulation Procedure

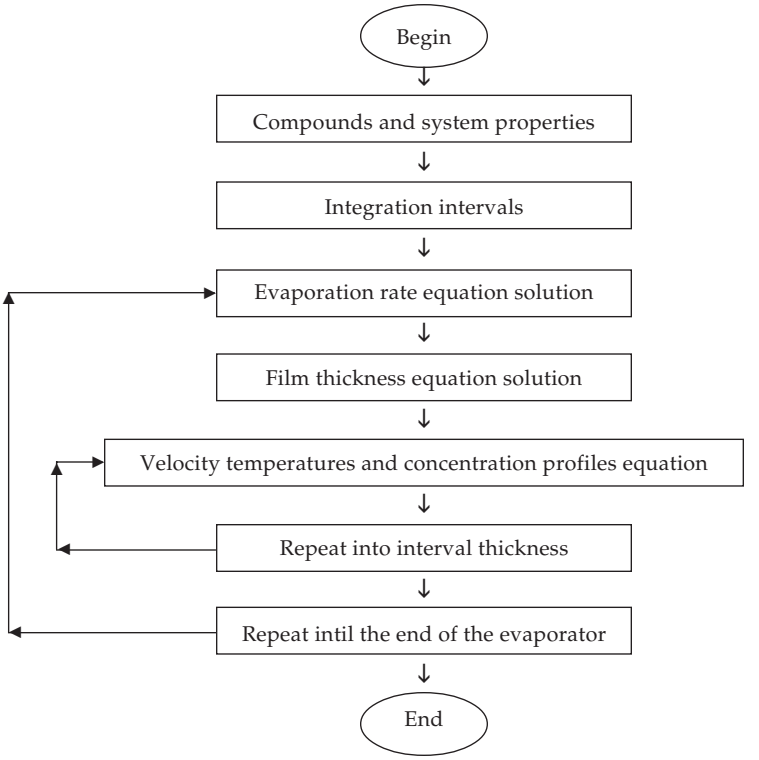

Component System Characteristics

Mean Free Path

The Clausius equation *(14)* gives the value of the mean free path, L, of a component at ideal conditions, i.e., path without collisions with residual gases:

$$L = \frac{1}{\sqrt{2}\,\pi\sigma^2 N} \tag{1}$$

in which

$$N = 9.66 \times 10^{18}\,\frac{P}{T}$$

(expression developed from the equation of state of an ideal gas);

$$\sigma = 8.09 \times 10^{-9}\,V_c^{1/3}$$

(15); L is the mean free path (cm); N is the number of molecules per volume unit (mol/cm^3); P is the pressure (mmHg); T is the temperature (K); V_c is the critical volume (cm^3/mol); and σ is the diameter of the molecule (cm).

Enthalpy of Vaporization

A pure component constant that is occasionally used in property correlations is the enthalpy of vaporization at the normal boiling point, ΔH_b^{vap}. In addition, several special estimation methods are suggested. The Chen equation *(15)* gives a relation among the enthalpy of vaporization, the reduced vapor pressure, and the reduced temperature. When applied to the normal boiling point, Eq. 2 is obtained, with an average error of 2%:

$$\Delta H_b^{vap} = \frac{RT_c T_{b_r}\left(3.978T_{b_r} - 3.958 + 1.555\ln P_c\right)}{1.07 - T_{b_r}} \tag{2}$$

For different temperatures, a widely used correlation between the enthalpy of vaporization and temperature is the Watson equation *(14)*, with an average error of 2%:

$$\Delta H^{vap} = \Delta H_b^{vap}\left(\frac{T_c - T}{T_c - T_{b_r}}\right)^{0.38} \tag{3}$$

in which P_c is the critical pressure (bar); T_b is the normal boiling temperature (K); T_c is the critical temperature (K); T_{br} is equal to T_b/T_c (reduced normal boiling temperature); ΔH^{vap} is the enthalpy of vaporization (J/mol); and ΔH_b^{vap} is the enthalpy of vaporization at normal boiling temperature (J/mol).

Mass Diffusivity

For a binary mixture of solute *A* in solvent *B*, the diffusion coefficient D_{AB}^o of *A* diffusing in an infinitely dilute solution of *A* in *B* implies that each molecule *A* is in an environment of essentially pure *B*. In engineering work, however, D_{AB}^o is assumed to be a representative diffusion coefficient even for concentrations of *A* up to 5 and, perhaps, 10 mol%.

An older, but still widely used, correlation for D_{AB}^o, the Wilke-Chang technique, is, in essence, an empirical modification of the Stokes-Einstein relation (Eq. 4). Several systems were studied by these investigators, and an average error of about 10% was noted:

$$D_{AB}^o = \frac{7.4\times10^{-8}\left(\phi M_B\right)^{0.5}T}{\eta_B V_{bA}^{0.6}} \tag{4}$$

in which D_{AB}^o is the mutual diffusion coefficient of solute *A* at very low concentrations in solvent *B* (cm^2/s); M_B is the molecular weight of solvent B (g/mol); *T* is the temperature (K); η_B is the viscosity of solvent B (cP); V_{bA} is the molar volume of solute *A* at its normal boiling temperature (cm^3/mol), and ϕ is the association factor of solvent *B* (dimensionless). Wilke and Chang recommend that ϕ be chosen as 2.6 if the solvent is water, 1.9 if it is methanol, 1.5 if it is ethanol, and 1.0 if it is unassociated.

In a binary liquid mixture, as already noted, a single diffusion coefficient was sufficient to express the proportionality between the flux and the concentration gradient. In multicomponent systems, the situation is considerably more complex, and the flux of a given component depends on the gradient of $n - 1$ components in the mixture. One important case of multicomponent diffusion results when a solute diffuses through a homogeneous solution of mixed solvents. When the solute is diluted, there are no concentration gradients for the solvent species and one can consider a single solute diffusivity with respect to the mixture D^o_{Am}. Perkins and Geankoplis evaluated several methods and suggested Eq. 5 *(15)*:

$$D^o_{Am}\,\eta_m^{0.8} = \sum_{j-1\neq A}^{n} x_j\, D^o_{Aj}\,\eta_j^{0.8} \tag{5}$$

in which D^o_{Am} is the effective diffusion coefficient for a diluted solute A into the mixture (cm^2/s); D^o_{Aj} is the infinite dilution binary diffusion of solute A into the solvent j (cm^2/s); x_j is the mole fraction of j; η_m is the mixture viscosity (cP); and η_j is the pure component viscosity (cP). When tested with data for ternary systems, errors were normally <20%. Perkins and Geankoplis also suggested that the Wilke-Chang equation might be modified to include the mixed solvent case, i.e., Eq. 6:

$$D^o_{Am} = \frac{7.4\times 10^{-8}\left(\phi M\right)^{0.5} T}{\eta_m V_A^{0.6}} \tag{6}$$

in which

$$\phi M = \sum_{j-1\neq A}^{n} x_j\,\phi_j\, M_j$$

Although not extensively tested, Eq. 6 provides a rapid, reasonably accurate estimation method.

Vapor Pressure

Antoine Vapor Pressure correlations have been widely used over limited temperature ranges *(15)*:

$$\text{Log}\, P^{vap} = A - B/\left(T + C\right) \tag{7}$$

in which A is a characteristic constant of a substance, to be adjusted; B is a characteristic constant of a substance, to be adjusted; C is a characteristic constant of a substance, to be adjusted; P^{vap} is the vapor pressure (bar); and T is the temperature (K).

Values of A, B, and C are tabulated for a number of materials. The applicable temperature range is not large and in most situations corresponds to a pressure interval of about 0.001–2 bar. The Antoine equation should never be used outside the stated temperature limits, since extrapolations beyond these limits may lead to absurd results. The constants A, B, and C form a set. It is recommended never to use one constant from one tabulation and other constants from different tabulation. Usually, in the

range of 0.01–2 bar, the Antoine equation provides an excellent correlating equation for vapor pressures *(15)*. When Antoine parameters are determined from data in this pressure range (as they usually are), the equation underpredicts vapor pressure at higher pressures.

For the systems studied in the present work, these constants are not available. However, a graphic is available that depicts the vapor pressure curve of fitosterols and tocopherols *(16)*. From this graphic, the constants *A*, *B*, and *C* of the Antoine equation were obtained. These values were introduced in the DISMOL simulator.

Characteristics of Mixture

Liquid Density

Even if no data are available, there are a number of techniques for estimating specific volumes or densities of pure liquid. An equation to estimate saturated volumes that was developed by Rackett and later modified by Spencer and Danner *(15)* is as follows:

$$V_S = \frac{RT_c}{P_c}\left\{Z_{RA}^{\left[1+\left(1-T_r\right)^{2/7}\right]}\right\} \tag{8}$$

in which Z_{RA} is a unique constant for each component. If a value of Z_{RA} is not available, it may be estimated by $Z_{RA} = 0.29056 - 0.08775\omega$.

Since $\rho = m/v$, Eq. 9 can be written as follows:

$$\rho_{eb} = \frac{MP_c}{RT_c\left\{Z_{RA}^{\left[1+\left(1-T_r\right)^{2/7}\right]}\right\}} \tag{9}$$

It is possible to correlate the density of a pure compound at any temperature through the Mathias' equation, with a maximum error of 2% *(14)*:

$$\rho = \rho_{eb}\left(\frac{2T_c - T}{2T_c - T_{b_r}}\right) \tag{10}$$

Mixing rules for both the modified Rackett and Hankinson equations have been published and are given below. The modified Rackett equation *(15)* for mixtures at their bubble points is

$$V_m = R\left(\sum_i \frac{x_i T_{ci}}{P_{ci}}\right) Z_{RA_m}^{\left[1+\left(1-T_r\right)^{2/7}\right]} \tag{11}$$

or, as shown in Perry and Green *(17)*

$$\rho_{eb} = \frac{P_{c,m}}{RT_{c,m}\left\{Z_{RA,m}^{\left[1+\left(1-T_{r,m}\right)^{2/7}\right]}\right\}}$$

in which

$$Z_{RA,m} = \sum_i x_i Z_{RA_i}; P_{c,m} = \sum_i x_i P_{c_i}; T_{c,m} = \sum_i x_i T_{c_i}; T_r = T/T_{cm};$$

M is the molecular weight (g/gmol); P_c is the critical pressure (bar); $P_{c,m}$ is the mixture critical pressure (bar); V_c is the critical volume (cm^3/mol); R is the universal gas constant (bar·cm^3/mol·K); T_c is the critical temperature (K); $T_{c,m}$ is the mixture critical temperature (K); T_b is the liquid temperature at its boiling point (K); Z_{RA} is the Rackett compressibility factor; T_r is the reduced temperature; x_i is the mole fraction of the component i; ρ is the liquid density (g/mL); ρ_{eb} is the liquid density at its boiling point (g/mL); ρ_i is the density of the component i (g/mL); ρ_m is the density of the liquid mixture (g/mL); and ω is the acentric factor.

Heat Capacity

Estimation methods applicable for liquid heat capacities fall into four general categories: theoretical, group contribution, corresponding states, and Watson's thermodynamic cycle. An assumption is made that various groups in a molecule contribute with a value to the total molar heat capacity, which is independent of other groups present.

Chueh and Swanson *(15)* have proposed values for different molecular groups to estimate molar liquid heat capacity, *Cp*, at room temperature (T = 293 K). This method is accurate and more general. Errors for the Chueh-Swanson method rarely exceed 2 to 3%:

$$Cp = \sum \Delta_{Cp} \tag{12}$$

in which Δ_{Cp} is the group contribution for the Chueh-Swanson method (J/mol·K).

For temperatures other than 20°C, the equation of Watson must be used *(14)*:

$$\frac{Cp_2}{Cp_1} = \left(\frac{W_1}{W_2}\right)^{2.8} \tag{13}$$

in which $W = 0.1745 - 0.0838T_r$.

For calculating the heat capacity of a liquid mixture, the following expression can be used *(14)*:

$$Cp_m = \sum \left(X_i\, Cp_i\right) \tag{14}$$

in which *Cp* is the heat capacity (J/mol·K); Cp_i is the heat capacity of the component i (J/mol·K); Cp_m is the heat capacity of the mixture (J/mol·K); T_r is the reduced temperature; W is the expansion factor of the liquid phase; X_i is the mass fraction of component i; 1 is temperature 1 (normally 20°C, reference temperature); and 2 is temperature 2 (operation temperature).

Thermal Conductivity

All estimation techniques for the thermal conductivity of pure liquids are empirical, and with only limited examination, they often appear rather accurate. Below the normal boiling point, the thermal conductivities of most organic, nonpolar liquids lie between 0.10 and 0.17 W/(m·K). With this fact in mind, it is not too difficult to devise various schemes for estimating λ_L within this limited domain. Sato *(15)* suggested that at the normal boiling point (Eq. 15)

$$\lambda_L\left(T_b\right) = \frac{1.11}{M^{1/2}} \tag{15}$$

in which λ_L (T_b) is the thermal conductivity of the liquid at the normal boiling point (at 1 atm) (W/[m·K]) and M is the molecular weight (g/mol).

To estimate λ_L at other temperatures, the Riedel *(15)* equation may be used:

$$\lambda_L = B\left[3 + 20\left(1 - T_r\right)^{2/3}\right] \tag{16}$$

Thus, by combining Eqs. 15 and 16, the thermal conductivity of a pure liquid can be estimated, with a maximum mean error of 20%, as described in Eq. 17:

$$\lambda_L = \frac{\left(\frac{1.11}{M^{1/2}}\right)\left[3 + 20\left(1 - T_r\right)^{2/3}\right]}{3 + 20\left(1 - T_{b_r}\right)^{2/3}} \tag{17}$$

The thermal conductivities of most mixtures of organic liquids are usually less than those predicted by either a mole or weight fraction average, although the deviations are often small *(15)*. Then, it can be calculated through the following expression *(14)*, with errors of about 4%:

$$\lambda_m = \Sigma\left(x_i \lambda_i\right) \tag{18}$$

in which M is the molecular weight (g/gmol); T_{b_r} is equal to T_b/T_c (reduced normal boiling temperature); T_r is the reduced temperature; x_i is the mole fraction of the component i; λ_L is the thermal conductivity (W/m·K); λ_i is the thermal conductivity of the component i (W/m·K); λ_m is the thermal conductivity of the liquid mixture (W/m·K).

Viscosity

The viscosity of a pure liquid can be determined as a function of the temperature when there are two or more values of viscosity for determining the constants A and B. The Guzman-Andrade equation *(14)*, presents maximum errors of 2%:

$$\eta = Ae^{B/T} \tag{19}$$

in which A is a characteristic constant of a substance, to be adjusted; B is a characteristic constant of a substance, to be adjusted; and T is the temperature (K).

The empirical equation of Kendall-Monroe is the best for calculating mixture viscosity *(14)*:

$$\eta_m^{1/3} = \Sigma X_i \eta_i^{1/3} \tag{20}$$

in which X_i is the mass fraction of the component i; η_i is the viscosity (cP); and η_m is the mixture viscosity (cP). This equation should not be used if $T_r > 0.75$.

Simulation Results of Falling Film Molecular Distillation Unit

Study of Tocopherols and Phytosterols from Crude DDSO

Figures 2 to 7 present simulation results of the quantity recovered of each component (except fatty acids) in the liquid and vapor phases in relation to its quantity in the feed stream (%) vs the operating temperature (°C) for feed flow rates ranging from 0.5 to 1.0 kg/h using the DISMOL simulator. Since fatty acids are the most volatile components and are recovered first at a lower temperature (approx 125°C), they were omitted in order to facilitate understanding the obtained results. By increasing the temperature, it is possible to recover tocopherols in the vapor phase with the diglyceride and the squalene. Phytosterols are recovered in the liquid phase, also called residue. Thermal decomposition was not calculated because, in these cases, it is very small.

It can be observed in Fig. 2 that for a feed flow rate of 0.5 kg/h and temperature of 170°C, the tocopherols were almost 100% recovered in the vapor phase (also called distillate). When the operating temperature was increased to 180°C (10°C above), part of the phytosterols began to be recovered in the vapor phase too; however, this is not of interest because at this temperature the phytosterols start to distillate and this reduces the purity of tocopherol. It was also observed that by increasing the feed flow rate from 0.5 to 1.0Kg/h (100%) (Figs. 2–7), a lower quantity of phytosterols was recovered in the vapor phase at 180°C.

The main objective of our study wasto recover tocopherols, but it is also possible to recover phytosterols, which are products with high added value, since they are used for the formulation of margarine and the syntheses of sexual hormones.

In addition, it was found that the higher the feed flow rate, the higher the required operating temperature to recover the same quantity of tocopherols (Figs. 2–7). Furthermore, for temperatures lower than 160ºC, practically all phytoesterols remained in the liquid phase (residue stream). It is also verified that tocopherols and diglycerides have similar behaviors, which implies that in the final product this mixture is obtained. Regarding tocopherol recovery (in the vapor phase), the best operating temperature was near 170ºC (feed flow rate = 0.6 kg/h); above this temperature, the problem of thermal decomposition can arise. Above a feed flow rate of 0.6 kg/h, the recovery decreases.

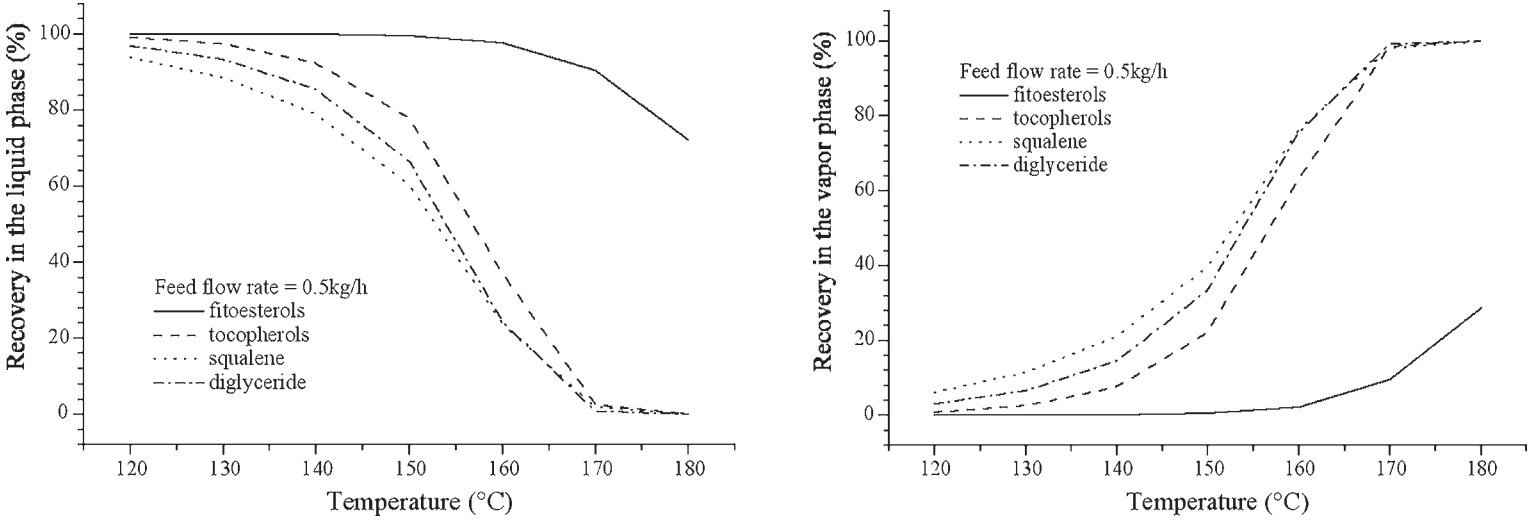

Fig. 2. Recovery of components in liquid and vapor phases in relation to quantity in feed vs temperature for feed flow rate of 0.5 kg/h.

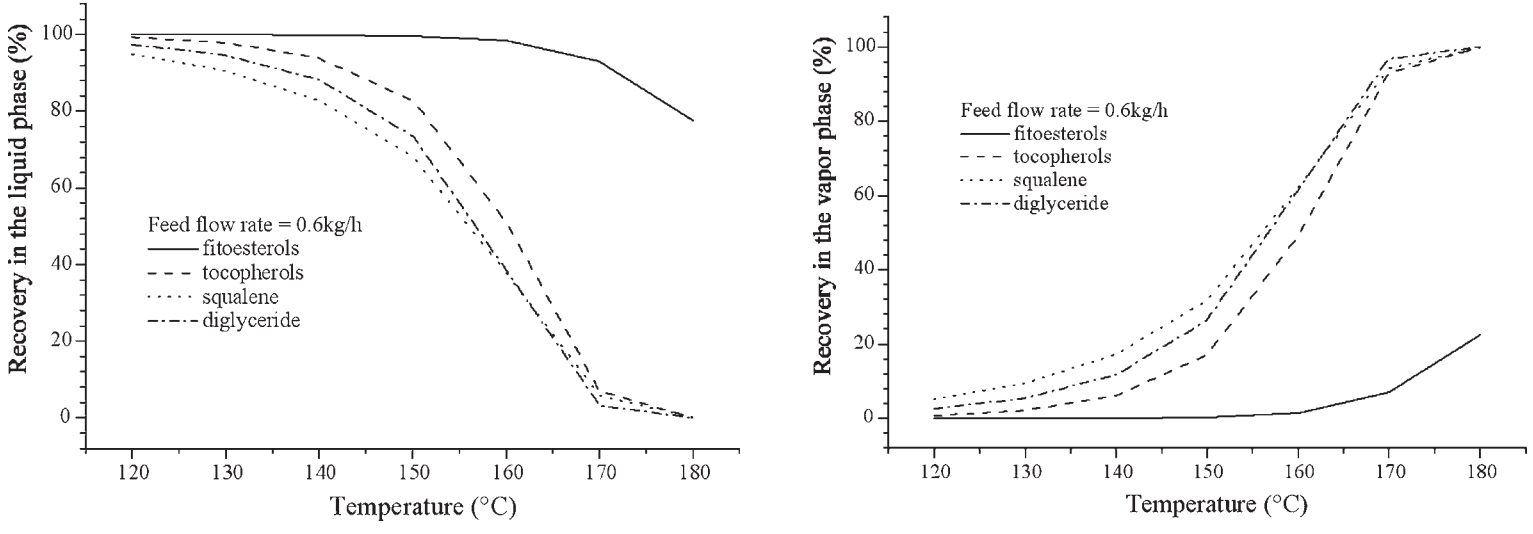

Fig. 3. Recovery of components in liquid and vapor phases in relation to quantity in feed vs temperature for feed flow rate of 0.6 kg/h.

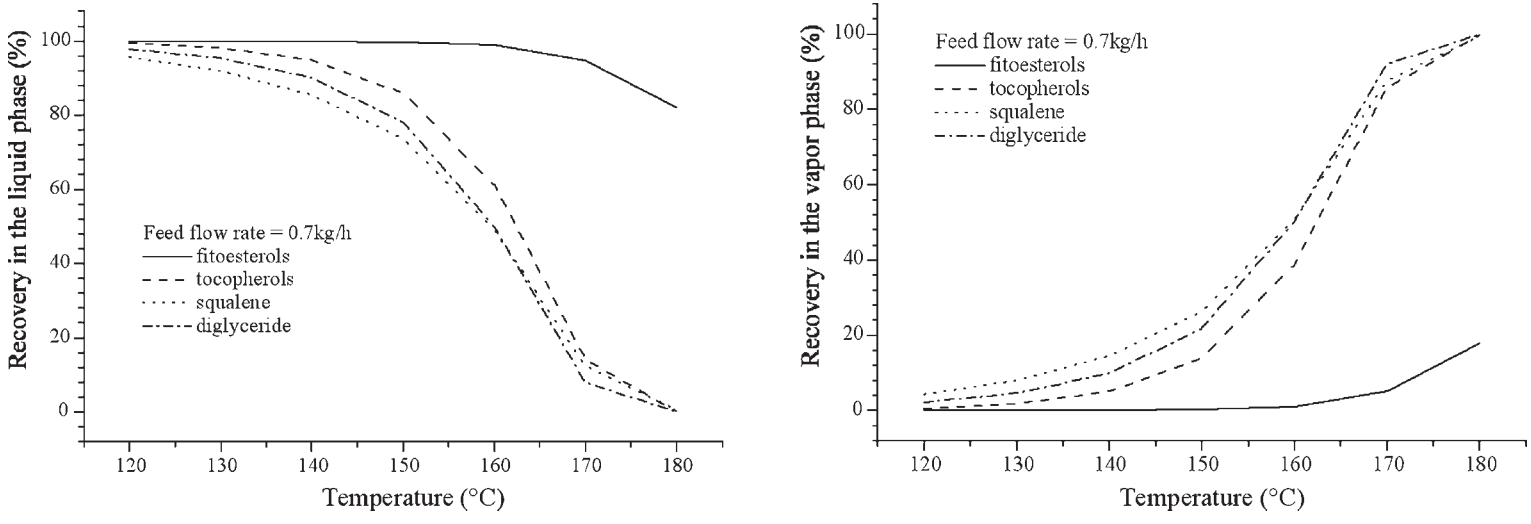

Fig. 4. Recovery of components in liquid and vapor phases in relation to quantity in feed vs temperature for feed flow rate of 0.7 kg/h.

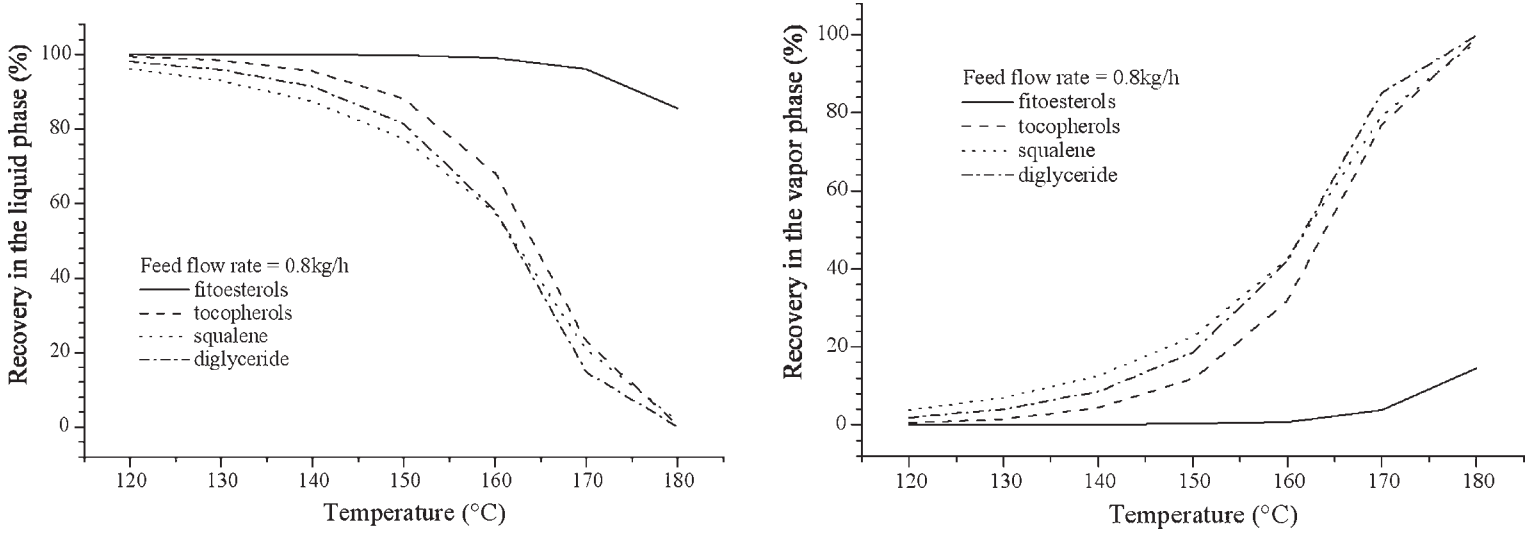

Fig. 5. Recovery of components in liquid and vapor phases in relation to quantity in feed vs temperature for feed flow rate of 0.8 kg/h.

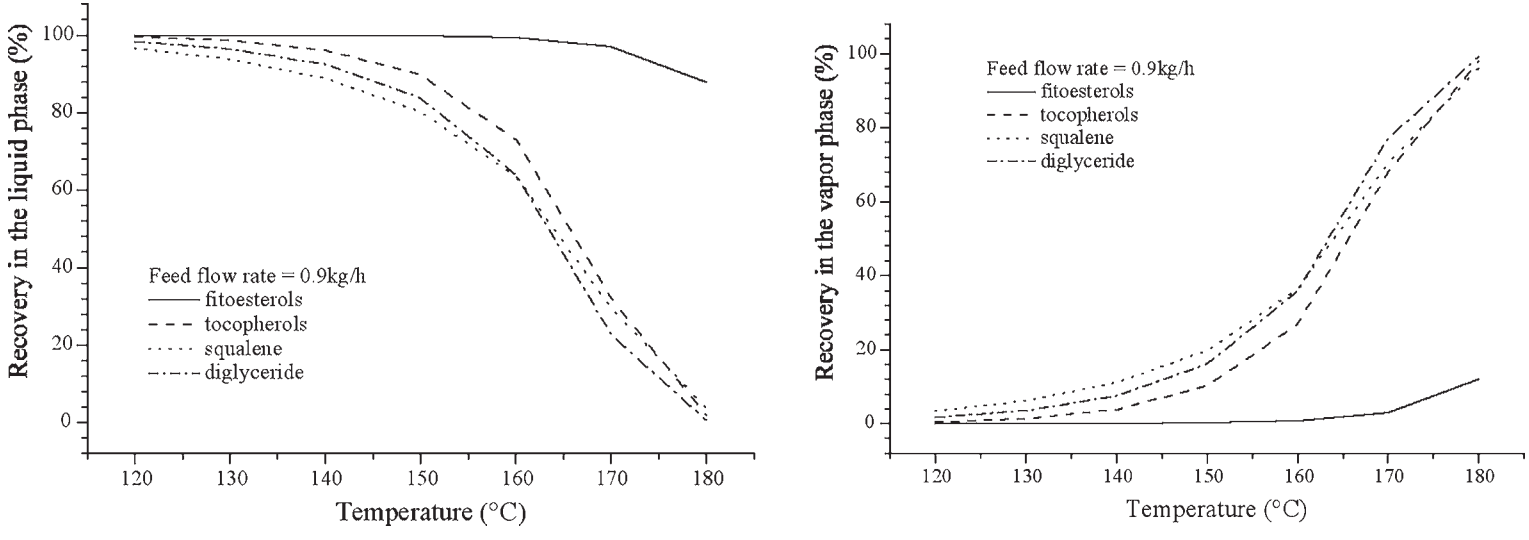

Fig. 6. Recovery of components in liquid and vapor phases in relation to quantity in feed vs temperature for feed flow rate of 0.9 kg/h.

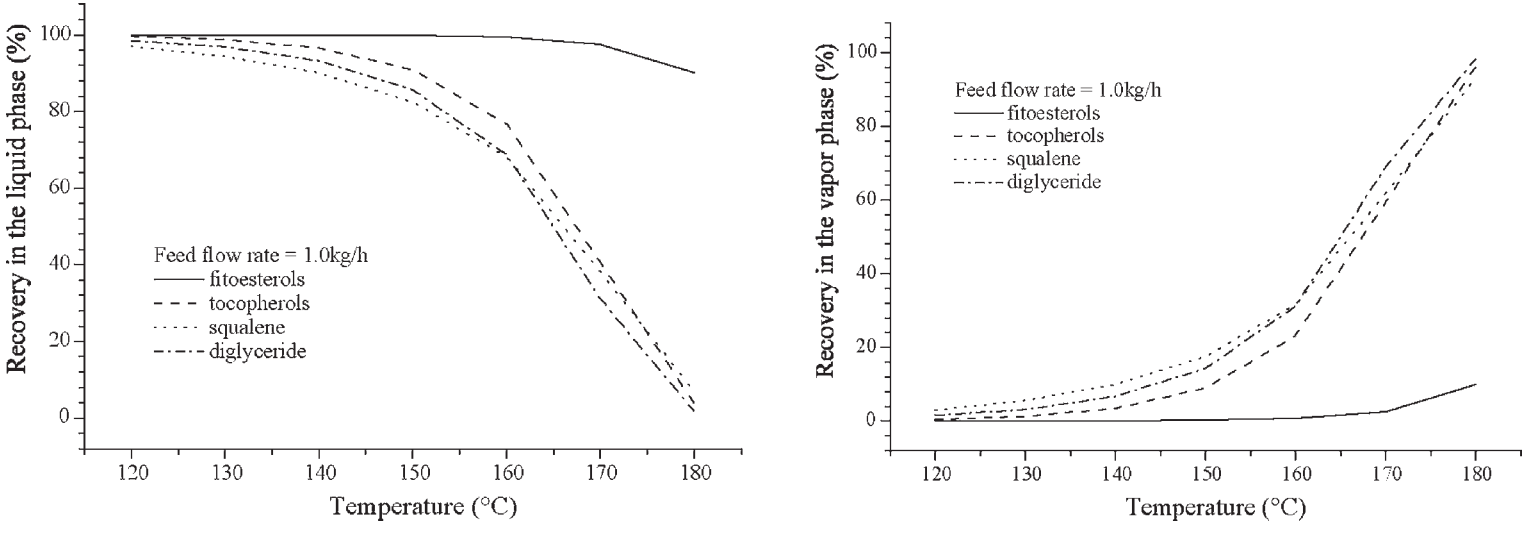

Fig. 7. Recovery of components in liquid and vapor phases in relation to quantity in feed vs temperature for feed flow rate of 1.0 kg/h.

Study of Tocopherol Concentration as Function of Distance Covered on Evaporator

Figures 8–10 show the curves of tocopherol concentration in the residue (% w/w) vs the percentage of the distance on the evaporator (from the feed point) for feed flow rate ranging from 0.5 to 1.0 kg/h for the falling film molecular distillation unit. The initial tocopherol concentration was 8.50% (w/w). For a feed flow rate of 0.5 kg/h (Fig. 8), it can be observed that at the end of the distillation, the tocopherol concentration in the residue will be higher, at 150°C (about 15% [w/w]). At 160°C, at 80% of the distillation, the tocopherol concentration reaches a maximum and then decreases, because the tocopherols are already recovered in the vapor phase. Figures 8–10 show that by increasing the feed flow rate at the same temperature (160°C), the tocopherol concentration can increase until it doubles the initial concentration (for a feed flow rate of 0.6 kg/h). From this point, it decreases, requiring an increase in the temperature to concentrate more (for a feed flow rate of 1.0 kg/h at 170°C). For all feed flow rates (Figs. 8–10), at 180°C, practically all the tocopherols are found in the vapor phase. With this study, it is possible to observe which temperature is the best in order to recover the fatty acids (first step = ±125°C) and, then, recover the tocopherols in the vapor phase (distillate) and the phytosterols in the liquid phase (residue) (second step = ±170°C). At the lowest temperature (120°C) the tocopherol recovery was minimum (about 5%). By increasing the feed flow rate from 0.5 to 1.0 kg/h (100%), the quantity of tocopherol in the residue at 170°C, e.g., increases, which means that the process performance has decreased.

Conclusion

The DISMOL simulator is a powerful tool for calculating the feasibility and performance of a process, as well as for identifying the best operating conditions to carry out the experiments. This means that it is possible to identify the operating conditions for recovering a large quantity of tocopherol. According to the results, a temperature of about 170°C and a feed flow rate of about 0.6 kg/h are the best operating conditions for the considered equipment. Simulation can result in a substantial reduction in the experimental time, process development, and optimization. The procedure for estimating the properties for complex systems is of crucial importance.

The results show that the feed flow rate and the temperature can be adequately chosen in order to obtain total tocopherol recovery. In addition, the behavior of the tocopherols on the evaporator as a function of the temperature and feed flow rate can be verified. In future works, the validation of the model and of the simulation will be demonstrated.

Acknowledgment

We are grateful to Fundação de Amparo à Pesquisa do Estado de São Paulo for financial support (scholarship) for this project (99/04656-9).

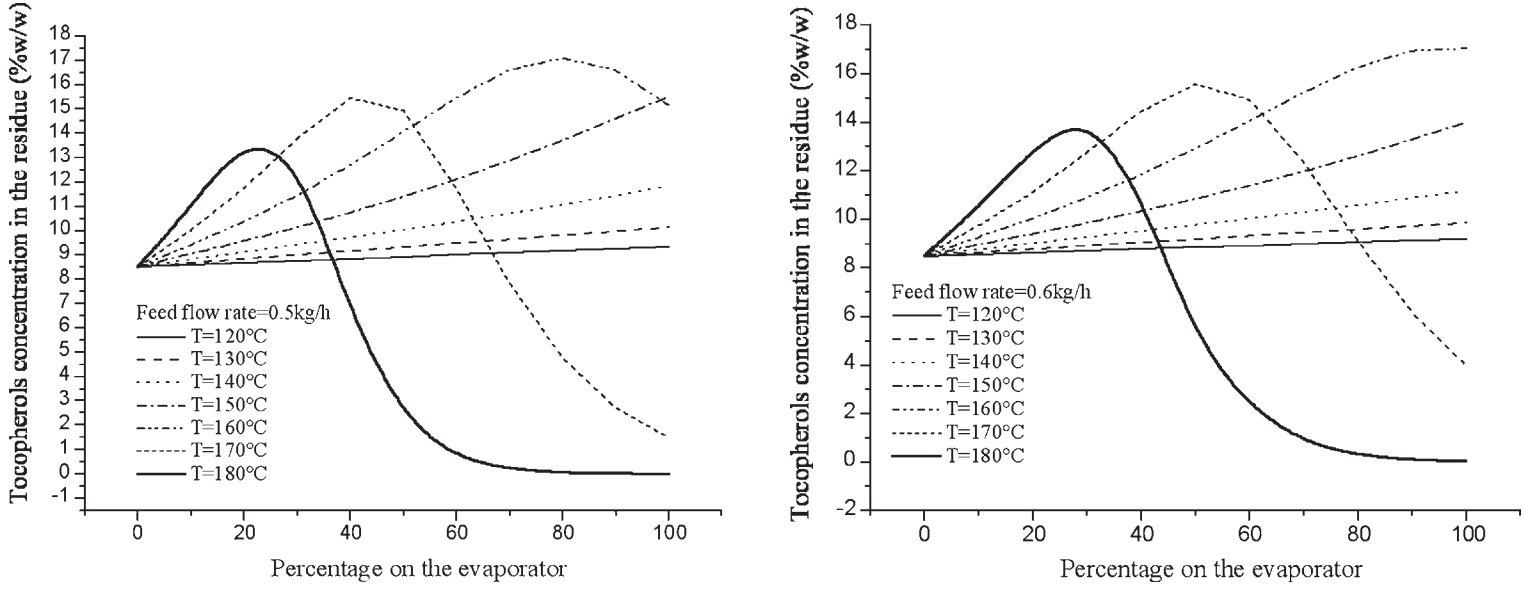

Fig. 8. Tocopherol concentration in residue vs distance covered on evaporator (%) for feed flow rate of **(A)** 0.5 and **(B)** 0.6 kg/h.

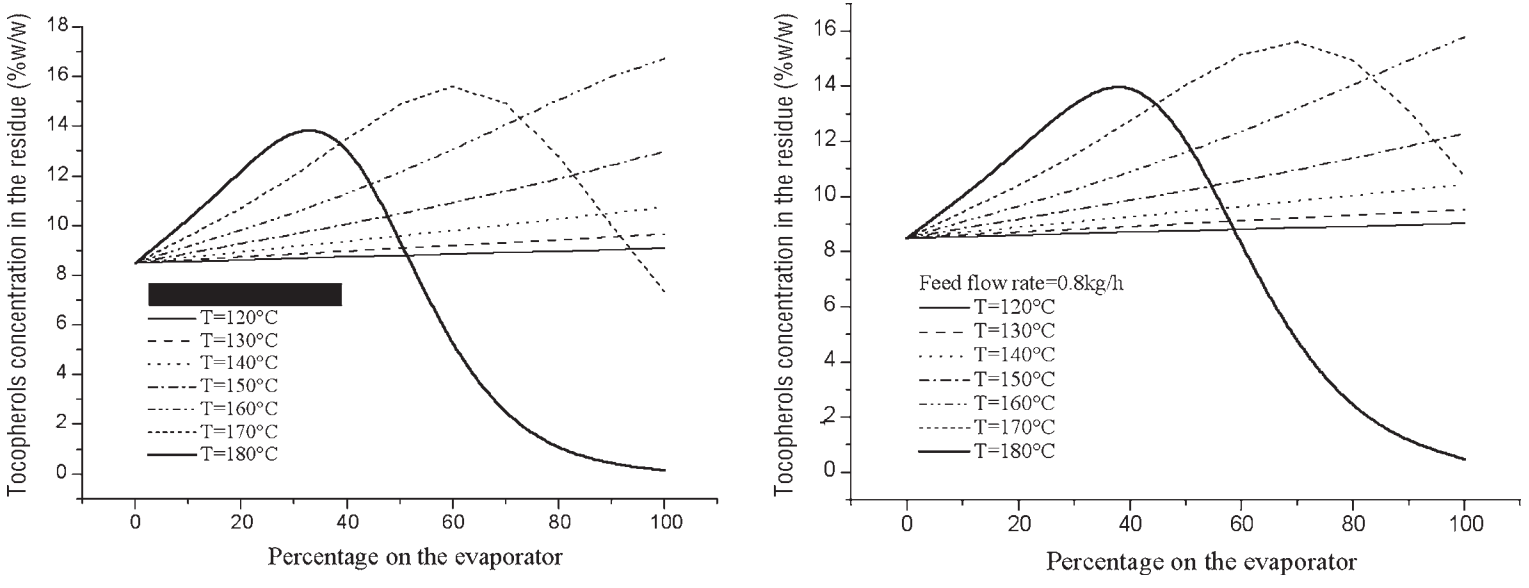

Fig. 9. Tocopherol concentration in residue vs distance covered on evaporator (%) for feed flow rate of **(A)** 0.7 and **(B)** 0.8 kg/h.

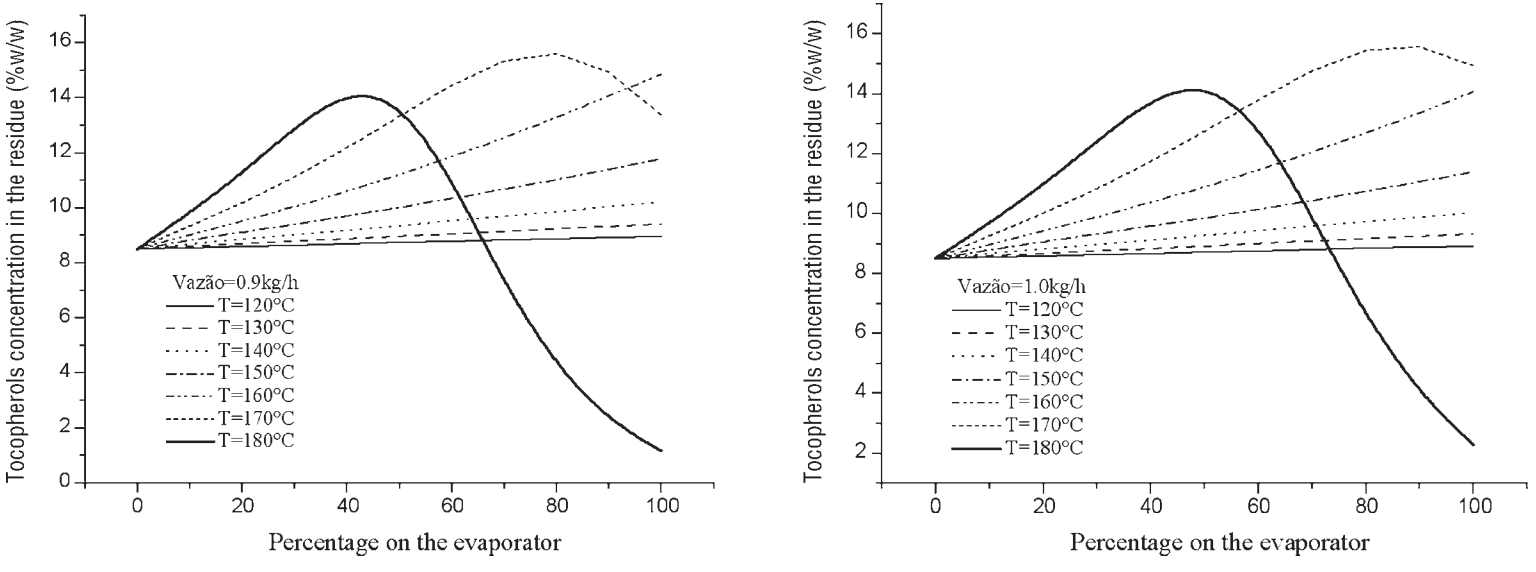

Fig. 10. Tocopherol concentration in residue vs distance covered on evaporator (%) for feed flow rate of **(A)** 0.9 and **(B)** 1.0 kg/h.

References

1. Cvengros J., Lutisan, J., and Micov, M. (2000), *Chem. Eng. J.* **78,** 61–67.
2. Batistella C. B. and Maciel, M.R.W. (1998), *Comput. Chem. Eng.* **22(Suppl.),** S53–S60.
3. Batistella, C. B., Moraes, E. B., Maciel Filho, R., and Maciel, M. R. W. (2002), *Appl. Biochem. Biotechnol.* **98(1–3),** 1187–1206.
4. Batistella, C. B., Moraes, E. B., Maciel Filho, R., and Maciel, M. R. W. (2002), *Appl. Biochem. Biotechnol.* **98(1–3),** 1149–1159.
5. Batistella C. B. and Maciel, M. R. W. (1996), *Comput. Chem. Eng.* **20(Suppl.),** S19–S24.
6. Batistella, C. B., Moraes, E. B., and Maciel, M. R. W. (1999), *Comput. Chem. Eng.* **(Suppl.),** S767–S770.
7. Batistella, C. B., Maciel, M. R. W., and Maciel Filho, R. (2000), *Comput. Chem. Eng.* **24(2–7),** 1309–1315
8. Maciel Filho, R., Wolf-Maciel, M. R., and Batistella, C. B. (2001), FRAMOL Project, UNICAMP/CENPES/PETROBRAS/FINEP.
9. Winters, R. L. (1990), in *World Conference Proceedings, Edible Fats and Oils Processing, Basic Principles and Modern Practices*, David, R., ed., American Oil Chemists' Society, Champaign, IL, pp. 402–405.
10. Winters, R. L (1986), in *Proceedings of the World Conference on Emerging Technologies in the Fats and Oils Industry*, Baldwin, A. R., ed., American Oil Chemists' Society, Champaign, IL, pp. 184–188.
11. Ramamurthi S. and McCurdy, A. (1993), *JAOCS* **70(3),** 287–295. *12*. Batistella C. B. (1996), MS thesis, UNICAMP, Campinas, SP, Brazil.
13. Augusto, M. M. M. (1988), MS thesis, UNICAMP, Campinas, SP, Brazil.
14. Perry, R. H. and Chilton, C. H. (1980), *Manual de Engenharia Química*, Seção 13, Ed. Guanabara II, Rio de Janeiro, RJ, Brazil.
15. Reid, R. C., Prausnitz, J. M., and Poling, B. E. (1987), *The Properties of Gases and Liquids*, McGraw-Hill, New York, NY.
16. Erickson, D. R. (1995), in *Practical Handbook of Soybean Processing and Utilization*, AOCS Press, Champaign, IL, and United Soybean Board, St. Louis, MO, pp. 203–217, 307.
17. Perry, R. H. and Green, D. (1984), *Perry's Chemical Engineers' Handbook*, 6th Ed., McGraw-Hill, Malaysia.

0273-2289/04/114/0713–0721/$25.00

High-Productivity Continuous Biofilm Reactor for Butanol Production

Effect of Acetate, Butyrate, and Corn Steep Liquor on Bioreactor Performance

Nasib Qureshi,*[,1] Patrick Karcher,[2] Michael Cotta,[1] and Hans P. Blaschek[2]

[1]United States Department of Agriculture,[†] National Center for Agricultural Utilization Research, Fermentation Biotechnology, 1815 N. University Street, Peoria, IL 61604, E-mail: qureshin@ncaur.usda.gov; and [2]University of Illinois, Biotechnology & Bioengineering Group, Department of Food Science & Human Nutrition, 1207 W. Gregory Drive, Urbana, IL 61801

Abstract

Corn steep liquor (CSL), a byproduct of the corn wet-milling process, was used in an immobilized cell continuous biofilm reactor to replace the expensive P2 medium ingredients. The use of CSL resulted in the production of 6.29 g/L of total acetone-butanol-ethanol (ABE) as compared with 6.86 g/L in a control experiment. These studies were performed at a dilution rate of 0.32 h^{-1}. The productivities in the control and CSL experiment were 2.19 and 2.01 g/(L·h), respectively. Although the use of CSL resulted in a 10% decrease in productivity, it is viewed that its application would be economical compared to P2 medium. Hence, CSL may be used to replace the P2 medium. It was also demonstrated that inclusion of butyrate into the feed was beneficial to the butanol fermentation. A control experiment produced 4.77 g/L of total ABE, and the experiment with supplemented sodium butyrate produced 5.70 g/L of total ABE. The butanol concentration increased from 3.14 to 4.04 g/L. Inclusion of acetate in the feed medium of the immobilized cell biofilm reactor was not found to be beneficial for the ABE fermentation, as reported for the batch ABE fermentation.

Index Entries: Immobilized cell biofilm reactor; butanol; corn steep liquor; sodium butyrate; *Clostridium beijerinckii* BA101; sodium acetate.

[†]Names are necessary to report factually on available data. However, the USDA neither guarantees nor warrants the standard of the product, and the use of the names by USDA implies no approval of the product to the exclusion of others that may also be suitable.

*Author to whom all correspondence and reprint requests should be addressed.

Introduction

Butanol, an industrially important chemical, can be produced by fermentation of carbohydrates using various solventogenic clostridia. In fact, this fermentation was commercially viable until after World War II when petrochemically produced butanol became available at competitive prices *(1)*. For several reasons, including fluctuating oil prices and the depletion of oil reserves, intensive research efforts on this fermentation have been made. Recent technological developments including the development of superior cultures, productive reactors, and efficient downstream processing have once again made this fermentation attractive. Although these developments are encouraging, certain problems, such as the use of economical substrates, need to be resolved before this fermentation will be able to become commercially viable.

The use of continuous immobilized cell biofilm reactors eliminates downtime and hence results in superior reactor productivity *(2,3)*. Adsorbed cell continuous biofilm reactors have been shown to favorably affect process economics *(4)*. Application of these reactors reduces capital and operational cost, thus making the process simpler. Within these reactors, cells are immobilized by adsorption, which is a simpler technique than other techniques such as entrapment and covalent bonding *(5)*. Adsorption is a simple technique and can be performed inside the reactors without the use of chemicals, whereas entrapment and covalent bonding are complicated techniques and require chemicals for bond formation. In anaerobic systems, such as butanol production, adsorption can be performed anaerobically within the reactor. An additional advantage of adsorption is that cells form uniform biofilm layers around the support, which lessens diffusion resistance compared to entrapped and covalently bonded cells. Hence, these reactors are called biofilm reactors. Because of reduction in diffusion resistance, the reaction rate is enhanced. For this reason, adsorption was chosen as the technique to be employed for *Clostridium beijerinckii* BA101 cell immobilization to produce butanol. In addition to being simple, it has the potential to be used in large-scale reactors. In the present study, clay brick was chosen as the cell adsorption support. It is available at a low cost and is easy to dispose of after use.

The previous cited studies were performed using P2 medium, which is composed of expensive chemicals such as biotin, thiamin, and yeast extract. The use of these chemicals at the commercial level would not be commercially viable. Hence, it is suggested that the use of cheaper and simpler nutrient sources be investigated. The use of corn steep liquor (CSL) has been reported in pilot plant trials for butanol batch production employing *C. beijerinckii* BA101 *(6)*. CSL is a byproduct of the corn wet-milling process and contains nutrients leached out of corn during the soaking process. The reader is advised that there are few studies on the use of CSL in continuous immobilized cell biofilm reactors. Similarly, the use of exogenous sodium butyrate and sodium acetate has not been reported in continuous immobilized cell biofilm reactors. Hence, these studies are

considered novel. The successful application of CSL, sodium butyrate, and sodium acetate is expected to benefit the economics of butanol production by fermentation.

One objective of the present study was to examine the effect of CSL on the performance of high-productivity biofilm reactors. Another objective was to study the effect of supplementing acetate and butyrate into the feed of the biofilm reactor. Supplementation of acetate to the feed medium of batch reactors (not continuous biofilm reactors) has been shown to be beneficial to this fermentation. It is also anticipated that butyrate added to the feed would be converted to butanol.

Materials and Methods

Organism and Culture Maintenance

For fermentation studies, the microorganism used was the *C. beijerinckii* BA101 hyperbutanol-producing strain *(7)*. Laboratory stocks of *C. beijerinckii* BA101 were routinely maintained as spore suspensions in sterile double-distilled water at 4°C. *C. beijerinckii* BA101 spores (200 µL) were heat shocked in 50 mL of cooked meat medium (CMM) for 10 min at 80°C followed by cooling in ice-cold water. Pyrex bottles (100-mL volume) containing heat-shocked spores were incubated anaerobically for 15 to 16 h at 36 ± 1°C before inoculating the reactor.

Fermentation Media

The feed medium contained glucose (60 g/L), yeast extract (Difco, Detroit, MI) (1 g/L), and P2 medium ingredients (buffer, minerals, and vitamins) *(8)* unless stated otherwise. Glucose and yeast extract solutions were sterilized separately at 121°C for 15 min followed by cooling to room temperature by sweeping oxygen-free N_2 gas across the surface of the medium. Stock solutions of buffer, mineral, and vitamins were added aseptically to the cooled glucose-yeast extract solution. The stock solutions were filter sterilized through a 0.2-µm filter. The medium was kept anaerobic by continuously sweeping oxygen-free N_2 across the surface. When needed, sodium butyrate or sodium acetate solutions were added to the P2 feed medium. The pH of the feed medium was adjusted to 6.8 prior to autoclaving.

Thirty-two grams of CSL (500 g/L of solids slurry) was added to each liter of CSL medium. The composition of CSL has been given elsewhere *(9)*. The CSL was dissolved in approx 300 mL of water and boiled for 30 min. After cooling to room temperature, the mixture was centrifuged to remove solids. To the supernatant, 60 g of glucose was added and the volume adjusted to 950 mL with water. The pH of the feed solution was adjusted to 6.8 prior to autoclaving at 121°C for 15 min. The autoclaved medium or solutions were cooled anaerobically by sweeping oxygen-free N_2 gas across the surface. One gram of cysteine hydrochloride was dissolved in 25 mL of water and filter sterilized (0.2 µm) before aseptically adding to the cooled

CSL medium. Twenty-five milliliters of $FeSO_4 \cdot 7H_2O$ (0.012 g) solution was made in water followed by filter sterilization (0.2 μm) and adding to the CSL medium. $FeSO_4 \cdot 7H_2O$ is an essential mineral for solventogenesis and was included in both P2 and CSL media. The CSL medium was fed to the reactor.

Bioreactor and Cell Immobilization

The reactor was composed of a 312-mL total volume jacketed polyacrylic (192 × 46 mm) vessel. The reactor was sterilized using 30% (v/v) ethanol solution for 48–72 h, after which it was drained and washed thoroughly with sterilized deionized water. Brick pieces (4 to 5 mm, total weight of 220 g) were washed with deionized water several times followed by sterilization in an oven at 250°C for 2 h. The particles were then cooled in an anaerobic chamber to room temperature. The void volume inside the reactor was 186 mL. The reactor was packed aseptically with the sterilized brick particles. After the reactor was packed, oxygen-free N_2 was passed through the column overnight. This was done to ensure that anaerobic conditions were attained inside the column and inside the particles.

Forty milliliters of actively growing *C. beijerinckii* cells from a CMM bottle were inoculated into the reactor, and the reactor was filled with fresh P2 medium. The composition of P2 medium has been published elsewhere *(8)*. Cell growth was allowed inside the reactor for 4 h, after which the P2 medium was continuously fed (using a peristaltic pump [Cole-Parmer, Vernon Hills, IL] and silicone tubing) at a flow rate of 92 mL/h (dilution rate of 0.29 h^{-1}). Water (35°C) was circulated through the jacket of the column to control temperature using a circulating water bath (Polystat; Cole-Parmer). Samples were taken after 3 d. The dilution rate was altered whenever a steady state was reached in terms of average solvent production and glucose utilization. Samples were collected over a period of five to seven steady-state residence times, with a sampling frequency of one residence time. Samples were centrifuged at 16,000*g* for 1 to 2 min. The supernatant was stored at –18°C in preparation for acetone, butanol, ethanol, and glucose analysis. Comparisons of the media were made in the same reactor (not in parallel reactors). The pH of the reactor effluents was not measured. The reader is advised that the pH inside the bioreactor was not controlled. Solventogenic clostridia regulate pH at approx 5.0. A schematic diagram of the reactor is shown in Fig. 1.

Analyses

Cell concentration in the reactor effluent was estimated by optical density (OD) and cell dry weight method using a predetermined correlation between OD at 540 nm and cell dry weight. Acetone-butanol-ethanol (ABE) and acids (acetic and butyric) were measured using a 6890 Hewlett-Packard gas chromatograph (Hewlett-Packard, Avondale, PA) equipped with a flame ionization detector and 6 ft × 2 mm glass column (10% CW-20M, 0.01% H_3PO_4, support 80/100 Chromosorb WAW). Productivity was calcu-

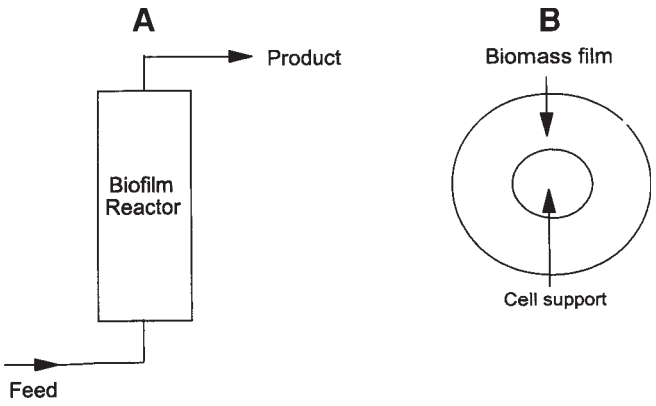

Fig. 1. Schematic diagram of butanol production in an immobilized cell biofilm reactor using *C. beijerinckii* BA101: **(A)** bioreactor; **(B)** biofilm particle of *C. beijerinckii* BA101.

lated as the average ABE concentration multiplied by dilution rate (h^{-1}). Dilution rate was defined as feed flow rate per reactor volume and is based on the total volume of the reactor. ABE yield was defined as grams of ABE produced per gram of glucose utilized.

Glucose concentration was determined using a hexokinase- and glucose-6-phosphate dehydrogenase– (Sigma, St. Louis, MO) coupled enzymatic assay. The fermentation broth was centrifuged (microfuge centrifuge) at 16,000*g* for 3 min at 4°C. A portion of the supernatant (10 µL) was mixed with glucose (HK) 20 reagent (1.0 mL) and incubated at room temperature for 5 min. Standard solutions of anhydrous D-glucose containing 1–5 g of glucose/L of distilled water were prepared. Ten microliters of each of the standard solutions was mixed with glucose (HK) 20 reagent (1.0 mL) and incubated at room temperature for 5 min. A blank (deionized water) (10 µL) was incubated with the reagent and used for zero adjustment of the spectrophotometer. After 5 min, the absorbance was measured at 340 nm using a Beckman DU 640 spectrophotometer, and the glucose content in the sample was computed by least squares linear regression using a standard curve.

Results and Discussion

Our previous biofilm reactor studies suggested that basal medium (1 g/L of yeast extract + 60 g/L of glucose) was a poor nutrient medium and did not promote good solventogenesis *(5)*. The reactor fed with this medium produced 3.75 g/L of total solvents compared with 11.90 g/L using P2 medium. This indicated that P2 or CSL medium may be required in this reactor design in order to produce solvents. As a result of those studies, the following studies were performed using P2 or CSL medium.

Table 1
Effect of CSL, Butyrate (NaBu), and Acetate (NaAc) on Butanol Production in Immobilized Cell Biofilm Reactor of *C. beijerinckii* BA101

Fermentation parameters and products	Dilution rate (0.32 h^{-1})					
	CSL		Butyrate		Acetate	
	Control	CSL	Control	NaBu [a]	Control	NaAc [b]
Acetone (g/L)	2.61	2.00	1.51	1.55	3.20	2.44
Butanol (g/L)	4.12	4.16	3.14	4.04	5.76	3.49
Ethanol (g/L)	0.13	0.13	0.12	0.11	0.16	0.12
Acetic acid (g/L)	1.83	1.84	0.42	2.70	0.40	2.45
Butyric acid (g/L)	0.53	0.45	1.14	0.85	0.73	1.83
Total ABE (g/L)	6.86	6.29	4.77	5.70	9.12	6.05
Total acids (g/L)	2.36	2.29	1.56	3.55	1.14	4.28
Glucose in feed (g/L)	65.50	67.50	59.10	59.70	64.40	64.40
Glucose utilization (%)	39.10	30.50	29.40	35.20	40.00	38.00
ABE Yield (g/g)	0.27	0.30	0.50	0.27	0.35	0.22
Productivity (g/(L·h])	2.19	2.01	1.53	1.82	2.92	1.94

[a] 2.5 g/L of butyrate added.
[b] 6.56 g/L (80 m*M*) of acetate added.

Initially the reactor was fed at 92 mL/h (dilution rate of 0.29 h^{-1}) with P2 medium until there were visible signs of cell mass accumulation. It took about 5 d to accumulate cell mass and for the reactor to be productive. The flow rate was then increased to 100 mL/h, and the reactor was allowed to achieve a new steady state. At this stage, a control experiment was run and the reactor was fed with P2 medium. At this dilution rate (0.32 h^{-1}), the reactor produced 6.86 g/L of total ABE and 2.36 g/L of total acids (Table 1). This resulted in an ABE productivity of 2.19 g/(L·h) and a yield of 0.27. This productivity is manyfold higher than the productivity achieved in a batch reactor (0.38 g/[L·h]) *(10)*. Glucose utilization was 39.1% of that available in the feed (65.5 g/L). In these reactors, high productivity is achieved but at the expense of a low ABE concentration in the effluent as well as low sugar utilization. To improve sugar utilization, the reactor effluent should be recycled back to the reactor after ABE removal *(11)*.

To compare the performance of the reactor and evaluate the effect of CSL incorporation into the feed, the reactor was fed with CSL medium. Fermentation conditions and the dilution rate were kept constant as in Table 1 for the duration of this experiment. The reactor produced 6.29 g/L of total ABE, of which acetone, butanol, and ethanol were 2.00, 4.16, and 0.13 g/L, respectively (Table 1). This resulted in a productivity of 2.01 g/(L·h) and a sugar utilization of 30.5% of that available in the feed (67.5 g/L). Compared to the control, the productivity was reduced by 10%. However, it is anticipated that it would be economical to use CSL compared with the P2 medium. This demonstrated that P2 medium can be replaced by economically available CSL. It is suggested, however, that the CSL

medium be optimized for further enhancement of ABE production in the immobilized cell reactor. It is also suggested that CSL be used to initiate the reactor and study the effect of CSL on cell growth and cell immobilization.

Next, an experiment was run in which 2.5 g/L of sodium butyrate was added to P2 medium to investigate whether it could be converted to butanol. A control experiment was run containing P2 medium. A separate control experiment was run before each experiment. This is essential because biomass accumulation in the reactor changes with time, thus affecting performance of the reactor *(5)*. The reactor produced 4.77 g/L of total ABE, of which acetone, butanol, and ethanol were 1.51, 3.14, and 0.12 g/L, respectively (Table 1). It resulted in a total ABE productivity of 1.53 g/(L·h) and a glucose utilization of 29.4% of that available in the feed of 59.1 g/L. The acid concentration in the effluent was 1.56 g/L. Following this, P2 medium was supplemented with sodium butyrate and the experiment was conducted at the same dilution rate. The reactor produced 1.55 g/L of acetone, 4.04 g/L of butanol, and 0.11 g/L of ethanol, for a total ABE concentration of 5.70 g/L, compared with 4.77 g/L in the control experiment. The productivity was 1.82 g/(L·h), compared with 1.53 g/(L·h) for the control experiment. These experiments suggested that butyrate was used by the culture to produce additional butanol. Note that 0.9 g/L of butanol was produced from 1.65 g/L of butyrate (2.5 g/L in feed, 0.85 g/L in effluent). The yield calculations do not include the amount of butyrate that was utilized by the culture.

In a previous study in which two reactors connected in series were used to produce butanol by *Clostridium acetobutylicum* P262, acids produced in the first reactor were converted to solvents (ABE) in the second reactor *(12)*. Ramey et al. *(13)*, and Ramey *(14)* used two immobilized cell series reactors to produce butanol from glucose. The first reactor contained immobilized cells of *Clostridium tyrobutyricum* to convert glucose to butyric acid and the second reactor contained immobilized cells of *C. acetobutylicum* ATCC 55025 to convert butyric acid (produced in the first reactor) to butanol. The product of the first reactor was fed to the second reactor without cell separation. It has been reported that the use of continuous two-stage reactors results in a significant increase in butanol yield. Furthermore, it has been demonstrated that application of such reactors eliminates production of all the ancillary byproducts (acetone, ethanol, and acetic acid) associated with butanol fermentation. Our investigations on the use of butyrate were performed with an ultimate objective of converting CO_2 to butyric acid and then to butanol. If successful, this would result in converting 53% of carbon that is lost to CO_2 in butanol fermentation. At this stage, we are attempting to isolate a culture that could convert CO_2 to butyric acid.

It has been reported that incorporation of 4.92–6.56 g/L (60–80 m*M*) of sodium acetate in the feed medium enhances levels of ABE production in a batch reactor from approx 25 to approx 33 g/L *(15)*. Additionally, it is also reported that levels of a number of key metabolic enzymes are elevated by the inclusion of acetate. Although the objective of the present investigation

was not to study the levels of these enzymes, we were interested in determining whether the inclusion of acetate in the feed medium of an immobilized call biofilm reactor would enhance the overall ABE production levels, thus improving productivity. A control experiment was therefore run with P2 medium. The reactor produced 9.12 g/L of total ABE, of which acetone, butanol, and ethanol were 3.20, 5.76, and 0.16 g/L, respectively. This resulted in a total productivity of 2.92 g/(L·h) at a dilution rate of 0.32 h^{-1}. The glucose utilization was 40% of that in the feed (64.4 g/L) (Table 1). When acetate was included in the feed medium, levels of these solvents decreased. Compared with 9.12 g/L of total ABE production in the control experiment, 6.05 g/L was produced, thus decreasing productivity to 1.94 g/(L·h) (Table 1). Total acid concentration was high, at 4.28 g/L. Interestingly, glucose utilization was 38% of that in feed of 64.4 g/L, similar to the control experiment. Although it has been reported that acetate is beneficial to butanol production in a batch reactor *(15)*, it does not improve the performance of the continuous biofilm reactor. Acetate may have hindered with the self pH regulation near pH 5.0. It may also have inhibited the fermentation owing to an increase in protonated acetate. Cell concentration in the effluent of the reactor varied from 0.6 to 1.5 g/L. We are aware of the significant variations in the results of control experiments. The reasons for these variations have been discussed elsewhere *(5)*. It is suggested that the different controls should not be compared because there have been varying concentrations of biomass in the controls. For these reasons, separate controls were run for all the treatments.

Conclusion

The use of CSL resulted in the production of 6.29 g/L of total ABE, compared with 6.86 g/L achieved in the control experiment. These studies were performed at a dilution rate of 0.32 h^{-1}. The productivities in the control and CSL experiments were 2.19 and 2.01 g/(L·h), respectively. Although the use of CSL resulted in a 10% decrease in ABE productivity, it is viewed that application of CSL would be economical for butanol production by fermentation. It was also demonstrated that inclusion of butyrate in the feed was beneficial to the butanol fermentation. A control experiment produced 4.77 g/L of total ABE, and the experiment supplemented with butyrate produced 5.70 g/L of total ABE. The butanol concentration increased from 3.14 to 4.04 g/L. Inclusion of acetate in the feed medium of the immobilized cell biofilm reactor was not beneficial to the ABE fermentation, as reported previously for the batch ABE fermentation.

Acknowledgments

This work was supported by grants from the Illinois Council on Food and Agricultural Research (IDA CF 02E-073-1 and IFA CF 03E116-1 FSHN) and Illinois Corn Marketing Board (ICMB 00-0126-01 BLASCHEK). CSL was kindly provided by A. E. Staley Manufacturing (Decatur, IL).

References

1. Dürre, P. (1998), *Appl. Microbiol. Biotechnol*. **49,** 639–648.
2. Davison, B. H. and Scott, C. D. (1988), *Appl. Biochem. Biotechnol*. **18,** 19–34.
3. Davison, B. H. and Thompson, J. E. (1993), *Appl. Biochem. Biotechnol*. **39,** 415–425.
4. Qureshi, N. and Blaschek, H. P. (2001), *Bioprocess Biosystems Eng*. **24,** 219–226.
5. Qureshi, N., Lai, L. L., and Blaschek, H. P. (2004), *Trans IChemE* **82(1),** 1–10.
6. Parekh, M., Formanek, J., and Blaschek, H. P. (1999), *Appl. Microbiol. Biotechnol*. **51,** 152–157.
7. Annous, B. A. and Blaschek, H. P. (1991), *Appl. Environ. Microbiol*. **57,** 2544–2548.
8. Qureshi, N. and Blaschek, H. P. (1999), *Biomass Bioenergy* **17,** 175–184.
9. Formanek, J. (1998) PhD thesis, University of Illinois, Urbana, IL.
10. Qureshi, N. and Blaschek, H. P. (1999), *Biotechnol. Prog*. **15,** 594–602.
11. Qureshi, N. and Maddox, I. S. (1991), *Bioprocess Eng*. **6,** 63–69.
12. Qureshi, N. and Maddox, I. S. (1988), *Bioprocess Eng*. **3,** 69–72.
13. Ramey, D. E., Ying, Z., and Yang, S. T. (2002), in *Proceedings of the 24th Symposium on Biotechnology for Fuels and Chemicals*, poster presentation, Gatlinburg, TN, p. 142.
14. Ramey, D. E. (1998) US patent no. 5, 753, 474.
15. Chen, C. K. and Blaschek H. P. (1999), *Appl. Microbiol. Biotechnol*. **52,** 170–173.

0273-2289/04/114/0723–0732/$25.00

Measurement of Rheology of Distiller's Grain Slurries Using a Helical Impeller Viscometer

Tiffany L. Houchin[1] and Thomas R. Hanley*[,2]

[1]Department of Chemical Engineering, University of Louisville, Louisville, KY 40292; and
[2]Auburn University, Office of the Provost, Auburn, AL 36849, E-mail: hanley@auburn.edu

Abstract

Current research is focused on developing a process to convert the cellulose and hemicellulose in distiller's grains into fermentable sugars, increasing both ethanol yield and the amount of protein in the remaining solid product. The rheologic properties of distiller's grain slurries were determined for concentrations of 21, 23, and 25%. Distiller's grain slurries are non-Newtonian, heterogeneous fluids subject to particle settling. Traditional methods of viscosity measurement, such as cone-and-plate and concentric cylinder viscometers, are not adequate for these fluids. A helical impeller viscometer was employed to measure impeller torque over a range of rotational speeds. Newtonian and non-Newtonian calibration fluids were utilized to obtain constants that relate shear stresses and shear rates to the experimental data. The Newtonian impeller constant, c, was 151; the non-Newtonian shear rate constant, k, was 10.30. Regression analysis of experimental data was utilized for comparison to power law, Herschel-Bulkley, and Casson viscosity models with regression coefficients exceeding 0.99 in all cases.

Index Entries: Distiller's grain slurries; rheologic properties; wet grains; calibration fluids; helical impeller.

Introduction

During corn dry mill ethanol manufacturing, the most common method for ethanol production in North America, the primary byproduct is dried distiller's grain (DDG). As production increases to meet demand, the supply of DDG will significantly increase. Thus, ethanol producers need to modify their processes for the sake of profitability. Technological

*Author to whom all correspondence and reprint requests should be addressed.

advances for alcohol producers will incorporate the improvement of ethanol yield and the creation of new products from DDG. Current research is focused on developing a process that converts the cellulose and hemicellulose in wet grains and fiber residues into fermentable sugars, increasing both the ethanol yield and the protein percentage in DDG.

To develop an optimum process, the rheologic properties of wet grains must be known. The rheologic properties of wet grain can be utilized to predict performance and behavior during the process, making it possible to design the process for optimal sugar conversion. Viscosity data will aid in the assessment of processability of wet grains when designing pumping and piping systems for the proposed process.

Wet grains are suspensions containing macroparticles. Because of this property, wet grains exhibit complex rheologic properties and are typically characterized as non-Newtonian fluids. Because of the complex relationship between shear rate and shear stress of wet grains, characterization of rheologic properties is more difficult than for simple Newtonian fluids. Conventional viscosity measurement devices, such as concentric cylinder, cone-and-plate, and pipeline viscometers, are prone to particle settling, slip velocity near the wall, and phase separation when measuring the rheology of suspensions. Therefore, an alternative method for measuring rheologic behavior must be used.

The impeller method is a technique commonly used to determine rheologic properties of fluids subject to particle settling. The impeller method utilizes a viscometer along with Newtonian and non-Newtonian calibration fluids to obtain constants that relate shear stresses and shear rates to experimentally measured values of torque and rotational speed. Newtonian calibration fluids are used to determine the impeller constant, c, and non-Newtonian calibration fluids are used to calculate the shear rate constant, k. These constants are then used to aid in the determination of rheologic properties of a selected non-Newtonian fluid, such as wet grains.

The aim of the present study was to determine rheologic characteristics of wet grain slurries using a helical impeller viscometer. The collected data were analyzed to develop a model describing the rheologic behavior of wet grain slurries.

Materials and Methods

Equipment

Two Brookfield viscometers were used to collect the data necessary for rheologic property studies of wet grains: a Brookfield RVDV III viscometer with a cone-and-plate spindle and a Brookfield HBDV III viscometer with a double helical ribbon impeller attachment. The Brookfield RVDV III had a full-scale torque of 7187 dyn-cm, and the HBDV III had a full-scale torque of 57,496 dyn-cm. Each viscometer had a maximum rotational speed of 250 rpm. Both viscometers had accuracy limits of ± 5% full-scale torque.

Howeever, inaccuracies were apparent for non-Newtonian calibration fluids and distiller's grain slurries up to ± 10% of the full-scale torque. Therefore, only measurements above 10% and below 90% torque were utilized for guar gum solutions and distiller's grain slurries. The experiments were conducted at a constant temperature of 25 ± 0.1°C.

The helical impeller was fashioned from nylon using selective laser sintering technology. The impeller had a diameter of 0.04 m and a pitch of 0.02 m. The impeller featured two helices, an ascending outer flight and a descending inner flight. The length of the impeller was 0.055 m, with an off-bottom clearance of 0.025 m.

The vessels used for Newtonian and non-Newtonian calibration were 1000-mL glass beakers. Because of particle settling, the vessel size utilized for wet grain slurries was reduced to 200 mL. Reducing the ratio of the helical impeller diameter to the vessel diameter allowed for more accurate rheology measurement of grain slurries. Although the effect of vessel size on helical impeller readings was not investigated in this study, previous researchers have been reported that vessel size has little or no effect *(1)*.

Calibration Fluids and Distiller's Grains

The Newtonian calibration fluids used were silicone oil and glycerol. The non-Newtonian calibration fluids used were guar gum solutions at relatively low concentrations (0.75 and 1.0% by weight) in deionized water. Distiller's grain particles were provided by a commercial source and had an average particle size of 0.361 × 0.565 mm, measured by electron microscopy. The distiller's grains were used to formulate wet grain slurries in solutions of 0.1% (w/v) xanthan gum in deionized water. The xanthan gum was found to have no effect on the viscosity of water and was used to aid in the suspension of grain particles. Wet grain slurries of 21, 23, and 25% (w/v) solids concentration were analyzed.

Impeller Viscometer Technique

Newtonian and non-Newtonian calibration fluids were used to determine the necessary calibration constants for the impeller method. It has been previously determined that the impeller method is only valid for a Reynolds number (Re) <10. Impeller rotational speed and torque data from Newtonian calibration fluids of known viscosity were employed to determine the Newtonian calibration constant, c. Cone-and plate-viscometer data from non-Newtonian calibration fluids were used to determine a viscosity vs shear rate relationship. Impeller rotational speed and torque data of the non-Newtonian calibration fluids combined with a determined viscosity vs shear rate correlation were utilized to calculate the shear rate constant, k. The impeller method calibration constants allow the calculation of viscosity, shear rate, and shear stress data of non-Newtonian suspensions. Metz et al. *(2)* have thoroughly discussed the equations utilized in the impeller method.

The Newtonian calibration constant is a function of Re and the power number:

$$P_N = \frac{2\pi NM}{\rho N^3 D_i^5} \tag{1}$$

in which Re can be expressed as

$$\mathrm{Re} = \frac{\rho N D_i^2}{\eta_a} \tag{2}$$

Assuming a Newtonian fluid ($\mu = \eta_a$) and combining Eqs. 1 and 2 results in an equation for impeller torque:

$$M = \frac{c}{2\pi} \mu N D_i^3 \tag{3}$$

For a given rotational speed, the measured torque combined with fluid viscosity and impeller diameter can be used to determine the Newtonian calibration constant, *c*.

The viscosity of a non-Newtonian fluid can be calculated using the Newtonian calibration constant, impeller speed and torque, and impeller diameter:

$$\eta_a = \frac{2\pi M}{c N D_i^3} \tag{4}$$

To calculate the shear rate constant, *k*, a relationship must be established between shear rate and viscosity of a non-Newtonian calibration fluid. A cone-and-plate viscometer is used to determine a correlation between shear rate and viscosity that can be fit to a power law model. The power law correlation is then applied to viscosity data calculated from the impeller viscometer and Eq. 4. The shear rate constant can be calculated as follows:

$$k = \frac{\dot{\gamma}_{AV}}{N} \tag{5}$$

Viscosity, shear stress, and shear rate can be calculated for any non-Newtonian suspension using the impeller method calibration constants. Viscosity is determined using Eq. 4. The shear stress can be calculated for any impeller speed and measured torque:

$$\tau = \frac{2\pi MK}{c D_i^3} \tag{6}$$

The shear rate can then be calculated:

$$\tau = \eta_a \dot{\gamma} \tag{7}$$

Rheologic Models

Three empirical models were utilized to fit the rheologic characteristics of the wet grain slurries: power law, Herschel-Bulkley, and Casson. The power law and Casson models are two-parameter models and are ideal for

Table 1
Newtonian Calibration Fluids

Calibration solution	Average viscosity (Pa·s)	Re
Glycerol	0.8465	0.47–7.25
Silicone oil 1 *M*	0.9537	0.42–5.87

Table 2
Average Newtonian Calibration Constants

Calibration solution	c_{avg}	c_{max}	c_{min}	SD
Glycerol	151.96	156.27	148.83	2.34
Silicone oil 1 *M*	150.68	153.39	148.57	1.50
Overall	151.00			

non-Newtonian rheologic modeling. The Herschel-Bulkley model is a three-parameter model that combines the power law with yield stress.

The power law, or Ostwald-de Waele, model is the simplest and most widely used rheologic empiricism. The power law states

$$\tau = K_{pl} \left| \dot{\gamma} \right|^{n_{pl}} \tag{8}$$

The Herschel-Bulkley model is shown as

$$\tau = \tau_0 + K_{HB} \dot{\gamma}^{HB} \tag{9}$$

The Casson model incorporates yield stress and is written as

$$\tau^{1/2} = \tau_0^{1/2} + K_c \dot{\gamma}^{1/2} \tag{10}$$

Results

Calibration

Average viscosity and helical impeller data were combined to determine the Newtonian calibration constant, c. Table 1 presents the measured average viscosities and R_e ranges for silicone oil and glycerol. Table 2 provides the average Newtonian calibration constants for each calibration fluid, standard deviation (SD) for each data set, and recorded c_{max} and c_{min} values. The overall average Newtonian calibration constant was 151. Figure 1 presents the power law fits for the guar gum solutions. Table 3 summarizes power law parameters calculated from these graphs. The average overall shear rate constant was calculated to be 10.3; and Table 4 summarizes shear rate constants.

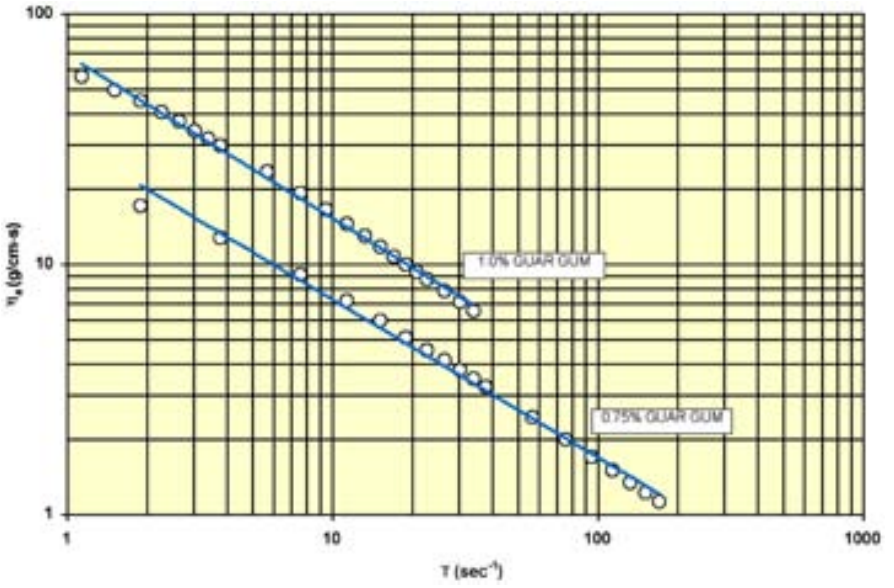

Fig. 1. Guar gum suspendsions: viscosity vs shear rate.

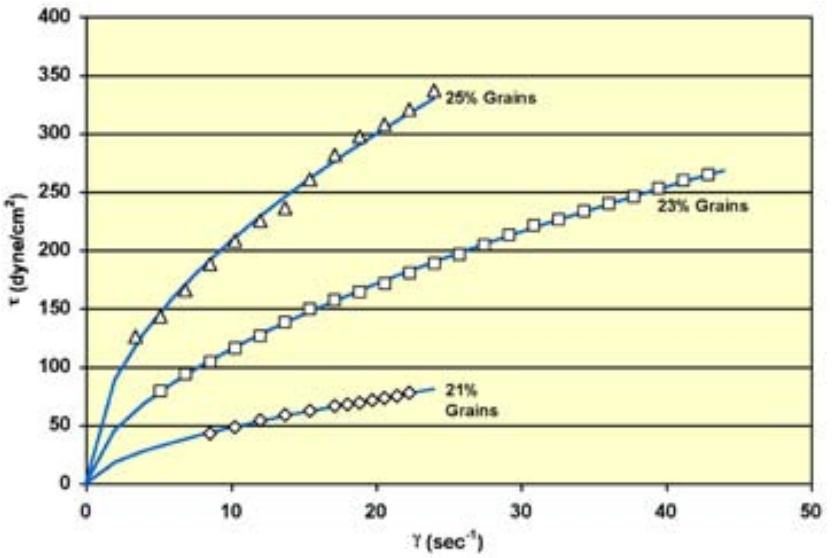

Fig. 2. Power Law model fit for distiller's grain slurries.

Wet Grain Slurries

Figure 2 shows the power law fits for the wet grain slurries. Table 5 summarizes the power law parameters for each slurry concentration. Figure 3 presents the experimental data fit to the Herschel-Bulkley model.

Table 3
Power Law Parameters for Guar Gum Solutions

Calibration solution	K_{pl}	n_{pl}	R^2
0.75% Guar gum	32.17	0.3534	0.9946
1.0% Guar gum	68.48	0.3469	0.9964

Table 4
Average Shear Rate Constants

Calibration solution	k_{avg}	k_{max}	k_{min}	SD
0.75% Guar gum	10.24	11.17	9.59	0.55
1.0% Guar gum	10.36	11.16	9.94	0.27
Overall	10.30			

Table 5
Power Law Parameters for Distiller's Grain Slurries

Slurry concentration	K_{pl}	n_{pl}	R^2
21% Solids	11.877	0.6019	0.9972
23% Solids	30.696	0.5727	0.9995
25% Solids	61.358	0.5291	0.9925

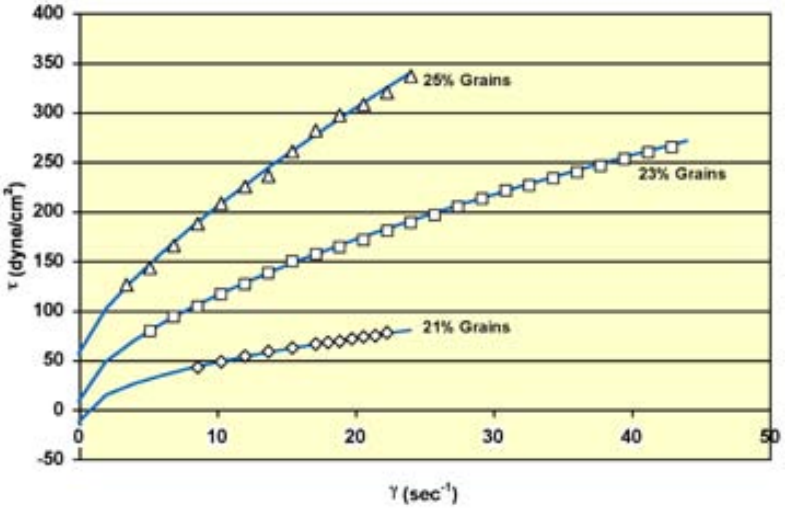

Fig. 3. Herschel-Bulkley model fit for distiller's grain slurries.

Table 6 summarizes the Herschel-Bulkley model parameters for each slurry concentration. Figure 4 represents the Casson model regression for 21, 23, and 25% grain slurries. Table 7 summarizes the Casson model parameters for each slurry concentration.

Table 6
Herschel-Bulkley Parameters for Distiller's Grain Slurries

Slurry concentration	K_{HB}	τ_{0HB}	n_{HB}	R^2
21% Solids	31.9580	–12.005	0.3919	0.9982
23% Solids	26.4580	8.306	0.6068	0.9996
25% Solids	26.9215	56.346	0.7409	0.9977

Table 7
Casson Parameters for Distiller's Grain Slurries

Slurry concentration	K_C	τ_{0C}	R^2
21% Solids	1.211	9.467	0.9972
23% Solids	1.697	28.478	0.9970
25% Solids	2.404	44.035	0.9977

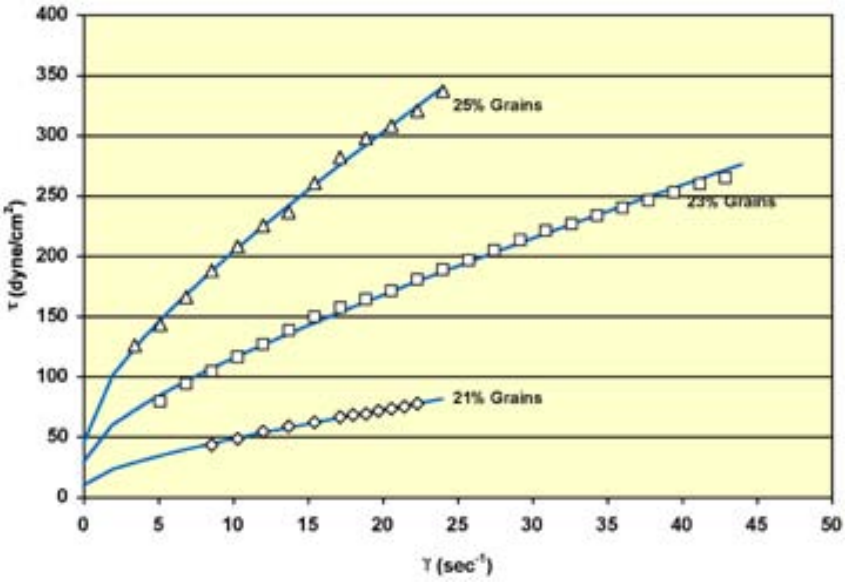

Fig. 4. Casson model fit for distiller's grain slurries.

Discussion

Calibration

The overall Newtonian calibration constant was 151, the same calibration constant obtained by Rieth *(3)* for the same helical impeller. Previously reported data by Donnelly *(4)* concluded that *c* was a function of R_e for vane and turbine impeller viscometers. It was concluded by Rieth *(3)* and confirmed in our study that *c* is a constant in the laminar region

of flow (Re < 10) for the helical impeller viscometer. Table 2 shows that the SD from the average Newtonian calibration constant was 2.34 for glycerol and 1.50 for silicone oil 1M.

The regression analysis of the power law models for 0.75 and 1.0% guar gum suspensions returned R^2 values exceeding 0.99 and are shown in Table 3. The power law model was an accurate representation of guar gum rheologic properties.

Table 4 lists calculated average shear rate constants and SDs of 10.24 ± 0.55 (0.75% guar gum solution) and 10.36 ± 0.27 (1.0% guar gum solution). The SDs are minimal. The average shear rate constant range calculated by Rieth *(3)* was 10.45–10.91 for the same helical impeller. The calculated overall average shear rate constant of 10.30 falls below the range reported by Rieth *(3)*.

Limitations of Grain Slurry Rheology Measurement

Grain slurries of 21, 23, and 25% solids were tested using the helical impeller viscometer. The grain slurry concentration range was selected based on trial-and-error impeller experimentation. The lower limit of grain slurry concentration (21%) was bound by R_e restrictions. The impeller method required that the R_e be held at values <10. Grain slurries of concentrations <21% resulted in Reynolds numbers >10 for suitable impeller speeds. The upper limit of grain slurry concentration (25%) was bound by the mixing capabilities of the helical impeller viscometer. Grain slurries of concentrations >25% were not mixed sufficiently by the helical impeller viscometer and therefore did not return accurate impeller torque readings.

Figures 2–4 show that no experimental data were recorded at low impeller shear rates. Experimental data began at $\gamma = 8.53\ s^{-1}$ for 21% solids, $5.15\ s^{-1}$ for 23% solids, and $3.43\ s^{-1}$ for 25% solids. The reason for the missing data is that the helical impeller viscometer has limitations. Owing to possible viscometer error, data were not recorded until the impeller torque was >10% of the full-scale torque. Therefore, no experimental data were recorded at low impeller rotational speeds. The lack of experimental data at low shear rates made comparison of rheologic models at low shear rates and the prediction of yield stress impossible.

Grain Slurry Rheologic Modeling

Experimental rheologic data were fit to the power law, Herschel-Bulkley, and Casson models. The power law model does not predict yield stress. Yield stress for 21% grain slurries predicted by the Herschel-Bulkley model was a negative value, as shown in Table 6. Yield stress values predicted by the Herschel Bulkley model for 23 and 25% solids were 8.31 and 56.3 dyn/cm^2, respectively. Predicted yield stress values from the Casson model were 9.47 dyn/cm^2 for 21% solids, 28.5 dyn/cm^2 for 23% solids, and 44.0 dyn/cm^2 for 25% solids.

Grain Slurry Rheology Predictions

Overall, each model accurately represented the experimental data for shear rates >5 s^{-1}. At shear rates between 0 and 5 s^{-1}, the empirical models disagree. Since no experimental data exist at low shear rates, it is impossible to determine which empirical model best represents the actual properties of the grain slurries. Further, all of the empirical models have comparable regression coefficients, as shown in Tables 5–7. Regression coefficient (R^2) ranges were 0.992–1.000 (power law), 0.998–1.000 (Herschel-Bulkley), and 0.997–0.998 (Casson).

Conclusion

The helical impeller viscometer method is an accurate technique for approximating rheologic behavior of distiller's grain slurries of concentrations between 21 and 25% solids. Power law and Casson empirical models are adequate methods for modeling rheologic behavior of distiller's grain slurries of concentrations between 21 and 25% solids. These data should help in the design and operation of the agitator, especially for the start of the fermentation.

Nomenclature

c = Newtonian calibration constant
D_i = impeller diameter
k = non-Newtonian calibration constant
M = torque
n_{pl}, K_{pl} = power law parameters
N = rotational speed
P_N = dimensionless power number
Re = dimensionless Reynolds number
η_a = apparent viscosity
γ = shear rate
μ = Newtonian viscosity
ρ = density
τ = shear stress
τ_0, K_C = Casson parameters
τ_0, K_{HB} = Herschel-Bulkley parameters

References

1. Metz, B. N., Kossen, W. F., and van Suijdam, J. C. (1979), *Adv. Biochem. Eng.*, **11,** 103–156.
2. Rieth, T. C. (1997), MS thesis, University of Louisville, Louisville, KY.
3. Svihla, C. K., Dronawat, S. N., and Hanley, T. R. (1995), *App. Biochem. Biotechnol.* **51/52,** 355–366.
2. Donnelly, J. A. (1995), MS thesis, University of Louisville, Louisville, KY.

0273-2289/04/114/0733–0745/$25.00

Computational Fluid Dynamics Simulation and Redesign of a Screw Conveyor Reactor

YINKUN WAN[1] AND THOMAS R. HANLEY*,[2]

[1]Department of Chemical Engineering, University of Louisville, Louisville, KY 40292; and
[2]Auburn University, Office of the Provost, Auburn, AL 36849, E-mail: hanley@auburn.edu

Abstract

National Renewable Energy Laboratory (NREL) designed a shrinking-bed reactor to maintain a constant bulk packing density of cellulosic biomass. The high solid-to-liquid ratio in the pretreatment process allows a high sugar yield and avoids the need to flush large volumes of solution through the reactor. To scale up the shrinking-bed reactor, NREL investigated a pilot-scale screw conveyor reactor in which an interrupted flight between screws was employed to mimic the "shrinking-bed" effect. In the experiments with the screw conveyor reactor, overmixing and uneven flow occurred. These phenomena produce negative effects on biomass hydrolysis. The flow behavior inside the reactor was analyzed to allow redesign of the screw to achieve adequate mixing and even flow. In the present study, computational fluid dynamics (CFD) was utilized to simulate the fluid flow in the porous media, and a new screw design was proposed. CFD analysis performed on the redesigned reactor indicated that an even flow pattern was achieved.

Index Entries: Screw reactor; computational fluid dynamics; modeling; backflow; hydrolysis.

Introduction

National Renewable Energy Laboratory (NREL) designed a shrinking-bed reactor *(1)* to maintain a constant bulk packing density of solid biomass in the reactor. As a result, high sugar concentrations were achieved owing to the high solid-to-liquid ratio and reduced liquid volume. NREL's work had experimentally proven that sugar yields higher than 95% from hemicellulose and higher than 85% from cellulose were attainable in a multiple percolation reactor system simulating countercurrent operation *(1)*.

Note: As a result of publishing restrictions, all color figures were changed to gray scale. The color copy is available upon the reader's request.

*Author to whom all correspondence and reprint requests should be addressed.

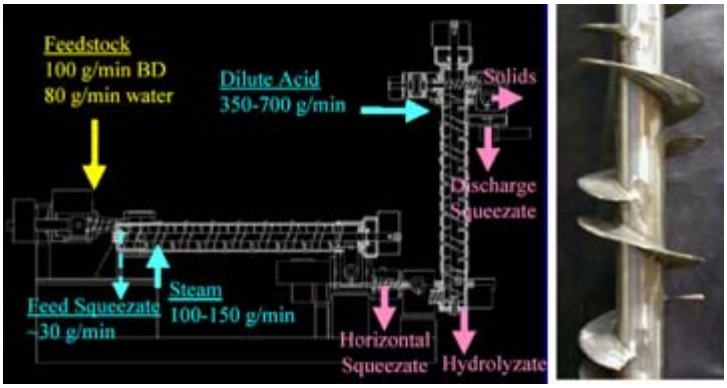

Fig. 1. Experimental arrangement and screw structure of NREL pilot-scale screw conveyor reactor for hardwood hydrolysis. (Adapted from ref. 7.)

Chen et al. *(2)* developed a kinetic model to describe the shrinking-bed reactor and found that the shrinking-bed operation increases the sugar yield by about 5% compared with the non-shrinking-bed operation. Lee et al. *(3)* also developed a mathematical model to simulate a countercurrent shrinking-bed reactor and showed that bed shrinking provides a positive effect on both hemicellulose and cellulose hydrolysis. Pettersson et al. *(4)* further expanded Lee et al.'s *(3)* modeling, adding new features including wood porosity, glucose diffusion, and absorption of hydrolysate at the bottom of the reactor. Pettersson et al. *(4)* found that both porosity and absorption of hydrolysate at the bottom of the reactor had small effects on the combined yield and concentration results at a given specified reactor solids loading. Converse *(5)* presented a model to simulate a cross-flow shrinking-bed reactor for the hydrolysis of lignocellulosics and found a trade-off between cross-flow and plug-flow shrinking-bed reactors. Cross flow allows one to obtain higher yields than plug flow but with a slight reduction in product concentration. Wan and Hanley *(6)* simulated the flow field inside the shrinking-bed reactor with computational fluid dynamics (CFD) and found that the flow inside the reactor is mostly plug flow and was ideal for biomass hydrolysis based on theoretical analysis.

Previous studies have shown the great potential of the shrinking-bed reactor for commercial application. To scale up the shrinking-bed reactor and to establish it as a practical process reactor, NREL further developed the shrinking-bed reactor into a screw conveyor reactor in which a vertical broken flight screw was employed as a moving-bed mechanism. Experiments with yellow poplar hardwood hydrolysis in pilot-scale (200 kg/d) screw reactors *(7)* produced soluble xylose yields of almost 90%. Glucose yields from cellulose were slightly less than predicted from bench work using a 5-min residence time at just under a normalized 25% yield. Figure 1 shows the arrangement and structure of pilot-scale screw conveyor reactor in the NREL hardwood hydrolysis experiment.

In the hardwood hydrolysis experiment with the screw reactor, NREL researchers found that overmixing and an uneven flow pattern existed in the reactor. These factors have a negative effect on biomass hydrolysis. To enhance the screw conveyor reactor's performance, it was necessary to redesign the reactor to achieve adequate mixing and an even flow pattern. In the present work, CFD was utilized to analyze the flow behavior in the screw conveyor reactor, and a new screw design was proposed based on CFD analysis.

Model and Method

The porous media model *(8)* is used to simulate flows through the biomass in a packed bed where biomass is the porous media. In this model, a momentum source term S_i is added to the standard fluid flow equation:

$$S_i = \sum_{j=1}^{3} D_{ij} \mu v_j + \sum_{j=1}^{3} C_{ij} \frac{1}{2} \rho \left| v_j \right| v_j \tag{1}$$

The first part of this equation is a viscous loss term and the second is an inertial loss term. For simple homogeneous porous media, S_i can be written as

$$S_i = \frac{\mu}{\alpha} v_i + C_2 \frac{1}{2} \rho \left| v_i \right| v_i \tag{2}$$

in which α is the permeability and C_2 is the inertial resistance factor.

In laminar flows through porous media, the pressure is proportional to velocity and C_2 can be taken as zero. Ignoring convective acceleration and diffusion, the porous media model can be changed into Darcy's Law:

$$\nabla P = - \frac{\mu}{\alpha} v \tag{3}$$

in which ∇P is the pressure drop.

For turbulent flows and the cases in which the permeability term can be eliminated, the porous media model can be rewritten as follows:

$$\frac{\partial p}{\partial x_i} = \sum_{j=1}^{3} C_{2ij} \left(\frac{1}{2} \rho v_j \left| v_j \right| \right) \tag{4}$$

For packed-bed and turbulent flows, Darcy's law can be rewritten as the Ergun equation *(9)*:

$$\nabla P = \frac{150 \mu}{D_p^2} \frac{\left(1 - \varepsilon\right)^2}{\varepsilon^3} v + \frac{1.75 \rho}{D_p} \frac{\left(1 - \varepsilon\right)^3}{\varepsilon^3} v v \tag{5}$$

For laminar flow, the second term of the Ergun equation may be dropped, resulting in the Blake-Kozeny equation:

$$\nabla P = \frac{150 \mu}{D_p^2} \frac{\left(1 - \varepsilon\right)^2}{\varepsilon^3} v \tag{6}$$

Comparing Eqs. 3 and 4 with Eq. 5,

$$\alpha = \frac{D_p^2}{150} \frac{\varepsilon^3}{(1-\varepsilon)^2} \tag{7}$$

$$C_2 = \frac{3.5}{D_p} \frac{(1-\varepsilon)}{\varepsilon^2} \tag{8}$$

in which D_p is the mean particle diameter, and ε is the void volume fraction of the packed bed. In this simulation, constant void volume fraction was assumed. From former research *(3)*, the void volume fraction was estimated to be 0.8.

Using the Blake-Kozeny equation, the screw conveyor reactor can be modeled as rotating equipment in which the fluid is moved by screw rotation. Although 10 small horizontal cylindrical baffles exist in the screw flights, the interaction between the screw and baffles can be ignored. For this case, the rotating reference frame was used instead of the inertial reference frame.

We used a commercial CFD package Fluent 6.0 to simulate the pilot-scale screw conveyor reactor. The geometry of the screw conveyor reactor is given in Table 1. The experimental conditions for hardwood hydrolysis for the vertical screw conveyor reactor are described in Table 2.

Results and Discussion

Flow Pattern of Screw Conveyor Reactor

Figure 2 shows the flow pattern in the upper part of the screw conveyor reactor along the vertical panel of baffles; also included a three-dimensional view of the flow pattern. It was found that the flow direction above the screw varies from the flow direction below the screw. The fluid between the two screws had the same flow direction. In most of the upper screw, the flow was downward; above the screw, some upward flow was found.

Figure 3 shows the flow pattern in the bottom part of the screw reactor along the vertical panel of baffles. Flow in the bottom zone is mostly rotational, with strong backflow observed in this area. Figure 4 shows the flow pattern in the horizontal panel along the baffle. Apparently, the flow along this panel can be divided into two zones, each of which moved along the reactor wall, met, and then moved downward.

Downward Plug Flow in Screw Conveyor Reactor

In the CFD simulation the downward axial flow was defined as negative axial velocity. Figure 5 shows the negative axial velocity contour along the vertical panel of the baffles. Except for the dilute-acid inlet and

Table 1
Parameters of Screw conveyor reactor geometry

Reactor diameter (m)	Reactor height (m)	Dilute acid inlet diameter (m)	Hydrolysate outlet diameter (m)
0.15	1.22	0.06	0.04

Table 2
Experimental Conditions for Hardwood Hydrolysis

Flow media	Dilute acid
Temperature (°C)	210
Flow type	Laminar
Screw rotation speed (rpm)	5
Inlet velocity (m/s)	2.95×10^{-3}
Outlet pressure (Pa)	350
Particle Diameter (D_p) (m)	0.001
Void volume fraction (ε)	0.8
$1/\alpha$	9.38×10^{6}
C_2	1.37×10^{6}

the bottom screw zones, the flow was downward plug flow. This kind of flow will promote good performance for biomass hydrolysis.

Backflow Along Bottom of Screw Conveyor Reactor

In the simulation definition, the downward axial velocity was calculated as a negative value, and the upward axial flow (the backflow) was calculated as positive axial velocity. To clearly describe the backflow, the positive axial velocity contour is shown in Fig, 6. Figure 6 shows that the backflow occurred between screws with >50% of the bottom zone showing backflow.

Backflow is detrimental to the overall chemical reaction and mass transfer process. For biomass hydrolysis, the backflow had a negative effect on sugar yield and toxic chemical production. As observed by the NREL researchers, backflow will cause overmixing and uneven flow. When backflow occurs, fluid with higher sugar concentrations will be transported where sugar concentration is lower, resulting in adverse effects on the hydrolysis reaction. Moreover, backflow will increase the residence time of the sugar solution, increasing the risk of deterioration of sugars into toxic byproducts.

The backflow in the screw conveyor reactor needed to be reduced. The bottom screw was therefore redesigned to minimize backflow.

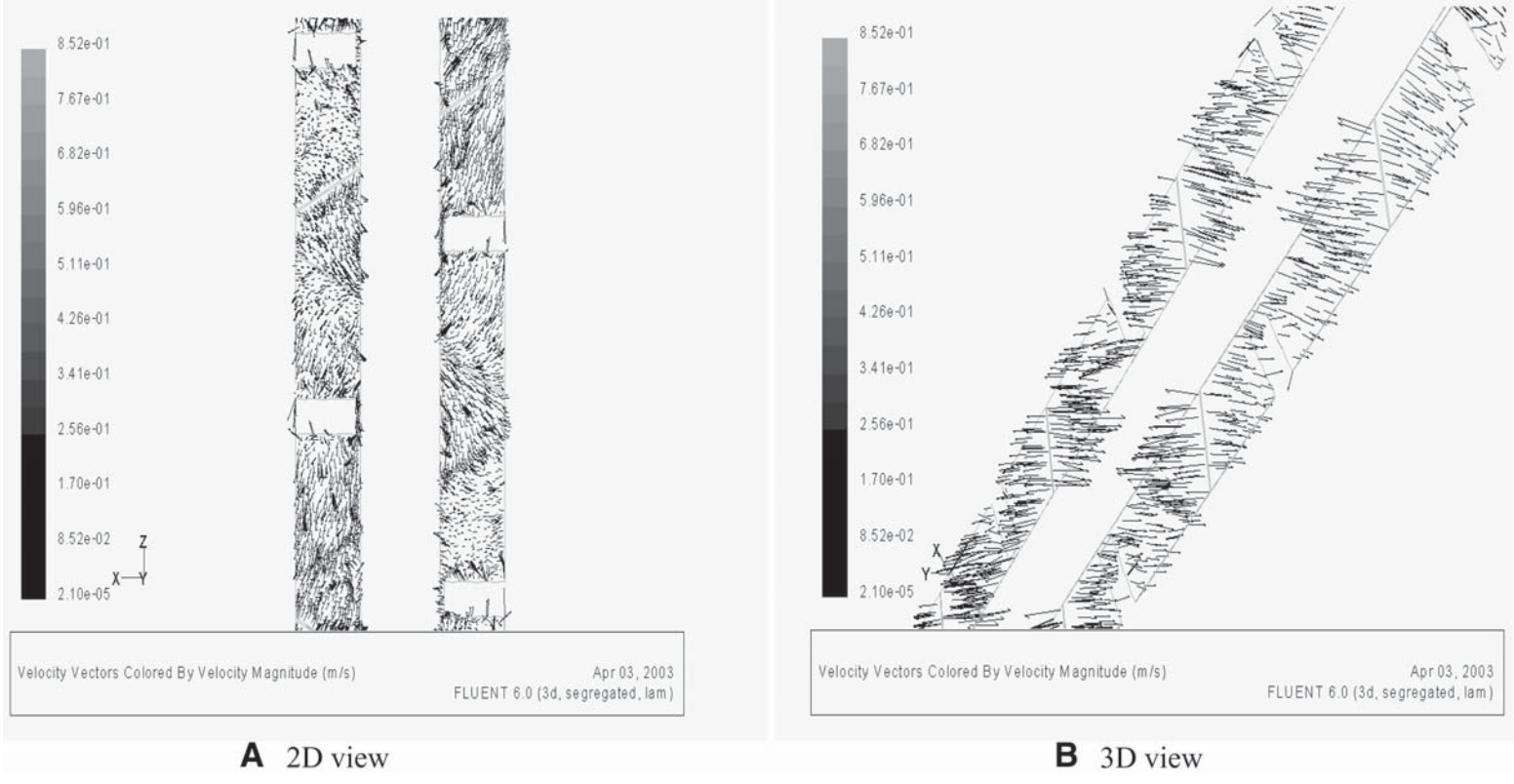

Fig. 2. Flow patterns in upper part of screw conveyor reactor: **(A)** two-dimensional view; **(B)** three-dimensional view.

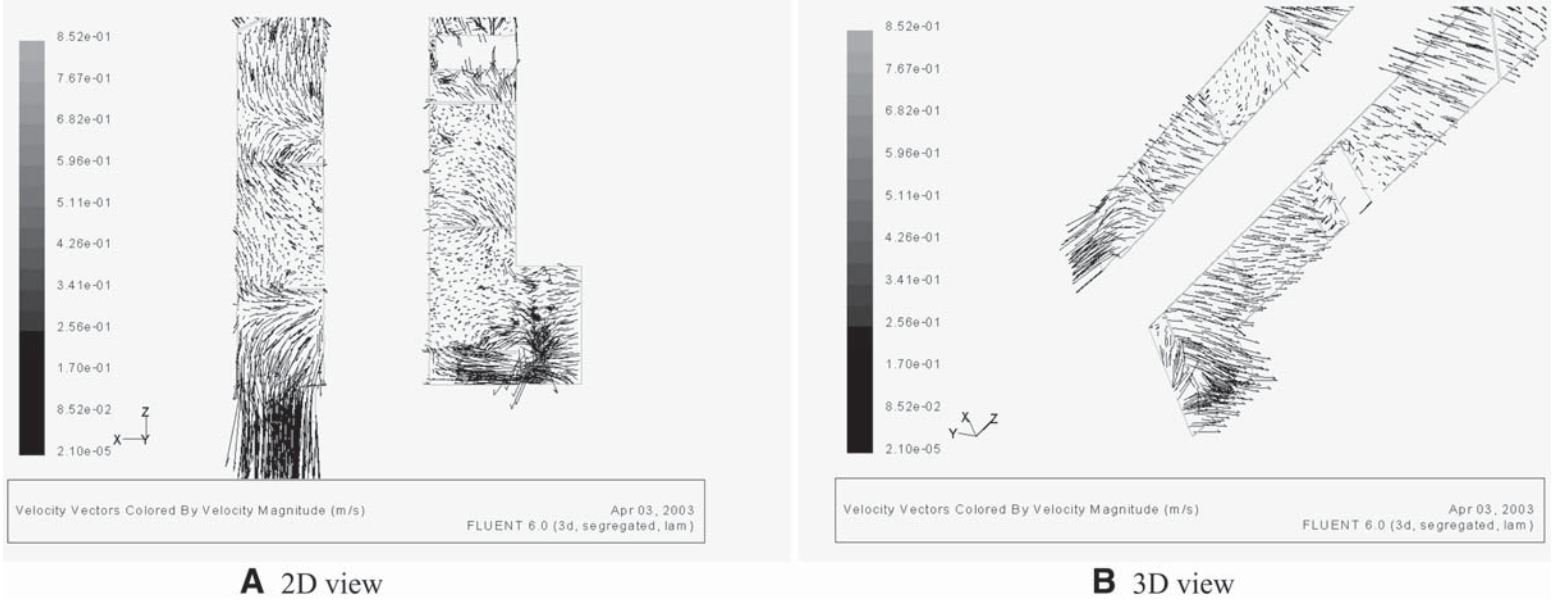

Fig. 3. Flow pattern in bottom part of screw reactor: **(A)** two-dimensional view; **(B)** three-dimensional view.

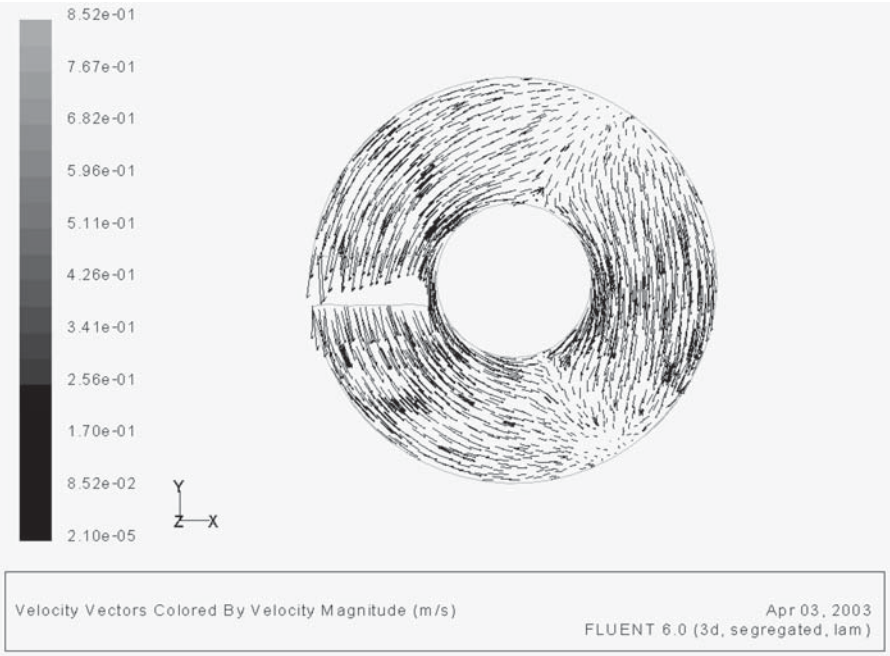

Fig. 4. Flow pattern of screw reactor along horizontal panel of baffle.

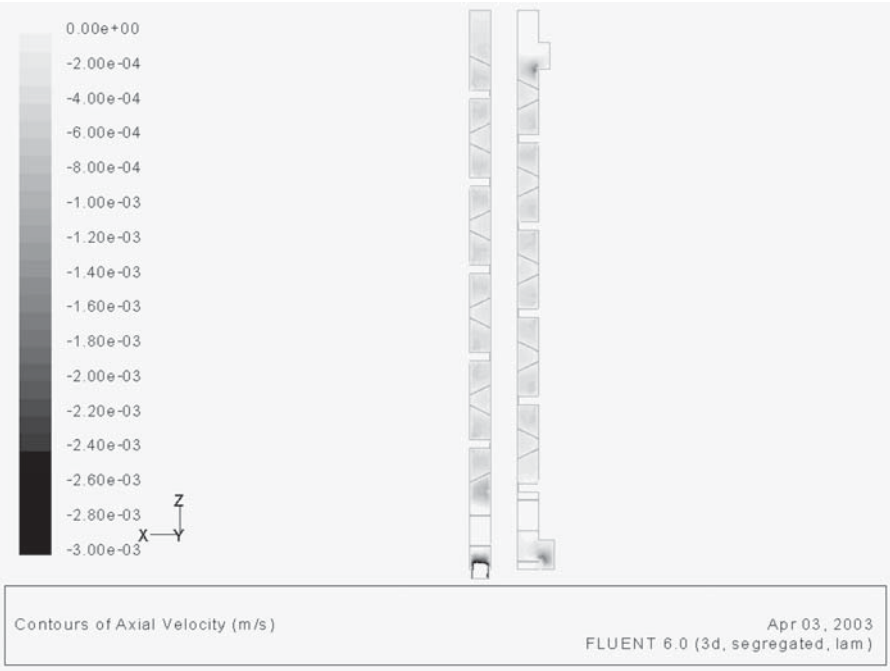

Fig. 5. Negative axial velocity contour (downward plug flow) along vertical panel of baffles.

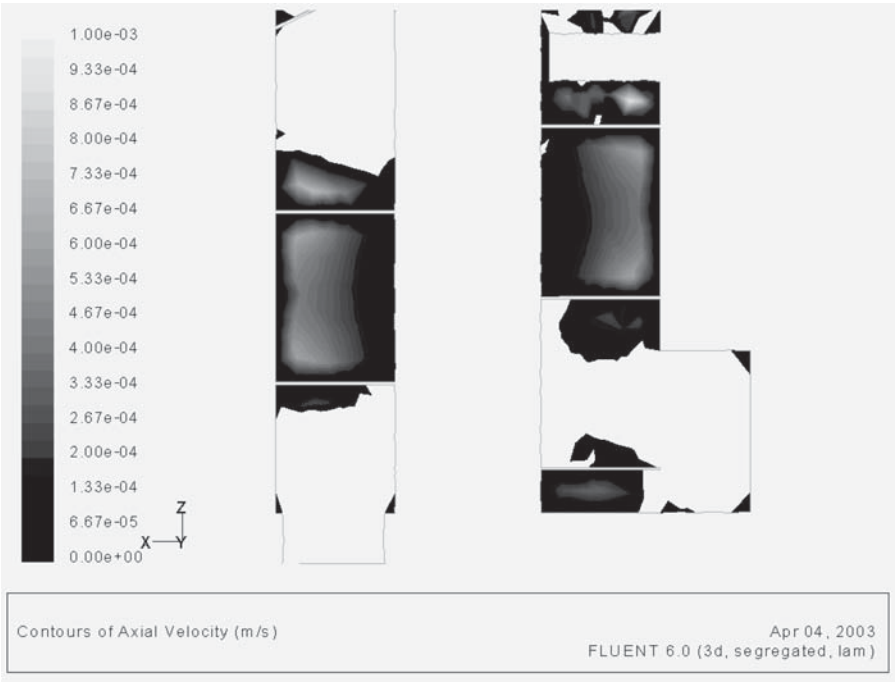

Fig. 6. Positive axial velocity contour (backflow) along bottom of screw conveyor reactor.

Redesign of Bottom Screw

Figure 7 showsn the original screw and Fig. 8 shows the redesigned bottom screw. The original cylindrical helical screw was converted into a conical helical lifter.

Backflow in Redesigned Bottom Screw

Figure 9 shows the positive axial velocity contour indicating backflow. Compared with the original screw reactor, the backflow in the redesigned screw reactor was diminished. The backflow area decreased from >50% in the original reactor to <30% in the redesigned one. Moreover, the maximum positive axial velocity in the original reactor was about 1.0×10^{-3} m/s, whereas in the redesigned reactor it was about 5×10^{-4} m/s, confirming that backflow was greatly reduced in the redesigned reactor. A better performance for biomass hydrolysis can be predicted with this redesigned screw reactor.

Comparison of Pathlines

Figure 10 shows the path lines in the bottom screw zone for the original screw reactor and the redesigned reactor. The path lines clearly show

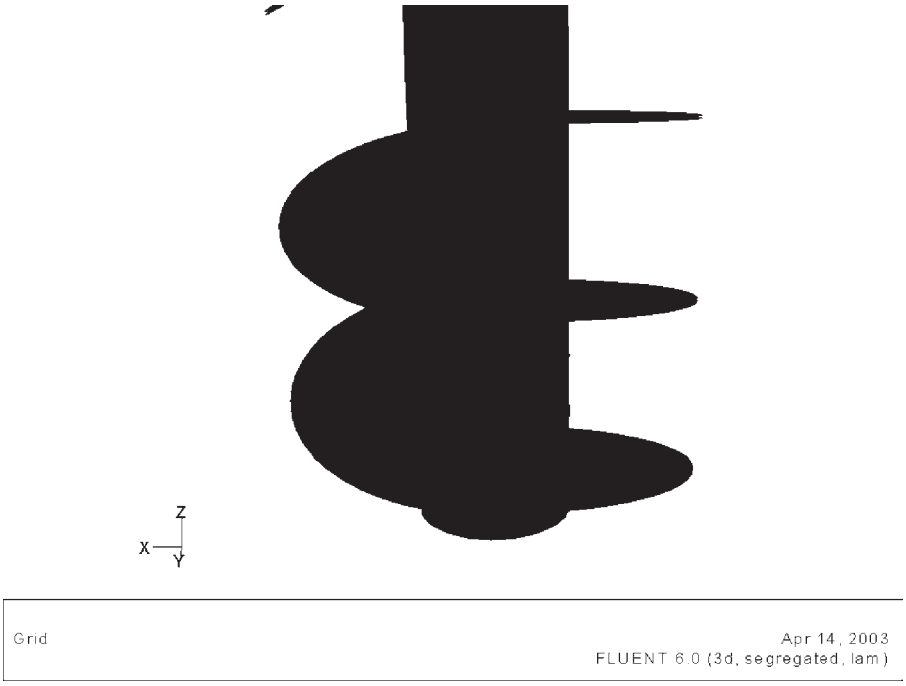

Fig.7. Original bottom screw.

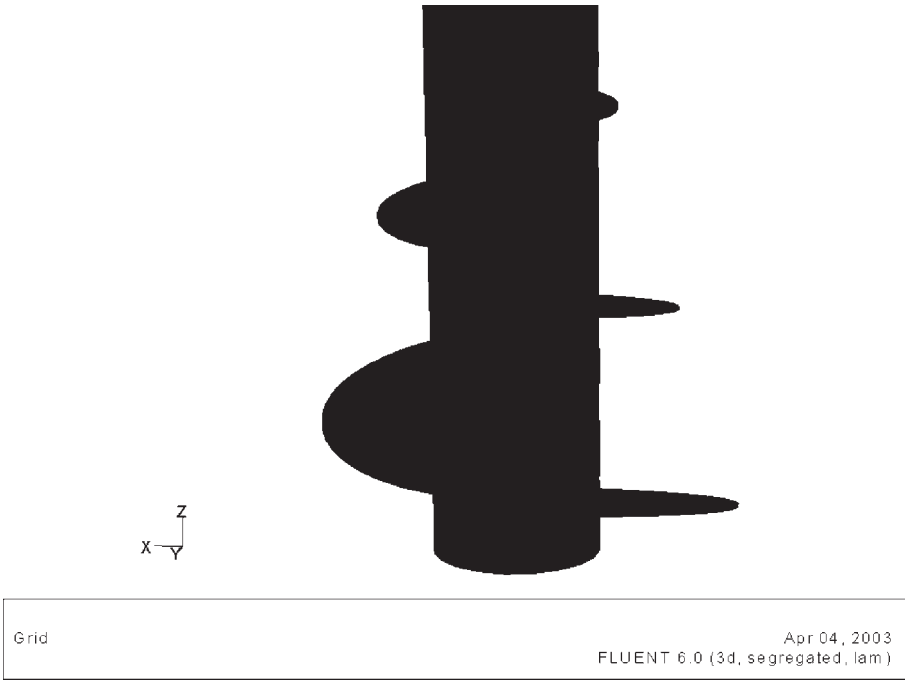

Fig. 8. Redesigned bottom screw.

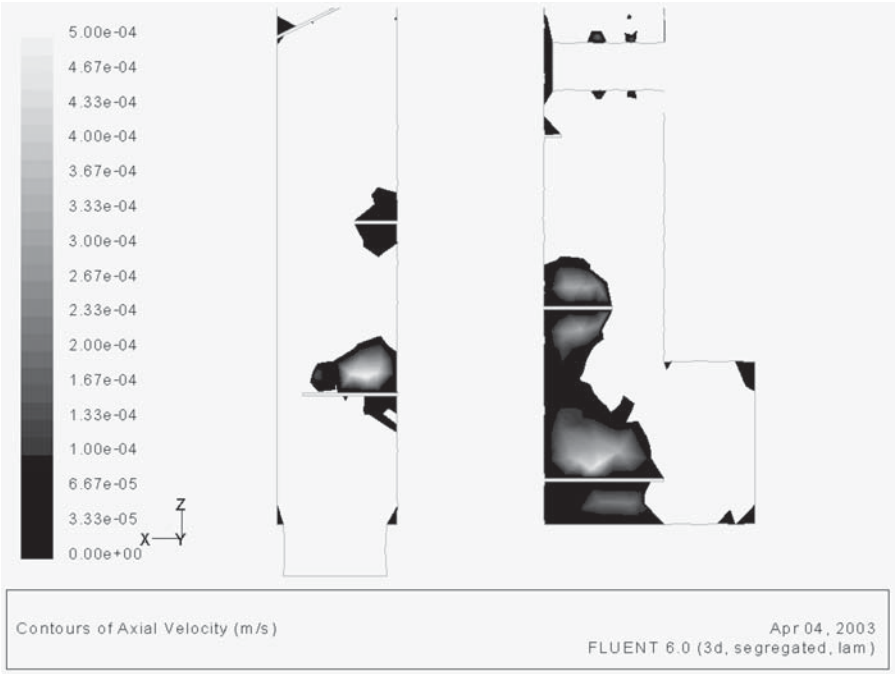

Fig. 9. Positive axial velocity contour (backflow) of redesigned screw reactor.

the random flow for the original reactor and the orderly flow for the redesigned reactor. This result further confirms that the backflow and overmixing inside the original reactor are reduced in the redesigned reactor.

Conclusion

Using the porous media model with a rotating reference frame, it was found that the overmixing and uneven flow inside the screw conveyor reactor resulted from the backflow in the bottom part of the screw. By redesigning the original cylindrical conical screw into a conical helical lifter, the backflow was reduced and even flow was achieved. As a result, this redesigned screw will decrease the risk of deterioration of sugars into toxic chemicals and improve the sugar yields. Further experimental work needs to be performed in this redesigned reactor to confirm the results of this simulation.

Nomenclature

C, C_2, D = matrix
D_p = particle diameter (m)
P = pressure (Pa)

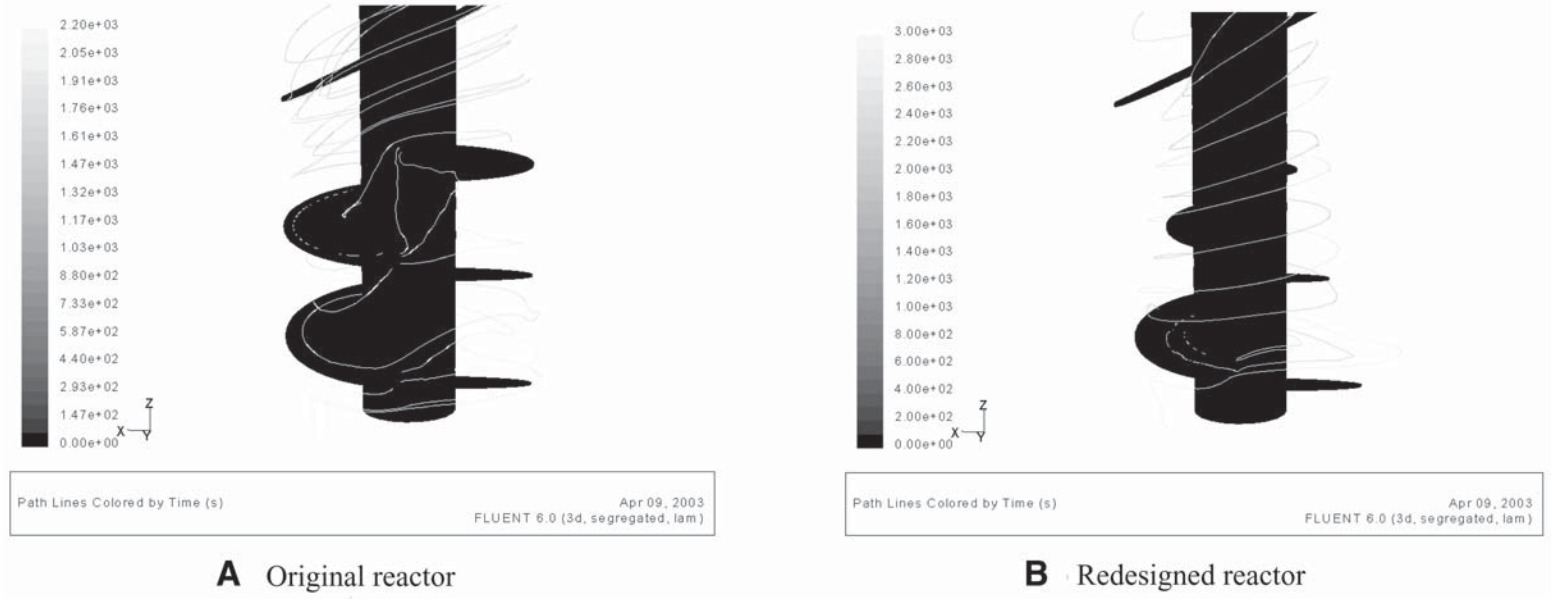

Fig. 10. Path lines of bottom part: **(A)** original reactor; **(B)** redesigned reactor.

S_i = source term for *i*th momentum equation
V_j = velocity of *i* direction
α = permeability
ε = void fraction
μ = molecular viscosity (kg/m·s)
ρ = density (kg/m^3)

Acknowledgment

This work was supported by the National Renewable Energy Laboratory (contract no. XCO-1-31016-01).

References

1. Torget, R. W., Hayward, T. K., and Elander, R. T. (1997), in the Proceedings of *Nineteenth Symposium on Biotechnology for Fuel and Chemicals*, presentation no. 4, Colorado Springs, CO.
2. Chen, R., Wu, Z., and Lee, Y. Y. (1998), *Appl. Biochem. Biotechnol*. **70–72,** 37–49.
3. Lee, Y. Y., Wu, Z., and Torget, R. W. (2000), *Bioresour. Technol.* **71,** 29–39.
4. Pettersson, P. O., Eklund, R., Saltin, J., and Zacchi, G. (2000), in Proceedings of *International Symposium on Alcohol Fuels XIII*, Stockholm, Sweden.
5. Converse, A. O. (2002), *Bioresour. Technol.* **81,** 109–116.
6. Wan, Y. and Hanley, T. R. (2003), *Appl. Biochem. Biotechnol.* **105–108,** 593–602.
7. Elander, R. T., Nagle, N. J., Tucker, M. P., Ruiz, R. O., Rohrback, B. T., and Torget, R. W. (2002), in Proceedings of *24th Symposium on Biotechnology for Fuel and Chemicals*, Gatlinburg, TN.
8. FLUENT. (2001), Fluent 6 User's Guide, vol.1, FLUENT, Lebanon, NH.
9. Ergun, S. (1952), *Chem. Eng. Prog*. **48(2),** 89–94.

0273-2289/04/114/0747–0758/$25.00

Production of Biodiesel Fuel by Transesterification of Rapeseed Oil

Gwi-Taek Jeong,[1] Don-Hee Park,[*,1–3] Choon-Hyoung Kang,[1] Woo-Tai Lee,[1] Chang-Shin Sunwoo,[1] Chung-Han Yoon,[4] Byung-Chul Choi,[5] Hae-Sung Kim,[6] Si-Wouk Kim,[7] and Un-Taek Lee[8]

[1]Faculty of Applied Chemical Engineering,
[2]Institute of Bioindustrial Technology,
[3]Biotechnology Research Institute,
[4]Department of Mineral and Energy Resources Engineering,
[5]School of Automotive Engineering, Chonnam National University, Kwangju 500-757, Korea, E-mail: dhpark@chonnam.ac.kr;
[6]Department of Chemical Engineering, Myongji University, Yongin 449-728, Korea,
[7]Department of Environmental Engineering, Chosun University, Kwangju 501-759, Korea; and
[8]Onbio Corporation, Pucheon-Si, Kyunggi-Do, 421-150, Korea

Abstract

Fatty acid methyl esters (FAMEs) show large potential applications as diesel substitutes, also known as biodiesel fuel. Biodiesel fuel as renewable energy is an alternative that can reduce energy dependence on petroleum as well as air pollution. Several processes for the production of biodiesel fuel have been developed. Transesterification processes under alkali catalysis with short-chain alcohols give high yields of methyl esters in short reaction times. We investigated transesterification of rapeseed oil to produce the FAMEs. Experimental reaction conditions were molar ratio of oil to alcohol, concentration of catalyst, type of catalyst, reaction time, and temperature. The conversion ratio of rapeseed oil was enhanced by the alcohol:oil mixing ratio and the reaction temperature.

Index Entries: Biodiesel fuel; transesterification; rapeseed oil; molar ratio; fatty acid methyl ester.

*Author to whom all correspondence and reprint requests should be addressed.

Introduction

Fatty acid methyl esters (FAMEs), which can be derived from vegetable oil and animal fats by transesterification reaction with alcohol, show large potential applications as diesel substitutes, also known as biodiesel fuel *(1–3)*. Biodiesel fuel as a renewable energy is an alternative that can reduce both energy dependence on petroleum and air pollution. Biodiesel fuels produced from various vegetable oils and animal fats have low viscosities similar to those of petrodiesel. In addition, characteristics of biodiesel fuels such as volumetric heating value, cetane number, and flask point are generally similar to those of petrodiesel *(4,5)*. The several advantages of using biodiesel fuel are that it may be an alternative renewable energy or a biodegradable nontoxic fuel; and that there is a reduction in air pollution from particulates, CO_2, SOx emissions, and recycling of CO_2 in short periods *(6)*.

Several processes for the production of biodiesel fuel have been developed by acid-, alkali-, and enzyme-catalyzed transesterification reactions *(7–10)*. Transesterification, called alcoholysis, is the displacement of alcohol from an ester by another alcohol in a process similar to hydrolysis. Transesterification is represented by a number of consecutive and reversible reactions. The reaction step is the conversion of triglycerides to diglycerides, followed by the conversion of diglycerides to monoglycerides and of monoglycerides to glyceride at each step *(11,12)*.

The transesterification process under alkali catalyst and short-chain alcohol gives a high level of conversion in short reaction times. At present, the most developed process using transesterification reactions employs an alkali-catalysis system. The main parameters affecting transesterification are molar ratio of vegetable oil to alcohol, catalysts, reaction temperature and time, contents of free fatty acids, and water in oils and fats *(8)*. Several alcohols were used for this process, including methanol, ethanol, propanol, butanol, and amyl alcohol. Methanol was utilized most broadly owing to low cost and its physical and chemical advantages such as polar and shorter-chain alcohol *(3)*. The bases used for the transesterification reaction include NaOH; KOH; carbonates; and alkoxides such as sodium methoxide, sodium ethoxide, sodium propoxide, and sodium butoxide. Sodium methoxide has been found to be more effective than NaOH, which produces a small amount of water by mixing NaOH and MeOH. However, NaOH and KOH are widely used in the industrial biodiesel production process owing to its low cost. For alkali-catalyzed transesterification, the oils and alcohol must be substantially anhydrous because water causes saponification with oil *(2,8)*. Ma et al. *(13)* suggested that the free fatty acid content of the refined oil should be as low as possible, below 0.5%. Another significant parameter affecting the conversion yield is the molar ratio of alcohol to vegetable oil. The stoichiometry of the transesterification reaction requires 3 mol of alcohol/mol of triglyceride to yield 3 mol of fatty esters and 1 mol of glycerol. Higher molar ratios result in greater conversion yields in a shorter reaction time *(8,14)*. The commonly used molar

Table 1
Fatty Acid Composition
and Characteristics of Rapeseed Oil

Characteristic	Content
Specific gravity	0.917
Moisture content (%)	0.01
Free fatty acid (%)	0.018
Unsaponifiable matter (%)	0.39
Fatty acid (% [w/w])	
Palmitic ($C_{16:0}$)	5.7
Stearic ($C_{18:0}$)	2.2
Oleic ($C_{18:1}$)	58.5
Linoleic ($C_{18:2}$)	24.5
Linolenic ($C_{18:3}$)	9.1

ratio of alcohol to glycerides is 6:1 *(8,9)*. The recommended amount of alkali catalyst for transesterification is between 0.1 and 1% (w/w) of oils and fats. Generally, reaction temperature was set at near the boiling point of alcohol. Higher reaction temperatures facilitate the reaction and shorten the reaction time *(14)*. Freedman et al. *(8)* reported the transesterification reaction of soybean oil and other vegetable oils in their investigation of the effects of the type of alcohol, molar ratio, type and amount of catalyst, and reaction temperature and time.

Biodiesel has become an attractive fuel but one problem remains: its production costs. There are two aspects of the cost of biodiesel production: the cost of raw materials (oil and alcohol) and the cost of process operation. The cost of raw materials accounts for approx 60–75% of the total biodiesel production cost *(15)*.

In the present study, we investigated the transesterification reaction of rapeseed oil with alcohol, examining the effects of the molar ratio of oil to alcohol, concentration of catalyst, type of catalyst, reaction time, and reaction temperature.

Materials and Methods

Rapeseed Oil, FAMEs, and Chemicals

Refined and bleached rapeseed oil were obtained from Onbio Co. Ltd. (Pucheon-Si, Korea). Table 1 presents the fatty acid composition and characteristics of rapeseed oil. Reference standards of FAMES such as palmitic, stearic, linolenic, linoleic, and oleic methyl ester of >99% purity were purchased from Sigma (St. Louis, MO). Methanol and catalysts such as KOH, NaOH, and sodium methoxide were analytical-grade chemicals.

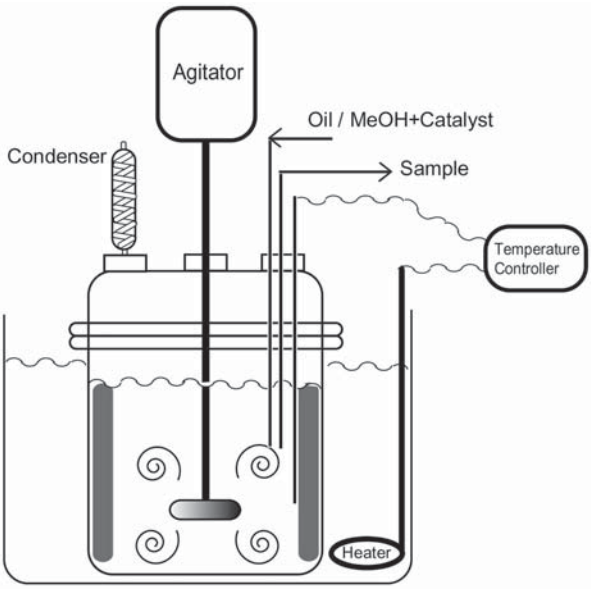

Fig. 1. Reactor setup for transesterification of rapeseed oil.

Apparatus

Transesterification reactions were performed in a 1-L four-necked reactor equipped with a reflux condenser, a thermometer, and a sampling port (Fig. 1). The reactor was immersed in a constant-temperature water bath controlled by a PID temperature controller, which was capable of controlling the temperature to within ±0.2°C of the setting point. Mixing was provided by an electric motor with a propeller-type impeller. During the experiments, samples were withdrawn with a 1-mL glass pipet through a sampling port of the reactor at various times.

Reaction Procedures and Conditions

Initially, the reactor was charged with 400 g of rapeseed oil and heated to the set temperature with agitation. Catalyst was dissolved in the required amount of methanol and heated to the set temperature. After reaching the set temperature of reactant and catalyst, methanolic catalyst was added to the base of the reactor to prevent evaporation of methanol. The reaction was timed immediately after the addition of catalyst and methanol. Reaction experiment parameters were designed to determine the conversion yield of rapeseed oil (Table 2).

Preparation and Analysis of Samples

Samples were drawn at preset time intervals. About 1 mL of sample mixture was collected in 10-mL test tubes, and 1 *N* HCl was added and vortexed immediately to neutralize the catalyst and stop the reaction.

Table 2
Proposed Operating Conditions
of Alkali-Catalyzed Transesterification

Process	Base-catalyzed alcoholysis
Fatty glyceride	Vegetable oil (rapeseed oil)
Alcohol	Methyl alcohol (above 99.8%)
Catalyst	Sodium methoxide, KOH, NaOH (0.1–1.2% [w/w])
Reaction condition	Reaction temperature: 30–65°C; oil:MeOH molar ratio:1:3–1:20
Purification and recovery	Distillation, centrifugation, washing

Pretreated samples were evaporated to remove nonreacted methanol and extracted by solvents (chloroform:*n*-hexane = 1:2) and centrifuged at low temperature to remove glycerin. One milliliter of supernatant was evaporated under vacuum and diluted with methanol (high-performance liquid chromatography [HPLC] grade) for HPLC analysis.

Samples were analyzed for FAMES using HPLC. An HPLC (Younglin) was equipped with a model 930D pump and an ultraviolet detector (M720, 205 nm). A Waters Spherisorb ODS2 column (4.6 × 250 mm with 5-μm particle size) was used for the separation. The mobile phase consisted of a 48:48:4 volumetric mixture of acetonitrile, acetone, and water. The mobile phase was degassed by sonication for 30 min. The pump was operated at a constant 1.0 mL/min flow rate, and the column temperature was maintained in a column chamber at 35ºC. The sampling injection volume was 20 μL, and peak identification was made by comparing the retention time between the sample and the standard materials. Using calibration curves of FAMES, the conversion yields were calculated.

Results and Discussion

For the alkali-catalyzed transesterification reaction of rapeseed oil, we investigated several operating conditions: reaction temperature, type and amount of catalyst, molar ratio of methanol to oil, and reaction time. In alkali-catalyzed transesterification, the amount of free fatty acid was assumed to be below 0.5% on the basis of oil weight, in order to obtain high conversion yield *(13)*. The conversion yield or percentage of conversion was calculated by dividing the amount of product by the maximum theoretical product. Because it has a high acid value, the activity of catalyst was diminished in the transesterification reaction. As reported in Table 1, the fatty acid content of rapeseed oil used for this experiment was 0.018%, which was lower than the proposed value (below 0.5%).

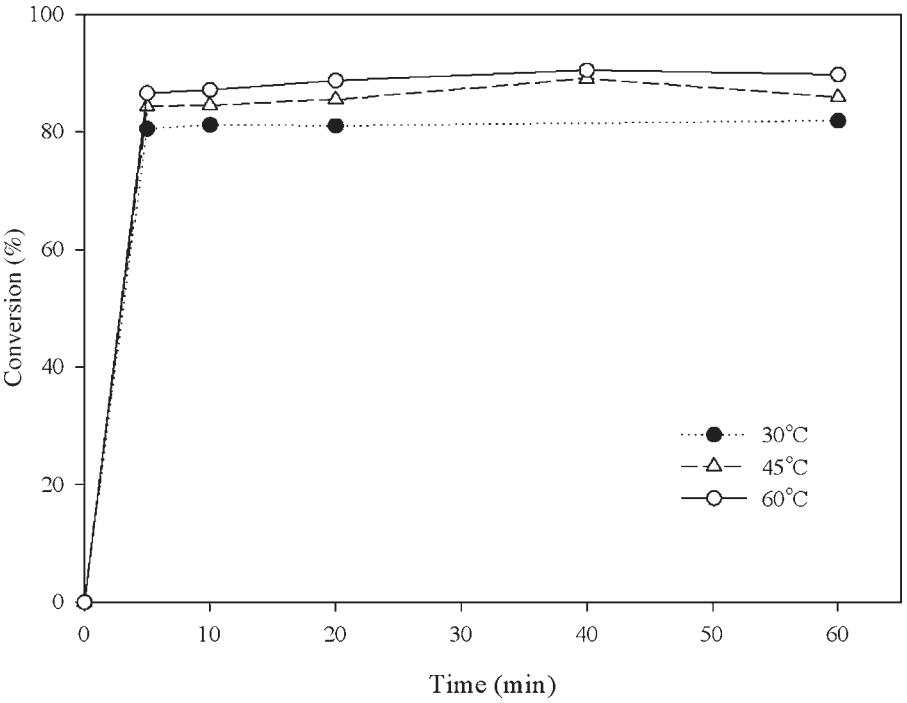

Fig. 2. Effect of reaction temperature onconversion at 1.0% (w/w) KOH at molar ratio of 1:6.

Effect of Temperature

Generally, alkali-catalyzed transesterification is performed near the boiling point of the alcohol, but several researchers have reported high conversion yield at room temperature *(8,14)*. Low reaction temperature was desirable, since reaction temperature was closely related to the energy cost of the biodiesel production process.

The effect of temperature on rapeseed oil transesterification reaction was investigated at 60, 45, and 30°C using the conditions of 1% (w/w), KOH as a catalyst and a methanol:oil molar ratio of 6:1 (Fig. 2). Reaction equilibrium was reached within 10 min at each temperature studied. After 10 min of reaction, the conversion yields were 87.1, 84.5, and 81.2% at 60, 45, and 30°C, respectively. The conversion yield of rapeseed oil had only a small difference at lower temperatures. Freedman et al. *(8)* reported the effect of temperature on transesterification of refined soybean oil using a molar ratio of 1:6 and 1% NaOH. After 0.1 h, conversion yields were 94, 87, and 64% at 60, 45, and 32°C, respectively *(8)*. Another study showed that the conversion of rapeseed oil at different temperature conditions (65, 50, and 40°C) with an oil:MeOH molar ratio of 1:6, and 1.7% NaOH began at 40, 20, and 5 min, respectively *(9)*. This study used longer reaction times than our experiments.

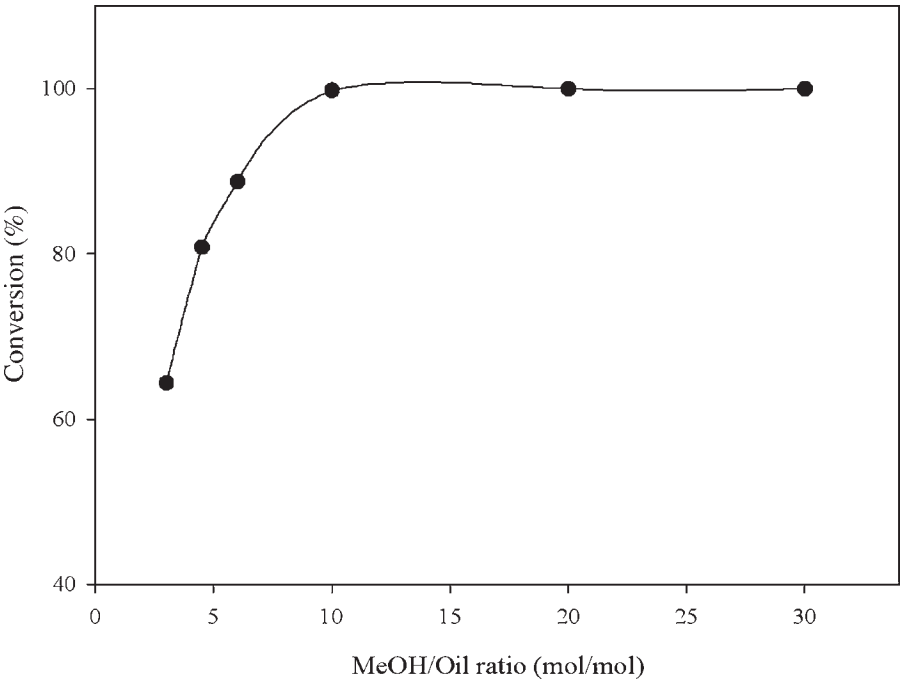

Fig. 3. Effect of methanol molar ratio on conversion at 1.0% (w/w) KOH, 60°C, and 60 min.

Effect of Molar Ratio

The most significant factor of alkali-catalyzed transesterification was the molar ratio of the alcohol and oil. The stoichiometry of alkali-catalyzed transesterification requires 3 mol of alcohol/1 mol of triglyceride to generate 3 mol of FAME and 1 mol of glycerol. Since the transesterification is composed of reversible and consecutive reactions, the increase in molar ratio of methanol will result in high conversion yields.

In this experiment, the effect of molar ratio was studied by varying it from 1:3 to 1:20 with a reaction temperature of 60°C, and 1% KOH on the basis of oil weight as catalyst for 60 min; the results are shown in Fig. 3. High conversion yield was obtained in a short period of reaction time for every molar ratio condition. After 20 min, conversion yields were equilibrated at 64~99%. Below a 1:10 molar ratio, conversion yields sharply increased with an increase in molar ratio. The increase in conversion yield was not noticed at a molar ratio higher than 1:10. In the alkali-catalyzed transesterification process, the conversion yield increased with added methanol, and total production costs increased when using high amounts of methanol. Despite high energy consumption by the addition of a large amount of methanol, it was concluded that a molar ratio of 1:6 to 1:10 was more suitable. Kim and Kang *(14)* reported an optimum molar ratio of 1:6 in an experiment using

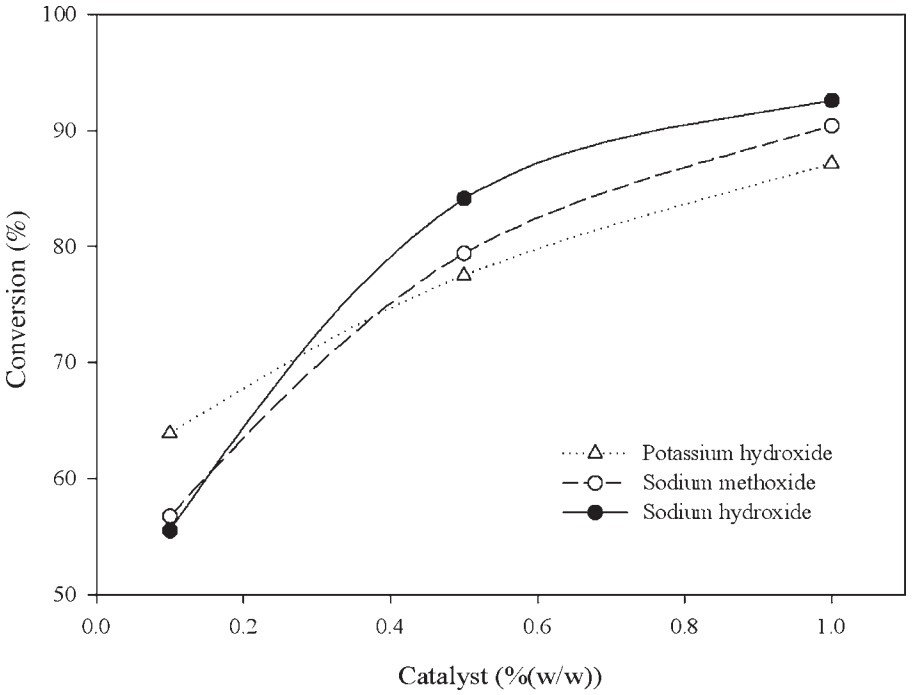

Fig. 4. Effect of catalyst type and concentration on conversion at molar ratio of 1:6, 60°C, and 20 min.

soybean oil with a high unsaturated fatty acid content and a reaction temperature above 60°C, whereas rapeseed oil with a high oleic acid content had an optimum molar ratio of 1:6 to 1:8 below 60°C.

Comparison of Alkali and Alkoxide

Alkali metal alkoxides such as KOH, NaOH, and CH_3ONa are the most effective catalysts in alkali-catalyst transesterification. When using KOH, NaOH, and CH_3ONa alkali-catalyst for FAME conversion, the active catalytic species were the methoxide anion (CH_3O^-), formed by the reaction between methanol and hydroxide ions of KOH and NaOH. In addition, the methoxide anion was formed by dissolution of sodium methoxide. Sodium methoxide causes the formation of several byproducts, mainly sodium salts, that have to be treated as waste and additionally require high-quality oil *(16)*. However, KOH has an advantage because it can be converted into KOH by reaction with phosphoric acid, which can serve as a fertilizer. Since KOH is more economical than sodium methoxide, it is the preferred choice for large-scale FAME production process.

Figure 4 compared the conversion yields of three different alkali catalysts at a molar ratio of 1:6, 60°C, and a reaction time of 20 min. All three alkali catalysts caused some difference in conversion yields. NaOH

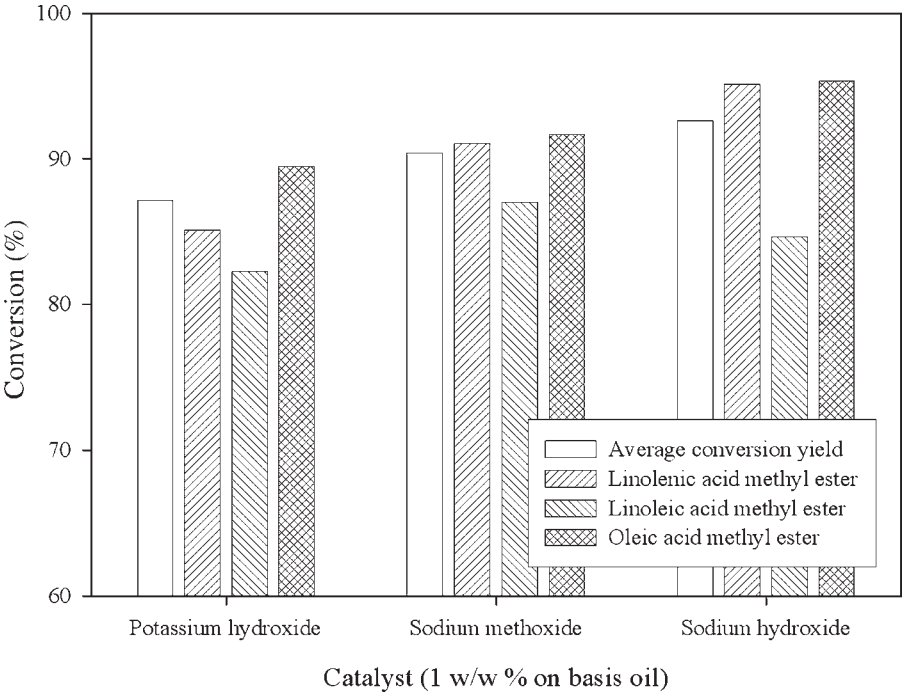

Fig. 5. Effect of catalyst type on FAME content after 10-min reaction with a catalyst of 1.0% (w/w) at a effect of molar ratio of 1:6, 60°C, and 10 min.

showed the best conversion yield, above 0.5% (w/w). NaOH has a lower molecular weight than KOH, so a smaller concentration (w/w) is required to achieve the same effect. In addition, its salts are less soluble in FAME solution than those of KOH. KOH was less effective than NaOH as a catalyst for FAME production from rapeseed oil. Freedman et al. *(8)* reported that methyl ester conversion yields were very similar to those of 1% NaOH and 0.5% $NaOCH_3$ used as catalyst in soybean oil with a 1:6 molar ratio. In our following experiments, KOH was used as alkali catalyst because of transesterification catalyzed by NaOH and CH_3ONa resulted in byproducts, as previously described.

Figure 5 compares the conversion yields of each FAME, transesterified from rapeseed oil, after a 10-min reaction with a 1.0%(w/w) catalyst at a molar ratio of 1:6 and 60°C. In all the catalysts studied, oleic acid was best converted to methyl oleate.

Effect of Catalyst Concentration

In alkali-catalyzed transesterification, the optimal catalyst and the amounts used were collected by optimal concentration instead of high conversion conditions, because a high catalyst concentration at a high conversion yield was decreased by a reverse hydrolysis reaction. Figure 6

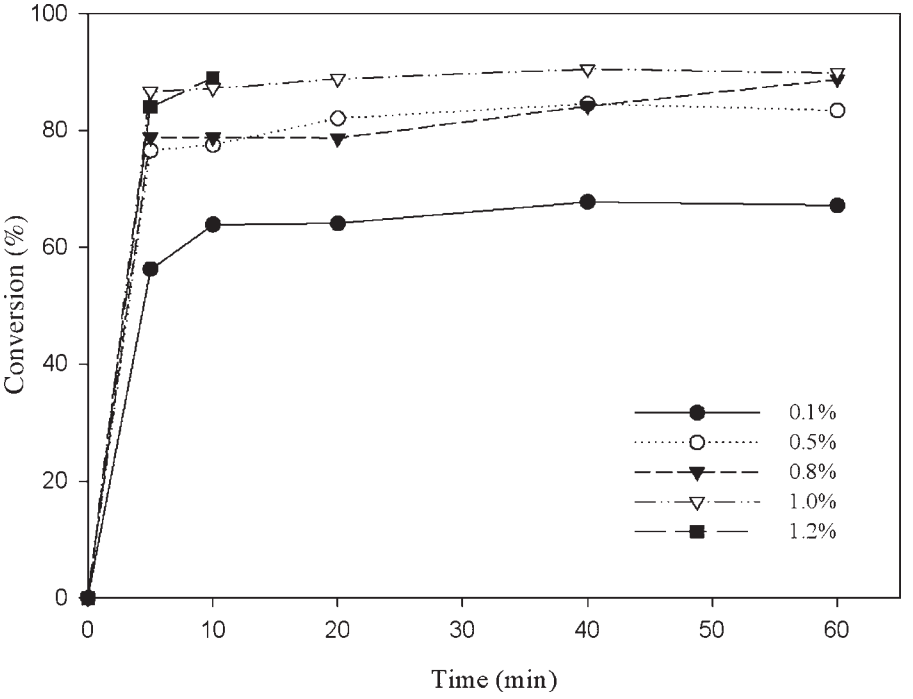

Fig. 6. Effect of KOH concentration on conversion at molar ratio of 1:6 and 60°C.

shows the effect of the concentration of KOH catalyst on the basis of oil weight at 60°C and a molar ratio of 1:6. The conversion yield was enhanced by increasing KOH concentration. The conversion rate increased rapidly within 5 min, and slowly after 10 min. At a low catalyst concentration (0.1%), the conversion rate was low. A small difference in FAME was shown at a conversion yield above 1.0% KOH. Some studies have shown that 1% KOH was optimum for transesterification of rapeseed oil *(17)*.

Effect of Reaction Time

Reaction temperature and time were significant operating parameters, which are closely related to the energy costs, of the biodiesel production process. Figure 7 shows the effect of reaction time on the transesterification of rapeseed oil at a catalyst concentration of 1%, molar ratio of 1:6, and 60°C. Within 5 min, the reaction was rapid. Rapeseed oil was converted to above 85% within 5 min and reached equilibrium state after about 10 min. Several researchers reported that the conversion of vegetable oils to FAME was achieved above 80% within 5 min with a sufficient molar ratio *(8,11)*. For a reaction time of 60 min, linoleic acid methyl ester was produced at a low conversion rate, whereas oleic and linolenic methyl ester were rapidly produced.

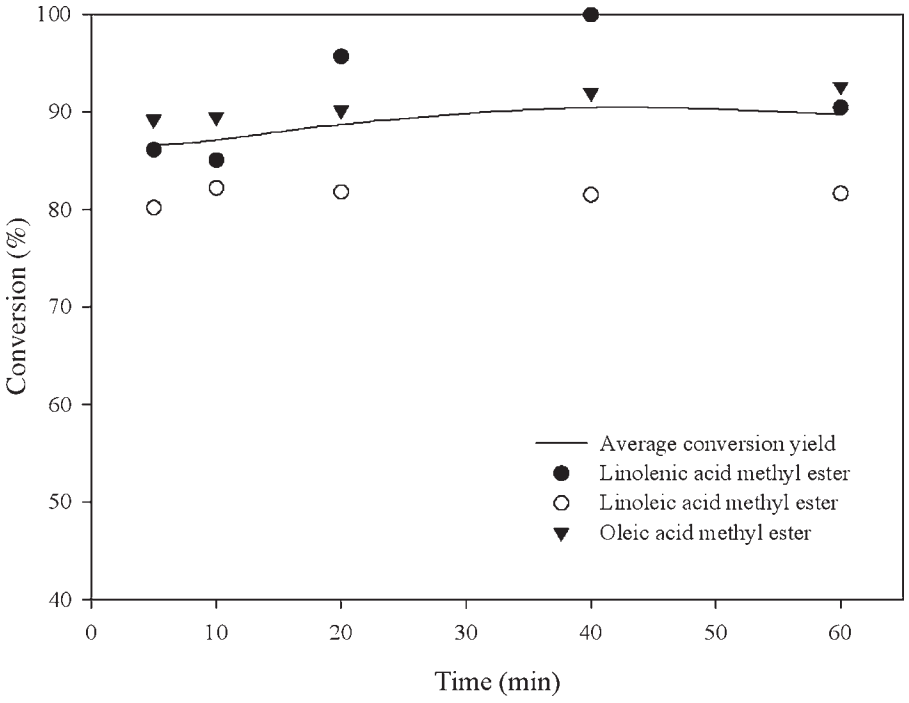

Fig. 7. Effect of reaction time on conversion and composition at 1.0% (w/w) KOH, molar ratio of 1:6 and 60°C.

Some studies have shown that the complete factorial design of KOH-catalyzed transesterification of refined rapeseed oil could be optimized at 50°C, 0.9% KOH, and an MeOH/oil ratio of 6:1; conversion was 80.3% *(18)*.

Conclusion

FAME production of rapeseed oil by alkali-catalyzed transesterification reaction was investigated. To obtain optimum conversion yield, anhydrous methanol and rapeseed oil with a free fatty acid content of <0.5% were used. The optimum conditions for alkali-catalyzed transesterification using KOH were determined as follows: an oil to methanol molar ratio of 1:8 to 1:10; KOH, 1.0% (w/w) on the basis of oil weight, as catalyst; a reaction temperature of 60°C; and reaction time of 30 min. At these conditions, the FAME conversion yield was approx above 98%. From the refined FAME product (biodiesel), the FAME purity was obtained above 99% through posttreatment such as washing and centrifugation.

Acknowledgment

We wish to thank Korea Energy Management Corporation for financial support.

References

1. Ramachandra Murty, V., Bhat, J., and Muniswaran, P. K. A. (2002), *Biotech. Bioproc. Eng.* **7(2),** 57–66.
2. Fukuda, H., Kondo, A. and Noda, H. (2001), *J. Biosci. Bioeng*. **92(5),** 405–416.
3. Ma, F. and Hanna, M. A. (1999), *Bioresour. Technol.* **70,** 1–15.
4. Lang, X., Dalai, A. K., Bakhshi, N. N., Reaney, M. J. and Hertz, P. B. (2001), *Bioresour. Technol.* **80,** 53–62.
5. Cvengros, J. and Povazanec, F. (1996), *Bioresour. Technol.* **55,** 145–152.
6. Graboski, M. S. and McCormick, R. L. (1998), *Prog. Energy Combust. Sci.* **24,** 125–164.
7. Ahn, E., Mittelbach, M., and Marr, R. (1995), *Sep. Sci. Technol.* **30(7–9),** 2021–2033.
8. Freedman, B., Pryde, E. H., and Mounts, T. L. (1984), *JAOCS* **61(10),** 1638–1643.
9. Karaosmanoglu, F., Akdag, A., and Cigizoglu, K. B. (1997), *Appl. Biochem. Biotechnol.* **61,** 251–264.
10. Nelson, L. A., Foglia, T. A., and Marmer, W. N. (1996), *JAOCS* **73(8),** 1191–1195.
11. Darnoko, D. and Cheryan, M. (2000), *JAOCS* **77(12),** 1263–1267.
12. Noureddini, H. and Zhu, D. (1997), *JAOCS* **74(11),** 1457–1463.
13. Ma, F., Clements, L. D., and Hanna, M.A. (1998), *Ind. Eng. Chem. Res*. **37,** 3768–3771.
14. Kim, H. S. and Kang, Y. M. (2001), *J. Korean Oil Chem. Soc*. **18(4),** 298–305.
15. Krawczyk, T. (1996), *INFORM* **7,** 801–829.
16. Ahn, E., Konear, M., Mittelbach, M., and Marr, R. (1995), *Sep. Sci. Technol*. **30,** 2021–2033.
17. Fillieres, R., Benjelloun-Mlayah, B., and Delmas, M. (1995), *Ibid*. **72,** 427–432.
18. Zmudzinska-Zurek, B. and Buzdygan, S. (2002), *Przemysl Chemiczny* **81(10),** 656–658.

Volume 115

Session 4

Biotechnology for Fuels and Chemicals—
Past, Present, and Future

Session 4

Biotechnology for Fuels and Chemicals—Past, Present, and Future

Charles D. Scott[1] and Charles E. Wyman[2]

[1]*Oak Ridge National Laboratory, Oak Ridge, TN; and*
[2]*Dartmouth College, Hanover, NH*

This session reflected on the evolution of biotechnology, industry, and this annual symposium for sustainable production of fuels and chemicals and speculated on future developments that can enhance their impacts. To structure a cohesive session covering areas appropriate for the silver anniversary meeting, presentations were invited in selected areas that offered complementary perspectives for the audience. Dr. Charles Scott, the founder of the annual symposium and its chair from 1978 through 1988, chaired this session, and the cochair was Dr. Charles Wyman, who was responsible for initiating alternate years in Colorado as symposium chair and cochair from 1988 to 1996.

Dr. Scott began the session with a brief review of the history of the symposium with his talk "Origins and Changes in the Annual Symposium on Biotechnology for Fuels and Chemicals." This presentation provided a sense of the evolution of the meeting from its initial comprehensive consideration of both biologic and thermal conversion of biomass and fossil sources and waste remediation to a gradual shift in focus to primarily biologic processing of biomass. The talk also described the change in venue from the single location at the Riverside Motor Lodge in Gatlinburg, TN, to alternate locations in Colorado and larger meeting facilities in Gatlinburg and described the growth in attendance for the symposium.

Next, Dr. Tom Jeffries from the United States Department of Agriculture Forest Products Laboratory and the University of Wisconsin presented a talk titled "Improvements in Applied Microbiology and Biochemistry for Bioprocessing." Dr. Jeffries, who was presented with the Charles D. Scott Award at the 25th symposium, provided an entertaining historical perspective on biomass conversion, describing some significant events and pioneers in both biological and thermochemical conversion technologies. He also provided some historical photographs that reminded us of many of these people and developments. He reviewed the frequent calls to substitute biomass for petroleum over many generations. The presentation reflected on some of the important advances realized to date and described many of the challenges that still remain.

Dr. Donald Johnson, recently retired from Grain Processing Corporation, followed with his overview "The Evolution of Industrial Bioprocessing." This interesting talk summarized many important developments in the field from such early processes as acetone/butanol production by Chaim Weizmann technology, to the use of fermentation ethanol during World War II to make rubber for tires, to penicillin and citric acid production. He also described the development of the industry for production of glucose from corn and its use in such high-growth products as high fructose corn syrup and ethanol. Finally, an interesting correlation was shown between symposium attendance and the price of crude oil.

Dr. David Glassner from Cargill Dow LLC provided a fascinating perspective titled "Startup of a New Business in Processing of Biomass to Chemicals." In particular, he discussed the emergence of technology now being commercialized for converting sugars to lactic acid that can be used to make new polymers with unique environmental and other attributes. His presentation described the current emphasis on corn glucose but also considered the value of moving toward conversion of cellulosic biomass. He provided interesting insight into the culture associated with fostering and applying new technology at such a large scale.

Dr. Charles Wyman from Dartmouth College then presented his thoughts in a talk titled "The Status, Synergies, and Benefits of Biological Processing of Cellulosic Biomass to Fuels and Chemicals." He pointed out that the cost of cellulosic biomass is competitive with petroleum now and the importance of reducing processing costs if products from this substrate are to compete. He further demonstrated that tremendous progress has been made in this direction over the last 20 yr, and that coproducing chemicals and other products in addition to fuel ethanol would offer economic synergies. However, he also reminded the audience that the key challenge facing commercialization of biologic processing of cellulosic biomass is the risk of introducing new technology. Thus, first plants will likely benefit by focusing on single products to control market and technology uncertainties. In addition, improving our collective understanding of biomass conversion will improve our ability to commercialize biologic processes with confidence and likely pay more immediate dividends than seeking to prematurely diversify the product slate.

The next speaker was Dr. Lee Lynd from Dartmouth College, whose presentation was titled "Advanced Technology Scenarios for Production of Fuels and Chemicals." He pointed out the need to transition to a sustainable world with an improved environment, greater energy security, more favorable balance of trade, healthier rural economies, and enhanced business opportunities. He also demonstrated the vital role that biomass can play in realizing that vision and the competitive cost of cellulosic biomass as a resource. He then discussed technology advances that would make processing costs competitive. Dr. Lynd included key insight into the impact of improved vehicle efficiency in supporting a transition to a sustainable world and the value of deriving multiple products to take advantage of the

diverse composition of biomass resources and reduce land-use demands. He left the audience with the message that integration of biomass resources with processing and end-use markets will facilitate production of a large fraction of our energy needs with modest resource demands and provide significant security, sustainability, and other benefits for the world.

Dr. David Morris from the Institute for Local Self Reliance, was the final speaker of the session. In his inspiring talk "The Future of the Carbohydrate Economy," he focused on public policy because regulations, statutes, tax incentives, and zoning ordinances all influence the direction of scientific ingenuity, entrepreneurial energy, and capital investments. He pointed out that policies impeding carbohydrate products and favoring petroleum and nuclear power moved us from the use of renewable products in the late nineteenth and early twentieth centuries. However, policies resulting from our growing environmental awareness are encouraging the revival of a carbohydrate economy, and the carbohydrate economy could take off again if the many constituencies work together, fossil fuels and their derivatives pay their full costs, the carbohydrate economy positions itself to be a major player, and local benefits are emphasized. He closed by noting that progress will only come when we develop the rules that channel scientific ingenuity and entrepreneurial energy and investment capital in directions that are compatible with the social and economic objectives that we seek.

0273-2289/04/115/0765–0769/$25.00

Origins of and Changes in the Symposium Series on Biotechnology for Fuels and Chemicals

Charles D. Scott*

Retired Director,
Bioprocessing Research and Development Center,
Oak Ridge National Laboratory,
109 Danbury Drive, Oak Ridge, TN 37830,
E-mail: cdscott1@aol.com

Abstract

More than two decades ago, a group of research engineers and applied scientists with interest in energy applications of bioprocessing initiated an annual symposium series ultimately entitled "Biotechnology for Fuels and Chemicals." The Department of Energy, several of the national laboratories, and various industrial firms have supported these symposia that are now held alternately in the mountains of Tennessee and Colorado. There has been wide acceptance of these meetings, with participants from the government, academia, and the commercial sector, and more than 20 different nations have been represented. The peer-reviewed proceedings have been published and are an important source for innovative bioprocessing research.

Index Entries: Symposium; biotechnology; fuels; chemicals; bioprocessing.

Introduction

About 26 yr ago when innovative bioprocessing concepts were receiving renewed attention, a group of research engineers and applied scientists with interest and involvement in energy applications got together to plan for a symposium series on bioprocessing in the energy area. The occasional specific sessions emphasizing this area at the various meetings of professional organizations, such as the American Institute of Chemical Engineers and the American Chemical Society, were appreciated, but a more sustained and structured series of meetings was desired.

*Author to whom all correspondence and reprint requests should be addressed.

It was decided that energy production and conservation would initially be emphasize. Furthermore, it was proposed that an appropriate location be used that could provide a facility that would accommodate 150 to 250 participants so they could engage in intense interactions on a scientific and technical basis. Since wide participation of the attendees was desired, oral presentations, unlimited poster presentations, and discussion topics were to be incorporated. Social functions were also to be planned that would encourage interpersonal interactions and detailed technical discussions. The first meeting was held in 1978.

Location

The Bioprocessing Research and Development Group at Oak Ridge National Laboratory (ORNL) agreed to host the first meeting. This first in the series was specifically entitled "Biotechnology in Energy Production and Conservation" and was held in the mountains of East Tennessee at Gatlinburg. The same location and title were used for the first four annual meetings; however, it became obvious that the more generic area of fuels and chemicals was of most interest. Therefore, the fifth and succeeding symposia were entitled "Symposium on Biotechnology for Fuels and Chemicals."

Later it was decided that the hosting duties would be shared between ORNL and the Solar Energy Research Institute (afterward named National Renewable Energy Laboratory, NREL), with the annual meetings alternating between the mountain areas of Tennessee and Colorado. It was found that alternating these sites provided a bit of welcomed variability, and maintaining the mountain locations provided a good sense of continuity. The use of the Tennessee site in the resort town of Gatlinburg has continued, and several different Colorado sites have also been used, mainly in resort areas such as Colorado Springs, Boulder, and now Breckenridge.

Symposium Support

The interest in and support of these symposia have been quite extensive. Several US Department of Energy (DOE) offices have been involved, including the Office of Alternative Fuels, the Office of Fuels Development, the Office of Waste Reduction Technologies, the Office of Industrial Technologies, the Office of Basic Energy Sciences, and the Office of Health and Environmental Research. Other US governmental agencies such as the National Institute of Standards and Technology and the Tennessee Valley Authority have also been sponsors. There has been international support from National Resources Canada, and numerous industrial firms continue to support the symposia. Several of the national laboratories have supported the meetings both monetarily and organizationally. These have included ORNL, NREL, Argonne National Laboratory, and Idaho National Engineering Laboratory.

Participants

There has been wide acceptance of these annual meetings with participants from the DOE and other government agencies, academia, national laboratories, and many commercial enterprises. There has also been a significant international involvement, with the attendees representing as many as 20 different countries. On average, about 25% of the attendees are international and about 30% are industrial. Typically, the attendance has been between 200 and 300 participants; however, there has been a significant increase in the last 3 yr, reaching a total of 450 for this 25th Symposium (Fig. 1). The total number of submitted manuscripts of the presented papers has also increased to a high of 150 for this symposium.

Publication of Proceedings

From the very beginning, it was decided that the presented papers would be compiled and published in appropriate international journals. This was to include both oral and poster presentations. The first several symposia were published in *Biotechnology and Bioengineering (1–8)*, and later proceedings have been published in *Applied Biochemistry and Biotechnology (9–24)*. These peer-reviewed proceedings have become an important resource for innovative bioprocessing research.

This annual symposium continues the tradition established 25 yr ago, and we look forward to many more in the future.

References

1. Scott, C. D., ed. (1979), *Biotechnol. Bioeng. Symp.* **8,** 1–513.
2. Scott, C. D., ed. (1980), *Biotechnol. Bioeng. Symp.* **10,** 1–353.
3. Scott, C. D., ed. (1981), *Biotechnol. Bioeng. Symp.* **11,** 1–666.
4. Scott, C. D., ed. (1982), *Biotechnol. Bioeng. Symp.* **12,** 1–493.
5. Scott, C. D., ed. (1984), *Biotechnol. Bioeng. Symp.* **13,** 1–672.
6. Scott, C. D., ed. (1984), *Biotechnol. Bioeng. Symp.* **14,** 1–697.
7. Scott, C. D., ed. (1986), *Biotechnol. Bioeng. Symp.* **15,** 1–741.
8. Scott, C. D., ed. (1986), *Biotechnol. Bioeng. Symp.* **17,** 1–781.
9. Scott, C. D., ed. (1988), *Appl. Biochem. Biotechnol.* **17,** 1–378.
10. Scott, C. D., ed. (1988), *Appl. Biochem. Biotechnol.* **18,** 1–420.
11. Scott, C. D., Greenbaum, E., and Wyman, C. E., eds. (1989), *Appl. Biochem. Biotechnol.* **20/21,** 1–872.
12. Greenbaum, E. and Wyman, C. E., eds. (1990), *Appl. Biochem. Biotechnol.* **24/25,** 1–936.
13. Greenbaum, E. and Wyman, C. E., eds. (1991), *Appl. Biochem. Biotechnol.* **28/29,** 1–934.
14. Wyman, C. E. and Woodward, J., eds. (1992), *Appl. Biochem. Biotechnol.* **34/35,** 1–834.
15. Woodward, J., Wyman, C. E., and Goodwin, B. J., eds. (1993), *Appl. Biochem. Biotechnol.* **39/40,** 1–809.
16. Wyman, C. E., Woodward, J., and Goodman, B. J., eds. (1994), *Appl. Biochem. Biotechnol.* **45/46,** 1–961.
17. Davison, B. H. and Wyman, C. E., eds. (1995), *Appl. Biochem. Biotechnol.* **51/52,** 1–823.
18. Wyman, C. E. and Davison, B. H., eds. (1996), *Appl. Biochem. Biotechnol.* **57/58,** 1–1030.
19. Davison, B. H., Finkelstein, M., and Wyman, C. E., eds. (1997), *Appl. Biochem. Biotechnol.* **63–65,** 1–897.

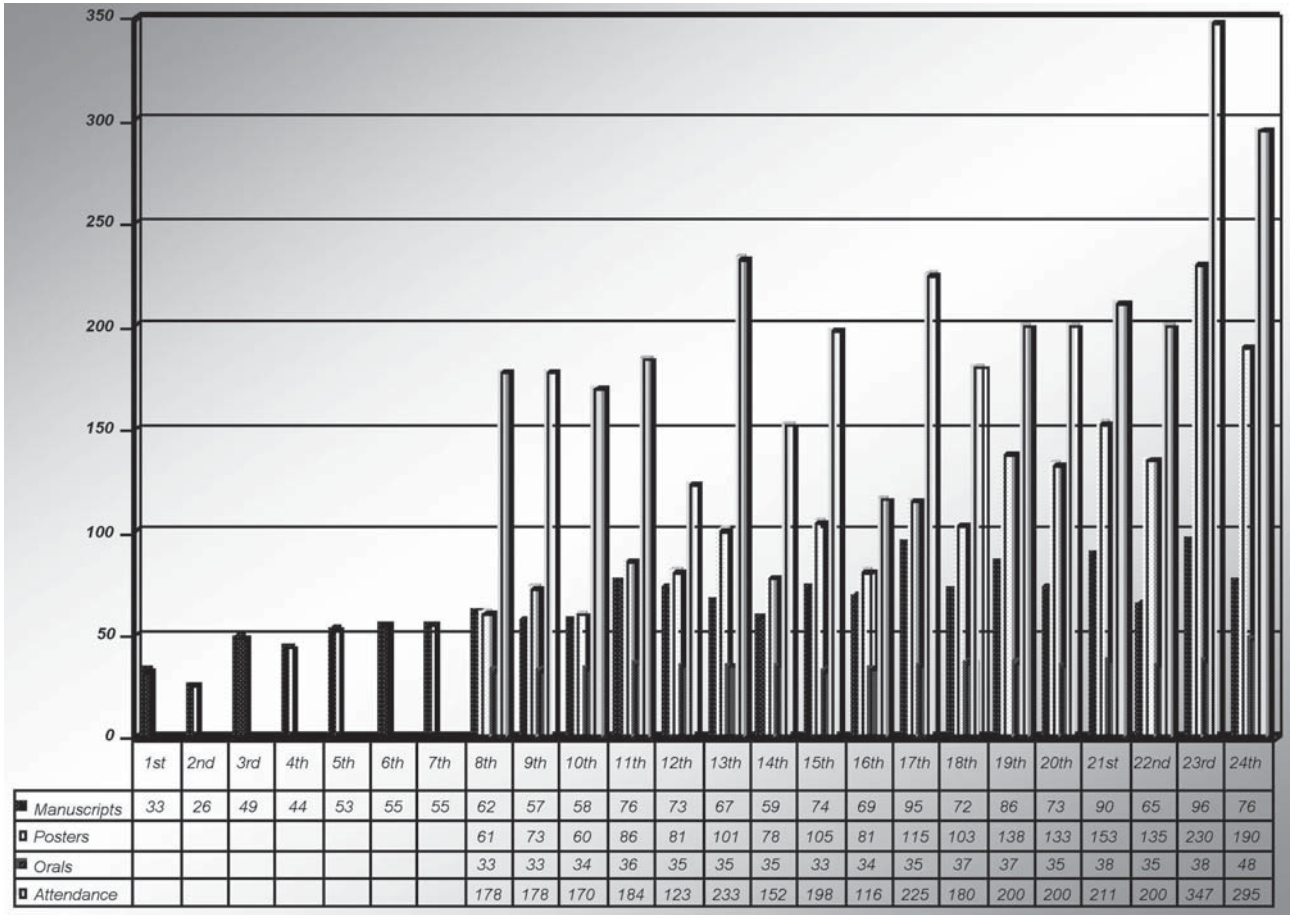

	1st	2nd	3rd	4th	5th	6th	7th	8th	9th	10th	11th	12th	13th	14th	15th	16th	17th	18th	19th	20th	21st	22nd	23rd	24th
Manuscripts	33	26	49	44	53	55	55	62	57	58	76	73	67	59	74	69	95	72	86	73	90	65	96	76
Posters								61	73	60	86	81	101	78	105	81	115	103	138	133	153	135	230	190
Orals								33	33	34	36	35	35	35	33	34	35	37	37	35	38	35	38	48
Attendance								178	178	170	184	123	233	152	198	116	225	180	200	200	211	200	347	295

Fig. 1. Growth patterns for this symposium series. Note that complete information for yr 1–7 was not available.

20. Finkelstein, M. and Davison, B. H., eds. (1998), *Appl. Biochem. Biotechnol*. **70–72,** 1–1015.
21. Davison, B. H. and Finkelstein, M., eds. (1999), *Appl. Biochem. Biotechnol*. **77–79,** 1–884.
22. Finkelstein, M. and Davison, B. H., eds. (2000), *Appl. Biochem. Biotechnol*. **84–86,** 1–1171.
23. Davison, B. H. and Finkelstein, M., eds. (2001), *Appl. Biochem. Biotechnol*. **91–93,** 1–798.
24. Finkelstein, M., McMillan, J. D., and Davison, B. H., eds. (2002), *Appl. Biochem. Biotechnol*. **63–65,** 1–1228.
25. Davison, B. H., Finkelstein, M., McMillan, J. D., and Lee, J. W., eds. (2004), *Appl. Biochem. Biotechnol*. **113–116** (this volume).

0273-2289/04/115/0771–0780/$25.00

Optimization of Enzymatic Production of Biodiesel from Castor Oil in Organic Solvent Medium

Débora de Oliveira, Marco Di Luccio, Carina Faccio, Clarissa Dalla Rosa, João Paulo Bender, Nádia Lipke, Silvana Menoncin, Cristiana Amroginski, and José Vladimir de Oliveira*

Department of Food Engineering, URI, Campus de Erechim, Av. Sete de Setembro, 1621-Erechim-RS, 99700-000, Brazil, E-mail: vladimir@uricer.edu.br

Abstract

We studied the production of fatty acid ethyl esters from castor oil using *n*-hexane as solvent and two commercial lipases, Novozym 435 and Lipozyme IM, as catalysts. For this purpose, a Taguchi experimental design was adopted considering the following variables: temperature (35–65°C), water (0–10 wt/wt%), and enzyme (5–20 wt/wt%) concentrations and oil-to-ethanol molar ratio (1:3 to 1:10). An empirical model was then built so as to assess the main and cross-variable effects on the reaction conversion and also to maximize biodiesel production for each enzyme. For the system containing Novozym 435 as catalyst the maximum conversion obtained was 81.4% at 65°C, enzyme concentration of 20 wt/wt%, water concentration of 0 wt/wt%, and oil-to-ethanol molar ratio of 1:10. When the catalyst was Lipozyme IM, a conversion as high as 98% was obtained at 65°C, enzyme concentration of 20 wt/wt%, water concentration of 0 wt/wt%, and oil-to-ethanol molar ratio of 1:3.

Index Entries: Alcoholysis; vegetable oils; lipases; reaction kinetics; biodiesel.

Introduction

Biotransformation of vegetable oils through the use of enzymes as catalysts has been a matter of intense investigation recently. The possibility

*Author to whom all correspondence and reprint requests should be addressed.

of using biodiesel as an additive to mineral diesel to result in a sulfur-free, higher-cetane-number fuel from a renewable resource has motivated efforts in the biomodification of vegetable oils in order to reduce environmental costs and import needs.

Lipases have been extensively used in triglyceride technology, mainly for the biotransformation of oils and fats. Among several important processes for lipid modification are the hydrolysis reactions, synthesis of esters, and transesterification of these materials in the presence of lipases. In these reactions, the triglyceride reacts with a fatty acid (acidolysis), an alcohol (alcoholysis), or another ester (interesterification), resulting in a rearrangement of the triglyceride fatty acid groups to produce a new triglyceride as a consequence of the competitive hydrolysis and esterification reactions.

Esters obtained from alcohols and fatty acids have many remarkable applications. Those from long chain acids (12–20 carbon atoms) and short chain alcohols (3–8 carbon atoms) have been widely employed in the food, cosmetic, and pharmaceutical industries *(1).* Natural esters such as those from jojoba oil, carnauba wax, and whale oil have been used. However, these oils are expensive and are not usually available in large amounts. Therefore, it is desirable to develop methods for the production of such esters using cheaper and more plentiful raw materials *(2).*

The establishment of the Brazilian National Program on Biodiesel and the expectation of commercial availability of the product within 2 yr throughout Brazil have prompted several studies on biodiesel production using different techniques and a variety of vegetable and animal sources. Among several raw materials available, castor oil is one of the most prominent. Besides the advantage of being a native plant in Brazil, the castor plant is versatile concerning climate and ground types, with a very high yield per hectare and high content of oil (¬^{a}50 wt%), affording a biofuel with a much higher cetane number (>60) than mineral diesel and has a good lubricity index. Of course, it should also be remembered that Brazil is one of the world's leading castor oil producers.

Chemical esterification methods use an alcohol and a carboxylic acid in the presence of a mineral acid as catalyst. Sulfuric acid, which is commonly used, leads to the formation of undesirable byproducts, requiring a difficult separation step *(3).* Moreover, in this case, the starting material is a high-value component (fatty acid). Consequently, researchers are interested in the alcoholysis reaction using a vegetable oil with low cost and largely produced in Brazil as a raw material for ester synthesis.

This reaction offers several advantages when compared to esterification of fatty acids, mainly owing to the possibility of using vegetable oils as substrates. In this case, a vegetable oil and an alcohol are used as substrates in the production of glycerol and fatty acid alkyl esters. Conventionally, acid and basic catalysts have been used *(4,5).* However, the use of acid catalysts usually results in low conversions. The use of basic catalysts require the utilization of vegetable oils with low free fatty acid con-

tent (3 mg of KOH/g). In spite of the high yields obtained (90%) when using pretreated acid oils, a decrease in conversion is observed owing to the soap-removing step. The use of enzymes minimizes this problem, since oils with a high acid content can also be used without a pretreatment and no enzymatic activity loss is observed.

Several researches have reported an alternative method to produce esters through enzymatic reactions using lipases as catalysts *(6–12)*. Because biocatalysts have high specific activity and a low impact on the environment, they have become increasingly important for industry. For example, immobilized lipases are used as catalysts for reactions involving biomodification of triglycerides *(13)*.

The main objective of the present work was the production of ethyl esters from the enzymatic alcoholysis of castor oil using *n*-hexane as solvent. Two commercial lipases, Novozym 435 and Lipozyme IM, were compared. The variables in these experiments were temperature, water and enzyme concentrations in the reaction medium, and the oil:ethanol molar ratio. An empirical model was built to evaluate the effects of process variables on the conversion, and thus to determine the operating conditions that maximize the production of esters for each enzyme.

Materials and Methods

Castor Oil

A commercial castor oil (Delaware-Brazil) was used as purchased without any pretreatment. The fatty acid composition was determined using a gas chromatograph (HP 5890) with a flame ionization detector. The following instrumentation and conditions were used: H_2 as carrier gas, modified polyethylene glycol column (FFAP 2 – 25 m × 0.20 mm id × 0.30-mm film), column temperature of 180–210°C (2°C/min), injector temperature of 250°C, and detector temperature of 280°C. Using this procedure, the approximate fatty acid composition in castor oil is 92 wt% ricinoleic acid and 8 wt% other acids. Ethyl alcohol (95 v/v%) (Merck) and *n*-hexane PA (Merck) were used as substrate and solvent, respectively.

Enzymes

Two commercial immobilized lipases were kindly supplied by Novozymes Brazil (Araucária, PR, Brazil): *Mucor miehei* (Lipozyme IM) immobilized on a macroporous anion-exchange resin (0.15 U/g and 4 wt% water) and *Candida antarctica* (Novozym 435) immobilized on a macroporous anionic resin (0.12 U/g and 1.4 wt% water).

Analytical Method

Samples of fatty acid esters were analyzed with a gas chromatograph interfaced with a mass selective detector (Model QP 5050A; Shimadzu) using a capillary column PE-5 (20 m × 0.18 mm × 0.25 mm). The following

Table 1
Range of Variables of Enzymatic Alcoholysis of Castor Oil

Variable	Range
[*T*] (°C)	35–65
[*W*] (wt/wt%)	0–10
[*E*] (wt/wt%)	5–20
[*R*]	1:3–1:10

column temperature gradient programming was adopted: 60–200ºC (3°C/min) and 200–300ºC (5°C/min). Identification and quantification of the samples (0.5 mL and 10 mL of heptane) were accomplished using ethyl ricinoleate (25 mg/mL) as internal standard. Helium was used as carrier gas, and the injection and detector temperatures were 280 and 320ºC, respectively. The injection of the internal standard with a known concentration allowed determination of the response factor according to the relation $C = A \times RF$, in which A is the peak area, RF is the response factor, and C is the concentration.

Experimental Procedure and Statistical Analysis

The experiments were performed in stoppered 300-mL Erlenmeyers flasks. Lipase was added to the mixture of oil-ethanol-solvent and the flasks were agitated at 200 rpm for 8 h in a controlled-temperature shaker. Samples were taken at each hour in order to follow the course of the reaction. The solvent was used with the purpose of reducing mass transfer limitations, thus promoting efficient contact between substrates (oil and ethanol). Based on previous works *(14,15)*, *n*-hexane was used as solvent medium in a fixed amount of 40 mL. A Taguchi experimental design with two levels and four variables (temperature [*T*], water [*W*] and enzyme [*E*] concentrations, and oil:ethanol molar ratio [*R*]) was adopted. The variable ranges adopted, as presented in Table 1, were based on previous results for a similar system and were chosen to cover the intervals commonly used *(14–16)*. The experimental runs were executed randomly, and duplicate runs were carried out for all experimental conditions providing an average SD of about 5%. The process conversion was then modeled by a polynomial model. The kinetic data, which demonstrated that for almost all experimental conditions the maximum conversions were obtained in 6 h, were used this time for evaluating the influence of the variables and process optimization.

Results and Discussion

The experimental results for Lipozyme IM, which exhibits specificity in the 1,3 positions, and Novozym 435, a nonspecific lipase, are presented

Table 2
Experimental Design and Conversions in Enzymatic Alcoholysis of Castor Oil

		Experimental Conditions (wt/wt %)			Maximum Conversion (%)	
Run	*T* (°C)	[*E*]	[*W*]	*R*	Lipozyme IM	Novozym 435
1	35	5	0	1:3	42.5	47.5
2	35	5	10	1:10	0.65	1.6
3	35	20	0	1:10	70.4	67.0
4	35	20	10	1:3	85.0	34.0
5	65	5	0	1:10	19.7	52.0
6	65	5	10	1:3	33.0	16.5
7	65	20	0	1:3	98.0	60.5
8	65	20	10	1:10	40.6	73.0
9	50	12.5	5	1:6.5	60.6	23.0

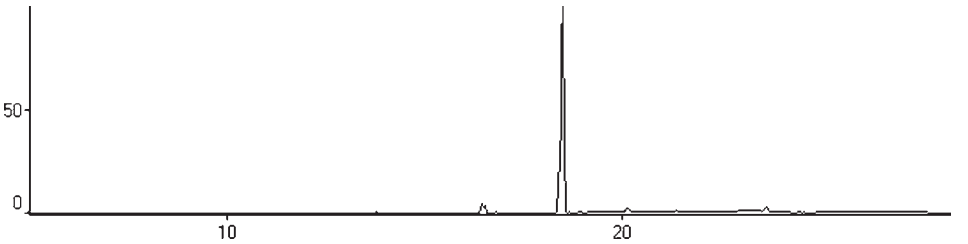

Fig. 1. Chromatogram obtained for biodiesel from castor oil. Experiment 3: time, 2h. The peak was identified as ethyl ricinoleate.

in Table 2. One can observe that the higher yield was achieved in the system with Lipozyme IM when compared with Novozym 435 (98 and 73%, respectively). Note that the enzymes exhibited different behavior probably because lipases generally have optimum working ranges and are affected mainly by the system temperature and water added to the reaction medium. Also note that the oil:ethanol molar ratio directly affected the process conversion and that the enzyme concentration had a positive effect on ester production. The results obtained here are similar to those from Oliveira and Alves (14), who performed lipase-catalyzed reactions using palm and palm kernel oil.

For the sake of brevity, Fig. 1 presents a typical chromatogram found for the biodiesel produced from castor oil using Lipozyme IM (experimental condition 3). Note the presence of a major peak referred to ethyl ricinoleate, which is the compound obtained from the alcoholysis of ricinoleic acid, the main component of castor oil.

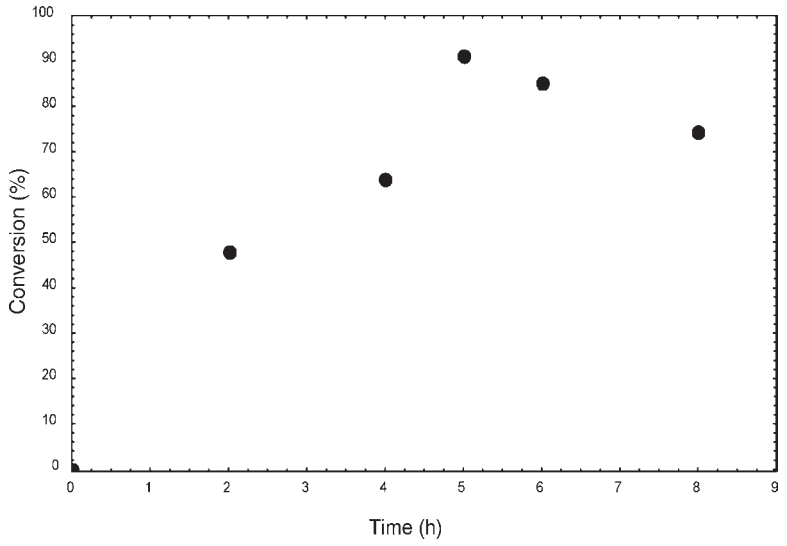

Fig. 2. Kinetics of lipase alcoholysis of castor oil in *n*-hexane for run 4 using Lipozyme IM.

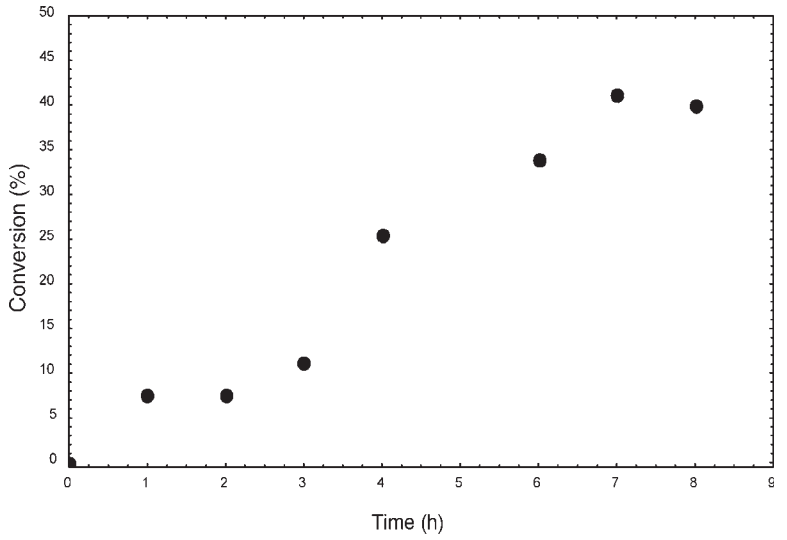

Fig. 3. Kinetics of lipase alcoholysis of castor oil in *n*-hexane for run 4 using Novozym 435.

As an example, Figs. 2–5 present kinetic curves obtained for runs 4 and 7 for each system studied up to 8 h of reaction. Undoubtedly, the knowledge of time evolution of the reaction plays an important role if one takes into account a possible scale-up of a continuous process.

Effects of Process Variables

The influence of temperature, water and enzyme concentrations, and oil:ethanol molar ratio, as well as the cross-interactions, was investigated.

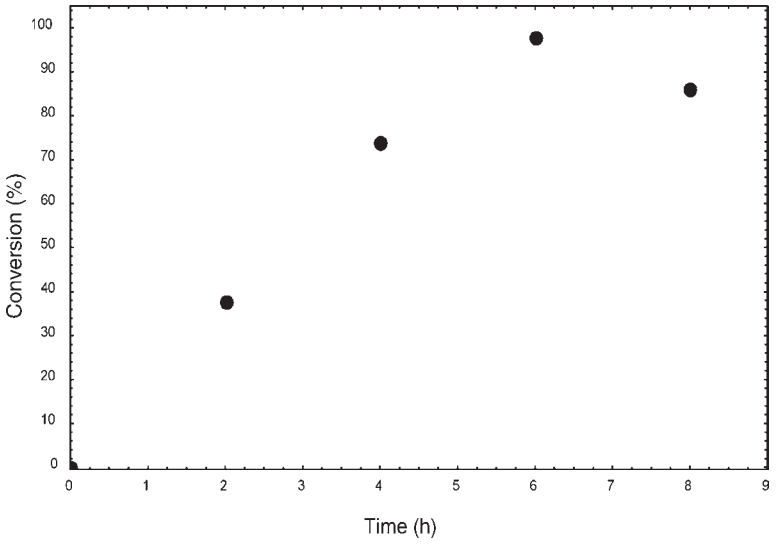

Fig. 4. Kinetics of lipase alcoholysis of castor oil in *n*-hexane for run 7 using Lipozyme IM.

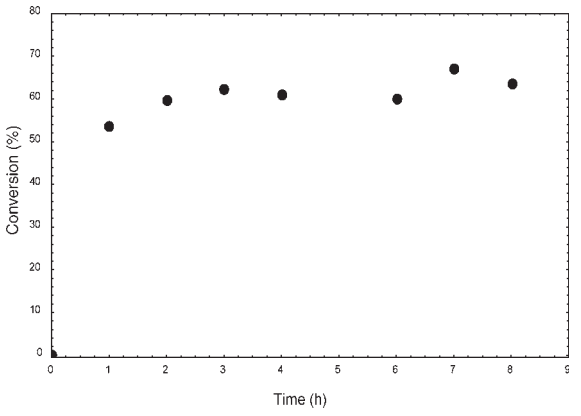

Fig. 5. Kinetics of lipase alcoholysis of castor oil in *n*-hexane for run 7 using Novozym 435.

To allow a direct comparison of each variable effect, the independent variables were normalized in the range of –1 to +1, according to

$$x_i = \frac{2\left(X_i - X_{\max}\right)}{\left(X_{\max} - X_{\min}\right)} - 1 \qquad (1)$$

in which x_i is the normalized value of the variable X at condition i; X_i is the actual value; and $X_{\min}$ and $X_{\max}$ are the lower and upper limit, respectively.

The "–1" level represents the lower limit, while the "+1" level represents the upper limit of each variable. A statistical modeling technique was used to obtain an empirical model able to reproduce the experimental data.

Table 3
Regression Results for Lipozyme IM System

$Y = a_0 + a_1R + a_2W + a_3E + a_4R^2 + a_5TE + a_6RE$

Average absolute deviation: 4.9 [a]

Parameter		SD
a_0	60.60	4.09
a_1	–15.79	1.45
a_2	–8.92	1.45
a_3	24.87	1.45
a_4	–11.97	4.34
a_5	–3.39	1.45
a_6	–2.21	1.45

[a]

$$\text{AAD\%} = \frac{1}{N}\sum_{i}^{N}\frac{\left|Y_i^{\text{exp}} - Y_i^{\text{calc}}\right|}{Y_i^{\text{exp}}} \times 100$$

in which the subscripts exp and calc are, respectively, the experimental and calculated values; and the quantity Y is the reaction conversion.

Empirical models were built by assuming that all variable interactions were significant, estimating the parameters related to each variable interaction and main variable effects, and discarding the meaningless parameters considering a confidence level of 95%, by using the student's *t*-test. The parameters were estimated through the maximum likelihood method *(17)*.

Reactions Catalyzed by Lipozyme IM

Regarding the system catalyzed by Lipozyme IM, the data in Table 3 show that the water added to the system, the oil:ethanol molar ratio, and the interactions of temperature–enzyme concentration and oil:ethanol molar ratio–enzyme concentration had a negative effect on the conversion. In addition, an excess of ethanol may inhibit the enzymatic reaction and the addition of water caused a negative effect on the conversion, corroborating the fact that excess water may change the reaction equilibrium, thus decreasing the formation of esters. Also note that the enzyme concentration had a strong positive influence on the biodiesel production. Once the effects of process variables were evaluated, the optimization was carried out. For this system, however, the optimum condition found from the experimental design was the same as observed for run 7 (Table 2), since the conversion value predicted by the empirical model was 99.6%, which agrees very satisfactorily with the experimental one, 98.0%.

Table 4
Regression Results for Novozym 435 System

$Y = a_0 + a_1 T + a_2 R + a_3 W + a_4 E + a_5 R^2 + a_6 TR + a_7 TW$

Average absolute deviation: 4.6[a]

Parameter		SD
a_0	23.01	4.64
a_1	6.48	1.64
a_2	4.39	1.64
a_3	-12.73	1.64
a_4	14.61	1.64
a_5	21.02	4.92
a_6	7.61	1.64
a_7	6.98	1.64

[a]

$$\text{AAD\%} = \frac{1}{N}\sum_{i}^{N}\frac{\left|Y_i^{\text{exp}} - Y_i^{\text{calc}}\right|}{Y_i^{\text{exp}}} \times 100$$

in which the subscripts exp and calc are, respectively, the experimental and calculated values; and the quantity Y is the reaction conversion.

Reactions Catalyzed by Novozym 435

From the results presented in Table 2 one can see that the greatest conversion was obtained at the upper limit of all process variables. Table 4 reveals that, as in the case of Lipozyme IM, the addition of water led to inhibition of the reaction. The enzyme concentration, the temperature, the oil:ethanol molar ratio, and the interactions temperature–oil:ethanol molar ratio and temperature–water addition had a positive effect on the production of biodiesel. Concerning temperature, the result obtained confirms the fact that the optimum temperature for this enzyme is about 70°C. As expected, the enzyme concentration, in the experimental range investigated, had a positive effect on the reaction conversion. Note also that for this system no alcohol inhibition was verified. The optimization for this system led to the following process variables values: T = 65°C, [E] = 20 wt/wt%, [W] = 0 wt/wt%, and R = 1:10, with a predicted maximum conversion of 82% in 6 h. The execution of the experiment resulted in an experimental value at these conditions of 81.4%, which agrees very well with the value predicted from the experimental model.

Conclusion

The use of an experimental design for the production of esters from the enzymatic reactions of vegetable oils proved to be a rational means to

investigate the influence of process variables on the conversion. Empirical models were built to represent experimental data and to allow the determination of process variables that maximize the conversion. The results obtained using Novozym 435 gave lower conversions when compared to the systems using Lipozyme IM. The results obtained here may be useful if one considers that a low-cost raw material, a renewable source, can be used for the production of high-value-added products and/or as a biofuel.

Acknowledgments

We thank Conselho Nacional de Desenvolvimento Científico e Tecnológico (CNPq), FAPERGS, and ANP/FINEP/PETROBRAS for financial support of this work and scholarships.

References

1. Carta, G., Gainer, J. L., and Zaidi, A. (1995), *Biotechnol. Bioeng.* **48,** 601–605.
2. Martinez, M., Torrano, E., and Aracil, J. (1988), *Ind. Eng. Chem. Res.* **27,** 2179–2182.
3. Al Saadi, A. N. and Jeffreys, G. V. (1981), *AIChE J.* **27,** 754–772.
4. Lago, R. C. A., Szpiz, R. R., Jablonka, F. H., Pereira, D. A., and Hartman, L. (1985), *Oléagineux* **40,** 147–154.
5. Lago, R. C. A., Szpiz, R. R., and Hartman, L. (1988), *Revista Química Ind.* **666,** 160–163.
6. Abramowicz, D. A. and Keese, C. R. (1989), *Biotechnol. Bioeng.* **33,** 149–156.
7. Barzana, E., Karel, M., and Klibanov, A. M. (1989), *Biotechnol. Bioeng.* **34,** 1178–1185.
8. Brunt, J. V. (1986), *Biotechnology* **4,** 611–615.
9. Dordick, J. S. (1989), *Enzyme Microb. Technol.* **11,** 194–211.
10. Stevenson, D. E. and Storer, A. C. (1991), *Biotechnol. Bioeng.* **37,** 519–527.
11. Yamane, T. (1988), *Biocatalysis* **2,** 1–9.
12. Yamane, T., Ichiryu, T., Nagata, M., Ueno, A., and Simizu, S. (1990), *Biotechnol. Bioeng.* **36,** 1063–1069.
13. Basri, M., Ampon, W. M. Z., Razak, C. N. A., and Salleh, A. B. (1995), *JAOCS* **72,** 407–411.
14. Oliveira, D. and Alves, T. L. M. (1999), *Appl. Biochem. Biotechnol.* **77–79,** 835–844.
15. Oliveira, D. and Alves, T. L. M. (2000), *Appl. Biochem. Biotechnol.* **84–86,** 59–68.
16. Mittelbach, M. (1990), *JAOCS* **67,** 168–170.
17. Pinto, J. C., Noronha, F. B., Monteiro, J. L., Lobão, M. W., and Santos, T. J. (1987), *ESTIMA: Um Pacote Computacional para Estimação de Parâmetros e Projeto de Experimentos*, PEQ/COPPE/UFRJ (in portuguese).

0273-2289/04/115/0781–0791/$25.00

Two-Step Preparation for Catalyst-Free Biodiesel Fuel Production

Hydrolysis and Methyl Esterification

Dadan Kusdiana and Shiro Saka*

Graduate School of Energy Science, Kyoto University, Yoshida-honmachi, Sakyo-ku, Kyoto, 606-8501, Japan, E-mail: saka@energy.kyoto-u.ac.jp

Abstract

Biodiesel fuel was prepared by a two-step reaction: hydrolysis and methyl esterification. Hydrolysis was carried out at a subcritical state of water to obtain fatty acids from triglycerides of rapeseed oil, while the methyl esterification of the hydrolyzed products of triglycerides was treated near the supercritical methanol condition to achieve fatty acid methyl esters. Consequently, the two-step preparation was found to convert rapeseed oil to fatty acid methyl esters in considerably shorter reaction time and milder reaction condition than the direct supercritical methanol treatment. The optimum reaction condition in this two-step preparation was 270°C and 20 min for hydrolysis and methyl esterification, respectively. Variables affecting the yields in hydrolysis and methyl esterification are discussed.

Index Entries: Supercritical methanol; biodiesel; methyl esters; transesterification; methyl esterification.

Introduction

Biodiesel fuel has long been considered an alternative or emergency fuel for diesel engines because its properties are close to those of petroleum diesel fuel. Generally, biodiesel fuel is produced through transesterification of vegetable oils/fats with alcohol (mostly methanol) in the presence of a catalyst *(1)*. This method, however, is only applicable for refined vegetable oils/fats or those with a low content of free fatty acids and water. In the case of high content of fatty acids and/or water, as found in crude oils/fats, waste-frying oil, and soap stocks, the yield of methyl esters is low since fatty acids and water inhibit the reaction. Therefore, a combination of acidic-

*Author to whom all correspondence and reprint requests should be addressed.

and alkaline-catalyzed processes has been developed to overcome this problem owing to the presence of fatty acids and water *(2–4)*.

Besides transesterification, there is another route for converting vegetable oil to methyl esters through hydrolysis and subsequent methyl esterification. Hydrolysis of vegetable oils is an old technology that can be traced back to the mid nineteenth century *(5)*. Several methods have been developed in vegetable oil hydrolysis including acidic/alkaline-catalyzed, lipase-catalyzed, and catalyst-free methods *(6–8)*. Both acidic- and alkaline-catalyzed methods are mostly practiced in commercial applications. In the acidic-catalyzed method, the reaction is performed in the presence of sulfonic acid at a boiling temperature of water and requires 20–48 h for a complete conversion. In the alkaline-catalyzed method, the reaction conditions are 185°C and 1 MPa for 6–10 h. In both methods, removal of the catalyst after the reaction is necessary. In the catalyst-free process, on the other hand, steam-based hydrolysis and subcritical water treatment of vegetable oils have been reported *(9)*.

Methyl esterification of fatty acids with methanol is generally conducted in the presence of acid catalyst at an elevated temperature close to the boiling point of methanol. Recently, we found that fatty acids could be successfully methyl esterified in supercritical methanol without the use of a catalyst *(10)*. In addition, from a comparative study between transesterification of vegetable oil and alkyl esterification of fatty acids with supercritical alcohols at 300°C in a batch-type reaction system, the reaction rates of alkyl esterification were found to be faster than those of transesterification *(11)*. An additional finding was that alkyl esterification of fatty acids could be performed at a lower reaction temperature than transesterification.

A catalyst-free supercritical methanol method for biodiesel fuel production was proposed with the optimum conditions of 350°C, 20 MPa, a molar ratio of 42 in methanol, and a 4-min treatment period *(12–13)*. This method has been proved to produce a high yield, because of simultaneous reactions of transesterification of triglycerides and methyl esterification of free fatty acids *(10)*. The only shortcoming of this one-step method is that it requires a severe reaction condition compared with the conventional commercial method with acid or alkaline catalyst. Consequently, our method would require a special alloy to cover the high temperature and high pressure of the reaction system.

Therefore, the purpose of the present work was to study an alternative method for biodiesel fuel production that has a lower reaction condition than the one-step supercritical methanol method, through the two-step preparation consisting of hydrolysis of triglycerides in subcritical water and subsequent methyl esterification of the fatty acids by supercritical methanol treatment. In this article, we present various parameters affecting the yield of fatty acids in hydrolysis from triglycerides followed by methyl esterification of the fatty acids. We also compare the one- and two-step preparation methods and propose a production scheme of the latter.

Materials and Methods

The vegetable oil used was rapeseed oil (Nacalai Tesque; Kyoto, Japan) without further treatment. The fatty acid content of the rapeseed oil mainly consisted of unsaturated fatty acids (93 wt%), with the saturated fatty acids of palmitic and stearic acids accounting for only a small amount (7 wt%). Various fatty acids of oleic ($C_{18\text{-}1}$), linoleic ($C_{18\text{-}2}$), linolenic ($C_{18\text{-}3}$), and palmitic ($C_{16\text{-}0}$) acids as well as their methyl esters were purchased from Nacalai Tesque. Anhydrous methanol and distilled water were also supplied by the same company.

Experiments were carried out in batch-type and flow-type supercritical biomass conversion systems. The batch-type reaction system was the same as reported previously *(14)*. In brief, it consisted of a tube reaction vessel (Inconel-625; 5 mL in volume) equipped with a thermocouple and a pressure gage. For hydrolysis reaction, 1 mL of rapeseed oil mixed with 4 mL of water was fully charged into the reaction vessel. The reaction vessel was then heated with molten tin preheated at desired temperatures. It took about 12 s to reach the reaction temperature. Subsequently, the vessel was moved into a water bath to quench the reaction. Reaction time was counted from the time a mixture reached the reaction temperature to when it was quenched. The obtained product was then kept for about 30 min until the two phases separated; the upper portion is the hydrolyzed product, while the lower is a mixture of water and glycerol. The upper portion was then evaporated in a vacuum evaporator to remove any water.

The same procedure and equipment for hydrolysis were used in the second step: methyl esterification of fatty acids by supercritical methanol treatment. Authentic fatty acids as well as fatty acids prepared by hydrolysis (the products of subcritical water treatment) and methanol were charged into the reaction vessel at a molar ratio of 42 in methanol for all runs.

The products obtained from hydrolysis and methyl esterification were analyzed for then composition by using high-performance liquid chromatography (HPLC) (LC -10AT; Shimadzu) consisting of a column (STR ODS-II, 25-cm length × 4.6-mm id; Shinwa) and refractive index detector (RID-10A; Shimadzu) operated at 40°C with a 1.0 mL/min flow rate of methanol as a carrier solvent. The methyl esters were also analyzed using a gas chromatography (GC-14B; Shimadzu) equipped with a flame ionization detector and thermogravimetric analysis (TGA-50; Shimadzu) with a 50 mL/min nitrogen purge flow.

To perform experiments at a constant pressure, a flow-type supercritical biomass conversion system was used. Major sections of the flow-type system consisted of pump stations, preheaters, supercritical treatment tube, cooling system, and separatory tank. The reaction time was calculated by dividing the volume of the treatment tube by the volumetric flow rate at the given conditions. Knowledge of the thermodynamic properties of the solvent, particularly correlation among temperature, pressure, and specific gravity, is important in order to accurately calculate the reaction treatment. Detailed information of the treatment with this equipment can

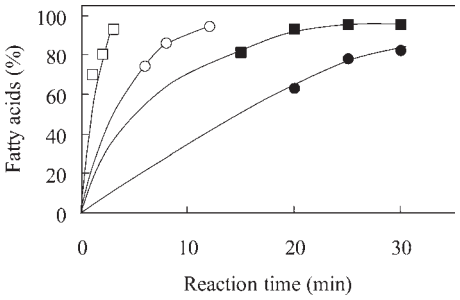

Fig. 1. Effect of reaction temperature on yield of fatty acids. The volumetric ratio of rapeseed oil to water was 1/4 (molar ratio: 1/217). □, 350°C; ○, 300°C; ■, 270°C; ●, 255°C.

be found elsewhere *(14)*. The experiment was performed at a temperature between 255 and 350°C and a pressure range from 5 to 20 MPa.

Results and Discussion

Hydrolysis of Rapeseed Oil with Subcritical Water

The hydrolysis reaction was carried out at various temperatures ranging from 255 to 350°C. Figure 1 demonstrates the effect of reaction temperature on the yield of fatty acids from triglycerides throughout the hydrolysis reaction. From Fig. 1, it is apparent that the course of the reaction for fatty acids formation was correlated with reaction temperature. At 350°C, a complete conversion could be achieved by 3 min of treatment. However, to get the same yield, it took 12 and 20 min at 300 and 270°C, respectively, while at 255°C only about 80% of the yield was achieved, and the yield was not increased for prolonged reaction treatment. Therefore, the reaction conditions of 270°C and 20 min were considered the mildest.

From Fig. 1 it can also be seen that the reaction rate was high at the beginning and tended to be lower in the prolonged treatment. We previously observed a similar trend in the transesterification reaction of rapeseed oil by supercritical methanol treatment *(13)*. This phenomenon is believed to be correlated with the reaction mechanism of vegetable oil/triglyceride in subcritical water which is known to consist of three stepwise reactions—triglyceride to diglyceride, diglyceride to monoglyceride and finally monoglyceride to glycerol—in which fatty acid is deliberated at each step. It was speculated that monoglyceride is the most difficult to be hydrolyzed, because monoglyceride is more stable than triglyceride and diglyceride.

The hydrolysis reaction is a reversible reaction, so it will be completed only if a large excess of water is used or if one of the products is removed from the reaction mixture. Therefore, we extended the experiment to study the effect of the amount of water on the hydrolysis reaction.

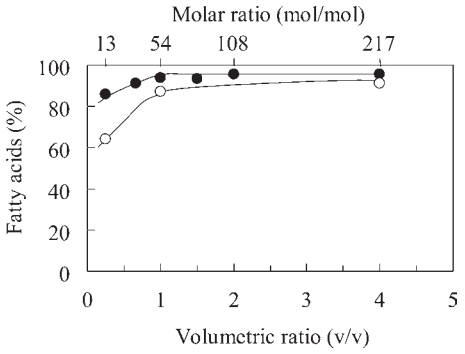

Fig. 2. Effect of volumetric ratio of water to rapeseed oil on yield of fatty acids treated at 270°C for 20 min. ●, Flow-type system; ○, batch-type system.

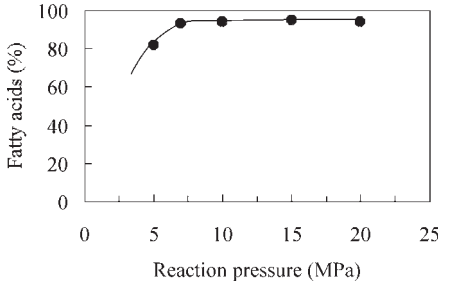

Fig. 3. Effect of reaction pressure on yield of fatty acids from rapeseed oil. Reaction conditions were 270°C and 20 min.

Figure 2 presents the effect of the various volumetric ratios of water to rapeseed oil on the yield of fatty acids as prepared with both flow- and batch-type reaction systems at 270°C for 20 min. The volumetric ratios of 1/4 and 4 correspond to the molar ratios of 13 and 217, respectively. For the batch-type system, the hydrolysis rate of triglycerides seemed to be affected more by the amount of water, and a slightly better conversion was seen with the flow-type reaction system. Even though the volumetric ratio of 1/4 is equivalent to the molar ratio of 13 in water, which is theoretically higher than its stoichiometry of 3, the formation of fatty acids in both reaction systems was obviously low. In addition, it was found that at a volumetric ratio less than 2/3, it was difficult to separate hydrolysis products from the water portion that contained glycerol. On the other hand, the presence of water in fatty acids would have a negative effect on the methyl esterification reaction *(15)*.

Figure 3 shows the effect of reaction pressure on the yield of fatty acids from rapeseed oil treated at 270°C for 20 min. It clearly demonstrates that a complete conversion of triglycerides to fatty acids was achieved when the

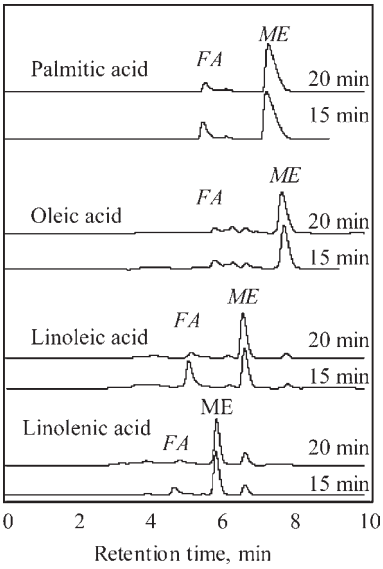

Fig. 4. HPLC chromatograms of various fatty acids treated in supercritical methanol at 270°C. FA corresponding fatty acids; ME, cooresponding methyl esters.

reaction pressure was above 7 MPa. Note that in the transesterification, the higher pressure was necessary to allow a complete conversion of triglycerides to methyl esters, as we observed previously *(13)*. However, as pressure was lowered to 5 MPa, a reduction in yield of fatty acids was apparent.

Hydrolysis is a homogeneous reaction that takes place in the water-oil phase as a result of rapeseed oil/triglycerides dissolving in the water. The capability of water to dissolve nonpolar triglycerides depends on the temperature and specific weight, which is further quantified as the dielectric constant. Under ordinary conditions, the dielectric constant of water and rapeseed oil is 80 and 3.1, respectively. To allow the reactants to form a soluble mixture, their dielectric constants should be close to each other. At 270°C, the dielectric constant of water tends to decrease to about 25, while that of rapeseed oil is 3.1 *(16,17)*. Judging from the results, it is then assumed that their dielectric constants at 270°C are close enough to form a homogeneous mixture.

Methyl Esterification of Fatty Acids with Supercritical Methanol

The second part of the present work deal with methyl esterification of fatty acids, the hydrolyzed products of triglycerides, in supercritical methanol treatment. We investigated the methyl esterification of several fatty acids present in rapeseed oil such as palmitic, oleic, linoleic and linolenic acids by supercritical methanol at 270°C and 17 MPa. Figure 4 shows

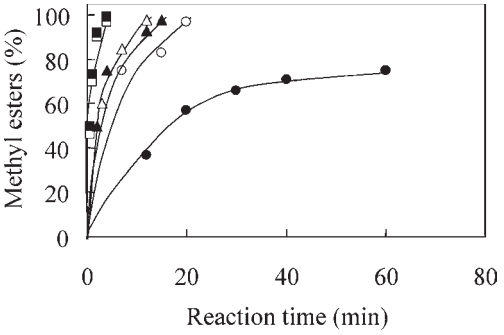

Fig. 5. Comparison in yield of methyl esters between transesterification of triglycerides and methyl esterification of fatty acids by supercritical methanol treatment at various temperatures. ●, Transesterification at 270°C; ▲, transesterification at 300°C; ■, transesterification at 350°C; ○, methyl transesterification at 270°C; △, methyl transesterification at 300°C; □, methyl transesterification at 350°C.

the obtained HPLC chromatograms. At a reaction time of 15 min, peaks of fatty acids marked by FA were present but disappeared mostly at 20 min of treatment. By contrast, the peaks of methyl esters dominate in the chromatograms.

Figure 5 shows a comparison of the yields of methyl esters between transesterification of triglycerides (rapeseed oil) and methyl esterification of fatty acids by supercritical methanol at various temperatures. At 350°C, both reactions could produce very similar results. At 300°C, transesterification produced about 90% methyl esters at 12 min of treatment, whereas methyl esterification resulted in a complete conversion. When triglycerides were transesterified at 270°C, a plateau was reached at about 40 min of treatment with a yield of about 76%. However, much higher yield could be achieved by methyl esterification at 20 min of treatment. These results, therefore, indicate that the reaction rate in methyl esterification is higher than that in transesterification.

The molar ratio of methanol to fatty acids is also an important parameter that controls the reaction. Figure 6 shows the obtained yields of methyl esters from oleic acid, a model of fatty acids, treated at various molar ratios of methanol to fatty acid. Interestingly, compared with the transesterification reaction shown by the dashed line *(13)*, methyl esterification proceeded more at the lower molar ratio, and it is apparent that at a molar ratio of 3, oleic acid was mostly converted to its methyl ester. This result is important in designing the production process, since a reaction with a low molar ratio requires less energy for the process.

Figure 7 shows a direct comparison of the yield of methyl esters between the one- and two-step supercritical methanol treatments at 270°C.

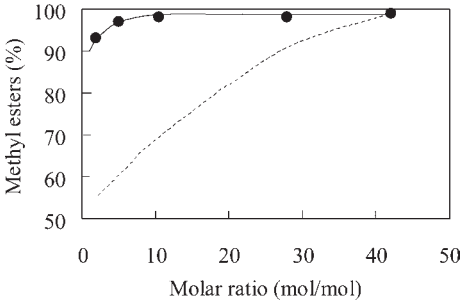

Fig. 6. Effect of molar ratio of methanol to oleic acid on yield of oleic acid methyl esters at 270°C for 20 min. The dashed line (- - -) represents data in transesterification from ref.*13*.

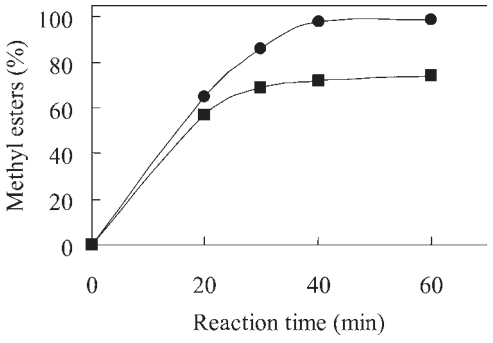

Fig. 7. Comparison of yields of methyl esters between one- and two-step supercritical methanol treatments at 270°C. ■, One-step supercritical methanol; ●, two-step supercritical methanol. The reaction time in the two-step method is a sum of those of hydrolysis and methyl esterification.

One-step treatment refers to a direct supercritical methanol method of rapeseed oil that involves mainly transesterification, while two-step treatment involves hydrolysis and subsequent methyl esterification. Figure 7 clearly demonstrates that at the same reaction time of 40 min, a significantly higher yield of methyl esters could be produced when the rapeseed oil was first treated with water, followed by methyl esterification of the hydrolyzed products.

Figure 8 shows a comparison of the HPLC chromatograms of rapeseed oil between one- and two-step preparation methods. As a comparison, the HPLC chromatogram of rapeseed oil treated with supercritical methanol in the presence of water is also shown. It is obvious that peaks of the two-step method only consist of methyl esters, whereas for other supercritical methanol methods, some peaks of intermediate compounds such as monoglycerides and diglycerides as well as unreacted triglycer-

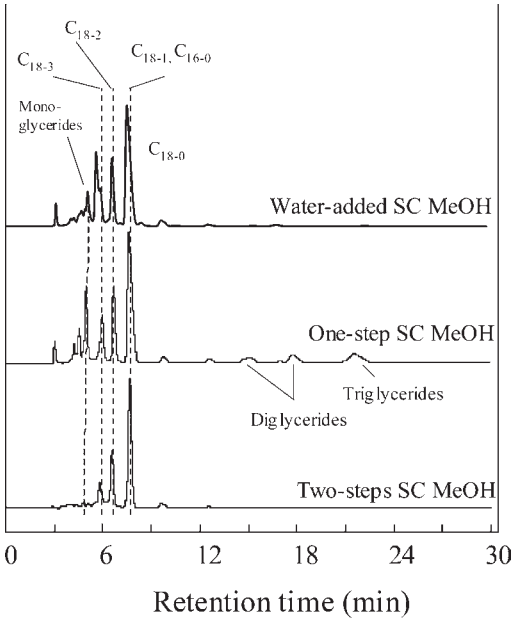

Fig. 8. Comparison in HPLC chromatograms of rapeseed oil treated using various supercritical methanol methods at 270°C for 40 min. SC MeOH, supercritical methanol.

ides are present. Compared with the one-step supercritical methanol method, a slightly higher conversion was achieved from the one-step supercritical methanol treatment in the presence of water *(15)*.

Figure 9 shows a schematic process of biodiesel production by the two-step supercritical methanol method. Several advantages have been attributed to the two-step reaction method. At temperature of 270°C, a common type of 316 stainless steel can fulfill the requirements of good corrosion resistance and cover the reaction condition *(5)*. Energy requirements may be less because mild reaction conditions for hydrolysis and methyl esterification are employed, whereas high-temperature treatment causes operational and equipment problems with, in some cases, the formation of undesirable degradation products. In addition, a reaction temperature of 270°C is commonly used in industries, so such a reaction condition is applicable for commercial applications.

Acknowledgments

This work was conducted through the 21st century COE program "Establishment of COE on Sustainable-Energy System" and received support through a Grant-in-Aid for Scientific Research (B) (2) (13556058, 2001.4-2003.3) from the Ministry of Education, Science, Sports and Culture, Japan.

Fig. 9. Schematic process of biodiesel production by two-step preparation.

References

1. Fukuda, H., Kondo, A., and Noda, H. (2001), *J. Biosci. Bioeng.* **92,** 405–416.
2. Haas, M. J. and Bloomer, S. (2000), *JAOCS* **77,** 373–379.
3. Frohlich, A., Rice, B., and Vicente, G. (2001), in *Proceedings of 1st World Conference on Biomass for Energy and Industry*, James & James (Science Publishers), London, UK, pp. 695–697.
4. Boocock, D. G. B. (2002), in *Proceedings of Kyoto University International Symposium on Post-Petrofuels in the 21st Century: the Prospects in the Future of Biomass Energy*, September 3–4, 2002, Montreal, Canada, pp. 171–177.
5. Muckerheide, V. J. (1952), *JAOCS* **28,** 490–495.
6. Mills, V. and McClain, H. K. (1949), *Ind. Eng. Chem.* **26,** 1982–1985.
7. Reinish, M. D. (1956), *JAOCS* **33,** 516–520.
8. Albasi, C., Bertrand, N., and Riba, J. P. (1999), *Bioprocess Eng.* **10,** 77–81.
9. Holliday, R. L., King, J. W. and List, G. R. (1997), *Ind. Eng. Chem. Res.* **36,** 832–935.
10. Kusdiana, D. and Saka, S. (2001), *J. Chem. Eng. Japan* **34,** 383–387.
11. Warabi, Y., Kusdiana, D., and Saka, S. (2004), *Bioresour. Technol.* **91,** 283–287.
12. Saka, S. and Kusdiana, D. (2001), *Fuel* **80,** 225–231.
13. Kusdiana, D. and Saka, S. (2001), *Fuel* **80,** 693–698.
14. Kusdiana, D., Minami, E., Ehara, K., and Saka, S. (2002), in *Proceedings of the 12th European Biomass Conference*, James & James (Science Publishers), London, UK, pp. 789–792.
15. Kusdiana, D. and Saka, S. (2004), *Bioresour. Technol.* **91,** 289–295.
16. Broll, D., Kaul, C., Kramer, A., Krammer, P., Richter, T., Jung, M., Vogel, H., and Zehner, P. (1999), *Angew. Chem. Int. Ed.* **38,** 2998–3014.
17. Rudan-Tasic, D. and Klofutar, C. (1999), *Acta Chim. Slov.* **46,** 511–521.

0273-2289/04/115/0793–0801/$25.00

Biodiesel Fuel from Vegetable Oil by Various Supercritical Alcohols

Yuichiro Warabi, Dadan Kusdiana, and Shiro Saka*

Graduate School of Energy Science, Kyoto University, Yoshida-honmachi, Sakyo-ku, Kyoto, 606-8501, Japan, E-mail: saka@energy.kyoto-u.ac.jp

Abstract

Biodiesel was prepared in various supercritical alcohol treatments with methanol, ethanol, 1-propanol, 1-butanol, or 1-octanol to study transesterification of rapeseed oil and alkyl esterification of fatty acid at temperatures of 300 and 350°C. The results showed that in transesterification, the reactivity was greatly correlated to the alcohol: the longer the alkyl chain of alcohol, the longer the reaction treatment. In alkyl esterification of fatty acids, the conversion did not depend on the alcohol type because they had a similar reactivity. Therefore, the selection of alcohol in biodiesel production should be based on consideration of its performance of properties and economics.

Index Entries: Supercritical alcohol; biodiesel; fatty acids alkyl ester; transesterification; alkyl esterification.

Introduction

Biodiesel is believed to be a promising alternative fuel to substitute petroleum-derived diesel fuel in diesel engines, and essentially no engine modifications are required to substitute biodiesel for diesel fuel. In addition, biodiesel is better than diesel fuel in terms of sulfur content, flash point, aromatic content, and biodegradability *(1)*. Research on the commercial application of biodiesel has therefore been started in European countries, the United States, and Japan *(2,3)*.

However, one of the limitations of using biodiesel fuel for diesel engines is higher cold flow properties compared with petroleum diesel fuel *(4)*. Cold properties consist of cloud point, pour point, and cold filter plugging point. The cloud point is a temperature at which the fuel starts to thicken and cloud, the pour point is a temperature at which the fuel thickens and no longer pours, and the cold filter plugging point is the lowest temperature at which fuel still flows through a specific filter. These

*Author to whom all correspondence and reprint requests should be addressed.

cold flow properties of biodiesel restrict its utilization in very cold weather.

Cold properties of biodiesel are highly correlated to the fatty acid composition. Biodiesel with a high content of saturated fatty acids, such as that from palm oil and coconut oil, possesses poor cold flow properties. On the other hand, biodiesel with a high content of unsaturated fatty acids possesses better flow properties at lower temperatures. However, biodiesel from highly unsaturated fatty acids with more than two double bonds has combustion problems. Therefore, in some countries, the content of highly unsaturated fatty acid methyl esters in biodiesel is kept low *(5)*.

To improve the cold properties of biodiesel, the use of alcohol with longer alkyl chain has been studied in the alkaline-catalyzed method. The cloud point for ethyl esters is approx 2°C lower than that of the corresponding methyl esters, while butyl esters are 10°C lower than methyl esters *(6)*. Furthermore, cetane number is appropriate for alkyl esters from the alcohol with the longer alkyl chain *(7)*.

In the alkaline-catalyzed method, however, the reaction condition should be adjusted as various alcohols are used, and sometimes, a complete conversion is difficult to achieve. Gauglitz and Lehman *(8)* studied the rate of transesterification using alkaline catalyst at 60°C, and found that an addition of one alkyl carbon to the alcohol doubled the reaction time. Additionally, Nimcevic et al. *(9)* found that transesterification of rapeseed oil by *n*-propanol or alcohol with longer alkyl chain always failed even after several hours of treatment at the boiling point of alcohol.

We have developed a catalyst-free method of biodiesel fuel production by supercritical methanol *(10–12)*, and we found that the process becomes much simpler and that the yield of biodiesel is higher compared with the alkaline-catalyzed method. The aim of the present work was, therefore, to investigate the possibilities of biodiesel fuel production from rapeseed oil with various alcohols by supercritical treatment. In addition, the supercritically prepared biodiesel fuel was studied for its cold properties.

Materials and Methods

Rapeseed oil and its fatty acids (stearic, palmitic, oleic, linoleic, and linolenic acids) were chosen as the samples of vegetable oil. The experiments were performed in the batch- and flow-type supercritical biomass conversion systems developed in our laboratory. For the batch-type system, a reaction vessel was made of Inconel-625 with a volume of 5 mL; for the flow-type system, the supercritical treatment tube was constructed from Hastelloy stainless steel (HC 276) with length of 84 m and an id of 1.2 mm, with the total volume being about 95 mL. Detailed information about the equipment can be found elsewhere *(13)*.

Rapeseed oil or fatty acid was mixed with alcohol in a molar ratio of 42:1 in alcohol to oil/fatty acids, and the mixture was treated at 300 and 350°C. In the batch-type system, the pressure was the maximum one

reached during the treatment in which the pressure depends on the kind of alcohol. On the other hand, the flow-type system allowed treatments in a constant reaction pressure. Reaction times ranged from 1 to 14 min at reaction pressures of 10–40 MPa. In transesterification, the treated oil was allowed to settle for about 30 min into three separate phases. The top phase, consisting of alcohol, was then pipetted away, and the remaining two phases were heated for 20 min to remove the alcohol further. The upper phase consisted of methyl esters, intermediates of methyl esters (diglycerides and monoglycerides), and unreacted rapeseed oil (triglycerides), while glycerol was present in the lower phase. In the case of esterification, the treated fatty acids were heated to remove the alcohol.

The products obtained were analyzed for composition using high-performance liquid chromatography (HPLC) (LC -10AT; Shimadzu, Kyoto, Japan), which consisted of a column (STR ODS-II, 25 cm in length $\times$4.6 mm in id; Shinwa Chemical, Osaka, Japan) operated at 40°C at a flow rate of 1.0 mL/min with methanol as a carrier solvent. The column was packed with silica particles (5-μm particle diameter and 12-nm pore diameter). The cloud and pour points of the obtained biodiesel were then determined by a mini–cloud/pour point tester (Model MPC-102; Tanaka Scientific, Tokyo, Japan) based on ASTM D2500 for cloud point and ASTM D6749 for pour point *(14)*.

Results and Discussion

To evaluate the reaction of rapeseed oil and fatty acids in supercritical treatment, five kinds of alcohols were selected: methanol, ethanol, 1-propanol, 1-butanol, and 1-octanol. Figure 1 shows the obtained HPLC chromatograms for rapeseed oil (triglycerides) treated in the batch-type reaction system with various alcohols under supercritical conditions at 350°C. The rapeseed oil consisted of 98.5% triglycerides. Therefore, it was considered a triglyceride. The peaks of the corresponding alkyl esters were slightly shifted as alkyl chains of alcohols became longer. Each alkyl ester emerged as a single peak. In addition, a distinct separation could be achieved for all kinds of alkyl esters, unreacted and intermediate compounds, in 30 min of retention time. By comparing them with the standard compounds, peaks of mono-, di-, and triglycerides were observed, respectively, at about 5 min, between 15 and 22 min, and after 22 min of retention time. From the HPLC chromatograms shown in Fig. 1, peaks of mono-, di-, and triglycerides were detected from treatments of 3 and 6 min. On the other hand, for the prolonged reaction times (10 and 14 min), peaks of alkyl esters were increased. Instead, peaks of unreacted and intermediate compounds decreased and further disappeared, demonstrating a formation of the alkyl esters.

Figure 2 shows changes in the yields of fatty acid alkyl esters treated in the batch-type reaction system with various supercritical alcohols at 350°C. In the case of methanol, >90% yield of methyl esters was achieved

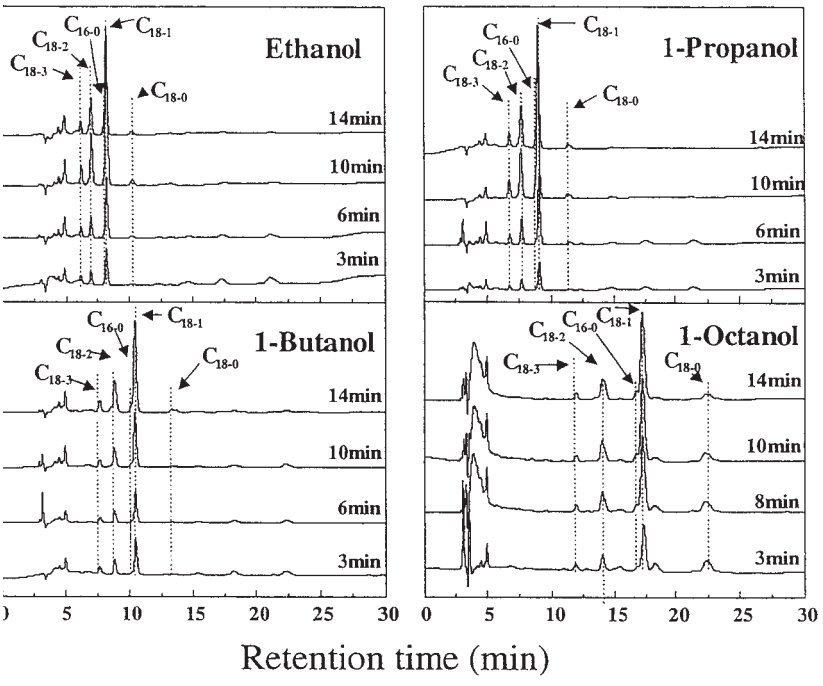

Fig. 1. HPLC chromatograms for rapeseed oil treated with various supercritical alcohols at 350°C in batch-type reaction system.

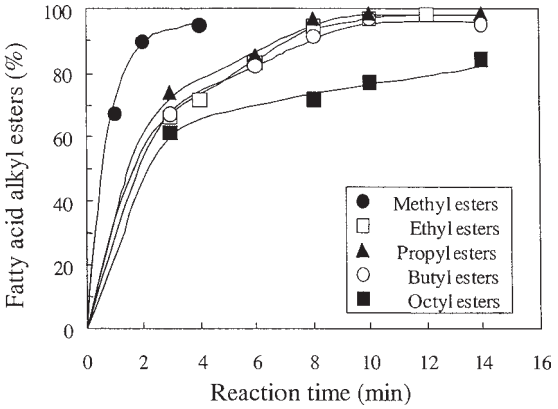

Fig. 2. Changes in yields of fatty acid alkyl esters of rapeseed oil treated with various supercritical alcohols at 350°C in batch-type reaction system.

after 2 min of treatment. On the other hand, it took 8 min for ethanol, 1-propanol, and 1-butanol to obtain the same yield of the corresponding alkyl esters, and even longer for 1-octanol. In the case of ethanol, 1-propanol, and 1-butanol, about 8–14 min of supercritical treatment was necessary to achieve almost complete conversions of triglycerides to fatty acid alkyl esters, while for 1-octanol, 20 min was required to obtain the same yield.

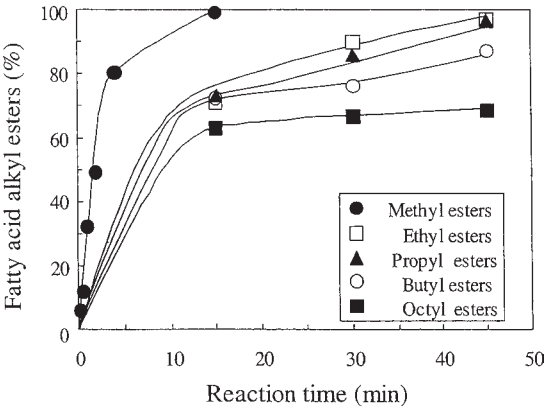

Fig. 3. Changes in yields of fatty acid alkyl esters of rapeseed oil treated with various supercritical alcohols at 300°C in batch-type reaction system.

These results demonstrate that the yields of fatty acid alkyl esters were not significantly different when rapeseed oil was treated in the batch-type system with ethanol, 1-propanol, and 1-butanol at 350°C.

Figure 3 presents changes in the yields of fatty acid alkyl esters as rapeseed oil treated at 300°C in the batch-type reaction system. As expected, the reaction rates were less than those in the 350°C treatment and there was an obvious difference in the reactivity for each alcohol. In all cases, the yield of alkyl esters increased as the reaction time was prolonged, while for identical reaction times, alcohols with the shorter alkyl chains gave better conversions. The highest yield of alkyl esters was obtained with 15 min of treatment with methanol, while ethanol and 1-propanol required 45 min to obtain the same yield. Under the same temperature condition, supercritical treatment with 1-butanol and 1-octanol produced only about 85 and 62% of the corresponding fatty acid alkyl esters, respectively. Therefore, it can be concluded that under the same temperature condition in the batch-type reaction system, the reaction time is correlated with the length of alkyl chain: the longer the alkyl chain of alcohol, the longer the supercritical treatment required to obtain comparable conversion of triglycerides to the alkyl esters.

In the batch-type reaction system, however, the pressure cannot be controlled during the treatment. Table 1 shows a maximum pressure for various supercritical alcohols at 300 and 350°C. It can be observed that at the same temperature, they gave different maximum pressure and that the pressure tended to be lower as the alkyl chain of the alcohol became longer. Previously, it was found that the reaction pressure is an important reaction parameter in enhancing the reaction rate *(11)*. Therefore, the flow-type reaction system, which can control the reaction pressure up to 50 MPa, was used to study the effect of the reaction pressure on the formation of alkyl esters. Reaction temperature and reaction time were set at 300°C and 20

Table 1
Critical State of Various Alcohols Studied and Their Maxiumum Temperature in Batch-Type Reaction System

Alcohol		Critical temperature (°C)	Critical pressure (MPa)	Pressure (MPa) 300°C	350°C
Methanol	(CH_3OH)	239	8.1	20	43
Ethanol	(CH_3CH_2OH)	243	6.4	15	25
1-Propanol	($CH_3[CH_2]_2OH$)	264	5.1	10	23
1-Butanol	($CH_3[CH_2]_3OH$)	287	4.9	9	23
1-Octanol	($CH_3[CH_2]_7OH$)	385	2.9	6	19

min, respectively. Figure 4 shows the relationship between the yield of fatty acid alkyl esters and reaction pressure. It is obvious that the higher reaction pressure slightly improved the yield through reaction rate enhancement, and that the pressure effect was lower for alcohols with a longer alkyl chain. However, compared with the results obtained with the batch-type system shown in Fig. 3, the yields were slightly lower. Therefore, it can be speculated that at pressures higher than the maximum one reached in the batch-type reaction system as shown in Table 1, the effect of the reaction pressure would not result in a significant increase in reaction rate. Thus, it further means that optimum reaction pressures are lower for a longer alkyl chain of alcohol. On the other hand, longer reaction times are required for alcohol with a longer alkyl chain.

The basic idea of supercritical fluid treatment is to take advantage of the relationship between pressure and temperature on thermophysical properties of the solvent (alcohol) such as dielectric constant, viscosity, specific gravity, and polarity. For example, the ionic product, which is an important parameter for chemical reaction, can be improved by increasing the pressure. Therefore, in the supercritical alcohol treatment of rapeseed oil, alcohol is expected to act, in addition to being a reactant, as an acid catalyst. Since the acidity of alcohol tends to decrease in the longer alkyl chain of alcohols, the reactivity would be correspondingly lower. This is one possible reason why the reaction rate is decreased in the longer alkyl chain of alcohol. Another factor might be that the smaller size of the alcohols could facilitate the simultaneous attack of alcohol on all three chains of triglycerides, resulting in the higher reaction rate of fatty acid alkyl ester formation as observed by others *(15)*.

Using similar reaction conditions with rapeseed oil, fatty acids were treated with various supercritical alcohols. From the HPLC analysis, it was shown that selective reactions could be obtained. Figure 5 presents the yields of alkyl esters of five fatty acids treated in various supercritical alcohols at 300°C. In the case of methanol, the reaction time for the complete conversion

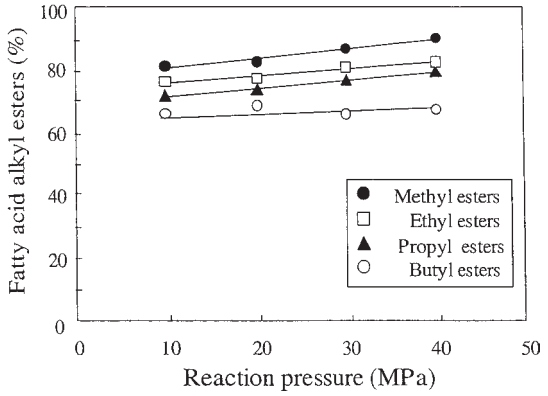

Fig. 4. Effect of reaction pressure on yield of fatty acid alkyl esters of rapeseed oil treated with various supercritical alcohols at 300°C for 20 min in flow-type reaction system.

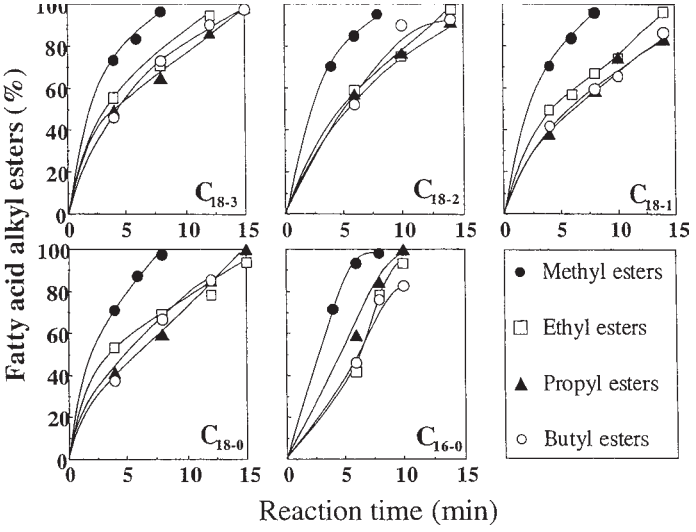

Fig. 5. Changes in yields of fatty acid alkyl esters from various fatty acids treated with supercritical alcohols at 300°C in batch-type reaction system.

of fatty acids to methyl esters was observed after 8 min of treatment. Interestingly, for other alcohols, 14 min of treatment was required to achieve complete conversions. The results with ethanol, 1-propanol, and 1-butanol show that saturated fatty acids of palmitic (C_{16-0}) and stearic (C_{18-0}) acids have slightly lower reactivity than those of unsaturated fatty acids such as oleic (C_{18-1}), linoleic (C_{18-2}), and linolenic (C_{18-3}) acids. This result is in good agreement with those found previously *(12)*.

Table 2
Cloud and Pour Point of Biodiesel Prepared by Supercritical Alcohol Treatment at 350°C and Alkaline-Catalyzed Method

Fatty acid alkyl esters	Cloud point (°C)	Pour point (°C)
Methyl esters	–4	–11
Ethyl esters	–7	–7
Propyl esters	–8	–10
Butyl esters	–10	–14
E-Oil[a]	–4	–12
Bio Super 3000[b]	–5	–12

[a] Biodiesel from waste rapeseed oil, used in Kyoto city from 1997 to 2002.
[b] Biodiesel from virgin rapeseed oil (from Austria).

Table 2 presents cloud and pour points of biodiesel prepared by our supercritical alcohol method at 350°C. For comparison, the results of the commercial biodiesel fuels are also shown. These results demonstrate that the cloud point of ethyl esters was 3°C lower than that of methyl esters, while that of butyl esters was even lower. The cloud point of methyl ester was similar to that of commercial biodiesel fuels.

Regardless of the kind of alcohols, our results revealed that supercritical treatment could convert both triglycerides and fatty acids to fatty acid alkyl esters. On the other hand, complete conversions are barely achieved by the alkaline-catalyzed method even at prolonged treatment. Considering the reactivity of triglycerides and fatty acids in various supercritical alcohols, it was noted that fatty acids are more reactive than triglycerides. With the exception of methanol, the alcohols studied had a similar reactivity in esterification of fatty acids under the same condition. Conversely, in transesterification, the formation of fatty acid alkyl esters greatly depended on the length of alcohol. The selection of alcohol in biodiesel production should therefore be based on its performance properties and economics.

Acknowledgments

This work was done in the 21 COE program "Establishment of COE on Sustainable-Energy System" and was supported by a Grant-in-Aid for Scientific Research (B) (2) (13556058, 2001. 4-2003. 3) from the Ministry of Education, Science, Sports and Culture, Japan.

References

1. Fukuda, H., Kondo, A., and Noda, H. (2001), *J. Biosci. Bioeng*. **92,** 405–416.
2. Ma, F. and Hanna, A. M. (1999), *Bioresour. Technol.* **70,** 1–15.

3. The Institute of Energy Economics, Japan. (1994), report on *Research on Feasibility of Utilization of Spent Vegetable Oils as Substitutes for Petroleum-Derived Oils*, (in Japanese), pp. 114–118.
4. Gomez, M. E. G., Hildige, R. H., Leahy, J. J., and Rice, B. (2002), *Fuel* **81,** 33–39.
5. Mittelbach, M. (1996), *Bioresour. Technol.* **56,** 7–11.
6. Lang, X., Dalai, K. A., Bakhshi, N. N., Reaney, J. M., and Hertz, B. P. (2001), *Bioresour. Technol.* **80,** 53–62.
7. Knothe, G., Matheaus, C. A., and Ryan, W. T. (2003), *Fuel* **82,** 971–975.
8. Gauglitz, E. J. and Lehman, L. W. (1963), *JAOCS* **40,** 197,198.
9. Nimcevic, D., Puntigam, R., Wörgetter, M., and Gapes, R. J. (2000), *JAOCS* **77,** 275–279.
10. Saka, S. and Kusdiana, D. (2001), *Fuel* **80,** 225–231.
11. Kusdiana, D. and Saka, S. (2001), *Fuel* **80,** 693–698.
12. Kusdiana, D. and Saka, S. (2001), *Chem. Eng. Japan* **34,** 383–387.
13. Kusdiana, D., Minami, E., Ehara, K., and Saka, S. (2002), in *Proceeding of 12th European Biomass Conference*, James & James (Science Publishers), London, UK, pp. 789–792.
14. Tanaka Scientific (2003), Mini-Pour/Cloud Point Tester, Instruction Manual, Ver. 1.01, Tokyo, Japan.
15. Freedman, B., Butterfield, R. O., and Pryde, E. H. (1986), *JAOCS* **63,** 1375–1380.

Session 5

Biobased Industrial Chemicals

Session 5

Biobased Industrial Chemicals

Douglas C. Cameron[1] and Jeff Lievense[2]

[1]Cargill, Incorporated, Minneapolis, MN; and
[2]Tate and Lyle, Decature, IL

Three Simple Rules for Biofulfillment

There are countless technically interesting biobased industrial chemical targets. This is readily appreciated by surveying the exponentially growing body of technical literature or, for those of us at this meeting, by appreciating the many fine papers and posters. It is therefore not difficult to find technically stimulating projects to work on. The greater challenge and one that leads to lasting personal fulfillment ("Biofulfillment") vs "interesting work" really comes from contributing to the commercialization of a new chemical or an improved process for an existing commercial chemical. Here are three simple rules for biofulfillment for your consideration. The papers given in this session on Biobased Industrial Chemicals all illustrate one or more of these rules. Ray Miller's talk on 1,3-propanediol (3GT) happens to address all three; it is cited for the examples it provides.

1. *The project should be business driven*. For example, Ray Miller explains the importance of bringing value to markets—a basic but critical concept. If a project is business driven, it has a much higher probability of resulting in commercial success and in a shorter time than if it is technically driven. In general, one can assess the business driver by the existence or absence of a business plan and a financial model for the project that identifies specific applications and customers for the product(s). The business plan and financial model must be validated by repeated, critical scrutiny by successful, informed businesspeople and investors.
2. *The project should leverage existing infrastructure*. This lowers the barriers to commercialization, such as reducing the capital requirements. For example, existing polymer plants can be inexpensively retrofitted to produce 3GT. Other general elements of leverage include using a feedstock that is already collected; integrating the new process into an existing manufacturing complex with a competitive cost structure and competent workforce already in place; implementing incremental (phased) introduction of a new product in order to lower capital risk.

3. *The project should provide for integration across the value chain*. This allows the commercial benefits to be maximized and often with modest incremental investment. However, it requires the ability and commitment to work through a broader spectrum of circumstances, technologies, and disciplines including integration of chemistry, biology, and engineering; and integration of products, customers, and markets. Ray Miller, in his talk on 3GT, explains the 3GT strategy that extends from starting materials to final consumer product, including consideration of the environmental footprint.

Failure in any one of the rules is a recipe for "biofrustration" (or "nobody really cares"). Biofrustration comes from investing a lot of time and resources in a project only to learn that it is not commercially viable. This is what happens in extreme cases of biofrustration:

1. *The project is strictly technically driven*. There was never a legitimate business driver. The project was funded based on unsound or insufficient business and financial groundwork. Commercializing technically driven projects is like "trying to shove a wet noodle through a hole": it can happen, it will be very messy, and you won't like the end result.
2. *The project is based solely on a "home run" vision*. There is a grandiose plan that requires too many years and too much money to yield any commercial success—otherwise known as "swinging for the fences." Just as in baseball, it is generally much smarter to play for walks, singles, and doubles. (Even the San Francisco home run king Barry Bonds gets three times more walks, singles, and doubles than home runs.) In other words, look for opportunities to realize earlier, although maybe smaller, commercial successes to build on as you strive to achieve the larger, longer-term vision.
3. *The project is a disconnected collection of functional experts with no incentive to work together*. In other words, integration is lacking. In reality, all links in the chain must be joined in order to realize commercial success. Or as Benjamin Franklin said, "We must all hang together, or assuredly we shall all hang separately." Strong project leadership is generally required to form the links and make them strong.

Although not as easy, it is much more fulfilling and, ultimately, productive to follow the three simple rules of biofulfillment.

0273-2289/04/115/0807–0825/$25.00

Effects of Trace Contaminants on Catalytic Processing of Biomass-Derived Feedstocks

Douglas C. Elliott,* Keith L. Peterson, Danielle S. Muzatko, Eric V. Alderson, Todd R. Hart, and Gary G. Neuenschwander

Pacific Northwest National Laboratory,
PO Box 999, Richland, WA 99352,
E-mail: dougc.elliott@pnl.gov

Abstract

Model compound testing was conducted in a batch reactor to evaluate the effects of trace contaminant components on catalytic hydrogenation of sugars. Trace components are potential catalyst poisons when processing biomass feedstocks to value-added chemical products. Trace components include inorganic elements such as alkali metals and alkaline earths, phosphorus, sulfur, aluminum, silicon, chloride, or transition metals. Protein components in biomass feedstocks can lead to formation of peptide fractions (from hydrolysis) or ammonium ions (from more severe breakdown), both of which might interfere with catalysis. The batch reactor tests were performed in a 300-mL stirred autoclave, with multiple liquid samples withdrawn over the period of the experiment. Evaluation of these test results suggests that most of the catalyst inhibition is related to nitrogen-containing components.

Index Entries: Catalysts; trace minerals; protein; catalytic hydrogenation; hydrolysates.

Introduction

In the United States, which is growing ever more dependent on imported oil, the use of biomass as a feedstock for chemical production provides an important opportunity for displacing petroleum and reducing this dependence. Converting biomass to value-added chemical products involves heterogeneous catalytic processing in aqueous phase, a relatively less studied area of chemical processing. Aqueous-phase processing requires specific catalyst formulations that are different from those typically used in more common petrochemical processing involving nonaqueous or gas-

*Author to whom all correspondence and reprint requests should be addressed.

phase reaction environments *(1,2)*. However, certain trace components in the biomass feedstocks (i.e., noncarbon, nonhydrogen, or nonoxygen components) are potential catalyst poisons, and their impact on the catalysts in aqueous phase processing must be considered. In this article, we discuss the results of extensive model compound tests conducted to evaluate the effect of trace contaminants on biomass processing rates and mechanisms.

Biomass is often referred to as a "clean" feedstock, most accurately pertaining to wood, which is low in mineral content; contains almost no sulfur or nitrogen; and is composed primarily of carbon, hydrogen, and oxygen. However, other potential biomass feedstocks are more problematic. Bark has more mineral, sulfur, and nitrogen, and leaves and twigs (juvenile wood) even more so. Herbaceous biomass has significant levels of mineral content, as much as 10–15 wt%, and a relatively high nitrogen (2–4%) content as well as sulfur. Aquatic biomasses, such as kelp or algae, have particularly high mineral contents, especially the marine species. Finally, waste biomass often can contain higher levels of minerals (concentrated in the residue after degradation of the organic portions) and be further contaminated with soil.

When considering biomass as a source of chemical feedstock, it is also important to remember that it is not a homogeneous organic structure. The carbohydrate structures of terrestrial plants are composed of both five-carbon and six-carbon sugar polymers. The lignin component, which binds the polymers together, is an aromatic polymer of nominally propyl-methoxyphenols. In addition, there are proteins and fatty acids/oils, as well as the trace biocomponents that incorporate much of the mineral content. Therefore, processing biomass to chemical products must take into consideration both its bulk chemical structure and its components.

In our program of process development for biobased chemical products, we conducted extensive model compound testing to evaluate the effect of various biomass contaminants on catalytic processing. Specifically, we evaluated catalytic hydrogenation of sugars to sugar alcohols in the aqueous phase, using a supported ruthenium metal catalyst. The experiments involve reagent glucose and/or xylose sugar as the model of the biomass-derived hydrolysates. To the sugar solutions, we added various chemicals to model the contaminants, which are derived from biomass feedstocks in actual process applications. The tests involved small batch reactor experiments to determine changes in the rate of reaction and mechanistic modifications caused by various contaminants. Some of these tests were undertaken as part of a project to evaluate the recovery of glucose derived from wheat millfeed starch hydrolysis. Other tests were part of a project that addressed recovery and purification of sugars derived from dairy manure solids hydrolysis.

Materials and Methods

The experiments were designed to model the hydrogenation process being developed for use in converting biomass-derived sugars into sugar alcohol products. The levels of the sugar solution contaminant tested were

based on the compositions of enzymatic hydrolysis product from wheat millfeed and acid hydrolysis product from dairy manure solids. In both cases, the sugars were relatively dilute. In the case of enzymatic hydrolysis of the millfeed, the sugar was primarily glucose from starch in the product solution. The manure was processed at two levels of severity to produce either a mixed xylose and glucose solution or a primarily glucose solution, as derived from mainly the hemicellulose or the cellulose, respectively.

A 300-mL Parr bomb reactor was operated in a semibatch mode wherein hydrogen pressure was maintained, and multiple liquid samples were removed over the 6-h period of the test. The sugar-water solution feedstock and catalyst particles (3 wt% ruthenium metal on rutile titania) were stirred in the reactor, which was maintained at constant temperature (100°C) and hydrogen overpressure (8.3 MPa). The product liquids were analyzed by high-performance liquid chromatography using a conventional carbohydrate column (Bio-Rad Aminex HPX-87H, 300 × 7.8 mm) at 65°C with a 5 m*M* H_2SO_4 mobile phase (isocratic) at a flow rate of 0.6 mL/min and a refractive index detector. Column calibration was maintained by continual analysis of standard compounds. Analysis of the products showed, in most cases, a very high selectivity to the sugar alcohol product. Traces of hydrogenolysis products (lower molecular weight polyols) were noted, as were trace yields of methane and CO_2. Glucose (or xylose) conversion is typically reported here based on reduction of sugar concentration, with time zero at temperature being the point when heating up of the reactor raised the aqueous temperature to 100°C.

The nonsugar components in the hydrolysates were determined to be a collection of metals, anions, and nitrogenous material. The inorganic elements (Ca, K, Mg, Na, S, P, Al, Si) were measured by an inductively coupled plasma-optical emission spectrometer (ICP-OES). Dissolved ammonium was measured with an ion-selective electrode.

The ICP was a Perkin-Elmer 3000DV with an AS90 Autosampler, which has an instrument detection limit of about 1 ppb (for most elements) with a linear calibration up to 100 ppm (for most elements). Solid samples were prepared via microwave digestion in concentrated nitric and hydrochloric acids, then diluted to volume. The ICP was calibrated and verified with two independent, certified standard sets. Spikes and dilutions were done for each batch of samples to check for and/or mitigate any matrix effects. The ICP process ran a constant pump rate of 1.5 mL/min for all samples and standards during analysis. A 3 mL/min rinse and initial sample flush were used to switch between each sample and standard. The plasma was run at 1450 W with argon flow. Trace metal-grade (sub-ppb) acids and two independently NIST-certified calibration standard sets were used for calibration and method verification.

Anions, including chloride, were measured by ion chromatography using a Dionex DX 500 ion chromatograph consisting of a GP40 Pump, an EG40 Elluent Generator, and an ED40 Electrochemical Detector, with an AS3500 autosampler. An ASRS-Ultra 4-mm suppressor was used (at 100

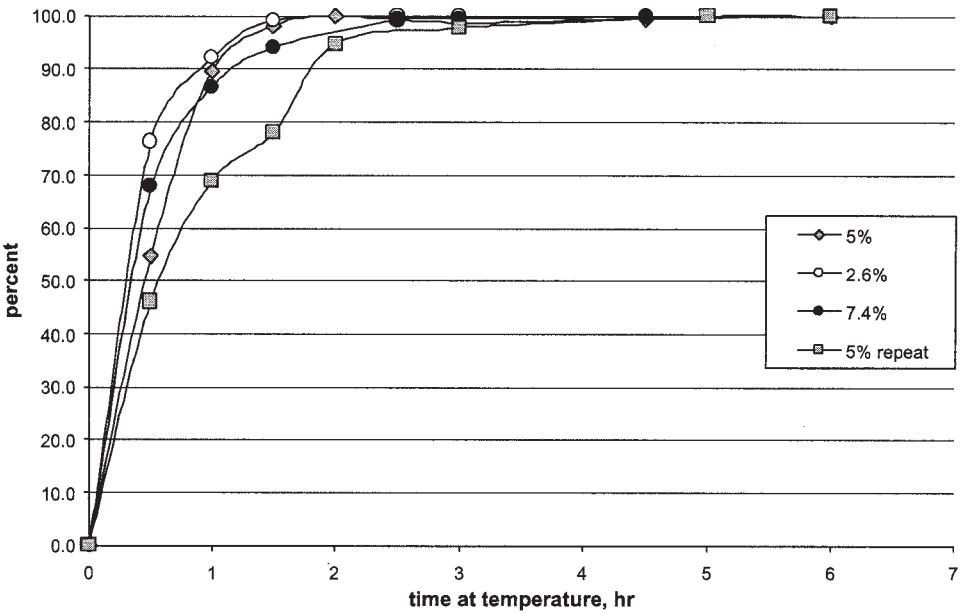

Fig. 1. Glucose conversion by catalytic hydrogenation at 100°C.

mW) to minimize baseline drift. Chromatography was performed using an AG-11 guard column and an AS-11HC column running at 30°C with a hydroxide gradient from 0.5 to 41 m*M* and a flow rate of 1.2 mL/min. Certified standards were used to calibrate the ion chromatography.

Results and Discussion

The experimental results are presented in several groups. The tests in the first group were performed with contaminant-free sugar solution to provide a baseline for comparison with the tests involving contaminants. The second group provides an overview of the range of the tests performed. The subsequent groups are more elaborate collections to evaluate certain contaminants perceived to be of greatest significance.

Sugar Hydrogenation

The tests to quantify the reaction rate and its reproducibility used reagent glucose (5 wt%) in deionized water as the feedstock. The test was repeated to evaluate the reproducibility of the reactor system. The glucose solution was also tested at two other concentrations, 2.6 and 7.4 wt%, to evaluate the effect of concentration. The results of these tests are depicted in Fig. 1. Overall, these results show the range of variability achieved with this test. The glucose conversion curves show a slight trend of increased rate of glucose conversion at lower concentration. In all cases, the glucose conversion reached 95% within 2 h at temperature.

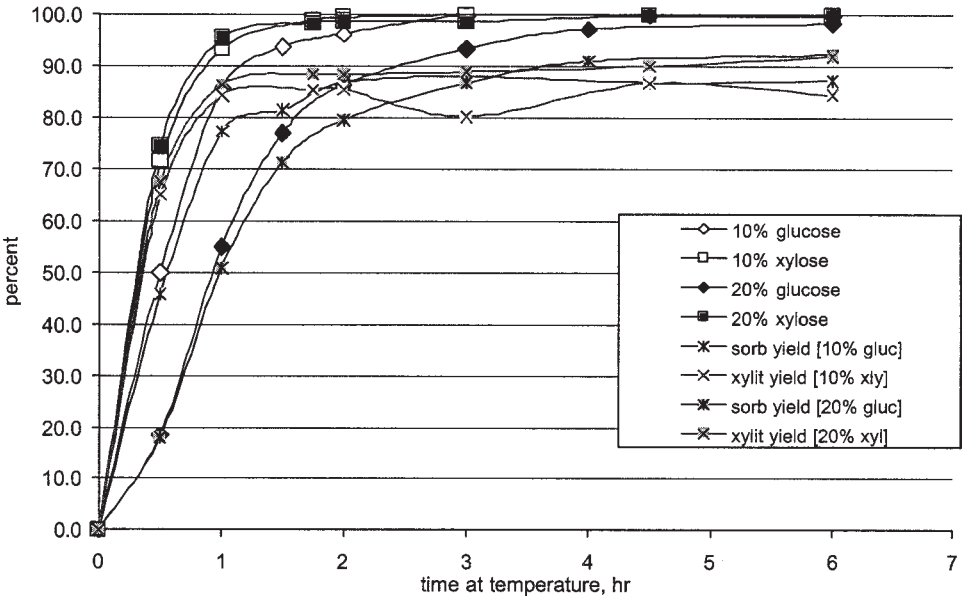

Fig. 2. Sugar conversion to sugar alcohol at 100°C.

Figure 2 shows the sugar hydrogenation and sugar alcohol production over the time of the tests for comparison of glucose and xylose. Clearly, xylose was hydrogenated more readily. These tests at higher concentrations of sugars show a concentration effect in the glucose case, but not in the xylose case; the reaction is so rapid that the concentration appears to have little impact. High selectivity (85–95%) to the sugar alcohol product is seen in all cases.

In another test with a mixed solution of 10% glucose and 10% xylose (20% total concentration), the interaction of the two sugars did not appear to occur. Figure 3 shows conversion curves for both glucose and xylose. As seen, the xylose reaction was very fast at either 10 or 20% concentration and at essentially the same rate with 10% glucose added to 10% xylose. The glucose reaction rate was reduced slightly by the competition of the 10% xylose, but not nearly as much as with the addition of the extra 10% glucose, which reacted more slowly.

Trace Contaminants

Based on the analyses of the trace contaminants conducted on the wheat millfeed–derived products, numerous potential problem components were identified, relative to catalyst activity *(3)*. These components (shown in Table 1) include sulfate (potential for metal sulfide formation); calcium, magnesium, and phosphate (potential for catalyst pore plugging by insoluble salt precipitation); sodium or potassium (alkali attack on the catalyst support); organic nitrogen components, such as amino acids (thiol

Table 1
Test Results with Trace Contaminants in Glucose

Contaminant	Form tested	Amount tested (ppm)	Amount in wheat millfeed hydrolysate (ppm)	Reduction in reactivity
Sodium	Sulfate	1000	18	None
Calcium	Hydroxide	100	77	None
Magnesium	Hydroxide	400	209	None
Potassium	Sulfate	1050	1050	None
Phosphorus	Phosphoric acid	950	510	None
Phosphorus	Phytic acid	430	510	None
Phosphorus	Dodeca-sodium phytate	550	510	None
Sulfate	Sodium sulfate	1000	1050	None
Chloride	Sodium chloride	49	56	None
Kjeldahl N	Urea	470	425	None
Cysteine	l-Cysteine	200	200 [a]	95–99%
Cysteine	DL-Cystine	200	200 [a]	None
Maltose	Crystalline	10,000	3000	None
Maltotriose	Crystalline	10,000	2000	None
Glucose oligomer	Maltodextrin 13-17	10,000	NA [b]	None
Glucose oligomer	maltodextrin 4-7	10,000	NA [b]	None

[a] Based on wheat analysis; amount in hydrolysate not analyzed.
[b] NA, not available.

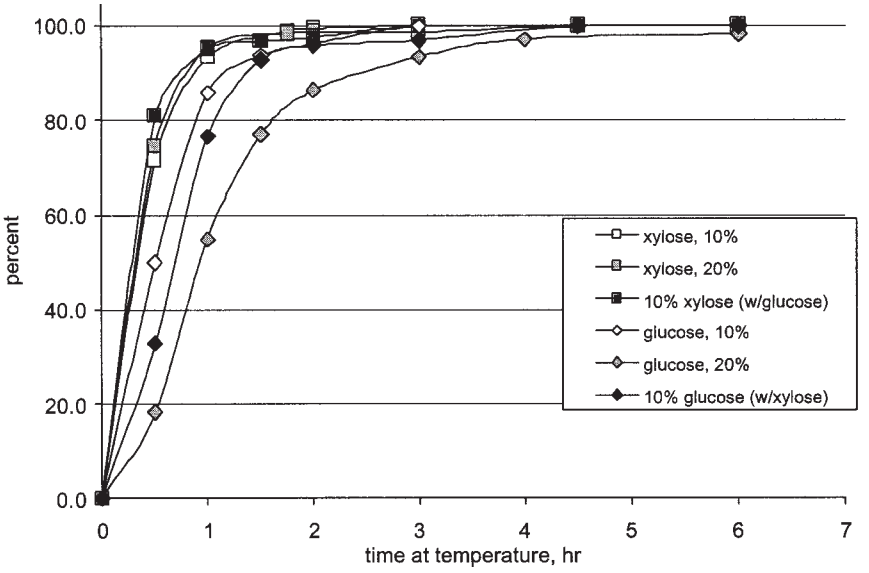

Fig. 3. Glucose/xylose conversion.

source for metal sulfide formation), proteins (pore plugging by precipitation of denatured forms), or urea (metal complex formation); chloride (reaction with the metal); phytic acid or sodium phytate (decompose and precipitate as phosphate); and maltose and maltodextrins (pore plugging or catalytic site plugging).

Tests were completed with added reagent chemicals (identified in Table 1) to model the various trace contaminants and, consequently, to identify any cause of catalyst inactivity. The results of the tests of glucose hydrogenation with these components added are summarized in Table 1. In this series of tests, no component was identified as the offending material. The components had an insignificant effect on either the rate of reaction or the total conversion achieved in the tests. The inorganic components were added as salts to the feedstock solution, as noted in Table 1. The phytic is a phosphorylated cyclohexanehexitol, which is found in wheat. It had no effect in either the acid or sodium salt form. In addition to the inorganic component results, the carbohydrate structures appeared to have little effect on activity. The nitrogenous materials were the one component that may not have been adequately modeled in these tests *(3)*.

Only the cysteine showed a deactivation of the catalyst; however, its deactivation was not reversible (by water wash of the catalyst), a characteristic of the wheat-derived material *(3)*. Therefore, we concluded that the cysteine deactivation was not analogous to the deactivation caused by wheat millfeed hydrolysates. Although cysteine is identified as a component of wheat protein structures, it is not likely to be found as cysteine in the hydrolysis products. More likely, it would be present as the bridged disulfide, cystine, following the oxidative reactions in the processing.

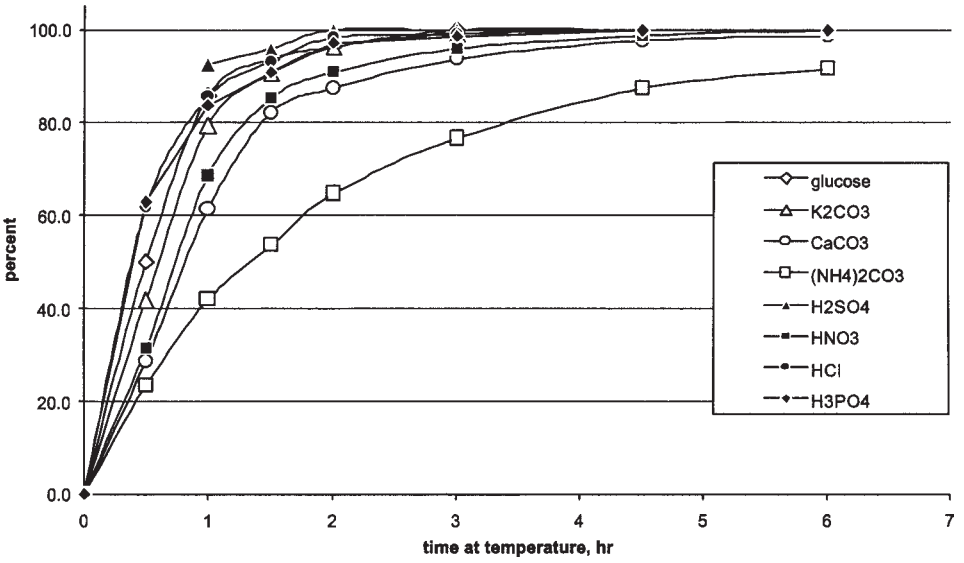

Fig. 4. Glucose conversion in presence of inorganic contaminants.

As cystine, there is no free thiol available to react with the catalyst metal and, therefore, no mechanism for catalyst deactivation. As seen in Table 1, the addition of cystine had no effect on the hydrogenation of glucose.

A subsequent series of glucose tests (10% concentration) was performed with added acids and bases to model expected anion and cation contaminants from manure hydrolysates (*see* Fig. 4). The contaminants were added at 100 ppm. The ammonium (added as carbonate) showed a decided inhibition of the catalysis. Calcium (added as carbonate) had a mild effect and the nitric acid contaminant even less, nearer the range of experimental variation. The effect of potassium (added as carbonate) was negligible (within experimental variation), as was the effect of the other acids.

Manure Hydrolysate Model Contaminants

Additional tests with added acids and bases were also performed to more accurately model expected anion and cation contaminants from manure; the results are shown in Fig. 5. The contaminants were added at the levels noted in Fig. 5, based on expected values in manure-derived feedstocks. The ammonium compounds showed a decided inhibition of the catalysis at this higher concentration, especially when added as carbonate but also to a lesser degree in the hydroxide form. Calcium (added as carbonate) had a mild effect. Neither the magnesium and the potassium bases nor the calcium sulfate appeared to have an effect at these concentrations.

A shorter companion series of tests was performed with xylose as the feedstock. As shown in Fig. 6, ammonium carbonate also inhibited the

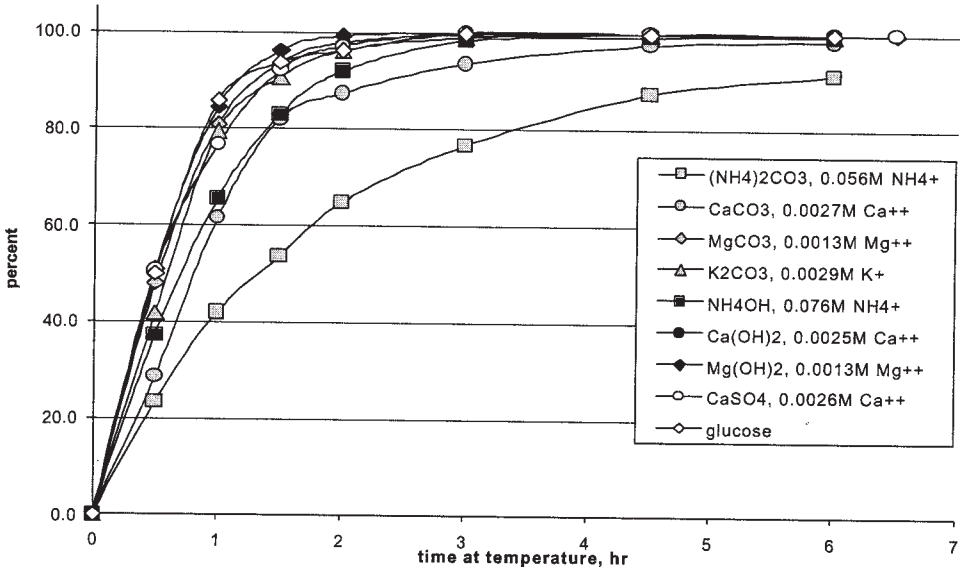

Fig. 5. Inhibition of glucose conversion by manure model contaminants.

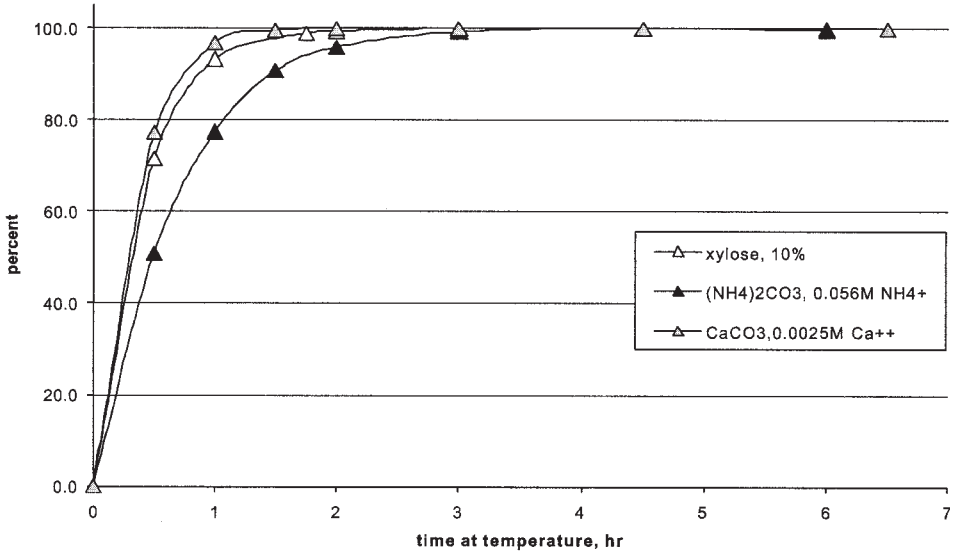

Fig. 6. Xylose conversion with contaminants.

hydrogenation of xylose. However, although the hydrogenation of xylose was noticeably faster than the hydrogenation of glucose, the effect of ammonium carbonate was less in the xylose case as compared to the glucose. Calcium carbonate appeared to have almost no impact on the hydrogenation of xylose at these concentrations.

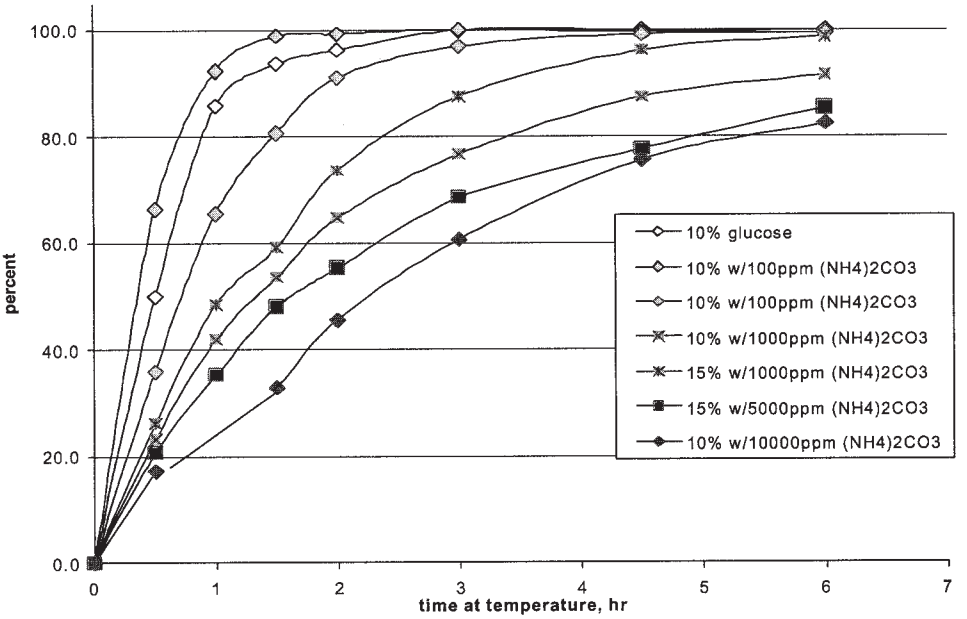

Fig. 7. Glucose conversion with ammonium present.

Ammonium Ion

The inhibition of ammonium carbonate was further studied with glucose to evaluate its scale of effect over a range of concentrations. As seen in Fig. 7, inhibition of glucose hydrogenation is a reproducible effect and is directly proportional to the concentration of the ammonium carbonate. Although there is some inconsistency in these simple batch test results, as shown by the two experimental results with 100 ppm, which bracket the 0-ppm test, the trend of reduced rate vs ammonium concentration is clear. Consequently, if the higher concentration of ammonium is present in the manure-derived feedstocks, there likely will be a significant effect on the rate of hydrogenation of the glucose. Also noted at the higher concentrations was the competitive reaction of isomerization of the glucose to form fructose. Correlating with this production of fructose is a reduction in the sorbitol product. As a result, the true inhibition of the glucose hydrogenation is even more severe than suggested by Fig. 7.

Additional tests with ammonium compounds were performed to address the effect of ammonium ion (*see* Fig. 8). It is clear that the catalyst inhibition was not based only on the presence of ammonium ion. Ammonium carbonate showed the largest inhibition of the glucose hydrogenation reaction, while chloride and hydroxide had lesser effects. Ammonium nitrate caused no apparent inhibition on glucose conversion. A similar lack of effect was shown with potassium nitrate. In the case of ammonium nitrate, the glucose conversion mechanism was affected, so that the sorbitol yield was reduced by about 20%, but numerous byproducts and overreaction products (lower molecular weight polyols) were evident.

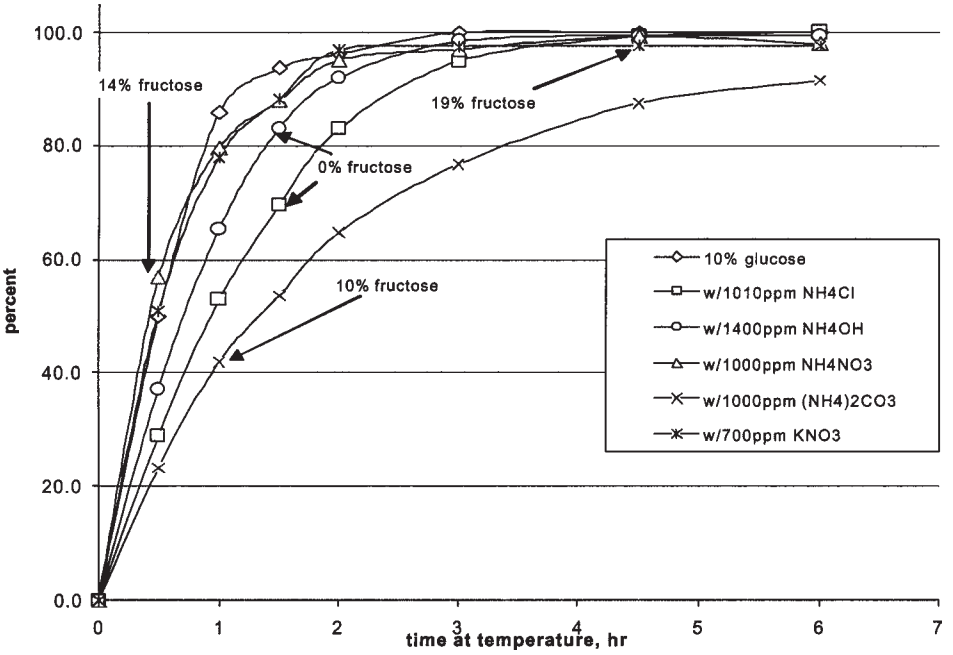

Fig. 8. Glucose conversion with ammonium and nitrates.

Calcium ion

The effect of calcium is not so straightforward. As seen in Fig. 9, the concentration of calcium carbonate appeared to have little effect on the extent of inhibition of the glucose conversion, which is low, and is about the same in all cases (i.e., from 100 to 5300 ppm). Calcium hydroxide appeared to have no inhibitory effect.

Comparison of Catalysts

Contaminant poisoning of the catalyst is likely to be catalyst specific. To evaluate this parameter, comparative tests of the ruthenium catalyst were made with a more conventional nickel catalyst (50% Ni metal on high-surface-area alumina). Figure 10 shows glucose conversion comparisons for two catalysts. The ruthenium and nickel catalysts exhibited similar activity in this batch test. However, although reaction inhibition was seen with the ruthenium catalyst in the presence of the ammonium carbonate (0.056 *M* NH_4^+), there was much less severe reaction inhibition when using the nickel catalyst in the presence of ammonium carbonate. Reaction inhibition was also seen with the ruthenium catalyst, with the addition of calcium carbonate (0.0025 *M* Ca^{++}), but the inhibition was not significant when using the nickel catalyst in the presence of the same amount of calcium carbonate.

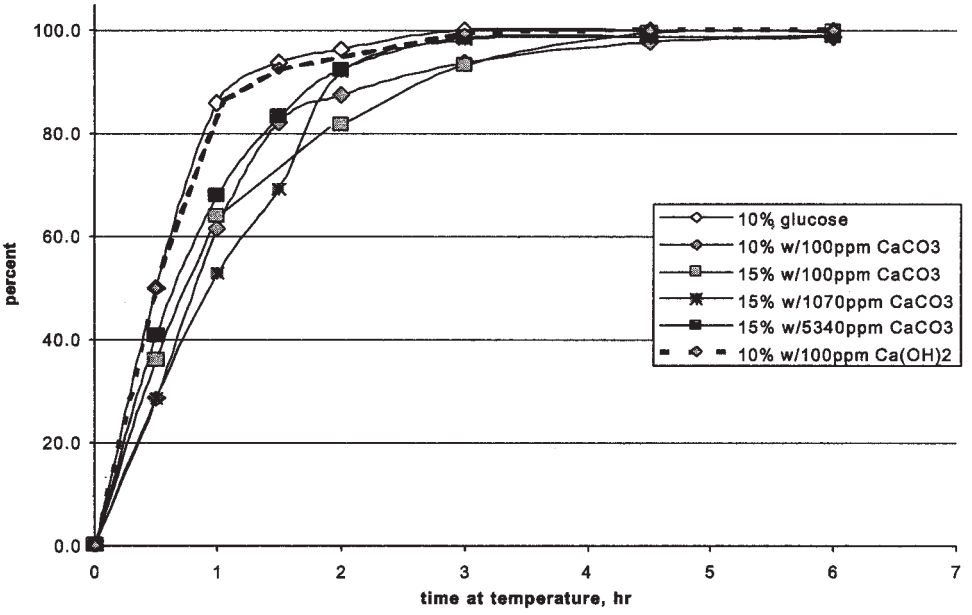

Fig. 9. Glucose conversion with calcium present.

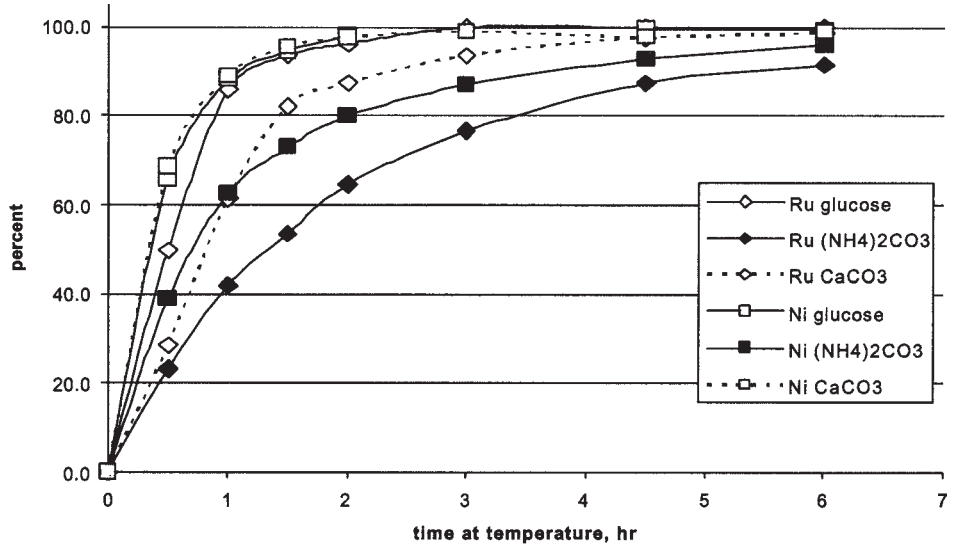

Fig. 10. Glucose conversion with different catalysts.

A model manure solution was prepared based on 10% glucose (as a carbohydrate hydrolysate model) with the various mineral components. The model solution was processed with three different catalyst formulations for comparison. The two nickel catalysts, ruthenium stabilized and copper stabilized *(4)*, exhibited no effects from the contaminants, while the ruthenium showed reduced activity similar to that already noted.

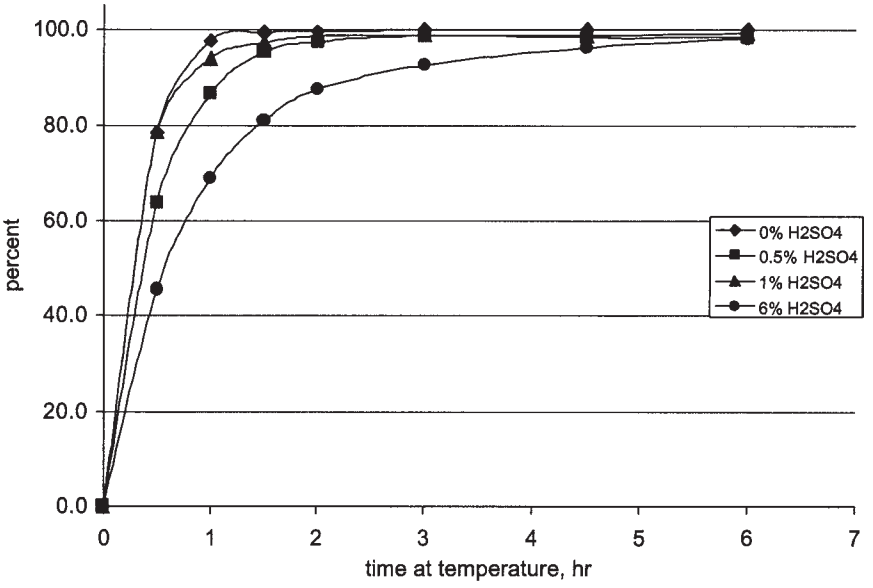

Fig. 11. Xylose (1%) conversion with H_2SO_4.

Sulfate and Ammonium

Initial analyses showed that the manure hydrolysis feedstocks were relatively dilute (~1% sugars) and mainly consisted of xylose when hydrolyzed at low temperature (~100°C). The H_2SO_4 remainder from hydrolysis can be significant. Hydrogenation tests with manure acid hydrolysates showed slow reaction rates in all cases, suggesting a large inhibition of the catalytic chemistry. Model tests were performed with 1% xylose in water with a range of H_2SO_4, from 0 to 6 wt%, to test the effect of the residual acid from the hydrolysis treatment. The results, depicted in Fig. 11, showed that H_2SO_4 had only a minor effect on the catalytic chemistry, noticeable only at the highest concentration tested and much too small to explain the results of the manure-derived feedstocks.

Analysis of ammonia performed on the manure hydrolysate samples showed ammonia concentrations of about 1300 ppm in the low-temperature acid hydrolysates and about 400 ppm in the moderate-temperature (135°C) acid hydrolysates. As already reported, model tests of ammonia at this concentration range appeared to show little or no effect. The sulfuric acid remaining in the samples from the hydrolysis ranges from 1 to 8 wt%. Again as reported, tests of H_2SO_4 in the range of the hydrolysates also appeared to have only a minor effect. A combination of the two (ammonia and H_2SO_4) might explain the catalyst inhibition; Table 2 summarizes the results. No significant effect on xylose hydrogenation was apparent at any of these sulfate concentrations with a clean xylose feedstock. The addition of ammonia with or without sulfate present also did not appear to affect xylose hydrogenation in a clean solution.

Table 2
Model Compound Xylose Hydrogenation Results

			Batch feed		6 h	
	Ammonium (ppm)	Sulfate (%)	Xylose (%)	Sulfate (area)	Xylose conversion (%)	Xylitol yield (%)
No additives	0	0	0.471	0	98	78
Low NH_4OH	445	0	0.471	0	98	92
Low $(NH_4)_2SO_4$	488	0.1	0.471	202,999	100	78
Low $(NH_4)_2SO_4 + H_2SO_4$	398	4.6	0.471	7,583,905	98	89
High NH_4OH	1258	0	3.94	0	99.3	79
High $(NH_4)_2SO_4$	1370	0.4	3.94	617,589	99.8	92
High $(NH_4)_2SO_4$ + low H_2SO_4	1524	1.5	3.94	1,815,351	99.8	99
High $(NH_4)_2SO_4 + H_2SO_4$	1258	7.1	3.94	12,429,875	99.7	82

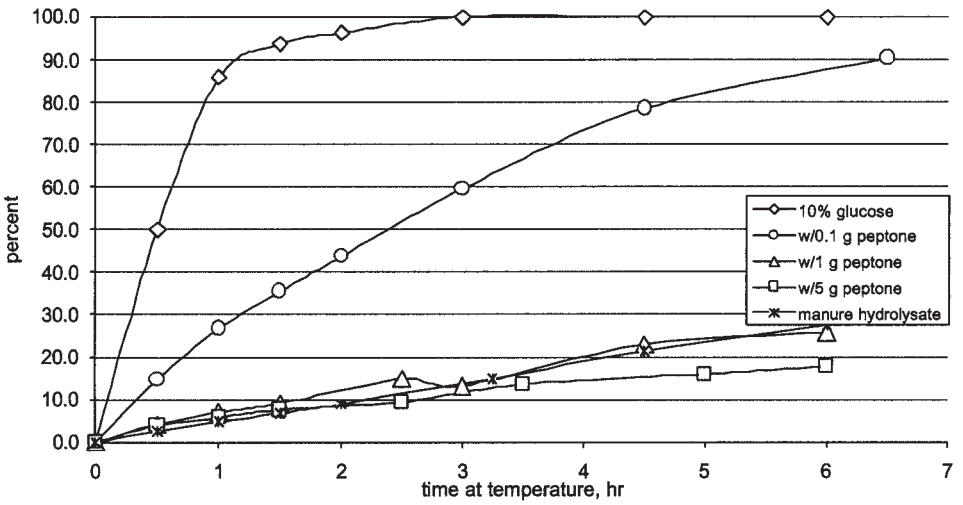

Fig. 12. Glucose conversion with addition of peptone.

Peptone Contaminant

One impurity in the manure hydrolysates is the protein-derived material, and peptone was added to the glucose solution to model the hydrolyzed protein material. Figure 12 shows a peptone concentration–dependent effect on the rate of glucose hydrogenation. As the peptone addition was increased from 0.1 to 1 g and to 5 g, glucose hydrogenation was slowed to the point that only a partial conversion was achieved after the full 6-h test compared with nearly complete conversion achieved in 2 h with reagent glucose alone. In addition, the reduction in rate of glucose hydrogenation was in the same range as that found in processing of the actual manure hydrolysates. The amount of peptone resulted in nitrogen contents similar to that found in the manure hydrolysates.

Catalyst Washing

Another important issue is the permanence of the catalyst inhibition or poisoning. The permanence of catalyst inhibition is dependent on the mechanism of the chemical interaction of the poison with the catalyst. Catalyst inhibition and the resulting reduction in reaction rate could result from competition between the poison and the preferred reactant at the catalytic site, either because of a high affinity of the poison for the catalyst site or because of its slow reaction once on the catalyst site. If the affinity is too high, as when the poison actually reacts with the catalyst to form a new compound, the catalyst is permanently poisoned. If the inhibition is only related to a slow rate of reaction, it may be possible to remove the poison from the catalyst surface and restore catalyst activity.

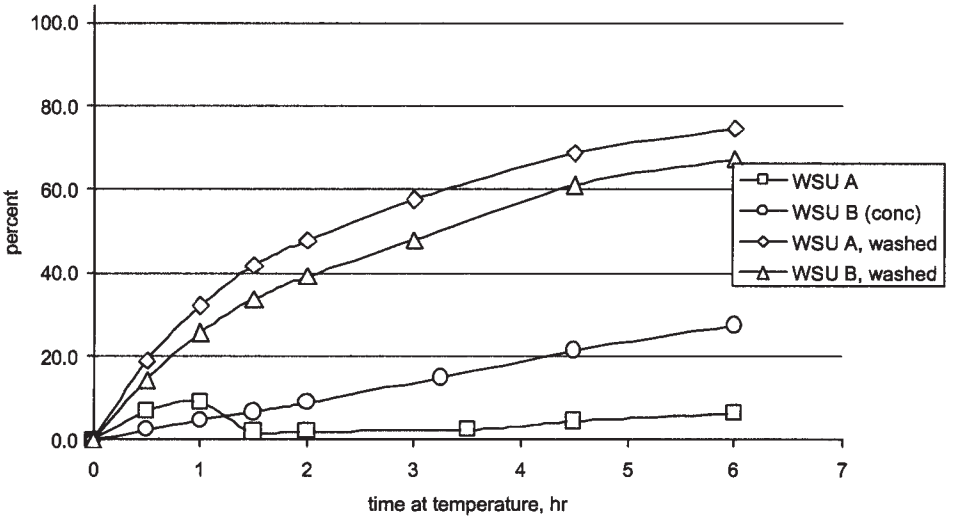

Fig. 13. Comparison of catalyst activity with raw hydrolysates and after washing.

Catalyst-washing tests were performed to determine whether catalyst activity could be recovered (*see* Fig. 13). Catalysts used in hydrogenation tests with manure hydrolysates were washed with water and reused to hydrogenate reagent glucose. The two high-temperature hydrolysates, designated solution A and solution B, gave low rates of conversion of glucose when hydrogenated directly as produced. The catalysts from those two tests, after washing, showed much improved reaction rates, approaching that of unused catalyst.

This reversibility of the poisoning is an important parameter. Two of the catalysts exhibiting inhibited activity shown in Fig. 8 were also tested following a water wash to determine the permanence of the deactivation. In the test results shown in Fig. 14, it is apparent that the catalyst deactivation noted in an initial test can be reversed by the water wash, and the catalyst activity can be returned to a level at or near that of unused catalyst. The effect was demonstrated for both ammonium carbonate and ammonium hydroxide.

Additional washing tests with the peptone-poisoned catalysts showed a similar relationship. As seen in Fig. 15, the washed catalysts showed greatly improved activity compared to the result initially with the peptone-contaminated environment. It appears that the water washing of the catalyst improved the activity equivalent to an order of magnitude reduction in the peptone contamination. However, in this case, there is not a total recovery of catalyst activity to the precontaminated state. This recovery of activity indicates that a significant portion of the catalyst deactivation

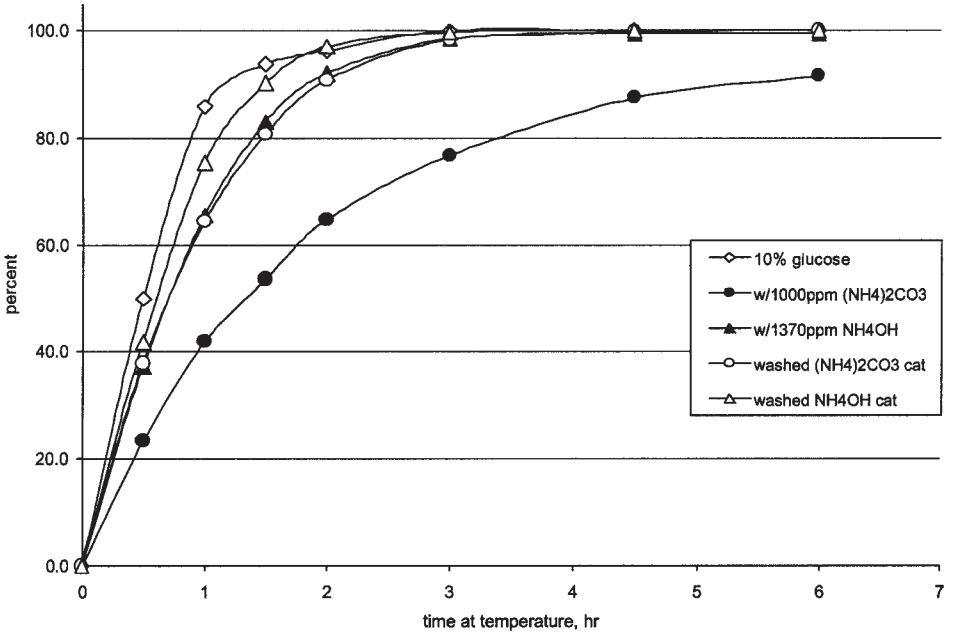

Fig. 14. Glucose conversion with reused catalyst.

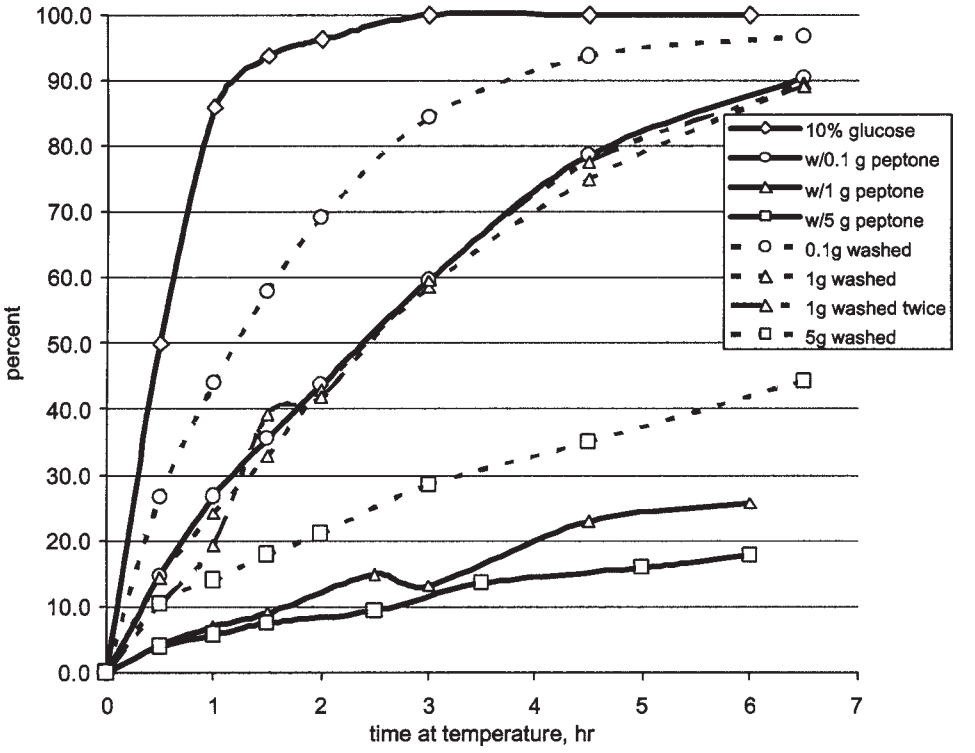

Fig. 15. Effect of washing peptone-contaminated catalysts.

results from a competition of the peptone or peptone-derived material (Maillard condensate) with the glucose for the catalytic site. In addition, also illustrated in these results is that a second wash does not improve the activity any further. This result appears to verify a combined effect of competition for the catalytic site with a more permanent poisoning of the catalytic site by the peptone.

A common thread that can link the ammonium and peptone catalyst poisoning results just described could be the Maillard reactions of amino acids with sugars *(5)*. Recent studies have shown that the ammonium ion is highly reactive, more so than substituted versions *(6)*. Its use as ammonium bicarbonate in developing flavoring compounds by Maillard reactions in extrusion cookers has been reported *(7)*. It is likely that such reactions could occur at our processing conditions. We can speculate that such products could have acted as catalyst surface poisons, which might have been subsequently washed from the catalyst, before it was reused in its active form.

Conclusion

Reaction rates for aqueous-phase catalytic hydrogenation will vary with different sugars. The C5 sugar, xylose, reacts more readily than the C6 sugar, glucose. However, our tests show that processing mixed sugars does not adversely affect the catalytic hydrogenation.

Some biomass-derived contaminants, on the other hand, may affect the catalytic processing rate. Ammonium shows significant inhibition; calcium may also have an effect. Potassium, though, appears to have too little interaction to be noticeable at the concentrations tested. The common acid anions phosphate, sulfate, and chloride appear to have no effect, while nitrate changes the conversion route and the product slate through a sugar isomerization mechanism. These tests show that while some contaminants may affect the catalytic processing rate, most have no impact, and there is no indication of a combinatorial effect on the catalyst when several of the contaminants are present in the feedstock. Consequently, the calcium and ammonium continue to be the key components of concern.

Peptone (hydrolyzed protein) appears to best mimic the catalytic inhibition experienced in the catalytic hydrogenation of sugars in manure hydrolysate solutions, suggesting that the inhibitory effect is owing to hydrolyzed protein in the solution. The inhibitory effect appears to stem from a combination of mechanisms, probably related to Maillard-type reactions forming condensed structures, which can block active catalyst sites. Some activity can be regained by simply washing the used catalyst with water. Thus, the suggested catalyst "poisoning" is more accurately an equilibrium competition effect or a site blocking. However, the washed catalyst does not regain its original activity level, suggesting that there is also a more permanent poisoning in this case.

Acknowledgments

We wish to acknowledge our collaboration with the Biological Systems Engineering Department of Washington State University, specifically Prof. Shulin Chen and his graduate students, Wei Liao and Chaunbin Liu, who produced the manure solids hydrolysate solutions. The testing and analyses described here were performed at the Pacific Northwest National Laboratory operated by Battelle for the U.S. Department of Energy under Contract DE-AC06-76RL01830.

References

1. Elliott, D. C., Sealock, Jr., L. J., and Baker, E. G. (1993), *Ind. Eng. Chem. Res.,* **32(8),** 1542–1548.
2. Elliott, D. C. (2001), in *Progress in Thermochemical Biomass Conversion*, Bridgwater, A. V., ed., Blackwell Science, Oxford, UK, pp. 1186–1196.
3. Elliott, D. C., Orth, R. J., Gao, J., et al. (2002), in *Proceedings of Bioenergy 2002, The Tenth Biennial Bioenergy Conference*, Crockett, J. and Peterson, C. L., ed., Pacific Regional Biomass Energy Program, Seattle, WA, p. 35.
4. Elliott, D. C. and Hart, T. R. (1999), US patent no. 5,977,013.
5. Kawamura, S. (1983), in *The Maillard Reaction in Foods and Nutrition, ACS Symposium Series 215*. Waller, G. R. and Feather, M. S., eds. American Chemical Society, Washington, DC, pp. 3–18.
6. Villota, R. and Hawkes, J. G. (1994), in *Thermally Generated Flavors Maillard, Microwave, and Extrusion Processes, ACS Symposium Series 543*. Parliament, T. H., Morello, M. J., and McGorrin, R. J., eds. American Chemical Society, Washington, DC, pp. 280–295.
7. Izzo, H.V., Hartman, T.G., Ho, C.-T. (1994), in *Thermally Generated Flavors Maillard, Microwave, and Extrusion Processes. ACS Symposium Series 543*. Parliament, T. H., Morello, M. J., and McGorrin, R. J. eds. American Chemical Society, Washington, DC, pp. 328–333.

0273-2289/04/115/0827–0836/$25.00

Characterization of Surfactin from *Bacillus subtilis* for Application as an Agent for Enhanced Oil Recovery

Kastli D. Schaller,* Sandra L. Fox, Debby F. Bruhn, Karl S. Noah, and Gregory A. Bala

Biotechnology Department,
Idaho National Engineering and Environmental Laboratory,
PO Box 1625, Idaho Falls, ID 83415-2203,
E-mail: schakd@inel.gov

Abstract

Surfactin produced by *Bacillus subtilis* (ATCC 21332) was used to examine the effect of altering salt concentration, pH, and temperature on surfactin activity (as measured by reductions in surface tension). These parameters are some of the conditions that define oil reservoir characteristics and can affect the application of surfactants. The Biotechnology for Oilfield Operations research program at the Idaho National Engineering and Environmental Laboratory (INEEL) has successfully produced surfactin from potato process effluents for possible use as an economical alternative to chemical surfactants for improved oil recovery. Surfactants enhance the recovery of oil through a reduction of the interfacial tension between the oil and water interfaces, or by mediating changes in the wettability index of the system. We investigated changes in surfactin activity under a range of conditions by measuring surface tension. Surface tension was determined using video image analysis of inverted pendant drops. Experimental variables included NaCl (0–10%), pH (3.0–10.0), and temperature (21–70°C). Each of these parameters, as well as selected combinations, resulted in discrete changes in surfactin activity. It is therefore important to consider the exploration of the studied surfactin as an enhanced oil recovery agent.

Index Entries: *Bacillus subtilis*; biosurfactant; surfactin; improved oil recovery; oil recovery agent.

Introduction

Surface-active molecules produced by microorganisms, called biosurfactants, could possibly replace costly and potentially toxic chemical

*Author to whom all correspondence and reprint requests should be addressed.

surfactants in several industries *(1)*. Industries that can use biosurfactants include textile, environmental bioremediation, and fossil fuel recovery *(2)*. Utilization is limited, however, by the cost of producing biosurfactants. This is determined by the process for growing the microorganisms that produce the surfactant, and the cost of purifying the biosurfactant from the culture fluid *(3)*. The Biotechnology for Oilfield Operations research program at Idaho National Engineering and Environmental Laboratory has successfully produced surfactin, the biosurfactant from *Bacillus subtilis* (ATCC 21332), from potato process effluents for possible use as an economical alternative to chemical surfactants for improved oil recovery *(3,4)*. Surfactants reduce interfacial tension between oil and water, thus decreasing the energy required to extract trapped oil in the matrix and displacing it into the mobile liquid phase. *B. subtilis* grown in low-solids (LS) potato process effluents produced surfactin with surface tensions of 25.5–26.5 mN/m *(3)*. The purpose of the present study was to evaluate the changes in surfactin activity of surfactin containing culture supernatant from *B. subtilis* grown on LS potato process effluents by altering pH, salt concentration, and temperature of the cell-free supernatant. We carefully considered typical oil reservoir conditions and the ultimate exploitation of this surfactin as an enhanced oil recovery agent.

Materials and Methods

Production of Surfactin

Surfactin was produced from *B. subtilis* (ATCC 21332) in a continuous stirred tank reactor (CSTR) utilizing LS potato process effluent, which was obtained from a southeast Idaho potato processor, as previously described by Noah et al. *(4)*. At the completion of a run, the culture fluid was centrifuged at 6084*g* for 30 min to remove cells and insoluble material. The supernatant containing surfactin was then stored in a sterile container at 4°C. The same supernatant from one single run was used throughout all experiments to provide continuity for comparison of each study.

Experimental Parameters and Procedures

Three experimental parameters and combinations thereof were investigated: (1) pH, (2) salt concentration, and (3) temperature. The effects on surfactin activity were measured by surface tension ($n = 5$).

Effects of pH

For each experiment, the supernatant was placed in 15-mL conical tubes, and the pH was adjusted with either 1 *N* KOH or 1 *N* HNO_3. The pH of the supernatant after the bioreactor run was 7.0. Simulated potato effluent (SPE) medium was used as a surfactin-free control and the pH adjusted likewise. SPE contained the following per liter of nanopure water: 5 g of potato starch, 3.5 g of peptone, 3.5 g of tryptone, 0.2 g of $MgSO_4 \cdot 7H_2O$, 0.1 g of yeast extract, and 0.8 g of $(NH_4)_2SO_4$.

Effects of Salt Concentration

For each experiment, up to 10% (w/v) NaCl was placed in 15-mL conical tubes. The supernatant was added and the tubes were gently stirred on a laboratory rotator for 2 h. With concentrations above 3%, the supernatant became cloudy with a precipitate that interfered with surface tension measurements. The supernatant was therefore left overnight in an upright position to allow the precipitate to settle out, and readings of surface tension were taken the following day. The SPE medium was used as a surfactin-free control and NaCl added likewise. When pH was included as a parameter in this experiment, NaCl was added first and the supernatant was stirred for 2 h. Then the pH of the supernatant was adjusted with either 1 *N* KOH or 1 *N* HNO_3.

Effects of Temperature

For each experiment, the supernatant was placed in 15-mL conical tubes and then incubated at temperatures up to 70°C. The supernatant was incubated for a minimum of 1 h. When experiments included NaCl and pH adjustments, the supernatant was incubated overnight, or longer, to allow for precipitate to settle out. For the surfactin stability experiment, supernatant was incubated at either 4 or 70°C for over 95 d. Surface tension was measured at elevated temperature using a special heated cell. The cell was made from stainless steel with channels drilled in the cell to accommodate attachment to a heated circulating water bath (Polystat Water Circulator; Cole-Parmer, Vernon Hills, IL). Density was determined for the supernatant used in all experiments by placing a little more than 1 mL in a 1-mL volumetric flask and incubating at 4, 21, 37, 51, and 70°C for 1 h. Afterward, the excess supernatant was removed to the 1-mL mark. The flasks were then weighed to determine the density of the fluid. The average density ($n = 2$) from this experiment was used in a quadratic equation to extrapolate density for each temperature in the range of 21–70°C.

Analytical Methods

Surfactin in the supernatant was confirmed and the concentration determined by high-performance liquid chromatography analysis as described by Noah et al. *(4)*. Surface tension was measured using video image analysis of inverted pendant drops as previously described *(5)*. All data points are an average of five measurements taken of the cell-free supernatant.

Results

Effects of pH

Figure 1 shows the effects of altering the pH of the supernatant containing surfactin. The starting pH of the supernatant produced from potato process effluents, without any pH adjustments, was 7.0 and the surface tension was 28.3 ± 0.1 mN/m. The effects of altering the pH were found to alter surface tension of the surfactin at pH values <6.0. The sharpest tran-

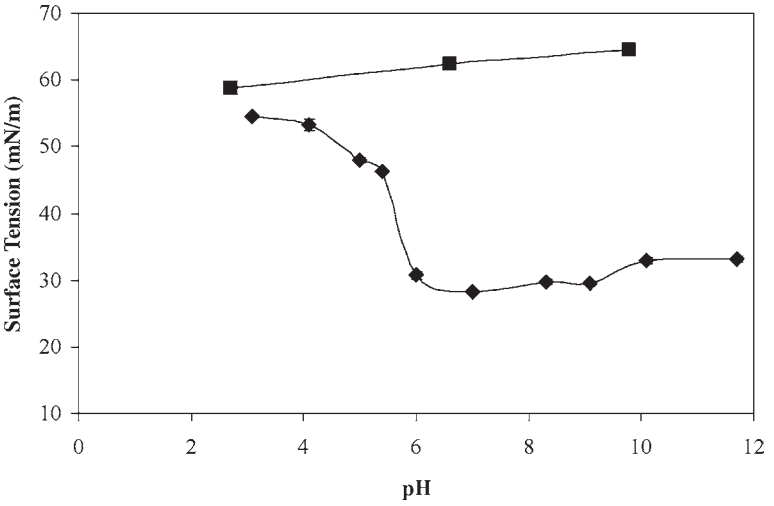

Fig. 1. Effects of pH on surfactin activity. The pH of the supernatant without any alteration in pH was 7.0. (◆) Surfactin; (■) surfactin-free control.

sition in surfactin quality, as indicated by an increase in surface tension, occurred between pH 6.0 (30.7 ± 0.5 mN/m) and 5.0 (47.9 ± 0.4 mN/m). Between pH 6.0 and 10.0 surface tensions remained almost unchanged and had a range of 28.3 ± 0.1 to 33.0 ± 0.4 mN/m. Since isolation procedures utilize the precipitation of surfactin under acidic conditions *(4)*, it was expected that a precipitate would form and surface tension would increase at pH <3.0. Indeed, a precipitate formed and surface tension increased to 54.5 ± 0.3 mN/m. When the sample was centrifuged and the resulting pellet resuspended in nanopure water, the surface tension returned to 32.2 ± 0.3 mN/m.

Effects of Salt Concentration

Figure 2 shows the effects of the addition of salt (NaCl) to the supernatant. The surface tension of the surfactin without any additions of NaCl was 29.4 ± 1 mN/m. Experiments found NaCl concentrations above 30 g/L to increase surface tension of surfactin. Between 30 and 50 g/L of NaCl, surface tension increased from 29.4 ± 0.1 to 46.2 ± 0.4 mN/m. Between 60 and 100 g/L of NaCl, surface tension remained at about 50 mN/m.

Effects of Temperature

Figure 3 shows the effects of incubating surfactin from 21 to 70°C. Although there was an apparent decrease in surface tension of surfactin at higher temperature, there was also a decrease in surface tension of water as

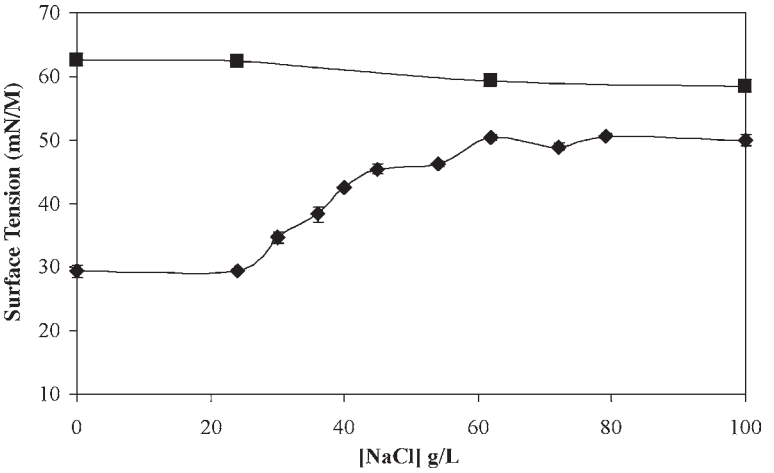

Fig. 2. Effects of salt concentration on surfactin activity. (◆) Surfactin; (■) surfactin-free control.

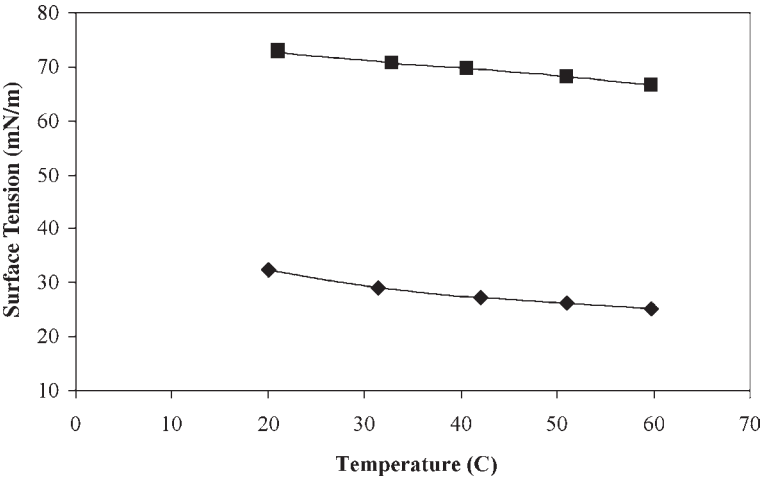

Fig. 3. Effects of temperature on surfactin activity. (◆) Surfactin; (■) water.

temperature increased. The difference in surface tension between water and surfactin remained the same, showing that there was no effect of temperature on surfactin. Furthermore, a stability experiment indicated no change in surface tension of surfactin when surfactin was incubated at 70°C for over 95 d (Fig. 4). There was also no change in surface tension of surfactin incubated at 4°C for 95 d.

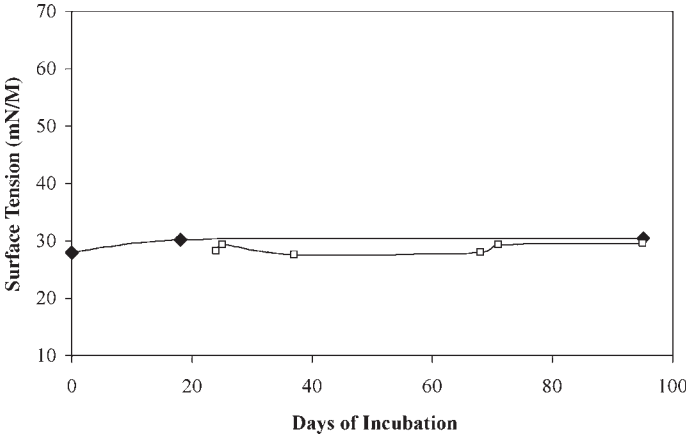

Fig. 4. Temperature stability of surfactin over time. (◆) Surfactin incubated at 70°C; (□) surfactin incubated at 4°C.

Effects of Temperature and pH

Temperature and pH effects were examined together to determine whether there were synergistic interactions that were not seen when each was tested alone. Figure 5 shows theresults from this experiment. Temperature alone did not alter surface tension of surfactin, nor did it alter the results seen from pH alone. The combination of temperature at 31 and 56°C and pH 5.0 did increase precipitate in the supernatant, which interfered with measurement of surface tension. Attempts to centrifuge did not remove the precipitate and still did not allow measurement of surface tension. However, visual observation of the pendant drop size indicated that surface tension had increased relative to the supernatant that had not been altered with KOH or HNO_3. At an incubation temperature of 70°C, pH 3.0 and pH 5.0 supernatants were cloudy, which interfered with surface tension measurements. Visual observation indicated that the surface tension was relatively high for these samples as well, since the pendant drop size was large compared to surfactin with surface tensions in the range of 27 to 28 mN/m.

Effects of Temperature and Salt Concentration

Figure 6 shows the results of the experiment on the effects of temperature and salt concentration. The supernatant was prepared as described in the Materials and Methods section, except that there was a 9-d incubation instead of overnight owing to the replacement of a burned-out lamp in the interfacial tension instrument. There were no significant differences among all salt concentrations at 21 and 45°C. However, at 70°C, the higher salt concentrations did not increase surface tension of surfactin, as did those at the lower temperatures. At 50 g/L of NaCl and 70°C, surface tension was 31.5 ± 1.3 mN/m compared with 50.9 ±0.3 and 53.4 ± 0.2 mN/m at 50 g/L of NaCl at 21 and 45°C, respectively.

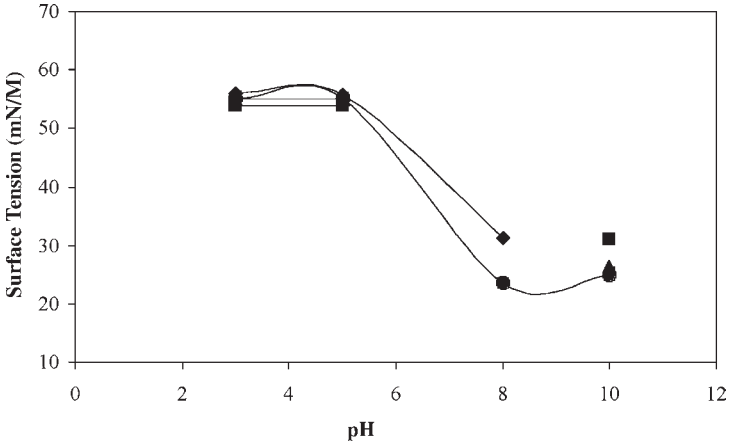

Fig. 5. Effects of temperature and alterations in pH on surfactin activity. (◆) Surfactin, 21°C incubation; (■) surfactin, 31°C incubation; (▲) surfactin, 56°C incubation; (●) surfactin, 70°C incubation.

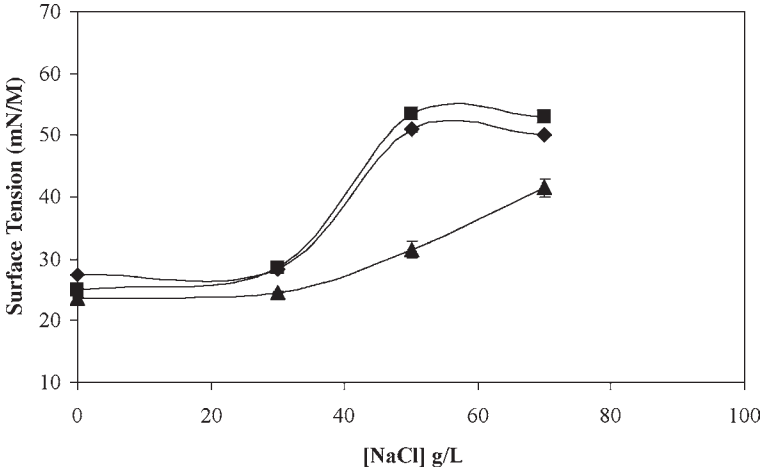

Fig. 6. Effect of temperature and salt concentration on surfactin activity. (◆) Surfactin, 21°C incubation; (■) surfactin, 45°C incubation; (▲) surfactin, 70°C incubation.

Effects of Temperature, Salt Concentration, and pH

Ther effects of the addition of NaCl (3–8%), alterations in pH (3.0–10.0), and temperature (21 and 70°C) were tested together to examine the effects of all three parameters combined. Figure 7 compares two experiments at 21 and 70°C. Samples were incubated overnight except for those at 70°C that were too cloudy to measure surface tension. These samples were incubated for 6 d until measurements could be taken. Incubation time was increased

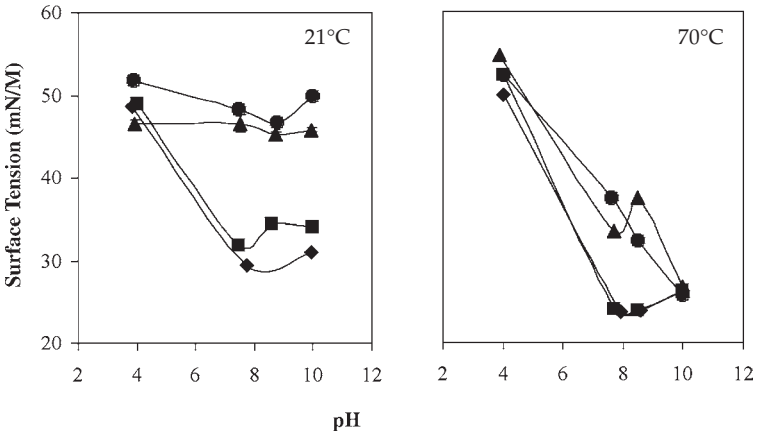

Fig. 7. Effect of temperature, salt concentration, and pH on surfactin activity. (◆) 0 g/L of NaCl; (■) 30 g/L of NaCl; (▲) 50 g/L of NaCl; (●) 70 g/L of NaCl at 21°C, 80 g/L of NaCl at 70°C.

because a high-temperature centrifuge was not available to remove the precipitate that had formed in the supernatant. It was observed that the effect of increasing surface tension by increasing salt concentration was moderated at higher temperature and basic pH. The surface tension of the supernatant at salt concentrations >50 g/L at 21°C remained between 45.2 ± 0.4 and 51.8 ± 0.3 mN/m. The surface tension of the supernatant at salt concentrations >50 g/L and 70°C, however, was lower. This was observed most at pH 10.0, where surface tension of the supernatant with 50 g/L of NaCl was 26.6 ± 0.2 mN/m, and the surface tension of the supernatant with 80 g/L of NaCl was 25.8 ± 0.1 mN/m. The surface tension of the supernatant with no addition of NaCl and no alterations in pH at 70°C was 23.7 ± 0.2 mN/m, and 29.4 ± 0.6 mN/m at 21°C.

Discussion

Supernatant containing surfactin, produced from LS potato process effluents in an airlift reactor, was characterized under various environmental parameters to better define appropriate conditions for its use as an agent for enhanced oil recovery. By itself, pH was found to increase surface tension of the surfactin below 6.0. Concentrations of NaCl a>30 g/L were seen to increase surface tension, with the highest surface tension occurring at about 50 g/L. When the effect of temperature was added to the pH experiment, there were no significant changes, and again, surface tension, at any temperature, increased at pH <6.0. Temperature alone, up to 70°C, did not alter surface tension of the surfactin. However, when temperature was added to experiments with salt concentration, increases in surface tension seen at 50 and 70 g/L of NaCl appeared to be somewhat moderated at 70°C.

This was further verified when all three parameters were combined in one experiment and no increase in surface tension was observed at 80 g/L of NaCl, pH 10.0, and 70°C. Temperature experiments did not go beyond 70°C, so the high temperature limit of the surfactin has yet to be determined.

Surfactin is an anionic, amphiphilic, lipopeptide compound. These properties are the reason for its ability to lower surface tension so effectively *(6)*. Surfactin is also an effective antimicrobial and antiviral, able to induce the formation of ionic pores in phospholipid bilayers *(7)* and transport cations across membranes *(8)*. Its cation-complexing property, owing to two negative charges on the aspartyl and glutamyl residues *(8)*, is probably fully utilized in our system containing ubiquitous amounts of Ca^{+2} and Na^{+} ions in the LS potato process effluent *(9)*. The increase in surface tension of surfactin with higher NaCl concentration and lower pH is more likely owing to a precipitation process commonly seen with proteins and used in protein purification. Precipitation of proteins can be achieved by adding salts, adding organic solvents, altering the pH, or altering the temperature *(10)*. In our study, we altered three of these variables. Furthermore, an increase in temperature to 70°C and an increase in pH to 10.0 probably decreased the hydrophobic effects caused by high salt concentration on the surfactin in the solution so that protein aggregation by association of hydrophobic surfaces did not occur.

These are favorable results for the application of this surfactin as an agent of enhanced oil recovery since high salt concentration, high temperature, and high pH describe the conditions of many oil reservoirs. This surfactin was also produced cheaply with potato process effluents, another attractive feature. Previous experiments with surfactin produced in minimal salts medium containing potato starch have shown similar results. However, note that changes in the process from which the feedstock is derived could have an impact on these results.

Future production of surfactin from potato process effluents will be used in core floods to characterize further its potential application as an agent for enhanced oil recovery.

Acknowledgments

We thank Jerry Casteel, Rhonda Lindsey, Suzanne M. Mehlhoff, Purna Halder, and Daniel Gurney of the US Department of Energy (DOE) National Petroleum Technology Office and Patricia St. Clair of the US DOE Idaho Field Office for their support. We also express our gratitude for the generous help and support from Basic American Foods, Blackfoot, ID. This work was supported by the US Department of Energy, Assistant Secretary for Fossil Energy, Office of Fossil Energy under contract no. DE-AC07-99ID13727.

References

1. Davis, D. A., Lynch, H. C., and Varley, J. (1999), *Enzyme Microb. Techno.* **25,** 322–329.
2. Fox, S. L. and Bala, G. A. (2000), *Bioresour. Technol.* **75,** 235–240.

3. Thompson, D. N., Fox, S. L., and Bala, G. A. (2000), *Appl. Biochem. Biotechnol.* **84–88,** 917–930.
4. Noah, K. S., Fox S. L., Bruhn, D. F., Thompson, D. N., and Bala, G. A. (2002), *Appl. Biochem. Biotechnol.* **98–100,** 803–813.
5. Herd, M. D., Lassahn, G. D., Thomas, C. P., Bala, G. A., and Eastman, S. L. (1992), in *Proceedings of the DOE Eighth Symposium on Enhanced Oil Recovery*, SPE/DOE 24206, Society of Petroleum Engineers (SPE), Tulsa, OK.
6. Gallet, X., Deleu, M., Razafindralambo, H., Jacques, P., Thonart, P., Paquot, M., and Brasseur, R. (1999), *Langmuir* **15,** 2409–2413.
7. Morikawa, M., Hirata, Y., and Imanaka, T. (2000), *Biochim. Biophys. Acta* **1488,** 211–218.
8. Grangemard, I., Wallach, J., Maget-Dana, R., and Peypoux, F. (2001), *Appl. Biochem. Biotechnol*. **90,** 199–210.
9. Thompson, D. N., Fox, S. L., and Bala, G. A. (2001), *Appl. Biochem. Biotechnol*. **91–93,** 487–501.
10. Ersson, B., Ryden, L., and Janson, J. C. (1998), in *Protein Purification*, Janson, J. C. and Ryden, L., eds., Wiley, New York, NY, pp. 3–40.

0273-2289/04/115/0837–0842/$25.00

Effect of Germ and Fiber Removal on Production of Ethanol from Corn

Elankovan Ponnampalam,* D. Bernie Steele, Deborah Burgdorf, and Darold McCalla

MBI International, 3900 Collins Road, Lansing, MI 48910, E-mail: ponnam@mbi.org

Abstract

Ethanol fermentations were conducted using both whole corn, and corn with 100% of the germ, and a portion (~74%) of the fiber removed. Ethanol production increased 11% in the germ and fiber-removed corn vs the whole corn. The protein content of distiller's dried grains and solubles increased from 30 to 36%, and phosphate levels were 60% lower in corn with germ and fiber removed vs whole corn. Removal of germ and fiber prior to fermentation allows higher starch loading and results in increased ethanol production. The integration of germ and fiber removal in the dry-grind ethanol industry could increase capacity and add valuable coproducts, resulting in increased productivity and profits.

Index Entries: Ethanol; germ; fiber oil; distiller's dried grains and solubles; fermentation.

Introduction

Of the current corn-to-ethanol processes, wet milling and dry grind, the dry grind has lower capital investment and produces more ethanol per bushel of corn, when compared with the wet-milling process *(1)*. Current wet-milling facilities utilize the corn germ and other nonfermentables as valuable coproducts that increase the profitability of their operations. Removal of the germ and hull during the dry-grind process would be expected to offer the same benefits to the dry-grind industry. Removal of these nonfermentables prior to fermentation is expected to increase ethanol production capacity in dry-milling operations. The increase in capacity and the production of germ and fiber byproducts, such as corn oil and corn fiber oil, could increase profit margins and reduce reliance on a single product.

*Author to whom all correspondence and reprint requests should be addressed.

There are currently several methods for the removal of the germ and fiber during dry-grind operations. The "Quick Germ" and "Quick Fiber" separations, developed at the University of Illinois, are examples of relatively inexpensive and simple methods for germ and fiber removal *(1,2)*.

Original assumptions by Singh and Eckhoff *(2)* predicted approx 7–10% increase in fermentation capacity using the Quick Germ process. The relative economics of using whole corn vs corn with the germ removed has been discussed previously *(2,3)*. Taylor et al. *(3)* estimated that the savings from the sale of germ (for production of corn oil) would be approx $0.094/gal of ethanol. This assumes a sale price of $0.25/lb for corn oil (current market price) and includes utility costs as well as capital-related costs for production. Wahjudi et al. *(1)* estimated an additional $0.04/gal from removal of the fiber.

The current study compared the fermentation of whole corn (as currently practiced in the dry-grind industry) with the high-density fermentation of corn with 100% of the germ and approx 74% of the fiber removed.

Materials and Methods

Feedstocks

Two corn samples (70 lb each) were received from Bunge Milling (Danville, IL) and stored in plastic bags at –20°C. The whole ground corn comprised of yellow dent corn kernels that had been reduced to a coarse meal granulation by passage through a Romer Mill, which is a laboratory-scale, burr-type mill. The proximate composition of this ground corn was essentially the same as the composition of the starting whole corn, since the entire stream was collected during the grinding process. The granulation profile for this ground corn sample was very broad but could be generally described as "minus 10/plus 50" with about 15% through the 50 sieve. The second sample was yellow dent corn with 100% of the germ and approx 74% of the fiber removed and henceforth referred to as "germ and fiber-removed corn" (G/F minus corn). This sample was prepared by physically blending a degermed corn grits product with a degermed corn meal product. This product also exhibited a "minus 10/plus 50" granulation profile with about 10% through the 50 sieve, although this granulation was not quite as broad as the whole ground corn sample.

Fermentations

Five pairs of ethanol fermentations (5 L) were completed. Each fermentor was loaded with 27.9% (w/w) dry mash. The pH was adjusted to 5.8 with NaOH. Amylase (Enzyme Biosystems, Beloit, WI) in the amount of 1367.4 U was added to the fermentors. The temperature was held at 85°C for 3 h with mixing. The temperature was then reduced to 60°C and the pH adjusted to 4.4 with H_2SO_4. Glucoamylase (Enzyme Biosystems) was then added in the amount of 274 U and the temperature maintained at 60°C for 2 h. The temperature was then lowered to 35°C, and a nitrogen

source was added to the fermentors (1.5 g/L of ammonium chloride). The fermentors were inoculated with 5% active yeast culture (*Saccharomyces cerevisiae* ATCC 4126). During the fermentations, the pH was maintained at 4.0 with 10% NaOH, and temperature was controlled at 35°C. Condensers were used on fermentor gas outlets to reduce the amount of ethanol loss owing to evaporation. Ten-milliliter samples were taken periodically during the process to monitor ethanol production and acid production, as well as glucose concentration, and to microscopically observe yeast cells. Samples were collected and stored at –20°C for further analysis. The initial samples were treated with enzyme for complete hydrolysis of the starch to obtain the glucose numbers necessary for yield calculations. The average initial glucose concentration after complete hydrolysis for the whole corn batches was 211.4 g/L and for the degermed corn batches was 248 g/L.

Fermentations were run until glucose concentrations were <1 g/L or the glucose concentration stopped decreasing. On completion of the fermentations, the whole broth was dried at 50°C and a coffee grinder was used to homogenize the dried samples. Samples from each of the fermentations (10 total) were sent to a commercial laboratory (Servi-Tech, Hastings, NE) for analysis of standard nutritional parameters and minerals for cattle feed.

Analytical Procedures

In all experiments, amyloglucosidase (A-3042; Sigma, St. Louis, MO) was used to convert starch to glucose. A biochemistry analyzer (YSI model 2700; Yellow Springs, OH) was used to measure glucose concentrations. A five-point external calibration curve was used for dextrose (0.5–100 g/L). Starch was determined using a standard protocol from the National Renewable Energy Laboratory (NREL) (Golden, CO), NREL LAP-016, 1996. Ethanol was measured by high-perfromance liquid chromatography. This assay used a Waters 600 Multisolvent Delivery System with a Waters 410 Differential Refractometer detector and an internal detector temperature of 35°C. The separation was performed on an Aminex HPX-87H column with a Cation H guard column maintained between 45 and 55°C using a Waters Column Heater Module with a mobile phase of 0.021 *N* H_2SO_4 and a flow rate of 0.5 mL/min. The mobile phase was prepared using 18.2 Mohm deionized water obtained from a Milli-Q system, and all samples were filtered through a 0.45-mm filter prior to injection using an Alcott 728 autosampler. Data werecollected by a TurboChrome 4 data acquisition package using a PE Nelson 900 series Interface. A five-point external calibration curve was used for ethanol (0.25–100 g/L).

Results

The fermentation profile shown in Fig. 1 is the average of five fermentations of whole corn and five fermentations with G/F minus corn.

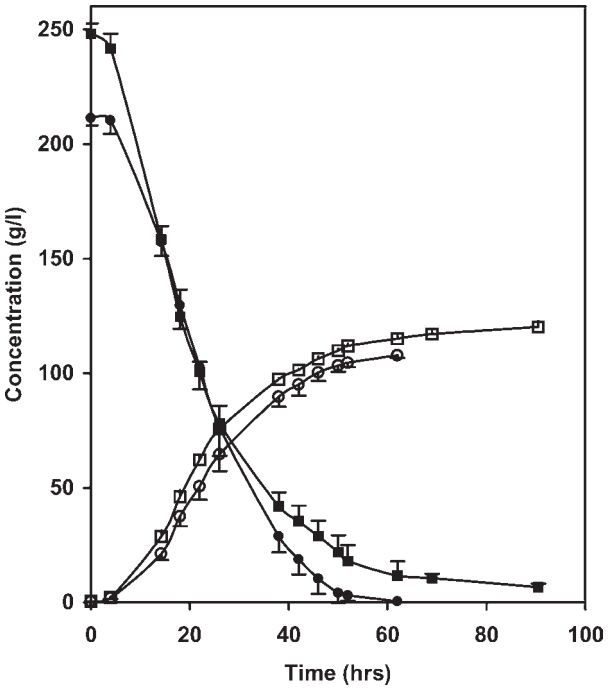

Fig. 1. Comparison of ethanol production from whole corn and G/F minus corn. (●) Whole-corn dextrose; (■) G/F minus corn dextrose; (○) whole-corn ethanol; (□) G/F minus corn ethanol.

The average ethanol concentration derived from whole corn fermentations was 106.8 g/L. The average ethanol concentration from G/F minus corn was 118.7 g/L, an 11% increase. While the whole-corn fermentations finished (residual glucose of <1 g/L), the G/F minus corn fermentations did not finish (residual glucose average of 6 g/L). The best G/F minus corn fermentation reached a peak ethanol production of 123.2 g/L with a residual glucose of 4.9 g/L. It is expected that yeast strains more tolerant to high-density fermentations could achieve ethanol concentrations of approx 125 g/L.

Table 1 shows the nutritional and mineral analysis of distiller's dried grains and solubles (DDs) from both whole-corn and G/F minus corn fermentations. Most significant are a 23% increase in protein concentration, a 58.5% decrease in neutral detergent fiber, a 45.5% decrease in fat, overall increases in net energy, and a 60.7% decrease in phosphorus.

Discussion

As the data have shown, the removal of the germ and fiber does allow higher starch loading, which results in an increase in ethanol production.

Table 1
Analysis of DDGs from Whole Corn and G/F Minus Corn

Parameter	G/F minus corn	Whole corn
Crude protein (%)	36.7 ± 4.50	29.8 ± 1.00
Neutral detergent fiber (%)	13.74 ± 1.57	33.14 ± 5.05
TDN[1] (%)	83.7 ± 2.20	78.3 ± 1.90
Net energy, main. (Mcal/lb)	0.97 ± 0.03	0.90 ± 0.02
Net energy, gain (Mcal/lb)	0.65 ± 0.03	0.58 ± 0.02
Phosphorus (%P)	0.33 ± 0.04	0.84 ± 0.04
Fat (% by acid hydrolysis)	9.63 ± 0.75	17.68 ± 1.63
Swine D.E. (Mcal/lb)	1.46 ± 0.08	1.27 ± 0.07
Swine M.E. (Mcal/lb)	1.29 ± 0.07	1.15 ± 0.06

This type of fermentation is generally limited by high suspended solids; however, removal of the germ results in lower suspended solids *(3)*. Taylor and colleages *(3,4)* also predicted that combining germ removal with continuous high-gravity fermentation with stripping could further improve economics. The estimated savings by combining continuous high-density fermentation with stripping with germ removal is approx 6–10 ¢/gal of ethanol *(3)*. Complete removal of the fiber could enhance the cost savings even further. Corn fiber oil contains phytosterols and other compounds shown to reduce cholesterol levels *(5,6)*. Extraction of this oil from corn fiber could offer a high-value coproduct that would result in even greater cost savings for an ethanol production facility.

The removal of the germ and fiber prior to fermentation results in significant changes to the DDGs produced during fermentation. Protein and digestible nutrients are increased while fat and fiber are reduced, although the increase in digestible nutrients and net energy could be attributed to residual glucose in the fermentation broth. A robust yeast strain capable of tolerating higher ethanol concentrations will be necessary to fully utilize the glucose in a high-density fermentation. The 60% reduction in phosphorus is significant in light of more stringent regulation of phosphate wastes in the livestock industry. The increased protein, lower fat and fiber, as well as the reduction in phosphate may offer a more valuable livestock feed.

In summary, removal of germ and fiber prior to fermentation allows higher starch loading and results in increased ethanol production. The integration of germ and fiber removal in the dry-grind ethanol industry could increase capacity and add valuable coproducts, resulting in increased productivity and profits. A more complete economic study of integrating germ and fiber removal into a dry mill ethanol plant is needed to determine the feasibility of such a strategy.

Acknowledgments

We wish to thank Heartland Grain Fuels, LLP and the Illinois Corn Marketing Board for supplying materials. This work was supported by US Department of Energy (DOE) Cooperative Agreement No. DE-FC36-02G012001 (DOE support does not constitute an endorsement by DOE of the views expressed in this article).

References

1. Wahjudi, J., Xu, Li., Wang, P., Singh, V., Buriak, P., Rausch, K. D., McAloon, A. J., Tumbleson, M. E., and Eckhoff, S. R. (2000), *Cereal Chem.* **77(5),** 640–644.
2. Singh, V. and Eckhoff, S. R. (1997), *Cereal Chem.* **74,** 462–466.
3. Taylor, F., Mcaloon, A. J., Craig, Jr., J. C., Yang, P., Wahjudi, J., and Eckhoff S. R. (2001), *Appl. Biochem. Biotechnol.* **94,** 41–49.
4. Taylor, F., Kurantz, M. J., Goldberg, N., McAloon, A. J., and Craig, Jr., J. C. (2000), *Biotechnol. Prog.* **16(4),** 541–547.
5. Moreau, R. A., Powell, M. J., and Hicks, K. B. (1996), *J. Agric. Food Chem.* **44(8),** 2149–2154.
6. Wilson, T. A., DeSimone, A. P., Romano, C. A., and Nicolosi, R. J. (2000), *J. Nutri. Biochem.* **11(9),** 443–449.

0273-2289/04/115/0843–0855/$25.00

Production of Fumaric Acid Using Rice Bran and Subsequent Conversion to Succinic Acid Through a Two-Step Process

Se-Kwon Moon, Young-Jung Wee, Jong-Sun Yun, and Hwa-Won Ryu*

School of Biological Sciences and Technology, Institute of Bioindustrial Technology, Chonnam National University, Gwangju 500-757, Korea, E-mail: hwryu@jnu.ac.kr

Abstract

The fungal production of fumaric acid using rice bran and subsequent bacterial conversion of succinic acid using fungal culture broth were investigated. Since the rice bran contains abundant proteins, amino acids, vitamins, and minerals, it is suitable material that fungi use as a nitrogen source. The effective concentration of rice bran to produce fumaric acid was 5 g/L. A large amount of rice bran caused excessive fungal growth rather than enhance fumaric acid production. In addition, we could produce fumaric acid without the addition of zinc and iron. Fungal culture broth containing approx 25 g/L of fumaric acid was directly employed for succinic acid conversion. The amount of glycerol and yeast extract required for succinic acid conversion was reduced to 70 and 30%, respectively, compared with the amounts cited in previous studies.

Index Entry: Fumaric acid; succinic acid; two-step process; fungal culture broth; rice bran.

Introduction

Succinic acid is a dicarboxylic acid produced as an intermediate of the tricarboxylic acid cycle and also as one of the fermentation products of anaerobic metabolism. It has been considered an important chemical because it can be used for the precursor of 1,4-butanediol, tetrahydrofuran, and γ-butyrolactone as well as for application in polymers, foods, pharmaceuticals, and cosmetics *(1,2)*. Currently, succinic acid is produced commercially through chemical synthesis. However, the production of

*Author to whom all correspondence and reprint requests should be addressed.

succinic acid by biological processes has recently been the focus of attention as an alternative chemical feedstock.

For the biological production of succinic acid, various studies, such as those on bioconversion of fumaric acid to succinic acid *(3–6)* and production from carbohydrate *(7–10)*, have been conducted. Although succinic acid was largely produced by anaerobic bacteria, succinic acid yield was low. In addition, there are some problems with succinic acid fermentation, such as the requirement of high-purity CO_2 gas because the related microorganism is a strict anaerobe, byproduct (acetic acid) formation, and product inhibition *(7,8)*. Although some investigations of the conversion of fumaric acid into succinic acid have been reported *(3–6)*, succinic acid production from fungal culture broth containing fumaric acid has rarely been reported so far.

In the present study, we evaluated a two-step process for succinic acid production. The first process was fumaric acid production by *Rhizopus* sp. using rice bran, and the second process was succinic acid production by *Enterococcus faecalis* RKY1 *(5–7)* using fungal culture broth obtained in the first process. We investigated the effects of rice bran on fumaric acid production and optimized the culture medium for fumaric acid fermentation. Furthermore, we optimized the culture conditions for succinic acid conversion from fumaric acid produced by the first process.

Materials and Methods

Microorganisms and Inocula

Rhizopus sp., a newly isolated fungus from brown rice, was used for producing fumaric acid. It was cultivated and maintained on potato dextrose agar slants. Spores from a 5-d-old slant at 35°C were suspended in sterile water. This spore suspension (approx 8×10^5 spores/mL) was inoculated into fermentation medium at a level of 0.3% (v/v).

E. faecalis RKY1 was used for converting the aforementioned fungal culture broth into succinic acid. Stock cultures were stored in the culture medium with 50% (v/v) glycerol at –20°C. The growth medium consisted of 10 g/L of glycerol, 20 g/L of fumaric acid, 18 g/L of Na_2CO_3, 15 g/L of yeast extract, and 5 g/L of K_2HPO_4. To prepare the inoculum, 1 mL of the glycerol stock culture was transferred into a 20-mL vial containing 15 mL of growth medium and cultivated at 38°C, 200 rpm for 6 h.

Production of Fumaric Acid

To optimize the culture medium for fumaric acid production, we investigated the effects of rice bran concentrations and various carbon sources. When rice bran was used as a nitrogen source, the effects of additional elements (phosphate, magnesium, zinc, and iron) on fumaric acid production were also investigated. The medium previously reported by Zhou et al. *(11)* was used as the basal medium. Fermentations were performed in 250-mL Erlenmeyer flasks containing 100 mL of medium.

Fumaric acid for succinic acid conversion was prepared using a 2.5-L jar fermentor (KF-2.5L; Korea Fermentor, Incheon, Korea). The pH was adjusted to 4.5 with $CaCO_3$ or 5 *N* Na_2CO_3.

Succinic Acid Conversion

The fungal culture broth containing fumaric acid was used as the medium for succinic acid conversion. Prior to the use of fungal culture broth, the fungi were removed by filtration through Whatman No. 1 filter paper, and then the pH of the broth was adjusted to 7.0. Glycerol, nitrogen source, and phosphate were aseptically added to pretreated fungal culture broth. We investigated the effects of added glycerol concentrations as hydrogen donor and corn steep liquor (CSL) concentrations as nitrogen source. Furthermore, we investigated the inhibition of gradually concentrated fungal culture broth on succinic acid conversion. To study the inhibition of fungal culture broth on succinic acid conversion, we concentrated fungal culture broth with a rotary vacuum evaporator (N-1NW; Eyela, Kyoto, Japan) at 70°C. Two, three, and four times concentrated broth were tested.

Analytical Methods

Glucose concentration was measured bya glucose oxidase–peroxidase method using a glucose E-kit (Young-Dong Pharmaceuticals, Seoul, Korea). Cell growth was measured as optical density at 660 nm (OD_{660}) with an ultraviolet (UV) spectrophotometer (UV-160A; Shimadzu, Tokyo, Japan). Dry cell weight was determined using precalculated standard curves by substituting OD_{660} values.

Succinic acid and fumaric acid concentrations were quantified using a high-performance liquid chromatography (Waters, Milford, MA) with an Aminex HPX-87H ion exclusion column (Bio-Rad, Hercules, CA) and a UV detector set at 210 and 260 nm, respectively. The mobile phase was 0.008 *N* H_2SO_4 at a flow rate of 0.6 mL/min. The temperature of the column was maintained at 38°C.

Results and Discussion

Production of Fumaric Acid

To investigate the effects of rice bran concentrations on fumaric acid production, various concentrations of rice bran ranging from 0 to 6 g/L were added to the medium. As shown in Fig. 1, the amount of glucose consumed was almost proportional to the rice bran concentration in the range of the experiment. When 6 g/L of rice bran was added, glucose was completely metabolized. Thus, it seemed that 1 g of rice bran was necessary to convert 9 g of glucose to fumaric acid. When a rice bran concentration above 6 g/L was used, fungal growth was predominant but an increase in fumaric acid production was not observed (data not shown). Since the culture pH dropped as fumaric acid was produced, it was necessary to add

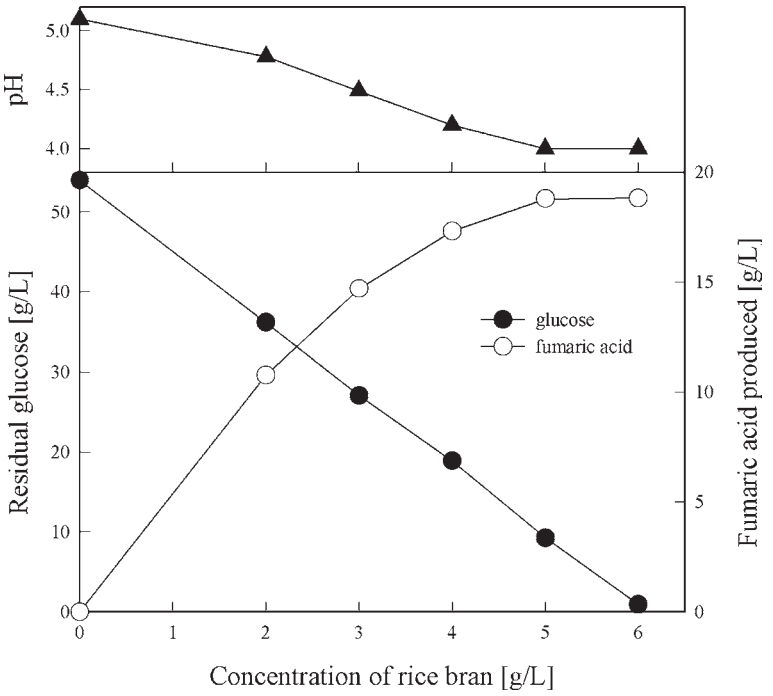

Fig. 1. Effect of rice bran concentration on fumaric acid production. The culture conditions were as follows: 250-mL flask containing 100 mL of medium at 35°C, 200 rpm for 4 d; 50 g/L of initial glucose; 15 g/L of $CaCO_3$; 0.6 g/L of KH_2PO_4; 0.5 g/L of $MgSO_4 \cdot 7H_2O$; 0.0179 g/L of $ZnSO_4 \cdot 7H_2O$; 0.498 mg/L of $FeSO_4 \cdot 7H_2O$.

more $CaCO_3$ to control the culture pH as a neutralizing agent. However, the amount of $CaCo_3$ did not influence fumaric acid production. Therefore, the optimal rice bran concentration for fumaric acid production was found to be 5 g/L.

To determine the optimal carbon source and its concentration on fumaric acid production, various carbon sources and their concentrations for fumaric acid production were examined. Figure 2 shows that *Rhizopus* sp. could metabolize glucose, fructose, maltose, and starch into fumaric acid. In view of industrial utilization, starch and rice bran might be used for economical carbon and nitrogen sources in the production of fumaric acid. Figure 3 shows that fumaric acid production was severely inhibited by the addition of high glucose concentration. Consequently, the optimum carbon source was found to be glucose, and maximum fumaric acid was obtained at 50 g/L of glucose.

Because rice bran contains various minerals, the effect of trace elements on fumaric acid production was investigated. Since the basal medium contained 0.6 g/L of KH_2PO_4, 0.5 g/L of $MgSO_4 \cdot 7H_2O$, 0.0179 g/L of $ZnSO_4 \cdot 7H_2O$, and 0.498 mg/L of $FeSO_4 \cdot 7H_2O$, 16 trials were carried out to determine the effect of four minerals; the results are shown in Table 1.

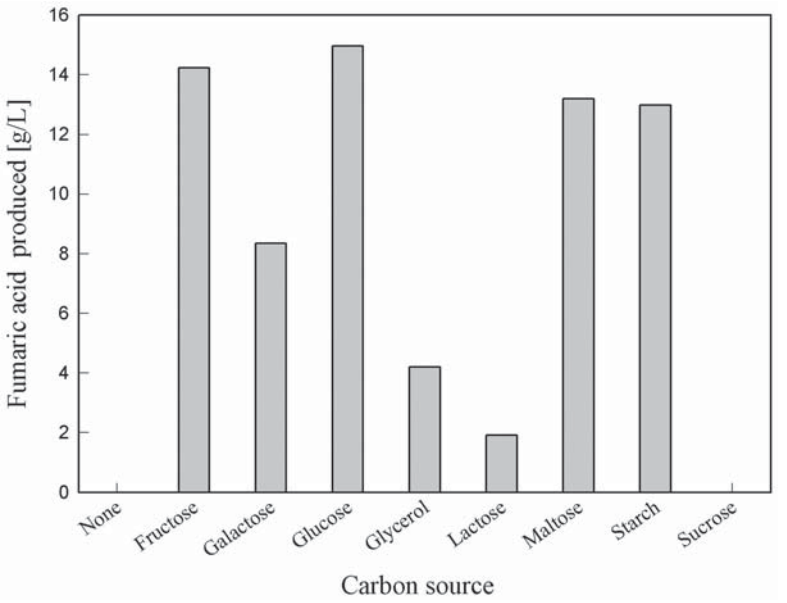

Fig. 2. Effect of different carbon sources on fumaric acid production. The culture conditions were as follows: 250-mL flask containing 100 mL of medium at 35°C, 200 rpm for 3 d; 50 g/L of initial carbon source; 5 g/L of rice bran; 15 g/L of $CaCO_3$; 0.6 g/L of KH_2PO_4; 0.5 g/L of $MgSO_4 \cdot 7H_2O$; 0.0179 g/L of $ZnSO_4 \cdot 7H_2O$; 0.498 mg/L of $FeSO_4 \cdot 7H_2O$.

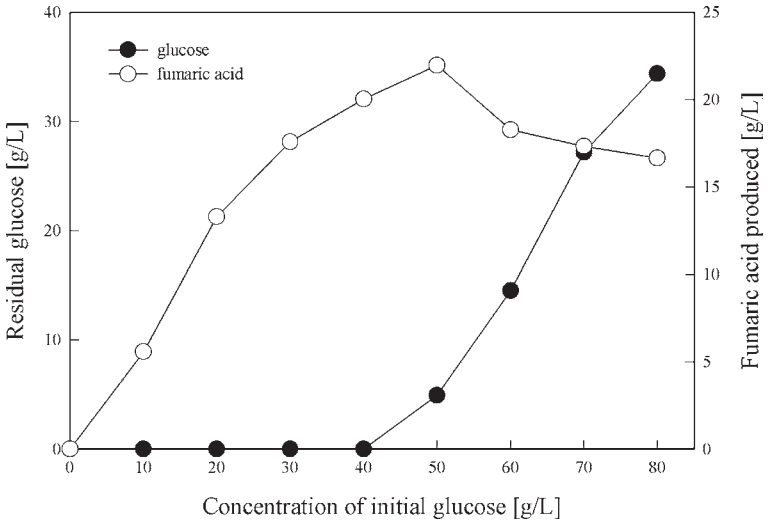

Fig. 3. Effect of initial glucose concentration on fumaric acid production. The culture conditions were as follows: 250-mL flask containing 100 mL of medium at 35°C, 200 rpm for 5 d; 5 g/L of rice bran; 15 g/L of $CaCO_3$; 0.6 g/L of KH_2PO_4; 0.5 g/L of $MgSO_4 \cdot 7H_2O$; 0.0179 g/L of $ZnSO_4 \cdot 7H_2O$; 0.498 mg/L of $FeSO_4 \cdot 7H_2O$.

Table 1
Effect of Phosphate, Magnesium, Zinc, and Iron on Fumaric Acid Production Using Rice Bran[a]

Trial	KH_2PO_4 (0.6 g/L)	$MgSO_4 \cdot 7H_2O$ (0.5 g/L)	$ZnSO_4 \cdot 7H_2O$ (0.0179 g/L)	$FeSO_4 \cdot 7H_2O$ (0.498 mg/L)	Residual glucose (g/L)	Fumaric acid produced (g/L)
1	○	○	○	○	1.19	22.49
2	○	○	○	×	2.09	22.72
3	○	○	×	○	3.56	21.69
4	○	×	○	○	2.35	21.76
5	×	○	○	○	6.45	7.78
6	○	○	×	×	2.67	22.71
7	○	×	○	×	1.51	22.30
8	○	×	×	○	5.85	21.33
9	×	○	○	×	10.16	8.28
10	×	○	×	○	5.80	6.65
11	×	×	○	○	6.64	9.49
12	○	×	×	×	6.02	19.84
13	×	○	×	×	5.42	7.77
14	×	×	○	×	12.66	8.21
15	×	×	×	○	16.44	6.34
16	×	×	×	×	12.47	8.58

[a]Culture conditions: 250-mL flask containing 100 mL of medium at 35°C, 200 rpm for 5 d; 50 g/L of initial glucose; 5 g/L of rice bran; 15 g/L of $CaCO_3$. ○, added ; ×, not added.

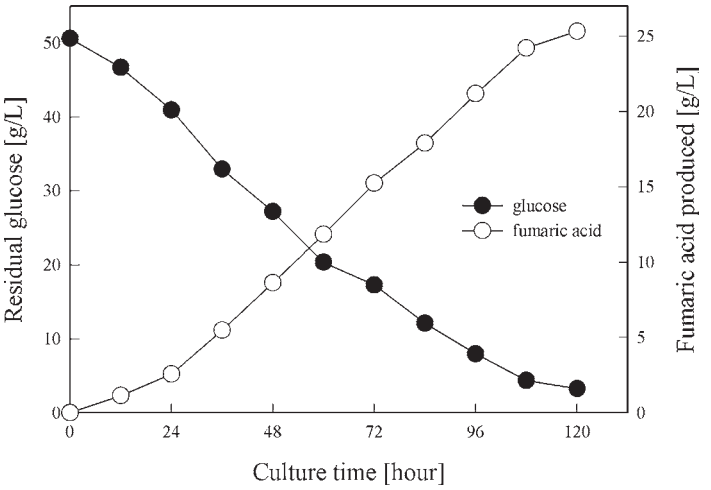

Fig. 4. Typical time course of fumaric acid production in fermentor by *Rhizopus* sp. The culture conditions were as follows: 2.5-L jar fermentor containinga 1-L working volume at 35°C, 200 rpm, 1 vvm, pH 4.5 adjusted with 5 *N* Na_2CO_3; 50 g/L of glucose; 5 g/L of rice bran; 1 g/L of KH_2PO_4; 0.5 g/L of $MgSO_4 \cdot 7H_2O$.

With the use of rice bran as a nitrogen source, we studied the effect of phosphate, magnesium, zinc, and iron on fumaric acid production. Although magnesium, zinc, and iron did not cause any effect (Mg^{2+}; trials 1 and 4, Zn^{2+}; trials 1 and 3, Fe^{2+}; trials 1 and 2), phosphate was crucial to fumaric acid production (trials 12 and 16).

Batch fermentations were carried out using rice bran and glucose as nitrogen and carbon sources, respectively. Figure 4 shows the profile of fumaric acid production in a 2.5-L jar fermentor. The fumaric acid concentration reached 25.3 g/L. The yield (fumaric acid produced/glucose consumed) and the productivity were 52% and 0.21 g/(L·h), respectively. For the following experiment, the fungal culture broth was used as a medium for the bioconversion of fumaric acid into succinic acid.

Bioconversion of Fumaric Acid into Succinic Acid

For the bioconversion experiments, we directly employed fungal culture broth containing fumaric acid as a basal medium. We optimized the culture medium for the production of succinic acid. Figure 5 represents the effects of glycerol on succinic acid production, fumaric acid consumption, and cell growth. When glycerol was not added to the culture medium, only 17 g/L the succinic acid was produced from the fungal culture broth. The quantity of glycerol added in the culture medium could be reduced to 70% compared with that of previous studies *(4–6)*. This result may imply that other hydrogen donors exist in fungal culture broth derived from fumaric acid fermentation.

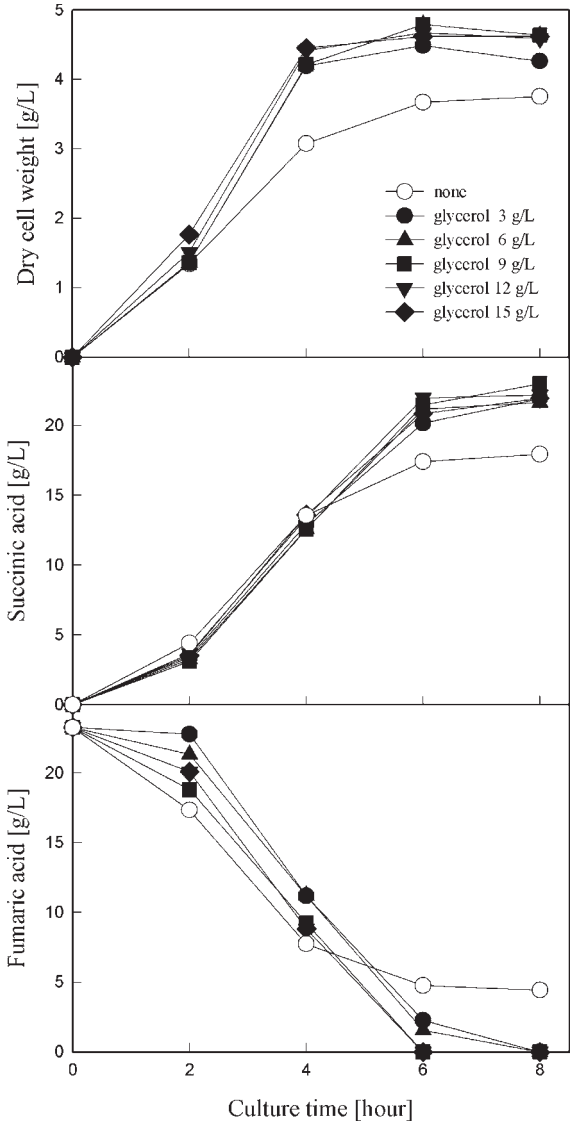

Fig. 5. Effect of glycerol concentration on succinic acid production, fumaric acid consumption, and cell growth. The culture conditions were as follows: 50-mL vial (40 mL of medium); 15 g/L of yeast extract; 5 g/L of K_2HPO_4; initial pH of 7.0.

To investigate the effect of yeast extract concentrations on succinic acid production, fumaric acid consumption, and cell growth, *E. faecalis* RKY1 was grown on culture medium containing from 0 to 20 g/L of yeast extract. As shown in Fig. 6, cell growth increased with increasing yeast extract. Succinic acid production and fumaric acid consumption were also enhanced by an increase in yeast extract up to 10 g/L, but they were not

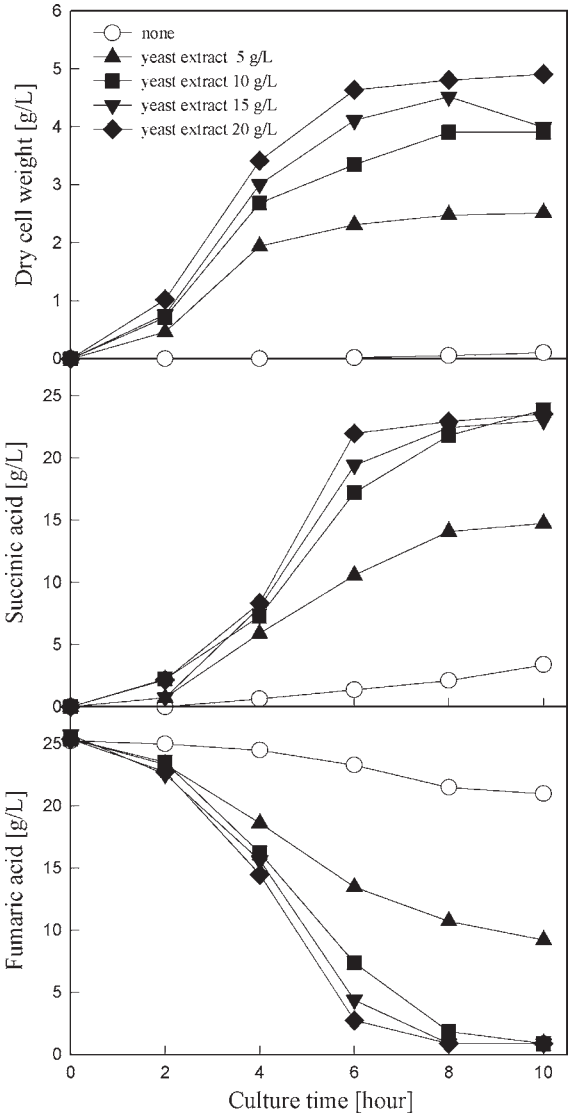

Fig. 6. Effect of yeast extract concentration on succinic acid production, fumaric acid consumption, and cell growth. The culture conditions were as follows: 50-mL vial (40 mL of medium); 3 g/L of glycerol; 5 g/L of K_2HPO_4; initial pH of 7.0.

significantly affected by yeast extract beyond 10 g/L. The amount of yeast extract could be reduced to approx 30% of that of previous reports *(4–6)* by using fungal culture broth. In this experiment, we could efficiently produce succinic acid from fungal culture broth containing approx 25 g/L of fumaric acid through the novel two-step bioconversion process. The maximum bioconversion yield and productivity were 97% and 2.4 g/(L·h), respectively.

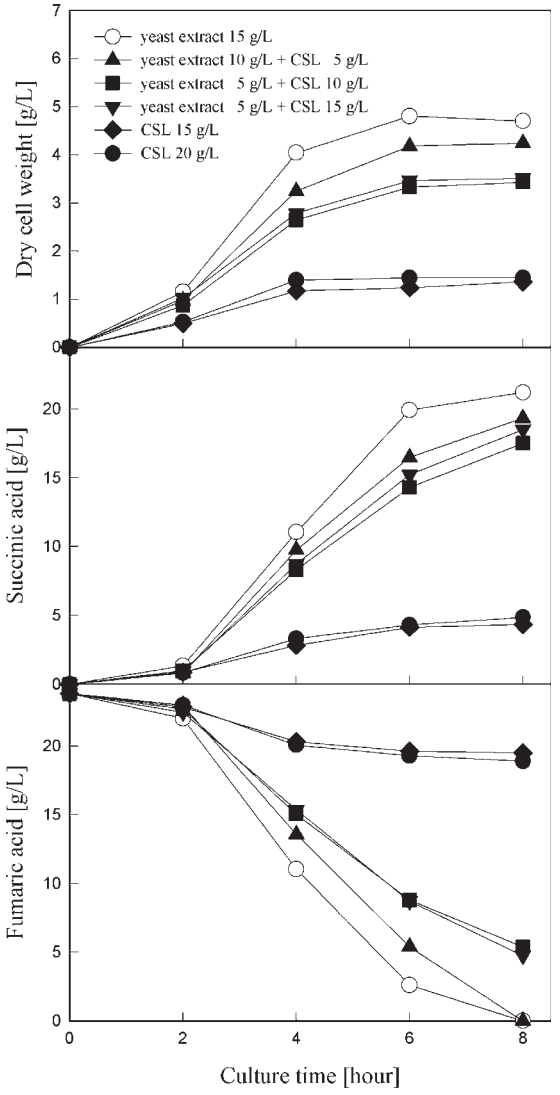

Fig. 7. Effect of addition of CSL on succinic acid production, fumaric acid consumption, and cell growth. The culture conditions were as follows: 50-mL vial (40 mL of medium); 3 g/L of glycerol; 5 g/L of K_2HPO_4; initial pH of 7.0.

Because yeast extract is very expensive, we studied the effect of CSL supplement in order to reduce the amount of yeast extract. CSL has been the focus of attention as an alternative nitrogen source *(8,12)*. As shown in Fig. 7, the bacterial conversion was very poor when only CSL was used as a nitrogen source. Even if yeast extract had a significant effect on cell growth, when 5 g/L of yeast extract and 15 g/L of CSL were used as nitrogen sources, a bioconversion yield and productivity of 95% and 2.2 g/(L·h), respectively, could be obtained.

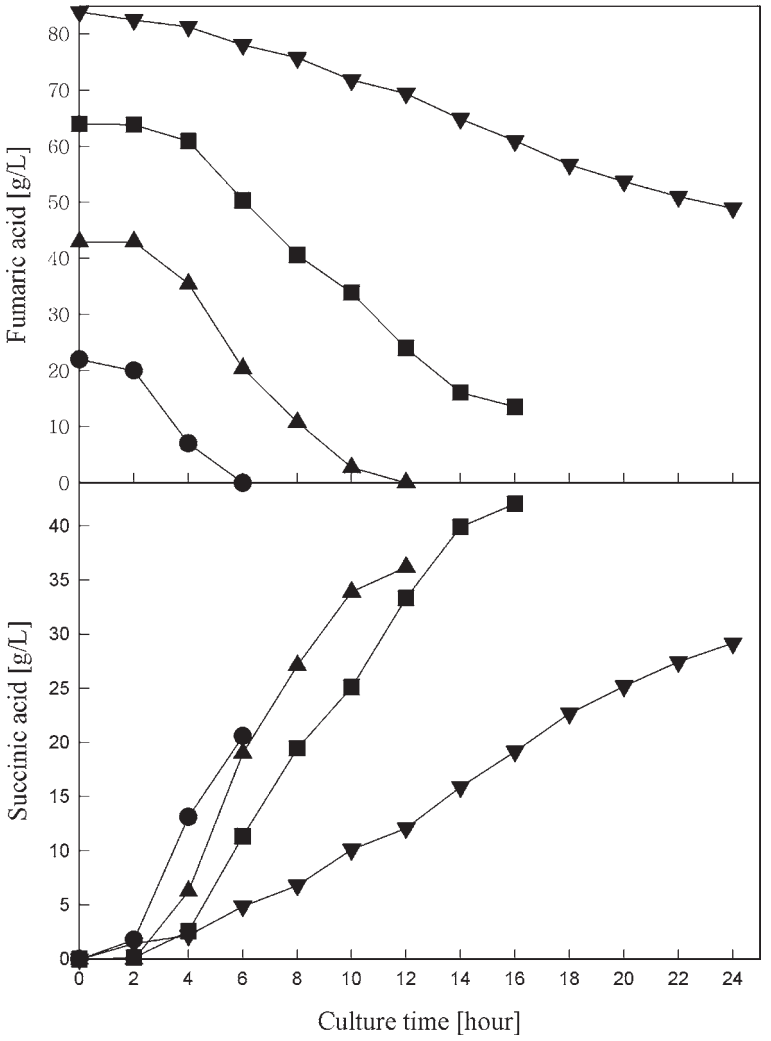

Fig. 8. Effect of broth concentration on succinic acid production and fumaric acid consumption. The culture conditions were as follows: 50-mL vial (40 mL of medium); 15 g/L of yeast extra; 5 g/L of K_2HPO_4; initial pH of 7.0. (–●–), Original broth; (–▲–), two-fold concentrated broth; (–■–), three-fold concentrated broth; (–▼–), four-fold concentrated broth.

Finally, we investigated the inhibition of concentrated fungal culture broth on succinic acid production and fumaric acid consumption. As shown in Fig. 8, we found that concentrated fungal culture broth slightly inhibited the bacterial conversion. Succinic acid could be efficiently produced from fungal culture broth until it was concentrated to three-fold (64 g/L of fumaric acid). However, the conversion time needed was severely prolonged when it was concentrated to more than four-fold (84 g/L of fumaric acid). Since *E. faecalis* RKY1 could efficiently convert fumaric acid

(to 100 g/L) into succinic acid *(5–6)*, the succinic acid conversion by concentrated fungal broth was not inhibited because the fumaric acid in the fungal culture broth was concentrated, but because other components in the broth were concentrated. Further investigations should be focused on the identification of inhibiting compounds in the fungal culture broth.

Conclusions

A novel two-step process was developed to produce fumaric acid using *Rhizopus* sp. and subsequently to convert the fungal culture broth containing fumaric acid into succinic acid using *E. faecalis* RKY1. Rice bran is a byproduct of the rice-milling process, however, the interest in rice bran has been focused on various fields of microbial propagation and enzyme and ethanol production because it contains various nutrients *(13–15)*. Therefore, rice bran was used as an additive to produce fumaric acid. First, we produced fumaric acid using rice bran and glucose. Fumaric acid was efficiently produced when 5 g/L of rice bran and 50 g/L of initial glucose were used as nitrogen and carbon sources, respectively, without the addition of zinc and iron. For the bioconversion of fumaric acid into succinic acid, the fungal culture broth was directly employed. Fumaric acid in fungal culture broth was efficiently converted into succinic acid with the addition of only 3 g/L of glycerol, 5 g/L of yeast extract, and 15 g/L of CSL. The bioconversion yield and productivity from fumaric acid to succinic acid were 95% and 2.2 g/(L·h), respectively. Our results suggest that this novel two-step process allows the respective production capacity to be controlled according to the commercial demand of fumaric acid and succinic acid.

Acknowledgment

This work was financially supported by grant no. R05-2000-000-00175-0 from the Korea Science & Engineering Foundation.

References

1. Datta, R. (1992), US patent no. 5,143,833.
2. Zeikus, J. G., Jain, M. K., and Elankovan, P. (1999), *Appl. Microbiol. Biotechnol.* **51,** 545–552.
3. Wang, X., Gong, C. S., and Tsao, G. T. (1998), *Appl. Biochem. Biotechnol*. **70–72,** 919–928.
4. Kang, K. H., Yun, J. S., and Ryu, H. W. (2000), *J. Microbiol. Biotechnol*. **10(1),** 1–7.
5. Ryu, H. W. and Wee, Y. J. (2001), *Appl. Biochem. Biotechnol*. **91–93,** 525–535.
6. Wee, Y. J., Yun, J. S., Kang, K. H., and Ryu, H. W. (2002), *Appl. Biochem. Biotechnol*. **98–100,** 1093–1104.
7. Lee, P. C., Lee, W. G., Kwon, S., Lee, S. Y., and Chang, H. N. (2000), *Appl. Microbiol. Biotechnol*. **54,** 23–27.
8. Lee, P. C., Lee, S. Y., Hong, S. H., Chang, H. N., and Park, S. C. (2003), *Biotechnol. Lett*. **25,** 111–114.
9. Chatterjee, R., Millard, C. S., Champio, K., Clark, D. P., and Donnelly, M. I. (2001), *Appl. Environ. Microb.* **67(1),** 148–154.
10. Vemuri, G. N., Eiteman, M. A., and Altman, E. (2002), *J. Ind. Microbiol. Biotechnol*. **28,** 325–332.

11. Zhou, Y., Du, J., and Tsao, G. T. (2000), *Appl. Biochem. Biotechnol*. **84–86,** 779–789.
12. Kim, J. S., Kim, H., Oh, K. K., and Kim, Y. S. (2001), *J. Ind. Eng. Chem*. **8,** 519–523.
13. Pessoa, A., Mancilha, I. M., and Sato, S. (1997), *J. Ind. Microbiol. Biotechnol*. **18,** 360–363.
14. Popanich, S., Klomsiri, C., and Dharmsthiti, S. (2003), *Bioresour. Technol*. **87,** 295–298.
15. Lima, K. G., Takahashi, C. M., and Alterthum, F. (2002), *J. Ind. Microbiol. Biotechnol*. **29,** 124–128.

0273-2289/04/115/0857–0869/$25.00

Catalytic Hydrogenation of Glutamic Acid

Johnathan E. Holladay,* Todd A. Werpy, and Danielle S. Muzatko

Pacific Northwest National Laboratory,
PO Box 999, MSIN: K2-12, 902 Battelle Boulevard,
Richland, WA 99352, E-mail: john.holladay@pnl.gov

Abstract

Technology to convert biomass into chemical building blocks provides an opportunity to displace fossil fuels and increase the economic viability of biorefineries. Coupling fermentation capability with aqueous-phase catalysis provides novel routes to monomers and chemicals, including those not accessible from petrochemical routes. Glutamic acid provides a platform to numerous compounds through thermochemical approaches including hydrogenation, cyclization, decarboxylation, and deamination. Hydrogenation of amino acids also provides access to chiral compounds with high enantiopurity. This article details aqueous-phase hydrogenation reactions that we have developed that lead to valuable chemical intermediates from glutamic acid. In addition, ^{13}C nuclear magnetic resonance and matrix-assisted laser desorption ionization mass spectral data are presented that provide a mechanistic picture of the reactions. The results show that hydrogenation of glutamic acid has unique characteristics from other amino acids and that paradigms in the literature do not hold up for this transformation.

Index Entries: Glutamic acid; catalytic hydrogenation; pyroglutaminol; pyroglutamic acid; phosphoric acid; prolinol.

Introduction

Aqueous-phase thermochemical catalysis offers an important and complementary role to biocatalysis for the conversion of biomass feedstocks into products. The diversity of products offered from catalysis, including the chemical building blocks for polymers, is of growing interest and particularly important for the economic sustainability of biorefineries. Starch/glucose derived from corn provides a significant opportunity to produce large-scale commodity chemicals without a significant impact on the food supply or on the infrastructure. Currently, the cost for carbon derived from corn is only about 10–15% higher than carbon derived from

*Author to whom all correspondence and reprint requests should be addressed.

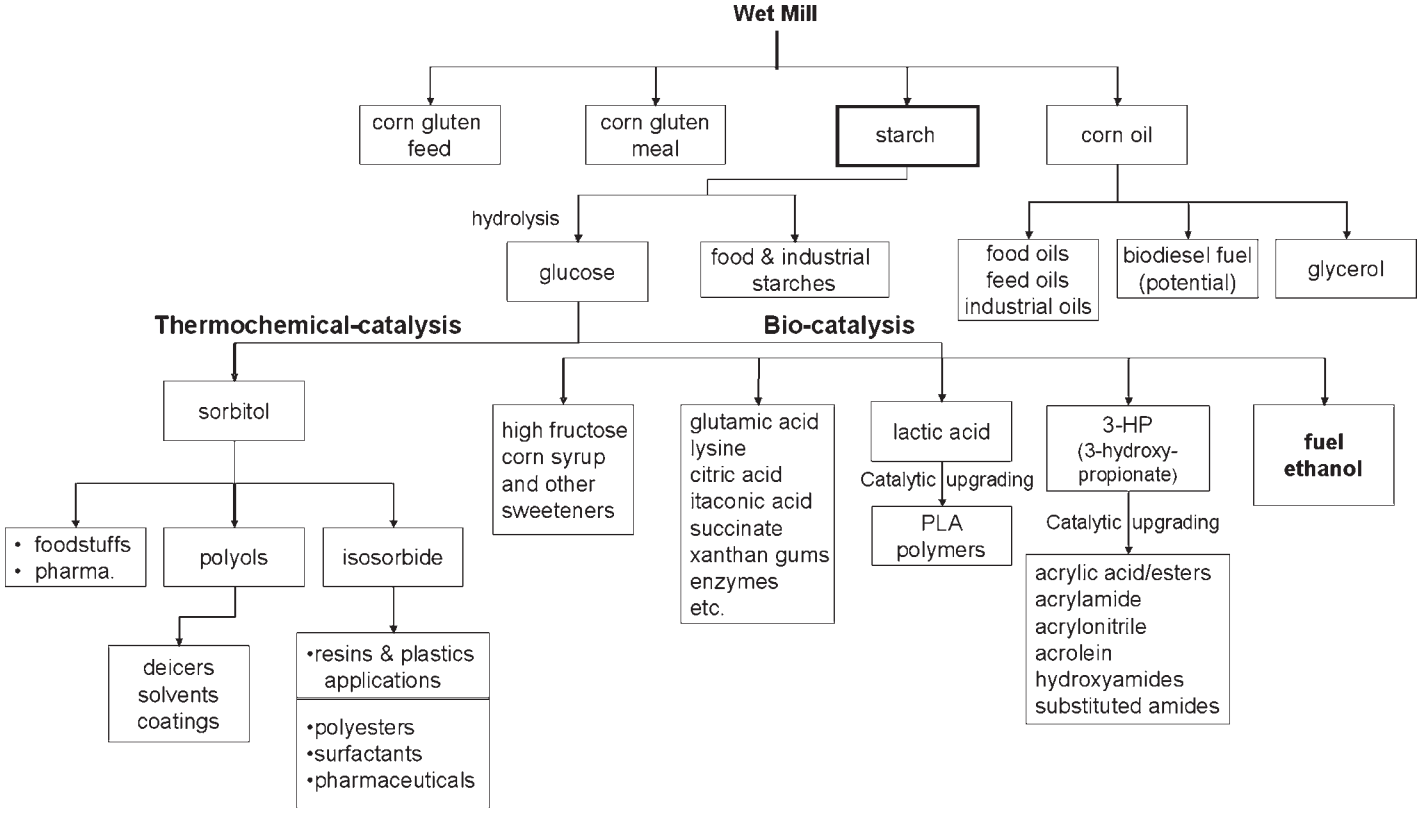

Fig. 1. Examples of products available from corn wet milling, one embodiment of a biorefinery.

Table 1
Chemical Building Blocks Derived from Crude Oil[a]

Carbon no.	Name	Example products
1	Methane	Methanol, methylene chloride, acetylene, cyanamide
2	Ethane/ethylene	Ethylene oxide, ethylene glycol, poly-ethylene
3	Propylene	Propylene oxide, propylene glycol, acrylonitrile
4	Butane	Maleic acid, THF, GBL, MTBE
5	N/A	N/A
6	Benzene/xylene	Styrene, adipic acid, phenol, acetone, toluene

[a] N/A, not available; THF, tetrahydrofuran; GBL, γ-butyrolactone; MTBE, methyl-t-butyl ether.

petrochemical sources. Coupled with low-temperature efficient processing, this makes chemicals derived from corn economically competitive with chemicals derived from nonrenewable petrochemical resources. Today glucose is converted into numerous compounds using fermentation, enzymatic catalysis, and thermochemical catalysis as depicted in a composite wet-mill operation shown in Fig. 1. Fermentation products can be further modified by catalysis to provide new polymers and monomers. The development of a diverse portfolio of products for economic sustainability is equally important to other biorefineries as it is for corn wet-milling operations.

The products developed by the petrochemical industry over the past 75 yr are based on feedstock supply and not necessarily the result of "products by design." The same opportunity exists for using a renewable feedstock. The petrochemical industry has several basic building blocks from which it derives products. Example building blocks from the refining of petroleum are presented in Table 1.

What is interesting, however, is some of the chemistry that is not present. For example, the petrochemical industry does not have a basic feedstock in the five-carbon area and thus we see few products derived from or based on five-carbon chemistry. Optical active compounds are also missing from the petrochemical-derived product list. For example, lactic acid is now made exclusively from glucose, with the reason being that the fermentation route provides stereochemical purity that is difficult to achieve from petrochemical building blocks.

The strategy for the development of products from biomass needs to be twofold. One approach is to identify those opportunities where we can compete economically with existing petrochemical products. Succinic acid–derived materials fit into this category (Fig. 1). The second approach must include the identification of products with novel functionality that cannot easily or cost effectively be derived from petrochemical building blocks. The challenge with developing new materials is that the market for these products must also be developed and the time and cost can be significant; however, the reward may also be substantial.

Amino acids, such as glutamic acid, derived from fermentation provide an excellent example of a "next-generation" platform intermediate beyond succinate. Recently, Ichimaru Pharcos announced the "volume production" of γ-polyglutamic acid for use in cosmetics, paints, water purification, and biodegradable plastics *([1])*. Aside from polyglutamic acid products, there are numerous monomeric intermediates that are possible to derive from glutamic acid. Such products offer unique functionality not provided by petrochemical intermediates including the five-carbon motif and chirality. In this article, we report our initial findings of the thermochemical conversion of glutamic acid into products and intermediates.

Background

Although catalytic hydrogenation has been part of the chemical landscape for many years, relatively little work has been directed toward the hydrogenation of amino acids *(2–7)* and even less directed toward the mechanism of hydrogenation *(8–9)*. On a practical level, the pioneering work of Adkin's group *(4)* in the 1930s and 1940s demonstrated that carboxylic acid esters can be converted into alcohols at mild temperatures (25–150°C) and high hydrogen pressures (>15 MPa). Important to this research group's work is the demonstration that carboxylic reduction can be done while maintaining a high degree of stereochemical purity. The catalyst systems of the day, nickel or copper and chromium oxides, worked well with esters but not with free acids. Development of ruthenium *(10)* and rhenium *(11)* catalysts in the 1950s solved this problem.

There has been a substantial body of work directed at hydrogenation of dicarboxylic acids *(12,13)*, particularly maleic and succinic acids *(14)*. An example is the development of 1,4-butanediol and tetrahydrofuran from butane-based maleic anhydride in the 1970s. The simple C_5 dicarboxylic acid, glutaric acid, and its alkyl esters have been the subject of numerous studies to produce 1,5-pentanediol as a product. Catalysts used include copper chromite *(15,16)*, palladium, and cobalt *(17)*. High selectivity (>95%) and high conversion (>98%) are achieved over the $CuCrO_x$ catalysts. Conversion over homogeneous ruthenium catalysts is also reported *(18,19)*. In general, achieving high selectivity to the diol product is easier with glutaric and adipic acids than with succinic acid, because of the thermodynamic favorability of succinic acid cyclization during reaction, which detracts from the formation of linear diol.

Direct hydrogenation of amino acids to amino alcohols was first examined by Bowden and Adkins *(4)* via the esters and recently was studied by Antons and colleagues *(5–7)* in a series of patents. Using Ru/C catalysts at high pressures (>14 MPa) and mild temperatures (70–150°C), Antons and colleagues demonstrated the conversion of carboxylic acids and amino acids with retention of optical activity in the product alcohols. High yields (>80%) and high enantiomeric purity (>97% in many cases) were achieved. In an earlier study, Broadbent et al. *(11)* demonstrated that under certain conditions hydrogenation of amino acids can be accompanied by deamination.

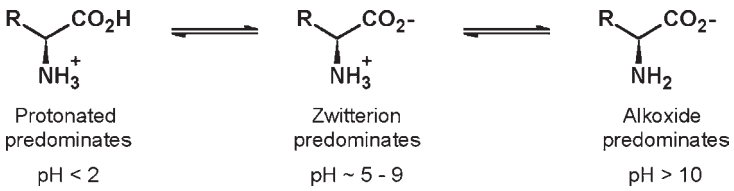

Scheme 1. Acidic, neutral, and basic forms of amino acids.

When we first considered glutamic acid, a search of the literature revealed no studies expressly directed at hydrogenating glutamic acid to a specific product. Indeed, the major role that glutamic acid plays in hydrogenation reactions is to act as an enantioselectivity enhancer *(20,21)*. Glutamic acid (or a number of other optically active amino acids) is added to solutions containing Raney nickel, supported nickel, palladium, or ruthenium catalysts and forms stereoselective complexes on the catalyst surface, leading to enantioselective hydrogenation of ketogroups to optically active alcohols. Under the reaction conditions used, no hydrogenation of glutamic acid takes place.

Since the inception of our work, Jere et al. *(22)* have published kinetic and stereochemical data on the hydrogenation of alanine. Important in their analysis is the observation that the amino acid must be in the protonated form to undergo facile hydrogenation. Since amino acids exist in their zwitterionic form, control of pH is important (*see* Scheme 1). A full equivalent of phosphoric acid was required to obtain high yields. Lower amounts resulted in a significant drop in yield since the product formed is basic.

Jere et al. *(22)* also reported the stereoretentive C-H bond activation in aqueous-phase catalytic hydrogenation of alanine. They demonstrated that hydrogenation of the carboxylic functionality is a stereoretentive process. Racemization occurs through a distinct process.

Also since the inception of our work, Antons at al. *(23)* reported the reduction of several amino acids including glutamic acid and pyroglutamic acid. Their study employed extremely high catalyst loadings of unsupported ruthenium and rhenium. The resultant products, glutaminol from glutamic acid and pyroglutaminol from pyroglutamic acid, were achieved in fair yields (58–65%) with high enantiomeric excess—i.e. high optical purity (*see* Fig. 2). However, the work clearly shows the need for catalyst improvement and leaves open the opportunity to identify other novel products. With these results in mind, we can now turn to our own work.

Materials and Methods

Glutamic acid, monosodium glutamate, pyroglutamic acid, and pyroglutaminol were purchased from commercial venders. Hydrogenation reactions were done using a 300-mL Parr autoclave using a continuous hydrogen gas feed at the pressure and temperature indicated. Reactant solutions contained 0.22 M substrate and 0–0.29 *M* phosphoric acid in deion-

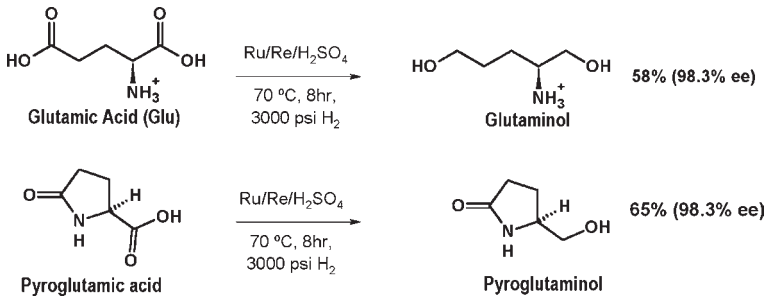

Fig. 2. Hydrogenation of glutamic acid and pyroglutamic acid (US patent no. 6,310,254; *see* ref. *23*).

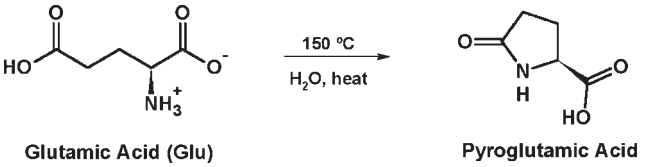

Scheme 2. Glutamic acid.

ized water. The catalysts used were various precious metals on carbon supports as provided by Engelhard (Iselin, NJ), Degussa (Calvert City, KY), or prepared in house and generally added at 1% loading. Analysis was done on either a Waters high-performance liquid chromatograph (HPLC) with RID detector or an Agilent HPLC using ultraviolet detection with various columns. Nuclear magnetic resonance (NMR) spectra were taken on a VXR-300 MHz spectrometer. Matrix-assisted laser description ionization (MALDI) mass spectral data were obtained on a Perceptive Biosystems MALDI mass spectrometer.

Results

Early in our work, we discovered that at elevated temperatures glutamic acid has a strong propensity to cyclize, even under dilute neutral or acidic aqueous media (*see* Scheme 2). The reaction is thermal and does not require a catalyst. However, the cyclization rate appears to be enhanced using metal on carbon catalysts. Ring opening is possible but requires base. The propensity for ring closing to form substituted pyrrolidinones provides additional possible products. Furthermore, it provides a method for selectively protecting the pendant carboxylic acid, allowing one to selectively reduce the amino acid. At temperatures below 100°C, cyclization is slow and was not noted in Antons et al. *(23)* work. An important consideration is that the amino group of pyroglutamic acid is considerably less basic than the amino group of glutamic acid. Thus, hydrogenation of the pendant carboxylic group does not require additional acid. In fact, as we shall see, the addition of acid promotes further chemistry.

For hydrogenations at 150°C, essentially identical results were obtained whether starting with glutamic acid or pyroglutamic acid. Pyroglutamic acid shows much greater water solubility and thus was easier to work with.

Under hydrogenation conditions further unexpected chemistry occurs. The results of two hydrogenations are shown in Fig. 3. Both were run using 0.22 *M* substrate in water. The catalyst was a 5% ruthenium on carbon support, and the reaction was carried out at 150°C at 13.7 MPa of hydrogen. In one case, 0.29 *M* phosphoric acid was added, and in the other no additional acid was used.

In the presence of phosphoric acid, the substrate was rapidly consumed within 2 h. An initial product was formed, pyroglutaminol, but it was not stable to the reaction conditions. Under the HPLC analytical method employed, no other products were observed. By comparison, in the absence of phosphoric acid, pyroglutaminol was stable and not consumed. Interestingly, the reaction halted after 1 h, before the substrate was fully consumed. Further inquiry verified that the catalyst was still viable; that is, it had not been poisoned. It was also noted, however, that there had been a sharp rise in the pH of the solution from about 3.0 to 9.0. Formation of pyroglutaminol, a neutral compound, could not account for the rise in pH. The possibility that ammonia was being released during the reaction, as observed by Broadbent et al. *(11)*, was considered. However, analysis demonstrated that this was not the case. A second troublesome observation was the apparent poor mass balance of HPLC detected products in both reaction mixtures but worse for the reaction that contained phosphoric acid. Gas analysis showed no significant formation of methane or other overhydrogenation products in either experiment. In fact a total organic carbon analysis showed that essentially no carbon was lost from the solution.

The hydrogenation reaction was repeated this time using pyroglutaminol as substrate. Both neutral and acidic media were used as before. The results are presented in Fig. 4. The experiment verified the instability of pyroglutaminol under hydrogenation conditions in the presence of acid. Under neutral hydrogenation conditions, pyroglutaminol was stable. A small amount of hydrogenolysis, forming 5-methylpyrrolidinone and 2-pyrrolidinone, was noted (these products were not observed in the presence of phosphoric acid).

^{13}C NMR was helpful in determining what had occurred in the two experiments. Reaction solutions from the experiments shown in Fig. 3 were concentrated and examined by NMR without any further modification. The spectra are shown in Fig. 5.

The NMR data showed that the reaction was very clean when phosphoric acid was present. Essentially a single product was formed. The product did not contain carbonyl functionality. The spectrum, however, was not that of glutaminol (the expected ring opened compound) but rather of prolinol (*see* Fig. 5). The minor peaks in the spectrum corresponded to a small amount of unreacted pyroglutaminol. Conversely, when acid was not added, the resultant solution contained a complex mixture of products.

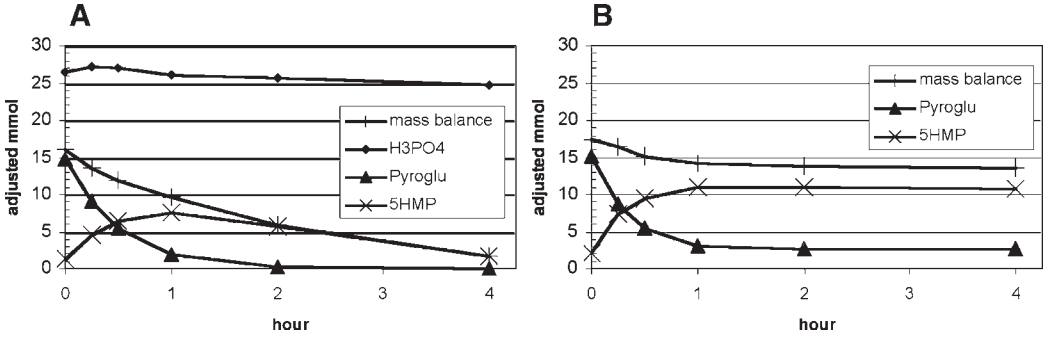

Fig. 3. Hydrogenation of pyroglutamic acid (0.22 *M*) in water at 150°C and 13.7 Mpa of H_2 with **(A)** 0.29 *M* phosphoric acid and **(B)** in absence of acid. 5HMP, pyroglutaminol (5-hydroxymethyl-2-pyrrolidinone). Note that small amounts of 2-pyrrolidinone and 5-methyl-2-pyrrolidinone were also formed. (Note: mass balance refers to HPLC identifiable product, not actual mass balance.)

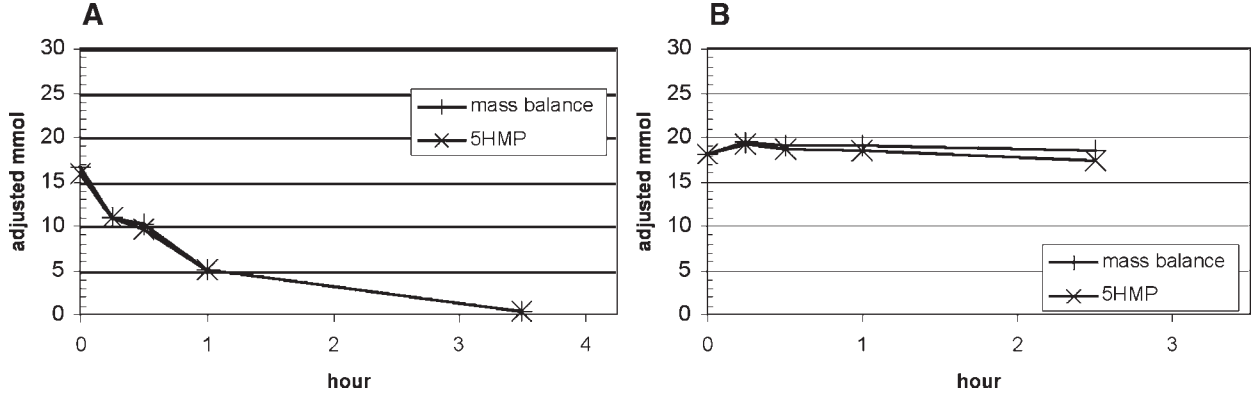

Fig. 4. Stability of pyroglutaminol (5HMP) (0.22 *M*) in water at 150°C. and 13.7 MPa of H_2 **(A)** in presence of 0.29 *M* phosphoric acid and **(B)** in absence of acid.

The spectrum showed resonances that we assigned to pyroglutamic acid and pyroglutaminol. In addition, there were resonances consistent with prolinol.

The ^{13}C NMR data were confirmed with MALDI mass spectral data. MALDI is a soft ionization technique able to transfer analytes into the gas phase as intact molecules without fragmentation. 2,5-Dihydroxybenzoic acid was used as the matrix to absorb nitrogen laser energy at 337 nm and assist in the ionization. The MALDI data verified the prolinol assignment (*see* Fig. 6). The data also showed that a minor amount of other pyrrolidines was formed including 2-methylpyrrolidine and pyrrolidine.

Discussion

The spectroscopic evidence provided the missing data required to explain the observations in Figs. 3 and 4. Key was the surprising observation that acid activates the lactam carbonyl toward reduction and thus produces prolinol *(24)*. Prolinol was not detectable using our HPLC method, which accounts for the apparent poor mass balance. A proposed mechanism for the transformation is shown in Fig. 7.

Under the reaction conditions, glutamic acid cyclizes to pyroglutamic acid. The cyclization can be done thermally, although the rate appears to be enhanced by the hydrogenation catalyst. The cyclization occurs at temperatures above 100°C even under dilute acidic conditions. Facile hydrogenation of pyroglutamic acid produces pyroglutaminol. Under strictly neutral conditions, pyroglutaminol is stable to the reaction conditions. However, in the presence of acid the carbonyl is activated. Hydrogenation of the resultant double bond followed by anchimeric assisted water loss and subsequent hydrogenation affords prolinol. Prolinol is a basic compound (pK_a of about 11.3). Under neutral conditions, pyroglutaminol is stable and the lactam carbonyl is not hydrogenated (Fig. 4). However, pyroglutamic acid is sufficiently acidic to promote a small level of lactam hydrogenation. In the absence of phosphoric acid, prolinol forms a salt with the substrate and the reaction halts before the pyroglutamic acid is fully converted. Phosphoric acid reprotonates the carboxylic acid, allowing high conversion to prolinol.

By careful control of reaction conditions and contact time, we were able to achieve high selectivity to either pyroglutaminol or prolinol. Under hydrogenation conditions in which phosphoric acid was present, prolinol was formed at about 98% selectivity with a 98% conversion (0.22 *M* glutamic acid, 0.29 *M* H_3PO_4, 5% Ru/C at 1% loading, 150°C, 2000 psig of H_2, 4 h). The absence of mineral acid, lower hydrogen pressure, and shorter residence time favor the formation of pyroglutaminol (0.22 *M* glutamic acid, 5% Ru/C at 1% loading, 150°C, 1000 psig of H_2, 1 h). The maximum selectivity we obtained was about 85% at 85–90% conversion. The major byproduct formed in this reaction was prolinol, which reacted with the substrate to inhibit higher conversion. Pyroglutamic acid can subsequently be ring opened under base-catalyzed conditions to form 4-amino-5-hydroxy pentanoic acid (*see* Fig. 8).

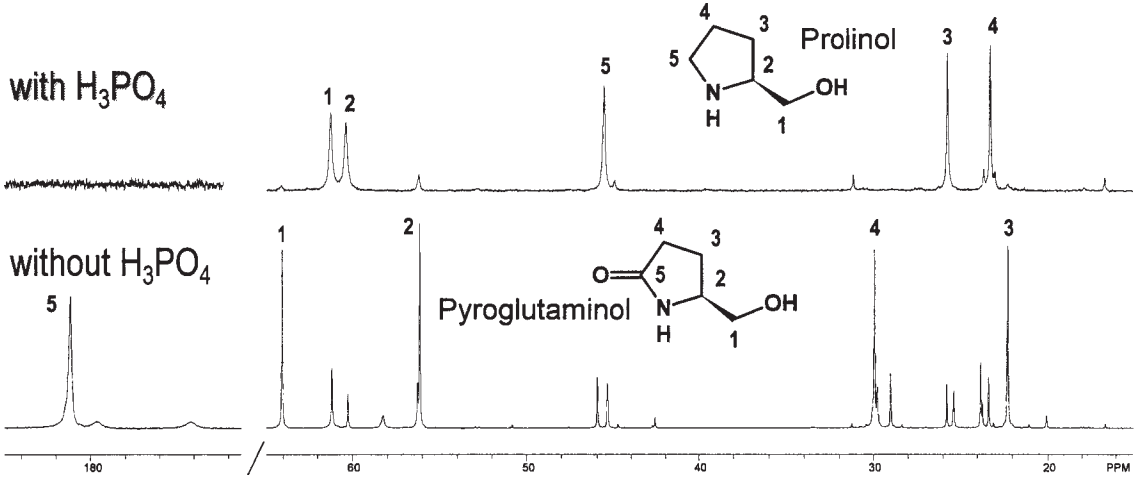

Fig. 5. ^{13}C NMR data of reaction solutions from Fig. 3.

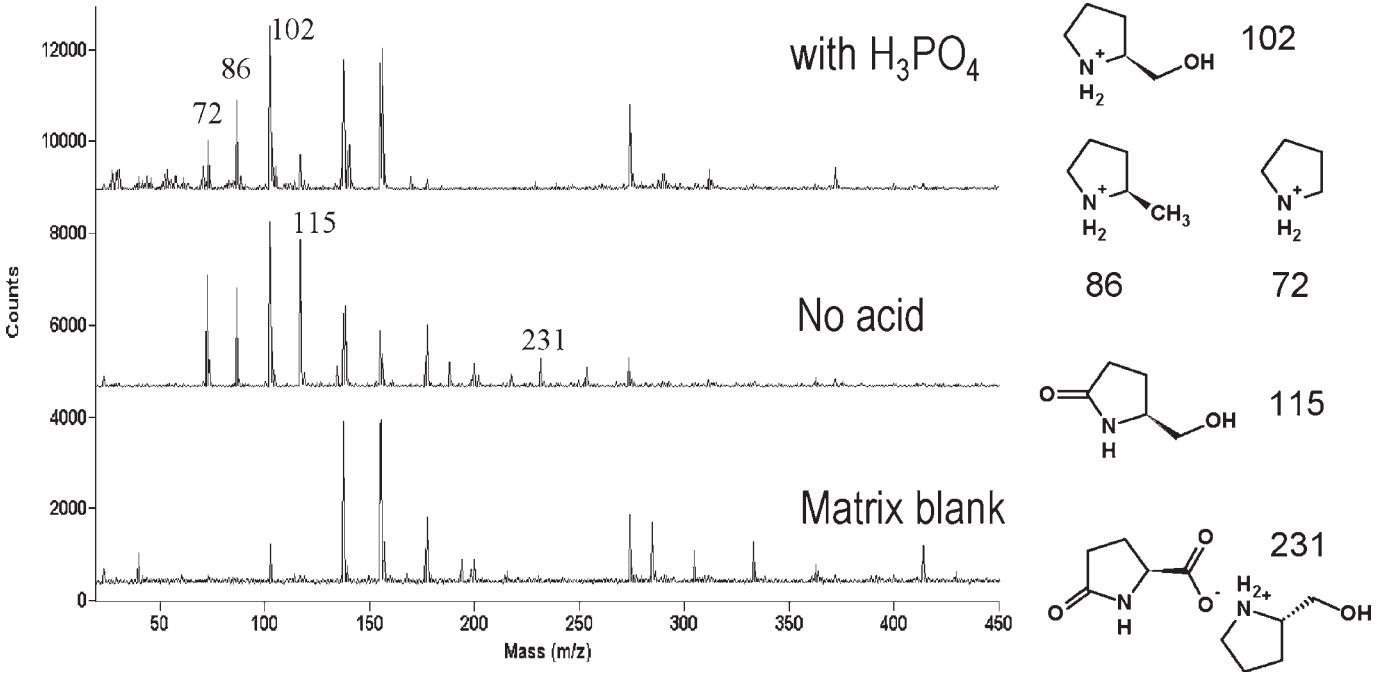

Fig. 6. MALDI mass spectral data confirming formation of prolinol.

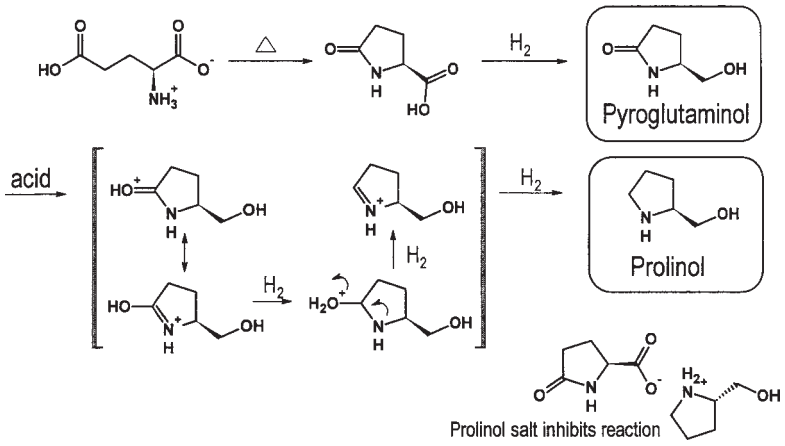

Fig. 7. Proposed reaction mechanism and products observed.

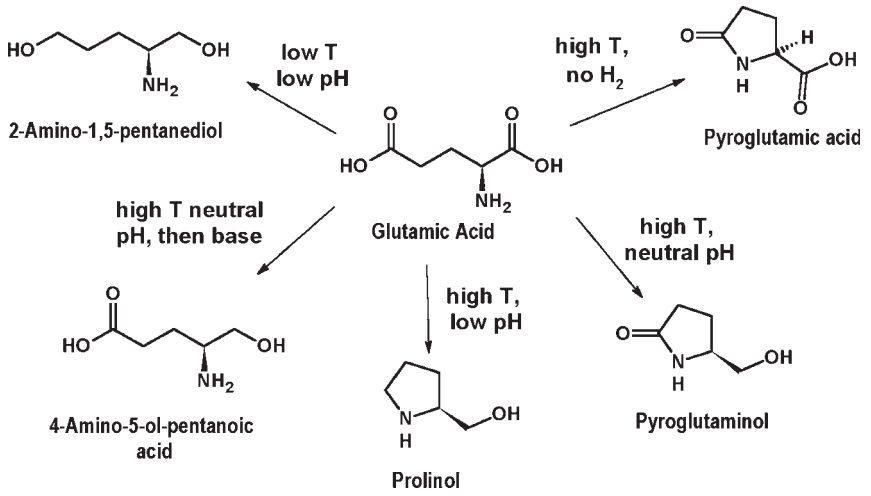

Fig. 8. Products demonstrated from glutamic acid.

In conclusion, we have presented various molecules available from glutamic acid via aqueous-phase thermochemical transformations. The chemistry highlights the dual role of acid in amino acid hydrogenation. Initially a catalytic amount of acid is required to protonate the zwitterionic amino acid. However, if a basic product is formed, stoichiometric amounts of acid are required to achieve high conversion. A caveat is present for glutamic acid: cyclization results in a lactam nitrogen that is significantly less basic than the amine. In this case, the addition of acid is not only unnecessary but in fact surprisingly promotes the subsequent hydrogenation of the less reactive lactam carbonyl. The various products that have been demonstrated thus far are shown in Fig. 8. Other products will be the subject of further research.

Acknowledgments

We acknowledge the help of April Getty with ^{13}C NMR and Catherine Petersen with MALDI mass spectra. Keith Peterson assisted in reactor support and Tom Wietsma in analytical support. We also thank Jim White and Dennis Miller for helpful discussions. This work was funded under a Laboratory Directed Research and Development grant administered by Pacific Northwest National Laboratory (PNNL). PNNL is operated by Battelle for the US Department of Energy.

References

1. (2003), *Japan Chemical Week*, April 24.
2. Bowden, E. and Adkins, H. (1934), *J. Am. Chem. Soc*. **56,** 689–691.
3. Adkins, H. and Billica, H. R. (1948), *J. Am. Chem. Soc*. **70,** 3118–3120.
4. Adkins, H. and Billica, H. R. (1948), *J. Am. Chem. Soc*. **70,** 3121–3125.
5. Antons, S. and Beitzke, B. (1996), US patent no. 5,536,879.
6. Antons, S. (1998), US patent no. 5,731,479.
7. Antons, S., Tilling, A. S., and Wolters, E. (1999), PCT Intl. Appl. World patent no. 9938838.
8. Rachmady, W. and Vannice, M.A. (2000), *J. Catal*. **192,** 322–334.
9. Santiago, M., Sanchez-Castillo, M., Cortright, R., and Dumesic, J. (2000), *J. Catal*. **193,** 16–28.
10. Carnahan, J., Ford, T., Gresham W., Grigsby, W., and Hager, G. (1955), *J. Am. Chem. Soc*. **77,** 3766–3768.
11. Broadbent, H., Campbell, G., Bartley, W., and Johnson, J. (1959), *J. Org. Chem*. **24,** 1847–1854.
12. Tahara, K., Tsuji, H., Kimura, H., Okazaki, T., Itoi, Y., Nishiyama, S., Tsuruya, S., and Masai, M. (1996), *Catal. Today* **28,** 267–272.
13. Toba, M., Tanaka, S., Niwa, S., Mizukami, F., Koppany, Z., Guczi, L., Cheah, K., and Tang, T. (1999), *Appl. Catal. A: Gen.* **189,** 243–250.
14. Turek, T., Trimm, D. L., and Cant, N. W. (1994), *Catal. Rev. Sci. Eng*. **36,** 645–683.
15. Nagahara, H., Ono, M., and Nakagawa, K. (1989), *Jpn. Kokai Tokkyo Koho*, Japanese patent no. 01085937 A2 19890330 Heisei.
16. Corry, A. (1986), British patent no. GB 2169896 A1 19860723.
17. Iliuta, I., Bulearca, M., and Lazar, L. (1995), *Romanian Rev. Chim. (Bucharest)* **46(8),** 725–729.
18. Mesich, F., Bedford, J., and Dougherty, E. (1971), German patent no. DE 2131696 19711230.
19. Bianchi, M., Menchi, G., Francalanci, F., Piacenti, F., Matteoli, U., Frediani,P., and Botteghi, C. (1980), *J. Organometallic Chem*. **188,** 109–119.
20. Smith, G. and Musoiu, M. (1979), *J. Catal*. **60,** 184–192.
21. Osawa, T., Harada, T., and Akira, T. (1990), *J. Catal*. **121,** 7–17.
22. Jere, F. T., Miller, D. J., and Jackson, J. E. (2003), *Org. Lett.* **5,** 527–530.
23. Antons, S., Tilling, A. S., and Wolters, E. (2001), US patent no. 6,310,254.
24. Sauer, J. C. and Adkins, H. (1948), *J. Am. Chem. Soc.* **60,** 402–406 (first example using a precious metal on carbon catalyst).

0273-2289/04/115/0871–0885/$25.00

Opportunities in the Industrial Biobased Products Industry

Tracy M. Carole,*[,1] Joan Pellegrino,[1] and Mark D. Paster[2]

[1]Energetics, Inc., 7164 Columbia Gateway Drive, Columbia, MD 21046, E-mail: tcarole@energetics.com; and [2]US Department of Energy, 1000 Independence Ave S.W., Washington, DC 20585

Abstract

Approximately 89 million metric t of organic chemicals and lubricants, the majority of which are fossil based, are produced annually in the United States. The development of new industrial bioproducts, for production in stand-alone facilities or biorefineries, has the potential to reduce our dependence on imported oil and improve energy security. Advances in biotechnology are enabling the optimization of feedstock composition and agronomic characteristics and the development of new and improved fermentation organisms for conversion of biomass to new end products or intermediates. This article reviews recent biotechnology efforts to develop new industrial bioproducts and improve renewable feedstocks and key market opportunities.

Index Entries: Bioproducts; thermoplastics; fermentation; solvents; platform chemicals.

Introduction

Industrial biobased products have enormous potential in the chemical and material industries. The diversity of biomass feedstocks (sugars, oils, protein, lignocellulosics), combined with the numerous biochemical and thermochemical conversion technologies, can provide a wealth of products that can be used in many applications. Targeted markets include the polymer, lubricant, solvent, adhesive, herbicide, and pharmaceutical markets. Industrial bioproducts have already penetrated some of these markets, but improved technologies promise new products that can compete with fossil-based products in both cost and performance.

Organic chemicals and lubricants represent the largest and most easily accessible target for bioproducts (Table 1). Within the organic chemicals

*Author to whom all correspondence and reprint requests should be addressed.

Table 1
Annual Domestic Organic Chemical Production *(1–9)*

Market (year of production data)	Annual production (million metric t)
Lubricants and greases (2001)	8.9
All organic chemicals [a]	79.6
Polymers (2001) [b]	45.9
Polyolefins (2001) [b]	22.4
Polyethylene terephthalate (2001) [b]	3.1
Polyvinyl chloride (2001) [b]	6.5
Styrenics (2001) [b]	4.1
Nylon (2001) [b]	0.5
Thermosets (2001) [b]	3.6
Other polymers (2001) [b]	5.7
Forest chemicals (1999 and 2000) [c]	1.3
Solvents (2001)	4.8
Glycols (2000)	1.4
Other organic chemicals (1997)	27.6

[a] The estimate represents the net volume of organic chemicals produced in the United States and does not double count volumes of intermediates and their derivatives.
[b] Data from ref. 2.
[c] Tall oil, gum rosin, and crude sulfate turpentine.

market, the polymer industry presents a tremendous opportunity, with an annual production of approx 46 million metric t *(2)*. Other market segments include organic acids, alcohols, solvents, and adhesives.

By using biotechnology and novel chemistries, biomass carbon can be rearranged to yield products that are equivalent or superior to the fossil-based products used today. New genetic mapping techniques allow researchers to sequence genes more quickly and to determine the relationship between structure and function *(10)*. These genetic tools are being used to create new and improved microorganisms to convert biomass components into end products or intermediates that can then be thermochemically upgraded *(11)*. The tools are also being used to improve biomass feedstocks by (1) increasing the content of desired components, (2) decreasing the content of components such as lignin, and/or (3) adding the capability to produce a new component (e.g., a new fatty acid in oilseeds) *(10)*. This article examines recent biotechnology efforts to develop new industrial bioproducts and improve renewable feedstocks and key market opportunities.

Polymers

Since 1976, plastics have been the most used material in the world *(12)*. According to the American Plastics Council, nearly 46 million metric t of polymers was produced in the United States in 2001 *(2)*. Plastics are often

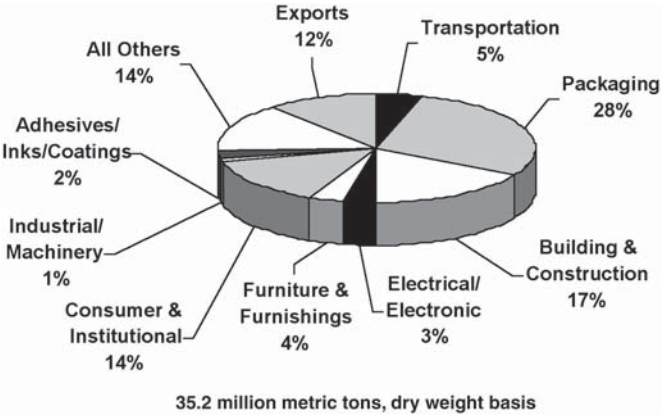

Fig. 1. US total sales and captive use of selected thermoplastic resins by major market for 2001. Major market volumes are derived from plastic resins sales and captive use data as compiled by VERIS Consulting, LLC and reported by the American Plastics Council's Plastic Industry Producers' Statistics Group. Selected thermoplastics are low-density polyethylene, linear low-density polyethylene, high-density polyethylene, polypropylene, nylon, polyvinyl chloride, thermoplastic polyester, engineering resins, acrylonitrile-butadiene-styrene, styrene-acrylonitrile, other styrenics, polystyrene, and styrene butadiene latexes. (Data from ref. *15*.)

selected over more traditional materials because of their superior properties (lightweight, corrosion and shatter resistant, long-lasting) and lower cost. Their versatility enables their use in applications ranging from clothing and packaging to high-tech composites, and they are found in nearly all end-use markets (Fig. 1). Biobased polymer manufacturers and researchers are currently targeting packaging and fiber/fiberfill applications, which represent two of the largest uses of polymers *(13,14)*.

Plastic packaging represents the largest single market for polymer resins and is a key focus for new biobased products. Since 1913 when cellophane (a bioproduct), the first fully flexible, waterproof wrap, was developed, the use of plastic packaging has grown owing to its ability to provide the same strength, barrier, and shatterproof properties with a reduction in the packaging weight and at a lower cost *(12)*. In 2000, nearly 10 million metric t of thermoplastics was consumed in packaging applications in the United States (Table 2) *(16)*.

Second behind packaging in the United States is the use of polymers in fiber and fiberfill applications that encompass the apparel, sports equipment, building and construction, electronic, furniture and furnishings, and industrial/machinery markets. In 1998, 4.8 million metric t of manufactured fiber was produced for use in traditional consumer products such as apparel, carpets, upholstered furniture, and bedding as well as in high-tech applications such as composite materials, medical devices, and electronic circuit boards *(17)*. Key fiber types include polyester, nylon, olefin,

Table 2
Thermoplastics Used in Packaging in 2000 in the United States *(16)*

Thermoplastic	Quantity (million metric t)	Percent
Low-density polyethylene	1.20	12.4
Linear low-density polyethylene	2.05	21.1
High-density polyethylene	3.38	34.9
Polypropylene	1.59	16.4
Polystyrene	0.59	6.1
Nylon	0.05	0.5
Polyvinyl chloride	0.44	4.6
Other	0.38	4.0
Total	9.68	100.0

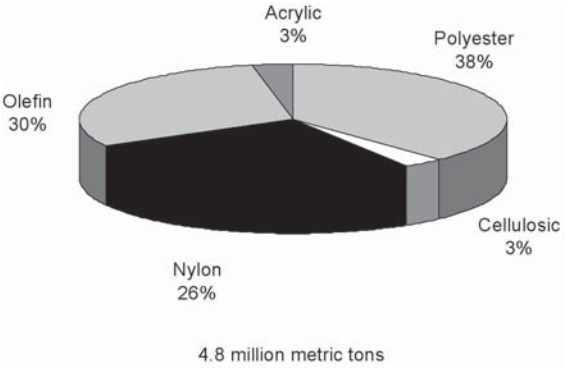

Fig. 2. US fiber production for 1998 *(17)*.

cellulosic, and acrylic (Fig. 2). Some of these are already biobased (cellulosic fibers, rayon, acetate), and there are opportunities for new industrial bioproducts to make inroads in the fiber industry.

Polylactide

Much has been written about Cargill Dow LLC's polylactide (PLA) polymer, also known as NatureWorks™ PLA. PLA is a thermoplastic produced from biomass sugars by fermentation. The fermentation product, lactic acid, is converted into a lactide that is purified and polymerized using a special ring-opening process *(18)*.

In April 2002, Cargill Dow started up its first large-scale PLA plant in Blair, NE. The plant has a capacity of 140,000 metric t, and demand for NatureWorks PLA has been so strong that construction of a second plant is likely to begin within a few years *(19)*. Cargill Dow projects a possible market of 3.6 million metric t by 2020 *(20)*.

PLA is cost-competitive with conventional polymers and offers performance properties equal to or greater than those offered by conventional

polymers such as polyethylene terephthalate (PET) and nylon. Cargill Dow is targeting the food-packaging and fiber/fiberfill applications markets. The high stiffness, superior clarity and gloss, dead-fold, grease resistance, and unique flavor and aroma barrier properties *(21)* of PLA combined with its environmentally friendly profile are opening inroads in the packaging industry. Cargill Dow has teamed with a number of domestic and international consumer product packaging companies including The Coca-Cola Company (soft drink cups) and Sony Pacific (blister packaging and film wrap for radios and minidiscs) *(22)*.

PLA fiber combines the most desired properties of natural fibers, such as wool, and synthetics, such as polyester. This combination of properties opens up a wealth of textile applications including clothing, carpet tiles, diapers/acquisition distribution layers, upholstery, furnishings, and filtration. PLA has a high dyeability, and in comparison with polyester in activewear, it displays superior wicking properties.

Cargill Dow currently relies on corn grain as a source of glucose for PLA production but is working to develop fermentation organisms that convert pentose sugars as well as glucose into polylactide *(11)*. This would enable the use of lignocellulosic material such as corn stover and rice straw, decreasing production costs and providing a higher value outlet for low-value agricultural residues.

Polyhydroxyalkanoates

Polyhydroxyalkanoates (PHAs) are a family of natural polymers produced by many bacterial species for carbon and energy storage that exhibit a broad spectrum of performance properties, enabling them to compete with a large share of the plastics market. PHAs can be produced through fermentation, and, more recently, researchers have been working to genetically modify a plant for direct production *(23)*. Since the 1970s, ICI, Zeneca, and, to some degree, Monsanto and others have pursued cost-effective fermentation production routes. In the 1990s, bacterial fermentation of PHAs, specifically poly(3-hydroxybutyrate-co-3-hydroxyvalerate) (PHBV), was performed commercially by Zeneca and then Monsanto under the trade name Biopol™; however, production costs of PHBV were high (more than $6.60/kg), and it could not compete with conventional petroleum-based plastics using the fermentation and separation technology available at the time *(24)*.

Metabolix has since developed lower-cost fermentation technology for PHAs, which the company claims would permit commercial-scale production for under $2.20/kg *(25)*. Production at this cost could open up a significant market for fermentation-based PHAs.

Researchers at the Hawaii Natural Energy Institute, University of Hawaii, have also developed a novel, two-step process that converts organic waste materials such as food scraps into poly(3-hydroxybutyrate) or PHBV *(26)*. Approximately 60% of the organic material is converted into PHAs, and the remaining 40% can be converted into fertilizers *(27)*. The first step

is an anaerobic digestion process that converts food scraps into four major organic acids: acetic, propionic, butyric, and lactic. The acids pass through a dialysis membrane, concentrating them, and then enter the second bioreactor to be consumed by an enriched *Ralstonia eutropha* culture to produce the PHAs. A polymer content of 72.6% of dry cell mass was obtained, comparable to PHA content through pure glucose fermentation *(26)*.

The estimated PHA production cost for the two-step process is between $2.20 and $4.40/kg *(27)*. The potential of this process has caught the attention of I-PHA BioPolymers, a Hong Kong–based company involved in environmental biotechnology development, which recently licensed the technology from the University of Hawaii. I-PHA BioPolymers plans to develop and build a pilot plant for the production of PHAs and fertilizers *(28)*.

A still lower-cost route to PHAs is genetic modification of plants to directly produce the final polymer. Monsanto (and others) pursued this approach and is currently being cofunded by the US Department of Energy (DOE) in a collaborative research project led by Metabolix. Switchgrass will be modified to produce PHAs, which can then be extracted from the plant material and processed to obtain a consistent composition and the desired material properties. The plant material remaining after PHA extraction can be used to produce fuels, power, or other products, creating the opportunity for a "plants as factories" biorefinery. Applications for polymers with properties similar to those of PHAs consume on the order of 13.6 million metric t annually, and it is possible that in the future PHAs will figure prominently in the plastics market.

1,3-Propanediol

Together with purified terephthalic acid, 1,3-propanediol is used to produce polytrimethylene terephthalate (PTT), a polymer with remarkable "stretch-recovery" properties. The desirable attributes of PTT have been known since the 1940s, but high production costs prevented its entrance into the polymer market *(29)*. In the 1990s, a new fossil-based route to 1,3-propanediol was developed enabling the production of PTT for higher-value applications, and PTT polymers were introduced into the market by DuPont and Shell Chemicals *(29,30)*.

For DuPont, the commercialization of 1,3-propanediol and PTT has opened up markets for industrial products from renewable resources. Through a partnership with Genencor International, DuPont has recently developed a lower-cost fermentation route that converts biomass sugars into 1,3-propanediol. DuPont plans to transition to the biobased process for 1,3-propanediol production in 2004 *(31)*.

PTT is used in apparel, upholstery, specialty resins, and other applications in which properties such as softness, comfort stretch and recovery, dyeability, and easy care are desired. The properties of PTT surpass nylon and PET in fiber applications, and polybutylene terephthalate and PET in resin applications such as sealable closures, connectors, extrusion coatings, and blister packs *(14)*.

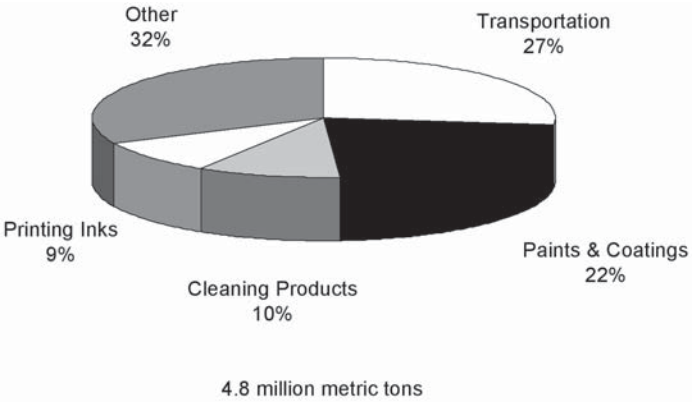

Fig. 3. US solvent demand for 2000 *(3)*.

DuPont expects PTT to stay at the same pricing level as nylon 6, though the company believes that the polymer's properties, and not price, will drive demand *(32)*. Based on its use in PTT, 1,3-propanediol has a potential 2020 market of 230,000 metric t.

In addition to its use in PTT, 1,3-propanediol can replace traditional glycols in urethane-based polymer systems, improving thermal and hydrolytic stability. As a partial substitute for traditional glycols in polyester systems, 1,3-propanediol can improve coating flexibility without affecting other key properties. Other applications include engine coolants and water-based inks *(33)*.

Solvents

Solvents are integral to our lifestyle today, contributing to the manufacture of numerous products such as pharmaceuticals, paints, inks, and microchips. They make it possible to process, apply, clean, or separate materials and are used across many industries (Fig. 3). Different applications require specific solvating or other properties, and solvents can be blended to achieve the properties necessary for a given application.

Growing concern over volatile organic compound and other emissions is motivating manufacturers to modify processes to capture and recycle solvents, reduce solvent use, or switch to solvents with better environmental profiles. A biobased solvent that is benefiting from this shift is ethyl lactate.

Ethyl Lactate

Ethyl lactate is another lactic acid derivative that has recently been commercialized. An environmentally benign solvent with properties superior to many conventional petroleum-based solvents, it can be blended with methyl soyate derived from soybean oil to create custom-tailored solvents for various applications.

Table 3
Selling Price of Common Solvents *(37)*

Product	Price ($/kg)
Methyl soyate	0.66–1.00
Aqueous cleaners	~2.65
Semiaqueous cleaners	~8.90
N-Methyl pyrrolidone	3.30–4.00
d-Limonene	Up to 0.88
Methylene chloride	0.66
Trichloroethylene	1.43
Methyl ethyl ketone	1.00
Perchloroethylene	0.77

Until recently, the use of ethyl lactate has been limited owing to high production costs; selling prices for ethyl lactate have ranged between $3.30 and $4.40/kg, compared with $2.00 and $3.75/kg for conventional solvents *(34)*. With advances in lactic acid fermentation, and separations and conversion technologies, retail costs have been driven down as low as $1.87/kg *(35)*. DOE has cofunded lactic acid separations technology involving the use of electrodialysis, advanced membranes, and reactive separations capable of converting the lactic acid salts made during fermentation directly into ethyl lactate.

More than 4.5 million metric t of solvents is used in the United States annually, and it has been suggested by industry experts that ethyl lactate could replace conventional solvents in more than 80% of these applications *(34)*. Vertec Biosolvents Inc. is currently using ethyl lactate in soy oil–solvent blends. Applications targeted by Vertec Biosolvents include conventional solvents that are under environmental scrutiny such as methylene chloride, methyl ethyl ketone, and *N*-methyl pyrrolidone *(36)*. Table 3 lists the selling prices of some common solvents.

Platform Chemicals

Platform chemicals are compounds that serve as building blocks for numerous chemical intermediates and end products. An example is ethylene, which serves as the feedstock for derivatives such as acetaldehyde, ethylene dichloride, ethylene oxide, polyethylene, vinyl acetate, and ethyl acetate. Biobased chemicals such as succinic acid, 3-hydroxypropionic acid (3-HP), and butanol also have the potential to be converted into multiple derivatives, some of which are commodity chemicals and others that are higher-value chemicals.

Succinic Acid

Succinic acid and its salts, produced through the fermentation of glucose, form a platform from which many chemicals can be produced. Since most fermentation organisms are not tolerant of acidic conditions, the fer-

mentation is typically neutralized, producing a salt of succinic acid. Conventional separation and recovery involves filtration to separate the solid cell mass, and reacidification of the succinate salt to form free succinic acid while precipitating out a salt.

There has been considerable research over the past 5–10 yr dedicated to improving microorganisms and separations technologies in order to reduce the overall cost of biobased succinic acid, much of which has been cofunded by DOE. This research has resulted in the development of the fermentation microorganism *Escherichia coli* strain AFP111, which exhibits greatly improved productivity. Fermentation with AFP111 to produce succinic acid has recently been successfully tested at commercial scale.

Separations research has resulted in the development of a two-stage desalting and water-splitting electrodialysis system that concentrates, purifies, and acidifies the succinic acid. The base is recycled back to the fermentation, where it is used for neutralization, eliminating the generation of gypsum salt, an unwanted neutralization byproduct that must be disposed of or sold *(38)*.

Succinic acid for industrial use is predominately produced from butane via maleic anhydride, whereas food-grade succinic acid is produced through older fermentation and separation technology. Both routes are costly and this has limited use to specialized areas. Consequently, the world market is relatively small at 15,000 metric t/yr *(39)*.

In 1992, the production costs of succinic acid fermentation ranged from $3.30 to $4.40/kg. Advances in fermentation, and especially separation technology for the biobased route, have reduced the potential production costs to about $1.10/kg. Ongoing advances could significantly reduce the cost of biobased succinic acid even more, and commercialization of these low-cost routes could have a significant impact on the demand for succinic acid, expanding current markets while opening up new markets for the acid and its derivatives.

As shown in Table 4, the real promise of succinic acid lies in its derivatives. A DOE-funded collaboration among Oak Ridge National Laboratory; Argonne National Laboratory; Pacific Northwest National Laboratory; National Renewable Energy Laboratory; and Applied CarboChemicals, Inc. investigated succinic acid derivatives such as tetrahydrofuran, 1,4-butanediol, γ-butyrolactone, and *N*-methyl pyrrolidone. More recently, Applied Carbochemicals has pursued succinate salts that can serve as de-icers and herbicide additives *(40,41)*.

Other companies showing strong interest in the production of biobased succinic acid and its derivatives are Mitsubishi Chemical and Ajinomoto Company, Inc., which have agreed to collaboratively develop a biobased process to convert sugars into succinic acid. These companies plan to construct a succinic acid plant in Japan with an initial capacity of 30,000 metric t/yr (MT) by 2006 *(42)*. Table 4 shows the current market estimates for the fossil-based chemicals, as well as 2020 market estimates for the biobased products potentially based on biobased succinic acid.

Table 4
Potential Near-Term Succinic Acid Derivatives *(39,40,43–46)*

Chemical	Current US market (metric t)[a]	Market Price ($/kg)[b]	Potential 2020 market size (metric t)[c]
Tetrahydrofuran	179,100	3.40	>22,700
1,4-Butanediol	373,200	1.40–2.00	>13,60?
γ-Butyrolactone	78,400	?	?
N-Methyl pyrrolidone	50,900	?	Could be displaced by ethyl lactate
2-Pyrrolidone	<29,500	Unknown	?
Succinate salts	Road de-icer: 9,090,900	0.05	Depends on demand for less-corrosive road de-icers
Succinate salts	Aviation de-icer: 91,000	1.00–1.95	Could replace 100% of airport de-icers
Succinate salts	Herbicide: small	?	Small

[a] This is the volume of market opportunities represented by the current and potential applications.
[b] This is the price of the current applications targeted by the biobased product and not the price of the biobased product.
[c] These are authors' estimates of the biobased market in 2020 based on the state of the technology development and current US market size.

Succinate salts (calcium, magnesium, diammonium, ammonium) show near-term market potential. They are produced through the neutralization of succinic acid, an intermediate step in the production of succinic acid by fermentation. Two key applications identified are herbicide additives and de-icing compounds for roads, aircraft, and airport runways. Although herbicide use is high, the active ingredients (herbicide and succinate salt enhancer) may comprise only a small amount of the product, between 0.5 and 3.0 wt% *(41)*. Conversely, in 1990, approx 9,090,900 metric t of salt was used on roads and highways and about 91,000 metric t of aviation de-icers is currently used each year *(40,45)*, and both types of de-icers are under pressure from environmental groups. Federal and state aviation and highway agencies are seeking de-icers with improved performance and reduced corrosiveness, and succinate salts are ideal for this purpose because they offer improved ice penetration characteristics and are less damaging to concrete, asphalt, metals, and the environment.

3-Hydroxypropionic Acid

The fermentation of glucose to 3-HP is just now being actively investigated. Many high-volume products can be made from 3-HP, giving it the

potential to be a platform intermediate similar to lactic acid and succinic acid. The synthesis of acrylic acid, and the salts and esters of acrylic acid derived from 3-HP, has been demonstrated in the laboratory. Other derivatives under consideration include acrylamide, 1,3-propanediol, malonic acid esters, and acrylonitrile *(47)*. As with PLA, there is no commercially viable production route of 3-HP from fossil fuel feedstocks.

The conversion of 3-HP into acrylic acid is expected to be "easier" and may require less energy than the oxidation of propylene to acrylic acid *(47)*. As conversion technologies are developed, the primary challenge will be to make them cost-competitive with the current fossil-based routes.

Butanol

Butanol is a platform chemical with several large-volume derivatives and is used as a solvent and in plasticizers, amino resins, and butylamines *(48)*. Butanol can also be used as a biobased transportation fuel and is more fuel efficient than ethanol on a volume basis.

In 1999, the domestic demand for butanol was 841,000 metric t and it is projected to increase 3% per year *(49)*. During the early twentieth century, the primary method of butanol production was anaerobic fermentation with *Clostridium acetobutylicum* to produce a mixture of acetone, butanol, and ethanol. The butanol yields were low, and as oil prices declined after World War II, petrochemical routes to butanol displaced the fermentation route *(50)*. The primary petrochemical route used today involves the hydrogenation of *n*-butyraldehyde *(49)*, and production costs hover around $0.66/kg *(24)*.

The US DOE's Small Business Technology Transfer Program is funding research to improve the biobased route to butanol and make it cost-competitive with the petroleum-based route. Researchers are attempting to increase butanol yield by using improved bacteria strains, employing advanced reactor technology, and separating the organic acid production and organic acid-to-alcohol phases into different vessels. A preliminary material and energy balance indicates that a yield of 9.5 L of butanol/bu of corn could be achieved *(51)*.

Feedstock Modification

Advanced genetic engineering techniques are being used to improve existing renewable feedstocks for the production of industrial bioproducts. In some cases, the feedstock composition is modified to increase the content of a desired component and/or decrease the content of an undesired component, whereas in others, a new metabolic pathway is inserted into the plant genes so that the modified plant produces an entirely new component. These research efforts are recent, and very little, if any, published information is currently available. However, we provide brief descriptions of the research activities to give perspective on the opportunities for new industrial bioproducts that may emerge from feedstock modification.

Adhesives and Resins from Soy Oil and Protein (10)

Researchers at the University of Delaware and Kansas State University are working together to optimize the soy oil and protein composition for use in resin and adhesive applications. Work is being performed to understand the relationship between the chemical structures of the oil and protein components, and their performance properties in resin and adhesive formulations. The results of this work will be used to modify the soybean varieties, using conventional breeding and genetic engineering to increase the percentage of specific fats and proteins.

Biobased Products from Optimized Sorghum Grain (10)

Sorghum grain is a very versatile feedstock and is used in a variety of consumer and industrial markets, including ethanol production. However, little has been done to optimize the grain composition or conversion into sugars and industrial products. As such, Orion Genomics, LLC is leading an effort to optimize grain composition for increased starch content and ease of processing to industrial bioproducts. The agronomic characteristics, such as yield per unit resource, will also be improved for more economical sorghum production.

Increased Natural Rubber Content in Guayule

Guayule, another emerging bioproduct-producing plant, is being developed by the US Department of Agriculture (USDA); Yulex Corporation; and Mendel Biotechnology, Inc. It is a desert shrub indigenous to the southwestern United States and northern Mexico and produces a natural rubber latex primarily in the cells of the bark *(52)*. Natural rubber, commonly used in medical device components, currently comes from the Brazilian rubber tree (*Hevea brasiliensis*) and is imported from Southeast Asian countries such as Thailand, Indonesia, and Malaysia. However, several factors, including increased global demand, diminished acreage, and pathogen attack, are endangering the dependability of the world's natural rubber supply.

Rubber production in guayule offers the potential to develop a domestic supply of natural rubber. In addition, guayule rubber does not contain the proteins present in *Hevea* rubber that can cause an allergic reaction. Natural rubber latex allergy has become an issue in the United States: approx 20 million Americans are allergic to the proteins found in *Hevea* rubber *(53)*. Initial target applications for guayule rubber include gloves and other products for which the strength and resiliency of natural rubber is desired without the potential allergic reaction.

Approximately 22.5–56.2 metric t of rubber can be produced per hectare of guayule (20,000–50,000 lb/acre) *(54)*, and researchers at Mendel Biotechnology are working to increase the rubber content of guayule without compromising rubber quality. They are identifying the *Arabidopsis thaliana* transcription factors that can activate promoters of genes in the rubber

synthesis pathway. These transcription factors will then be used to transform guayule for increased rubber yield *(55)*.

Plastics, Coatings, Adhesives, and Lubricants from Castor and Soy Oil (10)

The Dow Chemical Company, Castor Oil, Inc., and the USDA Western Regional Research Center are collaborating to develop the castor plant as a suitable oilseed for specialty oils that can be converted into lubricants, coatings, foams, adhesives, and engineering thermoplastics. Castor oil already contains ricinoleic acid, a fatty acid used in many industrial applications, but project partners hope to produce other industrially desirable fatty acids within the castor bean.

Conclusion

The chemical and lubricant markets represent an enormous opportunity for biobased products, but many obstacles must be overcome on the way to commercialization. To gain acceptance and supplant products made from petroleum, industrial bioproducts will need to be able to compete in terms of both cost and performance; advances in biotechnology will play a key role in surmounting these economic and technical barriers. Given the size of the potential markets and the considerable research under way, the future looks bright for a biobased economy.

Acknowledgments

The authors gratefully acknowledge the support of the US Department of Energy, Office of Energy Efficiency and Renewable Energy, Office of the Biomass Program; and the contributions and insights of experts in industry and within the US Department of Energy national laboratory system.

References

1. US Department of Commerce (1999), *1999 Annual Survey of Manufactures*, Bureau of the Census.
2. American Plastics Council (2003), (as compiled by VERIS Consulting, LLC and reported by the American Plastics Council's Plastic Industry Producers' Statistics Group). *APC Year-End Statistics for 2002, Production, Sales & Captive Use, 2002 vs. 2001*. Website: http://www.americanplasticscouncil.org/benefits/economic/03/YearEnd2002_Stats.pdf.
3. The Freedonia Group. (2001), *Solvents: Green & Conventional to 2005*, The Freedonia Group, Cleveland, OH.
4. US DOE. (2001), *Petroleum Supply Annual, Volume 1*. US Department of Energy, Energy Information Administration.
5. McPadden, M. (2001), *Chemical Market Reporter* **259(7),** 24.
6. De Guzman, D. (2000), *Chemical Market Reporter* **258(18),** 14.
7. (2000), Chemical Profile: Tall Oil, *Chemical Market Reporter*, May 15, 7.
8. (2001), Chemical Profile: Ethylene Glycol, *Chemical Market Reporter*, September 3.
9. (2001), Chemical Profile: Propylene Glycol, *Chemical Market Reporter*, September 24.
10. US DOE. (2001), *Bioproducts Project Fact Sheets*. US Department of Energy. Website: http://www.oit.doe.gov/agriculture.

11. Biomass Research and Development Initiative. "Awardees for U.S. Department of Energy, Energy Efficiency and Renewable Energy, Integrated Biomass R&D Solicitation," http://www.bioproducts-bioenergy.gov/pdfs/awardees.pdf (accessed October 11, 2003).
12. American Plastics Council. "About Plastics," Website: http://www.americanplastics council.org/benefits/about_plastics/about_plastics.html.
13. Cargill Dow LLC. "Cargill Dow LLC Products," Website: http://www.cargilldow.com/corporate/product.asp. (accessed October 16, 2003).
14. E.I. du Pont De Nemours and Company. "SoronaÆ in Use," Website: http://www.dupont.com/sorona/home3.html.
15. American Plastics Council (2003) (as compiled by VERIS Consulting, LLC and reported by the American Plastics Council's Plastic Industry Producers' Statistics Group). *Total Sales& Captive Use of Selected Thermoplsatic Resins by Major Market, 1998–2002. Revised 4/30/03*. Website: http://www.americanplasticscouncil.org/benefits/economic/03/98-02Maj_Mkt_Data.pdf.
16. Bohlmann, G. M. (2001), *Process Economics Program Report 115D*, SRI Consulting, Menlo Park, CA.
17. American Fiber Manufacturers Association, Inc. "Fiber Fact," Website: http://www.fibersource.com.
18. Cargill Dow LLC. "NatureWorks™ PLA," Website: http://www.cargilldow.com/corporate/natureworks.asp.
19. Cargill Dow LLC. (2000), "Cargill Dow LLC Commercialization Efforts in Full Swing," press release, June 19, 2000, Website: http://www.cargilldow.com.
20. Fahey, J. (2001), *Forbes Magazine*, November 26, 206.
21. Cargill Dow LLC. (2001), "New Food Service Alternative from Annually Renewable Resources Unveiled for Use in Major Venues," press release, March 5, 2001, Website: http://www.cargilldow.com.
22. Cargill Dow LLC (2003), "NatureWorks PLA Breaks Tradition in Packaging," press release, February 12, 2003, Website: http://www.cargilldow.com.
23. Metabolix, Inc. "Biotechnology Foundation: Plants," Website: http://www.metabolix.com/biotechnology%20foundation/plants.html
24. (2001), Process Economics Program Yearbook International, SRI Consulting, Menlo Park, CA.
25. (2002), *PR Newswire*, August 27.
26. Du, G. and Yu, J. (2002), *Environ. Sci. Technol*. **36,** 5511–5516.
27. Bolante, R. (2003), *Honolulu Magazine*, January, 12.
28. University of Hawaii. (2003), *UH News*, March 3, Website: http://www.hawaii.edu.
29. Elias, K. (2001), *Fashion Market Magazine*, April, 29.
30. Shell Chemicals Limited. "CORTERRA Polytrimethylene Terephthalate," Website: http://www.shellchemicals.com/corterra/1,1098,280,00.html.
31. Nieder, A. A. (2002), *California Apparel News*, November 15–22, 2.
32. Norberg, K. (2002), *International Fiber Journal* **17(6)**.
33. Shell Chemicals Limited. "1,3-Propanediol: experiment," Website: http://www.shell.com.
34. (1998), *Industrial Paint & Powder*, December, 13–14.
35. (1998), *Chemical Engineering*, April, 27–29.
36. Chang, J. (2002), *Chemical Marketing Reporter*, September 2, 4.
37. United Soybean Board. (2002), "Market Opportunity Summary: Soy-Based Solvents," Website: http://www.unitedsoybean.org.
38. Oak Ridge National Laboratory, Argonne National Laboratory, Pacific Northwest National Laboratory, National Renewable Energy Laboratory, and Applied Carbochemicals, Inc. (1999), CRADA Final Report for CRADA ORNL 96-0407.
39. Zeikus, J. G., Jain, M. K., and Elankovan, P. (1999), *Appl. Microbiol Biotechnol*. **51,** 545–552.
40. Berglund, K. A., Alizadeh, H., and Dunuwila, D. D. (2001), US patent no. 6,287,480 B1.
41. Coleman, R. (2001), US patent no. 6,218,336 B1.

42. Wood, A. (2003), *Chemical Week* **165(13),** 46.
43. (2002), Chemical Market Reporter, August 19–26, 12.
44. (2002), *Chemical Market Reporter*, September 23, 29.
45. Ritter, S. (2001), *C&E News*, January 1.
46. Reed Business Information. *Chemical News and Intelligence*. Website: http://cnionline.com.
47. Gokarn, R. R., Selifonova, O. V., Jessen, H., Gort, S. J., Selmer, T., and Buckel, W. (2002), International Patent Application, World Intellectual Property Organization, WO 02/42418 A2.
48. Ashford, R. D. (2001), *Ashford's Dictionary of Industrial Chemicals,* 2nd Ed., Wavelength Publications, London, UK.
49. (1999), *Chemical Market Reporter* **256(1),** 41.
50. Danner, H. and Braun, R. (1999*), Chem. Soc. Rev*. **28,** 395–405.
51. US DOE. (2001), Small Business Innovation Research and Small Business Technology Transfer Program, Public Abstract 58, grant no. DE-FG02-00ER86106, US Department of Energy, Website: http://www.science.doe.gov/sbir/#T2.
52. Yulex Corporation. (2002), Website: http://www.yulex.com/about.html.
53. Cornish, K., Brichta, J. L., Yu, P., Wood, D. F., McGlothlin, M. W., and Martin, J. A. (2001), *Agro-Food-Industry Hi-Tech*, November/December.
54. Wood, M. (2002), *Agricultural Research Magazine*, April.
55. US Department of Agriculture, Small Business Innovation Research, Cooperative State Research, Education, and Extension Service. "FY 2002 Phase I Public Abstract," Website: http://www.reeusda.gov/sbir/.

0273-2289/04/115/0887–0898/$25.00

Continuous Production of Butanol by *Clostridium acetobutylicum* Immobilized in a Fibrous Bed Bioreactor

Wei-Cho Huang,[1,2] David E. Ramey,[2] and Shang-Tian Yang*[,1]

[1]Department of Chemical Engineering, Ohio State University, 140 West 19th Avenue, Columbus, OH 43210, E-mail: yangst@che.eng.ohio-state.edu; and [2]Environmental Energy Inc., PO Box 15, 1253 N. Waggoner Road, Blacklick, OH 43004

Abstract

We explored the influence of dilution rate and pH in continuous cultures of *Clostridium acetobutylicum*. A 200-mL fibrous bed bioreactor was used to produce high cell density and butyrate concentrations at pH 5.4 and 35°C. By feeding glucose and butyrate as a cosubstrate, the fermentation was maintained in the solventogenesis phase, and the optimal butanol productivity of 4.6 g/(L h) and a yield of 0.42 g/g were obtained at a dilution rate of 0.9 h^{-1} and pH 4.3. Compared to the conventional acetone-butanol-ethanol fermentation, the new fermentation process greatly improved butanol yield, making butanol production from corn an attractive alternative to ethanol fermentation.

Index Entries: ABE fermentation; butanol; *Clostridium acetobutylicum*; fibrous bed bioreactor; dilution rate.

Introduction

Fermentation processes using anaerobic microorganisms provide a promising path for converting biomass and agricultural wastes into chemicals and fuels *(1)*. Acetone-butanol-ethanol (ABE) fermentation with the strict anaerobic bacterium *Clostridium acetobutylicum* was once (1917–1955) one of the largest fermentation processes ever developed in industry. However, with a few exceptions, anaerobic fermentation processes for production of fuels and chemicals, including ABE fermentation, usually suffer from a number of serious limitations including low yields, low productivity, and low final product concentrations *(2,3)*. It is unlikely that the fer-

*Author to whom all correspondence and reprint requests should be addressed.

mentation route will become competitive with petroleum-based solvent synthesis unless some of these limitations can be overcome *(4)*. However, U.S. legislation to produce strategic chemicals, fuels, and energy from domestic renewable resources and the need to lessen the dependence on the diminishing petroleum supplies have resulted in the renaissance of the fermentation process as a possible source of solvents *(5–7)*.

Butanol has many characteristics that make it a better fuel extender than ethanol, now used in the formulation of gasohol *(8)*. It can solve many problems associated with the use of ethanol. Butanol has the following advantages over ethanol:

1. It has 25% more British thermal units per gallon.
2. It is less evaporative/explosive with a Reid vapor pressure 7.5 times lower than ethanol.
3. It is safer than ethanol because of its higher flash point and lower vapor pressure.
4. It has a higher octane rating *(9)*.
5. It is more miscible with gasoline and diesel fuel but less miscible with water *(10)*.

Petroleum-derived butanol is currently used in food and cosmetic industries as an extractant *(11)*, but there are concerns about its carcinogenic aspects associated with the residual petroleum components. Many new uses will occur in these fields as "green" butanol becomes available to the market. Other uses include current industrial applications in solvents, rubber monomers, and break fluids. Butanol has the propensity to solve some infrastructure problems associated with fuel cell use. Dispersed through existing pipelines and filling stations and then reformed onboard the fuel cell vehicle, butanol offers a safer fuel with more hydrogen.

The present study on butanol fermentation has been focused primarily on the effects of pH and dilution rate *(D)* in continuous cultures of the mutant strain from *C. acetobutylicum* ATCC 55025. To overcome the problems of low productivity and yield of butanol, cell immobilization in a convoluted fibrous bed bioreactor (FBB) and feeding with dextrose and butyric acid as cosubstrates to produce butanol and reduce production of ancillary byproducts were used in the fermentation. By changing the dilution rate from 0.1 to 1.2 h^{-1} at pH 4.3 and varying the pH from 3.5 to 5.5 at the dilution rate of 0.6 h^{-1}, the optimal conditions for high productivity and butanol yield were investigated.

Materials and Methods

Bacterial Culture and Medium

C. acetobutylicum ATCC 55025 was cultured in 38 g/L of Reinforced Clostridial Medium (Oxoid CM149; Oxoid Limited, Hampshire, England) supplemented with 20 g/L of glucose (Sigma, St. Louis, MO).

Oxoid Reinforced Clostridial Medium has the following typical formula: 3.0 g/L of yeast extract, 10.0 g/L of "Lab-Lemco" powder, 10.0 g/L

of peptone, 1.0 g/L of soluble starch, 5.0 g/L of glucose, 0.5 g/L of cysteine hydrochloride, 5.0 g/L of sodium chloride, 3.0 g/L of sodium acetate, and 0.5 g/L of agar.

The medium was autoclaved at 121°C and 15 psig for 20 min. A butyric acid medium was used in the fermentation study. The butyric acid medium was prepared in an 18-L vessel (Kimax) and consisted of 7.0 g/L of CM149, 50–67 g/L of dextrose, and 3 to 4 g/L of butyric acid. The solution of dextrose and CM149 were autoclaved separately to prevent caramelization, a browning reaction, and then blended and sealed shortly after autoclaving to reduce oxygen contamination. After cooling, sterile nitrogen was added to break the vacuum formed during cooling. Reagent-grade butyric acid at 3 to 4 g/L (Aldrich) and 1 mL of 1 *N* Na_2S solution were added aseptically via filter membrane. The medium in the vessel was kept anaerobic by initially sweeping filtered oxygen-free N_2 across the surface and then by continuously keeping a low head pressure using a nitrogen-filled elastic bladder, which prevented vacuum formation as the medium was transferred out during the continuous fermentation study. The pH of the medium was adjusted between 3.5 and 5.5, depending on the fermentation conditions studied, by adding 12 *N* HCl or 5 *N* NaOH.

Fibrous Bed Bioreactor

Figure 1 shows the experimental setup of the continuous FBB system with medium recirculation. The FBB was made of a jacketed glass column (total volume: 800 mL) packed with a spiral wound fibrous matrix (packed volume: 200 mL) *(12)*. Before use, the reactor was sterilized at 121°C and 15 psig for 30 min and then cooled to room temperature while purging with sterile filtered nitrogen for 1 h to ensure that anaerobic conditions were attained inside the reactor. The reactor was then filled with 700 mL of sterile medium containing 20 g/L of dextrose. The medium of the pH was adjusted to 5.4 using 1 *N* NaOH or HCl, and the reactor temperature was controlled at 35°C. The medium was continuously circulated at 20–50 mL/min via a peristaltic pump and flushed with filtered nitrogen to ensure anaerobiosis. The reactor was then inoculated with the cells by injecting 3 mL of a stock culture, and approx 2 to 3 d were allowed for cell growth and immobilization in the fibrous matrix. Once solventogenesis occurred, the butyric acid medium described earlier was fed into the FBB continuously.

Fermentation Kinetics Study

The fermentation kinetics, mainly in solventogenesis phase, was studied with the FBB fed continuously with the butyric acid medium under strict anaerobiosis. The effects of pH (3.5–5.5) and dilution rate (0.1–1.2) were studied at 35°C with two FBBs. These two FBBs, reactor L and R, were used in parallel experiments to ensure the reproducibility of the data. The reactor performance at various dilution rates was first studied at pH 4.3. The effect of pH was then studied at a fixed dilution rate of 0.6 h^{-1}. For each condition studied, the reactor was operated under a constant feed condi-

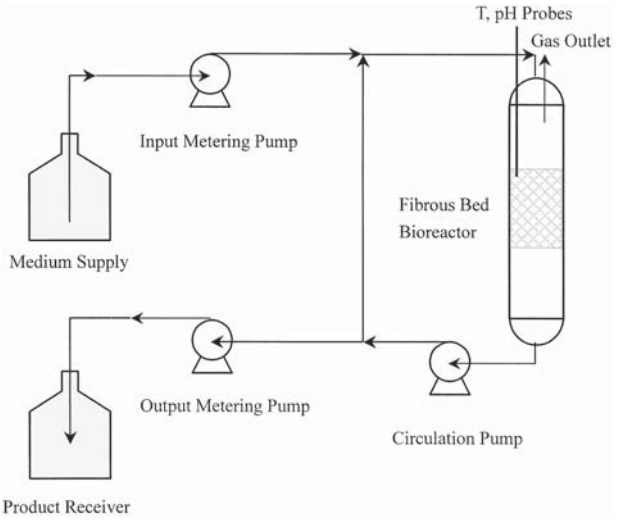

Fig 1. Continuous FBB system for ABE fermentation.

tion for ~100 h to allow the reactor to reach pseudo steady state before changing to the next feed condition. The dilution rate was estimated based on the reactor packed volume of 200 mL. With continuous medium recirculation and bubbling gas production in the fermentation, the reactor was sufficiently mixed and can be assumed to be well mixed.

Analytical Methods

At specified time intervals, 1 mL of sample was drawn aseptically. The cell density (data not shown) in the fermentation broth was measured by optical density (OD) at a 600-nm wavelength with a spectrophotometer (Model 3400; Sequoia-Turner, Mountain View, CA). The pH was measured with a pH/ORP Controller (model 5652-10; Cole Parmer, Vernon Hills, IL).

After removing the bacterial cells by centrifuging at 16,100*g* for 5 min, the clear fermentation broth was subjected to analysis for residual glucose and product concentrations. Glucose concentration was measured using a YSI model 2700 Select Biochemistry Analyzer (Yellow Springs, OH).

Acetone, butanol, ethanol, acetic acid, and butyric acid were determined using a gas chromatograph (Varian 3400 GC) equipped with a flame ionization detector and an SP4270 integrator. The glass column (2 m × 2 mm) (Supelco, Bellefonte, PA) was packed with 80/120 Carbopack BAW/6.6% Carbowax 20M. The oven temperature was programmed from 100°C to 185°C at a rate of 15°C/min after an initial holding time of 1 min. The injector and detector temperatures were set at 200 and 225°C, respectively. Nitrogen was the carrier gas, set at a flow rate of 20 mL/min.

Results

Effects of Dilution Rate

Figure 2 shows the concentration profiles of the outlet streams from the reactors operated at various dilution rates with the feed medium at pH 4.3. After the initial growth phase and the feed medium had been changed to butyric acid medium, reactor L was operated by gradually increasing the dilution rate from 0.1 to 0.3 h^{-1} at 102 h, 0.5 h^{-1} at 201 h, and 1.0 h^{-1} at 311 h, and then dropped to 0.8 h^{-1} at 407 h before increasing again to 1.2 h^{-1} at 503 h. By contrast, reactor R was initially operated at 0.9 h^{-1} and then gradually decreased to 0.6 h^{-1} at 109 h, 0.4 h^{-1} at 205 h, and 0.2 h^{-1} at 301 h. The dilution rate was then increased to 0.7 h^{-1} at 407 h and again to 1.1 h^{-1} at 500 h. As can be seen in Fig. 2, the outlet concentrations of substrates and products changed as the dilution rate changed and in general, they fluctuated before approaching a pseudo steady state toward the end of each operating condition period.

Although a clear steady state was not always achieved, there were clear trends in solvent production and substrate utilization as affected by the dilution rate. In general, as the dilution rate increased from 0.1 to 1.2 h^{-1}, the outlet concentrations of glucose, butyrate, and acetate also increased, whereas the concentrations of acetone, ethanol, and butanol decreased (reactor L). Consistent trends in reactor responses to decreasing the dilution rate were also observed (reactor R). These were expected results since at a higher dilution rate, the medium had shorter contact time with cells and, therefore, less substrates were consumed with less products formed in the fermentation. The highest concentration of butanol produced in the fermentation was 12.5 g/L at a dilution rate of 0.1 h^{-1}, whereas a low butanol concentration of ~3.5 g/L was obtained at higher dilution rates of 0.8–1.2 h^{-1}. The acetone concentration was approximately half that of butanol on average, consistent with the reported product ratio of 3:6:1 for ABE fermentation. On the other hand, ethanol production was relatively low compared to the other products. Note that the butyrate concentration in the reactor outlet was always lower than that in the feed medium, indicating that butyrate also was used as a carbon source in the solventogenic fermentation. However, a significant amount of acetate was still produced in the fermentation, especially at high dilution rates when there was significant cell growth or acidogenesis. As the dilution rate decreased, acetate concentration also decreased because the acetate produced in acidogenesis was reconsumed in solventogenesis.

The reactor volumetric productivities and product yields at pH 4.3 and various dilution rates were estimated based on the time course data in the pseudo steady state and are shown in Fig. 3. In general, production rates for butanol and acetate increased with an increase in the dilution rate from 0.1 to 1.2 h^{-1}, whereas acetone and ethanol remained relatively unaffected by the dilution rate except at 0.1 h^{-1}. A maximum butanol productivity of 4.6 g/(L·h) at a dilution rate of 0.9 h^{-1} was obtained with reactor R at the beginning of the solventogenic fermentation, whereas a lower productivity of

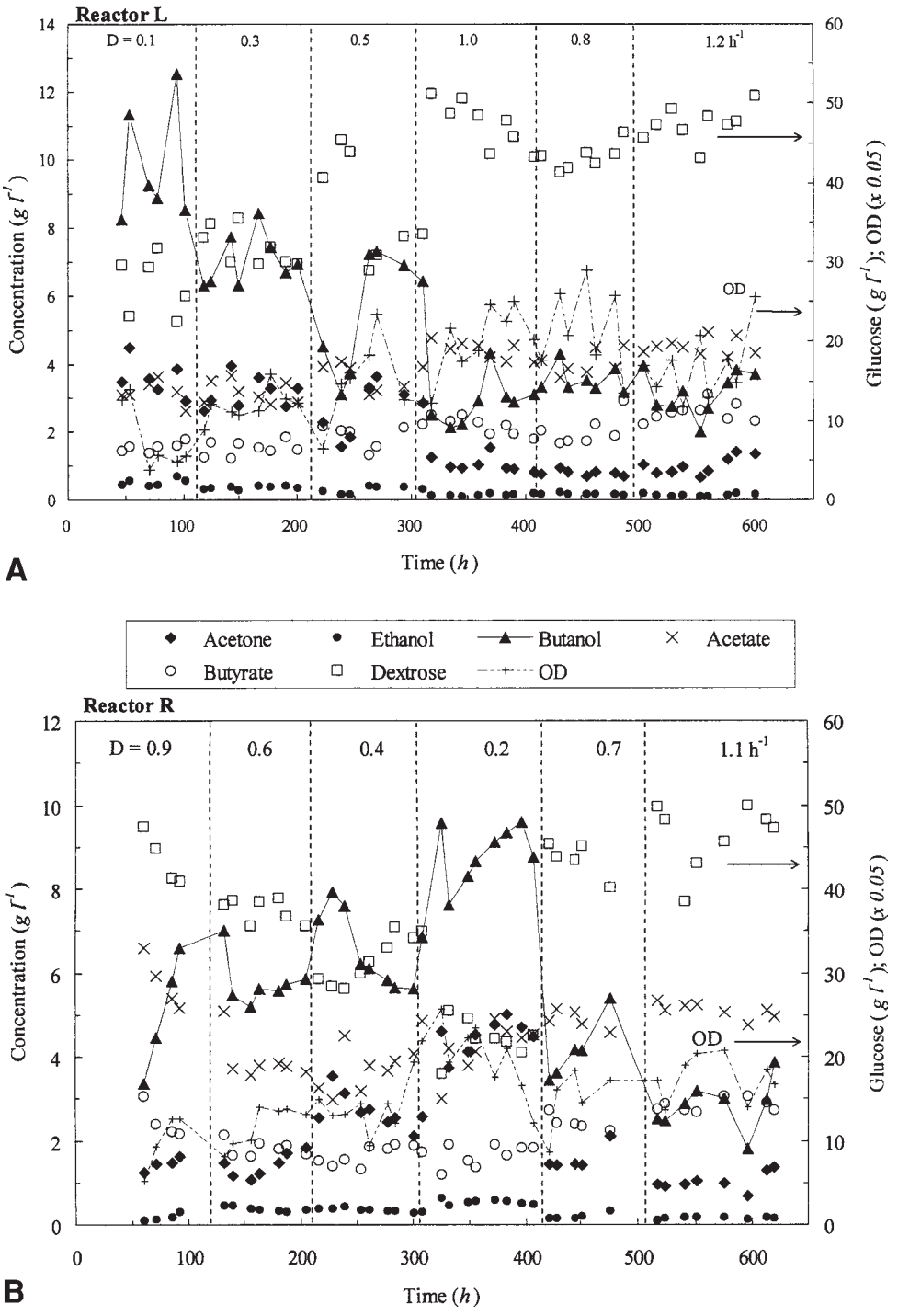

Fig. 2. Kinetics of continuous ABE fermentation at various dilution rates and pH 4.3. Glucose and OD are on the right axis; acetone, butanol, ethanol, acetate, and butyrate are on the left axis. **(A)** Reactor L; **(B)** reactor R.

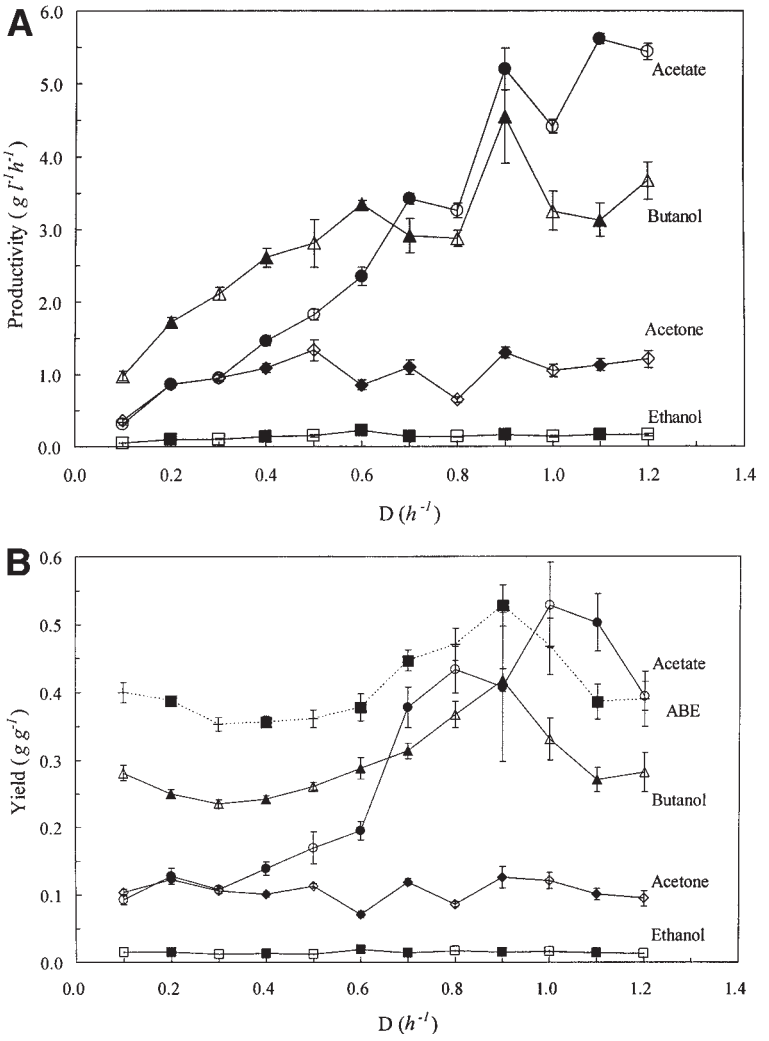

Fig. 3. Effects of dilution rate on productivities and product yields at pH 4.3. Open symbols: reactor L; solid symbols: reactor R. **(A)** Productivity; **(B)** yield.

~3.3 g/(L·h) at higher dilution rates was obtained after the reactor had been operated for a long period. It is not clear if the large difference was attributed to the effect of dilution rate or the culture age. Butanol is a strong inhibitor to the fermentation. A lower butanol productivity at a lower dilution rate where the butanol concentration was higher is therefore expected. The increased acetate productivity with an increase in the dilution rate was consistent with the higher cell growth rate because acetate is the main product in the acidogenic phase during which cell growth also occurs.

The product yields from glucose in the fermentation were based on the total consumption of glucose and butyrate, and each gram of butyric acid consumed was considered as 2 g of glucose in the feed since the butyric acid yield from glucose in butyric acid fermentation was ~50% *(12)*. As can be seen in Fig. 3B at pH 4.3, the butanol yield decreased slightly as the dilution rate increased from 0.1 to 0.3 h^{-1} but then increased with an increase in the dilution rate until reaching the maximum value of 0.42 g/g at 0.9 h^{-1}. The butanol yield was lower as the dilution rate continued to increase to 1.2 h^{-1}. By contrast, acetone and ethanol yields appeared to be not significantly affected by the dilution rate. The overall yield of solvents (acetone, butanol, and ethanol) was ~0.4 g/g, with a maximum value of 0.53 g/g obtained at 1.0 h^{-1}. The average product yields at all dilution rates studied were found to be 0.27, 0.12, and 0.015 g/g for butanol, acetone, and ethanol, respectively.

Effects of pH

After 606 h, the dilution rate in reactor L was decreased from 1.2 to 0.6 h^{-1}. When the pH was adjusted to 3.5 at 623 h, the concentrations of acetone, butanol, and ethanol decreased dramatically and reduced to almost 0 g/L by 700 h (*see* Fig. 4A). In the meantime, the concentrations of glucose and butyric acid increased with time to reach almost their feed concentrations. Coupled with the low OD value, these findings make it apparent that the fermentation had almost ceased at this low pH value.

However, the trends were reversed and the reactor started to recover after the feed pH was increased to 3.8 at 726 h. The product concentrations (ABE) continued to increase while substrates decreased as the feed pH was increased to 4.0 at 887 h. For reactor R, after reducing the dilution rate from 1.1 to 0.6 h^{-1} and increasing the feed pH from 4.3 to 5.3 at 661 h, the concentration of butanol increased rapidly and the concentrations of glucose and butyrate reduced (*see* Fig. 4B). This trend appeared to continue with time, although it slowed down as the pH changed to 4.7 at 733 h, even though the pH decreased to 4.5 at 795 h and then increased to 5.1 at 901 h, reaching a significantly higher butanol concentration of ~7.7 g/L at 956 h. The observed effects probably were mainly attributed to the change in the dilution rate and much less to the pH in the range studied (4.5–5.3). However, a further increase in the feed pH to 5.5 at 1028 h abruptly decreased butanol production in the fermentation, and the concentration of butanol dropped to below 4 g/L, with a corresponding increase in the glucose concentration. For both reactors, the concentration of acetic acid appeared to increase somewhat with an increase in the pH, consistent with the fact that acidogenesis is generally favored at a higher pH.

Although steady state might not have been reached in certain operating pH conditions studied, the productivities and product yields at the dilution rate of 0.6 h^{-1} and various feed pH values were estimated and are shown in Fig. 5. In general, the reactor productivity for butanol increased with an increase in the pH until reaching a maximum value of 4.6 g/(L·h)

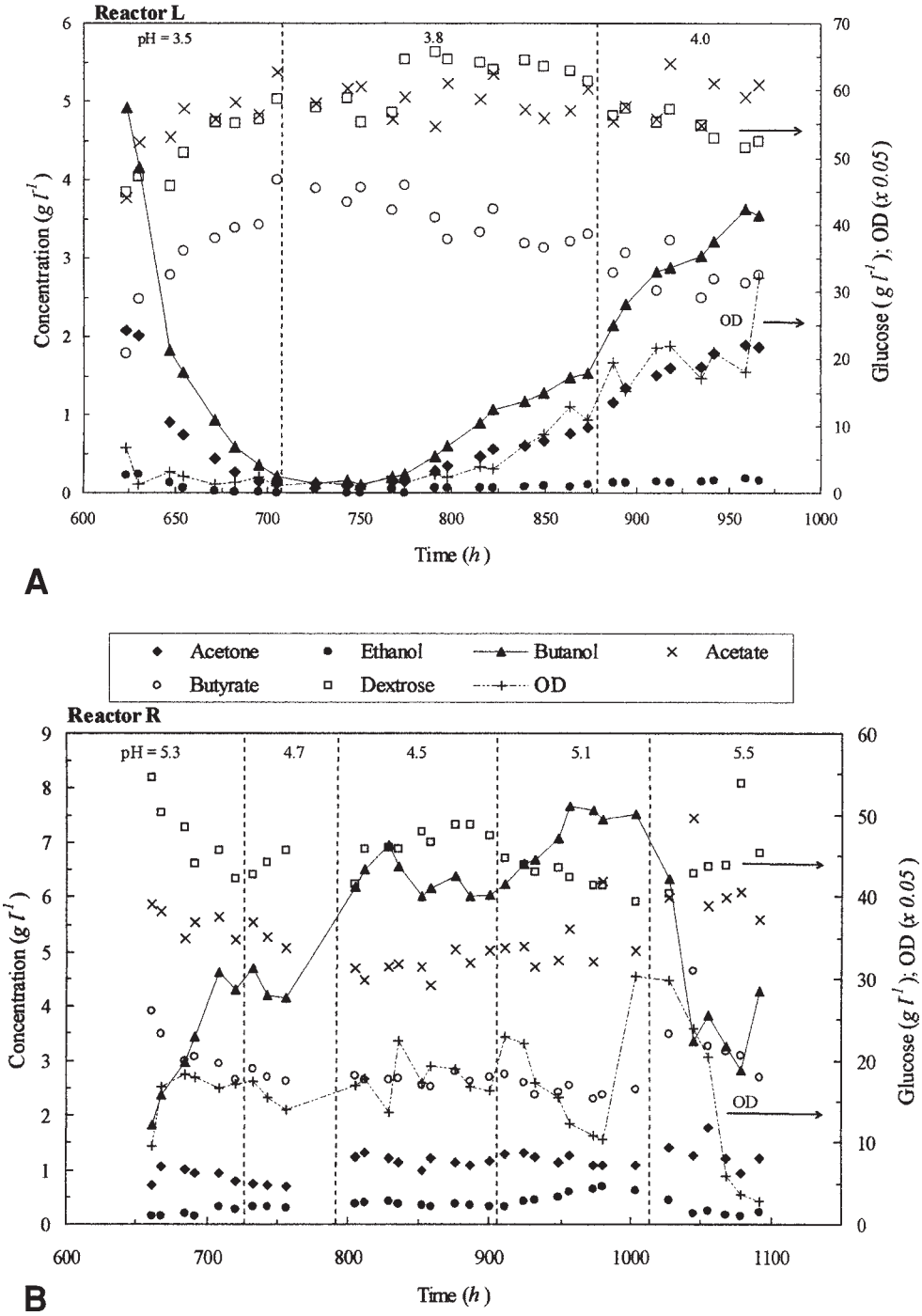

Fig. 4. Kinetics of continuous ABE fermentation at various pH values and 0.6 h^{-1} dilution rate. Glucose and OD are on the right axis; acetone, butanol, ethanol, acetate, and butyrate are on the left axis. **(A)** Reactor L; **(B)** reactor R.

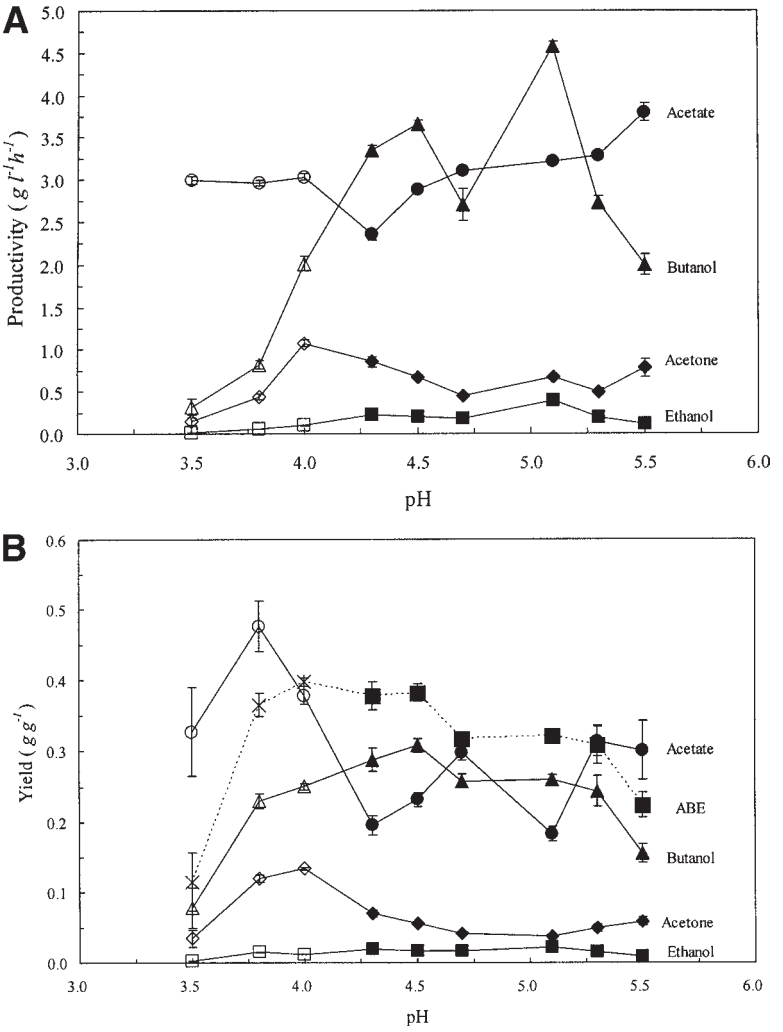

Fig. 5. Effects of pH on productivities and product yields at D = 0.6 h^{-1}. Open symbols: reactor L; solid symbols: reactor R. **(A)** Productivity; **(B)** yield.

at pH 5.1, but then it decreased as the pH increased further to 5.5. The effect of pH on the butanol yield appeared to be small in the range of 3.8–5.3, although the maximum value was found at pH 4.5. Butanol yield was significantly lower at pH 5.5, which is usually considered to be the pH value more favorable to acidogenesis. Both the productivity and butanol yield were low at pH 3.5, which appeared to be the lower limit for ABE fermentation. Acetone and ethanol production appeared to be much less sensitive to the pH in the range studied.

Discussion

Optimizing the ABE fermentation process has long been the aspiration of more than a century of research. Conventionally, the profitability of fermentation is influenced by the type and concentration of substrate, dilution rate, pH, culture medium, and product recovery. Even using cell recycle, cell immobilization, or extractive fermentation to increase cell density and productivity, the yield of the combined ABE production never exceeded 0.44 g/g *(13–15)*.

The production of butanol is usually associated with the uptake of various acids. In the present, we developed a continuous fermentation that improved the uptake of butyric acid and glucose by *C. acetobutylicum* in the FBB. The production of butanol via butyric acid converted from carbohydrates was efficient owing to the high density of viable cells maintained in the FBB through continual cell renewal *(16)*. An optimal butanol yield of 0.42 g/g and a productivity of 4.6 g/(L·h) were obtained in a 200-mL FBB at a dilution rate of 0.9 h^{-1}, pH 4.3, and 35°C with 54 g/L of glucose and 3.6 g/L of butyric acid in the feed stream. The concentration of butanol was 5.1 g/L on average. The conversions of glucose and butyric acid were 0.19 and 0.31, respectively. The optimum solvent (ABE) yield was 0.53 g/g under the same process conditions.

The higher butanol and total solvent yields obtained in our study can be attributed to feeding with butyrate as a cosubstrate, which greatly reduced acidogenesis and promoted solventogenesis. The increased butanol yield also could be owing to the dramatically reduced ethanol production. In addition, cell immobilization in the FBB allowed the bacteria to survive long in the solventogenic phase, allowing for long-term continuous solvent production without frequent cell regeneration.

Our study has shown that doubling the yield of butanol to approx 2.5 gal/bushel of corn (0.37 L/kg) in the conventional ABE fermentation can be achieved by converting carbohydrates into mainly butanol, which can make fermentation-derived butanol economically competitive with petrochemically derived butanol. Compared to the conventional ABE fermentation (the optimum butanol yield of 0.25 g/g and productivity of 4.5 g/(L·h), the FBB notably enhanced the yield of butanol and ABE (more than 68 and 20%, respectively) by *C. acetobutylicum*, making butanol production from renewable resource an attractive alternative to ethanol fermentation. Commercialization of this new technology has the propensity to reduce our the United States's dependence on foreign oil, protect its fuel generation grid from sudden disruption, develop its agricultural base, solve the hydrogen supply problem associated with fuel cells, and help reduce global warming.

Acknowledgments

We acknowledge Ying Zhu for helping to provide the information about butyric acid fermentation. This research was supported in part by a grant from the Department of Energy (DE-FG02-00ER86106).

References

1. Minton, N. P. and Clarke, D. J. (1989), *Clostridia, Plenum*, New York, NY.
2. Soni, B. K., Soucaille, P., and Goma, G. (1987), *Appl. Microbiol. Biotechnol*. **25,** 317–321.
3. Garcia, A., Ianotti, E. L., and Fischer, J. L. (1986), *Biotechnol. Bioeng*. **28,** 785–791.
4. Durre, P. (1998), *Appl. Microbiol. Biotechnol*. **49,** 639–648.
5. Mollah, A. H. and Stuckey, D. C. (1993), *J. Chem. Tech. Biotechnol.* **56,** 83–89.
6. Qureshi, N., Schripsema, J., Lienhardt, J., and Blaschek, H. P. (2000), *World J. Microbiol. Biotechnol*. **16(4),** 377–382.
7. Huang, J. and Meagher, M. M. (2001), *J. Membrane Sci*. **192,** 231–242.
8. Mollah, A. H. and Stuckey, D. C. (1993), *Enzyme Microb. Technol*. **15,** 200–207.
9. Ladisch, M. R. (1991), *Enzyme Microb. Technol*. **13,** 280–283.
10. Park, C.-H., Okos, M. R., and Wankat P. C. (1989), *Biotechnol. Bioeng*. **34,** 18–29.
11. Qureshi, N. and Blaschek, H. P. (1999), *Biotechnol. Prog*. **15,** 594–602.
12. Zhu, Y., Wu, Z., and Yang, S.-T. (2002), *Process Biochem*. **38(5),** 657–666.
13. Qureshi, N., Maddox, I. S., and Friedl, A. (1992), *Biotechnol. Prog*. **8,** 382–390.
14. Qureshi, N. and Blaschek, H. P. (2000), *Appl. Microbiol. Biotechnol*. **84–86,** 225–235.
15. Qureshi, N. and Blaschek, H. P. (2001), *Renewable Energy* **22,** 557–564.
16. Zhu, Y. and Yang, S.-T. (2003), *Biotechnol. Prog*. **19,** 365–372.

0273-2289/04/115/0899–0912/$25.00

Lipopeptide Surfactant Production by *Bacillus subtilis* Grown on Low-Cost Raw Materials

Fabíula A. S. L. Reis, Eliana Flavia C. Sérvulo,* and Francisca P. De França

Escola de Química, Universidade Federal do Rio de Janeiro, Centro de Tecnologia, Bloco E, Ilha do Fundão, 21.949-900, Rio de Janeiro, RJ, Brazil, E-mail: servulo@eq.ufrj.br

Abstract

The production of biosurfactant by *Bacillus subtilis* ATCC 6633 was investigated using commercial sugar, sugarcane juice and cane molasses, sugarcane juice alcohol stillage, glycerol, mannitol, and soybean oil. Commercial sugar generated the minimum values of surface tension, with the best results (28.7 mN/m, (relative critical micelle concentration [CMC^{-1}] of 78.6) being achieved with 10 g of substrate/L in 48 h. At a pH between 7.0 and 8.0, a higher production of surface-active compounds and a greater emulsifier activity was also observed. Enrichment of the culture medium with trace minerals and EDTA showed maximum yields, whereas supplementation with yeast extract stimulated only cell growth. The kinetic studies revealed that biosurfactant production is a cell growth–associated process; surface tension, CMC, and emulsification index values of 29.6 dyn/cm, 82.3, and 57%, respectively, were achieved, thus indicating that it is feasible to produce biosurfactants from a renewable and low-cost carbon source.

Index Entries: Biosurfactant; *Bacillus subtilis;* lipopeptide; surfactin; raw materials; commercial sugar.

Introduction

Surfactants are amphiphilic molecules widely used for different purposes in industrial processes, with a worldwide annual demand of about $10 billion *(1,2)*. The most used surfactants are produced from petrochemical sources *(3)*; however, compounds having surface activity characteristics may be synthetized by a wide variety of microorganisms *(4,5)*. Such compounds, called biosurfactants, when compared with the syn-

*Author to whom all correspondence and reprint requests should be addressed.

thetic ones offer important advantages such as biodegradability, low toxicity, and high specificity *(6,7)*. Furthermore, because some biosurfactants also present good thermal and chemical (pH, salinity) characteristics, they may be suited for environmental applications such as bioremediation, dispersion of oil spills, transportation of crude oil, heavy metal removal, and *in situ* microbial oil recovery *(7–14)*. In addition, biosurfactants can be used in a variety of food-processing, cosmetic, agricultural and pharmacologic applications *(15,16)*.

Among the microbial surfactant producers, *Bacillus subtilis* strains generate a lipopeptide called surfactin, one of the most effective biosurfactants known. This biomolecule is usually a cyclic compound consisting of seven amino acids bonded to a lipid moiety. Surfactin is effective in lowering the surface tension of water to <30 dyn/cm *(17)*, which is comparable with the values obtained by conventional synthetic surfactants. Additionally, surfactin preparations have other interesting characteristics, including antibiotic and antiviral properties *(18)*. In fact, surfactin is one of the few biosurfactants that has found commercial use *(19)*.

Despite the advantages of biosurfactants, they will not replace the synthetic ones unless there is a great improvement in biosurfactant production technology in order to reduce its costs. Thus, the use of renewable, readily available, and relatively inexpensive raw materials, considering that *B. subtilis* may synthesize biosurfactants from different carbon sources *(20,21)*, may account for the feasibility of this bioprocess.

Moreover, the establishment of fermentation conditions to maximize biosurfactant yield and productivity is essential for cost reduction and the large-scale production. Some previous works have evidenced some peculiarities about biosurfactant production. For instance, reports have appeared dealing with the use of locally available agricultural and food-processing residuals for promoting biosurfactant synthesis by different microorganisms *(21–24)*. Cooper et al. *(20)* have demonstrated that certain metals enhanced surfactant production by *B. subtilis*. In addition, the yield of the lipopeptide herbicolina A, produced by *Erwinia herbicola* A111 strain, was affected by the addition of amino acids or fatty acids but the structure of the molecule was not *(25)*. The aim of the present study was to evaluate the production of biosurfactant by *B. subtilis* ATCC 6633 using low-cost substrates in different culture conditions.

Materials and Methods

Microorganism

B. subtilis 6633, obtained from American Type Culture Collection (ATCC), provided by Dr. Leon Rabinovitch (Instituto Oswaldo Cruz/FIOCRUZ), was maintained on nutrient agar (Difco 0003) slants at 4ºC.

Media

Experiments on growth and biosurfactant production were performed on a mineral salt medium *(26)* containing 2.0 g/L of $NaNO_3$, 0.1 g/L of KCl,

0.5 g/L of KH_2PO_4, 1.0 g/L of K_2HPO_4, 0.01 g/L of $CaCl_2$, 0.5 g/L of $MgSO_4 \cdot 7H_2O$, and 5 mL of a trace metals solution *(27)*.

The initial pH of the medium was adjusted to 7.0. All chemicals were of analytical grade. The carbon sources (commercial sugar–sucrose, sugarcane juice and molasses, sugarcane juice alcohol stillage, glycerol, mannitol, soybean oil) were added in order to establish an initial substrate concentration of 20 g/L. In some cases, the medium was also aseptically supplemented with 0.1% (w/v) yeast extract and 0.001% (w/v) Na EDTA previously and separately sterilized by filtration through a Millipore membrane with a pore size of 0.22 μm.

Culture Conditions

The experiments were carried out using two types of vessels. Most experiments used 500-mL Erlenmeyer flasks, each containing 100 mL of the mineral salt medium, just described. Incubation was carried out in a rotary shaker at 150 rpm and 30°C for 48 h. For kinetics experiments, a 2-L MultiGen Fermentor (New Brunswick, Scientific) containing 1 L of medium was used. Temperature was controlled at 30°C, and aeration and agitation were set at 1 vvm and 300 rpm, respectively. For quantification analysis, culture samples were first centrifuged (10,000*g* for 15 min at 4°C) to remove cells. The culture supernatants obtained were stored at 4°C until monitored for surface tension, emulsification index, (E_{24}) and biosurfactant concentration, which was determined by relative critical micelle concentration (CMC^{-1}). The data presented represent the average of at least four measurements.

Inocula were prepared by adding a loopful of cells from the stock culture to 100 mL of Difco nutrient broth and incubating at 30°C for 16 h on a rotatory shaker at 150 rpm. Inoculation volumes corresponding to about 0.04 g/L of exponential-phase cells were used.

Analytical Methods

Biomass

The cell concentration was determined by dry weight by filtering through a 0.22-μm previously weighted Millipore membrane. Filtered samples of 5 mL culture broth under vaccuum, after being washed with 3 vol of distilled water (to remove broth components), were dried in a microwave until reaching constant weight *(7)*. The dry weights of sugarcane juice, molasses, and stillage media were also determined in the same manner, and the respective values accounted for biomass obtained in those nutritional conditions.

Sugar

Substrate concentration was measured enzymatically by the glucose oxidase method (Glucose Method God-Pap-Merck), based on the oxidation of glucose to gluconic acid and hydrogen peroxide. Samples of fermented broth were first centrifuged for cell removal and then hydrolyzed, after adequate dilution, by treating with 2 N HCl (1:1) and heating at 65–70°C for 10 min *(28)*.

Surface Tension

The changes in the culture's surface tension were evaluated by the ring Du Nouy method *(29)* using a SIGMA70 system unit (KSV Instruments, Trumbull, CT) tensiometer. Measurements were performed at 25ºC. The decrease in surface tension was used as a qualitative measurement of surfactant concentration and a quantitative indicator of efficiency.

Emulsification Index

The emulsifier activity of culture broth was determined according to Cooper and Goldenberg *(30)*. Four milliliters of cell-free culture samples was added to 6 mL of kerosene, vigorously mixed with a vortex for 2 min, and left undisturbed to stand for 24 h at room temperature. The E_{24} is given as a percentage of the height of emulsified layer (cm) divided by the total height of the liquid column *(31)*.

Critical Micelle Concentration

The biosurfactant yield was evaluated by CMC^{-1}. The CMC values were determined by measuring the surface tension for varying dilutions of cell-free broth (after centrifugation). The logarithms of the dilutions were plotted as a function of surface tension. The CMC is the point of abrupt increase in surface tension *(15)*. The surfactant concentration is a function of the inverse of CMC, i.e., CMC^{-1}.

Results and Discussion

Effect of Carbon Source

Table 1 presents the average values of cell growth and reduction in surface tension produced by *B. subtilis* ATCC 6633 using different carbon sources (commercial sugar, sugarcane juice and molasses, sugarcane juice alcohol stillage, glycerol, mannitol and soybean oil). When saccharine raw materials were used (commercial sugar and sugarcane juice), cell growth was favored similarly to that observed with glucose. However, in the presence of sugarcane molasses, biomass production doubled, demonstrating that such raw materials stimulate the microorganism's activity. The lipidic raw material (soybean oil) enhanced cell growth, reaching a value 37% greater than when glucose was used. Stillage, however, was not able to support growth of the *B. subtilis* strain, probably because of the presence of inhibitors to the bacterial metabolism. On the other hand, separate addition of polyalcohols such as glycerol and mannitol, which are stillage components, has caused less harmful effects on cell growth.

All carbon sources tested have favored extracellular production of active surface agent by *B. subtilis* ATCC 6633, which was estimated by the reduction in surface tension of the fermented broth. However, except for stillage, there was no relationship between cell growth and biosurfactant production. Similar results were reported by other investigators *(21,32,33)* not only with *B. subtilis* strains, but also with other species of bacteria. The

Table 1
Effect of Different Substrates on Growth
and Biosurfactant Production by *B. subtilis* ATCC 6633 [a]

Carbon source	Final pH	Biomass (g/L) [b]	Surface tension (dyn/cm) [c]
Glucose	8.0	2.4 ± 0.2	32.1 ± 0.6 (68.3)
Commercial sugar	8.0	2.0 ± 0.1	30.6 ± .09 (68.8)
Sugarcane juice	8.0	2.5 ± 0.2	34.8 ± 0.6 (42.4)
Sugarcane molasses	7.5	4.4 ± 0.6	34.4 ± 0.8 (52.5)
Stillage	7.6	0.6 ± 0.1	35.3 ± 1.3 (45.5)
Glycerol	7.7	1.3 ± 0.0	32.0 ± .07 (49.0)
Mannitol	7.9	1.9 ± 0.1	34.1 ± 0.9 (49.9)
Soybean oil	7.3	3.3 ± 0.5	35.3 ± 0.6 (50.4)

[a] Initial conditions: 20 g/L substrate concentration, 0.03 g/L cellular concentration; batch fermentation conditions: 100 mL of medium, pH 7.0, 150 rpm, 48 h.
[b] Mean ± SD.
[c] Values given in parentheses represent surface tension in culture broth before inoculation.

surface tension values differed concerning the raw material used, with the best results obtained with commercial sugar. The other sucrose raw materials (sugarcane juice and molasses) promoted different microorganism behavior regarding biosurfactant production. The probable presence of mineral salts in those carbon sources, mainly for molasses, may have favored cell growth to the detriment of biosurfactant production. Previous studies stated that biosurfactant is better produced in scarce quantities of certain elements such as amino acids *(34,35)*.

Makkar and Cameotra *(21)* comparing biomass and biosurfactant production by thermophilic strains of *B. subtilis* MTCC 2423 grown on different carbon sources, both soluble and insoluble, evidenced great variations in final concentrations of cells and lipopeptides. The maximum biomass values were reached for sucrose and hexadecane, 2.6 and 2.4 g/L respectively, whereas the bacterial growth on glucose resulted in only 1.85 g of cells/L. Low cell growth was also observed with the same bacteria growing on dodecane, decane, kerosene and sodium citrate, with values remaining between 0.34 and 0.75 g/L. The greatest reductions in surface tension—28, 29, and 30 dyn/cm—were achieved, respectively, when glucose, sucrose, and cow meat extract were used as carbon sources. In addition, although hexane favored cell growth, there was no evidence of biosurfactant production.

Other studies evidenced that *B. subtilis* ATCC 21332 was able to reduce the surface tension of potato and potato process effluents media below 36 dyn/cm, indicating surface activity from the production of surfactin *(23,24)*.

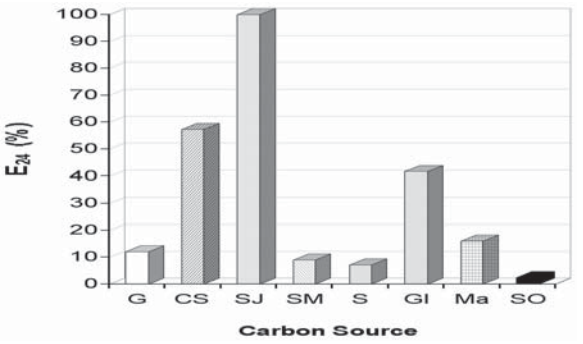

Fig. 1. E_{24} for surface-active compounds produced by *B. subtilis* ATCC 6633 in different substrates. G, glucose; CS, commercial sugar; SJ, sugarcane juice; SM, sugarcane molasses; S, sugarcane juice alcohol stillage; Gl, glycerol; Ma, mannitol; SO, soybean oil.

It was also found that potato alone could support growth, reducing the surface tension below 30 dyn/cm *(23)*.

As shown in Table 1 an increase in pH values was also observed. Fox and Bala *(23)* also noticed an increase in pH of different potato nonbuffered media from 6.2 to 8.5. Carvalho et al. *(36)* reported a similar behavior for *Planococcus citreus* growing on toluene, xylene, and olive oil.

A practical measurement of a surface-active compound utility is its ability to turn immiscible liquids into stable emulsions. Figure 1, shows that all samples were able to form stable emulsions with kerosene for 24 h. However, samples originated from glycerol, commercial sugar, and sugarcane juice were the most successful regarding emulsifying activity. Bacterial growth in mineral medium supplemented with commercial sugar yielded a biosurfactant with an E_{24} of 57.4%. This is a promising result compared with the values reported from biosurfactants produced by different microbial species. It should be emphasized that the best E_{24} was obtained with sugarcane juice as the raw material.

Effect of Initial pH

Certain microorganism have the ability to grow and produce biosurfactants in a wide pH range, rendering possible the microbial production of surfactant for *in situ* applications, such as bioremediation and enhanced oil recovery. According to Claus and Berkeley *(37)*, the active growth of *B. subtilis* was detected mainly in a pH range of 5.5–8.5, although this bacteria is able to grow at pH values lower or higher than these.

Figure 2 presents surface tension and E_{24} values obtained for fermented broth at different initial pH values in CS media. For all the pH values tested, a decrease in surface tension of the medium was noted before inoculation (62.5 dyn/cm) by the microorganism activity. These results indicate that the tested bacteria have the ability to produce biosurfactant at pH values ranging from 5.0 to 8.0 The minimum surface tension values of 30.1 and 31.5 dyn/cm were obtained when the medium's initial pH was 7.0 and 8.0, respectively.

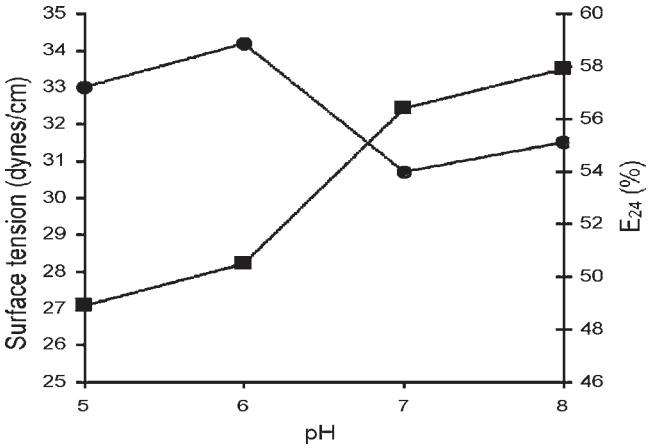

Fig. 2. Surface tension (●) and E_{24} (■) of *B. subtilis* ATCC 6633 fermented broth at various initial pH values, (20 g/L of commercial sugar, 0.03 g/L of initial cell concentration, 30ºC, 200 rpm, 48 h).

Regarding the emulsification index, it was observed the same behavior that is, all the fermented broth investigated, at all initial pH values tested, could emulsify kerosene forming stable emulsions. It has been also observed a relation between emulsification activity and initial pH, the best results been achieved for E_{24} at pH 7 (56,4%) and 8 (57,9%).

On the other hand, cell growth was not influence much by the initial pH value. For an initial pH of 5.0, the cell concentration attained was 3.6 g/L, and for the other initial pH values tested, cell growth remained about 2.5 g/L (data not shown).

Effect of Addition of Yeast Extract, Microsalts, and EDTA

The culture medium employed for biosurfactant production by *B. subtilis* generally presents similar chemical composition, being normally supplemented with microsalts varying, however, relative to the presence or absence of yeast extract and/or EDTA *(20,30,38)*. The addition of yeast extract is used in order to stimulate cell growth because it contains complex B vitamins, which are necessary to form enzymes and coenzymes, and also amino acids and other cell growth–stimulating compounds *(39,40)*. Furthermore, the addition of EDTA also may contribute to biosurfactant production *(41)*. EDTA acts at the cell wall, altering the cell wall's permeability or promoting biosurfactant removal when EDTA is attached to the wall, and/or can act as a metal-complexing agent to favor the metal's assimilation by the microorganism.

The addition of trace minerals (medium 2 and 3) considerably stimulated cell growth and had a stronger effect when yeast extract (medium 1) was added simultaneously, resulting in an increase of biomass in 40%, compared with medium 2 (Table 2). However, EDTA supplementation (medium 4) had practically no affect on cell growth, chiefly when it was

Table 2
Effect of Addition of Yeast Extract, Microsalts, and EDTA on Growth and Biosurfactant Production by *B. subtilis* ATCC 6633 [a]

Medium	Addition [b]			Final pH	Biomass (g/L) [c]	Surface tension (dyn/cm)	E_{24} (%)
	Yeast extract	Microsalts	EDTA				
1	Yes	Yes	Yes	8.4	3.5 ± 0.2	32.8 ± 0.7	49.4
2	No	Yes	Yes	8.2	2.3 ± 0.1	27.1 ± 0.8	51.2
3	No	Yes	No	8.2	2.6 ± 0.1	28.9 ± 0.8	51.8
4	No	No	Yes	8.2	1.4 ± 0.1	29.0 ± 0.9	39.8
5	No	No	No	8.3	0.9 ± 0.1	28.7 ± 1.0	47.8

[a] Initial conditions: (20 g/L substrate concentration, 0.05 g/L cellular concentration, 30°C, pH 7.0, 150 rpm, 48 h. Medium control: surface tension = 65.2 dyn/cm; E_{24} = 0.

[b] Yeast extract (1g/L); trace minerals (5 mL/L) (0.116 g/L of $FeSO.7H_2O$, 0.232 g/L of H_3BO_3, 0.41 g/L of $CoCl_26H_2O$, 0.008 g/L of $CuSO_45H_2O$, 0.008 g/L of $MnSO_4H_2O$, 0.022 g/L of $([NH_4]_6Mo_7O_{24}$, 0.174 g/L of $ZnSO_4$), EDTA (0.01 g/L).

[c] Mean ± SD.

done simultaneously with yeast extract and/or microsalts. In these experiments, the alkalinization of the final fermented broth was detected again.

In Table 2, the surface tension data of *B. subtilis* ATCC 6633 fermented broth according to different nutritional conditions are also given. There was expressive reduction in surface tension values, evidencing biosurfactant synthesis by this bacterial strain. Medium 1 (with the addition of yeast extract, trace minerals, and EDTA) showed the highest surface tension, indicating that nutritional supplementation does not favor biosurfactant production although it has stimulated cell growth. In the presence of microsalts (medium 3) or EDTA (medium 4), or even in the absence of those compounds (medium 5), surface tension values were similar. However, these results cannot be considered as an evaluation of the quantity of biosurfactant produced, because larger concentrations of that biosurfactant do not alter surface tension values, after having reached the minimum value, which is related to a maximum surface activity.

Furthermore, Fox and Bala *(23)* verified that although the addition of yeast extract could stimulate growth of a *B. subtilis* strain in an established potato medium, it did not decrease surface tensions. In fact, it has previously been related that the higher growth did not translate into lower surface tensions *(24)*. In reality, the reduction in surface tension is inversely related to cell growth.

All tested media produced a biosurfactant capable of emulsifying kerosene. However, except when EDTA was added alone (medium 4), the E_{24} values were satisfactory in comparison with those related to other emulsifiers produced by different microorganisms *(30)*.

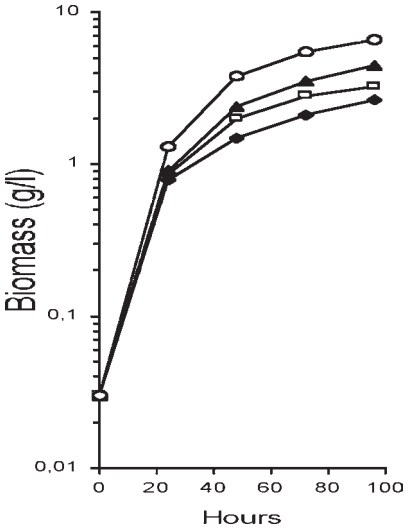

Fig. 3. Effect of initial substrate concentration on cellular growth of strain *B. subtilis* ATCC 6633: (▲) 5 g/L; (□) 10 g/L; (▲) 20 g/L; (○) 40 g/L.

Effect of Substrate Concentration

Normally, biosurfactant accumulation occurs when the microorganism is grown on a medium containing carbon source in excess, especially in relation to a limiting nutrient *(23,41)*. In most cases, the limiting nutrient is the nitrogen source, although limiting magnesium, iron, and phosphates can induce similar responses.

Cell growth of *B. subtilis* ATCC 6633 was proportional to the initial concentration of commercial sugar (Fig. 3). Regarding the kinetic profiles obtained, it can be concluded that cell growth rates were similar to those attained when 5 and 10 g/L of substrate were used, although the metabolic activity reached its peak at an initial concentration of 40 g/L. However, the values referring to specific cell growth velocities showed little variation, from 0.13 to 0.16 h^{-1}. Different media having potato process effluents as carbon source presented specific growth rates varying from 0.1 to 0.529 h^{-1} *(24)*. Substrate concentration had little effect owing to incomplete conversion (data not shown).

Biosurfactant production, expressed in terms of CMC^{-1}, reached maximum values within 48 h, practically the same for all substrate initial concentrations tested (Fig. 4); the corresponding values of surface tension were 28.7 and 29.3 dyn/cm (data not shown). These results are quite satisfactory when compared to values reported for more active biosurfactants, indicating a good performance of the product formed.

By contrast, Fox and Bala *(23)* observed that the degree of surface tension reduction was dependent on the amount of carbon source (potato) initially present in the medium.

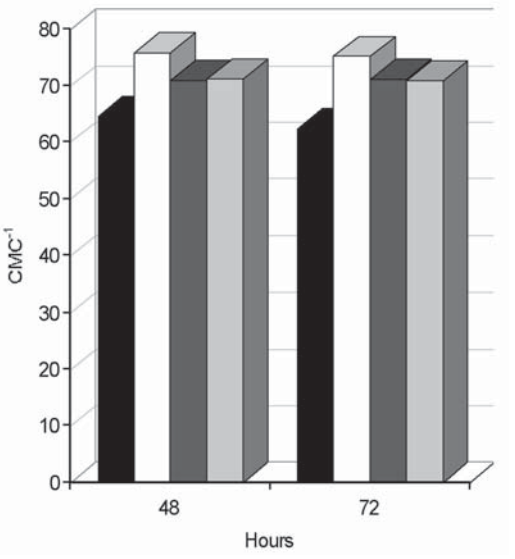

Fig. 4. Effect of initial substrate concentration on biosurfactant produced by *B. subtilis* ATCC 6633: (■) 5 g/L; (□) 10 g/L; (■) 20 g/L; (■) 40 g/L).

Analysis of the results obtained so far shows that substrate concentrations of 10, 20, and 40 g/L were quite adequate to produce biosurfactant by *B. subtilis* ATCC 6633, although the maximum concentration of the product was observed for 10 g/L of commercial sugar. Therefore, it should be concluded that the carbon/nitrogen relation in the range of 6.4–25.6 g/g had no affect on the biosurfactant synthesis.

Figure 5 shows some data referring to the ability of biosurfactant to emulsify kerosene produced by *B. subtilis* ATCC 6633 at the different substrate concentrations tested (5, 10, 20, and 40 g/L). Besides a decrease in surface tension, stabilization of hydrocarbon/water is frequently used as an indicator of surface activity. Note, however, that the quantity of biosurfactant produced should not be related to the E_{24} because that is an intrinsic property of the molecule. A similar behavior of the emulsifying activity in relation to the carbon source concentration and to the incubation period has been observed. The diverse initial concentrations of commercial sugar studied favor the formation of a surface-active compound, with an emulsifying activity >50% in a 48-h process. The maximum values for emulsion activity of 57.9 and 56.9% were determined for 10 and 20 g/L of substrate, respectively. It should be emphasized that there was a reduction in the E_{24} after a 96-h period of incubation. Carvalho et al. *(36)* reported similar results for cell-free fermented broth by *Bacillus sp*. emulsified in kerosene.

Kinetic Studies

The results of kinetic studies related to biosurfactant synthesis by *B. subtilis* ATCC 6633 cultivation in a fermentor containing a medium

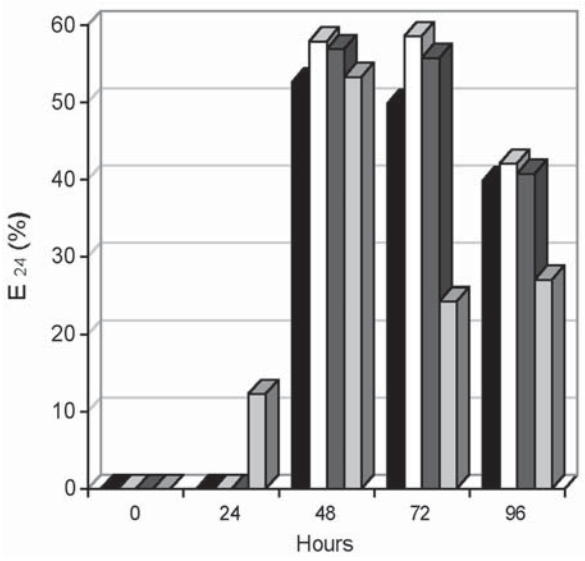

Fig. 5. Emulsification index (E_{24}) for biosurfactant produced by *B. subtilis* ATCC 6633 cultured in different initial substrate concentrations: (■) 5 g/L; (□) 10 g/L; (■) 20 g/L; (■) 40 g/L).

supplemented with microsalts and EDTA are shown in Fig. 6A. In these conditions, the growth rate and biosurfactant production profiles were similar to the ones obtained when the medium was not supplemented (Fig. 6B). However, the supplementation resulted in greater biomass production and product (CMC^{-1}), 1.5 g/L and 82.3, respectively.

By contrast, growth studies of *B. subtilis* ATCC 21332 using established potato media evidenced cells reaching early stationary phase whithin 12 h *(23)*. The addition of mineral salts to potato media resulted in a prolongation of the lag phase, the stationary phase being reached only 48 h after inoculation.

In the present work, the addition of microsalts and EDTA in the medium retarded biosurfactant synthesis, which was initiated only at the exponential phase of growth. The critical micelle concentration (CMC^{-1}) was reached at the onset of the stationary phase (after 50 h), although it is unknown whether surfactant production continued stationary phase.

The accumulation of the surface-active compound in the fermentation broth during the process was a function of the relative CMC^{-1} (Fig. 6A,B). Biosurfactant synthesis only started after 24 h, reaching its maximum after 50 h, thus confirming the kinetic profile of surface tension.

As shown in Fig. 6 (A,B), the synthesis of the surface-active agent took place in the late-exponential phase, achieving its maximum value at the beginning of the stationary growth phase. Therefore, it can be concluded that the biosurfactant produced by *B. subtilis* ATCC 6633 is a primary

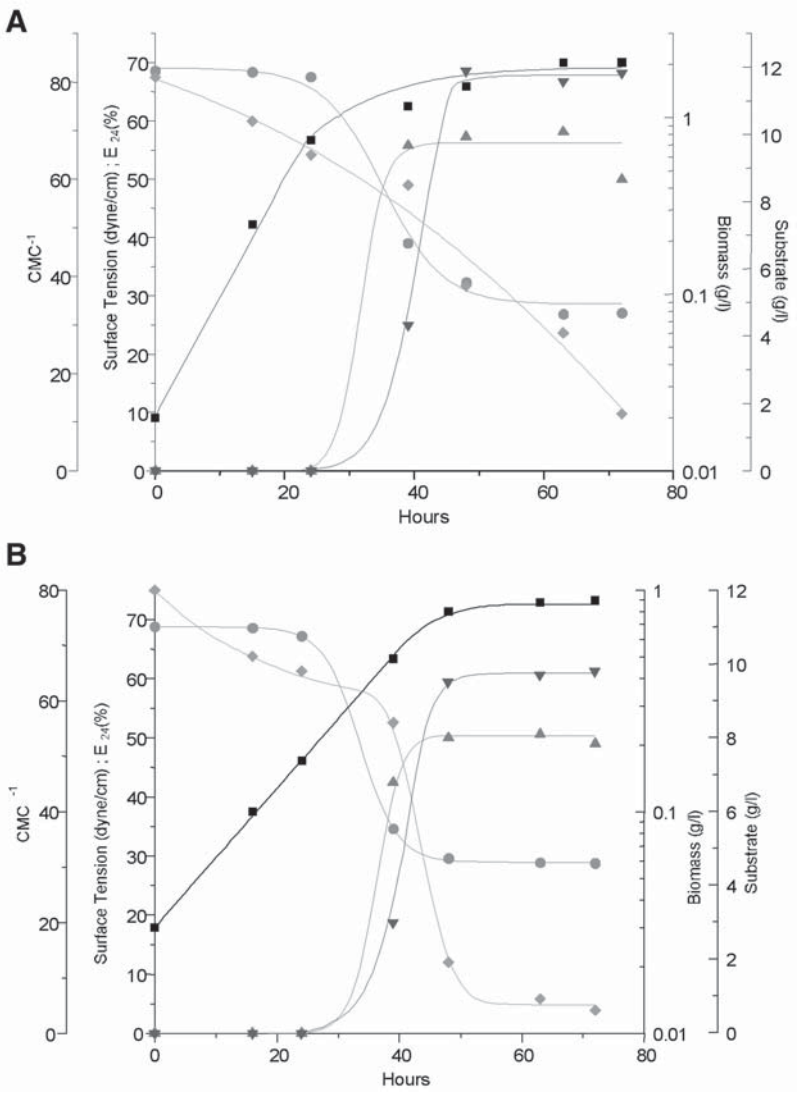

Fig. 6. Kinetics of growth and biosurfactant accumulation in batch culture of *B. subtilis* ATCC 6633 **(A)** with and **(B)** without supplementation of microsalts and EDTA: (●) surface tension; (▲) E24; (■) biomass; (◆) substrate; (▼) CMC^{-1}).

metabolite, which is in agreement with previous works *(20,35)*. This is also in agreement with the findings of previous reports that the onset of surfactin production occurred in the mid- to late-exponential phase *(20,24)*.

Thompson et al.'s *(24)* description of the kinetics of *B. subtilis* ATCC 21332 cultured in potato process waste streams medium presents the same correlation between biomass and surface tension. The minimum surface tension occurred near the onset of stationary phase. This behavior, as stated by these investigators, indicates a production of growth-associated surfactin.

As shown in Fig. 6B, a two-phase pattern occurred for the substrate uptake. It can be observed that during the exponential growth phase, sucrose assimilation by the bacteria was small, corresponding to about 20% of the initial amount introduced into the medium. However, after a 40-h process corresponding to the end of the growth phase, there was a rise in the substrate uptake, suggesting that the carbon source was directed to biosurfactant production, for the conditions tested. It should be emphasized that the fermentative process, when the medium was supplemented with microsalts and EDTA (Fig. 6A), generated a different substrate kinetics in comparison with that obtained for the nonsupplemented medium (Fig. 6B).

The addition of microsalts and EDTA resulted in a biomass yield on sucrose ($Y_{x/s}$) of 0.24 g/g and CMC^{-1}/dry cell weight of 54.5, quite different from that determined for the nonsupplemented medium, 0.08 g/g and 79.2, respectively. In a way, these results suggest that the presence of oligoelements stimulates cell growth rather than bioproduct synthesis.

Thompson et al. *(24)* also verified that the addition of trace minerals to potato process effluents has little effect on surfactin production by *B. subtilis* ATCC 21332. In fact, the addition of corn steep liquor had a detrimental effect on biosurfactant production, whereas the addition of trace minerals had no effect on surface tensions. On the other hand, growth rates were marginally higher with added nutrients.

Conclusion

Among the carbon sources tested, commercial sugar showed the best result for biosurfactant synthesis by *B. subtilis* ATCC 6633, reducing surface tension to 29.6 dyn/cm.

The maximum biosurfactant production was verified at pH 7.0 and 8.0. The addition of EDTA and microsalts favored microbial synthesis of surface-active compounds. On the other hand, the addition of yeast extract stimulated cell growth to the detriment of biosurfactant production. The most suitable concentration of commercial sucrose for biosurfactant synthesis was 10 g/L. Biosurfactant production occurred in the late-exponential phase, achieving its maximum value at the early stationary phase of growth. The values of surface tension that we obtained compare favorably with those obtained with commercial synthetic surfactants.

Acknowledgments

This work was supported by grants from Conselho Nacional de Desenvolvimento Científico e Tecnológico (CNPq) and Comissão de Aperfeiçoamento de Pessoal de Ensino Superior (CAPES).

References

1. Desai, J. D. and Banat, I. M. (1997), *Microbiol. Mol. Biol. Rev*. **61(1),** 47–64.
2. Kim, S. H., Lim, E. J., Lee, S. O., Lee, J. D., and Lee, T. H. (2000), *Biotechnol. Appl. Biochem*. **31,** 249–253.

3. Davis, D. A., Lynch, H. C., and Varley, J. (1999), *Enzyme Microb. Technol*. **25,** 322–329.
4. Morikawa, M., Hirata, Y., and Imanaka, T. (2000), *Biochim. Biophys. Acta* **1488,** 211–218.
5. Bicca, F. C., Fleck, L. C., and Ayub, M. A. Z. (1999), *Rev. Microbiol*. **30,** 231–236.
6. Ishigami, Y. (1993), *Inform* **4,** 1156–1165.
7. Lin, S.-C., Lin, K.-G., Lo, C.-C., and Lin, Y.-M. (1998), *Enzyme Microb. Technol*. **23,** 267–273.
8. Khire, J. M. and Khan, M.I. (1994), *Enzyme Microb. Technol*. **16,** 170–172.
9. Banat, I. M. (1995), *Acta Biotechnol*. **15,** 251–267.
10. Updegraff, D. M. (1990), *Dev. Ind. Microbiol*. **31,** 135–142.
11. Cassidy, D. P., Efendiev, S., and White, D. M. (2000), *Water Res*. **3(18),** 4333–4342.
12. Mulligan, C. N., Yong, R. N., Gibbs, B. F., James, S., and Bennet, H. P. J. (1999), *Environ. Sci. Technol*. **33(21),** 3812–3820.
13. Olivera, N. L., Commendatore, M. G., Moran, A. C., and Esteves, J. L. (2000), *J. Ind. Microbiol. Biotechnol*. **25(2),** 70–73.
14. Volkering, F., Breure, A. M., and Rulkens, W. H. (1998), *Biodegradation* **8,** 401–407.
15. Kim, H.-S., Yoon, B.-D., Choung, D.-H., Oh, H.-M., Katsuragi, T., and Tani, Y. (1999), *Appl. Microbiol. Biotechnol*. **52,** 713–721.
16. Vollenbroich, D., Ozel, M., Vater, J., Kamp, R. M., and Pauli, G. (1997), *Biologicals* **25,** 253–271.
17. Fox, S. L. and Bala, A. G. (2000), *Bioresour. Technol*. **75,** 235–240.
18. Davis, D. A., Lynch, H. C., and Varley, J. (1999), *Enzyme Microb. Technol*. **25,** 322–329.
19. Holmberg, K. (2001), *Curr. Op. Colloid Interf. Sci*. **6(2),** 148–159.
20. Cooper, D. G., MacDonald, C. R., Duff, S. J., and Kosaric, N. (1981), *Appl. Environ. Microbiol*. **42(3),** 408–412.
21. Makkar, R. S. and Cameotra, S. S. (1997), *J. Ind. Biotechnol*. **18,** 37–42.
22. Santa Anna, L. M., Sebastian, G. V., Pereira, N. Jr., Alves, T. L. M., Menezes, E. P., and Freire, D. M. G. (2001), *Appl. Biochem. Biotechnol*. **91-93,** 459–467.
23. Fox, S. L. and Bala, G. A. (2000), *Bioresour. Technol*. **75,** 235–240.
24. Thompson, D. N., Fox, S. L., and Bala, G. A. (2000), *Appl. Biochem. Biotechnol.* **84–86,** 917–930.
25. Greiner, M. and Winkelman, G. (1991), *Appl. Microbiol. Biotechnol*. **34,** 565–569.
26. Rosemberg, E., Zuckerberg, A., Rubinovitz, C., and Gutnick, D. L. (1979), *Appl. Environ. Microbiol*. **37(3),** 402–408.
27. Ramana V. K. and Karanth, N. G. (1989), *Biotechnol. Lett*. **11(6),** 437–442.
28. Trinder, D. (1969), *Ann. Clin. Biochem*. **6,** 24–27.
29. Cooper, D. G. and Zajic, j. E. (1980), *Adv. Appl. Microbiol*. **26,** 229–252.
30. Cooper, D. G. and Goldenberg, B. G. (1987), *Appl. Environm. Microbiol*. **53(2),** 224–229.
31. Iqbal, S., Khalid, Z. M., and Malik, K. A. (1995), *Lett. Appl. Microbiol*. **21,** 176–179.
32. Espuny M. J., Egido, S., Manresa, I. R. A., and Mercadé, M. E. (1996), *Biotechnol. Lett*. **18(5),** 521–526.
33. Robert, M., Mercadé, M. E., Bosch, M. P., Parra, J. L., Espuny, M. J., Manresa, M. A., and Guinea, J. (1989), *Biotechnol. Lett*. **11(12),** 871–874.
34. Peypoux F. and Georges, M. (1992), *Appl. Microbiol. Biotechnol*. **36,** 515–517.
35. De Roubien, M. R., Mulligan, C. N., and Gibbs, F. G. (1989), *Can. J. Microbiol*. **35,** 854–859.
36. Carvalho, D. F., Marchi, D. D., and Durrant, L. R. (1996), *In situ On-site Bioremed*. *4,* 91–96.
37. Claus, D. and Berkeley, R. C. W. (1984), in *Bergey's Manual of Systematic Bacteriology*, vol. II, Kieg, N. R. and Holt, J. G., eds., Williams & Wilkins, London, UK, pp. 1104–1130.
38. Banat, I. (1993), *Biotechnol. Lett*. **15(6),** 591–594.
39. Hawker, L. E., Linton, A. H., Folkes, B. F., and Carlile, M. J. (1964), *Elementos de Microbiologia General*. Editorial Acribia, Spain.
40. Pelczar, M. J. J., Chan, E. C. S., and Krieg, N. R. (1993), *Microbiology Concepts and Applications*, 5th Ed., McGraw-Hill, New York, NY.
41. Kosaric, N. (1996), in *Biosurfactantes*, Rehm, H.-J. and Reed, G. eds., VCH, Weinheim, Germany.

0273-2289/04/115/0913–0932/$25.00

Higher-Alcohols Biorefinery

Improvement of Catalyst for Ethanol Conversion

Edwin S. Olson,* Ramesh K. Sharma, and Ted R. Aulich

Energy & Environmental Research Center,
University of North Dakota,
PO Box 9018, Grand Forks, ND 58202-9018,
E-mail: eolson@undeerc.org

Abstract

The concept of a biorefinery for higher-alcohol production is to integrate ethanol and methanol formation via fermentation and biomass gasification, respectively, with conversion of these simple alcohol intermediates into higher alcohols via the Guerbet reaction. 1-Butanol results from the self-condensation of ethanol in this multistep reaction occurring on a single catalytic bed. Combining methanol with ethanol gives a mixture of propanol, isobutanol, and 2-methyl-1-butanol. All of these higher alcohols are useful as solvents, chemical intermediates, and fuel additives and, consequently, have higher market values than the simple alcohol intermediates. Several new catalysts for the condensation of ethanol and alcohol mixtures to higher alcohols were designed and tested under a variety of conditions. Reactions of methanol-ethanol mixtures gave as high as 100% conversion of the ethanol to form high yields of isobutanol with smaller amounts of 1-propanol, the amounts in the mixture depending on the starting mixture. The most successful catalysts are multifunctional with basic and hydrogen transfer components.

Index Entries: Biorefinery, alcohols; Guerbet reaction; methanol-ethanol mixtures; catalyst.

Introduction

Currently, most biorefineries are based mainly on a single product line with potentially one or two byproducts. Thus, an ethanol plant produces ethanol from corn starch, with distiller's grain as a byproduct. Greater product flexibility and, consequently, greater opportunities for profitability would derive from a plant producing a variety of alcohols, especially higher alcohols whose market prices range from $0.77 to $1.87/kg.

*Author to whom all correspondence and reprint requests should be addressed.

Alcohols with three to eight carbons are highly useful as solvents and chemical intermediates and are potentially useful as fuel oxygenate additives. The primary alcohols, such as 1-propanol, 1-butanol, 2-methyl-1-propanol, and 2-methyl-1-butanol, are now commercially produced from olefins in a multistep process that includes the oxo (hydrocarbonylation) reaction and subsequent hydrogenation and separation steps. The market for several of the higher alcohols is currently large and highly dependent on oil prices since they are derived from petroleum feedstocks. Lower-cost processes for higher alcohols could involve very efficient condensation reactions, starting with renewable CO_2-neutral ethanol and very inexpensive methanol. Expansion into the fuel additive market would likely be accelerated if superior performance and low-cost production could be demonstrated. Like ethanol, the higher alcohol fuel additives reduce engine emissions and improve performance but, unlike ethanol, do not generate high-volatility Reid vapor pressure and water-partitioning properties.

The condensation of inexpensive methanol and ethanol offers a relatively simple way to produce higher alcohols. This reaction is known as the Guerbet reaction and produces higher-value 1-butanol from self-condensation of ethanol or mixtures containing mainly 2-methyl-1-propanol (isobutyl alcohol) and 1-propanol from ethanol plus methanol. The Guerbet reaction is actually a multistep process occurring on a multifunctional catalyst at temperatures >300°C. The steps in the catalytic reaction involve dehydrogenation of the short-chain alcohols to aldehyde intermediates; condensation of the aldehyde intermediates to longer-chain aldehydes; and, finally, catalytic reduction to the larger alcohols. Earlier patents and studies used bases in combination with a hydrogenation/dehydrogenation catalyst component.

Development of a biorefinery concept for production of higher alcohols from ethanol depends on improvement of the catalyst required for the conversion. This article reviews the Guerbet condensation reactions developed for conversion of simple alcohols into higher alcohols and describes the testing of catalysts based on highly reactive catalytic carbons that function as the redox component of the catalytic system. The described research demonstrated the feasibility of a process for producing higher-alcohol mixtures from ethanol and methanol mixtures using novel catalytic processes. Methanol can be produced from biomass and other feedstocks via gasification and subsequent conversion of the syngas in high yield. Reactions of ethanol with itself and other alcohols will be described in future articles.

Guerbet Reactions

The condensation of methanol with ethanol produces a mixture of 1-propanol and 2-methyl-1-propanol (isobutyl alcohol), as well as small amounts of other branched alcohols, including 2-methyl-1-butanol, and nonalcohol components, depending on the catalyst and reactant ratios *(1–10)*. The reactions proceed through the formation of formaldehyde and

acetaldehyde (Eqs. 1 and 2), which condense and form propenal (Eq. 3), which is reduced to 1-propanol (Eq. 4). Further condensation of formaldehyde with propanal gives the branched 2-methyl-1-propanol (isobutyl alcohol) (Eqs. 5 and 6).

Other reactions are the acetaldehyde condensation to butanal (Eq. 7) followed by reduction to alcohol (Eq. 8) or reaction with formaldehyde to form 2-methylbutanal, which is reduced to the corresponding alcohol (Eq. 9). Other reactive combinations give condensation products, provided that one of the reactants has hydrogens on the carbon adjacent to the carbon bearing the hydroxyl group, so that the carbanion intermediate can form and add to the carbonyl formed on the other reactant.

$$CH_3OH \rightarrow CH_2{=}O + H_2 \tag{1}$$

$$CH_3CH_2OH \rightarrow CH_3CH{=}O + H_2 \tag{2}$$

$$CH_2{=}O + CH_3CH{=}O \rightarrow HOCH_2CH_2CH{=}O \rightarrow CH_2{=}CHCH{=}O + H_2 \tag{3}$$

$$CH_2{=}CHCH{=}O + 2H_2 \rightarrow CH_3CH_2CH_2OH\ (\text{1-propanol}) \tag{4}$$

$$CH_3CH_2CH{=}O + CH_2{=}O \rightarrow HOCH_2CH(CH_3)CH{=}O \tag{5}$$

$$HOCH_2CH(CH_3)CH{=}O + 2H_2 \rightarrow CH_3CH(CH_3)CH_2OH\ (\text{2-methyl-1-propanol}) \tag{6}$$

$$2CH_3CH{=}O \rightarrow CH_3CH{=}CHCH{=}O + H_2O \tag{7}$$

$$CH_3CH{=}CHCH{=}O \xrightarrow{H_2} CH_3CH_2CH_2CHO \xrightarrow{H_2} CH_3CH_2CH_2CH_2OH \tag{8}$$

$$CH_3CH_2CH_2CH{=}O + CH_2{=}O \rightarrow \rightarrow CH_3CH_2CH(CH_3)CH_2OH \tag{9}$$

There are two potential advantages of using a mixture of methanol and ethanol. First, the much lower cost of methanol allows its use in large excess so that very high conversions of ethanol might be obtained. Second, dehydrogenation of methanol produces formaldehyde, which is an especially reactive additive to carbanion intermediates in the condensation reactions.

These branched alcohol products are also useful in solvents, plasticizers, and monomers. For example, isobutyl alcohol is converted into the acetate ester, which is used extensively as a lacquer solvent. Isobutyl alcohol is also used in lubricating oils and in the production of amide resins. Propyl alcohol (59 million kg/yr) is used heavily in herbicide syntheses and in solvents for coatings and inks.

To effect the aldol condensation, reactions of liquid alcohols in a batch autoclave typically used a basic catalyst, such as sodium ethoxide or other alkali metal alcoholate *(11,12)*, phosphate *(13)*, or carbonate *(14)*, and a

relatively high temperature (230°C). To aid in the dehydrogenation and hydrogenation steps, nickel *(12)*, copper chromite *(14)*, platinum, palladium, ruthenium, or rhodium was used in a finely divided state. Moderate yields of alcohol products were obtained; however, several problems remain in commercializing the Guerbet reaction for higher-alcohol production. The starting alcohol is often converted into a large amount of carboxylic acid by a side reaction. Even when this is minimized by using an appropriate catalyst system, the catalyst systems are deactivated by the water byproduct of the reaction. Essentially, this is a hydrolysis of the sodium alkoxide to the less active hydroxide; thus, successive batch reactions required the addition of new sodium alkoxide.

The key to effecting economical condensation reactions of the Guerbet type is the use of a solid base catalyst bed in a continuous or flow-through reactor for the gas-phase reaction. In this mode, the water eliminated during the condensation does not accumulate in the reactor as it does in the batch reactor. Fuchs *(15)* described a reaction of mixed alcohols and hydrogen over MgO/CuO to give a mixture of alcohols (US patent no. 2,050,788). Matsuda *(8)* used a Cu-Ni alkaline catalyst in a similar reaction (US patent no. 4,518,810). Clark *(9)* described a gas-phase reaction with a catalyst composed of a platinum group metal and alkali metal impregnated on alumina for formation of the linear alcohols, but branched alcohols were not reported. Ueda et al. *(14)* reported using a magnesium oxide catalyst for the gas-phase reaction of ethanol and methanol. Conversions of 60% (ethanol basis) were obtained at 390°C at atmospheric pressure, with a selectivity of 80% for alcohols. The catalytic activity decreased with time, however, and methanol was converted into unwanted gases: CO, H_2, and CH_4. A magnesium oxide catalyst (no hydrogen-activating metal) was also patented (US patent nos. 5,095,156 and 5,364,979) *(16,17)*. The major problem with these processes is the high methane production and the loss of activity of the mixed metal oxides used in these reactions and sintering during attempted regeneration.

To improve process economics, further work is needed to improve catalyst lifetimes. A more stable system employed a noble metal-loaded potassium L-zeolite catalyst for the condensation of ethanol with methanol to produce a 1-propanol and 2-methyl-1-propanol (US patent no. 5,300,695) *(18)*. However, yields were small compared with the large amounts of CO and CO_2 produced from the methanol. More recently, Exxon patented a noble metal-loaded alkali metal-doped mixed metal (Zr, Mn, Zn) oxide (US patent nos. 6,034,141 and 5,811,602) *(19,20)*. The catalyst was used in a syngas atmosphere. As with other catalysts, the higher temperatures resulted in decomposition of methanol. Changes in catalyst composition were noted at higher temperatures, but the stability of the catalyst was not discussed. Recently, compositions including Ni, Rh, Ru, and Cu were investigated *(21,22)*.

Novel Catalysts for Higher-Alcohol Production

The formation of higher alcohols directly in one step from smaller alcohols via the Guerbet reaction was investigated by passing the alcohol

vapors through a catalytic bed and condensing the higher-alcohol products in a series of cold traps. The catalysts were tested in a tubular flow-through reactor with ethanol or with methanol-ethanol (5:1 mainly) mixtures in a nitrogen carrier gas in a matrix of temperature and pressure conditions. The liquid products were collected in dry ice–isopropanol traps and analyzed by gas chromatography (GC)–flame ionization detection. The gases were collected and analyzed by GC-thermal conductivity detector.

Novel, multifunctional fixed-bed catalysts for use in a continuous Guerbet process for higher-alcohol synthesis were prepared. To achieve high conversions in the Guerbet reaction over a stable multifunctional catalyst, we investigated the use of several catalytic carbons to function as the redox component of the catalytic system. Two commercial activated carbons were converted into more basic forms, denoted CM and FM. A highly active proprietary catalytic carbon (SO) prepared at the Energy & Environmental Research Center (EERC) was also treated to a more basic form. Thus, all three carbons were hypothesized to contain the needed redox and basic catalytic components for the Guerbet reaction. The activities of these modified carbons were compared with those of MgO catalysts on various supports and with those using a very high surface area aerogel magnesium oxide.

Materials and Methods

Preparation of Carbon-Based Catalysts

A commercial catalytic carbon (Centaur), a commercial activated carbon (Calgon 400), and the EERC SO carbon were impregnated with magnesium nitrate and calcined to produce the MgO-loaded carbons, denoted CM, FM, and SOM, respectively. Magnesium oxide (10 or 20 wt%)–impregnated carbons were prepared as follows. An aqueous solution of magnesium nitrate hexahydrate was impregnated on the carbon using the incipient wetness method. The resulting carbon was dried at 110°C. The dried carbon was placed in a 40-cm stainless steel reactor (2.5cm). The reactor was slowly heated to 360°C in a gentle flow of nitrogen. The carbon was heated at this temperature for 3 h to decompose the nitrate to oxide.

MgO-supported carbon catalyst was also prepared by impregnating an aqueous magnesium sulfate solution. The dried impregnated carbon was washed with concentrated ammonium hydroxide solution to convert the sulfate into magnesium hydroxide. This washed carbon was dried and heated in a tubular reactor as just described to convert the hydroxide to oxide.

Preparation of MgO Catalysts

Magnesium oxide was prepared by hydrolyzing an aqueous solution of magnesium sulfate with ammonium hydroxide. It was thoroughly washed with water until free of cations and anions and dried at 50°C under vacuum for 12 h. The dried product was then heated at 600°C in air *(13)*.

Magnesium oxide was also prepared by boiling 25 g of commercially available magnesium oxide in 500 mL of water with vigorous stirring in a

1-L flask equipped with a reflux condenser. After cooling, the slurry was filtered and the cake dried in an oven at 120°C. The dried product was broken into pieces and heated at 500°C under vacuum for 12 h. The product was stored under nitrogen *(23)*.

Ultrahigh-surface-area magnesium oxide (aerogel) was prepared according to the procedure described previously *(11,23)*. Magnesium turnings and analytical-grade methanol were used for the preparation of magnesium methoxide. Ten percent magnesium methoxide was prepared by stirring 7.2 g of magnesium (0.30 mol) with 300 mL of methanol in a 500-mL round-bottomed flask attached to a nitrogen supply. To prevent hydrolysis, a slow flow of nitrogen was maintained throughout the reaction. The stirring was carried out until all of the magnesium was gone (24 h).

The methoxide solution was placed in a round-bottomed flask, 300 mL of toluene was added, and the mixture was vigorously stirred. To the stirred mixture, 4.5 mL of water was added slowly. A white precipitate was observed on addition of water. After a few minutes, the mixture became clear and produced a syrup-like solution. The resulting mixture was stirred overnight to ensure completion of hydrolysis.

The hydroxide gel solution was transferred into an autoclave (300-mL glass-lined Parr reactor). The reactor was flushed with nitrogen and then pressurized with 200 cm^3 of nitrogen. The reactor was slowly heated from room temperature to 265°C. The temperature was allowed to equilibrate for 10 min before the reactor was vented to release the pressure. The operating pressure was 7.2 MPa. The pressure was released over a period of 0.5–0.8 min. The reactor was immediately removed from the heater and then flushed with nitrogen for 5–10 min. It was next allowed to cool to room temperature. The product was removed from the reactor and dried in an oven at 120°C for a few hours.

The dried product was activated by heating *in vacuo*. The dried product was placed in a quartz tube and evacuated. The quartz tube was then heated in a tubular furnace using a ramp-and-soak method as follows: ramped from room temperature to 220°C at 1°C/min; soaked at 220°C for 5 h, ramped from 220 to 500°C at 1°C/min, soaked at 500°C for 5 h. About 18 h was required for the heat treatment of the sample. The sample was allowed to cool to room temperature and then stored under nitrogen. The product was very light chunky powder. However, these chunks were very fragile; therefore, they could not be directly used for packed-bed reactors.

The ultrahigh-surface-area gel containing nickel and copper was prepared by adding nickel nitrate or copper nitrate (Ni or Cu was 3 wt% of metal of dried weight of MgO) to the gel prior to autoclave treatment *(12)*. For this product to be packed into a tube reactor, it was converted into a strong-enough granular form. This was accomplished as follows: Slurry was prepared by adding aerogel to an alcoholic solution of nickel nitrate hexahydrate. The amount of Ni in Ni/MgO was 3 wt%. Lava rock crushed to +8 mesh size was impregnated with this gel. The rock was thoroughly mixed and dried to remove solvent, and then activated by heating at 600°C for 2 h.

In another experiment, glass wool was added to the hydrolyzed magnesium methoxide gel prior to heating in the autoclave. The quartz wool coated with high-surface-area magnesium oxide was impregnated with nickel nitrate hexahydrate and activated as already described.

Continuous Catalytic Conversion of Methanol-Ethanol Mixtures

Flow-Through Reactions at Ambient Pressure

A tubular stainless steel reactor, 40 cm long (ID = 1 cm), was used for conducting catalytic runs at atmospheric pressure. The reactor was packed with the desired catalyst. The inlet of the reactor was attached to a pump and source of nitrogen gas. The outlet was attached to two ice-cooled traps. The reactor was placed in a tubular furnace maintained at 360°C. After the reactor had attained the desired temperature, the desired methanol-ethanol mixture was pumped into the reactor at the desired rate (0.1 or 0.5 mL/min). To facilitate the flow of alcohol vapors through the catalyst bed, a gentle flow (66 cm^3/min) of nitrogen was passed through the reactor. The products were condensed in the ice-cooled traps. After the desired time (60 min), alcohol flow was stopped. The flow of nitrogen was continued for an additional 10 min through the reactor to flush out any remaining product. The reactor was cooled to room temperature, and the catalyst was removed and stored under nitrogen. No liquid was present in the reactor. The distillate was analyzed by GC and GC-mass spectrometry (MS).

Flow-Through Reactions Under Pressure

In a flow-through reaction under pressure, the outlet of the reactor was attached to traps via a needle valve. The reactor was pressurized with 1.4 MPa of nitrogen, and the needle valve was closed. The alcohol mixture was pumped at 0.5 cm^3/min for 15 min. The pressure inside the reactor increased to 1.8–2.1 MPa. The valve was slightly opened to allow the product to condense into two ice-cooled traps by maintaining the pressure inside the reactor. The run was continued for another 15 min.

Batch Reaction

In a batch reaction, the reactants and catalyst were placed in a 15-mL tube reactor. The reactor was evacuated and sealed and then heated at 360°C for 30 min. The products were centrifuged, and liquid was collected and analyzed.

Product Analyses

Analyses of the starting material and products were carried out by GC and GC-MS analyses. For GC analyses, a Shimadzu gas chromatograph, GC-17A, was used. A 60-m-long narrow bore (0.25-mm) DB5 with 0.25-µm phase thickness supplied by J & W Scientific was used. The GC parameters were as follows: split injection (split ratio of 50:1), carrier gas of hydrogen at 1 cm^3/min at 30°C. The heating program was as follows: initial temperature of 30°C, initial time of 2 min, rate of 30–250°C at 3°C/min, final time

of 5 min. A variety of straight chain and branched alcohols (C_1-C_{10}) were calibrated using anisole as the internal standard. Reaction products from each run were mixed with 0.1 g of anisole (internal standard) and analyzed by GC. Conversions of the ethanol component were calculated by subtracting the ethanol recovered in the product mixture from the starting amount; this is reported in Tables 1, 2, and 4–10 as the percentage of ethanol conversion (EtOH conversion). Theoretical yields of each alcohol product were calculated by assuming that all of the ethanol that reacted was converted into that alcohol, and the percentage of theoretical is also reported in these tables for each alcohol component.

In many of the experiments, a small amount of the 2-methylpropanal (isobutyraldehyde) intermediate was formed. The amounts were determined and are reported in Tables 1, 2, and 4–10. Only in two of the experiments were formaldehyde and acetaldehyde analyzed, but it is assumed that small amounts of formaldehyde were present in all of the products. Other aldehyde intermediates, such as propanal and 2-methylbutanal, were not present in amounts large enough for detection. Besides the major higher-alcohol products and aldehyde intermediates described above, some other minor products were determined in the chromatograms of each product. These include esters, ethers, and aromatics formed in very small amounts. The sums of these are reported in Tables 1, 2, and 4–10 as "Other." The areas of these GC peaks were converted to millimoles by using approximate response factors appropriate for the molecular weight range of the peaks.

Results and Discussion

Effect of Reactor Temperature and Starting Composition

Reactions of ethanol-methanol mixtures were carried out with recovered CM catalyst at various temperatures. Several variations of the starting composition were utilized at 360°C. The results are shown in Table 1. The reaction at 310°C gave a very low conversion of the ethanol with small amounts of the higher alcohols being formed. The poor mass balance was assumed to have resulted from the formation of acetaldehyde, which was not analyzed in this experiment.

The reactions at 360°C gave high conversions of ethanol and good yields of 2-methyl-1-propanol, based on reacted ethanol, along with some of the other C_3 and C_5 alcohols, and small yields of nonalcohol products (carboxylic acids, esters, ethers). The high-temperature (400°C) experiment also gave a high conversion and respectable yields of higher alcohols. Mass balance closures were close to 100% based on reacted ethanol. Carbonaceous deposits may form but could not be identified because the catalyst is composed of carbon as well as metal oxide.

For reactions with the CM catalyst at 360°C, the higher molar ratios of methanol to ethanol resulted in considerably more ethanol being converted into products, reaching 98% conversion when the ratio was 9.7. For the higher methanol-to-ethanol ratios, yields of 2-methyl-1-propanol were

approximately the same. At the low ratio (3.3), yields of 2-methyl-1-propanol were much lower, and yields of 1-propanol and 2-methyl-1-butanol (formed from 2 mol of ethanol) were higher. Subsequent comparisons of catalysts were all conducted at 360°C with methanol-ethanol molar ratios of 7.2, corresponding to a 5:1 volume ratio.

Most of the reactions produced some 2-methylpropanal in the products. Not shown in Tables 1–6 are yields of formaldehyde and acetaldehyde, which were not measured in these initial experiments. A subsequent experiment with the SOM carbon was performed with several cold traps to determine formaldehyde and acetaldehyde concentrations in the products. The results are discussed below.

Comparison of Catalysts: Carbon-Based Catalysts

To determine the effect of the carbon structure on the catalytic conversion of methanol-ethanol mixtures to higher alcohols, three different carbons were investigated. The activity of a freshly prepared CM catalyst was compared with that of freshly prepared FM and SOM catalysts. Reactions of the pumped 5:1 methanol-ethanol mixture with all of these freshly prepared catalysts were performed in the flow reactor under identical conditions. Conversions and product composition results are given in Table 2. Very high conversions of ethanol were obtained with all three catalysts. The selectivity for 2-methyl-1-propanol was higher for the SOM and FM catalyst compared with CM. Typically, the catalyst activities degrade and selectivities for higher alcohols decrease with time. Further work is in progress to investigate these changes.

Gas Product Composition from Carbon Catalyst

For several of the experiments, gas products were collected in a gas bag following the liquid product traps. The gases were analyzed by GC with a thermal conductivity detector, and the total volume was determined from the gas flow rate. The amount of the gaseous product collected was 3.5 mmol. The major components in the gas phase were hydrogen, carbon monoxide, carbon dioxide, propane, acetylene, 1-butane, isobutane, *cis*- and *trans*-2-butenes, ethylene, methane, and oxygen. The composition of the gas mixture from a run with the SOM catalytic carbon is given in Table 3. The hydrogen is of some significance, since it derives from dehydrogenation of the alcohol but is not all retained on the carbon for subsequent hydrogenation of product aldehydes. Other gases were negligible.

Effect of Active Metal Incorporation

Earlier patents used catalysts containing a Group VIII metal to aid in the transfer of hydrogen (dehydrogenation and hydrogenation). The FM carbon catalyst in this project was similarly modified by the addition of 0.6 wt% of the active metal (nickel). The results using this catalyst are compared with those using FM catalyst in Table 4. The addition of nickel improved on

Table 1
Effects of Temperature and Starting Composition Molar Ratio on Conversion and Yields for Reactions of Methanol-Ethanol Mixtures[a]

Reactant ratio MeOH:EtOH (mmol)	Temperature (°C)	Recovered MeOH (mmol)	Recovered EtOH (mmol)	EtOH conversion (%)	2-Me propanal (mmol [%])	1-PrOH (mmol [%])	2-Me-1-PrOH (mmol [%])	2-Me-1-BuOH (mmol [%])	Other (mmol)
5.0/MeOH (97.95); EtOH (19.47)	310	94.42	16.64	15	0.00 (0)	0.44 (15)	0.59 (20)	0.00 (0)	0.20
9.7/MeOH (194.4); EtOH (20.00)	360	79.62	0.43	98	1.11 (5)	1.24 (6)	12.54 (64)	0.44 (4)	0.39
7.2/MeOH (125); EtOH (17.40)	360	88.00	0.96	94	0.84 (5)	0.65 (4)	10.64 (65)	0.28 (3)	3.40
3.3/MeOH (83.43); EtOH (25.44)	360	49.96	17.71	70	0.24 (1)	6.88 (39)	6.44 (36)	1.61 (18)	2.20
3.3/MeOH (91.28); EtOH (27.83)	400	37.36	2.40	91	0.92 (4)	4.20 (17)	14.48 (57)	1.80 (14)	2.60

[a] Catalyst, cm (recovered); carrier flow, 66cm^3/min. Percentages given in parenthesis refer to percent yield based on millimoles of product per millimole of ethanol converted.

Table 2
Effect of Carbon Precursor on Catalyst Activity and Conversions and Yields for Methanol-Ethanol Reactions[a]

Catalyst	Recovered MeOH (mmol)	Recovered EtOH (mmol)	EtOH conversion (%)	2-Me propanal (mmol [%])	1-PrOH (mmol [%])	2-Me-1-PrOH (mmol [%])	2-Me-1-BuOH (mmol [%])	Others (mmol)
CM	88.10	0.96	94	0.84 (5)	0.65 (4)	10.64 (65)	0.28 (3)	3.3
FM	89.03	0	100	1.13 (7)	0.44 (3)	13.19 (76)	0.88 (10)	1.2
SOM	82.61	0	100	1.12 (6)	0.30 (2)	14.81 (85)	0.42 (5)	0.8

[a] Flow rate, 0.1 mL/min; N_2 carrier flow, 66 cm^3/min; MeOH, 125 mmol (4.00 g); EtOH, 17.4 mmol (0.80 g); molar ratio, 7.2 temperature, 360°C; time, 60 min. Percentages given in parenthesis refer to percent yield based on millimoles of product per millimole of ethanol converted.

Table 3
Composition of Gas Formed in Methanol-Ethanol Reaction on SOM Catalyst

Gas	Weight (mg)	mmol	Composition (mmol%)
Hydrogen	3.0	1.500	8.40
Carbon dioxide	8.1	0.200	1.12
Propane	0.7	0.015	0.08
Acetylene	3.5	0.140	0.78
i-Butane	1.5	0.026	0.15
t-Butane	3.2	0.055	0.31
trans-2-Butene	1.6	0.028	0.16
cis-2-Butene	7.0	0.123	0.70
Ethene	1.2	0.040	0.22
Oxygen	2.8	0.087	0.49
Methane	4.0	0.230	1.30
Carbon monoxide	8.2	0.293	1.64
Nitrogen	424.6	15.153	84.65
Total	44.7	17.900	100.00

the high yields of the alcohol products, especially the 2-methyl-1-propanol (90%). Since the yield of 2-methylpropanal decreased substantially, the greater yield of 2-methyl-1-propanol may have resulted from the increased hydrogenation of 2-methylpropanal intermediate.

Effect of Base Composition on Activity

To determine whether a variation in base modification of the carbon catalyst has an effect on the activity, a second catalyst (CSM) was prepared from the Centaur commercial carbon by impregnating with magnesium sulfate and subsequently heating to decompose the salt to the oxide form. The resulting carbon was used as a catalyst for the conversion of the methanol-ethanol mixture; the results are given in Table 5. The CSM catalyst prepared using the alternative base precursor was less effective in converting the ethanol, and lower amounts of higher alcohols were obtained. Since the amount of 2-methylpropanal intermediate was higher, the results suggest that the sulfuric acid from the decomposition of the magnesium sulfate may have poisoned some of the catalytic sites for hydrogenation.

Magnesium Oxide Catalysts

Several patents and literature reports utilized inorganic basic catalysts for the Guerbet reaction. Several of these were prepared and utilized for the methanol-ethanol mixture. A very porous low-density aerogel form of MgO was prepared, but the material lacked any kind of strength and could not be packed by itself in a reactor tube. Thus, glass wool and lava rock were used as a support for MgO. For the lava rock support, MgO (aerogel) and nickel nitrate were slurried into ethanol and impregnated on lava rock. The product was dried at 110°C followed by activation at 160°C in nitrogen for 3 h.

Table 4
Effect of Transition Metal on Activity of Carbon Catalyst and Conversions and Yields of Methanol-Ethanol Reactions [a]

Catalyst	Recovered MeOH (mmol)	Recovered EtOH (mmol)	EtOH conversion (%)	2-Me propanal (mmol [%])	1-PrOH (mmol [%])	2-Me-1-PrOH (mmol [%])	2-Me-1-BuOH (mmol [%])	Others (mmol)
FM	89.03	0	100	1.13 (7)	0.44 (3)	13.19 (76)	0.28 (3)	1.3
Ni-FM	89.25	0	100	0.15 (1)	0.60 (3)	15.69 (90)	0.15 (2)	1.1

[a] Flow rate, 0.1 mL/min; carrier flow, 66 cm^3/min; MeOH, 125 mmol; EtOH, 17.4 mmol; temperature, 360°C; time, 60 min. Percentages given in parenthesis refer to percent yield based on millimoles of product per millimole of ethanol converted.

Table 5
Effect of Basic Precursor on Activity of Carbon Catalyst and Conversions and Yields for Methanol-Ethanol Reactions [a]

Catalyst	Recovered MeOH (mmol)	Recovered EtOH (mmol)	EtOH conversion (%)	2-Me propanal (mmol [%])	1-PrOH (mmol [%])	2-Me-1-PrOH (mmol [%])	2-Me-1-BuOH (mmol [%])	Others (mmol)
CM	88.00	0.96	94	0.84 (5)	0.65 (4)	10.64 (65)	0.28 (3)	3.4
CSM	99.26	3.26	81	2.76 (19)	0.20 (1)	9.50 (67)	0.00 (0)	1.4

[a] Flow rate, 0.1 mL/min; carrier flow, 66 cm^3/min; MeOH, 125 mmol; EtOH, 17.4;
temperature, 360°C; time, 60 min. Percentages given in parenthesis refer to percentage yield based on millimoles of product per millimole of ethanol converted.

Table 6
Activity of Supported MgO Catalyst and Conversions and Yields of Methanol-Ethanol Reactions [a]

Catalyst	Recovered MeOH (mmol)	Recovered EtOH (mmol)	EtOH conversion (%)	2-Me propanal (mmol [%])	C_3 (mmol [%])	2-Me-1-PrOH (mmol [%])	2-Me-1-BuOH (mmol [%])	Others (mmol)
Glass wool/ MgO	118.90	14.71	16	0.00 (0)	2.50 (93)	0.25 (9)	0 (0)	0
Glass wool/ MgO/Ni	109.61	9.25	47	0.61 (7)	7.01 (86)	0.00 (0)	0 (0)	1.3
Lava rock/ MgO/Ni	115.54	15.17	13	0.17 (8)	0.85 (38)	0.51 (23)	0 (0)	0

[a] Flow rate, 0.1 mL/min; carrier flow, 66 cm^3/min; temperature, 360°C; time, 60 min. Percentages given in parenthesis refer to percent yield based on millimoles of product per millimole of ethanol converted.

Table 7
Intermediate Formation and Conversions and Yields for Catalytic Conversion of Methanol-Ethanol Mixture to Higher Alcohols [a]

Time (h)	EtOH conversion (%)	H_2CO (mmol)	Ethanal (mmol)	2-Me propanal (mmol [%])	1-PrOH (mmol [%])	2-Me-1-PrOH (mmol [%])	2-Me-1-BuOH (mmol [%])	Other (mmol)
1	94	1.75	0.57	0.67 (8)	0.64 (4)	10.49 (64)	0.23 (3)	3.88
2	90	0.39	0.25	0.94 (12)	1.69 (11)	8.32 (53)	0.44 (6)	3.12
4 [b]	45	0.04	1.51	1.07 (9)	3.23 (14)	8.00 (34)	1.88 (16)	6.86

[a] Catalyst, CM; flow rate, 0.1 mL/min; carrier flow, 66 cm^3/min; temperature, 360°C; time, 60 min; MeOH, 125 mmol; EtOH, 17.4 mmol. Percentages given in parenthesis refer to percent yield based on millimoles of product per millimole of ethanol converted.
[b] MeOH/EtOH ratio, 1:1; MeOH, 75 mmol; EtOH, 52.17 mmol.

For the glass wool support, the glass wool was added to the autoclave prior to aerogel preparation. The resulting catalysts were used as a catalyst for the conversion of the methanol-ethanol mixture; the results are given in Table 6. Owing to the broadness of the peak corresponding to C_3 alcohols and aldehydes, a clear distinction could not be made as to the identity or identities of the C_3 species in these products; that is, the major component could be propanal.

The results show that these high-surface MgO catalysts are inferior to the carbon-based sorbents. Even with added nickel to aid in hydrogen transfer reactions, the conversions are lower than those obtained with the carbon catalysts. Although some condensation of the aldehyde intermediates to C_3 compounds must have occurred, the condensation reaction does not proceed as well to the C_4 compounds.

Formation of Aldehyde Byproduct

To further improve the mass balance during catalytic conversion of the methanol-ethanol mixtures into higher alcohols, products were collected in two traps cooled by dry ice–isopropyl alcohol slurry, and gases from the second traps were bubbled through another trap containing a known weight of 2-(2-methoxyethoxy)ethanol cooled in a dry ice–isopropyl alcohol bath. Products from all of these traps were weighed and analyzed by GC; the results are given in Table 7.

From the reaction of the methanol-ethanol mixture with freshly prepared catalyst, 98% of the products was trapped in the two traps cooled in a dry ice–isopropyl alcohol bath. The third trap containing 2-(2-methoxyethoxy)ethanol cooled in a dry ice–isopropyl alcohol bath showed only traces of several products. Therefore, it was assumed that the remaining 2% of the material was gaseous products, as observed in previous reactions. In addition to the products described in Table 7, formaldehyde (1.75 mmol) and acetaldehyde (0.57 mmol) were also identified. When the same reaction was carried out with the used catalyst, almost 100% of the products was trapped in the first two traps. The third trap showed only traces of product as before. Other products were formaldehyde (0.39 mmol) and acetaldehyde (0.25 mmol).

Reactions using a methanol-ethanol ratio of 1:1 with catalyst recovered from the experiment described in the paragraph above were also carried out under similar conditions. The products from the first two traps amounted to 95.3 wt%. Products in the third trap were insignificant. Formaldehyde (0.04 mmol) and acetaldehyde (1.51 mmol) were observed. It is assumed that the remaining 4.7% was gaseous products.

Effect of Hydrogen in Carrier Gas

Since the product gas composition indicated that some hydrogen was not being utilized for hydrogenation of the higher-aldehyde intermediate to form additional alcohols, the effect of adding hydrogen as a carrier gas to further improve the product yield and product slate was investigated.

Recovered Centaur–20% MgO catalyst was used as the catalyst. As before, products were collected in two traps cooled in a dry ice–isopropyl alcohol bath, and gases from the second traps were bubbled through another trap containing a known weight of 2-(2-methoxyethoxy)ethanol cooled in a dry ice–isopropyl alcohol bath. Products from all these traps were weighed and analyzed by GC; the results are given in Table 8.

There did not appear to be a significant difference in the conversion and yields in the reaction in hydrogen compared with the reaction in nitrogen. Since the 2-methylpropanal was actually higher in the reaction using hydrogen, this appears to show that the gas-phase hydrogen is probably not used as effectively as the spillover hydrogen on the carbon catalyst, resulting from dehydrogenation of the ethanol and methanol.

From both of these reactions, almost 98% of the products was trapped in the two traps cooled in a dry ice–isopropyl alcohol bath. The third trap containing 2-(2-methoxyethoxy)ethanol cooled in a dry ice–isopropyl alcohol bath showed only traces of several products. Therefore, it was assumed that the remaining 2% of the material was gaseous products, as observed in previous reactions. Formaldehyde (0.65 mmol) and acetaldehyde (0.55 mmol) were also identified.

Effect of Pressure on Catalytic Conversion

The effect of pressure was investigated by carrying out a flow-through reaction under mild pressure. The results (Table 9) were compared with the previous flow-through reactions at ambient pressure as well as with a batch reaction under similar conditions. The increased pressure in the flow-through run as well as the batch run resulted in very low conversions of the ethanol. There may have been destruction of the base catalyst under this condition.

Catalytic Conversion of Recycled Products

Some of the aldehyde intermediates in the Guerbet reaction were always present in the product mixture. These can obviously be converted into higher-alcohol products in subsequent reactions, by recycling either the entire product mixture or only the lower alcohol/aldehyde portion recovered by distillation. The latter would be expected to occur in the process. To investigate the feasibility of increased conversion by recycling the entire product mixture, products obtained from a continuous run for 5 h were used. The products from 2- to 5-h runs were mixed together, and the composite was recycled through the CM catalyst under identical conditions; the data are given in Table 10.

The composite was very low in ethanol, so the conversion was naturally 100% in the recycle run. The recycled feed produced a very high yield of 2-methyl-1-propanol. The reaction also resulted in an increased formation of 2-methylpropanal. Thus, recycling of the lower alcohols containing some lower aldehydes should be effective for increasing higher-alcohol product yields, but this experiment has not yet been completed.

Table 8
Effect of Carrier Gas Composition on Conversions and Yields for Catalytic Conversion of Methanol-Ethanol Mixture to Higher Alcohols [a]

Carrier gas	Recovered MeOH (mmol)	Recovered EtOH (mmol)	EtOH conversion (%)	2-Me propanal (mmol [%])	1-PrOH (mmol [%])	2-Me-1-PrOH (mmol [%])	2-Me-1-BuOH (mmol [%])	Others (mmol)
N_2	87.1	1.02	94	0.67 (4)	0.64 (4)	10.49 (64)	0.23 (3)	3.9
H_2	84.6	0.94	95	0.94 (6)	1.42 (9)	10.72 (65)	0.61 (7)	2.5

[a] Catalyst, CM; flow rate, 0.1 mL/min; carrier flow, 66 cm^3/min of N_2 or H_2; temperature, 360°C; time, 60 min; MeOH, 125 mmol; EtOH, 17.4 mmol. Percentage given in parenthesis refers to percent yield based on millimoles of product per millimole of ethanol converted.

Table 9
Effect of Pressure on Conversions and Yields for Catalytic Conversion of Methanol-Ethanol Mixture to Higher Alcohols [a]

Conditions/ ratios (mmol)[b]	Recovered MeOH (mmol)	Recovered EtOH (mmol)	EtOH conversion (%)	2-Me propanal (mmol [%])	1-PrOH (mmol [%])	2-Me-1-PrOH (mmol [%])	2-Me-1-BuOH (mmol [%])	Others (mmol)
Ambient flow/ MeOH (250); EtOH (35)	197.81	3.47	90	1.45 (5)	2.02 (6)	19.35 (62)	0.95 (6)	2.6
2.1 MPa flow/ MeOH (312); EtOH (43)	272.1	26.79	38	1.24 (8)	1.52 (9)	11.79 (71)	0.22 (3)	2.6
Batch/MeOH (130); EtOH (18)	124.6	17.8	2	Trace (0)	Trace (0)	Trace (0)	Trace (0)	Trace

[a] Catalyst, CM (recovered); temperature, 360°C. Percentage given in parenthesis refers to percent yield based on millimoles of product per millimole of ethanol converted.

[b] Ambient flow, injected at 0.1 mL/min using a syringe pump under ambient pressure for 120 min; 2.1 MPa flow, injected at 0.5 mL/min using a syringe pump under pressure for 30 min; batch, reaction carried out in a sealed-tube reactor for 30 min.

Table 10
Conversions and Yields for Catalytic Conversion of Recycled Products [a]

Sample	Recovered MeOH (mmol)	Recovered EtOH (mmol)	EtOH conversion (%)	2-Me propanal (mmol)	1-PrOH (mmol)	2-Me-1-PrOH (mmol)	2-Me-1-BuOH (mmol)	Other (mmol)
Initial product	97.19	2.98	—	1.53	1.32	8.35	0.63	2.68
Recyled product	88.57	0	100	1.86	1.28	10.87	0.80	3.09

[a] Catalyst, CM; flow rate, 0.1 mL/min; MeOH, 125 mmol; EtOH, 17.4 mmol; carrier flow, 66 cm^3/min; temperature, 360°C; time, 1 h.

Mixed Alcohol Fuel Production

A larger quantity of the actual higher-alcohol product mixture was desired for fuel characterization tests. The mixture of higher Guerbet alcohols was prepared by catalytic conversion of a methanol-ethanol mixture (5:1 volume ratio) with the CM catalytic carbon prepared during this project. Reactions were carried out continuously, and products were collected in dry ice–cooled traps and removed every 2 h for several days. The reactions were carried out under the following conditions: catalyst = CM; reactor = 40-cm-long, 2.5-cm-stainless steel reactor; feed = methanol-ethanol (5:1); flow rate = 0.5 mL/min; carrier gas = 66 cm^3/min of nitrogen; temperature = 360°C; pressure = ambient.

The alcohol mixture was distilled to remove the majority of methanol, ethanol, formaldehyde, acetaldehyde, and water. Remaining water was removed with the use of 3A molecular sieves. The composition of the alcohol mix after removal of most of the methanol and ethanol was as follows: (2.9%) methanol, (1.9%) ethanol, (11.9%) *n*-propanol, (81.3%) 2-methyl-1-propanol, (1.4%) 2-methyl-1-butanol, and (0.7%) other components. Attempts to remove the small amounts of residual methanol and ethanol using 4A molecular sieves were not successful.

No attempt was made to separate the higher alcohols by distillation, since purification is not needed for fuel-grade products. To obtain higher-purity 2-methyl-1-propanol, an alternative to distillation is to return the product mixture to the reactor to further convert 1-propanol to 2-methyl-1-propanol with excess methanol. Further methylation of either 2-methyl-1-propanol or 2-methyl-1-butanol was never observed. Identification of the minor products is in progress.

The distilled alcohol product mixture was also esterified by refluxing with glacial acetic acid in the presence of a catalytic amount of sulfuric acid. The product was extracted with water followed by extraction with saturated sodium bicarbonate solution. It was further washed with water and dried over anhydrous sodium sulfate. The crude ester was distilled, and the distillate was stored for further use. The percent yield of esters was 86%. The mixed ester was determined by GC to be composed of (1.3%) methyl acetate, (1.3%) ethyl acetate, (11.5%) *n*-propyl acetate, (81.7%) isobutyl acetate, (1.2%) 2-methyl-1-butyl acetate, and (1.9%) other components. The composition corresponded closely to that of the parent alcohol mixture. The fuel characteristics of the alcohol mixture and the ester mixture prepared from it were reported earlier *(24)*.

Conclusion

Base-modified carbons were highly effective for producing higher alcohols. In the methanol-ethanol (5:1) reactions, 90–100% of the ethanol was converted into products with the carbon catalysts. Selectivities for the major product, 2-methyl-1-propanol, vary from 65 to 85%, based on ethanol. Less than 3% of methanol was converted into gases. Other minor prod-

ucts were 1-propanol and 2-methyl-1-butanol. Small amounts of aldehyde intermediates were found. Best results were obtained at 360°C and ambient pressure. Adding hydrogen to the carrier had a negligible effect on yields. Adding nickel during the impregnation step in the preparation resulted in even higher yields of alcohol products.

For comparison with the carbon-based catalysts, several MgO catalysts were prepared on silica and alumina supports, and a very high-surface MgO aerogel was also prepared. Testing these under the same conditions gave very poor yields of the desired alcohols. It is clear that the carbon structures promote the activity, very likely by catalyzing the dehydrogenation and hydrogenation steps.

Although these high yield results and the low gas make were highly encouraging, the loss of activity with time was still a concern. Conversions dropped 20–30% after several days. Runs over longer time periods are currently being investigated to determine service life of the catalysts. Regeneration of spent carbon catalysts has been investigated and will be reported elsewhere.

Acknowledgments

This article was prepared with the support of the US Department of Energy (DOE) National Energy Technology Laboratory Cooperative Agreement No. DE-FC26-01NT41129. 1However, any opinions, findings, conclusions, or recommendations expressed herein are those of the authors and do not necessarily reflect the views of DOE.

References

1. Dvornikoff, M. N. and Farrar, M. W. J. (1957), *Org. Chem*. **22,** 540–542.
2. Radlowski, C. A. (1994), US patent no. 5,364,979.
3. Mueller, G. (1998), US patent no. 5,777,183.
4. Hagen, G. P. (1992), US patent no. 5,159,125.
5. Vanderspurt, T. H. (1996), US patent no. 5,493,064.
6. Young, D. A. (1991), US patent no. 5,068,469.
7. Barger, P. T. (1996), US patent no. 5,559,275.
8. Matsuda, M. (1985), US patent no. 4,518,810.
9. Clark, R. T. (1976), US patent no. 3,972,952.
10. Yates, J. E. (1976), US patent no. 3,979,466.
11. Utamapanya, S., Klabunde, K. J., and Schlup, J. R. (1991), *Am. Chem. Soc*. **3,** 175–181.
12. Parmaliana, A., Arena, F., Frusteri, F., and Glordano, N. J. (1990), *Chem. Soc. Faraday Trans*. **6(4),** 2663–2669.
13. Choudhary, V. R. and Pandit, M. Y. (1991), *Appl. Catal*. **71,** 265–274.
14. Ueda, W., Kuwabara, T., Ohshida, T., and Morikawa, Y. (1990), *J. Chem. Soc. Chem. Commun*. 1558–1559.
15. Fuchs, O. (1936), US patent no. 2,050,788.
16. Radlowski, C. A. and Hagen, G. P. (1992), US patent no. 5,095,156.
17. Radlowski, C. A., Hagen, G. P., Grimes, L. E., and Tatterson, D. F. (1994), US patent no. 5,364,979.
18. Radlowski, C. A. (1994), US patent no. 5,300,695.
19. Vanderspurt, T. H., Greaney, M. A., Leta, D. P., Koveal, R. J., Disko, M. M., Klaus, A. V., Behal, S. K., and Harris, R. B. (2000), US patent no. 6,034,141.

20. Vanderspurt, T. H. (1998), US patent no. 5,811,602.
21. Carlini, C., Di-Girolamo, M., Macinai, A., Marchionna, M., Noviello, M., Galletti, A. M. R., and Sbrana, G. (2003), *J. Mol. Catal. A: Chem*. **206,** 409–418.
22. Carlini, C., Macinai, A., Marchionna, M., Noviello, M., Galletti, A. M. R., and Sbrana, G. (2003), *J. Mol. Catal. A: Chem*. **200,** 137–146.
23. Klabunde, K. J., Stark, J., Kopper, O., Mohs, C., Park, D. G., Decker, S., Jiang, Y., Lagadic, I., and Zhang, D. (1996), *J. Phys. Chem*. **100,** 12,142–12,153.
24. Olson, E. S., Aulich, T. R., Sharma, R. K., and Timpe, R. C. (2003), *Appl. Biochem. Biotechnol*. **105–108,** 843–851.

Session 6A

Biomass Pretreatment and Hydrolysis

Session 6A

Biomass Pretreatment and Hydrolysis

Yong Y. Lee[1] and Bruce E. Dale[2]

[1]Auburn University, Auburn, AL; and
[2]Michigan State University, East Lansing, MI

This session deals with recent progress on pretreatment of lignocellulosic biomass, the peripheral reactions associated with pretreatment, and assessment of the effectiveness of pretreatment by enzymatic hydrolysis. Pretreatment is an essential element of the integral bioconversion process, and its objective is to enhance the susceptibility of cellulosic substrates to the action of cellulase enzymes.

Despite increased awareness of its importance and extensive research efforts in recent years, the pretreatment of biomass still remains one of the least understood subjects in biomass conversion technology. Recent research has broadened the database of pretreatment technology. However, the fundamental aspects of the pretreatment process are yet to be fully understood. It is still unclear which of the physical/chemical factors play major roles in pretreatment effectiveness and how they affect subsequent enzymatic hydrolysis. Among the known factors related to pretreatment are chemical composition (lignin, hemicellulose, buffering components), crystallinity, and surface area. What complicates this issue is that the lignocellulosic biomass varies widely in composition and physical characteristics depending on the species. The methods of pretreatment are often specific to each species of the biomass feedstock. This session was constructed with these thoughts in mind.

The session attracted papers covering a broad spectrum of pretreatment technologies. In the plenary session, the emphasis was placed on novel pretreatment methods and the fundamental understanding of pretreatments. A wide variety of feedstocks were introduced ranging from softwood to dry mill corn residues. Novel pretreatment methods based on organic solvents were introduced and their effectiveness on softwood was assessed. A considerable amount of hemicellulose is hydrolyzed in the acidic and neutral pretreatments. Several papers addressed this issue along with total hydrolysis (i.e., xylan and glucan) of biomass by dilute acid. While most papers addressed the fundamental aspects of pretreatment based on laboratory data, upscale process studies and data on mature technologies were also introduced. Comparative data reporting was presented describing the recent progress of pretreatment technologies being

developed by the Biomass Refining Consortium for Applied and Fundamental Innovation. It is noteworthy that the various pretreatment methods being developed by the consortium were evaluated by uniform test procedures and that the process economics of each process was also analyzed on a common basis.

A record number of papers were submitted for presentation in this session. A significant contribution came from overseas, perhaps a reflection of worldwide recognition of the importance of utilizing renewable resources for the production of fuels and chemicals. The information gathered here will contribute to the advancement and better understanding of pretreatment technology.

0273-2289/04/115/0937–0949/$25.00

Fermentation of "Quick Fiber" Produced from a Modified Corn-Milling Process into Ethanol and Recovery of Corn Fiber Oil

Bruce S. Dien,[*,1] Nick Nagle,[2] Kevin B. Hicks,[3] Vijay Singh,[4] Robert A. Moreau,[3] Melvin P. Tucker,[2] Nancy N. Nichols,[1] David B. Johnston,[3] Michael A. Cotta,[1] Quang Nguyen,[2] and Rodney J. Bothast[5]

[1]National Center for Agricultural Utilization Research, USDA,[†] Agricultural Research Service, 1815 North University Street, Peoria, IL 61604, E-mail: dienb@ncaur.usda.gov;
[2]Biotechnology Division for Fuels and Chemicals, National Renewable Energy Laboratory, 1617 Cole Boulevard, Golden, CO 80401;
[3]Eastern Regional Research Center, USDA, Agricultural Research Service, Wyndmoor, PA 19038;
[4]Department of Agricultural Engineering, University of Illinois, Urbana, IL 61801; and
[5]National Corn to Ethanol Research Pilot Plant, SIU Edwardsville, 1 N. Research Drive, Edwardsville, IL 62025

Abstract

Approximately 9% of the 9.7 billion bushels of corn harvested in the United States was used for fuel ethanol production in 2002, half of which was prepared for fermentation by dry grinding. The University of Illinois has developed a modified dry grind process that allows recovery of the fiber fractions prior to fermentation. We report here on conversion of this fiber (Quick Fiber [QF]) to ethanol. QF was analyzed and found to contain 32%wt glucans and 65%wt total carbohydrates. QF was pretreated with dilute acid and converted into ethanol using either ethanologenic *Escherichia coli* strain FBR5 or *Saccharomyces cerevisiae*. For the bacterial fermentation the liquid fraction was fermented, and for the yeast fermentation both liquid and solids were fermented. For the bacterial fermentation, the final ethanol concentration was 30 g/L, a yield of 0.44 g ethanol/g of sugar(s) initially present in the hydrolysate, which is 85% of the theoretical yield. The ethanol yield with yeast was 0.096 gal/bu of processed corn assuming a QF yield of 3.04 lb/bu.

*Author to whom all correspondence and reprint requests should be addressed.

The residuals from the fermentations were also evaluated as a source of corn fiber oil, which has value as a nutraceutical. Corn fiber oil yields were 8.28%wt for solids recovered following prtetreatment.

Index Entries: Bioethanol; corn fiber oil; *Escherichia coli*; pentose fermentations; *Saccharomyces cerevisiae*; β-glucosidase.

Introduction

In 2000, the United States produced more than 2 billion gallons of fuel ethanol, and >95% of this was from processed corn (Renewable Fuels Association, 2003). Ethanol is used as a fuel oxygenate, to meet goals required by the Clean Air Act 1990 amendment. Methyl *tert*-butyl ether (MTBE), which is made from petroleum-derived methanol, is the alternative oxygenate. However, MTBE has been identified as a major groundwater pollutant, and the federal government is moving to ban its use in gasoline. Fuel ethanol from corn is expected to double because it will be needed as a substitute for MTBE. Alternately, there is currently a proposal in the US Congress to relax the fuel oxygenate standard and require fuel ethanol usage as part of a National Renewable Fuel Standard.

Corn is processed for ethanol production by wet milling and dry grinding. Dry grinding accounts for 60% of the processed corn, and dry grind production capacity is growing more rapidly than wet milling. This growth in dry grinding capacity can be traced to the establishment of co-operatives owned by farmers, who favor this process because capital costs are much less than for wet mills. A major disadvantage of dry grinding compared to wet milling is the production of fewer coproducts.

Dry grind plants produce the following coproducts in addition to ethanol: carbon dioxide and a variety of high-fiber content animal feeds *(1)*. Carbon dioxide is produced during the fermentation, but because of its low selling price it is collected and sold by only a few of the dry grind ethanol processors. The animal feed products are manufactured from the fermentation residuals. The whole stillage is centrifuged or screened to yield distillers' wet grain (DWG) (more dense material) and thin stillage. The DWG is sometimes sold as is, but only locally because of its short shelf life. More often, it is combined with condensed thin stillage, dried, and sold as distillers' dried grains with solubles. By contrast, wet millers produce the following coproducts: corn oil, gluten meal, and corn gluten feed. Many wet millers also produce a variety of products from the starch in addition to ethanol. The final result is that the net cost of corn for ethanol production is lower for a wet mill compared to a dry grind operation.

The University of Illinois is developing a modified milling process, which would allow recoveries of the germ and hull fractions prior to fermentation *(2,3)*. The process involves soaking corn in water for a short period of time (12 h). The process has the following advantages over dry grinding: the potential for recovery of corn oil from recovered germ, an increased bioreactor capacity from prior separation of nonfermentables,

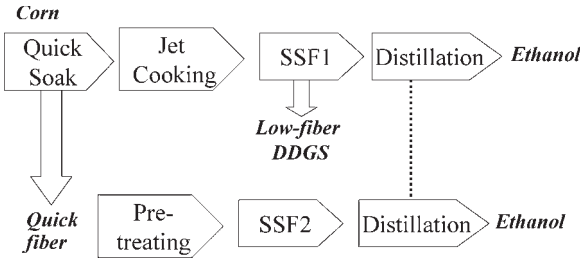

Fig. 1. Schematic of corn dry grind process with fiber conversion to ethanol. DDGS, distillers' dried grains with solubles.

and the ability to increase value and relative protein content for modified distillers' wet grains with solubles. It has been estimated that the modified process could generate an additional revenue of 5–7 ¢/gal *(4)*. The process is much less expensive to build than a traditional wet milling because of the shortened soaking time, fewer complex equipment needs, and avoidance of sulfuric acid steeping.

In the modified milling process, following steeping, the corn is milled and the germ and pericarp fiber are separated from the starch and gluten using hydroclones. The germ and pericarp fiber (quick fiber [QF]) are washed to recover additional starch, dried, and separated from each other by aspiration. The germ, which contains the corn oil, could be sold to an oil processor for extraction. The QF would be available for production of corn fiber oil, as well as an additional substrate for fermentation. Corn fiber oil has potential as a valuable coproduct because this oil contains relatively high levels of phytosterols *(5–7)*, which have been shown to lower cholesterol in several animal studies *(8,9)*. The phytosterol components include free phytosterols (St), phytosterol fatty acyl esters (St:E), and ferulate phytosterol esters (FPE). Corn fiber oil also contains stanols, which have additional value for lowering cholesterol.

QF has potential as a feedstock for ethanol fermentation because of its high carbohydrate content. A modified dry grind process that includes conversion of QF into ethanol is shown in Fig. 1. After fiber removal, the starch is liquefied, in part by jet cooking, and then undergoes simultaneous saccharification and fermentation (SSF1) to ethanol by the addition of yeast and glucoamylase. Converting QF to ethanol requires two additional processing steps: pretreatment and a SSF (SSF2). The ethanol streams for the starch and fiber fermentations can be mixed prior to distillation (Fig. 1, dotted line). Pretreatment prepares the cellulose for enzymatic saccharification and hydrolyzes the other carbohydrate components (i.e., residual starch and hemicellulose) into free sugars. The cellulose is saccharified enzymatically by cellulase. Fermentation of the fiber hydrolysate is more complicated than corn starch. The fiber contains a variety of carbohydrates including residual starch, hemicellulose, and cellulose. Hydrolyzing corn hemicellulose produces a mixture of sugars including arabinose, galactose, and xylose (ibid).

Saccharomyces cerevisiae ferments neither arabinose nor xylose. For the present study, these sugars along with glucose were converted to ethanol using recombinant ethanologenic *Escherichia coli* strain FBR5, which was developed by our laboratory *(10,11)*. This strain has been metabolically engineered to convert a wide spectrum of sugars to ethanol. Typical ethanol yields are 94% or greater of theoretical *(11)*. However, some mills may not wish to use recombinant organisms and, thus, fermentations were also carried out using *S. cerevisiae*. The yeast, however, is only capable of converting the sugars derived from cellulose and residual starch to ethanol.

Materials and Methods

Bacterial Strains, Growth Media, and Reagents

Media and protocols for routine maintenance of *E. coli* strain FBR5 have been previously described *(10)*. *S. cerevisiae* (Y-2034; ARS Culture Collection, Peoria, IL) was stored in 50% (v/v) glycerol stocks at –80ºC. The yeast culture was routinely maintained on YPD (10 g/L of yeast extract, 20 g/L of peptone, and 20 g/L of dextrose with 20 g/L of Difco agar added for solid medium) and incubated at 32ºC.

Enzymes were supplied by Novozyme (US Office: Franklinton, NC) and included cellulase (Celluclast® 1.5 L; 48 international filter paper units [IFPU]/mL), β-glucosidase (Novozym® 188; 66.8×10^3 IU/mL), and glucoamylase (Novozyme AMG300L). Sugars were purchased from Sigma (St. Louis, MO), and all other chemical and media reagents were from Fisher (Fairview, NJ).

Preparation of Quick Fiber

QF was prepared from no. 2 yellow dent corn as previously described *(2,12)*. Briefly, corn (1 kg) was soaked in water (2 L) for 12 h at 59°C. The corn was ground in a blender at 40% full power for 3 min followed by 46% full power for an additional 3 min, so as to separate out but not damage the germ. The germ, which is lighter than water, was isolated by flotation. The density of the remaining corn solution was adjusted by adding dried starch until the fiber fraction floated and could be removed by skimming off the surface. The coarse fiber was washed twice with water to remove added starch and stored at –20°C prior to hydrolysis.

Compositional Analysis of Biomass

Each sample was analyzed for moisture, carbohydrate, oil, and protein contents. Moisture was measured by drying the samples at 105°C until they reached a stable weight. Oil was measured using AOAC method 920.39 and protein by AOAC method 976.06, which is based on measuring total nitrogen. Starch was determined as previously reported *(13)*. Arabinose and xylose were determined by hydrolyzing the biomass with trifluoroacetic acid and analyzing for production of free sugars by high-

performance liquid chromatography (HPLC) as described previously *(14)*. Cellulose was determined using ASTM method E1758-95. Samples were analyzed for oil, protein, and starch by Analabs (Fulton, IL).

Optimizing Acid Loading for SSF Experiments

QF was pretreated with dilute acid for the *S. cerevisiae* SSF experiments. The amount of acid added per gram of biomass was optimized for complete hydrolysis of the hemicellulose and subsequent enzymatic hydrolysis of the cellulose. The QF (1.2 g) was mixed with 16 mL of various dilute H_2SO_4 solutions (0–12 g H_2SO_4/100 g of biomass [dry basis, db]) to give a solid loading of 7.0% (w of biomass, db/total w). The mixture was placed in stainless steel pipe reactors (40-mL working volume), which were placed in a fluidized sand bath (Model 01187-00 bath and 01190-72 temperature controller; Cole-Parmer, Vernon Hills, IL). The mixture was heated to and kept at 150ºC for 10 min before being quickly cooled in a water bath. The internal reactor temperature was monitored using a thermocouple probe inserted into one of the pipe reactors. The pretreated material was transferred to a test tube, neutralized with $Ca(OH)_2$ to pH 4.5, and citric acid buffer (pH 4.8, 50 m*M*) was added along with cellulase (0.3 mL) and β-glucosidase (0.3 mL); the total enzyme loading was 24 IFPU/g of QF. Thymol (0.025 mg/mL) was added to prevent microbial contamination. The biomass samples were incubated at 45°C with agitation for 48 h in a water bath (Dubnoff Metabolic Shaking Incubator; Precision Scientific, Chicago, IL). The hydrolysis reactions were sampled at 24 and 48 h for sugar concentrations. Each reaction was run in duplicate.

S. cerevisiae *SSF*

The biomass was pretreated as already described for the cellulase hydrolysis experiments with a 3.2% (w/w) H_2SO_4 loading. For SSF, 10.8 g (db) of pretreated material was placed in a 125-mL Erlenmeyer flask to which the following was added: cellulase (0.33% [v/v]), β-glucosidase (0.33% [v/v]), glucoamylase (0.046% [v/v]), and 10% (v/v) of a 10X YP stock (final concentration in medium: 10 g/L of Difco yeast extract, 20 g/L of Difco Proteose Peptone). The SSF was initiated by inoculation with *S. cerevisiae* to an OD_{600} of 0.5. The beginning solids for the SSF, including all additions, was 16.4% (w/w). The flasks were capped with rubber stoppers and pierced with a 22-gage needle to exhaust CO_2. The cultures were incubated at 32°C and agitated at 150 rpm (Refrigerated Innova® Shaker; New Brunswick Scientific, Edison, NJ) for 70 h. The fermentations were sampled each day for glucose and ethanol concentrations. All fermentations were run in duplicate.

E. coli *FBR5 Fermentations*

The QF was hydrolyzed using a different protocol than described for the *S. cerevisiae* fermentations, and, furthermore, the cellulose fraction was enzymatically hydrolyzed and fermented to ethanol. The QF was ground

with a coffee mill. The corn fiber was mixed with 1% (v/v) H_2SO_4 solution at a ratio of 1.2 g (db) biomass to 5.0 mL, placed in a shallow Pyrex® dish, covered with aluminum foil, and heated at 121°C for 1 h. After being allowed to cool, the liquid was separated from the solids by straining through cheesecloth. The recovered liquid portion was then treated as follows: first, the pH was adjusted to 10.0 by adding $Ca(OH)_2$. Second, 1 g/L of sodium bisulfite was added. Third, the liquid was warmed to 90°C and incubated at this temperature for 30 min. Finally, the liquid was neutralized with H_2SO_4 to pH 7.0. Following neutralization, the resulting precipitates, including gypsum, were removed by centrifugation (10,000*g*, 15 min). The recovered liquid was filter sterilized through a 0.22-µm membrane filter.

Bacterial fermentations were carried out in minibioreactors with automatic pH control that were constructed and operated as described previously *(14,15)*. Each 500-mL Fleaker® culture vessel contained 170 mL of hydrolysate supplemented with 20 mL of a 10X Luria-Bertani solution (10 g/L of tryptone and 5 g/L of yeast extract) and antifoam 289 (0.1 mL/L). Nitrogen was bubbled through the medium for 30 min prior to inoculation to remove oxygen. The fermentation vessels were each inoculated with a 5% (v/v) inoculum from an anaerobic culture of *E. coli* FBR5 grown overnight at 37°C. Fermentations were run at 35°C and stirred magnetically with 1 × 1 in. "X"-shaped stir bars at 300 rpm. The pH was set at 6.5 and maintained by the addition of a concentrated base solution (4 *N* KOH). Ethanol, sugars, organic acids, and optical densities (ODs) (550 nm) were determined periodically with 1.5-mL samples of cultures. Each experiment was run in duplicate.

Analytical Procedures

Activities for cellulase (FPU/mL) and β-glucosidase (IU/mL) were measured by the methods described previously *(16,17)*. ODs (1-cm light path) of cultures were monitored on a Beckman DU-640 Spectrophotometer (Fullerton, CA) at 550 (*E. coli*) or 660 nm (*S. cerevisiae*). Concentrations of sugars and ethanol were determined by HPLC using an Aminex HPX-87H column (300 × 7.8 mm; Bio-Rad, Richmond, CA) and refractive index detector. Samples were run at 65°C and eluted at 0.6 mL/min with 5 m*M* H_2SO_4.

Calculations

Ethanol yields and productivities for the fermentations were determined as previously described *(18)*. Ethanol yields for the QF are also reported on a per-bushel-of-corn-processed basis. The ethanol yield equation, which is similar to those derived in ref. *19*, is as follows.

$$\begin{aligned}\text{Ethanol}\,(\text{gal/bu}) = {} & \text{Dry Mass Yield}\,(\text{lb/bu corn}) \times \text{Carbohydrate Yield}\,(\text{lb/lb biomass}) \\ & \times 1.11\,(\text{lb free sugar/lb anhydrous sugar}) \\ & \times \text{Fermentation Yield}\,(\text{lb ethanol/lb fermented sugar}) \\ & \div 6.58\,(\text{lb ethanol/gal ethanol})\end{aligned}$$

Table 1
Comparison of QF and Corn Fiber[a]

Component	Corn fiber (% w/w db)[a]	QF (% w/w db)
Starch	11–23	15
Cellulose	12–18	17
Xylan	18–28	22
Arabinan	11–19	11
Protein	11–12	11
Oil	2	1

[a]Data from ref. *25*.

The dry biomass yield for QF (db) was assumed to be 3.04 lb/bu. The data on carbohydrate composition for QF (db) are provided in Table 1. The fermentation yield for a theoretical ethanol yield is 0.51 lb of ethanol/lb of sugar(s).

Results and Discussion

Composition of QF

QF samples contained 15% (w/w) starch and 17% cellulose (Table 1). The total carbohydrate composition was 65%. Protein and oils accounted for 12%. The components measured account for 78% of the dried material, the residual material (not tested for) includes ash, extractables, lignin, and lipids. The composition of the QF was, as expected, similar to that found for corn fiber. Corn fiber and QF are both derived from the pericarp and tip portions of the kernel. Most notably, the QF contained approx the same amount of residual starch, which suggests that the modified milling process is as effective at separating starch from the pericarp as a full steeping protocol. Starch recovery is significantly improved compared to previous results for which the starch content of the QF was 42–46% w/w *(2)*. The current study used an improved process that included an additional starch washing step.

Pretreatment and SSF of QF Using S. cerevisiae

The noncellulose carbohydrates present in QF were converted directly to free sugars by hydrolyzing with dilute H_2SO_4. Cellulose was hydrolyzed enzymatically using industrial cellulase preparations. QF was pretreated at various sulfuric acid loadings (0–4.8% g of H_2SO_4/g biomass [db]) to determine the optimal amount required for complete hydrolysis. The temperature for the pretreatment was set at 150°C as suggested *(20)* for the similar substrate of corn fiber. The glucose yield was maximum (92% of starch and cellulose recovered as glucose) at acid loadings of 0.8–3.2% (w/w) (Table 2).

Table 2
Dilute Acid Hydrolysis and Saccharification of QF

Acid Loading (% w/w)[a]	Glucose (%)[b]	Xylose (%)	Arabinose (%)	pH after heating
0 7	5 ± 0	16 ± 0	39 ± 0	4.41 ± 0.07
0.8	92 ± 2	50 ± 6	77 ± 2	2.78 ± 0.00
1.6	90 ± 1	74 ± 9	86 ± 3	2.12 ± 0.07
3.2	92 ± 3	98 ± 6	98 ± 4	1.89 ± 0.07
4.8	87 ± 4	98 ± 8	87 ± 0	1.56 ± 0.09

[a] % g of H_2SO_4/g of biomass.
[b] % of theoretical yield.

Maximum yields for arabinose (98% of available arabinose recovered as free sugar) and xylose (98% of xylan recovered as xylose) occurred at 3.2% (w/w) (Table 2). These percentage yields correspond to recoveries of 0.11 g of arabinose, 0.38 g of glucose, and 0.22 g of xylose/g of QF (db). Heating, even without adding a mineral acid, was sufficient to recover 0.32 g of glucose/g of QF (db) or 75% of the available glucan.

For the yeast fermentations, QF was treated at a high solid loading (14.1% w biomass [db]/total w) and an acid loading of 3.2% (w/w). The highest possible solid loading was used, such that the material formed a mixable slurry. The pretreated QF was neutralized; mixed with cellulase, β-glucosidase, and glucoamylase (to ensure complete starch hydrolysis); and inoculated with *S. cerevisiae*. The cellulase loading was 15 FPU/g of cellulose. The native β-glucosidase activity of the cellulase mixture was supplemented because adding extra β-glucosidase activity has been reported to enhance the rate of SSF *(21)*. The combined hydrolysis and fermentation was completed within 72 h (Fig. 2), and the final ethanol concentration was 23.4 ± 0.1 g/L. The ethanol yield was 0.153 g of ethanol/g of QF (db) or 85 ± 1% of maximum ethanol possible based on the total amount of glucans added and the theoretical ethanol yield from glucose. Assuming that 3.04 lb (db) of QF is recovered per bushel of corn, the fermentation results suggest that an additional 0.096 gal of ethanol/bu can be gained by fermenting QF with *S. cerevisiae*. The theoretical yield, based on the total glucan composition of QF, is 0.113 gal/bushel of corn.

The oils present in the QF differ from those found in the germ (corn oil) and in particular are enriched for phytosterols, which are cholesterol-lowering agents *(5–9)*. A prior study with corn fiber demonstrated that the oils withstood dilute-acid) pretreatment and became enriched in the pretreated solids *(22)*. Therefore, it was of interest to determine whether dilute-acid-pretreated QF solids might also serve as a source for these valuable nutraceutical chemicals. Following SSF, the solids residue was recovered and analyzed for the presence of oils. It was determined that only 1.12% oils was present in the residual solids (post-SSF, Table 3), which is comparable with that found in untreated QF (1.24–3.49% oil as noted in ref. *2*).

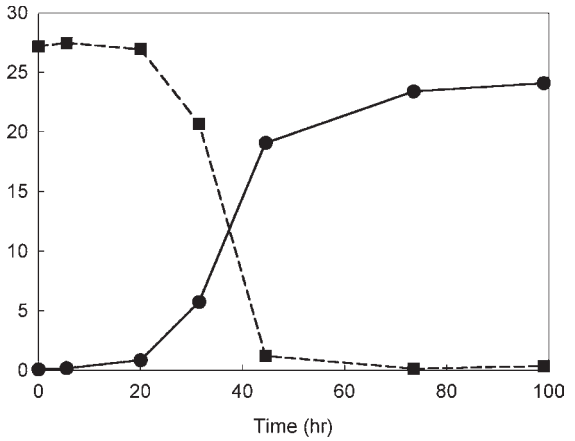

Fig. 2. H_2SO_4 loading was optimized for pretreating DWG for conversion to monomeric sugars. Each point is the average of duplicate runs. (■) Glucose; (●) ethanol.

Table 3
Recovery of Corn Fiber Oil from Process Fiber Residues

Fiber source	Total oil (% w/w)	Free sterol	FPE (wt% oil)	St:E (wt% oil)	Total sterols[a]
Pre-SSF[b]	8.15 ± 0.21	4.43 ± 0.19	3.27 ± 0.04	7.9 ± 0.1	15.6
Post-SSF[c]	1.12 ± 0.06	6.03 ± 3.74	5.82 ± 3.66	11.8 ± 5.7	23.6
Post-FBR5 ferm[d]	8.28 ± 0.14	5.80 ± 0.79	4.29 ± 0.69	12.2 ± 1.8	22.3

[a] Sum of prior three columns.
[b] Pretreated with dilute acid.
[c] Residual solids from SSF fermentation.
[d] Residual fiber from hydrolysate prepared for FBR5 fermentation.

One possible explanation for why the oils were not enriched is that they were diluted out by yeast and gypsum, from neutralizing with lime, mixed in with the recovered SSF residue. This possibility was partially tested by extracting the oils from the washed, pretreated QF prior to fermentation. The washed solids analyzed prior to neutralization and SSF contained 7 times more oil and 4.8 times more total phytosterols (pre-SSF, Table 3) than the recovered solid post-SSF. Therefore, pretreated QF is a valuable source of phytosterols, provided that they are recovered from the solids prior to SSF.

Pretreatment and Fermentation of QF Using E. coli *FBR5*

Sixty-five percent of the carbohydrates present in QF are in the form of pentoses, which *S. cerevisiae* does not ferment to ethanol. We have developed a recombinant *E. coli* strain that is capable of fermenting arabinose,

Table 4
Fermentation Results for Various Fibrous Feedstocks Using Ethanologenic Strain FBR5[a]

Feedstock	Initial sugar concentration			Maximum ethanol (% w/v)	Ethanol yield (g/g)	Ethanol productivity (g/[L·h])	Reference
	Arabinose (% w/v)	Glucose (% w/v)	Xylose (% w/v)				
QF	1.47	3.13	3.40	3.52 ± 0.03	0.44 ± 0.00	0.43 ± 0.04	This study
DWG[b]	0.79	1.96	1.23	2.12 ± 0.05	0.49 ± 0.01	0.71 ± 0.01	*11*
Corn fiber	2.00	2.80	3.70	3.74 ± 0.01	0.46 ± 0.00	0.77 ± 0.05	*11*

[a] Each result is based on duplicate fermentations.
[b] Broin Distiller wet grains.

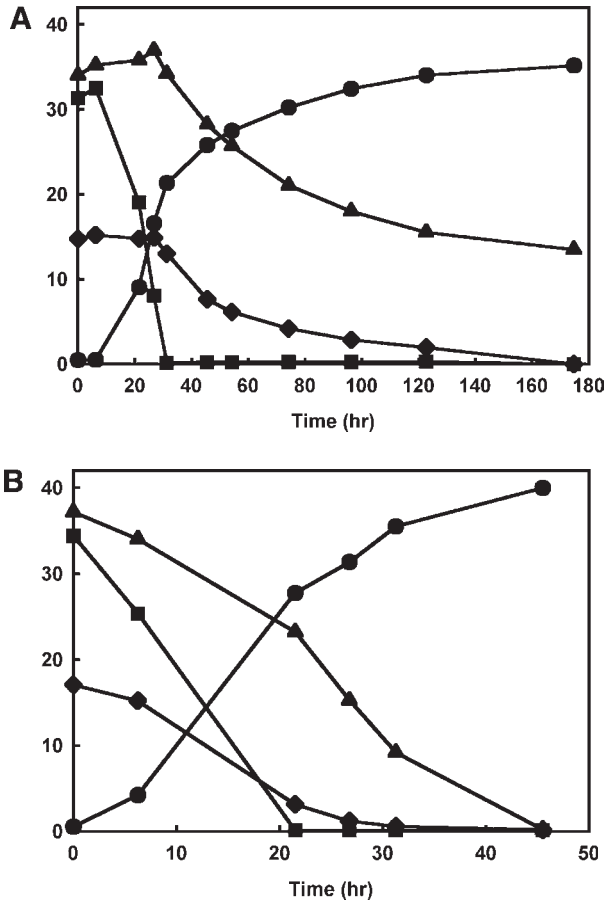

Fig. 3. **(A)** SSF of pretreated DWG with *S. cerevisiae.* Fermentations were performed in duplicate. **(B)** Fermentation of DWG liquid hydrolysate with *E. coli* FBR5. Fermentations were performed in duplicate. (▲) Xylose; (■) glucose; (◆) arabinose; (●) ethanol.

glucose, and xylose into ethanol *(10)*. The same pretreatment protocol was used for the present experiments as had been used previously for corn fiber produced by wet milling. Unlike the protocol described herein for the *S. cerevisiae* fermentations, only the liquid portion of the pretreated material was fermented to avoid a high solids content in the bioreactor. Cellulase was not added to the hydrolysate because cellulose partitions with the solids. The recovered liquid fraction from the hydrolysate contained 9.4% (w/v) total sugars (data not shown). *E. coli* FBR5 fermented all of the arabinose, glucose, and much of the xylose into ethanol (Fig. 3A). The final ethanol concentration was 3.51% (w/v), which is equal to 85% of the theoretical maximum ethanol yield based on the beginning sugar concentration of the medium (Table 4). The remaining 15% of the sugar(s) not converted to ethanol can be accounted for as residual xylose. The overall ethanol yield for FBR5 was 0.116 g of ethanol/g of QF (db).

A sugar mixture was prepared at a concentration similar to that of the QF hydrolysate using reagent-grade sugars. Fermentation of this sugar mixture served as a control. In contrast to the hydrolysate, all of the sugars were readily fermented (Fig. 3B), and the final production yield was 98% of theoretical. Furthermore, the ethanol productivity of the control fermentations was 57% faster than that of the hydrolysate. The difference in yield and rate can be attributed to microbial inhibitors that are formed during the hydrolysate preparation process *(23,24)*. Numerous inhibitors are formed during pretreatment and hydrolysis, and their effects are synergetic. One inhibitor that was detected in the QF was acetic acid (5 g/L), which arose from the acetyl side groups on the hemicellulose.

The additional yield per bushel of corn realized with FBR5 was 0.055 gal/bu. Ideally, 0.126 gal/bu would be realized by converting all of the pentosans and starch to ethanol at the theoretical ethanol yield (0.51 g of ethanol/g of fermented sugars). However, most of the loss in yield (73%) is associated with the pretreatment step. Fermentable sugars are lost during pretreatment by failing to recover all of the free sugars from the solid cake. The solids were not washed so as not to dilute the recovered sugars. Sugars can also be lost during pretreatment by degradation reactions; however, very little furfural and hydroxymethylfurfural were detected by HPLC in the hydrolysate (data not shown).

The residual solids from the QF pretreated for the FBR5 fermentation were analyzed for their oil content. The total oil content for the washed cake (Table 3) was 8.28% (w/dw) and the yield of total phytosterols was equal to 1.89% (w/dw). The yield compared favorably to that of an earlier study in which corn fiber was pretreated with dilute H_2SO_4 for which the yield of total phytosterols was 1.43% (w/dw) *(22)*. The pretreatment step concentrated the total phytosterols 26 times compared to untreated QF *(2)*.

As noted previously, QF is derived from the pericarp fraction of the corn. In dry grinding and wet milling, this fraction ends up in the DWG and corn fiber, respectively *(1)*. Both of these feedstocks have been converted to ethanol using *E. coli* FBR5 own this laboratory using the same protocol as described herein for QF (Table 4). Strain FBR5 produced the highest ethanol concentrations from corn fiber and QF, as expected because the prepared hydrolysates had approximately twice the concentration of sugars of the DWG. The ethanol production yields were also similar for corn fiber and QF, 86–90% of theoretical. However, FBR5 fermented the QF hydrolysate at a much slower rate (44% slower based upon average productivity) than the corn fiber hydrolysate. The slower rate suggests that the QF hydrolysate was more inhibitory to fermentation than the corn fiber. This result was unexpected and suggests that some difference in the collection of the two materials may be responsible. Possibly, the conventional steeping process "washes away" an inhibitor that is not removed during the much gentler steeping used to produce QF. One solution may be to include an additional step to further remove the inhibitors present following hydrolysis in addition to overliming.

Acknowledgments

We wish to thank Patricia J. O'Bryan and Loren Iten for their fine technical assistance.

References

1. Dien, B. S., Bothast, R. J., Nichols, N. N., and Cotta, M. A. (2002), *Int. Sugar J.* **104(1241),** 204–207.
2. Singh, V., Moreau, R. A., Doner, L. W., Eckhoff, S. R., and Hicks, K. B. (1999), *Cereal Chem.* **76(6),** 868–872.
3. Wahjudi, J., Xu, L., Wang, P., Singh, V., Buriak, P., Rausch, K. D., Mcaloo, A. J., Tumbleson, M. E., and Eckhoff, S. R. (2000), *Cereal Chem.* **77(5),** 640–644.
4. Taylor, F., Mcaloon, A. J., Craig, J. C., Yang, P., Wahjudi, J., and Eckhoff, S. R. (2001), *Appl. Biochem. Biotechnol.* **94(1),** 41–49.
5. Moreau, R. A., Hicks, K. B., and Norton, R. A. (1998), US patent no. 5,843,499.
6. Moreau, R. A., Powell, M. J., and Hicks, K. B. (1999), *J. Agric. Food Sci.* **44,** 2149–2154.
7. Moreau, R. A., Singh, V., Nunez, A., and Hicks, K. B. (2000), *Biochem. Soc. Trans.* **28,** 803–806.
8. Hicks, K. B. and Moreau, R. A. (2001), *Food Technol.* **55(1),** 63–67.
9. Moreau, R. A., Whitaker, B. D., and Hicks, K. B. (2002), *Prog. Lipid Res.* **41(6),** 457–500.
10. Dien, B. S., Hespell, R. B., Wyckoff, H. A., and Bothast, R. J. (1998), *Enzyme Micro. Technol.* **23(6),** 366–371.
11. Dien, B. S., Nichols, N. N., O'Bryan, P. J., and Bothast, R. J. (2000), *Appl. Biochem. Biotechnol.* **84–86,** 181–196.
12. Singh, V. and Eckhoff, S. R. (1996), *Cereal Chem.* **73(6),** 716–720.
13. Dien, B. S., Bothast, R. J., Iten, L. B., Barrios, L., and Eckhoff, S. R. (2002), *Cereal Chem.* **79(4),** 582–585.
14. Dien, B. S., Hespell, R. B., Ingram, L. O., and Bothast, R. J. (1997), *World J. Microbiol. Biotechnol.* **13(6),** 619–625.
15. Beall, D. S., Ohta, K., and Ingram, L. O. (1991), *Biotechnol. Bioeng.* **38(3),** 296–303.
16. Ghose, T. K. (1987), *Pure Appl. Chem.* **59(2),** 257–268.
17. Hespell, R. B., Wolf, R., and Bothast, R. J. (1987), *Appl. Environ. Microbiol.* **53(12),** 2849–2853.
18. Nichols, N. N., Dien, B. S., and Bothast, R. J. (2001), *Appl. Microbiol. Biotechnol.* **56(1–2),** 120–125.
19. Gulati, M., Kohlmann, K., Ladisch, M. R., Hespell, R., and Bothast, R. J. (1996), *Bioresour. Technol.* **58(3),** 253–264.
20. Grohmann, K. and Bothast, R. J. (1997), *Process Biochem.* **32(5),** 405–415.
21. Grohmann, K. (1993), in *Bioconversion of Forest and Agricultural Plant Residues*, 1st Ed., Saddler, J. N., ed., C.A.B. International, Wallingford, UK, pp. 183–210.
22. Singh, V., Johnston, D. B., Moreau, R. A., Hicks, K. B., Dien, B. S., and Bothast, R. J. (2003), *Cereal Chem.* **80(2),** 126–129.
23. Palmqvist, E. and Hahn-Hagerdal, B. (2000), *Bioresour. Technol.* **74(1),** 17-24.
24. Palmqvist, E. and Hahn-Hagerdal, B. (2000), *Bioresour. Technol.* **74(1),** 25–33.
25. Leathers, T. D. (1998), *Soc. Ind. Microbiol. News* **48(5),** 210–217.

0273-2289/04/115/0951–0963/$25.00

Ammonia Fiber Explosion Treatment of Corn Stover

Farzaneh Teymouri, Lizbeth Laureano-Pérez, Hasan Alizadeh, and Bruce E. Dale*

Department of Chemical Engineering and Materials Science, 2527 Engineering Building, Michigan State University, East Lansing MI 48824, E-mail: bdale@egr.msu.edu

Abstract

Optimizing process conditions and parameters such as ammonia loading, moisture content of biomass, temperature, and residence time is necessary for maximum effectiveness of the ammonia fiber explosion process. Approximate optimal pretreatment conditions for corn stover were found to be temperature of 90°C, ammonia:dry corn stover mass ratio of 1:1, moisture content of corn stover of 60% (dry weight basis), and residence time (holding at target temperature), of 5 min. Approximately 98% of the theoretical glucose yield was obtained during enzymatic hydrolysis of the optimal treated corn stover using 60 filter paper units (FPU) of cellulase enzyme/g of glucan (equal to 22 FPU/g of dry corn stover). The ethanol yield from this sample was increased up to 2.2 times over that of untreated sample. Lowering enzyme loading to 15 and 7.5 FPU/g of glucan did not significantly affect the glucose yield compared with 60 FPU, and any differences between effects at different enzyme levels decreased as the treatment temperature increased.

Index Entries: Ammonia fiber explosion; corn stover; enzymatic hydrolysis; simultaneous saccharification and fermentation; moisture content; residence time.

Introduction

Utilizing solar energy and extracting energy from the carbon fixed by photosynthesis in plants offers a potentially attractive solution to establish clean and sustainable resources for both energy demands and raw material needs. It has been estimated that 10^{11}–10^{12} tons of carbon is fixed annually around the world by photosynthesis of higher plants. Potentially, this renewable resource can provide approx 10 times our current energy demand from all sources *(1)*.

*Author to whom all correspondence and reprint requests should be addressed.

The potential for using lignocellulosic biomass material to produce energy carriers such as electricity, gases, and transportation fuels is well recognized. Biomass energy produced in an efficient and sustainable manner can offer numerous economic, environmental, and social benefits compared to fossil fuels. One liquid fuel that has the potential to match the convenient attributes of petroleum fuels is ethanol produced from lignocellulosic biomass. In ethanol production, enzymatic hydrolysis of cellulose to glucose is a very attractive route, because nearly theoretical yields of glucose are possible *(2,3)*.

A major problem in the commercialization of this potential is the inherent resistance of lignocellulosic materials toward conversion to fermentable sugars *(4)*. To improve the efficiency of enzymatic hydrolysis, a pretreatment step is necessary to make the cellulose fraction accessible to cellulase enzymes. Delignification, removal of hemicellulose, and decreasing the crystallinity of cellulose produce more accessible surface area for cellulase enzymes to react with cellulose *(5)*.

The ammonia fiber explosion (AFEX) process treats lignocellulosic biomass with liquid ammonia under pressure followed by explosive pressure release to enhance conversion of structural carbohydrates (cellulose and hemicellulose) to fermentable sugars. Instantly releasing the pressure in the AFEX process disrupts the fibrous structure of biomass and increases the accessible surface area, which improves the digestibility of the biomass. However, a previous study *(6)* has shown that increasing the blowdown pressure from 1.4 to 2.3 and 3 atm did not affect the reactivity of the treated biomass and the results were similar, but at higher pressure, 4 atm, less reactivity was observed. AFEX treatment also increases the digestibility of the biomass by decrystallizing cellulose, prehydrolyzing hemicellulose, and reducing lignin content of the treated material.

A major obstacle to the commercialization of enzymatic hydrolysis of biomass is the high cost of the enzymes. One way to reduce this cost is to use much less enzyme per unit of biomass hydrolyzed. Previous work has shown that the effective enzymatic hydrolysis of AFEX-treated biomass at enzyme loadings as low as 5 filter paper units (FPU)/g of dry biomass was achieved by adjusting the pretreatment parameters *(6)*. The objectives of the present study, were to determine the best AFEX conditions for pretreatment of corn stover, to employ different enzyme loading levels (60, 15, and 7.5, FPU/g of glucan), and to compare the enzymatic hydrolysis results and ethanol yield.

Materials and Methods

Substrate

The biomass material studied was corn stover (includes all aboveground portions of the corn plant except the grain and cob). Milled (passed through a 6-mm screen) and dried (about <10% moisture content) corn stover was provided by National Renewable Energy Laboratory (NREL)

Table 1
Composition of Corn Stover

Component	Mass percentage (dwb)
Glucan	36.1
Xylan	21.4
Arabinan	3.5
Mannan	1.8
Galactan	2.5
Lignin	17.2
Protein	4.0
Acetyl	3.2
Ash	7.1
Uronic acid (estimated)	3.6
Nonstructural sugars	1.2
Total	101.6

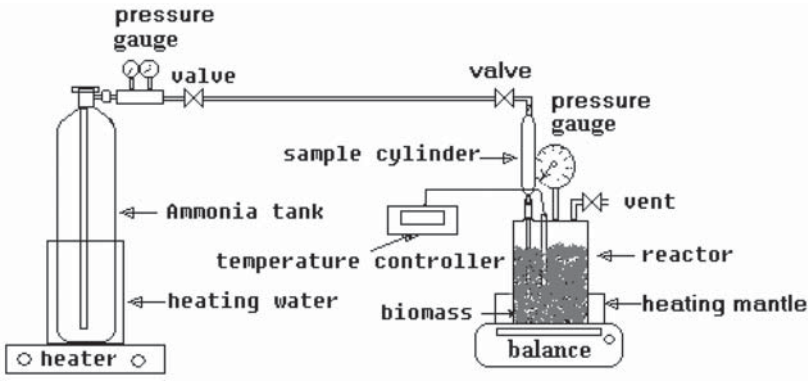

Fig. 1. Schematic diagram of laboratory AFEX apparatus.

(Golden, CO), as was its composition (Table 1). Liquid anhydrous ammonia was from AGA (Lansing, MI).

AFEX Treatment

The reactor consisted of a 300-mL stainless steel pressure vessel (Parr, Moline, IL) (Fig. 1). The vessel was loaded with prewetted corn stover (at desired moisture content). The vessel was topped up with stainless steel spheres (approx 1 mm in diameter) to occupy the void space and thus minimize transformation of the ammonia from liquid to gas during loading.

The lid was then bolted shut. Using the precalibrated ammonia sample cylinders, the predetermined amount of liquid ammonia was delivered to the vessel. The vessel was heated by a 400-W Parr heating mantle to the desired temperature. After holding the vessel at the target temperature for the selected residence time, the exhaust valve was rapidly opened to relieve the pressure and accomplish the explosion. Both pressure and temperature drop very rapidly. The treated samples were removed and allowed to stand overnight in a fume hood to evaporate the residual ammonia.

Treatment of the corn stover with ammonia resulted in a darkening of corn stover compared with untreated sample but did not otherwise change the macroscopic appearance of the substrate. The treated samples were kept in plastic bags in a refrigerator for further analysis.

Enzymatic Hydrolysis

We essentially followed the NREL standard biomass enzymatic hydrolysis protocol (LAP-009). The NREL standard protocols can be obtained from the following website: www.ott.doe.gov/biofuels/analytical_methods.html.

All the samples were hydrolyzed in a pH 4.8 citrate buffer with the desired cellulase enzyme (Celluclast 1.5 L [Novozyme] provided by NREL, CAS 9012-548; activity: 28 FPU/mL) loading (60, 15, and 7.5 FPU/g of glucan), and β-glucosidase from Sigma (St. Louis, MO) at 40 IU/g of glucan. All the samples were hydrolyzed at 50°C with gentle rotation (75 rpm) for a period of 168 h. At predetermined time intervals (0, 3, 6, 24, 48, 72, and 168 h), 1 mL of hydrolysate was taken for sugar analysis. Sugar analysis was performed using a Bio-Rad (Richmond, CA) high-performance liquid chromatography (HPLC) unit equipped with an Aminex HPX87P carbohydrate analysis column and a Bio-Rad Deashing Cartridge guard column. The mobile phase used was degassed HPLC water at a flow rate of 0.6 mL/min at 85°C. The injection volume used was 20 μL with a run time of 20 min.

Simultaneous Saccharification and Fermentation

Simultaneous saccharification and fermentation (SSF) experiments were conducted according to NREL standard protocol (LAP-008). Each SSF flask was loaded with 3% (w/w) glucan, 1% (w/v) yeast extract, 2% (w/v) peptone, 0.05 M citrate buffer (pH 4.8), the appropriate amount of cellulase enzyme to achieve 15 FPU/g of glucan, and the appropriate amount of *Saccharomyces cerevisiae* D_5A (provided by NREL) inoculum (starting optical density of 0.5). The SSF flasks were equipped with water traps to maintain anaerobic conditions and were incubated at 37°C with gentle rotation (130 rpm) for a period of 168 h.

At time intervals of 0, 3, 6, 24, 48, 72, 96, and 16 8h, a 2-mL aliquot was removed aseptically from each flask. The samples were centrifuged, and the supernatants were filtered for sugar analysis on HPLC and ethanol analysis by gas chromatography (GC). At the last time point, a sample from each SSF flask was streaked on a YPD (yeast extract, peptone, dextrose)

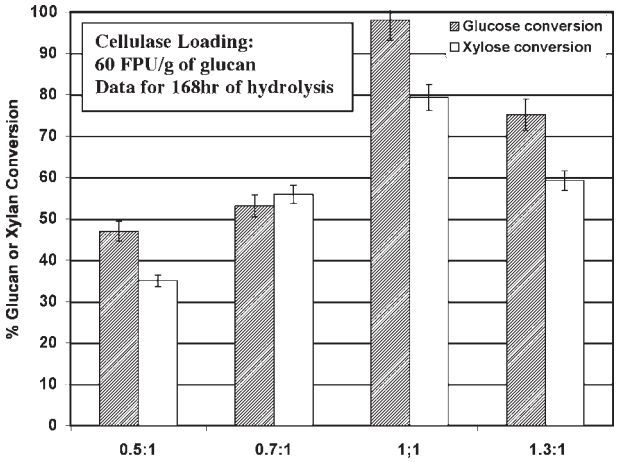

Fig. 2. Effects of ammonia loading (g of NH**3**:g of dry biomass) on enzymatic conversion of glucan and xylan for AFEX treatment of corn stover at 90°C and 60% moisture content (dwb). All the runs were kept at the set temperature for 5 min.

plate to check for any contamination. No contamination was observed in this series of SSF experiments.

The samples taken from fermentation at different time intervals were analyzed for ethanol yield by a GC 17 Shimadzu (Columbia, MD) unit. The injection temperature was 240°C and the detector temperature was 255°C. The column was first maintained at 80°C up to 3 min, followed by a temperature program at 15°C/min up to 125°C for 6 min.

Results and Discussion

Effects of Ammonia-to-Biomass Ratio on Enzymatic Hydrolysis of AFEX-Treated Corn Stover

Figure 2 shows the effect of ammonia-to-biomass ratio (0.5:1, 0.7:1, 1:1, and 1.3:1 g of anhydrous ammonia:g of dry biomass) on the subsequent enzymatic hydrolysis of AFEX-treated corn stover. Enzymatic hydrolysis was carried out for 168 h. Glucan conversion increased with increasing ammonia loading and attained a maximum value at a mass ratio of 1:1. Xylan conversion also showed the same trend as glucan conversion in response to ammonia loading. Ammonia at this loading provided maximum overall enhancement of reactivity during pretreatment. It is known that ammonia can react with lignocellulosic materials by ammonolysis of the ester crosslinks of some uronic acids with the xylan units and by cleaving the bonds linking hemicellulose and lignin *(7)*. However, it is evident from Fig. 2 that further increases in ammonia loading decreased glucan conversion. It is possible that extra liquid ammonia plasticizes *(8)* the cellulose and thereby reduces the disruptive effect of sudden pressure release.

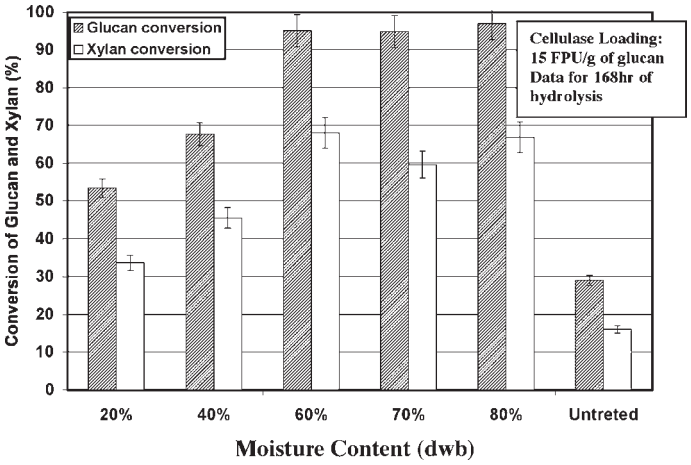

Fig. 3. Effects of moisture content on glucan and xylan conversion of AFEX-treated corn stover at 90°C and 1:1 ammonia loading. All runs were kept at the set temperature for 5 min.

Based on these observations, the ammonia ratio of 1:1 is considered to be the optimum ammonia loading ratio for AFEX treatment of corn stover. Previous work also recognized the same ammonia ratio as the optimum ratio for AFEX treatment of corn fiber *(9)*.

Effects of Moisture Content on the Enzymatic Hydrolysis of AFEX-Treated Corn Stover

Effects of different moisture contents (20, 40, 60, 70, and 80% dry weight bsis [dwb]; for example, to make 20% moisture content [dwb] 20 g of water was added to 100 g of dry corn stover) on the subsequent enzymatic hydrolysis are presented in Fig. 3. Glucan conversion increased with increasing moisture content and attained a maximum value at 60% moisture content. Xylan conversion also showed the same trend as glucan conversion in response to moisture content. Even though at higher moisture content, ammonia is more diluted, apparently the affinity of ammonia for biomass components (e.g., cellulose, hemicellulose) is still sufficiently strong so that the ammonia reacts adequately with the structural polymers (cellulose and hemicellulose). Previous studies have postulated that the moisture in the biomass allows formation of ammonium hydroxide, which hydrolyzes hemicellulose and thereby enhances the overall effect of AFEX treatment *(10)*. As Fig. 3 shows, further increases in moisture content beyond 60% (70 and 80% dwb), did not improve either glucan or xylan conversion. Dilution of ammonia at these moisture contents may reduce the affinity of ammonia for biomass. Based on these data, we have selected 60% moisture content (dwb) as the optimum moisture content for AFEX treatment of corn stover.

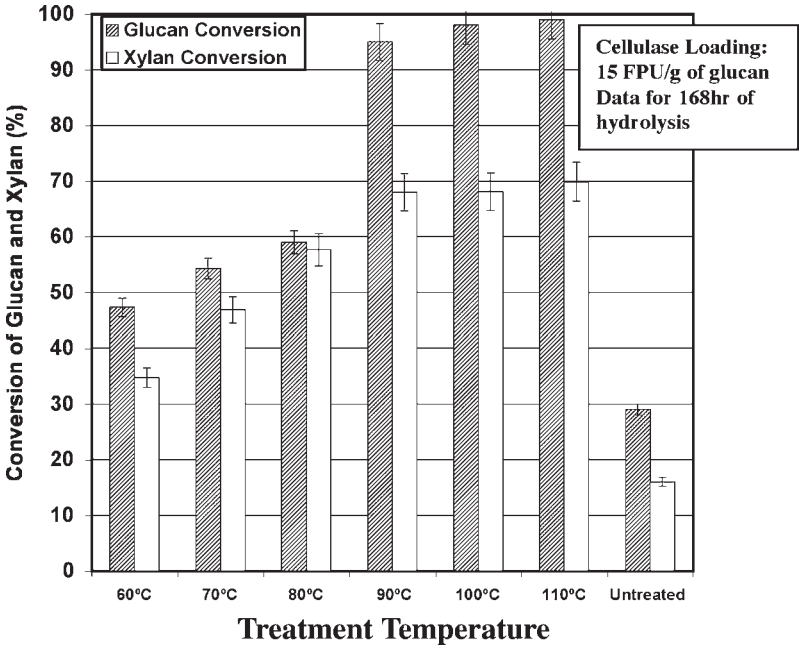

Fig. 4. Effects of treatment temperature on glucan and xylan conversion of AFEX-treated corn stover at 60% moisture content (dwb) and 1:1 ammonia loading. All the runs were kept at the set temperature for 5 min.

Effects of Temperature on the Enzymatic Hydrolysis of AFEX Treated Corn Stover

The data in Fig. 4 illustrate that increasing temperature dramatically enhances conversion of glucan to glucose. Pretreatment temperature is a very important variable, because it determines the amount of ammonia vaporized during the explosive flash and influences system pressure. At higher temperatures, more ammonia vapors flash, and, therefore, greater disruption of biomass fiber structure probably occurs. In addition, higher temperature accelerates the chemical reactions such as alkaline hydrolysis of hemicellulose. As Fig. 4 shows, increasing temperature from 90 to 100 and 110°C improved the conversion of glucan to glucose by only about 1%. Apparently further increases in treatment temperature beyond 90°C do not have much additional beneficial effect.

The ultimate goal of the AFEX treatment is to increase the yields of fermentation products such as ethanol by increasing the digestibility of the biomass. Therefore, selected runs that showed higher glucan and xylan conversion were chosen for further SSF analysis. The best treatment temperature is to be selected based on the fermentation results, not just on enzymatic hydrolysis; the fermentation results are presented later in this article.

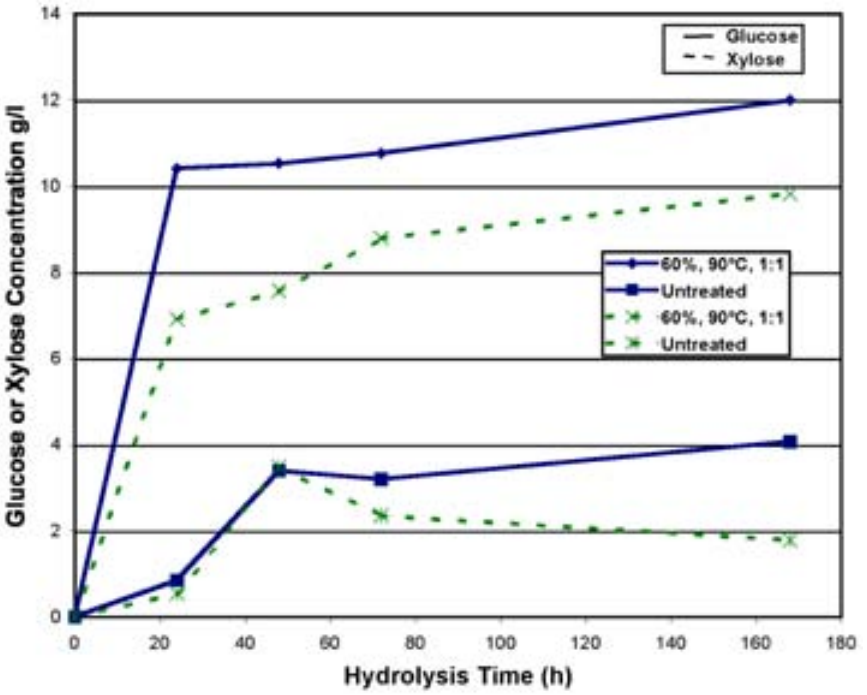

Fig. 5. Glucose and xylose concentration vs hydrolysis time at enzyme loading of 60 FPU/g of glucan.

Enzymatic Hydrolysis Time Profile

Figure 5 shows glucose and xylose production profiles of AFEX-treated and untreated corn stover samples at enzyme loading levels of 60 FPU/g of glucan. In all cases, the curves that describe sugar production vs time have a similar shape. The AFEX-treated sample showed a higher degree of digestibility than the untreated sample. Figure 5 also demonstrates that the initial rate of digestion of treated material was higher than of untreated corn stover. The 24-h yields of glucose and xylose from the AFEX-treated sample are more than 10 times the yields from untreated stover. As this data shows, AFEX treatment approximately doubled the yield of glucose and quadrupled the yield of xylose vs untreated corn stover.

Figure 6 illustrates glucose production vs time for our best AFEX run (60% moisture, 90°C, and 1:1 ammonia ratio), with the data normalized to the 3-d yield. The 3-d glucose yield is a convenient measure of enzymatic susceptibility of the AFEX-treated biomass. The normalized curve allows determination of glucose yield at times other than 3 d. Based on Fig. 6, about 96% of the 3-d glucose was released in 24 h and about 97% of glucose was released in 48 h. These data demonstrate the high digestibility of the AFEX-treated corn stover.

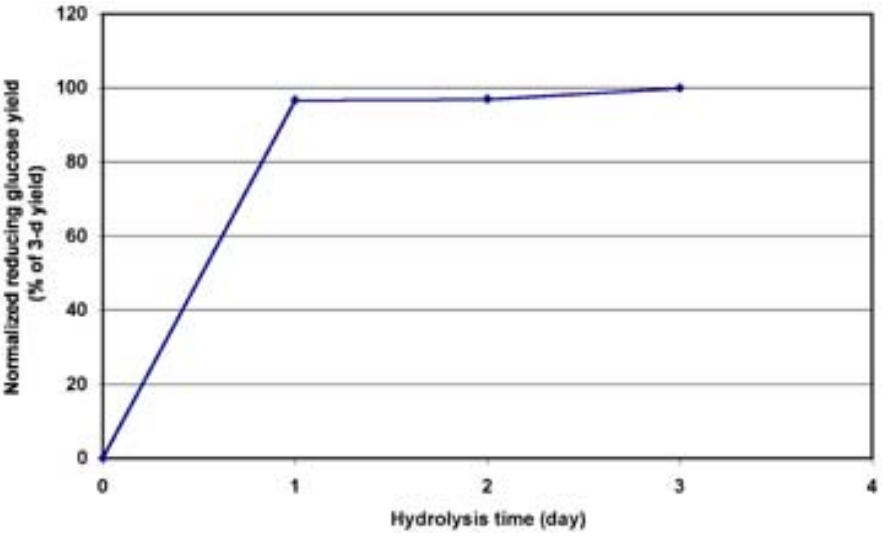

Fig. 6. Normalized hydrolysis profile for corn stover treated at 60% moisture content (dwb), 90°C, and 1:1 ammonia loading ratio, with enzyme loading of 60 FPU/g of glucan.

Simultaneous Saccharification and Fermentation

As Fig. 7 shows, throughout the SSF process, glucose produced by the cellulase enzyme was almost completely consumed by the yeast and converted to ethanol. The rate of ethanol production was quite rapid during the first 6 h of the fermentation. The AFEX-treated sample attained the maximum amount of ethanol after 96 h of the SSF process. As seen in Fig. 7, the AFEX-treated sample produced more than twice as much as ethanol compared with an untreated sample. Even though this sample showed slightly lower glucose yield in enzymatic hydrolysis compared with the samples treated under the same conditions except with higher temperature (100°C), as Fig. 8 shows, it still produced a higher ethanol yield. The higher temperatures may produce some inhibitory material, perhaps lignin fragments, that affects the performance of the yeast and reduces the SSF productivity.

On the other hand, the concentration of xylose produced consistently increased throughout the SSF process. Our yeast (*S. cerevisiae* D_5A) does not have the ability to utilize xylose and to convert it to ethanol. The data in Fig. 7 are also similar to those we observed in our enzymatic hydrolysis.

Effects of Longer AFEX Residence Time

In an effort to explore the effects of longer treatment time on the hydrolysis results, a series of AFEX experiments (temperature of 90–110°C, moisture content of 60–70% dwb, all at 1:1 ammonia loading ratio) were conducted; the reactor was maintained at the target temperature

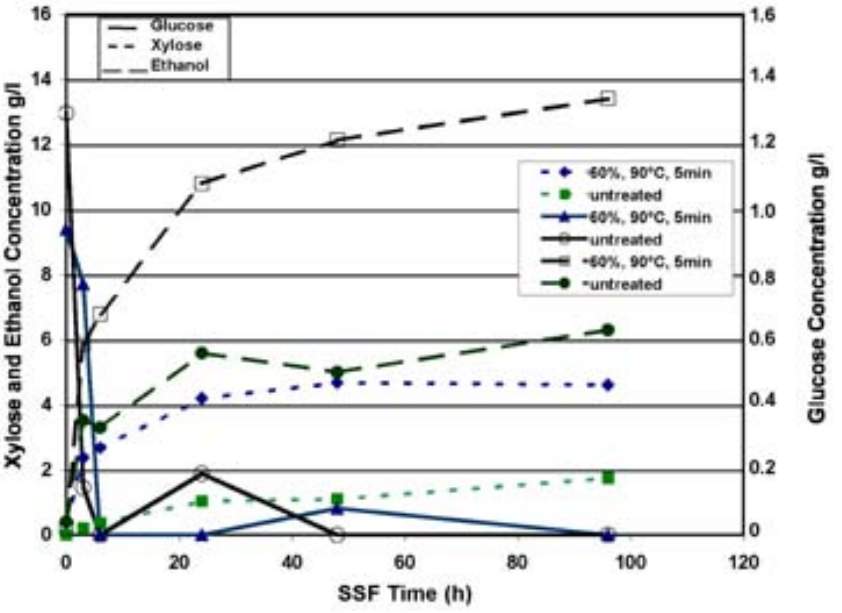

Fig. 7. SSF time profile for glucose, xylose and ethanol concentration.

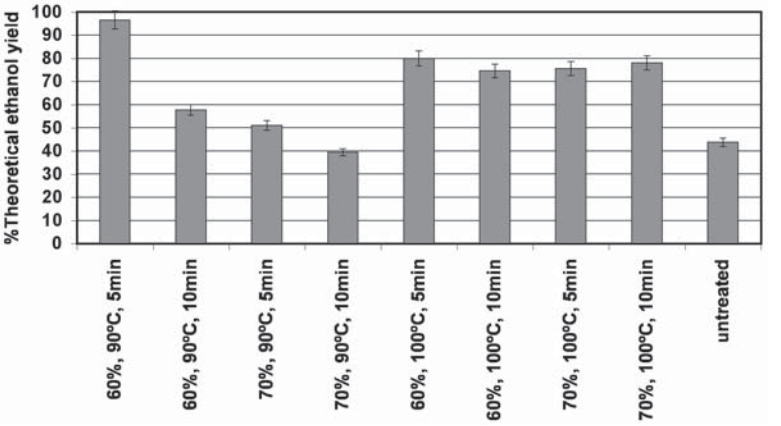

Fig. 8. SSF results of some AFEX runs with longer residence times.

for 5, 10, or 15 min. Increasing the treatment time in some cases slightly increased glucan and xylan conversion and in some cases decreased these conversions (data not shown). Since these effects were different in each set of AFEX runs, we were not able to find any correlation among the treatment time and other conditions of the AFEX runs. Therefore, to be able to choose the best treatment time, we selected some of the runs that showed greater glucan and xylan conversion with increasing time for further SSF experiments. The results of these SSF experiments are shown in Fig. 8.

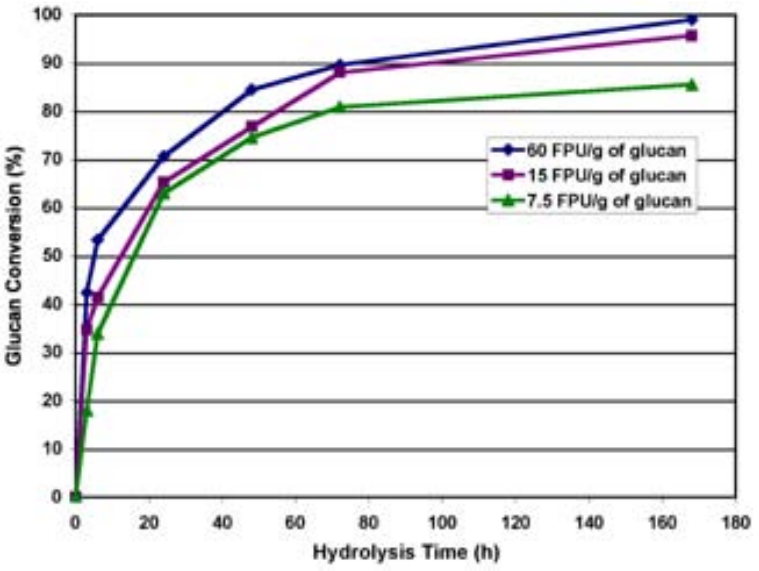

Fig. 9. Glucan conversion profile of AFEX-treated corn stover (60% moisture content [dwb], 1:1 ammonia loading, and 90°C) at different enzyme loadings.

Note that all the runs (with one exception) with longer treatment time showed lower ethanol yield. However, the hydrolysis results of these runs all showed greater glucan and xylan conversion. As mentioned previously, perhaps during longer treatment times some inhibitory materials were produced that in turn reduced the yield of the fermentation. Based on these findings, 5 min is currently considered the best residence time for the AFEX treatment of corn stover.

Effects of Different Cellulase Enzyme Loadings

The cost of enzyme used for saccharification of cellulosic materials strongly influences the overall economics of the biomass conversion process. One way to decrease enzyme cost is to use less enzyme per kilogram of biomass. Therefore, we performed enzymatic hydrolysis on AFEX-treated corn stover sample with three different cellulase loadings (7.5, 15, and 60 FPU/g of glucan). As Figs. 9 and 10 demonstrate, increasing cellulase loading from 15 to 60 FPU/g of glucan did not make an appreciable difference in glucan or xylan conversion of AFEX-treated samples. These data demonstrate the high digestibility of the AFEX-treated corn stover.

Conclusion

Optimum AFEX treatment conditions are quite broad. However, the highest glucan and xylan conversions and ethanol yields from AFEX-treated corn stover were achieved at about 1:1 kg of ammonia/kg of dry biomass, 60% (dwb) moisture content, 90°C, and 5-min residence time in a

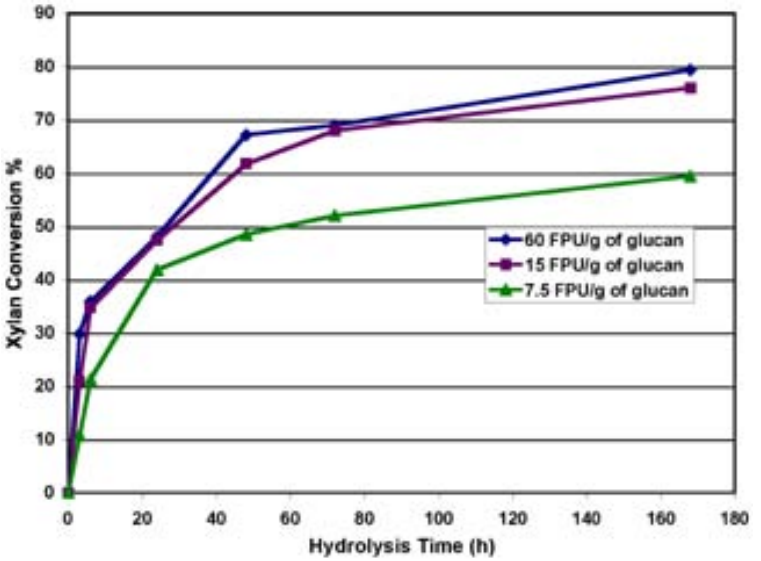

Fig. 10. Xylan conversion profile of AFEX-treated corn stover (60% moisture content [dwb], 1:1 ammonia loading, and 90°C) at different enzyme loadings.

batch AFEX reactor. It appears possible, at least within some limits, to achieve similar hydrolysis results by increasing temperature while reducing ammonia levels; that is, we can"trade off" these two parameters.

In addition, increasing temperature and moisture content enhanced the AFEX treatment, at least up to some limit. Above about 90°C, higher sugar yields by enzymatic hydrolysis were not accompanied by higher ethanol yields following SSF. Presumably, some fermentation inhibitors are formed, perhaps lignin fragments, at higher AFEX temperatures.

Furthermore, enzymatic hydrolysis of the corn stover treated under optimal AFEX conditions showed almost 98% glucan conversion and 80% xylan conversion vs 29 and 16% for untreated corn stover, respectively (at an enzyme loading of 60 FPU/g of glucan). Unlike acidic pretreatments, AFEX does not generate sugar monomers. The cellulase mixture in our study was developed for hydrolysis of acid-pretreated materials and has about 1% by weight xylanase activity (J. Cherry, personal communication, Nov. 2002). Enzyme cocktails with enhanced xylanase activity would presumably completely hydrolyze AFEX-treated xylans.

Moreover, lowering the cellulase loading from 60 FPU/g of glucan to 7.5 or 15 FPU/g of glucan did not make appreciable differences in glucan or xylan conversion of AFEX-treated corn stover. These results are very important in terms of process economics. We are doing additional studies to determine how low the cellulase loading can be made and still obtain high glucose and xylose yields.

Finally, AFEX-treated corn stover more than doubled the amount of ethanol production compared with untreated corn stover in an SSF process.

Acknowledgments

We thank the NREL for providing corn stover, cellulase enzyme, and yeast. We also thank Dr. Mariam Sticklen for the use of her laboratory and equipment. This work was supported by The USDA Initiative for Future Agricultural and Food Systems Program through contract no. 00-52104-9663.

References

1. Hall, D. O. (1979), *Solar Energy* **22,** 307–328.
2. Wyman, C. E. (1999), *Annu. Rev. Energy Environ.* **24,** 189–226.
3. Wyman, C. E. (1995), in *Enzymatic Degradation of Insoluble Carbohydrates*, ACS Symposium Series 618, Saddler, J. N. and Penner, M. H., eds., American Chemical Society, Washington, DC, pp. 272–290.
4. Walter, A. (2000), in *Industrial Uses of Biomass Energy*, Rosillo-Calle, F., Bajay, S. V., and Rothman, H., eds., Taylor & Francis, London, New York, pp. 200–253.
5. Lamptey, J., Moo-Young, M., and Robinson, C. W. (1986), in *Biotechnology and Renewable Energy*, Moo-Young, M. and Laptey, J., eds., Elsevier Applied Science, London, UK, pp. 46–56.
6. Holtzapple, M. T., Jun, J., Ashok, G., Patibandla, S. L., and Dale, B. E. (1991), *Appl. Biochem. Biotechnol.* **28/29,** 59–74.
7. Wang, P. Y., Bolker, H. I., and Pruves, C. B. (1967), *Tappi* **50(3)**, 123–124.
8. O'Conner, J. J. (1972), *Tappi* **55(3),** 353–358.
9. Moniruzzaman, M., Dale, B.E., Hespell, R.B., and Bothast, R.J. (1997), *Appl. Biochem. Biotechnol.* **67,** 113–126.
10. Dale, B. E., Henk, L. L., and Shiang, M. (1985), *Dev. Ind. Microbiol.* **26,** 223–233.

0273-2289/04/115/0965–0976/$25.00

Initial Evaluation of Simple Mass Transfer Models to Describe Hemicellulose Hydrolysis in Corn Stover

Michael A. Brennan and Charles E. Wyman*

Thayer School of Engineering, Dartmouth College,
8000 Cummings Hall, Hanover, NH 03755,
E-mail: Charles.Wyman@Dartmouth.edu

Abstract

The uncatalyzed hydrolysis and removal of xylan from corn stover is markedly enhanced when operation is changed from batch to continuous flowthrough conditions, and the increase in hemicellulose removal with flow rate is inconsistent with predictions by widely used first-order kinetic models. Mass transfer or other physical effects could influence the hydrolysis rate, and two models reported in the literature for other applications were adapted to investigate whether incorporation of mass transfer into the kinetics could explain xylan removal in both batch and continuous flowthrough reactors on a more consistent basis. It was found that a simple leaching model and a pore diffusion/leaching model could describe batch and flowthrough data with accuracy similar to that of conventional batch models and could provide a more rational explanation for changes in performance with flow rate.

Index Entries: Pretreatment; flowthrough; batch; mass transfer; hemicellulose hydrolysis.

Introduction

Cellulosic biomass can be pretreated by removing the hemicellulose fraction to expose cellulose to enzymes and recover sugars in high yields for fermentation to fuels and chemicals with unique and powerful economic, environmental, and strategic benefits *(1)*. Accurate, predictive tools would be valuable in scaling up pretreatment by hemicellulose hydrolysis and in defining opportunities to advance pretreatment, but current hemicellulose hydrolysis kinetic models, which have changed little since the mid-1940s, display some inconsistencies that call into question their mechanistic valid-

*Author to whom all correspondence and reprint requests should be addressed.

ity *(2)*. For example, significant differences are observed in predicting whether or not sugar yields increase or decrease with increasing acid concentration or temperature. In addition, hemicellulose removal has been observed to change with solids concentration and flow through the solids, contrary to conventional first-order kinetic model predictions *(3–5)*. Furthermore, one would not expect homogeneous first-order reaction kinetics to necessarily describe solid-liquid reactions in which mass transfer, solubility limitations, and nonhomogeneous reactions at the solid-liquid interface could be important *(2,3,6)*. Oligomers could also play an important role in governing the performance of hemicellulose hydrolysis, and understanding their behavior could help explain some of the deviations from first-order kinetics *(7)*. Jacobsen and Wyman *(2)* postulated that limitations in the solubility of hemicellulose oligomers in hydrolysate liquid coupled with mass transfer could account for the differences among batch, cocurrent, and flowthrough/countercurrent systems.

In the present study, two mass transfer models were adapted from other applications, and preliminary comparisons were made to conventional reaction-only models to assess their abilities to describe hemicellulose hydrolysis in batch and flowthrough reactors. Particular attention was paid to including production and diffusion of oligomers in these models with the intent of exploring whether this approach holds promise for explaining the performance of batch and flowthrough systems in a more consistent manner.

Conventional Kinetic Models

In 1945, Saeman *(8)* described acid hydrolysis of cellulose as a homogeneous two-step first-order reaction, in which acid catalyzes the breakdown of cellulose to glucose followed by the breakdown of the glucose released to form hydroxymethylfurfural and other degradation products. This modeling approach has since been applied to hemicellulose hydrolysis with the hemicellulose portion hydrolyzed to xylose, which breaks down to form furfural and other degradation products *(9)*. These reactions are assumed to follow a first-order dependence on reactant concentration with an Arrhenius temperature relationship for the rate constant. Additional refinements were made to improve such models in describing hemicellulose hydrolysis *(2)*. For example, Kobayashi and Sakai *(10)* incorporated two fractions of hemicellulose with independent kinetic constants into a biphasic model, with one fraction hydrolyzing faster than the other.

While the previous models assume that oligomers break down to monomers so quickly that they can be neglected, Mehlberg and Tsao *(11)* suggested a reaction mechanism for hemicellulose hydrolysis in which oligomers formed during reaction have varying degrees of polymerization (DPs) and their reaction rates vary with their respective DP value (lower DP corresponds to a faster reaction). Another reaction model incorporated two types of oligomers, some with high DPs and the rest with lower DPs, and assumed that xylan is hydrolyzed to the high-DP oligomers that further react to lower-DP oligomers *(12)*. This model showed that the oligomers

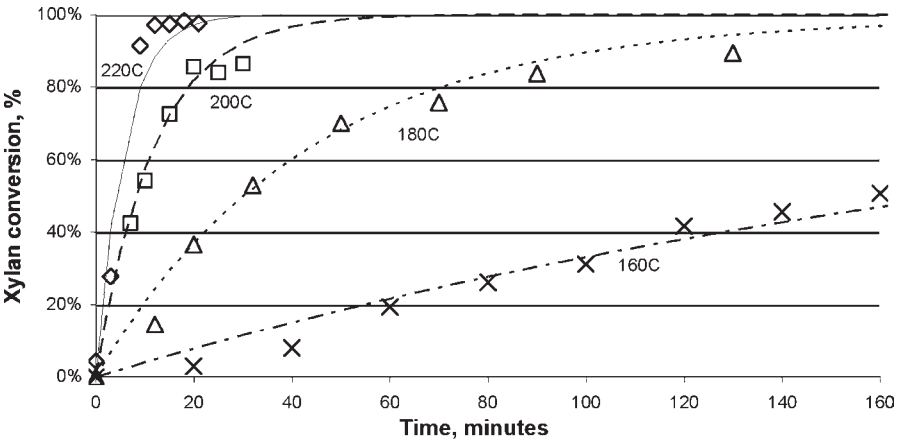

Fig. 1. Data and biphasic chemical reaction model predictions of xylan conversion vs time for batch pretreatment of corn stover with only water at 160, 180, 200, and 220°C and 5% solids concentration.

could either directly form degradation products or be converted to monomers that can then degrade.

On the basis of these approaches, the following biphasic equation can be applied to describe the amount of xylan left in the solid phase for hemicellulose hydrolysis:

$$M_A(t) = F_{fast} \times \exp\left(-k_1 t\right) + \left(1 - F_{fast}\right) \times \exp\left(-k_2 t\right) \quad (1)$$

in which $M_A(t)$ is the mass fraction of the initial xylan left in the solids; F_{fast} is the fraction of the total xylan that hydrolyzes more rapidly for a biphasic reaction; k_1 and k_2 are the first-order rate constants for hydrolysis of the fast and slow fractions of xylan, respectively; and t is the time. We applied this expression throughout this analysis to describe hydrolysis of xylan for batch and flowthrough pretreatment of corn stover for varying temperatures, solids concentrations, acid levels, and flow rates. The fast fraction F_{fast} was determined to minimize the sum of the squares of the differences between experimental and predicted yields for application of Eq. 1 to batch data collected at different reaction conditions for dilute-acid (T. Lloyd and C. Liu, personal communication, March 2002) and water-only pretreatment of corn stover *(13)*. Then, the kinetic constants k_1 and k_2 were fit to the data using the Solver Routine in Excel to minimize the sum of the squares of the differences between the experimental data and predicted values for batch and flowthrough data.

Figures 1 and 2 present some representative results for the application of Eq. 1 to describe data for hydrolysis of hemicellulose in corn stover in only water by batch and flowthrough systems, respectively. In Figs. 1 and 2, xylan conversion is calculated as the initial mass of xylan minus the mass of xylan at a time t all divided by the initial mass of xylan. Although the data are not presented, acid-catalyzed systems behaved similarly.

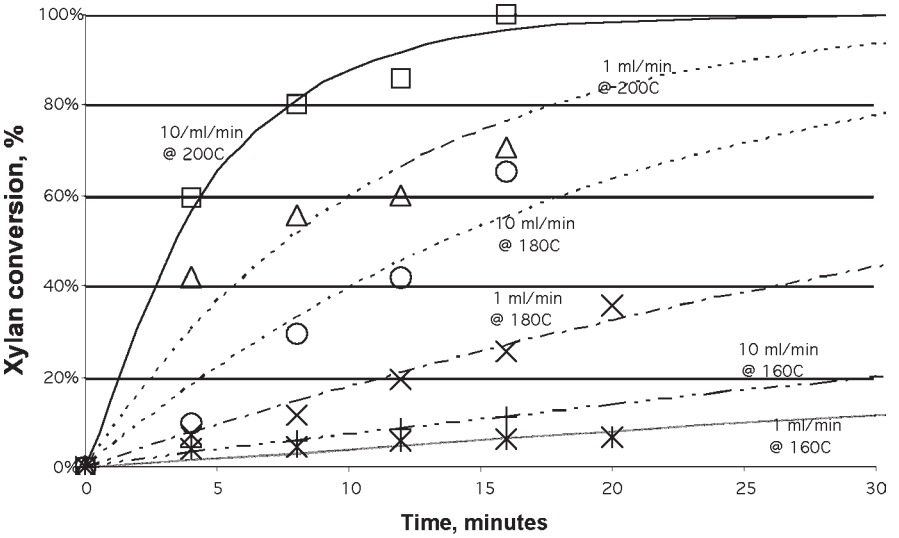

Fig. 2. Data and biphasic chemical reaction model predictions of xylan conversion vs time for flowthrough pretreatment of corn stover with only water at 160, 180, and 200°C and flow rates of 1 and 10 mL/min.

Table 1
Rate Constants for Biphasic Chemical Reaction and Leaching Kinetic Models at 180°C

		Reaction only		Leaching-only model	
Reactor	Condition	k_1	k_2	k_1	k_2
Batch					
No acid	5% Solids	0.81396	0.2268	0.03336	0.0
	10% Solids	0.21252	0.1884	0.02193	0.00011
	20% Solids	0.11568	0.0060	0.02417	0.06310
0.5% Acid	25% Solids	81.389	78.984	89.418	0.01580
1.0% Acid	25% Solids	120	—	120	224
Flowthrough					
No acid	10 mL/min	0.51320	0.008366	0.04946	0.000120
	1 mL/min	0.19820	0.003252	0.01397	0.001584

Table 1 summarizes the rate constants for this model, and Table 2 presents the sum of squares of the differences (SS_E) between the experimental data and the results predicted from application of Eq. 1. Interestingly, the plots of ln(k) vs ($1/T$) (not shown) yield straight lines, suggesting that an Arrhenius relationship is appropriate.

Table 2
Sum of Square of Differences Between Experimental Data and Predicted Results (SS_E) for Flowthrough and Batch Reactors Without Acid Addition at 180°C

Reactor	Condition	Reaction only (SS_E)	Leaching (SS_E)	Branched pore (SS_E)
Batch	5% Solids	840	2491	3408
	10% Solids	479	210	1477
Flowthrough	10 mL/min	2638	1104	8522

Mass Transfer Considerations

Although the rate constants in Eq. 1 can be fit to describe hemicellulose hydrolysis in both batch and flowthrough systems, the change in rate constants with flow is not consistent with chemical reaction control. Thus, one would expect that mass transfer or other physical effects could be important. For example, Table 3 summarizes the effect of some key process variables on kinetics and their implications for control by chemical reactions vs mass transfer *(6)*. Although many hemicellulose hydrolysis studies have pointed out the significance of solids concentrations, relative densities, viscosities, particle size, and reactor design on the overall removal of hemicellulose sugars from biomass *(3,7)*, Table 3 illustrates that such factors should not affect purely chemical reactions but should be indicative of a role of mass transfer in governing hemicellulose hydrolysis. Yet mass transfer considerations have not been incorporated into hemicellulose hydrolysis models *(2)*. Thus, while current models may be useful for data regression, their inability to describe rationally the effect of flow and other inconsistencies could undermine their accuracy in predicting the effects of scale-up or technology improvements.

Biphasic Mass Transfer Leaching Model

Mass transfer models have been used to describe the leaching of soluble substances from porous particles into solution. Such models include a concentration difference that drives the concentration of soluble components in the solids and solution to equilibrate *(14)*. Application of one such model *(14)* to track release from a solid into solution results in the following equations when applied to xylan conversion in a batch system:

Solid
$$\frac{dc_A}{dt} = -\frac{k_c A_s}{V_c}\left(c_A - c_{A\infty}\right) \tag{2}$$

Solution
$$\frac{dc_{A\infty}}{dt} = -\frac{k_c A_s}{V_t}\left(c_A - c_{A\infty}\right) \tag{3}$$

Table 3
Qualitative Relationships Among Performance and Process Parameters for Control by Mass Transfer and Chemical Reaction *(6)*

	Variables affecting observed reaction rate		
Controlling step	Major influence	Minor influence	Insignificant influence
Liquid-solid mass transport (liquid reactant)	• Amount of catalyst • Catalyst particle size • Concentration of reactant in liquid phase	• Temperature • Agitation rate • Reactor design • Viscosity • Relative densities	• Concentration of gas-phase reactant • Concentration of active components on catalyst
Chemical reaction (with insignificant pore diffusion resistance)	• Temperature • Amount of catalyst • Reactant concentrations • Concentration of active components on catalyst		• Stirring rate • Reactor design • Catalyst particle size

Table 4
Rate Constants for Branched Pore Model at 180°C

Reactor		Conditions	k_1	k_2	k_3
Batch	No acid	5% Solids	0.7200	0.00120	—
		10% Solids	0.057768	0.23514	—
		20% Solids	0.024168	0.63096	
Batch	1.0% Acid	25% Solids	60.00	—	—
	0.5% Acid	25% Solids	53.77	84.00	—
Flowthrough	No acid	10 mL/min	0.63284	0.011880	—
		1 mL/min	0.23521	0.055030	—
	0.05% Acid	10 mL/min	3.6498	0.150324	$8.06e^{-4}$
		1 mL/min	0.8474	0.393264	$8.86e^{-6}$
		0 mL/min	1.8338	1.696000	—
	0.10% Acid	10 mL/min	9.6000	2.2530	—
		5 mL/min	5.9110	0.9721	—
		1 mL/min	3.6240	9.8269	1.8166
		0 mL/min	0.7632	0.2446	0.08748

in which c_A is the concentration of the xylan in the solid, $c_{A\infty}$ is the concentration of xylan in solution, k_c is a mass transfer coefficient, A_s is the surface area of the particles, V_c is the volume of the solid, and V_t is the total volume of solution. The concentrations in both phases change with time, and these two mass balance equations are coupled. c_A and $c_{A\infty i}$ can be related by dividing Eq. 2 by Eq. 3 and integrating with the initial concentrations c_{Ai} and $c_{A\infty i}$ to give

$$c_{A\infty} - c_{A\infty i} = -V_r\left(c_A - c_{Ai}\right) \tag{4}$$

Substituting this relationship into the solid mass balance, Eq. 2, one obtains a single equation for c_A:

$$\frac{dc_A}{dt} + \left(\frac{k_c A_s}{V_c}\right)\left(1 + V_r\right) c_A - \left(\frac{k_c A_s}{V_c}\right)\left(c_{A\infty i} + V_r c_{Ai}\right) \tag{5}$$

in which $V_r = \dfrac{V_c}{V_t}$.

Based on the solution developed by Plawsky *(14)*, the concentration of xylan in the solid is described by

$$c_A(t) = c_{Ao}\exp\left[-\left(\frac{k_c A_s}{V_c}\right)\left(1 + V_r\right)t\right] + \left(\frac{c_{A\infty o} + V_r c_{Ao}}{1 + V_r}\right)\times \left\{1 - \exp\left[-\left(\frac{k_c A_s}{V_c}\right)\left(1 + V_r\right)t\right]\right\} \tag{6}$$

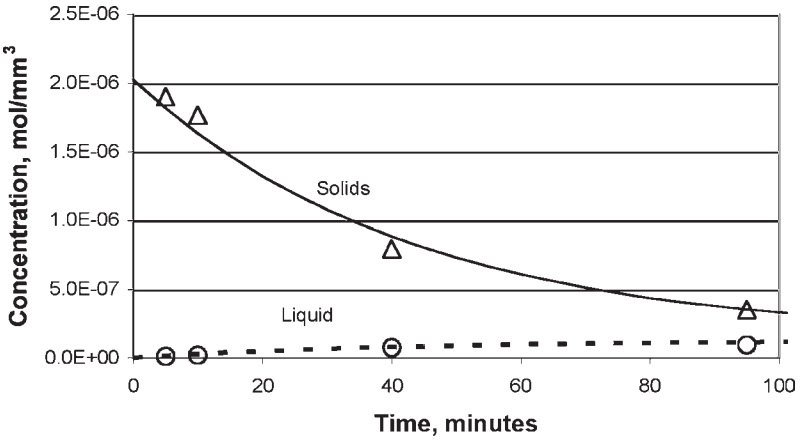

Fig. 3. Data and biphasic mass transfer leaching model predictions of xylan concentrations in solids and solution vs time for water-only batch tube hydrolysis of corn stover at 180°C and 10% solids.

while the concentration in solution is predicted to be:

$$c_{A\infty}(t) = c_{A\infty o} - V_r \left\{ \left(\frac{c_{A\infty o} + V_r c_{Ao}}{1 + V_r} - c_{Ao} \right) \left(1 - \exp\left[- \left(\frac{k_c A_s}{V_c} \right) \left(1 + V_r \right) t \right] \right) \right\} \quad (7)$$

It was found that applying the biphasic concept of Eq. 1 to Eq. 6 improved the results, and the constants k_1 and k_2 and the fraction of faster reacting material were calculated using the Solver Routine in Excel to minimize SS_E for batch tube *(13)* and flowthrough systems (T. Lloyd and C. Liu, personal communication, March 2002).

Figure 3 shows that the leaching model predicts that xylan will dissolve until it equilibrates with its concentration in solution for batch systems. However, as seen in Fig. 4, although there is an initial spike in solution concentration for the flowthrough system, the solution concentration drops quickly owing to continual replacement of solution with fresh water, and as a result, a concentration gradient is maintained throughout the period as c_A is maintained larger than $c_{A\infty}$. Thus, equilibrium between the xylan concentration in the solute and solution cannot be met for the flowthrough reactor until all of the xylan is exhausted from the solids. Table 1 presents mass transfer coefficients for the leaching model, and Table 2 summarizes SS_E for this model. Overall, the predicted and measured values agree reasonably well for both batch and flowthrough reaction systems with only water.

Branched Pore Leaching Model

Cao et al. *(15)* developed a branched pore leaching model in order to simulate the leaching of water-soluble organic carbon from soil in a column

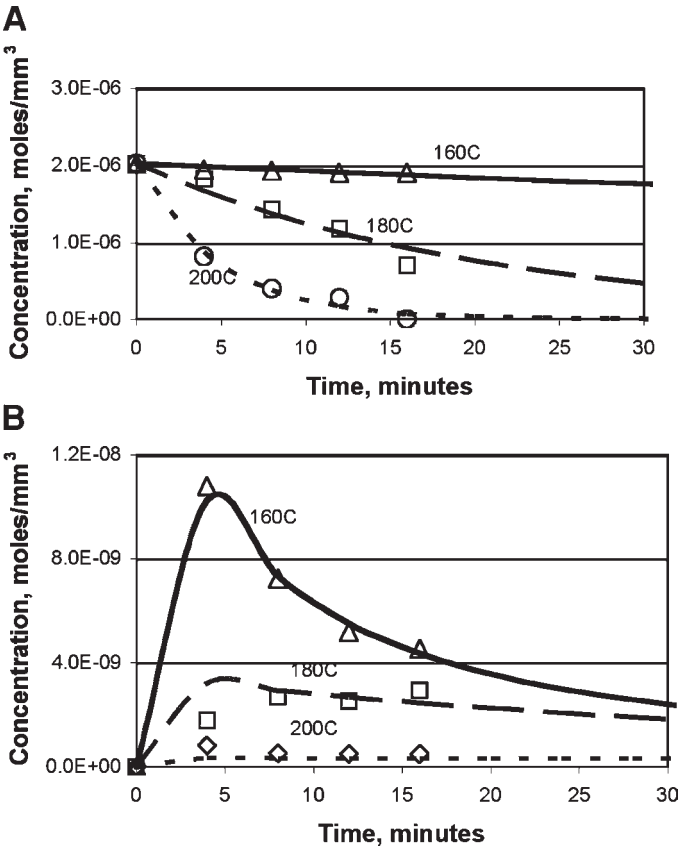

Fig. 4. **(A)** Data and biphasic mass transfer leaching model predictions of xylan concentration in solids vs time for flowthrough pretreatment of corn stover with only water at 160, 180, and 200°C and flow rate of 10 mL/min; **(B)** xylan concentrations in solution vs time for same conditions.

leaching system. The model and its extension to xylan hydrolysis can be depicted as the release of material (xylan) inside the solid matrix (biomass) to internal capillary and gravitational pores in four sequential steps: (1) degradation of insolubles (xylan) to form solubles (xylose oligomers), (2) desorption of the solubles into capillary pore water, (3) diffusion of solubles from capillary pores into the gravitation pore water, and (4) leaching of the solubles from gravitational pore water into the bulk solution by convection. Furthermore, the overall kinetics are described by three additive terms for degradation, desorption/diffusion, and convection. Because there is no turbulence in capillary pore water, the solute migrates through the pores by molecular diffusion alone, and the rate of molecular diffusion can be much slower than the rate of desorption, through which the solubles that are sorbed on the surface of the particles enter the capillary pore water.

Therefore, steps 2 and 3 can be combined into a single step, and the overall kinetics can then be described in three compositional fractions: the permanent (formed from insolubles), the resistant (in capillary pores and sorbed within aggregates), and the labile (in gravitational pores). The contribution of the permanent fraction (the insoluble portion) to the soluble portion in the leachate is proportional to its concentration. The release of the resistant fraction is represented by mass transfer, and the translocation of the labile fraction relates to convection flow and dispersion.

The overall release of water soluble organic carbon from soil, on which this model for xylan hydrolysis is based, was expressed as three additive terms *(15)*:

$$C_t = C_1 e^{-k_1 t^2} + C_2 e^{-k_2 t} + C_3 \left(1 - e^{-k_3 t}\right) \tag{8}$$

in which C_t is the concentration of leachate at time t; k_1, k_2, and k_3 are the transfer rate constants for the labile, the resistant, and the permanent fractions, respectively; C_1 and C_2 are concentration components of the solute for the first two fractions in the matrix at time zero; and C_3 is the equilibrium concentration of the solute from degradation as time becomes infinite. The k values (kinetic coefficients) are plotted for each velocity, and it is postulated that they should be related to a power function of the form

$$k_1 = AV^n \tag{9}$$

in which A is a constant, V is the velocity, and n is some power close to unity.

This model was applied to the same data for batch and flowthrough systems with and without acid addition as for the previous two models, and some of the xylan conversion predictions calculated from the data and concentration predictions via Eq. 8 are summarized in Figs. 5 and 6 for batch and flowthrough systems, respectively. Tables 4 and 2 present the parameters and the SS_E values for the branched pore model, respectively. Overall, although some data are better matched than others, hemicellulose hydrolysis models based on mass transfer alone can predict performance in batch and flow systems as well as, if not better than, reaction-only models. In addition, the changes in mass transfer coefficient with flow are consistent with expectations for a mass transfer model but not for strictly a chemical reaction.

Conclusion

This preliminary study suggests that mass transfer models could describe many features of xylan hydrolysis with accuracy similar to that of conventional first-order reaction-only models that have been long used to describe such systems. For example, a simple leaching model can describe release of xylan into solution as the product of a concentration gradient times a mass transfer coefficient. This model predicts that flowthrough operation could improve xylan release compared to a batch system by reducing the concentration in solution and thereby increasing the concen-

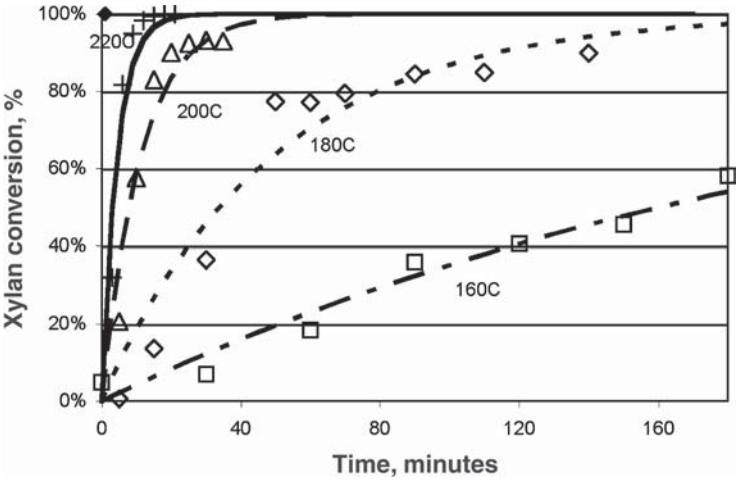

Fig. 5. Data and branched pore leaching model predictions of xylan conversion vs time for batch pretreatment of corn stover with only water at 160, 180, 200, and 220°C and 20% solids concentration.

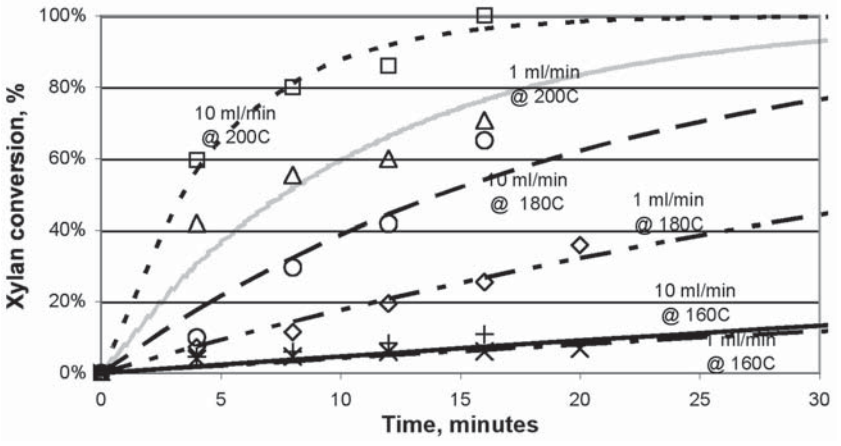

Fig. 6. Data and branched pore leaching model predictions of xylan conversion vs time for flowthrough pretreatment of corn stover with only water at 160, 180, and 200°C and flow rates of 1 and 10 mL/min.

tration difference that drives solubilization. In addition, the film thickness of a diffusive film around particles would be expected to decrease with introduction of flow, increasing the mass transfer coefficient and enhancing release of xylan. Although similar accuracy can be obtained for a conventional chemical reaction-only model, only temperature and acid concentration should impact performance in this case, and no rational explanation can be offered as to why flow rate would enhance xylan removal.

A branched pore leaching model as applied to release of water-soluble carbon from soil incorporates reaction to soluble compounds coupled with pore diffusion within the solids and leaching into the bulk solution. Application of such a model appears to describe hemicellulose hydrolysis reasonably well but not significantly better than chemical reaction only or simple leaching models.

These results could suggest that what has been traditionally been described as "biphasic" behavior may reflect a combination of chemical reaction and mass transfer effects, with each limiting xylan reaction and removal at different stages or modes of operation. This effect might be better described by a model that incorporates reaction of solids to form soluble species as a function of temperature and acid concentration coupled with a second mass transfer step that is affected by flow. On this basis, we plan to investigate whether the pore leaching model could be simplified and adapted in this way to better describe hemicellulose hydrolysis.

Acknowledgments

This work was made possible through the funding of the Office of the Biomass Program of the United States Department of Energy through contract nos. DE-FC36-00GO010589 and DE-FC36-01GO11075. We also appreciate the support of the Thayer School of Engineering at Dartmouth College for making this research possible.

References

1. Wyman, C. E. (1999), *Annu. Rev. Energy Environ.* **24,** 189–226.
2. Jacobsen, S. E. and Wyman, C.E. (2000), *Appl. Biochem. Biotechnol.* **84–86,** 81–96.
3. Jacobsen, S. E. and Wyman, C. E. (2002), *Ind. Eng. Chem. Res.* **41(6),** 1454–1461.
4. Brennan, M. A., Liu, C., Wyman, C. E., and Yang, B. (2002), in *24th Symposium on Biotechnology for Fuels and Chemicals*, Oral presentation 3-02, Gatlinburg, TN.
5. Bobleter, O. (1994), *Prog. Polym. Sci.* **19,** 797–841.
6. Fogler, H. S. (1999) *Elements of Chemical Reaction Engineering*, 3rd Ed., Prentice Hall, Upper Saddle River, NJ.
7. Abatzoglou, N., Chornet, E., Belkacemi, K., and Overend, R. (1992), *Chem. Eng. Sci.* **47(5),** 1109–1122.
8. Saeman, J.F. (1945), *Ind. Eng. Chem.* **37,** 42–52.
9. Lee, Y. Y., Iyer, P., and Torget, R. W. (1999), *Adv. Biochem. Eng. Biotechnol.* **65,** 93–115.
10. Kobayashi, T. and Sakai, Y. (1956), *Bull. Agric. Chem. Soc. Jpn.* **20,** 1–7.
11. Mehlberg, R. and Tsao, G. T. (1979), in *Abstracts of Papers of 178th ACS National Meeting*, American Chemical Society, Washington, DC, p. 36.
12. Garrote, G., Domínguez, H., and Parajó, J. C. (1999) *Holz als Roh– und Werkstoff* **57,** 191–202.
13. Stuhler, S. L. (2002), MS thesis, Thayer School of Engineering, Dartmouth College, Hanover, NH.
14. Plawsky, J. L. (2001), *Transport Phenomena Fundamentals*, Marcel Dekker, New York, NY.
15. Cao, J., Tao, S., and Li, B. G. (1999), *Chemosphere* **39(11),** 1771–780.

0273-2289/04/115/0977–0987/$25.00

Impact of Fluid Velocity on Hot Water Only Pretreatment of Corn Stover in a Flowthrough Reactor

Chaogang Liu and Charles E. Wyman*

Thayer School of Engineering, Dartmouth College, 800 Cummings Street, Hanover, NH 03755, E-mail: charles.wyman@dartmouth.edu

Abstract

Flowthrough pretreatment with hot water only offers many promising features for advanced pretreatment of biomass, and a better understanding of the mechanisms responsible for flowthrough behavior could allow researchers to capitalize on key attributes while overcoming limitations. In this study, the effect of fluid velocity on the fate of total mass, hemicellulose, and lignin was evaluated for hot water only pretreatment of corn stover in tubular flowthrough reactors. Increasing fluid velocity significantly accelerated solubilization of total mass, hemicellulose, and lignin at early times. For example, when fluid velocity was increased from 2.8 to 10.7 cm/min, xylan removal increased from 60 to 82% for hot water only pretreatment of corn stover at 200°C after 8 min. At the same time, lignin removal increased from 30 to 46%. Dissolved hemicellulose was almost all in oligomeric form, and solubilization of hemicellulose was always accompanied by lignin release. The increase in removal of xylan and lignin with velocity, especially in the early reaction stage, suggests that chemical reaction is not the only factor controlling hemicellulose hydrolysis and that mass transfer and other physical effects may also play an important role in hemicellulose and lignin degradation and removal.

Index Entries: Pretreatment; hot water; hemicellulose hydrolysis; fluid velocity; corn stover.

Introduction

Lignocellulosic, often termed cellulosic, biomass is the most abundant renewable resource on Earth, and large-scale production of organic fuels and chemicals from this low-cost sustainable resource would provide unparalleled environmental, economical, and strategic benefits *(1–5)*.

*Author to whom all correspondence and reprint requests should be addressed.

However, cellulosic biomass must be pretreated prior to biologic conversion to achieve the high yields vital to economical success, because a complex hemicellulose-lignin structure shields cellulose in native cellulosic biomass and limits cellulose accessibility to organisms or enzymes. Pretreatment is the most expensive single step in conversion of biomass to ethanol and other products and also greatly influences the cost of biological steps that collectively comprise the largest costs *(5)*. Thus, low-cost advanced pretreatment technologies must be developed if biomass conversion is to be economical *(5)*.

Many favor dilute sulfuric acid pretreatment because both high hemicellulose recovery and good cellulose digestibility can be achieved *(6–8)*. Moreover, most of the soluble sugars from dilute-acid pretreatment are released as monomers that can be readily fermented to ethanol by recombinant organisms *(9,10)*. Pretreatment with just hot water or steam, termed *uncatalyzed hydrolysis* or *autohydrolysis*, eliminates chemical additives, lowers the cost of materials of construction, and generates less waste, but hemicellulose and cellulose yields from batch systems are limited.

Passing hot water continuously through a stationary biomass bed could result in higher hemicellulose sugar recoveries, more lignin removal, more digestible cellulose *(11–15)*, and less inhibitors in the hydrolysate liquid *(16)* compared to conventional systems. Antal and colleagues also reported complete xylan dissolution and >90% recovery of pentosans for hot water pretreatment of sugarcane bagasse in their flowthrough reactor *(17,18)*. Torget and colleagues *(19,20)* achieved both high xylan recovery and high simultaneous saccharification and fermentation conversion while applying extremely dilute sulfuric acid (0.07 %[w/w]) in a countercurrent flowthrough configuration.

Using water instead of steam *(21)* also increases yields for just water pretreatment. However, the high quantities of water used increase energy demands in pretreatment and product recoveries, and equipment selection presents challenges. A better understanding of the mechanisms responsible for flowthrough behavior could allow researchers to capitalize on its key attributes while overcoming its limitations. Our previous study showed that increasing flow rate can not only significantly increase hemicellulose solubilization but also increase recovered hemicellulose sugar yields and lignin removal, and high flow rate is especially favorable for runs at high temperatures *(22)*. Bobleter et al examined the effect of flow rate in a small range with a maximum flow rate less than one-third of reactor volume per minute *(12)* and reported that increasing flow rate can enhance total mass solubilization. However, no one has systematically evaluated the impact of fluid velocity on pretreatment of biomass. In the present study, the effect of fluid velocity on the fate of total mass, hemicellulose, and lignin was evaluated for hot water only pretreatment of corn stover in a flowthrough reactor.

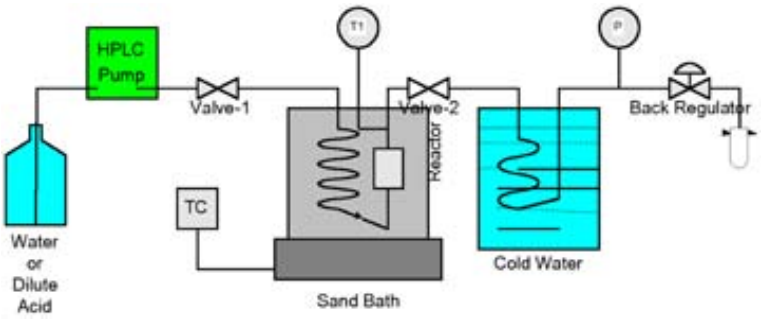

Fig. 1. Schematic diagram of flowthrough system. TC, Thermal controller; T1, thermal couple; P, pressure gauge.

Materials and Methods

Substrate

Corn stover was graciously provided by the National Renewable Energy Laboratory (NREL) in Golden, CO, from a large maintained supply that it obtained from Harlan, IA. Material was ground to a particle size of 250–420 μm using a laboratory knife mill (Model 4, Arthur H. Thomas Company, Philadelphia, PA) and passed through 35-mesh sieves to produce a particle small enough size to facilitate additions to the small reactors used. Samples prepared in this manner were kept in a freezer at –4°C for use in all tests. The composition of a representative sample was 36.1% glucan, 21.4% xylan, 2.5% galactan, 3.5% arabinan, 1.8% mannan, and 17.2% Klason lignin, as determined by the NREL according to its published methods *(22)*.

Flowthrough Apparatus and Experiments

A schematic of the flowthrough system is shown in Fig. 1. We used a set of 10.9 mm id × 180 mm long, 15.7 id × 87 mm long, and 21.2 id × 47 mm long tubular reactors with the same internal volume of 16.8 mL to investigate the impact of fluid velocity at constant residence time. Each reactor was constructed of VCR fitting parts with two gasket filters with an average pore size of 5 μm at each end of the reactor body. All of these parts were made of 316 stainless steel and obtained from the Maine Valve and Fitting Co. (Bangor, ME). We used 316 stainless steel tubing for a 1/4 in. od × 0.035 in. wall thickness preheating coil and a 1/8 in. od × 0.028 in. wall thickness cooling coil as well as to connect the reactor with other system components. The preheating coil was long enough to allow the incoming water to reach the desired temperature before it entered in the reactor, as measured experimentally. A 1/8 in. stainless steel thermocouple (Omega Engineering, Stamford, CT) was installed at the outlet of the reactor to monitor temperature. A high-pressure pump (Acuflow Series III Pumps;

Fisher, Puerto Rico) with a flow rate range of 0–40 mL/min, a pressure gage (Cole-Parmer, Vernon Hills, IL) with a pressure range of 0–1500 psi, and a back-pressure regulator (Maine Valve and Fitting, Bangor, ME) were used to control water pressure and flowthrough the system.

To operate the flowthrough unit, about 2.5 g of corn stover was loaded into the reactor, and the reactor was then connected to the preheating and outlet coils. Distilled water at room temperature was pumped through the reactor for a few min to purge air, completely wet the biomass in the reactor, and pressurize the system to a pressure of 350–400 psig by controlling the back-pressure regulator. Next, the preheating coil was submerged in a 4-kW model SBL-2D fluidized sand bath (Techne, Princeton, NJ) set at the target temperature for 3 min to make sure the preheating coil reached the desired temperature. Then the reactor was also submerged in the same sand bath. At the same time, defined as time zero, the pump was turned on, and liquid fractions were collected continuously over 4-min intervals. When the target reaction time was reached, the pump was turned off, and the reactor and preheating coil were immediately transferred to an ice-water bath to quench the reaction. Once the temperature in the reactor dropped to about 50°C, cold water was pumped through the system to purge liquid remaining in the reactor and coils until about 10 mL of additional effluent was collected.

Sample Analysis

The pH of each liquid fraction was promptly measured on cooling to room temperature. Then, a portion of each was dried under vacuum at 60°C until weight loss ceased to determine the fraction of the total mass dissolved in the liquid fraction. The rest of the sample was used for sugar analysis. The entire solid residue in the reactor was washed into a glass vial, dried at 105°C, and weighed for sugar analysis and determination of Klason lignin as described below. The amount of lignin removed was calculated as the difference between the dry mass of Klason lignin in the feed material and that in the solid residue and expressed as the percentage of the dry mass in the feed material.

Compositional analyses of all solid samples were carried out by the standard methods as provided by NREL *(23,24)*. Sugar monomers in the liquid portion were analyzed quantitatively by a Waters high-performance liquid chromatography (HPLC) model no. 2695 system equipped with a 2414 refractive index detector and a Waters 2695 autosampler using Millenium^{32} chromatography manager 3.2 software (Milford, MA). A Bio-Rad Aminex HPX-87P column (Hercules, CA) was employed for sugar analysis. Total xylose as both monomers and oligomers in the liquid fraction was determined after post-hydrolysis with 4 wt% sulfuric acid at 121°C for 1 h *(25)*. Xylooligomers in the liquid were calculated as the difference between the total xylose and monomeric xylose measurements and expressed as a percentage of the original total xylose in the feed solids. All the experiments were performed in duplicate, with the average value reported.

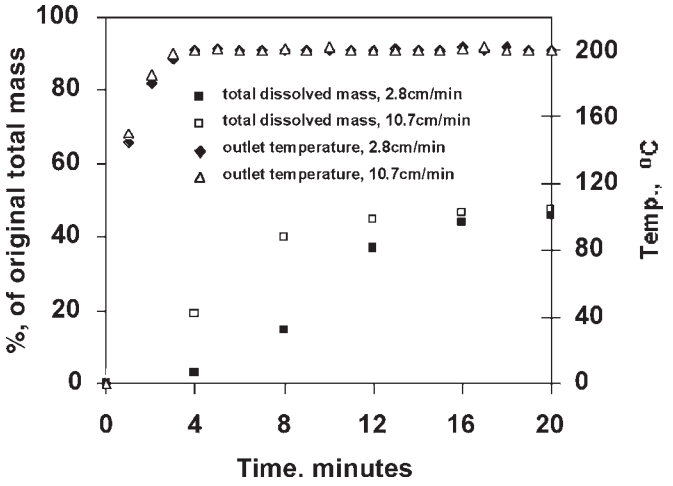

Fig. 2. Overall dissolved mass profiles for hot water only pretreatment of corn stover at 200°C.

Results and Discussion

Our previous research showed that increasing flow rate can significantly enhance solubilization of hemicellulose, lignin, and total mass *(22)*. Research by several teams has recently shown that hemicellulose solubilization and sugar recovery increase with water content in batch systems, suggesting that flowthrough behavior may benefit from the large amounts of water used *(21,26–28)*. However, water quantities alone cannot explain the differences between batch and flowthrough operation, because even at low flow rates (1 mL/min), more total mass, hemicellulose, and lignin was removed under otherwise identical conditions. To investigate whether factors other than water quantities could be responsible for the behavior of flowthrough operations, we examined the effect of fluid velocity during hot water only pretreatment of corn stover in a flowthrough reactor. Hot water without the addition of acid at 200°C was applied in the three reactors described earlier with the flow rate kept constant at 10 mL/min. Thus, fluid velocities of 10.7, 5.2, and 2.8 cm/min result, and average liquid residence time is the same for each reactor (1.68 min).

Solubilization of Total Mass

Figure 2 presents total dissolved mass yields as a function of reaction time for hot water only pretreatment of corn stover in the smallest-diameter and largest-diameter reactors. Total dissolved mass yields increased with reaction times with about 45% of the original total mass dissolved after 20 min for hot water only flowthrough pretreatment of corn stover at 200°C.

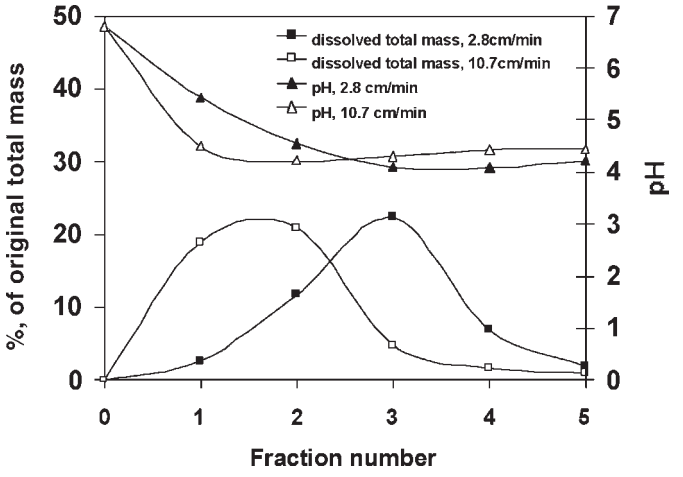

Fig. 3. Total dissolved mass in liquid fraction and pH of each fraction collected over 4-min intervals for hot water pretreatment of corn stover at 200°C.

The important finding is that total mass solubilization for the high-fluid-velocity (10.7 cm/min) run is more rapid than that for the low-fluid-velocity (2.8 cm/min) run, especially in the first 8 min. The heating rate is the same for all reactors for these small flowthrough systems, suggesting that delayed solubilization of total mass at lower fluid velocity did not arise from heat transfer effects (Fig. 2). The effect of velocity is more obvious when one examines changes in total dissolved mass and pH for each liquid fraction collected over 4 min intervals for flowthrough pretreatment (Fig. 3). The peak in total mass removal was delayed by about 4 min for the lowest-velocity run, although the maximum value was about the same as for the highest velocity. The pH for each fraction first dropped as total dissolved mass yield increased and then increased as total dissolved mass yield decrease for both runs, suggesting that acetyl groups are released with solubilization of biomass.

Hemicellulose Hydrolysis

Figure 4 present sugars concentration of each liquid fraction (collected in 4-min intervals) after posthydrolysis. Most of the hemicellulose dissolved in flowthrough operations was in oligomeric form, and very little monomeric sugars were produced for hot water only pretreatment of corn stover under the conditions run. This is in a good agreement with our previous results and those of other researchers *(21,26,27)*. As expected, most of the sugar was xylose, but some glucose, galactose, arabinose, and mannose were also detected in some fractions. As for total mass, the xylose concentration for lower-velocity operation peaked about 4 min after that for higher-velocity operation. However, the maximum xylose concentration for

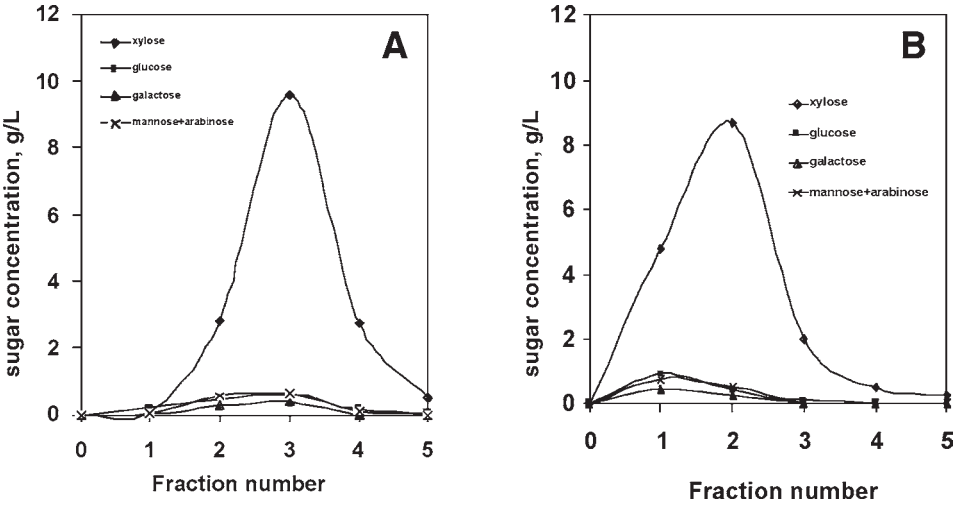

Fig. 4. Sugar concentrations in liquid fractions collected over 4-min intervals for hot water only pretreatment of corn stover at 200°C at velocities of **(A)** 2.8 cm/min and **(B)** 10.7 cm/min.

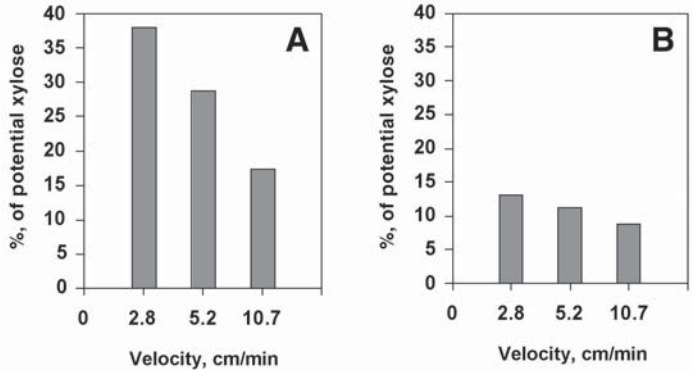

Fig. 5. Xylan remaining in solid residue for hot water only pretreatment of corn stover at 200°C after **(A)** 8 min and **(B)**16 min.

lower-velocity runs (about 9 g/L) was higher than that for higher-velocity runs (about 8 g/L) at the same flow rate. The hydrolysis rate of other hemicellulose sugars (glucan, arabinan, and mannan) increased with fluid velocity (Fig. 4B).

Xylan remaining in solid residues was also analyzed. As seen in Fig.5, increasing velocity significantly increased xylan removal, especially in the first 8 min. For example, xylan removal for operation at 2.8, 5.2, and 10.7 cm/min was 60, 70, and 82% for hot water only pretreatment of corn stover at 200°C after 8 min. However, after 16 min, the differences in xylan removal were less for all velocities run, suggesting that fluid velocity has less impact on the overall degree of hemicellulose hydrolysis.

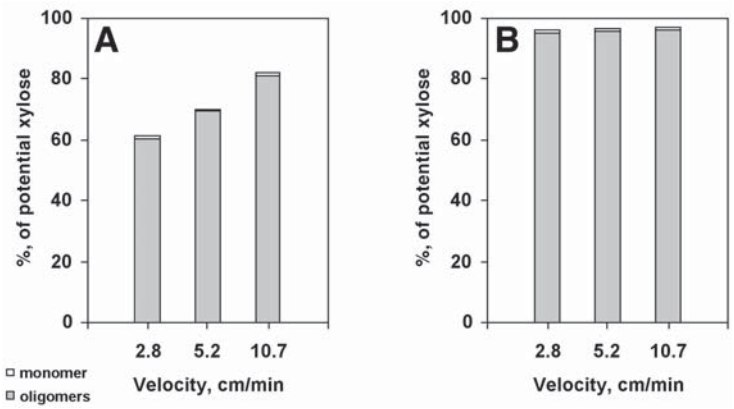

Fig. 6. Monomeric and oligomeric xylose yields for hot water only pretreatment of corn stover at 200°C after **(A)** 8 min and **(B)** 16 min.

Total xylose (monomeric and oligomeric xylose together) yield also increased with fluid velocity early in the reaction (Fig. 6). For example, when fluid velocity was increased from 2.8 to 10.7 cm/min, total xylose yield was increased from 60 to 82% for hot water only pretreatment of corn stover at 200°C after 8 min. Thus, the dissolved xylan was virtually completely recovered for all velocities. In addition, increasing reaction time increased total xylose yields, and about 95% of the potential xylose was recovered for all runs at this temperature after 16 min.

Lignin Removal

Figure 7 displays changes in lignin removal with fluid velocity. Lignin removal increased significantly with increasing fluid velocity in a manner similar to that for xylose removal. For example, when fluid velocity was increased from 2.8 to 10.7 cm/min, lignin removal increased from 30 to 45% after 8 min. However, the maximum lignin removal was almost the same (65% of the original Klason lignin) for both low- and high-velocity operations after 16 min, implying that fluid velocity has less impact on the degree of delignification of biomass than on the rate.

Figure 8 shows the change in total sugar and nonsugar compound concentrations collected in the liquid fractions at 4-min intervals. Total sugar concentration is defined as the sum of xylose, glucose, galactose, arabinose, and mannose concentration analyzed after posthydrolysis of each liquid fraction. Nonsugar compounds are defined as the difference between the total dissolved mass and the total sugar concentration in each fraction. The nonsugar fraction could also be roughly referred to as "dissolved" lignin, because most of the nonsugar compounds are lignin. The total sugar concentration for the highest-velocity operation peaked 4 min ahead of that for the lowest-velocity run, but the maximum total sugar

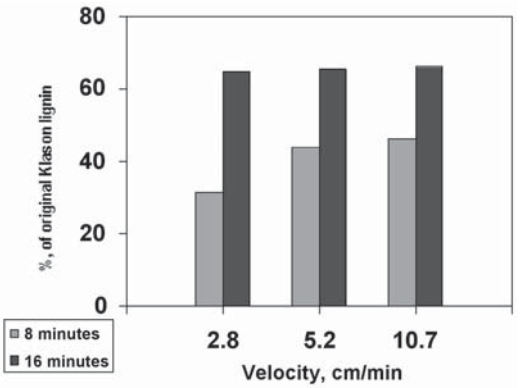

Fig. 7. Change in lignin removal with fluid velocity for hot water only pretreatment of corn stover.

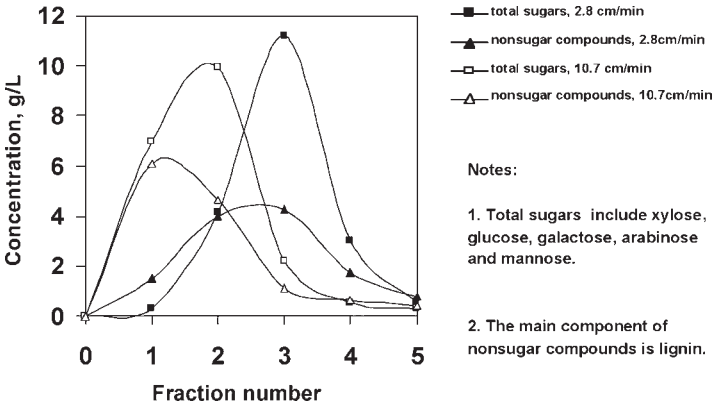

Fig. 8. Sugar and nonsugar collected in liquid fractions over 4-min intervals for hot water only pretreatment of corn stover at 200°C.

concentration was lower (10 g/L) compared with that for the low-velocity run (11 g/L), at the same flow rate. The important finding is that the nonsugar compound concentration peaks much earlier (about 8 min ahead) for high- vs low-velocity runs. However, unlike xylose, the maximum nonsugar compound concentration for the higher-fluid-velocity run was much higher than for lower velocity (6 vs 4 g/L). This strongly suggests that increasing fluid velocity significantly accelerates delignification of biomass in a flowthrough reactor with hot water only pretreatment. In addition, the nonsugar compound concentration increased as total sugar concentration increased, showing that lignin release always accompanies hemicellulose solubilization. Furthermore, at low fluid velocity, nonsugar compounds were extracted ahead of any sugar, suggesting that some nonsugar compounds such as tannin, protein, fat, and even a small portion of lignin are easily extracted.

Conclusion

Fluid velocity has a significant impact on hot water only pretreatment of biomass in a flowthrough reactor. Increasing fluid velocity significantly accelerated solubilization of total mass, hemicellulose, and lignin for hot water only pretreatment even at the same liquid residence time. For example, when fluid velocity was increased from 2.8 to 10.7 cm/min, xylan removal increased from 60 to 82% for hot water only pretreatment of corn stover at 200°C after 8 min. At the same time, total xylose yield increased from 60 to 82% and lignin removal increased from 30 to 46%. The dissolved hemicellulose is almost all in oligomeric form and always accompanied by lignin removal. The increase in xylan removal and lignin with velocity, especially in the early reaction stage, cannot be explained by traditional first-order reaction models developed from batch experiment data in which rate should only change with temperature and acid concentration. All these results suggest that chemical reaction factors (temperature, acid concentration) are not the only ones controlling hemicellulose hydrolysis and delignification reactions, and that mass transfer and other physical effects may play an important role in hemicellulose and lignin degradation. It is also important to note that these effects were all observed at the same residence time, suggesting that more time for xylose degradation or lignin reactions did not dominate compared to the influence of velocity. This result could be attributed to the influence of velocity on the thickness of the liquid film surrounding biomass particles and supports a possible role for mass transfer.

Acknowledgments

We wish to thank the National Renewable Energy Laboratory for kindly providing the corn stover. In addition, we acknowledge the Thayer School of Engineering at Dartmouth College for providing facilities and equipment to carry out our research. We would also like to recognize our partners in this project for their ongoing input: Dr. Y. Y. Lee from Auburn University, Dr. Bruce Dale from Michigan State University, Richard Elander from NREL, Dr. Michael Ladisch from Purdue University, and Dr. Mark Holtzapple from Texas A&M University. This work was funded by The United States Department of Agriculture Initiative for Future Agricultural and Food Systems Program through contract no. 00-52104-9663.

References

1. Lynd, L. R., Cushman, J. H., Nichols, R. J., and Wyman, C. E. (1991), *Science* **251,** 1318–1323.
2. Wyman, C. E., ed. (1996), *Handbook on Bioethanol: Production and Utilization, Applied Energy Technology Series*, Taylor & Francis, Washington, DC.
3. Lynd, L. R., Wyman, C. E., and Gerngross, T. U. (1999), *Biotechnol. Prog.* **15,** 777–793.
4. Wyman, C. E. (1999), *Ann. Rev. Energy Environ.* **24,** 189–226.
5. Lynd, L. R., Elander, R. T., and Wyman, C. E. (1996), *Appl. Biochem. Biotechnol.* **57/58,** 741–761.

6. Grohmann, K., Torget, R. W., and Himmel, M. E. (1985), *Biotechnol. Bioeng*. **15,** 59–80.
7. Torget, R., Walter, P., Himmel, M., and Grohmann, K. (1991), *Appl. Biochem. Biotechnol.* **28/29,** 75–86.
8. Lee, Y. Y., Iyer, P., and Torget, R. W. (1999), *Adv. Biochem. Eng/Biotechnol*. **65,** 93–115.
9. Asghari, A., Bothast, R. J., Doran, J. B., and Ingram, L. O. (1996), *J. Ind. Microb.* **16,** 42–47.
10. Ingram, L. O. and Doran, J. B. (1995), *FEMS Microbial. Rev.* **16,** 235–241.
11. Bobleter, O. (1994), *Prog. Polym. Sci.* **19,** 797–841.
12. Bobleter, O., Bonn, G., and Concin, R. (1983), *Alt. Energy Sources* **3(3),** 323–332.
13. Hormeyer, H. F., Schwald, W., Bonn, G., and Bobleter, O. (1988), *Holzforschung* **42,** 95–98.
14. Bonn, G., Horemeyer, H. F., and Bobleter, O. (1983), *Wood Sci. Technol.* **17,** 195–202.
15. van Walsum, G. P., Allen, S. G., Spencer, M. J., Laser, M. S., Antal Jr., M. J., and Lynd, L. R. (1996), *Appl. Biochem. Biotechnol*. **57/58,** 157–170.
16. Hormeyer, H. F., Tailliez, P., Millet, J., Girard, H., Bonn, G., Bobleter, O., and Aubert, J.-P. (1988), *Appl. Microbial. Biotechnol*. **29,** 528–535.
17. Mok, W. and Antal, M. J. (1992), *Ind. Eng. Chem. Res*. **31,** 1157–1161.
18. Allen, S. G., Kam, L. C.; Zemann, A. J., Antal, M. J. (1996), *Ind. Eng. Chem. Res.* **35,** 2709–2715.
19. Torget, R. W., Hayward, T. K., and Elander, R. (1997), *Proceedings of the 19th Symposium on Biotechnology for Fuels and Chemicals*, Oral presentation, Colorado Springs, CO.
20. Torget, R. W., Kadam, K. L., Hsu,T.-A., Philippidis, G. P., and Wyman, C. E. (1998), US patent no. 5,705,369.
21. Laser, M., Schulman, D., Allen, S. G., Lichwa, J., Antal, M. J., Lynd, L. R. (2002), *Bioresour. Technol.* **81,** 33–44.
22. Liu, C. and Wyman, C. E. (2003), *Ind. Eng. Chem. Res.* **42,** 5409–5416.
23. Ruiz, R. and Ehrman, T. (1996), Determination of carbohydrates in biomass by performance liquid chromatography, in *Laboratory Analytic Procedure LAP-002*, National Renewable Energy Laboratory, Golden, CO.
24. Templeton, D. and Ehrman, T. (1995), Determination of acid-insoluble lignin in biomass, in *Laboratory Analytic Procedure LAP-003*, National Renewable Energy Laboratory, Golden, CO.
25. Ruiz, R. and Ehrman, T. (1996), Dilute acid hydrolysis procedure for determination of total sugars in the liquid fraction of process samples, in *Laboratory Analytic Procedure LAP-014*, National Renewable Energy Laboratory, Golden, CO.
26. Jacobsen, S. E. and Wyman C. E. (2002), *Ind. Eng. Chem. Res.* **41,** 1454–1461.
27. Stuhler, S. L. (2002), MS thesis, Dartmouth College, Hanover, NH.
28. Allen, S. G., Schulman, D., Lichwa, J., Antal, M. J., Laser M., and Lynd, L.R. (2001), *Ind. Eng. Chem. Res.* **40,** 2934-2941.

0273-2289/04/115/0989–1002/$25.00

Combined Steam Pretreatment and Enzymatic Hydrolysis of Starch-Free Wheat Fibers

Beatriz Palmarola-Adrados, Mats Galbe, and Guido Zacchi*

Department of Chemical Engineering 1, Lund University, PO Box 124, SE-221 00, Lund, Sweden, E-mail: guido.zacchi@chemeng.lth.se

Abstract

Steam treatment of an industrial process stream, denoted starch-free wheat fiber, was investigated to improve the formation of monomeric sugars in subsequent enzymatic hydrolysis for further bioconversion into ethanol. The solid fraction in the process stream, derived from a combined starch and ethanol factory, was rich in arabinose (21.1%), xylose (30.1%), and glucose (18.6%), in the form of polysaccharides. Various conditions of steam pretreatment (170–220°C for 5–30 min) were evaluated, and their effect was assessed by enzymatic hydrolysis with 2 g of Celluclast + Ultraflo mixture/100 g of starch-free fiber (SFF) slurry at 5% dry matter (DM). The highest overall sugar yield for the combined steam pretreatment and enzymatic hydrolysis, 52 g/100 g of DM of SFF, corresponding to 74% of the theoretical, was achieved with pretreatment at 190°C for 10 min followed by enzymatic hydrolysis.

Index Entries: Wheat fibers; steam pretreatment; enzymatic hydrolysis; starch-free fiber; microwave oven.

Introduction

In the production of starch from wheat, several byproduct streams are obtained *(1)*. The starch-free fiber (SFF) stream used in the present investigation originated from a combined starch and ethanol factory. Currently, this SFF stream is marketed as low-cost animal feed. Hemicellulose and glucan (cellulose) are the major components of this stream, comprising about 70% of its dry weight. Recovery of the monomeric sugars that compose this material (i.e., xylose, arabinose, and glucose) by performing some sort of hydrolysis would increase the amount of sugars available for ethanol production. Thus, utilization of this stream in the

*Author to whom all correspondence and reprint requests should be addressed.

very same plant where it is generated and where ethanol is already produced could decrease the ethanol production cost, since the cost of the feedstock is one of the major contributors to the relatively high production cost of fuel ethanol *(2)*.

In a previous investigation on another batch of SFF, the optimal conditions for pretreatment were determined using heat treatment in a microwave oven followed by enzymatic hydrolysis. The severity factor, $\log(R_o)$, which combines the temperature and residence time parameters, was used to compare the results at different conditions:

$$\mathrm{Log}\left(R_o\right) = \mathrm{Log}\left\{t \cdot \exp\left[\frac{\left(T_r - T_b\right)}{14.75}\right]\right\} \quad (1)$$

in which t is the reaction time (min); T_r is the reaction temperature (°C); and T_b is the reference temperature, which is set to 100°C (3). A severity factor of 3.65 resulted in the highest total sugar yield (4). In the present study, the same pretreatment was repeated on the new SFF batch to determine whether there were any differences in the materials. Combined acid hydrolysis in a microwave oven and enzymatic hydrolysis was performed mainly to allow analysis of the maximum amount of carbohydrates available. Because pretreatment using microwave irradiation is not feasible on a large scale, steam pretreatment was investigated as a means of pretreatment of SFF on an industrial scale. This method, consisting of high-pressure steaming, remains one of the best ways of increasing the enzyme digestibility of fibers and is regarded as one of the key technologies in the cost-effective manufacture of bioethanol *(2,5–7)*. The effect of enzyme loading on the direct enzymatic hydrolysis of SFF and on enzymatic hydrolysis following pretreatment was also investigated.

Materials and Methods

Figure 1 shows the experimental procedure used to evaluate the hydrolysis methods of SFF. First, the SFF material was subjected to saccharification with amyloglucosidase to determine the amount of starch available in the material. Second, the material was subjected to pretreatment in either a steam pretreatment unit or a microwave oven, followed by enzymatic hydrolysis. Pretreatment in a microwave oven was performed both with and without the addition of acid. Direct enzymatic hydrolysis was also performed.

Raw Material

Wheat SFF material was kindly donated by Amylum UK (Nesle, France). The material had a dry matter (DM) content of 18.5% and was stored in buckets at –18°C. The composition, analyzed by combined acid hydrolysis with 1% H_2SO_4 followed by enzymatic hydrolysis with cellulolytic and hemicellulolytic enzymes, is given in Table 1.

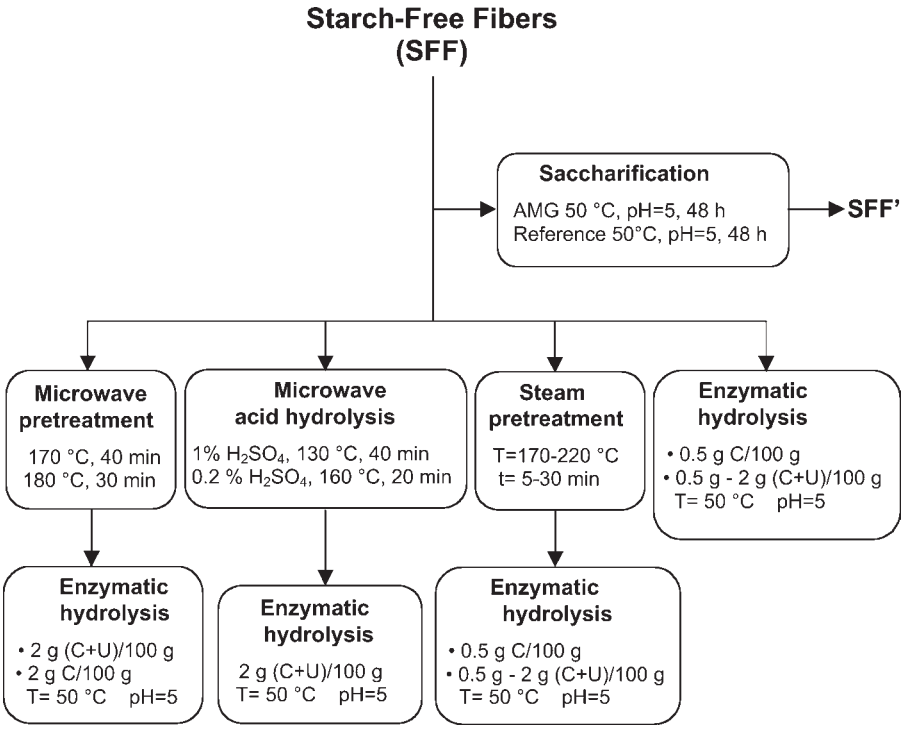

Fig. 1. Experimental procedure used for assessment of various methods for the hydrolysis of SFFs.

Table 1
Composition of SFF Material

	g/100 g SFF (dry wt basis)
Arabinose [a]	21.1
Xylose [a]	30.1
Glucose [a]	18.6
Galactose [a]	2.0
Acid-soluble lignin [b]	4.0
Acid-insoluble lignin [c]	15.2
Ash [d]	1.1
Total	92.1

[a] Determined by acid hydrolysis with 1% H_2S0_4 at 130°C for 40 min followed by enzymatic hydrolysis with 2 g of Celluclast + Ultraflo/100 g of slurry (5% DM).

[b] NREL standard method for determination of acid-soluble lignin (LAP-004).

[c] NREL standard method for determination of acid-insoluble lignin (LAP-003).

[d] NREL standard method for determination of ash (LAP-005).

Saccharification

The SFF was saccharified with amyloglucosidase (AMG 300L; Novozymes A/S, Bagsvaerd, Denmark) to determine the starch (or dextrin) content. The material was diluted to an 8 wt% DM slurry, the pH was adjusted to 5.0 and AMG was added at a concentration of 1.2 mL/100 g of SFF slurry. Enzymatic hydrolysis was carried out using a 1-L Rotavapor (Büchi Labortechnik AG, Flawil, Switzerland) containing 800 g of slurry, at 50°C for 48 h. A reference SFF slurry not containing AMG was subjected to the same conditions. The liquid fractions were analyzed regarding glucose, arabinose, xylose, and galactose contents.

Steam Pretreatment

Pretreatment was performed in a steam pretreatment unit. This equipment consists of a 2.4-L vessel into which steam from a boiler saturated up to 40 bar is introduced. The saturated steam permeates the SFF material and causes a high internal pressure. After a certain time, the pressure is suddenly released by opening a valve in the reactor to atmospheric pressure. The rapid change in pressure leads to expansion of the cellulose/hemicellulose structure. The heat treatment provides partial hydrolysis, which, in combination with the expansion following decompression, improves the action of enzymes. Pretreated material is collected in a cyclone connected to the outlet of the pressurized vessel. A computer, ABC 800 (Luxor AB, Motala, Sweden), is used to control valve operation and to record the temperature. The pretreatment vessel was preheated with steam prior to loading 1 kg of the original SFF material (18.5% DM), corresponding to approx 2 L in volume. The material was heated by steam to the desired temperature, and when the preset pretreatment time had elapsed, the material was discharged into the cyclone. Then steam was introduced into the reactor for a short period of time (usually 30 s) at the same temperature to rinse out any remaining material. The time required to attain the desired temperature was approx 20 s. Temperatures of 170, 180, 190, 200, 210, and 220°C and times of 5, 10, 15, 20, and 30 min, were investigated (Table 2).

The liquid fraction of the pretreated material was analyzed for glucose, arabinose, xylose, galactose, furfural, and hydroxymethylfurfural. The slurry was further hydrolyzed with enzymes.

Heat Treatment in Microwave Oven

A microwave oven, MLS-1200 Mega Microwave workstation, from Milestone (Sorisole, Italy), described in a previous study *(4)*, was used to pretreat a 5% DM SFF slurry. Heat treatment was performed at 170°C for 40 min and at 180°C for 30 min. Acid hydrolysis was performed with 1% H_2SO_4 at 130°C for 40 min and with 0.2% H_2SO_4 at 160°C for 20 min. These pretreatment experiments were performed to allow analysis of the material, as well as to compare the SFF material with that used in a previous investigation *(4)*.

Table 2
Experimental Conditions in Pretreatment Step Performed with Steam Gun

Run no.	Severity (Log[R_o])	Temperature (°C)	Time (min)	DM content after pretreatment (%)[a]
1	3.24	170	15	10.2
2	3.35	190	5	12.4
3	3.36	170	20	9.8
4	3.36	180	10	10.5
5	3.53	180	15	9.3
6	3.64	200	5	12.2
7	3.65	190	10	10.5
8	3.66	180	20	9.3
9	3.83	180	30	9.1
10	3.94	200	10	10.1
11	3.94	210	5	10.5
12	3.95	190	20	8.4
13	4.23	220	5	9.8
14	4.24	210	10	11.3
15	4.53	220	10	9.8

[a] DM includes material recovered by rinsing steam.

Enzymatic Hydrolysis

The hemicellulose-degrading enzymes (Ultraflo L) and the cellulases (Celluclast 1.5L) were kindly donated by Novozymes A/S. Celluclast 1.5L had a filter paper activity of 80 filter paper units/mL, determined according to the procedure of Mandels *(8–9)*. For the present study the most important side activities of Ultraflo L were endo-1,4-β-xylanase, β-xylosidase, and α-arabinofuranosidase *(10)*.

The DM content of the steam-pretreated SFF was adjusted to 5% and the pH set to 5.0 with NaOH. Enzymatic hydrolysis was performed using a Celluclast + Ultraflo mixture (1:1) at a ratio of 2 g of enzyme/100 g of slurry *(10)*. Hydrolysis was carried out for 72 h in 100-mL shake flasks maintained at 50°C and shaken at 200 rpm in a laboratory rotary shaker-incubator (LSR/L-V; Adolf Kühner AG) for 72 h. Samples were withdrawn after 0, 2, 4.5, 7.5, 11, 14, 24, 31, 38, 48, 60, and 72 h for analysis of monosaccharides. Direct enzymatic hydrolysis of a 5% DM SFF slurry was also performed as a reference to evaluate the effect of steam pretreatment on the yield.

Enzyme Loadings

Pretreatment was applied at three levels of severity—220°C for 5 min, Log(R_o) = 4.23; 190°C for 10 min, Log(R_o) = 3.65; and 170°C for 15 min, Log(R_o) = 3.24—for enzymatic hydrolysis with the addition of 0.5 g of Celluclast + Ultraflo mixture/100 g of SFF slurry and 0.5 g of Celluclast/100 g of SFF slurry.

Analysis

The DM content of the samples was determined by drying duplicate samples for 16 h in an oven at 105°C according to the National Renewable Energy Laboratory (NREL) standard method for determination of total solids in biomass, LAP-001 *(11)*. Total ash content was determined by ashing samples in triplicate at 575°C in a muffle furnace according to the NREL standard method for ash in biomass, LAP-005 *(12)*.

Samples for high-performance liquid chromatography analysis were withdrawn from the liquid fraction of the SFF slurry after starch hydrolysis, heat pretreatment, acid hydrolysis, and enzymatic hydrolysis. All samples were analyzed regarding arabinose, galactose, glucose, and xylose content using a high-performance liquid chromatography (Shimadzu, Kyoto, Japan) equipped with a refractive index detector (Shimadzu). Separation was performed using an Aminex HPX-87P column (Bio-Rad, Hercules, CA) at 80°C with deionized water at a flow rate of 0.5 mL/min as the mobile phase. The contents of furfural and hydroxymethylfurfural (HMF) were determined in the samples taken after heat pretreatment and after acid hydrolysis of the SFF slurry. Furfural and HMF were separated on an Aminex HPX-87H column (Bio-Rad) at 65°C using 5 m*M* H_2SO_4 as the mobile phase at a flow rate of 0.5 mL/min. All samples were filtered through 0.2-µm filters before analysis.

Soluble and insoluble lignin were determined with the NREL standard biomass analytical methods for the analysis of acid-insoluble and acid-soluble lignin in biomass, LAP-003 and LAP-004, respectively *(13–14)*. NREL's laboratory analytical procedure for the determination of carbohydrates in biomass, LAP-002, without correction for hydrolysis losses was performed to determine the sugar content *(15)*.

Results and Discussion

The material denoted SFF investigated, was the solid fraction obtained after liquefaction of wheat starch fibers with α-amylase and subsequent separation and washing from the glucose syrup. This procedure was carried out at the wheat-milling industry providing the material. Table 1 shows the composition of the SFF material. All values are given on a DM basis. Carbohydrates, determined by acid hydrolysis with 1% H_2SO_4 followed by enzymatic hydrolysis, comprised about 70 wt% of the SFF. These sugar values agreed well with the values determined with the NREL standard analytical method for the determination of carbohydrates, consisting of two-stage acid hydrolysis. The latter resulted in slightly lower sugar values: 28.4 g of xylose, 20.9 g of arabinose, and 18.1 g of glucose/100 g of SFF.

Analysis showed high values of lignin content, which may comprise compounds formed by the degradation of monosaccharides, as well as other compounds. No references in the literature have been found. The raw material also contained a small amount of ash, equal to 1.1 g/100 g of SFF. The analyzed compounds accounted for 92.1% of the DM.

Table 3
Sugar Yields After Pretreatment and Acid Hydrolysis
Performed in Microwave Oven Followed by Enzymatic Hydrolysis

	Yield (g/100 g of SFF)			
	Arabinose	Xylose	Glucose	Total
Pretreatment				
170°C, 40 min + EH	10.8	17.7	17.9	46.4
	7.9	**12.0**	**15.6**	**35.5**
180°C, 40 min + EH	10.7	18.4	18.5	47.6
	6.2	**11.4**	**15.0**	**32.6**
Acid hydrolysis				
0.2% H_2SO_4, 160°C, 20 min + EH	16.5	26.1	18.1	60.7
	6.8	**16.3**	**14.1**	**37.2**
1% H_2SO_4, 130°C, 40 min + EH	21.1	30.1	18.6	69.8
	7.2	**17.4**	**14.1**	**38.7**

[a]EH, enzymatic hydrolysis. The values in boldface are from a previous investigation *(4)* on similar material and are given for comparison.

No starch saccharification was performed on the SFF material used in this study, and therefore some starch-glucose could still be present as dextrins (malto-dextrins) in the material. For this reason, saccharification with AMG was performed in order to determine the starch-glucose still present in the material. The results showed that only 2 g of glucose/100 g DM of SFF was released during saccharification. It was thus decided that starch hydrolysis of the SFF prior to steam pretreatment to hydrolyze the hemicellulose/cellulose was unnecessary. Surprisingly, 3 g of xylose and 2 g of arabinose were also released per 100 g of SFF during hydrolysis with AMG. To investigate whether this depended on the heat treatment (50°C for 48 h) or was owing to the AMG preparation, a further experiment was carried out using the same pH and temperature conditions for 48 h but without the addition of AMG. The results showed that no sugar was released when the SFF material was subjected to hydrolysis conditions without the addition of enzyme. Thus, it appears that the AMG preparation also contains some hemicellulolytic activity.

Comparison of Two Different Batches

Table 3 shows the sugar yields obtained after pretreatment and enzymatic hydrolysis of the SFF material used in the present study and the SFF material utilized in a previous study (boldface in Table 3) *(4)*. The sugar yields obtained with acid hydrolysis in a microwave oven followed by enzymatic hydrolysis are also given. Unless otherwise stated, the yields following pretreatment and enzymatic hydrolysis are expressed as g/100 g of dry SFF. Galactose was present at very low amounts in both materials.

Therefore, only xylose, arabinose, and glucose were used for evaluation of the yields. These two batches were collected at different times and stages of the process at the starch factory, so some difference in composition could therefore be expected.

The material used in the present study contained higher amounts of carbohydrates. The higher sugar content can, to some extent, be ascribed to the fact that the material was withdrawn before the saccharification step in the factory, in contrast to the old material. As already mentioned, starch saccharification releases some pentoses as well. If these monosaccharides, released in the saccharification step, are subtracted from the sugar yields obtained with the new material, the difference in yield between the two materials diminishes. However, the new material still has a higher amount of carbohydrates.

Steam Pretreatment Followed by Enzymatic Hydrolysis

Pretreatment was performed in a steam pretreatment unit in which the SFFs were exposed to steam at high pressure. Owing to continued introduction of steam into the reactor during steam pretreatment, the SFFs are diluted, resulting in a slurry with lower DM content, between 9 and 12% (*see* Table 2), than the initial material, 18.5%.

The total yield of (fermentable) sugars after both pretreatment and combined pretreatment and enzymatic hydrolysis is shown in Fig. 2. Steam pretreatment did not have a significant effect on the sugar yield but enhanced the following enzymatic hydrolysis. The steam pretreatment that resulted in the highest release of monomer sugars, 6.4 g of total sugars/100 g, was 200°C and 10 min, which corresponds to a severity factor of 3.94. Steam pretreatment at 190°C for 10 min (Log[R_o] = 3.65) resulted in the highest total sugar yield, 51.8 g/100 g, after subsequent enzymatic hydrolysis. This yield, which consists of 13.4 g of arabinose, 21.2 g of xylose, and 17.2 g of glucose, corresponds to 74.2% of the theoretical. However, similar yields, between 44 and 49 g/100 g, were achieved over the entire range of pretreatment conditions tested. The main improvement in steam pretreatment at 190°C for 10 min was seen on the glucose yield, which increased to 92.4% of the theoretical, while the yield of pentoses only increased to 69.4 and 55.5% for xylose and arabinose, respectively. A severity factor of 3.65 proved to be optimal in obtaining the maximum total sugar yield by heat pretreatment followed by enzymatic hydrolysis, using either a microwave oven (at 170°C for 40 min) or a steam pretreatment unit (at 190°C for 10 min).

Figure 3 shows the yield of individual sugars after combined pretreatment and enzymatic hydrolysis. Most of the arabinose was released at low severity (severity factors between 3.3 and 3.7). The highest arabinose yield, about 13.5 g/100 g of SFF, was obtained at 170°C, 15 min; 170°C, 20 min; 180°C, 15 min; and at 190°C, 10 min. At lower severity, somewhat less arabinose was released, while higher severities resulted in partial degradation. A severity factor of about 3.65 was required to obtain the maximum yield of xylose, reaching a yield of 21.2 g/100 g of SFF, at 190°C for 10 min.

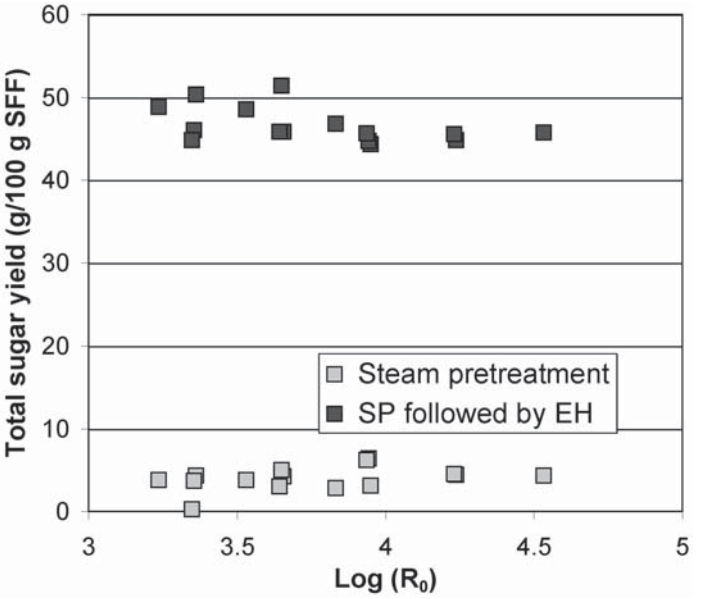

Fig. 2. Effect of severity factor (Log[R_o]) on total sugar yield after steam pretreatment (SP) and after combined SP and enzymatic hydrolysis (EH).

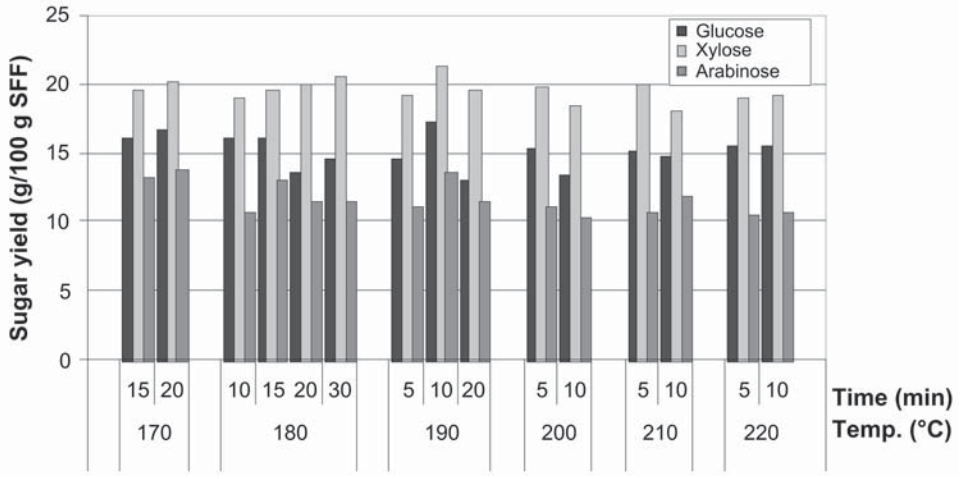

Fig. 3. Effect of pretreatment conditions on yield of individual sugars after combined steam pretreatment and enzymatic hydrolysis.

The same conditions also resulted in the maximum glucose yield, 17.2 g/100 g of SFF. At the pretreatment conditions used, the formation of fermentation-inhibiting compounds was very low (results not shown) *(16)*. The concentration of furfural in the slurry pretreated at 190°C for 10 min was about 0.3 g/L. No HMF was detected.

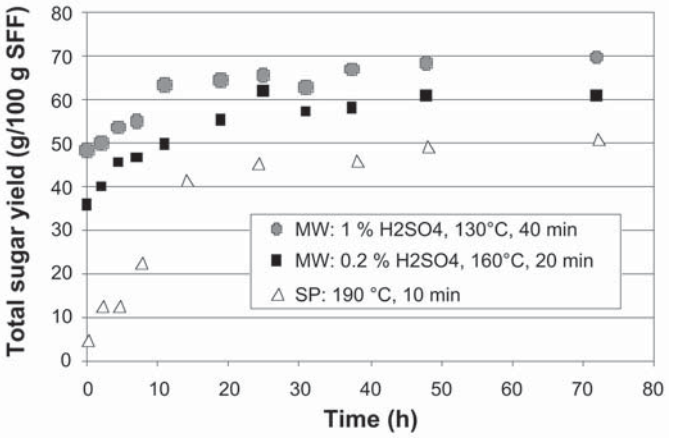

Fig. 4. Sugar yields as a function of enzymatic hydrolysis time. Comparison of best combination of pretreatment and enzymatic hydrolysis methods using either microwave oven (MW) or steam pretreatment (SP).

Further comparison of the maximum yields obtainable with the different hydrolysis methods showed that the addition of acid during pretreatment substantially increased the total sugar yield (Fig. 4). The analytical method consisting of combined acid hydrolysis with 1% H_2SO_4 at 130°C for 40 min followed by enzymatic hydrolysis released the highest amount of total sugars, corresponding to about 70 wt% of the total DM. This value was taken as the maximum achievable, i.e., 100% of theoretical. Direct acid hydrolysis with 1% H_2SO_4 resulted in 69% of the theoretical. The concentrations of furfural and HMF were 0.15 and 0.01 g/L, respectively.

Acid hydrolysis with 0.2% H_2SO_4 at 160°C for 20 min resulted in 50% of the theoretical sugar yield. This is approximately the same yield as that obtained with direct enzymatic hydrolysis. When the acid hydrolysis was followed by enzymatic hydrolysis, the sugar yield increased to 88% of the theoretical. Analysis of furfural and HMF showed that only 0.2 g/L of furfural was present in the slurry and no HMF was formed.

Besides two different hydrolysis methods (i.e., acid hydrolysis and pretreatment without the addition of acid), two different pieces of pretreatment equipment were used to perform the experiments (Fig. 4). Acid hydrolysis was conducted in a microwave oven, while pretreatment was performed in a steam pretreatment unit. The microwave oven provides a closed system where the amount of water added is fixed and there is no loss of material during the process *(17–18)*. On the other hand, the samples have to be rather diluted for the microwave oven to be efficient. Another disadvantage is that the microwaves penetrate the material only a few centermeters, and therefore this method is not feasible on a large scale. The microwave oven may, however, still be of interest in the laboratory as a screening method to analyze the composition of feedstock as well as to determine a range of optimal conditions for steam pretreatment.

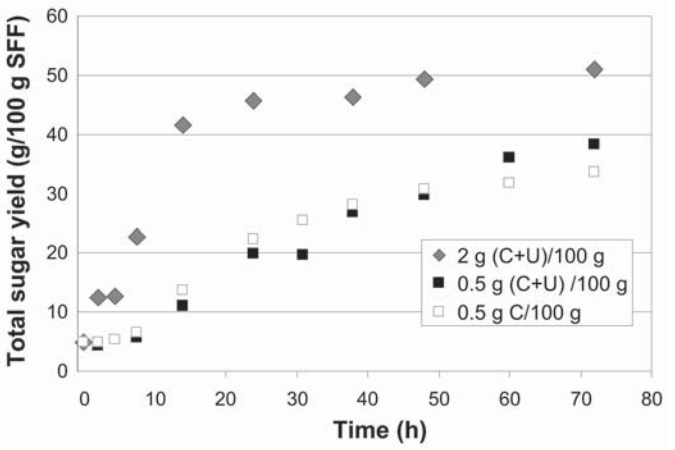

Fig. 5. Effect of enzyme loading in enzymatic hydrolysis of material after steam pretreatment at 190°C for 10 min.

Enzyme Loading

The effect of reducing the enzyme loading was also evaluated. Enzymatic hydrolysis after microwave pretreatment was performed previously both with and without the addition of Ultraflo to Celluclast. Only a small increase in total sugar yield (4%) was observed when using a mixture of 2 g of Celluclast + Ultraflo instead of 2 g of Celluclast/100 g of SFF slurry (5% DM content) following microwave pretreatment at 170°C for 40 min and 180°C for 30 min (results not shown).

To investigate further the effect of enzyme loading, three materials pretreated at different degrees of severity (i.e., 220°C for 5 min, 190°C for 10 min, and 170°C for 15 min) were selected for enzymatic hydrolysis with dosages of 0.5 g of Celluclast + Ultraflo mixture/100 g of SFF slurry and 0.5 g of Celluclast/100 g of SFF slurry. Figure 5 shows the maximum total sugar yield obtained at these enzyme loadings for the material pretreated at 190°C for 10 min. The yield obtained with 2 g of Celluclast + Ultraflo/100 g of SFF is also shown for comparison.

When 0.5 g of Celluclast + Ultraflo/100 g of SFF was used, a total yield of 38.4 g of sugars/100 g of SFF, corresponding to 55% of the theoretical, was obtained. When only Celluclast was used the total sugar yield was reduced to 33.5 g/100 g of SFF. The materials pretreated at 220°C for 5 min and at 170°C for 15 min showed curves similar to those presented in Fig. 5 although the yields were slightly lower than those obtained with the material pretreated at 190°C for 10 min.

Direct enzymatic hydrolysis with the supplementation of Ultraflo to the Celluclast resulted in a significant increase in yield compared with when Celluclast alone was used (Fig. 6). The maximum sugar yield for direct enzymatic hydrolysis, 36.6 g/100 g, corresponding to 52% of the

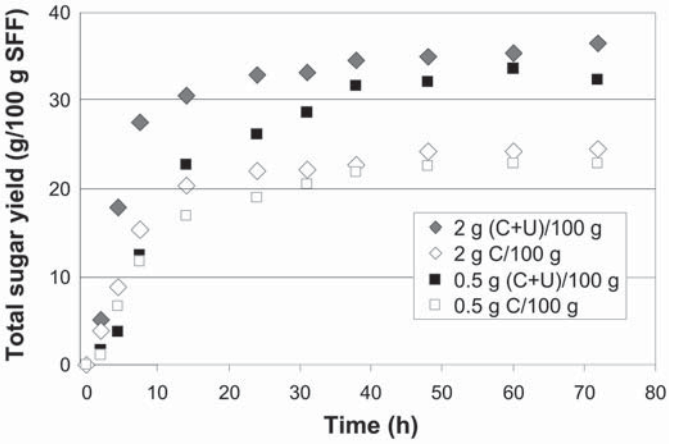

Fig. 6. Total sugar yield as function of time for direct enzymatic hydrolysis with enzyme loadings of 0.5 g of Celluclast + Ultraflo/100 g of SFF slurry, 0.5 g of Celluclast/100 g of SFF, 2 g of Celluclast + Ultraflo/100 g of SFF slurry, and 2 g of Celluclast/100 g of SFF.

theoretical, was achieved with 2 g of Cellulcast + Ultraflo mixture/100 g of slurry. When only Celluclast was used at the same enzyme loading, the yield decreased to 35.8% of the theoretical.

On the other hand, no significant difference in total sugar yield was observed between the 0.5- and 2-g loading for either two- or one-enzyme preparations, but the conversion rate was faster when the higher loading was used.

By contrast, a much less pronounced difference was observed between one- and two-enzyme preparations when enzymatic hydrolysis was preceded by pretreatment. Table 4 presents the yields of individual and total sugars obtained after direct enzymatic hydrolysis for 72 h, and after combined pretreatment and enzymatic hydrolysis with the different enzyme loadings.

At the lowest enzyme loading, pretreatment prior to enzymatic hydrolysis had a significant effect only on the glucose yield, since most of the pentosan could be readily hydrolyzed by direct enzymatic hydrolysis.

Conclusion

Wheat SFF, consisting of about 70 wt% carbohydrates on a DM basis, proved to be a suitable substrate to release sugars for ethanol production. If all the sugars in the SFF could be utilized, this would correspond to more than 25% of the glucose available in the starch fraction, which is used for ethanol production today. Pretreatment of the SFF could thus substantially improve the ethanol yield. Steam pretreatment at the optimal conditions,

Table 4
Individual and Total Sugar Yields Following Direct Enzymatic Hydrolysis of SFF and Following Combined Steam Pretreatment at 190°C for 10 min and Enzymatic Hydrolysis.

	Arabinose	Xylose	Glucose	Total
SP: 190°C for 10 min followed by EH				
2 g (C + U)/100 g SFF	13.4	21.2	17.2	51.8
0.5 g (C + U)/100 g SFF	8.8	15.5	14.1	38.4
0.5 g C/100 g SFF	6.6	12.5	14.4	33.5
Direct EH				
2 g (C + U)/100 g SFF	9.0	17.6	10.0	36.6
2 g C/100 g SFF	4.0	11.3	9.2	24.5
0.5 g (C + U)/100 g SFF	8.1	15.9	8.4	32.4
0.5 g C/100 g SFF	4.2	10.4	8.3	22.9

[a] SP, steam pretreatment; EH, enzymatic hydrolysis; C, celluclast; U, ultraflo.

190°C for 10 min, followed by enzymatic hydrolysis with 2 g of Celluclast + Ultraflo resulted in a total sugar yield of 74% of the theoretical. When a loading of 0.5 g of Celluclast + Ultraflo/100 g of SFF slurry was used, the total sugar yield decreased to 55% of the theoretical. Nevertheless, this yield is slightly higher than the overall total sugar yield obtained by direct enzymatic hydrolysis with 2 g of Celluclast + Ultraflo/100 g of SFF slurry, which resulted in 36.5 g/100 g of SSF, corresponding to 52% of the theoretical yield. Thus, pretreatment prior to enzymatic hydrolysis could reduce the enzyme loading without a reduction in the sugar yield.

Acid hydrolysis with 0.2% H_2SO_4 at 160°C for 20 min followed by enzymatic hydrolysis resulted in 88% of the theoretical yield. Because some acid is already used in the process to adjust the pH before fermentation, the addition of small amounts of acid in a pretreatment step could be a possibility.

A higher increase in sugars was obtained with acid hydrolysis using 1% H_2SO_4 at 130°C for 40 min followed by enzymatic hydrolysis, which resulted in approx 70 g/100 g of SFF. Because the addition of acid presents several drawbacks, such as the requirement of corrosion-resistant construction materials and a need for neutralization prior to fermentation, this higher acid concentration may not be feasible *(2)*.

To evaluate the different hydrolysis options, a study of economic feasibility, considering the possible increase in ethanol yield and the overall process cost, must be performed.

Acknowledgment

This work was financed by the European Commission Framework V, contract no. QLK3-CT-1999-00080.

References

1. Pomeranz, Y. (1988), in *Wheat Chemistry and Technology*, Pomeranz, Y., ed., American Association of Cereal Chemists (AACC), St. Paul, MN.
2. Von Sivers, M. and Zacchi, G. (1996), *Bioresour. Technol.* **56,** 131–140.
3. Overend, R. P. and Chornet, E. (1987), *Philos. Trans. R. Soc. Lond.* **A321(1561),** 523–536.
4. Palmarola-Adrados, B., Galbe, M., and Zacchi, G. (2003), *Biotechnol. Prog.*, in press.
5. Hsu, T. (1996), in *Handbook on Bioethanol: Production and Utilization*, Wyman, C. E., ed., Taylor & Francis, Bristol, PA, pp. 179–212.
6. Sun, Y. and Cheng, J. (2002), *Bioresour. Technol.* **83 ,** 1–11.
7. Söderström, J., Pilcher, L., Galbe, M., and Zacchi, G. (2002), *Appl. Biochem. Biotechnol.* **98–100 ,** 5–21.
8. Mandels, M., Andreotti, R., and Roche, C. (1976), *Biotechnol. Bioeng.* **6,** 21–33.
9. Ghose, T. K. (1987), *Pure Appl. Chem.* **59,** 257-268.
10. Sørensen, H. R., Meyer, A. S., and Pedersen, S. (2003), *Biotechnol. Bioeng*. **81,** 726–731.
11. Ehrman, T. (1994), Chemical Analysis and Testing Task Laboratory Analytical Procedure, LAP-001, US Department of Energy, National Renewable Energy Laboratory, Golden, CO.
12. Ehrman, T. (1994), Chemical Analysis and Testing Task Laboratory Analytical Procedure, LAP-005, US Department of Energy, National Renewable Energy Laboratory, Golden, CO.
13. Templeton, D. and Ehrman, T. (1995), Chemical Analysis and Testing Task Laboratory Analytical Procedure, LAP-003, US Department of Energy, National Renewable Energy Laboratory, Golden, CO.
14. Ehrman, T. (1996), Chemical Analysis and Testing Task Laboratory Analytical Procedure, LAP-004. US Department of Energy, National Renewable Energy Laboratory, Golden, CO.
15. Ruiz, R. and Ehrman, T. (1996), Chemical Analysis and Testing Task Laboratory Analytical Procedure, LAP-002. US Department of Energy, National Renewable Energy Laboratory, Golden, CO.
16. Larsson, S., Palmqvist, E., Hahn-Hagerdal, B., Tengborg, C., Stenberg, K., Zacchi, G., and Nilvebrant, N. O. (1999), *Enzyme Microb. Technol.* **24,** 151–159.
17. Azuma, J. I., Tanaka, F., and Koshijima, T. (1984), *J. Ferment. Technol.* **62,** 377–384.
18. Junel, L. (1999), Licenciate thesis, Lund University, Lund, Sweden.

0273-2289/04/115/1003–1012/$25.00

Application of Xylanase from *Thermomyces lanuginosus* IOC-4145 for Enzymatic Hydrolysis of Corncob and Sugarcane Bagasse

Mônica Caramez Triches Damaso,[1] Aline Machado de Castro,[1] Raquel Machado Castro,[1] Carolina Maria M. C. Andrade,[2] and Nei Pereira Jr.[*,2]

[1]Departamento de Engenharia Bioquímica da Escola de Química da Universidade Federal do Rio de Janeiro, PO Box 68542, CEP 21945-970, Rio de Janeiro, RJ, Brazil, E-mail: nei@eq.ufrj.br; and
[2]White Martins Gases Industriais LTDA, Duque de Caxias, CEP 25225-170, Rio de Janeiro, RJ, Brasil

Abstract

Xylanases have significant current and potential uses for several industries including paper and pulp, food, and biofuel. For the biofuel industry, xylanases can be used to aid in the conversion of lignocellulose to fermentable sugars (e.g., xylose). We investigated the thermophilic fungus *Thermomyces lanuginosus* was yielded for xylanase production and found that the highest activity (850 U/mL) was yielded after 96 h of semisolid fermentation. The enzyme was used for hydrolyzing agricultural residues with and without pretreatment. Such residues were characterized in relation to the maximum xylose content by total acid hydrolysis. The highest xylose yields realized by enzymatic hydrolysis were 24 and 52%, achieved by using 3000 U/g (dried material) of sugarcane bagasse and corncob, respectively, which received both alkali and thermal pretreatment.

Index Entries: Xylanase; *Thermomyces lanuginosus*; agricultural residues; enzymatic hydrolysis; corncob; sugarcane bagasse.

Introduction

Hemicellulases, similar to the cellulase complex, are seldom found in isolation but are usually present as part of a multicomponent system.

*Author to whom all correspondence and reprint requests should be addressed.

The complete degradation of hemicellulose becomes more complex than that of cellulase, since substituent-hydrolyzing activities are also necessary. With heteroxylans, apart from endo-1,4-β-xylanase, which catalyzes the hydrolysis of internal β-1,4-xylan links and β-xylosidase, which catalyzes the hydrolysis of xylooligossacharides, mainly xylobiose into xylose, other enzymes must act to accomplish complete hydrolysis, such as acetyl xylan esterase, α-glucuronidase, and α-L-arabinofuranosidase *(1)*.

Xylanases have a wide range of potential biotechnological applications. They catalyze the hydrolysis of internal β-1,4-D-xylose units and are used in bread making, in recovery of textile fibers, in clarification of beer and juices, and in hydrolysis of xylan-containing lignocellulosic materials to D-xylose, which can be converted to a variety of bioproducts with high aggregate value *(1–3)*. In addition, there has been increasing interest in using thermostable cellulase-free xylanases in the paper and pulp industry to modify pulp properties by removing hemicelluloses without disturbing the cellulose fiber strength of paper products *(4,5)*.

Xylanases are produced by a wide variety of microorganisms, and among them the fungi are the most potent producers. The *Thermomyces lanuginosus* strain IOC-4145, isolated from Brazilian soil, secreted cellulase-free xylanase activity in submerged and semisolid fermentation using corncob as substrate *(6)*. Some properties of the crude enzyme preparation have been published *(6,7)*, and the efficient use of this thermophilic preparation in the bleaching of acetosolv *(8)* and ethanol/water *(9)* bagasse pulps has also been reported.

There are very few articles reporting the use of xylanase in enzymatic hydrolysis of xylan-containing raw materials to obtain xylose *(10,11)*. Xylose is a fermentable sugar with high market price. Thus, the utilization of enzymatic hydrolysis to obtain xylose from agricultural residues is of great interest in modern biotechnology, because it is a cleaner and more specific procedure compared with the conventional technology to produce this abundant pentose.

In this article, we describe the production of xylanase by *T. lanuginosus* IOC-4145 in semisolid cultivation using corncob as raw material in optimized conditions. Furthermore, we describe the pretreatment effect on corncob and sugarcane bagasse and the enzymatic hydrolysis of these lignocellulosic materials using the produced thermophilic xylanase.

Materials and Methods

Chemicals

All chemicals were of analytical grade and obtained from Sigma (St. Louis, MO) unless otherwise stated. Agar-agar and meat extract were purchased from Merck.

Organism and Growth Conditions

The strain of *T. lanuginosus* used was isolated from soil at IBILCE/UNESP/SP, Brazil, and identified by Fundação Instituto Oswaldo Cruz

(Rio de Janeiro, Brazil), under the code IOC-4145. This strain was maintained on slants of oat agar: 50.0 g/L of oats, and 30.0 g/L of agar at 4°C. The composition of the growth medium (GPMKC) was as follows: 10.0 g/L of peptone, 10.0; 10.0 g/L of meat extract, 10.0 g/L of NaCl, 1.0 g/L of KH_2PO_4, 15.0 g/L of glucose. The production medium (PPMKC) had the following composition: 2.0 g/L of peptone, 2.0 g/L of meat extract, 2.0 g/L of NaCl, and 1.0 g/L of KH_2PO_4. The semisolid medium was composed of 15 g of corncob and 22.5 mL of PPMKC medium. The corncob was kindly supplied by Empresa Brasileira de Pesquisa Agropecuária (EMBRAPA), Brazil).

Spore and Mycelium Suspensions

Spores suspensions were prepared by adding 3 mL of 0.1% Tween-80 to slant cultures and gently scraping off the surface with a sterilized wire loop. These spores were counted in a Neubauer chamber, and a standardized amount (10^6 spores/mL) was inoculated in the GPMKC medium. The experiments were carried out by inoculating the GPMKC medium (pH6.0) with a mycelium suspension, germinated previously for 20 h at 45°C and 150 rpm.

Xylanase Production in Semisolid Fermentation

Twenty percent (v/v) mycelium suspension was used to inoculate 500-mL conical flasks containing 15 g of corncob as carbon source and 22.5 mL of PPMKC medium (pH6.0) as optimized by Damaso et al. *(6)*. After inoculation, the flasks were incubated in a stationary manner at 45°C for 6 d in a laboratory electric incubator. At each sampling time, the culture medium was vacuum filtered using filter paper (Whatman, no. 4, fast-flow rate), and the filtrate was used for further enzyme assays. During the cultivation, two or more flasks were sampled daily.

Enzyme Assays

Xylanase was assayed using birchwood xylan as substrate. The solution of xylan and the enzyme at appropriated dilution were incubated at 75°C for 3 min, and the reducing sugar was determined by the dinitrosalicylic acid procedure *(12)* with xylose as standard. The released color development was measured spectrophotometrically at 540 nm. One unit of enzyme activity was defined as 1 μmol of reducing sugar released 1 min under the described assay conditions. Protein concentration was measured by the Lowry method *(13)* using bovine serum albumin as standard.

All experiments were performed in duplicate and the analytical measurements at least in triplicate.

Acid Hydrolysis of Corncob and Sugarcane Bagasse

Samples of 1 g of lignocellulosic material were weighed and placed in 100-ml beakers. This material was treated with 5 mL of 72% H_2SO_4 and continuously stirred with a glass rod at 45°C for 7 min. The reaction was

stopped with the addition of 50 mL of distilled water. Then, the samples were transferred to 250-mL conical flasks, and water was added to a total volume of 137 mL. For total hydrolysis, the flasks were closed and treated thermally for 30 min at 121°C. The reaction mixtures were then filtered using filter paper, and the hydrolysates were transferred to 250-mL volumetric flasks and completed with distilled water *(14)*.

A 20-mL aliquot of hydrolysate was diluted with distilled water in a 25-mLvolumetric flask after the pH of the solution was increased from 0.6 to 5.0 with 2 *N* NaOH. The hydrolysate samples were filtered and checked for xylose yield by high-performance liquid chromatography (HPLC).

Enzymatic Hydrolysis of Corncob and Sugarcane Bagasse

The enzymatic hydrolysis of agricultural substrates was carried out as follows: Corncob, already dried (supplied by EMBRAPA), and sugar cane bagasse (supplied by Usina São Martinho, São Paulo, Brazil), dried in an oven at 60°C for 24 h, were milled in a mill of knives model 6010, at 15 A, and 15 V; Primelétrica LTDA, Brazil to powder form and sieved (42 mesh size). These lignocellulosic materials were not pretreated or were pretreated thermally or pretreated both chemically and thermally. The thermal pretreatment was carried out using approx 20 g of lignocellulosic material and 450 mL of water, for 90 min at 121°C, while the chemical pretreatment was carried out with alkali at similar conditions, using 2 *N* NaOH instead of water, at 30°C for 20 h. The alkali-pretreated samples were washed with distilled water followed by separation to remove the alkali. The lignocellulosic substrate pretreated or not (1.25 g dry wt) was placed into water or universal buffer (0.04 M H_2PO_4, 0.04 *M* CH_3COOH, and 0.04 *M* H_2BO_3 adjusted to pH6.0 with 0.2 *N* NaOH) or phosphate buffer (0.2 *M* NaH_2PO_4 and 0.2 *M* Na_2HPO_4 adjusted to pH6.0) in 500-mL conical flasks, and a desired amount of crude xylanase was added to start the reaction, for a total volume of 35 mL. The hydrolysis reaction mixture was kept under constant shaking at 120 rpm (model G-25, New Brunswick Scientific Co., Edison, NJ); at 40°C, and a control reaction was carried out at the same conditions, substituting the active enzyme with its denaturated form. The hydrolysate samples were withdrawn after different incubation times, filtered, and checked for xylose measurements by HPLC.

Enzymatic Hydrolysis of Xylan

The enzymatic hydrolysis of soluble birchwood xylan was carried out as follows: The substrate (0.5 g) was placed universal or phosphate buffer in 500 mL conical flasks, and 1500 U of crude xylanase was added to start the reaction, for a total volume of 25 mL. The hydrolysis and control reactions were accomplished at the same conditions described for enzymatic hydrolysis of lignocellulosic materials.

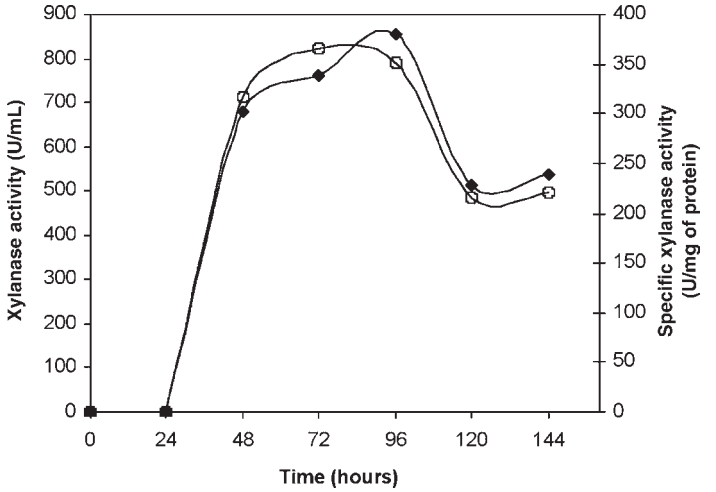

Fig. 1. Kinetic profile of xylanase production (—◆—) by *T. lanuginosus* IOC-4145 and its specific activity (—○—) using corncob as sbustrate on semisolid fermentation. The values correspond to the average of five and three measurements, respectively, and the error was –10%.

End Product Analysis by HPLC

The end products of acid and enzymatic hydrolysis of corncob and sugarcane bagasse were analyzed by using a high-performance liquid chromatograph (Waters, Milford, MA) equipped with a Rheodyne automatic injector with a 20-µL injection capacity loop, a Shodex Sugar SC 1011 column, and an integrator model 747 with a model 410 RI detector. The mobile phase was deionized water, and the flow rate was adjusted to 0.8 mL/min.

Results and Discussion

Kinetics of Xylanase Production in Semisolid Fermentation

The kinetic profile of the enzymatic production by *T. lanuginosus* IOC-4145 in semisolid medium using corncob as substrate was obtained after cultivation at 45°C for 144 h. The maximum peaks of xylanase production and specific activity occurred after 96 and 72 h of cultivation, respectively (Fig. 1). Note that most of the protein produced is related to the xylanase secreted by the fungus. High activities (850 U/mL and 365 U/mg of protein) were obtained using corncob, denoting that this residue is a good substrate for xylanase production by *T. lanuginosus* IOC-4145. When compared with other data reported in the literature employing the same or different lignocellulosic materials and other microorganisms *(15–17)*, the strain used in the present work proved to be a promising microorganism for xylanase production. The production of xylanases by *Aspergillus niger* on semisolid cultures supplemented with wheat bran revealed a

Table 1
Xylose Yield of Corncob and Sugarcane Bagasse With and Without Pretreatment

	Xylose yield (% w/w)[a]	
Pretreatment	Corncob	Sugarcane bagasse
None	22.2 ± 3.5	20.3 ± 2.4
Thermal	18.2 ± 2.1	16.8 ± 1.4
Alkali and thermal	12.2 ± 1.8	10.4 ± 0.9

[a] On dry basis.

xylanase level of 40 U/mL *(16)*, and that reached by *Aspergillus terreus* in semisolid fermentation led to an enzyme level of about 22 U/mL *(15)*.

Determination of Xylose in Sugarcane Bagasse and Corncob by Acid Hydrolysis

Acid hydrolysis was used to determine the amount of xylose present in the lignocellulosic materials without pretreatment, after thermal pretreatment, and after both alkali and thermal pretreatments.

Table 1 shows the percentage of xylose present in corncob and sugarcane bagasse with and without pretreatments. The values are in accordance with those reported in the literature *(18)*. The results also revealed that xylose content decreased when pretreatments were applied (alkali and thermal), particularly when both of them were used.

Enzymatic Hydrolysis of Xylan, Sugarcane Bagasse, and Corncob With and Without Pretreatments

Enzymatic hydrolysis of sugarcane bagasse and corncob was carried out with a concentration of solids of 36 g of biomass TL using different amounts of xylanase as well as different incubation times and conditions of the reaction.

Table 2 depicts the results of the enzymatic hydrolysis of sugarcane bagasse after thermal pretreatment with different enzyme concentrations (1000, 2000, 3000, 4000, and 5000 U/g of dried material) using universal buffer. Hydrolysis was carried out with different intervals of time, and the samples were analyzed to evaluate the degree of hydrolysis. In the initial times of hydrolysis (2 and 6 h of incubation), lower values of the degree of hydrolysis were obtained, independently of the enzyme concentration. On the other hand, after 24 h of incubation, the degree of hydrolysis increased and the best result was achieved with 3000 U/g of dried material, decreasing with higher enzyme concentration (4000 and 5000 U/g of dried material), which might be owing to any steric hindrance effect.

The second set of experiments was carried out using sugarcane bagasse and corncob both pretreated either thermally or with alkali and thermally, using a fixed amount of enzyme (3000 U/g of dried material).

Table 2
Degree of Hydrolysis of Thermally Pretreated Sugarcane Bagasse After Incubation with Xylanase from *T. lanuginosus* IOC-4145

Total enzyme (U)/g of dried material	Relative degree of hydrolysis (%) [a]		
	2 h	6 h	24 h
1000	11.0	12.3	19.4
2000	9.6	12.1	47.2
3000	12.7	11.3	100.0
4000	8.7	11.2	50.6
5000	12.0	6.2	57.4

[a] The degree is expressed as the percentage of the maximum hydrolysis obtained with 3000 U of xylanase g of dried material after 24 h of incubation. The values correspond to the average of two measurements and the error was 12.5%.

Table 3
Effect of Enzymatic Hydrolysis Using 3000 U of Xylanase from *T. lanuginosus* IOC-4145 g of Sugarcane Bagasse Under Different Conditions After 24 h of Incubation

Condition [a]	Xylose yield (mg/g of bagasse) [b]	Degree of hydrolysis (%)[b]
1 (A, T, W)	1.4	1.4
2 (A, T, PB)	25.2	24.3
3 (A, T, UB)	19.6	18.9
4 (T, W)	0.0	0.0
5 (T, PB)	0.4	0.2
6 (T, UB)	4.4	2.6

[a] A, T, W: alkali and thermal pretreatments and the presence of water; A, T, PB: alkali and thermal pretreatments and the presence of phosphate buffer; A, T, UB: alkali and thermal pretreatments and the presence of universal buffer; T, W: thermal pretreatment and the presence of water; T, PB: thermal pretreatment and the presence of phosphate buffer; T, UB: thermal pretreatment and the presence of universal buffer.

[b] The values correspond to the average of two measurements and the error was <15%.

In addition, the effect of water, and universal and phosphate buffer, on the degree of hydrolysis was investigated (Tables 3 and 4). It can be observed that it was necessary to use both pretreatments (conditions 1, 2, and 3) to obtain higher amounts of xylose. Probably, this could be ascribed to the fact that these pretreatments had opened up the pores of the cell wall structure, enhancing the enzyme's access to the substrate

Table 4
Effect of Enzymatic Hydrolysis Using 3000 U of Xylanase from *T. lanuginosus* IOC-4145/g of Corncob Under Different Conditions After 24 h of Incubation

Condition[a]	Xylose yield (mg/g of corncob)[b]	Degree of hydrolysis (%)[b]
1 (A, T, W)	25.0	20.5
2 (A, T, PB)	33.4	27.3
3 (A, T, UB)	63.4	51.9
4 (T, W)	0.5	0.3
5 (T, PB)	0.6	0.4
6 (T, UB)	0.8	0.5

[a]A, T, W: alkali and thermal pretreatments and the presence of water; A, T, PB: alkali and thermal pretreatments and the presence of phosphate buffer; A, T, UB: alkali and thermal pretreatments and the presence of universal buffer; T, W: thermal pretreatment and the presence of water; T, PB: thermal pretreatment and the presence of phosphate buffer; T, UB: thermal pretreatment and the presence of universal buffer.

[b]The values correspond to the average of two measurements and the error was <12.8%.

and, consequently, improving the hydrolysis yield. Additionally, the presence of buffer during the enzymatic hydrolysis (conditions 2 and 3), instead of simple addition of water (condition 1), was fundamental for higher xylanase efficiency.

Finally, the best condition for enzymatic hydrolysis was attained using corncob treated both with alkali and thermally in medium containing the universal buffer, achieving a degree of hydrolysis of 52%, which corresponds to 63.4 mg of xylose per gram of dried corncob. Comparison of these results with those obtained with enzymatic hydrolysis of soluble substrate xylan (Fig. 2), in which the best results (107 mg of xylose g of xylan and degree of hydrolysis of 21%) were also obtained using universal buffer, shows that after 24 h of incubation, the efficiency of xylanase in pretreated corncob was corroborated (Table 4).

Christov and Prior *(10)* used a crude xylanase preparation from *Aurebasidium pullulans* to remove hemicellulose from unbleached sulfite pulp in which the pulp was pretreated with 0.03 g of NaOH 1 h of pulp at 80°C for 1 h and with 2.5% pulp consistency. After 24 h of incubation, 12.8 mg of reducing sugar 1 g of pulp was produced, fivefold lower than the value achieved in the present work (63.4 mg of xylose 1 g of dried corncob), although different pretreatment conditions had been employed.

Gokhale et al. *(11)* studied the application of a yeast cellulase-free xylanase in agrowaste materials, such as bleached bagasse pulp, jute fiber, and corncob powder. The best result was achieved using bleached bagasse pulp with a degree of hydrolysis of 19.4%.

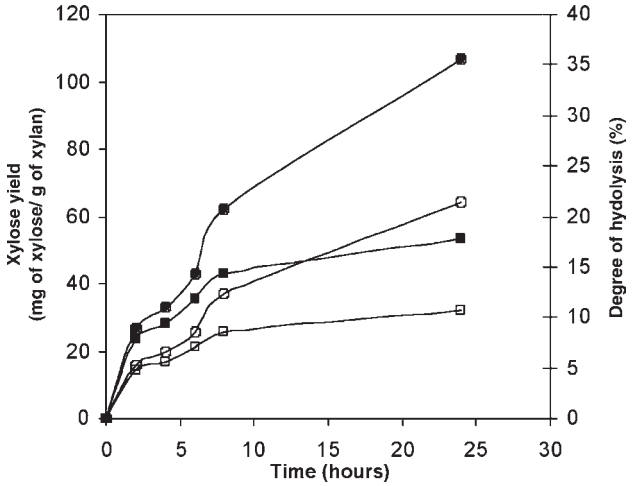

Fig. 2. Influence of phosphate and universal buffers in enzymatic hydrolysis of soluble birchwood xylan (Sigma) using 3000 U of xylanase from *T. lanuginosus* IOC-4145/g of substrate: (●) xylose yield–universal buffer; (○) degree of hydrolysis–universal buffer; (■) xylose yield–phosphate buffer; (□) degree of hydrolysis–phosphate buffer. The values correspond to the average of two measurements, and the error was <9.5%.

In conclusion, although the accessory enzyme activities needed to complete the degradation of the hemicellulose fraction in the crude extract were not all determined it was evident that the *T. lanuginosus* was capable of producing them. This novel, isolated, filamentous fungus has shown the capacity to produce appreciable amounts of xylose from corncob and sugarcane bagasse, which are abundant residues from the agroindustry. These residues have no production costs attached to them and are environmental polluters. Their enzymatic hydrolysis is a clean technology, of innovative approach and poorly exploited, needing further investigation in order to improve the xylose yield, and consequently the degree of hydrolysis.

Acknowledgments

This work was supported by grants from Rio de Janeiro Research Foundation (FAPERJ), Conselho Nacional de Desenvolvimento Científico e Tecnológico (CNPq), and FINEP/PRONEX (014/98).

References

1. Subramaniyan, S. and Prema, P. (2002), *Crit. Rev. Biotechnol*. **22,** 33–64.
2. Biely, P. (1985), *Trends Biotechnol*. **3,** 286–290.
3. Prade, R. A. (1995), *Biotechnol. Genet. Eng. Rev.* **13,** 101–131.
4. Haarhoff, J., Moes, C. J., Cerff, C., Van Wyk, W. J., Gerischer, G., and Janse, B. J. H. (1999), *Biotechnol. Lett*. **21,** 415–420.
5. Bissoon, S., Christov, L., and Singh, S. (2002), *Process Biochem*. **37,** 567–572.
6. Damaso, M. C. T., Andrade, C. M. M. C., and N. Pereira, Jr. (2000), *Appl. Biochem. Biotechnol*. **84–86,** 821–834.

7. Damaso, M. C. T., Andrade, C. M. M. C., and N. Pereira Jr. (2002), *Braz. J. Microbiol*. **33,** 1–6.
8. Gonçalves, A. R., Andrade, C. M. M. C., Ruzene, D. S., Damaso, M. C. T., and N. Pereira Jr. (2000), in *Proceedings of the Sixth European Workshop on Lignocellulosics and Pulp—Advances in Lignocellulosics Chemistry Towards High Quality Process and Products*, Paris, France, pp. 337,338.
9. Gonçalves, A. R., Ruzene, D. S., Andrade, C. M., Damaso, M. C., and Pereira, Jr., N. (2001), in *Proceedings of the 8th International Conference on Biotechnology in the Pulp and Paper Industry*, Helsinki, Finland, pp. 205,206.
10. Christov, L. P. and Prior, B. A. (1994), *Appl. Microbiol. Biotechnol*. **42,** 492–498.
11. Gokhale, D. V., Patil, S. G., and Bastawde, K. B. (1998), *Bioresour. Technol*. **63,** 187–191.
12. Miller, G. L. (1959), *Anal. Chem*. **31,** 426–428.
13. Lowry, O. H., Rosebrough, N. J., Farr, A. L., and Randall, R. J. (1951), *J. Biol. Chem*. **193,** 265–275.
14. American Society for Testing and Materials. (1956), *Standard Test for Lignin in Wood*, D 271–248, American Society for Testing and Materials, Philadelphia, PA.
15. Ghanem, N. B., Yusef, H. H., and Mahrouse, H. K. (2000), *Bioresour. Technol*. **73,** 113–121.
16. Couri, S., Terzi, S. C., Pinto, G. A. S., Freitas, S. P., and Costa, A. C. A. (2000), *Process Biochem*. **36,** 255–261.
17. Park, Y. S., Kang, S. W., Lee, J. S., Hong, S. I., and Kim, S. I. (2002), *Appl. Microbiol. Biotechnol*. **58,** 761–766.
18. Lee, J. (1997), *J. Biotechnol*. **54,** 1–24

0273-2289/04/115/1013–1022/$25.00

Predicted Effects of Mineral Neutralization and Bisulfate Formation on Hydrogen Ion Concentration for Dilute Sulfuric Acid Pretreatment

Todd A. Lloyd and Charles E. Wyman*

Thayer School of Engineering, Dartmouth College,
8000 Cummings Hall, Hanover, NH 03755,
E-mail: charles.e.wyman@dartmouth.edu

Abstract

Dilute acid and water-only hemicellulose hydrolysis are being examined as part of a multiinstitutional cooperative effort to evaluate the performance of leading cellulosic biomass pretreatment technologies on a common basis. Cellulosic biomass, such as agricultural residues and forest wastes, can have a significant mineral content. It has been shown that these minerals neutralize some of the acid during dilute acid pretreatment, reducing its effectiveness, and the higher solids loadings desired to minimize costs will require increased acid use to compensate. However, for sulfuric acid in particular, an equilibrium shift to formation of bisulfate during neutralization can further reduce hydrogen ion concentrations and compound the effect of neutralization. Because the equilibrium shift has a more pronounced effect at lower acid concentrations, additional acid is needed to compensate. Coupled with the effect of temperature on acid dissociation, these effects increase acid requirements to achieve a particular reaction rate unless minerals are removed prior to hydrolysis.

Index Entries: Pretreatment; dilute acid; hemicellulose hydrolysis; bisulfate; neutralization.

Introduction

Cellulose ethanol has the potential to displace a significant amount of petroleum in the United States, reducing the nation's dependence on foreign imports *(1)*. The biologic processes favored for producing ethanol from lignocellulosic biomass require a pretreatment step before high yields can be realized, and the accessibility of cellulose to cellulase enzymes has

*Author to whom all correspondence and reprint requests should be addressed.

been shown to increase with removal of hemicellulose *(2)*. Furthermore, the addition of dilute acid accelerates the breakdown of hemicellulose through the generation of greater concentrations of hydrogen ions and also improves recovery of hemicellulose sugars for later fermentation to ethanol and other products *(3)*. Although many different acids have been used in dilute-acid pretreatment including nitric and hydrochloric, sulfuric acid is often favored because of its low cost *(4)*, but pretreatment is still among the most costly steps in a biomass-to-fuels-and-chemicals process *(5,6)*.

When considered for process design, several factors are responsible for the high capital and operating costs of dilute-acid pretreatment processes. First, dilute sulfuric acid requires expensive materials for construction. Second, the high temperatures used result in high pressures and compound containment costs. Third, feeding solid materials to high pressure operations is costly, and substantial energy is required to heat up the biomass to pretreatment temperatures. Finally, although sulfuric acid is relatively low in cost, the quantities required are substantial, and additional costs are incurred for neutralization and conditioning chemicals prior to cellulose hydrolysis and hydrolysate fermentation as well as disposal of neutralization products.

Overall, these factors suggest that it would be desirable to reduce acid use and the severity of the reaction conditions if the costs of hemicellulose hydrolysis by pretreatment are to be reduced. Kinetic models could provide some insight into tradeoffs between acid consumption and yields, and a review by Jacobsen and Wyman *(7)* describes how acid has been incorporated into previous hemicellulose hydrolysis models. Most of these models include acid concentration but on a mass basis *(8)*. Several include acid neutralization by minerals in biomass *(9)*. Because the acid dissociation constant is a function of temperature, it has also been shown that the concentration of active hydrogen ion decreases with pretreatment temperature for sulfuric acid *(10)*. For example, Springer and Harris *(11)*, as well as others, raise the acid concentration to an empirical power apparently as a means of accounting for these effects. Unfortunately, although such models can describe the data from which they were derived, there can be inconsistencies among studies using the same substrate, limiting their utility for tuning acid concentration while maintaining acceptable yields.

Experimental results in the literature for many sulfuric acid–catalyzed pretreatment studies with a variety of feedstocks show that hemicellulose sugar recovery increases with acid addition, at least initially, and some acid is desirable to achieve high sugar yields from pretreatment and subsequent enzymatic hydrolysis of cellulose *(12–15)*. In addition, previous studies have shown that minerals in biomass can neutralize some of the added acid, increasing acid demand to reach a pH targeted for high yields *(13)*. A third effect not previously reported for hemicellulose hydrolysis is that neutralization of sulfuric acid forms bisulfates that also reduce the hydrogen ion concentration (increase pH) *(16)*. Thus, the present study was directed toward understanding how acid concentra-

tion, temperature, and the coupled effects of sulfuric acid neutralization by minerals and bisulfate formation could interplay and impact hemicellulose hydrolysis.

Predicting Catalytic Effect of Acid on Hemicellulose Hydrolysis

It is often assumed that hemicellulose hydrolysis is a first-order homogeneous reaction in hemicellulose, that is

$$H + H_3O^+ \xrightarrow{k_h} X + H_3O^+ \quad (1)$$

in which H is hemicellulose, H_3O^+ is the hydronium ion, and *X* is xylose.

A typical model applies a rate constant of the form

$$k_h = Ae^{-E/RT} \quad (2)$$

in which the preexponential factor *A* is a function of acid concentration, but the activation energy *E* is considered independent of temperature and acid concentration. This expression can be rewritten to explicitly include the effect of acid concentration:

$$A = A_0 C^m \quad (3)$$

in which *C* is the acid concentration in percent added prior to hydrolysis, and *m* is an arbitrary constant that varies with the type of biomass being pretreated.Equations 2 and 3 can be combined to give

$$k_h = A_0 C^m e^{-E/RT} \quad (4)$$

Typical values of *m* of between about 0.4 and 1.6 have been reported in the literature *(13)*. The use of percent acid in this expression appears to be arbitrary. Other investigators have used normality or molarity of the added acid, and yet others have used the pH taken at room temperature after hydrolysis. This arbitrary use of the acid concentration may explain why the power term *m* and the kinetic rate constants vary so widely, even for investigations using the same substrate, underscoring the need for consistent use of this term.

Effect of Acid Neutralization

Both Eqs. 3 and 4 show that hydrogen ion concentration should affect the rate of hemicellulose hydrolysis, but the neutralization capacity of biomass is not always taken into consideration in models reported in the literature. Neutralization is caused by basic minerals containing potassium, sodium, calcium, iron, and other cations present in biomass reacting with sulfuric acid and reducing available hydrogen ions stoichiometrically *(17)*:

$$N_2^{m+}O_m + mH_2SO_4 = N_2^{m+}(SO_4)_m + mH_2O \quad (5)$$

in which N^{m+} is the cation and *m* is its valence. Because mineral content varies from species to species, neutralization capacity must be determined

experimentally, although it may be possible to correlate neutralization capacity from mineral analyses. In a dry method described in Tappi standard method T-211 *(18)* a biomass sample is ashed, and the ash is neutralized with an excess of sulfuric acid, which is backtitrated with sodium hydroxide.To understand how neutralization by minerals impacts hydrogen ion concentration, one starts with dissociation of sulfuric acid as described by the following coupled equations:

$$H_2SO_4 \xleftrightarrow{K_1} H^+ + HSO_4^- \tag{6}$$

$$HSO_4^- \xleftrightarrow{K_2} H^+ + SO_4^= \tag{7}$$

From this, the equilibrium concentrations of each species can be predicted from the dissociation constants K_1 and K_2 as follows:

$$K_1 = \frac{\left[H^+\right]\left[HSO_4^-\right]}{\left[H_2SO_4\right]} \tag{8}$$

$$K_2 = \frac{\left[H^+\right]\left[SO_4^=\right]}{\left[HSO_4^-\right]} \tag{9}$$

Assuming K_1 to be large (i.e., the first dissociation reaction is essentially complete), then the total hydrogen ion concentration is primarily affected by the second dissociation reaction, and Eq. 9 can be rearranged to

$$\left[SO_4^=\right] = K_2 \frac{\left[HSO_4^-\right]}{\left[H^+\right]} \tag{10}$$

When partial neutralization of added sulfuric acid occurs because of minerals in the biomass, a sulfate imbalance occurs: some of the hydrogen ion is converted to water and some sulfate is then associated with mineral cations (Eq. 5). That is, for every equivalent of sulfuric acid neutralized, an equivalent amount of sulfate ions associated with mineral cations is created. The sulfate imbalance is equal to the number of moles of sulfuric acid neutralized, and if one lets M = concentration of sulfuric acid remaining after neutralization and N = sulfate concentration resulting from neutralization, then the sulfate balance can be expressed as follows:

$$\left[HSO_4^-\right] + SO_4^= - M - N = 0 \tag{11}$$

Substituting the expression for $\left[SO_4^=\right]$ from Eq. 10 into Eq. 11, one obtains

$$\left[HSO_4^-\right] + K_2 \frac{\left[HSO_4^-\right]}{\left[H^+\right]} - M - N = 0 \tag{12}$$

The charge balance can be expressed as

$$\left[H^+\right] + 2N - \left[HSO_4^-\right] - 2\left[SO_4^=\right] = 0 \tag{13}$$

or

$$\left[H^+\right] + 2N - \left[HSO_4^-\right] - 2K_2\frac{\left[HSO_4^-\right]}{\left[H^+\right]} = 0 \tag{14}$$

Then from the sulfate balance (Eq. 12) one can obtain

$$\left[HSO_4^-\right] = \frac{\left[H^+\right](M+N)}{\left[H^+\right] + K_2} \tag{15}$$

Substituting this result into the charge balance (Eq. 14) and eliminating $\left[HSO_4^-\right]$, the following quadratic equation results:

$$\left[H^+\right]^2 + \left(K_2 + M - N\right)\left[H^+\right] - 2K_2 M = 0 \tag{16}$$

Solving for $[H^+]$ leads to

$$\left[H^+\right] = \frac{-\left(K_2 + M - N\right) + \sqrt{\left(K_2 + M - N\right)^2 + 8K_2M}}{2} \tag{17}$$

Effect of Sulfate on Hydrogen Ion Activity

A second effect on hydrogen ion activity not previously considered in dilute-acid hydrolysis of hemicellulose is the shift to bisulfate that occurs with neutralization. Neutralization products are water and mineral sulfates (Eq. 5). These mineral sulfates, if not removed from the system, will form bisulfates from some of the remaining hydronium ions to reestablish equilibrium as follows (Eq. 7):

$$HSO^+ + SO_4^= \overset{K_2}{\longleftrightarrow} HSO_4^-$$

This further reduces the hydronium ion concentration, and this effect is even greater at elevated temperatures because the equilibrium constant decreases.

Effect of Temperature on Hydrogen Ion Activity

Equation *(17)* can predict the hydrogen ion activity for dilute sulfuric acid solutions containing neutralization salts with a concentration of *N* mol/L at a standard temperature such as 25°C for which dissociation constants have been tabulated. However, modifications are required to predict the hydrogen ion activity at elevated temperatures of about 100°C to >200°C, typical for hemicellulose hydrolysis. Increasing temperature accelerates rates via an Arrhenius effect but also affects the activity of hydrogen ions, i.e., the effective ion concentration after accounting for solution nonidealities. Although a pH meter measures hydrogen ion activity, it is

difficult if not impossible to measure pH reliably above about 100°C, and hydrogen ion activity generally must be estimated for higher temperatures. In this case, the solution dissociation constant K_2 in Eq. 17 is related to the thermodynamic dissociation constant K_2^0 (solution dissociation constant extrapolated to infinite dilution) by

$$K_2^0 = \frac{a_{H^+} a_{SO_4^=}}{a_{HSO_4^-}} = \frac{[H^+][SO_4^=]}{[HSO_4^-]} \frac{\gamma_{H^+}\gamma_{SO_4^=}}{\gamma_{HSO_4^-}} = K_2 \frac{\gamma_{H^+}\gamma_{SO_4^=}}{\gamma_{HSO_4^-}} \tag{18}$$

$$K_2 = K_2^0 \frac{\gamma_{HSO_4^=}}{\gamma_{H^+}\gamma_{SO_4^=}} \tag{19}$$

in which a_i is the ionic activity (mol/L), and γ_i is the ionic activity coefficient. The relation developed by Marshall from experiments determining the solubility of calcium sulfate in sulfuric acid solutions at elevated temperatures can then be used to estimate the values of the thermodynamic dissociation constant, K_2^0, as a function of temperature *(19)*:

$$\text{Log } K_2^0 = 56.889 - 19.8858 \text{ Log } T - 2307.9/T - 0.006473T \tag{20}$$

in which T is the temperature in Kelvin. For the activity coefficients γ_i, we used an empirical correlation by Davies *(20)*, which is a modification of the Debye-Hückel limiting law:

$$-\text{Log } \gamma_i = Az^2 \left(\frac{\sqrt{I}}{1+\sqrt{I}} - 0.2I \right) \tag{21}$$

in which I is the ionic strength $\frac{1}{2}\Sigma n_i z_i^2$; γ_i is the ionic activity coefficient; A is the Debye-Hückel constant = $1.825 \times 10^6 (\varepsilon T)^{-1.5}$; ε is the dielectric constant of water = 132.88-.208T; z is the ionic charge; n is the ion molarity; and T is the temperature (K).Assuming that the two monovalent activity coefficients are equal, the expression for the solution dissociation constant after rearranging Eq. 19 becomes

$$K_2 = \frac{K_2^0}{\gamma_{SO_4^=}} \tag{22}$$

By substituting this result into Eq. 17 and remembering that the activity of the hydrogen ion $a_{H+} = [H^+]\,\gamma_{H^+}$ (in which a_{H^+} is in mol/L) one now has

$$a_{H^+} = \left\{ -\left(\frac{K_2^0}{\gamma_{SO_4^=}} + M - N \right) + \left[\left(\frac{K_2^0}{\gamma_{SO_4^=}} + m - n \right)^2 + 8 \frac{K_2^0}{\gamma_{SO_4^=}} M \right]^{1/2} \right\} \frac{\gamma_{H^+}}{2} \tag{23}$$

This expression predicts the hydrogen ion activity for any concentration of neutralization products and at any temperature. By inserting this result in the kinetic rate expression of Eq. 4 in place of the acid term, one obtains:

$$k_h = A_0\, a_{H^+}\, e^{-E/RT} \tag{24}$$

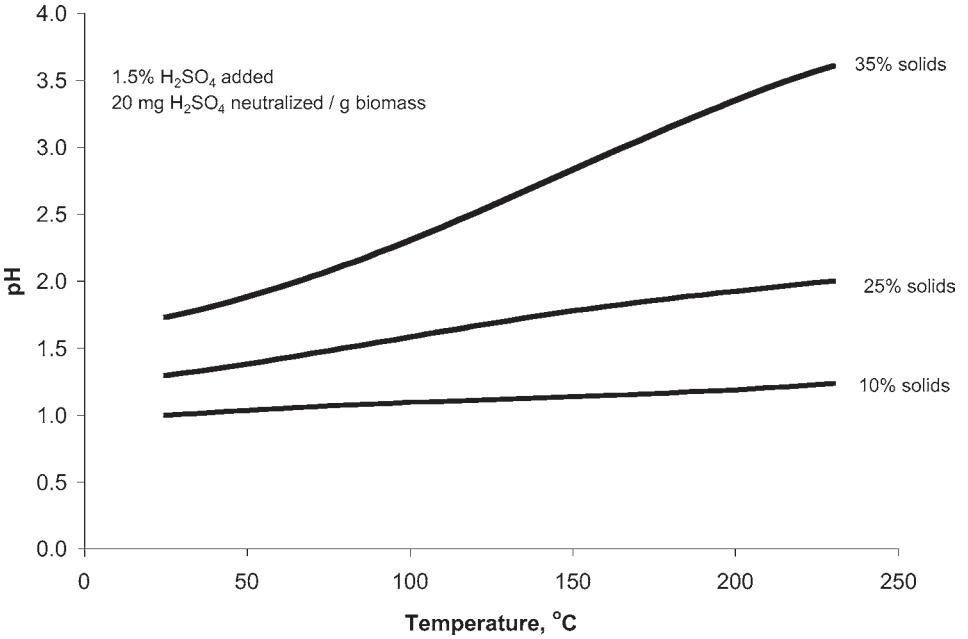

Fig. 1. Change in pH with temperature and solids loadings for solution originally containing 1.5% H_2SO_4 (w/w).

To make Eq. 24 dimensionally consistent with Eq. 4, one can convert a_{H^+} to mole fraction from molarity by dividing by the overall mole density of solution (also a function of temperature). One now has an expression that includes the effect of temperature and neutralization on added acid and can be used to predict pretreatment hydrolysis performance.

Combined Effects of Neutralization, Sulfate, and Temperature

To illustrate how acid neutralization, sulfate formation, and temperature could potentially affect hemicellulose hydrolysis, suppose several different concentrations of biomass solids were added to a 1.5% H_2SO_4 solution and treated over a temperature range of 25–160°C. Further assume that 20 mg of sulfuric acid is neutralized per g of dry biomass, and pH, defined as $pH = -Log_{10} a_{H^+}$ is taken as the measure of hydrogen ion concentration. For this case, Fig. 1 illustrates how pH would vary with temperature based on Eq. 24 at 10, 25% and 35% solids concentrations and hence three different neutralization product (sulfate salt) concentrations. A sharp rise in pH with increasing temperature in the presence of neutralization products occurs owing to an equilibrium shift of the hydrogen ion to bisulfate ion via Eq. 8 and the impact of temperature on hydrogen ion activity via Eq. 24. Furthermore, this effect is magnified with increasing temperature, and the pH rises about 0.15 units for a solids loading of 10%

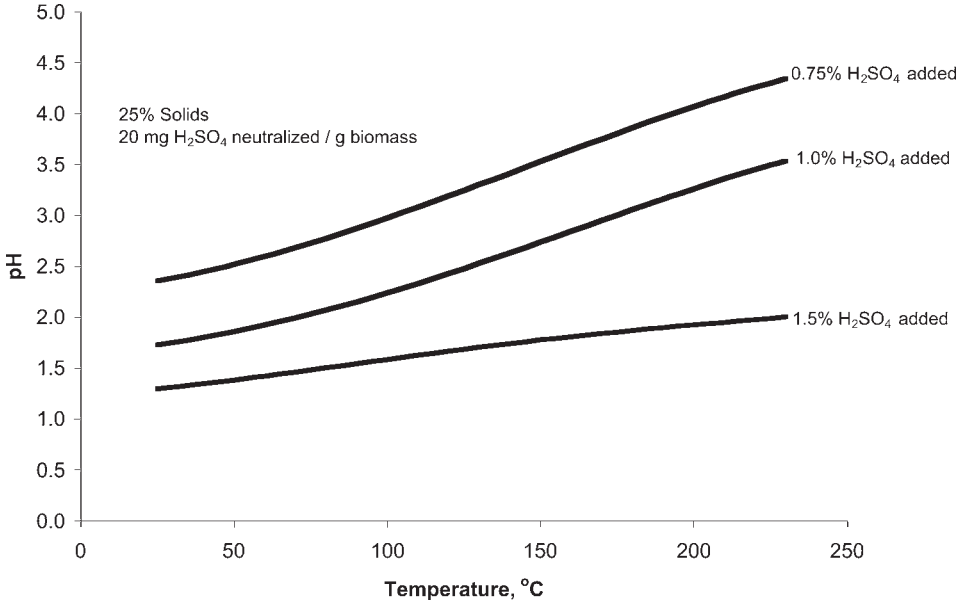

Fig. 2. Effect of acid concentration on pH as function of temperature for three different initial H_2SO_4 concentrations assuming 25% solids and 20 mg of acid/g of biomass neutralization capacity.

and about 1.2 units for a solids loading of 35%, corresponding to about a 29 and a 94% reduction in hydrogen ion activity, respectively. By contrast, if there had been no neutralization, the pH would rise just 0.11 units, from 0.89 to 1.00, over the same temperature range regardless of solids loading corresponding to a 22% reduction in hydronium ion activity.

Figure 2 shows the effect of initial acid concentration again assuming that 20 mg of sulfuric acid is neutralized/g of dry biomass and 25% solids loading. As the ratio of neutralization products to sulfuric acid increases (added acid is decreased), pH becomes increasingly temperature dependent. As an example of this effect, consider a batch pretreatment at 25% solids performed at 160°C. Adding a sulfuric acid solution with an initial concentration of 1.5% (w/w) before 20 mg/g of biomass neutralization occurs, and assuming that neutralization products are not removed, the pH shown in Fig. 2 is 1.81. Intuitively, one would expect that cutting the acid concentration in half would also cut the hydrogen ion activity in half, but Fig. 2 shows that a pH of 3.64 would be obtained for an initial sulfuric acid concentration of 0.75% at 160°C, a reduction of >98% rather than the 50% level one might expect. By contrast, if there had been no neutralization, reducing the acid addition from 1.5 to 0.75% at 160°C would result in the pH rising from 1.00 to 1.26, corresponding to a 45% reduction in hydronium ion. This is somewhat less than the 50% expected owing to the favorable equilibrium shift to the hydronium ion.

Conclusion

Neutralization of sulfuric acid by the minerals in biomass reduces the hydrogen ion activity and must be taken into account for models to accurately predict the performance of dilute-acid hemicellulose hydrolysis. Furthermore, in the case of sulfuric acid, the neutralization products lead to a bisulfate ion shift, further reducing active hydrogen ion. Neutralization and formation of bisulfate can have particularly significant effects for low acid concentrations or high solids loadings. Thus, it may be worthwhile to remove minerals or neutralization products prior to hydrolysis if one wishes to reduce acid consumption for hemicellulose hydrolysis while maintaining high sugar yields. Further experiments are required to validate the predicted effects of mineral neutralization, bisulfate formation, and temperature on dilute-acid pretreatment of biomass.

Acknowledgments

We wish to recognize our partners from Auburn, Michigan State, Purdue, and Texas A&M universities and the National Renewable Energy Laboratory for their valuable interactions during this study. We also appreciate the Thayer School of Engineering at Dartmouth College for making our work possible. Finally, we gratefully acknowledge the United States Department of Agriculture Initiative for Future Agricultural and Food Systems Program for funding our pretreatment work (contract 00-52104-9663).

References

1. Wyman, C. E. (1999), *Annu. Rev. Energy Environ*. **24,** 189–226.
2. Torget, R., Hatzis, C., Hayward, T. K., Hsu, T.-A., and Philippidis, G. D. (1996), *Appl. Biochem. Biotechnol*. **57/58,** 85–101.
3. Allen, G. A., Schulman, D., Lichwa, J., and Antal, Jr., M. J. (2001), *Ind. Eng. Chem. Res*. **40,** 2352–2361.
4. Hsu, T. A., Himmel, M., Schell, D., Farmer, J., and Berggren, M. (1996), *Appl. Biochem. Biotechnol*. **57/58,** 3–18.
5. Wooley, R. Ruth, M., Glassner, D., and Sheehan, J. (1999), *Biotechnol. Prog*. **15,** 794–803.
6. Lynd, L. R., Elander R. T., Wyman C. E. (1996). *Appl. Biochem. Biotechnol*. **57/58,** 741–761.
7. Jacobsen, S. E., and Wyman, C. E. (2000), *Appl. Biochem. Biotechnol*. **84-86,** 81–95.
8. Belkacemi, N., Abatzoglou, N., Overend, R. P., and Chornet, E. (1991), *Ind. Eng. Chem. Res*. **30,** 2416–2425.
9. Maloney, M. T. and Chapman, T. W. (1985), *Biotechnol. Bioeng*. **27,** 355–361.
10. Adamson, A. W. (1973), *A Textbook of Physical Chemistry*, Academic, New York, NY.
11. Springer, E. L., Harris, and J. F. (1985), *Ind. Eng. Chem. Prod. Res. Dev*. **24,** 485–489.
12. Grethlein, H. E., Allen, D. C., and Converse, A. O. (1984), *Biotechnol. Bioeng*. **26,** 1498–1505.
13. Esteghlalian, A., Hashimoto, A. G., Fenske, J. J., and Penner, M. H. (1997), *Bioresour. Technol. 59,* 129–136.
14. Torget, R. and Hsu, A. T. (1994), *Appl. Biochem. Biotechnol*. **45/46,** 5–21.
15. Bhandari, N., MacDonald, D. G., and Bakhshi, N. N. (1984), *Biotech. Bioeng*. **26,** 320–327.
16. Readnour, J. M. and Cobble, J. W. (1969), *Inorg. Chem*. **8(10),** 2174–2182.
17. BeMiller, J. N. (1967), *Adv. Carbohydr. Chem*. **22,** 25–108.

18. TAPPI. (2002), Ash in wood, pulp, paper and paperboard: combustion at 525°C, in *Documenty number TAPPI T-211*, Technical Association of the Pulp and Paper Industry, Norcross, GA.
19. Marshall, W. L. and Jones, E. V. (1966), *J. Phys. Chem*. **70/12,** 4028–4040.
20. Davies, C. W. (1930), *The Conductivity of Solutions and the Modern Dissociation Theory*, J. Wiley & Sons, New York, NY.

0273-2289/04/115/1023–1031/$25.00

Enhancement of Enzymatic Digestibility of Recycled Newspaper by Addition of Surfactant in Ammonia–Hydrogen Peroxide Pretreatment

Sung Bae Kim* **and Jin Won Chun**

Division of Applied Chemical Engineering and EBRC, Gyeongsang National University, Jinju 660-701 Korea, E-mail: sb_kim@nongae.gsnu.ac.kr

Abstract

The effect of surfactant on enzymatic digestibility was investigated during the pretreatment stage. Newspaper was pretreated with an ammonia–hydrogen peroxide mixture on a shaking bath at 40°C and 130 strokes/min for 3 h. Two kinds of nonionic surfactants, NP series and Tween series, were utilized. The effect of hydrophile-lipophile balance (HLB) value of both series surfactants on digestibility was found to be negligible, even though de-inking efficiency was improved as HLB value was increased. The effect of surfactant loading on digestibility was small, below 0.5 wt%, and negligible above 0.5 wt% at 60 international filter paper units (IFPU). The percentage improvement in digestibility increased as enzyme loading decreased. Digestibility of NP-5-added sample relative to control sample, increased significantly at an enzyme loading <60 IFPU, i.e., 19 and 13% at 15 and 30 IFPU, respectively. Such an increase in digestibility was not explained clearly from the experimental results. It was also found that ink removal before enzymatic hydrolysis is very important to enhance digestibility.

Index Entries: Pretreatment; newspaper; ammonia; hydrogen peroxide; enzymatic digestibility; surfactant.

Introduction

The widespread use of papers has created an enormous amount of wastepaper; however, it is not easy to recycle this resource because of the high cost of its utilization process. In the past, recycled wastepaper was used only two to three times before the fibers became unacceptably short *(1)*. This wastepaper can be used in the bioethanol process as inexpensive

*Author to whom all correspondence and reprint requests should be addressed.

carbohydrate substrate *(2)*. Cellulose, the major component of wastepaper, can be converted into fermentable sugars by enzymatic hydrolysis. However, raw biomass generally resists enzymatic hydrolysis because sites available for enzyme attack are limited *(3)*. Thus, effective pretreatment is an essential prerequisite to enhance the digestibility of lignocellulosic materials *(4,5)*.

Numerous pretreatment methods have been developed to improve cellulose hydrolysis by physical, chemical, or biochemical methods *(6)*. In a number of pretreatment studies, there have been very limited examinations of already delignified biomass such as wastepaper *(7–11)*. However, pretreatment methods used in most of these studies were the same as those used in conventional woody and herbaceous materials. Recent work *(5,12)* has shown that wastepaper did not require such an extensive pretreatment as developed for lignocellulosic materials.Researchers used much milder conditions than conventional conditions, such as 4% ammonia and 2% hydrogen peroxide (H_2O_2) mixture at 40°C *(5)* and 0.25% H_3PO_4 at 20°C *(12)*. According to these researchers, the ink components and some additives used in paper production hindered enzyme access to substrate. Previous studies *(4,5,13,14)* revealed that an ammonia-H_2O_2 mixture proved to be very effective in pretreating lignocellulosic materials. Ammonia helps to separate ink from cellulosic fibers and H_2O_2 to swell fibers. Thus, the enzymatic digestibility of ammonia-H_2O_2- treated substrate was much higher than that of untreated substrate. It was also found that ink had a significant effect on enzymatic digestibility.

In addition to ammonia and H_2O_2, surfactant can be added in a pretreatment process to improve de-inking, which also enhances enzymatic hydrolysis. In a de-inking process, surfactant can aid in reducing the adhesion of the ink to the fibers *(15)*. Furthermore, cellulose hydrolysis is improved when surfactants are present, because they help cellulase to desorb easily from the cellulose surface after hydrolysis reaction *(16)*. Therefore, it was deduced that surfactants could enhance the enzymatic digestibility if they were added in our pretreatment system. The main purpose of our study was to investigate the effect of surfactant on enzymatic digestibility when it was added in our pretreatment stage. Pretreatment was conducted in an ammonia-H_2O_2 mixture on a shaking bath at 40°C and 130 strokes/min for 3 h.

Materials and Methods

Newspaper and Surfactants

A mixture of three newspapers issued in Korea was used as substrate. Newspaper was cut into approx 0.5 × 0.5 cm pieces. The moisture of the paper was 6.8 wt% with the following composition: 56.2 wt% glucan, 13.9 wt% xylan + mannan + galactan (XMG), 15.0 wt% klason lignin, and 7.4 wt% ash. The nonionic surfactants (TCI; Tokyo Kasei Kogyo, Tokyo, Japan) used are listed in Table 1.

Table 1
Nonionic Surfactants[a]

Surfactant	*Chemical composition*	*Appearance*	*EO content (mol)*	*HLB*
NP-5	Polyethylene glycol	Oily liquid	5	10.0
NP-10	Mono-4-nonylphenyl	Oily liquid	10	13.3
NP-20	Ether	White solid	20	16.0
TW-80 (n=1)	Polyoxyethylene	Light yellow liquid		15.0
TW-85 (n=3)	Sorbitan n-oleate	Light yellow liquid		11.0

[a] EO, ethylene oxide: HLB, hydrophile-lypophile balance.

Pretreatment

Petreatment was performed on a reciprocating shaking water bath. Five grams of substrate was added to a 500-mL autoclavable bottle with 100 g of 4 wt% ammonia–2 wt% H_2O_2 solution. The concentration of each component was expressed as wt% based on the total amount of the solution. Then 0.1–1.5 wt% of a surfactant was added to this solution. The concentration of the surfactant was calculated as wt% based on the 5 g of dry substrate. The bottle was placed for 3 h on a shaker operating at 40°C and 130 strokes/min. After pretreatment, the wet solid was washed with deionized water until neutral and then separated into two portions. One was oven dried at 105°C overnight to measure moisture content, and subsequently, the weight loss on pretreatment. It was further subjected to composition analysis. The other was to be used in carrying out the enzymatic digestibility test stored in a refrigerator.

Enzyme and Digestibility Test

Commercial cellulase and β-glucosidase (Novo Nordisk, Bagvaerd, Denmark) supplied from Novozymes Korea were used. A mixture of Celluclast (80 IU or international filter paper units [IFPU]/mL) and Novozym 188 (792 cellobiase units [CBU]/mL) was used with a ratio of 4 IU of Celluclast/CBU of Novozym to alleviate end-product inhibition by cellobiose.

Enzymatic digestibility of pretreated substrate was performed in duplicate according to National Renewable Energy Laboratory (NREL) standard procedure no. 009 *(17)*. The amount of solid required to give 0.5 g of glucan in 50 mL was added to a 250-mL flask. The buffer solution was 0.05 *M* citrate, pH 4.8, and the cellulase enzyme loading was 60 IFPU/g of glucan. The content of the flask was preheated to 50°C before the enzyme was added. The flask was placed on a shaking bath operating at 50°C and 90 strokes/min. A sample was taken periodically and analyzed for glucose using high-performance liquid chromatography (HPLC). The glucose content after 72 h of hydrolysis was used to calculate the enzymatic digestibility.

Analytical Methods

The solid biomass sample was analyzed for moisture, sugars, klason lignin, and ash by NREL standard procedures no. 001–005 *(17)*. Sugars were measured by HPLC (Thermo Separation Products) using a Bio-Rad HPX-87H column (conditions: 0.6 mL/min, 65°C, 0.005 *M* H_2SO_4). Because this column does not resolve xylose, mannose, and galactose, the combined value of XMG is used in this article.

Results and Discussion

Newspaper exhibits low enzymatic digestibility because of its high lignin content. Additionally, chemicals such as ink, fillers, and other additives make it difficult to hydrolyze enzymatically. Our previous studies *(5,14)* showed that ink had a significant effect on digestibility when newspaper was pretreated with ammonia-H_2O_2. Furthermore, Nikolov et al. *(12)* reported that fillers and other additives used in the process of paper production made an adhesive "envelope" around the cellulose fibers, and this envelope was effectively removed with 0.25% H_3PO_4. In their study, the deliginified waste-cellulose fibers left from the processing of paper product, which was not printed, were used as substrate. Therefore, in the pretreatment of lignocellulosic materials, it is important to develop a proper pretreatment method suitable to a specific substrate.

Effect of Hydrophile-Lipophile Balance Value on Digestibility

The hydrophile-lipophile balance (HLB) represents the relative affinity of an emulsifier for water and for oil. The HLB scale goes from 0 to 20. Generally, values below 7 refer to hydrophobic agents and values above 7 to hydrophilic ones. In a de-inking process, the ink particles released from the fiber surface are removed from the slurry either by washing or flotation. The efficiency of de-inking depends on the ink properties and the paper quality used *(15)*. Surfactants are added in the de-inking process to decrease adhesion of the printing ink to the fibers at approx pH 9.0–10.0. The addition of H_2O_2 also helps ink removal by breaking chemical crosslinkages between the binders of the ink.

The optimum HLB value is dependent on ink composition *(18)*. For a washing de-inking, the values are usually above 10, and typical surfactant loadings are 0.25–1.5% relative to dry paper weight. Since nonionic surfactants are most common in de-inking *(15)*, two kinds of nonionic surfactants, NP series and Tween series were selected, as listed in Table 1.

Figure 1A shows the effect of HLB value of NP series surfactant on digestibility at a surfactant loading of 0.5 wt%. The HLB values of NP-5, -10, and -20 are 10.0, 13.3, and 16.0, respectively (Table 1). Here, control sample means a substrate pretreated without surfactant. After pretreatment, a dark-colored band consisting of ink components was observed in the upper portion of the bottle in the control sample, whereas no dark-colored band was observed in the NP-added samples (not shown). It was

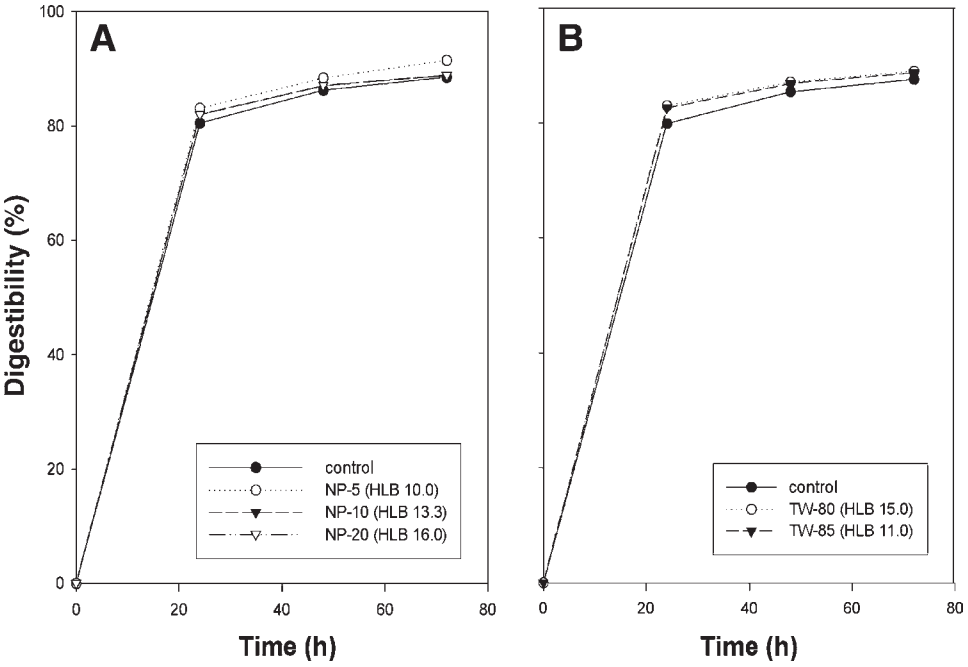

Fig. 1. Effect of HLB value on enzymatic digestibility at surfactant loadings of 0.5 wt%: **(A)** NP series; **(B)** TW series.

apparent that the dark-colored components were emulsified by the addition of surfactant, so these components were evenly distributed among the fibers. After washing pretreated samples, it was also observed that the higher the HLB value used, the whiter the swollen sample obtained. This means that de-inking efficiency is improved with this surfactant. In spite of such improvement, Fig. 1 shows that the digestibilities of NP-5-added samples were almost the same as those of the control one, resulting in the conclusion that digestibility did not depend on the HLB value using a surfactant loading of 0.5 wt%.

Figure 1B shows the effect of HLB value of the two Tween (TW) series surfactants on digestibility using a surfactant loading of 0.5 wt%. The HLB values of TW-85 and TW-80 are 11.0 and 15.0, respectively (Table 1). Unlike NP series surfactants, the dark-colored components were not distributed among the fibers (not shown). However, a slightly thicker band than the one formed in the control sample was observed in the upper portion of the bottle. As in NP series surfactant, digestibility did not depend on the HLB value. From the results shown in Fig. 1, it can be said that surfactants can improve ink removal efficiency, but not enzymatic digestibility.

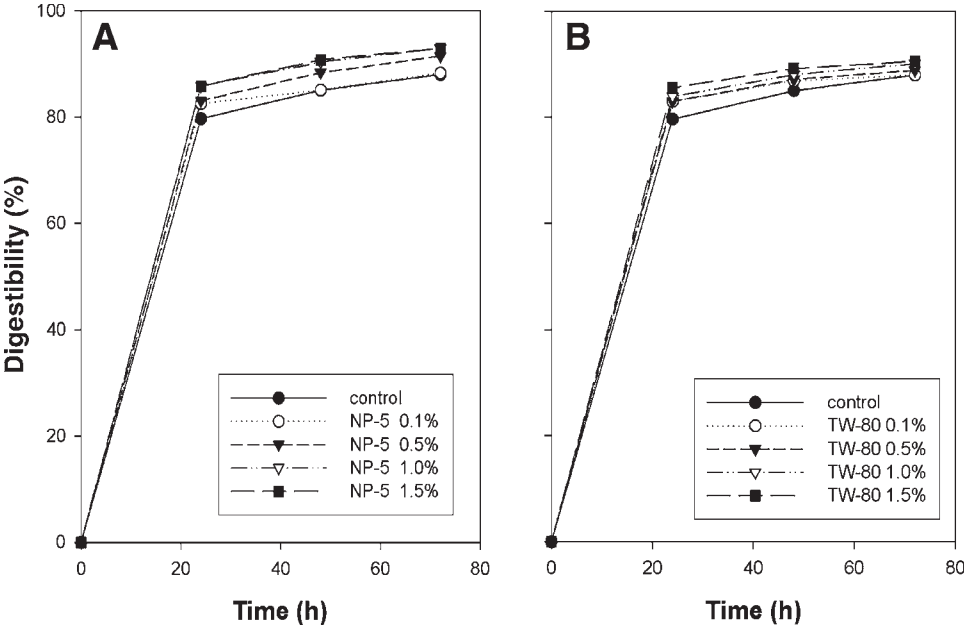

Fig. 2. Effect of surfactant loading on enzymatic digestibility: **(A)** NP-5; **(B)** TW-80.

Effect of Surfactant Loading on Digestibility

NP-5 and TW-80 were selected to examine the effect of surfactant loading on digestibility. As shown in Fig. 2, the increase in surfactant loading from 0.1 to 1.5 wt% caused a small increase in digestibility. With both surfactants, digestibilities were almost the same above 0.5 wt%, even though de-inking efficiency increased as surfactant loading increased. Surfactant is beneficial to enzymatic hydrolysis, but excess surfactant can create excessive foam and inhibit cell growth in the later fermentation process *(19)*. Therefore, an optimum surfactant loading of 0.5 wt% was selected for further experiments.

Effect of Enzyme Loading on Digestibility

As already revealed, the enzymatic digestibility was not increased as much as the de-inking efficiency. This difference may be explained by the fact that there were already detached ink re-deposits on the fiber surface after washing, which interfered with enzyme access to the substrate. Nevertheless, detached ink particles were observed in the control experiment that did not include any surfactant. It has also been reported that liquid-phase ink does not inhibit cellulase activity when ink is added to de-inking newspaper sludge at a concentration up to four times the average ink content *(20)*. Thus, the enzyme loading based on 1 g of glucan was changed from 60 to 15 IFPU and 30 IFPU because it was thought that digestibility was too high to compare the surfactant effect at 60 IFPU.

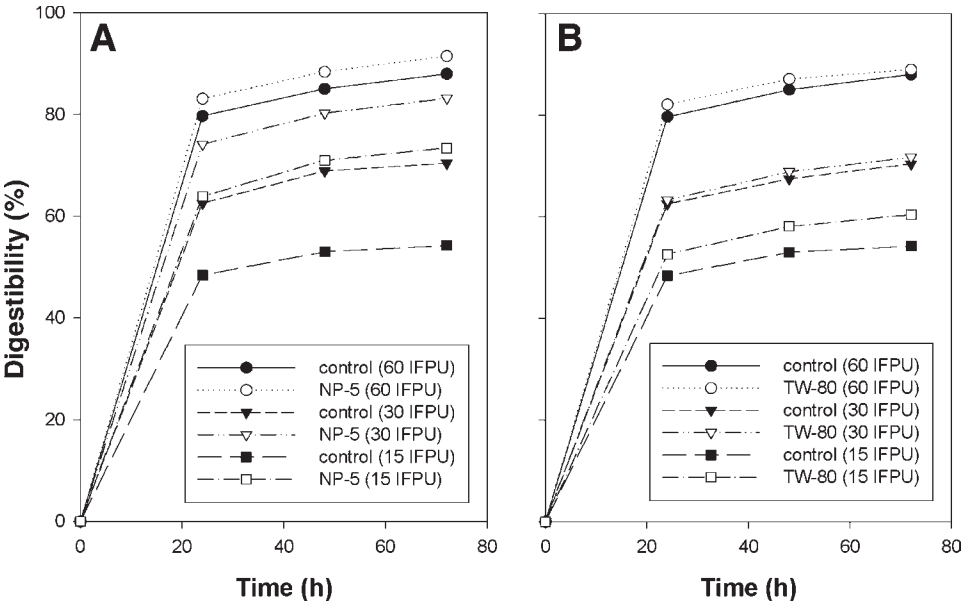

Fig. 3. Effect of enzyme loading on enzymatic digestibility at surfactant loadings of 0.5 wt%: **(A)** NP-5; **(B)** TW-80.

Figure 3 shows the effect of enzyme loading on digestibility at surfactant loadings of 0.5 wt%. As seen in Fig. 3A, the digestibility of NP-5-added sample increased more significantly than that of the control sample—from 54 to 73% for 15 IFPU and from 70 to 83% for 30 IFPU. In the case of TW-80, digestibility remained almost the same except for the lowest enzyme loading, 15 IFPU. This means that a small amount of NP-5 can reduce enzyme loading significantly and digestibility depends on the type of nonionic surfactant. Since the cost of cellulase enzyme accounts for a major portion of total cost in bioethanol production, the use of surfactant can reduce a substantial portion of production cost *(21)*. For both surfactants, the percentage improvement in digestibility increased as enzyme loading decreased. This coincides with the fact that surfactant was much more effective at low enzyme loading *(16)*.

Effect of Residual Surfactant on Digestibility After Pretreatment

Pretreated samples in our study were washed with water until neutralized to pH 7.0, but this step required a lot of water, about 300 times the weight of substrate used, because the pretreated sample was sticky and swollen. It was theorized that there was still a small amount of surfactant left in the washed fibers, and that residual surfactant may help enzymatic hydrolysis. Figure 4 shows the effect of residual surfactant after pretreatment on digestibility at 72 h. To see this effect, newspaper was pretreated without surfactant, and then a given amount of surfactant was added to

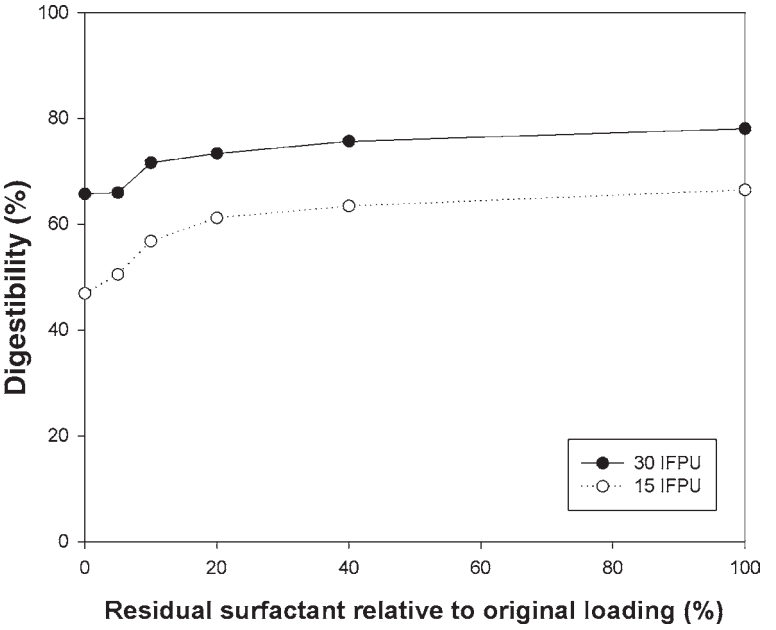

Fig. 4. Effect of residual surfactant on enzymatic digestibility after pretreatment (original NP-5 loading = 0.5 wt% of dry paper weight).

the pretreated sample at enzymatic hydrolysis. The *x*-axis value in Fig. 4 means the surfactant percentage left in pretreated sample relative to original surfactant loading (0.5 wt% of dry paper weight). As expected, digestibility increased significantly at residual surfactant levels below 20%, but marginally above 20%. Since surfactant was mostly removed in our pretreated sample, it can be expected that residual surfactant is not solely responsible for enhancement of digestibility at lower enzyme loadings.

One thing to be noted here is that digestibility depends on which stage of surfactant is added, i.e., pretreatment or enzymatic hydrolysis. As already discussed, the digestibility when surfactant was added in the pretreatment stage was 73% for 15 IFPU and 83% for 30 IFPU. When the same amount of NP-5 was added in the enzymatic hydrolysis stage, 100% in Fig. 4, digestibility was 67% for 15 IFPU and 78% for 30 IFPU. This means that the addition of surfactant in pretreatment stage is more effective on cellulosic hydrolysis. Therefore, the results confirm that ink removal by adding surfactant to pretreatment before enzymatic hydrolysis is very important to enhance digestibility at an enzyme loading <60 IFPU.

Conclusion

The effect of surfactant on enzymatic digestibility was investigated when it was added in ammonia-H_2O_2 pretreatment. The impact of digestibil-

ity depended on the type of nonionic surfactant. A small amount of NP-5 can reduce enzyme loading, resulting in substantial cost reduction in the bioethanol process. Ink removal before enzymatic hydrolysis was shown to be very important to enhance digestibility at low enzyme loading.

Acknowledgments

This work was supported by a grant from the Korea Science and Engineering Foundation (KDSEF) to the Environmental Biotechnology Research Center (grant no. R15-2003-012-02002-0)

References

1. Scott, C. D., Davison, B. H., Scott, T. C., Woodward, J., Dees, C., and Rothrock, D. S. (1994), *Appl. Biochem. Biotechnol*. **45/46,** 641–653.
2. Wyman, C. E. (1994), *Bioresour. Technol*. **50,** 3–16.
3. Gregg, D. J. and Saddler, J. N. (1996), *Biotechnol. Bioeng*. **51,** 375–383.
4. Kim, S. B., Um, B. H., and Park, S. C. (2001), *Appl. Biochem. Biotechnol*. **91–93,** 81–94.
5. Kim, S. B. and Moon, N. K. (2003), *Appl. Biochem. Biotechnol*. **105–108,** 365–373.
6. McMillan, J. D. (1992), *Process for Pretreating Lignocellulosic Biomass: A Review*, NREL/TP-421-4978, November, National Renewable Energy Laboratory, Golden, CO.
7. Khan, A. W., Labrie, J., and McKeown, J. (1987), *Radiat. Phys. Chem*. **29,** 117–120.
8. Zheng, Y., Lin, H., and Tsao, G. T. (1998), *Biotechnol. Prog*. **14,** 890–896.
9. Holtzapple, M. T., Lundeen, J. E., Sturgis, R., Lewis, J. E., and Dale, B. E. (1992), *Appl. Biochem. Biotechnol*. **34/35,** 5–21.
10. Kim, J. S., Lee, Y. Y., and Park, S. C. (2000), *Appl. Biochem. Biotechnol*. **84–86,** 129–139.
11. Capek-Menard, E., Jollez, P., Chornet, E., Wayman, M., and Doan, K. (1992), *Biotechnol. Lett*. **14,** 985–988.
12. Nikolov, T., Bakalova, N., Petrova, S., Benadova, R., Spasov, S., and Kolev, D. (2000), *Bioresour. Technol*. **71,** 1–4.
13. Kim, S. B. and Lee, Y. Y. (1996), *Appl. Biochem. Biotechnol*. **57/58,** 147–156.
14. Moon, N. K. and Kim, S. B. (2001), *Korean J. Biotechnol. Bioeng*. **16,** 446–451.
15. Lassus, A. (2000), in *Recycled Fiber and Deinking, Book 7*, Gottsching, L., ed., Gummerus Printing, Jyvaskylä, Finland, pp. 241–264.
16. Helle, S. S., Duff, S. J. B. and David, G. C. (1993), *Biotechnol. Bioeng*. **42,** 611–617.
17. Chemical Analysis and Testing Standard Procedures (1996), National Renewable Energy Laboratory, Golden, CO.
18. Borchardt, J. K. (1997), Recycling, Paper, in *Kirk-Othmer Encyclopedia of Chemical Technology*, John Wiley & Sons, New York, NY.
19. Wu, J. and Ju, L. (1998), *Biotechnol. Prog*. **14,** 649–652.
20. Duff, S. J. B., Moritz, J. W., and Casavant, T. E. (1995), *Biotechnol. Bioeng*. **45,** 239–244.
21. Kadam, K. L. (1996), in *Handbook on Bioethanol: Production and Utilization*, Wyman, C. E., ed., Taylor & Francis, Washington, DC, pp. 213–252.

0273-2289/04/115/1033–1039/$25.00

Study on Methane Fermentation and Production of Vitamin B_{12} from Alcohol Waste Slurry

Zhenya Zhang,[*,1] Taisheng Quan,[2] Pomin Li,[3] Yansheng Zhang,[4] Norio Sugiura,[1] and Takaaki Maekawa[1]

[1]Institute of Agricultural and Forest Engineering,
[2]Master Program of Biosystem Studies,
[3]Doctoral Program of Agricultural Science, University of Tsukuba,
1-1-1 Tennodai, Tsukuba, Ibaraki 305-8573, Japan,
E-mail: tyou6688@sakura.cc.tsukuba.ac.jp; and
[4]Water Conservancy and Civil Engineering College,
China Agricultural University, Peking,
Haidian District, Qinhua Dong Road, China

Abstract

We studied biogas fermentation from alcohol waste fluid to evaluate the anaerobic digestion process and the production of vitamin B_{12} as a byproduct. Anaerobic digestion using acclimated methanogens was performed using the continuously stirred tank reactor (CSTR) and fixed-bed reactor packed with rock wool as carrier material at 55°C. We also studied the effects of metal ions added to the culture broth on methane and vitamin B_{12} formation. Vitamin B_{12} production was 2.92 mg/L in the broth of the fixed-bed reactor, twice that of the CSTR. The optimum concentrations of trace metal ions added to the culture liquid for methane and vitamin B_{12} production were 1.0 and 8 mL/L for the CSTR and fixed-bed reactor, respectively. Furthermore, an effective method for extracting and purifying vitamin B_{12} from digested fluid was developed.

Index Entries: Vitamin B_{12}; methane; acclimated methanogens; trace metal ions; rock wool.

Introduction

Vitamin B_{12} is an important cofactor in many biochemical reactions and is widely used in chemotherapy and animal feed. Until now, vitamin

*Author to whom all correspondence and reprint requests should be addressed.

B_{12} was produced industrially only by microbiological means, using propionic bacterium cultivated with sugar. The conventional method results not only in low production of vitamin B_{12}, but also in remarkable organic acid inhibition *(1,2)*. Vitamin B_{12} production by methanogens may have the following advantages over conventional vitamin B_{12} production: (1) the concentration of vitamin B_{12} in the culture broth is 10 times greater than that using propionic acid–utilizing microbes *(3)*; (2) the main product, methane, does not inhibit growth of methanogens and could provide a high cell density culture system; and (3) methanol, CO_2, and acetic acid used as substrates are inexpensive, relatively stable, and renewable.

On the other hand, because of the low growth rate of methanogens compared to aerobic microbes, a long substrate residence time is required to make the fermentation facility larger. To maintain a high density of methanogens in the fermentation reactor, a method for immobilizing microbial cells onto various supports has often been used *(4,5)*. Mazumder et al. *(6)* attempted continuous fermentation of extracellular vitamin B_{12} compounds using a diatomaceous clay fixed-bed bioreactor. The concentration of vitamin B_{12} was about 4 mg/L, and total cell mass retained in the reactor was 39.6 g dry cell L^{-1} *(6)*. However, only a few research studies have examined the production of vitamin B_{12} from alcohol waste fluid using acclimated methanogens, and none of these studies were carried out from continuous methane fermentation with a fixed-bed bioreactor packed with rock wool. The aim of the present study was to investigate the optimum operating conditions including the effect of trace metal ions on the production of vitamin B_{12} compounds from alcohol waste fluid utilizing acclimated methanogens in a fixed-bed anaerobic digester.

Materials and Methods

Reactor System

A schematic of the experimental system is shown in Fig. 1. One liter of culture liquid was added to a 2.8-L cylindrical glass column reactor, and 300 mL of cylindrical carrier was packed with rock wool. All of the tubing connections, stoppers, and seals in the column were made of butyl rubber. To prevent photodecomposition of vitamin B_{12}, the outside of the whole device was covered with a vinyl sheet to shut out light. The digestion was carried out at 55°C and 20 d of hydraulic retention time (HRT).

Culture Medium and Reactor Operation

Microbial inoculum was collected from an urban waste treatment plant, and alcohol waste fluid was obtained from a local brew plant. Sugar content was used as an organic load index, and the feed of the alcohol waste fluid to the reactor was diluted to 5% sugar content (as glucose) with distilled water. The basal medium consisted of the following components (per liter of distilled water): 3.40 g of KH_2PO_4, 3.40 g of K_2HPO_4, 2.54 g of Na_2CO_3, 2.0 g of yeast extract, and 0.75 g of NH_4Cl. First, 400 mL of the alcohol waste

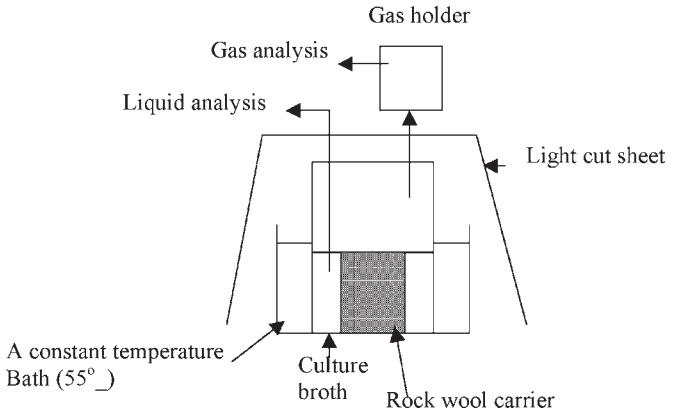

Fig. 1. Schematic of batch fermentation system with rock wool carrier.

Table 1
Composition of Trace Metal Solution

Compound	Concentration (mg/L)
$MgSO_4 \cdot 7H_2O$	600
$MnSO_4 \cdot H_2O$	5
$NiCl_2 \cdot 6H_2O$	125
$FeSO_4 \cdot H_2O$	28
$CoCl_2 \cdot H_2O$	10
$CaCl_2 \cdot H_2O$	40
$ZnSO_4 \cdot H_2O$	30
$CuSO \cdot H_2O$	8
$AlK(SO_4)$	1
H_3BO_3	1
$NaMoO_4 \cdot H_2O$	1.5

fluid and 400 mL of basal medium were added to the reactor, and then this was inoculated with 200 mL of inoculum to the reactor. To begin fermentation, the HRT of the alcohol waste fluid to the reactor at the initial stage of fermentation was set as 30 d, and then increased to 20 d gradually. The composition of trace metal solution is shown in Table 1.

Analysis Method

The concentrations of the gas-phase components were analyzed by a gas chromatograph (Shimadzu GC-8A; Kyoto, Japan) equipped with a thermal conductivity detector connected to a data analyzer (Shimadzu C-R4A Chromatopac). A stainless steel column packed with Porapak-Q was used.

The detector and injector temperature were both 60°C and the column temperature was 80°C. N_2 was used as the carrier gas at an inlet pressure of 199 kPa and outlet pressure of 150 kPa. This allowed very accurate determination of CO_2, H_2, and CH_4.

Vitamin B_{12} was analyzed by high-performance liquid chromatography (HPLC) (*[2]*; Jasco Culliver 1550) equipped with a Crest Pak C_{18} column at 40°C with an ultraviolet detector (355 nm). HPLC was performed with an automated gradient controller. KH_2PO_4 (10 m*M*) + $CH_3(CH_2)_5SO_3Na$ (2 m*M*) with an initial pH of 3.0 and methanol (100% [v/v]) were mixed as degassed solvent components A and B, respectively. The gradient condition was designed at response times of 0.0, 30.0, 35.0, and 35.1 min, and A/B ratios of 100/0, 50/50, 50/50, and 100/0. Solvents were used at a flow rate of 1 mL/min and at a maximum pressure of 46 kg/cm^2. The cyanocobalamin (Wako) was used as standard. A digital refractometer (ATAG; PR-101) was used to measure the sugar content as glucose.

Extraction and Purification of Vitamin B_{12}

Extraction and purification of vitamin B_{12} were performed as described by Sado *(8)*, Chanto et al *(7)*, and Mazumder et al. *(9)*. Finally, the following method modified by us was used throughout the study. A 4-mL sample of fermentation broth was centrifuged at 7000*g* for 4 min. The liquid (containing few or no bacterial cells) was directly passed through an Amberlite XAD-2 column (2 cm diameter × 10-cm length). After washing the column with water, the liquid with 0.01% (wt/v) KCN at pH 4.5 was passed through the same column once more and the absorbed corrinoids were changed to cyanocobalamin. The absorbed cyanocobalamin was eluted with 80% methanol containing 0.01% (wt/vol) KCN and 20% distilled water. The cyanocobalamin fraction was flash evaporated to dryness and dissolved in a small volume of water. In addition, vitamin B_{12} extraction and purification from a standard cyanocobalamin aqueous solution was tested using the modified method.

Results and Discussion

Extraction and purification of vitamin B_{12} were carried out by the method reported by Sado *(8)*; however, no vitamin B_{12} peak was determined by HPLC. Another method reported by Chanto et al. *(7)* showed that the culture broth was autoclaved for 10 min and then analyzed by HPLC. With this method, several peaks were present and the real peak of vitamin B_{12} could not be detected. It could not be isolated clearly because of determination errors. Then a modified isolation method of vitamin B_{12} was attempted using a column filled with Amberlite XAD-2 *(9)*. The details of the modified method was described above. A good recovery rate (about 90%) was obtained.

The effect of the concentration of trace metal ions on the conversion rate and vitamin B_{12} production was investigated first. As shown in the Figs. 2

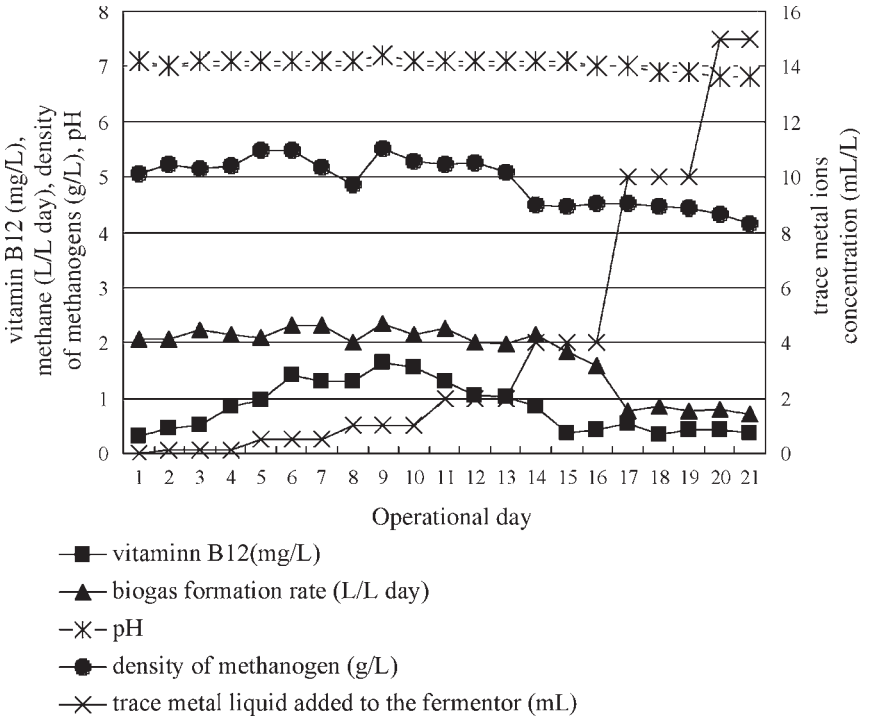

Fig. 2. Course of vitamin B_{12} production, methane production, and methanogen density with different trace metals ion added using a complete liquid stirred reactor.

and 3, the optimum concentration of trace metal ions added to the culture liquid for methane and vitamin production were 1.0 and 8 .0 mL/L for the CSTR and fixed-bed reactor, respectively. When fermentation was carried out at the optimum concentration of trace metal ions, the methane production rate and methanogen density were 2.35 L/(L·d) and 5.50 mg/L for the CSTR, and 3.90 L/(L·d) and 4.04 g/L for the fixed-bed reactor. Lower methanogen density in the broth of the fixed-bed reactor could be considered because most of the methanogens were fixed by rock wool. A corrinoid, such as vitamin B_{12}, containing cobalt ions is known to bind to coenzyme M (CoM) methylase, and therefore cobalt is essential for vitamin B_{12} synthesis *(10)*. To raise the production of vitamin B_{12}, the optimum trace metal ions added to the fermentation liquid should be a very important factor. As shown in the Figs. 2 and 3, inhibition of growth of methanogens occurred when the trace metal ion concentration was greater than 1.0 mL/L in the case of CSTR, and 8.0 mL/L in the fixed-bed reactor. At this concentration of trace metals ion, vitamin B_{12} yield and CH_4 formation decreased sharply. The maximum yield of vitamin B_{12} obtained was 0.3 mg/g of methanogens with the CSTR and 0.72 mg/g of methanogens with the fixed-bed reactor.

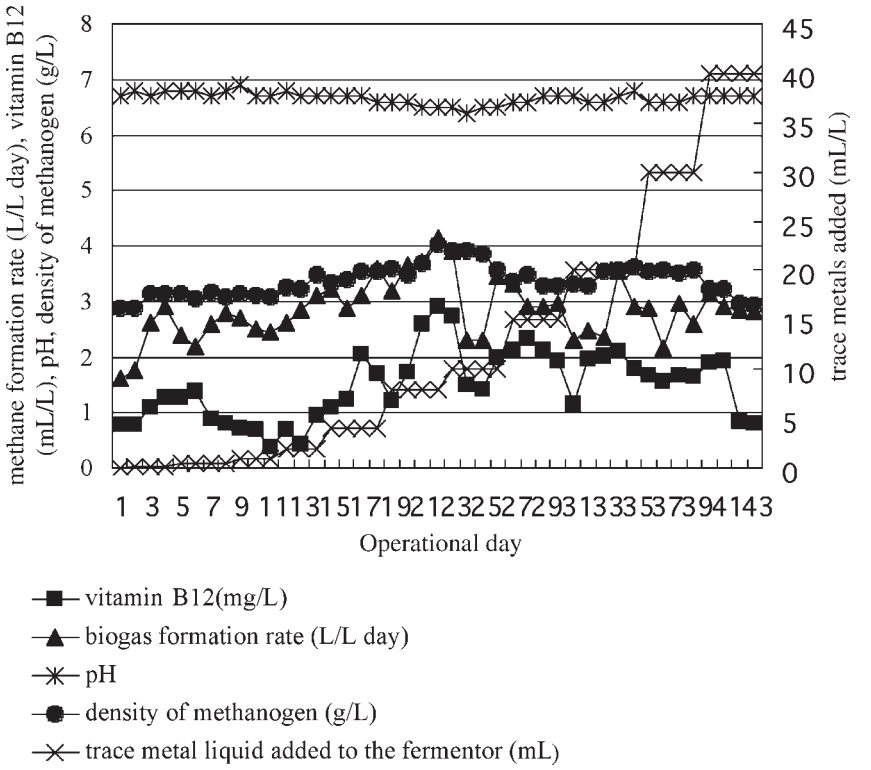

Fig. 3. Course of vitamin B_{12} production, methane production, and methanogen density with different concentrations of trace metals ion added using rock wool fixed-bed reactor.

Krzycki and Zeikus *(11)* reported that the highest corrinoid level of 5.6 mg/L was obtained from *Methanosarcina bakeri* strain MS using MeOH as substrate. The results presented herein show that alcohol waste fluids utilizing acclimated meth-anogens have a lower level of corrinoids. Methanol may be considered a stimulatory factor, and additional studies are in progress.

The results in the present study show that rock wool is effective at improving the performance of the fermentor. It could be possible that, owing to the rock wool, the fixed-bed has a higher porosity, and the methanogens immobilized on the rock wool support system have the potential to offer a high methane production rate and high vitamin B_{12} concentration in the culture broth. We checked the rock wool carrier after 42 d of digestion, and although it looked black, it maintained its original shape and did not collapse during the long digestion period.

References

1. Hill, D. T., Cobb, S. A., and Bolte, J. P. (1987), *Trans. ASAE* **30,** 496–501.
2. Marchaim, U. and Krause, C. (1993), *Bioresour. Technol.* **43,** 195–203.

3. Zhang, Z. Y., Yang, Y. N., Lu, J., and Maekawa, T. (2001), Determination of extracelluar vitamin B12 compounds in anaerobic microbial, in *Environment Protection and Technology*. China Ocean Publishing Company, 69–80.
4. Christof, H., Martin, W., Karl-Heinz, R., and Georg, M. G. (2002), *Bioresour. Technol.* **81,** 19–24.
5. Andersson, J. and Björnsson, L. (2002), *Bioresour. Technol.* **85,** 51–56.
6. Mazumder, T.K., Fukuzaki, S., and Nagai, S. (1987), *Appl. Microbiol. Biotechnol.* **26,** 511–516.
7. Chanto, A. Q., Meyer, A. C., Fucher, S., Jonas, M. F., Koechtopp, P., and Jonas R. (1998), *Biotechnol. Tech.* **12(1),** 75–77.
8. Sato, K. (1983), *Vitamins (Japan)*, 57 **(11),** 609–616.
9. Mazumder T. K., Nishio N., and Nagai, S. (1986), *Biotechnol. Lett.* **8(12),** 643–648.
10. Kenealy, W. R. and Zeikus, J. G. (1981), *J. Bacteriol.* **146,** 133.
11. Kida, K., Shigematsu, T., Kijima, J., Numaguchi, M., Mochinaga, Y., Abe, N., and Morimura, S. (2001), *J. Biosci. Bioeng.* **91(6),** 590–595.

0273-2289/04/115/1041–1058/$25.00

Comparison of Two Posthydrolysis Processes of Brewery's Spent Grain Autohydrolysis Liquor to Produce a Pentose-Containing Culture Medium†

Luís C. Duarte,[1] Florbela Carvalheiro,[1] Sónia Lopes,[1] Susana Marques,[1] Juan Carlos Parajó,[2] and Francisco M. Gírio*,[1]

[1]INETI, Departamento de Biotecnologia, Estrada do Paço do Lumiar 22, 1649-038 Lisboa, Portugal, E-mail: francisco.girio@ineti.pt; and [2]Universidade de Vigo-Ourense, As Lagoas, 32004 Ourense, Spain

Abstract

A readily fermentable pentose-containing hydrolysate was obtained from Brewery's spent grain by a two-step process consisting of an autohydrolysis (converting the hemicelluloses into oligosaccharides) followed by an enzymatic or sulfuric acid–catalyzed posthydrolysis (converting the oligosaccharides into monosaccharides). Enzymatic hydrolyses were performed with several commercial enzymes with xylanolytic and cellulolytic activities. Acid-catalyzed hydrolyses were carried out at 121°C under various sulfuric acid concentrations and reaction times, and the effects of treatments were interpreted by means of a corrected combined severity factor (*CS**), which varied in the range of 0.80–2.01. Under the tested conditions, chemical hydrolysis allowed higher pentose yields than enzymatic hydrolysis. Optimized conditions (defined by *CS** = 1.10) allowed both complete monosaccharide recovery and low content of inhibitors. Liquors subjected to posthydrolysis under optimal conditions were easily fermented by *Debaryomyces hansenii* CCMI 941 in semiaerobic shake–flask experiments, leading to xylitol and arabitol as major fermentation products. The bioconversion process was improved by hydrolysate concentration and supplementation of fermentation media with casamino acids.

† The authors wish it to be known that the first two authors should be regarded as joint First Authors.

*Author to whom all correspondence and reprint requests should be addressed.

Index Entries: Arabitol; *Debaryomyces hansenii*; hemicellulose hydrolysate; combined severity; xylitol.

Introduction

Brewery's spent grain (BSG) is the residue of malt and grain remaining in the mash kettle after the liquefaction and saccharification of starch to produce the wort. Since the manufacture of just 1 L of beer leads to about 0.04 kg of dry BSG, this material is largely available throughout the year. BSG is only used in low added-value applications such as feed, and therefore upgrading solutions are needed.

Even though the chemical composition of BSG may vary depending on the brewing conditions and ingredients used, its content of polysaccharides is remarkable (between 40 and 56% dry wt). Since hemicellulose constitutes the major fraction of BSG polysaccharides *(1–4)*, there arises the possibility of manufacturing hemicellulosic hydrolysates from BSG that could be utilized as fermentation medium, following the same principles already studied for the bioconversion of other agricultural or agroindustrial residues (such as corn cobs or sugarcane bagasse) into fuel (e.g., ethanol) or fine chemicals (e.g., polyols such as xylitol or arabitol) *(5–8)*. The remaining solid residue from BSG processing (made up of cellulose and lignin) could be upgraded by further processing as has been proposed for other raw materials *(7,9–11)*.

Several technologies for hemicellulose hydrolysis are available, including direct dilute-acid hydrolysis *(12)*, steam explosion *(13)*, and autohydrolysis *(2)*. The latter two are less severe than dilute-acid processes, and present several advantages, namely limited solubilization of lignin, low generation of degradation products, and low usage of chemicals, all of which are positive economic and environmental factors *(14)*. However, steam explosion and autohydrolysis lead to large amounts of oligomeric saccharides *(2)*, which have to be converted into monosaccharides (by acid or enzymatic catalysis) before fermentation. Studies exploring similar strategies for other raw materials have been reported *(15–17)*.

The main advantage of enzymatic posthydrolysis over the acidic process is the milder operation, which leads to reaction medium free of sugar- or lignin-degradation compounds that can limit microbial performance. Conversely, the acid process is faster, and the catalyst is cheap and allows high monosaccharide recovery. To make a correct choice, the performance of the raw material under consideration must be studied for each process.

The main factors affecting monosaccharide recovery in dilute-acid hydrolysis are catalyst concentration, reaction time, and temperature, whereas enzymatic hydrolysis is also dependent on additional factors such as substrate structure, and type and ratio of enzymatic activities present in the commercial enzyme preparations. The most important enzymes for xylan hydrolysis are endo-1,4-β-xylanases (which attack the main chain); β-xylosidases (which hydrolyze xylooligosaccharides to xylose); and accessory enzymes, such as acetyl xylanesterases, α-glucu-

ronidases, and α-arabinofuranosidases (which liberate substituents from the main chain). These enzymes act synergistically, since the xylanase activity is highly dependent on the presence of debranching enzymes and vice versa *(1,17–19)*.

The present work deals with a two-step procedure of autohydrolysis followed by posthydrolysis to obtain a fermentable, monosaccharide-rich liquor from the hemicellulose fraction of BSG. The autohydrolysis step was carried out under preoptimized conditions, and both enzymatic and chemical posthydrolysis were evaluated. Preliminary studies are also reported on the production of polyols from such liquor by *Debaryomyces hansenii*, a polyol-overproducing yeast *(20–25)*.

Materials and Methods

Feedstock and Pretreatment

BSG was obtained from Sociedade Central de Cervejas (Vialonga, Portugal). The raw material was mixed with water at an 8:1 (w/w) liquid-to-solid ratio and pretreated in an autoclave (Uniclave 88, AJC, Lisbon, Portugal) for 1 h at 100°C for residual starch removal. The solid was separated by filtration, washed and dried at 50°C to reach a moisture below 10% (w/w) *(2)*, homogenized to obtain a uniform lot, and stored in PA/PE vacuum-sealed bags.

Autohydrolysis

Starch-free BSG was subjected to reaction with water (autohydrolysis) in a 2-L stainless steel Parr reactor model 4532 (Moline, IL), to cause the hydrolytic degradation of hemicelluloses, operating under optimized conditions (liquid-to-solid ratio of 8:1 [w/w], standard heating temperature profile up to 190°C, isothermal reaction at 190°C for 2.5 min) *(2)*. After the reactor was cooled down, the oligosaccharide-containing liquor (OCL) was separated from the residual solid by filtration (Whatman no. 1 filter paper).

Posthydrolysis

Enzymatic Posthydrolysis

The pH of the OCL was adjusted to 5.5 using $Ca(OH)_2$, and the OCL was centrifuged at 6000*g* for 20 min (Beckman Coulter centrifuge; Fullerton, CA) and sterilized in an autoclave at 121°C for 15 min. Enzymatic hydrolyses were carried out in closed universal flasks at 35°C operating at 150 rpm in an orbital incubator (Unitron; Infors AG, Bottmingen, Switzerland) for 96 h. Commercial enzyme preparations were properly diluted in 0.05 *M* sodium citrate buffer (pH 5.5), and 1 mL of diluted enzyme solution was added to 25 mL of OCL. Seven commercial enzymatic preparations containing hemicellulolytic and cellulolytic activities were tested: Celluclast 1.5L®, Novozym 342®, Viscozyme L®, Pentopan 500BG® and Pulpzyme HC® from Novozymes, Denmark; and Multifect Xylanase® and

Multifect GC® from Genencor, Rochester, NY. The enzyme solutions were characterized by the following activities: endo-1,4-β-xylanase, β-xylosidase, acetylesterase, α-L-arabinofuranosidase, and filter paper activity (FPase, which describes the overall cellulolytic activity). The dilutions were calculated to provide 100 U of xylanase/g of total xylose in the reaction medium. Hydrolysis reactions were stopped by boiling for 5 min to inactivate enzymes and clarified by centrifugation prior to analysis. A blank OCL sample was assayed identically to enzyme-treated OCL using water instead of the enzyme solution. Control experiments were carried out for each enzyme, in which buffer replaced the OCL. All the hydrolysis trials were performed in duplicate.

Chemical Posthydrolysis

Defined volumes of 72% (w/w) H_2SO_4 were added to OCL to reach final concentrations of 1, 2, 3, or 4% (w/w) sulfuric acid in the reaction medium. Hydrolyses were carried out in an autoclave at 121°C for 15 or 60 min. Heating time from 100 to 121°C was 7 min. pH and weight of solutions were measured before and after autoclaving. No water losses were detected during autoclave treatments. All hydrolyses were done at least in duplicate.

Microorganism and Growth Conditions

Microorganism

D. hansenii CCMI 941 *(26)* was used in all experiments. The yeast was maintained on YM-xylose agar slants containing 20 g/L of xylose, 3 g/L of yeast extract, 3 g/L of malt extract, 5 g/L of peptone, and 20 g/L of agar.

Preparation of Media

The hydrolysate obtained by acid posthydrolysis with 2% sulfuric acid (15 min) was centrifuged as described above. To adjust pH of the hydrolysate to 5.5, NaOH, CaO, or $Ca(OH)_2$ was added. When needed, precipitates formed were removed by centrifugation as described above. To obtain a fermentation medium with a higher monosaccharide content, a concentration step (1.8-fold) was carried out in an evaporation system comprising a Syncore orbital shaker equipped with four evaporation flasks, a vacuum pump VAC® v-500, and a vacuum controller B-721 (all from Büchi, Flawil, Switzerland). The operational conditions were as follows: lower plate temperature, 100°C; upper plate temperature, 70°C; pressure, 200 mbar; stirring, 175 rpm; volume per flask, 100 mL. Under these conditions, the concentrated hydrolysates were obtained in about 3 h.

When required, media were supplemented with casamino acids (Difco, Detroit, MI) to a final concentration of 5 g/L. Four different media were tested: hydrolysate (H), supplemented hydrolysate (SH), concentrated hydrolysate (CH), and concentrated and supplemented hydrolysate (CSH). To prevent additional medium decomposition, all media were filter sterilized using 0.22 μm Gelman membrane filters (Pall, Ann Arbor, MI).

Growth Conditions

Two 24-h-grown slants were used to seed 150 mL of nonsupplemented and nonconcentrated medium in a 1000-mL baffled Erlenmeyer flask. After 24 h, the cell biomass was centrifuged at 8500*g* under sterile conditions in a Sigma 3K15 centrifuge (Osterode am Harz, Germany), and a similar flask was inoculated with all the cell biomass. After 24 h, the cell biomass was centrifuged again and used to seed the final culture, in an initial cell dry weight concentration of about 2.8 g/L. All experiments were carried out aerobically in 500-mL Erlenmeyer flasks capped with cotton wool stoppers containing 200 mL of medium in an Infors Unitron orbital incubator set at 30°C and 150 rpm. All assays were done at least in duplicate.

Enzymatic Activities

All enzyme assays were carried out at 35°C in 0.05 *M* sodium citrate buffer (pH 5.5) similar to the conditions used for the enzymatic hydrolyses of OCL. Endo-1,4-β-xylanase (EC 3.2.1.8) and FPase activities were determined by measuring (after an incubation time of 30 min) the release of reducing sugars from the following substrates: 1% (w/v) oat spelts xylan (Sigma, Steinheim, Germany) and Whatman no. 1 filter paper (about 50 mg), respectively. Reducing sugars released were assayed by the dinitrosalicylic acid method *(27)*.

β-D-Xylosidase (EC 3.2.1.37), acetylesterase (EC 3.1.1.6), and α-L-arabinofuranosidase (EC 3.2.1.55) activities were determined using the synthetic substrates 1 m*M* *p*-nitrophenyl-β-D-xylopyranoside, 5 m*M* *p*-nitrophenyl-acetate, and 5 m*M* *p*-nitrophenyl-α-L-arabinofuranoside (all from Sigma). Release of *p*-nitrophenol was monitored spectrophotometrically at 410 nm using a Jasco V-530 Spectrophotometer.

One unit of enzymatic activity was expressed as 1 μmol of xylose, glucose, or *p*-nitrophenol released per minute under the specified conditions.

Analytical Methods

D-Xylose; D-glucose; L-arabinose; formic, acetic, and levulinic acids; ethanol; hydroxymethylfurfural (HMF), and furfural were quantified by high-performance liquid chromatography (HPLC) using an Aminex HPX-87H column from Bio-Rad (Hercules, CA). The HPLC system was a Waters LC module 1 plus (Millford, MA) equipped with both a refractive index and an ultraviolet detector set at 280 nm (used to detect HMF and furfural). The mobile phase was 5 m*M* H_2SO_4, the column temperature was 50°C, and the flow rate was 0.4 mL/min. The system was equipped with a Micro-Guard Cation-H Refill Cartridge from Bio-Rad prior to the HPX-87H column. In the fermentation experiments, owing to the partial overlap of arabinose, xylitol, and arabitol, samples were also analysed by HPLC using a Waters Sugar Pak 1 column. It was used with a Merck Hitachi HPLC system (Tokyo, Japan) equipped with a refractive index detector (L-7490).

The mobile phase was 50 mg/L of calcium EDTA, the column temperature was 90°C, and the flow rate was 0.5 mL/min. Once this method no longer allowed us to distinguish between D- and L-arabitol, the latter was used as arabitol standard. All samples were filtered with 0.45-µm Gelman membrane filters prior to analysis.

Total phenolic compounds content was assayed spectrophotometrically using a modified Prussian blue method as described by Graham *(28)* employing an LKB Biochrom Ultrospec II spectrophotometer (Cambridge, England). Tannic acid was used as calibration standard.

Cellular dry weight concentration was quantified gravimetrically by filtering of 5 mL of culture broth through 0.45-µm Gelman membrane filters, washing with an equal volume of water, and drying overnight at 100°C to constant weight.

Calculations

Monosaccharide, aliphatic acids, furan derivatives, and phenolic compound recoveries after posthydrolysis were calculated as the ratio between the concentration determined in the reaction media and the concentration that resulted from the quantitative acid hydrolysis *(29)* of oligosaccharides into monosaccharides and other compounds. In enzymatic treatments, the concentrations obtained were corrected by subtracting the corresponding concentration in the respective control assays, since the commercial enzymes contain mono-, di-, and oligosaccharides. The dilution factor introduced by adding the dilute enzyme preparation or the different volumes of sulfuric acid in posthydrolysis were also accounted for.

In the same way as reported in the literature *(30)*, the severity of operational conditions in acid post hydrolysis was comparatively assessed by means of a combined severity parameter *CS** (*see* below).

The volumetric substrate consumption rates, Q_s (g/[L·h]), were based on grams of substrate consumed per liter of culture medium/h at designated times. The product volumetric production rate (productivity), Q_p (g/[L·h]), was based on grams of product produced per liter of culture medium/h at designated times. The product yield, $Y_{p/s}$ (g/g), was calculated as the amount of product formed per gram of designated consumed substrates.

Results and Discussion

Autohydrolysis enables the selective hydrolysis of hemicelluloses to a mixture mainly consisting of oligosaccharides and monosaccharides. The monosaccharide content can be increased under harsher reactor conditions, but then monosaccharides can undergo decomposition reactions, thereby increasing the content of potential fermentation inhibitors in hydrolysates.

Under the BSG autohydrolysis conditions used herein, most of the hemicelluloses are converted mainly into oligosaccharides. To obtain a monosaccharide-rich hydrolysate, the OCLs have to be further hydrolyzed.

Two different processes (enzymatic posthydrolysis and acid posthydrolysis) were assayed for this purpose.

Enzymatic Posthydrolysis

Unlike starch or cellulose, BSG hemicellulose has a complex structure, which is still present, in part, on its autohydrolysis products. Oligosaccharides from BSG hydrolysis consist mainly of branched arabino-xylo-glucurono oligosaccharides that are not highly acetylated when compared to other xylans, such as from *Eucalyptus* wood *(31)*. The action of several enzymatic activities including endo-1,4-β-xylanase; β-xylosidase; and accessory activities such as acetyl xylanesterase, α-glucuronidase, and α-arabinofuranosidase is therefore required for the complete hydrolysis of OCL to monosaccharides.

Table 1 shows the main activities present in the various reaction mixtures using Celluclast 1.5L, Novozym 342, Viscozyme L, Pentopan 500BG, Pulpzyme HC, Multifect Xylanase, and Multifect GC. Although most endoxylanases present in the commercial preparations exhibit optimal activity near 50°C, hydrolysis assays were carried out at a lower temperature (35°C) to increase enzyme stability and to reduce the possibility of inactivation of other enzymatic activities having unknown stability profiles.

The monosaccharides and acetic acid recoveries obtained on enzymatic posthydrolysis are also provided in Table 1. The concentrations of formic and levulinic acids, HMF, and furfural concentrations were also determined, but in all cases, they remained unchanged throughout the enzymatic process. The same trend was observed for the total phenolic content (data not shown).

The lowest recovery for monosaccharides and acetic acid was obtained with Pulpzyme HC. This can be explained by the fact that this preparation only exhibits endo-1,4-β-xylanase activity, lacking the debranching enzymatic activities. The best total sugar recovery was obtained using either Celluclast 1.5L or Viscozyme L, enabling about 75% arabinose recovery, 63% xylose recovery, and almost total glucose recovery, with no additional production of microbial inhibitors, except acetic acid. Because BSG oligosaccharides are not highly acetylated, a residual acetyl xylanesterase activity may be sufficient to completely remove the linked acetyl groups.

The incomplete degradation of the main xylan backbone might be partially explained by its complex structure having several steric hindrances. On the other hand, the ratios of the assayed enzymes present in the commercial preparations tested might not be adapted to the structure of the BSG-derived oligosaccharides, suggesting that improved yields could be obtained by using mixtures of these preparations and, additionally, by applying sequential enzyme treatments *(32)*.

Besides these factors, the synthetic nitrophenyl derivatives used for estimating β-xylosidase, acetyl xylanesterase, and α-arabinofuranosidase activities may not provide suitable information to be applied to a real, complex substrate and/or additional enzymes (such as α-glucuronidases)

Table 1
Enzyme Activity Levels Present in Reaction Mixture for Different Commercial Enzyme Preparations Used and Respective Monosaccharides and Acetic Acid Recoveries for Enzymatic Posthydrolysis of BSG OCL[a]

	Enzyme activities (U/g xylose)					Recovery (%)			
Enzyme formulations	β-xylanase	β-xylosidase	Acetyl esterase	α-arabino-furanosidase	FPase	Glucose	Xylose	Arabinose	Acetic Acid
Celluclast 1.5L	100	0.53	ND	3.41	3.84	94	63	77	115
Novozym 342	100	0.04	0.09	0.09	0.25	52	36	79	92
Viscozyme L	100	0.08	0.52	37.91	2.01	119	63	74	105
Pentopan 500BG	100	0.69	ND	1.45	0.63	44	32	77	96
Pulpzyme HC	100	ND	ND	ND	vest.	9	12	52	68
Multifect Xylanase	100	vest.	0.01	0.01	0.03	9	28	60	86
Multifect GC	100	0.12	0.02	0.13	1.95	13	46	69	90

[a]The data are relative concentrations compared to the quantitative acid hydrolysis *(29)*. ND, not detected; vest., <0.01 U/g of xylose.

could play a role in saccharification. Finally, possible inhibitory effects on enzymatic activities caused by the phenolic compounds present in OCL could limit the extent of oligosaccharide saccharification *(18)*.

Acid Posthydrolysis

Acid posthydrolysis was studied as an alternative to enzymatic posthydrolysis, since limited monosaccharide recoveries were achieved with that technology. When compared to the enzymatic hydrolysis process, significant monosaccharide degradation reactions may occur during acid posthydrolysis. Examples of such reactions are the degradation of pentoses to furfural, hexoses to HMF, and both these furans to aliphatic acids such as formic and levulinic acids. Therefore, high monosaccharide recovery requires balanced operational conditions. In our case, the severities of treatments were modified by varying the concentrations of sulfuric acid (in the range of 1–4 % [w/w]) and reaction times of 15 or 60 min.

To provide a comparative assessment on the effects caused by the severity of operational conditions in acid-catalyzed media, the joint effects of temperature, reaction time and catalyst have been interpreted in terms of the parameter *CS (30)*. For isothermal conditions,

$$CS = \log\left\langle t \exp\left[(T - 100)/\omega\right]\right\rangle - \mathrm{pH} \quad (1)$$

in which t is the isothermal reaction time (min), T is the temperature (°C), and ω is a parameter dependent on the activation energy of the reaction that usually is assumed to be 14.75.

The parameter *CS* is an extension of the severity concept *(33)* that has been mainly used for the hydrolysis of lignocellulosic biomass with chemically defined catalysts. However, the application of *CS* to OCL hydrolysis might not be straightforward owing to the necessity of setting a suitable pH for the reaction. It can be noted that pH cannot be calculated from the molar H_2SO_4 concentration considering that 2 mol of H_3O^+/mol of sulfuric acid is produced, as generally assumed *(34,35)*. This may be justified by the facts that OCL has a complex polyelectrolite nature, that compounds with buffering activity exist in the reaction media and that side reactions involving pH alteration (e.g., hydrolysis of acetyl groups) occur throughout the posthydrolysis process. Considering this, and on the basis of the pK_a for the second dissociation of sulfuric acid for the temperatures and catalyst concentrations used in the present work, a simplified combined severity parameter (*CS**) was defined as:

$$CS^* = \log\left\langle t \exp\left[(T - 100)/\omega\right]\right\rangle - \log\left[\mathrm{H_2SO_4}\right] \quad (2)$$

in which $[H_2SO_4]$ is the molar concentration of sulfuric acid. It can be noted that *CS* and *CS** take the same value if 1 mol of (H_2SO_4) results in the net release of 1 mol of H_3O^+. This hypothesis was supported by the fair agreement found between the pH of post-hydrolyzed media measured experimentally at room temperature and the pH calculated assuming a net release

Table 2
Operational Conditions, *CS**, and Relative Composition of Posthydrolysis Liquors (Measured by Monosaccharides and Furan Derivatives) Expressed as Percentages of Concentrations Obtained on Quantitative Acid Hydrolysis (*CS** = 2.01)[a]

Operational conditions			Relative composition[b] (%)				
H_2SO_4 (% [w/w])	Time (min)	*CS**	Glucose	Xylose	Arabinose	HMF	Furfural
1	15	0.80	28	70	101	42	38
2	15	1.10	81	105	102	61	63
3	15	1.28	90	107	105	60	64
4	15	1.41	96	105	102	68	66
4	60	2.01	100	100	100	100	100

[a]All posthydrolysis assays were carried out at 121°C.
[b]Aliphatic acids content and total phenolic compounds did not change significantly with severity and were omitted from the table.

of 1 mol of H_3O^+/mol of sulfuric acid. Additional calculations showed that the values of *CS** corresponding to the heating stages were negligible in comparison with the corresponding results determined for the isothermal reaction stage.

Table 2 shows the operational conditions, the respective *CS**, and the chemical composition of BSG posthydrolysis liquors for the different posthydrolysis conditions tested. Compositions of posthydrolyzed liquors were expressed as percentages regarding to the concentrations determined by quantitative acid hydrolysis *(29)*.

Under the mildest operational conditions tested, arabinose was totally solubilized and not significantly degraded to furfural (a fact that may explain the 101% recovery with respect to the quantitative acid hydrolysis conditions), but both xylose and glucose recoveries were rather low. Sugar recovery increased with increasing severity, reaching a maximum for pentoses at a *CS** of 1.28. Further increases in severity led to pentose degradation, as indicated by higher furfural concentrations, with a negative impact in pentose recovery. Conversely, glucose recoveries always increased with the increase in severity, indicating that the gluco-oligosaccharides were more difficult to hydrolyze than the hemicellulosic oligosaccharides. The levels of aliphatic acids and total phenolic compounds were also measured, but only slight concentration changes were detected (data not shown). Aliphatic acids exhibited average concentrations of approx 1.3 g of acetic acid/L, 0.5 g of formic acid/L, and <0.2 g of levulinic acid/L, with minor increases with respect to their concentrations in autohydrolysis of OCL *(2)*. The concentrations of total phenolic compounds obtained after acid posthydrolysis were also similar to the results determined in autohydrolysis of OCL, indicating that these compounds do not react significantly during acid posthydrolysis.

Although the higher recovery of pentoses was obtained at *CS** 1.28, if the dilution effect (owing to the addition of acid) is accounted for, the recovery of pentoses obtained at *CS** 1.10 becomes similar to that obtained at *CS** 1.28, whereas only slightly lower glucose recovery was achieved. Since aliphatic acid and furan derivative recoveries were also similar, the least severe condition should be considered the most adequate condition for acid posthydrolysis, once it decreases acid and later also alkali requirements, both with a positive impact on process economics.

Similar conditions have been described for posthydrolysis of steam-exploded Douglas fir wood chips performed at 120°C, but longer hydrolysis time was required *(15)*. Similar to our results, increasing catalyst also increased monosaccharide recovery and higher participation of degradation reactions. For corn cobs *(36)*, a material similar to BSG, the posthydrolysis of OCL autohydrolysis was carried out at *CS** 1.66 (calculated from the reported operational conditions: 125°C, 0.5% H_2SO_4, 165 min), a more severe condition than the optimal conditions determined in the present work for BSG.

The total monosaccharide composition of OCL acid posthydrolysate is approx 26 g/L of monosaccharides, with a ratio of 2:5:3 for glucose: xylose:arabinose. Compared to other hydrolysates, it has higher arabinose but lower xylose contents than rice straw *(37)*, sugarcane bagasse *(38)*, *Eucalyptus* wood *(16)*, and corncobs *(36)*, where the latter two hydrolysates were also obtained in a similar two-step procedure. Nevertheless, the total monosaccharide content is in the same range, e.g., as rice straw, *Eucalyptus* wood, or corncobs.

A significant comparative advantage of this BSG hydrolysate lies with the low level of microbial inhibitors; it is among the lowest reported in the literature *(16,37)*. In fact, the more relevant inhibitors usually considered for lignocellulosic-based hydrolysates, acetic acid and furfural, are present at 1.2 and 0.6 g/L, respectively, which is lower than the levels of microbial inhibition presented in the literature, at 4 and 1 g/L respectively *(39)*.

Polyol Production by D. hansenii

Polyols, namely arabitol and xylitol, have potential chemical, pharmaceutical, and food applications. The latter polyol is currently produced by chemical means, in spite of xylitol bioproduction receiving increased interest *(40)*. Previously it was shown *(22)* that *D. hansenii* CCMI 941, under oxygen limitation conditions, coproduces both of arabitol and xylitol in chemically defined medium. In the present work, we evaluated the polyol production by *D. hansenii* grown on the BSG acid posthydrolysate.

Although other researchers have reported the use of detoxification steps for other hydrolysates to be utilized by yeast *(5,7,38,41)*, considering the low level of inhibitors present in the BSG OCL acid posthydrolysate, no special detoxification treatment was carried out, except adjustment of the hydrolysate pH to 5.5. For pH adjustment of the hydrolysate, several alkalis were tested, namely NaOH, CaO and $Ca(OH)_2$. CaO, induced high foam

formation during pH adjustment, whereas NaOH-treated hydrolysates turn to a gel-like consistency during the evaporation step used to obtain the concentrated hydrolysates. Therefore, $Ca(OH)_2$ was chosen for the pH adjustment because it did not present any significant operational problems, and it limited the loss of monosaccharides (<6%), while providing complete removal of levulinic acid and a partial removal of HMF (9%), furfural (15%), and phenolic compounds (10%).

Figure 1 shows the kinetics of polyol production by *D. hansenii* grown in both hydrolysate medium (Fig. 1A) and concentrated hydrolysate medium (Fig. 1B). During the hydrolysate concentration, a minor loss of monosaccharide occurred and furfural was evaporated. All other components were concentrated, although some components such as acetic acid were partially lost during evaporation. Significant foam formation was observed during evaporation and vacuum filtration.

During fermentation glucose was the preferred monosaccharide, being depleted from the culture medium in about 48-h. Concomitantly, HMF, furfural, and formic acids were also metabolized (data not shown). Acetic acid was slowly consumed compared with formic acid (data not shown). Xylose was consumed after a short lag phase (Fig. 1A) albeit at a slower rate compared to glucose assimilation. Arabinose was only slightly consumed. Arabitol was the major polyol formed for both hydrolysate and concentrated hydrolysate media. Xylitol was also produced, but at a far lesser extent. Glycerol, another important metabolite usually accumulated in *D. hansenii*, was not detected. Ethanol was produced mostly at the expense of glucose consumption, and after glucose depletion no further ethanol accumulation occurred from pentose catabolism. Conversely, some ethanol was presumably oxidized to biomass and CO_2 concomitantly with the pentose metabolism.

Previous reports in the literature suggest that media supplementation with complex nutrient sources can increase both xylitol yield and productivities *(41)*. Therefore, a second set of experiments were carried out by adding casamino acids to both hydrolysate (Fig. 2A) and concentrated media (Fig. 2B). In both conditions, casamino acids induced changes in the yeast metabolism in relation to nonsupplemented media. Besides glucose, both xylose and arabinose were consumed more quickly and a simultaneous consumption of glucose-xylose and xylose-arabinose was observed, as already described for this yeast when grown in chemically defined media *(22,42)*. Table 3 shows the yields and volumetric rates for the metabolic products from *D. hansenii* grown under different hydrolysate media compositions. The xylose consumption rate was higher for supplemented media being for casamino acids–supplemented hydrolysate and concentrated and supplemented hydrolysate media, 0.19 and 0.30 g/(L·h), respectively. HMF, formic acid, and acetic acid were consumed slightly faster in these experiments, and again formic acid was depleted before acetic acid (data not shown).

Ethanol volumetric production rate did not differ significantly between nonsupplemented and supplemented media, but ethanol was no longer

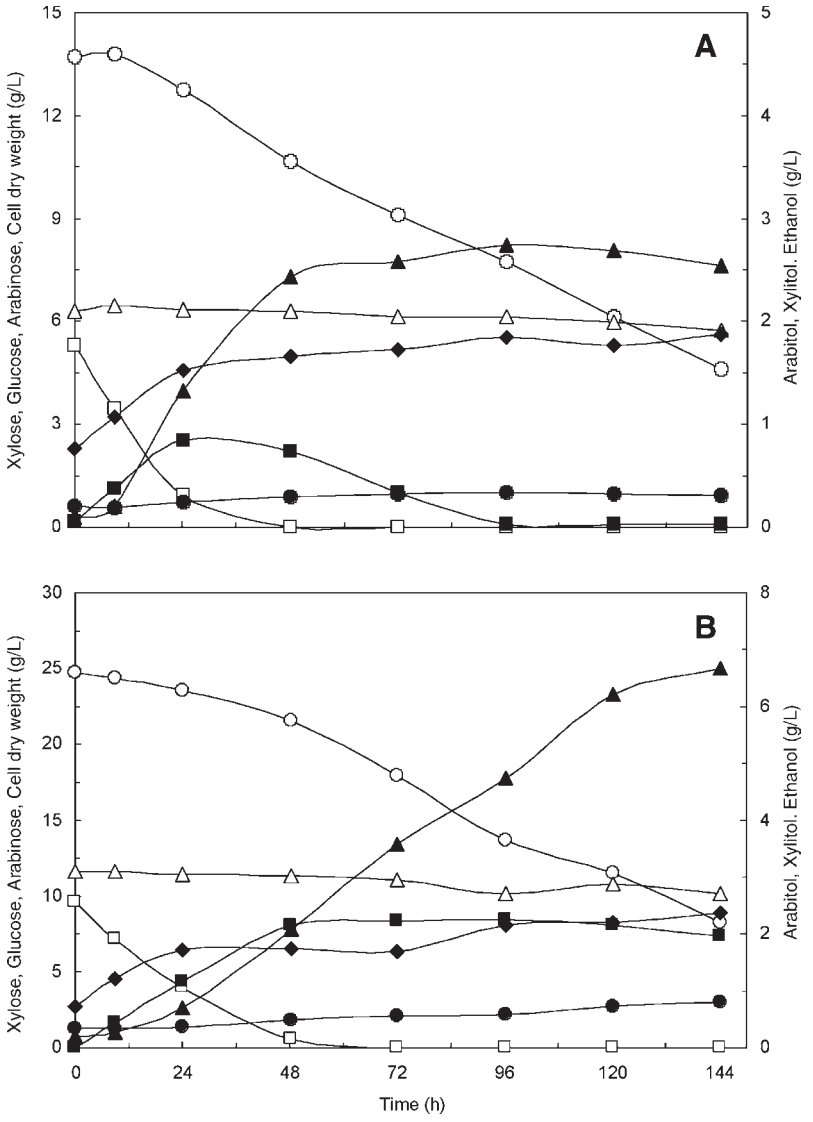

Fig. 1. Time course of substrates, cell dry weight, and metabolic products in fermentation of BSG OCL posthydrolysate (H medium) **(A)** and concentrated posthydrolysate (CH medium) **(B)** by *D. hansenii* CCMI 941. (□) Glucose, (○) xylose, (△) arabinose, (◆) cell dry weight, (■) ethanol, (●) xylitol, and (▲) arabitol.

exclusively derived from glucose metabolism for supplemented medium. In the latter medium, pentose metabolism becomes the greater contributor to ethanol production. Although ethanol production in this strain has been mainly correlated with glucose metabolism, ethanol from pentoses has also already been reported *(22)*. Arabitol was accumulated almost throughout the fermentation, but in both cases, when sugars were close to depletion it was also used as a carbon source.

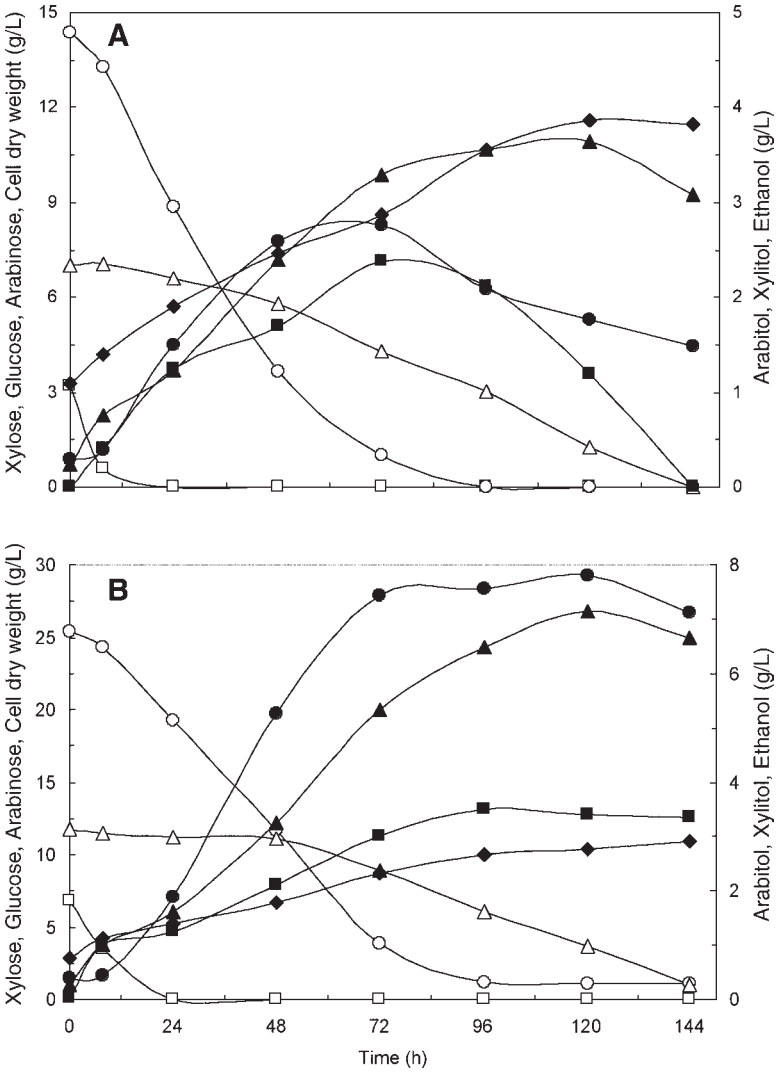

Fig. 2. Time course of substrate, cell dry weight, and fermentation products in fermentation of casamino acids supplemented with BSG OCL posthydrolysate (SH medium) **(A)** and casamino acids supplemented concentrated posthydrolysate (CSH medium) **(B)** by *D. hansenii* CCMI 941. (□) Glucose, (○) xylose, (△) arabinose, (◆) cell dry weight, (■) ethanol, (●) xylitol, and (▲) arabitol.

The major change in yeast metabolism induced by casamino acids supplementation was the marked increase in xylitol production, being the major metabolic product by *D. hansenii* grown in supplemented concentrated medium (Fig. 2B). Both arabitol and xylitol production in yeast are described to be augmented under stress conditions. Arabitol is usually found as a product of arabinose metabolism in oxygen-limited conditions *(8,22)*, but arabitol production is not restricted to arabinose metabolism,

Table 3
Maximal Volumetric Production Rates and Yields for Cell Biomass, Ethanol, Arabitol, and Xylitol Obtained with *D. hansenii* CCMI 941 Yeast for Different Tested Conditions

	Ethanol			Arabitol			Xylitol		
Exp[a]	Time (h)	Q_p (g/[L·h])	$Y_{p/s}$ (g/g)	Time (h)	Q_p (g/[L·h])	$Y_{p/s}$ (g/g)	Time (h)	Q_p (g/[L·h])	$Y_{p/s}$ (g/g)
H	24	0.03	0.18[b]	48	0.05	0.77[c]	—	0.00	0.00
CH	48	0.04	0.24[b]	120	0.05	0.45[c]	—	0.00	0.00
SH	72	0.03	0.12	72	0.04	0.19[d]	72	0.03	0.15[d]
CSH	72	0.04	0.10	72	0.07	0.21[d]	72	0.10	0.29[d]

[a] H, hydrolysate; CH, concentrated hydrolysate; SH, casamino acids–supplemented hydrolysate; CSH, concentrated and supplemented hydrolysate.
[b] Based on consumed glucose.
[c] Based on consumed xylose.
[d] Based on consumed pentoses.

since it has also been described for *Saccharomyces cerevisiae* grown in anoxic conditions in a glucose/xylulose mixture *(43)* and for *Pichia stipitis* grown in xylose with a severe respiratory inhibition *(44)*. Furthermore, its production as a compatible solute in the yeasts *Zygosaccharomyces rouxii* and *D. hansenii* is also well documented, where arabitol accumulation is part of the yeast response to osmotic stress, regardless of the carbon source being utilized *(23,45,46)*.

Thus, the relatively constant arabitol production in all tested conditions can probably be explained by a combination of factors, such as high oxygen limitation and possible osmotic effects (e.g. induced by sulfate ions not fully precipitated with calcium) that may act synergistically. Arabitol yields and productivities found in the present work are similar to reported values in the literature *(8,22)*.

On the other hand, higher xylitol production is usually correlated to, among other factors, oxygen limitation, high xylose concentrations and high xylose uptake rates *(41)*. Casamino acids induce an increase in xylose uptake rate, therefore increasing xylitol production that is further enhanced by the hydrolysate concentration. Although the maximal obtained yields and volumetric production rates for xylitol are in the range usually described for this yeast *(42)*, they are below the reported values for optimized conditions *(25)*, which for xylitol production usually requires higher xylose concentrations and oxygen availability. Therefore, this system can still be improved in order to further increase both polyol yields and productivities.

Conclusions

Enzymatic posthydrolysis enabled monosaccharide recoveries in the range usually attained for other feedstocks to be obtain *(17,18)*. The higher recoveries were obtained with Celluclast 1.5L and Viscozyme L, with arabinose recoveries close to 75%, xylose recoveries of 63%, and close to total glucose recovery. Furthermore, no additional production of microbial inhibitors occurs during the enzymatic step, with the exception of acetic acid. However, the long incubation time and catalyst costs may constitute important constraints for the near-term implementation of an enzyme-based conversion process to the conversion of OCL to monosaccharides.

Since dilute-acid posthydrolysis with 2% (w/w) H_2SO_4 at 121°C for 15 min enables hydrolysis of the oligosaccharides with a good recovery of pentoses and only a slight increase in microbial inhibitors, no attempt was made to optimize the enzymatic process (namely, in terms of enzyme dosage, incubation time or by applying mixtures of enzymes). The acid posthydrolysate was therefore used for *D. hansenii* cell biomass and polyol production without any detoxification treatment, except pH adjustment to 5.5. Hydrolysate concentration led to higher polyol productivities, and supplementation with casamino acids favored xylitol production, pointing out a possible direction for further studies in polyol production optimization. *D. hansenii* is a particularly interesting yeast for that purpose since the ratio between both polyols can be modulated by simple manipulation of culture conditions.

Acknowledgments

We wish to thank Carlos Barata for technical support in the autohydrolysis work. We are also grateful to the Commission of the European Communities for financial support of this work (project FAIR-CT98-3811).

References

1. Beldman, G., Hennekam, J., and Voragen, A. G. J. (1987), *Biotechnol. Bioeng.* **30,** 668–671.
2. Carvalheiro, F., Esteves, M. P., Parajó, J. C., Pereira, H., and Gírio, F. M. (2004), *Bioresour. Technol.* **91(1),** 93–100.
3. Faulds, C. B., Sancho, A. I., and Bartolomé, B. (2002), *Appl. Microbiol. Biotechnol.* **60,** 489–493.
4. Santos, M., Jiménez, J. J., Bartolomé, B., Gómez-Cordovés, C., and del Nozal, M. J. (2003), *Food Chem.* **80,** 17–21.
5. Roberto, I. C., Felipe, M. G. A., Lacis, L. S., Silva, S. S., and Manchilha, I. M. (1991), *Bioresour. Technol.* **36,** 271–275.
6. Roberto, I. C., Felipe, M. G. A., Manchilha, I. M., Vitolo, M., Sato, S., and Silva, S. S. (1995), *Bioresour. Technol.* **51,** 255–257.
7. McMillan, J. D. (1994), in *Enzymatic Conversion of Biomass For Fuels Production*, Himmel, M. E., Baker, J. O., and Overend, R. P., eds., ACS Symposium Series No. 566, American Chemical Society, Washington, DC, pp.411–437.
8. Saha, B. C. and Bothast, R. J. (1996), *Appl. Microbiol. Biotechnol.* **45,** 299–306.
9. Ballesteros, I., Oliva, J. M., Negro, M. J., Manzanares, P., and Ballesteros, M. (2002), *Process Biochem.* **38,** 187–192.

10. Curreli, N., Agelli, M., Pisu, B., Rescigno, A., Sanjust, E., and Rinaldi, A. (2002), *Process Biochem.* **37,** 937–941.
11. Tengborg, C., Galbe, M., and Zacchi, G. (2001), *Biotechnol. Prog.* **17,** 110–117.
12. Grohmann, K., Torget, R., and Himmel, M. (1985), *Biotechnol. Bioeng. Symp.* **15,** 59–80.
13. Heitz, M., Capekmenard, E., Koeberle, P. G., Gagne, J., Chornet, E., Overend, R. P., Taylor, J. D., and Yu, E. (1991), *Bioresour. Technol.* **35,** 23–32.
14. Garrote, G., Domínguez, H., and Parajó, J. C. (1999), *J. Chem. Technol. Biotechnol.* **74,** 1101–1109.
15. Shevchenko, S. M., Chang, K., Robinson, J., and Saddler, J. N. (2000), *Bioresour. Technol.* **72,** 207–211.
16. Garrote, G., Domínguez, H., and Parajó, J. C. (2001), *Bioresour. Technol.* **79,** 155–164.
17. Vázquez, M. J., Alonso, J. L., Domínguez, H., and Parajó, J. C. (2001), *World J. Microbiol. Biotechnol.* **17,** 817–822.
18. Walch, E., Zemann, A., Schinner, F., Bonn, G., and Bobleter, O. (1992), *Bioresour. Technol.* **39,** 173–177.
19. Puls, J. and Poutanen, K. (1989), in *Enzyme Systems for Lignocellulosic Degradation*, Coughlan, M. P., ed., Elsevier Applied Science, London, UK, pp. 151–165.
20. da Costa, M. S., and Nobre, M. F. (1989), in *Microbiology of Extreme Environments and Its Potencial for Biotechnology*, da Costa, M. S., Duarte, J. C. and Williams, R. A. D., eds., Elsevier Applied Science, London, UK, pp. 310–327.
21. Domínguez, J. M. (1998), *Biotechnol. Lett.* **20,** 53–56.
22. Gírio, F. M., Amaro, C., Azinheira, H., Pelica, F., and Amaral-Collaço, M. T. (2000), *Bioresour. Technol.* **71/3,** 245–251.
23. Nobre, M. F. and Da Costa, M. S. (1985), *Can. J. Microbiol.* **31,** 467–471.
24. Parajó, J. C., Domínguez, H., and Domínguez, J. M. (1998), *Bioresour. Technol.* **65,** 203–212.
25. Roseiro, J. C., Peito, M. A., Gírio, F. M., and Amaral-Collaço, M. T. (1991), *Arch. Microbiol.* **156,** 484–490.
26. Amaral-Collaço, M. T., Gírio, F. M., and Peito, M. A. (1989), in *Enzyme Systems for Lignocellulosic Degradation*, Coughlan, M. P., ed., Elsevier Applied Science, London, UK, pp. 221–230.
27. Miller, G. L. (1959), *Anal. Chem.* **31,** 426–428.
28. Graham, H. D. (1992), *J. Agric. Food Chem.* **40,** 801–805.
29. Browning, B. L. (1967), in *Methods of Wood Chemistry*, vol. 2, Sarkeanen, K. V. and Ludwig, C. H., eds., John Wiley & Sons, New York, NY, pp. 795–798.
30. Chum, H. L., Johnson, D. K., Black, S. K., and Overend, R. P. (1990), *Appl. Biochem. Biotechnol.* **24/25,** 1–14.
31. Kabel, M. A., Carvalheiro, F., Garrote, G., Avgerinos, E., Koukios, E., Parajó, J. C., Gírio, F. M., Schols, H. A., and Voragen, A. G. J. (2002), *Carbohydr. Polym.* **50,** 47–56.
32. Hespell, R. B., O'Bryan, P. J., Moniruzzaman, M., and Bothast, R. J. (1997), *Appl. Biochem. Biotechnol.* **62,** 87–97.
33. Overend, R. P. and Chornet, E. (1987), *Phil. Trans. R. Soc. Lond.* **A321,** 523–536.
34. Nguyen, Q. A., Tucker, M. P., Keller, F. A., and Eddy, F. P. (2000), *Appl. Biochem. Biotechnol.* **84/86,** 561–576.
35. Tengborg, C., Stenberg, K., Galbe, M., Zacchi, G., Larsson, S., Palmqvist, E., and Hahn-Hägerdal, B. (1998), *Appl. Biochem. Biotechnol.* **70/72,** 3–15.
36. Rivas, B., Domínguez, J. M., Domínguez, H., and Parajó, J. C. (2002), *Enzyme Microb. Technol.* **31,** 431–438.
37. Roberto, I. C., Mancilha, I. M., Souza, C. A., Felipe, M. G. A., Sato, S., and Castro, H. F. (1994), *Biotechnol. Lett.* **16,** 1211–1216.
38. Domínguez, J. M., Gong, C. S., and Tsao, G. T. (1996), *Appl. Biochem. Biotechnol.* **57/58,** 49–56.
39. Garrote, G., Domínguez, H., and Parajó, J. C. (2001), *Appl. Biochem. Biotechnol.* **95,** 195–207.
40. Parajó, J. C., Domínguez, H., and Domínguez, J. M. (1998), *Bioresour. Technol.* **65,** 191–201.

41. Parajó, J. C., Domínguez, H., and Domínguez, J. M. (1998), *Bioresour. Technol.* **66,** 25–40.
42. Tavares, J. M., Duarte, L. C., Amaral-Collaço, M. T., and Gírio, F. M. (2000), *Enzyme Microb. Technol.* **26,** 743–747.
43. Jeppsson, H., Yu, S., and Hahn-Hägerdal, B. (1996), *Appl. Environ. Microbiol.* **62,** 1705–1709.
44. Jeppsson, H., Alexander, N. J., and Hahn-Hägerdal, B. (1995), *Appl. Environ. Microbiol.* **61,** 2596–2600.
45. Groleau, D., Chevalier, P., and Yuen, T. L. S. T. (1995), *Biotechnol. Lett.* **17,** 315–320.
46. Jovall, P. A., Tunblad-Johansson, I., and Adler, L. (1990), *Arch. Microbiol.* **154,** 209–214.

0273-2289/04/115/1059–1072/$25.00

Optimization of Brewery's Spent Grain Dilute-Acid Hydrolysis for the Production of Pentose-Rich Culture Media

Florbela Carvalheiro, Luís C. Duarte, Raquel Medeiros, and Francisco M. Gírio*

INETI, Departamento de Biotecnologia,
Estrada do Paço do Lumiar 22, 1649-038 Lisboa, Portugal,
E-mail: francisco.girio@ineti.pt

Abstract

Dilute-acid hydrolysis of brewery's spent grain to obtain a pentose-rich fermentable hydrolysate was investigated. The influence of operational conditions on polysaccharide hydrolysis was assessed by the combined severity parameter (*CS*) in the range of 1.39–3.06. When the *CS* increased, the pentose sugars concentration increased to a maximum at a *CS* of 1.94, whereas the maximum glucose concentration was obtained for a *CS* of 2.65. The concentrations of furfural, hydroxymethylfurfural (HMF), as well as formic and levulinic acids and total phenolic compounds increased with severity. Optimum hydrolysis conditions were found at a *CS* of 1.94 with >95% of feedstock pentose sugars recovered in the monomeric form, together with a low content of furfural, HMF, acetic and formic acids, and total phenolic compounds. This hydrolysate containing glucose, xylose, and arabinose (ratio 10:67:32) was further supplemented with inorganic salts and vitamins and readily fermented by the yeast *Debaryomyces hansenii* CCMI 941 without any previous detoxification stage. The yeast was able to consume all sugars, furfural, HMF, and acetic acid with high biomass yield, 0.68 C-mol/C-mol, and productivity, 0.92 g/(L·h). Detoxification with activated charcoal resulted in a similar biomass yield and a slight increase in the volumetric productivity (11%).

Index Entries: Brewery's spent grain; dilute-acid hydrolysis; pentose-rich media; *Debaryomyces hansenii*.

Introduction

Lignocellulosic agroindustrial byproducts are renewable, widespread, and generally an inexpensive source of biomass. Brewery's spent grain (BSG) is a disposal residue generated throughout the year in large amounts, for

*Author to whom all correspondence and reprint requests should be addressed.

which new uses are needed, owing to its low value and negative environmental impact. Like other hemicellulose-rich agroindustrial residues, it may be used for the production of added-value products such as functional oligosaccharides by selective hydrolysis *(1,2)*, and fuel or chemicals by fermentation processes *(3–6)*. In the latter case, complete polysaccharide hydrolysis is required to ensure an efficient fermentation process. During hydrolysis several potential inhibitory compounds are cogenerated, resulting in a decrease in yield and productivity. To overcome this well-documented effect, several physicochemical detoxification treatments have been reported, such as overliming, sulfitation, extraction with organic solvents, activated charcoal adsorption, ion-exchange resins, and evaporation or biologic treatments using peroxidase and laccase enzymes from fungi *(5,7)*, which are the main reason for the increase in the overall bioprocessing cost.

Thus, it is important to look for hydrolytic processes to overcome the need for detoxification. Mild processes using very dilute sulfuric acid, water, or steam alone have been mainly used as a pretreatment in the biomass-to-ethanol process *(8–11)*. Although these processes allow a high solubilization of hemicellulose to be obtained *(11–13)*, the high quantity of sugars in the oligomeric form *(10,11,14)* or the reduced sugar recoveries *(15)* are drawbacks that limit the use of these processes for producing hydrolysates for yeast fermentation, at least without subsequent post-hydrolysis *(16–18)*.

Dilute-acid hydrolysis is therefore the main choice for the hydrolysis of hemicellulose to monosaccharides once it is a fast and efficient method *(19)*. However, a careful optimization of operational conditions used for hydrolysis is important to ensure high monosaccharide recovery and minimize coformation of microbial inhibitors.

In the present work, we studied the hydrolysis of BSG using the combined severity concept *(20)*, which combines the effects of time, temperature, and acid concentration into a single parameter (combined severity factor [*CS*]), with the aim of establishing the operational conditions leading to the maximum yield of pentoses. The inhibitory byproducts recovered in the hydrolysates, such as acetic acid, furfural, hydroxymethylfurfural (HMF), formic acid, levulinic acid, and total phenolics, were also evaluated. The pentose-rich hydrolysate obtained was further used as culture medium for the pentose-assimilating and xylitol-overproducing yeast *Debaryomyces hansenii*. Hydrolysate toxicity was assessed by comparing the yeast growth kinetic parameters on detoxified vs nondetoxified dilute acid hydrolysates.

Materials and Methods

Preparation of Feedstock

BSG, kindly supplied by Sociedade Central de Cervejas (Vialonga, Portugal), was pretreated in an autoclave (liquid-to-solid ratio of 8 [w/w]) at 100°C for 1 h in order to remove the residual starch. The solid was fil-

tered, washed, and dried at 50°C until reaching a moisture content <10% (w/w). The feedstock material was screened (>0.5 mm retained) and stored in polyamide-polyethylene vacuum-sealed bags prior to use. On average, the pretreated BSG contained 19.6% glucan, 19.8% xylan, 9.4% arabinan, 1.4% acetyl groups, 22.8% Klason lignin, 23.5% protein, and 1.0% ash.

Dilute-Acid Hydrolysis

The feedstock was mixed with 3% (w/w) sulfuric acid solution in 500-mL closed universal flasks with a liquid-to-solid ratio of 8 (w/w). The moisture content of the samples was included as water in the material balances. The mixtures were allowed to stand for 10 min at room temperature in order to equilibrate the acid concentrations between the bulk phase and biomass. Hydrolysis was performed in an autoclave at 130°C for preestablished isothermal periods ranging from 2 to 240 min. The flasks were placed inside the autoclave at 100°C, and the heating time to reach 130°C was recorded. After the reaction time had elapsed, the autoclave was rapidly cooled down and the hydrolysate and solid phase were recovered by filtration (Whatman no. 1 filter paper). All experiments were done at least in duplicate.

The solid phase was washed with water, dried at 40°C, and the yield and composition (xylan, arabinan, glucan, Klason lignin) were determined.

The severity of the treatments was measured using the *CS (20)*, which relates the effect of acid catalysts with severity factor R_0 (Eq. 1) *(21)* into a single parameter (Eq. 2):

$$R_0 = \int_0^t \exp\left(\frac{T-100}{14.75}\right) \cdot dt \tag{1}$$

$$CS = \text{Log } R_0 - \text{pH} \tag{2}$$

in which t is time (min) and T is the temperature (°C). The heating periods from 100 to 130°C were considered for R_0 calculations. The pH was calculated from the amount of sulfuric acid added *(22,23)*.

Detoxification of Dilute-Acid Hydrolysate

For CS 1.94, several treatments were performed as described above in order to obtain enough volume of hydrolysates for fermentation experiments. Thereafter the hydrolysates were mixed, stored at 4°C and several detoxification methods, including activated charcoal and anion-exchange resin treatments, were applied. Nondetoxified hydrolysate was adjusted to pH 5.5 by adding $Ca(OH)_2$. After 1 h the precipitate was removed by centrifuging (Avanti J-25i; Beckman Coulter, Fullerton, CA) at 7500*g* for 25 min.

The detoxification treatments were done as follows.

Activated Charcoal Treatment

Granular activated charcoal about 2.5 mm from Merck (Darmstadt, Germany) was washed with water and equilibrated with HCl (0.4 *M*),

washed again with water and dried at room temperature. The charcoal was mixed with the pH 5.5 hydrolysates (10% [w/v]) and stirred for 1 h at room temperature. The detoxified hydrolysate was recovered by filtration (Whatman no. 1 filter paper). Thereafter, the pH was adjusted to 5.5 with $Ca(OH)_2$ or H_2SO_4 and, if needed, centrifuged at 7500*g* for 25 min.

Anion-Exchange Resin Treatment

Weak anion-exchange resins (Dowex Marathon WBA, 25–50 mesh) obtained from Aldrich (Milwaukee, WI) were equilibrated with 0.1 *M* NaOH and then washed with water and filtered until a neutral effluent was obtained. The hydrolysate was treated with resins in a batch process at room temperature. The amount of resins added to the hydrolysate was sufficient to obtain pH 5.5. Thereafter, the resin beads were removed by filtration (Whatman no. 1 filter paper).

Microorganism and Growth Conditions

D. hansenii CCMI 941 was used in all experiments. Stock cultures were maintained at 4°C on YM-xylose agar slants containing 20 g/L of D-xylose, 3 g/L of yeast extract, 3 g/L of malt extract, 5 g/L of peptone, and 20 g/L of agar.

Prior to fermentation, the hydrolysates (obtained at CS 1.94) were sterilized using 0.22-µm Gelman membrane filters (Ann Arbor, MI). pH-adjusted and detoxified hydrolysates were supplemented with salts, vitamins, nitrogen, phosphate, and magnesium sources. The nutrients were added in concentrated stock solutions to final concentrations as described before *(24)*, except citric acid, which was replaced with EDTA (final concentration of 0.19 g/L). In the nonsupplemented medium, the supplements were replaced with sterile water.

D. hansenii YM-xylose slants incubated at 30°C for 24 h were used to inoculate 1-L baffled Erlenmeyer flasks containing 80 mL of pH-adjusted (to 5.5) and nonsupplemented hydrolysate. Inocula cultures were grown in an Unitron orbital incubator (Infors, Bottmingen, Switzerland) at 150 rpm and 30°C for 16 h. Ten milliliters of inoculum culture was used to seed 1-L baffled Erlenmeyer flasks containing 80 mL of nondetoxified or detoxified hydrolysates, both nonsupplemented and supplemented with nutrients. Cultivations were run for 24 h at 30°C and 150 rpm. All experiments were carried out at least in duplicate.

Analytical Methods

Feedstock material and processed solids were analyzed for glucan, xylan, arabinan, and acetyl groups by quantitative acid hydrolysis according to standard methods *(25)*. The acid-insoluble residue was considered as Klason lignin, after correction for the acid-insoluble ash (determined by igniting the contents at 575°C for 5 h).

Protein content in the feedstock was estimated by the Kjeldahl method *(26)* using the $N \times 6.25$ conversion factor. Moisture content of the samples was determined by oven drying at 105°C to constant weight.

Glucose, xylose, arabinose, acetic acid, formic acid, levulinic acid, glycerol, ethanol, HMF, and furfural were analyzed by high-performance liquid chromatography (HPLC) (Waters, Milford, MA) using an Aminex HPX-87H (Bio-Rad, Hercules, CA) column operating at 50°C in combination with a cation H^+-guard column (Bio-Rad). The mobile phase was 5 m*M* H_2SO_4, and the flow rate was 0.4 mL/min. Detection was performed using an RI detector (Waters 2410) except in the case of furfural and HMF, in which an ultraviolet detector (Waters 486) set at 280 nm was used.

In fermentation samples, owing to the partial overlap of arabinose, xylitol, and arabitol, in the column Aminex HPX-87H, those components were also analyzed using a Sugar-Pak I column (Waters) operating at 90°C in a Merck-Hitachi HPLC system (Merck) equipped with an RI detector (L-7490; Merck). The mobile phase was 50 mg/L of calcium EDTA at a flow rate of 0.5 mL/min.

The total soluble phenolics were determined by a modification of the Prussian blue method *(27)* using tannic acid as standard. Cell mass was determined by optical density measurements at 600 nm using an LKB spectrophotometer (Biochrom II, Cambridge, UK) and gravimetrically at the beginning and end of fermentations as follows: Five-milliliter samples were vacuum filtered through 0.45-µm dried filters (Gelman), washed with 10 mL of ultrapure water, and dried overnight at 100°C to constant weight.

The elemental composition (C, H, N) of the cell mass was measured in a Leco CHN-2000 analyzer (St. Joseph, MI), while the oxygen content was obtained by the difference after correction for ash. Total organic carbon (TOC) of fermentation medium at the beginning and end of fermentations was analyzed with a TOC analyzer (Shimadzu 5050A; Kyoto, Japan) by the combustion technique with nondispersive infrared detection.

Results and Discussion

Dilute-Acid Hydrolysis of BSG

The effects of the operational conditions in the hydrolysates and solid composition were compared using *CS* in the range of 1.39–3.06. Sulfuric acid concentration and reaction temperature were kept constant for all runs. The severity was varied by setting the isothermal period from 2 to 240 min.

Figure 1 shows the variation in monosaccharide yield obtained after hydrolysis as a function of *CS*. Xylose and arabinose yield increased to a maximum at *CS* 1.94 and 2.04, respectively. Because only a slightly higher arabinose yield was obtained for *CS* 2.04 compared with *CS* 1.94, it was considered that maximum recovery of pentoses was obtained at CS 1.94. The highest pentose yields were 18.9 g/100 g for xylose and 9.0 g/100 g for arabinose. At these conditions, 95% of the feedstock xylan was recovered as xylose and 96% of the feedstock arabinan as arabinose. Further increases in *CS* resulted in lower recoveries of pentoses owing to their degradation. Note that a large part of the feedstock hemicellulose was released to the medium for the lowest severity assayed. At the highest severity, xylose and

arabinose recoveries were only 59 and 69% of the original feedstocks xylan and arabinan, respectively.

Glucose concentrations increased with the severity up to *CS* 2.65. A further increase in *CS* led to a slight decrease in glucose concentration. The highest glucose concentration obtained corresponds to a yield of 4.7 g/100 g.

The high pentose yields obtained in the current study are favorable when compared to those previously reported for dilute-acid hydrolysis in batch processes *(28–31)*. However, the hemicellulosic sugar yield reported in the literature is often expressed as xylose equivalents, which is difficult to compare to monosaccharide recovery. The highest monosaccharide recovery was obtained with low *CS* values, which is in agreement with previous findings for sulfuric acid–catalyzed steam explosion, in which also better hemicellulosic sugar recoveries were obtained at relatively low severities *(28,32)* of <2.2 *(22)*.

Since we aim to use the BSG acid hydrolysate for yeast growth, special attention was paid to the compounds that can have a potential inhibitory effect on fermentation. These are generated both from the hydrolysis of lignocellulosic components, such as acetic acid and phenolic compounds, and by degradation reactions, such as furfural, HMF, formic acid, and levulinic acid. The concentrations of all measured inhibitory byproducts increased with severity, with the exception of acetic acid, which reached a maximum at *CS* 2.04 (Fig. 2), where 100% of the acetyl groups present in the feedstock were recovered as free acetic acid in the hydrolysate. For *CS* >2.04, acetic acid concentration remained quite stable. The maximum yields of furfural and HMF were 2.3 and 0.26 g/100 g, respectively. However, in the conditions leading to the highest recovery of pentoses (*CS* 1.94), the concentrations of both furan derivatives were quite low: 0.35 g/100 g for furfural and 0.02 g/100 g for HMF, which corresponds to 1.6% of feedstock xylan and 0.12% of feedstock glucan, respectively.

Levulinic acid was detected only for *CS* values >1.94, and the maximum yield obtained was 0.37 g/100 g for the severest conditions. The maximum yields of formic acid and total soluble phenolics found were 0.45 and 1.43 g/100 g. However, at *CS* 1.94 (maximum recovery of pentoses), those yields were much lower: 0.19 g/100 g for formic acid and 0.75 g/100 g for total phenolics.

The low yields of all inhibitory byproducts obtained here for BSG dilute-acid hydrolysates compare favorably with those of other agroindustrial residues for which higher inhibitory byproducts recoveries were obtained *(33)*, even when lower sulfuric acid concentrations were used *(34)*.

Note that near the maximal recovery of pentoses, inhibitor concentrations were quite stable, except for furfural, whose concentration increased steadily with *CS*, which is an advantage since it allows a broader range in operating conditions.

Since dilute-acid hydrolysis mainly solubilizes the hemicellulose components, the changes in solid yield (a measure of dry weight loss) are useful for monitoring the progress of the treatment. Table 1 shows the yield and

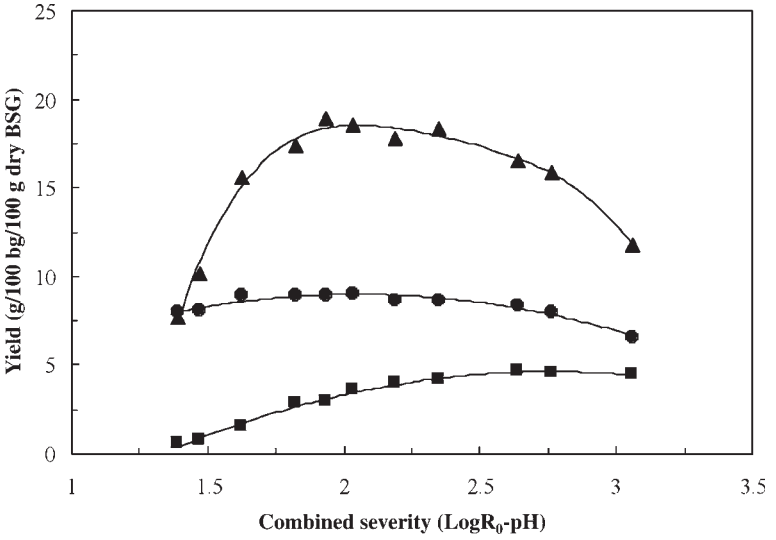

Fig. 1. Yield of monosaccharides after dilute-acid hydrolysis of BSG as a function of *CS*. (▲), Xylose; (●), arabinose; (■), glucose. The lines only show trends.

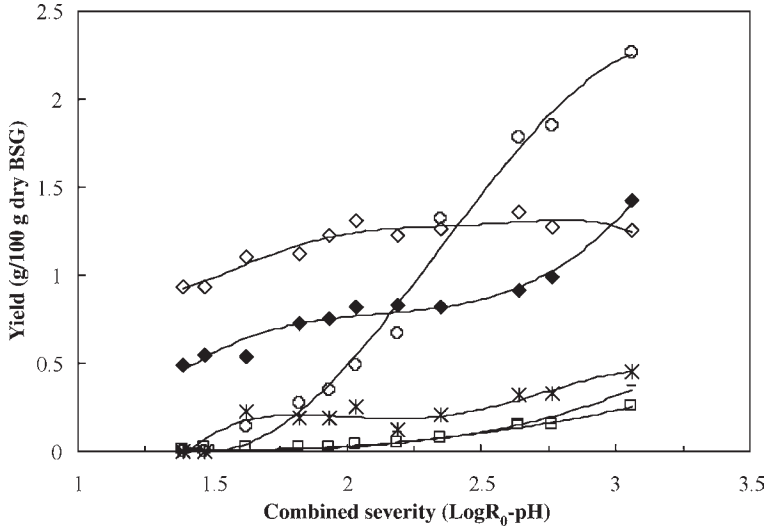

Fig. 2. Yield of inhibitory byproducts after dilute-acid hydrolysis of BSG as a function of *CS*. (◇), Acetic acid; (○), furfural; (□), HMF; (∗), formic acid; (—), levulinic acid; (◆), total phenolic compounds. The lines only show trends.

composition of the processed solids as a function of hydrolysis severity. The amount of solubilized xylan increased with *CS* reaching 100% for the severest operating conditions assayed, *CS* 3.06. Despite being solubilized slightly faster than xylan at low severities, traces of arabinan (0.8%) were still found in the solid at *CS* 3.06.

Table 1
Effect of *CS* Parameter on Solid Yield and Polymeric Composition of Processed Solids Obtained After Dilute-Acid Hydrolysis of BSG

	CS (Log R_0 – pH)[a]										
	1.39 (2)	1.48 (3.5)	1.63 (5)	1.83 (10)	1.94 (15)	2.04 (20)	2.19 (30)	2.36 (45)	2.65 (90)	2.77 (120)	3.06 (240)
Solid yield (%)[b]	70.2	69.3	64.4	61.4	60.7	59.2	56.2	50.2	48.2	49.3	46.8
Xylan (%)[c]	9.4	8.1	6.7	5.9	6.2	5.7	5.0	4.2	1.6	1.6	0.0
Arabinan (%)[c]	3.1	3.1	2.0	1.9	2.0	2.1	1.7	1.3	1.1	1.2	0.8
Glucan (%)[c]	25.5	26.5	29.2	28.8	32.9	31.1	33.3	36.5	38.4	38.4	37.1
Klason lignin (%)[c]	37.5	38.8	37.0	38.8	39.1	40.5	41.9	43.9	47.2	46.7	53.8

[a] Values in parentheses indicate the duration of the isothermal period (min).
[b] (g/100 g feedstock).
[c] (g/100 g processed solids).

Table 2
Composition of BSG Dilute-Acid Hydrolysate Obtained at *CS* Factor of 1.94

Compound	Concentration (g/L)
Xylose	26.7
Arabinose	12.8
Glucose	4.0
Acetic acid	1.5
Formic acid	0.23
Furfural	0.29
HMF	0.02
Total phenolics	0.91

Glucan was not significantly affected by the hydrolytic treatment, and the maximal glucan solubilization was only 11% for the severest conditions. Torget et al. *(11)* also reported a low solubilization of glucan when *CS* is relatively low.

Under the present conditions of acid hydrolysis, no significant removal of lignin was expected to occur. However, for all the experiments performed, the percentage of Klason lignin (measured as the acid-insoluble residue) increased with the increase in *CS* and its recovery ranged from 97 to 118%. The greater than 100% yield could be owing to the condensation of lignin with sugar and/or sugar degradation products such as furfural *(15,35,36)* to give insoluble reaction products, causing an increase in apparent Klason lignin yield. Moreover, since the Klason lignin procedure allows direct estimation of all components that are insoluble in both concentrated and hot dilute sulfuric acid, the Klason lignin value could also include part of the protein *(29)*.

From the reported data (Figs. 1 and 2, Table 1) the optimum condition to obtain a pentose-rich hydrolysate from dilute-acid hydrolysis of BSG at 130°C was 15 min (*CS* 1.94). Such hydrolysate contains about 43.5 g/L of glucose, xylose, and arabinose (ratio of 10:67:32), together with a low content of furfural, HMF, acetic acid, formic acid, and total phenolic compounds (Table 2). This condition was chosen for subsequent production of hydrolysates for fermentation.

Detoxification and Fermentation of BSG Acid Hydrolysates

The inhibitory effect caused by the acid hydrolysis byproducts depends mainly on the chosen microorganism and on the overall composition of the hydrolysate. Moreover, interaction effects involving several inhibitors are most likely implicated *(37)*.

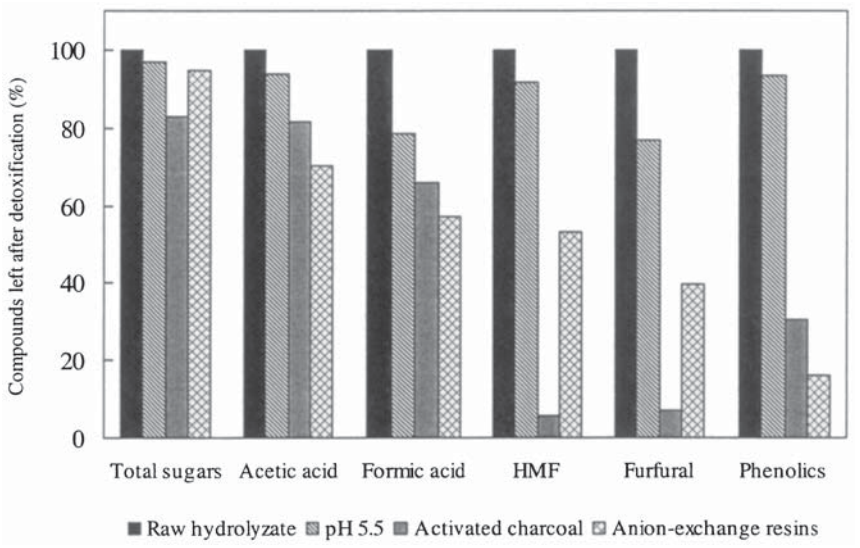

Fig. 3. Influence of detoxification methods on composition of BSG hydrolysates. Values are expressed as the percentage of the concentration of compounds left after treatment relative to the raw hydrolysate.

To evaluate the degree of microbial growth inhibition caused by the hydrolysate used, *Debaryomyces hansenii* was grown in detoxified hydrolysates and in a hydrolysate only subjected to a pH correction, both nonsupplemented and supplemented. As detoxification methods, anion-exchange resins and activated charcoal treatments were chosen because both enable the reduction of most of the fermentation-inhibiting compounds *(7,38,39)*.

Figure 3 shows the effect of pH correction to 5.5 and of the detoxification treatments assayed (anion-exchange resins and activated charcoal) on hydrolysate composition relative to the raw hydrolysate. Activated charcoal treatment was the most effective method for removal of furan derivatives, whereas the anion-exchange resin treatment enabled the highest removal of phenolics, which is in agreement with previous studies *(40–42)*. Resins were also slightly better than activated charcoal for the removal of aliphatic acids. Contrary to what happened with activated charcoal treatment, no significant loss of sugars was obtained with anion exchangers, which is in agreement with our previous findings *(43)*. Both detoxification treatments removed more inhibitors than the simple pH adjustment, which had only a minor effect on inhibitor removal.

Figure 4 shows the growth profiles of *D. hansenii* in nondetoxified (pH 5.5) and detoxified hydrolysates, both nonsupplemented and supplemented with several nutrients. Similar specific growth rate and biomass yield were observed for all nonsupplemented hydrolysates regardless of the utilization of a detoxification step (Table 3). A similar pattern occurred

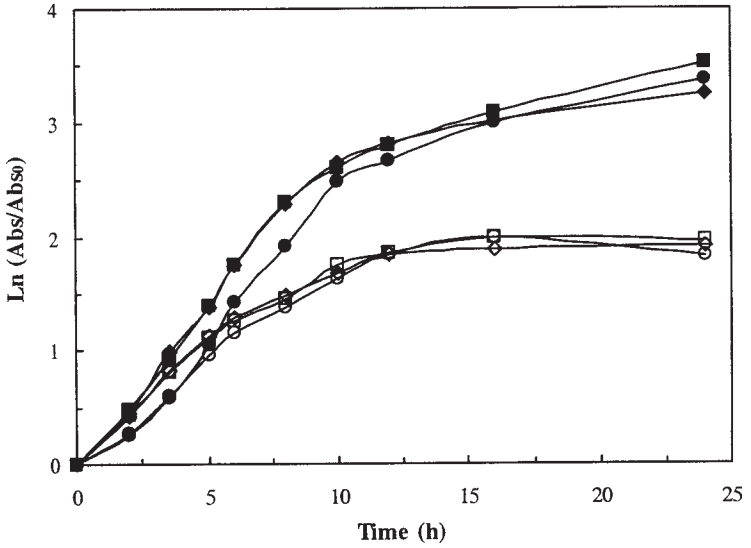

Fig. 4. Effect of detoxification and/or supplementation of BSG dilute-acid hydrolysates on growth profile of *D. hansenii* CCMI 941. Nonsupplemented: (○), pH 5.5 hydrolysate; (◇), activated charcoal detoxified hydrolysate; (□), anion-exchange resins detoxified hydrolysate; supplemented: (●), pH 5.5 hydrolysate; (◆), activated charcoal detoxified hydrolysate; (■), anion-exchange resins detoxified hydrolysate.

Table 3
Kinetic and Stoichiometric Parameters of *D. hansenii* CCMI 941 Batch Growth in Nonsupplemented and Supplemented Nondetoxified, Activated Charcoal Detoxified and Anion-Exchange Resins Detoxified BSG Dilute-Acid Hydrolysates[a]

	Nondetoxified		Activated charcoal		Anion-exchange resins	
	NS	S	NS	S	NS	S
μ (h^{-1})	0.22	0.29	0.22	0.31	0.21	0.31
Q_S (g/[L·h])	0.28	1.24	0.30	1.32	0.38	1.31
Q_X (g/[L·h])	0.14	0.92	0.15	1.04	0.14	0.66
Y_{XS} (g/g)	0.50	0.74	0.49	0.79	0.37	0.50
Xyl cons. (%)	10	90	15	99	17	93
Ara cons. (%)	1	44	2	100	3	49
Ac cons. (%)	90	100	96	100	91	100
Form cons. (%)	0	14	15	100	5	100

[a]μ, specific growth rate; Q_S, overall volumetric sugar consumption rate; Q_X, volumetric biomass production rate; Y_{XS}, biomass yield from total monosaccharides; Xyl cons., Ara cons., Ac cons., and Form cons. are the percentages of consumption of xylose, arabinose, acetic acid, and formic acid, respectively. All parameters, except μ, were calculated after 24 h. NS, nonsupplemented; S, supplemented.

for supplemented hydrolysates. Therefore, the use of a previous detoxification step before yeast growth seems to be unnecessary. Conversely, hydrolysate supplementation by itself greatly improved the specific growth rate and biomass yield. Supplementing the hydrolysates increased the specific growth rate and biomass yield by 1.3–1.5 and 4.7–6.9 fold, respectively.

The final biomass yield increased for the supplemented hydrolysates and was higher than expected, even when taking into account the consumption of compounds other than monosaccharides, such as furfural, HMF, acetic acid, and formic acid. High biomass yields (0.53–0.58 g/g) have already been ascribed to *D. hansenii* in xylose-limited chemostat cultures *(24)*. Since the concentration of total soluble phenolics remained unchanged at the end of fermentation, and the sugar oligomers present in the hydrolysate (about 1.3 g/L) were not consumed (data not shown), our results suggest that other compounds in the hydrolysate, which are not quantified by the current analytical methods used, contributed to the high biomass yields. To elucidate this statement, TOC in the experiments with the nondetoxified and supplemented media was measured at the beginning and end of fermentation. Based on these results, and on the carbon content of biomass as determined by elemental analysis (46.5%), the new, adjusted biomass yield obtained, 0.68 C-mol/C-mol, was close to the values reported in the literature for this yeast, 0.67 C-mol/C-mol *(24)*.

The overall volumetric sugar consumption rate showed the same trend as specific growth rate, since much lower values were obtained in nonsupplemented hydrolysates (Table 3). The highest final biomass concentration was obtained in the supplemented hydrolysates treated with activated charcoal, corresponding to a volumetric productivity of 1.04 g/(L·h). Only a slight decrease in biomass productivity (11%) was observed in the nondetoxified hydrolysates. Furthermore, xylose was almost completely exhausted when the hydrolysate was supplemented, whereas a slight tendency to increase xylose consumption rate was noticed when the hydrolysate was detoxified but not supplemented. In the nonsupplemented hydrolysates, arabinose consumption was almost negligible whereas in supplemented hydrolysates it increased from 44 to 100%.

For all conditions tested, *D. hansenii* was able to consume all furfural and HMF, regardless of the type of hydrolysate (data not shown). Acetic acid consumption ranged from 90 to 100%. Formic acid was only fully consumed for detoxified and supplemented hydrolysates. The complete consumption of acetic acid in hydrolysates has already been reported by other investigators *(44,45)*.

Besides biomass and CO_2, no significant amount of extracellular products was detected. Xylitol and arabitol were only accumulated in small amounts, with a maximum of 2.0 and 3.8 g/L, respectively. Other metabolic products usually associated with the pentose metabolism of *D. hansenii*, such as ethanol and glycerol *(46,47)*, were only found in trace amounts, less than 0.5 and 0.3 g/L, respectively.

Conclusion

Dilute-acid hydrolysis of BSG enables a high solubilization of hemicellulose at a low severity (*CS* 1.94) with almost total pentose recovery (close to 96%). This pentose-rich hydrolysate was found to exhibit a low level of fermentation-inhibiting compounds, namely aliphatic acids, furan derivatives, and total phenolics. In fact, the use of nondetoxified hydrolysate as culture medium for *D. hansenii* gave similar growth performances compared with detoxified hydrolysates. This strongly suggests that a detoxification procedure is not required for BSG dilute-acid hydrolysate. This is a significant advantage over other hemicellulosic hydrolysates and can lead to lower operative costs at the industrial level.

Acknowledgments

We wish to thank M. Helena Nogueira for conducting the total organic carbon analysis. We also gratefully acknowledge Dr. J. Seabra e Barros for help with the elemental analysis.

References

1. Gírio, F. M., Carvalheiro, F., Esteves, M. P., Amaral-Collaço, M. T., Parajó, J. C., Domínguez, H., et al. (2003) Portuguese patent no. 102563.
2. Kabel, M. A., Schols, H. A., and Voragen, A. G. J. (2002), *Carbohydr. Polym.* **50,** 191–200.
3. Roberto, I. C., Felipe, M. G. A., Lacis, L. S., Silva, S. S., and Mancilha, I. M. (1991), *Bioresour. Technol.* **36,** 271–275.
4. Roberto, I. C., Felipe, M. G. A., Mancilha, I. M., Vitolo, M., Sato, S., and Silva, S. S. (1995), *Bioresour. Technol.* **51,** 255–257.
5. McMillan, J. D. (1994), in *Enzymatic Conversion of Biomass for Fuels Production*, Himmel, M. E., Baker, J. O., and Overend, R. P., eds., ACS Symposium Series 566, American Chemical Society, Washington, DC, pp. 411–437.
6. Saha, B. C. and Bothast, R. J. (1996), *Appl. Microbiol. Biotechnol.* **45,** 299–306.
7. Palmqvist, E. and Hahn-Hägerdal, B. (2000), *Bioresour. Technol.* **74,** 17–24.
8. van Walsum, G. P., Allen, S. G., Spencer, M. J., Laser, M. S., Antal, M. J., and Lynd, L. R. (1996), *Appl. Biochem. Biotechnol.* **57/58,** 157–170.
9. Allen, S. G., Schulman, D., Lichwa, J., Antal, M. J., Jennings, E., and Elander, R. (2001), *Ind. Eng. Chem. Res.* **40,** 2352–2361.
10. Allen, S. G., Schulman, D., Lichwa, J., Antal, M. J., Laser, M., and Lynd, L. R. (2001), *Ind. Eng. Chem. Res.* **40,** 2934–2941.
11. Torget, R., Hatzis, C., Hayward, T. K., Hsu, T. A., and Philippidis, G. P. (1996), *Appl. Biochem. Biotechnol.* **57/58,** 85–101.
12. Allen, S. G., Kam, L. C., Zemann, A. J., and Antal, M. J. (1996), *Ind. Eng. Chem. Res.* **35,** 2709–2715.
13. Mok, W. S. L. and Antal, M. J. (1992), *Ind. Eng. Chem. Res.* **31,** 1157–1161.
14. Saska, M. and Ozer, E. (1995), *Biotechnol. Bioeng.* **45,** 517–523.
15. Heitz, M., Capek-Ménard, E., Koeberle, P. G., Gagne, J., Chornet, E., Overend, R. P., Taylor, J. D., and Yu, E. (1991), *Bioresour. Technol.* **35,** 23–32.
16. Garrote, G., Domínguez, H., and Parajó, J. C. (2001), *Appl. Biochem. Biotechnol.* **95,** 195–207.
17. Duarte, L. C., Carvalheiro, F., Lopes, S., Marques, S., Parajó, J. C., and Gírio, F. M. (2004), *Appl. Biochem. Biotechnol.* **113–116,** 1139–1056.
18. Vázquez, M. J., Alonso, J. L., Domínguez, H., and Parajó, J. C. (2001), *World J. Microbiol. Biotechnol.* **17,** 817–822.

19. Domínguez, J. M., Cao, N. J., Gong, C. S., and Tsao, G. T. (1997), *Bioresour. Technol.* **61,** 85–90.
20. Chum, H. L., Johnson, D. K., Black, S. K., and Overend, R. P. (1990), *Appl. Biochem. Biotechnol.* **24/25,** 1–14.
21. Overend, R. P. and Chornet, E. (1987), *Phil. Trans. R. Soc. Lond.* **A321,** 523–536.
22. Nguyen, Q. A., Tucker, M. P., Keller, F. A., and Eddy, F. P. (2000), *Appl. Biochem. Biotechnol.* **84–86,** 561–576.
23. Tengborg, C., Stenberg, K., Galbe, M., Zacchi, G., Larsson, S., Palmqvist, E., and Hahn-Hägerdal, B. (1998), *Appl. Biochem. Biotechnol.* **70–72,** 3–15.
24. Nobre, A., Duarte, L. C., Roseiro, J. C., and Gírio, F. M. (2002), *Appl. Microbiol. Biotechnol.* **59,** 509–516.
25. Browning, B. L. (1967), in *Methods in Wood Chemistry*, Sarkanen, K. V. and Ludwig, C.H., eds., John Wiley & Sons, New York, NY.
26. AOAC. (1975), *AOAC Official Methods of Analysis*, AOAC International, Washington, DC.
27. Graham, H. D. (1992), *J. Agric. Food Chem.* **40,** 801–805.
28. Carrasco, J. E., Sáiz, M. C., Navarro, A., Soriano, P., Sáez, F., and Martínez, J. M. (1994), *Appl. Biochem. Biotechnol.* **45/46,** 23–34.
29. Torget, R., Werdene, P., Himmel, M., and Grohmann, K. (1990), *Appl. Biochem. Biotechnol.* **24/25,** 115–126.
30. Torget, R., Walter, P., Himmel, M., and Grohmann, K. (1991), *Appl. Biochem. Biotechnol.* **28/29,** 75–86.
31. Grohmann, K., Torget, R., and Himmel, M. (1985), *Biotechnol. Bioeng. Symp.* **15,** 59–80.
32. Taherzadeh, M. J., Eklund, R., Gustafsson, L., Niklasson, C., and Liden, G. (1997), *Ind. Eng. Chem. Res.* **36,** 4659–4665.
33. Martín, C., Galbe, M., Nilvebrant, N. O., and Jönsson, L. J. (2002), *Appl. Biochem. Biotechnol.* **98–100,** 699–716.
34. Neureiter, M., Danner, H., Thomasser, C., Saidi, B., and Braun, R. (2002), *Appl. Biochem. Biotechnol.* **98–100,** 49–58.
35. Aoyama, M., Seki, K., and Saito, N. (1995), *Holzforschung* **49,** 193–196.
36. Montané, D., Salvadó, J., Farriol, X., Jollez, P., and Chornet, E. (1994), *Wood Sci. Technol.* **28,** 387–402.
37. Palmqvist, E., Grage, H., Meinander, N. Q., and Hahn-Hägerdal, B. (1999), *Biotechnol. Bioeng.* **63,** 46–55.
38. Domínguez, J. M., Gong, C. S., and Tsao, G. T. (1996), *Appl. Biochem. Biotechnol.* **57/58,** 49–56.
39. Parajó, J. C., Domínguez, H., and Domínguez, J. M. (1996), *Bioresour. Technol.* **57,** 179–185.
40. Miyafuji, H., Danner, H., Neureiter, M., Thomasser, C., Bvochora, J., Szolar, O., and Braun, R. (2003), *Enzyme Microb. Technol.* **32,** 396–400.
41. Larsson, S., Reimann, A., Nilvebrant, N. O., and Jönsson, L. J. (1999), *Appl. Biochem. Biotechnol.* **77–79,** 91–103.
42. Nilvebrant, N. O., Reimann, A., Larsson, S., and Jönsson, L. J. (2001), *Appl. Biochem. Biotechnol.* **91–93,** 35–49.
43. Carvalheiro, F., Duarte, L. C., Lopes, S., Parajó, J. C., Pereira, H., and Gírio, F. M. (2003), submitted.
44. Roberto, I. C., Mancilha, I. M., Souza, C. A., Felipe, M. G. A., Sato, S., and Castro, H. F. (1994), *Biotechnol. Lett.* **16,** 1211–1216.
45. Pessoa, A., Mancilha, I. M., and Sato, S. (1996), *J. Biotechnol.* **51,** 83–88.
46. Roseiro, J. C., Peito, M. A., Gírio, F. M., and Amaral-Collaço, M. T. (1991), *Arch. Microbiol.* **156,** 484–490.
47. Tavares, J. M., Duarte, L. C., Amaral-Collaço, M. T., and Gírio, F. M. (2000), *Enzyme Microbiol. Technol.* **26,** 743–747.

0273-2289/04/115/1073–1086/$25.00

Comparison of Microbial Inhibition and Enzymatic Hydrolysis Rates of Liquid and Solid Fractions Produced from Pretreatment of Biomass with Carbonic Acid and Liquid Hot Water

Damon M. Yourchisin[1] and G. Peter Van Walsum[*,2]

[1]US Army Maneuver Support Center (MANSCEN), Directorate of Combat Developments, Chemical Division (Concepts), 320 Manscen Loop, Suite 141, Fort Leonard Wood, MO 65473-8929; and [2]Department of Environmental Studies and Glasscock Energy Research Center, Baylor University, PO Box 97266, Waco, TX, 76798-7266, E-mail: GPeter_van_Walsum@Baylor.edu

Abstract

This research quantified the enzymatic digestibility of the solid component and the microbial inhibition of the liquid component of pretreated aspen wood and corn stover hydrolysates. Products of liquid hot water and carbonic acid pretreatment were compared. Pretreatment temperatures tested ranged from 180 to 220°C, and reaction times were varied between 4 and 64 min. Both microbial inhibition rates and enzymatic hydrolysis rates showed no difference between pretreatments containing carbonic acid and those not containing no carbonic acid. Microbial inhibition increased as the reaction severity increased, but only above a midpoint severity parameter of 200^0C for 16 min. Both the rates and yields of enzymatic hydrolysis displayed an increase from the lowest tested reaction severity to the highest tested reaction severity.

Index Entries: Carbonic acid; pretreatment; hydrolysis; corn stover; aspen wood.

Introduction

Conversion of lignocellulosic material to ethanol requires hydrolysis of carbohydrate polymers to their constituent sugars. Enzymatic hydrolysis is a common approach to hydrolysis and offers the benefits of mild

*Author to whom all correspondence and reprint requests should be addressed.

reaction conditions and selective hydrolysis. To achieve useful rates of enzymatic hydrolysis, the lignocellulose must first be pretreated to reduce the recalcitrance of the substrate to hydrolysis. Pretreatment accomplishes many alterations of the biomass. Depending on the technology chosen, these effects typically include, to varying degrees; hydrolysis of the hemicellulose, solubilization of lignin and carbohydrate oligomers, and increased accessibility of the cellulose to cellulase enzymes *(1)*. Several pretreatment methods have been explored to varying degrees. The most commonly reported technologies include dilute-acid pretreatment, in which H_2SO_4 used in low concentrations (on the order of 1%) and at temperatures usually less than 200°C *(2–6)*, and steam explosion, which exposes the substrate to steam at elevated temperature and then explosive decompression to physically break apart the plant fibers *(7–9)*. Often, steam explosion is coupled with acid catalysis by impregnating the substrate with sulfur dioxide prior to steam treatment *(10–12)*. Other techniques include ammonia fiber explosion, which breaks down the lignin using ammonia and explosive decompression *(13–15)*, treatment with organic solvents *(16,17)*; and treatment with liquid hot water *(18–21)*. Some methods that have been examined less thoroughly include treatment with supercritical fluids *(22)* and carbonic acid *(23–25)*.

Steam explosion and dilute-acid pretreatment have undergone research and development for many years. Much of this research has been devoted to fuel production from biomass. Dilute-acid pretreatment offers good performance in terms of recovering hemicellulose sugars but suffers from its use of H_2SO_4. H_2SO_4 is highly corrosive and its neutralization results in copious production of solid wastes *(25)*. In situations in which landfill costs are high, disposing of the gypsum precipitate can be prohibitively expensive. The calcium sulfate resulting from neutralization also has problematic solubility characteristics in that it becomes less soluble at higher temperatures, such as those encountered in a reboiler *(25)*. Compared to dilute-acid pretreatment, steam explosion makes no use of H_2SO_4 and is less corrosive both to equipment and as a recovery product. However, steam explosion yields lower amounts of hemicellulose sugars. Studies suggest an 80% recovery of five-carbon sugars with dilute-acid pretreatment compared with 65% with steam explosion *(3,26)*. SO_2-catalyzed steam explosion achieves higher recovery of hemicellulose sugars, but this again introduces a reliance on sulfur acids and the requisite neutralization.

One process that may offer benefits of acid catalysis without the drawbacks of H_2SO_4 is the use of carbonic acid. The pH of carbonic acid is determined by the partial pressure of CO_2 in contact with water, and thus it can be neutralized by releasing the reactor pressure. Carbonic acid is relatively mild and hence does not offer the same hydrolytic capability of H_2SO_4. However, van Walsum *(25)* has demonstrated that at temperatures on the order of 200°C, carbonic acid does exhibit a catalytic effect on the hydrolysis of xylan. Van Walsum *(25)* observed an enhanced release of xylose and low-degree-of-polymerization xylan oligomers compared to pretreatment

using hot water alone. Puri and Mamers *(24)* compared steam explosion of biomass with and without CO_2 pressurization and reported enhanced enzymatic degradation with the carbonic acid-enhanced steam explosion. Contrary to these results, McWilliams and van Walsum *(23)* reported that compared to liquid hot water, carbonic acid offered no improvement in xylose yields for pretreatment of aspen wood. They proposed that this may have been owing to the high level of endogenous acid produced by the highly acetylated substrate and suggested that a less acidic substrate may show benefits from carbonic acid. This idea was confirmed by Shi and van Walsum *(27)*, who observed enhanced hydrolysis activity for carbonic acid pretreatment of corn stover, noting both increased xylose and furan yields when liquid hot water pretreatment was pressurized with CO_2.

The present study investigated the inhibition of *Saccharomyces cerevisiae* by the liquid hydrolysate and the kinetics of enzymatic hydrolysis of the solid components produced by the pretreatment of aspen wood and corn stover by liquid hot water and hot carbonic acid. Inhibition of yeast was determined by measuring the rate of glucose consumption by yeast growing in hydrolysates produced at various reaction severities. The enzymatic hydrolysis rates of pretreated solids was determined by measuring rates of sugar accumulation of enzyme-digested pretreated solids.

Materials and Methods

Experimental Design

A series of laboratory experiments compared products from reactions of biomass with water with those of biomass with water and carbonic acid. The three parameters that determined reaction severity were the reaction temperature, reaction duration, and carbonic acid concentration (psi of CO_2) *(25)*. The parameters tested were 180, 190, 200, and 220°C; 0 (at room temperature) and 800 psi (at room temperature); and 4, 8, 16, 32, and 64 min. Using the severity function as defined by Overend and Chornet *(28)*,

$$t \times \exp\left(\frac{\mathrm{T} - 100}{14.75}\right) \tag{1}$$

in which t is the time, min and T is the temperature in °C, and the severity conditions for these parameters varied from $R_o = 1813.8$ to $R_o = 109{,}242.9$. Broad categories of low, medium, and high severities were determined using the Log of the severity function (Log R_o). These broad categories were defined as having the following Log R_o: low (3.3–4.1), medium (4.2–4.5), and high (4.6–5.0). Table 1 shows some results representing the basic layout of the experimental design and inhibition/hydrolysis results in these severity ranges.

Preparation of Feedstock

Aspen wood chips were kindly supplied by the USDA Forest Products Laboratory (Madison, WI) and corn stover by the National Renewable

Table 1
Selected High-, Medium-, and Low-Severity Yeast Inhibition/
Enzymatic Hydrolysis Experiments on Aspen Wood and Corn Stover

	Severity parameters[a]					Inhibition[b]			Enzyme hydrolysis[c]			Final pH range
	T	*t*	*P*	R_o	Log R_o	No. of rep	No. of exp	%inh	No. of rep	No. of exp	T+24 (g/L yld)	
Aspen Wood												
	180	8	0	1813.78	3.3	2	1	4	6	4	0.58	5.69–4.97
	180	8	800	1813.78	3.3	2	1	0	2	1	0.55	5.69–4.97
	200	16	0	14,076.33	4.2	6	1	26	6	4	1.31	5.69–4.97
	200	16	800	14,076.33	4.2	6	1	22	6	4	1.71	5.69–4.97
	220	32	0	109,242.90	5.0	4	1	92	1	1	1.97	5.69–4.97
	220	32	800	109,242.90	5.0	4	1	84	1	1	2.09	5.69–4.97
Corn stover												
	180	8	0	1813.78	3.3	2	1	0	2	1	0.65	5.87–4.97
	180	8	800	1813.78	3.3	2	1	0	2	1	0.09	5.87–4.97
	200	16	0	14,076.33	4.2	4	2	4	4	2	1.06	5.87–4.97
	200	16	800	14,076.33	4.2	4	2	6	4	2	1.06	5.87–4.97
	220	32	0	109,242.90	5.0	2	1	18	2	1	1.5	5.87–4.97
	220	32	800	109,242.90	5.0	2	1	24	2	1	1.56	5.87–4.97

[a] R_o, severity = $t \times \exp[(T - 100)/14.75]$.
[b] No. of rep, number of replicates of the sample analysis; no. of exp, number of experiments in which the samples were generated; % inh, percent of microbial inhibition.
[c] T + 24 g/L yld, g/L of glucose produced at T + 24 of the experiment.

Energy Laboratory (Golden, CO). CO_2 was standard laboratory grade, and water was of standard laboratory deionized quality. Feedstock was first ground in a manual grinder to reduce particle size and then further ground in a domestic coffee grinder. Particles were sifted to give a uniform particle size of 0.6–1 mm. Moisture content of the ground biomass was determined by oven drying at 100°C for several days.

Pretreatment

Two 1.25-g samples of uniform particle-size feedstock were each weighed out and placed in separate 150-mL, 316 stainless steel reactors, along with 100 mL of deionized water each. The reactors were filled and emptied by removing a swage connection on one end. One reactor was pressurized with 800 psi of CO_2 at room temperature, and the other was left with air in the headspace at atmospheric pressure. For reactions using CO_2, a stainless steel tubing connection and valve with pressure gage were fitted to the reactor. Two sand baths (model SBL 2D in (Techne, Oxford UK,), with temperature controller (model TC-8D; Techne) were used for temperature control, one heated to the desired reaction temperature, and the second to 40°C above the desired reaction temperature. The higher-temperature sand bath was used for preheating the reaction vessels for 3 min to quickly attain the desired reaction temperature *(25)*. After preheating, the reactors were transferred to the reaction-temperature sand bath for the desired reaction duration. The reaction was quenched in an ice bath immediately after the reaction was complete. Previous research by McWilliams and van Walsum, *(23)* had determined that a temperature range of 180 to 220°C was optimal for xylose production from aspen wood. Reaction times ranged from 4 to 64 min.

Preparation of Hydrolysates

Solids were filtered out from the hydrolysate samples using a vacuum filter and microfilter paper. The filtrate was further clarified by centrifuging with a Fisher Marathon 21000R centrifuge and 04-976-006 rotor at 4000*g*, generating approx 3000 RCF, for 15 min at 15°C. The solids remaining on the filter paper were washed with deionized water three times (12 mL od deionized water total), with the final rinse dewatered under vacuum for 3 min prior to shutting off the vacuum. The filtered solids were placed in weighing tins and stored in a 100% humidity equilibrium chamber for 72 h. Half of each sample was analyzed for dry weight by drying in an oven at 101°C for 72 h. Dried portions of the samples were then available for quantitative saccharification, while the remaining moist sample was used for the enzymatic hydrolysis tests.

Microbial Culturing

A new batch of yeast malt agar (Y-3127; Sigma, St. Louis, MO), yeast malt broth (Y-3752; Sigma) and yeast (Fleishman's) were prepared for each

experiment according to the manufacturers directions. With each experiment, a new batch of baker's yeast was prepared according to the manufacturer's directions: two and a quarter teaspoons of yeast was added to 1/4 cup of water at 37°C with 1 teaspoon of glucose. The mixture was left to stand for 10 min. Once growth of yeast was confirmed, the mixture was plated for isolation under a laminar flow hood using fresh yeast agar plates. An isolated colony from the plate was aseptically transferred into the 10 mL of broth in the culture tube using a loop. The culture tubes were placed into the incubator at 30°C for 48 h.

Preparation of Test Vials

Twenty milliliters of the previously generated liquid hydrolysate was placed in serum vials containing from 0 to 100% hydrolysate, with the balance being deoinzed water. Dry yeast broth (21 g/L) and dextrose (10 g/L) were weighed and placed in each serum vial to serve as nutrient and energy sources. Vials were purged with N_2 for 30 s, sealed, and placed in an autoclave for 20 min at 121°C. The pH for each of these samples was also tested and was within the preferred tolerance range of yeast, varying from 4.97 for the most severe pretreatment to 5.87 for the least severe pretreatment *(29)*.

Inhibition

Batch culture experiments were performed to measure the rate of glucose consumption. Once the seed yeast had been incubated for exactly 48 h, the serum vials were each injected with 0.2 mL of freshly vortexed yeast. The moment of inoculation became time zero ($t = 0$) for the experiment. Viable cell counts taken at time zero showed the initial cell concentration to be on the order of 100,000 colony-forming units/mL. Samples were taken every 2 h over the next 12 h, except for the first 4 hours, and analyzed for glucose.

Glucose Assay

The glucose assay used was the Infinity™ Glucose Reagent Kit from Sigma. The procedure used was Procedure 17-UV provided with the kit. For each sample, 0.2 mL of liquid was removed from the serum vials and placed in a 1-mL microcentrifuge tube. The glucose assay was found to give a linear response up to 3 g/L of glucose, so samples were sufficiently diluted to put their glucose content into this range, depending on the anticipated concentration of the sample. Next, 1500 µL of glucose reagent was placed into a 2-mL cuvet for each sample. Prior to adding the sample, UV measurements of the reagent were made at 340 nm. Then, 15 µL of each sample was added to its dedicated cuvet. The cuvets were covered and incubated for 14 min (at room temperature). The absorbance was again measured at 340 nm. The difference in absorption units was then used to determine glucose content. A glucose standard of 2 g/L was run at each sampling time. A control was also used for each yeast inhibition experiment by running a sample that contained 0% hydrolysate but all the other components of the nutrient broth.

For the enzymatic hydrolysis samples, the control used contained citrate buffer, preservative, and cellulase enzymes.

Quantitative Saccharification

Quantitative saccharification was done in accordance with NREL LAP-002 *(30)*. Duplicate samples of approx 0.4 g were dispensed into separate test tubes. A standard of pure cellulose (Avicel) was analyzed in triplicate each experiment. Tubes and vials were placed on ice during manipulations to minimize reaction during untimed periods. H_2SO_4 (72%) was added to each of the tubes to create an acid-to-sample ratio of 0.01 mL/mg, after which they were placed in a reciprocal water bath set at 30°C. The tubes were immersed in the shaker bath for 2 h and stirred every 15 min with dedicated glass stirring rods. At the end of the 2 h period, each sample was diluted with deionized water into a serum vial to give a final concentration of 0.27 mL/mg of sample. Each serum vial was then capped, sealed, and autoclaved for 1 h. Once the autoclaving was complete, the serum vials were cooled and analyzed for glucose using the enzymatic glucose assay.

Enzymatic Hydrolysis Tests

A pH 5.0 citrate buffer solution was prepared with 0.5% sodium benzoate as a preservative. Taking into account the moisture and cellulose content of each pretreated sample, vials were prepared to achieve a glucose level no greater than 2 g/L (assuming 100% conversion of cellulose) in 20 mL of buffer solution. Each sample was done in duplicate. Cellulase (Iogen IG) was added at a loading of 20 cellulase units/g of solid residue. Quantitative saccharification of the residues found that most samples, prepared across various severities, had a cellulose content of approx 64%; thus, the cellulase loading translates to about 31 U/g of cellulose. β-Glucosidase (Novo 188) was added at a ratio of 5 U/U of cellulase. The addition of the enzymes defined time zero. Immediately after taking the samples at time zero, the testing vials were placed in a shaking water bath at 40°C. The serum vials were removed for testing every 2 h for up to 12 h. They were further sampled at 24 h, 48, and 120 h.

Results

Inhibition Testing

Two metrics were used to quantify inhibition: total consumed glucose and consumption rate. Figures 1–3 show average values derived from replicate samples within single experiments.

Figure 1 shows that with aspen wood as the substrate, glucose consumption by yeast was inhibited by the hydrolysate and that the inhibition increased as the severity of the pretreatment increased. However, there was no difference in the amount or rate of glucose consumed between samples that were pretreated with CO_2 and samples pretreated without CO_2.

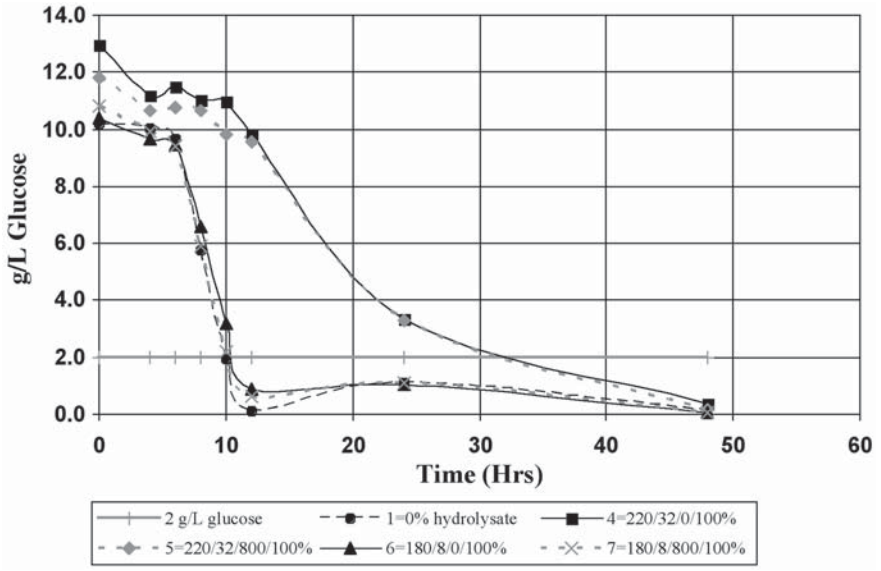

Fig. 1. Glucose consumed for samples with and without CO_2 for aspen wood.

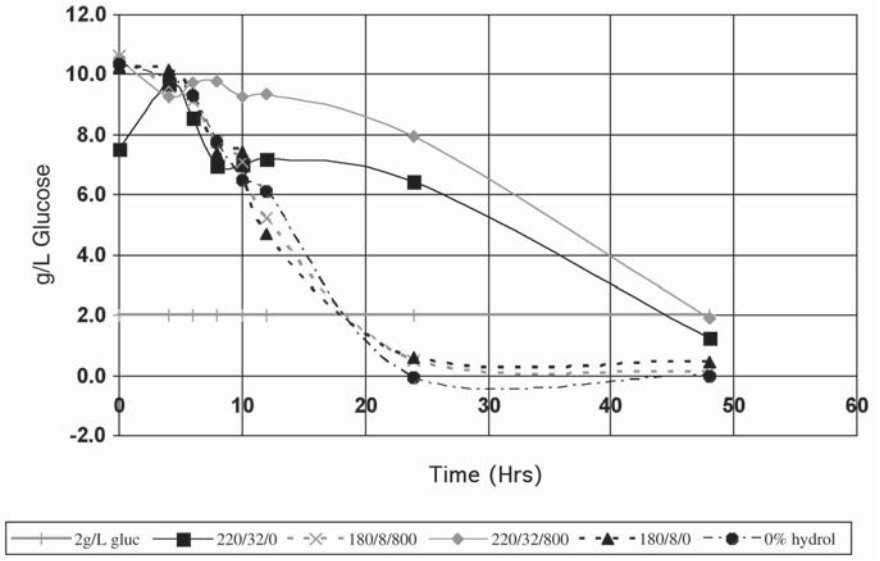

Fig. 2. Glucose consumed for samples with and without CO_2 for corn stover.

Figure 2 shows that for corn stover at the highest tested severity parameter of 220°C for 32 min, inhibition of the yeast regarding to the control was as extreme as with the aspen wood samples shown in Fig. 1. It took more than double the amount of time for the higher-severity sample yeast to consume 50% of the glucose than in all the other samples, just as with the aspen wood sample at 220°C for 32 min.

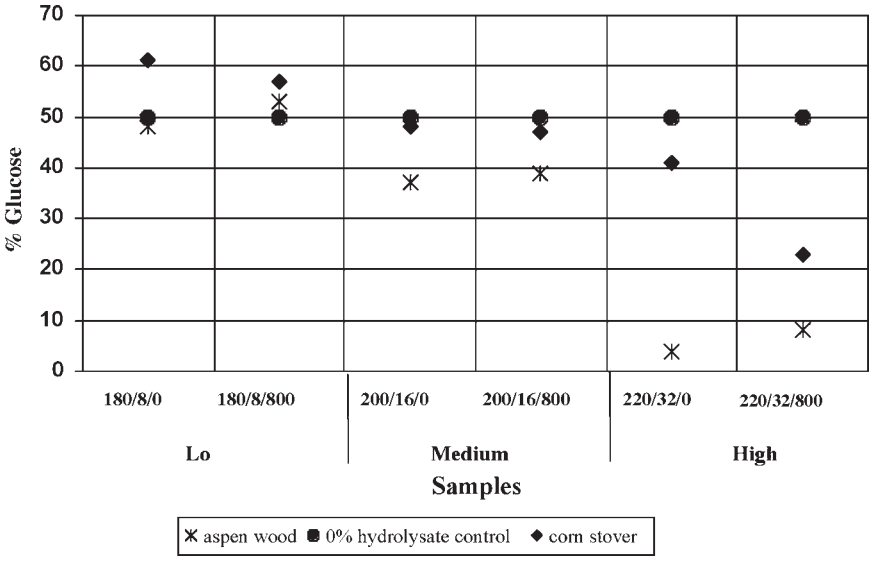

Fig. 3. Glucose consumption comparing aspen wood and corn stover for low-, medium-, and high-severity pretreatment.

At the lowest tested severity parameter of 180°C for 8 min, there was almost no inhibition when compared to the control that was run at each experiment. However, at the highest tested severity parameter of 220°C for 32 min, there was an almost 50% reduction in the rate of glucose consumption by the yeast. This division of inhibition as it correlates to severity is well defined for both the aspen wood and corn stover samples. However, between the aspen wood and corn stover samples there appeared to be a difference in inhibition rates, as a comparison of Figs. 1 and 2 shows. However, for this distinction to be conclusive, a side-by-side experiment would need to be conducted, giving a more standardized inoculum between the two experiments. Both Figs. 1 and 2 show the lowest and highest tested severity parameters. The response of mid-level severity was similar to that observed for the low level severities (data not shown).

Figure 3 shows a comparison of the glucose consumption among a low-severity (Log R_o = 3.3), medium-severity (Log R_o = 4.2), and high-severity (Log R_o = 5.0) pretreatment with and without carbonic acid. Glucose consumption for different severity hydrolysates was measured at the time when the 0% control hydrolysate had achieved 50% utilization. A trend is shown that the yeast was more inhibited as the severity of the pretreatment increased. Figure 3 also shows a difference between corn stover samples and aspen wood samples for the same pretreatments. Aspen wood was more inhibitory than corn stover for all three pretreatment conditions, and the difference between the two continued to increase as the severity of the pretreatment increased.

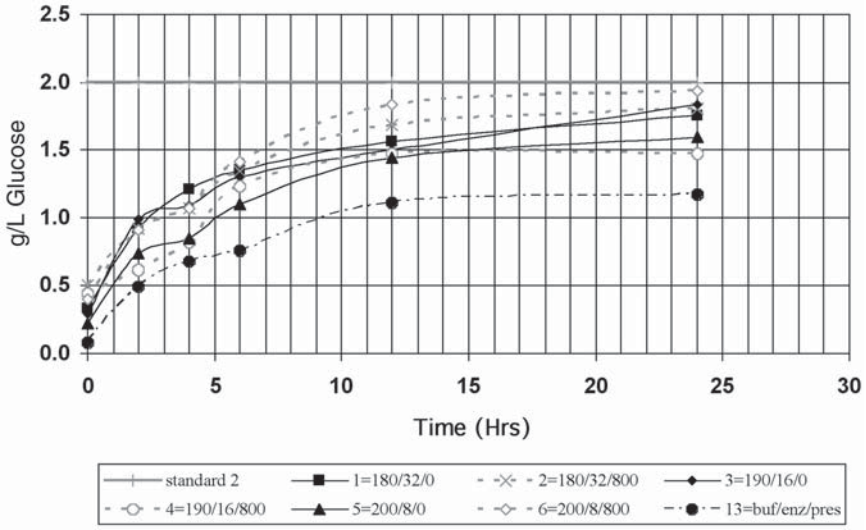

Fig. 4. Rate and yield of enzymatic hydrolysis vs reaction severity of medium-severity pretreatments only for aspen wood samples.

Enzymatic Hydrolysis Rates

Two metrics of hydrolysis efficacy were used: total recovered glucose and reaction rate.

Different combinations of time and temperature parameters that result in a low to mid range severity (Log R_o ~ 3.84) are shown in Fig. 4. The relative consistency between the experiments indicates that the severity of the different conditions is comparable and also that there appears to be no significant difference between samples pretreated with or without carbonic acid. After 24 h there was little difference in the yield, and this remained so even when the testing continued for 120 h (data not shown), the time it is thought to take for enzymes to achieve about 90% hydrolysis. Figure 5 shows that reaction severity played a major role in the rate and yield of enzymatic hydrolysis and that as the reaction severity increased, so too did the rate and final yield of the enzymatic hydrolysis throughout the range of severities. Increased severity also appeared to enhance initial glucose concentrations, which indicates that some glucose was released during pretreatment. In Fig. 6, the grams per liter of glucose produced from enzymatic hydrolysis was determined for the low, medium and high severities at t + 24. Aspen wood consistently produced more glucose than did the corn stover, and more glucose was produced with increased severity for both substrates.

Discussion

Inhibition

The midpoint pretreatment condition of 200°C for16 min could be an optimal condition for reduced microbial inhibition. For severities around

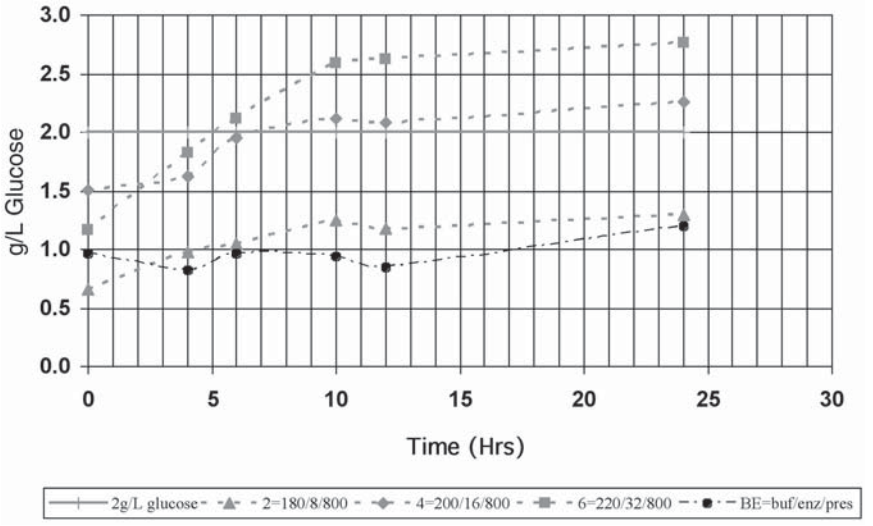

Fig. 5. Rate and yield of enzymatic hydrolysis vs reaction severity of low-, medium-, and high-severity pretreatment for corn stover samples.

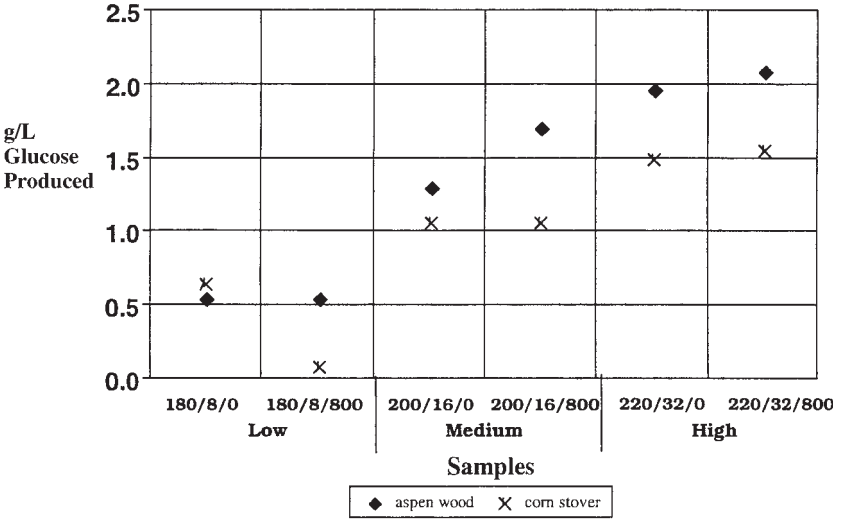

Fig. 6. Glucose produced from enzymatic hydrolysis at t = 24 h comparing aspen wood and corn stover for low-, medium-, and high-severity pretreatment.

the midpoint and below, there was no improvement in the reduction of microbial inhibition. This is promising because McWilliams and van Walsum *(23,31)* found that the midpoint severity of 200°C for 32 min to produce the optimal yield of xylose monomers during pretreatment: lower severities produced less; higher severities led to degradation.

It is possible that a toxicity threshold is not achieved at lower severities, reducing the inhibition from these conditions. The corn stover samples were consistently less inhibitory than the aspen wood samples. This is likely owing to the fact that fewer acids are inherent in the corn stover biomass than in the aspen wood biomass. For example, it was found that the pH of the corn stover hydrolysates was higher than the pH of aspen hydrolysates. Further testing is warranted to investigate the difference in the inhibition of the substrates and also to determine whether scatter is to blame for the appearance of a difference between pretreatments with and without carbonic acid when assessing the percent inhibition from Fig. 3. Pretreatment severity showed a marked effect on the degree of inhibition suffered by yeast cultures, but the presence or absence of carbonic acid appears to have had no influence on inhibition. Between the aspen wood and corn stover samples, there appeared to be a difference in inhibition rates.

Hydrolysis Rates

It is clear that the midpoint severity of 200°C for 32 min that produces the maximum xylose recovery as found by McWilliams and van Walsum *(23,31)* from the pretreatment step is not the optimal severity for enzymatic hydrolysis. The rates and yields of enzymatic hydrolysis continued to increase as the reaction severity of the pretreatment increased. It is possible that the enzymatic hydrolysis rates and yields would continue to increase past the maximum severity that was tested, 220°C for 32 min. A possible explanation for this result is that the more severe reaction conditions are continuing to break down the hemicellulose and solubilize the lignin, allowing the enzymes more and easier access to the cellulose without destroying the cellulose. Thus, optimization of this pretreatment appears to involve a compromise among maximized xylose yield, minimized inhibition, and maximal rates of enzymatic hydrolysis. The differences between the substrates and their glucose yield at t +24 is very interesting. A possible cause of this phenomenon is that the lower pH of the aspen hydrolysate enhances the pretreatment effectiveness as time continues. These acids may assist in the degradation of the hemicellulose and lignin, allowing more exposure of the cellulose for the enzymes to hydrolyze. Further investigation of the differences shown between the substrates is warranted.

Conclusion

Both microbial inhibition rates and enzymatic hydrolysis rates showed no differences between pretreatments containing carbonic acid and those not containing carbonic acid. Additionally, when the microbial inhibition and enzymatic hydrolysis rates were tested at varying reaction severities and between different substrates, this remained true.

When microbial inhibition rates were examined with increasing reaction severity, the inhibition increased as the reaction severity increased, but

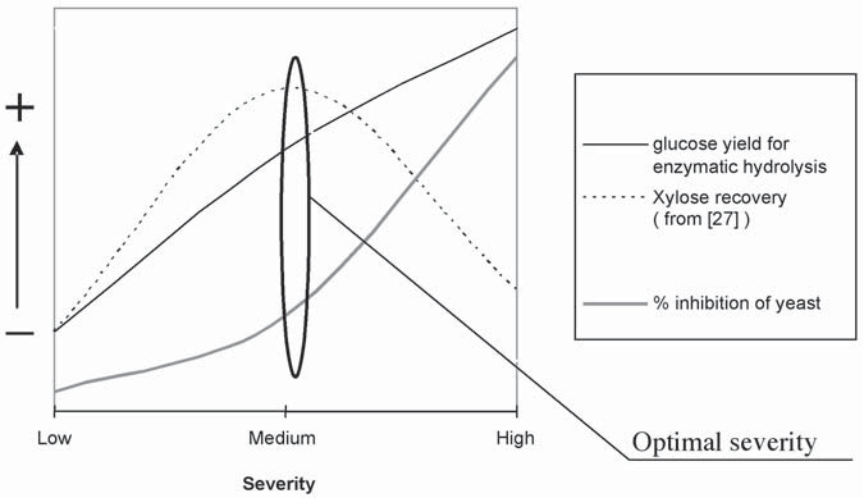

Fig. 7. Optimization of severity parameters.

only above the midpoint severity parameter. Below the midpoint severity parameter, there was little to no inhibition to the yeast. When enzymatic hydrolysis rates and yields were examined with increasing reaction severity, both the rates and yields displayed an increase from the lowest tested reaction severity to the highest tested reaction.

It is possible to theorize that between the two tests performed, there is an optimal severity that will maximize the glucose yield and rate from enzymatic hydrolysis while minimizing the inhibition to the yeast. This can further be optimized when using the severity parameters that produce the greatest amount of xylose monomer as detailed in previous research by McWilliams and van Walsum *(23)*. Figure 7 provides a possible view of the optimization of the severity parameters. While the inhibition of yeast is still minimal in the midseverity range, the amount of xylose is at its highest point. Finally, the glucose produced from enzymatic hydrolysis is at a median point.

Acknowledgments

Support for this study was provided by the Department of the Army, the US Army Chemical Corps, Advanced Civil Schooling program; the Department of Environmental Studies and Glasscock Energy Research Center at Baylor University; and the US Department of Energy contract no. DE-FC36-01GO11070, A000.

References

1. McMillan, J. D., (1994), in *ACS Symposium Series No. 566*, Himmel, M. E., Baker, J. O., and Overend, R. P., eds., American Chemical Society, Washington, DC, pp. 292–324.

2. Bouchard, J., Overend, R. P., and Chornet, E., (1992), *J. Wood Chem. Technol*. **12(3),** 335–354.
3. Quang, A. N., Tucker, M. P., Keller, F. A., and Eddy, F. P., (2000), *Appl. Biochem. Biotechnol*. **84–86,** 561–576.
4. Torget, R., Hatzis, C., Hayward, T. K., Hsu, T., and Phillipidis, G.P., (1996), *Appl. Biochem. Biootechnol*. **57/58,** 85–101.
5. Torget, R. W., Kim, J. S., and Lee, Y. Y., (2000), *Ind. Eng. Chem. Res*. **39,** 2817–2825.
6. Wooley, R., Ruth, M., Glassner, D., and Sheehan, J., (1999), *Biotechnol. Prog*. **15,** 794–803.
7. Boussaid, A. L., Esteghlalian, A. R., Gregg, D. J., Lee, K. H., and Saddler, J. N., (2000), *Appl. Biochem. Biotechnol*. **84–86,** 693–705.
8. Brownell, H. H. and Saddler, J. N., (1987), *Biotechnol. Bioeng*. **29,** 228–235.
9. Montane, D., Farriol, X., Salvado, J., Jollez, P., and Chornet, E., (1998), *J. Wood Chem. Technol.* **18(2),** 171–191.
10. Clark, T. A., Mackie, K. L., Dare, P. H., and McDonald, A. G., (1989), *J. Wood Chem. Technol*. **9(2),** 135–166.
11. Mackie, K. L., Brownell, H.H., West, K. L., and Saddler, J. N., (1985), *J. Wood Chem. Technol*. **5(3),** 405–425.
12. Schell, D., Nguyen, Q., Tucker, M., and Boynton, B., (1998), *Appl. Biochem. Biotechnol*. **70–72,** 17–24.
13. Dale, B. E., Weaver, J., and Byers, F. M., (1999), *Appl. Biochem. Biotechnol*. **77–79,** 35–45.
14. Holtzapple, M. T., Lundeen, J. E., Sturgis, R., Lewis, J. E., and Dale, B. E., (1992), *Appl. Biochem. Biotechnol*. **34/35,** 5–21.
15. Wang, L., Dale, B. E., Yurttas, L., and Goldwasser, I., (1998), *Appl. Biochem. Biotechnol*. **70–72,** 51–66.
16. Avgerinos, G. C. and Wang, D. I. C.,(1983), *Biotechnol. Bioeng*. **15,** 67–83.
17. Bouchard, J., Lacelle, S., Chornet, E., Vidal, P. F., and Overend, R. P., (1993), *Holzforschung* **47(4),** 291–296.
18. Allen, S. G., Kam L. C., Zemann, A. J., and Antal Jr., M. J. (1996), *Ind. Eng. Chem. Res*. **35(8),** 2709–2715.
19. Allen, S. G., Schulman, D., Lichwa, J., Antal, M. J., Laser, M., and Lynd, L.R., (2001), *Ind. Eng. Chem. Res*. **40,** 2934–2941.
20. Mok, W. S. L. and Antal Jr., M. J. (1992), *Ind. Eng. Chem. Res*. **31(4),** 1157–1161.
21. van Walsum, G. P., Allen, S. G., Spencer, M. J., Laser, M. S., Antal, M. J., and Lynd, L.R., (1996), *Appl. Biochem. Biotechnol*. **54/55,** 157–170.
22. Sasaki, M., Fang, Z., Fukushima, Y., Adschiri, T., and Arai, K., (2000), *Ind. Eng. Chem. Res*. **39,** 2882–2890.
23. McWilliams, R. C. and van Walsum, G. P., (2002), *Appl. Biochem. Biotechnol*. **98–100,** 109–134.
24. Puri, V. P. and Mamers, H., (1983), *Biotechnol. Bioeng*. *25,* 3149–3161.
25. van Walsum, G. P. (2001), *Appl. Biochem. Bioetechnol*. *91–93,* 317–329.
26. Heitz, M., E. Capek-Menard, P. G. Koeberle, J. Gagne, E. Chornet, E., Overend, R. P., and Taylor, E. Y. (1991), *Bioresour. Technol*. **35,** 23–32.
27. Shi, H. and van Walsum, G. P. (2004) *Bioresourc. Technol.*, in press.
28. Overend, R. P. and Chornet, E., (1987), *Philos. Trans. R. Soc. Lond*. *A321:* 523–536.
29. Palmqvist, E. and Hähn-Hagerdal, B. (2000), *Bioresour. Technol*. **74,** 17–24.
30. Ruiz, R. and Ehrman, T. (1996), *Determination of Carbohydrates in Biomass by High Performance Liquid Chromatography*, Laboratory Analytical Procedure No. LAP-002, National Renewable Energy Laboratory, Golden, CO.
31. McWilliams, R. (2002), MS thesis, Department of Environmental Studies, Baylor University, Waco, TX.

0273-2289/04/115/1087–1102/$25.00

Modeling of Carbonic Acid Pretreatment Process Using ASPEN-Plus®

KEMANTHA JAYAWARDHANA AND G. PETER VAN WALSUM*

Department of Environmental Studies, Baylor University,
PO Box 97266, Waco, TX 76798-7266,
E-mail: gpeter_van_walsum@baylor.edu

Abstract

ASPEN-Plus® process modeling software is used to model carbonic acid pretreatment of biomass. ASPEN-Plus was used because of the thorough treatment of thermodynamic interactions and its status as a widely accepted process simulator. Because most of the physical property data for many of the key components used in the simulation of pretreatment processes are not available in the standard ASPEN-Plus property databases, values from an in-house database (INHSPCD) developed by the National Renewable Energy Laboratory were used. The standard non-random-two-liquid (NRTL) or renon route was used as the main property method because of the need to distill ethanol and to handle dissolved gases. The pretreatment reactor was modeled as a "black box" stoichiometric reactor owing to the unavailability of reaction kinetics. The ASPEN-Plus model was used to calculate the process equipment costs, power requirements, and heating and cooling loads. Equipment costs were derived from published modeling studies. Wall thickness calculations were used to predict construction costs for the high-pressure pretreatment reactor. Published laboratory data were used to determine a suitable severity range for the operation of the carbonic acid reactor. The results indicate that combined capital and operating costs of the carbonic acid system are slightly higher than an H_2SO_4-based system and highly sensitive to reactor pressure and solids concentration.

Index Entries: Acid pretreatment; carbonic acid; ASPEN-Plus model; alcohol fuels; biomass.

Introduction

Computer-aided design and simulation gives the process engineer the ability to evaluate more design alternatives in more detail than was

*Author to whom all correspondence and reprint requests should be addressed.

possible by hand calculations. Simulation, as used in this article, refers to the creation of a mathematical model or representation of a chemical process. ASPEN-Plus® (Aspen Technologies, Cambridge, MA) software is used to model biomass conversion processes at the Department of Environmental Studies at Baylor University. It is capable of solving steady-state material and energy balances, calculating phase equilibria, and estimating physical properties for thousands of chemical compounds. It can also estimate capital costs of equipment. Originally developed for the Department of Energy (DOE) by the Massachusetts Institute of Technology in 1987, ASPEN-Plus required the user to write an input file containing process specifications. More recent versions of ASPEN-Plus incorporate a graphical user interface, making the simulation software more user friendly.

Although ASPEN-Plus is widely used to simulate petrochemical processes, its uses for modeling biomass processes are limited owing to the limited availability of physical properties that best describe biomass components such as cellulose, xylan, and lignin. For example, Lynd et al. *(1)* used conventional methods to calculate the economic viability of a biomass-to-ethanol process. However, with the development by the National Renewable Energy Laboratory (NREL) of an ASPEN-Plus physical property database for biofuels components, modified versions of ASPEN-Plus software can now be used to model biomass processes *(2)*. Wooley et al. *(3)* used ASPEN-Plus simulation software to calculate equipment and energy costs for an entire biomass-to-ethanol process that made use of dilute-H_2SO_4 acid pretreatment.

Carbonic acid has been proposed as an alternative to dilute sulfuric acid for biomass pretreatment. Proposed advantages of carbonic acid include reduced cost of materials owing to less corrosive conditions and reduced costs associated with the neutralization of H_2SO_4 and consequent disposal of calcium sulfate *(4)*. Recent laboratory studies on carbonic acid have shown that it can enhance hydrolysis of xylan compared to liquid hot water pretreatment, but that hydrolysis falls short of the normal performance range for dilute H_2SO_4 *(4,5)*. Studies on aspen wood have shown little advantage of carbonic acid over liquid hot water pretreatment *(6,7)*, whereas a study on corn stover did show elevated hydrolysis compared to liquid hot water *(8)*. A study conducted by Puri and Mamers *(9)* reported enhanced enzymatic hydrolysis following CO_2-pressurized steam explosion. The central hypothesis of the present study is that reduced metallurgy and waste disposal costs for carbonic acid pretreatment will result in a negative incremental cost for the carbonic acid pretreatment process compared to the H_2SO_4 process. In other words, it is hypothesized that the reduced corrosivity and neutralization requirements for the carbonic acid system will result in cost savings compared to the H_2SO_4 process. Because carbonic acid pretreatment has not been investigated or optimized to the extent achieved with dilute H_2SO_4, conversion effectiveness and final ethanol yield are not factored into this comparison.

Method

Process Design and Simulation

The process flow diagram (PFD) was developed by selecting all the necessary unit operation blocks from the ASPEN-Plus model library. Once the PFD was sketched out, ASPEN-Plus software was used to build the process model. Figure 1 depicts the carbonic acid pretreatment process flowsheet generated by ASPEN-Plus. The reactor (B1) in this pretreatment process was modeled as a stoichiometric reactor (RSTOIC), since kinetic data for many of the pretreatment reactions were not available. RSTOIC models a reactor when stoichiometry and conversion are known but kinetics are unknown or unimportant. It can also perform product selectivity and heat of reaction calculations. Laboratory investigations carried out at the Department of Environmental Studies at Baylor University showed that a pressure of 2000 psi and reaction severity conditions (as defined by Overend and Chornet *[10]*) on the order of $\text{Log}(R_o) = 4.2$ would produce an effective pretreatment for aspen wood *(7)*. CO_2 compression to 2000 psi is difficult and expensive to implement in commercial scale; therefore, the process was modified to inject the CO_2 into the biomass and water stream (stream no. 4) at a lower temperature (28°C) and pressure (800 psi). The lower temperature increases the solubility of CO_2 in water and requires a pressure of only 800 psi to deliver sufficient CO_2 into the pretreatment reactor. Hence, the compression duty was lowered by a factor of 2.5. To raise the CO_2 pressure from 1 atm (14.7 psi) to 800 psi, a multistage compressor (B13) was used. Stream no. 1, which contains biomass and water, was pressurized to 800 psi using pump B7. The mixing of CO_2 into stream no. 4 (biomass and water at 800 psi) was carried out using an in-line CO_2 mixer (B8). The mixer model in ASPEN-Plus determines the combined outlet stream temperature and phase conditions by performing an adiabatic-phase equilibrium flash calculation on the composite feed streams. A heat exchanger (B11) was employed to preheat the incoming stream using the filtrate (stream no. 16) from a Pneumapress filter (B10) as heat source. Then, the preheated stream no. 5 was pressurized to 2000 psi using pump B12. Heater B9 was employed to further heat stream no. 12 to 220°C. In this manner, high pressure in the pretreatment reactor (B1) was maintained, and the carbonic acid feed was delivered in a liquid state, eliminating the need for compression of gaseous CO_2 to 2000 psi.

The product stream from the reactor (B1) was flash cooled using a flash drum (B3) to separate vapors from the liquid phase. The flash models available in ASPEN-Plus determine the thermal and phase conditions of a mixture with one or more inlet streams. A separator (B6) was employed to separate CO_2 and steam. The resulting recycle streams no. 10 and no. 9 were sent to B13 and B7, respectively. The liquid stream (no. 14) from the flash drum was sent to a Pneumapress filter (B10), where it was separated into filter cake (stream no. 13) and filtrate (stream no. 8). This separation was done to facilitate heat extraction from the product stream for heat exchanger B11.

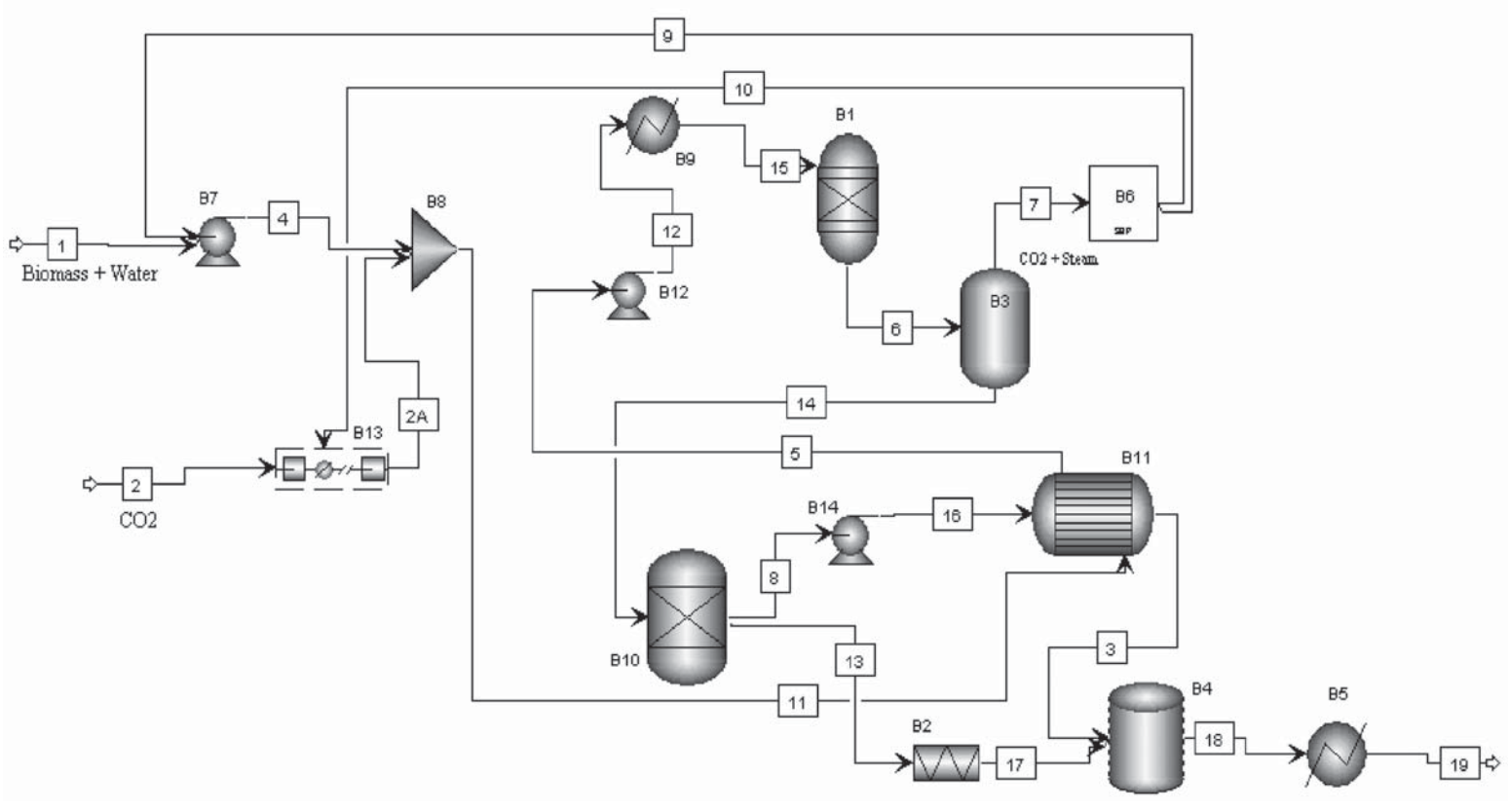

Fig. 1. ASPEN-Plus PFD of carbonic acid pretreatment process as analyzed in this study. B1, pretreatment reactor (Rstoic); B2, screw mixer; B3, blowdown tank and screw conveyor; B4, slurrying tank and tank agitator; B5, cooler; B6, reflux drum and condenser; B7, feed pump; B8, in-line CO_2 mixer; B9, heater; B10, pneumapress filter; B11, heat exchanger; B12, loading pump; B13, CO_2 compressor; B14, primary filtrate pump.

To minimize the pressure differential across the heat exchange surfaces in B11, stream no. 8 was pressurized to 800 psi using pump B14. The filter cake was sent to a mixing tank (B4) through a screw conveyor (B2). At the mixing tank B4, filtrate and cake were thoroughly mixed in order to obtain a slurry. This product slurry was cooled using a cooler (B5) before being sent on to the next stage of the biomass conversion process.

Component Data and Databases

Physical property data for many of the key components used in the simulation for the ethanol-from-lignocellulose process are not available in the standard ASPEN-Plus property databases *(11)*. Indeed, many of the properties necessary to successfully simulate this process are not available in the standard biomass literature. The physical properties required by ASPEN-Plus are calculated from fundamental properties such as liquid, vapor, and solid enthalpies and density. In general, because of the need to distill ethanol and to handle dissolved gases, the standard nonrandom two-liquid (NRTL) or renon route is used. This route, which includes the NRTL liquid activity coefficient model, Henry's law for the dissolved gases, and Redlich-Kwong-Soave equation of state for the vapor phase, is used to calculate properties for components in the liquid and vapor phases. It also uses the ideal gas at 25°C as the standard reference state, thus requiring the heat of formation at these conditions.

Inputs and Basis

After careful investigation of the NREL model, the scale for the carbonic acid model was selected to be 2000 dry metric t/d of biomass. This number represents a scale that would have an economically feasible collection distance for biomass *(3)*.

Biomass: 2000 dry t/d = 2,000,000 dry kg/d = 83,333 dry kg/h.

Moisture content at 52% dry solids = 76,923 kg of water/h.

Total feed = 160,256 kg moist biomass/h.

The composition of poplar wood was used as a model for the feedstock composition; however, as used in this simulation, the poplar is modeled as consisting of only cellulose, xylan, and lignin, with compositions of 49.47, 27.26, and 23.27%, respectively. Laboratory results for carbonic acid pretreatment are relatively scarce, so for the purpose of this comparative study, stoichiometry of pretreatment reactions was assumed to be equal to those used in the comparison model *(3)*: cellulose conversion to glucose; 6.5%; xylan conversion to xylose; 75; and lignins solubilized; 5%. Thus, economic comparisons made with this model assess different equipment and operating costs but not product yields. For the successful convergence of the carbonic acid model, the simulation required initial specification of several variables. These variables included initial estimates for stream variables and inputs for the unit operation blocks.

Results and Discussion

An ASPEN-Plus model was used to calculate the heat and energy demands of the process units. Simulation results were generated for 15 different pretreatment conditions, consisting of a full factorial design comprising three temperatures (180, 200, and 220ºC) and five pressures (800, 1000, 1200, 1600, and 2000 psi). Then, equipment and energy costs were calculated in 2001 US $. For each set of parameters, a corresponding material and energy balance sheet was generated by the ASPEN-Plus software.

Calculation of Reactor Wall Thickness

The use of carbonic acid for pretreatment results in mild acidity inside the pretreatment reactor, with pH in the range of 3.5–4.0 *(4,8)*. Owing to this only moderately corrosive environment, fabrication of pretreatment reactors could be carried out using commonly used metal alloys. In the present study, it is assumed that pretreatment reactors are fabricated using stainless steel 316 L (SS316), which has been found to stand up well in laboratory experiments on carbonic acid.

Pretreatment reactor residence time was varied from 2 to 10 min, and the corresponding reactor sizes and wall thicknesses were calculated for all the pretreatment conditions (i.e., from 800 psi, 180°C to 2000 psi, 220°C).

The thickness of the reactor walls can be calculated using Eq. 1 *(12)*:

$$t = P \times R/(S \times E - 0.6 \times P) \quad (1)$$

in which t is the reactor wall thickness (in.); R is the radius of the reactor (in.); P is the pressure of the reactor (psi); S is the maximum allowable stress (psi); and E is the joint efficiency, set to 0.85 *(12)*.

As can be seen from Eq. 1, increasing the radius will proportionately increase the required thickness of the reactor walls. To accommodate the large quantity of biomass flowing through the system, the use of a single reactor would necessitate a very large reactor, with a correspondingly large diameter. This increases the thickness of the reactor walls, making it difficult and expensive to build the reactor. The use of several smaller reactors in parallel can be a more economically feasible method, because it diminishes the wall thickness and total amount of metal needed. However, the use of multiple reactors will multiply the requirements for auxiliary equipment and process control instrumentation. By optimizing between the cost of a single large, expensive reactor and multiple parallel units, the optimum number of reactors for the pretreatment process was determined to be three. For 12-m-long reactors with 10% headspace and a pretreatment residence time of 4 min, the required reactor radius is 0.376 m. Wall thickness and cost for these reactors were calculated for different conditions of temperature and pressure and are presented in Table 1; for comparison, the conditions of the single NREL model reactor, at the pressure of saturated water at 190°C (representative of dilute H_2SO_4 pretreatment), is included.

NREL reported that the pretreatment reactor built using Hastelloy C would cost $2,505,084, which is 50% more expensive than to build with

Table 1
Reactor Wall Thickness and Cost Calculation
at Different Pretreatment Conditions (Residence Time: 4 min)

Parameter	R_D (m)	S	Wall thickness (m)	Material volume (m^3)	Original price (2000 US$)
CO2 model (3 needed)					
2000 psi, 220ºC	0.376	13,080	0.07587	2.153	4,846,878
2000 psi, 200ºC	0.376	13,342	0.07421	2.105	4,740,436
2000 psi, 180ºC	0.376	13,846	0.07120	2.020	4,548,291
1600 psi, 220ºC	0.376	13,080	0.05927	1.681	3,785,890
1600 psi, 200ºC	0.376	13,342	0.05799	1.645	3,704,670
1600 psi, 180ºC	0.376	13,846	0.05570	1.580	3,557,842
1200 psi, 220ºC	0.376	13,080	0.04342	1.232	2,773,880
1200 psi, 200ºC	0.376	13,342	0.04251	1.206	2,715,716
1200 psi, 180ºC	0.376	13,846	0.04086	1.159	2,610,421
NREL reactor (1 needed)					
179 psi, 190ºC	0.7933	13,594	0.0124	0.742	1,670,056

SS316 *(3)*. The same reactor design built of SS316 would cost only $1,670,056 (2000 US$). Reactor costs for carbonic acid pretreatment were calculated by using the reactor wall thickness to determine the volume of metal required to meet the demands of various temperature and pressure conditions. The material volume for fabrication of the reactor was calculated using Eq. 2:

$$V = 2 \times \pi \times R \times h \times t \quad (2)$$

in which V is the volume of metal in the reactor (m^3), R the radius (m), h the reactor height (m), and t is the wall thickness (m). With these data, reactor cost can be calculated for different pretreatment conditions as given in Table 1.

Calculation of Equipment Cost

The equipment requirements were determined from the ASPEN-Plus model. The quantity and size of each piece of equipment was determined on the basis of the mass flow rate through the equipment. From the thickness calculations, it was found that three reactors were optimal to accommodate a mass flow rate of 83,333 dry kg/h. It was also found that the solids concentration of the pretreated material made it necessary to use more than one Pneumapress filter.

The installation and scaling factors were taken from the NREL modeling report *(3)*. For the reactor, the installation factor was taken as 1.7, which is appropriate when SS316 is used as the material of construction *(3)*. Table 2 lists equipment costs for this scenario at 2000 psi, 220°C, and 4-min residence time. Equipment costs were obtained from vendor quotations when possible; however, the majority of the equipment costs were derived from NREL's economic model *(3)*.

Table 2
Equipment Cost for Carbonic Acid Pretreatment Process (2000 psi, 220°C, 4 min)

Equip no.	Qty. required (spare)	Equipment name	Scaling stream	Stream flow (kg/h)	Scale exp.	Inst'n factor	Installed cost (2001 US$)
B8	1	In-line CO_2 mixer	11	208,280	0.48	1	2951
B7	1 (1)	Feed pump	4	203,879	0.7	2.8	235,516
B12	1 (1)	Loading pump	5	208,280	0.7	2.8	239,064
B3	1	Blowdown tank	6	208,280	0.93	1.2	61,924
B3	1	Screw conveyor	14	160,401	0.78	1.3	60,810
B10	3	Pneumapress filter	SLD 14	62,647	0.6	1.05	5,694,196
B14	1 (1)	Primary filtrate pump	8	97,012	0.79	3.56	178,184
B11	1 (1)	Heat exchanger	Area/ft^2	6805	0.68	2.1	377,755
B13	1 (1)	CO_2 compressor	2A	4401	0.34	1.3	253,336
B9	1 (1)	Heater	Duty (cal/s)	3,890,560	0.68	2.1	428,191
B2	1	Screw conveyor	17	63,390	0.78	1.3	29,477
B4	1	Tank agitator	18	160,401	0.51	1.2	29,394
B4	1	Slurrying tank	18	160,401	0.71	1.2	31,138
B5	1 (1)	Cooler	Duty (cal/s)	2,185,707	0.68	2.1	524,086
B1	3	Reactor	15		1	1.7	24,869,613
B6	1	Separator (condenser)	Duty (cal/s)	5,556,935	0.68	2.1	494,241
B6	1	Separator (reflex drum)	Duty (cal/s)	5,556,935	0.93	2.1	415,773
						Total	33,925,650
		Additional equipment					
A205	1	Hydrolysate mix tank agitator					35,068
C202	1	Hydrolysate washed solid belt conveyor					116,103
H200	1	Hydrolysate cooler					127,051
P205	2 (1)	Pneumapress feed pump					154,290
P225	1 (1)	ISEP elution pump					43,462
P226	1 (1)	ISEP reload pump					74,798
S221	1	ISEP					2,739,939
T205	1	Hydrolysate mixing tank					39,812
						Total	3,330,522
						Grand total	37,256,172

Table 3
Electricity Cost

Equipment	Number (NREL no.)	Power (kW)	Cost ($/h)	Cost (2001 $/yr)
Feed pump	B7	268	10.72	84,902
Loading pump	B12	451	18.04	142,877
Primary filtrate pump	B14	162	6.48	51,322
Compressor	B13	235	9.4	74,448
Reactor screw (3 nos.)	B1 (WM 202)	863.08	34.5	273,424
Screw conveyor	B3 (WC 201)	36.96	1.5	11,709
Screw conveyor	B2 (WC 202)	44.59	1.8	14,126
Tank agitator	B4 (WT 232)	25.55	1.0	8094
Press filter (3 nos.)	B10 (WS 202)	133.8	5.4	42,388
Total		2219.98		703,290
Total for H_2SO_4 system *(3)*		1754.17		555,721

Scaling of process equipment was done using the following exponential scaling expression *(13)*:

$$\text{New cost} = \text{Original cost} \times \left(\frac{\text{New size}}{\text{Original size}}\right)^{s} \quad (3)$$

in which *S* is the scaling exponent, determined separately for each type of equipment. Instead of size, a characteristic that is linearly related to size, such as mass throughput, can be used in Eq.3. Another characteristic that can be used in Eq.3 is heat duty for a heat exchanger when the temperature differentials are held constant. For equipment that is not listed in a standard reference such as *Handbook of Chemical Engineering (12)*, the scaling exponents were obtained from the NREL dilute-acid report *(3)*. To maintain consistency between models, the installation costs were also taken from the NREL economic model. Since original equipment costs were calculated in different cost years, the chemical engineering cost indices *(14)* were used to calculate their cost in 2001 US$.

Calculation of Energy Cost

Energy cost of the pretreatment section was determined using energy demand values generated by the ASPEN-Plus model. Assumptions made for the economic analysis included 7920 operating hours per year and utilities valued at 4 ¢/kwh for electricity, 5.5¢ 1000 lb of 15°C cooling water, and 2000 psi steam at $4.50/1000 lb. For pumps and compressors such as B7, B12, B14, and B13, the power requirements were determined by the ASPEN-Plus model. However, some internal components of major process units such as reactor screws and tank agitators were not explicitly modeled in this process. Because these are standard types of process equipment, power requirements for these devices were assumed to be the same as those provided in the NREL economic model *(3)*. For example, the power requirement for reactor screw (B1) was taken to be the same as WM202 given in the NREL model. The total electricity cost was calculated as given in the Table 3.

Table 4
Cooling and Heating Duty and Costs

Equipment name	Number	Duty (kW)	Flow rate (kg/h)	Cost ($/yr)
Cooler	B5	9151	461,395	442,164
Separator/condenser	B6	23,266	284,890	273,016
Compressor cooler	B13	689	59,057	56,596
Total cooling			80,5342	771,775
Heater	B9	16,289	23,422	1,836,506
Total heating				1,836,506

Table 5
Annual Total Energy Cost

Energy type	Energy cost ($/yr)	Energy cost ($/gal)
Electricity	703,290	0.0137
Cooling duty	771,775	0.0150
Heating duty	1,836,506	0.0358
Total energy cost (2001 US$)	3,311,571	0.0645

Table 3 also includes the total power requirements for the pretreatment section of the NREL model *(3)*. The cooling duty and the heating duty of different process units were also determined by the ASPEN-Plus model. These data were used to calculate the total cooling and heating duties for the carbonic acid pretreatment and finally the total energy cost of the pretreatment process. These results are summarized in Tables 4 and 5.

Sensitivity Analyses

Sensitivity analyses were conducted to address the question of whether there is an optimum pretreatment condition that could be used for carbonic acid pretreatment. Laboratory results from Yourchisin and van Walsum *(7)* and McWilliams and van Walsum *(6)* indicate that optimal reaction severity would be in the range of $\text{Log}(R_o) = 4.2$, where the severity R_o is as defined by Overend and Chornet *(10)*. Relatively high temperature (220°C) and short retention time (4 min) were chosen to achieve this severity, since reactor costs dominate the economics and longer retention times would increase capital costs significantly. Pretreatment temperatures and pressures were varied for this study to determine the sensitivity of the cost to adjustments in these parameters.

In its economic model *(3)*, NREL used the discounted cash flow method to calculate the yearly total equipment cost for different process sections. To simplify economic comparisons between the two pretreatment designs,

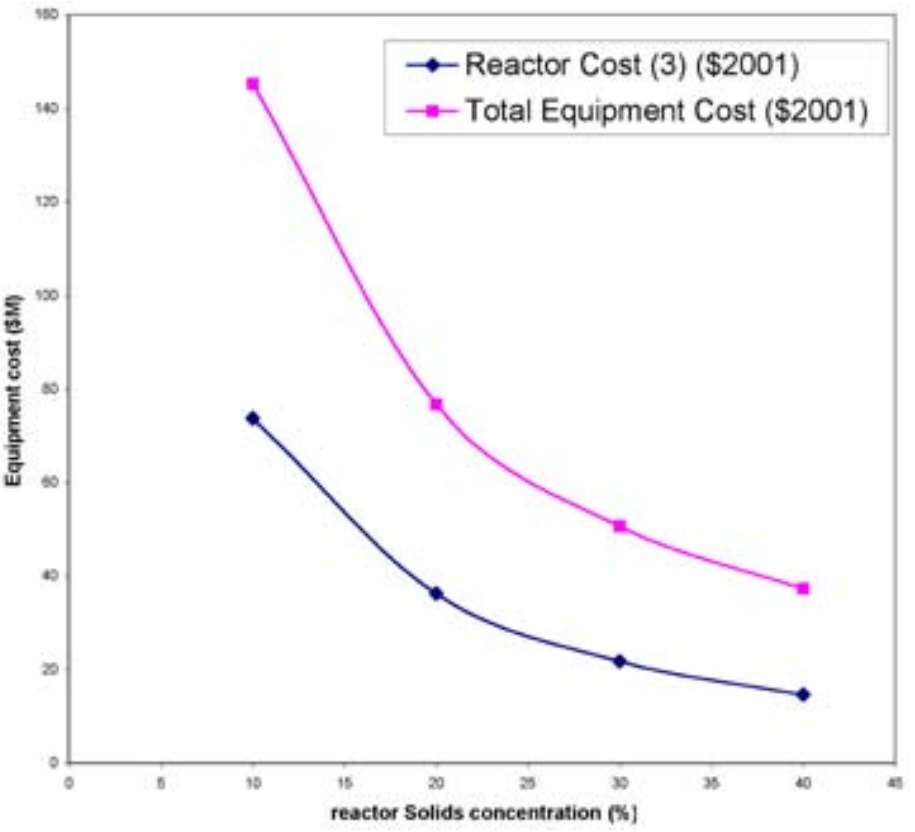

Fig. 2. Sensitivity of carbonic acid equipment costs to reactor solids concentration.

we assumed for both cases a 20% per year capital recovery factor to give the contribution of capital. This value was chosen to be consistent with investment returns for mature, low-risk technology *(1)*. With this assumption, it was possible to calculate total cost of pretreatment per year for different pretreatment conditions as given in Table 6. All values are in 2001 US$.

Variation of Equipment Cost with Reactor Solids Concentration

Experimental results for carbonic acid pretreatment have been generated at low solids concentration *(6,8,9)*, but no data are available for pretreatment conversions at higher solids concentrations, as are available for dilute H_2SO_4. The equipment costs for carbonic acid pretreatment were calculated for different solids concentrations (Fig. 2), and it can be seen that equipment costs are highly sensitive to solids concentration. For comparison to the dilute-acid system, a high reactor solids concentration of 40% was chosen to enable direct comparison with the NREL model.

Table 6
Variation of Total Cost at Constant Pressure

Parameters		Total equipment cost ($)	Equipment cost (per yr)($)	Operating cost (per yr) ($)	Total cost ($/yr)	Total cost ($/gal)
Pressure (psi)	Temp (°C)					
2000	220	37,256,172	7,451,234	3,311,571	10,762,805	0.210
2000	200	36,642,711	7,328,542	2,742,546	10,071,088	0.190
2000	180	35,659,532	7,131,906	2,208,698	9,340,604	0.180
1600	220	31,758,432	6,351,686	3,280,963	9,632,649	0.187
1600	200	31,342,841	6,268,568	2,712,051	8,980,619	0.175
1600	180	30,591,542	6,118,308	2,178,089	8,296,397	0.162
1200	220	26,580,118	5,316,024	3,250,150	8,566,174	0.167
1200	200	26,282,500	5,256,500	2,681,126	7,937,626	0.155
1200	180	25,743,721	5,148,744	2,147,277	7,296,021	0.142
1000	220	24,080,135	4,816,027	3,234,846	8,050,873	0.157
1000	200	23,834,986	4,766,997	2,665,821	7,432,818	0.145
1000	180	23,401,891	4,680,378	2,131,973	6,812,351	0.133
800	220	21,636,822	4,327,364	3,219,542	7,546,906	0.147
800	200	21,448,875	4,289,775	2,650,517	6,940,292	0.135
800	180	21,105,669	4,221,134	2,116,669	6,337,803	0.123

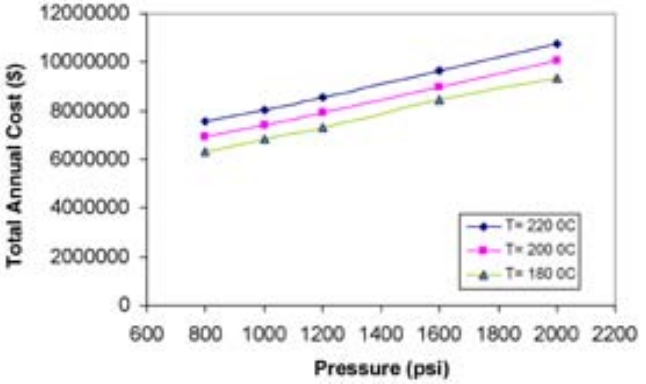

Fig. 3. Sensitivity of total (capital and operating) cost with variation in pretreatment pressure and temperature.

Variation of Total Cost with Temperature and Pressure

As explained in previous sections, equipment and operating costs were calculated for different pretreatment conditions. Reactor solids concentration and residence time remained constant at 40% and 4 min, respectively, throughout these calculations. Figure 3 depicts the variation of the total cost with pressure at different reaction temperatures. It is evident that the pressure of the system strongly affects the overall cost and is a dominant concern for cost reduction. Likewise, temperature also affects cost, with higher temperatures costing more. Increased temperature and pressure both increase reaction severity, although for some substrates such as aspen wood, only increased temperature results in clearly enhanced pretreatment effectiveness *(6,7)*. As a result, reducing pressures is more likely to improve overall economics than reducing temperatures.

Comparison of Carbonic Acid Pretreatment and H_2SO_4 Pretreatment

The central hypothesis of this research is that there will be negative incremental cost for the carbonic acid pretreatment process compared with the H_2SO_4 process. However, the equipment and energy costs for the carbonic acid system as calculated in this study are higher than those for the H_2SO_4 system. Although the cost of materials was reduced by making use of SS316, these savings were lost to provide the extra wall thickness needed for the higher pressures. The energy cost associated with CO_2 compression is not highly significant; for example, the power requirement for the reactor screw, which is common to both the carbonic and H_2SO_4 systems, is four times as great as that of the CO_2 compressor. Cost results are as follows:

Total equipment cost (2001 US$) = $37,256,172

Annual energy cost (2001 US$) = $3,311,571

A comparison of sulfuric and carbonic acid pretreatment flowsheets shows that some operations associated with processing requirements of

Table 7
Cost of Reagents and Waste Disposal in Dilute H_2SO_4 Pretreatment Process *(3)*

Component	Stream no.	kg/h	t/yr	Price ($/t)	Year	Total cost ($/yr)
H_2SO_4	STRM0710	2128	16,854	25	2001	421,344
Lime	STRM0745	913	7231	70	2001	506,167
Gypsum disposal		2433	19,269	22	2001	423,926
Total						1,351,437

Table 8
Comparison of Costs of Carbonic Acid and Sulfuric Acid Processes

Pretreatment method	Pretreatment equipment cost ($)	Pretreatment capital cost ($/yr)	Variable operating cost (2001 US$) at 2000 t/d	Total annual cost ($/yr)	EtOH (gal/yr)	EtOH ($/gal)
Carbonic acid	37,256,172	7,451,235	3,311,571	10,762,805	51,300,000	0.210
H_2SO_4	29,235,023	5,847,005	4,515,439 (approx)	10,435,565	51,300,000	0.202

the H_2SO_4 process that are absent from the carbonic acid system. These include the use of acid-neutralizing reagents and the resulting disposal of the waste calcium sulfate precipitate. Results compiled from the NREL report *(3)* are used to quantify these additional costs (Table 7). For the purpose of comparison, these costs are rolled into the operating cost of the H_2SO_4 pretreatment. Because the pretreatment section of the NREL model is embedded in a much larger model of the entire biomass-to-ethanol process, it was not possible to accurately determine steam and cooling water costs associated with only the pretreatment section. For the purpose of this comparison, energy costs for steam and cooling in the H_2SO_4 system were approximated as being equal to those calculated for the carbonic acid pretreatment. With this assumption, the total variable operating cost for the H_2SO_4 system is given in Table 8 as approx 4.5 million US$. Cost contributions to final ethanol selling price for the two pretreatment systems (assuming equal ethanol yields) are comparable, with dilute H_2SO_4 being slightly more economical.

Dilute H_2SO_4 is a well-studied pretreatment system that has been shown to be effective but expensive. Limited studies on carbonic acid have shown that this mild acid offers some benefit compared to liquid hot water *(4,5)*, but that performance is generally less effective than optimized dilute H_2SO_4. Laboratory investigations of carbonic acid pretreatment have shown that pretreatment effectiveness is primarily a function of time and temperature, and that high CO_2 pressure enhances hydrolysis on some substrates such as corn stover *(8)* but offers little benefit on aspen wood *(6,7)*. Thus, for certain substrates such as aspen wood, lower pressure values are likely to offer performance similar to higher pressures. To date, no study integrating carbonic acid pretreatment, enzymatic hydrolysis, and fermentation has been carried out to determine the overall ethanol yield compared to similar.

Conclusion

Although at the beginning of the design process it was hypothesized that reactor cost could be lowered owing to the use of stainless steel instead of Hastelloy C, the pretreatment reactor turned out to be the most expensive piece of equipment in the carbonic acid pretreatment, costing about twice as much as the NREL reactor constructed of Hastelloy C. High pressures associated with carbonic acid pretreatment made it extremely expensive to build reactors out of SS316 L. One option that can be used to minimize this cost is to clad the reactor with polymeric material such as Teflon and to reinforce it with stainless steel; this approach would likely offer similar benefits to the dilute H_2SO_4 system as well. Energy requirements for compression of CO_2 were relatively minor and did not greatly affect overall process economics. This was partly owing to the ambient temperature (high solubility) conditions at which CO_2 was dissolved into solution. About 50% of the total operating cost is owing to the heat demand of the process. This appears to be unavoidable because of difficulties in process heat recovery.

Acknowledgments

We greatly appreciate contributions made by the following departments and organizations: Department of Environmental Studies, Baylor University; NREL; and the US Department of Energy (contract DE-FC36-01GO11070, A000).

References

1. Lynd, L., Elander, R. T., and Wyman, C. E. (1996), *Appl. Biochem. Biotechnol*. **54/55,** 741–749.
2. Wooley, R. and Putsche V. (1996), NREL/MP-425-20685, National Renewable Energy Laboratory, Golden, CO.
3. Wooley, R., Ruth, M., Ibsen, K., Sheehan, J., Majdeski, H., and Galvez, A. (1999), NREL/TP-580-26157, National Renewable Energy Laboratory, Golden, CO.
4. van Walsum, G. P. (2001), *Appl. Biochem. Biotechnol*. **91/93,** 317–328.
5. van Walsum, G. P., McWilliams, R., and Shi, H. (2002), in *Proceedings of the 12th European Conference and Technology Exhibition on Biomass for Energy, Industry and Climate Protection*. p 809–812.
6. McWilliams, R. C. and van Walsum G. P. (2002), *Appl. Biochem. Biotechnol*. **98/100,** 109–134.
7. Yourchisin, D. and van Walsum, G. P. (2004), in *Appl. Biochem. Biotechnol*. submitted.
8. van Walsum, G. P. and Shi, H. (2004), *Bioresour. Technol*., submitted.
9. Puri, V. P. and Mamers, H. (1983), *Biotechnol. Bioeng*. **25,** 3149–3161.
10. Overend, R. P. and Chornet, E. (1987), *Phil. Trans. R. Soc. Lond*. **A321,** 523–536.
11. Wooley, R. and Ibsen, K. (2000), *Rapid Evaluation of Research Proposals Using Aspen Plus*, presentation at Aspen World 2000, February, 4–7, Orlando, FL.
12. Perry, H. R. and Green, D. W. (1993), in *Handbook of Chemical Engineering*, 5th Ed. McGraw-Hill, New York, NY, pp.10,136–10,156.
13. McAloon A., Taylor F., Yee W., Wooley R., and Ibsen K., (2000), DOE-AC36-99-GO103337, National Renewable Energy Laboratory, Golden, CO.
14. American Institute of Chemical Engineers. (2001), Chemical Engineering Plant Cost Index, *Chemical Engineering Progress*, p. 134.

0273-2289/04/115/1103–1114/$25.00

Enhanced Enzymatic Hydrolysis of Steam-Exploded Douglas Fir Wood by Alkali-Oxygen Post-treatment

Xuejun Pan, Xiao Zhang, David J. Gregg, and John N. Saddler*

Forest Products Biotechnology, Faculty of Forestry, University of British Columbia, 2424 Main Mall, Vancouver, BC, Canada, V6T 1Z4,
E-mail: saddler@interchange.ubc.ca

Abstract

Good enzymatic hydrolysis of steam-exploded Douglas fir wood (SEDW) cannot be achieved owing to the very high lignin content (>40%) that remains associated with this substrate. Thus, in this study, we investigated the use of alkali-oxygen treatment as a posttreatment to delignify SEDW and also considered the enzymatic hydrolyzability of the delignified SEDW. The results showed that under optimized conditions of 15% NaOH, 5% consistency, 110°C, and 3 h, approx 84% of the lignin in SEDW could be removed. The resulting delignified SEDW had good hydrolyzability, and cellulose-to-glucose conversion yields of over 90 and 100% could be achieved within 48 h with 20 and 40 filter paper units/g of cellulose enzyme loadings, respectively. It was also indicated that severe conditions, such as high NaOH concentration and high temperature, should not be utilized in oxygen delignification of SEDW in order to avoid extensive condensation of lignin and significant degradation of cellulose.

Index Entries: Steam explosion; Douglas fir; oxygen delignification; enzymatic hydrolysis; lignin.

Introduction

During the twentieth century, fossil fuels were the major driving force for economic growth in the world. In particular, a cheap and abundant oil supply has brought North America tremendous economic benefits, a profusion of products, and a high quality of life. However, consumption of fossil fuels on an ever-expanding scale has also led to adverse changes in

*Author to whom all correspondence and reprint requests should be addressed.

our climate and a dramatic increase in air pollution. Mann at al. *(1)* study has suggested that the increasing concentrations of carbon dioxide and other greenhouse gases in the atmosphere during the past century have played a significant role in global warming. Detrimental compounds found in automobile emissions, such as carbon monoxide, nitrogen oxides, volatile hydrocarbons, sulfur oxides, and benzene, have been identified as the underlying cause of a number of human health problems. Thus, there are environmental and health-related incentives to develop alternative sources of energy to alleviate our dependence on fossil fuels.

The Kyoto protocol had identified the development of an alternative biofuel from biomass as one of several areas deserving of research support, since this type of renewable fuel could help reduce greenhouse gas emissions. The use of bioethanol as a viable motor fuel to replace or augment gasoline is an attractive component of an integrated strategy to reduce the release of detrimental hydrocarbons, carbon monoxide, nitrogen oxide, sulfur dioxide, and aromatics *(2–3)*.

Lignocellulosics are the most abundant renewable organic materials in the biosphere. They account for approx 50% of the total biomass in the world, with an estimated annual production of $1–50 \times 10^9$ t *(4)*. Lignocellulosic materials, particularly the residues obtained from wood processing, are usually much cheaper than sugar- and/or starch-derived feedstock, such as sugarcane and corn. They also have no competitive use as human or animal foodstuffs.

Softwoods are the predominant species of tree in Canada. In British Columbia, an estimated 2.2 million t of surplus wood residues are generated each year *(5)*, which until now have been of limited use as a commercial product. Bioconversion of these residues into biofuel ethanol and valuable chemicals provides an attractive opportunity for the sustainable development of both renewable energy and Canada's forest resources.

A typical wood-to-ethanol bioconversion process consists of at least three major steps: pretreatment, hydrolysis, and fermentation. The pretreatment stage has been shown to be the key step to providing a substrate susceptible to the subsequent hydrolysis. Steam explosion is one of the most intensively studied pretreatment methods for bioconversion of softwood materials *(6–10)*.

The steam explosion process uses high temperature and pressure followed by sudden release to separate individual fibers within the woody substrate. One of the problems with the steam explosion process is that it does not significantly delignify the wood; most of the lignin remains in the resulting cellulosic substrate. This high lignin content is one of the reasons that pretreated substrate continues to be very resistant to enzymatic hydrolysis. Our previous work *(11)* has shown that the enzymatic digestibility of steam-exploded Douglas fir wood (SEDW) can be enhanced with a peroxide posttreatment step. However, the high hydrogen peroxide consumption involved in this process makes it impractical for industrial use. There is, therefore, a need to develop a cost-effective posttreatment method capa-

ble of reducing the lignin content of the SEDW and enhancing its hydrolyzability.

Oxygen delignification has been widely used in the pulp and paper industry to remove lignin in both pulping and bleaching processes *(12)*. A typical commercial oxygen delignification operation is able to remove about 50% of the lignin present in a Kraft pulp without significant impact on pulp yield and strength. There is little information in the existing literature describing the application of oxygen delignification to high-lignin-containing substrates, such as SEDW, and those few studies that were carried out were generally unsuccessful *(13)*. Thus, the aim of the present work was to evaluate the potential of using oxygen delignification as a posttreatment to enhance the susceptibility of SEDW.

Materials and Methods

Preparation of SEDW

Douglas fir (*Pseudotsuga menziesii*) was chipped and screened to a relatively homogeneous chip size of approx 3 × 3 × 0.3 cm. The chips were initially impregnated with 4.5% (w/w) gaseous SO_2 and then steam exploded in a 1-L steam gun in batches of 50 g of dry chips at 195°C for 4.5 min, as previously described by Boussaid et al. *(14)*. The steam-exploded wood samples of each batch were collected, combined, washed, and finally defibrillated on a refiner to produce a homogeneous feedstock.

Oxygen Delignification

Oxygen delignification of SEDW was carried out in a 1-L steel reactor equipped with a motorized stirrer. The SEDW (30 g for each batch), NaOH, and water was premixed in a beaker and transferred to the reactor. The amount of NaOH and water were adjusted according to the reaction conditions (alkali dosage and consistency; *see* Table 1). All experiments were conducted under an oxygen pressure of 0.5 MPa. Magnesium sulfate (0.5% on SEDW [w/w]) was added to prevent the cellulose from degrading during oxidation. At the end of the reaction, the suspension was removed from the reactor. The oxygen-delignified SEDW in the suspension was separated from waste liquor using filtration, washed with distilled water, then stored in a refrigerator for subsequent analysis and hydrolysis.

Enzyme Preparations

The enzyme preparations were provided by Novo Nordisk. Cellulase (Celluclast) possessed 115 filter paper units (FPU)/mL; β-glucosidase (Novozym 188) had 570 cellobiose units (CBU)/mL.

Enzymatic Hydrolysis

All hydrolysis experiments were conducted with a combination of cellulase (Celluclast) and β-glucosidase (Novozym 188) at a ratio of 1:2

Table 1
Oxygen Delignification of SEDW

		Oxygen-delignified SEDW[a]					
Sample ID	SEDW	O-1	O-2	O-3	O-4	O-5	O-6
Delignification conditions							
NaOH (% on oven dry pulp)		20	20	15	15	15	10
Consistency (%)		12	10	10	5	5	5
Temperature (°C)		140	110	110	110	100	110
Time (h)		1.5	1.5	1.5	3	3	3
Pulp yield, %	100.0	59.6	66.5	71.5	58.5	61.8	71.7
Total lignin (%)	42.8	47.1	49.0	49.1	12.0	14.8	23.8
Klason lignin (%)	41.7	46.7	48.6	48.7	11.5	14.3	23.3
Acid-soluble lignin (%)	1.1	0.4	0.4	0.4	0.5	0.5	0.5
Carbohydrate composition (%) [b]	100.0	100.0	100.0	100.0	100.0	100.0	100.0
Arabinose	0.5	ND	ND	ND	ND	ND	ND
Galactose	0.7	ND	0.5	0.5	ND	ND	ND
Glucose	87.7	93.3	93.2	92.6	96.8	96.6	96.9
Xylose	8.3	5.0	4.5	5.1	1.4	1.5	1.3
Mannose	2.8	1.7	1.8	1.8	1.8	1.9	1.8

[a] ND, not detected.
[b] Percentage of sugars in total carbohydrates..

(FPU/CBU). β-Glucosidase was added to avoid end-product inhibition owing to cellobiose accumulation. Batch hydrolysis experiments were conducted at 2% consistency of cellulose in 50 m*M* acetate buffer, pH 4.8, with 4 mg of tetracycline/100 mL of buffer as antibiotic. The hydrolysis incubation was performed at 45°C on a rotary shaker at 150 rpm. Samples of the supernatants were taken at assigned intervals for sugar analysis. All hydrolysis experiments were performed in duplicate, and the averages were reported.

Analytical Procedure

Sugar concentrations of hydrolysates were determined using a Dionex high-performance liquid chromatography system (DX-500) equipped with an AS3500 autosampler, a GP40 gradient pump, an anion-exchange column (Dionex CarboPac™ PA1), and an ED40 electrochemical detector. Deionized water was used as an eluent at a flow rate of 1 mL/min; NaOH (1 *M*) was used to equilibrate the column after elution of sugars. To optimize baseline stability and detector sensitivity, 0.2 *M* NaOH was added postcolumn. After being filtered through 0.45-µm nylon syringe filters (Chromatographic Specialties), a 20-µL sample was injected.

Klason lignin determination of substrates was carried out according to TAPPI standard method T-222. The hydrolysate from the Klason lignin determination was collected and analyzed for sugars and acid-soluble lignin. Sugars were determined as just described, with the exception that the mixture of sugar standards was autoclaved at 120°C for 1 h to compensate for sugar changes during autoclaving. Acid-soluble lignin was determined by ultraviolet spectra, as described by Dence *(15)*.

Results and Discussion

Oxygen Delignification Operations

Oxygen delignification, a delignification method using combined oxygen and alkali, has been widely utilized in the bleaching of pulps in the paper industry. In most cases, the lignin content of a brown stock prior to bleaching is about 5% (w/w). Because of the poor selectivity of oxygen, the extent of oxygen delignification is typically limited to 45–50% lignin removal in order to avoid the undesired degradation of cellulose and resulting negative impact on pulp strength *(12)*.

The main process parameters of an oxygen delignification operation include alkali (NaOH) charge, temperature, pulp consistency, reaction time, and oxygen pressure. Previous work *(16)* has shown that approx 1% NaOH (per oven dry pulp) is required to remove each percentage of lignin from the pulp. An increase in temperature will accelerate the delignification rate; however, there is a simultaneous increase in the risk of cellulose degradation. In general, higher consistency produces improved delignification at a fixed NaOH loading. Typical oxygen delignification operations are carried out at 90-115°C, at 10–20% pulp consistency, over 30–80 min of reaction time and 0.5–0.7 MPa of oxygen pressure.

Distinct from kraft pulp, SEDW has a very high lignin content (about 40%), and the lignin present in SEDW has been shown to be highly condensed and less reactive than is found in commercial pulps *(17)*. To assess the potential of oxygen delignification on SEDW lignin removal, a series of oxygen delignification experiments was designed with different reaction conditions (Table 1). The severity of the treatments was controlled by a combination of reaction parameters including temperature, substrate consistency, and alkali charge. The severities of different oxygen delignification experiments vary, with the O-1, O-2, and O-3 group representing relatively severe treatment conditions, and the O-4, O-5, and O-6 group corresponding to relatively mild treatment conditions.

The chemical composition of oxygen-delignified SEDW at different conditions was determined and compared with the control, untreated SEDW. There was a significant loss in the sample yield, varying from 58.5 to 71.7%, after oxygen delignification. The glucose fraction of the total carbohydrate increased in all treated samples, when compared to untreated SEDW, probably owing to the removal of the hemicellulose present in the substrates. Among the different hemicellulose sugars, arabinose and galac-

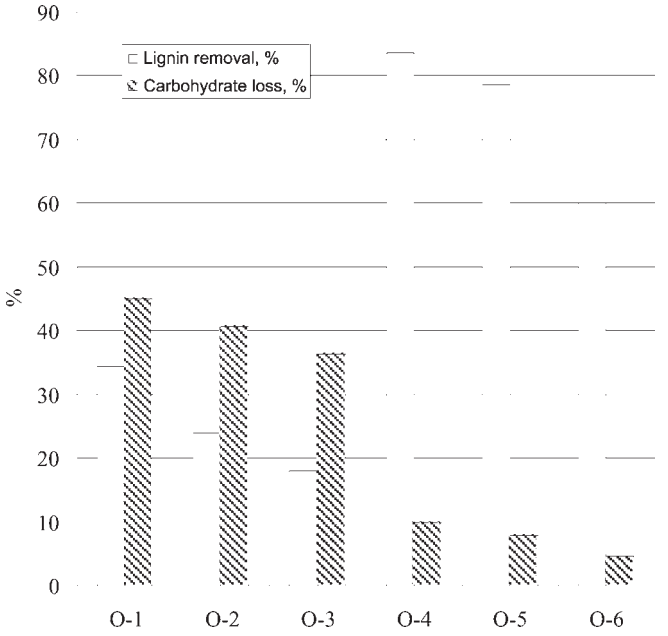

Fig. 1. Effect of oxygen delignification conditions on lignin removal and carbohydrate loss.

tose were totally removed and a considerable decrease in the amount of xylose and mannose was detected. However, the changes in the lignin content after oxygen delignification were somewhat unexpected. The lignin content increased after oxygen treatments under relatively severe conditions (O-1, O-2, and O-3), whereas there was a significant removal of lignin under milder conditions (O-4, O-5, and O-6). The reason for substantial delignification under mild conditions was further investigated.

Effect of Oxygen Delignification on Removal of Lignin and Yield of Carbohydrates

The degree of delignification was plotted against the loss of carbohydrates after each treatment. As shown in Fig. 1, there was a significant loss of carbohydrates, from 37–44.9%, under severe treatment conditions (O-1, O-2, and O-3). Conversely, mild treatment conditions (O-4, O-5, and O-6) resulted in less degradation of the carbohydrates. It was anticipated that higher alkalinity combined with higher temperature would increase delignification. The results from our experiments proved otherwise, showing that mild conditions removed much more lignin than severe conditions. These results can be postulated by the reaction mechanisms of carbohydrate and lignin during oxygen delignification.

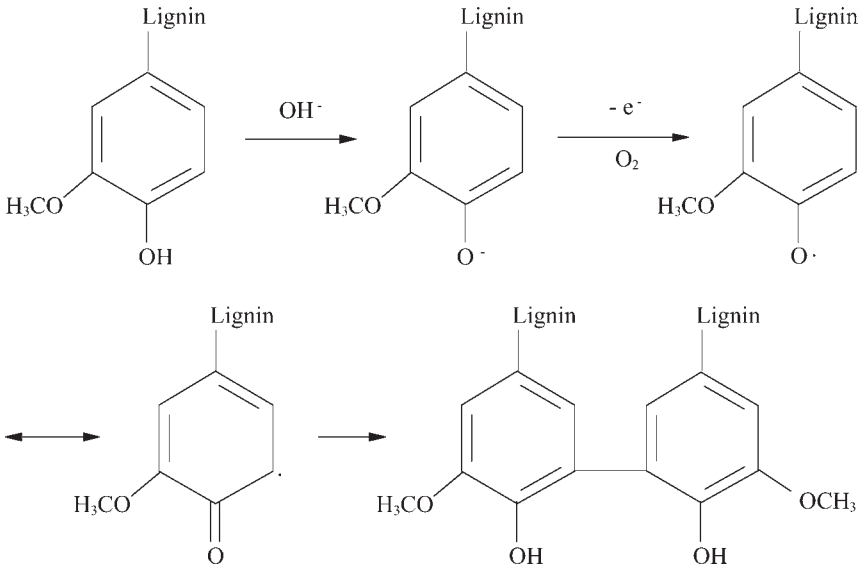

Fig. 2. Condensation reaction of lignin during oxygen delignification.

In general, there are two types of reactions that would lead to cellulose degradation during oxygen delignification *(12)*. The first is random chain cleavage (alkaline hydrolysis), which occurs at any point along the cellulose chain. The first step in this chain cleavage process is the oxidation of a hydroxyl group to a carbonyl group. The enol form of the ensuing carbonyl-containing unit will then undergo a β-elimination reaction to cleave the glycosidic bond and break the cellulose chain *(18)*. The second is the "peeling" reaction, during which the reducing units (containing the carbonyl group) on the end of the chain are attacked and successively removed. Random chain cleavage will promote the peeling reaction by producing new reducing ends *(12)*. Both higher temperature and alkaline conditions will typically enhance random chain cleavage and the peeling reaction.

It is known that free-radical reactions are also involved in oxygen delignification *(19)*. Free phenolic groups on the lignin have been shown to play a key role in these reactions. Under alkaline conditions, the phenolic groups can be ionized to form the phenoxide ion, which has a high electron density. The phenoxide ions are very susceptible to molecular oxygen and form phenoxy radicals. The propagation of this radical reaction will result in the consecutive rupture of the lignin structure, formation of degraded compounds, and consequent removal of lignin. However, throughout the lignin degradation reactions, the phenoxy radicals can also undergo coupling (condensation) reactions (Fig. 2) that lead to the formation of new carbon-carbon bonds between lignin subunits *(20)*. Severe treatment conditions, such as high temperature and high alkali concentration, can facilitate these coupling and condensation reactions.

The SEDW substrate has a very high lignin content and therefore has the potential to form a considerable number of phenoxy radicals in high alkaline concentration and high temperatures. It is probable that the more severe treatment conditions (O-1, O-2, and O-3) caused a significant condensation of the SEDW lignin, thereby limiting its removal. Meanwhile, the milder treatments encountered in the O-4 and O-5 treatments were more favorable to the lignin degradation. However, the insufficient alkali charge also led to limited lignin removal under O-6 treatment.

It is apparent that an increase in alkalinity and temperature during oxygen delignification of SEDW does not correlate with the extent of delignification. Different treatment parameters need to be optimized in order to minimize lignin condensation and carbohydrate degradation. Among the tested conditions, a relatively mild treatment (O-4) with 15% NaOH for 3 h at 110°C was shown to optimize the delignification of SEDW at a 5% substrate consistency. This treatment removed 83.6% of the lignin from SEDW, originally comprising 42.8% lignin. The carbohydrate yield after oxygen delignification (O-4) was 90%. The loss of carbohydrates was mainly owing to the removal of hemicellulose sugars. The glucose yield of O-4 was 99%. Our previous research *(11)* showed that the carbohydrate yield after steam explosion was 88%. Therefore, the overall yield of carbohydrates (steam explosion + oxygen delignification) was 79.2%.

Enzymatic Hydrolyzability of Oxygen-Delignified SEDW

The hydrolyzability of untreated SEDW was determined at several enzyme loadings, from 20 to 80 FPU/g of cellulose (Fig. 3). Poor enzymatic hydrolyzability was observed on the SEDW substrate even at a high enzyme loading. A 72-h-incubation resulted in approx 35, 58, and 75% cellulose-to-glucose conversions at Celluclast loadings of 20, 40, and 80 FPU/g of cellulose, respectively. Complete cellulose hydrolysis was not observed even after extended incubation for another 2 d.

The hydrolyzability of SEDW after oxygen delignification was also determined and compared with controls (Figs. 4 and 5). An enzyme loading at 20 FPU/g of cellulose was used to hydrolyze the delignified SEDW. As shown in Fig. 4, after more severe treatments (O-1, O-2, and O-3), SEDW demonstrated improved digestibility over untreated SEDW, with an increase in cellulose-to-glucose conversion yields from 8 to 21%. However, note that the O-1-, O-2-, and O-3-treated samples contained higher lignin when compared to the untreated SEDW. Although the amount of lignin present has been shown to correlate with the digestibility of a lignocellulosic substrate, it is also recognized that the nature and distribution of lignin within the substrate can also have a detrimental effect on enzyme accessibility to the substrate and subsequent hydrolysis efficiency *(21)*. Besides acting as a physical barrier to hinder enzyme accessibility, lignin has been shown to be able to irreversibly adsorb cellulase enzymes and impair the efficiency of enzymatic hydrolysis. Free phenolic groups on lignin have also been shown to play a critical role in the adsorption of

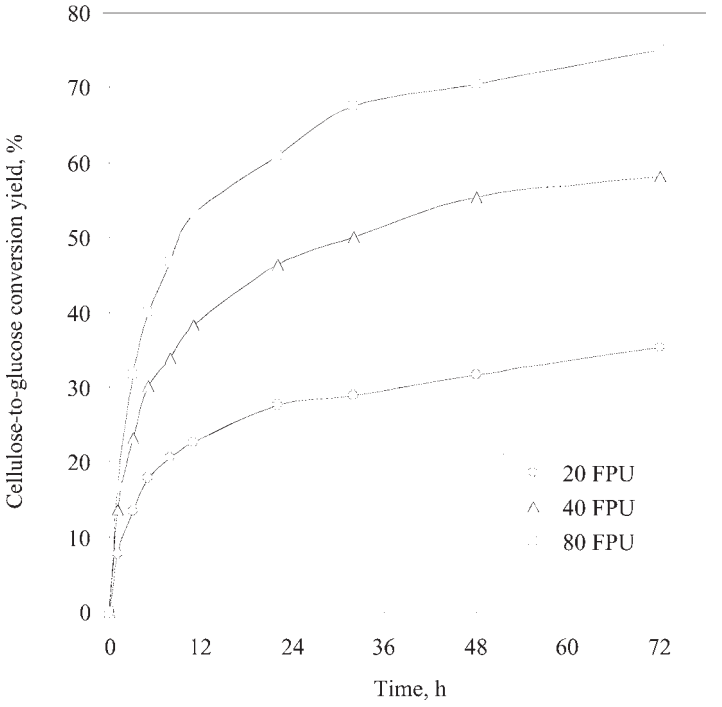

Fig. 3. Enzymatic hydrolysis of untreated SEDW.

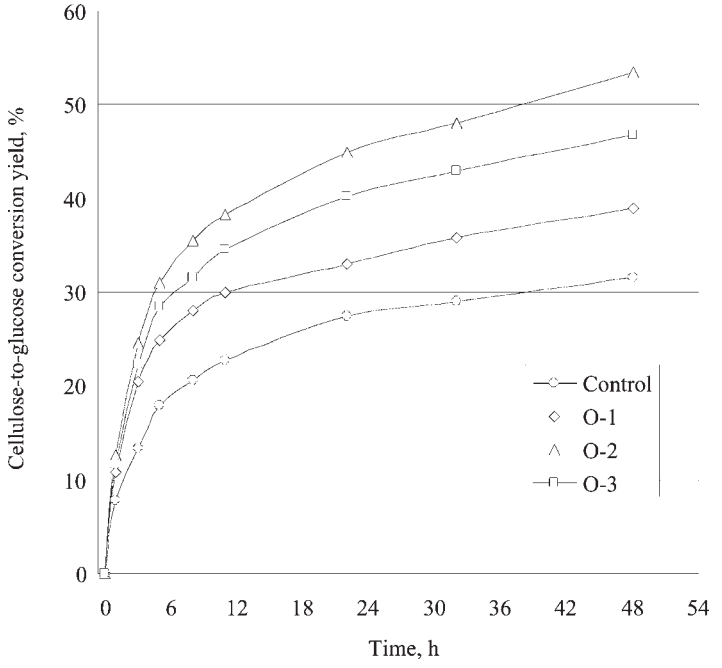

Fig. 4. Enzymatic hydrolysis of SEDWs oxygen delignified under severe conditions (cellulase loading: 20 FPU/ g of cellulose).

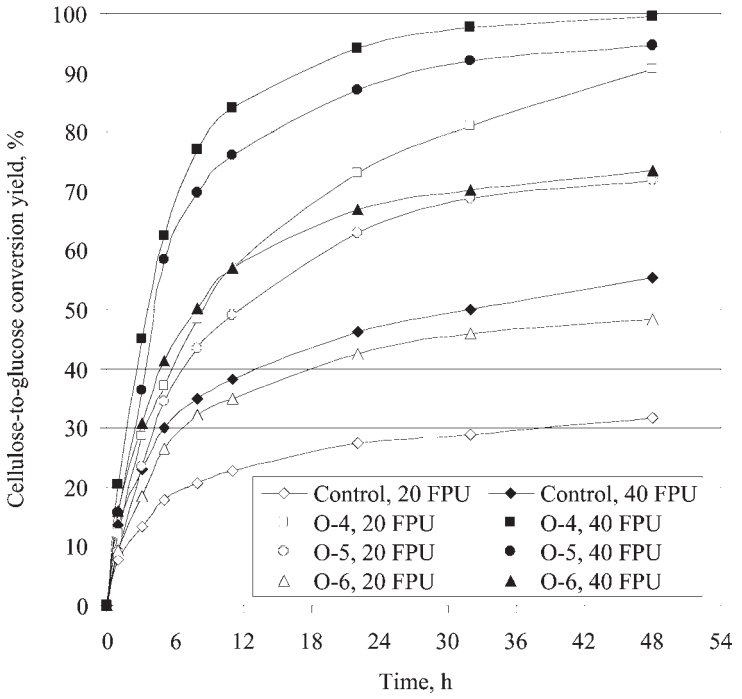

Fig. 5. Enzymatic hydrolysis of SEDWs oxygen delignified under mild conditions.

enzymes by mediating the binding between lignin and proteins *(22,23)*. Oxygen treatment reduced the number of phenolic groups present in the lignin, producing a more condensed structure *(12,24,25)*. Therefore, it is conceivable that the increased hydrolyzability of the O-1, O-2, and O-3 samples is owing to the modifications in the lignin structures making lignin less detrimental to the cellulase enzyme.

When the digestibility of O-4-, O-5-, and O-6-treated samples was compared to the control SEDW at both enzyme loadings of 20 and 40 FPU/g of cellulose, significant increases in cellulose-to-glucose conversion yield were observed (Fig. 5). A completed hydrolysis was obtained with the O-4-treated sample after 48 h of incubation with an enzyme loading of 40 FPU/g of cellulose. At the same enzyme loading, the hydrolysis of O-5 and O-6 samples produced 95 and 73% cellulose-to-glucose conversion, respectively. At the lower enzyme loading (20 FPU/g of cellulose), the O-4-treated SEDW was still able to reach a 90% conversion yield after 48 h of hydrolysis, compared with a 70% conversion yield on O-5-treated samples and a close to 50% conversion yield when the O-6-treated sample was used. It is apparent that significant decreases in the lignin content, resulting from oxygen delignification under mild conditions, were the main reason for the enhanced hydrolyzability of treated samples. It is also likely that the modifications to

the nature of steam-exploded lignin contributed to some improvement in the digestibility of the O-4-, O-5-, and O-6-treated samples.

The overall glucose yield of SEDW was 91%, as reported previously *(11)*. As mentioned earlier, the glucose yield of O-4 after oxygen delignification was 99%. The cellulose-to-glucose conversion yields after 48 h of enzymatic hydrolysis of sample O-4 were 90% after an enzyme loading of 20 FPU/g of cellulose, and 100% after an enzyme loading of 40 FPU/g of cellulose. Thus, the overall wood-to-glucose conversion yield of the whole process (steam explosion pretreatment + oxygen posttreatment + enzymatic hydrolysis) was between 81 and 90%, which is considerably higher than has been reported previously *(26)*.

Conclusion

High-lignin-containing SEDW behaved differently to normal low-lignin-containing pulps during oxygen delignification. Severe reaction conditions (high NaOH concentration and high temperature) resulted in the condensation of lignin and destruction of cellulose rather than delignification. However, relatively mild conditions resulted in substantial delignification of SEDW without significant degradation of cellulose. The optimal conditions tested were 15% NaOH, 5% consistency, 110°C, and 3 h, which facilitated the removal of approx 84% of lignin in SEDW with only 10% loss of carbohydrates.

Untreated SEDW had poor hydrolyzability, and a complete hydrolysis was not observed even at a high enzyme loading. However, the oxygen-delignified SEDW showed a significant improvement in hydrolyzability. Cellulose-to-glucose conversion yields of 90 and 100% could be achieved within 48 h with enzyme loadings of 20 and 40 FPU/g of cellulose, respectively.

Acknowledgments

We thank Dr. Bill Cruickshank for his advice and Ian Cullis for kindly providing the SEDW. This research was financially supported by Natural Resources Canada.

References

1. Mann, M. E., Bradley, R. S. and Hughes, M. K. (1998), *Nature* **392,** 779–787.
2. Bailey, B. K. (1996), in *Handbook on Bioethanol: Production and Utilization*, Wyman, C.E., ed., Taylor & Francis, Bristol, PA, pp. 37–60.
3. Wheals, A. E., Basso, L. C., Alves, D. M. G., and Amorim, H. V. (1999), *Trends Biotechnol.* **17,** 482–487.
4. Claassen, P. A. M., Sijtsma, L, Stams, A. J. M, De Vries, S. S., and Weusthuis, R. A. (1999), *Appl. Microbiol. Biotechnol.* **52,** 741–755.
5. BW McCloy & Associates Inc. (2003), Report prepared for NRCan, Ottawa, Canada.
6. Clark, T. A. and Mackie, K. L. (1987), *J. Wood Chem. Technol.* **7,** 373–403.
7. Ramos, L. P., Breuil, C., and Saddler, J. N. (1992), *Appl. Biochem. Biotechnol.* **34–35,** 37–48.

8. Nguyen, Q. A., Tucker, M. P., Keller, F. A., Beaty, D. A., Connors, K. M., and Eddy, F. P. (1999), *Appl. Biochem. Biotechnol.* **77–79,** 133–142.
9. Boussaid, A., Esteghlalian, A. R., Gregg, D. J., Lee, K. H., and Saddler, J. N. (2000), *Appl. Biochem. Biotechnol.* **84–86,** 693–705.
10. Stenberg, K., Tengborg, C., Galbe, M., and Zacchi, G. (1998), *J. Chem. Technol. Biotechnol.* **71,** 299–308.
11. Yang, B., Boussaid, A., Mansfield, S. D., Gregg, D. J., and Saddler, J. N. (2002), *Biotechnol. Bioeng.* **77,** 678–684.
12. McDonough, T. J. (1996), in *Pulp Bleaching—Principles and Practice*, Dence, C. W. and Reeve, D. W, eds., TAPPI, Atlanta, GA, pp. 213–239.
13. Draude, K. M.; Kurniawan, C. B., and Duff, S. J. B. (2001), *Bioresour. Technol.* **79,** 113–120.
14. Boussaid, A., Jarvis, J., Gregg, D. J., and Saddler, J. N. (1997), in *Proceedings of the Third Biomass Conference of the Americas*, vol. 2 Montreal, Canada, Overend, R. P. and Chornet, E., eds., Pergamon, New York, NY, pp. 873–880.
15. Dence, C. W. (1992), in *Methods in Lignin Chemistry*, Lin, S. Y. and Dence, C. W., eds., Springer-Verlag, Berlin, Germany, pp. 33–61.
16. Tench, L. and Harper, S. (1987), in *1987 TAPPI International Oxygen Delignification Conference Proceedings*, TAPPI, Atlanta, GA, pp. 1–11.
17. Shevchenko, S. M., Beatson R. P., and Saddler, J. N. (1999), *Appl. Biochem. Biotechnol.* **77-79,** 867–876.
18. Gratzl, J. S. (1990), in *1990 Tappi Oxygen Delignification Symposium Notes*, TAPPI, Atlanta, GA, pp. 1–10.
19. Gierer, J. (1993), in *Proceedings of the 7th International Symposium on Wood and Pulping Chemistry*, Vol. 1, CTAPI, Beijing, pp. 301–307.
20. Dence, C.W. (1996), in *Pulp Bleaching—Principles and Practice*, Dence, C. W. and Reeve, D. W., eds., TAPPI, Atlanta, GA, pp. 113–124.
21. Mansfield, S. D., Mooney, C., and Saddler, J. N. (1999), *Biotechnol. Prog.* **15,** 804–816.
22. Kawamoto, H., Nakatsubo, F., and Murakami, K. (1992), *Mokuzai Gakkaishi* **38,** 81–84.
23. Sewalt, V. J. H., Glasser, W. G., and Beauchemin, K. A. (1997), *J. Agric. Food Chem.* **45(6),** 1823–1828.
24. Hagstrom-Nasi, C. (1988), *J. Wood Chem. Technol.* **8,** 299–311.
25. Akim, L. G., Colodette, J. L., and Argyropoulos, D. S. (2001), *Can. J. Chem.* **79,** 201–210.
26. Galbe, M. and Zacchi, G. (2002), *Appl. Microbiol. Biotechnol.* **59,** 618–628.

0273-2289/04/115/1115–1126/$25.00

Effects of Sugar Inhibition on Cellulases and β-Glucosidase During Enzymatic Hydrolysis of Softwood Substrates

ZHIZHUANG XIAO, XIAO ZHANG,[†]
DAVID J. GREGG, AND JOHN N. SADDLER[*]

Forest Products Biotechnology, University of British Columbia, 4033-2424 Main Mall, Vancouver BC, V6T 1Z4 Canada, E-mail: saddler@interchg.ubc.ca

Abstract

A quantitative approach was taken to determine the inhibition effects of glucose and other sugar monomers during cellulase and β-Glucosidase hydrolysis of two types of cellulosic material: Avicel and acetic acid–pretreated softwood. The increased glucose content in the hydrolysate resulted in a dramatic increase in the degrees of inhibition on both β-Glucosidase and cellulase activities. Supplementation of mannose, xylose, and galactose during cellobiose hydrolysis did not show any inhibitory effects on β-Glucosidase activity. However, these sugars were shown to have significant inhibitory effects on cellulase activity during cellulose hydrolysis. Our study suggests that high-substrate consistency hydrolysis with supplementation of hemicellulose is likely to be a practical solution to minimizing end-product inhibition effects while producing hydrolysate with high glucose concentration.

Index Entries: β-Glucosidase; cellulase; degree of inhibition; softwood; glucose; hydrolysate.

Introduction

The utilization of renewable lignocellulosic resource, such as wood and agricultural residues, for ethanol production provides a promising means to decrease the greenhouse effect and alleviate the shortage of fossil fuel energy *(1,2)*. An integrated lignocellulose-to-ethanol biocon-

[†]Present address: Paprican, 570 St. Jean Blvd., Pointe Claire, Quebec, H9R 3JR, Canada.

*Author to whom all correspondence and reprint requests should be addressed.

version process consists of at least the following steps: removal of lignin and hemicellulose by pretreatment, hydrolysis of cellulose to fermentable sugars, and fermentation of sugars to ethanol. The hydrolysis of cellulose to glucose has been shown to be the key step in the bioconversion of lignocellulosic biomass. Cellulose hydrolysis can be carried out by either acidic or enzymatic treatment. The maximum yields of glucose obtained from batch and bed-shrinking flow-through reactors, through acidic treatment, were about 60 and 90%, respectively, for α-cellulose *(3)*. The enzymatic process converts cellulose to glucose in high yields without sugar degradation products and has been recognized as the method of choice for future wood-to-ethanol processes *(4,5)*. However, currently, there are some limitations associated with cellulase enzymes that hinder the application of enzyme at industrial scale *(6–8)*. Unlike many other enzymes, cellulase is not a single enzyme but a family of at least three groups of enzymes: endoglucanase (EC 3.2.1.4), cellobiohydrolase (CBH) (EC 3.2.1.91), and β-Glucosidase (EC 3.2.1.21). A synergistic action among these enzymes is required to effectively break down cellulose to glucose. A typical cellulose hydrolysis pattern in a batch mode enzymatic process is characterized by a two-phase curve, with an initial logarithmic phase followed by an asymptotic phase *(9)*. A rapid release of glucose is normally observed in the initial phase with about half of the cellulose hydrolyzed in less than 24 h. On the other hand, the hydrolysis of the remaining cellulose requires more than 2 days to complete *(10)*. Several mechanisms have been proposed for this insufficient hydrolysis phenomenon *(11–13)*. However, end-product inhibition has been shown to play a major role in hindering a continuously fast hydrolysis rate *(14)*, and glucose, cellobiose, and ethanol have demonstrated significant inhibitory effects on the activity of both β-glucosidase and cellulase mixtures *(8)*.

A considerable amount of research has been carried out to elucidate the mechanism of end-product inhibition on cellulase enzyme systems during cellulose hydrolysis *(6,8)*. However, there have been few attempts to quantitatively determine the degree of sugar inhibition on the cellulase enzymes during cellulose hydrolysis. Because of the intricate nature of lignocellulosic material, most of the mechanisms proposed for pure cellulose substrates, such as Avicel, and Solka Floc, are typically not representative of what happens on these never-dried substrates with various degrees of noncellulosic contaminants *(9)*. There is also a lack of information on whether monosaccharides other than glucose will have inhibitory effects on cellulase activity during cellulose hydrolysis.

In the present study, we quantified the degree of inhibition on both β-glucosidase and cellulase mixtures by glucose and cellobiose at different concentrations. We also determined the inhibitory effects of mannose, galactose, and xylose on both β-glucosidase and cellulase activities and assessed the potential to increase the final sugar concentration by supplementing cellulosic substrate hydrolysis with hemicellulose-rich stream-obtained from steam exploded softwood (prehydrolysate).

Materials and Methods

Enzymes and Hydrolysis

The complete cellulase system (Celluclast®) and β-glucosidase (Novozym 188®) used were obtained from Novo Nordisk Biochem (Franklinton, NC). The cellulolytic activities determined in the Celluclast preparation are 121 filter paper units (FPU)/mL, and 45 cellobiase units (CBU)/mL. The activities of Novozym 188 are 570 CBU/mL and 2.0 FPU/mL. The enzyme activities were measured according to standard procedures *(15)*. All the hydrolysis experiments were conducted in 500-mL Erlenmeyer flasks at 50°C using 50 mM sodium acetate buffer (pH 4.8) with shaking at 150 rpm. The substrate consistency during acetic acid–pretreated softwood hydrolysis is 10% and the enzyme loading is 40 FPU of Celluclast®/g of cellulose supplemented with 80 CBU of β -glucosidase.

The concentration of glucose released during the hydrolysis was measured using a YSI 2700 Select Biochemistry Analyzer (Yellow Springs Instruments, Yellow Springs, OH), and the concentrations of mannose, galactose, and xylose were measured by high-performance liquid chromatography *(16)*.

Substrates and Chemicals

The sugars used as inhibitors were glucose (Sigma, St. Louis, MO), mannose (Sigma), galactose (G-0750; Sigma), and xylose (Fisher Scientific, Fair Lawn, NJ). Avicel, cellobiose, *p*-nitrophenyl-β-D-glucopyranoside (pNPG) and all the sugar monomers were obtained from Sigma. Acetic acid-pretreated softwood substrate was prepared as described previously.

Removal of End Products During Acetic Acid–Pretreated Softwood Hydrolysis Through Ultrafiltration

After 24 h and 48 h of hydrolysis, the hydrolysate was separated from the residue solids by centrifuging at 11,950*g* for 10 min. The supernatant was then filtered through a 10-kDa membrane at 4°C in a 160-mL Amicon ultrafiltration unit (Beverly, MA). Fresh buffer was added during the filtration to remove the soluble end products. The retained enzymes in the Amicon unit were added back to the solid residues, and fresh buffer was added to the initial volume without any additional enzymes.

Determination of Degree of Inhibition Caused by Sugar Monomers

The degree of inhibition was based on the ratio of the hydrolysis rates with and without the presence of supplemented sugars, V_I/V., in which V_I is the amount of glucose (g) produced from the substrate in the presence of supplemented sugars/30 min, and V is the amount of glucose (g) produced from the substrate without sugar supplementation/30 min. The hydrolysis rates were determined after 30 min of hydrolysis. The short hydrolysis period was selected to minimize the inhibitory effects of the released sugars.

Results and Discussions

Significance of End-Product Inhibition on Hydrolysis of Lignocellulosic Substrates

In an earlier work, we showed that acetic acid pulping is an effective pretreatment method for converting softwoods. The pulped substrate contained very low amounts of lignin (~5%) and hemicellulose and showed a lower degree of polymerization and crystallinity in the cellulose when compared to the raw material. The acetic acid–pretreated softwood substrate showed a greater degree of hydrolyzability to cellulase, which was superior to many other cellulosic substrates including Avicel, and steam-exploded pulp This greater digestibility enables hydrolysis at higher substrate concentrations (10–20%).

A 72-h hydrolysis profile of a 10% acetic acid–pretreated softwood substrate (Fig. 1) represents a typical enzymatic cellulose hydrolysis course with the majority of the cellulose (up to 70%) broken down within the first 24 h. However, the conversion of the remaining cellulose (~30%) was incomplete, even after another 2 d of incubation. The decrease in the hydrolysis rate in the latter phase is likely owing to accumulation of end products. To demonstrate that the end products played a major inhibitory role, we removed the produced sugar from the hydrolysate through ultrafiltration. Fresh buffer was then added to the retained protein and the residual substrate to attain the initial volume, and the hydrolysis was continued under the same condition. As shown in Fig. 1, significant increases in the hydrolysis rate were observed after the sugar removal at both 24 h and 48 h of incubation, with complete hydrolysis attained after 48 h and 60 h of incubation respectively.

Enzymatic hydrolysis of cellulose can be separated into two major steps. The first step depolymerizes and hydrolyzes cellulose into soluble cellobiose, and the subsequent step converts cellobiose to glucose by β-glucosidase. Several cellulolytic enzymes are involved in the first hydrolysis step, and the β-glucosidases are the predominant group of enzymes that carry out the latter step of the conversion. As a final product, glucose has a direct inhibitory effect on β-glucosidase activity. Kinetic studies of glucose inhibition on β-glucosidase have been an area of debate *(8),* although the actual inhibition mechanism is largely dependent on the sources of enzymes *(7,17–19)*.

In the present study, rather than try to distinguish the nature of inhibition, we tried to determine the degree of inhibition on β-glucosidase activity by adding different amounts of glucose to the hydrolysate. The inhibitory effects of several other monosaccharides, including mannose, galactose, and xylose, were also determined. The degree of inhibition was expressed by the ratio between the hydrolysis rate in the presence of possible inhibitor (V_I) and hydrolysis rate of a control cellulose hydrolysis without any sugar supplementation (V). The hydrolysis rate was calculated based on the glucose released from the substrates, pNPG—cellobiose,

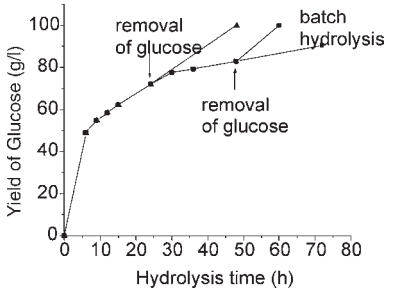

Fig. 1. Effects of glucose removal on the hydrolysis rate of acetic acid–pretreated wood.

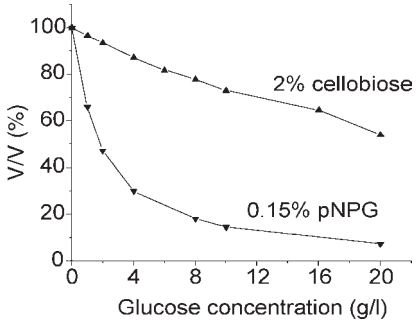

Fig. 2. Degree of Inhibition on β-glucosidase activity caused by addition of glucose during hydrolysis of cellobiose and pNPG.

Avicel, and acetic acid–pretreated softwood—after a 30-min incubation with respective enzymes.

Degree of Inhibition on β-glucosidase Activity by Different Amounts of Glucose

The degree of inhibition on β-glucosidase activity in the presence of glucose from 0 to 20 g/L was tested (Fig. 2) using two different types of substrate: pNPG and cellobiose. Although pNPG is a substrate analog to cellobiose, the pNPG assay provides a quick and simple method to determine the effect of supplemented glucose on β-glucosidase activity. However, because the measurement of sugar is based on colorimetry, only very low substrate (pNPG) concentrations, 5 m*M* (0.15% [w/v]), were used, whereas the concentration of cellobiose used in the hydrolysis was 2% (w/v). The β-glucosidase (Novozym188) loading was 80 CBU/g of the substrate, either pNPG or cellobiose. A significant inhibitory effect was observed on the hydrolysis rate even at very low glucose concentration when pNPG substrate was used (Fig. 2). The reaction rate was reduced by >80% when the glucose concentration exceeded 10 g/L. A steady decrease in the hydrolysis rate with increases in glucose concentration was also observed when cellobiose was subjected to β-glucosidase hydrolysis.

However, the degree of glucose inhibition at the same glucose concentration on the 2% cellobiose hydrolysis was less significant than that obtained on the pNPG. Since the ratio between the enzyme and the substrate is constant, higher substrate concentration means higher enzyme input. Thus, the reason for the reduced impact on inhibition, as the consistency increases, is probably owing to the higher enzyme-to-inhibitor ratio encountered in the cellobiose hydrolysis system compared with that in the pNPG hydrolysis system.

The degree of glucose inhibition on β-glucosidase activity at different substrate concentrations was further investigated. Three cellobiose consistencies were selected—2, 5, and 10%—along with a β-glucosidase loading of 80 CBU/g of cellobiose. The maximum amounts of glucose supplementation—20, 50, and 100 g/L—were chosen to correlate with the three different substrate consistencies at 2, 5, and 10%, respectively. Again, the effects of inhibition at the same glucose supplementation levels became less significant as the substrate concentration increased from 2 to 10% (Fig. 3). However, since the degree of inhibition was determined at the same enzyme-to-glucose ratio, all three experiments seemed to give similar results. The degrees of inhibition were 53, 51, and 48% correlated to 20, 50, and 100 g/L of glucose supplementation in 2, 5, and 10% cellobiose hydrolysates, respectively (Fig. 3).

Degree of Inhibition on Cellulase Activity by Different Amounts of Glucose

The degree of glucose inhibition on the cellulase activity was also determined using Avicel as a substrate. Two substrate concentrations, 2 and 10%, and glucose supplementation from 0 to 100 g/L were tested. The enzyme loading was 40 FPU (Celluclast) with 80 CBU (Novozym188)/g of cellulose. The addition of glucose resulted in significant inhibitory effects on the cellulase activity. The results agree with many previous findings *(12,20,21)*. It was interesting to find that at the same glucose supplementation, a higher degree of inhibition was observed on the cellulase activities than on the β-glucosidase (Fig. 4) at both substrate concentrations. As mentioned earlier, cellulase is a family of multiple enzymes, including at least endoglucanase, CBH, and β-glucosidase. This result seemed to indicate that the glucose may have a direct inhibitory effect on the cellulase enzymes other than just β-glucosidase. Previous research has shown that glucose has a significant impact on endoglucanase and CBH activity *(22,23)*. It has also been shown that cellobiose exhibits a greater impact than glucose on cellulase activity during cellulose hydrolysis *(6–8,24)*. It is probable that the high glucose content in the hydrolysate leads to the accumulation of cellobiose, which then acts as a secondary inhibitor. Therefore, the combined inhibitory effects have a greater impact on the overall cellulase activity than that of single sugar. Other studies have also shown that cellobiose is more inhibitory to the overall cellulase activity than is glucose *(25–27)*.

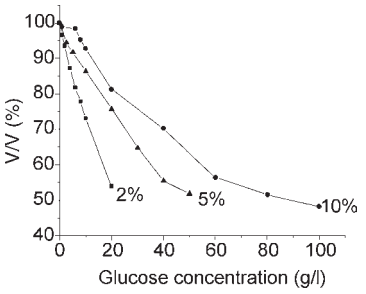

Fig. 3. Degree of Inhibition on β-glucosidase activity caused by the addition of glucose during hydrolysis of cellobiose at three different substrate concentrations: 2, 5, and 10% (w/v).

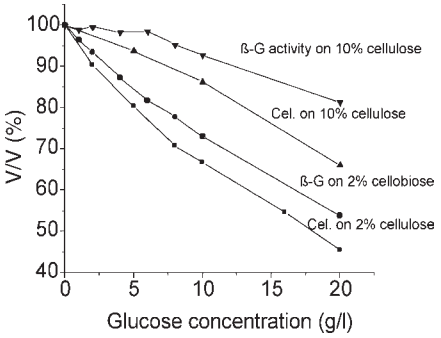

Fig. 4. Comparison of degree of glucose inhibition on cellulase and β-glucosidase activities during hydrolysis of cellulose and cellobiose at two substrate consistencies: 2 and 10% (w/v). Cel, cellulase; β-G, β-glucosidase.

Inhibitory Effects of Mannose, Galactose, and Xylose on β*-glucosidase*

Mannose, galactose, and xylose are the major monosaccharides formed in the hemicellulose-rich fraction of steam-exploded softwoods. Most of these sugars are present in the dilute water-soluble fraction after various pretreatment processes. Low ethanol concentration after the fermentation of this stream resulted in high costs associated with the subsequent evaporation and recovery process steps *(28,29)*. High sugar concentrations are desirable after enzymatic hydrolysis in order to minimize the cost of the overall bioconversion process. Cellulose hydrolysis supplemented with the hemicellulose-rich water-soluble stream obtained after steam explosion provides a potential way to enhance the final sugar concentration. Little information has been published on the inhibitory effect of hemicellulose-derived sugars on β-glucosidase and cellulase activities, although Dekker *(7)* reported a 13% decrease in β-glucosidase activity that was detected at 5% D-xylose supplementation.

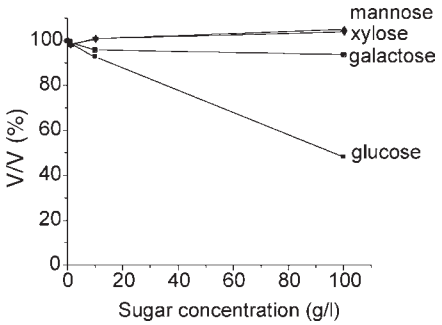

Fig. 5. Degrees of Inhibition on β-glucosidase activity caused by addition of mannose, galactose, and xylose.

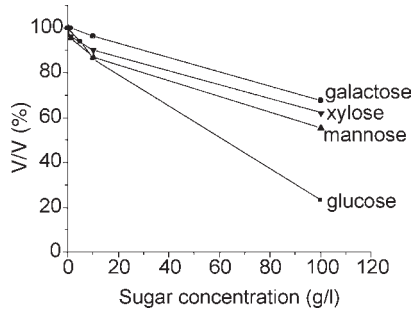

Fig. 6. Degrees of Inhibition on cellulase activity caused by addition of mannose, galactose, and xylose.

None of the monosaccharides in our study showed any observed inhibition on β-glucosidase at concentrations up to 100 g/L (Fig. 5). Other research has also shown that arabinose, galactose, mannose, and xylose were not inhibitory at concentrations up to 56 m*M (30,31)*. β-Glucosidase has been shown to be quite specific in its response to the nature of the inhibitors *(8,32)*, and β-glucosidases obtained from different origins have been shown to have different responses to these various inhibitors *(7,30,31)*.

Mannose, galactose, and xylose supplementation demonstrated significant inhibition of hydrolysis rate (Fig. 6). Hydrolysis rates decreased by 32, 38, and 45% after supplementation with galactose, xylose, and mannose, respectively, at 100 g/L. The hemicellulose-derived sugars seemed to have a direct inhibitory effect on the cellulase enzymes. The detailed inhibitory mechanisms of these sugars on the cellulase activities were not clear and are currently under investigation. However, it is likely that the mechanisms will depend on both the characteristics of the specific inhibitors and the structure of the different enzymes.

Inhibitory Effect of Synthetic Hemicellulose-Rich Water-Soluble Fraction on High-Cellulose Consistency Hydrolysis

Previous research indicated that the biomass-to-ethanol process could be more economically feasible by incorporating the hemicellulose-rich, water-soluble fraction with the enzymatic hydrolysis of the solid fraction *(14)*. We have shown that inhibitory effects caused by the hemicellulose-derived sugars were less significant than glucose. Our results also indicate that increases in substrate concentration during hydrolysis may reduce the degree of inhibition caused by the same amount of inhibitors. Since the water-soluble stream obtained after steam explosion of softwoods are typically low in sugar concentration (1–5%), we next examined the potential to enhance the effects of final sugar concentration by combining the cellulose hydrolysis stream with hemicellulose-rich water-soluble stream. A synthetic sugar mixture containing glucose, galactose, and mannose at a ratio of 1:1:3 was prepared. This mixture represents the predominant sugars derived from softwood hemicellulose, and the ratio reflects the composition of these sugars found in most softwood species *(33,34)*. Two different concentration levels, 1 and 2%, were used in combination with the 2% glucose stream.

Hydrolysis was carried out at 50°C for 48 h with an enzyme loading of 40 FPU + 80 CBU/g of cellulose. The substrate used was acetic acid pulp at a 10% substrate concentration. The yields of glucose released from the three sugar-supplemented hydrolysis samples were lower than that obtained with control sample (without any sugar addition) over the 48-h incubation time (Fig. 7). As expected, 20 g/L of glucose exhibited the strongest inhibition on the hydrolysis, followed by 20 g/L and 10 g/L of sugar supplementation in the hydrolysate. The degree of inhibition was measured over the hydrolysis period (Fig. 8), and it was apparent that the presence of 10 g/L and 20 g/L of hemicellulose sugars decreased the hydrolysis rate by 10–15% in the first hours of hydrolysis, and a 45% reduction in hydrolysis rate was observed for the sample supplemented with 20 g/L of glucose. However, as the hydrolysis proceeded, the three hydrolysis curves approached the control hydrolysis curve. After 48 hours of incubation, the rates of all four hydrolysis runs were comparable. This is probably because the inhibitory effects of the produced glucose surpassed the inhibitory effects of the supplemented sugars.

As mentioned earlier, the purpose of carrying out cellulose hydrolysis in the presence of hemicellulose-rich, water-soluble fraction was to enhance the overall sugar concentration in the final hydrolysate prior to the fermentation. When total sugar concentrations were also monitored during the 48-h hydrolysis (Fig. 9), although the supplemented sugars showed various degrees of inhibition on the hydrolysis, the total sugar concentrations present in the three sugar-supplemented hydrolysates after 48 h of hydrolysis were higher than that obtained with control. Total sugars concentrations of 101.8, 95.4, and 98.1 g/L were obtained, respectively, in the presence of the 2% hemicellulose-derived sugars, 1% hemicellulose-derived sugars, and

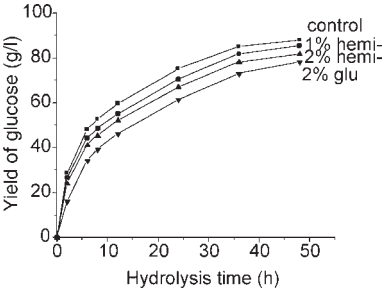

Fig. 7. Inhibitory effects of supplemented hemicellulose-derived sugars on hydrolysis of 10% acetic acid-pretreated softwood.

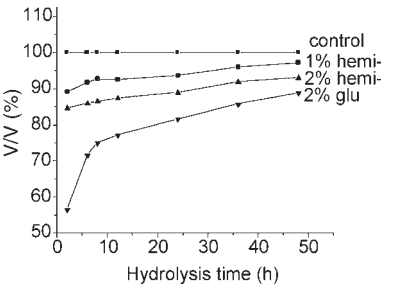

Fig. 8. Degree of Inhibition caused by supplemented hemicellulose-derived sugars on hydrolysis of 10% acetic acid-pretreated softwood.

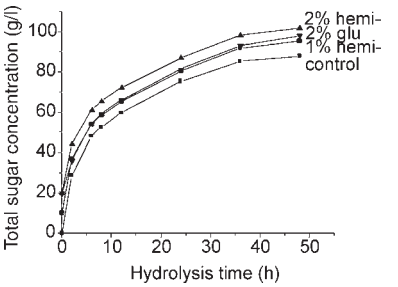

Fig. 9. Total sugar concentrations during combined hydrolysis (10% acetic acid–pretreated softwood substrate with prehydrolysate).

2% glucose-supplemented hydrolysate after 48 h of hydrolysis compared with 87.9 g/L obtained in the control hydrolysate.

Conclusions

The degree of inhibition of glucose on both β-glucosidase and cellulase activities was determined at glucose supplementation levels up to 100 g/L.

It was apparent that glucose had a greater inhibitory effect on the overall cellulase activity than it had on the β-glucosidase. Although the higher substrate concentration seemed to be able to alleviate some of the inhibitory effects at the same glucose concentrations, the degree of inhibition measured based on the same enzyme-to-inhibitor ratio was comparable. No adverse effects were detected on the β-glucosidase activity in the presence of mannose, galactose, and xylose at concentrations up to 100 g/L, and these sugars seemed to show some inhibition towards, the other cellulase components. Combining the cellulose hydrolysis with the hemicellulose sugars present in the water-soluble stream obtained from steam-exploded softwood was shown to be a promising strategy for enhancing the final sugar concentration. The results from our study suggest that high-substrate consistency hydrolysis with supplementation of hemicellulose could be a practical solution for minimizing end product-inhibition effects while producing a hydrolysate with high glucose concentration.

Acknowledgment

Funding for this work was provided by Natural Resources Canada and National Science and Engineering Research Council of Canada. We would especially wish to thank Dr. William Cruickshank for continued enthusiastic support and direction.

References

1. Galbe, M. and Zacchi, G. (2002), *Appl. Microbiol. Biotechnol*. **59,** 618–628.
2. Sun, Y. and Cheng, J. Y. (2002) *Bioresour. Technol*. **83,** 1–11.
3. Kim, J., Seok, L. Y. Y., and Torget, R. W. (2001), *Appl. Biochem. Biotechnol*. **91–93,** 331–340.
4. Duff, S. J. B. and Murray, W. D. (1996), *Bioresour. Technol*. **55,** 1–33.
5. Hsu, T. (1996), *Handbook of Bioethanol: Production and Utilization,* Wyman, C. E., ed., Taylor & Francis, Washington, DC, pp. 179–212.
6. Gusakov, A. V. and Sinitsyn, A. P. (1992), *Biotechnol. Bioeng*. **40,** 663–671.
7. Dekker, R. F. H. (1986), *Biotechnol. Bioeng*. **28,** 1438–1442.
8. Holtzapple, M., Cognata, M., Shu, Y., and Hendrickson, C. (1990), *Biotechnol. Bioeng*. **36,** 275–287.
9. Ramos, L. P., Breuil, C., and Saddler, J. N. (1993), *Enzyme Microbial. Technol.* **15,** 19–25.
10. Gregg, D. J. and Saddler, J. N. (1996), *Biotechnol. Bioeng*. **51,** 375–383.
11. Ohmine, K., Ooshima, H., and Harano, Y. (1983), *Biotechnol. Bioeng*. **25,** 2041–2053.
12. Holtzapple, M. T., Caram, H. S., and Humphrey, A. E. (1984), *Biotechnol. Bioeng*. **26,** 753–757.
13. Scheiding, W., Thoma, M., Ross, A., and Schuegerl, K. (1984), *Appl. Microbiol. Biotechnol. 20,* 176–182.
14. Tengborg, C., Galbe, M., and Zacchi, G. (2001), *Enzyme Microbial. Technol*. **28,** 835–844.
15. Wood, T. M. and Bhat, K. M. (1988), in *Methods in Enzymology*, vol. 160, Wood, W. and Kellogg, S., eds., Academic, New York, NY, pp. 87–112.
16. Boussaid, A. L., Esteghlalian, A. R., Gregg, D. J., Lee, K. H., and Saddler, J. N. (2000), *Appl. Biochem. Biotechnol*. **84–86,** 693–705.
17. Gong, C.-S., Ladisch, M. R., Tsao, G. T. (1977), *Biotechnol. Bioeng*. **19,** 959–981.
18. Montero, M. and Romeu, A. (1992), *Appl. Microbiol. Biotechnol*. **38,** 350–353.
19. Yeoh, H. H., Tan, T. K., and Koh, S. K. (1986), *Appl. Microbiol. Biotechnol*. **25,** 25–28.
20. Asenjo, J. A. (1983), *Biotechnol. Bioeng*. **25,** 3185–3190.

21. Rao, M., Seeta, R., and Deshpande, V. (1989), *Biotechnol. Appl. Biochem*. **11,** 477–482.
22. Beltrame, P. L., Carniti, P., Focher, B., Marzetti, A., and Sarto, V. (1984), *Biotechnol. Bioeng*. **26,** 1233–1238.
23. Mosolova, T. P., Kalyuzhnyi, S. V., Varfolomeyev, S. D., and Velikodvorskaya, G. A. (1993), *Appl. Biochem. Biotechnol*. **42,** 9–18.
24. Hadj-Taieb, N., Chaabouni-Ellouz, S., Kammoun, A., and Ellouz, R. (1992), *Appl. Microbiol. Biotechnol*. **37,** 197–201.
25. Murray, W. D. (1987), *Biotechnol. Bioeng. 29, 1151–1154.*
26. Breuil, C., Chan, M., and Saddler, J. N. (1990), *Appl. Microbiol. Biotechnol.* **34,** 31–35.
27. Dekker, F. F. H. and Wallis, A. F. A. (1983), *Biotechnol. Bioeng*. **25,** 3027–3048.
28. Zacchi, G. and Axelsson, A. (1989), *Biotechnol. Bioeng*. **34,** 223–233.
29. Larsson, M., Galbe, M., and Zacchi, G. (1997), *Bioresourc. Technol.* **60,** 143–151.
30. Saha, B. C., Freer, S. N., and Bothast, R. J. (1994), *Appl. Environ. Microbiol.* **60,** 3774–3780.
31. Yun, S. I., Jeong, C.-S., Chung, D.-K., and Choi, H.-S. (2001), *Biosci. Biotechnol. Biochem.* **65,** 2028–2032.
32. Klyosov, A. A., Sinitsyn, A. P., and Rabinowitch, M. L. (1980), *Enzyme Eng.* **5,** 153–165.
33. Sjostrom, E. (1981) *Wood Chemistry: Fundamentals and Applications*, Academic, San Diego, CA.
34. Fengel, D. and Wegener, G. (1984), *Wood: Chemistry, Ultrastructure, Reactions,* Walter de Gruyter, Berlin, Germany.

0273-2289/04/115/1127–1138/$25.00

Kinetics of Glucose Decomposition During Dilute-Acid Hydrolysis of Lignocellulosic Biomass

Qian Xiang,[1] Yong Y. Lee,[*,1] and Robert W. Torget[2]

[1]Department of Chemical Engineering, Auburn University, Auburn, AL 36849, E-mail: yylee@eng.auburn.edu;
[2]National BioEnergy Center, National Renewable Energy Laboratory, 1617 Cole Boulevard., Golden, CO 80401

Abstract

Recent research work in-house both at Auburn University and National Renewable Energy Laboratory has demonstrated that extremely low concentrations of acid (e.g., 0.05–0.2 wt% sulfuric acid) and high temperatures (e.g., 200–230°C) are reaction conditions that can be effectively applied for hydrolysis of the cellulosic component of biomass. These conditions are far from those of the conventional dilute-acid hydrolysis processes, and the kinetic data for glucose decomposition are not currently available. We investigated the kinetics of glucose decomposition covering pH values of 1.5–2.2 and temperatures of 180–230°C using glass ampoule reactors. The primary factors controlling glucose decomposition are the reaction medium, acid concentration, and temperature. Based on the experimental data, a kinetic model was developed and the best-fit kinetic parameters were determined. However, a consistent discrepancy in the rate of glucose disappearance was found between that of the model based on pure glucose data and that observed during the actual process of lignocellulosic biomass hydrolysis. This was taken as an indication that glucose recombines with acid-soluble lignin during the hydrolysis process, and this conclusion was incorporated accordingly into the overall model of glucose decomposition.

Index Entries: Reaction kinetics; glucose decomposition; dilute acid hydrolysis; kinetic modeling; acid-soluble lignin; acid-base catalysis rules.

Introduction

Saccharification of cellulosic biomass by dilute acid has a much longer history than the enzymatic process. The initial acid-catalyzed wood saccharification was in operation in Germany as early as the 1940s *(1)*. In recent

*Author to whom all correspondence and reprint requests should be addressed.

years, however, treatment of lignocellulosic biomass with dilute H_2SO_4 has been primarily used as a means of pretreatment for enzymatic hydrolysis of cellulose. A concerted research and development effort was phased into the enzymatic hydrolysis process owing to its potential to convert cellulose to glucose nearly quantitatively *(2–3)*. Despite the diminished interest in acid technology, there has been a continual research effort on the subject and a significant advance has also been made in this area *(4)*, including the study of various reactor configurations. The fundamental knowledge and chemistry of biomass processing are still a focus of research interest today. There have also been new developments in kinetic investigations, with the exploration of a broader range of reaction conditions in terms of temperature and acid concentration *(5)*. These activities have contributed to a phenomenal improvement in dilute-acid hydrolysis technology, making it competitive with the enzymatic process *(4)*.

The primary challenge for dilute-acid hydrolysis processes is how to raise glucose yields higher than 70% in an economically viable industrial process while maintaining a high cellulose hydrolysis rate and minimizing glucose decomposition. Percolation reactors have been used in most of the wood sugar processes. Glucose yields of 45–55% and 2–4 wt% sugar concentrations have been generally reported *(1,6–7)*. A significant fraction of the glucan is unaccounted for when the yield is compared with the prediction of percolation process based on two consecutive pseudo-first-order hydrolysis kinetic models developed by Saeman *(8)*. The goal of our research effort was to elucidate the underlying chemistry that limits the yield of glucose in the dilute-acid hydrolysis process.

There have been several improvements to Saeman's original kinetic pattern, and these new models were developed to elucidate the outcomes from actual dilute-acid operations. The explanations for low yields include the following: First, once glucose is formed under reaction conditions, it can be derivatized and/or degraded at a significant rate *(9)*. Second, cellulose has been chemically altered after about 70% conversion *(10)*. Third, 30% of the hydrolyzed cellulose gives rise to oligomers which cannot be converted to glucose *(11)*. These kinetic models predict that glucose yields higher than 65–70% are not attainable using dilute H_2SO_4 for both batch and flow-through type reactors. However, Torget et al. *(12)*, using a simulated countercurrent shrinking-bed reactor system for the aqueous fractionation of yellow poplar, have produced glucose yields higher than 85% by applying 0.07% (w/w) H_2SO_4 and 225°C. The same results have been reproduced in our laboratory. These findings cannot be explained by previously published kinetic models. Further investigation is needed to verify the kinetic pattern and to provide an explanation for the high yields of glucose obtained.

We have therefore studied the kinetics of cellulose hydrolysis and glucose decomposition under extremely dilute H_2SO_4 (0.05–0.2 wt%, pH 1.5–2.2) and high-temperature (200–230°C) conditions. Our ultimate goal is to better understand the kinetics of dilute-acid hydrolysis of biomass and develop promising acid hydrolysis processes that can give both high

glucose yields and sugar concentrations. In the present study, we examined glucose decomposition in both pure solution and hydrolysate liquor medium. An additional pathway for glucose disappearance may exist through the reattachment reaction between glucose and acid-soluble lignin (ASP). In studying "dilute" H_2SO_4 hydrolysis, previous researchers commonly used acid concentration of 0.4 wt% to 1 to 2 wt% *(8,9,13)*. However, those conditions require the use of exotic alloys in the construction of the hydrolysis reactor in order to ensure corrosion resistance. In addition, the higher the acid concentration, the more gypsum is produced owing to lime input for neutralization. The extremely low-acid conditions used in our research work allow the use of lower-cost alloys for the construction of industrial-scale reactors and also reduce the amount of gypsum. Additionally, Zucher-Hammet plots of cellobiose hydrolysis *(14)* and glucose degradation *(15)* indicated that an acid concentration equivalent to a pH (measured at ambient conditions) of 2.2 would favor higher glucose yields.

Materials and Methods

Chemicals and Substrate

All chemicals were purchased from Sigma-Aldrich. d-(+)-Glucose has the product no. G-8270 and lot no. 89H0150, with 99.5% minimum content. α-Cellulose (product no. C8002) contained 92.2% glucan, 3.4% xylan, and 3.2% mannan on dry basis. The ash content was negligible. *Liriodendron tulipifera* L. (yellow poplar) sawdust substrate was provided by the National Renewable Energy Laboratory (NREL) and was used to generate prehydrolysate solution containing ASL. The chemical composition of a representative yellow poplar sample was 42.8 wt% glucan, 14.8 wt% xylan, 2.5 wt% mannan, 0.9 wt% galactan, 0.5% arabinan, 24.3 wt% Klason lignin, 2.8 wt% ASL, and 0.7 wt% ash content based on samples dried at 45°C for over night.

Experimental Apparatus and Procedures

Glucose decomposition studies were conducted in glass ampoule reactors made from 7-mm (Pyrex) glass tubing with a capacity of 2.0 mL. Ampoules were charged with 1 mL of 0.125 *M* glucose solution, sealed, and reacted in a thermostatically controlled bath. The heat transfer tests showed that the contents in the ampoules reached the bath temperature in about 1 min. A correction time of 0.3 min was applied to all the results to compensate for this short warm-up period. After the reaction, the ampoules were quenched in a second bath of cold water, and the contents of the ampoules were collected for analysis by breaking one end and transferring the reacted solutions to vials. The solutions were then analyzed directly by high-performance liquid chromatography (HPLC) for glucose and other components.

Analytical Methods

When aqueous and solid samples were analyzed for moisture and content of sugars, lignin and other chemicals, the procedures described in the NREL Chemical Analysis & Testing Standard Procedure LAP no. 001-014 *(16)* were followed. The analysis of aqueous samples was carried out by two HPLC units: a Bio-Rad (Hercules, CA) Aminex HPX-87P column for analysis of sugars, and a Bio-Rad Aminex HPX-87H column for analysis of acid and other compounds, respectively. Samples were run at 65°C and eluted at 0.6 mL/min with 5 m*M* H_2SO_4 for the HPX-87H column, and 85°C and 0.55 mL/min with pure water for the HPX-87P column.

Results and Discussion

Glucose Decomposition Profile and Rate Constant

Figure 1 shows the profiles of glucose disappearance and the formation of decomposition products at 200°C with an initial pH of 1.8 (0.1 wt% H_2SO_4) and 0.125 *M* concentration of glucose. The major products of glucose decomposition that were identified by HPLC included hydroxymethulfurfural (HMF), 1,6-anhydroglucose, levulinic acid, and formic acid. Other products in the liquor included fructose, cellobiose, acetic acid, humic solid (precipitates), and other gaseous products. When the experimental data for the logarithm of the glucose concentration were plotted with time, a linear relationship was observed. The decomposition rate of glucose at constant temperature and pH is regarded as a pseudo-first-order reaction. Generally, the Arrhenius equation and acid-base catalysis rules are applied to glucose decomposition *(17)*:

$$k^{\mathrm{Glu}} = \left[k_{\mathrm{H_2O}} + k_{\mathrm{H^+}} \times \left(\mathrm{H^+}\right)\ \mathrm{k}_{\mathrm{OH^-}} \times \left(\mathrm{OH^-}\right)\right] \times \exp\left(-\frac{E^{\mathrm{Glu}}}{RT}\right) \qquad (1)$$

in which k^{Glu} is the first-order rate constant for glucose degradation, E^{Glu} is the activation energy, T is the reaction temperature, and R is the gas constant. By acid-base catalysis rules, the preexponential factor comprises three major parts: acid factor (k_{H+}), base factor (k_{OH-}), and solvent factor (k_{H2O}), respectively.

A series of experiments were conducted under various temperatures and pH conditions, and the decomposition profiles were obtained accordingly. The effect of pH on the decomposition is shown in Fig. 2. Surprisingly, the rate of glucose decomposition is found to level off within the pH range of 2.2–7.0, where the decomposition rates are almost identical. This indicates that the solvent term (equal to solvent factor) is the dominance factor of decomposition because the change in pH does not have much of an effect on the overall rate constant. Thus, the acidic term (equal to acid factor times concentration of H^+) has very little effect on overall decomposition, and so does the base term (equal to base factor times OH^-) within this pH range. An SAS nonlinear regression program was then formulated to

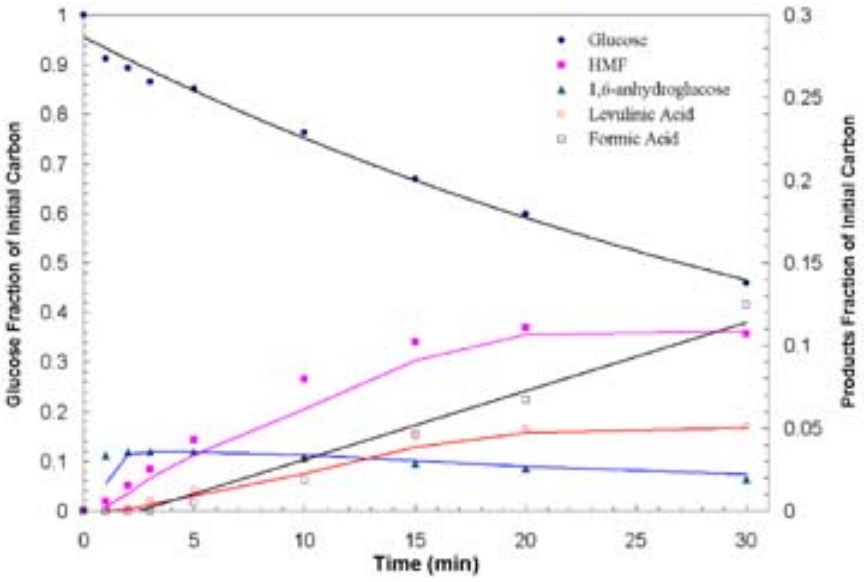

Fig. 1. Profiles of glucose disappearance and formation of decomposition products (under conditions of 200°C, initial 0.125 *M* glucose concentration, and pH 1.8)

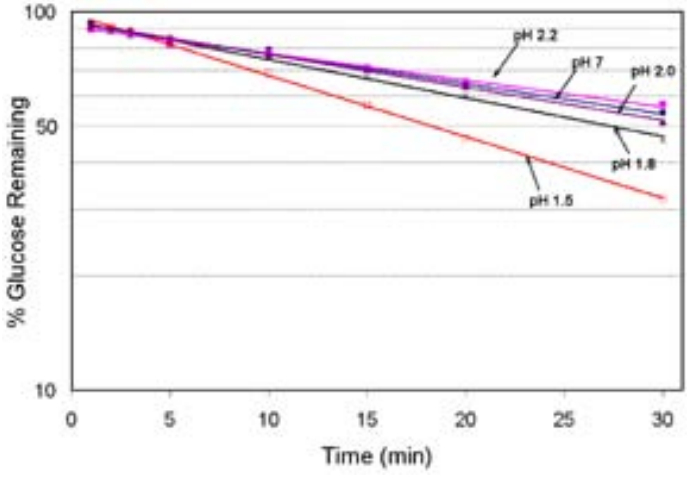

Fig. 2. Profiles and trend lines of glucose decomposition at various pH values and 200°C.

determine the kinetic parameters of Eq. 1 for glucose decomposition in acidic conditions ignoring the effect of OH^- term. The best-fit kinetic parameters give the complete Arrhenius equation in the acidic medium, shown as follows:

$$k^{\mathrm{Glu}} = \left(2.132 \times 10^{13} + 2.148 \times 10^{15} \times 10^{-\mathrm{pH}}\right) \times \exp\left(-\frac{139{,}000}{RT}\right) \qquad (2)$$

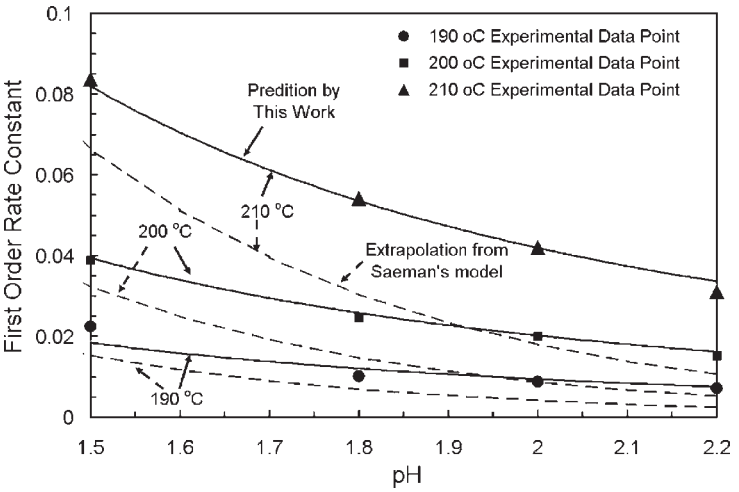

Fig. 3. Rate constants experimentally determined and calculated by proposed model and Saeman's (1945) model under conditions of pH 1.5–2.2 and 190–210°C.

Rate constants (min^{-1}) were calculated by Eq. 2 for given pH values and temperatures. The simulation results were found to be quite consistent with the experimental data as shown in Fig. 3. The estimated activation energy for glucose decomposition, 139 kJ/mol, is consistent with the previously reported data of McKibbins et al. *(17)*, 137 kJ/mol, which was determined from glucose decomposition for a temperature range of 140–250°C and a higher pH region than for our work. At 180–230°C, the glucose decomposition rate approximately doubled for every 10°C increase. Figure 3 also compares the experimental data with the predictions of this model and that of Saeman. The kinetic model developed by this work can accurately predict the first-order rate constants under acidic conditions, especially in extremely low acid concentration ranges (e.g., pH 1.5–2.2). Saeman's model, however, underestimates the rate constants because it ignores the solvent term in decomposition kinetics. When acid concentration is increased (pH is decreased), the trend lines of the two kinetic models eventually merged. This means that the solvent term is less important than the acid term and can thus ignored at high acid concentration range, which is what Saeman's model assumed.

Reversible Reaction in Glucose Decomposition

From the experimental results in Figs. 1 and 2, the first-order reaction trend lines could not be traced back to the origin (time at 0 and a glucose fraction at 1) on extrapolation. This phenomenon can be observed in most previously reported data. It indicates that the reversible reactions are much faster than irreversible glucose decomposition and equilibrium is attained at early phase of the reaction. Conner et al. *(9)* suggested an

extended kinetic model for glucose decomposition and cellulose hydrolysis that incorporates the reversible reactions of glucose.

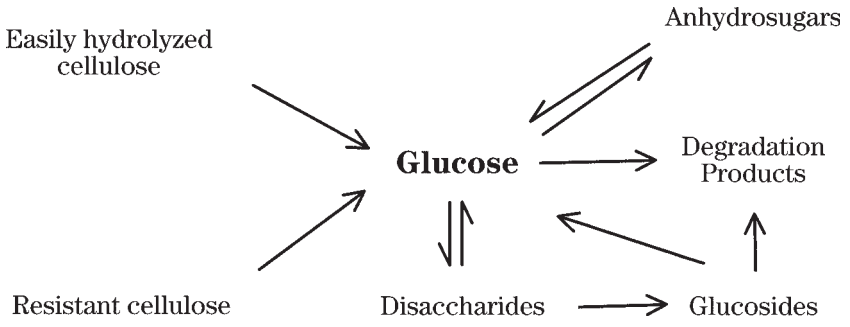

Conner's Hydrolysis Model

A complicated mathematic model was also developed for cellulose saccharification that includes glucose decomposition, reversible reactions, and disaccharide dehydration. With the implementation of the modified kinetic model, such as inclusion of the reversible reactions with 1,6-anhydrosugars and disaccharides, the fit of experimental data to the predicted model has been greatly improved. A number of researchers who have conducted mechanistic studies of glucose reactions in aqueous solutions found that the isomerization of glucose to fructose (and mannose) was found to be an important reaction pathway, especially under extremely low acid or pure-water conditions *(18)*. Fructose itself is also subject to decomposition and other reversible reactions after being formed from glucose through the reversible isomerization reactions. If one adds these reversible isomerization reaction pathways to the kinetic model in the above scheme, along with the decomposition of the fructose pathway, a more complicated kinetic model is expected.

Assuming that the glucose decomposition reaction (excluding all reversible reactions) follows first order kinetics, certain conclusions can be drawn from the glucose residual profiles of the actual experimental data. First, the overall reversible reactions, including isomerization and dehydration, have a much greater reaction rate than glucose decomposition, and equilibrium is reached at the early phase of the reaction. Second, straight lines are obtained once the equilibria are established. This indicates that the components produced from the reversible reaction are also subject to decomposition, which occurs at approximately the same reaction rate level as glucose decomposition. This ensures the first-order reaction nature of the decomposition reaction. Third, acid concentration and temperature will affect both the glucose decomposition rate and the reversible reactions rate. Based on these conclusions, we propose a simplified mathematical model for the glucose decomposition mechanism, which is discussed in the next section.

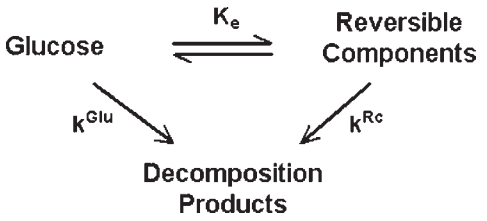

Fig. 4. Simplified kinetic model for glucose decomposition.

Kinetic Model for Glucose Decomposition Involving Reversible Reactions

Figure 4 shows the scheme of a simplified kinetic model for glucose decomposition involving reversible reactions. It was developed based on following assumptions: First, all reversible reactions are combined into one reaction with a single equilibrium constant, K_e. Second, since the reversible reaction is very rapid, equilibrium is attained instantly. Third, reversible components are also subject to degradation at the same rate level as glucose. Therefore, the reversible reaction does not affect the first-order reaction pattern of glucose disappearance once the equilibrium is established. Fourth, both the rate constant k^{Glu} and equilibrium constant K_e are functions of pH and temperature. In acidic conditions, they are governed by both Arrhenius equation and general acid-base catalysis rules. Therefore, reaction kinetics are expressed by the following equations, omitting the term for hydroxyl ion (OH^-) under the acidic conditions:

$$k^{Glu} = \left[K_{H_2O} + K_{H^+}\left(H^+\right)\right] \times \exp\left(-\frac{E^{Glu}}{RT}\right) \tag{3}$$

$$k_e = \left[K_{e_{H_2O}} + K_{e_{H^+}}\left(H^+\right)\right] \times \exp\left(-\frac{\Delta H}{RT}\right) \tag{4}$$

And the glucose profile is expressed from the model as follows:

$$\frac{Glu}{Glu_0} = \frac{\exp\left(-K^{Glu} \times t\right)}{\left(1 + K_e\right)} \tag{5}$$

in which Glu_0 is the initial glucose concentration. Best-fit kinetic parameters within the pH range of 1.5–2.2, as determined by SAS nonlinear regression analysis, are as follows:

$$k^{Glu} = \left[2.132 \times 10^{13} + 2.148 \times 10^{15} \times \left(H^+\right)\right] \times \exp\left(\frac{-139{,}000}{RT}\right) \tag{6}$$

$$k_e = \left[1.2531 - 35.37 \times \left(H^+\right)\right] \times \exp\left(\frac{-10{,}640}{RT}\right) \tag{7}$$

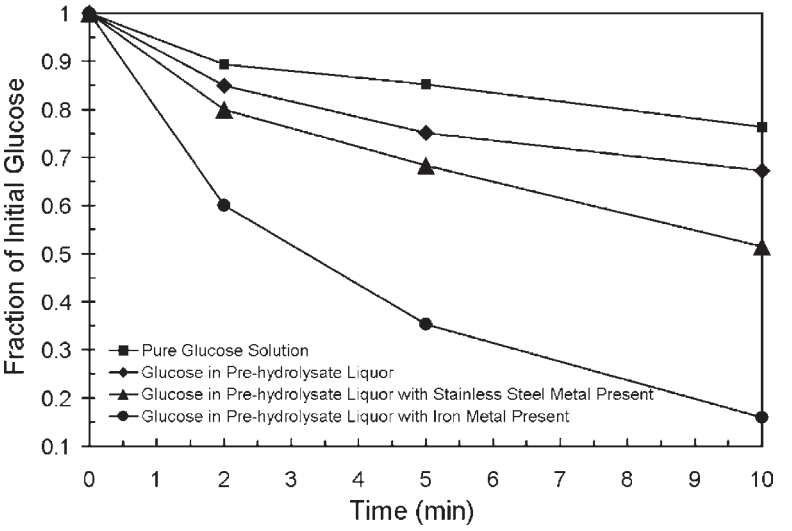

Fig. 5. Glucose decomposition affected by presence of ASL and by presence of metals.

This model includes the reversible reaction pathways, which predict the glucose decomposition behavior better than the pseudo-first-order kinetic model, especially when both pH and temperature are high. Because of the reversible decomposition reactions, under the conditions applied in this investigation (200°C and pH 1.5–2.2) and with the use of percolation or shrinking-bed reactors, this model predicts that there is 4–8% glucose loss owing to reversible reactions (after liberation from biomass). We note that the kinetic parameters determined in this work may not be applied to high pH region.

Other Factors Affecting Glucose Decomposition

To study how other factors affect glucose decomposition during the biomass hydrolysis process, reaction media are made up with biomass-prehydrolysis liquor, which contains ASL, to simulate glucose decomposition of lignocellulosic biomass. The results are summarized in Fig. 5. The data indicate that glucose undergoes faster decomposition in prehydrolyzed acidic liquor than in pure acidic medium. We believe that this is caused by an additional glucose degradation pathway through a recombination reaction with ASL. Additional evidence for this is presented in our previous research *(19)*. With ASL in the acidic medium, the presence of protons causes formation of reactive intermediates of various types such as protonized glucose. They would have high affinity for any positively charged molecules including nucleophilic reaction partners. This system is primarily involved as a reaction partner in lignin fragmentation or lignin condensation reactions, depending on the type of the

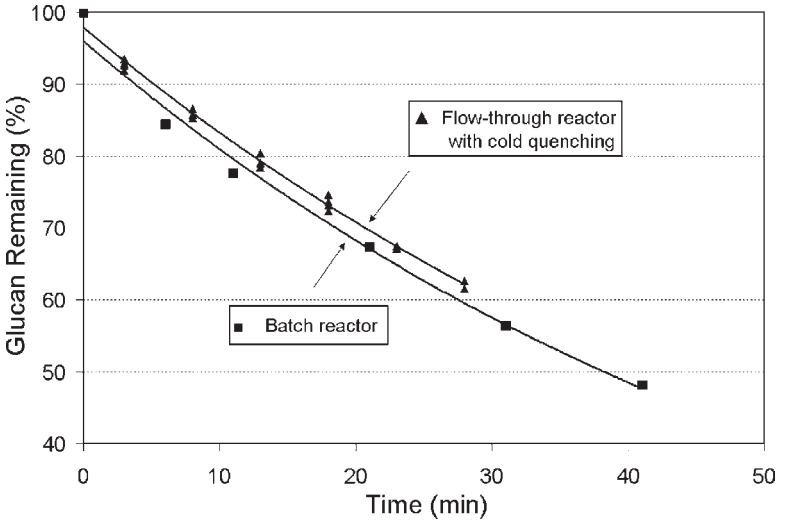

Fig. 6. Comparison of hydrolysis of α-cellulose at 205°C, pH 2.2 between batch and flow-through reactors.

active nucleophile *(20)*. Thus, the active sites on ASL will lead to the combination reaction between ASL and glucose or oligomers as follows:

$$\text{ASL} + \text{Glucose} \rightarrow \text{ASL-Glucose}$$
$$\text{ASL} + \text{Oligomer} \rightarrow \text{ASL-Oligomer}$$

This provides an explanation for the unaccounted glucose loss during the acid hydrolysis process. It also gives an explanation for the generally low yield for dilute acid hydrolysis processes and previously unclosed carbon mass balance.

More evidence exists for the combination of glucose with ASL. After comparing the hydrolysis performance in different reactor systems, Torget et al. *(21)* reported that the observed kinetics of biomass hydrolysis could be much different for various reactor configurations, and the difference is indeed phenomenal. A flow-through reactor with yellow poplar as feedstock exhibits a hydrolytic reaction rate two to three times that of a batch reactor, whereas about two-thirds of the total lignin is dissolved into the liquid during both types of processing. However, when nonlignin feedstocks such as α-cellulose are subjected to the same comparison, very little difference in hydrolysis rate is found as shown in Fig. 6. The rate constants are 0.0171 min^{-1} for the batch reactor and 0.0162 min^{-1} for the flow-through reactor under the same hydrolysis conditions. The principal molecular mechanism of acid-catalyzed hydrolysis of cellulose (cleavage of β-1-4-glycosidic bond) has been described to proceed in three steps. The reaction starts with a proton from the acid interacting rapidly with the glycosidic oxygen linking two sugar units, forming a conjugate acid. The cleavage of the C–O bond and breakdown of the conjugate acid to the

cyclic carbonium ion then takes place, which adopts a half-chair conformation. After a rapid addition of water, free sugar and a proton are liberated *(22–25)*. The formation of the intermediate carbonium ion takes place more rapidly at the end than in the middle of the polysaccharide chain. When ASL is presented in the reaction medium at high temperature, it combines with oligomers at the reducing end, thus preventing the formation of such carbonium ion. The hydrolysis rate with yellow poplar in a batch reactor is therefore slowed down. The lignin can be effectively removed in a flow-through reactor and a higher hydrolysis rate is obtained. Since α-cellulose does not contain lignin, the exhibited hydrolysis rates are identical in both batch and flow-through reactors under the same conditions.

Experimental runs have also been conducted in the presence of different metals to demonstrate how various metals for the construction of industrial hydrolysis reactors may affect the overall degradation of glucose during the real process of biomass dilute-acid hydrolysis. The glucose decomposition profiles in the presence of stainless steel (S.S.) and iron are also presented in Fig. 5. Comparing four different metals, we found that copper and Hastelloy C-276 have very little effect on glucose decomposition, whereas stainless steel has a significant effect. Most notably, iron has the strongest impact on glucose decomposition, causing a very fast disappearance of residual glucose in the reaction medium.

Conclusion

The kinetic pattern for glucose decomposition is affected by many factors, including the reaction medium, reactor configuration, and temperature. Based on glucose decomposition kinetic data obtained from glass ampoule reactors, a simplified kinetic model was developed taking all reversible pathways into consideration. The best-fit parameters were determined by nonlinear regression analysis. However, the glucose decomposition rate in actual hydrolysis processes is found to be faster than the predictions based on the kinetic model obtained from ampoule glass reactors. A new pathway for glucose disappearance through a combined reaction between glucose and ASL is believed to be partly responsible for previously unaccounted for glucose decomposition. Metal and/or metal ions can also catalyze glucose decomposition; thus, the material used in the construction of reactor must be carefully selected.

The kinetic model established by our work can accurately predict the rate constants of glucose decomposition over a broad range of acid concentrations including extremely low acid conditions (pH 1.5–2.2) in which Saeman's model fails to hold.

Acknowledgments

This research was sponsored by the US Department of Energy under Cooperative Agreement DE-FC36-01GO11072, and by National Renewable Energy Laboratory under subcontract ACO-1-31003-01.

References

1. Faith, W. L. (1945), *Ind. Eng. Chem. Res.* **37,** 1–9.
2. Wyman, C. E. (1994), *Bioresour. Technol*. **50,** 3–16.
3. van Walsum, P., Allen, S. G., Laser, M. S., Spencer, M. J., Antal, M. J., and Lynd, L. R. (1996), *Appl. Biochem. Biotechnol*. **57/58,** 157–170.
4. Lee, Y. Y., Iyer, P., and Torget, R. W. (1999), *Adv. Biochem. Eng.* **65,** 93–115.
5. Torget, R. W., Hayward, T. K., Hatzis, C., and Philippidis, G. P. (1995), in *17th Symposium on Biotechnology for Fuels and Chemicals*, Vail, Co.
6. Gilbert, N. G., Hobbs, I. A., and Levine, J. D. (1952), *Ind. Eng. Chem.* **44,** 1712.
7. Harris, E. E. (1949), *Adv. Carbohydr. Chem.* **4,** 153–188.
8. Saeman, J. F. (1945), *Ind. Eng. Chem. Res*. **37,** 43–52.
9. Conner, A. H., Wood, B. F., Hill, C. G., and Harris, J. F. (1986), in *Cellulose: Structure, Modification and Hydrolysis*, Young, R. A. and Rowell, R. M., eds., John Wiley and Sons, New York, NY, pp. 281–296.
10. Bouchard, J., Abatzoglou, N., Chornet, E., and Overend, R. P. (1989), *Wood Sci. Technol*. **23,** 343–355.
11. Mok, W. S., Antal, M. J., and Varhegyi, G. (1992), *Ind. Eng. Chem. Res.* **31**, 94–100.
12. Torget, B., Nagle, N., Hayward, T. K., and Elander, R. (1997), in *19th Symposium on Biotechnology for Fuels and Chemicals,* Colorado Springs, CO.
13. Harris, J. F., Baker, A. J., Connor, A. H., Jeffries, T. W., Minor, J. L., Pettersen, R. C., Scott, R. C., Springer, E. L., Wegner, T. H., and Zerbe, J. L. (1985), *General Technical Report FPL-45*, US Department of Agriculture Forest Products Laboratory, Madison, WI.
14. Bobleter, O., Schwalk, W., Concin, R., and Binder, H. (1986), *J. Carbohyd. Chem*. **5(3),** 387–399.
15. Popoff, T. and Theander, O. (1976), *Acta Chem. Stand.* **30,** 397–402.
16. Ehrman, C., Ruiz, R., Templeton, D., Adney, W. S., Baker, J. D., and Hsu, D. (1995), *Chemical Analysis & Testing Standard Procedure, LAP no. 001–014*, National Renewable Energy Laboratory, Golden CO.
17. McKibbins, S. W., Harris, J. F., Saeman, J. F., and Neill, W. K. (1962), *Forest Prod. J.* **12,** 17.
18. Kabyemela, B. M., Adschiri, T., Malaluan, R. M., and Arai, K. (1999), *Ind. Eng. Chem. Res.* **38(8),** 2888–2895.
19. Xiang, Q., Kim, J. S., and Lee, Y. Y. (2003), *Appl. Biochem. Biotechnol*. **105–108,** 337–352.
20. Fengel, D. and Wegener, G. (1984), *Wood—Chemistry, Ultrastructure, Reactions*. Walter de Gruyter, Berlin, Germany.
21. Torget, R. W., Kim, J. S., and Lee, Y. Y. (2000), *Ind. Eng. Chem. Res.* **39,** 2817–2825.
22. Shafizadeh, F. (1963), *TAPPI* 46, 381–383.
23. Timell, T. E. (1964), *Can. J. Chem. 42*, 1456–1472.
24. Harris, J. F. (1975), *Appl. Polym. Symp*. **28,** 131–144.
25. Philipp, B., Jacopian, V., Loth, F., Hirte, W., and Schulz, G. (1979), in *Hydrolysis of Cellulose: Mechanisms of Enzymatic and Acid Catalysis*, Adv. Chem. Ser. 181, Brown, Jr. R. D. and Jurasek, L., eds., American Chemical Society, Washington, DC, pp. 127–143.

0273-2289/04/115/1139–1159/$25.00

Conversion of Distiller's Grain into Fuel Alcohol and a Higher-Value Animal Feed by Dilute-Acid Pretreatment

Melvin P. Tucker,*[,1] Nicholas J. Nagle,[1] Edward W. Jennings,[1] Kelly N. Ibsen,[1] Andy Aden,[1] Quang A. Nguyen,[1] Kyoung H. Kim,[2] and Sally L. Noll[3]

[1]National Renewable Energy Laboratory, National Bioenergy Center, Bioprocess Engineering Group, 1617 Cole Boulevard, Golden, CO 80401, E-mail: melvin_tucker@nrel.gov; [2]Department of Food Science, Korea University, Seoul 136-701, S. Korea; and [3]Animal Science Laboratory, 405B Haecker Hall, University of Minnesota, 1364 Eckles Avenue, St. Paul, MN 55108-6118

Abstract

Over the past three decades ethanol production in the United States has increased more than 10-fold, to approx 2.9 billion gal/yr (mid-2003), with ethanol production expected to reach 5 billion gal/yr by 2005. The simultaneous coproduction of 7 million t/yr of distiller's grain (DG) may potentially drive down the price of DG as a cattle feed supplement. The sale of residual DG for animal feed is an important part of corn dry-grind ethanol production economics; therefore, dry-grind ethanol producers are seeking ways to improve the quality of DG to increase market penetration and help stabilize prices. One possible improvement is to increase the protein content of DG by converting the residual starch and fiber into ethanol. We have developed methods for steam explosion, SO_2, and dilute–sulfuric acid pretreatment of DG for evaluation as a feedstock for ethanol production. The highest soluble sugar yields (~77% of available carbohydrate) were obtained by pretreatment of DG at 140°C for 20 min with 3.27 wt% H_2SO_4. Fermentation protocols for pretreated DG were developed at the bench scale and scaled to a working volume of 809 L for production of hydrolyzed distiller's grain (HDG) for feeding trials. The pretreated DG was fermented with *Saccharomyces cerevisiae* D_5A, with ethanol yields of 73% of theoretical from available glucans.

*Author to whom all correspondence and reprint requests should be addressed.

The HDG was air-dried and used for turkey-feeding trials. The inclusion of HDG into turkey poult (as a model non-ruminant animal) diets at 5 and 10% levels, replacing corn and soybean meal, showed weight gains in the birds similar to controls, whereas 15 and 20% inclusion levels showed slight decreases (–6%) in weight gain. At the conclusion of the trial, no negative effects on internal organs or morphology, and no mortality among the poults, was found. The high protein levels (58–61%) available in HDG show promising economics for incorporation of this process into corn dry-grind ethanol plants.

Index Entries: Distiller's grain; corn dry-grind; pretreatment; enzymatic hydrolysis; ethanol; animal feed.

Introduction

Seventy-four ethanol plants were in operation in the United States in mid-2003, with nearly sixteen more expected to come on line by the end of 2004 *(1)*. The majority of these new plants are corn dry-grind ethanol plants. Approximately 2.5–2.7 gal of ethanol, 17.5 lb of dried distiller's grain (DDG), and 17 lb of carbon dioxide are produced from each bushel of corn processed through a corn dry mill *(2)*. Since 1980, process improvements in enzymes, thermal-tolerant yeasts, molecular sieves, and cogeneration have achieved a 50% reduction in the energy required to produce ethanol from corn *(2)*. Further improvements in efficiencies and reductions in production costs can be expected in the future.

Currently 3.8 million t of distiller's grain (DG) per year is produced as a coproduct of corn dry mill ethanol production. This amount is expected to rise to 7 million t/yr when ethanol production reaches 5 billion gal/yr in 2005 *(3)*. The present DDG and distiller's dried grain with solubles (DDGS) animal feed markets are not expected to absorb these increases without erosions of price and profit margins. The resultant loss in income will affect the economic viability of both current and future dry mills. The primary use of DG residues (DDG and DDGS) is in feed formulations for dairy and beef cattle. However, a higher-protein and lower-fiber-content DG residue would allow the market to expand by penetrating the swine and poultry feed markets. Converting the residual starch and fiber into DG for ethanol production would raise ethanol yields and result in hydrolyzed distiller's grain (HDG) residues with a higher protein content. HDG would compete with soybean meal in animal feed markets, provided that the high protein content is of a high-quality, digestible protein. The increase in ethanol yield is also a significant benefit to corn dry-grind operators because corn costs represent a significant portion of the production costs for a gallon of ethanol.

Acceptance of DDG and DDGS products as animal feed supplements is limited by the variable "quality" of DDG and DDGS among ethanol plants and the relatively low crude protein content *(4)*. This variability is caused by differing amounts of residual starch and crude protein in DG products. Crude protein content depends in part on preserving protein during the drying step. A study conducted by the Department of Animal

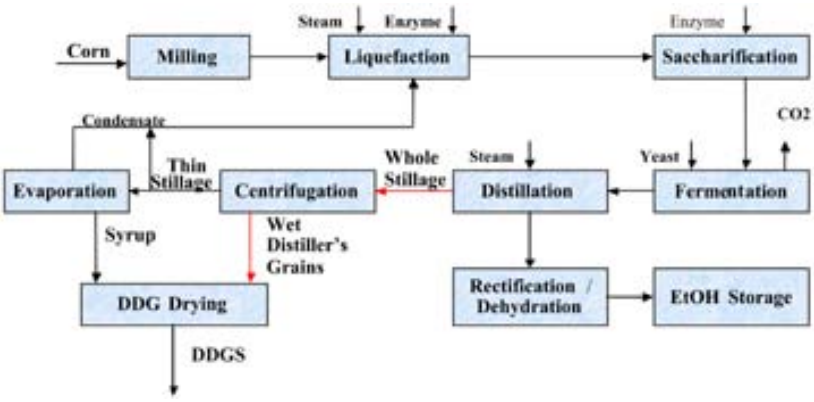

Fig. 1. Process flow diagram for typical dry-grind ethanol process.

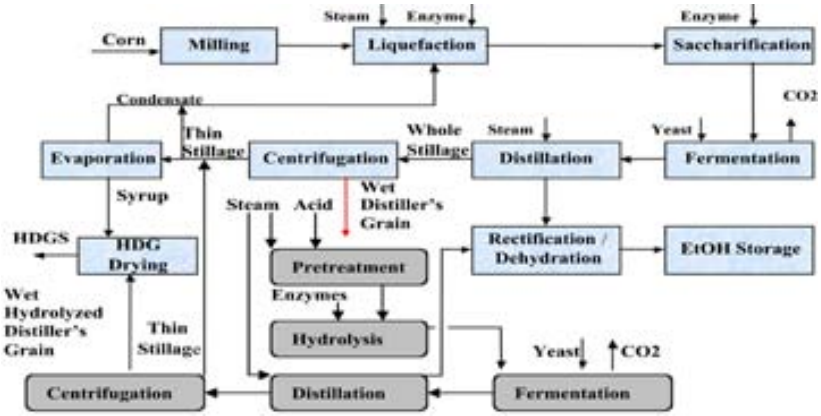

Fig. 2. Dry-grind process with pretreatment option for production of HDG.

Sciences at the University of Minnesota comparing six Minnesota dry mill ethanol plants concluded that crude protein content of DDG and DDGS ranged from 28.7 to 31.6 % *(4)*. Additional findings from this study confirm that the lysine, phosphorous, and fat content of DDG or DDGS vary considerably among the corn dry-grind ethanol producers. Crude protein content is one of the currently accepted baseline indicators for essential amino acid content *(4)*. As a result, quality control (QC) programs for DG residues that include protein content have begun to be implemented in several dry mills. Programs and services, such as those at the University of Minnesota DDGS QC program, offer certification to dry-grind ethanol plants that produce DG residues that meet established standards *(5)*. Certification allows dry-grind ethanol plants to command a higher price for their DG residue.

Figure 1 shows an elementary schematic diagram for process flows within a typical dry mill operation. A proposed process for converting the residual starch and fiber in wet DG into ethanol and HDG and hydrolyzed distiller's grain with solubles (HDGS) is shown schematically in Fig. 2.

Modifications to an existing dry mill plant include a pretreatment section added after the first centrifugation step, in which dilute acid and steam are used to convert the residual starch and fiber in wet DG into fermentable sugars. Next, an enzymatic hydrolysis step is inserted to convert oligomeric sugars freed by pretreatment to fermentable monomeric sugars, which are sent to a secondary fermentation step. Whole stillage from the second distillation column is sent to a second centrifugation step for separation into concentrated HDG and thin stillage. Finally, concentrated HDG is sent to the dryer and combined with evaporated thin stillage syrup to form the dried, higher-protein-content HDGS.

Producing higher-quality HDG and HDGS products requires overcoming several technical challenges. A major challenge is pretreatment with sufficient severity to allow solubilization of the carbohydrate fraction from both the residual starch and the fiber while limiting protein degradation and acid catalyst consumption. Neutralization of the acid in the fermentation section results in salt formation, which can be detrimental to animals fed these residues. The most difficult hurdle for producing high-quality HDGS is minimizing deleterious Maillard reactions between amino acids and reducing sugars during pretreatment *(6)*. Pretreatment of corn fiber residues from corn wet-milling operations has been found to generate fewer Maillard reactions as a consequence of the lower protein content in corn fiber residues *(7–13)*. Maillard reactions are known to lead to sugar and essential amino acid losses, produce enzyme inhibitors and degradation products, cause undesirable color changes in products, and impart off flavors that some animals (especially poultry) are sensitive to *(14–16)*. Several strategies can be employed to reduce Maillard reactions in pretreatment of DG feedstocks, including reducing the protein content of wet DG feedstocks prior to pretreatment *(17)*, reducing pretreatment severity by lowering the concentration of acid catalyst, reducing reaction temperature and residence times, and sulfation of the sugars with SO_2 during pretreatment. Opportunities also exist for reducing browning and charring during the drying step by incorporating new filter technologies to replace energy-intensive dryers (S. Benesi, personal communication, April 30, 2003).

Pretreatment of DG followed by fermentation was shown to increase ethanol yield and may be of economic benefit for a corn dry-grind ethanol producer. The resulting HDG was shown to be low in fiber with increased digestible protein content, which may increase markets for this residue. Preserving the "high-quality" protein in the residues in pretreated DG is the major challenge facing the incorporation of HDG and HDGS production into the typical dry mill. Several of the unit operations proposed in the modified dry mill (Fig. 2) process were tested at the bench or pilot scale, and the results are reported herein. Animal feeding trials with turkey poults were also conducted to determine the effects of pretreatment on residual protein "quality" in HDG in relation to growth and other performance parameters. We have shown that increases in ethanol yield are possible

from pretreatment of DG, and that a lower-fiber, high-protein residue is produced that can be successfully incorporated into nonruminant animal feeds. The turkey poults were used as a model animal, and the feeding trial results suggest that HDG may be used as a high-protein feed supplement in other nonruminant animals.

Materials and Methods

Feedstock

Three 55-gal drums of wet DG (28.7 wt% total solids) were received at the National Renewable Energy Laboratory (NREL) via overnight shipment from a centrifuge in the production line of a dry-grind ethanol plant. The material was spread as soon as received on rubber-coated tarpaulins in a cool (~10°C) enclosed building and partially air-dried for 4 d using fans. The spread wet DG was mixed twice per day to promote even drying to a final concentration of approx 74.5 wt% solids. The partially air-dried DG was sieved to pass through a 6-mm screen with the large pieces broken up before screening. Thorough mixing of the screened material was achieved by the method of cone and quarter mixing three times prior to acid impregnation and pretreatment. The partially air-dried DG was stored at 4°C for a few days prior to completing acid impregnation. Pretreatment was completed within 2 wk of receiving the wet DG. The results of the solids compositional analysis of the mixed, partially air-dried feedstock are given in Table 1. The drying and sieving of DG was performed to ensure even acid distribution in the acid impregnation step, described next. Note that drying DG may not be necessary for acid impregnation using industrial high-speed mixers such as pug mill mixers.

Acid Impregnation

Impregnation of DG with SO_2 was accomplished by injecting a known weight of SO_2 gas into a sealed polyethylene bag containing DG. For dilute-H_2SO_4 impregnation, the acid solution was sprayed on 3 kg of partially air-dried DG while mixing in a 30-qt bread dough mixer. Tests using a red dye and salt tracer with the bread dough mixer were promising, showing an even distribution of both the dye and salt tracer. Preparing acid-impregnated feedstock for the poultry feeding trial required mixing 42 individual batches with acid using the bread dough mixer, with all batches combined and mixed by the method of cone and quarter mixing before pretreatment. Approximately 176 kg of feedstock at approx 50 wt% solids and 1.9 wt% H_2SO_4 in the liquid fraction was obtained. H_2SO_4 concentrations used in the pretreatment experiments given in Table 2 were determined by titration with NIST traceable NaOH solutions.

Pretreatment

Pretreatment screening experiments of partially air-dried DG were carried out in both a 4-L steam explosion reactor *(18,19)* and a 4-L

Table 1
Survey by NREL of Composition of Corn Dry-Grind DG (wt%)

Sample	Crude protein	Total carbohydrates	Nonstarch glucan	Starch	Galactan	Mannan	Xylan	Arabinan	Extractives	Acetyl	Total ash	Acid insoluble residue
Plant A	35.2	39.0	12.4	5.60	2.2	1.5	10.1	7.2	18.5	1.6	2.6	3.2
Plant B	34.0	38.2	10.6	5.80	2.2	1.6	10.5	7.4	18.4	1.6	2.4	3.2
Plant B [a]	32.0	41.0	11.0	7.30	2.3	1.5	11.2	7.7	20.0	1.5	2.6	3.2
Plant C	31.2	41.2	11.5	6.20	2.4	1.4	11.7	7.9	15.7	1.7	2.8	3.2
Plant D	31.9	41.2	12.1	6.30	2.3	1.6	11.0	7.7	13.8	1.5	2.5	4.3
Air Dried DG [b]	33.9	42.7	12.1	8.40	2.2	7.4	10.2	7.4	20.3	1.4	2.7	3.1
Pretreated DG	42.8	30.3	15.7	2.80	1.4	2.4	6.9	2.4	ND [c]	ND [c]	0.5	20.1
HDG [d]	60.6	14.0	4.5	0.82	1.0	1.8	4.6	1.8	22.6	0.6	1.2	12.6

[a] Sample taken at same plant months later.
[b] Partially dried to 74.5% solids.
[c] ND, not detected.
[d] Used for feeding trials.

Table 2
DG Pretreatment Conditions, Yields, and Conversions

Experiment	Reactor[a]	Catalyst (wt%)	Time (min)	Temp (°C)	CS[b]	Glucose yield (%)[c]	Xylose yield (%)[c]	Total soluble sugar yield (% total carbohydrates in DG)[c]
1	SG	Steam	20	160	2.35	14.1 (2.6)	17.1 (2.1)	20.4 (8.7)
2	SG	SO_2 (2%)	15	160	2.42	25.8 (4.7)	35.9 (4.3)	36.2 (15.5)
3	SG	H_2SO_4 (1.1%)	5	185	2.35	41.5 (7.2)	57.4 (6.5)	50.1 (20.4)
4	ZC	H_2SO_4 (3.27%)	20	140	2.17	65.1 (13.0)	93.4 (11.7)	77.2 (35.0)
5	ZC	H_2SO_4 (3.27%)	30	140	2.34	65.1 (11.2)	77.3 (8.7)	68.9 (28.0)
6	ZC	H_2SO_4 (3.27%)	40	140	2.76	47.6 (9.5)	50.7 (6.4)	49.0 (22.2)
7	ZC	H_2SO_4 (3.27%)	12	150	2.23	59.1 (11.8)	90.2 (11.3)	70.1 (31.7)
8	ZC	H_2SO_4 (3.27%)	16	150	2.35	59.5 (11.9)	86.3 (10.8)	71.3 (32.3)
9	ZC	H_2SO_4 (3.27%)	20	150	2.42	59.0 (11.8)	75.7 (9.5)	65.9 (29.8)
10	SG	H_2SO_4 (3.27%)	12	150	2.35	59.3 (11.8)	85.9 (10.8)	73.2 (33.2)
11	SG	H_2SO_4 (3.27%)	16	150	2.23	55.2 (11.0)	76.5 (9.6)	64.5 (29.2)
Production	SG	H_2SO_4 (1.9%)	8	160	2.10	47.5 (9.8)	57.2 (5.8)	54.7 (24.1)

[a] SG, 4-L steam explosion reactor (steam gun); ZC, 4-L Zipperclave stirred reactor.
[b] $CS = Log_{10}(R_o) - pH$; $R_o = t_r \cdot \exp[(T_r - 100)/14.75]$.
[c] Parentheses indicate g of soluble sugar yield/100 g of dry input feedstock.

Zipperclave® stirred reactor (Autoclave Engineers, Erie, PA). The Zipperclave reactor was equipped with an anchor-type mixer and a 2.5-L Hastelloy® pail to reduce condensate accumulation in the pretreated slurry. The pretreatment screening conditions used in the two reactors are presented in Table 2. Comparisons of sugar yield obtained from various pretreatment conditions are simplified using the severity concept of combining time and temperature *(20,21)*. The combined severity factor (CS) used in our study also includes acid concentration and is represented as $CS = \log_{10}(R_o) - pH$ *(22)*, with reaction ordinate (R_o) defined as $R_o = t_r \cdot \exp[(T_r - 100)/14.75]$. The factor t_r is defined as reaction time (min), and T_r is the reaction temperature (°C). In our study, the value of pH used in the CS calculation is from the measurement of pH in the pretreated slurry after pretreatment. No attempt was made to estimate the pH during the reaction time course within the feedstock at temperature because the dynamics of acid dilution with steam condensate and activity of the acid within the feedstock during pretreatment were not known. Producing HDG for conducting the poultry-feeding trials required the pretreatment of 104 individual 1.7-kg acid-impregnated batches using the 4-L steam explosion reactor. All pretreated batches were mixed together prior to fermentation.

The H_2SO_4 concentration was decreased to 1.9 wt% for the HDG production run to further reduce the amount of salt formed during neutralization of acid in the fermentation step. This was done because animals (especially poultry) become distressed if they are given feed containing high salt concentrations (S. Noll, personal communication, 2002). In addition to lowering the acid loading, the CS of the production experiment was lowered from the optimum found during the pretreatment screening experiments to reduce the possibility of excessive protein hydrolysis, and protein as well as sugar losses through Maillard degradation reactions.

Fermentation

An initial set of fermentation screening experiments was carried out using pretreated DG (Table 2, experiment 4) to test for fermentation inhibitors, the efficacy of various commercial enzymes in hydrolyzing the oligomeric sugars formed during pretreatment, and the benefits of coculture fermentation. Fermentation screening experiments consisted of duplicate 100-mL working volume flasks with bubble traps and solids loading of 10 wt% pretreated DG. A cellulase enzyme loading of approx 15 filter paper units (FPU)/g of cellulose using Iogen cellulase enzyme preparation (lot no. BRC191095; Iogen, Ottawa, Canada) was added to the pretreated DG residue. This was supplemented with four commercially available glucoamylase and xylanase enzymes at 20 times the manufacturer's recommended dosage to ensure that the level of enzyme loading was not limiting. Xylanase MX® and Xylanase XL® preparations from Genencor (Richmond, CA) and UHP Xylanase® preparation from Iogen were used to test the efficacy of these enzymes on residual xylan in pretreated DG. The glucoamylase preparation, Distillase L-400® (Genencor), was used to hydrolyze residual starch

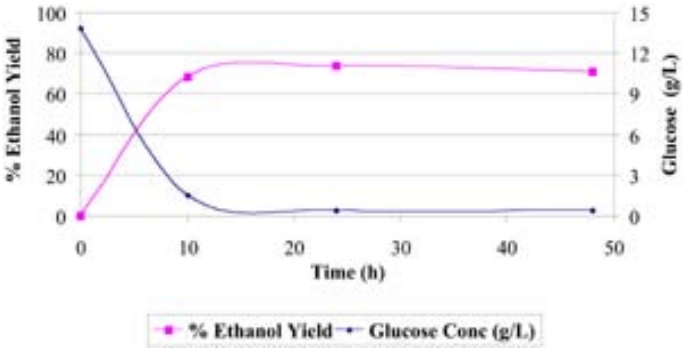

Fig. 3. Ethanol yield from pilot-scale fermentation of pretreated DG. Starch and cellulose in the pretreated DG slurry (10% [w/w]) were saccharified using glucoamylase and cellulose enzymes for 24 h prior to fermentation to ethanol using *S. cerevisiae* D_5A yeast at 32°C, pH 5.0, and 75-rpm agitation.

and amylodextrins. Prior to inoculation of the flasks with yeasts, enzyme cocktails were added and incubated with the solids at 48°C for 24 h and 150 rpm in a shaking incubator to hydrolyze residual carbohydrates in the flasks. Three sets of flasks were run as cocultures using the yeasts *Saccharomyces cerevisiae* D_5A (ATCC 200062) and *Pichia stipitis* strain NPw9 (ATCC PTA-3717) *(23)*, and a D_5A control. The flasks were supplemented after saccharification with corn steep liquor (CSL) to 1 wt% and then inoculated with yeasts (10% [v/v]) at an optical density at 600 nm (OD_{600nm}) of 0.50 for D_5A and 0.48 for NPw9. The fermentation conditions for the screening experiments were 32°C, pH 5.0, and 150 rpm in the shake flasks.

Pilot-Scale Fermentation

HDG was obtained from an 809-L fermentation of pretreated DG. The pretreated DG was diluted in a 1450-L fermentation vessel to a 10 wt% slurry. Enzymatic saccharification of the pretreated DG slurry was performed at 48°C for 24 h using an enzyme cocktail with a cellulase (Iogen) loading of 15 FPU/g of cellulose and a glucoamylase (Genencor Distillase L-400) loading of 0.08 times the weight of starch in the solids (Table 1). After saccharification, the 809-L fermentation was cooled to 32°C and CSL was added to 1 wt%. The yeast *S. cerevisiae* D_5A was inoculated using an 80-L culture at an OD_{600nm} of 0.50 (~10% [v/v] final). Fermentation was carried out at 32°C and pH 5.0, with agitation set at 75 rpm, and air overlay at an airflow rate of 50 L/min, with backpressure set to 0.1 bar (10 kPa). The results of the pilot-scale fermentation are presented in Fig. 3. Samples for enzymatic saccharification steps were taken at 0 and 24 h, and postinoculation fermentation samples were taken at 0, 10, 24, and 48 h. Samples were analyzed for sugars, ethanol, and organic acids using NREL's Laboratory

Table 3
Protein Mass Balance for HPG Production

Operation	Protein (wt%)[a]	Protein balance (% recovery)
Feedstock	33.9 [b]	100.0
Pretreatment	41.7	108.0 [c]
Fermentation	42.8	99.9
Centrifuged solids	55.6	53.1 [d]
Supernatant	23.2	25.4
Final feed	60.6	56.0 [e]

[a] Protein was measured using the crude protein method *(25)*.
[b] Analysis of the percentage of protein may be low, leading to mass balance error.
[c] This amount is used as 100% protein mass from feedstock for subsequent calculations.
[d] This mass includes solids from Pneumapress filter and Boch centrifuge.
[e] The amount shown here is larger than that from the centrifuge because we processed the supernatant twice through the centrifuge.

Analytical Procedures *(24)*. Crude protein analyses on the combined solid/liquid fraction of the 0- and 48-h postinoculation samples were performed using carbon–hydrogen–nitrogen analysis *(25)* with a protein conversion factor of 6.25 × nitrogen content.

Solid/Liquid Separation

The spent fermentation broth from the pilot-scale fermentation was separated in a Bock centrifugal extractor, model 775 (Bock, Toledo, OH) operating at 1725 rpm (~1600*g*). Approximately 86 kg of solids (36 wt% solids) was collected. The supernatant was recycled through the centrifuge again to remove additional solids. A small quantity of spent broth was filtered using a Pneumapress® model 3-C-276 automatic pressure filter (Pneumapress Filter, Richmond, CA) to test the benefits of new filtration technologies. Solids collected using the Pneumapress filter (~50% moisture) were mixed with the centrifuged solids and dried (~93 wt% solids) in a pan-type forced hot-air oven by an outside laboratory (Hazen Research, Golden, CO) using air heated to a maximum of 45°C. The low-temperature air-drying step was specified to reduce Maillard reactions.

The dried fermentation residues were broken up to pass through a 6-mm screen and mixed three times by the method of cone and quarter mixing. The dried and screened HDG (~32 kg) was available for poultry-feeding trials (Table 3). The supernatant from the centrifugation step and filtrate from the filter belt were not evaporated to form concentrated syrup to be added to the dried HDG to form HDGS because of lack of pilot-scale equipment to accomplish the evaporation step.

Table 4
Comparison of NRC (1994) Corn and Corn Coproducts vs NREL HDG[a]

Parameter	Corn (4-02-935)[b]	DDG (5-28-235)[b]	DDGS (5-28-236)[b]	HDG (NREL)
DM (%)	89.0	97.0	93.0	95.86
ME (kcal/kg)	3350	1972	2480	2008
TME (kcal/kg)	3470	—	3097	2566
Protein (%)	8.5	27.8	27.4	57.8
Ether extract (%)	3.8	9.2	9.0	14.6
Linoleic acid (%)	2.2	—	4.55	—
Crude fiber (%)	2.2	12.0	9.10	3.90
Calcium (%)	0.02	0.10	0.17	0.02
Total phosphorus (%)	0.28	0.40	0.72	0.22
Nonphytate phosphorus (%)	0.08	0.39	0.39	0.11
Potassium (%)	0.30	0.17	0.65	0.19
Chlorine (%)	0.04	0.07	0.17	0.03
Sodium (%)	0.02	0.09	0.48	0.16
Magnesium (%)	0.12	0.25	0.19	0.07
Manganese (%)	0.0002	0.0022	0.0024	0.00
Aluminum (%)	—	—	—	0.00
Iron (%)	0.0045	0.0300	0.028	0.04
Zinc (%)	0.0018	0.0055	0.008	0.00
Copper (%)	—	—	—	0.00
Ash (%)	—	—	—	1.43
Starch (%)	—	—	—	1.60
Sugars (%)	—	—	—	<2.0

[a] Data from NCR reports for standardized poultry rations *(26).*
[b] International feed no.

Poultry-Feeding Trials

Poultry-feeding trials were carried out in two phases as follows.

Phase 1

Initial feed ingredient evaluation and compositional characterization were carried out for HDG using proximate analyses by an outside laboratory for protein, fat, fiber, ash, moisture, mineral composition (major and trace elements), starch, and sugars and were compared to standard reference feed materials (National Research Center [NRC], 1994 methods) *(26)* (Table 4). An amino acid profile was obtained on HDG and compared to standard reference corn and corn coproduct feeds to determine the digestible amino acids present in the HDG feed (Table 5). In vivo metabolizable energy (ME) and digestible amino acids were determined by feeding a known quantity of HDG to eight cecatomized roosters (Table 4). The feces were quantitatively collected for a 48-h time period after feeding, and amino acids and digestibility were based on quantitative measurement of input feed and output feces. Endogenous secretions were corrected for by having eight nonfeed roosters. True metabolizable energy (TME) was similar to ME, except that intact turkeys were used (Table 4). Excreta were freeze-dried, ground, and analyzed for nitrogen and gross energy content.

Table 5
Amino Acid and Digestible Amino Acid Composition of Soybean Meal, NRC Feeds, and HDG

	Amino acid as % of protein					Disgetible amino acid as % of protein			
	Composition (NRC 1994)					Composition (NRC 1994)			
	Soybean meal (5-04-612)	Corn (4-02-935)	DDG (5-28-235)	DDGS (5-28-236)	NREL HDG Analyzed [a]	Soybean meal (5-04-612)	Corn (4-02-935)	DDGS (5-28-236)	NREL HDG Analyzed [a]
Aspartic acid					5.20				3.75
Threonine	3.94	3.41	1.76	3.38	3.28	3.46	2.87	2.44	2.47
Serine	5.22	4.35	2.52	5.92	3.56	11.70			
Glutamic acid					14.87				11.70
Proline					7.60				6.14
Glycine	4.32	3.88	1.76	2.10	2.99				
Alanine					6.44				5.27
Cysteine	1.52	2.12	0.86	1.47	2.00	1.24	1.80	1.13	1.56
Valine	4.67	4.71	4.24	4.78	4.76	4.25	4.14	3.87	3.66
Methionine	1.41	2.12	1.44	2.21	2.08	1.30	1.93	1.85	1.78
Isoleucine	4.46	3.41	3.56	3.68	3.79	4.15	3.00	3.09	2.94
Leucine	7.87	11.76	10.83	8.09	12.15	7.24	10.94	7.20	10.08
Tyrosine	4.11	3.53	3.02	2.72	4.19				3.61
Phenylalanine	4.93	4.47	3.38	0.74	5.29	4.53	4.07	0.65	4.46
Histidine	2.69	2.71	2.23	2.43	2.26	2.37	2.54	1.82	1.74
Lysine	6.23	3.06	2.81	2.76	1.99	5.67	2.48	1.79	1.35
Arginine	7.33	4.47	3.49	3.60	2.66	6.74	3.98	2.27	2.10
Tryptophan	1.56	0.71	0.72	0.70	0.39				0.25

[a] International feed numbers are given in parentheses.

Table 6
Composition of Poult Diets

Ingredient (%)	Incorporation of HDG				
	Control (%)	5%	10%	15%	20%
Corn, ground	39.49	38.32	37.10	35.88	34.65
Soybean meal[a]	50.38	45.92	41.46	37.01	32.56
Poultry byproduct meal	4.0	4.0	4.0	4.0	4.0
HDG	0.0	5.0	10.0	15.0	20.0
Dicalcium phosphate[b]	2.35	2.35	2.35	2.35	2.35
Calium carbonate	1.14	1.14	1.14	1.14	1.14
Sesquicarb (sodium bicarbonate)[b]	0.152	0.157	0.179	0.200	0.222
Salt	0.250	0.229	0.194	0.160	0.125
99% DL-Methionine	0.175	0.138	0.101	0.064	0.027
L-Lysine HCl	0.000	0.067	0.177	0.287	0.396
Starter vitamin mix	0.35	0.35	0.35	0.35	0.35
Prestarter vitamin mix	0.08	0.08	0.08	0.08	0.08
Trace mineral mix	0.12	0.12	0.12	0.12	0.12
60% Choline chloride	0.175	0.175	0.175	0.175	0.175
Animal fat	1.34	1.96	2.57	3.19	3.80
Total	100.00	100.00	100.00	100.00	100.00

[a] Protein content of soybean meal is 47 wt%.
[b] Dicalcium phosphate, calcium carbonate, sodium carbonate, trace mineral, and vitamins.

Phase 2

Feed ingredient evaluation was carried out at low levels of HDG inclusion to test the effects of this protein source on viability, organ weight gains, and other measures of turkey performance. A corn-soybean meal–based diet with some meat and bone meal was used as the control. HDG was incorporated into the diet (replacing corn and soybean meal) at levels of 5, 10, 15, and 20%. Diets were formulated to provide similar levels of ME, lysine, methionine, calcium, and phosphorus. In addition, all of the poult diets contained the necessary vitamins and trace minerals, salt, and added fat (choice white grease or tallow). Major ingredients (corn, soybean meal, and meat bone meal) were analyzed prior to the start of the trial. Mixed diets were analyzed for protein content. The composition of feed rations fed to the turkey poults are given in Table 6.

Prior to the start of the feeding trial, newly hatched poults (420 male commercial turkey poults) were randomly placed into 42 cage battery brooder units. All poults received the control starter diet up until 3 d of age. At d 3 each poult was wing banded, weighed, and approx 20% of the poults (heaviest and lightest) was discarded. The remaining 350 poults were sorted into 50 cages (7 poults/cage) with each bird of approximately equivalent body weight. Each diet was fed to 10 replicate cage units from 3 to 21 d of age. Body weights were taken at 3, 7, 14, and 16 d of age. Feed intake records for each pen were kept. No mortality was found. At the end of the trial, two poults per pen were randomly selected, weighed, and euthanized using

approved procedures, and the weights of internal organs (spleen, heart, liver, gastrointestinal tract, bursa) were recorded. Analysis of variance was conducted to determine the effect of HDG inclusion in the feed on the probability of treatment differences for each of the measured criteria on poult performance and organ characteristics.

Results and Discussion

Composition

The compositional variation of samples of wet DG received from a number of different corn dry mill ethanol plants is given in Table 1. Two of the entries show the variation between samples of wet DG removed from the production line centrifuge of a dry-grind ethanol plant several months apart. The crude protein content was found to vary among the different plants from 31.2 to 35.2%. These results can be compared with those of a study of six Minnesota dry-grind ethanol plants conducted by the Department of Animal Sciences at the University of Minnesota that found crude protein content of DDG and DDGS from these plants ranging from 28.7 to 31.6 % *(4)*. This variation is of some concern to animal feedlot operators.

Table 3 provides the increase in protein content as a result of the pretreatment of DG with dilute H_2SO_4, followed by enzymatic hydrolysis and fermentation of the pretreated DG. The residual protein content in the HDG was found to increase from approx 33.9 to 60.6 wt%. Analysis by an independent laboratory places the crude protein content of the HDG produced at 57.8% (Table 4).

Pretreatment

The sugar yields and sugar conversion recoveries for the dilute-acid-pretreated DG are given in Table 2. Sugar yields and conversions were low in steam pretreatment (experiment 1) without the addition of acid catalysts, indicating a recalcitrant form of starch and fiber in the DG. However, when SO_2 and dilute-acid impregnation were not homogeneous throughout the feedstock before pretreatment, soluble sugar yields and conversions suffered, as shown for experiments 2 and 3. Visual investigation of the pretreated slurries from experiments 2 and 3 clearly showed areas of partial pretreatment, indicating nonhomogeneous acid impregnation. Higher yields and conversions were found in pretreatment experiments 4 through 11 and the production experiment when a bread dough mixer was used for acid impregnation.

Gravimetric mass balance closure around each pretreatment experiment in Table 2 ranged from 95 to 100%, with an average of 96.7 ± 1.9% (data not shown), indicating losses owing to unaccounted for volatile components. The Zipperclave reactor showed the highest level of solubilization of residual carbohydrates, suggesting that internal mixing and direct steam injection enhances pretreatment kinetics within the Zipperclave reactor. Less mixing of the acid-impregnated feedstock with steam within the steam

explosion reactor was expected because it lacks an impeller mixer such as that found in the Zipperclave, thus decreasing performance. The highest total soluble sugar yield was found using the Zipperclave reactor, where approx 77% of the carbohydrates available in the DG was solubilized (experiment 4). The soluble xylose yield from the hemicellulosic fraction in experiment 4 was found to be 93.4%, while 65% of the available glucan was solubilized during this pretreatment. Approximately 35 g of total soluble sugar was produced/100 g of dry DG under these pretreatment conditions. The steam explosion reactor gave slightly lower total soluble sugar yields. At the maximum, approx 73% of available carbohydrate was solubilized with pretreatment using this reactor (experiment 10). The soluble xylose and glucose yields were slightly lower in the steam explosion reactor for experiment 10, compared with the stirred Zipperclave reactor, giving 85.9 and 59.3%, respectively. The steam explosion reactor produced a maximum of 33.2 g of total soluble sugar/100 g of dry DG. However, the mechanical simplicity of the steam explosion reactor, compared with the Zipperclave reactor with mixer, is of economic advantage because of lower capital and operating costs associated with this design.

Pretreating wet DG with SO_2 (experiment 2) resulted in higher solubilization of residual carbohydrates than uncatalyzed steam explosion (experiment 1), however, higher yields and conversions are possible if homogeneous absorption of the acid gas can be accomplished. Careful examination of the SO_2-pretreated residue indicated nonhomogeneous pretreatment because the SO_2 appears to have been absorbed only at the surface of the particles and did not penetrate far into the interior. However, less expensive pretreatment reactors are possible if SO_2 is used as the catalyst, as opposed to dilute-acid pretreatment, because exotic alloys may not be needed.

Consistent steam explosion reactor performance was found during the 104-batch production experiment, with uniform temperatures measured throughout the production run. However, DG feedstock baked onto the internal walls of the reactor and charring occurred over the extended period of time needed to produce the required quantities of pretreated DG. The baked-on material was collected and analyzed separately for mass. Overall gravimetric mass balance for the production run was lower, 93.3%, as a result of this charring, compared to the screening experiments, in which approx 97% mass recovery was found. Removing corn oil prior to pretreatment may decrease this tendency of the feedstock to stick to, and bake on, the walls of the pretreatment reactor. Total soluble sugar recoveries of 24.1 g/100 g of dry input material were found for the production experiment. These recoveries were less than those found in the screening experiments for both the Zipperclave and steam gun reactors (Table 2). This may be owing to the less severe pretreatment conditions chosen to reduce protein hydrolysis and Maillard reactions, nonhomogeneous acid impregnation, and nonuniform heat transfer effects caused by charring on the walls of the reactor. Homogeneous acid impregnation is one of the technical challenges limiting yields for the conversion of DG.

Fermentation

Fermentation screening studies using two different yeasts showed that pretreated DG does not contain significant levels of inhibitors (data not shown). Screening shake-flask fermentations were complete in 17 h, with ethanol yields reaching 82% from all available hexose sugars in the pretreated DG. Crude protein levels increased from 43 to a high of 58 wt% (data not shown). The combined cellulase and glucoamylase enzymes were effective in increasing the amount of soluble glucose, while the three commercial xylanases were ineffective in solubilizing residual xylan with this pretreated material (high-performance liquid chromatography data not shown).

The NREL *Pichia* strain NPw9 was equivalent to the D_5A yeast in ethanol production; however, it did not utilize xylose under the anaerobic conditions used in the screening experiments (data not shown). However, the *Pichia* strain NPw9 has been shown to ferment xylose in toxic pretreated softwood hydrolysates under microaerophilic conditions *(23)*.

Saccharification of the residual carbohydrates in the pretreated DG slurry for the pilot-scale production experiment increased the glucose concentration from 4.4 to 15.1 g/L in 24 h at 48°C. Following inoculation with D_5A yeast, the initial glucose was consumed in 10 h with ethanol concentration reaching 8.81 g/L at 24 h (Fig. 3) with 73% ethanol yield from glucan and starch. Mannose, galactose, arabinose, and xylose were not utilized by *S. cerevisiae* D_5A in this fermentation (data not shown), thus lowering the ethanol yield from available hexose and pentose sugars. A different microorganism would be needed to utilize these sugars and increase ethanol yields. The ethanol concentration decreased slightly after 48 h, suggesting that the residual cellulose in the HDG was not digestible by the cellulase enzyme after the initial saccharification period.

Feeding Trial

Analysis of the international NRC standardized (1994) *(26)* corn (4-02-935), DDG (5-28-235), and DDGS (5-28-236) feeds, and NREL HDG indicates that HDG had the highest crude protein content, with high levels of glutamine, alanine, proline, and asparagine (Table 4). With the exception of lysine, the amino acid content of HDG was in the range reported for the NRC standardized corn, DDG, and DDGS feeds *(26)*. More important, the in vivo metabolically determined relative digestibility and percentage of digestible amino acids indicate that amino acid digestibility is in the range reported for international corn, DDG, and DDGS feeds. The exception is lysine, for which the percentage of composition in the crude protein was reduced along with the availability. Typical amino acid digestibility coefficients for soybean meal are 95%. This reduction in availability may have occurred during pretreatment in the steam gun, which was conducted at 160°C for 8 min. Other essential amino acids (e.g., histidine, arginine, cysteine, methionine, and tryptophan) demonstrated reduced digestibility. However, factoring in the amount and percentage of availability of these amino acids in HDG, the range of values is equal to or greater than those

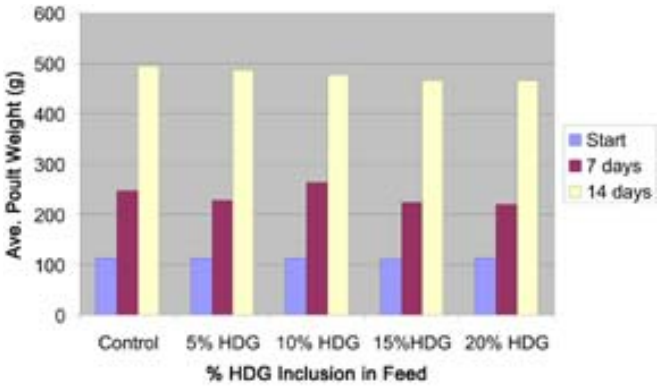

Fig. 4. Average turkey poult weight gain over 14 d with inclusion of HDG in diet.

reported for the NRC feeds. We speculate that including nutrients from evaporated supernatant from the solid-liquid separation step to produce HDGS may reduce the amino acid compositional differences between HDG and the NRC feeds reported in Tables 4 and 5.

The preliminary results reported in Fig. 4 from the 16-d feeding trial of poults are promising. These poults consumed the blended material without separating out the HDG from the base feed ration, their weight gain tracked the control group, there was no mortality in the group, there was no toxicity of HDG to the poults. Small (–6%), but significant differences in the total weight gain between the control group and the experimental group incorporating HDG in the feed at the 15 and 20% level were found (Fig. 4).

Economic Analysis

A preliminary economic analysis performed early in the project before pretreatment testing began showed that if the protein content and type, and hence value, of the hydrolyzed DG was comparable to soybean meal (estimated at 52 wt% with a value of $200/dry t), and the ethanol yield was at least 92% of all hexose sugars available in the DG feed, the payback period for the additional process equipment needed could be as short as 2 yr. The effects of adding additional capital equipment for conversion of DG to an existing corn dry-grind ethanol plant are presented in Table 7. Three preliminary process scenarios are presented that include new equipment for dilute-acid pretreatment, fermentation, distillation, and cellulase enzyme costs. A hot water pretreatment process scenario is also included to show the effects of issues regarding pretreatment reactor materials of construction on costs of the overall process. Adding additional solid/liquid separation equipment increases the costs. The pilot-scale fermentation achieved 73% theoretical yield from available hexoses, lower than the 92% target; however, the overall initial results are very promising and suggest that additional research could result in an economically viable process to convert DG into ethanol and a higher-value

Table 7
Effects of Additional Ethanol Production on Minimum Ethanol Selling Price for Various Pretreatment and Process Options on Existing 25 Million Gallon Per Year Dry-Grind Ethanol Plant

Process	Capital investment ($million)	Annualized capital cost ($) (capital charge factor, 0.17)	Minimum ethanol selling price ($/gal ethanol) Conversion of hexose to EtOH[a] 80%	84%	88%	92%
Basic using hot water pretreatment[b]	10.5	1,784,142	0.86	0.84	0.83	0.81
Basic using dilute-acid pretreatment	10.9	1,860,225	0.90	0.88	0.87	0.85
Basic using dilute-acid pretreatment and solid/liquid separation	11.5	1,954,394	0.94	0.92	0.90	0.88
Additional ethanol (gal/yr)			2,060,606	2,499,186	2,560,200	2,638,917

[a] Conversion of all hexose monomers, meaning glucose, galactose, and mannose.
[b] Basic processing refers to DG pretreatment, simultaneous saccharification and fermentation with cellulase enzyme and *Saccharomyes*, and ethanol recovery via distillation.

animal feed. The annual production of ethanol could increase an additional 2.0–2.6 million gal/yr.

Conclusion

Pretreatment of wet DG with dilute H_2SO_4 was shown to solubilize significant (~77%) amounts of carbohydrates from the wet DG. Pretreatment with SO_2 may give equivalent results if homogeneous absorption of the acid gas can be accomplished. Less expensive reactors are possible when using SO_2 as the catalyst. Homogeneous acid impregnation of wet DG feedstocks was found to be a showstopper requirement for obtaining high soluble sugar yields and recoveries.

Fermentation of pretreated DG slurries is readily accomplished because of the low toxicity of the pretreated slurries. Soluble monomeric sugars (mostly glucose) were fermented to ethanol by the yeasts *S. cerevisiae* D_5A and *P. stipitis* NPw9; however, the soluble oligomeric sugars were not converted by the added enzymes and decreased ethanol yields to 82% of theoretical. The use of cellulase enzymes in the saccharification and fermentation step decreased the nonstarch glucan from ~12 to ~4% in the pretreated DG residue, indicating that the pretreatment enhanced the cellulose digestibility.

The 14-d feeding trial using turkey poults as a model nonruminant animal is promising. These poults consumed the blended material without separating out the HDG from the base feed ration, their weight gain tracked the control group, there was no mortality in the group, no toxicity of the HDG to the poults was observed, and there were no significant differences between the morphology of the control or any of the experimental groups after necropsy. However, small (–6%) but significant differences in the total weight gain between the control group and the experimental group receiving the HDG mix at the inclusion level of 15 and 20% level were found.

Our study successfully demonstrated that increases in ethanol production and increases in protein level of HDG can be achieved with less severe pretreatment of DG and subsequent fermentation of the pretreated DG to produce HDG. The HDG residue had a crude protein content near 61 wt%, comparing favorably with soybean meal, which has a range of 44–52 wt%. The total amount of digestible amino acids available to turkey poults in HDG was comparable to NRC feeds *(26)*, with the exception of the levels of lysine.

Preliminary economic analysis of the process indicates economically feasible scenarios for the incorporation of pretreatment and fermentation of wet DG into existing corn dry-grind ethanol plants. The production of high-quality, high-protein animal feed and the additional production of 2.0–2.6 million gal of ethanol could lead to a payback period of 2 yr. The payback period and projected rate of return depend heavily on the "quality" of the high-protein animal feed and the price per ton that the market might be willing to pay for this new product. Other factors that can affect the economics include ethanol yield and whether all the hexose and pentose sugars can be utilized in fermentation.

Acknowledgment

This work was supported by the US Department of Energy, Office of the Biomass Program.

References

1. BBI International. (2003), *U.S. Ethanol Production Existing and Planned Capacity*. BB International. (Website: http://www.bbibiofuels.com/plant.production/usuc.html). Last modified on 10/13/2003.
2. BBI International. (2001), *The U.S. Dry-Mill Ethanol Industry.* (Website: http://www.bioproduct-bioenergy.gov/existsite/pdfs/drymill_ethanol_industry.pdf).
3. National Corn Growers Association. (2003), *Distillers Grains Defined*, (Website: www.ncga.com/ethanol/co_products/definition_production.htm). Last modified 6/03/03.
4. Knott, J., Shurson, J., and Gohil, J. (2003), *Effects of the Nutrient Variability of Distiller's Solubles Within Ethanol Plants and the Amount of Distiller's Solubles Blended With Distiller's Grains on Fat, Protein and Phosphorus Content of DDGS*, (Website: http://www.ddgs.umn.edu/research-quality/nutrientvariability.pdf). Department of Animal Science University of Minnesota. Last modified 9/11/03.
5. Knott, J., Shurson, J., and Gohil, J. (2003), *Variation in Particle Size and Bulk Density of Distiller's Dried Grains with Solubles (DDGS) Produced by "New Generation" Ethanol Plants in Minnesota and South Dakota*, (Website: http://www.ddgs.umn.edu/research-quality/variation.pdf). Department of Animal Science University of Minnesota. Last modified 9/11/03.
6. Morales, F. J. and Boekel, M. A. J. S. (1998), *Int. Dairy J.* **8(10/11),** 907–915.
7. Bura, B., Mansfield, S. D., Saddler, J. N., and Bothast, R. J. (2002), *Appl. Biochem. Biotechnol.* **98–100,** 59–72.
8. Dale, B. E., Leong, C. K., Pham, T. K., Esquivel, V. M., Rios, I., and Latimer, V. M., (1996), *Bioresour. Technol.* **56,** 111–116.
9. Weil, J. R., Sarikaya, A., Rau, S. L., Goetz, J., Ladisch, C. M., Brewer, M., Hendrickson, R., and Ladisch, M. R., (1998), *Appl. Biochem. Biotechnol.* **73,** 1–17.
10. Moniruzzaman, M., Dale, B. E., Hespell, R. B., and Bothast, R. J. (1997), *Appl. Biochem. Biotechnol.* **67,** 113–126.
11. Moniruzzaman, M., Dien, B. S., Ferrer, B., Hespell, R. B., Dale, B. E., Ingram, L. O., and Bothast, R. J. (1996), Biotechnol. Lett. 18, 985–990.
12. Allen, S. G., Schulman, B., Lichwa, J., Antal, M. J., Laser, M., and Lynd, L. R. (2001), *Ind. Eng. Chem. Res.* **40,** 2934–2941.
13. Grohmann, K. and Bothast, R. J. (1997), *Process Biochem.* **32(5),** 405–415.
14. Knerr, T., Lerche, H., Pischetsrieder, M., and Severin, T. (2001), *J. Agric. Food Chem.* **49(4),** 1966–1970.
15. Oste, R. E., Brandon, D. L., and Bates, A. H. (1990), *J. Agric. Food Chem.* **38(1),** 258–261.
16. Glomb, M. A. and Pfahler, C. (2001), *J. Biol. Chem.* **276(45),** 41,638–41,647.
17. Dien, B. S., Hespell, R. B., Ingram, L. O., and Bothast, R. J. (1997), *World J. Microbiol. Biotechnol.* **13,** 619–625.
18. Nguyen, Q. A., Tucker, M. P., Boynton, B. L., Keller, F. A., and Schell, D. J. (1998), *Appl. Biochem. Biotechnol.* **70–72,** 77–87.
19. Nguyen, Q. A., Tucker, M. P., Keller, F. A., and Eddy, F. P. (2000), *Appl. Biochem. Biotechnol.* **84–86,** 561–576.
20. Overend, R. P., and Chornet, E. (1987), *Phil. Trans. R. Soc. Lond. A* **321,** 523–536.
21. Tengborg, C., Stenberg, K., Galbe, M., Zacchi, G., Larsson, S., Palmqvist, E., and Hahn-Hagerdal, B. (1998), *Appl. Biochem. Biotechnol.* **70–74,** 3–15.
22. Chum, H. L., Johnson, D. K., Black, S. K., and Overend, R. P. (1990), *Appl. Biochem. Biotechnol.* **24–25,** 1–14.
23. Keller, F. A. and Nguyen, Q. A. (2002), US patent no. 6,498,029.

24. Hames, B. R. (1996), *HPLC Analysis of Liquid Fractions of Process Samples for Byproducts and Degradation Products*, Laboratory Analytical Procedure No. 015, (Website: http://www.afdc.doe.gov/pdfs/4698.pdf.
25. Association of Official Analytical Chemists. (1990), *Official Methodfs of Analysis in Protein (Crude) in Animal Feed: Combustion Method*, AOAC Method 990.03, 15th Ed., Helrich, K., ed., AOAC, Arlington, VA.
26. National Research Center for the National Academy of Science. (1994), *Nutrient Requirements for Poultry*, 9th Rev. Ed., National Academy Press,Washington, DC.

Volume 116

Session 6B

Plant Biotechnology and Feedstock Genomics

Session 6B

Plant Biotechnology and Feedstock Genomics

James S. McLaren[1] and Steven R. Thomas[2]

[1]StrathKirn Inc., Chesterfield, MO; and
[2]National Renewable Energy Laboratory, Golden, CO

Over the first part of the twentieth century, it is expected that a large increase in the utilization of renewable bioresources will occur. The possibility for change arises from the broad range of research projects that are currently under way, and the drivers for change continue to include sustainable economic growth and national energy security, and to minimize anthropogenic effects on the environment.

The recent research focus on conversion of conventional lignocellulose biomass will provide useful results in clarifying potential application within various processing mills. However, additional technical approaches will also contribute to successful implementation of the overall biomass platform. For example, if the raw input material were to be "designed" to be more easily converted to a sugar platform, then the system efficiency, practical application, and economic viability would all increase. The recent significant advances in genomics and biotechnology applications provide a new opportunity to utilize renewable resources in ways that will help ensure sustainable enterprises.

The knowledge and understanding of genome sequences, gene function, gene expression, protein interactions, and metabolic control mechanisms will form the basis for future biotech-based alterations in primary production, which is the key underlying renewable resource. The participants in this session provided an exciting view, covering state-of-the-art developments in several relevant areas. Details are provided in the individual papers and an overview of the session is as follows:

Nathan Lakey (Orion Genomics) introduced the exciting capability to uncover the sequences of genes within the genome, without the need to sequence all the nongene DNA space. The technique takes advantage of a chemical difference between repetitive junk DNA, which is methylated and comprises ~90% of plant genomes, and genes, which remain unmethylated and occupy only 10% of the genome. This approach has been demonstrated in all of the major plant species and is estimated to provide the "genespace" sequence at a 10-fold lower cost and much faster than previous methods. The ultimate application to plants used for bioenergy would provide an operational base for significant improvements, primary

productivity, and composition, leading to much lower cost of input "sugars" and easier bioconversion to intermediates of interest.

Mike Lassner (Verdia Inc.) presented examples of the usefulness of directed molecular evolution as an in vitro process that more easily achieves what was traditionally attempted via reproductive crossing and recurrent selection (plant breeding). Proteins may be engineered that have specific desirable characteristics via methods that "evolve" the basic underlying DNA. For example, the outcome can be enzymes with improved kinetic properties that result in enhanced primary production, or proteins that remain operational under extreme conditions. In addition, compositional proteins may be enhanced to provide functional performance that was not achievable via conventional methods.

Justin Stege (Diversa Corporation) discussed the molecular evolution of enzymes for particular pathways, with a focus on the modification of oil composition. Oleochemical applications for such enzymes include applications as biocatalysts for fatty acid modifications. In a program to integrate production and processing, such enzymes can be used to modify the fatty acid content of vegetable oils *in planta*. Results show that expressing such new enzymes in oilseed crops has resulted in altered oil composition, and that the features may be used to better design plant-based oils for use as biofuels and as improved renewable feedstocks.

Mariam Sticklen (Michigan State University) presented results showing the successful expression of three different full-length polhydroxybutyrate (*phb*) genes in maize, and accumulation of the poly-(*R*)-3-hydroxybutyrate (PHB) enzymes within maize chloroplasts. PHB is a potentially useful polymer for use in the plastic markets and is currently produced via fermentation. PHB from transgenic plants was first demonstrated using Arabidopsis, but expression in major crops has added economic implications. This paper also reported work on codon-optimized *Trichoderma reesi cbh1* and wild-type *Acidothermus cellulolyticus e1* genes regulated by the rice *rbcS* promoter. Many maize plants were transformed with evaluations of protein targeting to various subcellular organelles.

Steve Thomas (National Renewable Energy Labortory) described the use of near-infrared (350–2500 nm) reflectance spectroscopy as a genetic screening tool to identify individual plants with particular cell-wall compositions. A broad range of corn genotypes was evaluated, including mutant populations, and the chemical composition was aligned with the phenotypic characteristics. Quantification of plant cell walls is an essential component if lignocellulose biomass is to become a major contributor to a biobased economy. Through such measurements it will be possible to better match biocatalysis to input composition, and to enhance raw material inputs through modified composition with more desirable characteristics.

Deborah Samac (USDA-ARS, Minnesota) reported that more than 100 genes are involved in cell-wall biosynthesis, and that many of these genes have now been cloned to better understand how modification could be achieved. Experiments on alfalfa involving the expression of a soybean

UDP-glucose dehydrogenase cDNA under the control of two promoters active in vascular tissues showed good expression in greenhouse tests. Other results provided evidence that altering the expression of a single gene may have only minor effects. Multigene changes or finding specific regulatory genes may be required to improve the ability to modify plant cell walls to have more useful features.

Overall the participants in this session covered a wide range of topics and clearly demonstrated the importance of genomics and biotechnology to the future of renewable resources. The major underlying threads seemed to be the following:

1. Rapid advances in the technology are opening the door for novel opportunities.
2. Enzymes can be improved via molecular evolution, and for use *in planta*.
3. Single gene changes may not be enough for coordinated pathway engineering.
4. Compositional quantification is important for baseline and useful modifications.

Above all, there was general agreement that the integration of these approaches may be much more productive than just exploring limited single areas. The true biorefinery concept requires integration of all the available science—to enable a broad range of input types along with an output portfolio that includes biofuels and a selected range of economically acceptable biobased products.

0273-2289/04/116/1167–1182/$25.00

Expression of UDP–Glucose Dehydrogenase Reduces Cell-Wall Polysaccharide Concentration and Increases Xylose Content in Alfalfa Stems

Deborah A. Samac,[*,1,2] Lynn Litterer,[3] Glena Temple,[4] Hans-Joachim G. Jung,[1,3] and David A. Somers[3]

[1]USDA-ARS-Plant Science Research, 495 Borlaug Hall, 1991 Upper Buford Circle, University of Minnesota, St. Paul, MN 55108, E-mail: dasamac@umn.edu; [2]Department of Plant Pathology, 495 Borlaug Hall, 1991 Upper Buford Circle, University of Minnesota, St. Paul, MN 55108; [3]Department of Agronomy and Plant Genetics, 411 Borlaug Hall, 1991 Upper Buford Circle, University of Minnesota, St. Paul, MN 55108; and [4]Biology Department, Viterbo University, 815 Ninth Street South, LaCrosse, WI 54601

Abstract

The primary cell-wall matrix of most higher plants is composed of large amounts of uronic acids, primarily D-galacturonic acid residues in the backbone of pectic polysaccharides. Uridine diphosphate (UDP)–glucose dehydrogenase is a key enzyme in the biosynthesis of uronic acids. We produced transgenic alfalfa (*Medicago sativa*) plants expressing a soybean UDP–glucose dehydrogenase cDNA under the control of two promoters active in alfalfa vascular tissues. In initial greenhouse experiments, enzyme activity in transgenic lines was up to seven-fold greater than in nontransformed control plants; however, field-grown transgenic plants had only a maximum of 1.9-fold more activity than the control. Cell-wall polysaccharide content was lower and Klason lignin content was higher in transgenics compared to the nontransformed control. No significant increase in pectin or uronic acids in the polysaccharide fraction was observed in any line. Xylose increased 15% in most transgenic lines and mannose concentration decreased slightly in all lines. Because of the complexity of pectic polysaccharides and sugar biosynthesis, it may be necessary to manipulate multiple steps in carbohydrate metabolism to alter the pectin content of alfalfa.

*Author to whom all correspondence and reprint requests should be addressed.

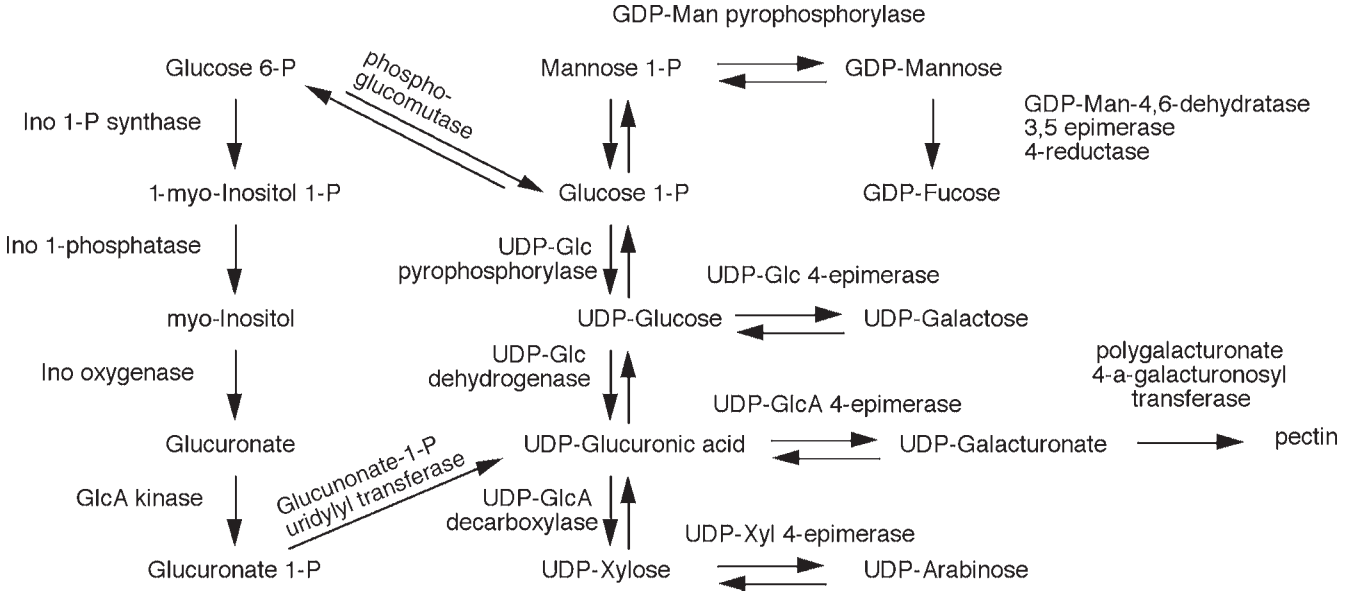

Fig. 1. Monosaccharide biosynthesis pathways.

Index Entries: Carbohydrate**;** forage; homogalacturonan; lucerne; protein utilization.

Introduction

Alfalfa (*Medicago sativa*) is an important forage crop for ruminant animals in temperate regions of the world. Forage consumed by ruminants is first digested in the rumen, where a large proportion of the nutrients is converted to microbial biomass. Remaining nutrients and the microbial biomass pass into the small intestine, where further digestion of forage material and microbes takes place *(1)*. Alfalfa leaf proteins are rapidly degraded in the rumen; however, the resulting free amino acids cannot be completely captured through bacterial growth if there is insufficient energy from carbohydrate fermentation. Although alfalfa stems contain large amounts of cell-wall carbohydrates (approx 70% of stem dry weight), the majority of the cell walls, specifically the cellulose and hemicellulose fractions, are poorly digested in the rumen. Currently, dairy producers feed large amounts of starch to partially reduce protein wastage from alfalfa. However, starch fermentation in the rumen often leads to acidosis and other health problems *(2)*.

A possible alternative to using starch-containing feeds for efficient capture of alfalfa protein is to increase the amount of pectic polysaccharides in alfalfa stems. Pectin, the major component of the cell-wall matrix, is highly digestible by ruminants with a rate of digestion similar to that of alfalfa proteins. In situ rates of pectin degradation from alfalfa range from 9% h^{-1} to >25% h^{-1}, compared with 4% h^{-1} for degradation of cellulose and hemicellulose *(3)*. The rate of pectin degradation is also faster than starch degradation (5 to 12% h^{-1}) from grains *(4)*. More important, pectin fermentation does not result in the rumen health problems associated with starch fermentation because pectin does not yield lactic acid as an end product *(5)*.

Pectin is a mixture of heterogeneous, branched, highly hydrated polysaccharides rich in galacturonic acid *(6)*. The most prevalent monomers for pectic cell-wall polysaccharides are derived from UDP–glucuronic acid (UDP-GlcA) (Fig. 1). Homogalacturonan, a homopolymer of (1→4) α-D-galacturonic acid, accounts for approx 50% of the alfalfa stem pectin *(7)*. The other pectic polysaccharides are rhamnogalacturonan-I, composed of repeated units of galacturonic acid and rhamnose with side chains predominately of neutral sugars, and rhamnogalacturonan-II, a polymer of galacturonic acid residues with heteropolymeric side chains. The primary neutral sugar in alfalfa pectin is arabinose (20–25% of the pectin), with smaller amounts of galactose, rhamnose, glucose, mannose, and fucose present. Pectin composition is relatively stable throughout alfalfa stem maturation *(7)*, supporting the general opinion that pectin is deposited in the middle lamella and primary cell wall and is not present in the secondary cell wall, which is synthesized during maturation of stem tissues.

Biochemical and developmental studies suggest that production of UDP-GlcA is a key control point in regulating the flux of UDP-monomers into pectin *(8,9)*. There is evidence for two distinct pathways leading to UDP-GlcA, which may be developmentally regulated *(10)*. However, the majority of UDP-GlcA in plant cell walls is apparently synthesized by conversion of UDP-Glc to UDP-GlcA by UDP–glucose (Glc) dehydrogenase (EC 1.1.1.22). The reaction is irreversible and apparently rate limiting *(11)*. By modifying expression of UDP–Glc dehydrogenase, it may be possible to enhance UDP-GlcA synthesis and, therefore, UDP-monomers for pectin biosynthesis.

The prime targets for enhancing pectin content in stems are xylem cells. Epidermal, collenchyma, and cortical fiber tissues in alfalfa stems develop very thick primary walls that are rich in pectin *(12)*. These thick primary walls never lignify and remain completely digestible by rumen microbes throughout stem maturation. However, xylem tissues develop lignified secondary walls rapidly and become indigestible with maturity. Because xylem tissue forms a continuous cylinder in alfalfa stems, the indigestibility of this tissue slows particle size reduction in the rumen. If increased pectin biosynthesis results in a thick, pectin-rich primary wall in xylem, then the rate of xylem tissue fragmentation and clearance from the rumen should increase. Because milk production by dairy cows is strongly related to feed intake, any increase in digesta clearance rate from the rumen should increase feed intake and animal productivity *(13)*.

Two gene promoters have been shown to direct transgene expression in alfalfa vascular tissue. In experiments to identify promoter elements involved in nodule-enhanced expression, a 536-bp sequence of the phospho*enol*pyruvate carboxylase promoter (P4) was found to be a strong promoter for expression in alfalfa vascular tissue, particularly xylem, throughout the plant *(14)*. Expression in phloem tissue was observed when an *Arabidopsis* class III chitinase promoter::GUS gene was expressed in alfalfa (unpublished). Transgenic alfalfa plants were produced containing a UDP–glucose (Glc) dehydrogenase cDNA from soybean (*Glycine max*) controlled by these vascular tissue–specific promoters. UDP–Glc dehydrogenase enzyme activity, pectin concentration, and cell-wall composition were measured for field-grown plants.

Materials and Methods

Isolation of Soybean UDP–Glc Dehydrogenase cDNA

An *Arabidopsis* cDNA library (Stratagene, La Jolla, CA) was hybridized with an *Arabidopsis* expressed sequence tag (EST)–derived probe (GenBank H36268) homologous to the previously sequenced bovine enzyme (SwissProt P12378) *(15)*, and a full-length 1732-bp cDNA (AD4) was isolated. This clone was used to probe a soybean seed cDNA library (a gift from Dr. C. Vance, USDA-ARS, St. Paul, MN) prepared from developing seed from the cultivar Lambert in the late cotyledon stage (120–160

mg/seed). Approximately 150,000 plaques were screened using the *Arabidopsis* AD4 cDNA as a probe. Screening was carried out using standard protocols *(16)*. Washes were performed at low stringency (2X saline sodium citrate, 0.1% sodium dodecyl sulfate [w/v] at 22°C). Plaques that were positive on duplicate filters were excised from the original plates and eluted in 100 m*M* NaCl; 10 m*M* $MgSO_4$; 0.01% gelatin (w/v); and 50 m*M* Tris-HCl, pH 7.5 (SM buffer) with 2% $CHCl_3$ (v/v). Positive plaques were purified three times to obtain pure preparations. Inserts were obtained by the in vivo excision method according to the manufacturer's instructions (Invitrogen, Carlsbad, CA). Clones were submitted to the Advanced Genetic Analysis Center, University of Minnesota, for DNA sequencing.

Plant Transformation Vectors

The soybean cDNA (SD5) putatively encoding UDP–Glc dehydrogenase was modified by polymerase chain reaction (PCR) to contain an *Sma*I restriction site immediately 5' of the initiating ATG and an *Sst*I site immediately 3' of the stop codon. Primers used were SmaI-SD5 (5'-CTGCCC GGGATGGTGAAGATTTGCTGC-3') and SD5-SstI (5'-CTGGAGCTCTT ATGCCACAGCAGGCAT-3'). Reactions consisted of approx 50 pg of DNA in a 50-mL reaction with 1.5 m*M* $MgCl_2$, 50 pmol of each primer, 0.25 m*M* each dNTP, and 1 U of *Taq* DNA polymerase (Promega, Madison, WI) in the reaction buffer provided by the manufacturer. Reactions were carried out for 30 cycles of 94°C for 30 s, 55°C for 1 min, and 72°C for 1 min. The 1450-bp PCR product was purified using a QIAquick spin column (Qiagen, Valencia, CA) and cloned into pBluescript KS+ digested with *Sma*I and *Sst*I. The insert was sequenced to confirm that the coding sequence was unchanged from the original sequence. Two transformation vectors were constructed with promoters controlling the expression of SD5: an *Arabidopsis* class III chitinase promoter (Atchit) and a 536-bp portion of the alfalfa phospho*enol*pyruvate carboxylase promoter (P4). To construct the phloem-enhanced expression vector pARC205 (Atchit::SD5), the 1.5-kbp *Arabidopsis* acidic chitinase promoter was excised from pMON8896 *(17)* with *Sal*I and *Bgl*II and ligated into the *Sal*I and *Bam*HI sites of pBI101.2 to produce pARC201. The GUS coding region of pARC201 was removed by digestion with *Sma*I and *Sst*I and replaced with the modified SD5 fragment digested with *Sma*I and *Sst*I. To construct the xylem-enhanced expression vector pARC206 (P4::SD5), the modified SD5 was inserted into the *Sma*I-*Sst*I site of pBI101.2 from which the GUS gene had been removed. The *Xba*I-*Rsa*I P4 promoter fragment *(14)* was inserted into this clone digested with *Xba*I and *Sma*I. All vectors contained *nptII* controlled by the *nos* promoter for selection of transgenic plants. Vectors were mobilized into *Agrobacterium tumefaciens* strain LBA4404 by triparental mating *(18)*.

Transformation and Culture of Plants

Alfalfa leaf explants from a highly regenerable clone of Regen-SY *(19)* were cocultured with *A. tumefaciens* containing each binary vector, and

somatic embryos were produced essentially as described by Austin et al. *(20)* using kanamycin selection. After establishing plants in soil, DNA was extracted from young leaves using a Puregene Kit (Gentra, Minneapolis, MN) according to the manufacturer's instructions. Plants were tested by PCR for the presence of *nptII* using specific primers (NPTII forward: 5'-GCT ATGACTGGGCACAACAGAC-3'; NPTII reverse: 5'-CGTCAAGAAG GCGATAGAAGG-3') and subsequently for the presence of the modified SD5 cDNA using the primers *Sma*I-SD5 and SD5-*Sst*I. Reactions consisted of 1 µg of DNA in a 50-µL reaction with 2.0 m*M* $MgCl_2$, 50 pmol of each primer, 0.25 m*M* each dNTP, and 1 U of *Taq* DNA polymerase (Promega) in the reaction buffer provided by the manufacturer. Reactions were carried out for 30 cycles of 94°C for 30 s, 58°C for 1 min, and 72°C for 1 min using NPTII primers. For SD5 amplification, an annealing temperature of 55°C was used.

Because of the obligate outcrossing nature of alfalfa, all experiments were carried out using vegetative cuttings of primary transformants. Nodal stem sections were placed in sterile, moist vermiculite for approx 14 d to stimulate adventitious root production, then transferred to a mix of sand and soil (1:1 [v/v]) in 3.8 × 21 cm plastic cone-tainers (Stuewe & Sons, Corvallis, OR) and fertilized monthly with soluble 10:10:10 (N:P:K) fertilizer.

For field experiments, vegetative cuttings were made of Regen-SY, five independent lines containing the Achit::SD5 transgene (pARC205-3, -16, -17, -23, -24) and seven independent lines containing the P4::SD5 transgene (pARC206-2, -6, -8, -11, -16, -20, -22). On June 2, 1999, the plants were established in a field plot at the Minnesota Agricultural Experiment Station, St. Paul, MN. Each plot consisted of seven plants of the same line at 0.33-m intervals, with three replicate blocks. Starting July 1, 1999, plants were sprayed with Ambush (0.78 kg/ha) for potato leafhopper control at approx 15 d intervals. Plots were hand weeded and no fertilizer was applied. On July 6, plants were clipped to approx 4 cm to remove insect-damaged material. Plots were harvested on August 27, 1999 (plants in early bud), and September 28, 1999 (plants vegetative). For each plot, 15 random stems were clipped at ground level for enzyme assays. Stems were placed on ice until processed in the laboratory. Leaves and secondary branches were removed from stem samples and the stems were stored at –80°C. The remainder of each plot was clipped to approx 4 cm and the foliage dried at 55°C for 7 d and then weighed. Plots were harvested as before on June 13 and July 14, 2000, when the plants were in early flower.

RNA Extraction and Reverse Transcriptase Polymerase Chain Reaction

Total RNA was extracted from the third internode of field-grown stems from the June 13, 2000, harvest. Frozen stems were ground in liquid nitrogen using a mortar and pestle, and then the RNA was extracted using an RNeasy kit (Qiagen) as specified by the manufacturer. RNA in 50 µL of RNase-free water was treated with 1 U of RQ1 RNase-free DNase (Promega) for 1 h at 37°C according to the manufacturer's directions. RNA was puri-

fied using RNeasy columns and eluted in 100 µL of RNase-free water. Reverse transcriptase polymerase chain reaction (RT-PCR) was performed using the Access RT-PCR System (Promega) according to the supplier's instructions using 0.5 µg of RQ1-treated RNA with the primers NPTII forward and NPTII reverse with an annealing temperature of 59°C and the primers *Sma*I-SD5 and SD5-*Sst*I with a 55°C annealing temperature. The predicted products from amplification with NPTII primers and SD5 primers are 670 and 1450 bp, respectively. A 20-µL aliquot of each completed reaction was electrophoresed through 1% agarose gels in 1X TAE buffer (40 m*M* Tris-acetate, 1 m*M* EDTA), gels were stained with ethidium bromide, and bands were visualized under ultraviolet light.

Preparation of Extract and UDP–Glc Dehydrogenase Assay Procedure

UDP–Glc dehydrogenase activity was measured in stems from initial transformed plants grown in the greenhouse and in plants from the first harvests in 1999 (August 27, plants in early bud stage) and 2000 (June 13, plants in early flower stage). Extracts from field-grown plants were prepared from stem samples harvested from plants in three replicate plots. In 1999, enzyme activity was measured from the topmost three internodes of sampled stems, whereas in 2000 activity was measured from the middle three internodes of stems to decrease variation in activity owing to primary cell-wall synthesis found in younger tissues. Approximately 0.75 g of stem tissue (all stem samples were selected to have comparable diameters) was ground in a chilled mortar and pestle in 3 mL of extraction buffer (40 m*M* Tris-HCl, pH 7.5, containing 0.5 m*M* NAD^+, 1 m*M* EDTA, 2.5 m*M* dithiothreitol, 0.5% [w/v] PVPP, and 0.5 m*M* phenylmethylsulfonyl fluoride). The homogenate was filtered through cheesecloth and centrifuged at 16,000*g* for 10 min. The supernatant was removed and transferred to a new tube and centrifuged again at 16,000*g* for 10 min. The low-molecular-mass solutes were removed from the resulting supernatant by passage through an Econo-Pac10 DG column (Bio-Rad, Hercules, CA) as previously described *(21).* UDP–Glc dehydrogenase activity was measured spectrophotometrically by monitoring the appearance of NADH at 340 nm during the linear phase of the reaction. The standard assay volume was 1 mL (75 µmol of Tris-HCl, pH 8.4; 3 µmol of NAD^+; and 1 µmol of UDP-glucose). The reactions were initiated by the addition of the enzyme extract (150 µL) and monitored for 8 min. Two enzyme assays were completed per extract, and the results reported are an average of the two assays. Activity levels were calculated as previously described *(21).* Protein content was determined with Bradford reagent (Sigma-Aldrich, St. Louis, MO) according to the suppliers' instructions, using bovine serum albumin as a standard.

Analysis of Cell-Wall Components

Dried material from both harvests in 1999 was separated into leaf and stem samples. Stems were ground through a 1-mm screen in a cyclone-type

mill prior to analysis. Neutral sugar composition of the cell-wall polysaccharides was determined by the Uppsala Total Dietary Fiber procedure *(22)*, a two-stage sulfuric acid hydrolysis followed by gas chromatogrphy analysis, which measures monosaccharide composition and Klason lignin. Uronic acids were measured colorimetrically *(23)*. Based on the work of Hatfield *(7)*, alfalfa pectin can be estimated as the sum of cell-wall uronic acids, galactose, arabinose, and rhamnose. Hemicellulose sugar residues included xylose, mannose, and fucose. Glucose residues were assumed to be derived primarily from cellulose.

At the first harvest in 1999, stem internode pieces from the middle of two stems from each plot were immediately preserved in 50% ethanol. Thin sections were examined by light microscopy with and without staining for pectin to determine whether changes in the pattern of pectin accumulation occurred. Ruthenium red was used to visualize the presence of pectin in stem thin sections *(12)*.

Statistical Analyses

The field experiment was planted in three replicate blocks. Data were analyzed separately by year for enzyme activity and biomass yield. Enzyme activity data were statistically analyzed as a randomized complete block design with line as the main effect. Data for plant yield were analyzed as a randomized complete block design with line as the main effect, and harvest and its interaction with line as a split plot arrangement of treatments. Cell-wall concentration and composition data were analyzed as randomized complete block design with line as the main effect, and harvest and the line times harvest interaction as the split plot. The appropriate error terms were used to test main and split plot effects. For those traits that showed a significant *F*-test for differences among lines, individual transgene line means were compared to the nontransformed control line using the least-significant difference method. Data were considered significant at the $p < 0.05$ level. The GLM procedure in the SAS/STAT Users Guide *(24)* was used for all statistical analyses.

Results

Identification of Soybean Seed UDP–Glc Dehydrogenase cDNA

The initial screening of the soybean seed library yielded five identical partial-length cDNA clones. One of these clones was used as a probe to rescreen the library. The rescreening yielded 10 positive clones of which one contained a full-length UDP–Glc dehydrogenase cDNA. A full-length cDNA clone (SD5) was isolated that is 1738 bp long with a 71-bp 5' untranslated region, 1443-bp coding region, and 224-bp 3' untranslated region. The clone is 99.5% identical to a soybean cDNA sequence from suspension cultured cells (GenBank U53418) *(9)*. The *Arabidopsis* cDNA clones AD4 and SD5 are 72% identical at the nucleotide level and 91% identical at the amino acid level.

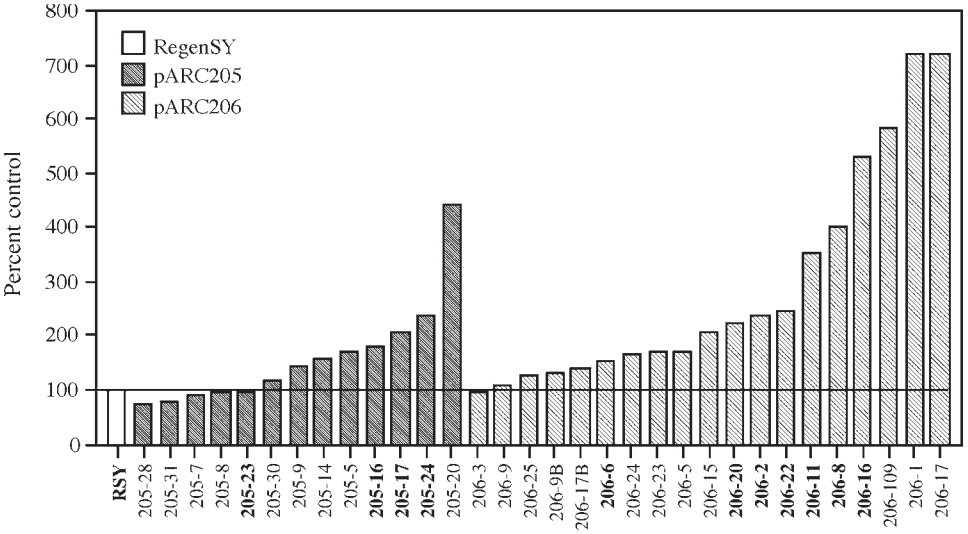

Fig. 2. UDP–Glc dehydrogenase activity in control and transgenic alfalfa plants. Stem internodes of uniform age from greenhouse-grown plants were assayed for production of UDP-GlcA. Activity is expressed as percentage of the untransformed control Regen-SY. Plant lines in bold were selected for field testing.

Selection of Transgenic Alfalfa for Field Testing

In total, 13 independent transformed plants with the Atchit::SD5 construct (pARC205) for phloem-enhanced expression and 19 plants with the P4::SD5 construct (pARC206) for xylem-enhanced expression were generated and confirmed to contain the selectable marker gene and promoter–UDP–Glc dehydrogenase cDNA constructs by PCR. Assays for UDP–Glc dehydrogenase activity were carried out twice on young plants in the greenhouse to select those with reproducibly enhanced enzyme activity for testing in the field. Control untransformed plants (Regen-SY) had a mean activity of 3.7 U $\times$ 10^{-6}/mg of protein (U = µmole of UDP-GlcA/min). Plants from 5 of the 13 lines containing the Atchit::SD5 transgene (pARC205) had activities equal to or less than the control, while 8 lines had greater activity (Fig. 2). Plants containing the transgene driven by the xylem-enhanced promoter, P4, had the greatest UDP–Glc dehydrogenase activity. In 10 lines enzyme activity was more than 200% of the activity in control plants. Based on enzyme activity and plant vigor, the following lines were selected for field testing: pARC205-16, -17, -23, -24; pARC206-2, -6, -8, -11, -16, -20, -22. Lines with the highest levels of activity (pARC205-20; pARC206-1, -10, -17) had low vigor and produced insufficient numbers of rooted cuttings for field testing.

Table 1
Enzyme Activity and Plant Biomass Yield
from Field-Grown Plants

	Control activity (%)		Yield (g/plant)[a,b]	
	1999	2000	1999	2000
Regen-SY	100	100	15.6	58.3
pARC205-16	171[d]	156[d]	4.2[d]	25.3[d]
pARC205-17	154	141[d]	6.4[d]	42.0
pARC205-23	112	122	9.1[d]	37.9
pARC205-24	87	91	5.5[d]	46.1
pARC206-6	153	151[d]	4.8[d]	44.7
pARC206-11	169[d]	109	6.2[d]	(52.2)
pARC206-16	188[d]	170[d]	5.5[d]	(24.0)
pARC206-20	151	138[d]	8.4[d]	52.0
pARC206-22	194[d]	109	4.8[d]	47.7
SEM[c]	26	13	1.2	7.4

[a] Dry matter yield averaged over two harvests each year.
[b] Yield data in parentheses were not included in statistical analysis because an insufficient number of plants survived the preceding winter.
[c] Standard error of the mean.
[d] Transgenic line was significantly different from the nontransformed Regen-SY control line ($p < 0.05$).

UDP–Glc Dehydrogenase Activity and Plant Biomass of Field-Grown Plants

Carbohydrate composition in alfalfa is strongly influenced by environmental conditions and tissue maturity. Field testing of transgenic plants provided a means to evaluate whether increasing UDP–Glc dehydrogenase activity would have a practical and quantitative impact on stem pectin content or composition in mature plants. For lines pARC206-2 and –8, an insufficient number of plants survived to assess biomass production, enzyme activity, or cell-wall composition. Table 1 shows the dry matter yield (stems and leaves) per plant for the control and remaining transgenic lines averaged across the two harvests in both years of the experiment. The line times harvest interaction was non-significant ($p > 0.05$) in either year. In the establishment year, 1999, the nontransformed control line (Regen-SY) had significantly greater biomass accumulation than the lines containing the UDP–Glc dehydrogenase transgenes. Stem biomass paralleled total biomass production (data not shown). During the second year, biomass accumulation of Regen-SY plants and six lines containing UDP–Glc dehydrogenase transgenes was similar. Data for the pARC206-11 and -16 lines could not be analyzed for the second year because insufficient plants survived the preceding winter.

The mean UDP–Glc dehydrogenase activity in Regen-SY plants in 1999 was 1.26 U × 10^{-6}/mg of protein and in 2000 the mean activity was 5.10 U × 10^{-6}/mg of protein. Because the amount of measured enzyme activity was much greater in 2000 than 1999, and the manner in which the stems were sampled varied somewhat between years, the UDP–Glc dehydrogenase activity of the transgenic lines was calculated as a percentage of Regen-SY in each year. Under field conditions, transgenic lines showed small increases in enzyme activity, compared to the control (Table 1). In 1999, the activity in lines pARC205-16, and pARC206-11, -16, and -22 (2.15, 2.12, 2.37, and 2.45 U × 10^{-6}/mg protein, respectively) was significantly greater ($p < 0.05$) than activity in Regen-SY. In 2000, significant differences from Regen-SY were observed in pARC205-16 and pARC206-6, -16, and -20 (7.96, 7.70, 8.65, and 7.05 U × 10^{-6}/mg protein, respectively).

To determine whether expression of transgenes was occurring in field-grown plants, RNA was extracted from the third internodes of stems from the June 13, 2000, harvest. RT-PCR reactions were carried out using primers specific for *nptII* and the engineered soybean UDP–Glc dehydrogenase cDNA (SD5). Reactions from all transgenic lines resulted in the expected band of 670 bp using the primers for *nptII*. Reactions from all lines containing the UDP–Glc dehydrogenase transgenes contained the expected band of 1450 bp using the primers for SD5. Reactions from the nontransformed control were negative for both PCR products (data not shown).

Stem Cell-Wall Composition

Dry matter from the first and second harvests in 1999 was separated into leaf and stem fractions to measure pectin concentration and composition in stems. Data for cell-wall concentration and composition are presented in Table 2. The results are averaged across harvests because there were no significant ($p < 0.05$) line times harvest interactions. Alfalfa stems from the second harvest were less mature with lower cell-wall concentrations (638 and 591 g/kg of organic matter; $p < 0.05$) and lower amounts of cell-wall lignin (217 and 197 g/kg of cell wall; $p < 0.05$). Averaged across the harvests, pARC205-16 and pARC206-22 had more ($p < 0.05$) cell-wall material than the Regen-SY control. Polysaccharide content of the cell walls was lower ($p < 0.05$) and Klason lignin content was higher ($p < 0.05$) in all transgenic lines compared to Regen-SY. No significant increase in cell-wall glucose, galactose, or uronic acids owing to the presence of a transgene was observed in any line. Xylose and rhamnose were consistently present in higher proportions ($p < 0.05$) in the cell-wall polysaccharides of the transgenic lines, with the exception of no difference for xylose in pARC205-17, than found in Regen-SY. This increase was relatively greater for rhamnose (36%) than xylose (15%), but in absolute terms the increase in xylose deposition in the transgenics was much greater than the increase in rhamnose. Line pARC205-17 had significantly more arabinose than the Regen-SY, and several other transgenic lines tended toward an increase in arabinose. Mannose content of the cell-wall polysaccharides was consis-

Table 2
Stem Cell-Wall Concentration and Composition of Control and Transgenic Alfalfa Plants Averaged Across Two Harvests from 1999[a]

				Pectic sugars (g/kg polysaccharide)				Hemicellulosic sugars (g/kg polysaccharide)			
	CW (g/kg OM)	Poly (g/ kg CW)	KL (g/ kg CW)	UA	Gal	Ara	Rha	Xyl	Man	Fuc	Glc
Regen-SY	597	824	176	206	44	51	12	163	34	4.1	486
pARC205-16	640[b]	782[b]	218[b]	183	42	53	16[b]	194[b]	29[b]	3.6	480
pARC205-17	587	799[b]	201[b]	211	44	58[b]	17[b]	172	30[b]	3.2	464
pARC205-23	620	793[b]	207[b]	190	41	54	16[b]	187[b]	29[b]	3.1	479
pARC205-24	586	793[b]	207[b]	197	41	50	16[b]	182[b]	31[b]	2.5[b]	481
pARC206-6	627	787[b]	213[b]	193	41	55	16[b]	191[b]	30[b]	2.7[b]	472
pARC206-11	600	800[b]	200[b]	195	45	57	18[b]	182[b]	31[b]	4.5	468
pARC206-16	628	771[b]	229[b]	193	45	54	16[b]	184[b]	29[b]	3.1	476
pARC206-20	608	788[b]	212[b]	192	43	54	16[b]	182[b]	31[b]	3.2	479
pARC206-22	654[b]	778[b]	222[b]	176	39	49	16[b]	200[b]	29[b]	3.3	489
SEM	15	7	7	10	1	2	0.3	5	1	0.4	8

[a] CW, cell wall; Poly, polysaccharides; KL, Klason lignin; UA, uronic acids; Gal, galactose; Ara, arabinose; Rha, rhamnose; Xyl, xylose; Man, mannose; Fuc, fucose; Glu, glucose; OM, organic matter; SEM, standard error of the mean.

[b] The transgenic line was different from the nontransformed Regen-SY control line ($p < 0.05$).

tently reduced ($p < 0.05$) in the transgenic lines by approx 12% compared to the control. Two lines (pARC205-24 and pARC206-6) had minor decreases ($p < 0.05$) in fucose content compared to Regen-SY.

No obvious differences in tissue distribution, shape, or staining for the presence of pectin were observed among the alfalfa lines. The transgenic lines appeared normal in tissue structure.

Discussion

In plants, more than 100 genes are involved in cell-wall biosynthesis. Pectic polysaccharides play a critical role in plant cell-wall structure and in plant growth and development. Although degradation of pectin, primarily owing to enzymatic activity by pathogenic microbes, has been well characterized, comparatively little is known about the process of pectin biosynthesis. Several genes encoding enzymes in the pathways for production of the monosaccharide constituents of the cell-wall matrix have recently been cloned *(25)*, paving the way for manipulating polysaccharide composition and content. Because of the central role of UDP-GlcA in pectin biosynthesis, UDP–Glc dehydrogenase appeared to be an ideal candidate for ectopic expression to manipulate the composition of alfalfa cell walls. In young, rapidly growing plants, we saw enhanced enzyme activity in a number of transgenic lines. However, enhanced activity was not retained in mature field-grown plants. The lower enzyme activity may be a result of reduced promoter activity in mature stem tissues. Although the P4 and Atchit promoters were found to be active in vascular tissue of greenhouse-grown plants, their activity in more mature tissues is not known. However, transcripts were detected in mature stems from each transgene by RT-PCR suggesting that both promoters retained activity in older stems. It is highly likely that UDP–Glc dehydrogenase is subject to feedback regulation, which would impact activity and pectin synthesis. Dalessandro and Northcote *(11)* presented evidence for feedback inhibition of UDP–Glc dehydrogenase by UDP-xylose. In addition, other enzymes involved in pectin biosynthesis are subject to feedback regulation. For example, the activity of UDP-GlcA 4-epimerase from *Streptoococcus pneumoniae* is inhibited by UDP-GalA and UDP-xylose *(26)*.

Two distinct pathways exist in plants for synthesis of UDP-GlcA, one from UDP-Glc by action of UDP–Glc dehydrogenase and an alternative pathway by way of oxidation of *myo*-inositol (Fig. 1). It is possible that UDP-GlcA synthesis in alfalfa stems occurs primarily from *myo*-inositol. However, growing evidence supports a primary role for UDP–Glc dehydrogenase in the synthesis of UDP-GlcA for primary cell-wall construction. Radioactive labeling of squash hypocotyls with ^{3}H-inositol or ^{14}C-Glc resulted in approx 1% of the label incorporated into the cell wall coming from *myo*-inositol and 40% from Glc *(27)*. Inhibitor studies with soybean callus cells showed that cell-wall synthesis continues at a normal rate when the *myo*-inositol pathway is inhibited *(28)*. Tissue-specific expression of

UDP–Glc dehydrogenase also supports a role for this enzyme in providing precursors for cell-wall synthesis. In *Arabidopsis*, UDP–Glc dehydrogenase activity occurs in root and apical meristems, young leaves, and vascular tissue of young leaves *(10).* Similarly, in soybean, expression is highest in root tips, epicotyls, and expanding leaves *(9).* Additionally, the soybean cDNA of UDP–Glc dehydrogenase from suspension cultured cells shares 82–90% DNA sequence identity with *Medicago truncatula* ESTs (GenBank AW695554, BE326183) from developing stems. The alternative pathway for synthesis of UDP-GlcA, the *myo*-inositol oxidation pathway (Fig. 1), was found to be active in *Arabidopsis* cotyledons and hypocotyls, where it may play a role in turnover of phytate *(10).*

Plants with the largest increase in UDP–Glc dehydrogenase activity (pARC205-16 and pARC206-16) appeared to accumulate less dry matter than most transgenic lines in both years, possibly owing to expression level of the transgenes. The moderate increase in UDP–Glc dehydrogenase activity in alfalfa stems led to increased xylose and rhamnose, and a decrease in mannose in the cell-wall polysaccharide fraction of most transgenic lines. Possibly by increasing concentrations of UDP-GlcA, more substrate was available for synthesis of xylose and less available for synthesis of mannose (Fig. 1). Why rhamnose content of the pectic polysaccharides increased is unclear. It appears that the pathways for monosaccharide biosynthesis are highly interconnected and that altering production of a single enzyme in this pathway may not increase the yield of such a complex end product as pectin. Dörmann and Benning *(29)* found that overexpression of the gene for UDP-Glc 4-epimerase, which catalyzes the reversible conversion of UDP-Glc to UDP-galactose, increased enzyme activity threefold in *Arabidopsis* but did not alter the ratio between UDP-Glc and UDP-galactose. Antisense expression of the gene decreased enzyme activity by 90% but did not alter the cell-wall composition. Nonetheless, pectin composition and content have been altered by single gene changes. The *mur1* mutant of *Arabidopsis* is deficient in l-fucose, a component of xyloglucan and the pectic polysaccaharides rhamnogalacturonan I and II *(30).* Pectic polysaccharide composition has also been altered by ectopic gene expression. In transgenic potato (*Solanum tuberosum* L.), expression of genes for lytic enzymes such as rhamnogalacturonan lyase led to a large reduction in galactosyl and arabinosyl residues in rhamnogalacturonan I *(31)*, and expression of endo-α-1,5-arabinanase resulted in a 70% reduction in arabinose content in tubers *(32).*

To achieve a change in the pectin content in plants, it may be necessary to redirect UDP-Glc from cellulose biosynthesis. In *Nicotiana benthamiana* transient silencing of a cellulose synthase gene caused a 25% reduction in cellulose with a concomitant increase in homogalacturonan *(33).* Possibly, by reducing cellulose synthesis, more glucose was available for pectin synthesis. An alteration in pectin composition was also observed in cell walls of the *Arabidopsis* dwarf mutant *korrigan,* which is deficient in a membrane-bound endo-1,4-β-glucanase. Cell walls of these plants have increased

amounts of homogalacturonan and a decrease in rhamnogalacturonan *(34)*. Although endo-1,4-β-glucanase is not directly involved in pectin biosynthesis, its elimination results in substantial changes in cell-wall composition, further supporting the complexity of regulation of the enzymes directing pectin biosynthesis. In both cases, alteration of pectin content resulted in aberrant cell or plant growth. Thus, constitutive changes in pectin content cannot be made without serious impacts on plant development. Most pectin in alfalfa stems is located in tissues that do not lignify during maturation such as chlorenchyma and collenchyma *(35)*. Alfalfa genotypes differing in stem pectin content have been identified (unpublished). Analysis of gene expression in these genotypes may yield clues to successful modification of alfalfa for increased pectin content and rumen digestibility.

Acknowledgments

We gratefully acknowledge technical assistance from Sheila Lutz, Todd Miller, and Ted Jeo and field plot assistance from Keith Henjum. This research was funded in part by Pioneer Hybrid International and Forage Genetics. This article is a joint contribution from the USDA–Agricultural Research Service and the Minnesota Agricultural Experiment Station. Mention of a trademark, proprietary product, or vendor does not constitute a guarantee or warranty of the product by the USDA and does not imply its approval to the exclusion of other products and vendors that might also be suitable.

References

1. Beever, D. E. and Mould F. L. (2000), in *Forage Evaluation in Ruminant Nutrition,* Givens, D. I., Owen E., Axford R. F. E., and Omed, H. M. eds., CAB International, Wallingford, UK, pp. 15–42.
2. Galyean, M. L. and Goetsch, A. L. (1993), in *Forage Cell Wall Structure and Digestibility*, Jung, H. G., Buxton, D. R., Hatfield, R. D., and Ralph, J., eds., American Society of Agronomy-Crop Science Society of America-Soil Science Society of America (ASA-CSSA-SSSA), Madison, WI, pp. 33–72.
3. Hatfield, R. D. and Weimer, P. J. (1995), *J. Sci. Food Agric.* **69,** 185–196.
4. Nocek, J. E. and Russell, J. B. (1988), *J. Dairy Sci.* **71,** 2070–2107.
5. Strobel, H. J. and Russell, J. B. (1986), *J. Dairy Sci.* **69,** 2941–2947.
6. Aman, P. (1993), in *Forage Cell Wall Structure and Digestibility,* Jung, H. G., Buxton, D. R., Hatfield, R. D., and Ralph, J. eds., American Society of Agronomy-Crop Science Society of America-Soil Science Society of America (ASA-CSSA-SSSA), Madison, WI, pp. 183–200.
7. Hatfield, R. D. (1992), *J. Agric. Food Chem.* **40,** 424–430.
8. Robertson, D., Beech, I., and Bolwell, G. P. (1995), *Phytochemistry* **39,** 21–28.
9. Tenhaken, R. and Thulke, O. (1996), *Plant Physiol.* **112,** 1127–1134.
10. Seitz, B., Klos, C., Wurm, M., and Tenhaken, R. (2000), *Plant J.* **21,** 537–546.
11. Dalessandro, G. and Northcote, D. H. (1977), *Biochem. J.* **162,** 267–279.
12. Engles, F. M. and Jung, H. G. (1998), *Ann. Bot.* **82,** 561–568.
13. Hatfield, R. D., Ralph, J., and Grabber, J. H. (1999), *Crop Sci.* **39,** 27–37.
14. Pathirana, S., Samac, D. A., Roeven, R., Vance, C. P., and Gantt, S. J. (1997), *Plant J.* **12,** 293–304.

15. Hempel, J., Perozich, J., Romovacek, H., Hinich, A., Kuo, I., and Feingold, D. S. (1994), *Protein Sci.* **3,** 1074–1080.
16. Ausubel, F. M., Brent, R., Kingston, R. E., and Moore, D. (1995), *Short Protocols in Molecular Biology: A Compendium of Methods from Current Protocols in Molecular Biology*. John Wiley & Sons, New York, NY.
17. Samac, D. A. and Shah, D. M. (1991), *Plant Cell* **3,** 1063–1072.
18. Bevan, M. (1984), *Nucleic Acids Res.* **12,** 8711–8720.
19. Bingham, E. T. (1991), *Crop Sci.* **31,** 1098.
20. Austin, S., Bingham, E. T., Matthews, D. E., Shahan, M. N., Will, J., and Burgess, R. R. (1995), *Euphytica* **85,** 381–393.
21. Stewart, D. C. and Copeland, L. (1998), *Plant Physiol.* **116,** 349–355.
22. Theander, O., Aman, P., Westerlund, E., Andersson, R., and Petterson, D. (1995), *J. A.O.A.C. Int.* **78,** 1020–1044.
23. Ahmed, A. E. R. and Labavitch, J. M. (1977), *J. Food Biochem.* **1,** 361–365.
24. SAS Institute (1988), *SAS/STAT Users Guide*, Release 6.03 Ed., SAS Institute, Cary, NC.
25. Reiter, W.-D. and Vanzin, G. F. (2001), *Plant Molec. Biol.* **47,** 95–113.
26. Muñoz, R., López, R., de Frutos, M., and García, E. (1999), *Mol. Microbiol.* **31,** 703–713.
27. Wakabayashi, K., Sakurai, N., and Kuraishi, S. (1989), *Plant Cell Physiol.* **30,** 99–105.
28. Biffen, M. and Hanke, D. E. (1991), *Plant Sci.* **75,** 203–213.
29. Dörmann, P. and Benning, C. (1998), *Plant J.* **13,** 641–652.
30. Bonin, C. P., Potter, I., Vanzin, G. F., and Reiter, W.-D. (1997), *Proc. Natl. Acad. Sci. USA* **94,** 2085–2090.
31. Oomen, R. J. F. J., Doeswijk-Voragen, C. H. L., Bush, M. S., Vincken, J.-P., Borkhardt, B., van den Broek, L. A. M., Corsar, J., Ulvskov, P., Voragen, A. G. J., McCann, M.C., and Visser, R. G. F. (2002), *Plant J.* **30,** 403–413.
32. Skjøt, M., Pauly, M., Bush, M. S., Borkhardt, B., McCann, M. C., and Ulvskov, P. (2002), *Plant Physiol.* **129,** 95–102.
33. Burton, R. A., Gibeaut, D. M., Bacic, A., Findlay, K., Roberts, K., Hamilton, A., Baulcombe, D. C., and Fincher, G. B. (2000), *Plant Cell* **12,** 691–705.
34. His, I., Driouich, A., Nicol, F., Jauneau, A., and Höfte, H. (2001), *Planta* **212,** 348–358.
35. Jung, H. G. and Engels, F. M. (2002), *Crop Sci.* **42,** 524–534.

0273-2289/04/116/1183–1191/$25.00

Effects of Ammonia Fiber Explosion Treatment on Activity of Endoglucanase from *Acidothermus cellulolyticus* in Transgenic Plant

Farzaneh Teymouri,[1] Hasan Alizadeh,[1] Lizbeth Laureano-Pérez,[1] Bruce Dale,[*,1] and Mariam Sticklen[2]

[1]Department of Chemical Engineering and Material Science, 2527 Engineering Building, E-mail: bdale@msu.edu; and [2]Crop and Soil Sciences Department, 361 Plant and Science Building, Michigan State University, MI 48824

Abstract

A critical parameter affecting the economic feasibility of lignocellulosic bioconversion is the production of inexpensive and highly active cellulase enzymes in bulk quantity. A promising approach to reduce enzyme costs is to genetically transform plants with the genes of these enzymes, thereby producing the desired cellulases in the plants themselves. Extraction and recovery of active proteins or release of active cellulase from the plants during bioconversion could have a significant positive impact on overall lignocellulose conversion economics. The effects of ammonia fiber explosion (AFEX) pretreatment variables (treatment temperature, moisture content, and ammonia loading) on the activity of plant-produced heterologous cellulase enzyme were individually investigated via heat treatment or ammonia treatment. Finally, we studied the effects of all these variables in concert through the AFEX process. The plant materials included transgenic tobacco plants expressing E1 (endoglucanase from *Acidothermus cellulolyticus*). The E1 activity was measured in untreated and AFEX-treated tobacco leaves to investigate the effects of the treatment on the activity of this enzyme. The maximum observed activity retention in AFEX-treated transgenic tobacco samples compared with untreated samples was approx 35% (at 60°C, 0.5:1 ammonia loading, and 40% moisture). Based on these findings, it is our opinion that AFEX pretreatment is not a suitable option for releasing cellulase enzyme from transgenic plants.

*Author to whom all correspondence and reprint requests should be addressed.

Index Entries: Ammonia fiber explosion; endoglucanase; *Acidothermus cellulolyticus*; transgenic tobacco; E1cd.

Introduction

In ethanol production, enzymatic hydrolysis of cellulose to glucose is an attractive route, because nearly theoretical yields of glucose are possible *(1,2)*. Cellulase enzymes are currently produced from microorganisms by expensive large-scale fermentation. The cost of enzyme-based processes has been reduced by about a factor of four *(1)*, and additional improvement opportunities have been identified that may make the technology even better *(3)*. However, enzyme production costs through microbial systems are still very high and tend to dominate the economics of enzyme-based bioconversion processes. These costs might conceivably be reduced by genetically transforming plants with cellulase genes to produce the desired enzymes, and perhaps even to release active cellulases from the plants during bioconversion.

Transgenic plants are an attractive and cost-effective alternative to microbial systems for production of biomolecules *(4)*. Advances in biotechnology are enabling plants to be exploited as bioreactors for the production of proteins, carbohydrates *(5,6)*, lipids *(7,8)*, and industrial enzymes *(9–11)* in bulk quantities with minimal inputs of raw materials and energy. As this technology continues to grow and improves the production efficiencies of biomolecules in plants, the development of downstream processing technology to extract and recover these biochemicals will increasingly determine progress in this area.Enzymes and other proteins produced in transgenic crops have very high value. Recovering and utilizing valuable bioactive plant proteins and enzymes in an overall process for producing fuels and chemicals from biomass may improve the lignocellulose conversion economics.To process cellulase-containing transgenic plants, the following technical options can be envisioned:

1. Harvest the cellulase-containing transgenic plants while they are green, macerate them, and separate the solid to produce an enzyme concentrate, which can later be used in the enzymatic hydrolysis of pretreated biomass. Depending on the production level of this enzyme in transgenic plants, the need for externally added cellulases in the enzymatic hydrolysis step might be avoided or minimized.
2. Harvest the cellulase-containing transgenic plants at the end of the season (dry), grind this material to release enzyme, and subsequently use it in the enzymatic hydrolysis of lignocellulosic biomass for ethanol production.
3. Harvest the cellulase-containing transgenic plants at the end of the season, use biomass pretreatment to rupture plant cells to facilitate the release of enzyme, and then combine this material with lignocellulosic biomass in enzymatic hydrolysis.

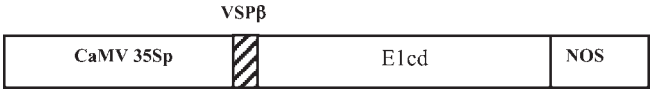

Fig. 1. Schematic representation of E1cd expression cassette. CaMV 35Sp, cauliflower mosaic virus promoter; NOS, nopaline synthase transcription termination signal; E1cd, catalytic domain of E1 gene; VSPβ, soybean vegetative storage protein β leader sequence to target the protein to apoplast *(15)*.

The success of any of these approaches depends on having a sufficiently high level of cellulase in the transgenic plant to make hydrolysis effective. Research such as that reported here is required to define which option(s) might prove favorable under specific circumstances.

A high recovery yield of plant proteins from biomass depends on extensive cell maceration. The more cell walls are disrupted, the more protein can be recovered *(12)*. Therefore, a pretreatment that disrupts plant cells may be useful in protein recovery processes.

An integrated pretreatment that improves protein recovery and increases the conversion of cellulose and hemicellulose to fermentable sugars could significantly enhance the biomass process economics. Many pretreatment processes that increase the conversion of cellulose to fermentable sugars operate under harsh conditions that tend to degrade the sugars, biomass proteins, and enzymes. However, previous studies *(13,14)* have shown that under limited treatment conditions, the AFEX process not only increases the conversion of cellulose and hemicellulose to simple sugars, but also allows the recovery of plant proteins in their native functional form.In the present study, we explored the third option that we just discussed. We investigated the potential of using AFEX as an integrated pretreatment process to enhance the release of active cellulase enzyme from transgenic plant while simultaneously increasing the digestibility of the biomass.

Material and Methods

Plant Material

Seeds of the transgenic tobacco plants expressing E1cd (catalytic domain fragment of E1 endo-1,4-β-glucanase from *Acidothermus cellulolyticus*) were obtained from Dr. Sandra Austin-Phillips from the University of Wisconsin–Madison. Figure 1 shows the plasmid that has been used by Dr. Austin-Phillips's group to transform tobacco plants to express the E1cd in apoplast.

Transgenic plants were grown, harvested (leaves), and dried at Michigan State University greenhouses. As Fig. 2 shows, the expression of E1cd did not cause any obvious phenotypic effect in plants and did not affect their normal growth.

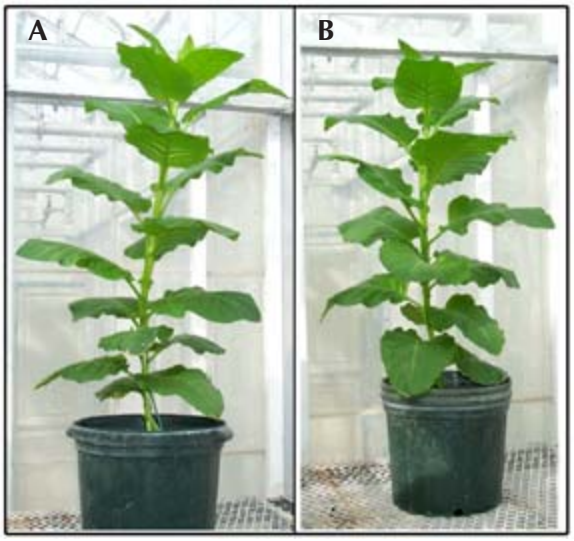

Fig. 2. **(A)** Nontransgenic and **(B)** transgenic tobacco plants grown in a greenhouse.

Identification of Transgenic Plant Expressing E1cd

After seedlings developed their first true leaves, samples were removed for enzyme assay to identify transgenic plants. Enzyme assay was conducted according to Ziegelhoffer et al. *(15)*. E1cd activity was determined by subtracting the background contributed by W38 control extracts, and fluorescence values were compared with values obtained with purified E1cd (provided by Steven R. Thomas, National Renewable Energy Laboratory [NREL], Golden, CO). The expression level of E1cd in transgenic plants was up to 2.5% of total soluble proteins. Transgenic plants were grown to maturity, and leaves were harvested, dried, and collected for AFEX treatment. Since each independently transformed plant had a different level of expression, the dried leaves were ground and well mixed before AFEX treatment to ensure the homogeneity of the samples.

AFEX Treatment

The AFEX reactor consisted of a 300 ml stainless steel pressure vessel (Parr Instrument, Moline, IL) (Fig. 3). The vessel was loaded with prewetted transgenic tobacco leaves with the desired moisture content (a range of moisture content was tested to determine the effect of moisture content on the activity of cellulase in AFEX-treated transgenic plants). The vessel was topped up with stainless steel pellets (approx 1 mm in diameter) to occupy the void space and thus minimize transformation of the ammonia from liquid to gas during loading, and then the lid was bolted shut. Using precalibrated ammonia sample cylinders, a predetermined amount of liquid ammonia was delivered to the vessel. The vessel was heated by a 400-W Parr heating mantle to the desired temperature.

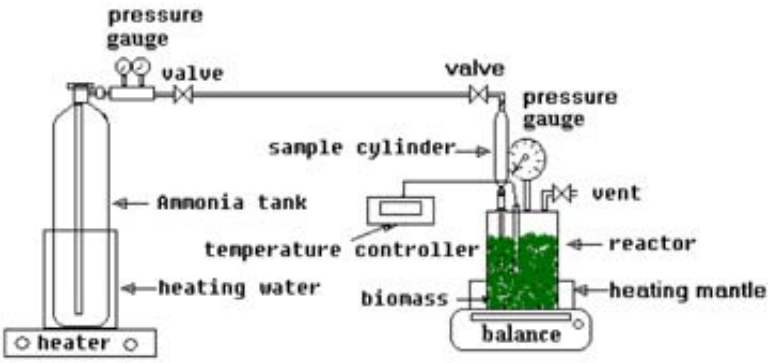

Fig. 3. Schematic diagram of laboratory AFEX apparatus.

After holding the vessel at the target temperature for 5 min, the exhaust valve was rapidly opened to relieve the pressure and accomplish the explosion. The treated samples were removed and left in a fume hood overnight at atmospheric conditions to evaporate the residual ammonia. AFEX-treated samples were darker than untreated sample, and other than this no visible physical change was observed.

Heat Treatment of Transgenic Tobacco Plants Expressing E1cd

The prewetted samples were placed in the AFEX unit, and the vessel was sealed and warmed to the desired temperature as described in the previous section. To avoid overheating, the reactor was taken out of the heater at approx 10°C less than the target temperature, and if needed the unit was placed in a bath of cold water to maintain the system at the set temperature. The system was kept at the target temperature for 5 min. Since there was no ammonia in this system, no increase in pressure was observed during the experiment. At the end of 5 min, the heat-treated samples were removed from the vessel and kept in plastic bags at 4°C until further analysis.

Ammonia Treatment of Transgenic Tobacco Plants Expressing E1cd

The prewetted samples were placed in the pressure vessel of the AFEX unit. The vessel was sealed as already explained. A predetermined amount of ammonia was delivered to the pressure vessel. To ensure that the desired amount of ammonia was delivered, the reactor vessel was weighed before and after loading. The vessel was left in the fume hood at room temperature (without heating) for 10 min. During the experiment, some of the liquid ammonia converted to gaseous ammonia and increased the pressure from 90 to 105 psi (after 10 min), and since the vessel was not heated, the system temperature was decreased (initial temperature was 34°C and final temperature was about 28°C).

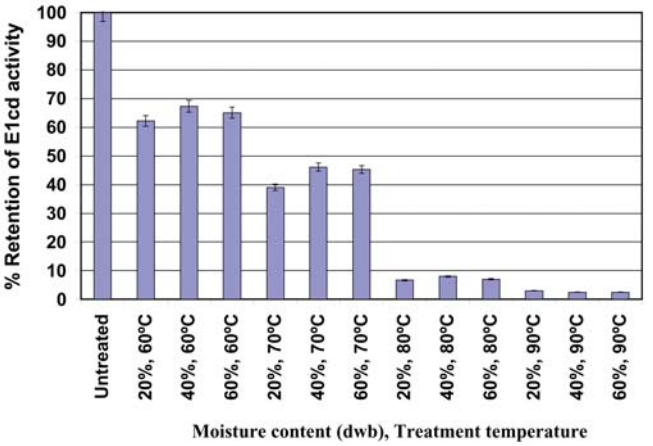

Fig. 4. Activity retention of E1cd extracted from heat-treated transgenic tobacco plants.

Measurement of Activity of E1cd Enzyme In Transgenic Tobacco Plants After Treatments

All the treated and untreated transgenic tobacco plant samples were ground and sieved to 40 mesh prior to the E1cd activity assay. E1cd was extracted from the treated and untreated samples as described by Ziegelhoffer et al. *(15)*. The total protein of each of the extracts was measured by the Bradford *(16)* method using bovine serum albumin as a standard. Subsequently the appropriate amount of extract containing the same amount of total protein was subjected to the activity assay.

Results and Discussion

Transgenic tobacco plants were treated at different temperatures (60–90°C) and at different levels of ammonia (0.5:1, 0.7:1, and 1:1 kg of ammonia:kg of dry tobacco sample) to assess the individual effect of each AFEX variable on the E1cd enzymatic activity. All results are the mean of two replicates, and they have been compared with the untreated transgenic tobacco sample. In all the runs the moisture contents are based on the sample dry weight.

Ziegelhoffer et al. *(15)* tested the stability of the apoplast-targeted E1cd in transgenic tobacco plants. In their study, the apoplast-targeted E1cd enzyme extracted from tobacco plants, along with the purified microbial E1cd, was subjected to different temperatures (60–90°C) for 10 min. Both enzymes showed similar high thermal stability throughout the experiment. Their results showed that at 60°C up to 95%, at 70°C up to 90%, at 80°C up to 80%, and at 90°C up to 40% of the enzymes' activity was retained. However, as seen in Fig. 4, our heat stability test showed sur-

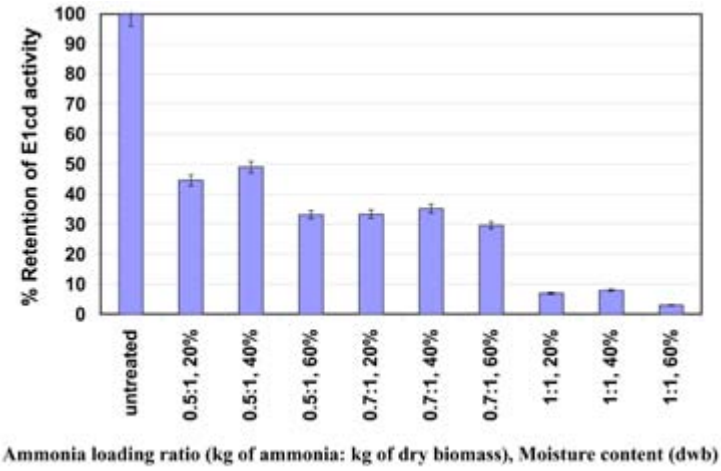

Fig. 5. Activity retention of E1cd extracted from ammonia-treated transgenic tobacco plants. dwb, dry weight basis.

prisingly different results from those reported by Ziegelhoffer et al. *(15)*. The E1cd extracted from transgenic tobacco plants treated at 60°C showed a maximum 67% and at 70°C showed a maximum 46% activity retention compared to E1cd extracted from untreated transgenic tobacco plants. The E1cd extracted from the samples treated at 80 and 90°C was almost completely inactive.

Figure 5 shows that at any moisture content, as the ammonia loading increased, the percentage of E1cd activity retention decreased, and at a 1:1 loading ratio, the E1cd enzyme was almost completely inactive. The highest percentage activity retention (49%) was observed at 0.5:1 ammonia loading with 40% moisture content. As Figs. 4 and 5 demonstrate, at any temperature and any ammonia loading, 40% moisture content showed the highest activity retention.

The transgenic tobacco samples were AFEX treated under different conditions. These experimental conditions were selected based on the results of our heat and ammonia treatment of transgenic tobacco plants; we chose the conditions that showed the highest enzymatic activity retention for E1cd. The results of these experiments are presented in Fig. 6.

E1cd enzyme showed better survival rates with individual heat or ammonia treatment (up to 67 and 49%, respectively), but the combination of heat and ammonia in AFEX treatment caused a drastic loss in the activity of E1cd. The maximum observed activity retention in AFEX-treated transgenic tobacco plants was only 35% at 60°C, 0.5:1 ammonia loading ratio, and 40% moisture content. Future studies may be able to clarify the mechanistic bases for these observations.

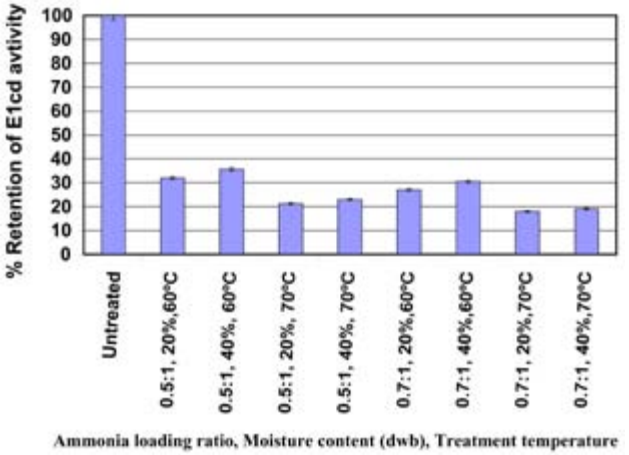

Fig. 6. Activity retention of E1cd extracted from AFEX-treated transgenic tobacco plants. dwb, dry weight basis.

Conclusion

Originally, pretreatment techniques were developed for various end uses of lignocellulosic biomass with an emphasis on ethanol production. Pretreatment processes have been used to enhance enzymatic hydrolysis of biomass to increase ethanol production and improve lignocellulosic conversion economics. Advances in biotechnology are enabling plants to become economically important systems for producing heterologous proteins such as cellulase enzymes. Therefore, expanding the application of biomass pretreatment to the release and recovery of these proteins might significantly improve biorefinery economics. We examined the potential of the AFEX treatment to recover active cellulase. As the data show, the maximum E1cd activity retention in AFEX-treated transgenic tobacco plant (under 60°C, 0.5:1 ammonia loading, and 40% moisture conditions) was only 35%. The glucan conversion of corn stover treated under the same conditions was only 47% of theoretical with 60 filter paper units/g of glucan of cellulase enzyme *(14)*. Based on these findings, it is our opinion that AFEX pretreatment is not a suitable option for releasing cellulase enzyme from transgenic plants. Considering the fact that other biomass pretreatments (e.g., steam explosion, acid treatment) operate under even harsher conditions, it is reasonable to assume that none of these pretreatments are a suitable choice for this purpose. Using pretreatment to release the cellulase enzymes from transgenic plants was only one of our technical options, therefore exploring the potential of other options (mentioned in Introduction) merits future study.

Based on these results and previous research *(15)*, we believe that E1cd extracted from transgenic plants is thermostable if it is heated in the

extraction buffer (at the enzyme's preferred pH of 5.5), but its thermal stability drastically decreases if plants expressing the enzyme are heated directly.

Acknowledgments

We are grateful to NREL for providing purified E1 enzyme, and Dr. Sandra Austin-Phillips for providing seeds for transgenic tobacco plants expressing E1cd enzyme. We also thank Mitra Sticklen for greenhouse assistance, and Majed Hammud for laboratory assistance. This work was supported by the USDA Initiative for Future Agricultural and Food Systems Program through contract no. 00-52104-9663.

References

1. Wyman, C. E. (1999), *Annu. Rev. Energy Environ*. **24,** 189–226.
2. Wyman, C. E. (1995), in *Enzymatic Degradation of Insoluble Carbohydrates*, ACS Symposium Series 618, Saddler, J. N. and Penner, M. H., eds., American Chemical Society, Washington, DC, pp. 272–290.
3. Lynd, L. R., Elande, R. T., and Wyman, C. E. (1996), *Appl. Biochem. Biotechnol.* **57/58,** 741–61.
4. Goddijn, O. J. M. and Pen, J. (1995), *Trends Biotechnol*. **13,** 379–387.
5. Kidd, G. and Devorak, J. (1994), *Bio/Technology* **12,** 1328–1329.
6. Stark, D., Timmermann, K. P., Barry, G. F., Preiss, J., and Kishore G. M. (1992), *Science* **258,** 287–292.
7. Grayburn, W. S., Collins, G. B., and Hildebrand, D. F.(1992), *Bio/Technology* **10,** 675–678.
8. Poirier, Y., Nawrath, C., and Somerville, C. (1995), *Bio/Technology* **13,** 142–150.
9. Austin, S., Koegel, R. G., Matthews, D., Shahan, M., Strau, R. J., and Burgess, R. (1994), *Ann. NY Acad. Sci*. **721,** 234–244.
10. Pen, J., Molendijk, L., Quax, W. J., Sijmons, P. C., van Ooyen, A. J. J., van den Elzen, P. J. M., Rietveld, K., and Hoekema, A. (1992), *Bio/Technology* **10,** 292–296.
11. Pen, J., Verwoerd, T. C., van Paridon, P. A., Beudeker, R. F., van den Elzen, Geerse, K., van den Klis, J. D., Versteegh, H. A. J., van Ooyen, A. J. J., and Hoekema, A.(1993), *Bio/Technology* **11,** 811–814.
12. Carroad, P. A., Anaya-Serrano, H., Edwards, R. H., and Kohler, G. O. (1981), *J. Food Sci*. **46(2),** 383–386.
13. De la Rosa, L. B., Dale, B. E., Reshamwala, S. T., Latimer, V. M., Stuart, E. D., and Shawky, B. T. (1994), *Appl. Biochem. Biotechnol*. **45/46,** 483–497.
14. Teymouri, F. (2003), PhD thesis, Department of Chemical Engineering and Material Sciences, Michigan State University, East Lansing, MI.
15. Ziegelhoffer, T., Raasch, A., and Austin-Phillips, S. (2001), *Mol. Breeding* **8,** 147–158.
16. Bradford, M. (1976), *Anal. Biochem*. **72,** 248–254.

0273-2289/04/116/1193–1203/$25.00

Effects of Inoculum Conditions on Growth of Hairy Roots of *Panax ginseng* C.A. Meyer

Gwi-Taek Jeong,[1] Don-Hee Park,[*,1,2] Hwa-Won Ryu,[1] Baik Hwang,[3] and Je-Chang Woo[4]

[1]Faculty of Applied Chemical Engineering,
[2]Institute of Bioindustrial Technology, [3]Department of Biological Sciences,
Chonnam National University, Kwangju 500-757, Korea,
E-mail: dhpark@chonnam.ac.kr; and
[4]Department of Biology, Mokpo National University,
Chonnam 534-729, Korea

Abstract

Plants have a potential to produce a large number of important metabolites such as pharmaceuticals, food additives, pigments, flavors, fragrances, and fine chemicals. Large-scale plant cell and tissue cultures for producing useful products has been considered an attractive alternative to whole plant extraction for obtaining valuable chemicals. In plant cell and tissue cultures, cell growth and metabolite production are influenced by nutritional and environmental conditions as well as physical properties of the culture system. To obtain a high growth rate of plant cell and tissue cultures, the culture conditions should be maintained at an optimum level. We studied the relationship between inoculum conditions and the growth of *Panax ginseng* hairy root culture, and found that the growth rate varied with the inoculum conditions such as the number of root tips, the length of root tips, the part of root tips, and the inoculum size and age of hairy roots.

Index Entries: *Panax ginseng*; transformed hairy root; inoculum condition; inoculum age; root culture.

Introduction

Plants are known as a potential source of a large number of important biochemical constituents *(1–3)*. In recent years, transformed hairy roots have been studied as a potential large-scale source for production of plant-derived useful compounds such as pharmaceuticals. They have several advantages compared to plant cell suspension culture, such as high growth rate, high and stable secondary metabolite productivity, autotrophy of

*Author to whom all correspondence and reprint requests should be addressed.

plant growth hormones, and inherent genetic stability reflected in stable growth and reproduction *(4,5)*.

Several bioreactor designs have been demonstrated for large-scale culture of hairy roots *(6,7)*. Bioreactors used for hairy root culture are more complex owing to continuous growth of hairy root and must compensate for the heterogeneous, cohesive, structured, and entangled nature of fibrous roots *(4)*. Hairy root cultures may be feasible for large-scale applications, but many problems with the hairy root culture system are still unsolved *(6–9)*.

In plant cell culture, the growth rate is generally affected by inoculum conditions such as cellular age and preculture period *(10)*. For many years, it has been known that inoculum size is a significant factor affecting the performance of plant cell suspension cultures. Inoculum size affects the activities of enzymes in plant cell cultures for a synthesis of secondary metabolites *(11)*. If the inoculum size is sufficiently high, the lag phase may be eliminated or diminished. The root growth morphology may be an important consideration factor in the development of large-scale processes using hairy roots *(12)*. The development of suitable large-scale inoculation techniques and strategies to provide uniform root distribution within bioreactors has met with obstacles *(13)*.

Very few investigations have been carried out on the effect of inoculum conditions on hairy root cultures *(11)*. In recent research of the root culture system, the inoculum studies have often focused on the physical structure and physiologic status of roots *(14)*. Bhadra and Shanks *(15)* reported that the length of individual root tips was an important factor on growth, while the number of tips used in the inoculum had relatively little effect on *Catharanthus roseus* hairy root culture.

Panax ginseng C.A. Meyer, which belongs to the Araliaceae family, is one of the most famous oriental medicinal plants and is found in the Korean peninsula and China. Ginseng plants have many beneficial bioactive effects on human health, such as hemostatic qualities and abilities to promote blood circulation, relieve pain, cure bleeding wounds and trauma, relieve stress, and improve immune functions. The major compounds of pharmaceutical interaction in ginseng have been identified to be saponin (ginsenosides), polysaccharides, antioxidants, peptides, fatty acids, alcohols, vitamins, and phenolic compounds *(16,17)*. The aim of the present work was to investigate the effect of inoculum conditions on the growth and metabolite biosynthesis of *P. ginseng* C.A. Meyer hairy root culture.

Materials and Methods

Hairy Roots and Culture

The hairy roots of *P. ginseng* C.A. Meyer were initiated and maintained as described previously *(18)*. In all experiments, the hairy roots were cultivated in liquid hormone-free 1/2 MS medium *(18)* containing 30 g/L of sucrose. The pH of the medium was adjusted to 5.8 with 2 *N* NaOH, and

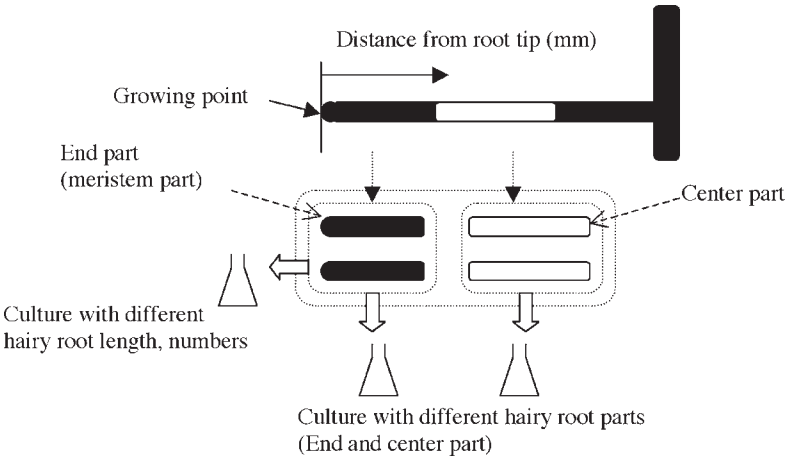

Fig. 1. Schematic of root segment preparation used for inoculum conditions of *P. ginseng* hairy root.

the medium was autoclaved at 121°C for 15 min and cooled to 23°C prior to use. Cultures were incubated at 23°C in the dark in 250-mL Erlenmeyer flask on a rotary shaking incubator (Vision Scientific) operated at 70 rpm.

Experimental Procedure

Shake-flask experiments were carried out to investigate the effect of inoculum conditions on hairy root growth and metabolite biosynthesis. To investigate the effect of the root tip on hairy root growth for 30 d, the end part (meristem part) of the primary root tip was excised about 10 mm from the apical meristem, and the center part was used to 10 mm length after the end part root tips (Fig. 1) *(19)*. Each flask contained 30 mL of medium/100-mL flask and three root tips. To investigate the effect of root tip number and length on hairy root growth, the number of root tips was set at one, three, six, or nine with each 10 mm long, and the root tip length was set at 5–25 mm with three root tips. Each experiment was performed in a 100-mL flask containing 30 mL of medium for 30 d. To determine optimum inoculum age, 5- to 30-d-old cultured roots were used as an inoculant with 1% (w/v) g fresh weight for 30 d in a 250-mL Erlenmeyer flask containing 100 mL of medium. To determine optimum inoculum size in flask culture, 0.2–3.0 % (w/v) inoculum size was tested for 15 d in a 250-mL Erlenmeyer flask containing 100 mL of medium.

For scale-up of inoculum conditions of hairy root cultivation, a 1-L bioreactor (working volume of 800 mL) was used. This bioreactor had a height/diameter aspect ratio of 7.14. The bubble bioreactors had no internal mechanical agitation parts. The supplied aeration rate was 0.1 vvm at the bottom by sparger. Each bioreactor was inoculated with 0.2–2.0 % (w/v) g fresh weight of hairy roots and cultured for 32 d.

Analytical Methods

To determine cell mass, the hairy roots were harvested, rinsed with distilled water, and the extra water was eliminated. Treated hairy roots were measured as fresh weight and dry weight. The dry weight was measured gravimetrically after drying the roots at 60°C for 24 h.

Extraction and Analysis of Crude Saponin and Intracellular Polysaccharide

To determine crude saponin, 100 mg of powdered dry hairy roots was suspended in 5 mL of water-saturated *n*-BuOH, sonicated for 2 h, and centrifuged twice at 5030*g* for 10 min. The collected supernatant was used to determine crude saponin by the vanillin-H_2SO_4 gravimetric methods *(18)*.

To determine intracellular polysaccharide, 100 mg of powdered dry hairy roots was suspended in 10 mL of distilled water, sonicated for 1 h, and centrifuged twice at 5030*g* for 10 min. The collected supernatant was used to determine intracellular polysaccharide by the phenol–sulfuric acid method *(19)*.

Calculation of Growth Rate

Cell growth was evaluated in terms of average cell growth rate (GR). Average growth rate was defined as follow:

GR = (final cell mass – initial cell mass)/initial cell mass/time

The presented data are the average value from three independent experiments each repeated twice.

Results and Discussion

Hairy roots show species- and culture-dependent branching patterns *(20)*. A general characteristic of hairy roots is their prolific branching tendency, resulting in generation of many new root tips and relatively high specific growth rates *(12)*. The physical structure of hairy roots presents handling problems for preparation of inoculum in large-scale cultivation. The management of branching pattern in hairy root cultures is important because branching can influence growth rate and production of metabolites, but branching patterns are not simply related to the inoculum conditions *(20)*. We investigated the effect of inoculum conditions such as inoculum size, root parts, age, and root number on the growth and metabolite production in *P. ginseng* hairy root culture.

Figure 2 shows the effect of the inoculated root tip part on the growth of *P. ginseng* hairy roots. The end part, whose apical meristem of root tip had been excised prior to inoculation, was grown to a total biomass 1.6 times greater than that of the center parts, which are the root tip part after being excised about 10 mm from the end part. In all experiments, new lateral branch formation was observed on the inoculated main root tip.

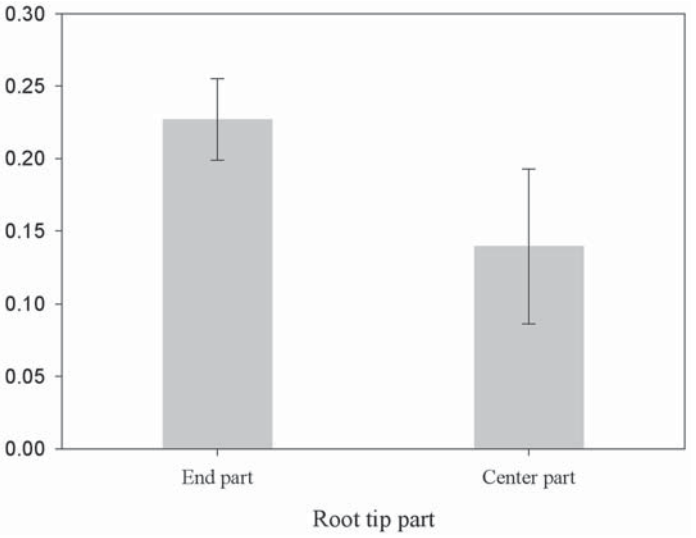

Fig. 2. Effect of inoculated root tip parts on biomass growth in flask culture for 30 d (used root tip length of 5-mm).

The root tip with apical meristem showed length enhancement with lateral root formation. However, the center root tip formed lateral roots without length enhancement of the original root tip (Fig. 3). Some researchers have reported the effect of the apical dominance on growth, which was observed as an increase in specific growth rate for inocula formed by branched roots *(12,14).*

Medium conditioning by increasing cell density is known to be an important factor in plant cell suspension culture *(21).* Increasing the number of inoculated root tips in root culture would be expected to promote more rapid conditioning of the medium and therefore show better growth, but it did not affect the growth in the hairy root experiments reported here. At the beginning of hairy root culture, when the flasks contain only a few root tips, the total oxygen demand is minimal; thus, the mass transfer does not interfere significantly. During the growth period of hairy roots, mass-transfer limitations were not believed to reduce the growth rate of hairy root cultures *(11).* The growth rate depends on the generation of new meristematic growth regions. If the ratio between the number of root tips per length decreases as the root culture grows, the specific growth rate would decline *(14).*

Some suggest the concept that diversity of the hairy root tip—cell division, elongation, and maturation regions—is necessary for optimal growth rate *(15).* The best growth of root tips is consistent with the formation of new branches in maturation zones and enhancement of apical dominance *(14).*

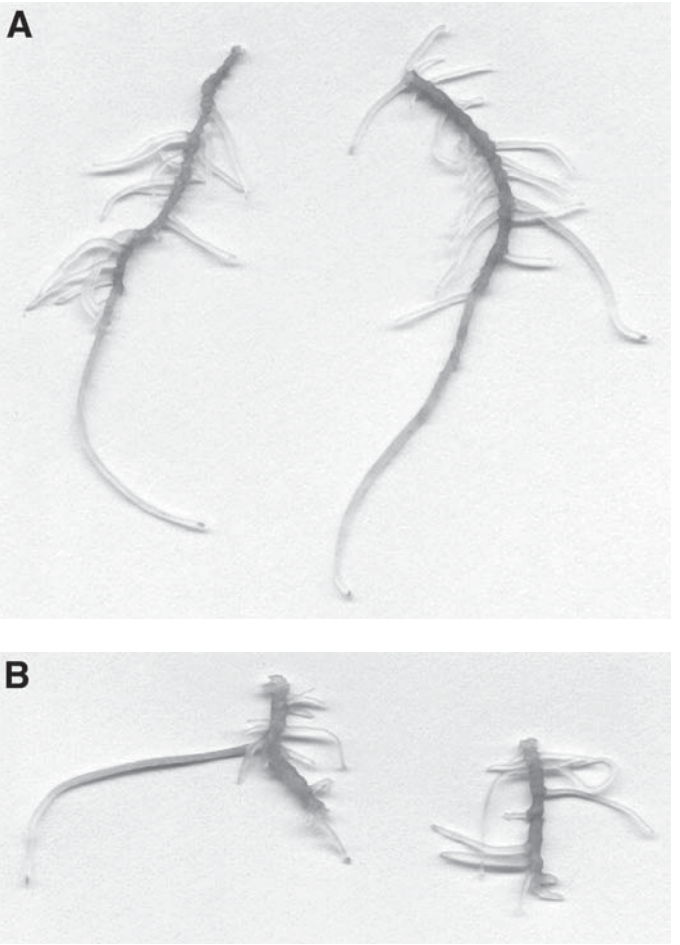

Fig. 3. Growing root segments of *P. ginseng* hairy root in solid culture for 10 d: **(A)** end part; **(B)** center part.

Figure 4 shows the effect of the number of root tips in the inoculum. Increasing the number of root tips from one to six enhanced growth rate. However, the growth rate was reduced by 21% at 9 root tips. These results were caused by several factors, including medium conditioning, mass-transfer resistance, and interactive effect of root tips. The number of inoculated root tips and the initial medium volume had relatively little effect on culture growth for *Catharanthus roseus* hairy roots, and increasing the number of tips from three to nine reduced growth rates by up to 40% in *Atropa belladonna* hairy root culture *(11,15).*

Figure 5 shows the effect of different lengths of root tips in shake-flask cultures. By inoculating shake flasks with root tips of different lengths (5–25 mm), the highest growth rate was obtained for 5-mm-long root tips.

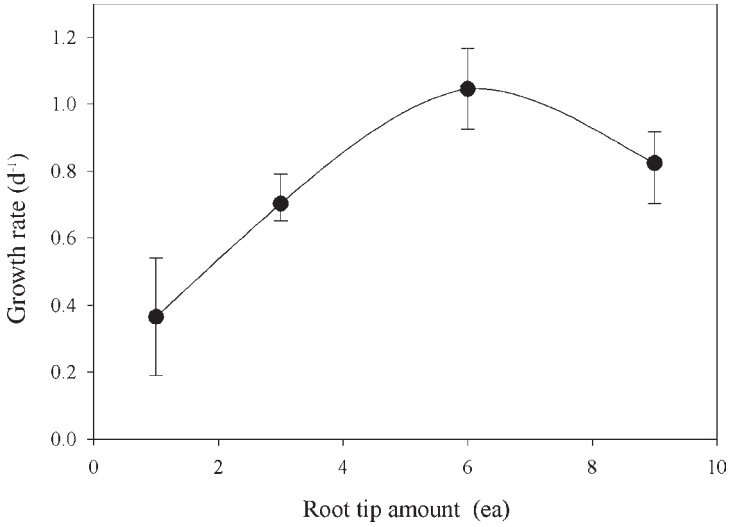

Fig. 4. Effect of inoculated root tip number on biomass growth in flask culture for 30 d.

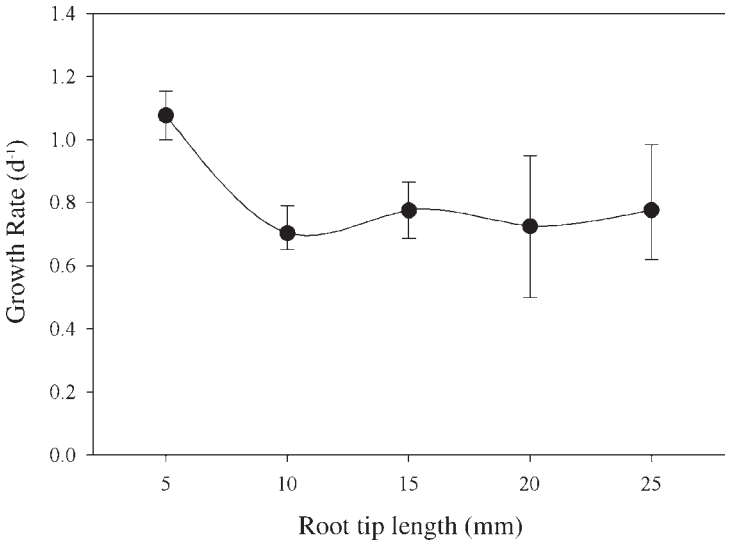

Fig. 5. Effect of inoculated root tip length on biomass growth in flask culture for 30 d (each experiment was performed using three root tips).

Longer tips (10–25 mm) containing apical meristem and maturation zone all had a lower growth rate. We believe that the suppression of growth was caused by a physiologic status of inoculated root tips affected largely by enhancing their apical dominance in spite of retarding the appearance of new lateral branches in the maturation zone. By contrast, Bhadra and Shanks *(15)* have reported that the specific growth rates of culture for 35 to 40-mm-long root tips was 20–60% higher than for cultures with 10 to 15-mm-long root tips in *C. roseus* hairy root culture.

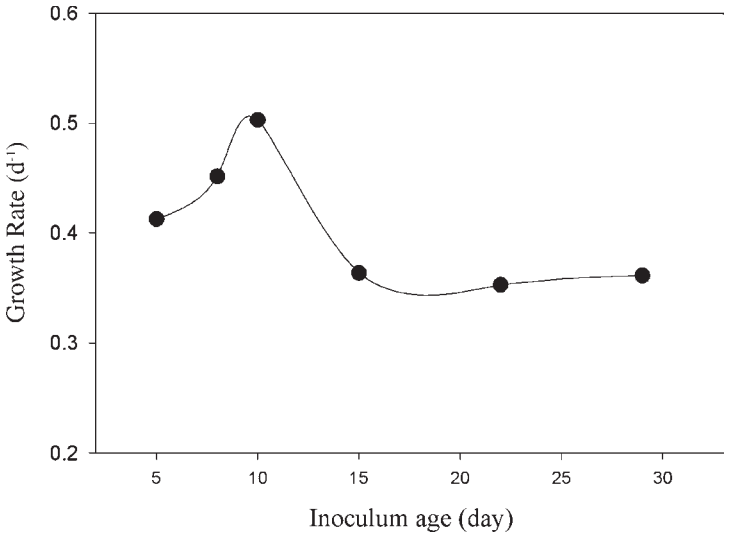

Fig. 6. Effect of inoculum age on biomass growth in flask culture for 30 d.

To investigate the influence of inoculum condition such as precul-tured age of root inoculant, the hairy roots were incubated for various periods (5–30 d) in 250-mL shake flasks. Figure 6 shows the effect of inoculum age on the growth of *P. ginseng* hairy roots with 100 mL of medium in 250-mL flask cultures. Hairy roots inoculated about 1 g fresh weight per 100 mL of medium for this experiment. The maximum growth rate was obtained using inoculum precultured for 10 d in liquid shake-flask cultures. The doubling time of *P. ginseng* hairy roots was about 6.5 d in 1% (w/v) flask cultures *(19),* so the maximum growth rate of hairy roots presented at 8- to 10-d precultured periods. It appears that the higher initial growth rate of precultured inoculum results in shorter lag phase for growth of hairy roots. In *Beta vulgaris* hairy roots, biomass growth was at a maximum in 14-d-old inoculum on solid and liquid medium culture at precultured conditions for 7–21 d *(22).*

Plant cell suspension cultures inoculated at low cell concentrations resulted in a typical growth rate reduction by long lag phase periods, whereas plant root cultures showed an improvement in growth rate. These contrasting growth patterns can be explained as a result of the basic physical and physiologic differences such as the high specific surface area of cells as compared to roots and the differentiated structure of roots *(14).*

Figure 7 shows the effect of inoculum size on growth rate in 250-mL flask cultures. Maximum growth rate occurred with an inoculum size of 0.4% (w/v). Above 0.7% (w/v) growth rate was declined. The final cell growth was not proportional to the increase in inoculum size. This result, caused by the growth rate reduction at higher root tissue concentration,

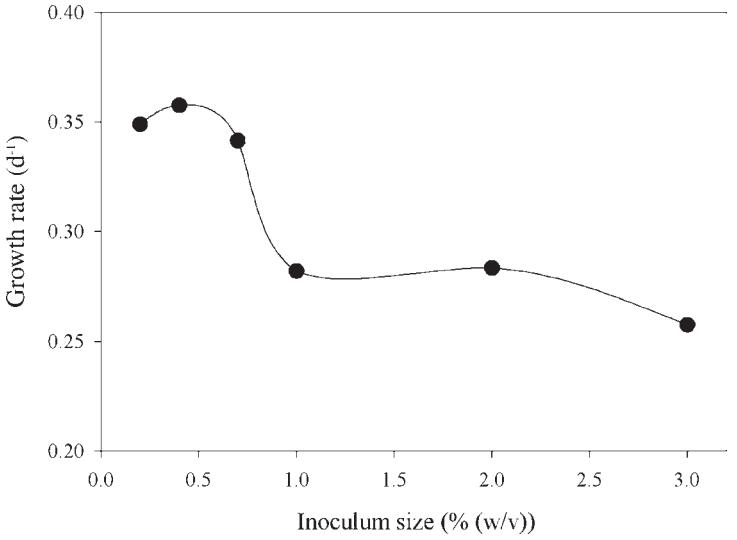

Fig. 7. Comparison of hairy root growth rate on inoculum size in flask culture at 15 d.

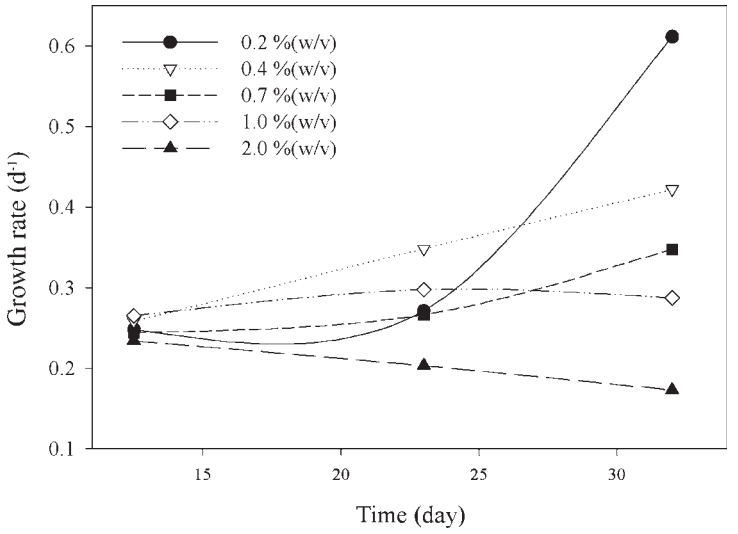

Fig. 8. Effect of inoculum size on biomass growth rate in bioreactor culture for 32 d.

may be owing to the liquid mass-transfer limitations and the depletion of medium nutrients. In root and suspension cultures of *Hyoscyamus muticus*, effective specific growth rates steadily increase as inoculum size decreases, whereas cell suspensions show a marked decline in growth rate *(14)*.

For large-scale culture, inoculum size is one of the most significant factors affecting plant cell/tissue culture systems. Figure 8 shows the time course of the change in growth rate as inoculum size in bioreactor cultures.

Table 1
Comparison of Metabolite Content on Root Tip Parts of *P. ginseng* Hairy Roots

	Crude saponin (%)	Intracellular polysaccharide (g/g)
End part	10.2	0.201
Center part	17.6	0.174
Whole hairy root	16.4	0.191

The growth rate of hairy roots did not greatly differ for an initial growth period of 13 d. At below 1% (w/v) inoculum size, growth rates were enhanced for 34-d culture periods. In particular, a sharp increase in growth rate for long cultivation periods was observed at 0.2% (w/v) inoculum size. By contrast, the declining growth pattern was above 1% (w/v). As inoculum becomes smaller, there are very few hairy roots in large volume of medium in large-scale culture. As a result of the small amount of hairy roots, the influence of the physiologic and physical status of inoculated hairy roots on overall growth rate becomes important. In fact, the higher growth rate at reduced optimum inoculum tends to reduce the time required to reach the final mass concentration *(14).*

The distribution of metabolites in *P. ginseng* hairy roots cultured in shake flasks for 30 d is shown in Table 1. The crude saponin and polysaccharide content were about 16.4% and 0.191 g/g, respectively, in the whole hairy roots. The metabolite contents of different hairy root sections were as follows: meristem part of root tip (below 10 mm), 10.2 and 0.201; maturation part of root tip (10–20 mm), 17.6 and 0.174 on a dry weight basis. These results are owing to the fact that the meristem part has younger periderm and cortex tissue, which is distributed with oil canal, than the maturation part of hairy root. Root hair and lateral root parts of field-cultured *P. ginseng* roots showed higher crude saponin content than main root parts. In the natural *P. ginseng* roots, saponin content is higher in the periderm and cortex than in the xylem. However, the main part on natural roots has a higher polysaccharide content than the lateral root or root hairs *(19).* Ramakrishnan et al. *(13)* reported that for biomass and specific hyoscyamine content, the total amount of hyoscyamine in the whole roots was equal to the sum of the amounts in the tips and mature parts.

Conclusion

We investigated the effect of inoculum conditions such as the part, number, and length of root tips; age of the hairy roots; and size of inoculant on the growth and metabolite biosynthesis of *P. ginseng* C.A. Meyer hairy root culture. The growth of *P. ginseng* hairy roots in shake-flask cultures was found to vary depending on the inoculum conditions. The end part, whose apical meristem of root tip had been excised prior to inoculation,

was grown to a total biomass 1.6 times that of the center parts, which are the root tip parts after excision about 10 mm from the end part. Root tip with apical meristem showed length enhancement with lateral root formation. However, the center root tip formed lateral roots without length enhancement of the original root tip. Increasing the number of inoculated root tips from one to six enhanced growth rates, but the growth rate reduced by 21% at 9 root tips. By inoculating with root tips of different lengths (5–25 mm), the highest growth rate was obtained for 5-mm-long root tips. At precultured age of root inoculant, maximum growth rate was obtained using inoculum precultured for 10 d. For the experiment on the effect of inoculum size on growth rate in 250-mL flask cultures, maximum growth rate at 0.4% (w/v). Above 0.7% (w/v) inoculum size, growth rate declined. The results of the experiment on the change in growth rate as the result of inoculum size in 1-L bioreactor cultures showed that the growth rate of hairy roots did not differ greatly with an initial growth period of 13 d. At below 1% (w/v) inoculum size, growth rates were enhanced for 34-d culture periods. In particular, a sharp increase in growth rate with long cultivation periods was observed at 0.2% (w/v) inoculum size. By contrast, the declining pattern was shown above 1% (w/v).

References

1. Banthorpe, D. V. (1994), *Nat. Prod. Rep.* **11,** 303–328.
2. Chattopadhyay, S., Farkya, S., Srivastava, A. K., and Bisaria, V. S. (2002), *Biotechnol. Bioprocess Eng.* **7(3),** 138–149.
3. Prakash, G., Bhojwani, S. S., and Srivastava, A. K. (2002), *Biotechnol. Bioprocess Eng.* **7(4),** 185–193.
4. Giri, A. and Narasu, M. L. (2000), *Biotechnol. Adv.* **18,** 1–22.
5. Nilsson, O. and Olsson, O. (1997), *Physiologia Plantarum* **100,** 463–473.
6. Nobuyuki, V. and Takesh, K. (1994), in *Advances in Plant Biotechnology*, Ryu, D.D.Y. and Furusaki, S., eds., Elsevier, Amsterdam, pp. 307–338.
7. Jeong, G. T., Park, D. H., Hwang, B., and Woo, J. C. (2003), *Appl. Biochem. Biotechnol.* **105–108,** 493–503.
8. Bais, H. P., Suresh, B., Raghaoarao, K. S. M. S., and Ravishankar, G. A. (2002), *In Vitro Cell. Dev. Biol.-Plant* **38,** 573–580.
9. Liu, C. Z., Guo, C., Wang, Y. C., and Ouyang, F. (2003), *Process Biochem.* **39(1),** 45–49.
10. Takahashi, Y., Hitaka, Y., Kino-Oka, M., Taya, M., and Tone, S. (2001), *Biochem. Eng. J.* **8,** 121–127.
11. Kanokwaree, K. and Doran, P.M. (1997), *J. Ferment. Bioeng.* **84(4),** 378–381.
12. Falk, L.R. and Doran, P.M. (1996), *Biotechnol. Lett.* **18(9),** 1099–1104.
13. Ramakrishnan, D., Salim, J., and Curtis, W. R. (1994), *Biotechnol. Tech.* **8(9),** 639–644.
14. Carvalho, E .B. and Curtis, W. R. (1999), *Biotechnol. Bioprocess Eng.* **4,** 287–293.
15. Bhadra, R. and Shanks, J. V. (1995), *Biotechnol. Tech.* **9(9),** 681–686.
16. Jung, N. P. and Jin, S. H. (1996), *Korean J. Ginseng Sci.* **20(4),** 431–471.
17. Wu, J. and Zhong, J. J. (1999), *J. Biotechnol.* **68,** 89–99.
18. Jeong, G. T., Park, D. H., Ryu, H. W., Lee, W. T., Park, K., Kang, C. H., Hwang, B., and Woo, J. C. (2002), *Appl. Biochem. Biotechnol.* **98–100,** 1129–1139.
19. Kino-Oka, M., Hitaka, Y., Niomiya, K., Taya, M., and Tone, S. (1999), *J. Biosci. Bioeng.* **88(6),** 690–692.
20. Woo, S. H., Park, J. M., and Yang, J. W. (1997), *Plant Cell Tissue Organ Cult.* **48,** 131–134.
21. Zhang, C .H., Wu, J. Y., and He, G. Y. (2002), *Appl. Microbiol. Biotechnol.* **60,** 396–402.
22. Pavlov, A., Georgiev, V., and Kovatcheva, P. (2003), *Biotechnol. Lett.* **25,** 307–309.

Special Session A

Microbial Pentose Metabolism

Special Session A

Microbial Pentose Metabolism

Chair: Bärbel Hahn-Hägerdal

University of Lund, Sweden

Co-chair: Neville Pamment

University of Melbourne, Australia

Introduction

Speakers were asked to provide quantitative data on the performance of different xylose- (or, in one instance, arabinose-) fermenting strains in laboratory media and, where possible, in "industrial" media prepared by hydrolysis of native lignocellulosic substrates. The data provided are presented in Table 1, which gives an indication of the performance of the various strains but should not be taken as a rigorous comparison. In particular, there is considerable variation in the extent of nutritional supplementation of the various media and the degree of detoxification of the hydrolysates. References provided by some of the speakers are also given *(1–6)*.

Speakers

L. R. Lynd, Dartmouth College, Hanover, NH
S. A. Underwood, University of Florida, Gainesville, FL
B. S. Dien, USDA NCAUR Laboratories, Peoria, IL
M. Zhang, NREL, Golden, CO
T. W. Jeffries, USDA Forest Products Laboratory, Madison, WI
R. Benson, Tembec Chemical Products, Temiscaming, Quebec, Canada
J. Becker, Institute for Microbiology, Frankfurt, Germany
A. Nilsson, University of Lund, Lund, Sweden
S. Helle, University of British Columbia, Vancouver, Canada

References

1. Becker, J. and Boles, E. (2003), *Appl. Environ. Microbiol.* **69,** 4144–4150.
2. Nigam, J. N. (2001), *J. Ind. Microbiol. Biotechnol*. **26,**145–150.
3. Shi, N. Q., Cruz J., Sherman F., and Jeffries T. W. (2002), *Yeast* **19,** 1203–1220.

Table 1
Performance of Some Recombinant and Native Xylose-Fermenting Organisms Under Laboratory Conditions and on Native Lignocellulosic Hydrolysates

	Laboratory conditions [a]			"Industrial" conditions [b]	
Strain	Xylose concentration (g/L)	Ethanol yield (g/g) [c]	Ethanol productivity (g/[g cells·h]) [d]	Ethanol yield (g/g) [c]	Ethanol productivity (g/[g cells·h]) [d]
Thermoanaerobacter thermosaccharolyticum [e]	72 [m]	0.33 [m]	0.4 [m]	—	—
Escherichia coli KO11 [f]	90	0.47	0.38	0.49 [q]	0.37 [q]
E. coli FBR5 [g]	40	0.43	0.29	0.46 [r]	0.214 [r]
Zymomonas mobilis 8b [h]	100	0.47	1.13 [p]	0.42 [s]	—
Pichia stipitis CBS 6054 [i]	80	0.40	0.347	—	—
P. stipitis FPL-Shi21 [i]	80	0.46	0.43	—	—
P. stipitis NRRL Y-7124 [i]	—	—	—	0.41 [t]	0.44 [t]
P. stipitis CBS 5773 [j]	—	—	—	0.35 [u]	0.05 [u]
	—	—	—	0.44 [v]	0.083 [v]
Saccharomyces cerevisiae JBY25-4M [k]	20 [n]	0.3 [n]	0.08 [n]	—	—
S. cerevisiae TMB 3006 [l]	—	—	—	0.37 [w,x]	0.66 [w,x]
S. cerevisiae TMB 3400 [l]	20	0.25 [o]	0.10 [o]	0.43 [w,x]	0.25 [w,x]

[a] Synthetic medium containing xylose or arabinose and one or more complex ingredients (unless otherwise indicated).
[b] Mixed sugar hydrolysate of native lignocellulosic substrate lacking complex medium ingredients. Detoxification applied unless otherwise indicated.
[c] Based on initial sugar concentration.
[d] Based on time to produce 95% of final ethanol concentration.
[e] Data supplied by L.R. Lynd.
[f] Data supplied by S. Underwood.
[g] Data supplied by B. S. Dien.
[h] Data supplied by M. Zhang.
[i] Data supplied by T. W. Jeffries.
[j] Data supplied by R. Benson.
[k] Data supplied by J. Becker and E. Boles; arabinose fermenting strain.
[l] Data supplied by A. Nilsson.
[m] Chemostat data on 72 g/L xylose feed
[n] Carbon source: arabinose.
[o] Defined mineral medium (no complex ingredients).
[p] High specific productivity in part reflects low inoculum size.
[q] Bagasse hemicellulose hydrolysate, mainly xylose (100 g/L of total sugars). Supplemented with 2.5% (w/v) corn steep liquor.
[r] Corn stover hydrolysate (37 g/L of xylose, 28 g/L of glucose, 20 g/L of arabinose).
[s] Eighty percent overlimed corn stover hydrolysate (50 g/L of xylose, 75 g/L of glucose).
[t] Data of Nigam, 2001, for fermentations on spent sulfite liquor.
[u] Industrial scale continuous fermentations on rotoevaporated spent sulfite liquor (hardwood pulping, y softwood pulping).
[v] Industrial scale continuous fermentations on rotoevaporated spent sulfite liquor (softwood pulping).
[w] Undetoxified hydrolysate.
[x] Dilute acid hydrolysate of forest residuals, mainly spruce (6 g/L of xylose, 13 g/L of mannose, 16 g/L of glucose, 3 g/L of galactose, 1 g/L of arabinose), fed-batch fermentation.

4. Shi, N. Q., Davis B., Sherman F., Cruz J. and Jeffries T. W. (1999), *Yeast* **15,** 1021–1030.
5. Underwood, S. A., Zhou, S., Causey, T. B., Yomano, L. P., Shanmugam, K. T., and Ingram, L. O. (2002), *Appl. Environ. Microbiol.* **68,** 6263–6272.
6. Wahlbom, C. F., van Zyl, W. H., Jonsson, L. J., Hahn-Hagerdal, B., and Otero, R. R. C. (2003) *FEMS Yeast Res.* **3,** 319–326.

Special Session B

International Energy Agency—Bioenergy
Current State of Fuel Ethanol Commercialization

Special Session B

International Energy Agency—Bioenergy

Current State of Fuel Ethanol Commercialization

Warren E. Mabee,* David J. Gregg, and John N. Saddler

Forest Products Biotechnology Group,
University of British Columbia, 2424 Main Mall,
Vancouver, BC, Canada V6T 1Z4

The International Energy Agency (IEA) was founded in 1974 as an autonomous body within the Organization for Economic Co-operation and Development to implement an international energy program in response to the oil shocks. IEA Bioenergy was created in 1978 by the parent organization with the aim of improving cooperation and information exchange between countries that have national programs in bioenergy research, development, and deployment. The goal of IEA Bioenergy Task 39, "Liquid Biofuels," is to successfully introduce biofuels for transportation into the marketplace. To meet this objective, the members of Task 39 have taken on the job of reviewing both technical and policy or regulatory issues that are related to commercializing the technology for fuel ethanol production. It is our belief that these issues are strongly related, and that successful commercialization of the technology will require advances in both areas. In this session, the Task 39 group worked to create a forum in which the interrelated issues of policy and technology could be reviewed and explored.

The production of raw biomass material and its subsequent conversion to fuels creates local jobs, provides regional economic development, and can increase farm and forestry incomes. Environmental benefits associated with the use of ethanol include a net reduction of carbon dioxide emissions and improved waste utilization. The cost of ethanol manufacture remains relatively high, however; consequently, ethanol fuels presently have significant impact only in those locations where governments provide policies and incentives that encourage their use. The positive social and environmental aspects of ethanol will always make this technology an attractive policy option, but the long-term success of the ethanol industry will require technological breakthroughs and refinements as well as political support. In the short term, governmental policies and incentives allow the infrastructure for biofuels to be established, and they

*Author to whom all correspondence and reprint requests should be addressed.

start the transition from a petroleum-only economy. At the same time, governments are also sponsoring research and development efforts to reduce the cost of biofuels so they can compete more effectively in the marketplace. The long-term viability of biofuels will require both that the infrastructure for biofuels exists and that economically competitive processes are available.

Participants in the commercialization of fuel ethanol may be characterized according to a number of factors, including the size of the participant, the participants interest in the process, and the policies under which the organization must operate. A greater chance of success in commercialization may be realized by linking participants with complementary characteristics. Small, entrepreneurial companies are often leaders in developing the technology and processes required for bioconversion; larger companies have access to the resources required to support long-term development goals and are connected to the marketplace and able to introduce new products more effectively than an entrepreneurial venture. Some participants are involved because of their interest in inputs to or outputs from the bioconversion process; others focus on creating the technology and improving the process. Finally, the policies of the state, province, or nation in which the participant is based have a large impact on their chances of success. A significant difference in the levels of subsidy, incentive, and mandated use exists among different nations, and these political realities must be incorporated into a commercialization plan.

One of the most difficult tasks in the commercialization process is identifying policies or actions that are effective in incubating the ethanol industry. We asked each of the oral presenters in our session to identify the actions that they would like to see their respective government take. Because our participants' roles in the ethanol industry are characterized quite differently, the responses that they gave were quite different. When taken individually, the suggestions provided in this session tracked very closely to the specialty of the participant. It is expected, however, that effective policy recommendations for the commercialization of ethanol must incorporate the full range of these suggestions.

Author Index

Subject Index